Environmental Assessment of the Alaskan Continental Shelf

Annual Reports of Principal Investigators for the year ending March 1977

Volume XIV. Transport

DISCLAIMER

The Environmental Research Laboratories do not approve, recommend, or endorse any proprietary product or proprietary material mentioned in this publication. No reference shall be made to the Environmental Research Laboratories or to this publication furnished by the Environmental Research Laboratories in any advertising or sales promotion which would indicate or imply that the Environmental Research Laboratories approve, recommend, or endorse any proprietary product or proprietary material mentioned herein, or which has as its purpose an intent to cause directly or indirectly the advertised product to be used or purchased because of this Environmental Research Laboratories publication.

VOLUME XIV

TRANSPORT

CONTENTS

* indicates final report

ANNUAL REPORT

Project No: RW0000 R7120856

Research Unit: No. 48

Reporting Period: April 1, 1976
     March 31, 1977

No. of Pages: 5

Development and Operation of HF Ocean Current Mapping Radar Units

Principle Investigator: Donald E. Barrick

Submitted: April 1, 1977

CURRENT-MAPPING RADAR PROGRAM

Progress Report 1 January 1977

I. Abstract

The first simultaneous two-site data were obtained in mid-October of 1976. Surface current maps were generated by combining the data from the two sites, one at Fort Lauderdale and one at South Mission Beach. This map shows surface currents consistent with previously measured Gulf-Stream flows in the area off the southern coast of Florida. To this date, two-site data have been taken on October 19, 20, 26, 27, 28, 29, 30 and December 14. An example of the map is shown at the back of the report.

At this time, there is no direct supporting surface current measurements made during our radar operations. However, the results are consistent with the general magnitudes, directions, and shear of the Gulf Stream in that area, giving confidence that the radar system and data processing techniques are working properly.

II. Objectives

The primary objectives of the program has been twofold: (i) to implement a proven radar concept into a transportable, easily assembled and operated pair of units capable of producing a map of near-surface currents on location in real time, and to calibrate the system as to its accuracy; (ii) to operate the radars at coastal areas of interest along the Gulf of Alaska seacoast in support of the OCSEAP objectives in physical oceanography. It is planned that the first Alaskan operations of the radar unit-pair will be in the Lower Cook Inlet, with one site near Anchor Point (above Homer), and the other at Point Naskowhak (near Seldovia). Experiments may be conducted in other areas of Alaska and the continental United States in conjunction with other research groups for specific scientific purposes, such as correlation of observed oil trajectories with the output of our radar.

Other objectives of the current mapping radar program for the next calander year are to: 1) Improve the reliability of existing hardware, 2) Optimize the field software through ground truth testing, 3) Determine the accuracy of the maps via ground truth testing, 4) Interpret current data from Alaska.

III. Field Activities

1. A major milestone point in the Florida field tests was reached on 24 July: namely, experimental evidence that the field radar system works! A summary of the details of accomplishment is the following. Signals were broadcast and received through the antenna system, converted to digital bit streams, filtered, and Fourier-transformed in the field in real time.

The outputs are digital sea-echo Doppler spectra for different ranges. These spectra contain all of the information about the surface currents, which are deduced therefrom by mathematical formulas already tested in software form in the laboratory. The several sets of Doppler spectra we measured thus far contain all of the identifying features of the Gulf Stream, indicating that the basic operation of the system was proper.

2. A second major field event consisted in moving the entire radar unit to the beach and operating it from a van with power from a portable gasoline generator; field operations in this mode were conducted for nearly one week, with no serious interruptions due to hardware failures. Of further interest is the fact that the team continued these operations throughout a tropical storm (which later became a hurricane), with winds of 50 knots and waves of 15 feet. Much of the time the antennas on the beach were awash, but data continued to be recorded. Sea-echo signals were detected to ranges exceeding 90 km. The very harsh conditions encountered during this three-day period in Florida will most likely exceed those anticipated in Alaska. Hence the continued operation of the radar during this period gives us confidence that the system should function well in the future.

Later field operation at two sites were in the Miami-Ft. Lauderdale area in October and December and has resulted in two-site surface-current maps. Direct comparisons of drifter measured surface currents were not possible until March because of weather or because the ship was unavailable. However, the early results are consistent with the known Gulf-Stream patterns; the fact that the system produced there results in an indication that the agreement between the radar output and other surface current observations in the upper 50 cm of the ocean will be close. To this date, two site data have been collected on October 19, 20, 26, 27, 28, 29, 30, December 14, 1976 and the week of March 20, 1977.

The drifter comparisons to establish the current map accuracy involved returning to Florida, and taking surface current observations with the dual-site radar simultaneous with a surface drifter observations. The drifters were put into the water at various distances from shore and tracked with a ship for about 15 minutes to determine the surface velocity. This was done on a line halfway between the two radars from 10 km at the nearest point from shore to a maximum of 60 km.

Preliminary analysis shows a good comparison with the radar derived velocity fields.

IV. System Design, Construction, Calibration and Modifications

During the past year the following tasks were accomplished:

1. Designs. All system-level designs have been completed. All of the hardware components being constructed in-house were designed.

3

2. Procurements. Major hardware items which were purchased commercially include: (i) the electronic laboratory test gear; (ii) computer support facilities; (iii) the radar receivers; (iv) the mini-computers for the field units. All of these major hardware items have been delivered.

3. In-House Fabrication. Several hardware items were designed and constructed in-house. These included: (i) transmitter-drivers; (ii) transmitter power amplifiers; (iii) receiving antennas; (iv) transmitting antennas; (v) radio telemetry gear (between sites); (vi) fast Fourier-transform digital hardware; (vii) array-processing digital hardware; (viii) data-acquisition board, consisting of the sample and hold circuits, the analog-to-digital converters, and the digital pre-averaging circuits; (ix) semi-conductor buffer memory; (x) graphic display hardware; (xi) systems-integration hardware, including special high-efficiency power supplies, power sequencing circuitry, and fault-analysis circuitry. All of these items were built and checked out in their final form for the field units.

4. System Integration. All of the hardware items which were procured or fabricated in-house were assembled into the two units constituting the radar pair; this assembly was completed 15 June. The only item which was not integrated into the field units is the fast-Fourier transform processor; for the present, this function is being done by minicomputer software. Each radar unit consists of two weather-proof fiberglass cases containing shock-mounted racks; these racks contain all of the RF and digital gear necessary for producing real-time current maps in the field. Each case stands 44 inches high and weighs about 175 pounds, capable of being handled in the field by two men.

5. System Performance Analyses. Based upon the system design specifications, an analysis of system performance was completed. This study shows that the maximum range from each radar unit should be of the order of 70 km. An analysis of azimuthal angle-of-arrival accuracy shows that insignificant position errors will result when signal-to-noise ratio exceeds 10 decibels. An optimization study indicates that the ideal separation between the two units is approximately 40 km.

6. System Software. Integration of operating-system software for control of the various hardware components was completed. Graphics and display software (for making on-site current maps) has been completed. The radar-signal data-processing software was completed and checked out. This software has already operated satisfactorily in the field.

7. System Simulation. Using the graphics/display software and the signal data-processing software, simulations were run in the laboratory. These simulations — instead of using actual radar signals — employ simulated signals consisting of the (random) sea-echo signal and a (random) noise signal, as would be received by the actual radar at each of the

three antenna terminals. The sea-echo signal includes the effect of the current pattern on the Doppler shift. Any desired current pattern can be inserted on the signal. These simulated signals are then processed by the same software to be used in the field. Hence, such simulations permit one to: (i) debug and check out the system software before actually going into the field; (ii) obtain a feel for the accuracy of the output product (i.e., the current maps); (iii) modify and improve the system software where certain inaccuracies and weaknesses are detected from the simulations.

8. Antennas. The transmitting antenna system was conceived to be moderately directive, so that (i) higher signals could be obtained from desired ocean regions, and (ii) signals from unwanted areas (for example, behind the radar) could be eliminated. A design study contract was given to Lawrence Livermore Laboratories, which has an international reputation in the area of numerical antenna analysis. Based on their study (now completed), we selected and constructed Yagi monopole antennas consisting of both three vertical elements (for a wider pattern) and four vertical elements (for a narrower pattern). (The vertical elements are about 9 feet high, and the entire device can be erected on the beach in about 1/2 hour.) The antenna has been checked out electrically, and the measured parameters agree very closely with those predicted by Livermore. (The agreement was far better than expected.)

The receiving antenna system consists of three short elements. While one version has been built and checked out, we redesigned (in-house) this antenna system to be much smaller and more lightweight. The receiving antenna dimensions are much less critical than those of the transmitting antenna.

9. Operating Frequencies. We have recently received frequency allocations from IRAC for all of our upcoming operations. We are permitted to select any frequencies in the band between 25.330 and 28.000 MHz; these allocations we presently consider satisfactory for all of our operations.

10. Theoretical Analyses. Several non-system, oceanographic factors will limit the accuracy of the system for measuring near-surface currents. One of these is the nonlinear interactions of surface waves, which generate Doppler-shift errors that are not associated with the currents. Examination of this mechanism theoretically shows that such errors — expressed in terms of radial current velocity — can always be expected to be less than 10 cm/s, with typical errors of the order of 5 cm/s.

11. Modifications. Repairs have been made to some of the components corroded by the humid salt air of Florida. Steps were taken to improve the reliability in the field, and modifications were made to bring the nearest range gate closer than 12 to 15 km from shore. The receiver was modified in order to obtain better signal-to-noise ratios at the near ranges, and this will possibly improve this ratio at the more distant ranges.

5

Because of problems with antenna cables, antenna switches were built to eliminate two of the four receiver antenna cables. Before that, they had to be within 1/4 inch in length relative to each other, a difficult task when each cable is 1500 feet long. Special care had to be taken not to stretch them when moving them. These switches are now located at the antennas, and thus the extra two cables can be eliminated; mismatched cable lengths will therefore no longer be a problem.

Additional work done on the system since returning from Florida includes a new calibration circuit to check-out the entire data flow loop, a new lighter power supply, a modification of the solid state buffer to reduce parity errors, and a new video display that can plot the time series data and FFT in real time. The latter will be useful for ascertaining that the data is good.

Since the October tests much effort has been devoted to software development for the field system. This involves various kinds of signal processing techniques of the two-site data to remove some of the random-like fluctuations from the derived currents. These techniques include the averaging of several two-minute runs together, statistical thresholding tests, and filtering techniques. New data from other locations are now needed to verify how these techniques work where the flow is not as uniform as the Gulf Stream. Another concept is being tried to increase the area covered by the two radars. The software for these techniques has been completed.

V. Results

Appended to this report are surface current maps, perhaps the most concise form of our results so far. This shows part of the Gulf Stream between the Miami-Ft. Lauderdale area. The first one, Fig. 1, show the results with little signal filtering to remove the noise, the second, Fig. 2, is the result of more signal processing. Both of these were made from the same data taken on October 20, 1976. The long line denotes the shoreline, and the two lines perpendicular to the shore line denote the location of the sites at Ft. Lauderdale and S. Miami Beach.

VI. Preliminary Interpretations of Results

In the map, one can see a definite increase in the current magnitude as a function of the distance from the shore. The maximum current is about 2 m/s. Publications by Duing and others show that these values are reasonable, but are subject to some temporal variations. We did observe a variation of as much as 50% in the magnitude of the current during the times of our observations.

6

VII. Problems Encountered/Recommended Changes

Most of the problems we have encountered thus far have been hardware related. Since returning with the radars to Boulder, effort has been made to eliminate these problems in the field. We found the very moist salt air to be the most damaging to the hardware.
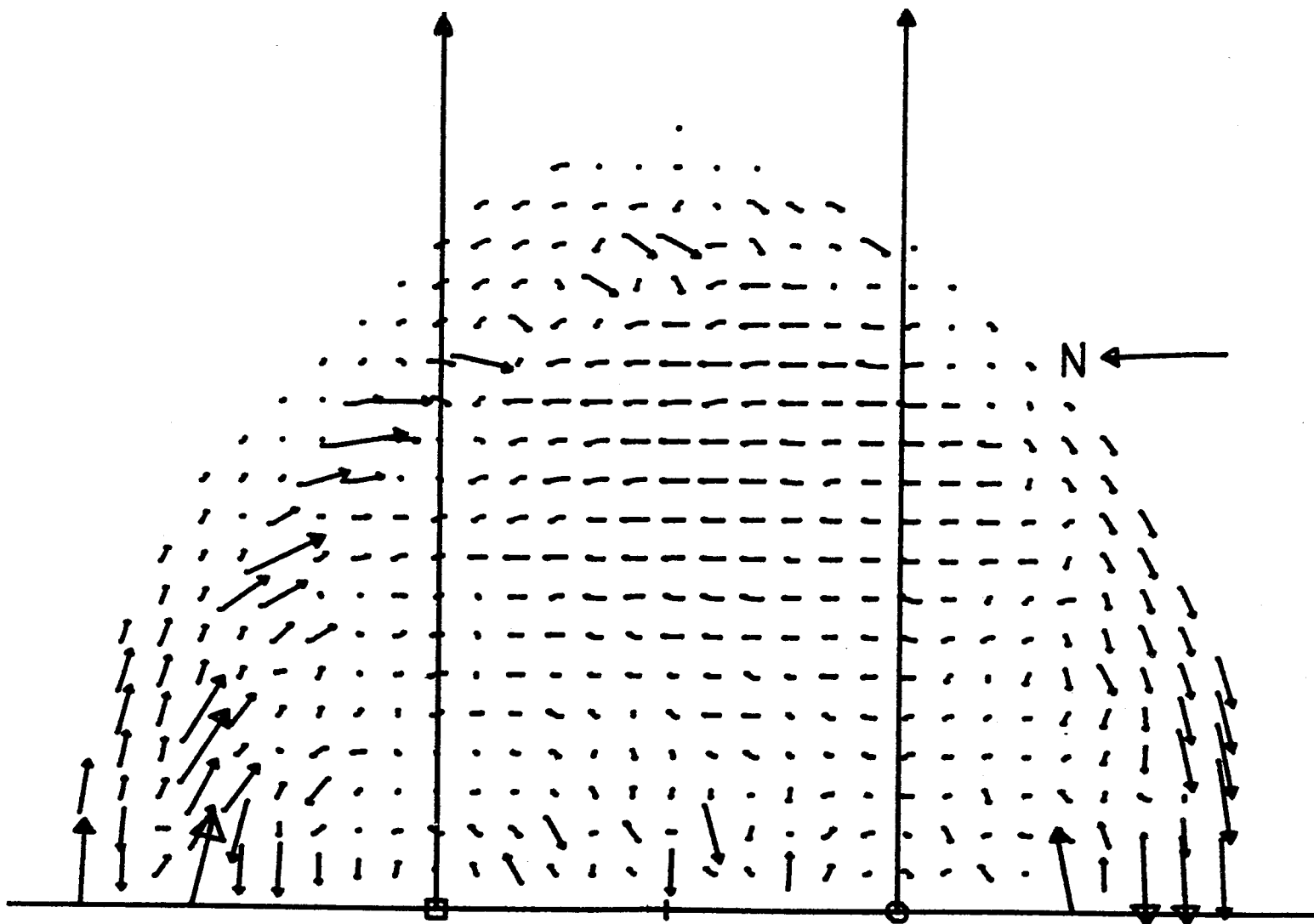
Figure 1.   Reduced data from Ft. Lauderdale and Miami Beach with no numerical processing.   The two vertical lines represent the separation between Ft. Lauderdale and Miami Beach.
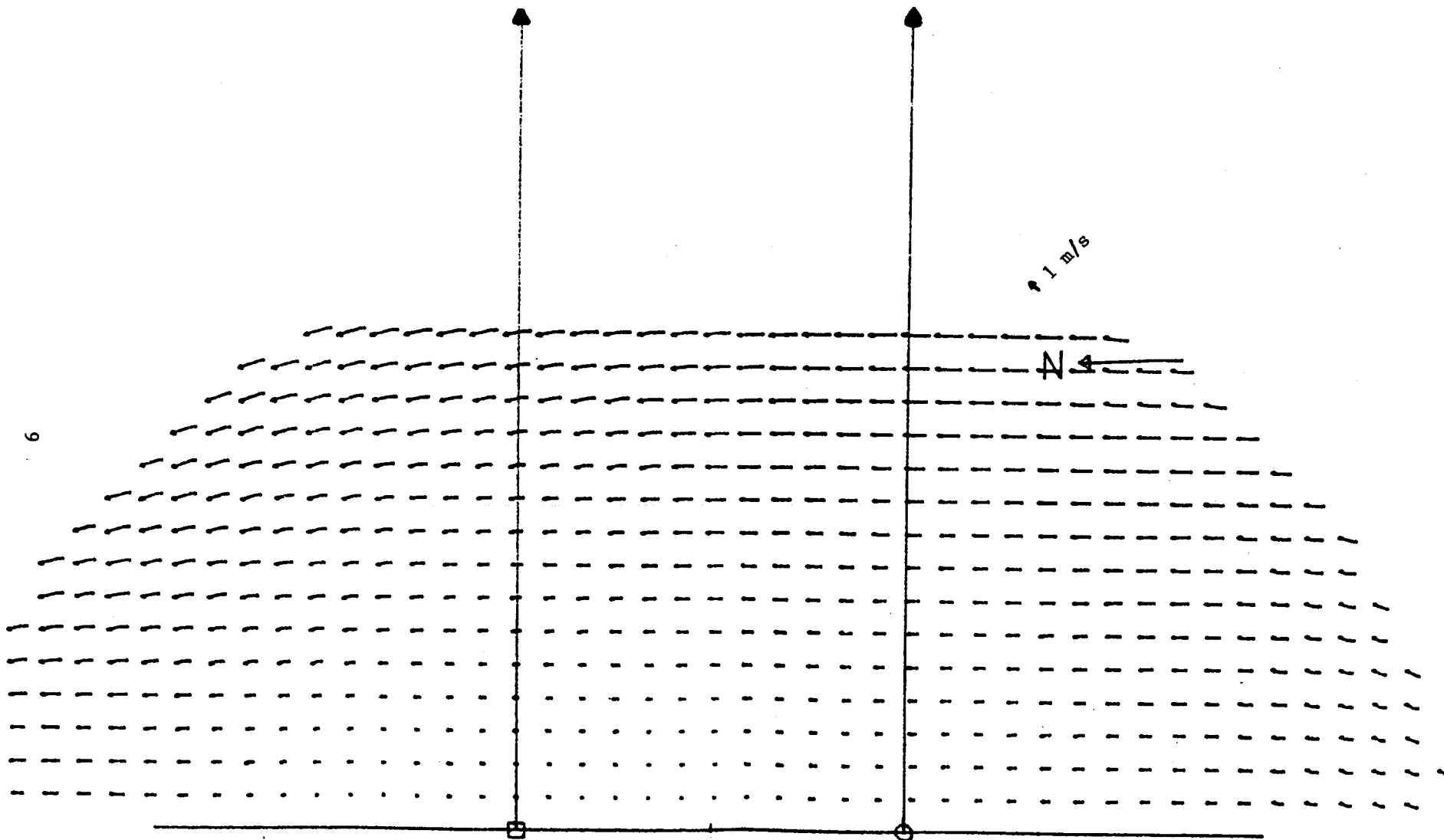
Figure 2. The same data with numerical processing.

SURFACE CURRENTS OF THE NORTHEAST CHUKCHI SEA

BY

G. L. HUFFORD, B. D. THOMPSON, AND L. D. FARMER

FINAL REPORT

RU - 81

ENVIRONMENTAL ASSESSMENT OF THE ALASKAN CONTINENTAL SHELF

SPONSORED BY

UNITED STATE DEPARTMENT OF INTERIOR
BUREAU OF LAND MANAGEMENT

APRIL 1977

INTRODUCTION

A knowledge of the surface current patterns along the north Alaskan coast
is of both economic and environmental interest. The discovery of oil reserves
along the coast has brought development and exploitation on shore with offshore
drilling on the continental shelf certain to be undertaken within the next few
years. Even the best of planning and the most modern techniques cannot insure
that accidental oil spills will not occur. The initial movement of the spilled
oil during the summer would be determined primarily by the local surface currents.
Thus a working knowledge of the surface currents along the north Alaskan coast
is imperative.

During August 1976, a detailed study of the surface currents of the northern
Chukchi Sea and western Beaufort Sea coasts was attempted from helicopters from
the icebreaker USCGC GLACIER. The objective of this report is to describe the
surface circulation during open water.

DESCRIPTION OF STUDY AREA

The investigation was conducted primarily in the region between Icy Cape
(70°09'N, 161°55'W) and Point Barrow (71°20'N, 156°40'W) and seaward to the pack
ice edge. A chart of this study area is shown in Figure 1. A few stations were
occupied at Harrison Bay in the Beaufort Sea. (See Figure 9.)

The bathymetry of the Chukchi Sea has been discussed by Creager and McManus
(1966). The Chukchi is a continential shelf sea, essentially flat with depths
generally <60m. The most prominant feature in the northeast Chukchi Sea is
Barrow Canyon with depths >50m found as far south as Cape Franklin. The canyon
shows a sectional asymmetry, with the steepest side next to the coast.

The most comprehensive analysis of the physical oceanography of the Chukchi
Sea to date has been that of Coachman et al (1976). Using data from the cruises
of the NORTHWIND (1962), BROWN BEAR (1960), NORTHWIND (1963), GLACIER (1970),
and OSHORO MARU (1972), they have based their analysis on two regional water mass
groupings, ACW (Alaskan Coast Water) and BSW (Bering Sea Water). In the summer
BSW (1-7°C, 32.2-33.0 o/oo) dominates the central and western part of the Chukchi
Sea. ACW (2-10°C, <32.2 o/oo) is found in the eastern part of the sea with a
recognizable demarcation between it and BSW. The ACW is characterized by lateral
gradation from a relatively cold and saline faction on the west, to a warm and
less saline faction close to the coast.

The ACW flows north along the Alaskan coast. Near Icy Cape, data from
Fleming and Heggarty (1966) show that ACW is often found to spread above a colder,
more saline water. They interpreted the cold water to be residual Chukchi Sea
winter water.

Current measurements of the surface waters of the Chukchi Sea north of
Cape Lisburne are few. The most comprehensive measurements are those from the
BROWN BEAR (Fleming and Heggarty, 1966) and the OSHORO MARU (unpublished, 1972).
Most of the measurements were of durations of less than one hour. The observa-
tions reveal that in the summer surface (0-10m) currents along the Alaskan coast
flow northerly parallel to the coast. Speeds of 15 to 25 cm sec^{-1} are indicated.
Near Point Hope there is an acceleration of the flow ($\sim$40cm sec^{-1}). Another
small acceleration appears to occur near Icy Cape ($\sim$30cm sec^{-1}). The few
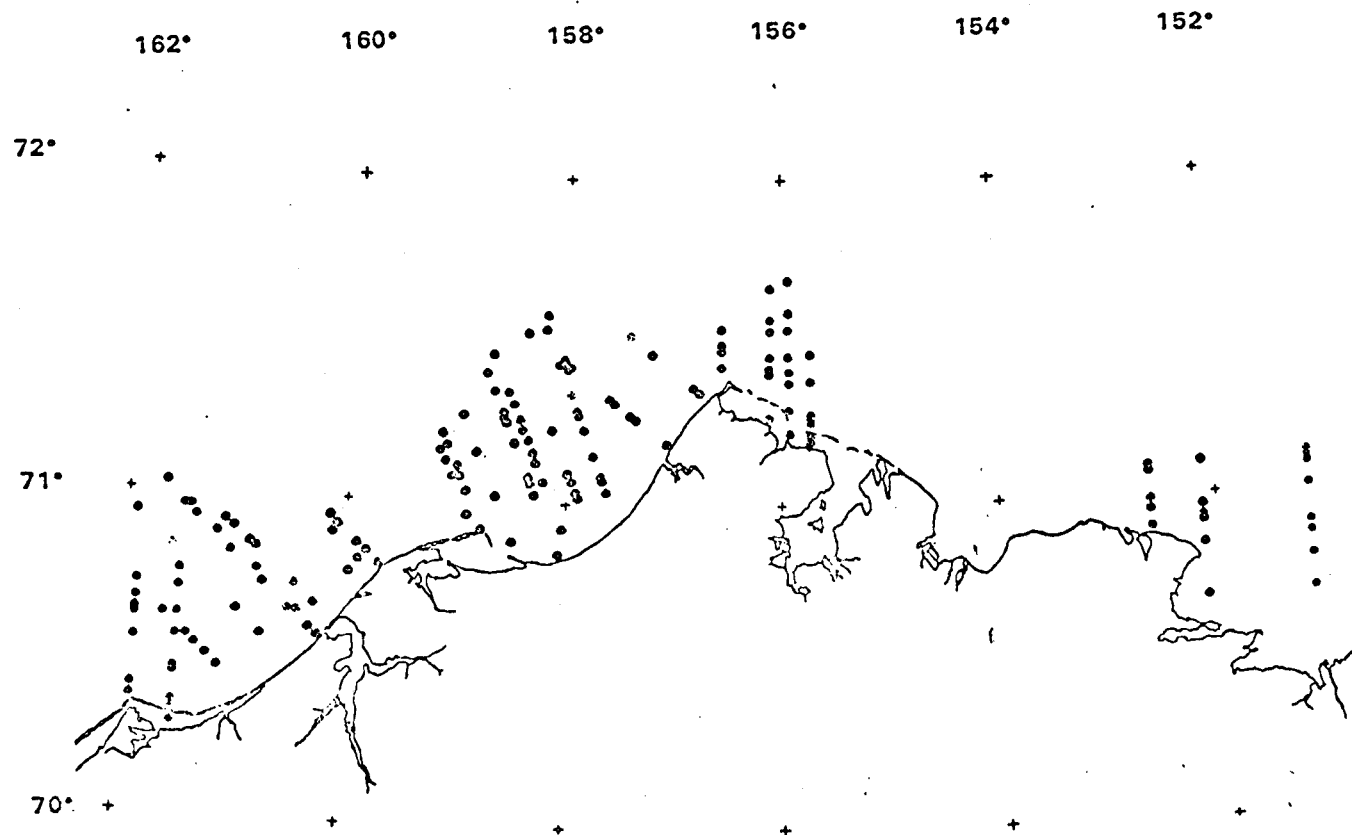
11

Figure 1. Location of stations taken in the northeast Chukchi Sea and Beaufort Sea.

measurements of currents indicate a considerable complexity and great variability in the flow. Aagaard (1964) reports that offshore of the northeast coast when winds were from the southwest, the surface flow was about 20-50cm sec^{-1} toward the northeast. When the winds were from the northeast, the surface flow was slowed or reversed.

Wiseman et al. (1974) have examined current flow in the nearshore region of the northeast Chukchi Sea. The currents appeared to be wind driven and severely controlled by bottom topography. The mean velocity of flow for July and August was 21.8cm sec^{-1} to the north. A small semi-diurnal tidal component was present; the amplitude was only about 1cm sec^{-1}. A major feature of the summer flow was significant reversals in direction associated with changes in wind direction.

No comphensive picture of the surface water motions in the northeast Chukchi Sea can be obtained from the scattered measurements discussed above. Location of stations have been hampered in the past by the presence of ice. Even in the summer, the polar pack is never far off the coast and can advance onto the shore usually in response to northerly and northwesterly winds. In addition, because of the draft of the icebreakers from which most of the data are obtained, few measurements have been taken shoreward of the 20m depth contour.

Long-term wind data are available from two locations along the northeast Chukchi Sea coast: Cape Lisburne and Barrow (Figure 2). The predominant summer winds are from the east-northeast and are dominated by the presense of the Polar High centered in the eastern Beaufort Sea (Campbell, 1965). Wind speed rarely exceeds 10m sec^{-1} in the summer. Southwesterly winds occur about 30 percent of the time and are caused by the passage of low pressure systems. These storms originate in either northern Siberia or the Bering Sea (Klein, 1957). During an average summer, six or seven low pressure systems will pass the region affecting the winds.

Wind stress measurements have been made over Chukchi Sea waters. Results by Walters (1975) indicates the appropriations of a single drag coefficient to describe momentum transfer from the wind to the water. The computed drag coefficient was 1.7×10^{-3}, very similar to the value (1.4×10^{-3}) of Banke and Smith (1971) for the Beaufort Sea coastal waters.

SURFACE CURRENT EXPERIMENT

The surface current study along the northeast Chukchi Sea coast was conducted using air-deployed ESCP (expendable surface current probes). The ESCP, developed by Richardson et al (1972), essentially consists of a plastic tube containing two floats, each with a dye packet, and a timing mechanism which releases the floats once they have reached the bottom of the body of water into which they have been dropped. At a preset time, a red plastic float is released, and later a white plastic float is released. These floats rise under their own buoyancy, and upon surfacing, the floats disperse a bright yellow-green fluorescein dye at the surface. Assuming that the current from the surface to the bottom has not changed during the delay time ($\sim$3 minutes) between float releases and that the floats rise at the same rate:
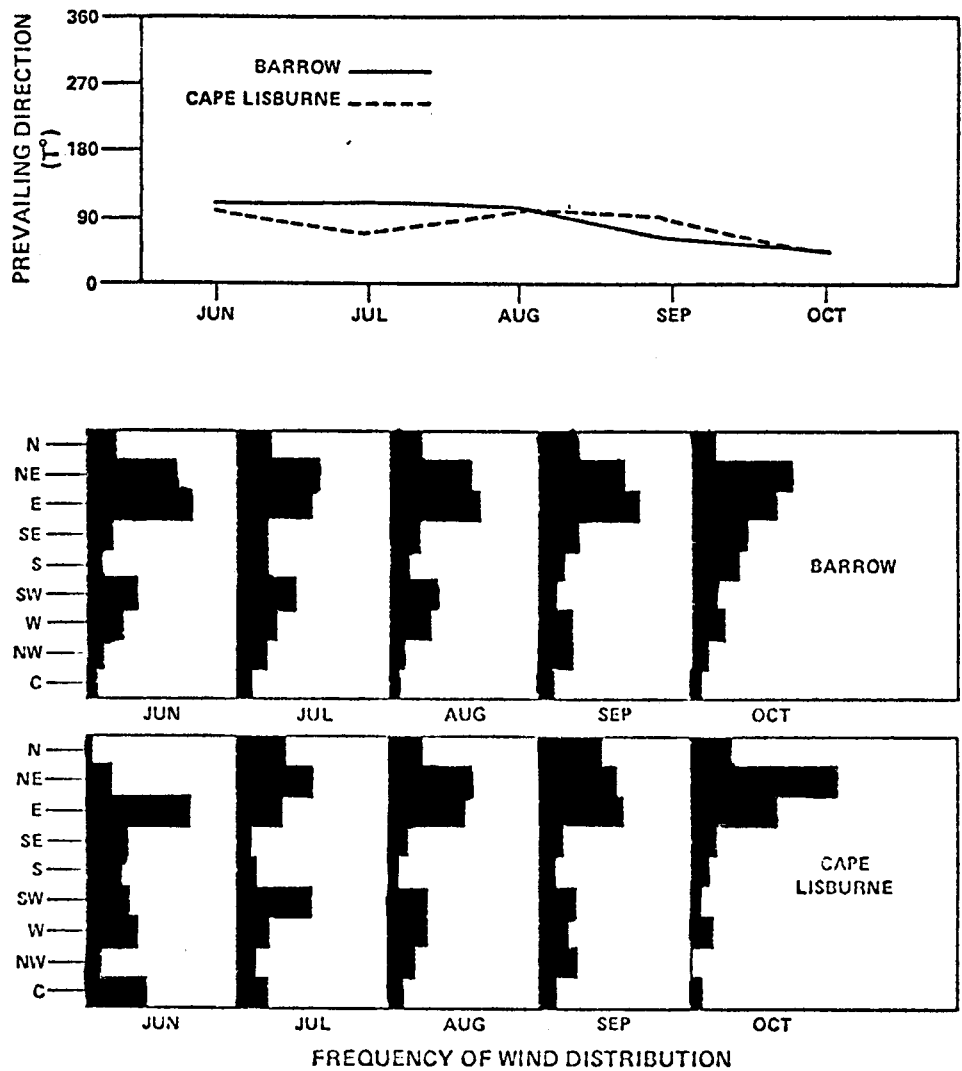
Figure 2.   Characteristics of the wind at Barrow and Cape Lisburne, Alaska.

14

$$\vec{V}_s = \frac{\vec{x}_{RW}}{t_D} \quad \ldots \ldots \ldots \ldots \ldots \ldots \ldots (1)$$

where $\vec{V}_s$ is the surface current, $\vec{x}_{RW}$ is the vector separation between the red and white floats, and t_D is the time delay between their releases. The direction of flow is the heading from the white float to the red float.

The ESCP's were launched from an open door of a HH-52 helicopter hovering at 8m above the water. A second helicopter follows at the appropriate time at 300m and photographs the dye marks on the surface. The aerial photographs were obtained with two nadir-viewing, motor-driven, 70mm Hasselblad cameras mounted side by side on a frame mounted in the door of the helicopter. One camera was equipped with ordinary daylight color film. The other camera contained black-and-white film and was equipped with a green filter. A total of 3 to 4 frames were taken at each probe drop station. The helicopter always flew on a heading from white to the red float.

The photographs from each station are screened to determine the one most suitable for further analysis. The chosen photograph is then expanded to 2x for easier removal of the information. A Cartesian coordinate system is superimposed on the photograph and the X and y positions of the floating dye sources are determined. These position locations along with the helicopter's altitude and heading are then used to obtain distance and direction between the two floats. This data along with the time delay (preset) is then used to compute current speed and direction. The accuracy of the reading system for photographs taken at an altitude of 300m is ±2m. Float separations are typically 75m.

A total of 167 surface current speed-and-direction measurements were collected along the northeast Chukchi Sea coast between 6 and 19 August 1976 (Figure 1). The measurements were taken along transects perpendicular to the coast. Each transect contained 10 stations (unless the pack ice limited the amount of open water). Position of drop stations was determined by using the ship's search radar and vectoring the helicopter to the site. Station locations are probably accurate to ±2km offshore and ±0.5km inshore.

Climatological data were collected hourly onboard the CGC GLACIER during the entire study. The ship was never more than 37km from the most distant surface current station. Hourly wind data was also obtained from Barrow, Alaska.

During the study, hydrographic stations were occasionally taken for another project (RU #359). That data will be used in this report to determine the hydrography of the region during the current measurement study.

RESULTS

Water Properties

Analysis of the hydrographic data collected for project RU #359 agrees with descriptions given for the area. ACW (Alaskan Coast Water), characterized by salinities <32.0 o/oo, was found from the surface to 20m at those stations

south of Cape Franklin and from surface to 15m at those stations north of Cape Franklin (Figure 3). ACW was found overlying a cold (<0°C), saline (>32.0 o/oo) water at all the stations. This cold water is probably residual Chukchi Sea winter water. (See Fleming and Heggarty, 1966.)

The pcynocline between 15 and 20m creates a dynamic barrier to convection affecting the dispersion of any potential oil spill. First it will limit the layer through which the wind drift current can act. Consequently, the wind drift 'current in time may approach a constant velocity through the entire shallow surface layer (assuming the upper layer is not affected by semi-permanent currents). Second, it will affect the rate and depth of descent of the oil after it has lost its volatile and light fractions.

Winds

Winds observed at Barrow and the CGC GLACIER are shown in Figure 4. There appears to be good agreement between the winds observed at the two stations. As expected, there are small differences in speed and direction. The increased effect of friction over land compared to over sea will cause the wind over land to be slower (this is evident in the record for the period of 7-13 August) and cause a greater deflection in direction.

Three low pressure systems passed through the study area on 8-10, 13-16, and 17-18 August. The winds associated with the systems all showed the same pattern: a shift from easterly winds abruptly to northerly and more gradually to westerly. Wind speed increased as the storms entered the area and decreased as the storm passed by. It must be emphasized that the wind measurements at sea reported here are for a relatively short sampling period during one month only; nevertheless, the winds in the study area offshore appear to correspond closely with the Barrow wind patterns. The minor deviations are probably attributable to the combination of land versus sea location and wide spatial separation between stations.

Currents

Surface current measurements taken during the periods of 8-9, 11-15, 16, 17, and 20 August are shown in Figure 5 through 9. The currents off the coast at Wainwright (Figure 5) show a weak and variable flow (5-30cm sec^{-1}) toward the northeast. This surface flow is part of the Alaskan Coastal Water. Inshore of the 20m depth contour, the surface flow is opposite in direction to the offshore currents. Speeds of 5 to 24cm sec were observed. The 8-9 August period was dominated by easterly to northeasterly winds with these components having a mean speed of 8.9m sec^{-1}. It should be noted that the winds were predominantly westerly from 3-7 August. The currents in Figure 5 probably represent a transient state. According to Ekman (1905), a wind-driven current in shallow water near a coast should reach steady state within 1 or 2 pendulum days.

Three transects were occupied on 11 August off Icy Cape (Figure 6). The interesting feature is the anticyclonic gyre located inshore of the ACW flow and in the lee of Icy Cape. The diameter of the gyre is estimated at 20km. In the southern Chukchi Sea an anticyclonic eddy has been observed in the lee

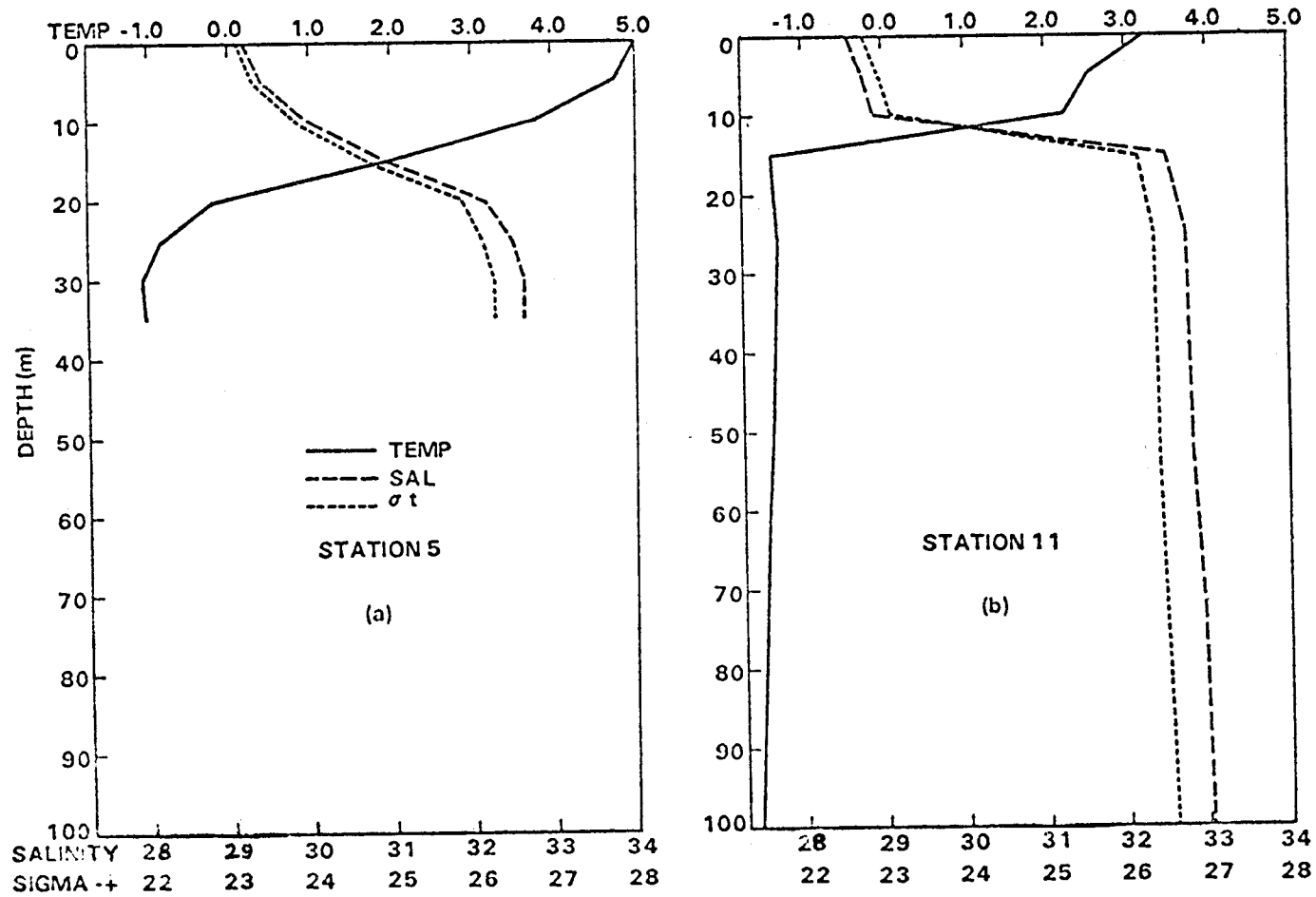Figure 3. Temperature, salinity and sigma-t of stations 5 and 11.
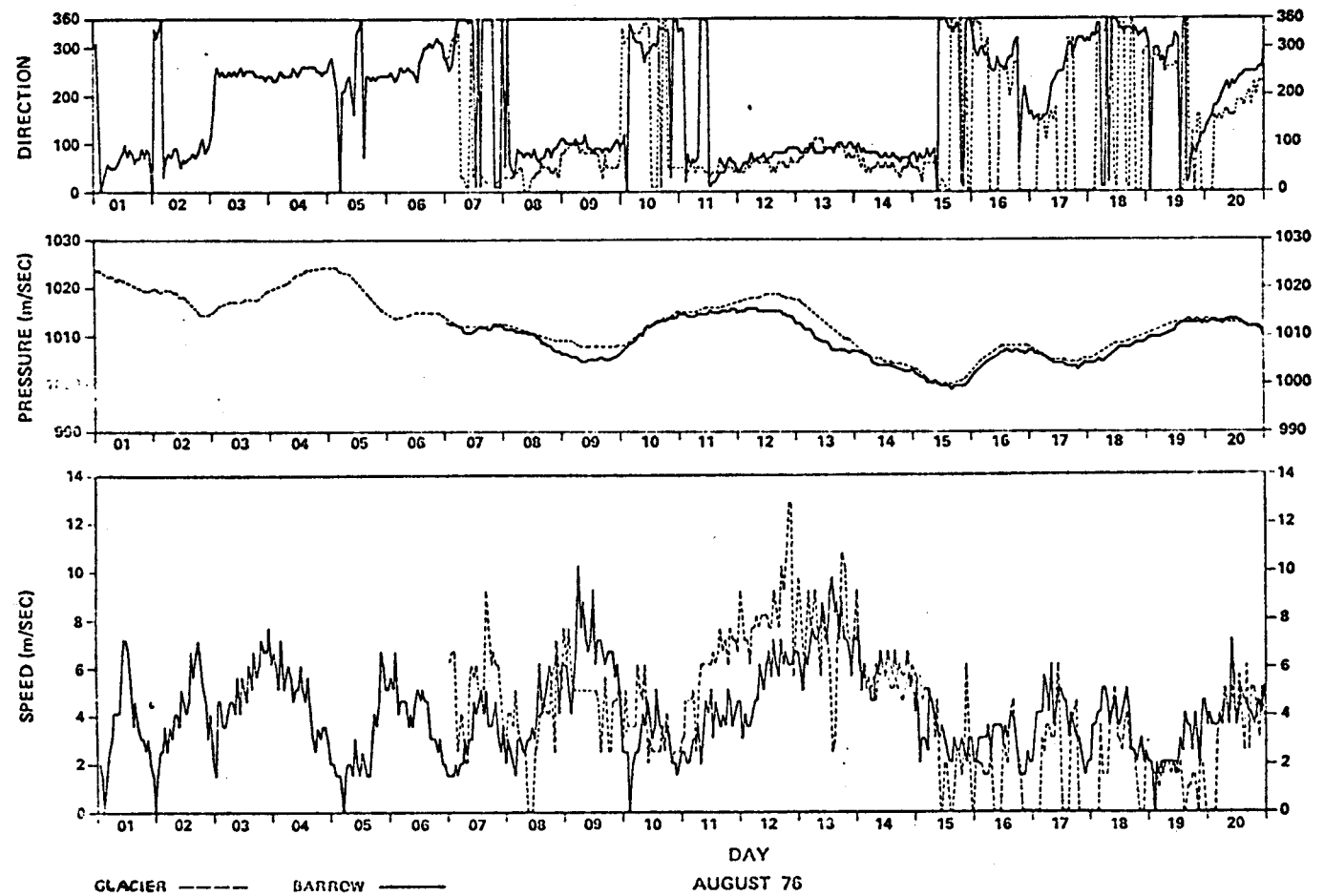
Figure 4. Winds observed at Barrow and the CGC GLACIER, August 1976.

162°   160°   158°
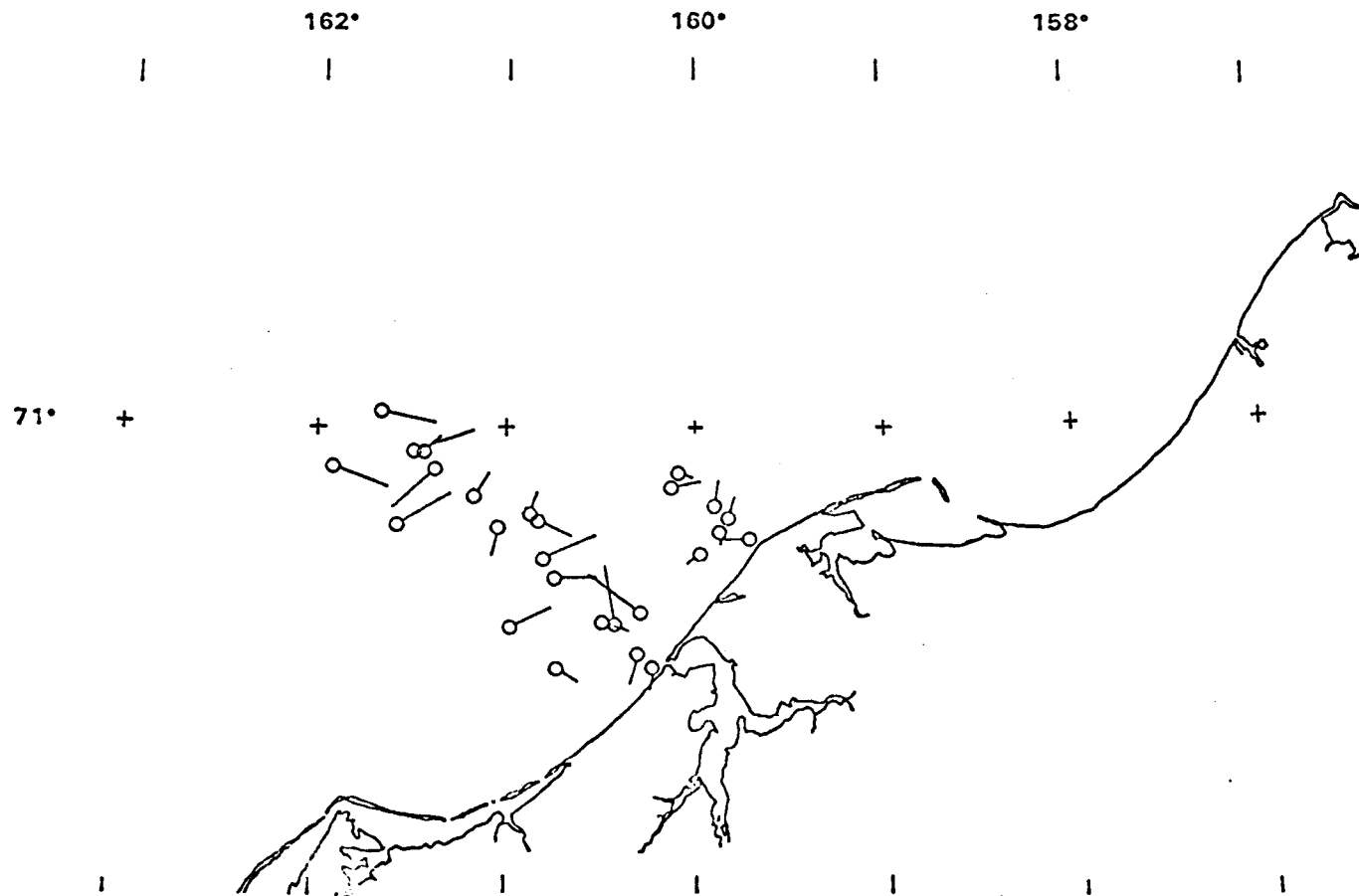
71° +

Figure 5.   Surface currents off the Chukchi Sea coast at Wainwright, Alaska
8-9 August 1976

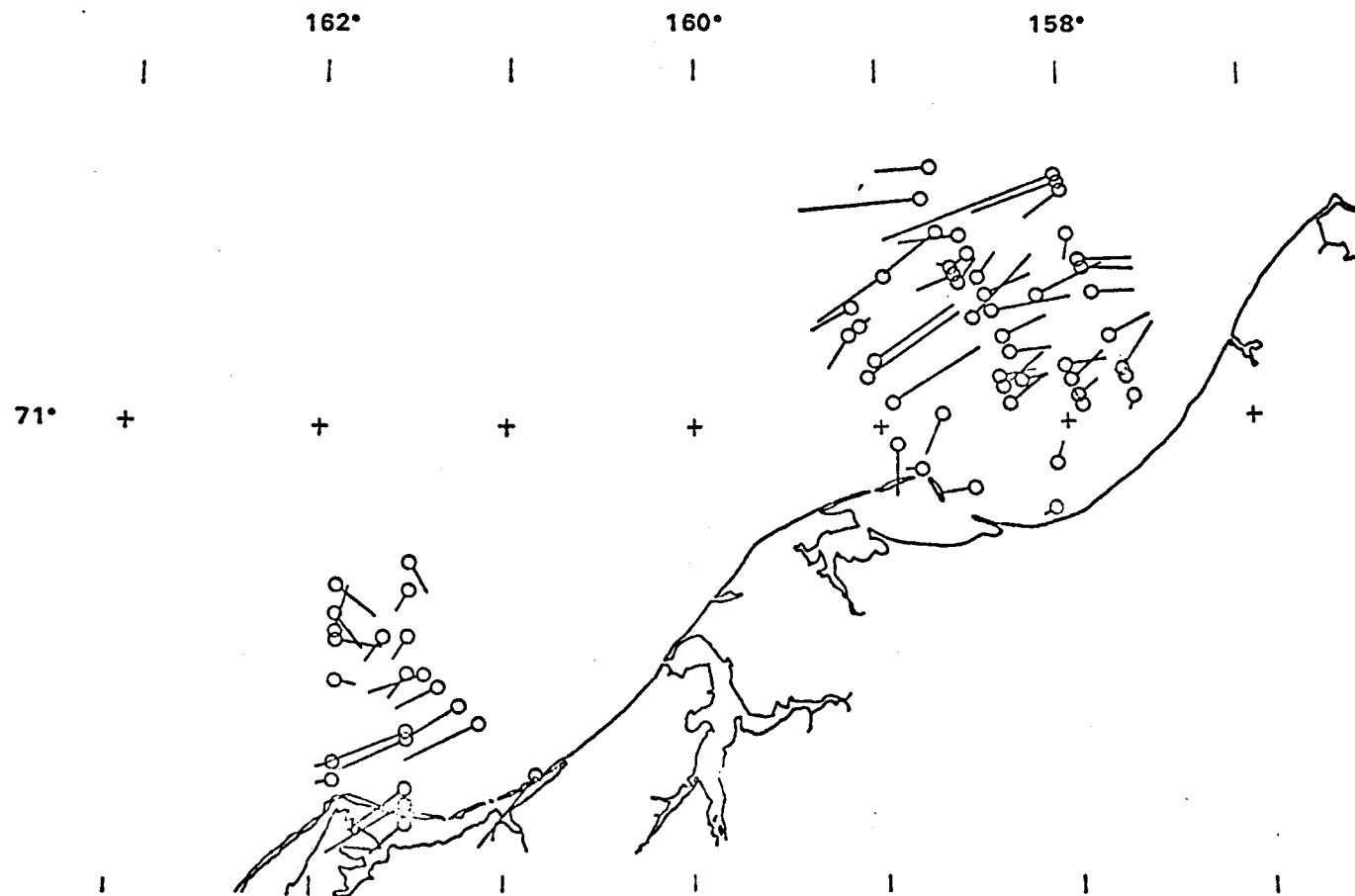162°   160°   158°

71° +

Figure 6. Surface currents off the Chukchi Sea coast from Icy Cape to Peard Bay

11-15 August 1976

of the Point Hope-Cape Lisburne peninsula (Ingham and Rutland, 1971). Thus it is not surprising that an eddy should be found in the lee of Icy Cape. However, this is the first documentation of this feature.

The major feature of the surface currents observed off Peard Bay (Figure 6) is a a three "banded" current regime: a southerly flow inshore and offshore separated by a northeasterly flow. Previous evidence of the southerly flow offshore only 70km from the coast does not exist in the literature. Speeds of 30 to 71cm sec^{-1} were measured. There appears to be a general acceleration of the northeasterly flow (to ∿55cm sec^{-1}) near Cape Franklin.

The currents measured off of Point Barrow on 16 August (Figure 7) show the ACW flow to be found close to shore and to exhibit an acceleration in speed. The currents just east of Point Barrow and near shore appear to be wind driven. The winds on 16 August were predominantly westerly. Current direction was to the northeast. Those stations were nearly reoccupied on 17 August (Figure 8) when the predominant winds were southeasterly. The current direction was to the northwest.

Three transects were occupied near Cape Halkett in the Beaufort Sea on 20 August (Figure 9). Wind direction was predominantly southeasterly. The currents show a flow offshore. The currents in the southern end of Harrison Bay appear to be controlled by bottom topography. Current speeds (3-27cm sec^{-1}) and direction suggest the surface flow is wind driven.

DISCUSSION

A study of the surface currents along the northeast Chukchi Sea coast in August 1976 shows that the flow is dominated by the northeasterly flow of ACW. This relatively warm current has its source in the Bering Strait (Coachman et al, 1976). This warm coastal current is close to the coast and narrow. It is as narrow as 25-40km in places and even narrower (∿20km) near Point Barrow. The highest current speeds were observed near Cape Franklin and Point Barrow. The current seems constrained to follow bottom contours. Once the warm coastal current reaches Point Barrow, the current turns sharply to the right 40km northeast of Point Barrow again following the bottom contours.

It is interesting to note that northeasterly winds during the study period (3 to 10m sec^{-1}) were not intense enough to cause current reversal of the warm coastal current. On 8-9 August during northeasterly winds (mean of 8.9m sec^{-1}), the surface flow was reduced in speed and variable in direction, but did not reverse.

During periods of easterly-northeasterly winds, nearshore currents were found to flow towards the south parallel to the bottom topography, as one would expect from Ekman dynamics (Ekman, 1905). During westerly winds the nearshore currents were northerly just south of Barrow. A scatter diagram for wind speed versus current speed is shown in Figure 10. The linear correlation between wind and current speed yields a correlation coefficient of +0.77 at the 0.95 confidence level. The relationship is of greater significance than is indicated by the numerical coefficient, since the effects of time lags in the response of the currents to changes in the wind regime are not taken into account.

21

Figure 7.   Surface currents off Point Barrow, 16 August 1976.

72°

158°   **156°**   **154°**

71°
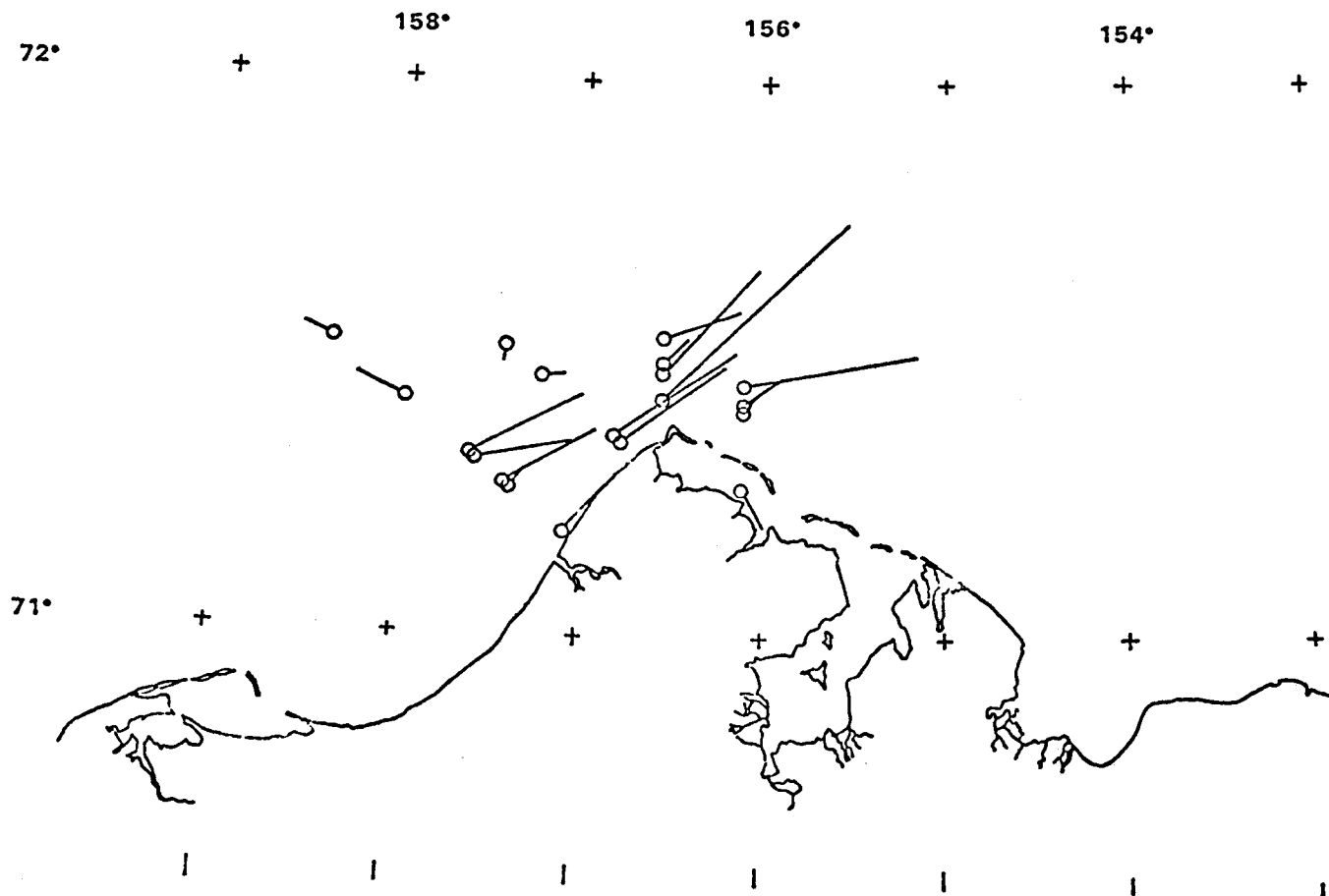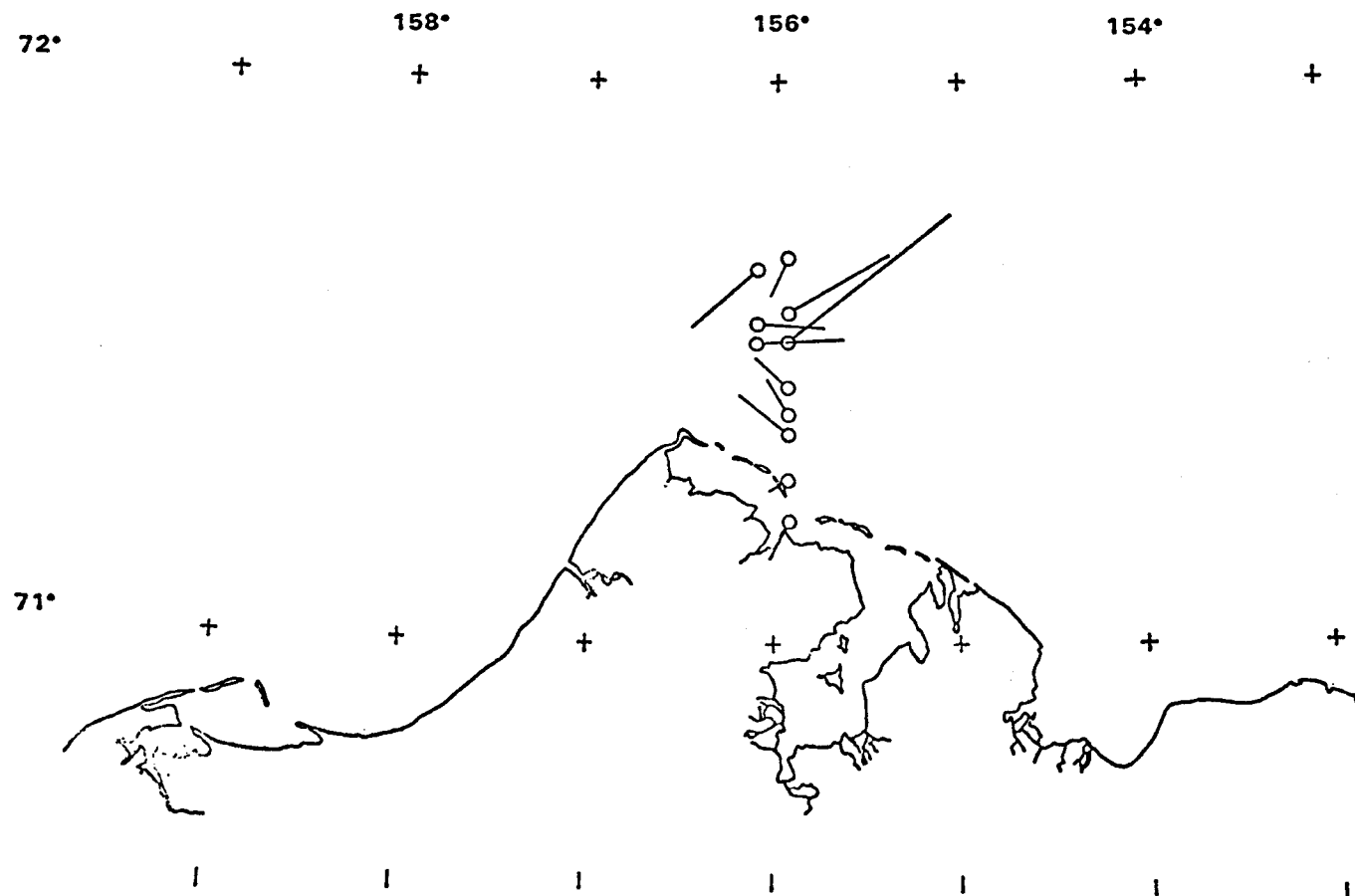
Figure 8. Surface currents off Point Barrow, 17 August 1976.
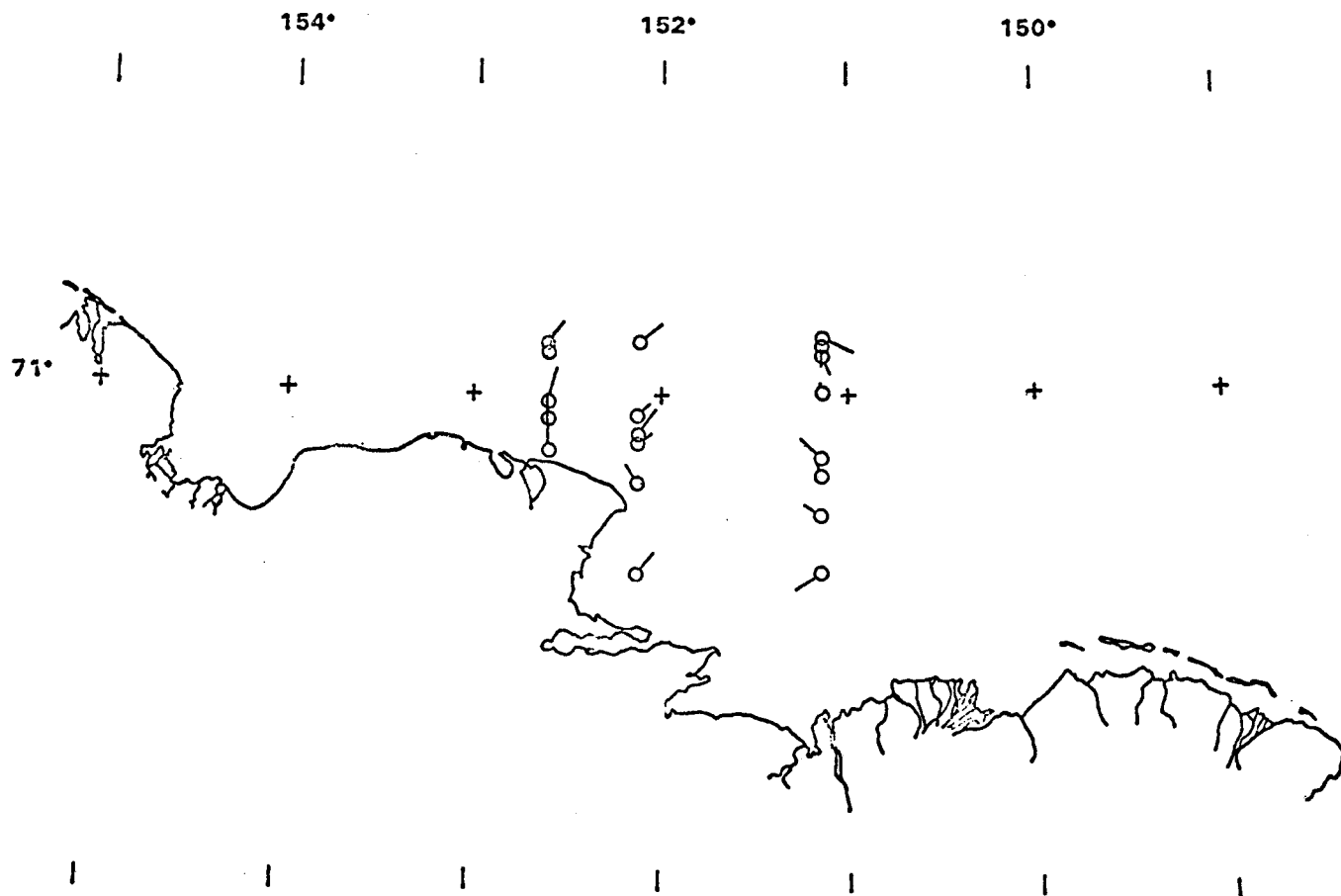
Figure 9. Surface currents off Harrison Bay, 20 August 1976.
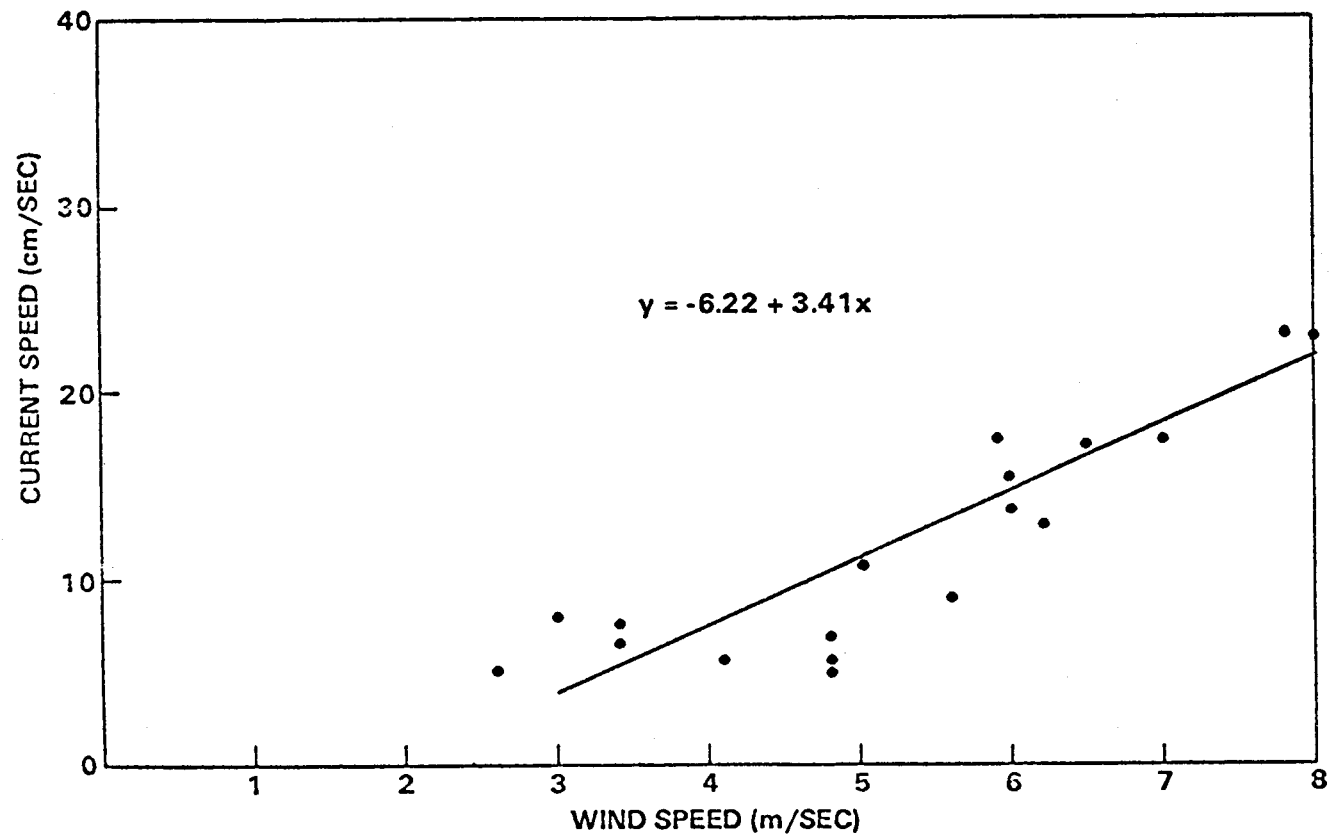
Figure 10. Scatter diagram of wind speed versus current speed for the northeast Chukchi Sea.

25

A scatter diagram for wind speed versus current speed for the surface currents of eastern Harrison Bay is shown in Figure 11. It should be mentioned that this diagram only represents the relationship of the currents to the wind when the winds are from the south. Although there is an obvious qualitative correlation between high wind speed and high current speed, the data do not justify any attempt to fit a curve through the sample points.

Analysis of the surface currents inside the 18m depth contour taken in August 1976 in the Chukchi Sea show a southerly flow under the influence of the prevailing easterly-northeasterly winds and that this flow is reversed with little observable time lag when the wind is from the southwest or west. The statistical correlation between wind and water movement gives a means for predicting the rate of movement of pollutants released into this arctic coastal environment.

The southwesterly surface current flow seaward of the warm northeasterly flow has not been described in the literature. Current speeds greater than 70cm sec^{-1} were measured indicating that the wind is not the primary driving force. There is no way to determine from this data whether the current is a semipermanent or a transient feature. There is some circumstantial evidence that the southerly flow occurs in May and June. Drifter buoys released into the ice as part of the AIDJEX ice drift studies were found to drift from the Beaufort Sea south into the Chukchi Sea and then reverse back to the northwest in late June and early July (Bob Pritchard, personal communication).

The importance of this southerly flow is that if oil moving offshore or a spill were to occur offshore, oil could become entrained into the current and be carried south rather than north as the surface currents closer to shore might suggest.

Transport per unit width of the water column (m^2 sec^{-1}) was calculated for the transects off Peard Bay (Figure 6) to examine in more detail the three "banded" current (Figure 12). The two southerly current regimes are quite evident indicating that the flow also occurs at depth. Mass transport was calculated (Table 1) for each section. The totals shows that the offshore southerly flow dominated. The transport (Sv) for the area is shown in Figure 13.

This should not be treated as representative of the transport for this area. We know that transports through the system can vary by a few tenths of a Severdrup in one or two days (Couchman et al., 1976). However, the calculations do give some quantitative aspects of the passage of this offshore water to the south.

TABLE 1

TRANSPORT (Sv; + = north) THROUGH SECTIONS OFF PEARD BAY
(STATION NUMBERS FROM APPENDIX)

NEARSHORE FLOW	COASTAL CURRENT	OFFSHORE FLOW
-0.1	0.2	-0.6
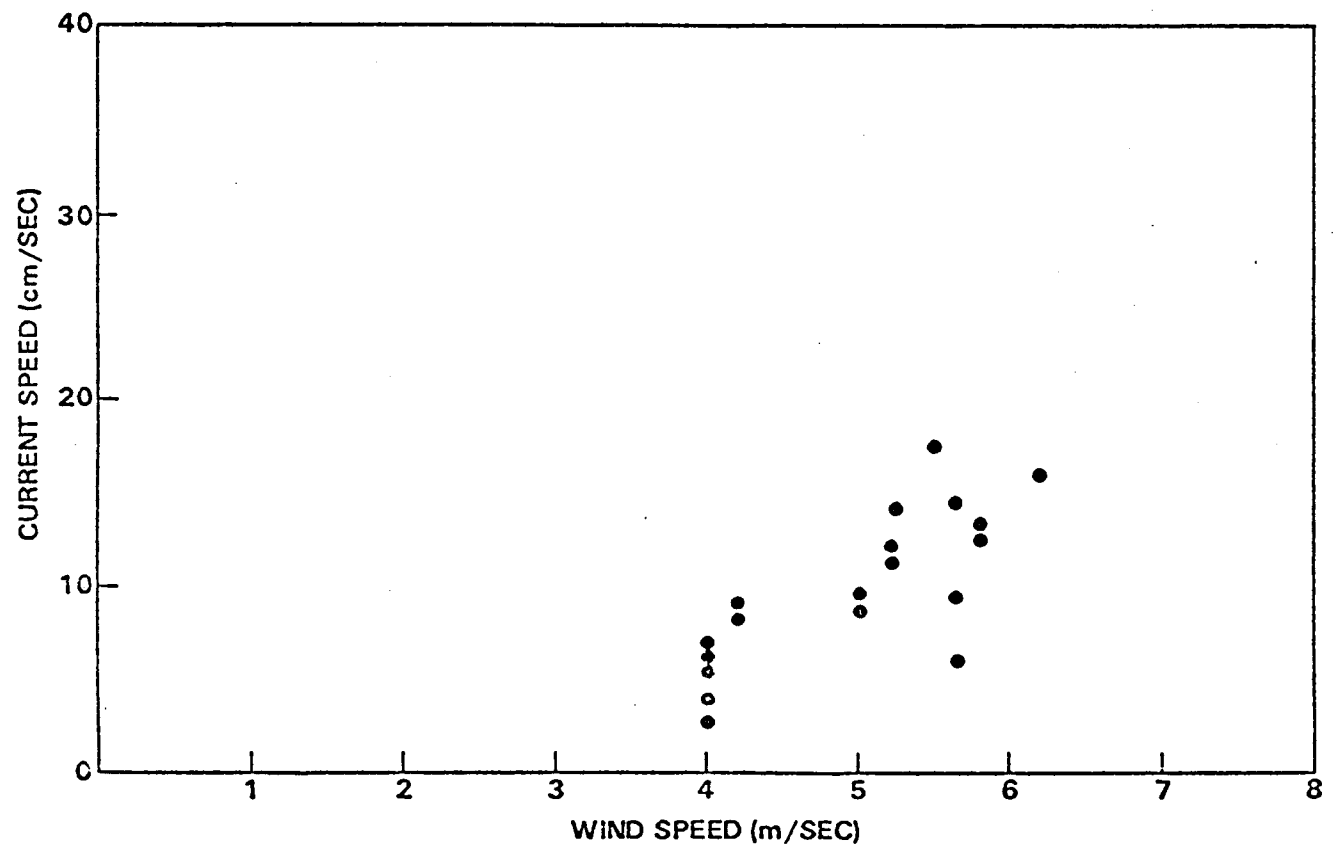
Figure 11. Scatter diagram of wind speed versus current speed for the area
near Harrison Bay.
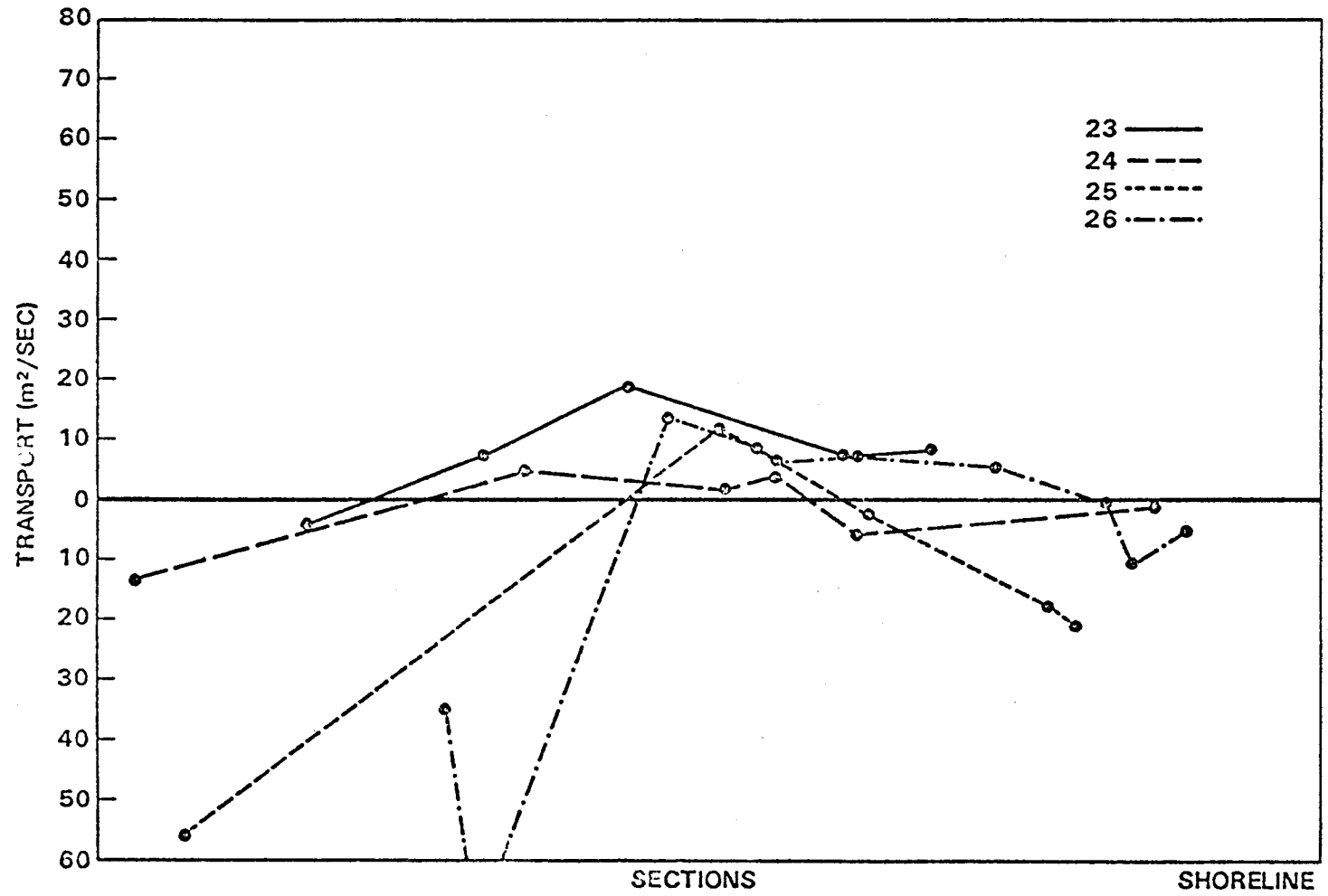
Figure 12. Transport (m^2/sec) for sections off Peard Bay (see appendix for station location).
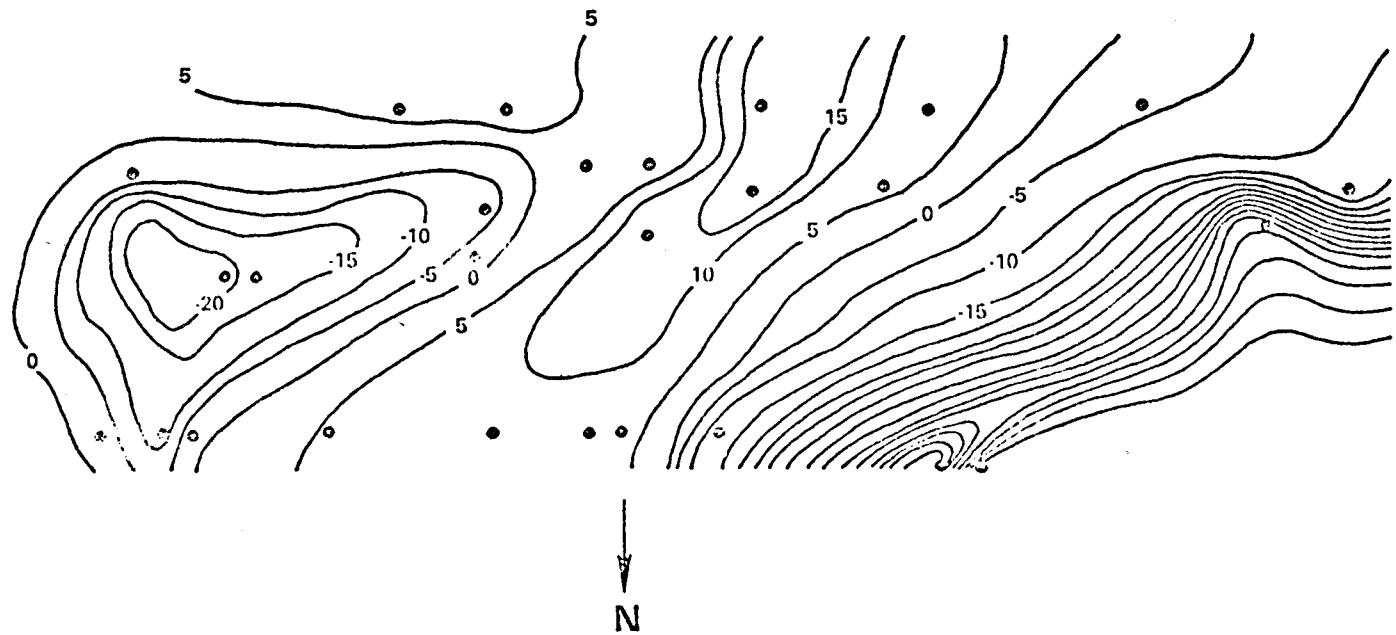
Figure 13. Transport plotted for the sections off Peard Bay.

SUMMARY

Our knowledge of the surface currents of the northeast Chukchi Sea is quite inadequate for forecasting the flow. This stems largely from the lack of a dedicated oceanographic program to the area. Because of this lack of knowledge, only a descriptive approach can be taken for presenting the observed conditions rather than an analytical approach to understand processes.

The dominant surface flow in the northeast Chukchi Sea is the warm coastal current which originates in the Bering Strait and flows toward the northeast turning to the right into the Beaufort Sea northeast of Point Barrow. This current can be classified as a semi-permanent flow showing slowing and sometimes reversal for short periods especially during northeast winds.

An anticyclonic eddy has been observed in the lee of Icy Cape. The importance of this feature is that it can be a "trap" for oil spilled on the area. More data is needed to determine if this eddy is a semi-permanent feature like the eddy in the lee of Point Hope-Cape Lisburne.

Nearshore currents along the northeast Chukchi Sea coast are wind driven and show a southwesterly flow under the influence of easterly-northeasterly winds and northeasterly flow during westerly-southwesterly flow. Analysis of these nearshore currents with the winds produced a means of predicting the rate of movement of oil spilled into this area. This means of predicting local wind drift current patterns should have considerable utility until more precise knowledge of the coastal currents is available.

The southwesterly current observed 70km off the Alaskan coast is an unknown feature. Current data presented by Coachman et al (1976) suggest southerly flow in the north central region of the Chukchi Sea near 164°W. There is no evidence to indicate that the flow in the central part of the sea has shifted closer to the Alaskan coast. Future study of this southwesterly flowing current is necessary to determine the processes affecting the flow.

REFERENCES

Aagard, K.. Features of the Physical Oceanography of the Chukchi Sea in the Autumn. Univ. Washington Department, Oceanography, M.S. thesis, 41 pp. (1964).

Banke, E. G. and Smith, S. D. Wind Stress Over Ice and Over Water in the Beaufort Sea. Journal of Geophysical Research, 76:7368-7374 (1971).

Campbell, W. J. The Wind Driven Circulation of Ice and Water in a Polar Ocean. Journal of Geophysical Research, 70:3279-3301 (1965).

Coachman, L. K. Aagaard, K., and Tripp, R. B. Bering Strait: The Regional Physical Oceanography. University of Washington Press, Seattle, Washington, 172 pp. (1976).

Creager, J. S. and McManus, D. A. Geology of the Southeastern Chukchi Sea. Environment of the Cape Thompson Region, Alaska. U.S. Atomic Energy Commission Report, Division of Technical Information (1966).

Ekman, V. W. On the Influence of the Earth's Radiation on Ocean Currents. Ark. f. Mat. Astron. och Fysek, 2(11):1-53 (1905).

Fleming, R. H. and Heggarty, D. Oceanography of The Southeastern Chukchi Sea. Environment of The Cape Thompson Region, Alaska. U. S. Atomic Energy Commission Report, Division of Technical Information (1966).

Ingham, M. C. and Rutland, B. A. Physical Oceanography of the Eastern Chukchi Sea Off Cape Lisburne-Icy Cape. WEBSEC 70, An Ecological Survey in the Eastern Chukchi Sea, September-October 1970. U. S. Coast Guard Oceanographic Report No. 50, 206 pp. (1971).

Klein, W. H. Principal Tracks and Mean Frequencies of Cyclones and Anticyclones in the Northern Hemisphere. Weather Bureau Research Paper No. 40, Washington, DC (1957).

Walters, C. D. Drag Coefficient and Roughness Length Determinations on an Alaskan Arctic Coast During Summer. Boundary-Layer Meteorology 8:235-237 (1975).

Wiseman, W. J. Suhayda, J. N., Hsu, S. A., and Walters, C. D. Characteristics of Nearshore Oceanographic Environment of Arctic Alaska. The Coast and Shelf of the Beaufort Sea, Arctic Inst. North Am., Arlington, VA (1974).

Sta. I.D.	Position Latitude	Longitude	Date	Time	Speed (cm/sec)	Heading (°T)	
5A	70°47.7'	159°43.1'	8 Aug	1545	13.0	267°	
5B	70°49.7'	159°49.4'	8 Aug	1547	9.3	017°	
5C	70°51.1'	159°54.1'	8 Aug		11.8	008°	
5D	70°54.2'	160°5.1'	8 Aug		5.8	111°	
5E	70°55.2'	160°8.1'	8 Aug				
6B	70°53.2'	160°9.0'	8 Aug	1417	14.6	079°	
6A	70°48.4'	159°52.4'	8 Aug		3.8	178°	
7A	70°46.1'	159°58.3'	8 Aug		5.6	231°	
8A	70°40.3'	160°17.8'	9 Aug	0956	35.7	306°	
8C	70°43.7'	160°27.9'	9 Aug	1024			
8E	70°50.4'	160°52.8'	9 Aug	1040	18.0	115°	
8F	70°51.6'	160°55.5'	9 Aug	1048	8.3	020°	
8G	70°53.7'	161°2.4'	9 Aug	1054			
8H	70°54.9'	161°6.6°	9 Aug	1101			
9B	70°39.4'	160°27.5'	9 Aug	1337	32.6	350°	
9D	70°45.4'	160°48.7'	9 Aug	1410	30.3	066°	
9G	70°57.2'	161°28.1'	9 Aug	1457	12.6	032°	
9H	70°59.6'	161°36.9'	9 Aug	1503	9.5	048°	
10A	70°34.6'	160°15.7'	9 Aug	1648	9.0	190°	
10B	70°35.7'	160°19.8'	9 Aug	1655	15.6	196°	
10C	70°39.0'	160°31.1'	9 Aug	1658	13.3	110°	
10F	70°43.5'	160°47.6'	9 Aug	1718	21.1	089°	
10G	70°48.6'	161°5.3'	9 Aug	1635	12.8	194°	
10J	70°54.7'	161°25.3'	9 Aug	1758	31.3	228°	
10K	70°56.8'	161°32.9'	9 Aug	1807	33.9	071°	
9K	71°1.1'	161°42.0'	9 Aug	1820	29.6	102°	

Sta. I.D.	Position Latitude	Longitude	Date	Time	Speed (cm/sec)	Heading (°T)
11K	70°54.3'	161°42.5'	9 Aug	1830	30.7	111°
11J	70°48.4'	161°34.6'	9 Aug	1838	33.1	060°
11B	70°33.6'	160°45.2'	10 Aug	1928	11.9	122°
11C	70°38.3'	161°0.6'	10 Aug	1945	23.6	064°
19A	70°23.2'	161°49.4'	11 Aug	0925	6.61	259°
19B	70°25.5'	161°49.4'	11 Aug	0935	7.82	253°
19D	70°34.3'	161°49.4'	11 Aug	0956	9.81	103°
19E	70°37.8'	161°49.4'	11 Aug	1017	25.0	099°
19F	70°38.8'	161°49.4'	11 Aug	1025	24.6	016°
19G	70°43.6'	161°49.4'	11 Aug	1030	22.1	143°
19H	70°44.4'	161°49.4'	11 Aug	1040	26.7	128°
18B	70°16.4'	161°26.1'	11 Aug	1403	23.3	228°
18C	70°24.0'	161°26.1'	11 Aug	1408	52.9	238°
18D	70°21.6'	161°26.1'	11 Aug	1416	39.4	233°-
18E	70°25.6'	161°26.1'	11 Aug	1422	40.0	245°
18F	70°26.8'	161°26.1'	11 Aug	1427	53.3	248°
18G	70°32.7'	161°26.1'	11 Aug	1443	14.4	217°
18H	70°36.9'	161°26.1'	11 Aug	1448	12.0	213°
18J	70°41.7'	161°26.1'	11 Aug	1458	11.1	210°
18K	70°44.3'	161°26.1'	11 Aug	1505	17.4	150°
15A	70°22.3'	160°50.2'	11 Aug	1645	53.0	217°
15B	70°27.4'	161°6.7'	11 Aug	1655	46.6	243°
15C	70°29.7'	161°14.6'	11 Aug	1706	35.5	238°
15D	70°31.5'	161°20.7'	11 Aug	1718	24.2	243°
15E	70°32.8'	161°25.5'	11 Aug	1731	31.9	251°
15F	70°36.5'	161°37.2'	11 Aug	1742	13.0	217°

Sta. ID	Position Latitude	Longitude	Date	Time	Speed (cm/sec)	Heading (°T)	
20D	71°9.3'	159°8.0'	14 Aug	1642	19.2	214°	
20C	71°7.3'	159°5.8'	14 Aug	1658			
20B	71°4.7'	159°3.1'	14 Aug	1704	64.7	056°	
20A	70°57.0'	158°54.9'	14 Aug	1711	27.0	082°	
21A	70°55.0'	158°43.1'	14 Aug	1726	7.4	267°	
21A	70°55.0'	158°43.1'	14 Aug	1730	5.0	267°	
21C	71°2.9'	158°49.2'	14 Aug	1743	58.8	061°	
21C	71°2.9'	158°49.2'	14 Aug	1745	60.0	058°	
21D	71°5.7'	158°50.9'	14 Aug	1750	Failure		
21E	71°7.6'	158°52.3'	14 Aug	1804	55.9	056°	
21F			14 Aug				
21G	71°13.6'	158°56.9'	14 Aug	1820	14.5	242°	
22G	71°16.2'	158°46.4'	14 Aug	2050	44.5	236°	
22E	71°10.8'	158°42.0'	14 Aug	2108			
22D	71°1.4'	158°35.1'	14 Aug	2120	23.7	204°	
22C	70°53.0'	158°28.2'	14 Aug	2131	17.5	262°	
23G	71°16.6'	158°25.1'	14 Aug		20.0	249°	
23A	70°50.6'	158°5.1'	14 Aug	2201	5.4	242°	
23B	71°2.3'	158°13.7'	15 Aug	1040	24.9	052°	
23C	71°4.1'	158°15.1'		1046	28.1	050°	
23D	71°5.5'	158°16.3'		1056	18.7	081°	
23E	71°11.6'	158°21.1'		1145	48.1	044°	
23F	71°13.7'	158°23.9'		1200	14.0	036°	
23H	71°17.7'	158°26.0'		1206	3.9	284°	
23J	71°21.2'	158°28.9'		1223	36.6	232°	
23K	71°24.6'	158°31.4'	15 Aug	1233	70.4	266°	

34

Sta. I.D.	Position Latitude	Longitude	Date	Time	Speed (cm/sec)	Heading (°T)
25K	71°26.9'	158°27.4'	15 Aug	1239	60.7	254°
24K	71°29.6'	158°27.1'		1242	28.0	267°
24/25J	71°21.8'	158°21.4'		1301	32.4	264°
24/25H	71°21.1'	158°20.3'		1309	11.2	226°
24G	71°16.3'	158°17.3'		1325	14.1	036°
24F	71°14.5'	158°15.7'		1528	26.1	068°
24E	71°12.8'	158°14.4'		1535	44.4	081°
24D	71°10.1'	158°12.6!		1541	25.1	066°
24C	71°7.7'	158°10.8'		1550	20.5	085°
24B	71°4.8'	158°8.3'		1558	10.6	079°
24A	70°55.3'	158°1.8'		1606	8.2	197°
25A	71°1.4'	157°54.9'		1629	7.1	332°
25B	71°2.3'	157°56.0'		1631	10.1	052°
25C	71°4.2'	157°58.1'		1634	21.8	048°
25D	71°8.5'	158°3.5'		1644	21.4	084°
25F	71°12.9'	158°9.1'			40.7	065°
26A	71°1.6'	157°39.1'			4.8	200°
26B	71°3.7'	157°41.7'			6.3	002°
26C	71°4.8'	157°43.0'			29.9	034°
26D	71°8.2'	157°47.2'			23.0	064°
26E	71°12.8'	157°52.8'			20.8	090°
26F	71°15.3'	157°55.9'			26.2	093°
26G	71°16.2'	157°57.7'			27.4	090°
26H	71°18.9'	158°1.6'			11.8	189°
26J	71°29.3'	158°8.1'				
26K	71°30.7!	158°17.1'	15 Aug			

35

Sta. ID.	Position Latitude	Longitude	Date	Time	Speed (cm/sec)	Heading (°T)	
27K	71°33.5'	158°15.4'	15 Aug				
27H	71°26.3'	158°6.4'	15 Aug		108.1	250°	
27G	71°24.4'	158°4.0'	15 Aug		51.9	251°	
27F	71°23.4'	158°2.9'	15 Aug		23.8	234°	
29A	71°11.5'	157°3.7'	16 Aug	1650	34.2	041°	
29B	71°13.1'	157°9.9'		1704	11.7	036°	
29C	71°16.3'	157°22.0'		1710	60.4	059°	
29D	71°18.4'	157°29.8'		1720	56.1	078°	
29E	71°19.5'	157°34.5'		1734	74.5	061°	
29F	71°25.9'	158"0.0'		1744	29.1	295°	
29G	71°27.5'	158°5.6'		1752	15.8	294°	
30D	71°30.5'	157°24.1'		1814	5.8	189°	
30D	71°30.5'	157°24.1'		1815	5.5	185°	
30C	71°27.8'	157°13.0'		1820	9.8	084°	
30B	71°21.6'	156°49.5'		1855	87.0	054°	
30A	71°20.8'	156°46.8'		1907	75.6	052°	
1B	71°25.1'	156°34.2'		1943	156.7	045°	
1C	71°28.1'	156°34.2'		2006	84.1	041°	
1D	71°29.1'	156°34.2'		2017	17.3	045°	
1E	71°32.1'	156°34.2'	16 Aug	2024	46.7	070°	
2A	71°15.7'	156°6.6'	17 Aug	1620	22.7	151°	
2B	71°23.7'	156°6.6'	17 Aug	1635	12.2	040°	
2C	71°24.7'	156°6.6'	17 Aug	1642	25.3	055°	
2D	71°26.7'	156°6.6'	17 Aug	1649	113.8	079°	
2E	71°31.7'	156°6.6'	17 Aug	1838	48.2	087°	
2F	71°33.7'	165°6.6'	17 Aug	1846	36.3	093°	

36

Sta. ID	Position		Date	Time	Speed (cm/sec)	Heading (°T)
	Latitude	Longitude				
2G	71°39.7'	156°6.6'	17Aug	1900	49.7	228°
3H	71°41.7'	155°54.6'		1911	21.9	204°
3G	71°35.7'	155°54.6'		1921	66.9	059°
3F	71°32.7'	155°54.6'		1930	122.8	051°
3E	71°27.7'	155°54.6'		1940	23.7	313°
3D	71°24.7'	155°54.6'		1945	20.9	329°
3C	71°22.7'	155°54.6'		1953	34.7	309°
3B	71°17.7'	155°54.6'		1958	9.8	238°
3A	71°13.7'	155°54.6'	17 Aug	2014	22.1	207°
4G	71°28.0'	155°42.6'	19 Aug	1758	81.7	086°
4F	71°23.0'	155°42.6'		1806	9.3	354°
4E	71°17.0'	155°42.6'		1821	14.7	279°
4D	71°16.0'	155°42.6'		1828	13.7	274°
4D	71°16.0'	155°42.6'		1834	11.8	274°-
4C	71°15.0'	155°42.6'		1845	29.1	230°
4B	71°13.0	155°42.6'	19 Aug	1855	20.4	273°
4A	71°12.0'	155°42.6'	19 Aug	1900	20.5	295°
8E	71°5.0'	152°35.4'	20 Aug	1145	12.1	037°
8D	71°4.0'	152°35.4'		1153	9.5	018°
8C	70°59.0'	152°35.4'		1201	17.5	016°
8B	70°57.0'	152°47.4'		1208	11.7	358°
8A	70°54.0'	152°35.4'		1217	26.9	359°
9A	70°39.4'	152°6.6'		1242	12.6	041°
9B	70°50.4'	152°6.6'		1301	9.2	329°
9C	70°54.4'	152°6.6'		1312	6.0	050°
9D	70°55.4'	152°6.6'	20Aug	1317	14.5	036°

Sta. I.D.	Position Latitude	Longitude	Date	Time	Speed (cm/sec)	Heading (°T)	
9E	70°59.4'	152°6.6'	20 Aug	1326	6.3	050°	
9H	71°0.4'	152°6.6'		1335	13.4	052°	
11K	71°6.3'	151°8.4'		1539	16.1	115°	
11J	71°5.3'	151°8.4'		1545	8.5	182°	
11H	71°4.3'	151°8.4'		1555	7.0	153°	
11G	71°0.3'	151°8.4'		1607	2.7	341°	
11G	71°0.3'	151°8.4'		1609	4.0	330°	
11F	70°53.3'	151°8.4'		1625	14.4	313°	
11E	70°51.3'	151°8.4'		1637	4.7	340°	
11D	70°47.3'	151°8.4'		1646	9.1	303°	
11D	70°47.3'	151°8.4'		1646	9.1	303°	
11C	70°41.3'	151°8.4'	20 Aug	1655	14.4	237°	

4—

Annual Report

Current Measurements in Possible Dispersal Regions

of the Beaufort Sea

Knut Aagaard

Department of Oceanography

Dean Haugen

Applied Physics Laboratory

University of Washington

Seattle, Washington   98195

29 March 1977

I. Summary

At least in late winter the currents on the inner shelf appear to be slow, generally less than 5 cm sec^{-1}. Long-term mean currents are extremely small, representing net displacements over a week of only 1-2 km. The two measurements made north of Narwhal Island showed these small displacements to have been west-southwest. Tidal currents are probably not much above 1 cm sec^{-1} in winter.

On the outer shelf an entirely different situation prevails. Measurements made at 100 m under the ice from May-September showed the flow to reach over 55 cm sec^{-1}, and even over a 3-month period the mean flow was 13 cm sec^{-1} toward the east. Pollutants reaching the outer shelf at sub-surface depths could thus be transported 1000 km eastward in three months. The most remarkable feature observed was the dominance of the motion by low-frequency variations with a typical time scale of 10 days. These oscillations represent bursts of speed as high as 50 cm sec^{-1} or more; they are directed eastward and are aligned approximately with the shelf edge. Between the bursts there were shorter periods of westward motion, the maximum observed speed toward the west being 26 cm sec^{-1}. The cause of these motions is for the present unknown. Tidal currents are in the neighborhood of 5 cm sec^{-1}, and a diurnal inequality probably prevails at times of high lunar declination.

The implication of these measurements with respect to the transport and dispersal of pollutants on the Beaufort shelf is that the ice-covered inner and outer shelf represent very different advective regimes. Over the former, currents are weak and net displacements are small. However, over the outer shelf there are strong currents and pollutants can be transported very long distances.

II. Introduction

The objective of this work is to obtain long-term Eulerian time series of currents at selected locations on the shelf and slope of the Beaufort Sea. Such measurements are necessary to describe and understand the circulation on the shelf and the exchange between the shelf and the deep Arctic Ocean. This circulation and exchange are in turn the physical mechanisms which transport and dispense pollutants and substances of biological and geological importance. The water motion also influences the ice distribution and drift. The current time series must be long enough to define the important temporal scales of motion.

III. Current state of knowledge

Prior to the previous work, there had been only one time series current measurement of significant length on the Beaufort shelf. This was from a single instrument moored in water 54 m deep about 70 km east-northeast of Barrow during 15 days of August 1972. Other current measurements are also from summer and have been made in water shallower than 20 m; the records are of very short duration. During the spring and summer of 1973 we obtained two four-month long current records from the inner part of Barrow Canyon, whence waters enter onto the Beaufort shelf. By piecing together these observations, along with indirect evidence such as that provided by summer hydrographic measurements, one can arrive at some general ideas about the circulation on the Beaufort Sea shelf, primarily during summer.

Water originating in the Bering Sea and modified by its passage through the Chukchi flows northeast through Barrow Canyon at speeds as high as 100 cm sec^{-1}. Subsequently the majority of this flow probably turns eastward and enters the Beaufort Sea. On the shelf some 70 km east-northeast of Barrow, the eastward motion has been observed to average 60 cm sec^{-1} during a six-day interval. The eastward flow, concentrated on the outer shelf, can be traced through hydro-graphic evidence at least as far as Barter Island at 143°W. Measurements have shown that changes in the meridional atmospheric pressure gradient can temporarily reverse the flow in Barrow Canyon, and apparently also on the western Beaufort shelf.

Summer observations have also indicated the likelihood of an intermittent upwelling regime on the eastern part of the shelf. It is hypothesized that the upwelling is a response to locally strong easterly winds, and that the water upwelled onto the shelf moves westward.

While tidal effects are probably small, storm surges and related effects may be important in promoting significant changes of short time scales.

Earlier studies have contributed essentially nothing to knowledge of the advective exchange between the shelf and the deep basin.

IV. Study area

The area of interest extends eastward from Pt. Barrow along the entire northern Alaska coast, *i.e.*, from about 156°30'W to 141°W, a lateral distance of 600 km. The shelf is narrow, with the shelf break typically 80-90 km offshore. The total runoff is relatively small, highly seasonal, and concentrated in a very few rivers of any consequence, the largest of which is the Colville. Tidal amplitudes are small, with a probable mean spring range of about 15 cm; the tides are mixed, predominantly semi-diurnal. The entire area is covered by sea ice, both first and multi-year, through all but 2-3 months. Even during the height of summer, ice is usually found well onto the shelf.

V. Data collection

It is obviously impossible to attempt intensive time series coverage of the entire region. One is in practice limited to measurements at a few points, hopefully key ones. The first year of the present work we picked three sites. The first was in Barrow Canyon, at a point down-canyon from our earlier measure-ments, where the Bering Sea source waters for the Beaufort shelf presumably have begun turning eastward. We also selected two sites more nearly midway along the shelf, at about 150°W. One of these was on the outer shelf and one part-way down the slope, the idea being to get not only a representation of the shelf and adjacent slope flow regimes, but also to examine the possible exchanges between these regimes. These moorings were installed in April 1976 and were designed to measure until fall. At that time a new set of current meters was deployed north of Lonely, in coordination with the CTD work being performed there (see this year's annual report, Research Unit No. 151). All moorings carried two current meters each.

All of these sites can in general be expected to be covered by ice. Since anchored current meters record internally, so that data retrieval is dependent upon instrument recovery (a fairly formidable task in ice-covered waters), we decided on an alternative set of approaches that provide redundancy in data recovery. The first approach was to transmit the data acoustically. This involves storing the data in such a way that they can be recalled at very high rates upon command, the recall being done from the ice on an opportunity basis. This method has two side benefits, *viz.* that the current meters can be left in place as long as they continue to function, and that data recovery can be made as often as desired, *i.e.*, more nearly in real-time. The second approach to data recovery was to have the instruments record internally as usual, equip them with acoustic releases, and provide the arrays with an acoustic ranging and bearing system to enable pinpointing their position under the ice after having been released and risen to the under-ice surface. A hole can then be cut in the ice and divers used to attach recovery lines; the mooring is dragged laterally to the hole and brought up.

Each instrumentation system was thus to be comprised of an anchor, an acoustic anchor release, a lower current meter, a data buoy, an upper current meter, and appropriately distributed floatation. The current meters provide current speed, direction, and temperature in binary code. The data buoy is linked acoustically to the current meters. The buoy houses power supply, digital tape recorder, timing and control electronics, and acoustic telecommunication subsystems.

In addition we used the opportunity provided by the radar ice tracking program conducted from Narwhal Island in the spring of 1976 to obtain two shorter current records. In that case one internally recording current meter was simply hung through a hole cut in the ice adjacent to each of two radar targets. The ice tracking provided a description of the ice movement, so that vectorial summation of the ice and relative water motion gave a representation of true currents.

VI. Results

There have been very substantial difficulties and delays with the acoustically telemetering data buoy system. In consultation with the project office we therefore had to modify our original plans. The first modification occurred in spring 1976 when none of the data buoys were ready for deployment. Some of the reasons for this were discussed in the annual report of 26 March 1976. Rather than delay instrument deployment, we chose to put the moorings out with the intent to recover them the next fall through the ice. At that time two new moorings were to be deployed offshore from Lonely, complete with telemetry system. During 24-29 April the three moorings were installed as planned. Details have been provided in the quarterly report of 30 June 1976.

Meanwhile the two current meters offshore from Narwhal Island had also been deployed and recovered. These current records cover the three-and-a-half weeks 28 March-22 April.

In early fall it became apparent that there would be further delays in completing the data buoys. Again we decided to deploy with only the internal recording capability. This then required picking up the moorings the following March and re-deploying new moorings at that time, complete with acoustic telemetry.

The Barrow Canyon mooring was duly recovered on 6 October 1976 and the inshore Oliktok mooring, at 149°53'W, on 25 October. The third mooring released successfully, but was lost in a storm on 27-28 October before it could be brought up through the ice. Due to what we believe to have been faulty magnetic tapes only partial current meter records were obtained from these moorings, one of about five days duration in Barrow Canyon and another with at least 95 days of clear records from north of Oliktok. On 15 October the inshore mooring north of Lonely was deployed, but an attempt to put in the deeper mooring on 17 October failed because of an echo sounder malfunction that required factory repairs. These activities have all been discussed in the quarterly report of 31 December 1976.

We have just now, on 23 March, recovered the Lonely mooring installed last spring. Both current meters had leaked through the external electrical terminal, so that the tape recorders had run only part of the time. These leaks occurred despite our having pressure tested the assemblies before deployment. They were probably due to thermal stressing as the moorings were put out. To prevent recurrence on the next deployments, we are removing the electrical connectors and inserting pressure hull plugs. The two new Lonely moorings will be deployed within the next few days. Only the deeper one of the two will carry a telemetering data buoy, however, as the second unit could not be completed on time. Present plans are to recover both of these moorings through the ice in October 1977. Meanwhile we'll attempt to interrogate the outer mooring on several occasions later this season.

VII. Discussion

We begin with what we shall call the Narwhal Island records. Current meter no. 433 was situated adjacent to radar target R3, and meter no. 437 adjacent to target R5. Both meters were suspended 10 m below the ice. Target R5 was in water less than 30 m deep and did not move more than 20 m the entire time. Target R3 was in water 35-40 m deep; it moved an appreciable distance only during the last 6 days of recording. Meter 433 recorded from 2340 GMT on 28 March to 1040 on 19 April, and meter 437 from 0107 on 28 March to 0027 on 22 April.

Figures 1-6 show the east (U) and north (V) components of velocity at meter 433 before correcting for ice drift (Fig. 7), and Figures 8-11 show the components of true current, $i.e.$, the vectorial sum of the relative current and the ice drift. The currents are generally small, less than 5 cm sec^{-1}, except during a few periods in the latter part of the record when they reached close to 10 cm sec^{-1}. These periods of higher speed coincided with the movement of the ice itself, which first achieved an appreciable velocity on 14 April. Comparison of Figures 12 and 13, which respectively are the progressive vector diagrams for the ice drift and the true current, show that during the last five days of record both the ice and the water moved in a similar manner: east or east-northeast during 14-15 April and then west-southwest during 16-19 April (the time ticks are 12 hours apart). This can also be seen by comparing Figure 7 with Figures 10 and 11.

Parts of the record suggest small oscillations of tidal frequency, with an amplitude of perhaps 1-2 cm sec^{-1}.

The mean motion over the entire period of measurement was nearly negligible. The mean relative water velocity was 0.2 cm sec^{-1} toward 243°T; the mean ice drift was 0.1 cm sec^{-1} toward 69°T; and the mean true water velocity was 0.1 cm sec^{-1} toward 240°T.
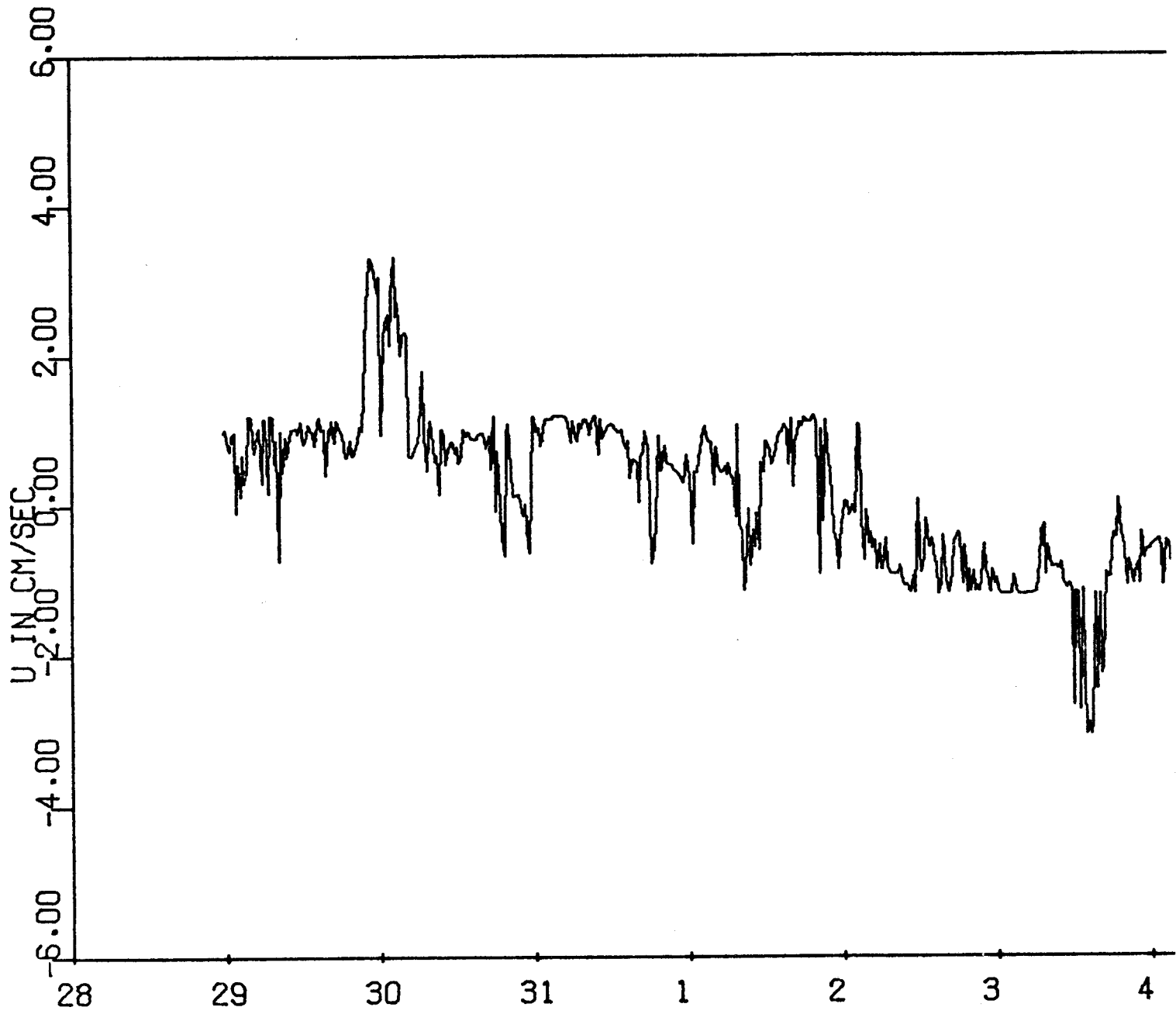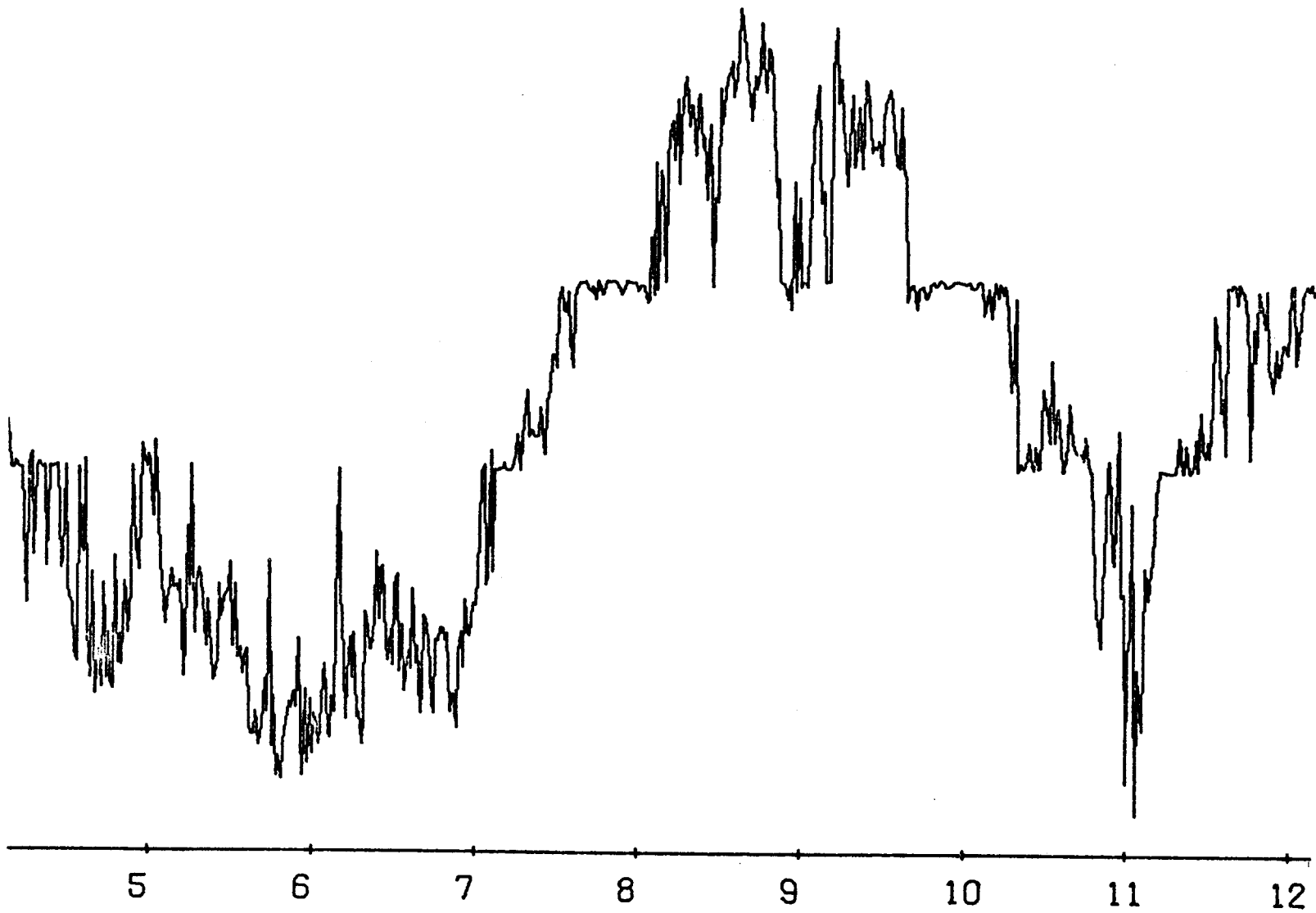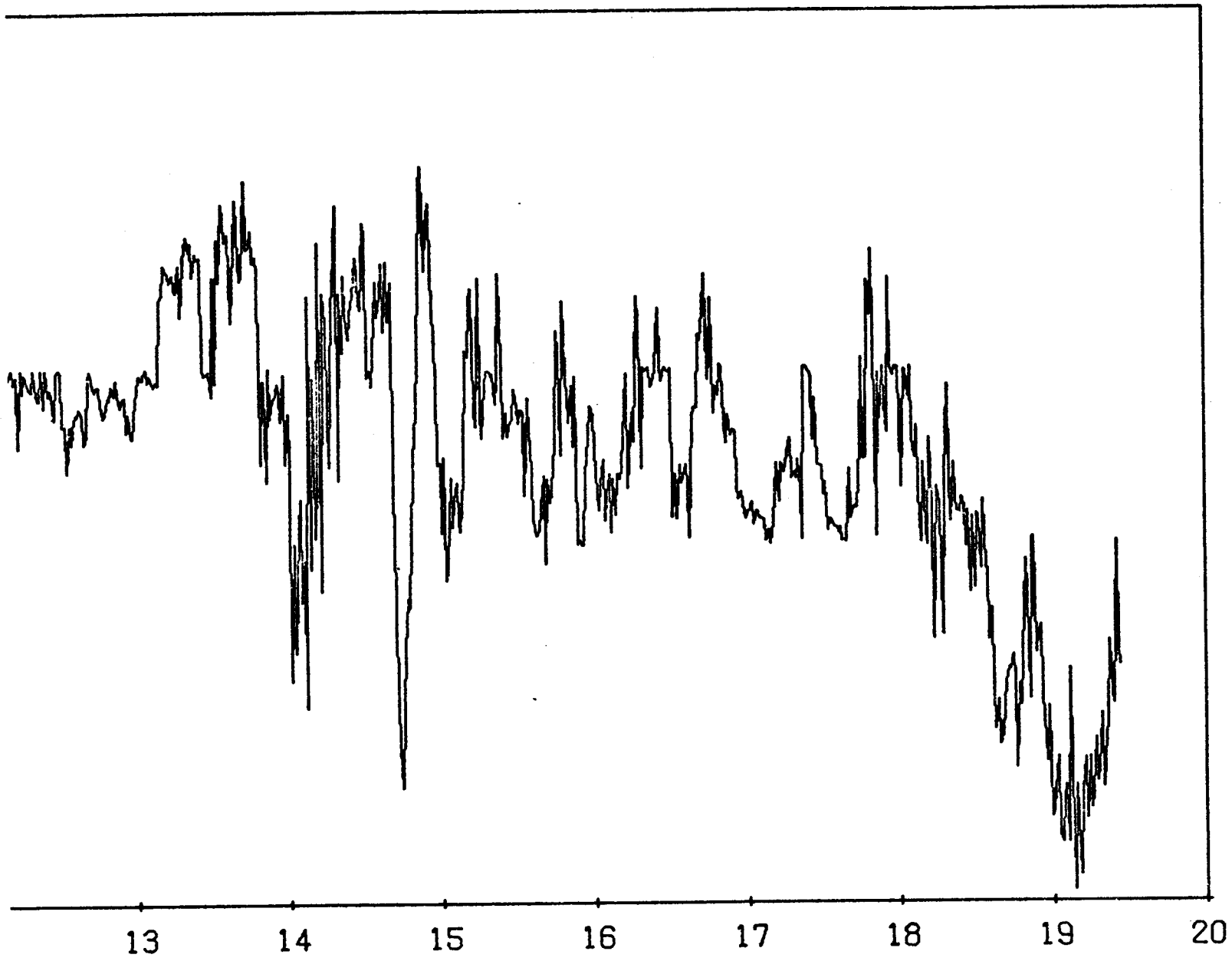
Figure 1
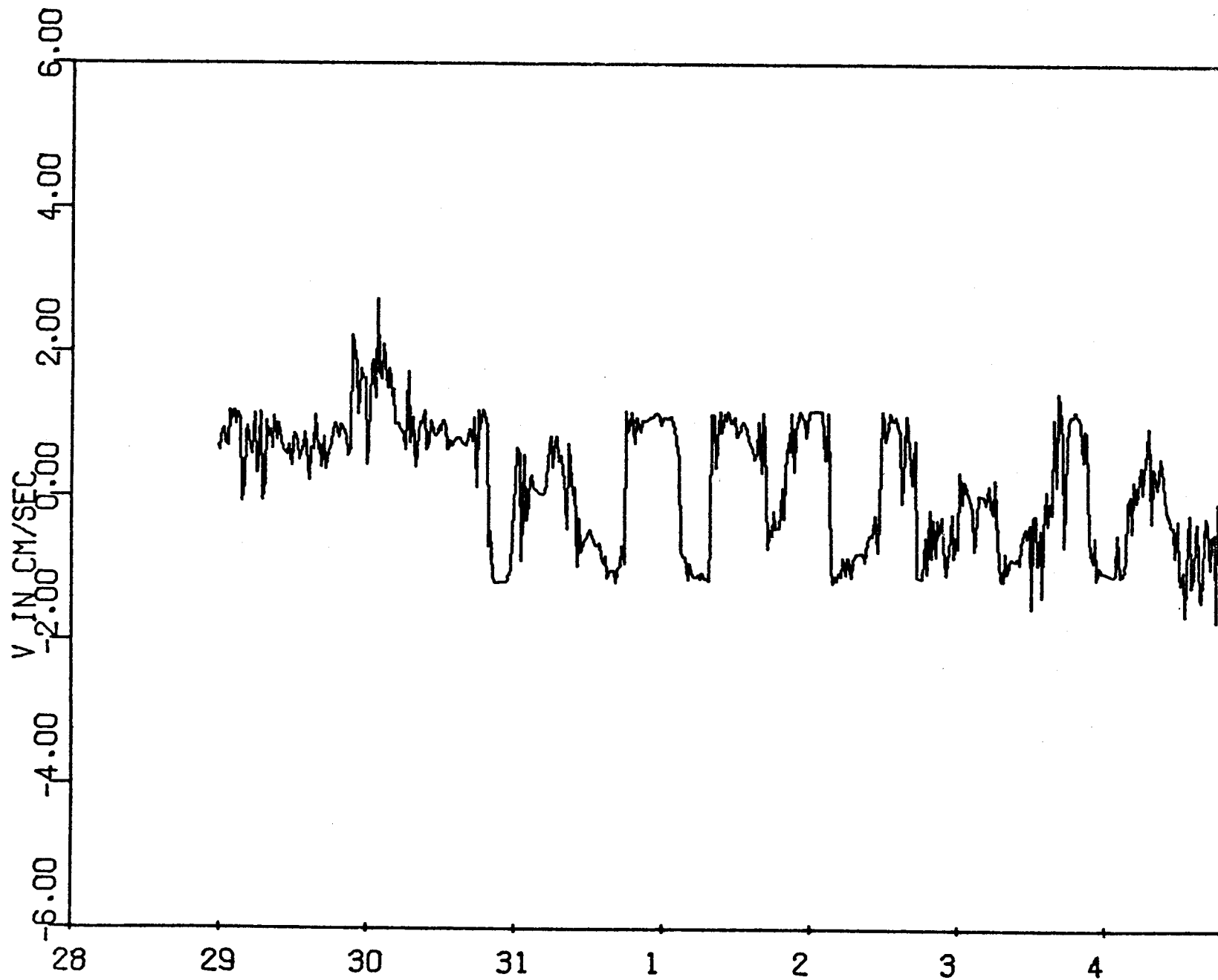
Figure 2
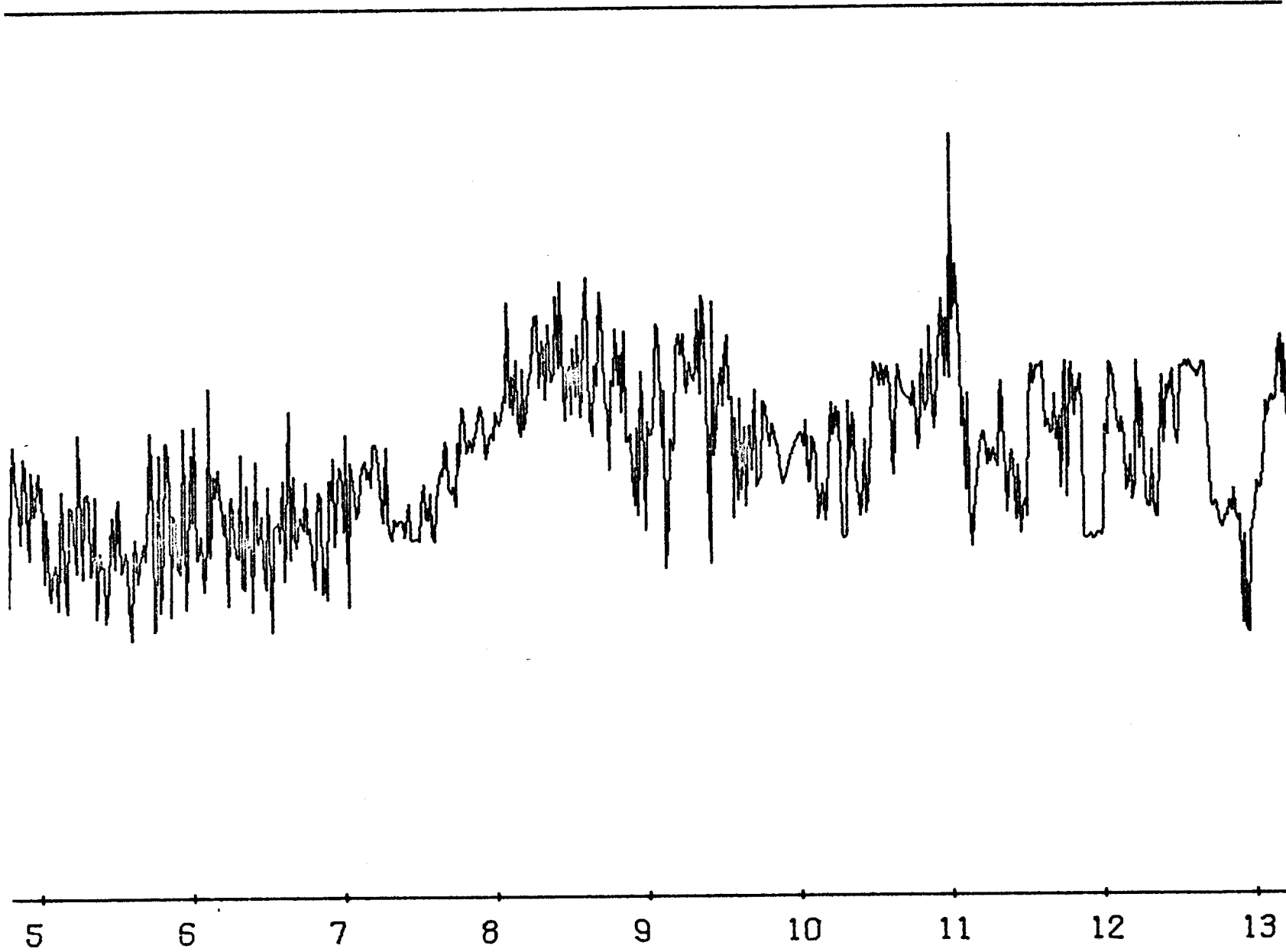
Figure 3

Figure 4

Figure 5
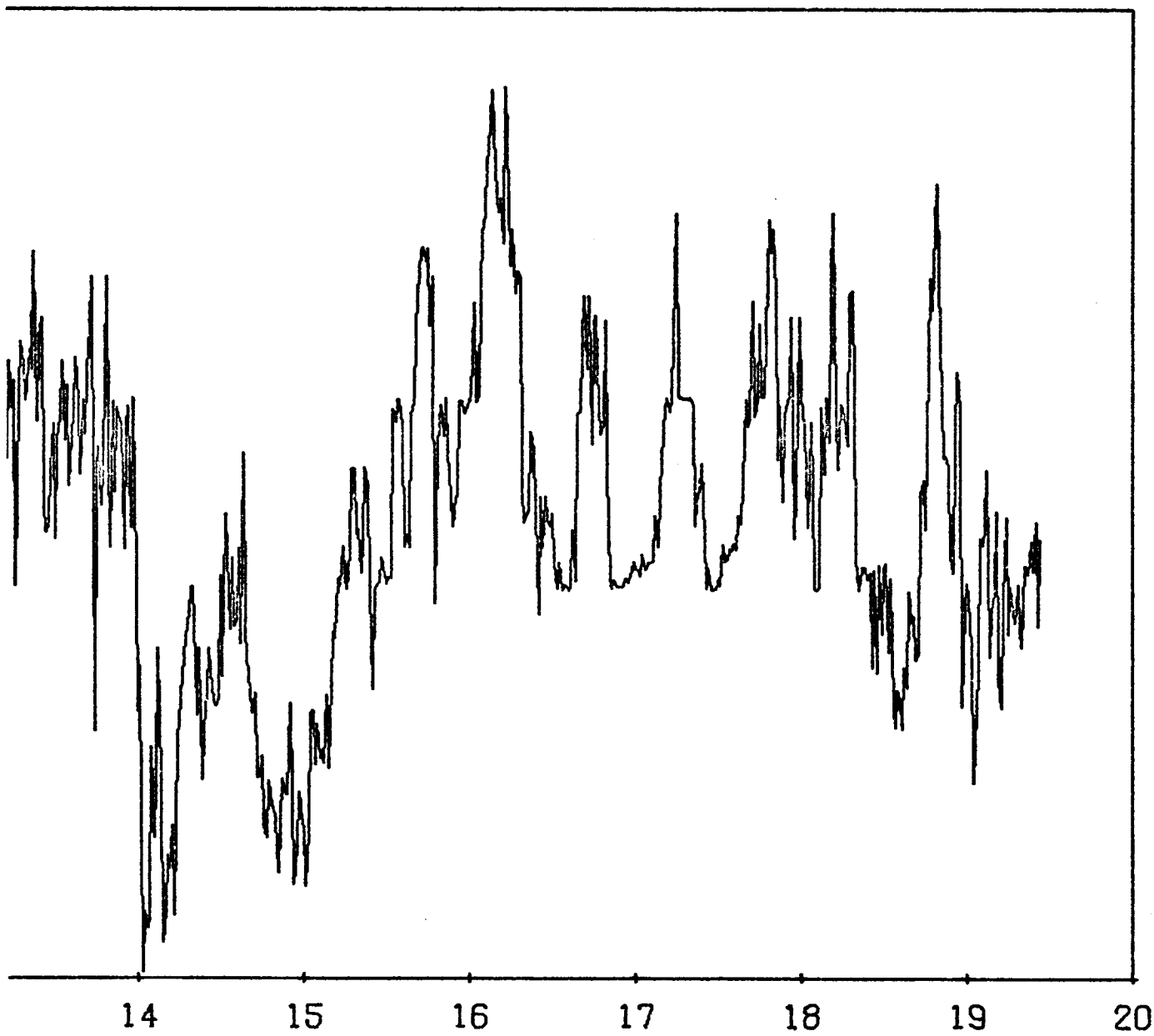
Figure 6
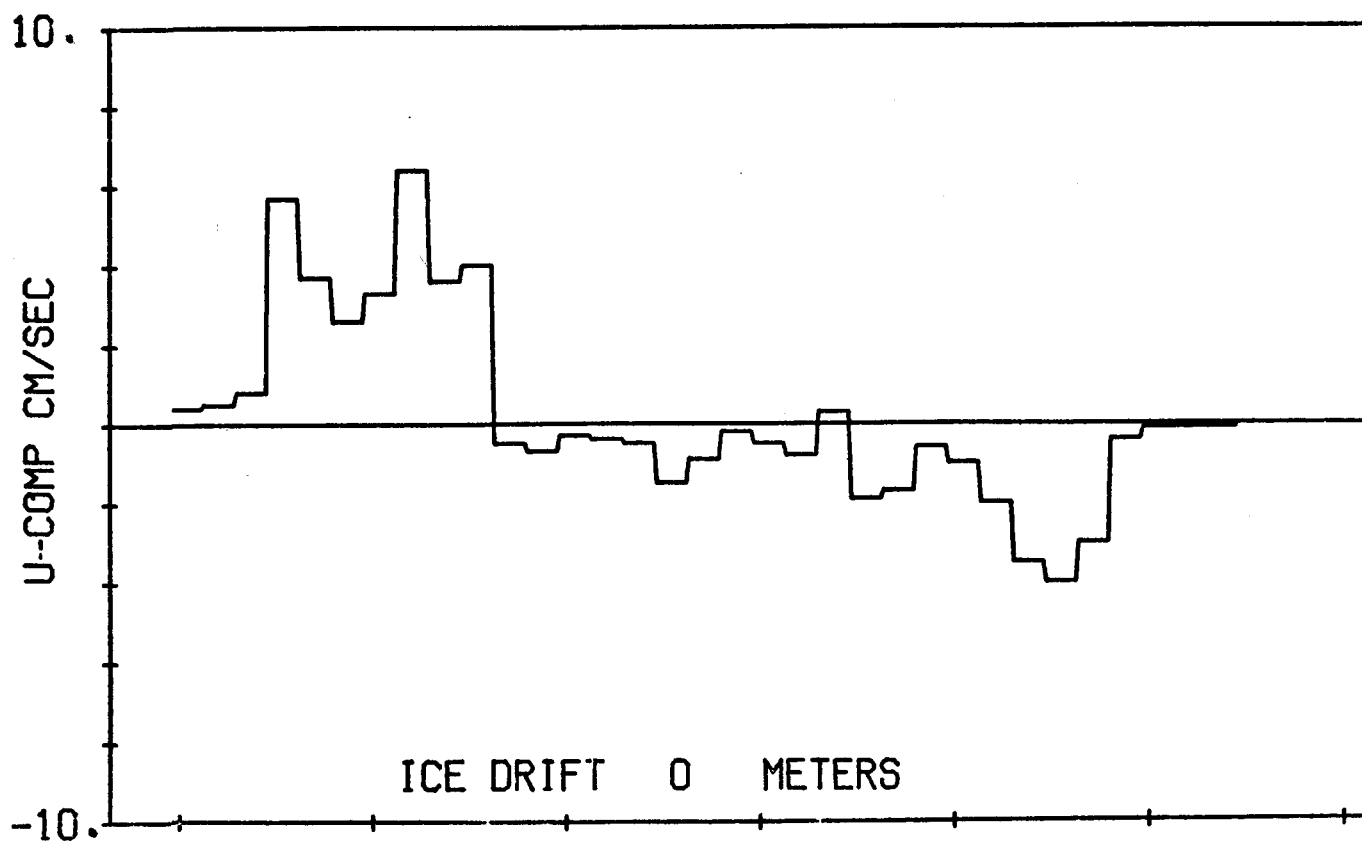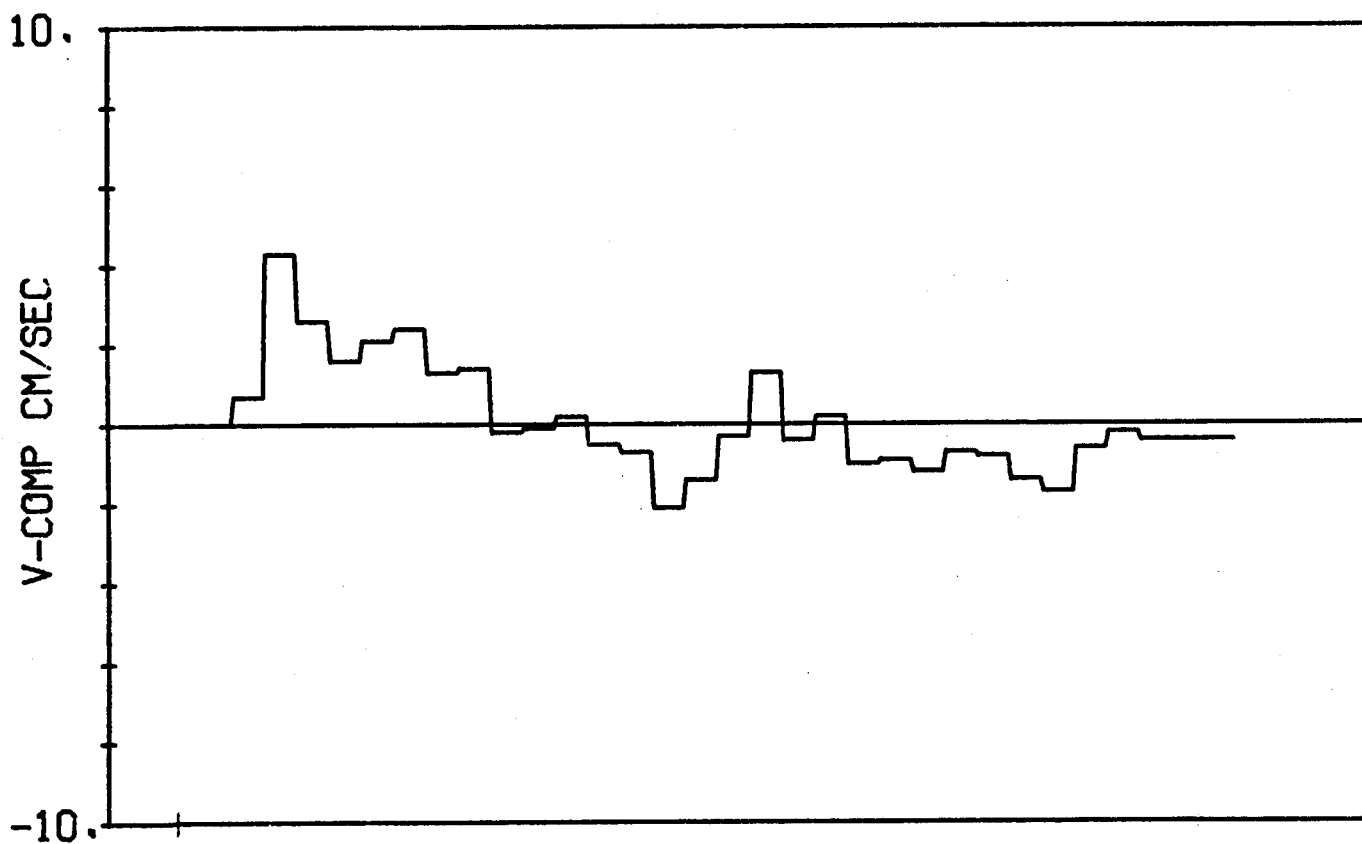
ICE DRIFT 0 METERS

04/14/76   Figure 7   04/20/76
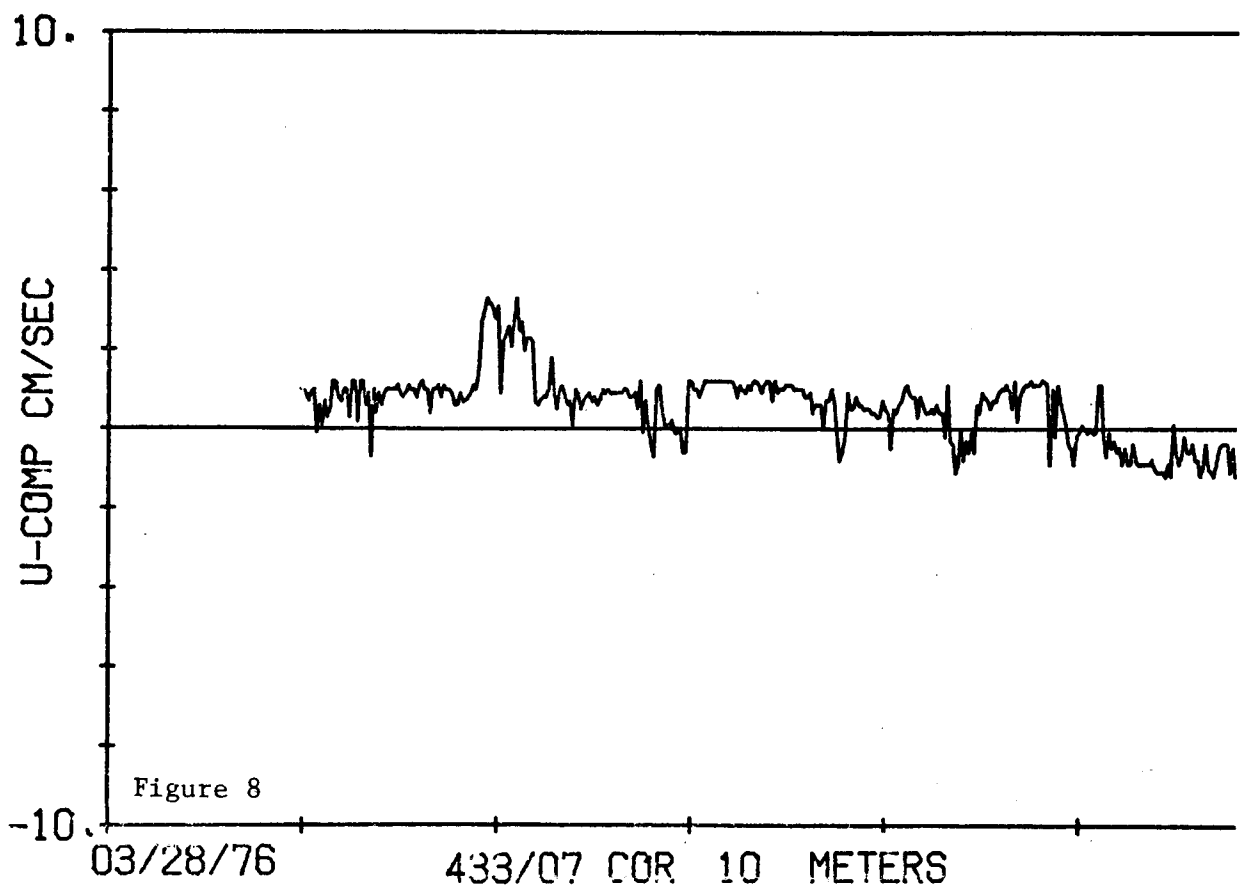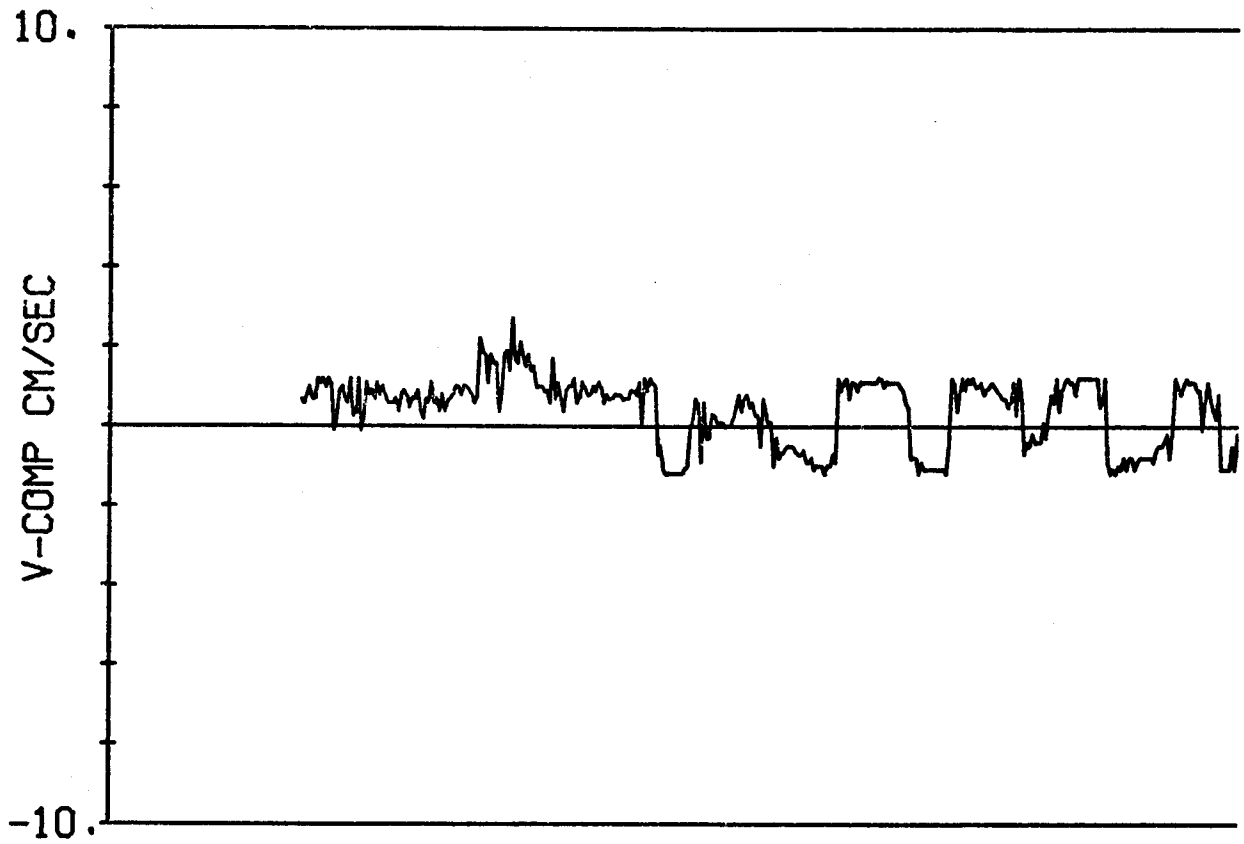
Figure 8

03/28/76   433/07 COR 10   METERS

04/03/76   Figure 9   04/09/76

Figure 10

04/10/76   04/16/76

Figure 11

04/21/76

ICE DRIFT   START DATE 413761920
PLOTTED AT 2.0 KM/INCH

Figure 12

433/07CORR   START DATE 328762340
PLOTTED AT   2.0 KM/INCH   Figure 13

Figures 14-19 show the components of motion at meter 437. The speeds were even lower than at meter 433, never exceeding 6 cm sec^{-1}. With the possible exception of the events during 4-6 April, when there was a burst of motion toward the southwest, there is no apparent correlation between water motion at the two meters. Figure 20 is the progressive vector diagram for meter 437; it can be compared with Figure 13.

Again the record suggests small oscillations of tidal frequency with amplitude in the range 1-2 cm sec^{-1}, and with no clear phase difference between components.

The mean motion was comparable to that at meter 433, being 0.3 cm sec^{-1} toward 248°T.

The spectra for the two records are shown in Figure 21-26. The energy levels are of course very low, and only for the east component at meter 433 is there a low-frequency maximum. Relatively strong signals appear in both the diurnal and semi-diurnal tidal bands, corresponding to an amplitude of about 1 cm sec^{-1}, or a bit more. The spectral estimates indicate the presence of the K_1 component at both meters, but can distinguish M_2 only at meter 437. The K_1 signals in the east and north components are coherent at each meter and in phase, but the M_2 signals are incoherent.

These two records thus show motion on the inner shelf to have been small, generally with a 20-minute mean of 5 cm sec^{-1} or less, and only on a few occasions approaching 10 cm sec^{-1} (and then only at the outer meter). The mean motion over more than three weeks was very small, one-fourth kilometer per day or less, and directed west-southwest. Tidal currents were of order 1 cm sec^{-1}, with comparable energy in both the diurnal and semi-diurnal bands. However, only the K_1 component was clearly identifiable in both records.

We turn now to the mooring on the outer shelf north of Oliktok. Current meter no. 660 was suspended at a nominal depth of 100 m, in water 225 m deep. Figures 27-42 show the east (U) and north (V) components of velocity at this meter from 1215 GMT on 27 May 1976 to 1200 GMT on 14 July, and from 1215 GMT on 16 July to 0830 GMT on 1 September. The two-day gap in the middle of the record, along with the truncated end and beginning are due to noise and other data reduction problems which have not yet been satisfactorily resolved. The portions of the records shown here were relatively clean.

The difference between these currents and those observed on the inner shelf is remarkable. The speeds are a full order of magnitude greater than those observed on the inner shelf. The velocity varied between 56 cm sec^{-1} easterly and 26 cm sec^{-1} westerly. The entire 95-day record is dominated by large low-frequency oscillations which have a typical peak-to-peak amplitude exceeding 50 cm sec^{-1} and a time scale of order 10 days. The oscillations are not centered about the line of zero velocity, but rather are offset in the direction of positive U-component. In effect, therefore, the oscillations represent long bursts of high easterly velocity separated by shorter periods of lesser flow toward the west. Between the easterly bursts there were frequently smaller oscillations with amplitude and time scale of order 10 cm sec^{-1} and 2 days, respectively.

The flow did not alternate strictly between east and west, for there were also appreciable north-south motions. Rather there was a tendency for the water
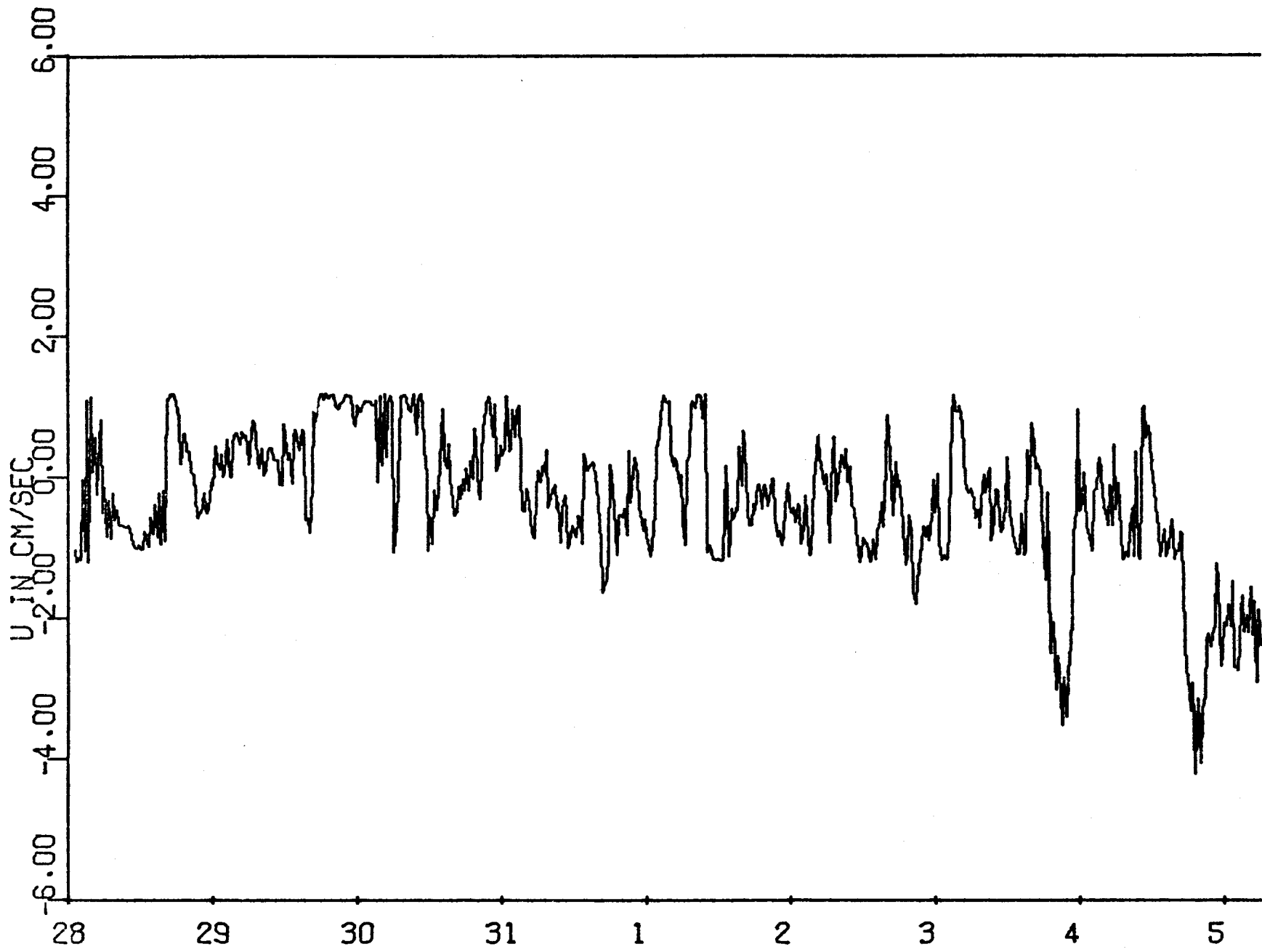
Figure 14
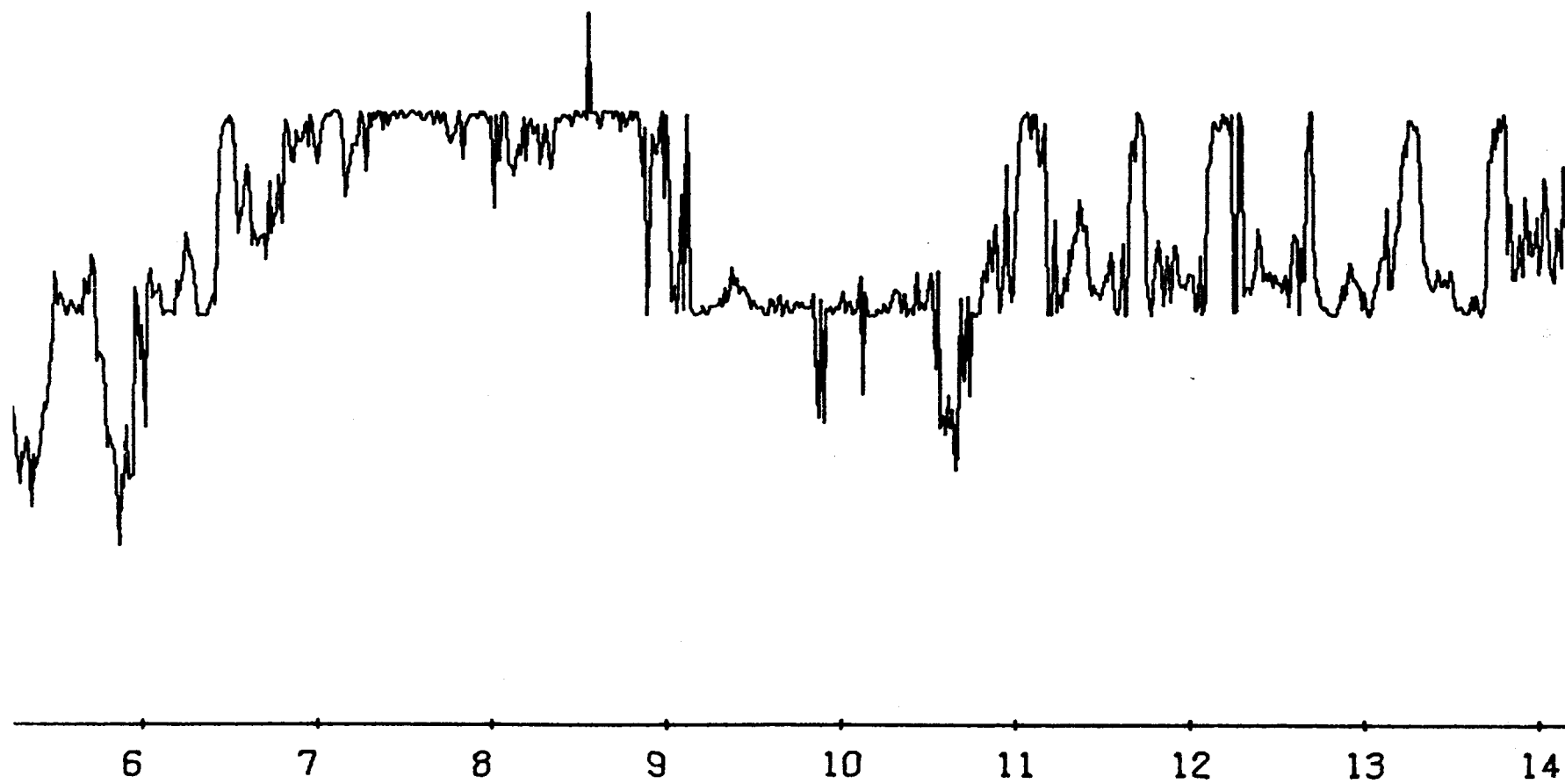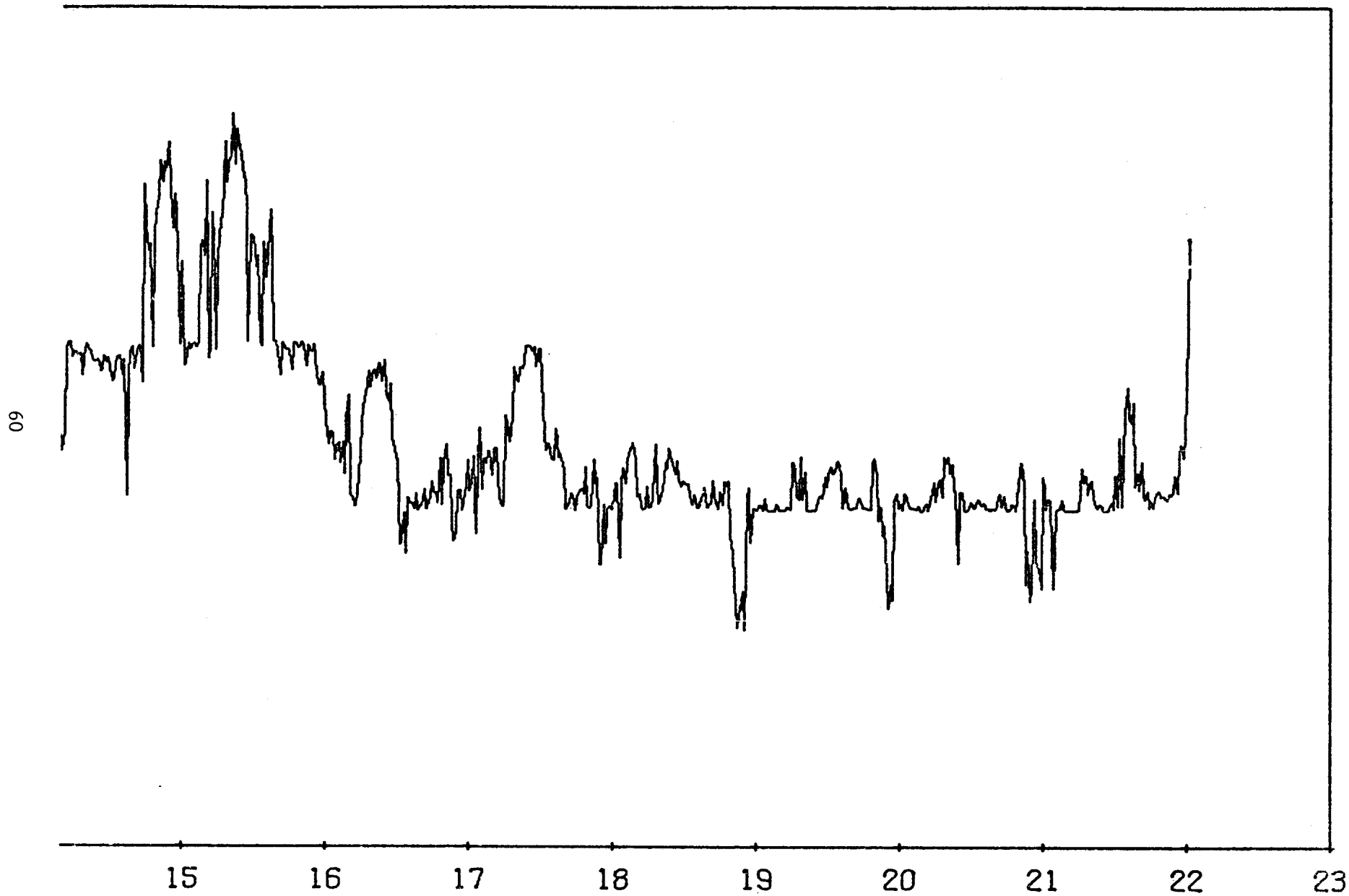
Figure 15

Figure 16
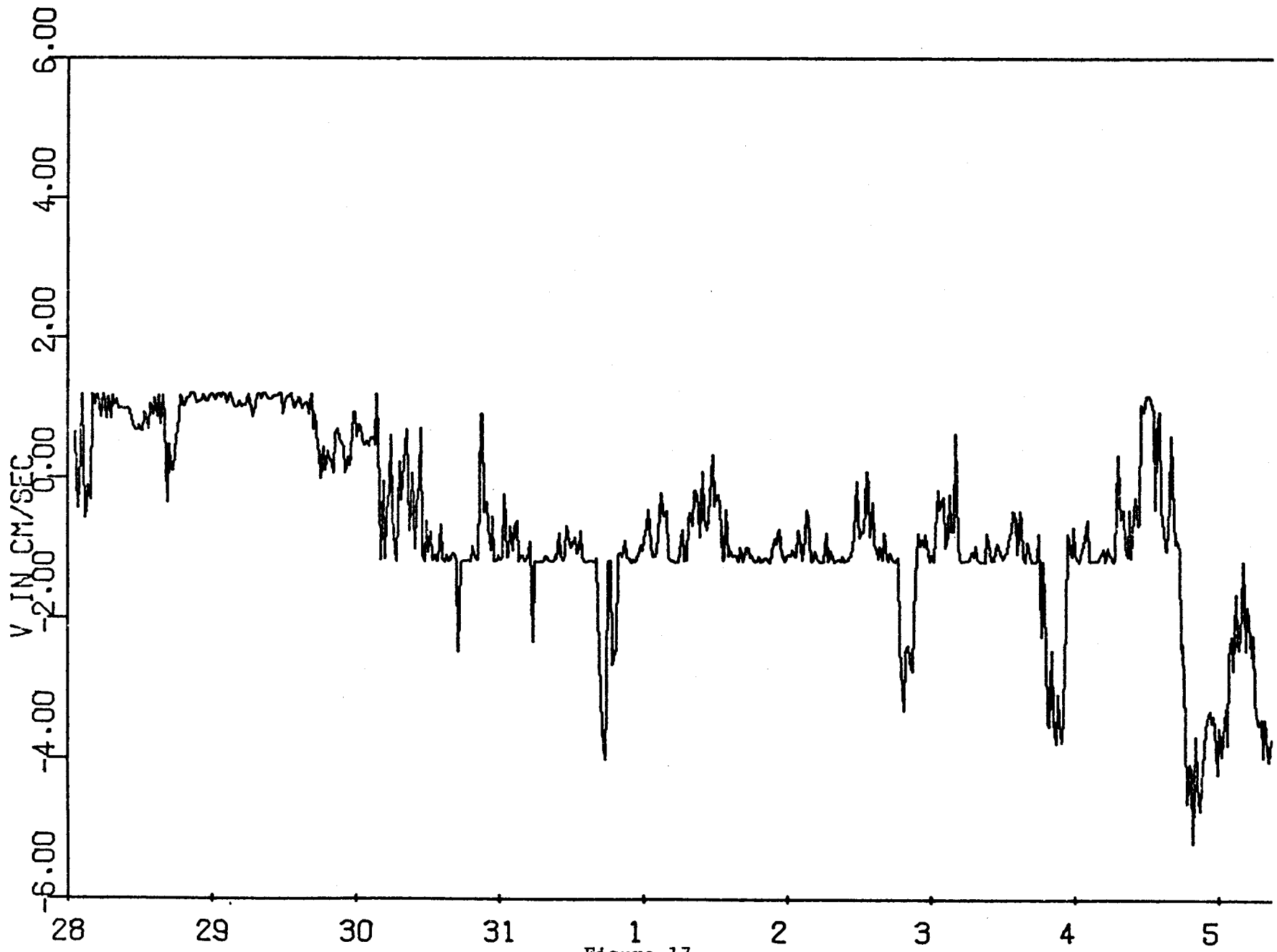
Figure 17
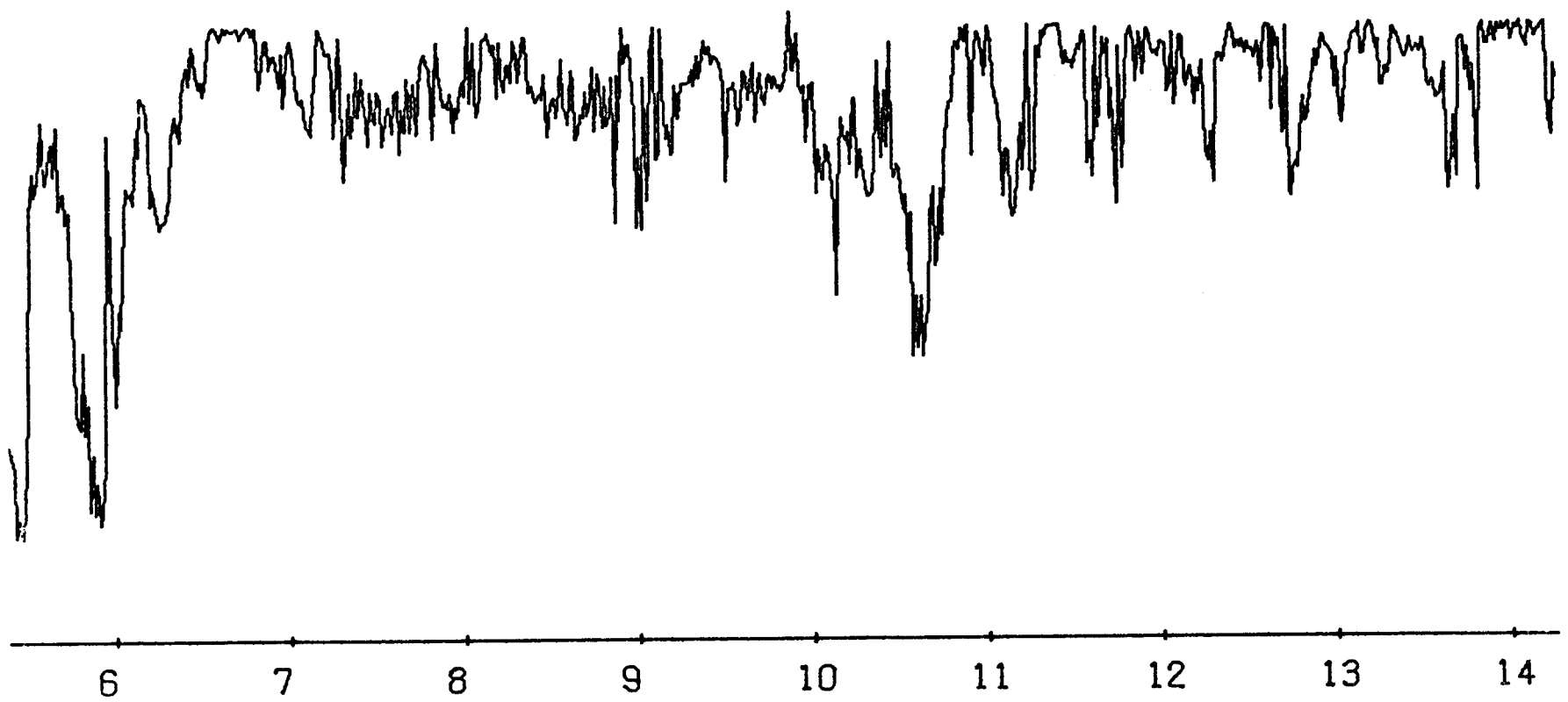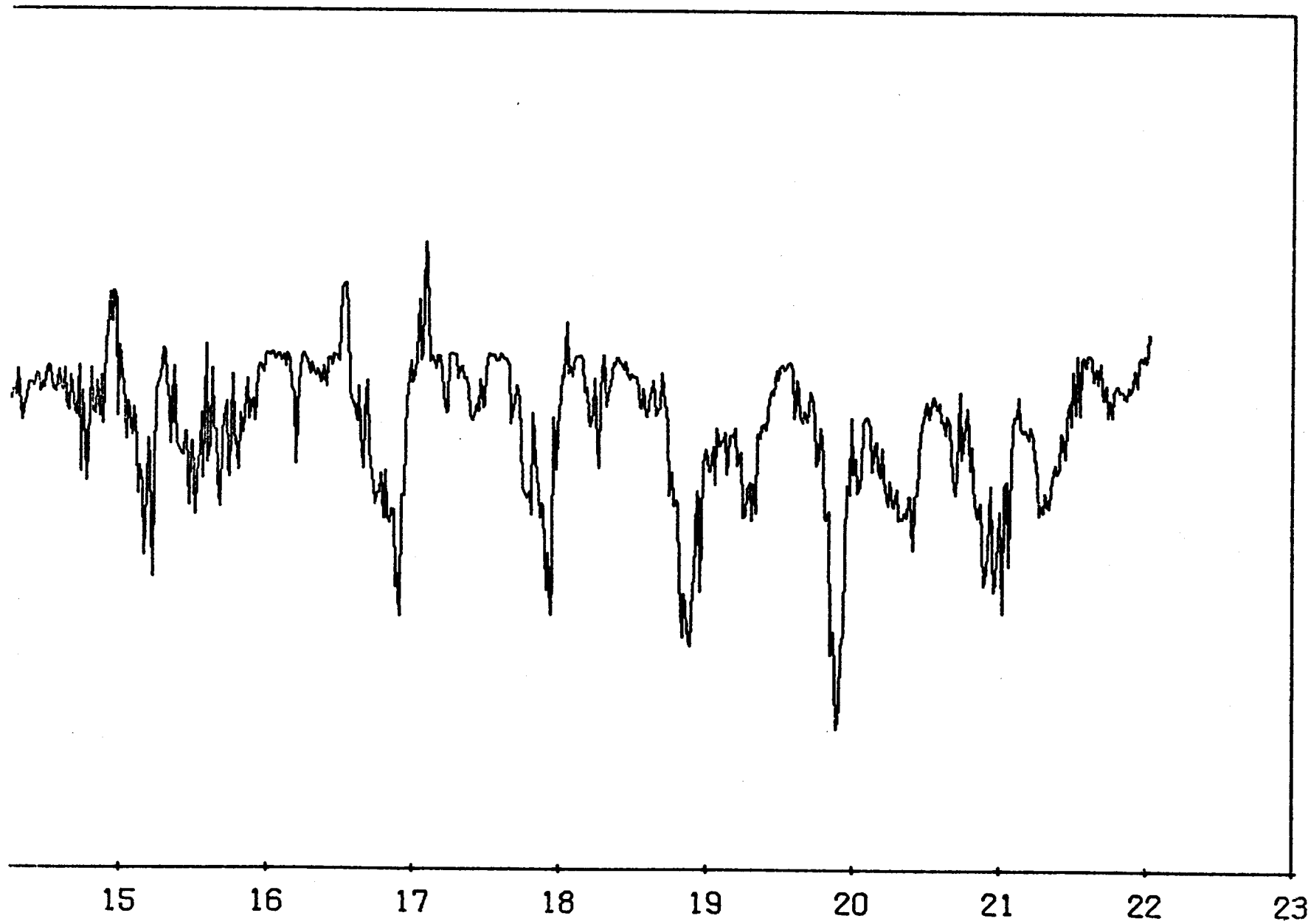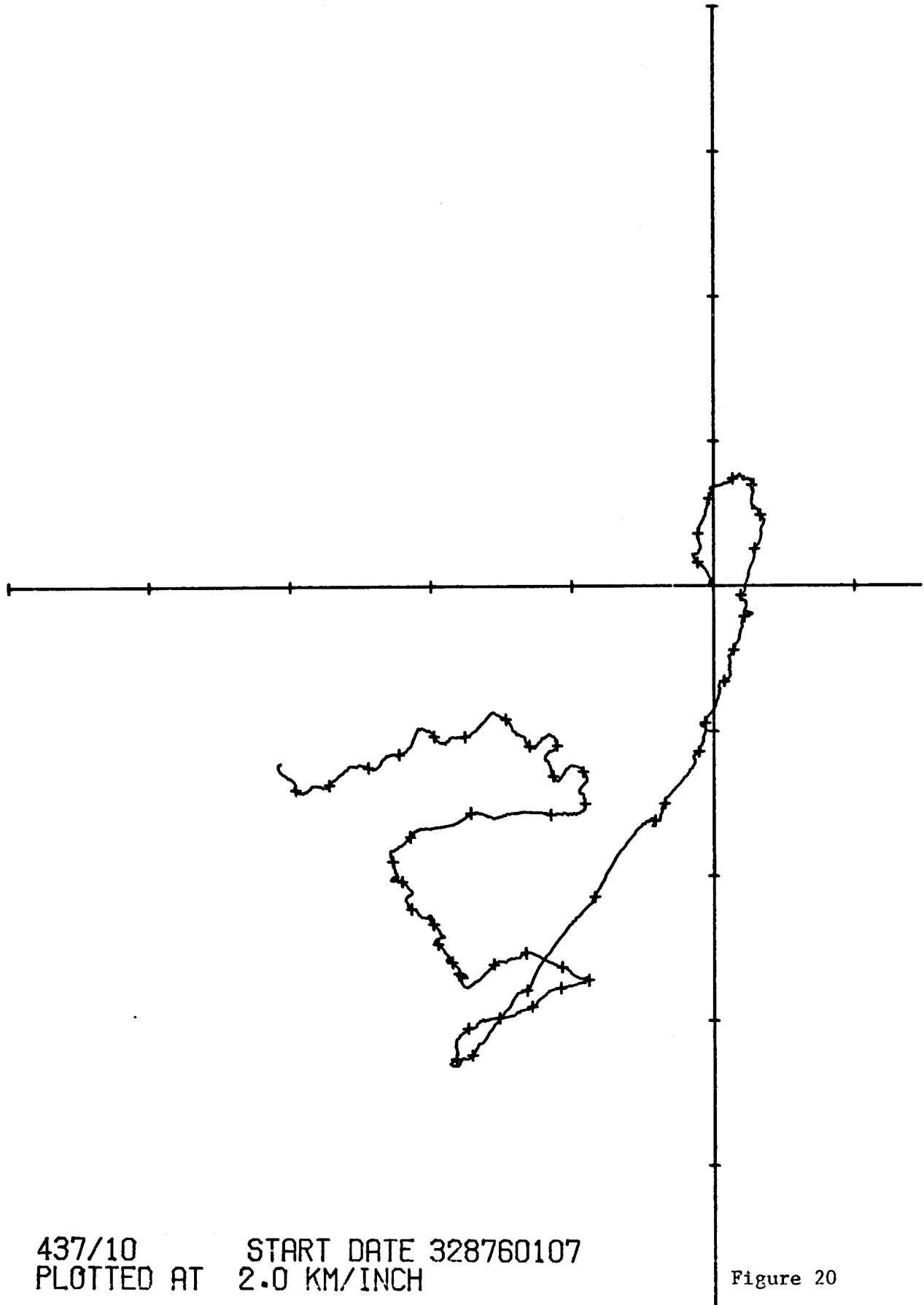
Figure 18
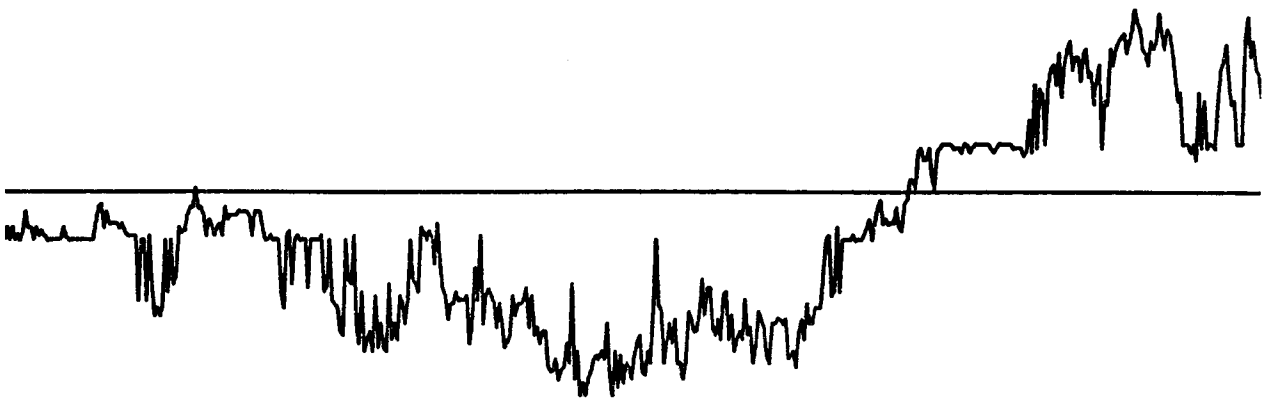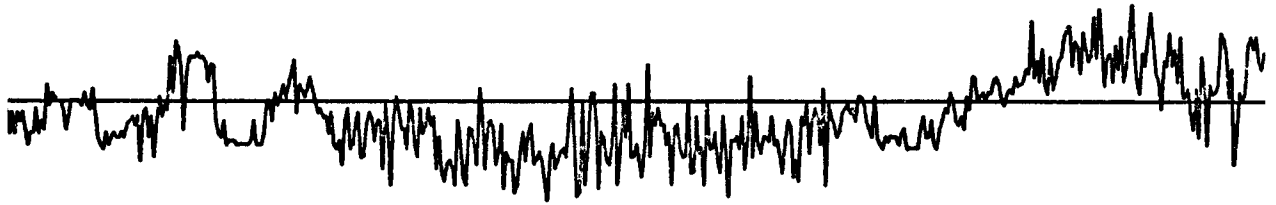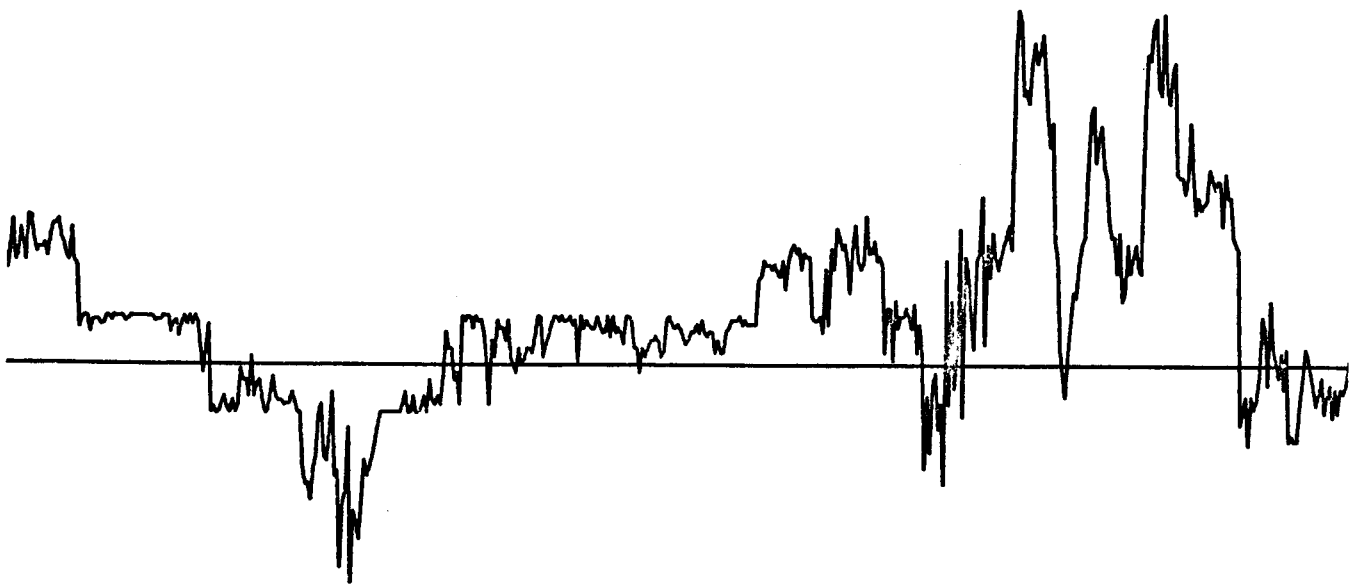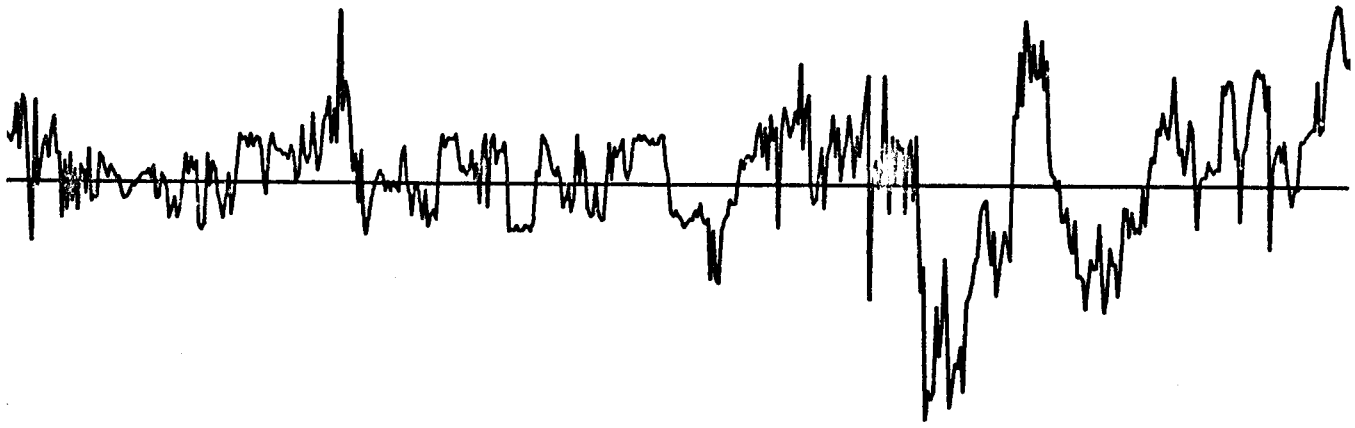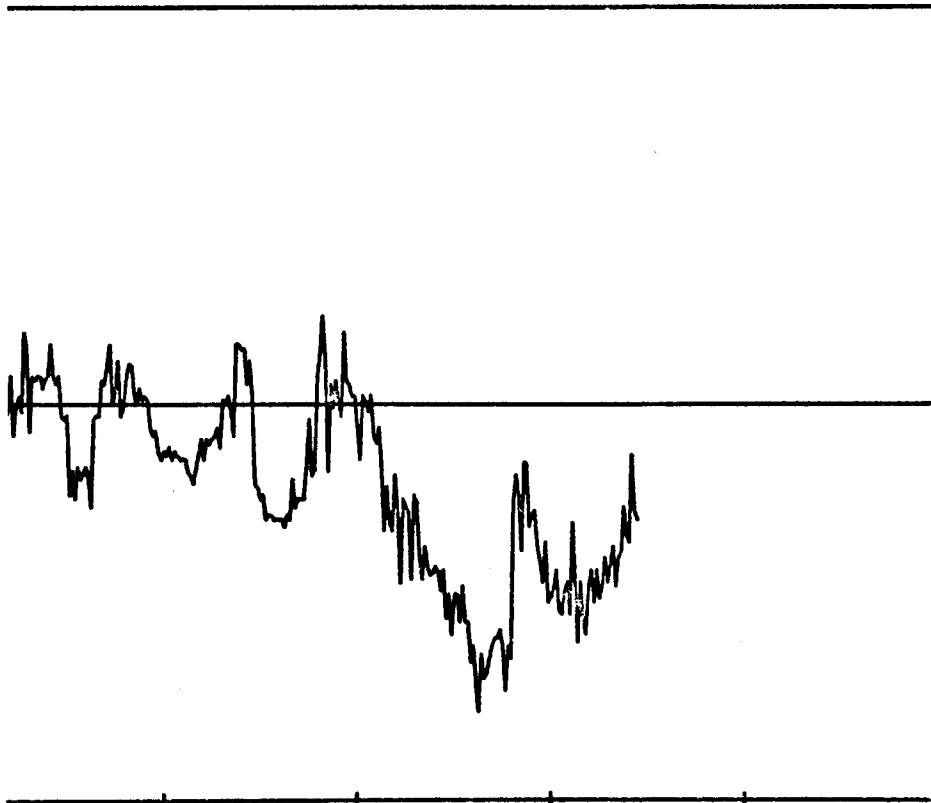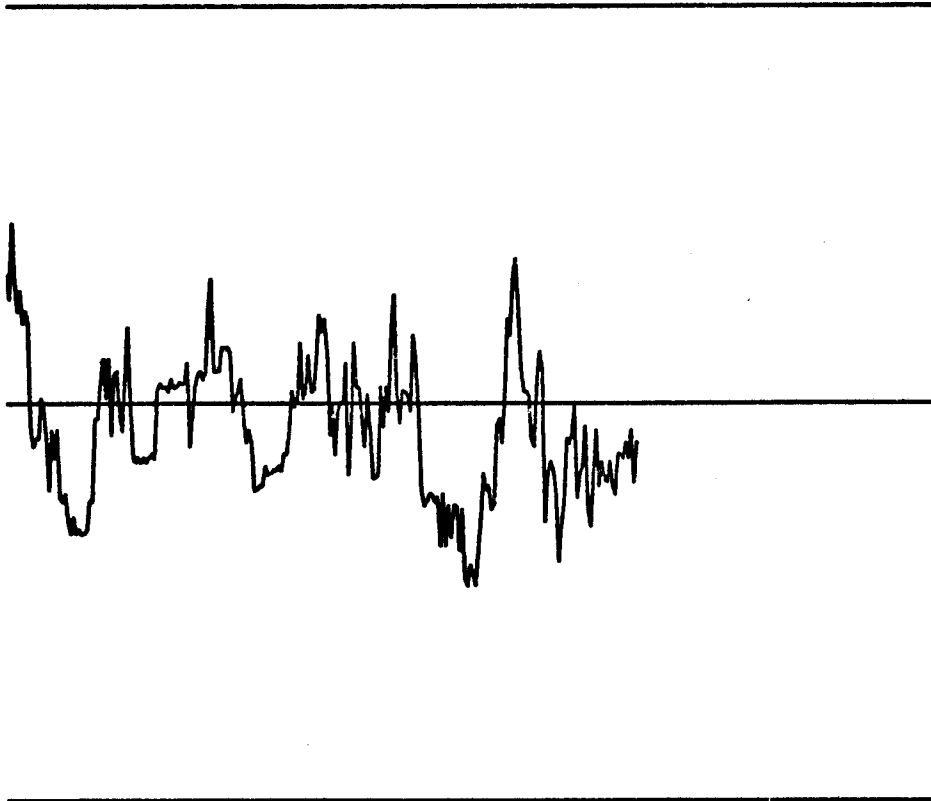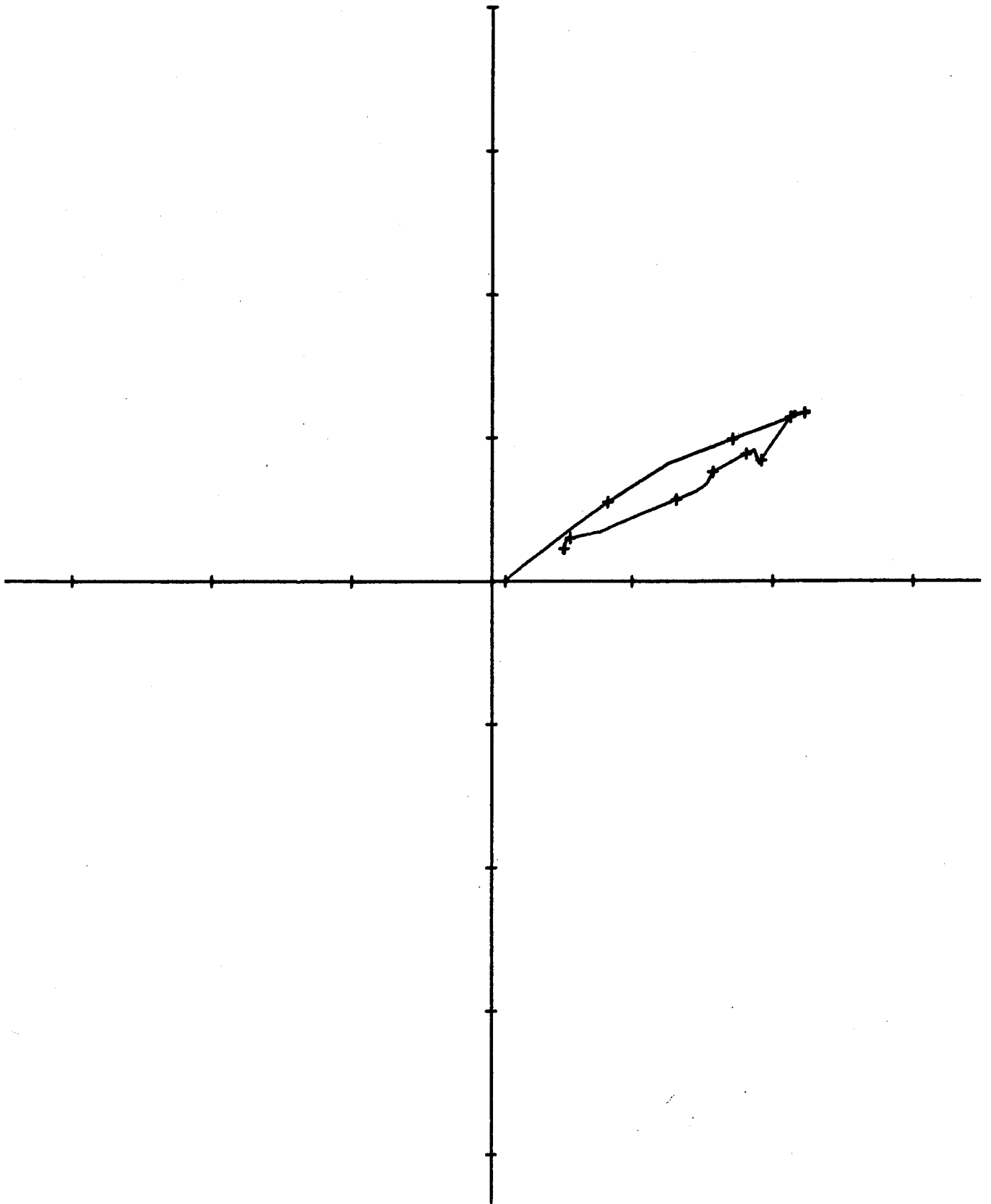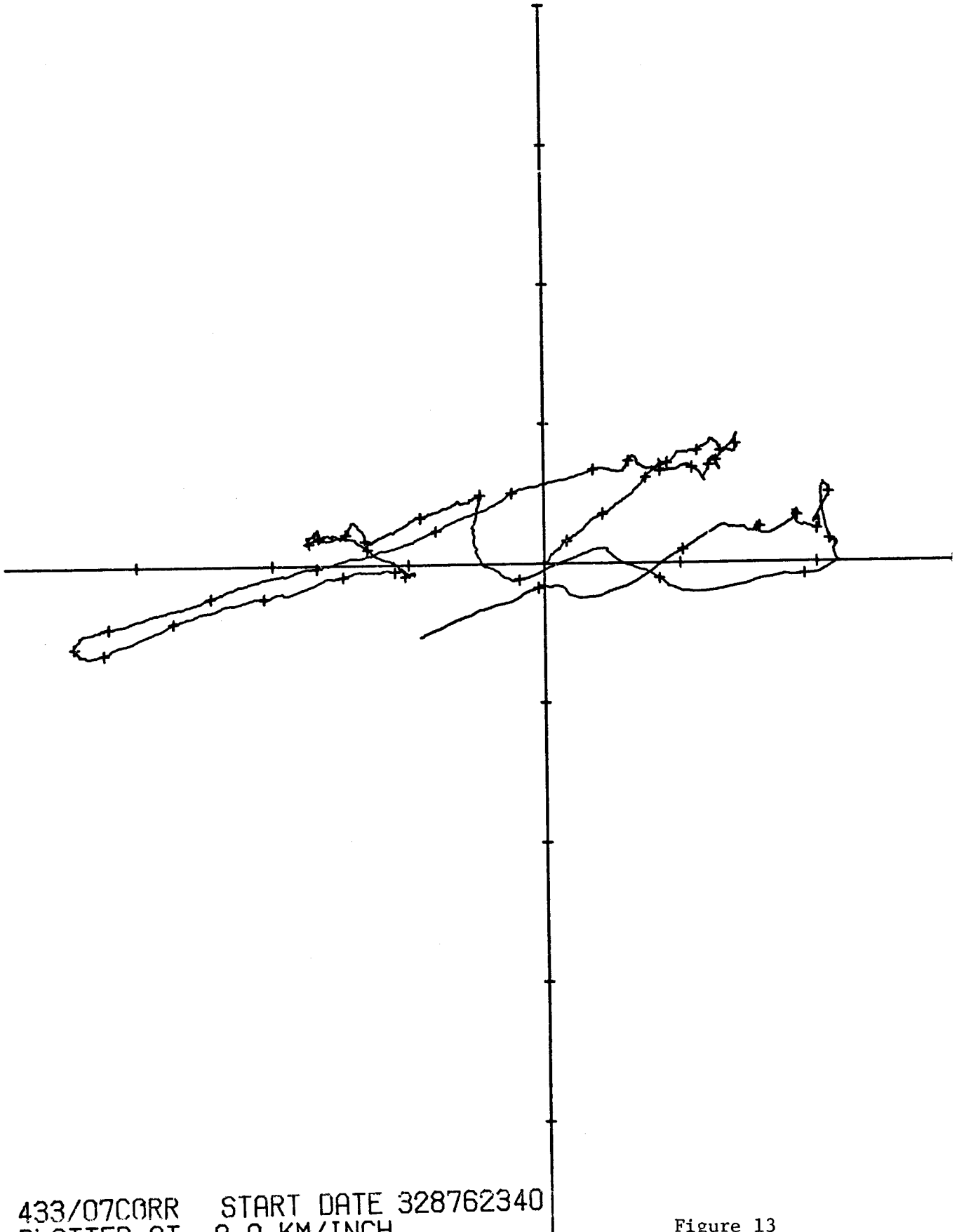
Figure 19

437/10   START DATE 328760107
PLOTTED AT   2.0 KM/INCH

Figure 20

U-COMP   METER 433/07 CORRECTED FOR DRIFT
3/28/76 2340   DELTA-T =20 MIN

Figure 21

V-COMP METER 433/07 CORRECTED FOR DRIFT
3/28/76 2340   DELTA-T =20 MIN

Figure 22

U-COMP   METER 433/C7 CORRECTED FOR DRIFT
V-COMP   METER 433/07 CORRECTED FOR DRIFT

Figure 23

U-COMP   METER 437/10
3/28/76 0107   DELTA-T =20 MIN
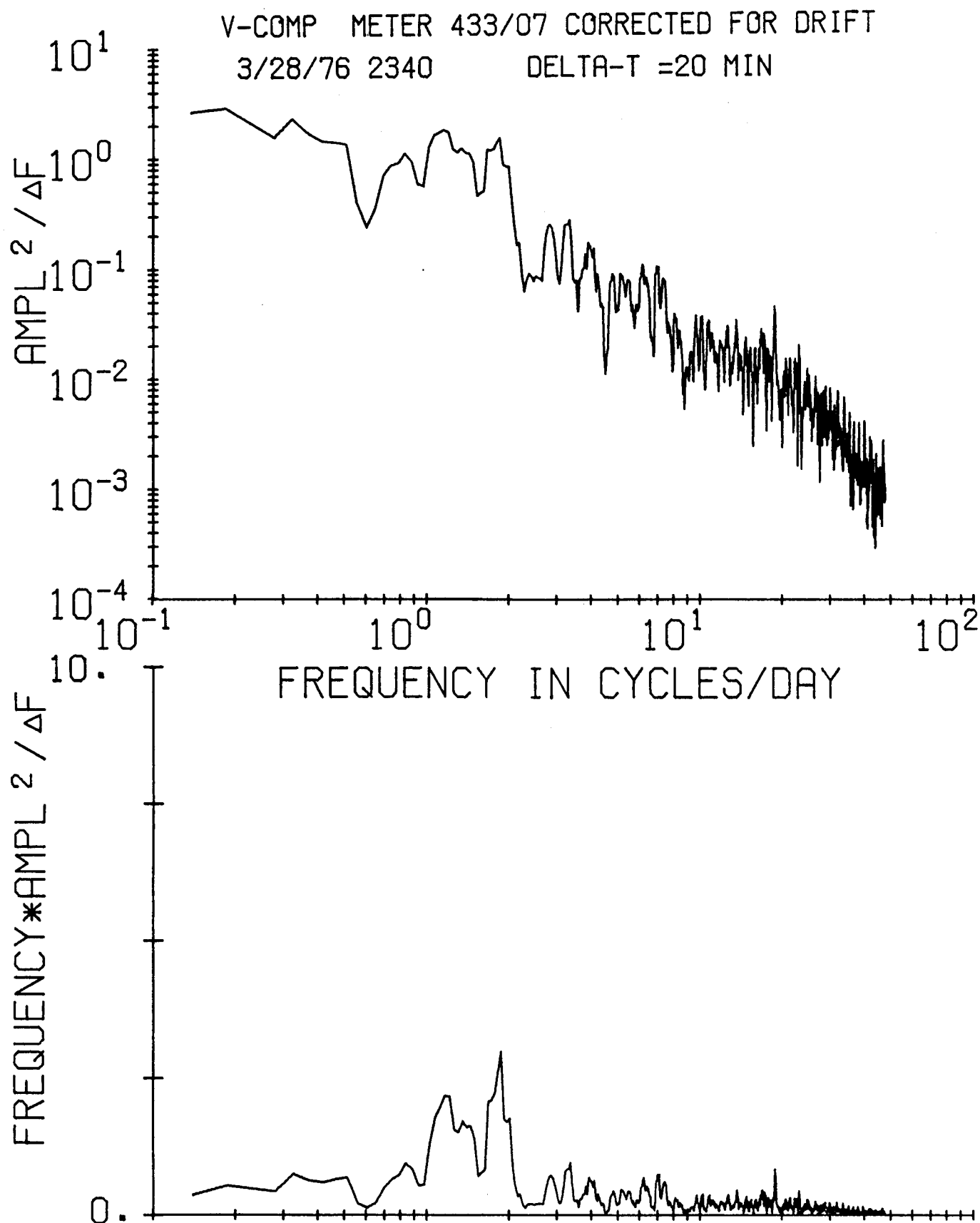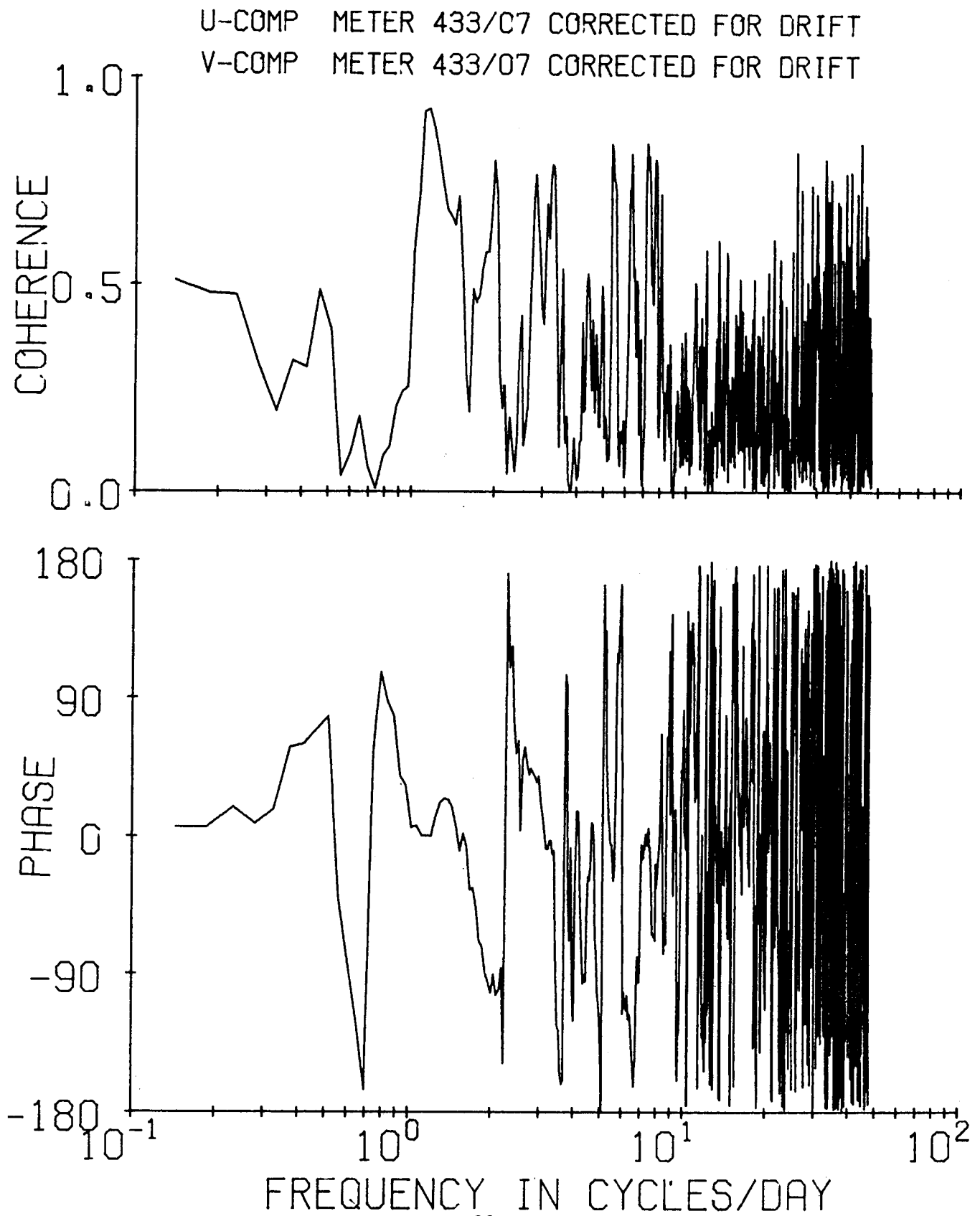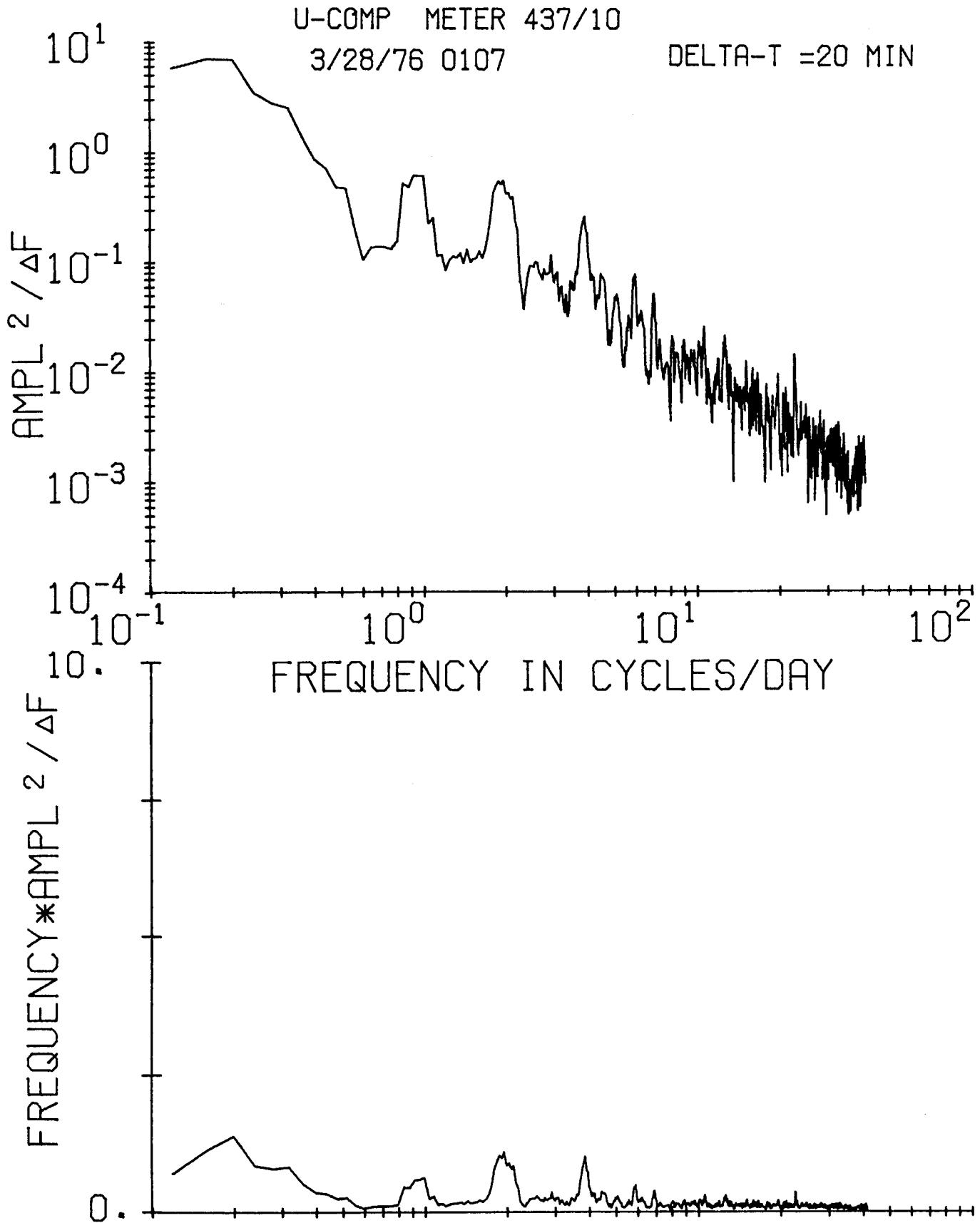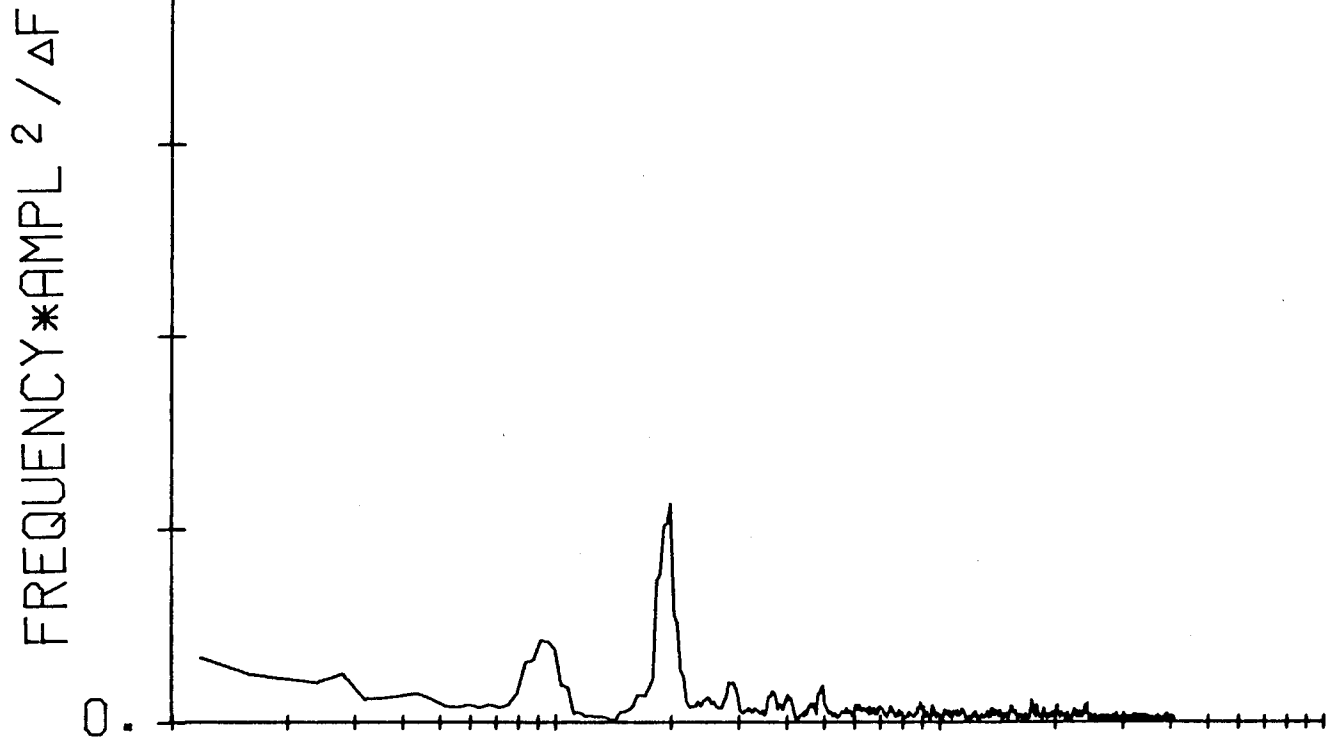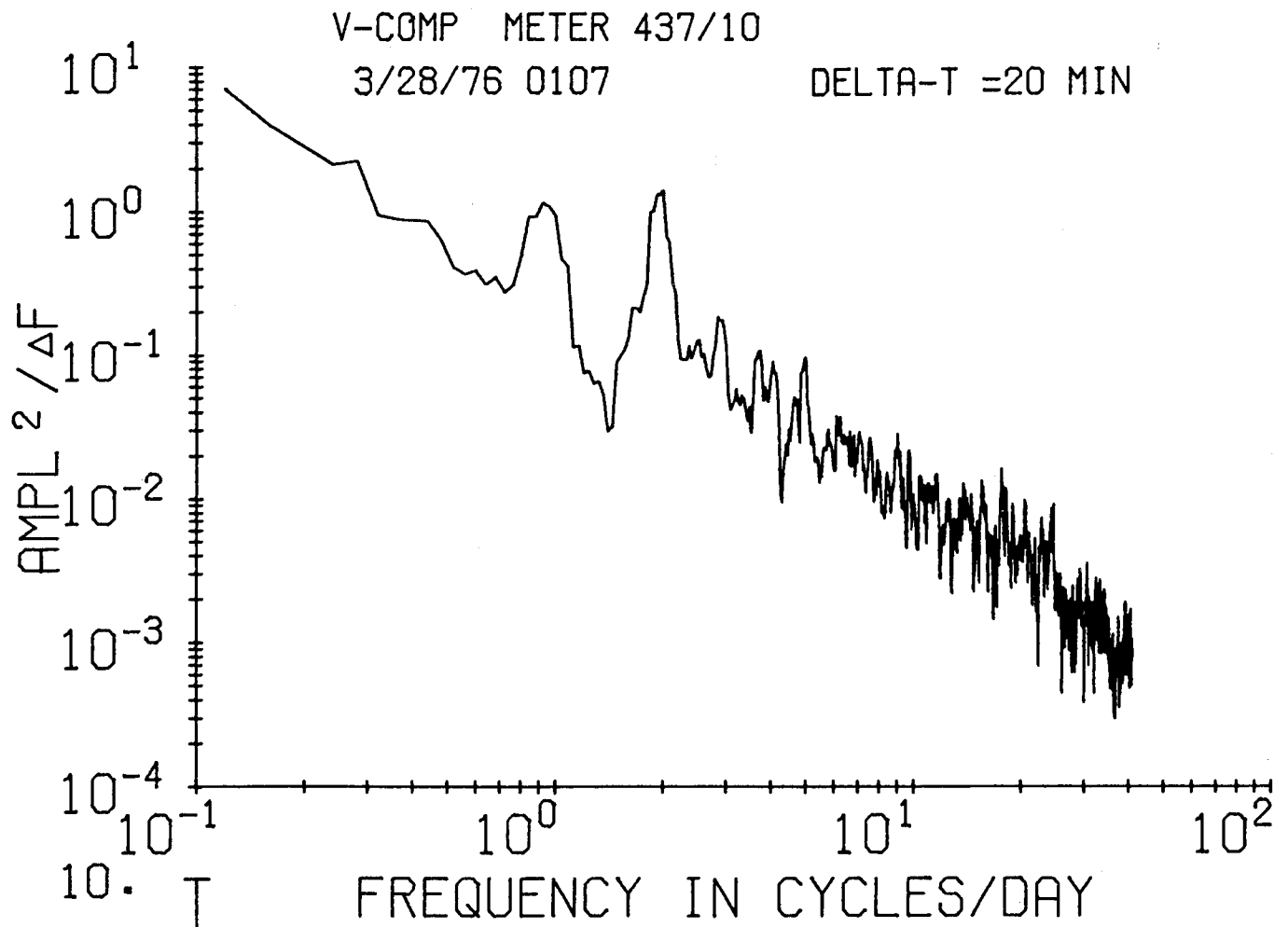
Figure 24

Figure 25

U-COMP   METER 437/10
V-COMP   METER 437/10
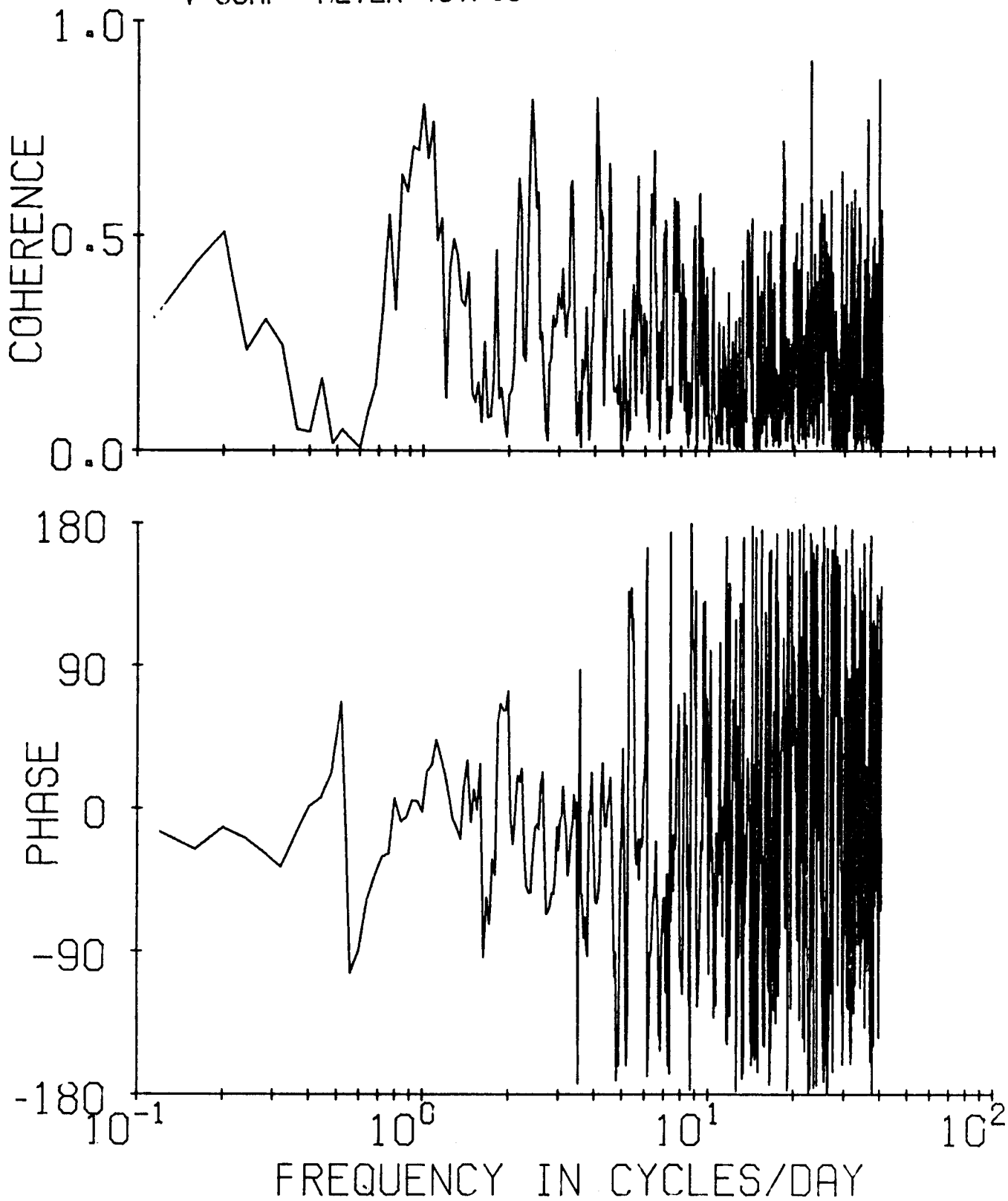
Figure 26
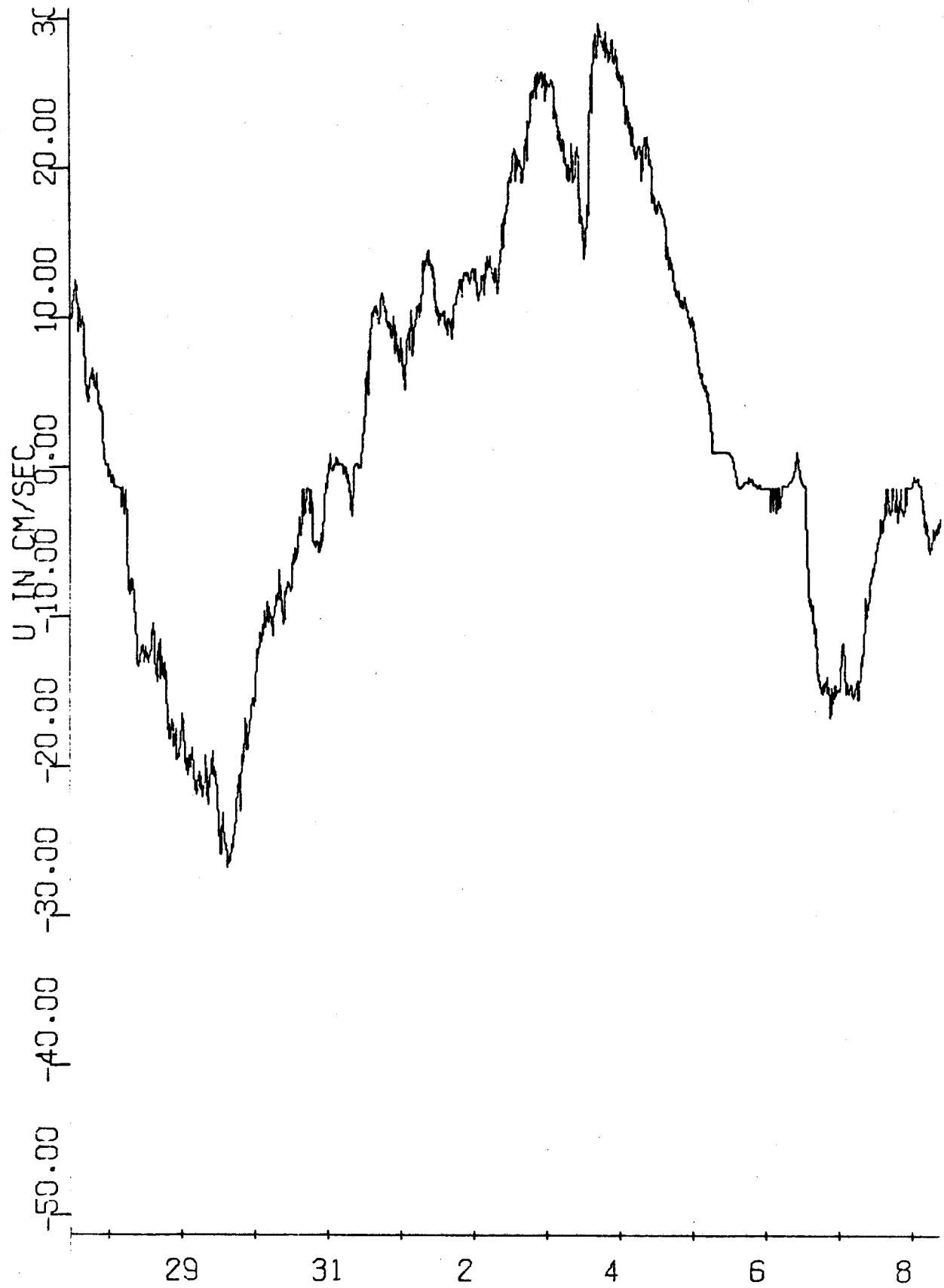
Figure 27
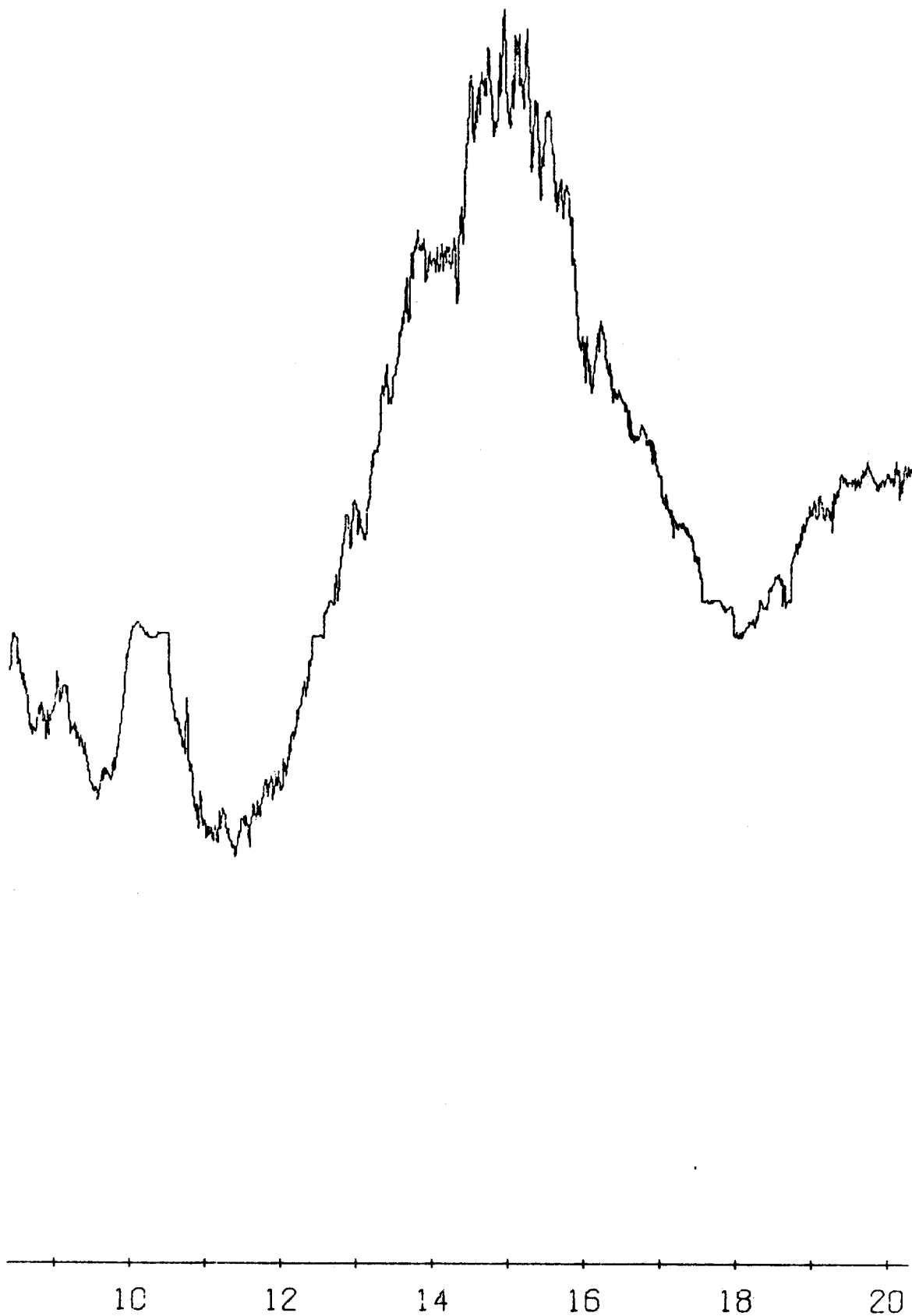
Figure 28
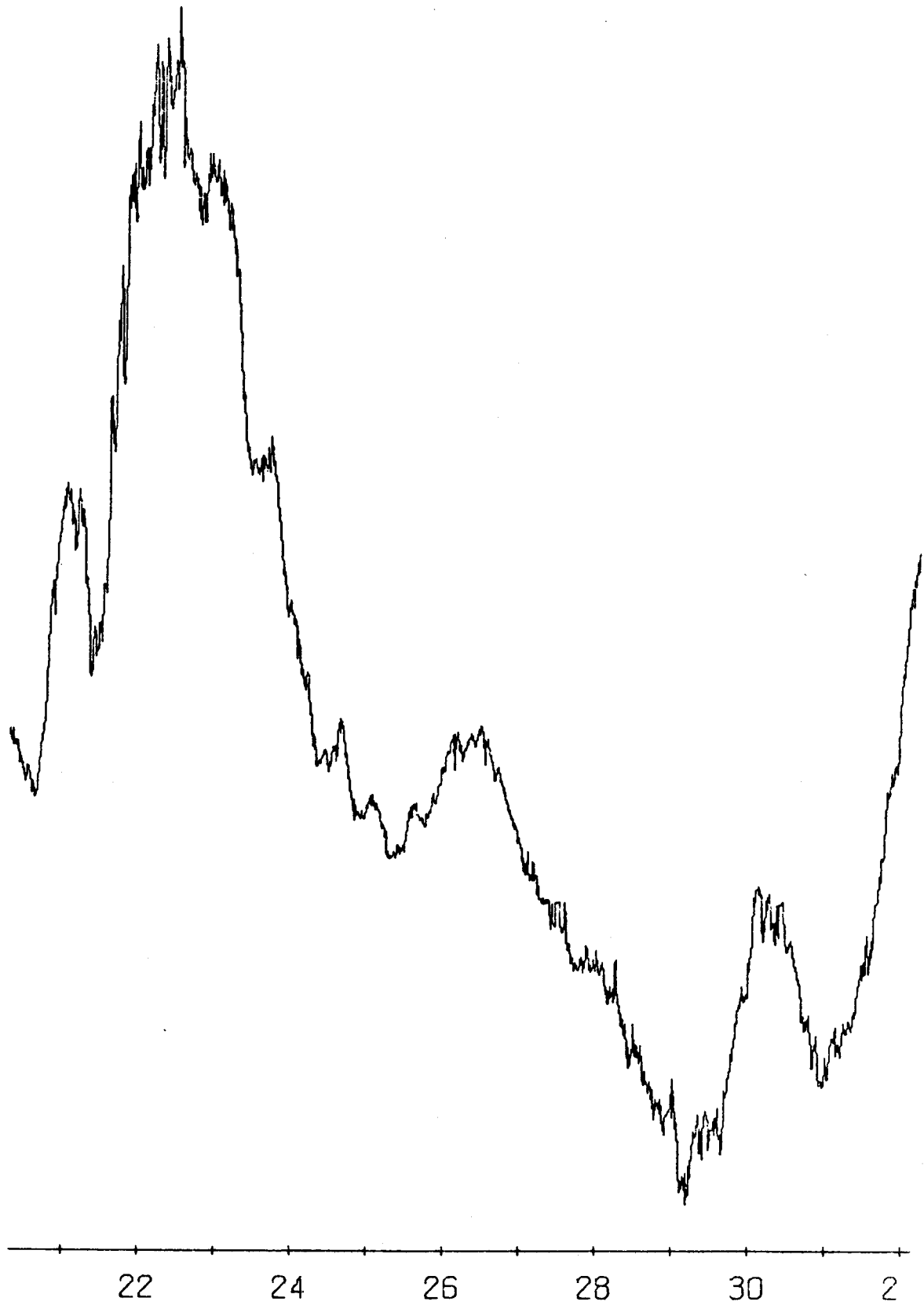
Figure 29
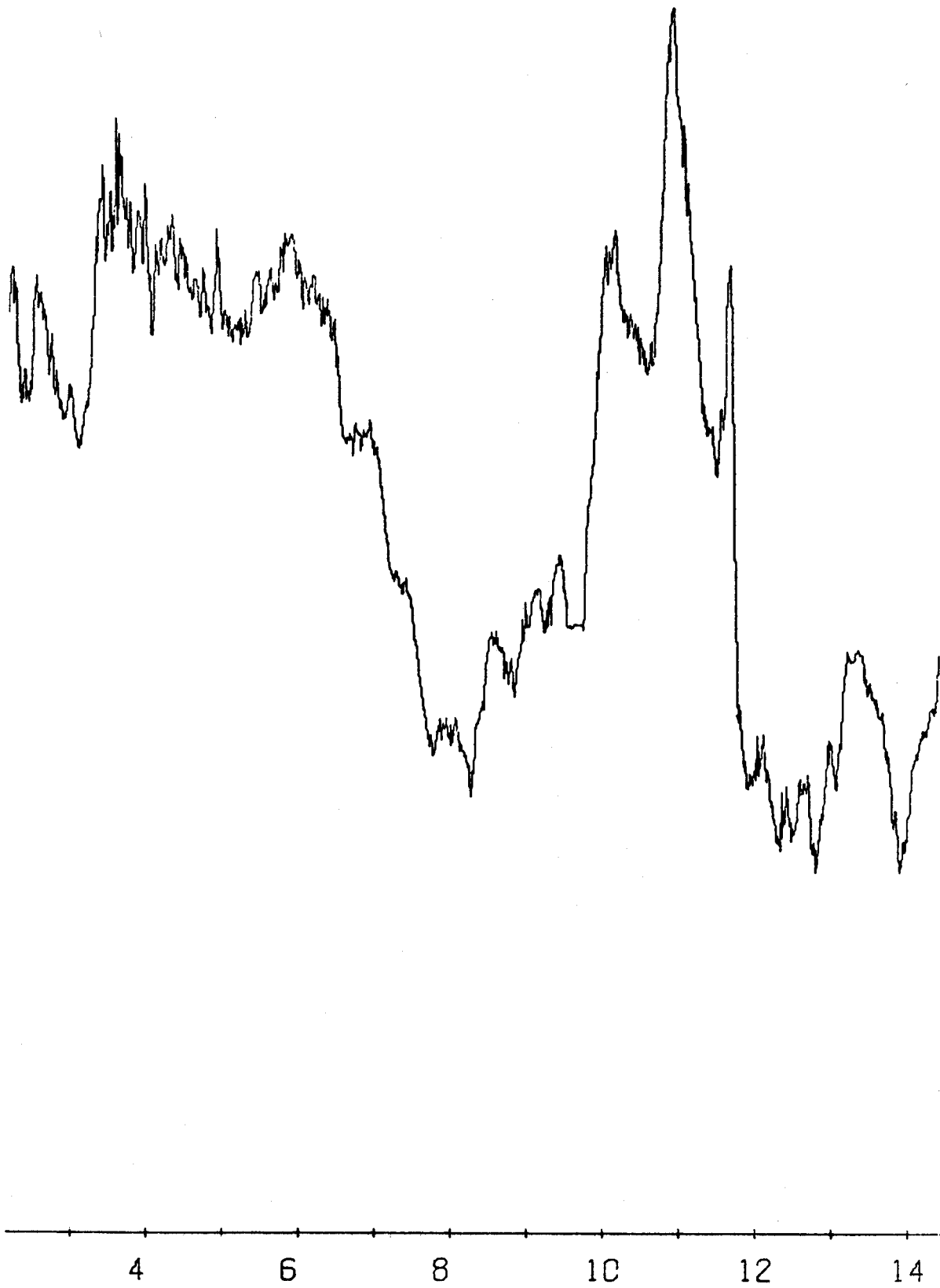
Figure 30
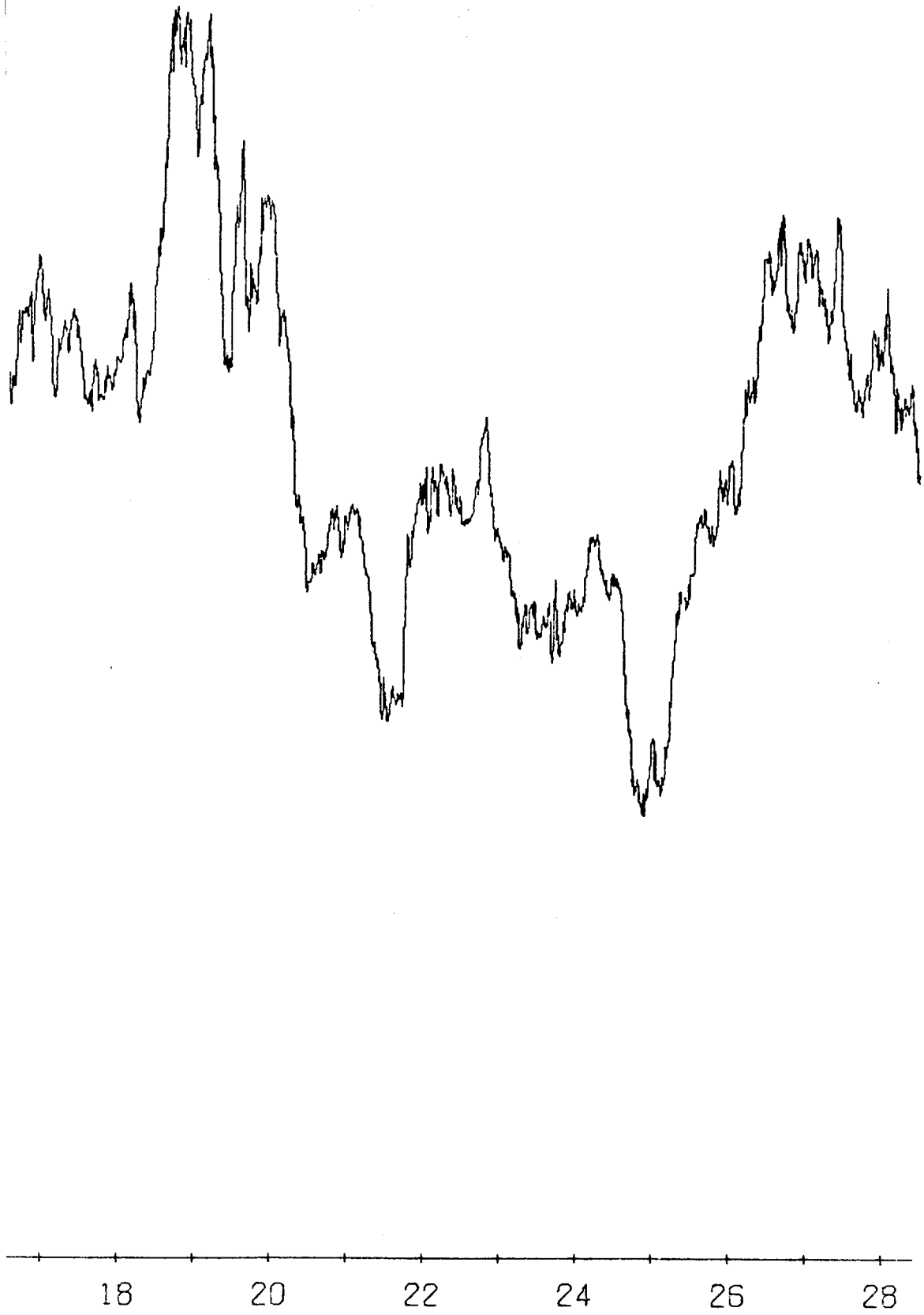
Figure 31
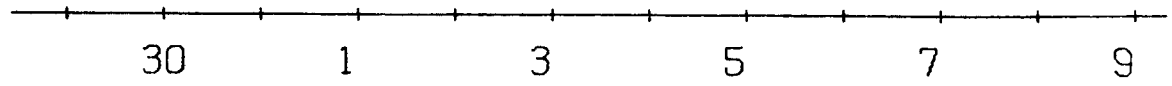
Figure 32
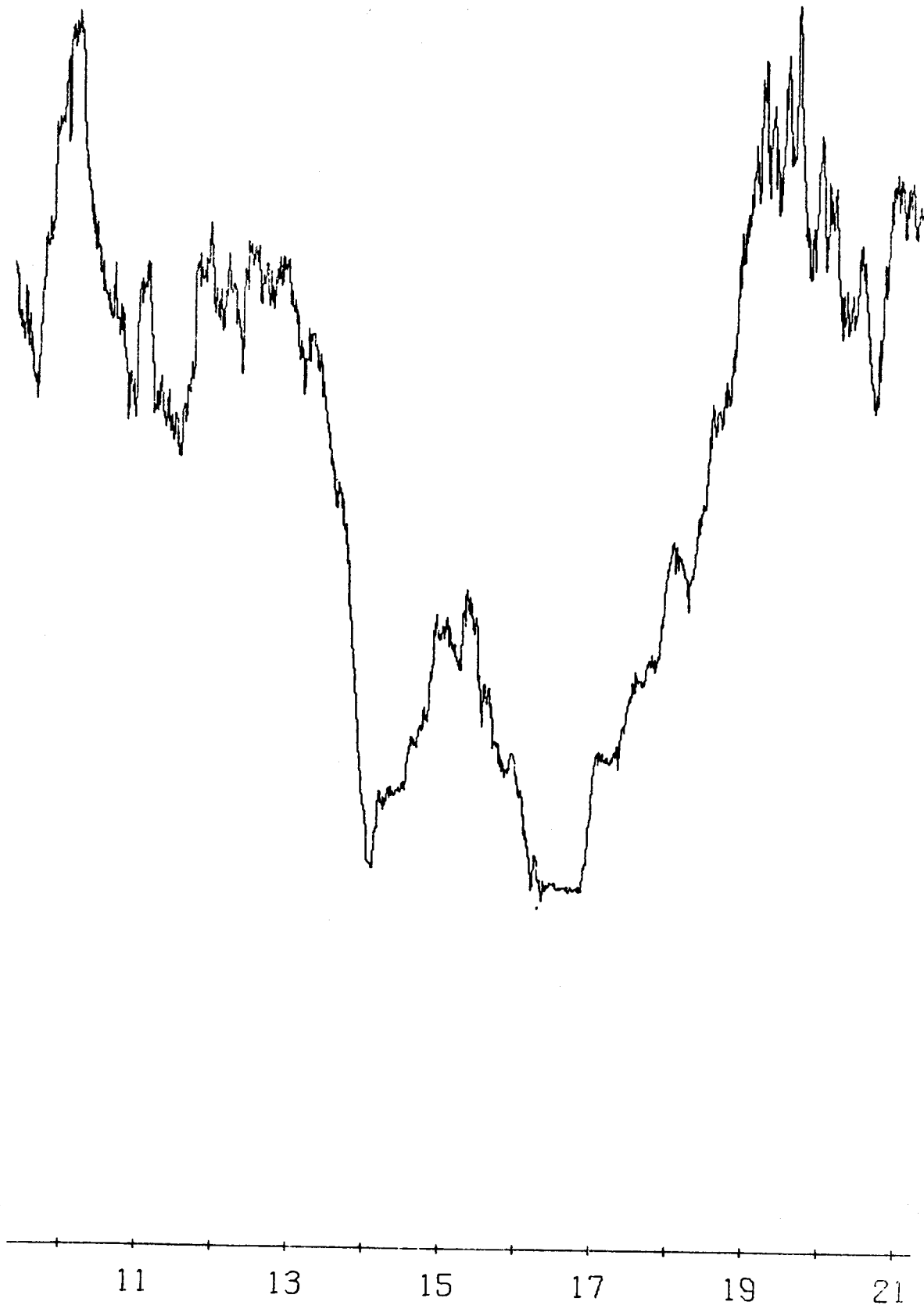
Figure 33

Figure 34

40
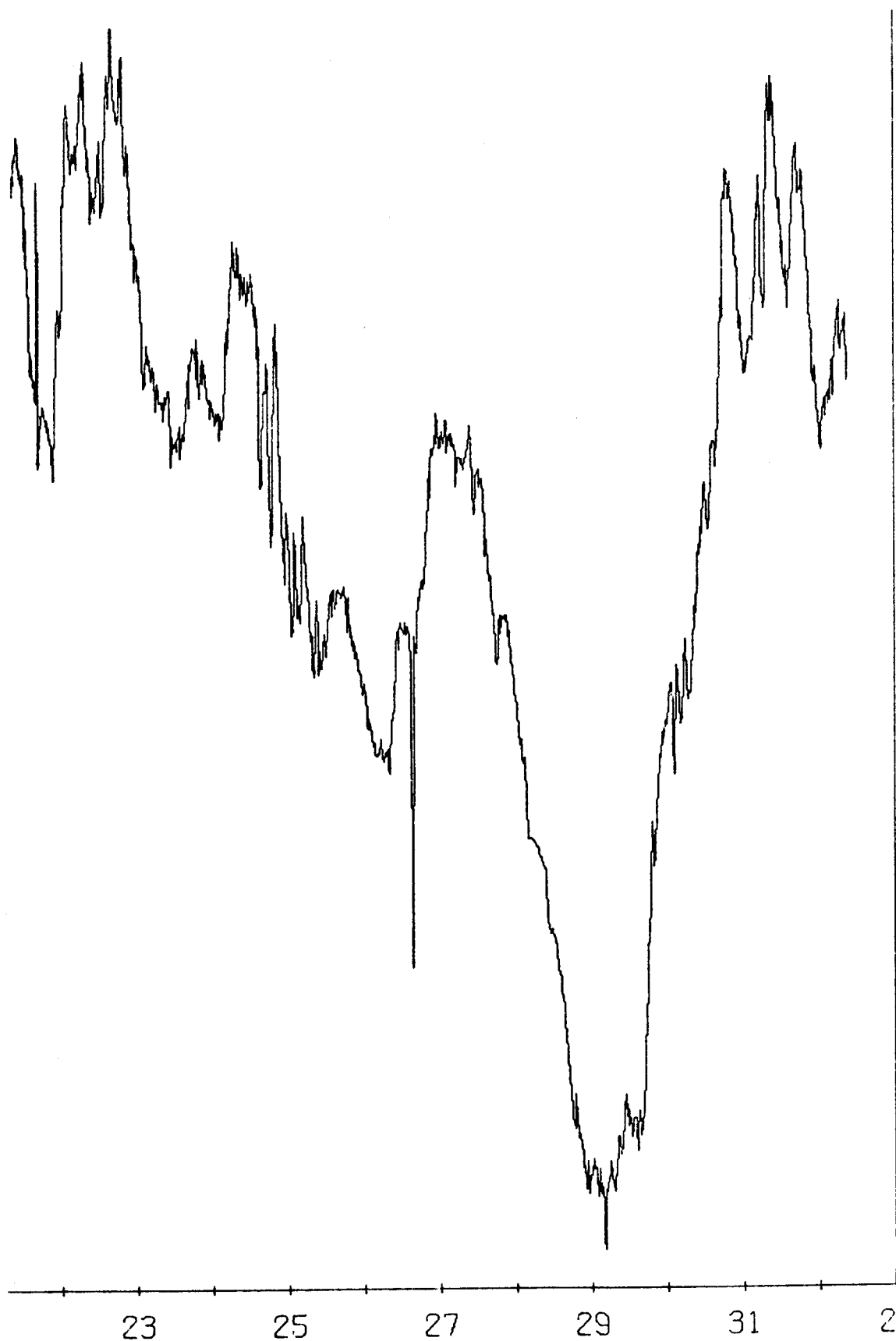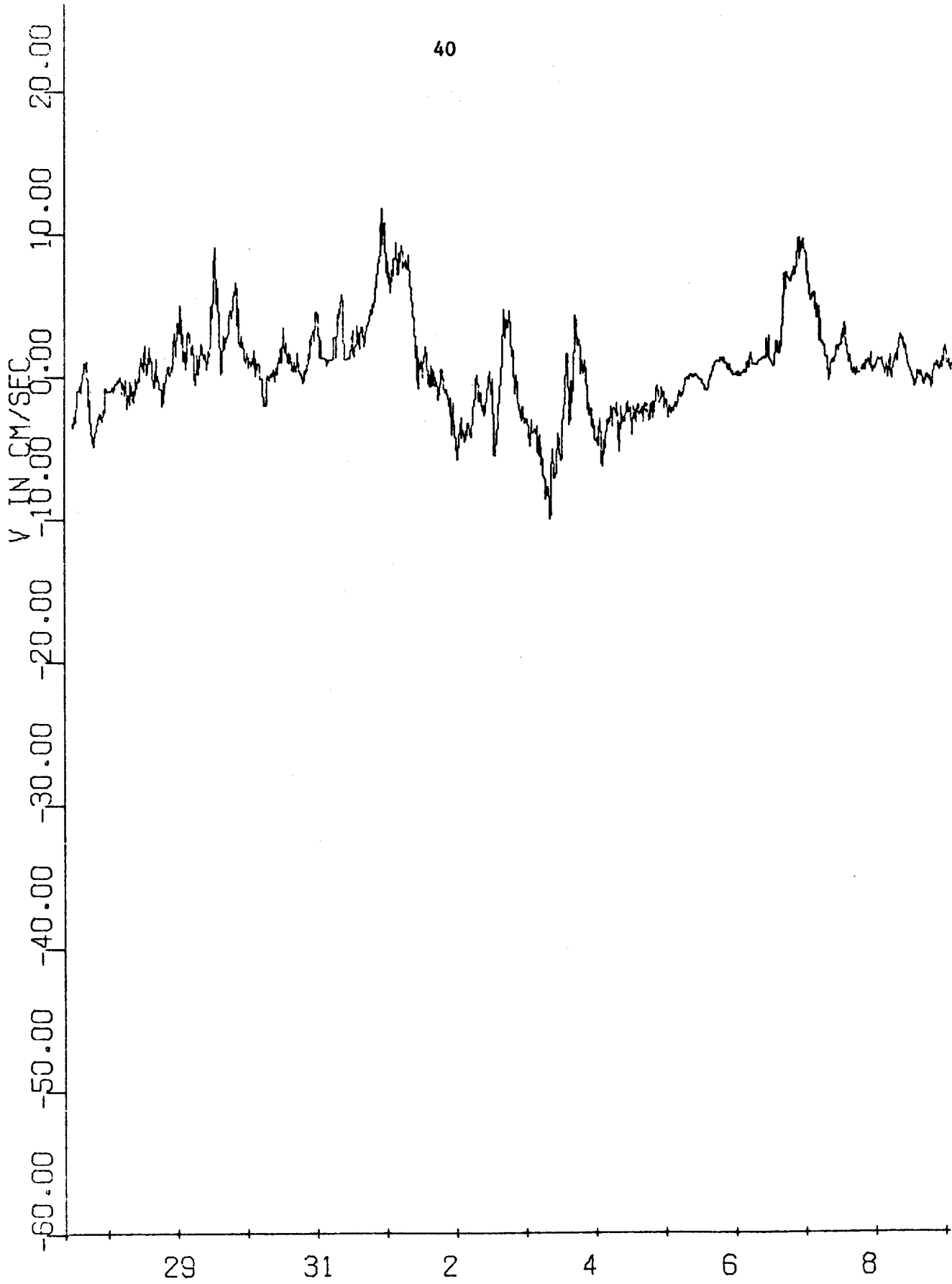
Figure 35

Figure 36

24   26   28   30   2   4
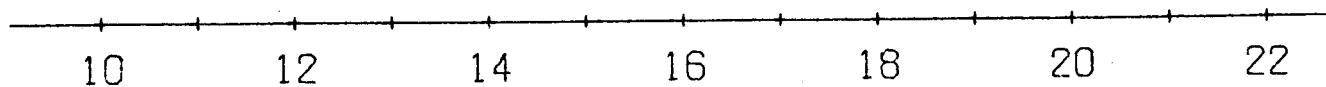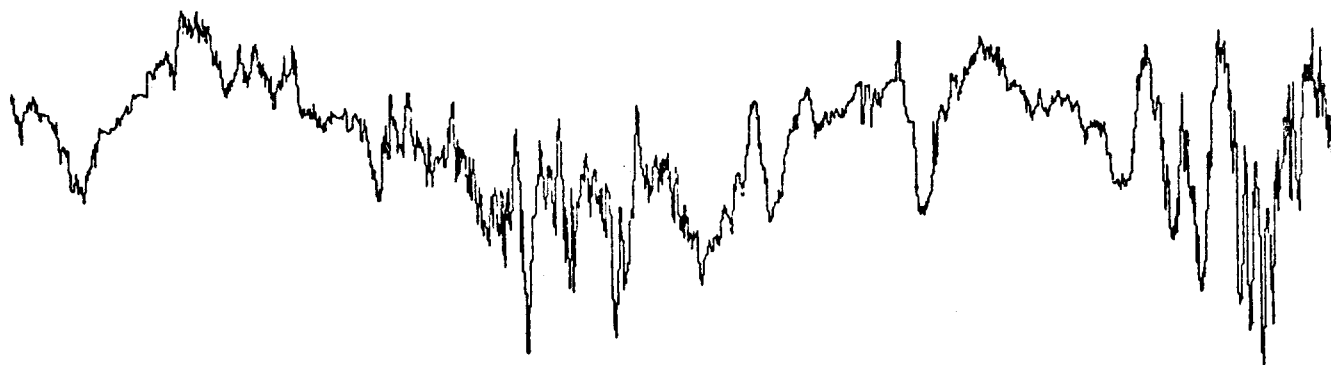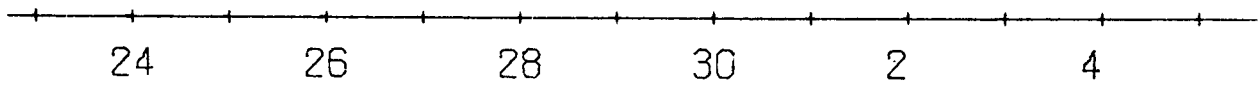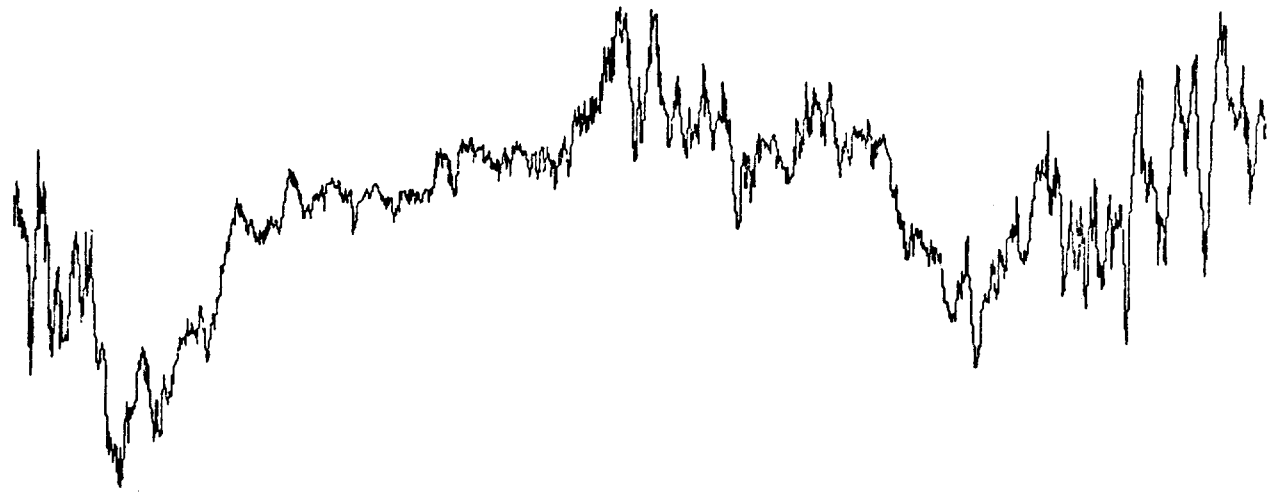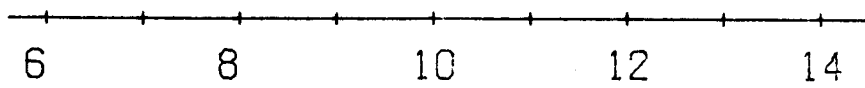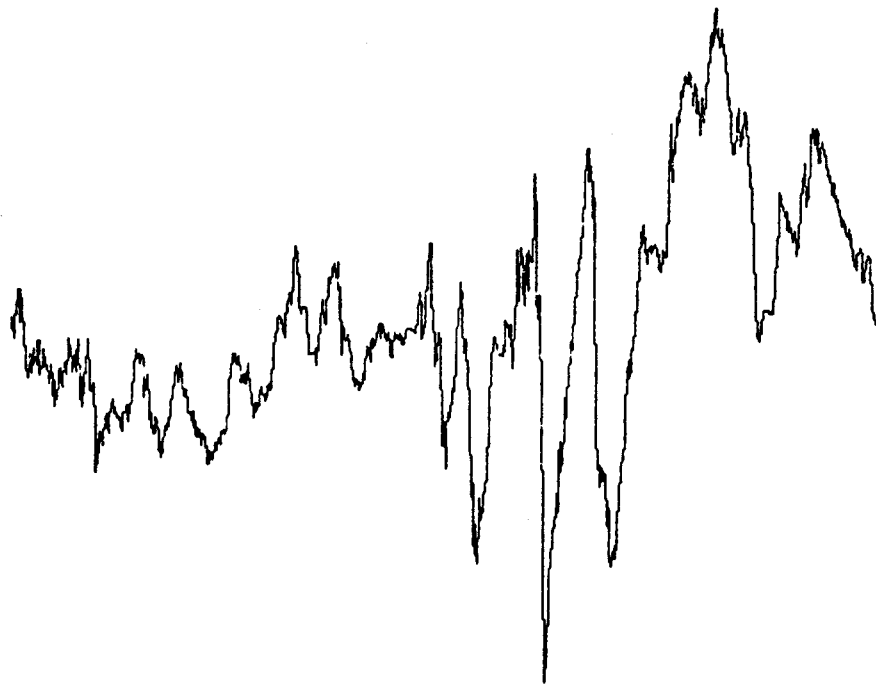
Figure 37

Figure 38
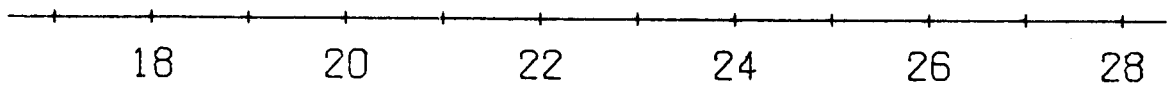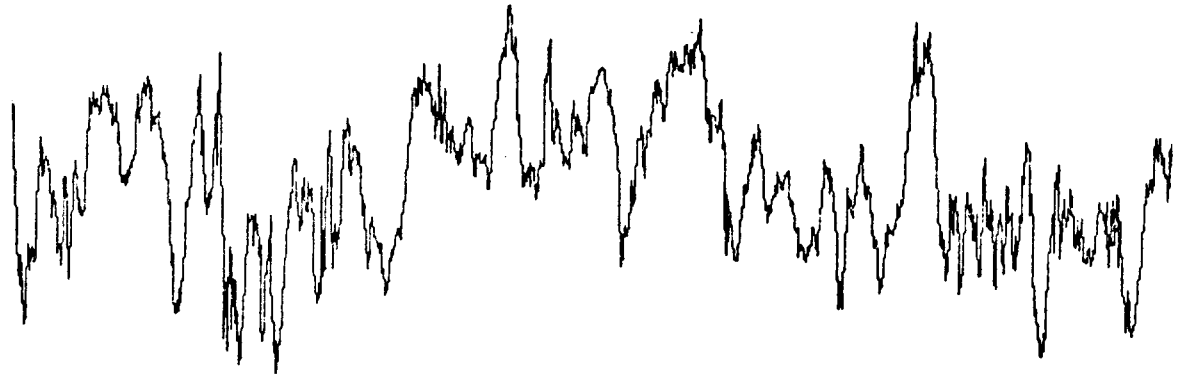
Figure 39
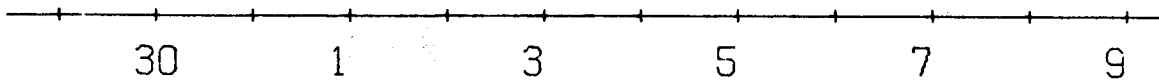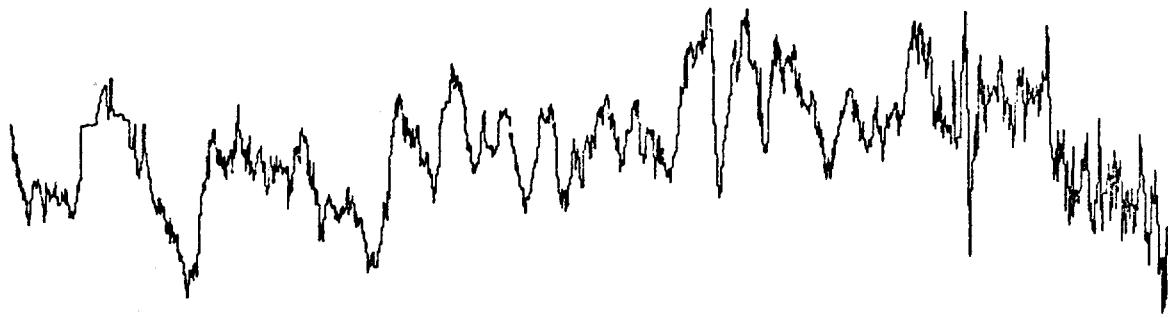
Figure 40

Figure 41

23   25   27   29   31   2
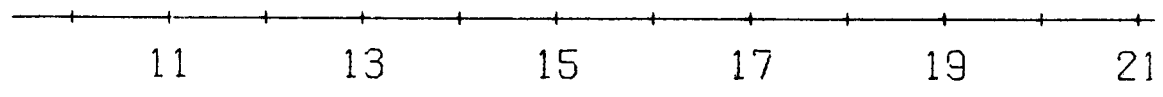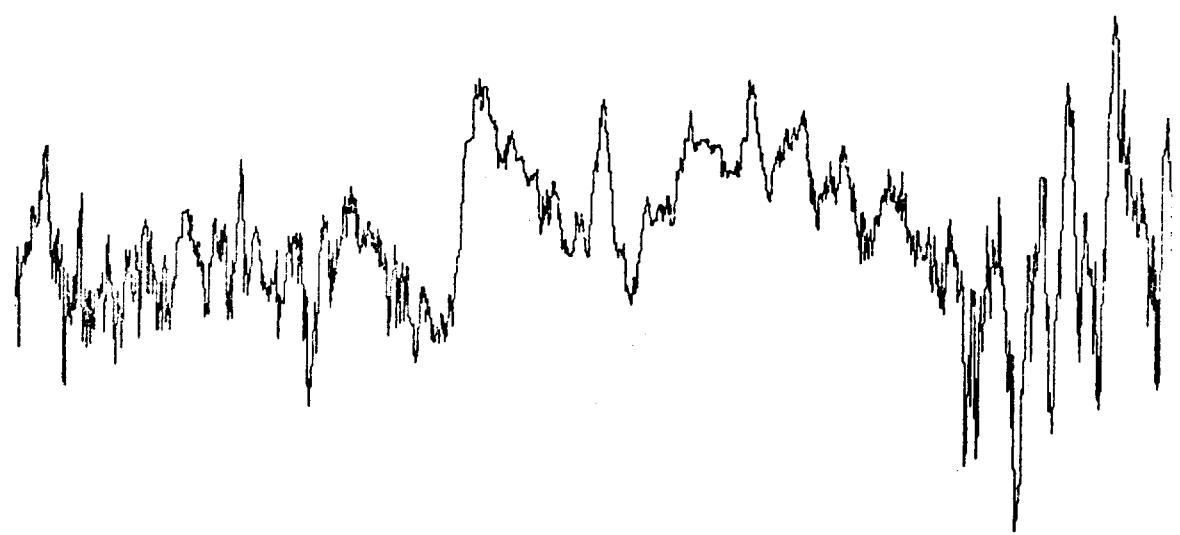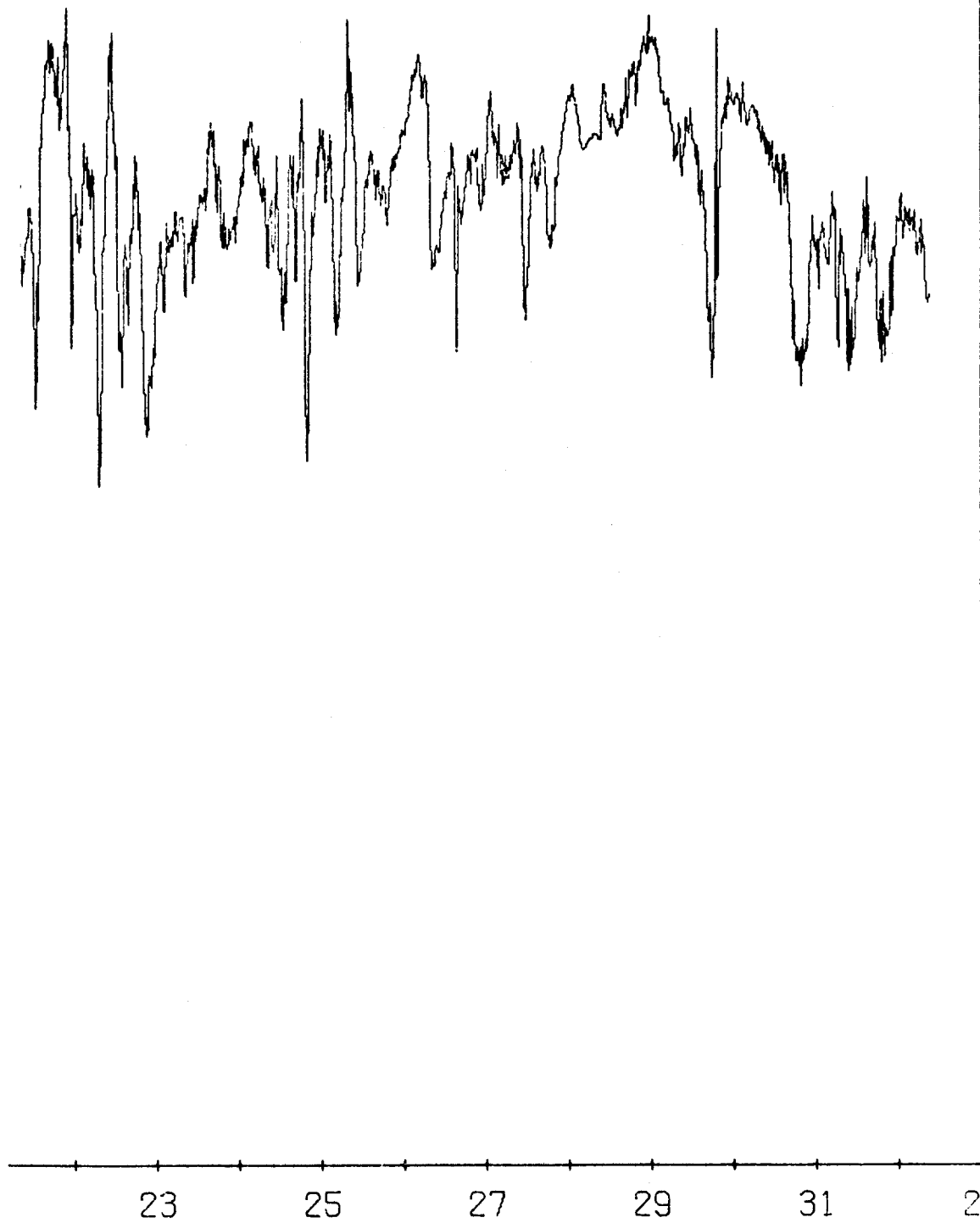
Figure 42

to have a southerly component of motion when moving east, and northerly when moving west. An example can be seen in the records between 19-27 June, when the easterly burst was accompanied by a smaller southerly component, and vice versa during the ensuing period 27 June-2 July. Since the trend of the isobaths is about 100°-280°T, the oscillations nearly represent alternating motion along the shelf edge.

The mean motion also appears to be steered by the bathymetry. During 27 May-14 July the mean set was 7.0 cm sec^{-1} toward 100°T and during 16 July-1 September 18.5 cm sec^{-1} toward 98°T, coincident with the estimated trend of the isobaths in the region.

Figures 27-42 also indicate rather clear tidal signals, again considerably larger than those inshore. The tidal amplitude is in the neighborhood of 5 cm sec^{-1}, and appears to have a diurnal inequality. For example, an inequality is indicated in the record of north velocity component during the period centered about 21 August. In this connection I note that the maximum lunar declination was on 20 August.

The spectra are shown in Figure 43-48. They are of course dominated by the low-frequency bands, the energy scaling of which obscures the higher spectral estimates. While the low-frequency bands are somewhat noisy, the coherence and phase spectra show that at the low-frequency coherence peaks, the east and south components tend to be approximately out of phase. This corresponds to the current alternating between either shelf-edge direction. Examination of the spectral estimates in the tidal band shows typical amplitudes of 2-4 cm sec^{-1} for the M_2, S_2, K_1 and O_1 constituents, although in any given series (*e.g.*, U-component, part 2) all may not be clearly identifiable. Except at the M_2 and S_2 frequencies in the first half of the record, the coherence between velocity components is very low at the four tidal frequencies indicated. For the M_2 and S_2 constituents in the first half of the record, the north component leads the east component by 90°, so that the tidal ellipse rotates anti-cyclonically.

On the outer shelf, then, we have observed a very active field of motion. The mean flow was aligned with the shelf edge and in the eastward direction. The mean speed over the 95-day record was nearly 13 cm sec^{-1}, representing an eastward displacement of more than 1000 km during the 95 days. There was a very large low-frequency oscillation, approximately along the shelf edge, representing long bursts of speed as high as 56 cm sec^{-1} toward the east. These bursts alternated with shorter periods of slower westward motion. The relationship between these low-frequency motions and the on-shelf flooding by dense water reported in the STD work (see this year's annual report, Research Unit No. 151) is not clear. The directly observed maximum speeds at 100 m were comparable to those calculated from the CTD work for the sub-surface core at about the same depth, but directed oppositely. Conceivably the calculated current represents the between-bursts westward flow observed north of Oliktok. However, the latter did not clearly involve an onshore component, as did the flow cal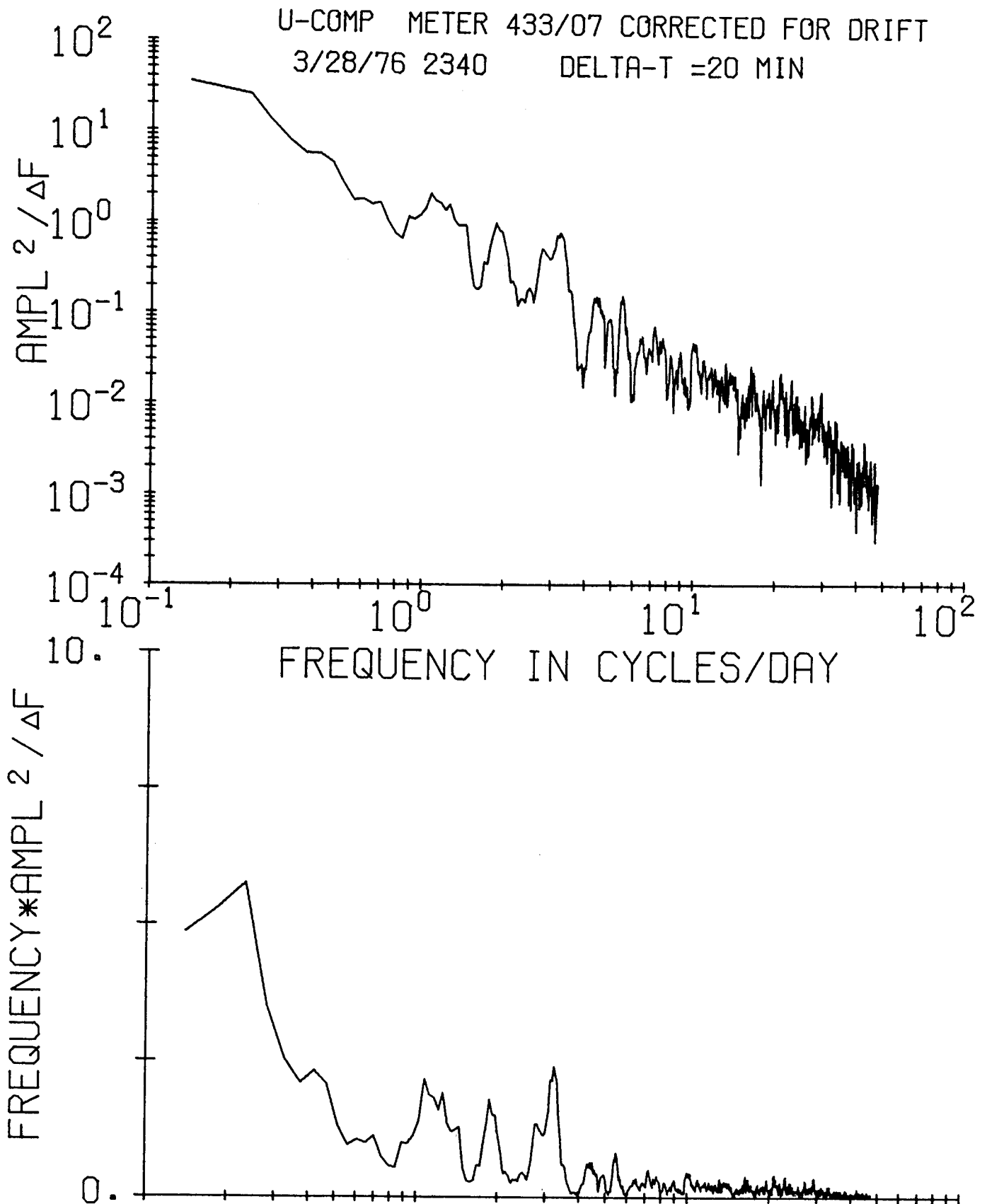culated from the CTD work north of Lonely. Nor did the temperature recorder on the current meter show any water warmer than about -1.4°C. For the present, the issue remains unresolved. Tidal currents were of order 5 cm sec^{-1}, and at least the semi-diurnal tide rotates clockwise.
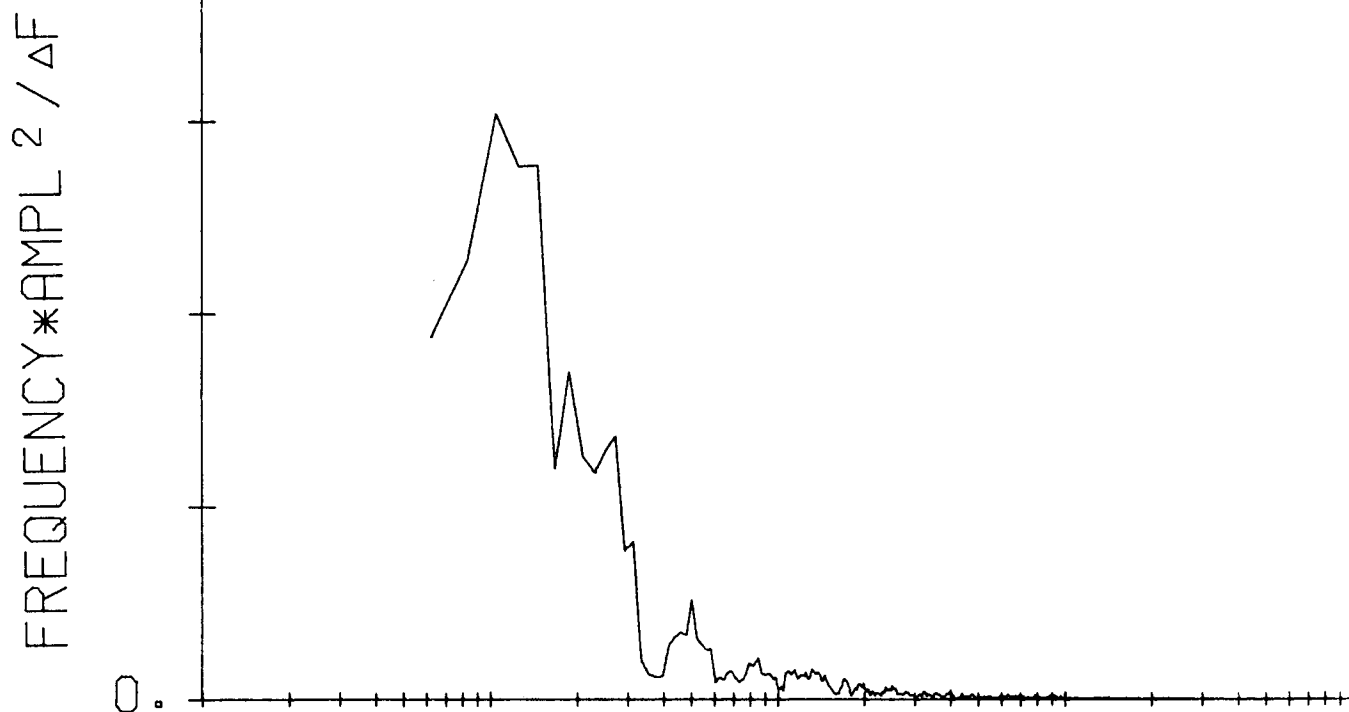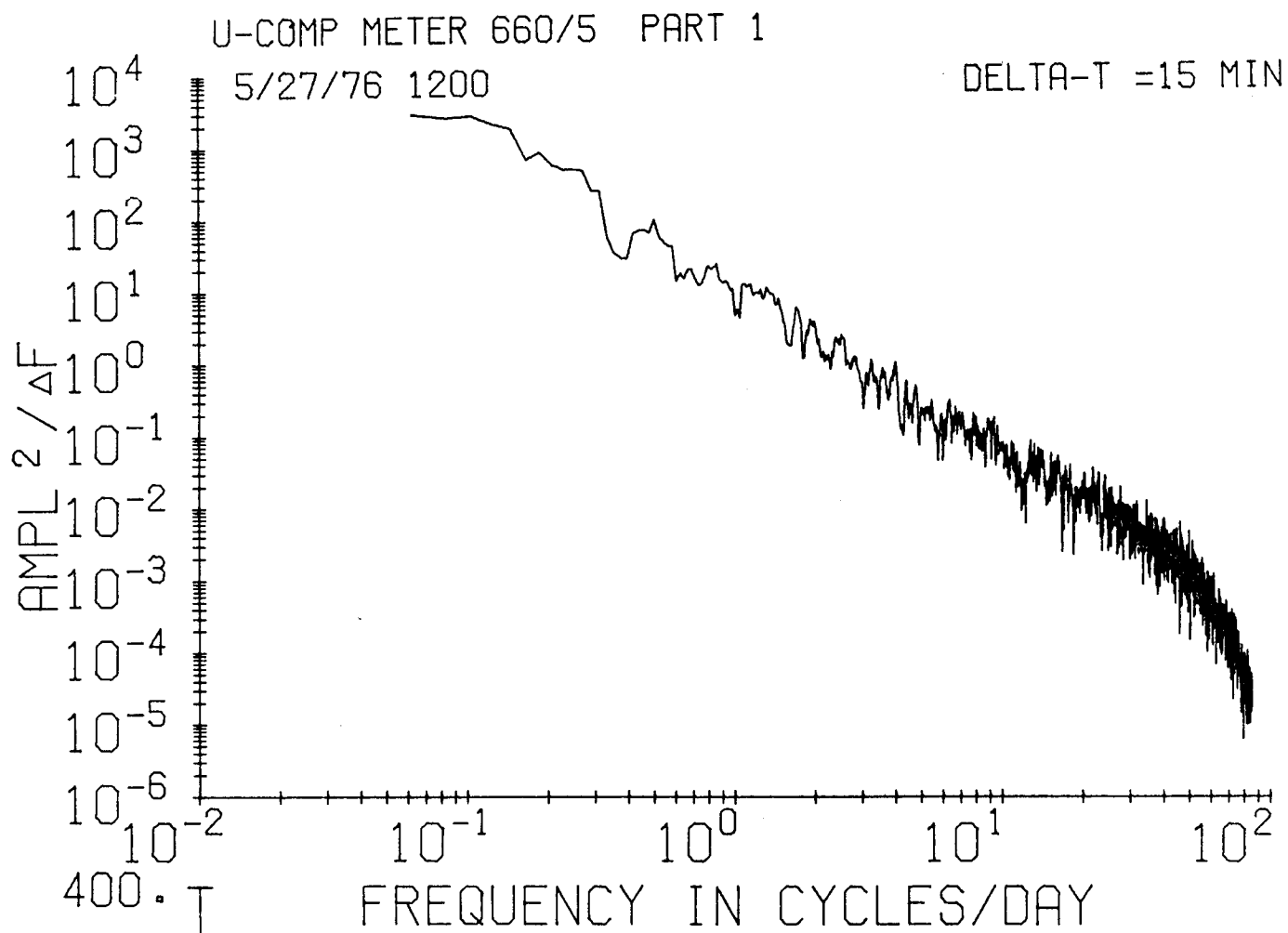
U-COMP METER 660/5   PART 1
5/27/76 1200   DELTA-T =15 MIN

FREQUENCY IN CYCLES/DAY
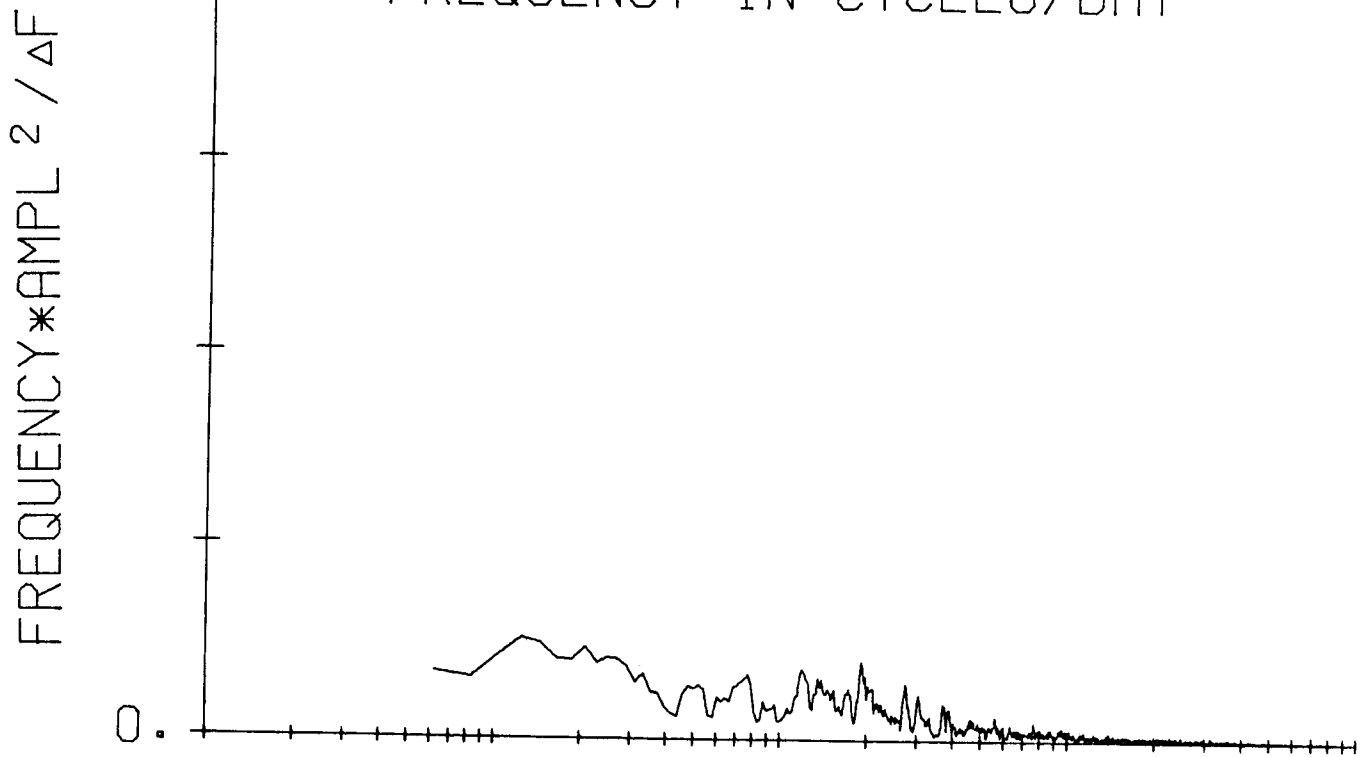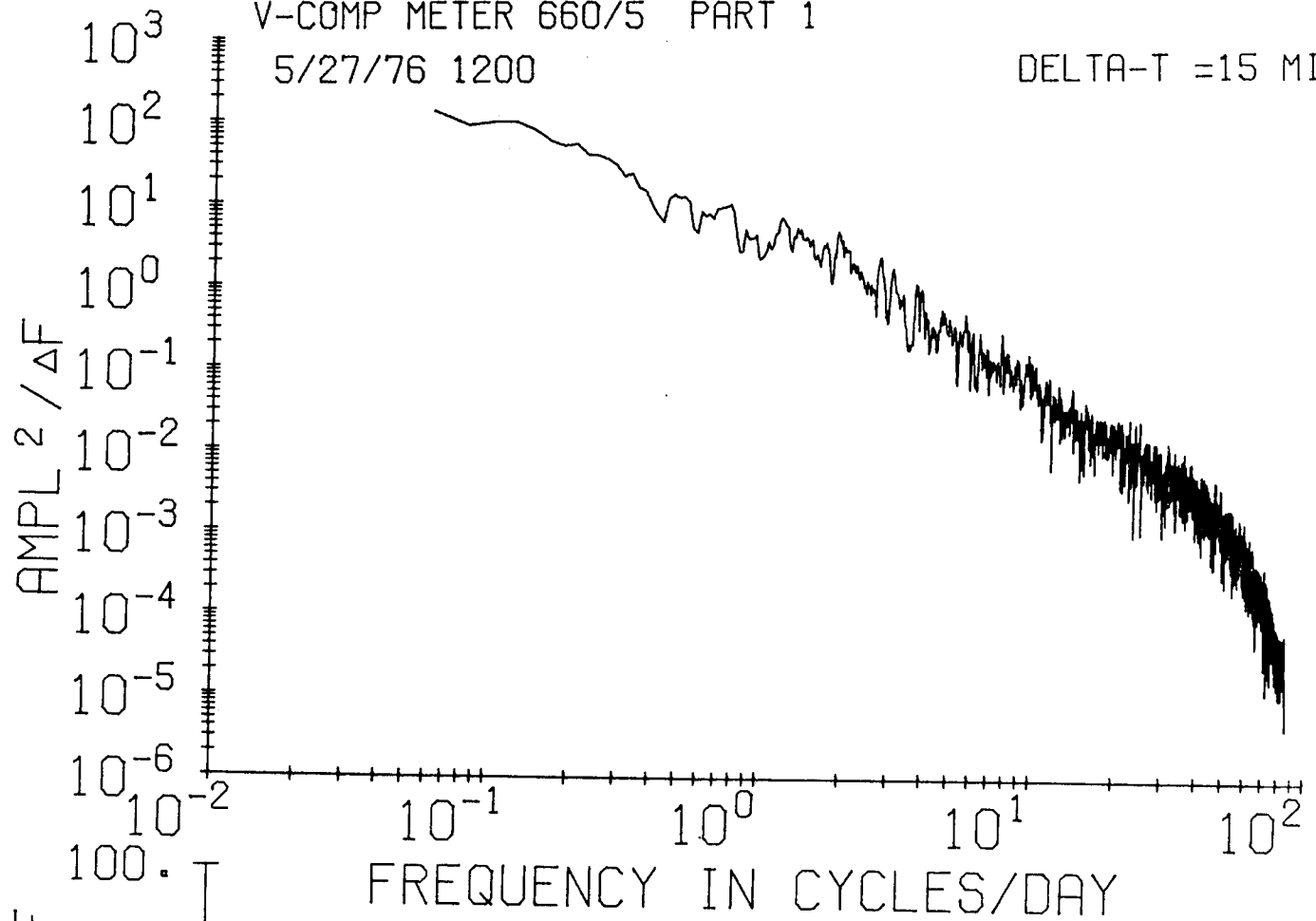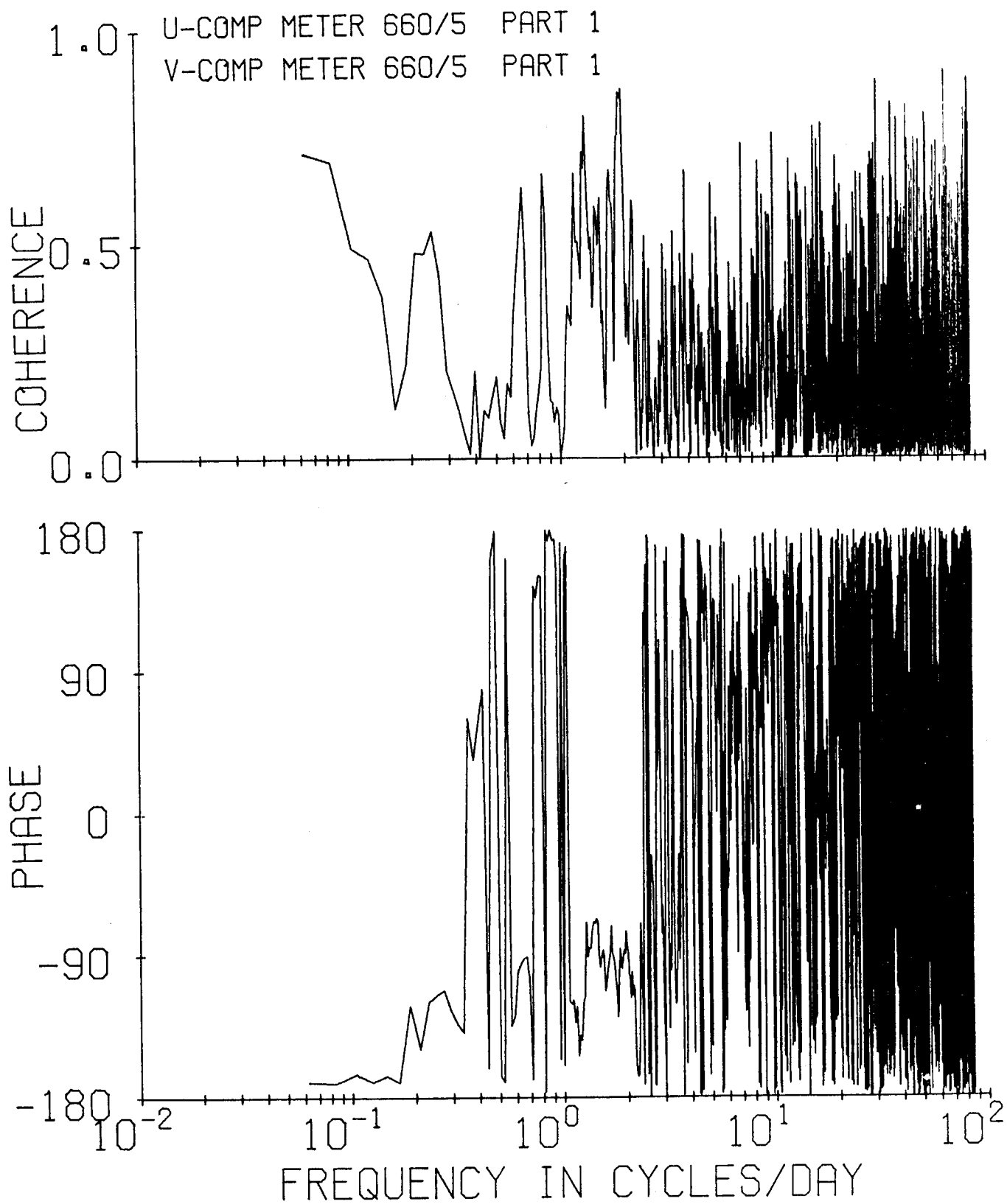
Figure 43

Figure 44

Figure 45

U-COMP METER 660/5 PART 2
7/16/76 1200
DELTA-T =15 MIN
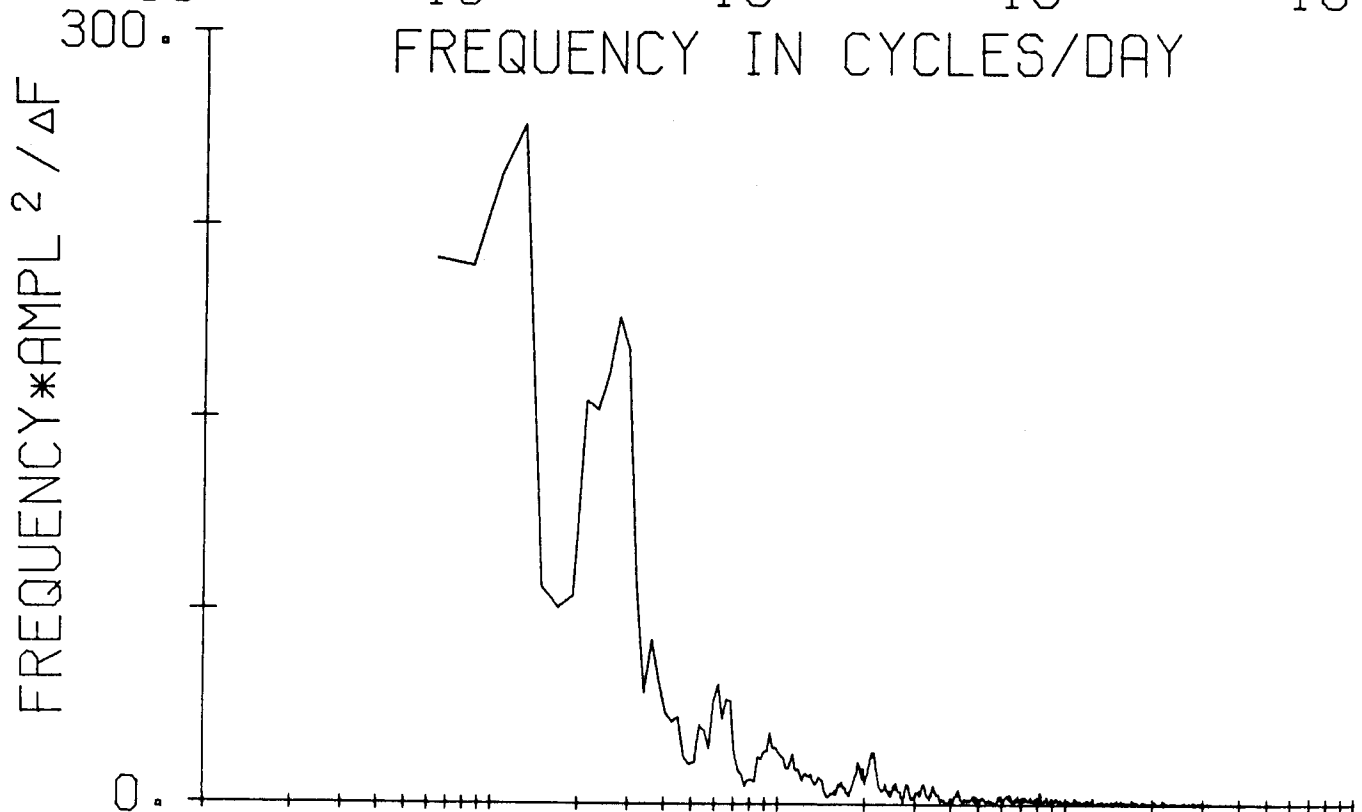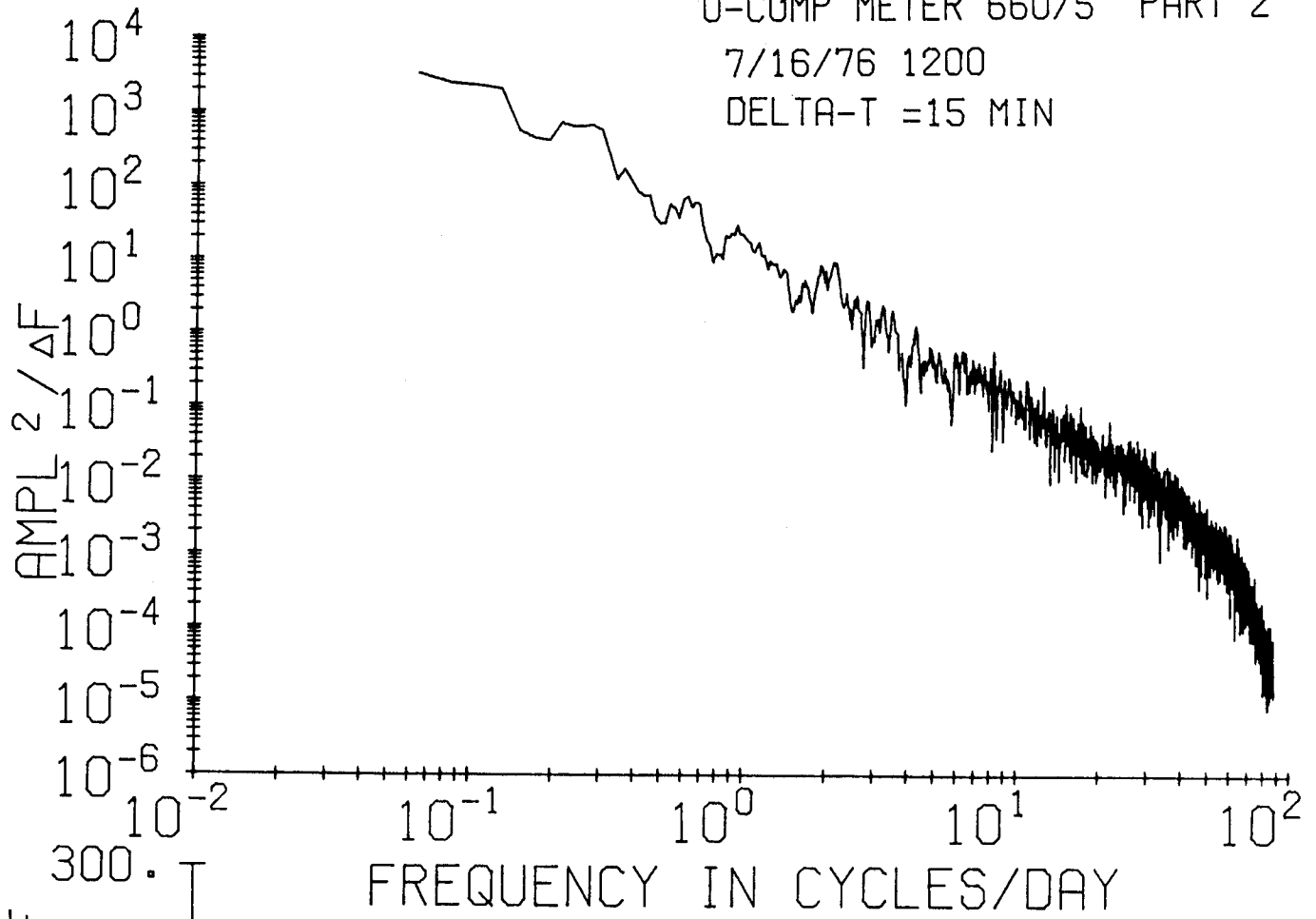
Figure 46

V-COMP METER 660/5 PART 2
7/16/76 1200
DELTA-T =15 MIN
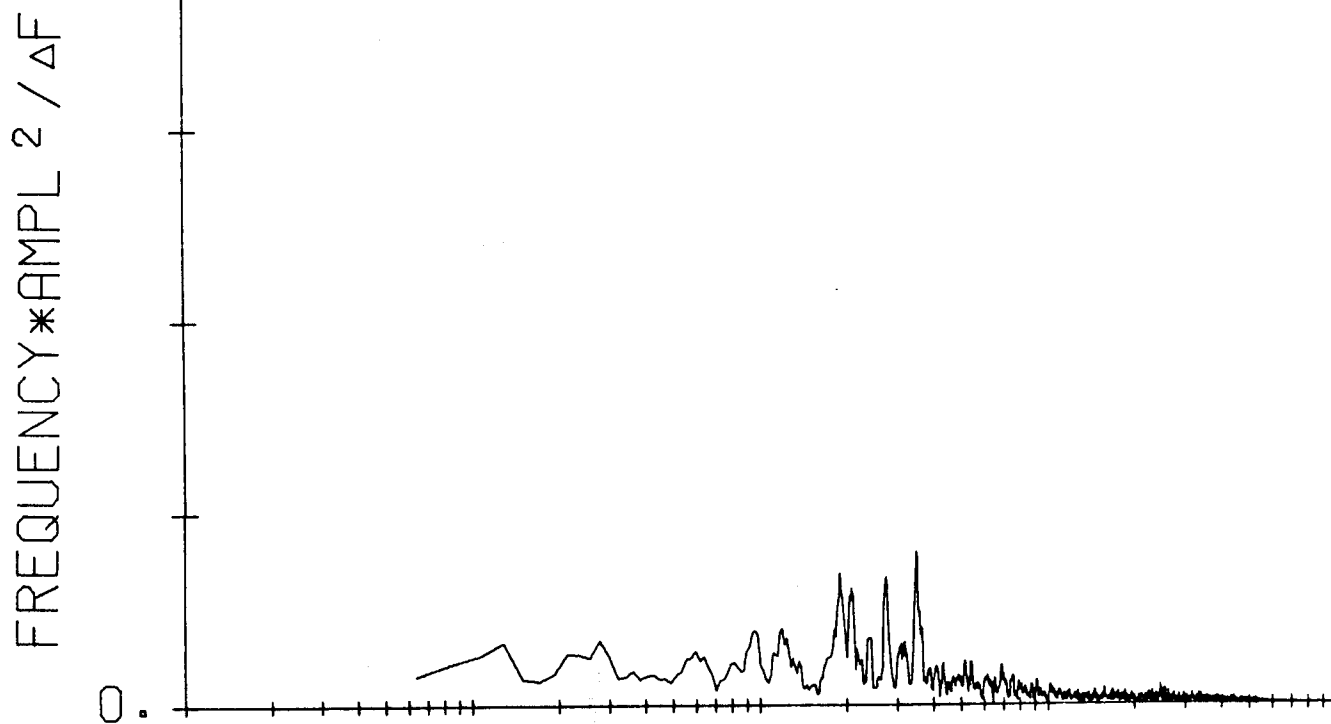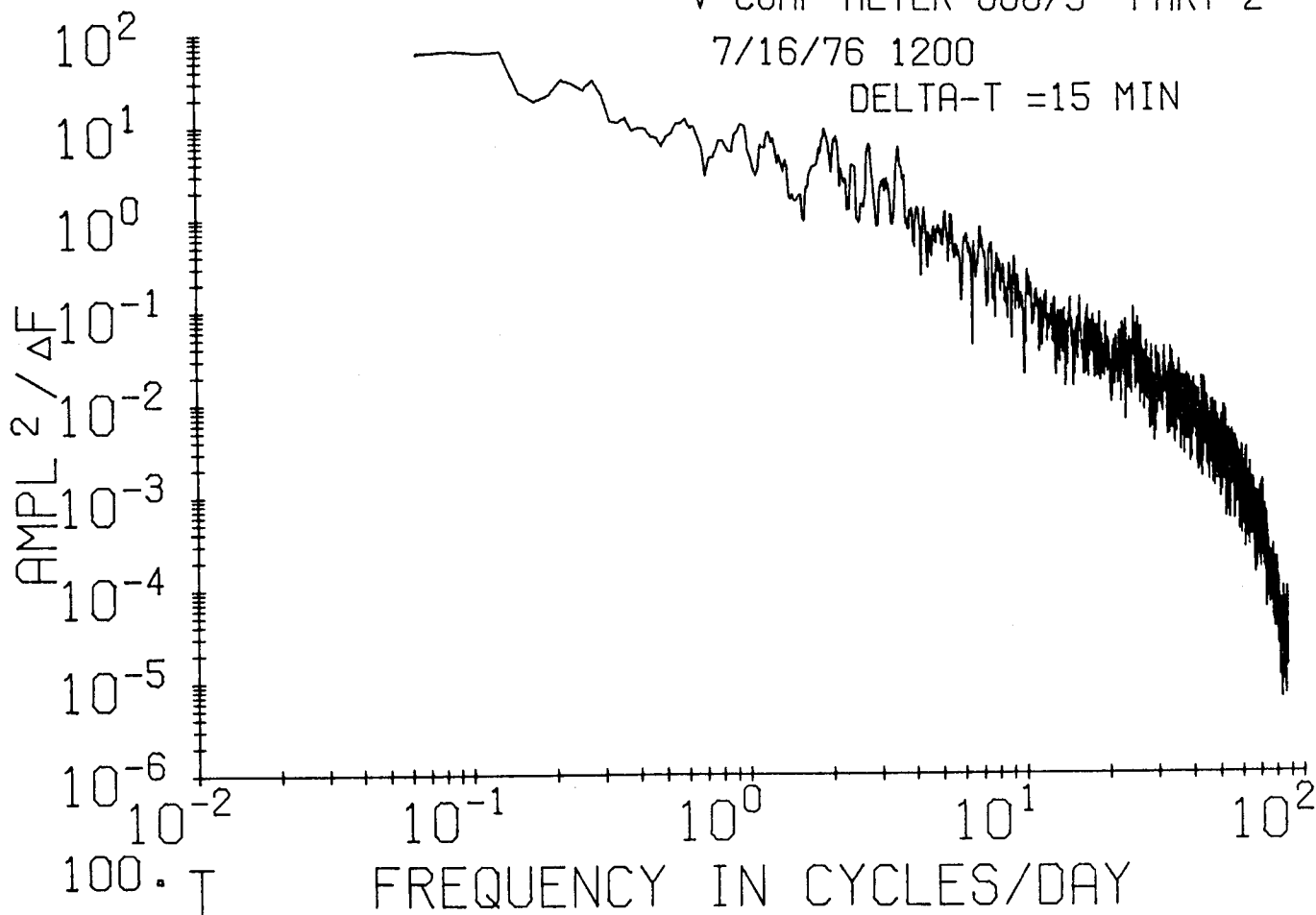
Figure 47
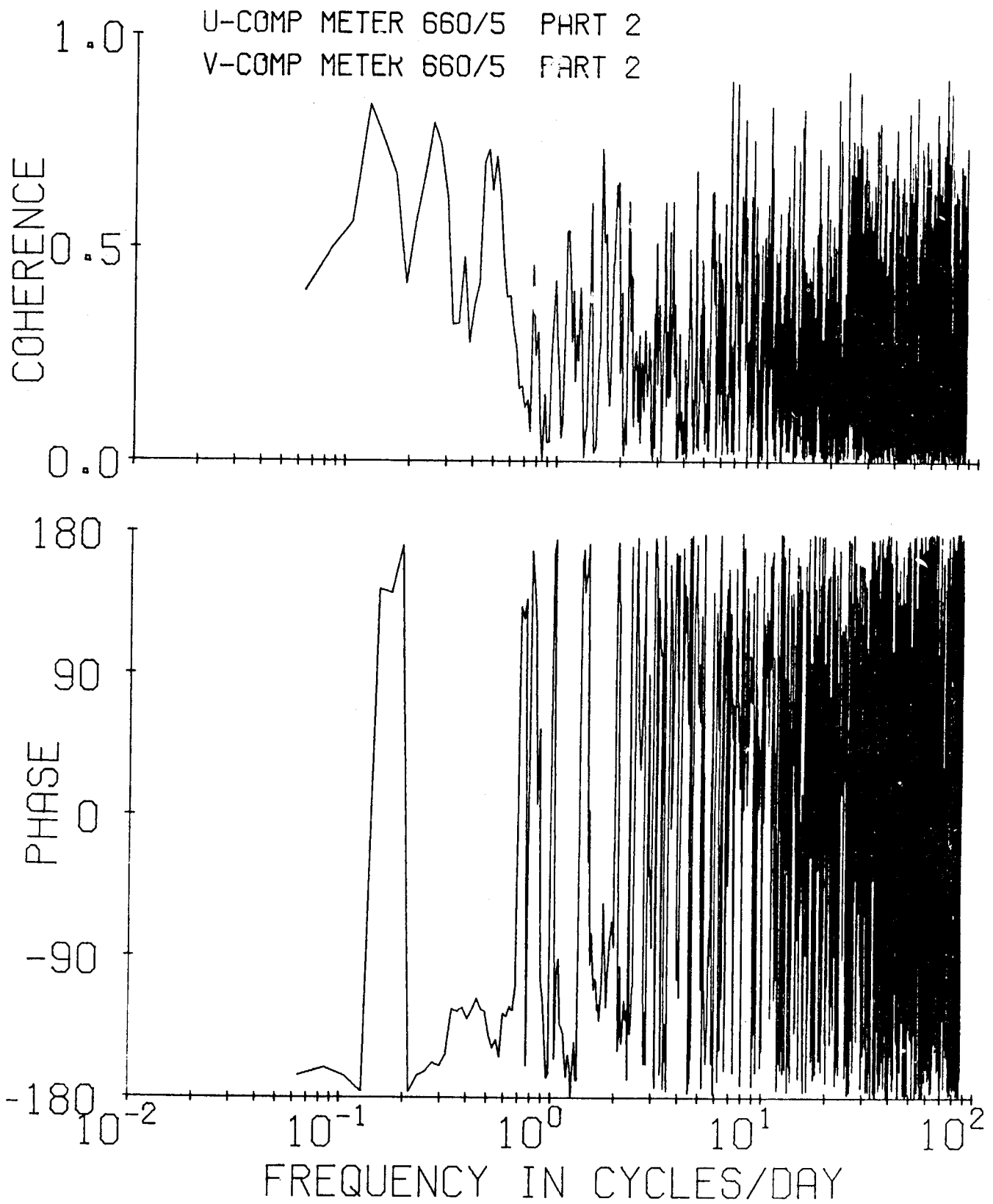
Figure 48

VIII. Conclusions

At least in late winter the currents on the inner shelf appear to be slow, generally less than 5 cm sec^{-1}. Long-term mean currents are extremely small, representing net displacements over a week of only 1-2 km. The two measurements made north of Narwhal Island showed these small displacements to have been west-southwest. Tidal currents are probably not much above 1 cm sec^{-1} in winter.

On the outer shelf an entirely different situation prevails. Measurements made at 100 m under the ice from May-September showed the flow to reach over 55 cm sec^{-1}, and even over a 3-month period the mean flow was 13 cm sec^{-1} toward the east. Pollutants reaching the outer shelf at sub-surface depths could thus be transported 1000 km eastward in three months. The most remarkable feature observed was the dominance of the motion by low-frequency variations with a typical time scale of 10 days. These oscillations represent bursts of speed as high as 50 cm sec^{-1} or more; they are directed eastward and are aligned approximately with the shelf edge. Between the bursts there were shorter periods of westward motion, the maximum observed speed toward the west being 26 cm sec^{-1}. The cause of these motions is for the present unknown. Tidal currents are in the neighborhood of 5 cm sec^{-1}, and a diurnal inequality probably prevails at times of high lunar declination.

IX. Needs for further study

The outer shelf is an extremely active area, and it would appear worthwhile to attempt a further year of time series between the 100- and 200-m isobaths. This could best be done by deploying two more moorings north of Lonely when the present moorings are picked up in October. The new ones would remain out til late May following.

X. Summary of 4th quarter operations

A. Field operations

Field work is presently in progress.

B. Estimate of funds expended by Department of Oceanography, University of Washington to 28 February 1977.

Total allocation (5/16/75-9/30/77)		$188,542
A. Salaries, faculty and staff	$17,611	
B. Benefits	2,087	
C. Expendable supplies & equipment	21,202	
APL direction homing unit $957		
Floatation $2,700		
D. Permanent equipment	47,680	
Acoustic releases $12,739		
E. Travel	4,352	
F. Computer	439	
G. Other Direct Costs	6,349	
Freight $4,734	4,734	

H. Indirect costs   7,714

    Total expenditures   112,168

    Remaining balance   76,374

    C.   Estimate of funds expended by Applied Physics Laboratory, University of Washington to

    Total allocation (5/16/75-9/30/77) $150,418

    (Breakdown information not available at time of report preparation.)

FINAL REPORT

EFFECTS OF SEASONABILITY AND VARIABILITY

OF STREAMFLOW ON NEARSHORE COASTAL AREAS

Robert F. Carlson, Director
Institute of Water Resources
University of Alaska
Fairbanks, Alaska 99701
SS #395-40-5203

This report was prepared by:

Richard Seifert, Research Hydrologist
Douglas Kane, Assistant Professor
Water Resources and Civil Engineering
Institute of Water Resources
University of Alaska
Fairbanks, Alaska 99701

31 March 1977

TABLE OF CONTENTS

LIST OF TABLES

LIST OF FIGURES

I. SUMMARY OF OBJECTIVES WITH RESPECT TO OCS OIL AND GAS DEVELOPMENT

An understanding of the seasonability and variability of streamflow is of considerable engineering importance to the imminent oil and gas development in nearshore coastal areas. Streamflow variability, effects of seasonal ice, sediment characteristics, and ice-jam flooding all have considerable impact on nearshore and estuarine areas. This is especially so in areas where sea-ice remains intact after the initiation of river break-up. This phenomenon occurs in nearly all rivers and streams in the North Bering, Chukchi, and Beaufort Seas, and is attributable to the extensive shorefast ice formed annually in these areas. The estuarine and shorefast areas are presently being developed and leased and this development is likely to continue throughout the Outer Continental Shelf (OCS) program. An analysis of the annual seasonability of streamflow, expected break-up data, expected freeze-up data, and sediment character-istics are all necessary information to ensure safe and efficient off-shore development.

However, the higher precipitation and comparatively reduced effects of offshore ice on the coast of the Gulf of Alaska, together with the sparseness of available data, have made it necessary to establish indices of seasonability and variability to allow for extrapolation to ungaged streams in order to estimate streamflow variation and spring flooding.

II. INTRODUCTION

A. General nature and scope of the study:

This study examines the variability of streamflow in all gaged Alaskan rivers and streams which terminate in the ocean. Forty-one such streams have been gaged for varying periods of time by the U. S. Geological Survey, Water Resources Division. Attempts have been made to characterize streamflow statistically using standard hydrological methods. The analysis scheme which was employed is shown in the flow chart which follows. In addition to the statistical characterization, the following will be described for each stream when possible:

1. average period of break-up initiation (10-day period)

2. average period of freeze-up (10-day period)

3. miscellaneous break-up and freeze-up data.

4. relative hypsometric curve for each basin

5. observations on past ice-jam flooding

6. verbal description of annual flow variation

7. original indices developed in this study to relate stream-flow variability to basin characteristics and regional climate.

B. Specific Objectives:

1. The primary objective of this study is the development of a characterization of coastal streams in Alaska which is relevent for engineering applications, useful to the imminent OCS petroleum development, and which may also be generally useful to as many other agencies, individuals, and commercial interests as may have need for such information.

2. Realizing that characterization of streams in other regions of the United States may not be adequate to describe Alaskan streams, an original approach was developed in order to derive an index for stream characterization in this study. After trying several indices, it was decided that graphic plot of the ratio of the 1-, 3-, 7-, 10-, and 30-day maximum cumulative daily flows to the mean annual flow was an adequate characterization index. This index is a good expression of short-term variability.

3. A grouping of most ungaged streams is accomplished using regional and physical similarities to gaged streams as criteria. This grouping is intended to be a guide for extrapolation of the characterization of gaged streams to streams which have similar basin areas, climate, and elevation distributions, but which are not gaged by the U. S. Geological Survey.

4. An attempt is made to establish a relationship between precipitation and elevation in order to better characterize snowmelt patterns.

5. NOAA and LANDSAT satellite imagery are used as major sources of information to characterize snowmelt in both gaged and ungaged basins.

C. Relevance to problems of petroleum development:

1. Spring break-up presents critical engineering problems which need to be considered for nearshore oil development and exploration. Logistics and scheduling may be severely

disrupted by unforeseen or unknown problems related to rivers, spring run-off, and ice. A problem unique to the Arctic is that of flooding of the shorefast ice at the mouths of rivers during spring break-up. Satellite observations of several ungaged streams in the Arctic indicate that this event is endemic, but the timing of the initial flooding is variable. Ice jams are a problem, especially on the Yukon River. A major danger from ice jams in the possibility of a rapid break of the jam which could release dammed water and cause flooding downstream. Floating ice is also an engineering hazard. Ice jams will be discussed further in the results sections.

Snow cover and snowmelt characteristics which will be investigated in this study should lead to a better understanding of snowmelt rate. The relationships which exist between melt rate and runoff may also become more evident. A knowledge of these influences on nearshore development will be important to petroleum development as well as the planning and public works agencies of government.

III. CURRENT STATE OF KNOWLEDGE

As stated in our original proposal, we know of no directly related research being carried out by others. A bibliographic search was made using the OASIS system. A report entitled "Environmental Studies of an Arctic Estuarine System" (EPA, 1975) contains baseline information on the effects of river flow in an Arctic estuary, which is relevant to this work. Many papers address the problem of coastal breakup in

Arctic areas (Newburg, 1974; Antonov, *et al.*, 1972; Reimnitz, *et al.*, 1974; Barnes, *et al.*, 1973; Walker, 1973; McCloy, 1970; Reimnitz, *et al.*, 1972; and Walker, 1970). Carlson (1972) repsents discussion of the land hydrology of the southcenteral Alaska coastal zone. A regional discussion of sediment yield in Alaskan streams is given by Guymon (1974).

Some correlative studies of snow measurements made on the ground with remote sensing observations have been done by Bilello (1974). Poulin (1974) used infrared staellite imagery to determine the hydrologic characteristics of snow-covered terrain.

Carlson (1974) and Newburg (1974) both address the effects of permafrost on river hydrology. Permafrost or glacial influences affect nearly all major hydrologic systems in Alaska.

The general state of knowledge for characterizing streams in lieu of coastal development is inadequate. More hydrologic research has been done in the Beaufort Sea drainage than elsewhere in Alaska and no area of Alaska has been or is being as well studied.

IV. STUDY AREAS

This report includes characterization of all gaged streams in all the OCS areas of interest:

1. Gulf of Alaska

2. Southern Bering Sea

3. Northern Bering - Chukchi Seas

4. Beaufort Sea

106

V. SOURCES, METHODS

The major source of data for this study is the U. S. Geological Survey streamflow records. Programs were written in order to extract the statistical parameters and hydrograph records from a tape containing all the stream records of interest. This data enabled us to characterize the seasonability and variability of streamflow.

To obtain break-up and freeze-up information, the standard U. S. Geological Survey annual water resources data catalogs were examined for evidence of those events in the record. Some data on break-up and freeze-up were also available from the U. S. Weather Service and from the Environmental Atlas of Alaska (Johnson and Hartman, 1969).

The snowmelt characterization was accomplished using both NOAA - VHRR (Very High Resolution Radiometer) and LANDSAT satellite imagery.

Much of our data have been updated to include the 1974 data which recently have become available.

Our computer processing work has been additionally aided by existing programs supplied by the Alaska district of the U. S. Army Corps of Engineers in Anchorage. The selection of the 1-, 3-, 7-, 10-, and 30-day maximum period flows has been accomplished through one of the Corps' programs. By determining the ratio of these flow durations to the mean annual flow, a quantitative indicator of streamflow variability has been established.

VI. RESULTS

Presentation of the results of the statistical analyses and supplementary information is graphical wherever possible. Freeze-up and break-up information is tabulated.

The characterizations of the streams follow closely the character-ization flow chart (Table 1). For ease of drafting, each set of para-meters was grouped together for each region, i.e. all the flow duration curves are in a series followed by all the short-term variability indices, etc. The order of presentation of the streams is the same as that used by the U. S. Geological Survey in presenting the streamflow data in its annual publications. The order is established by following a traverse along the coast starting (in this case) with the Copper River and traveling westward along the coast; rivers are similarly ordered.

Explanatory notes precede each graphical presentation.

A.   Notes on determination of break-up and freeze-up date: Since both break-up and freeze-up are variable from year to year and depend greatly upon weather conditions, it is not possible to arrive at an average single date of freeze-up or break-up. Rather, a most likely 10-day period for each annual event is determined from the streamflow data. Freeze-up is determined by the period, usually in October or November, when the streamflow record is monotonically decreasing for 10 consecutive days; or, if there is a field note describing the termination of streamgage function due to ice formation, that data is used as the mid-date of the 10-day freezing period. Freeze-up is difficult to determine because its occurrence in the steamflow records is much more subtle and few direct observations of the freezing date are available.

Break-up, in this description, is used in the broadest sense of the term, implying snowmelt runoff initiation as well as the break-up of river ice. Break-up was determined to

108

TABLE 1

FLOW CHART - OCS STREAM CHARACTERIZATION

```
┌─────────────────────────────────────────────────┐
│ U.S. Geological Survey Streamflow Data            │
└─────────────────────────────────────────────────┘
                        │
        ┌───────────────────────────────────────┐
        │          Extreme Hydrographs:          │
        │  Record High Year, Record Low Year     │
        └───────────────────────────────────────┘
                        │
              ┌───────────────────────┐
              │   Flow Duration Curve  │
              └───────────────────────┘
                        │
              ┌───────────────────────┐
              │    Flow Mass Curve     │
              │     (Cumulative)       │
              └───────────────────────┘
                        │
              ┌───────────────────────┐
              │    Exceedance Series   │
              └───────────────────────┘
                        │
      ┌───────────────────────────────────────────┐
      │       Short Term Variability Index          │
      │  1-, 3-, 7-, 10-, 30-Day Duration Series    │
      │       In Ratio to Mean Annual Flow          │
      └───────────────────────────────────────────┘
                        │
        ┌───────────────────────────────────────┐
        │  Statistical Streamflow Parameters:     │
        │                                         │
        │               Mean                      │
        │               Mode                      │
        └───────────────────────────────────────┘
      ┌───────────────────────────────────────────┐
      │  Range (over complete duration series)      │
      └───────────────────────────────────────────┘
                        │
              ┌───────────────────────────┐
              │  Snowmelt Characterization  │
              └───────────────────────────┘
                        │
            ┌───────────────────────────────┐
            │  Total Stream Characterization │
            └───────────────────────────────┘
```

109

be that period of the streamflow record during which the discharge begins a steady increase after having reached minimum discharge for the year. Because this is an indirect method of determining break-up and freeze-up, it is very possible that the measurements involve instances of error. This is another reason why the term "most probably period" of break-up or freeze-up is used instead of attempting to narrow the estimates to a single mean date. The stated ranges will be the mean 10-day period during which the streamflow record indicated a snowmelt flow contribution or a steady decline to a baseflow condition.

Variations from this method of determining the break-up dates may occur in river analysis if other direct observations are used as input, such as LANDSAT or NOAA satellite imagery. Satellites were used to aid break-up determinations for large or rapidly responsive rivers such as the Yukon and the Kvichak Rivers. In these streams, flow is large all year. Large changes in stage and flow volume can take place in a river such as the Yukon, before the ice is swept away or broken. According to the empirical definition of break-up in this study, the Yukon River should have been ice-free and flowing by April 26-May 5, 1975. From satellite imagery it is evident that the Yukon was still ice covered in Alaska on May 8 and was not ice-free in the Yukon flats until on or about May 12 Ice often persists as much as a week or two later in the lower Yukon nearer the delta than it does upstream. Other large rivers may also be subject to large increases in stage over

its minimum level before the ice is removed, especially the
Kuskokwim, Kobuk, Copper, Susitna, Kvichak, and Wood Rivers.

The method of estimating break-up and freeze-up is only
useful after 1965. Before this period, gages were not usually
in operation before break-up in the spring, and were removed
before freeze-up in autumn. Estimates were usually poor when
ice cover prevailed since ice affected the stage-discharge
relationship. Records of break-up and freeze-up dates are
shown in Table 2 and additional records of freeze-up and
break-up from the U. S. Coast and Geodetic Survey (1964) are
presented in Table 3 for further historical information.

B.   Hypsometric curves:

These curves (Figures 1-3), which are essentially area-
altitude curves, relate the horizontal cross-sectional area
of a drainage basin to relative elevation above the basin
mouth. Through use of dimensionless parameters (a/A = area
of interest/Total basin area, h/H height of interest/highest
elevation), curves can be read and compared irrespective of
true scale. Curves show distinctive differences both in form
and proportionate area below the curve. Further development
of the uses of the hypsometric curve is discussed by Strahler,
1952.

Practical applications of hypsometric curves have value
in many areas. The area-altitude relation provides a means of
estimating the mean depth of snow over a basin, or its
water equivalent. Because precipitation normally increases
with elevation, the hypsometric curve can be used to estimate

111

TABLE 2
1976 Tabulation of Breakup and Freezeup Dates
of Alaskan Coastal Rivers
Determined from Streamflow Measurements

River Name	Most Probable Break-Up Dates	Most Probable Freeze-Up Dates	Other Data	Comments
Copper R.	May 3-12	Oct. 17-26		
Power Cr.	Apr. 23-May 2	Nov. 24-Dec. 3		Fluctuations throughout winter
Olsen Bay Cr.(W.fork)	Apr. 12-21	Nov. 18-27		
Nellie Juan R.	Apr. 25-May 4	Nov. 14-23		
Resurrection R. (Seward)	Apr. 23-May 2	Nov. 10-19		
Lowell Cr.	Apr. 26-May 5	Nov. 26-Dec. 5		
Spruce Cr.				Insufficient record length
Bradley R.	May 4-13	Nov. 4-13		
Anchor R.	Apr. 18-27	Nov. 4-13		
Ninilchik R.	Apr. 17-26	Nov. 6-15		
Kasilof R.	Apr. 5-14	Nov. 3-12	4/13 breakup USWS 16-yr. avg.	Difficult to determine from record
Kenai R. (Soldotna)	Apr. 22-May 1	Nov. 5-14	4/16 breakup USWS 15-yr. avg.	
Resurrection Cr. (Hope)	Apr. 22-May 1	Nov. 1-10		
Glacier Cr.	Apr. 10-19	Nov. 7-16		
Campbell Cr.	Apr. 22-May 1	Nov. 5-14		Freeze-up difficult to determine
Chester Cr.	Apr. 9-18	Oct. 31-Nov. 9		
Ship Cr.(Elmendorf)	Apr. 30-May 9	Dec. 3-12		Power plant probably affects freeze-up
Eagle R.	May 4-13	Nov. 1-10		
Knik R.	Apr. 24-May 3	Oct. 26-Nov. 4		
Matanuska R.	Apr. 26-May 4	Oct. 24-Nov. 3		

TABLE 2 Continued

River Name	Most Probable Break-Up Dates	Most Probable Freeze-Up Dates	Other Data	Comments
Little Susitna R.	May 2-11	Oct. 22-Nov. 1		
Susitna R. (Gold Cr.)	May 5-14	Oct. 16-25	5/9 breakup USWS 9-yr. avg. @ Talkeetna	
Chakachatna R.	May 16-25	Oct. 16-25		
Terror R.				No freeze cycle detectable
Myrtle Cr.	Mar. 24-Apr. 5	Dec. 2-11		
Uganik R.				same as above
Kvichak R.	May 10-19	Nov. 27-Dec. 6		Freeze-up difficult to determine
Nuyakuk R.	May 10-19	Oct.31-Nov. 9		
Kuskokwim R. (Crooked Cr.)	Apr. 28-May 27	Oct. 23-Nov. 2	5/8 breakup 10/30 freezeup USWS 10-yr. avg.	
Kuzitrin R.	May 9-18	Oct. 17-26		
Kobuk R. (Ambler)	May 12-21	Oct. 9-18	5/21 breakup 10/12 freezeup USWS 11-yr. avg.	
Kuparuk R.	May 29-June 8	Sept. 20-29		
Putuligayuk R.	June 3-12	Sept. 26-Oct 5		
Sagavanirktok R.	May 13-22	Sept. 27-Oct. 6		
Wood R.	Apr. 26-May 5	Nov. 3-12		

TABLE 3

HISTORICAL DATES OF ICE BREAKUP AND FREEZEUP (FROM U. S. COAST AND GEODETIC SURVEY, 1964)

Place	Waters	Ice breakup			Ice freezeup			Avg. Years Record	Period
		Average	Earliest	Latest	Average	Earliest	Latest		

Gulf of Alaska

Place	Waters	Average	Earliest	Latest	Average	Earliest	Latest	Years Record	Period
Susitna	Susitna R.	May 1	4/12/41	5/10/46	Nov 1	10/19/33	11/14/36	12	1933 - 1946
Talkeetna	do	May 8	4/12/41	5/25/52	Dec 2	11/12/39	12/23/47	12	1919 - 1952
Kasilof	Kasilof R.	Apr 13	3/27/41	4/29/46	Dec 3	11/13/45	12/24/48	10	1937 - 1947
Kenai	Kenai R.	Apr 2	3/18/52	4/14/51	Dec 10	11/23/51	12/26/37	6	1937 - 1952
Anchorage	Ship Cr.	Mar 29	2/16/44	4/17/42	Nov 24	11/10/35	12/10/36	21	1915 - 1953

Bering Sea

Place	Waters	Average	Earliest	Latest	Average	Earliest	Latest	Years Record	Period
Egegik	Egegik R.	Apr 14	3/16/41	5/01/39	Dec 12	11/12/42	1/11/39	10	1937 - 1952
Naknek	Naknek R.	Apr 9	3/19/41	4/25/49	Nov 17	10/17/39	12/15/17	7	1916 - 1951
Koggiung	Kvichak R.	May 4	4/26/38	5/13/40	Dec 22	11/23/39	1/30/41	3	1937 - 1940
Dillingham	Nushagak Bay	May 9	4/25/26	5/27/52	Nov 7	10/16/32	12/22/40	19	1919 - 1952
Kanakanak	do	May 2	4/17/40	5/22/39	Nov 20	10/14/42	12/21/38	4	1937 - 1943
Platinum	Goodnews Bay	May 1	4/08/42	5/25/52	Nov 19	10/23/30	12/12/47	12	1928 - 1952
Kwinhagak	Kuskokwim Bay	May 1	4/10/45	5/17/46	Nov 15	10/20/29	12/20/38	10	1929 - 1952
Bethel	Kuskokwim R.	May 15	4/24/40	5/28/52	Oct 29	10/08/28	11/24/51	27	1923 - 1952
Crooked Creek	do	May 7	4/22/40	5/23/52	Nov 18	11/03/39	12/02/52	12	1937 - 1952
McGrath	do	May 10	4/24/40	5/24/52	Nov 5	10/23/41	11/15/52	12	1939 - 1952
Mekoryuk Nunivak Is.	Mekoryuk R.	May 12	4/18/50	5/30/46	Nov 27	11/20/52	12/13/47	5	1943 - 1951
Gambel, St. Lawrence Is.		May 26	5/01/43	7/01/50	Nov 21	10/15/49	12/14/40	10	1940 - 1952
Savoonga, St. Lawrence Is.		May 26	4/25/48	6/17/45	Nov 19	9/30/30	12/13/40	10	1929 - 1949
Hooper Bay	Hooper Bay	May 26	5/15/42	6/04/45	Nov 12	10/19/26	11/20/41	4	1926 - 1945
St. Michael	Norton Sound	Jun 9	5/19/12	7/03/01	Nov 10	10/10/84	12/07/81	53	1874 - 1952
Unalakleet	Unalakleet R.	May 17	4/28/40	5/30/52	Oct 25	10/08/39	11/19/37	14	1937 - 1952
Moses Point	Kwiniuk R.	May 24	5/02/51	6/11/49	Oct 20	10/01/51	11/02/52	6	1943 - 1952
Golovin	Golivnin Bay	May 23	5/13/40	6/14/39	Nov 2	10/08/42	11/19/37	6	1937 - 1943
White Mountain	Fish R.	May 21	5/05/40	6/02/37	Oct 14	9/27/31	11/01/25	24	1923 - 1951
Solomon	Solomon R.	May 20	5/01/42	5/30/45	Oct 29	10/10/40	11/29/48	10	1940 - 1952
Council	Nuikluk R.	May 17	4/27/40	5/31/52	Oct 30	10/13/20	11/09/40	12	1920 - 1952
Nome	Norton Sound	May 29	4/28/42	6/28/48	Nov 12	10/13/18	12/13/47	50	1900 - 1952
Teller	Grantley Harbor	Jun 7	5/12/36	6/18/39	Nov 10	10/13/42	12/26/50	16	1936 - 1952

Yukon River

Place	Waters	Average	Earliest	Latest	Average	Earliest	Latest	Years Record	Period
Akulurak	Kwikluak Pass	May 27	5/20/42	6/04/20	Oct 24	10/11/39	11/07/23	14	1917 - 1948
Hamilton	22	May 22	5/06/40	6/05/52	Oct 25	10/15/39	11/02/38	14	1938 - 1952
Azacharak	85	May 20	5/03/38	6/06/52	Nov 13	11/01/39	12/22/49	12	1937 - 1952
Pilot Station	115	May 17	5/01/26	5/24/24	Nov 8	10/27/24	11/13/25	5	1924 - 1943
Russian Mission	195	May 12	4/25/40	5/25/39	Nov 4	10/21/28	11/15/37	8	1928 - 1944
Holy Cross	257 Nautical	May 17	4/25/40	5/28/52	Oct 31	10/12/31	11/30/34	32	1917 - 1952
Galena	481 Miles	May 17	5/08/51	5/26/52	Nov 6	10/11/47	12/08/50	10	1943 - 1952
Ruby	526 Above	May 15	4/30/40	5/22/20	Nov 7	10/28/17	11/18/37	11	1917 - 1946
Tanana	628 Apoon	May 14	4/29/40	5/25/35	Nov 4	10/13/30	11/22/37	33	1917 - 1952
Rampart	688	May 16	5/01/30	5/25/52	Nov 6	10/13/30	11/23/45	21	1917 - 1952
Ft. Yukon	896	May 14	5/07/40	5/22/27	Oct 28	10/14/41	11/15/52	30	1918 - 1952
Coal Creek	1002	May 12	5/07/43	5/18/45	Nov 9	11/01/38	11/20/40	8	1938 - 1950
Eagle	1089	May 9	4/25/40	5/18/52	Nov 19	10/18/30	12/11/49	29	1917 - 1952
Dawson, Canada	1197	May 8	4/28/40	5/16/45	Nov 17	11/03/41	12/18/42	12	1917 - 1947

Arctic Ocean

Place	Waters	Average	Earliest	Latest	Average	Earliest	Latest	Years Record	Period
Wales	Bering Strait	Jun 8	5/15/47	6/30/49	Dec 3	10/08/48	1/08/51	16	1927 - 1952
Shishmaref	Arctic Ocean	Jun 22	5/30/36	7/08/33	Nov 10	10/06/39	12/18/34	18	1921 - 1952
Candle	Kiwalik R.	May 18	5/05/43	5/27/27	Oct 17	10/10/42	10/23/43	8	1922 - 1950
Deering	Inmachuk R.	Jun 4	5/11/43	6/30/41	Oct 23	10/03/46	11/04/41	4	1937 - 1948
Kotzebue	Kotzebue Sound	May 31	5/17/40	6/08/45	Oct 23	10/02/39	11/05/38	14	1929 - 1952
Selawik	Selawik R.	May 28	5/13/40	6/07/45	Oct 17	10/03/46	10/30/38	12	1927 - 1952
Noorvik	Kobuk R.	May 29	5/18/25	6/11/22	Oct 11	9/26/48	10/25/22	17	1918 - 1952
Kiana	do	May 18	5/07/40	5/29/39	Oct 18	10/10/39	11/04/38	6	1938 - 1944
Kobuk	do	May 19	5/11/43	5/29/45	Oct 21	10/09/39	11/02/38	12	1937 - 1952
Shungnak	do	May 21	5/12/41	5/29/45	Oct 16	10/07/19	10/25/40	8	1919 - 1950
Kivalina	Kivalina R.	May 22	5/15/43	5/27/49	Oct 25	10/15/48	11/01/46	6	1943 - 1952
Point Hope	Arctic Ocean	Jun 20	5/30/27	7/08/46	Nov 11	10/06/42	12/19/47	8	1927 - 1951
Point Lay	do	Jun 24	6/01/43	7/10/53	Nov 4	10/12/43	11/27/48	4	1943 - 1953
Wainwright	do	Jun 29	6/07/44	7/26/48	Oct 2	9/26/48	10/09/45	7	1939 - 1953
Point Barrow	do	Jul 22	6/15/44	8/22/31	Oct 3	8/31/27	12/19/47	31	1920 - 1953
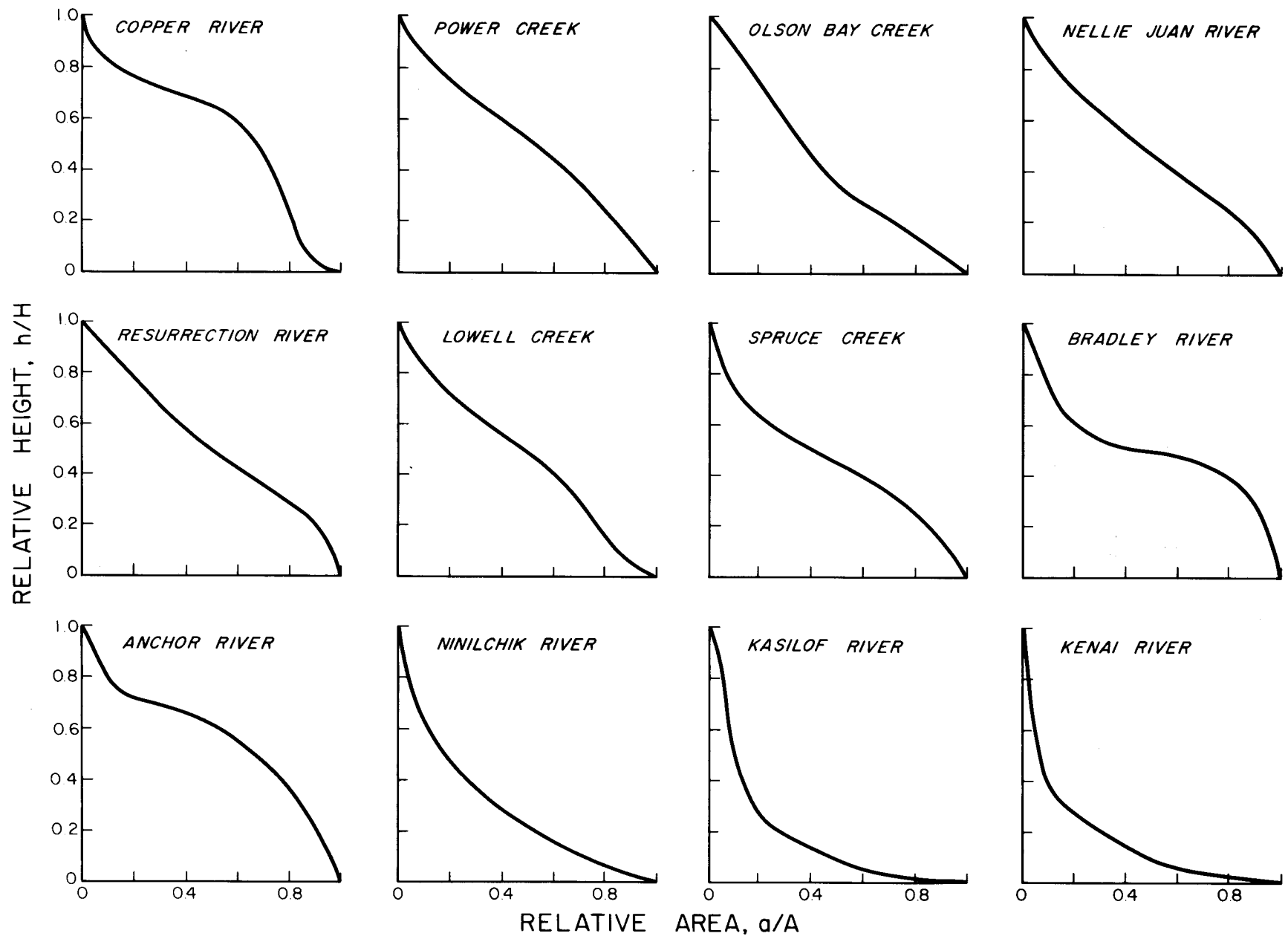
FIGURE 1 - HYPSOMETRIC CURVES
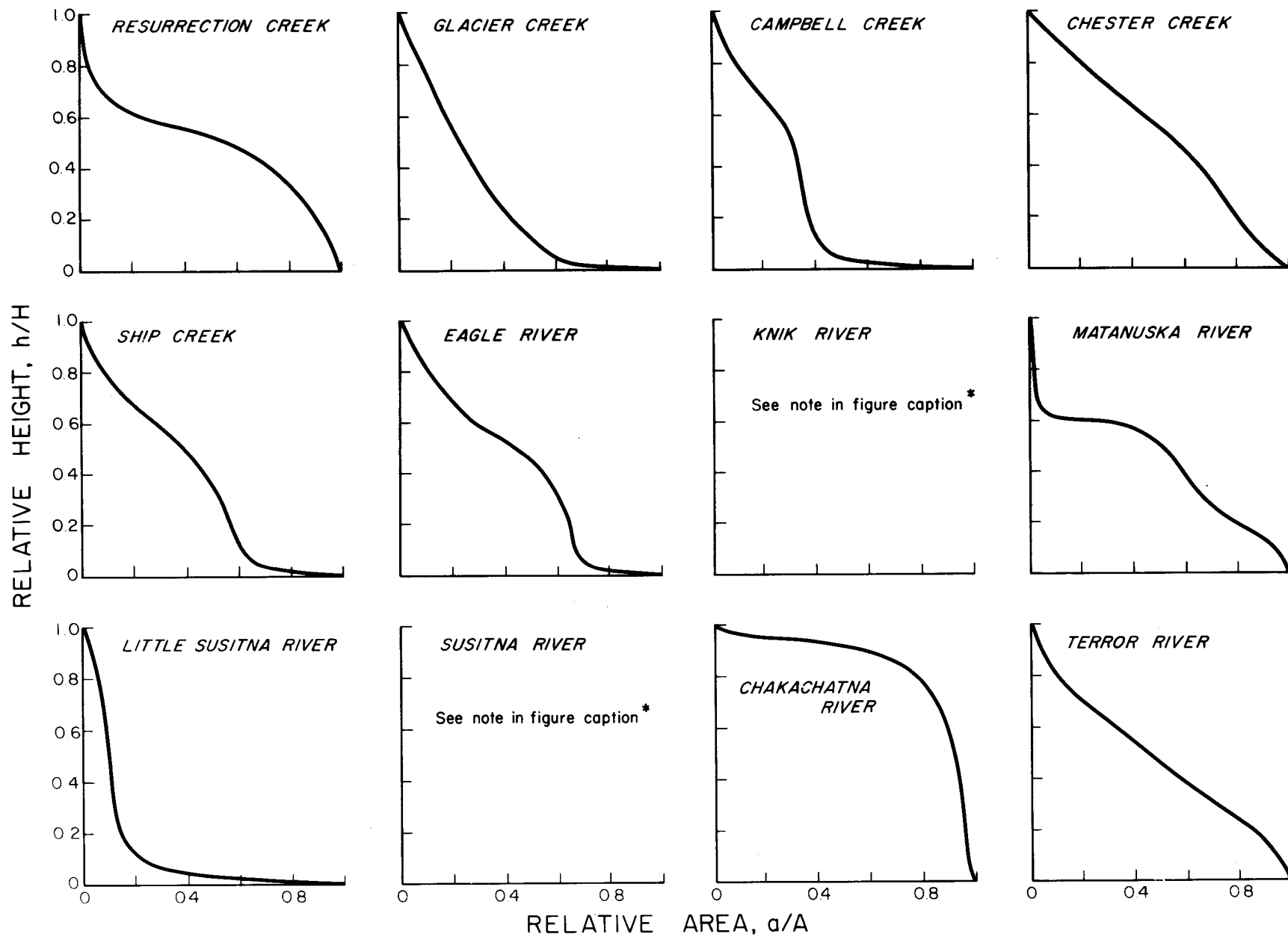
FIGURE 2 - HYPSOMETRIC CURVES

THE KNIK AND SUSITNA RIVERS HAVE INADEQUATE MAPS AVAILABLE FOR ACCURATE HYPSOMETRIC ANALYSIS

116
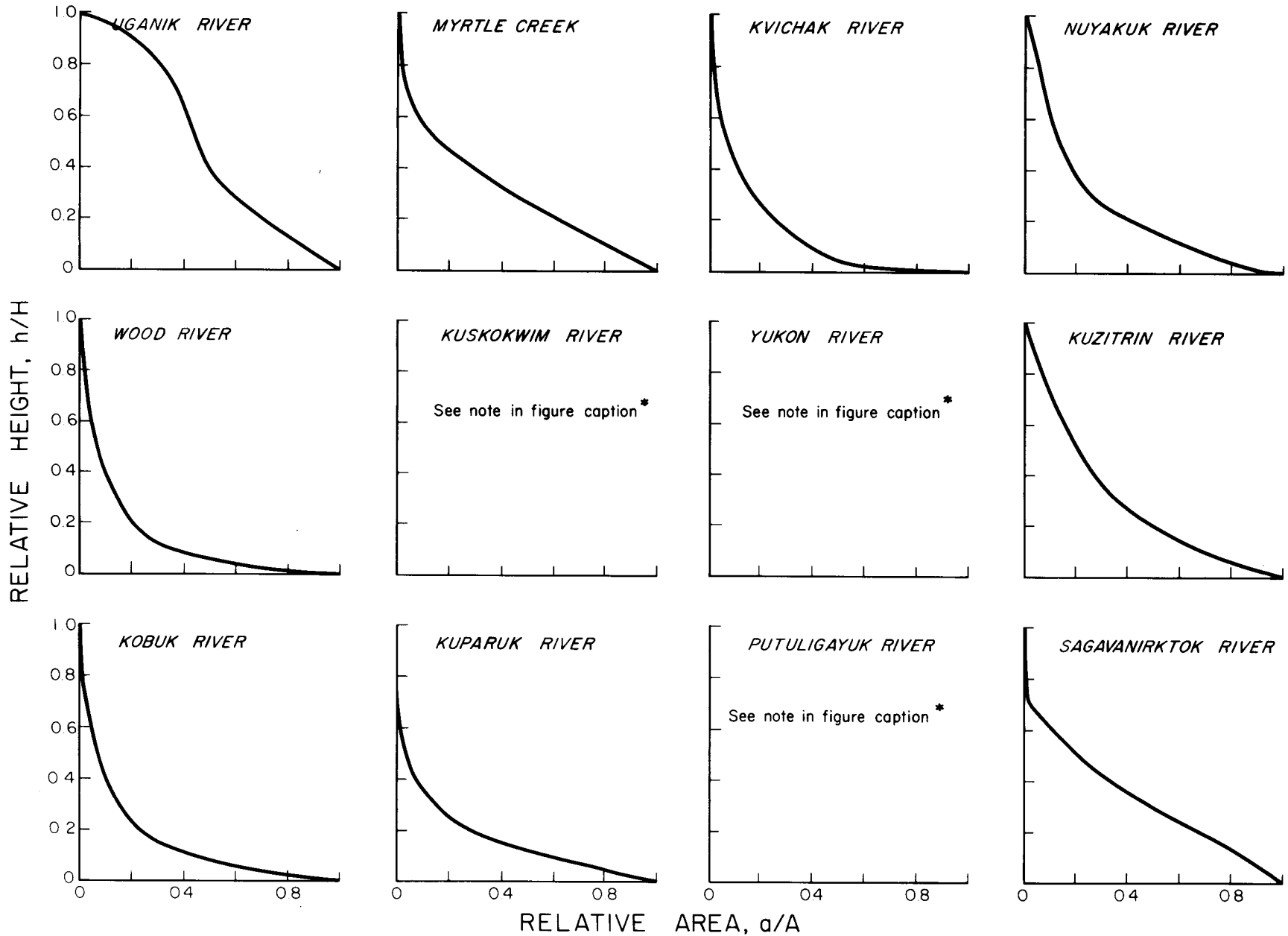
FIGURE 3 - HYPSOMETRIC CURVES

THE KUSKOKWIM RIVER HAS INADEQUATE MAP AVAILABLE FOR ACCURATE HYPSOMETRIC ANALYSIS. BECAUSE OF ITS BASIN SIZE, A HYPSOMETRIC ANALYSIS OF THE YUKON RIVER WAS NOT FELT TO BE MEANINGFUL. THE PUTULIGAYUK RIVER IS CONFINED TO ELEVATIONS LESS THAN 50 METERS.

precipitation at elevations where measurements are not made directly. The use of satellite imagery in snowcover mapping is aided by the use of hypsometric curves, making it a simple matter to calculate the areal coverage of snow if the mean "snow line" is determined, or to find the mean elevation of snowcover if the areal coverage of snow is more easily measured.

In order to more easily use the hypsometric curves, the highest elevation in each basin (H), and the basin area (A) are tabulated on Table 4.

C. Extreme hydrographs:

Both the record high and record low year of flow (based on mean annual flow) is shown for each river of interest, Figures 4 through 21. This information is available from the U. S. Geological Survey Water Resources division and is presented here in graphical form. Although some of the records are of short duration, these hydrographs provide an indication of the range of flow of each river for a relatively dry year and a relatively wet year.

TABLE 4
HYPSOMETRIC DATA

River Basin	Highest Elevation (H)	Basin Area (A)	
		mi^2	km^2
Copper River	19,850 ft. (6616 m)	20,600	53,400 @ Chitna
Power Creek	4,660 ft. (1420 m)	20.5	53.1
WF Olson Bay Creek	3,720 ft. (1133 m)	4.78	12.38
Nellie Juan River	6,182 ft. (1884 m)	125	322
Resurrection River (Seward)	5,309 ft. (1618 m)	169	438
Lowell Creek	4,003 ft. (1220 m)	4.02	10.4
Spruce Creek	4,003 ft. (1220 m)	9.26	23.98
Bradley River	4,921 ft. (1500 m)	54.0	139.9
Anchor River	2,060 ft. (628 m)	133	344
Ninilchik River	2,010 ft. (612 m)	131	339
Kasilof River	6,560 ft. (2000 m)	738	1,910
Kenai River (Soldotna)	5,520 ft. (1680 m)	2,010	5,210
Resurrection Creek (Hope)	5,079 ft. (1548 m)	149	386
Glacier Creek	5,202 ft. (1586 m)	62	160.6
Campbell Creek	3,940 ft. (1200 m)	69.7	180.5
Chester Creek	1,148 ft. (350 m)	20.0	51.8
Ship Creek (Elmendorf)	6,370 ft. (1941 m)	115	298
Eagle River	4,920 ft. (1500 m)	192	497
Knik River	10,610 ft. (3230 m)	1,180	3,060
Matanuska River	13,176 ft. (4016 m)	2,070	5,360
Little Susitna River	1,937 ft. (590 m)	61.9	160.3
Susitna River (Gold Creek)	20,320 ft. (6190 m)	160	15,950
Chakachatna River	9,350 ft. (2850 m)	1,120	2,900
Terror River	4,405 ft. (1340 m)	15.0	38.9
Uganik River	4,405 ft. (1340 m)	123	319
Myrtle Creek	2,079 ft. (630 m)	4.74	12.28
Kvichak River	10,197 ft. (3110 m)	6,500	16,800
Nuyakuk River	6,000 ft. (1829 m)	1,490	3,860
Wood River	2,950 ft. (900 m)	1,110	
Kuskokwim River (Crooked Creek)	11,670 ft. (3560 m)	31,100	80,500
Yukon River (Ruby)	20,300 ft. (6190 m)	259,000	671,000
Kuzitrin River	2,682 ft. (817 m)	1,720	4,450
Kobuk River (Ambler)	8,800 ft. (2680 m)	6,570	17,020
Kuparuk River	1,968 ft. (600 m)	3,130	8,107
Putuligayuk River	230 ft. (15 m)	176	456
Sagavanirktok River	7,370 ft. (2246 m)	2,208	5,719
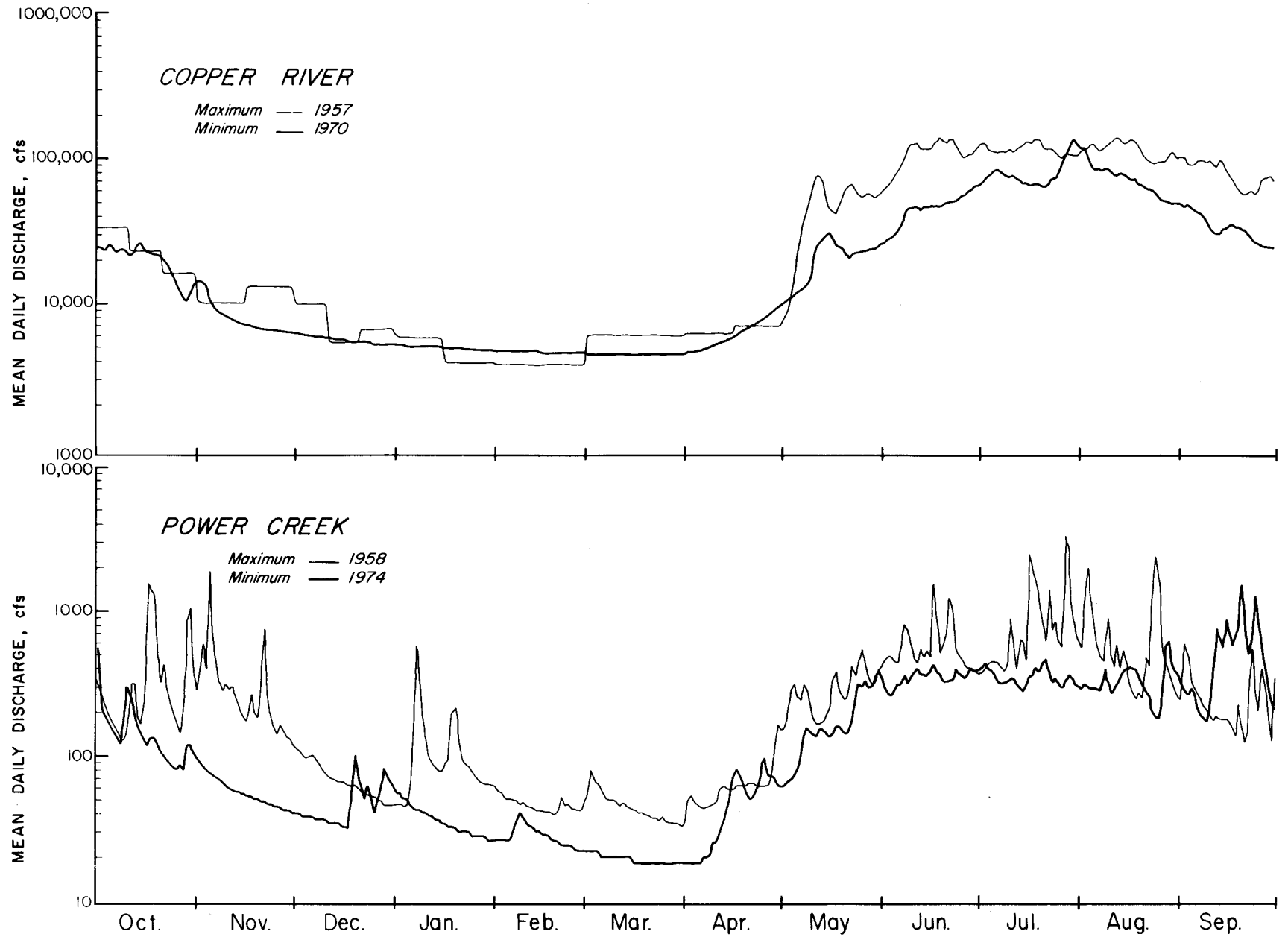
FIGURE 4 – HYDROGRAPHS – Copper River / Power Creek

120
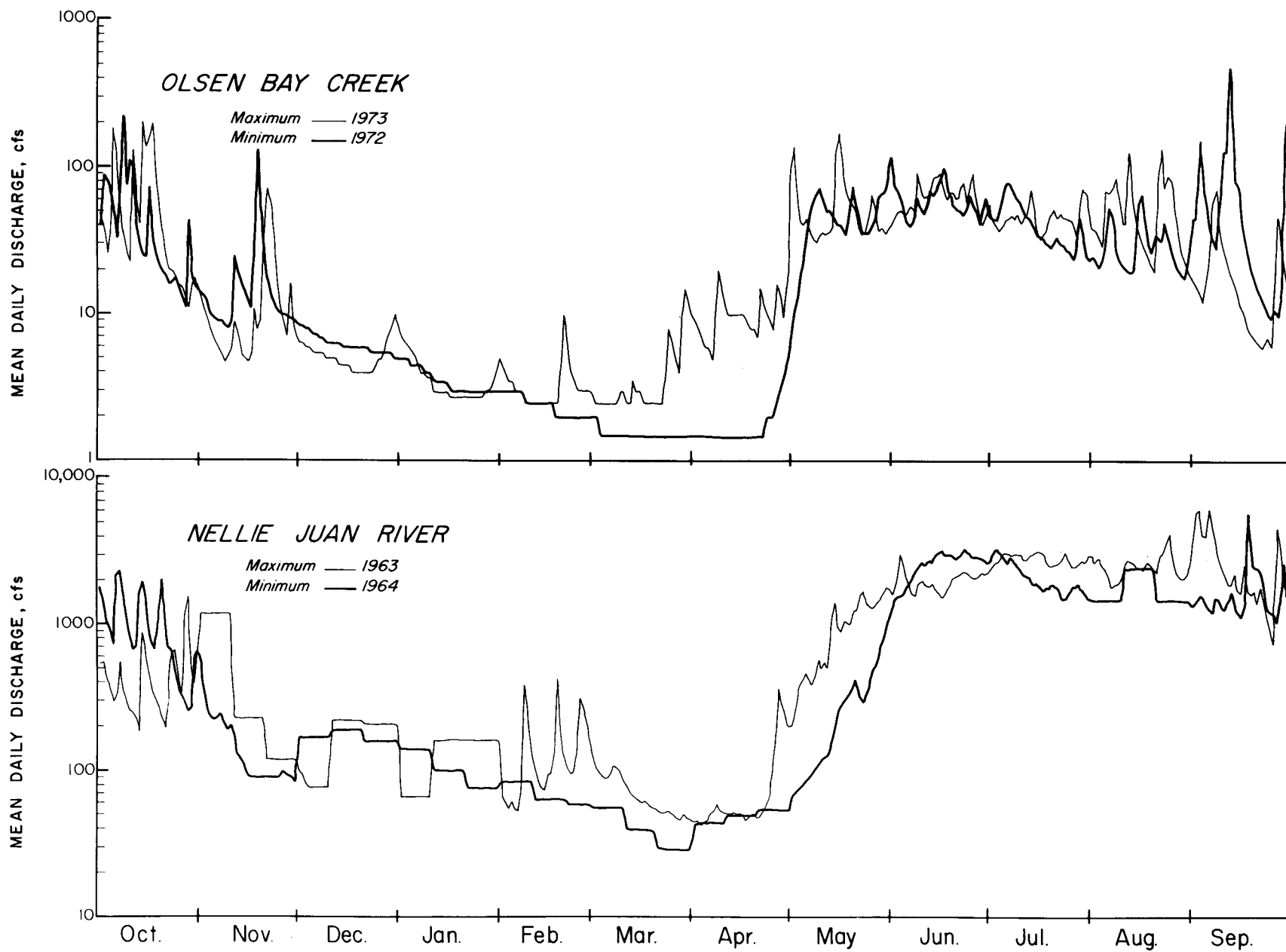
FIGURE 5 — HYDROGRAPHS – Olsen Bay Creek / Nellie Juan River
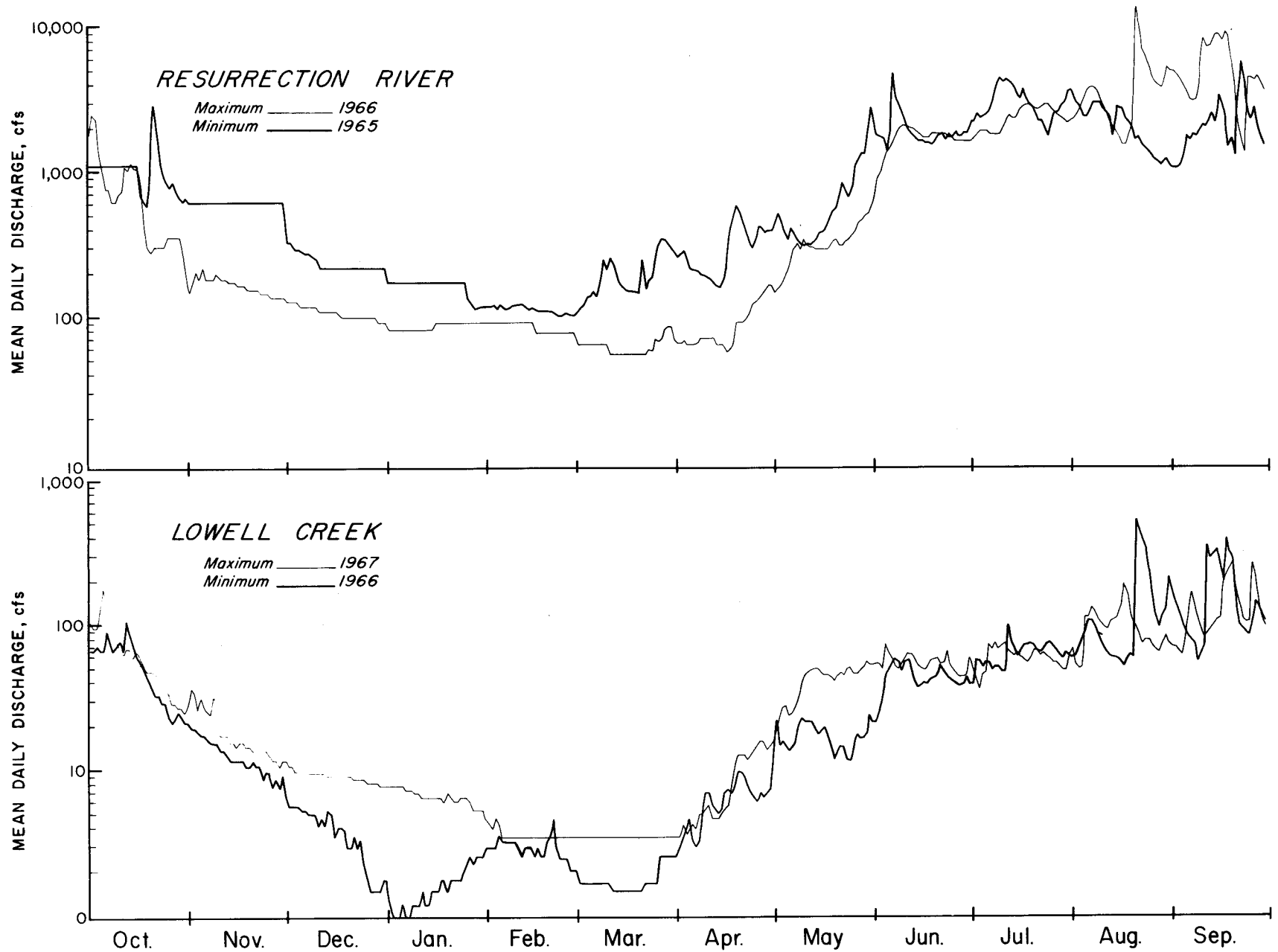
FIGURE 6 – HYDROGRAPHS – Resurrection River / Lowell Creek

SPRUCE CREEK

Maximum _____ 1970
Minimum _____ 1968

MEAN DAILY DISCHARGE, cfs

10,000

1,000

100

10

BRADLEY RIVER

Maximum _____ 1970
Minimum _____ 1962

MEAN DAILY DISCHARGE, cfs

10,000

1,000

100

10

Oct.   Nov.   Dec.   Jan.   Feb.   Mar.   Apr.   May   Jun.   Jul.   Aug.   Sep.
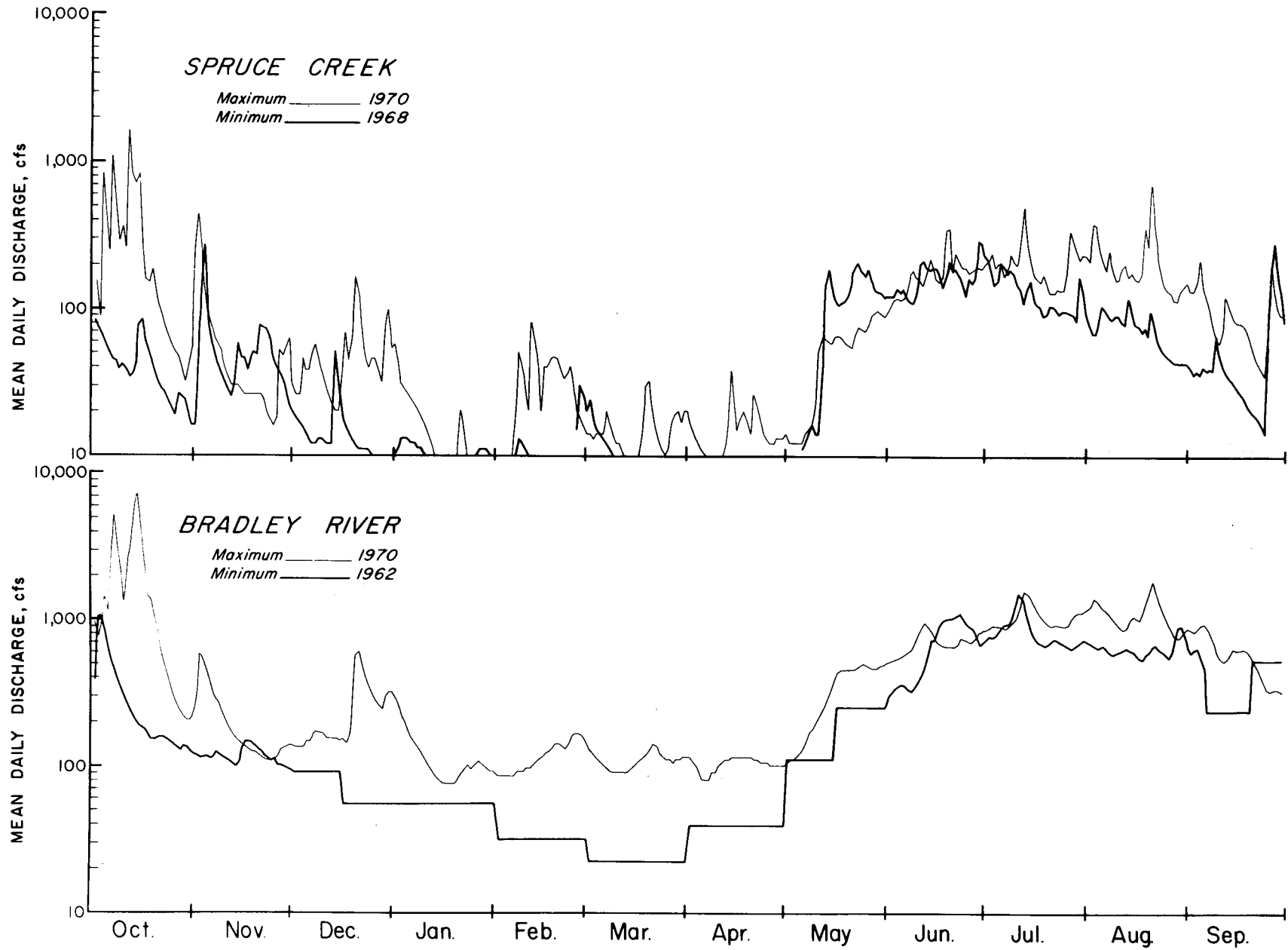
FIGURE 7 – HYDROGRAPHS – Spruce Creek / Bradley River
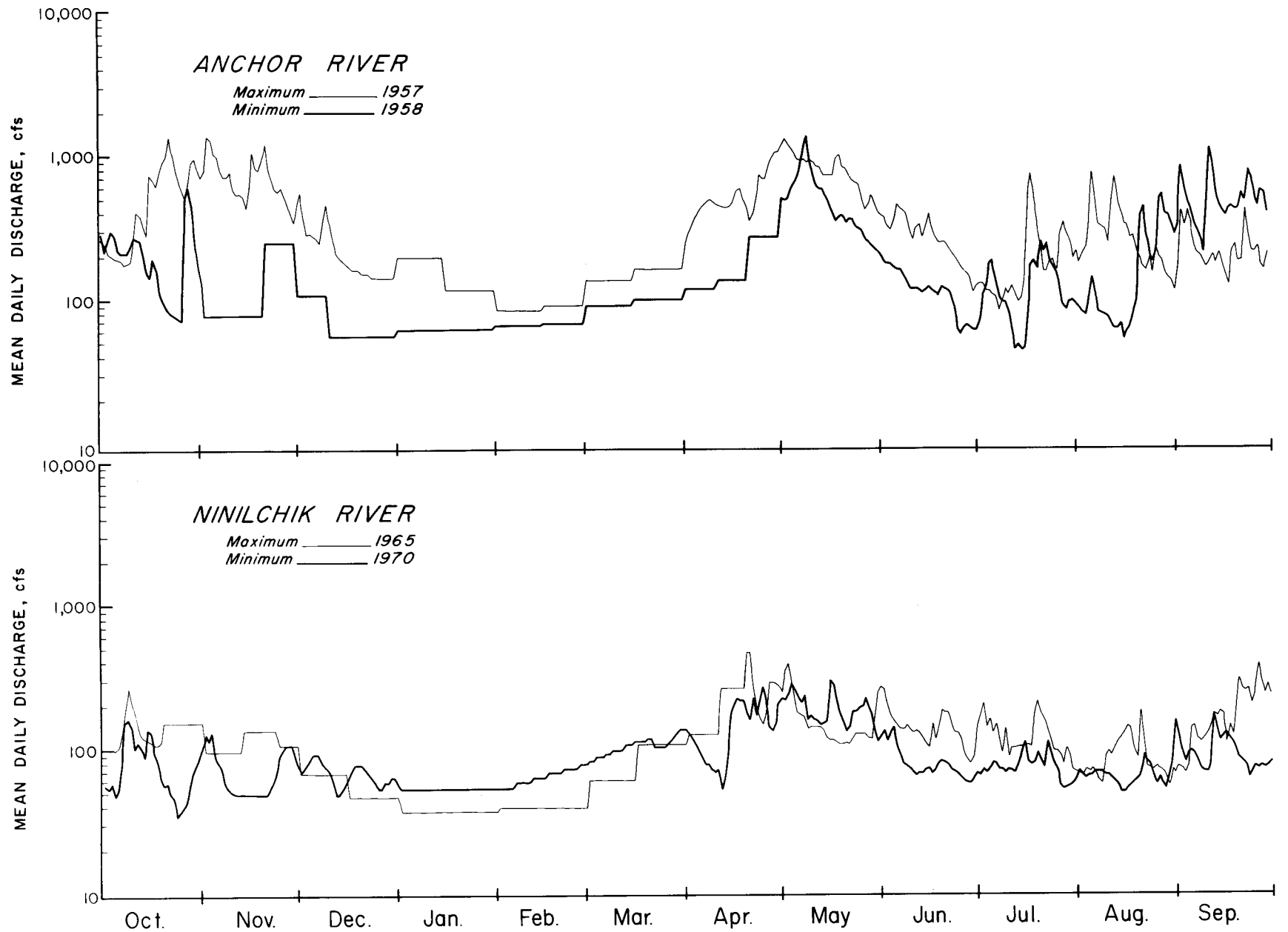
FIGURE 8 – HYDROGRAPHS - Anchor River / Ninilchik River
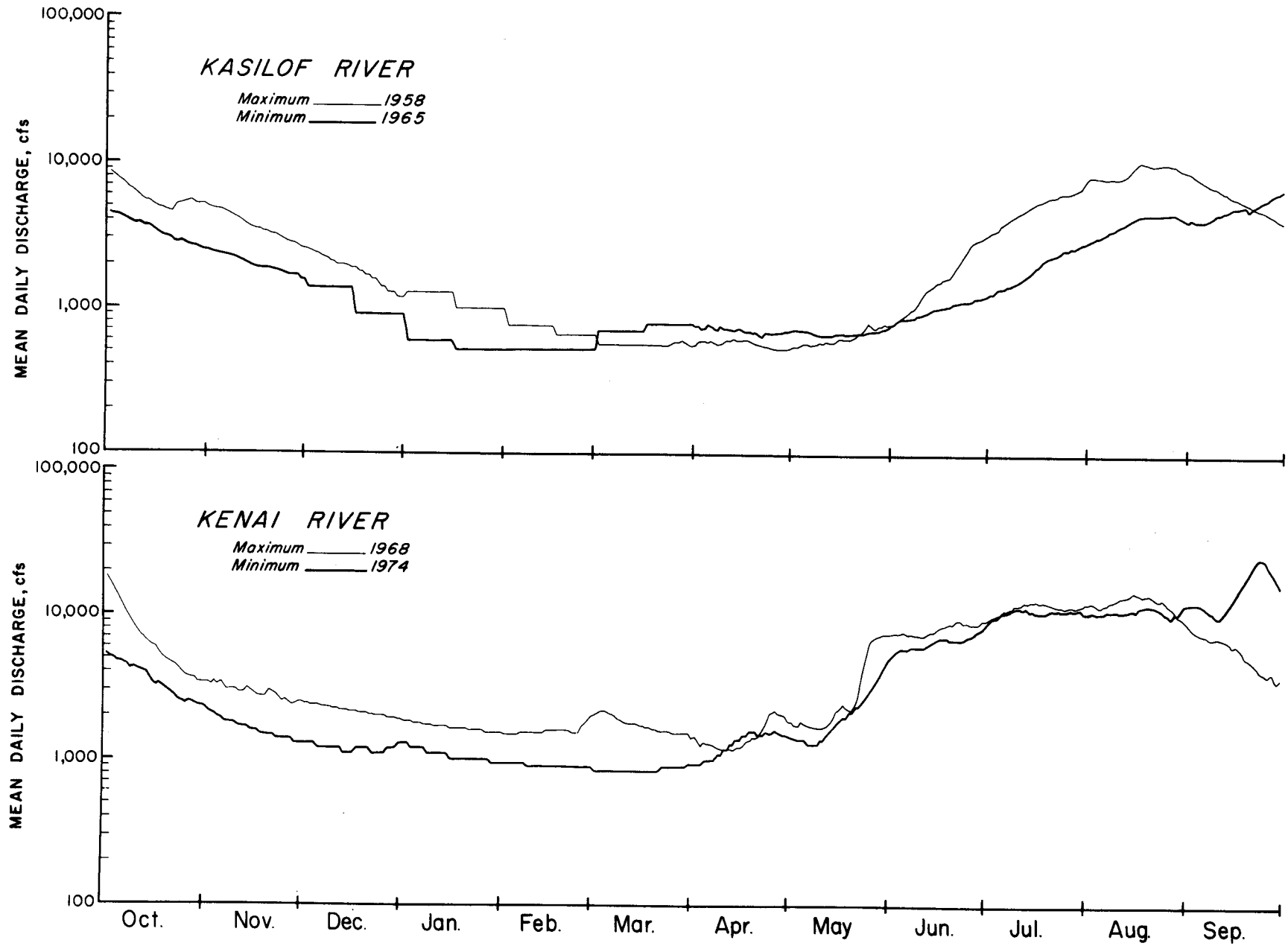
FIGURE 9 - HYDROGRAPHS - Kasilof River / Kenai River
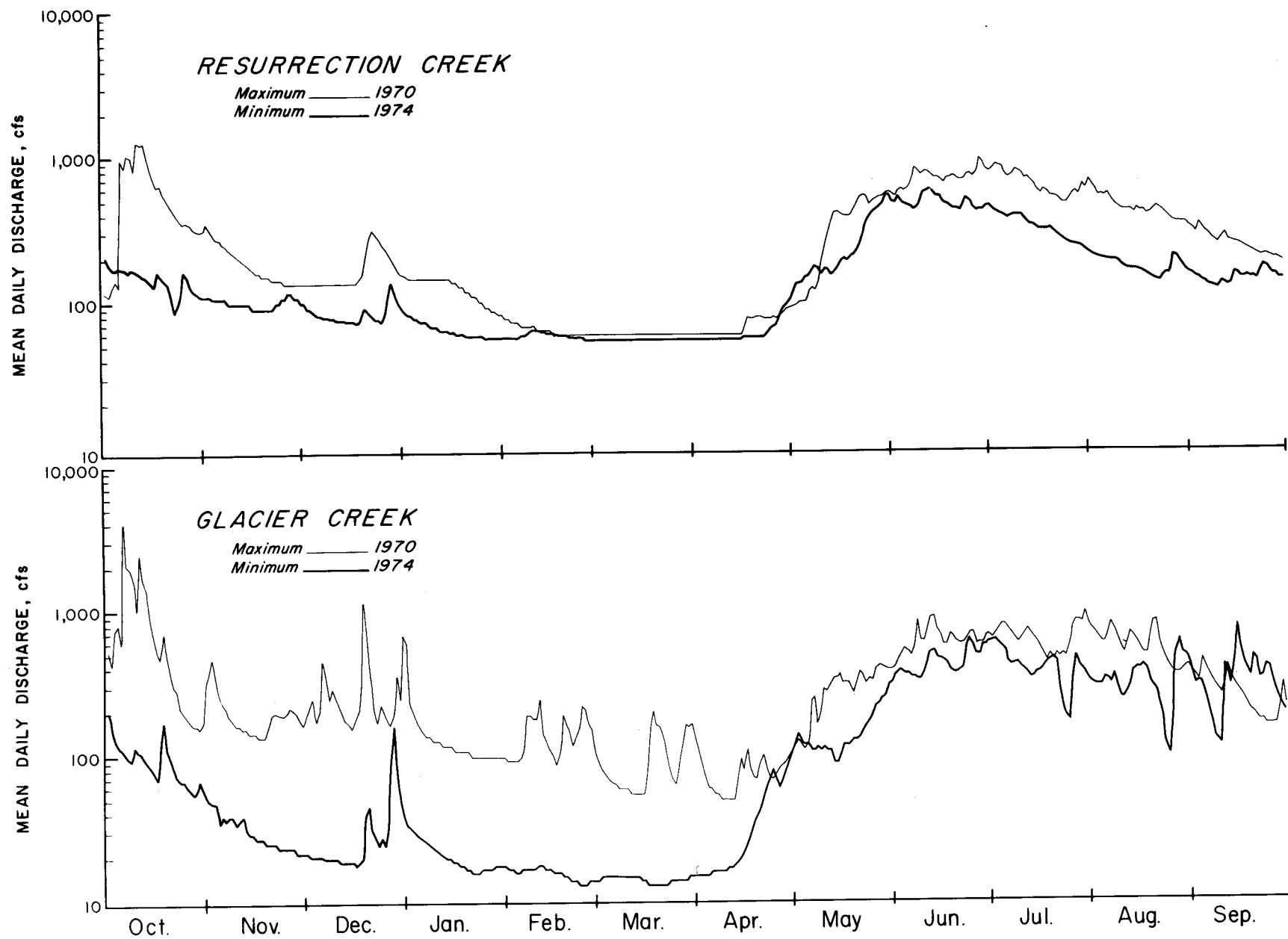
FIGURE 10 - HYDROGRAPHS - Resurrection Creek /Glacier Creek
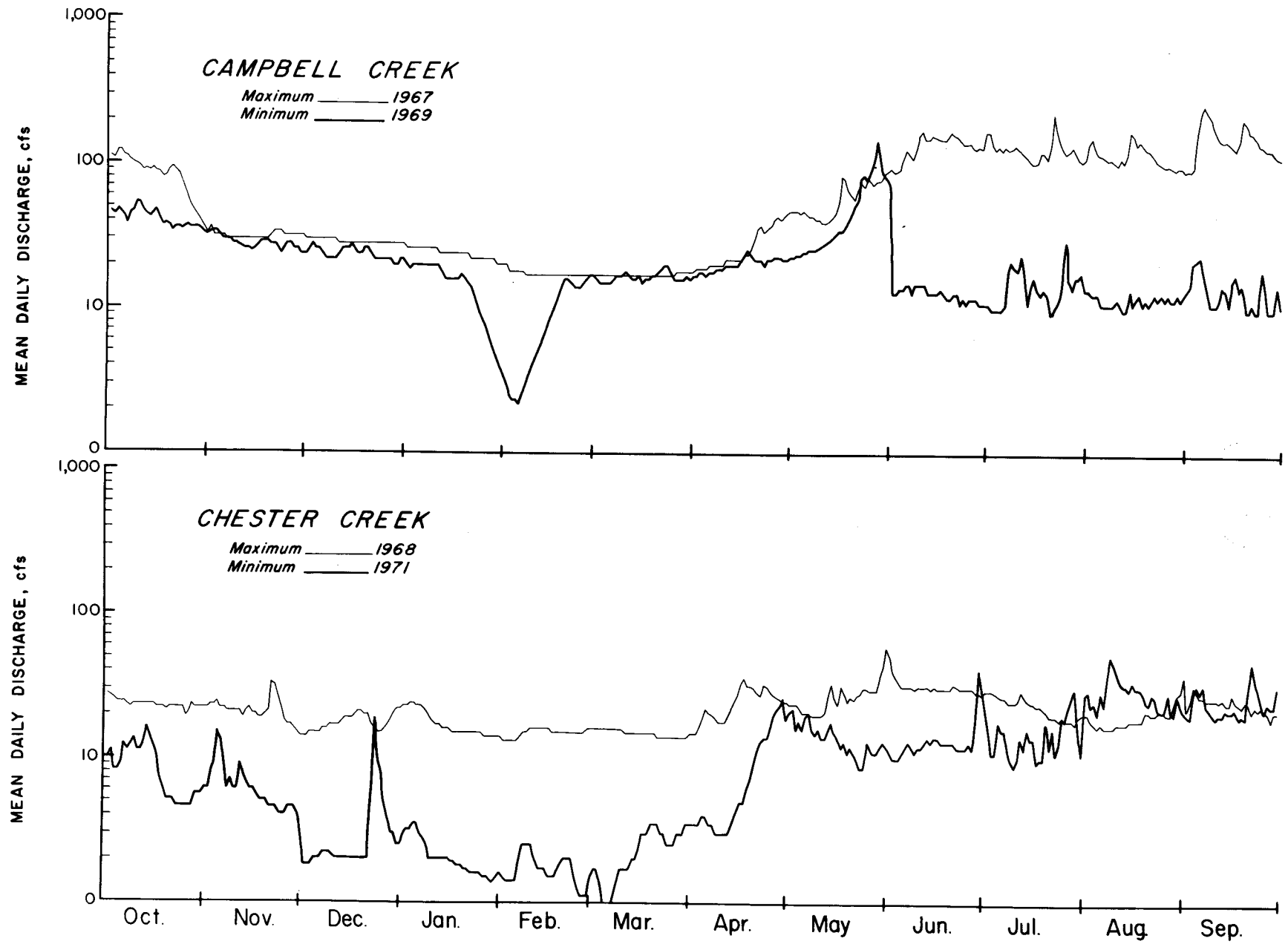
FIGURE 11 – HYDROGRAPHS – Campbell Creek / Chester Creek
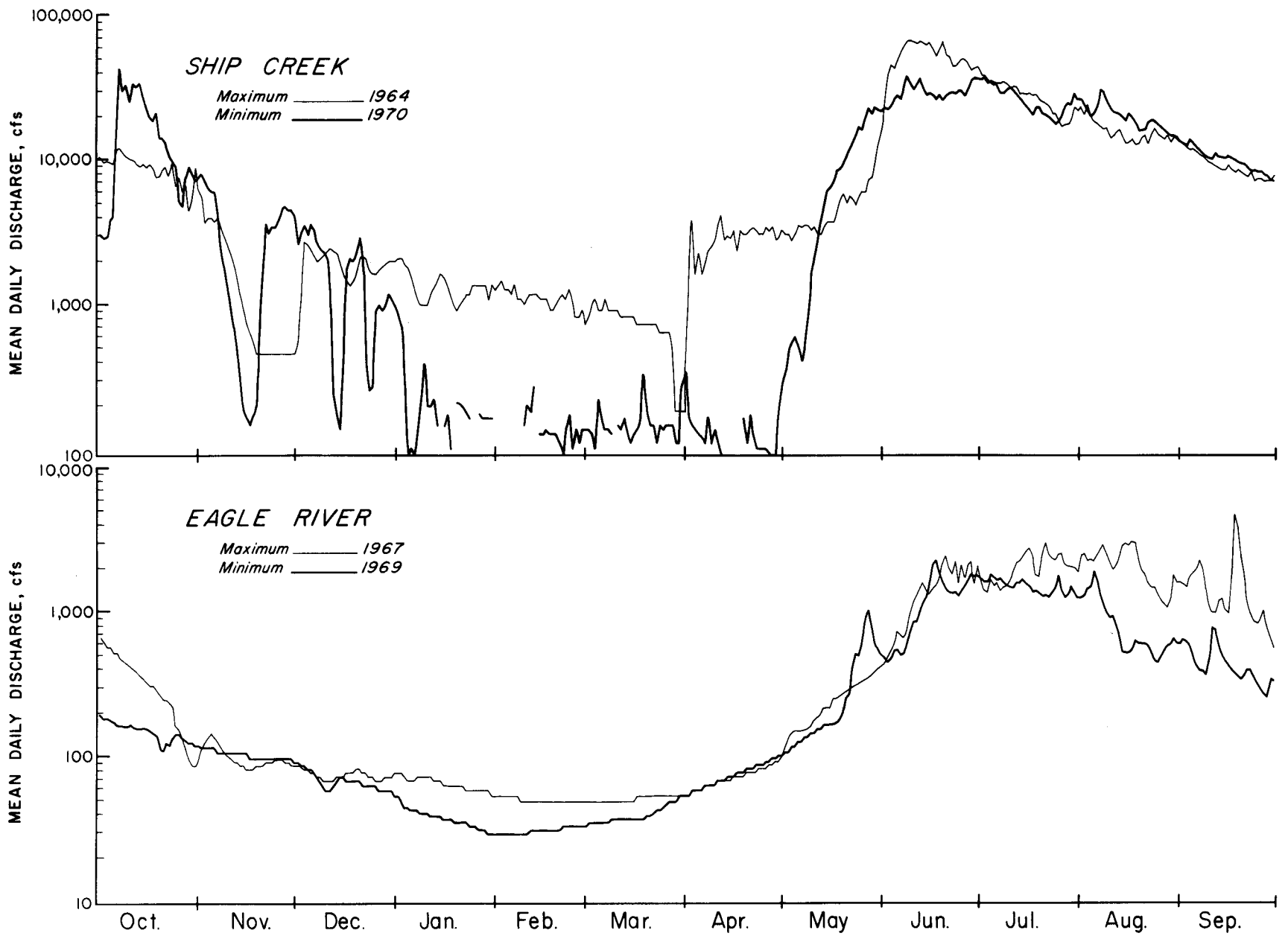
FIGURE 12 — HYDROGRAPHS — Ship Creek / Eagle River

128
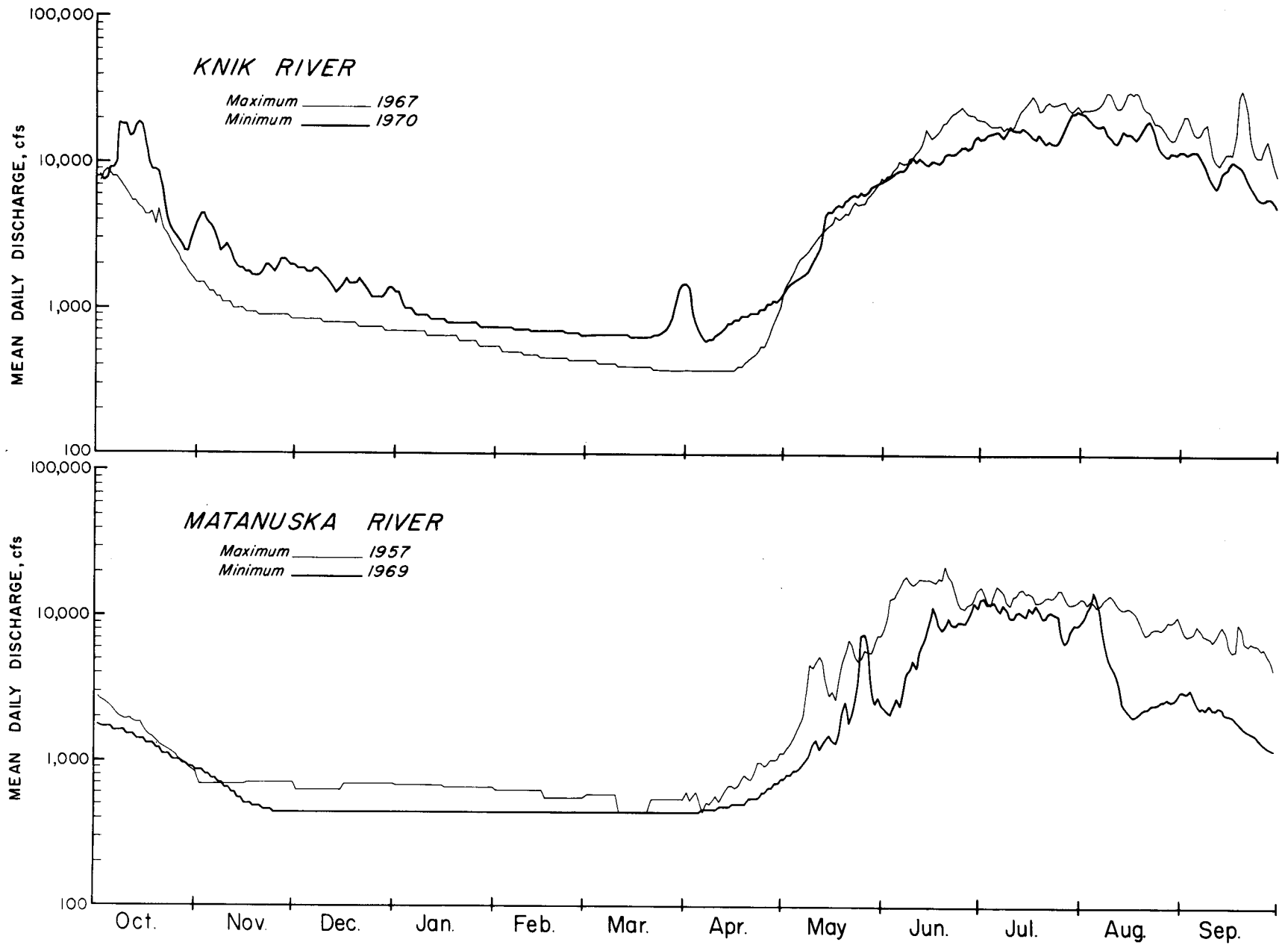
FIGURE 13 - HYDROGRAPHS - Knik River / Matanuska River
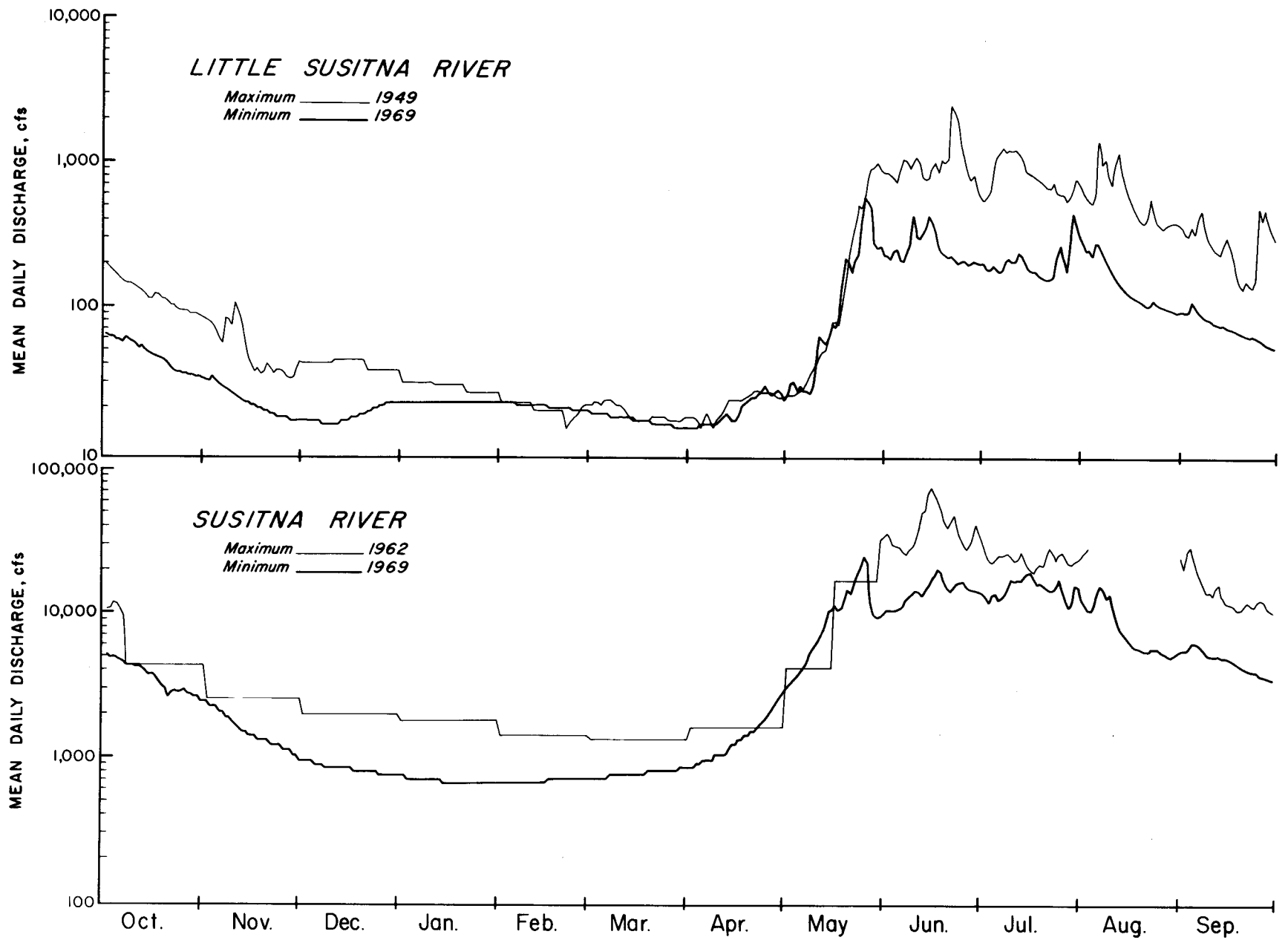
FIGURE 14 – HYDROGRAPHS – Little Susitna River / Susitna River

CHAKACHATNA RIVER
Maximum ——————— 1971
Minimum ————— 1970

TERROR RIVER
Maximum ———— 1967
Minimum ———— 1966
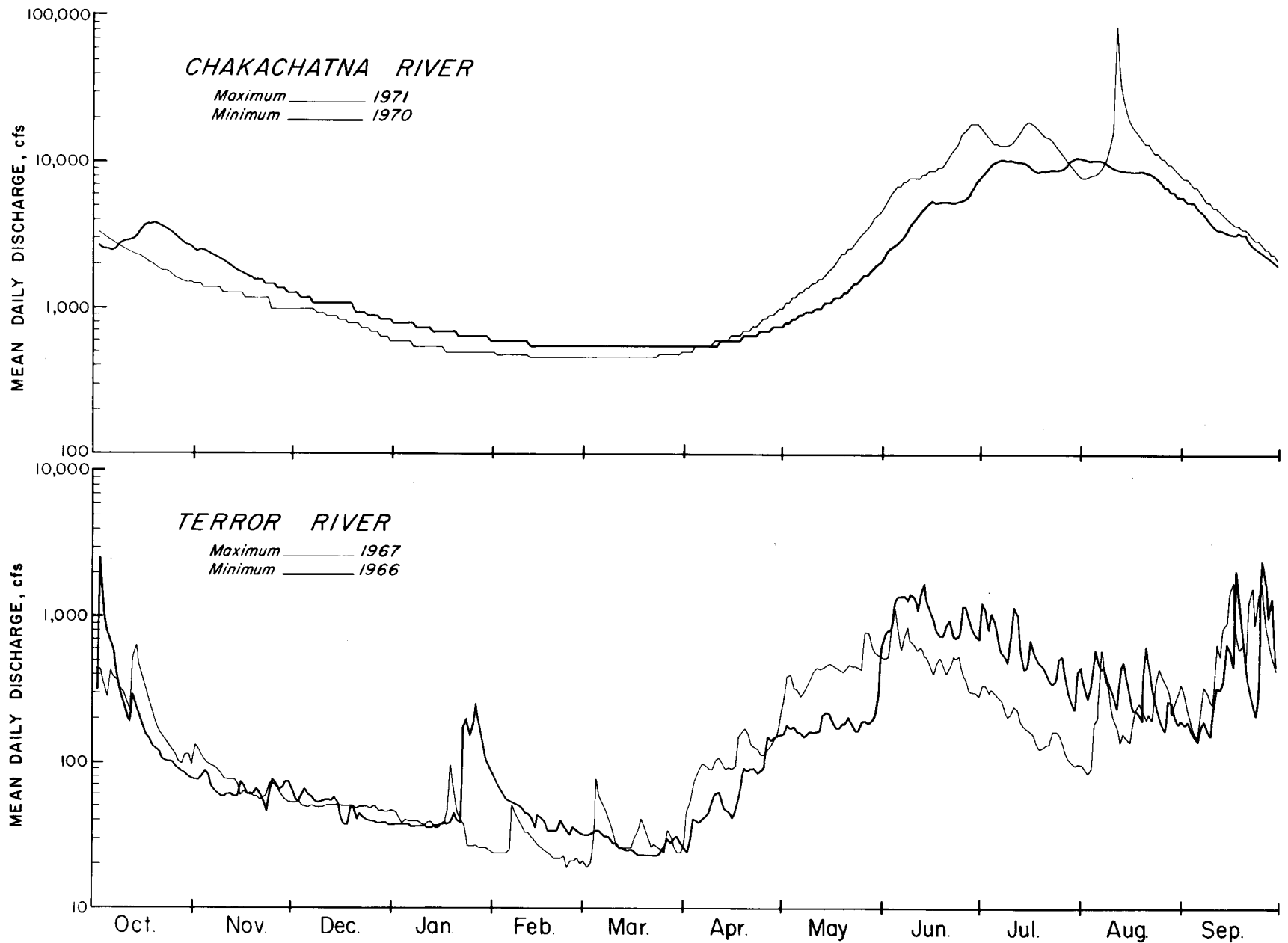
FIGURE 15 - HYDROGRAPHS - Chakachatna River / Terror River

131
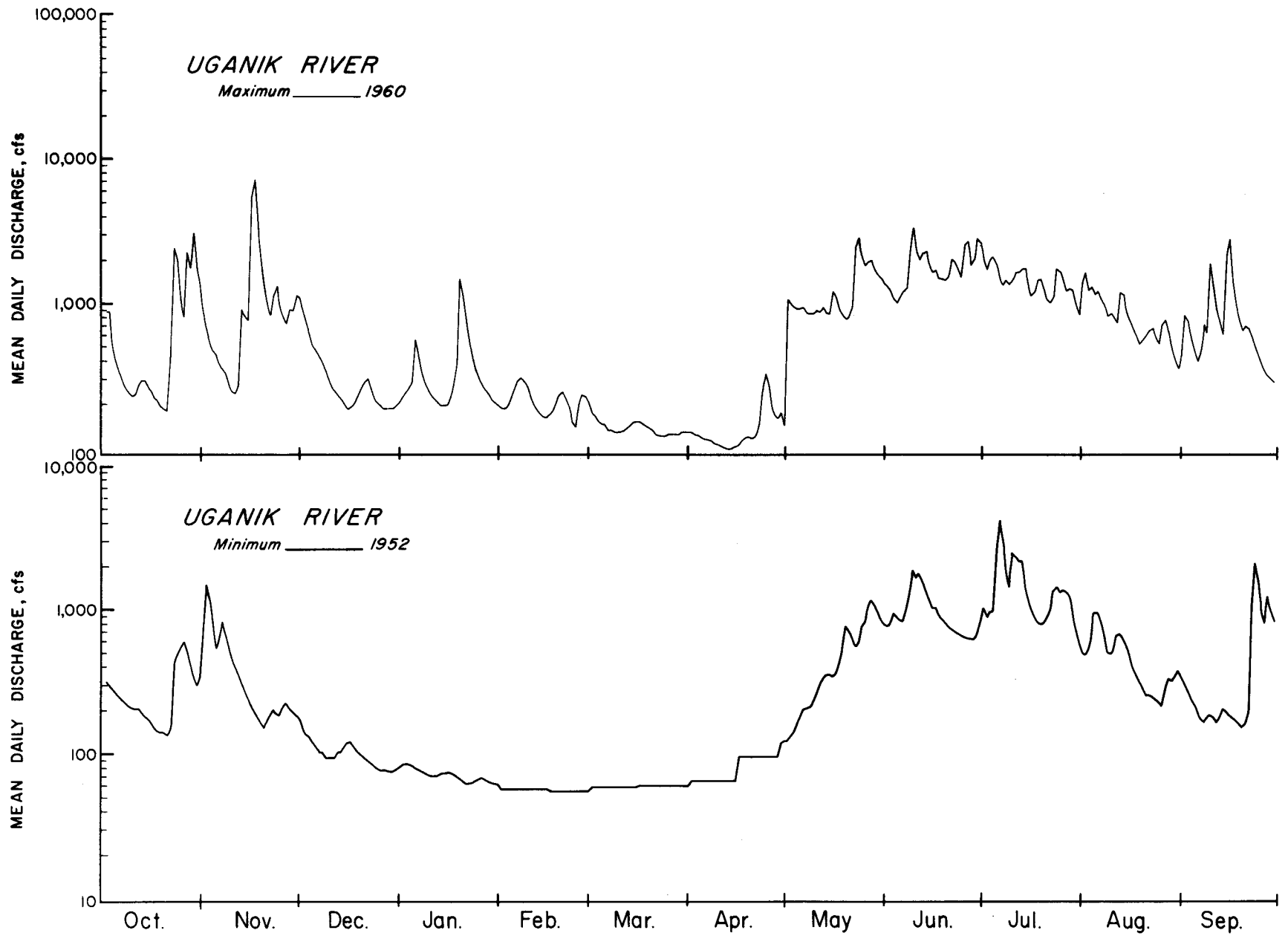
FIGURE 16-HYDROGRAPHS-Uganik River
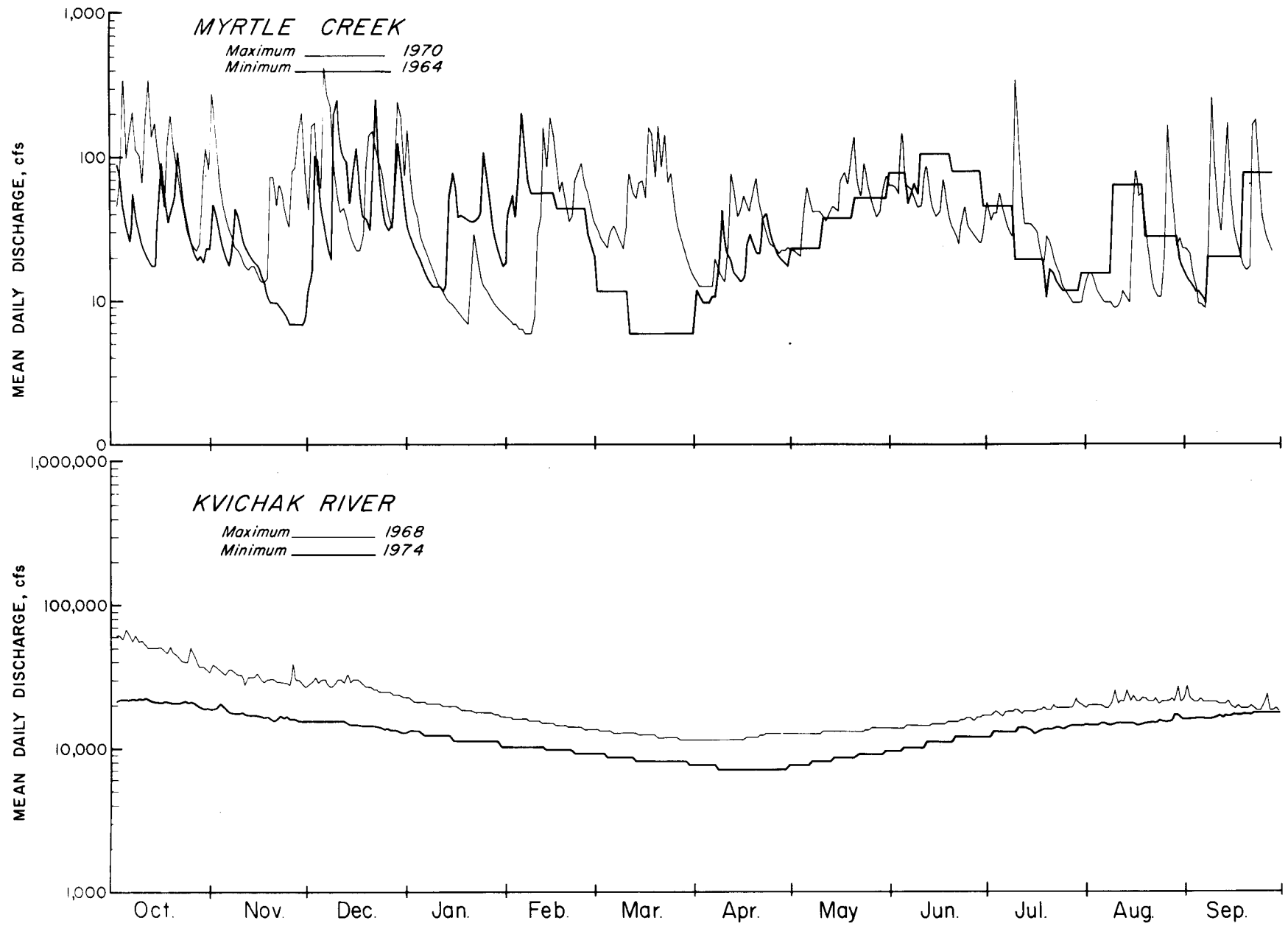
FIGURE 17 – HYDROGRAPHS – Myrtle Creek / Kvichak River
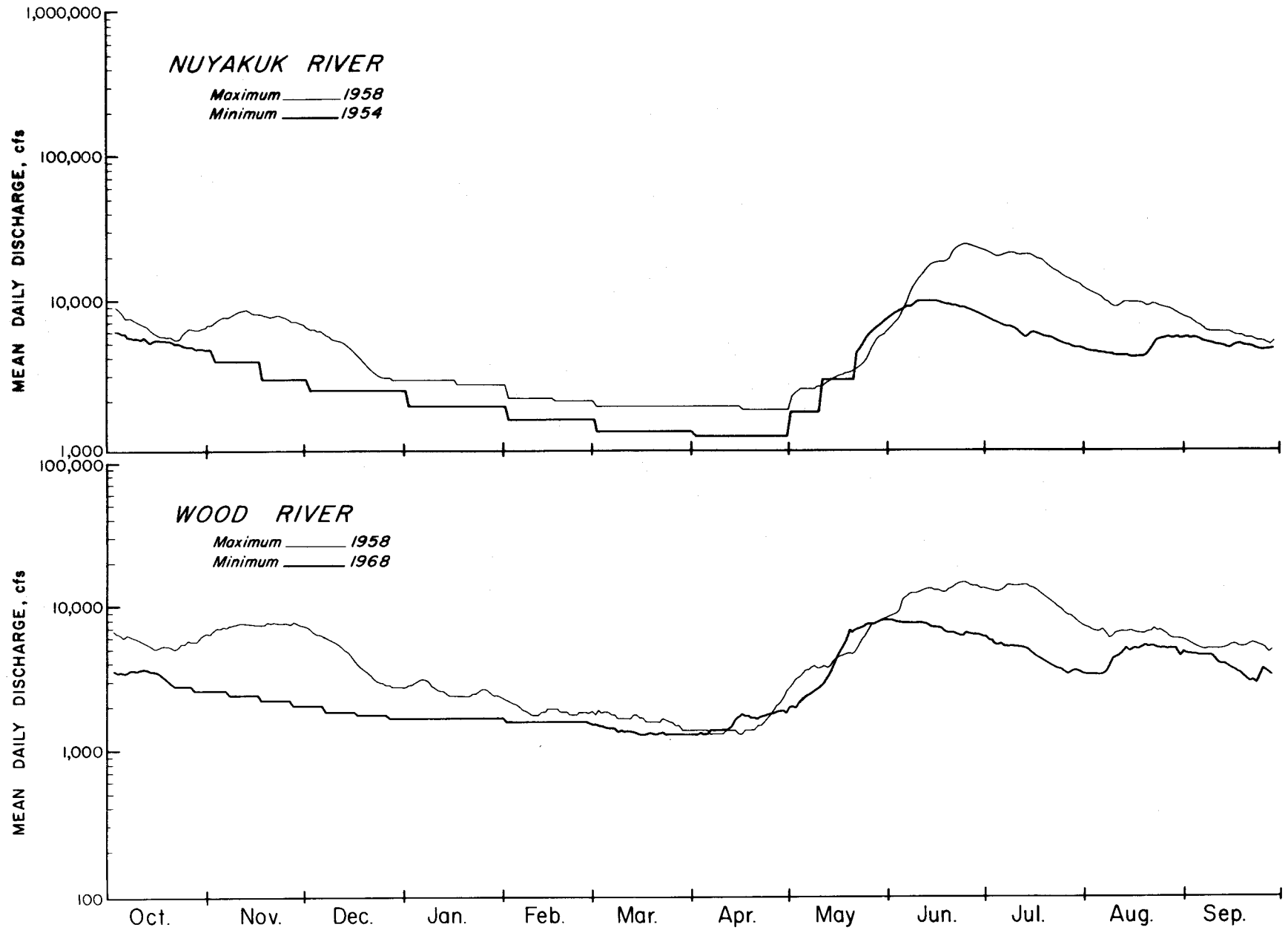
FIGURE 18 – HYDROGRAPHS – Nuyakuk River / Wood River

134
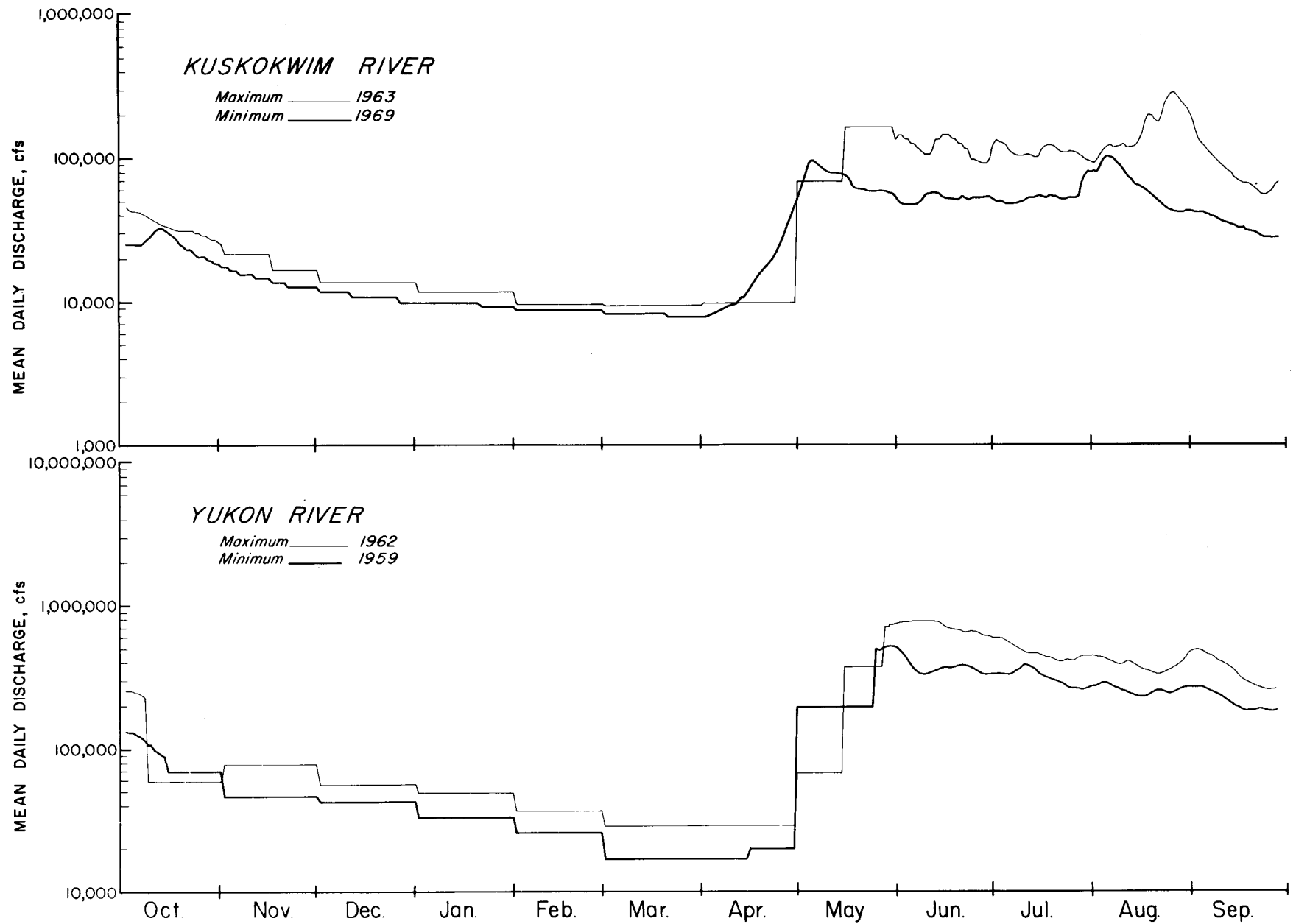
FIGURE 19 – HYDROGRAPHS – Kuskokwim River / Yukon River
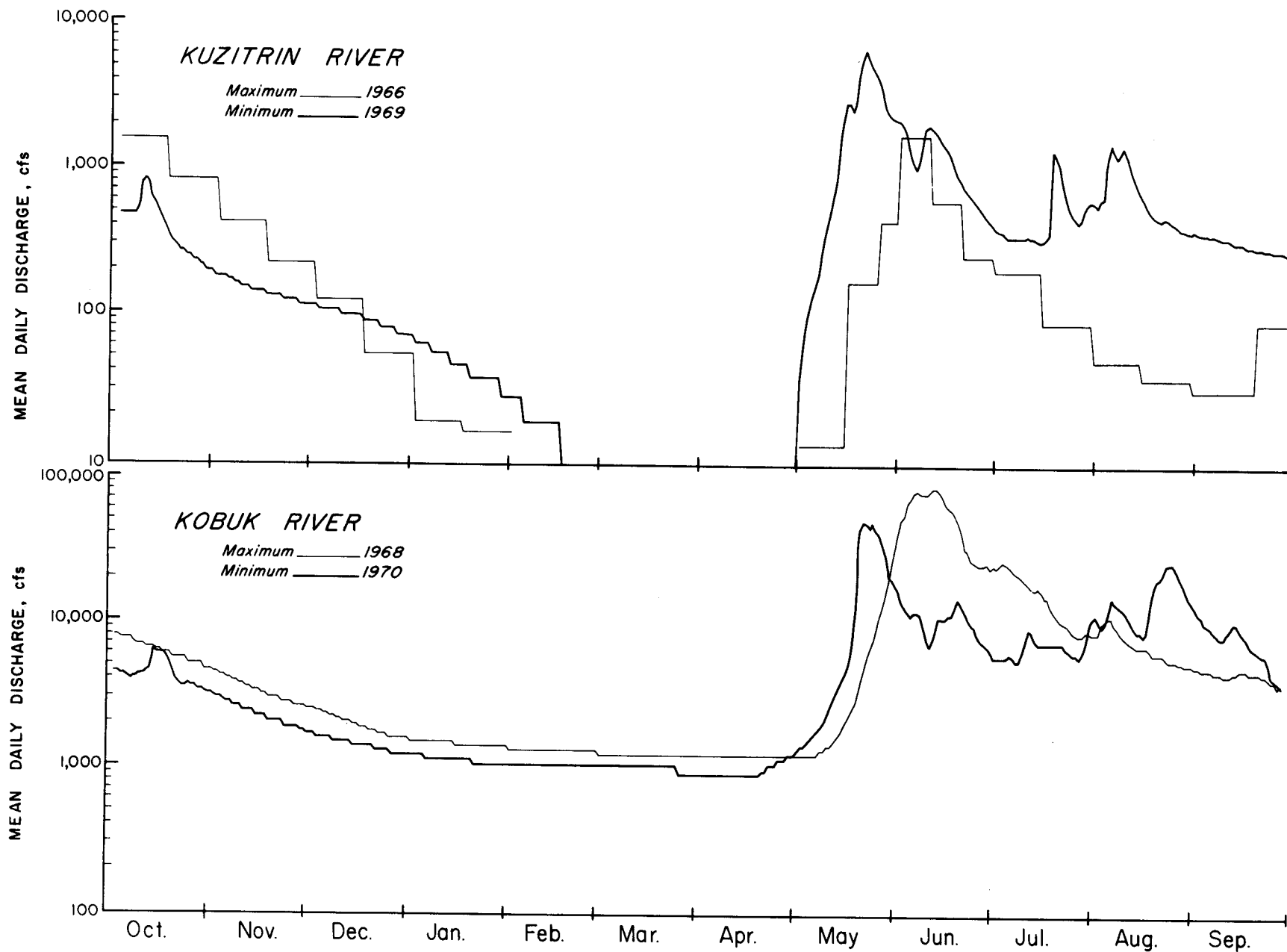
FIGURE 20 – HYDROGRAPHS – Kuzitrin River / Kobuk River
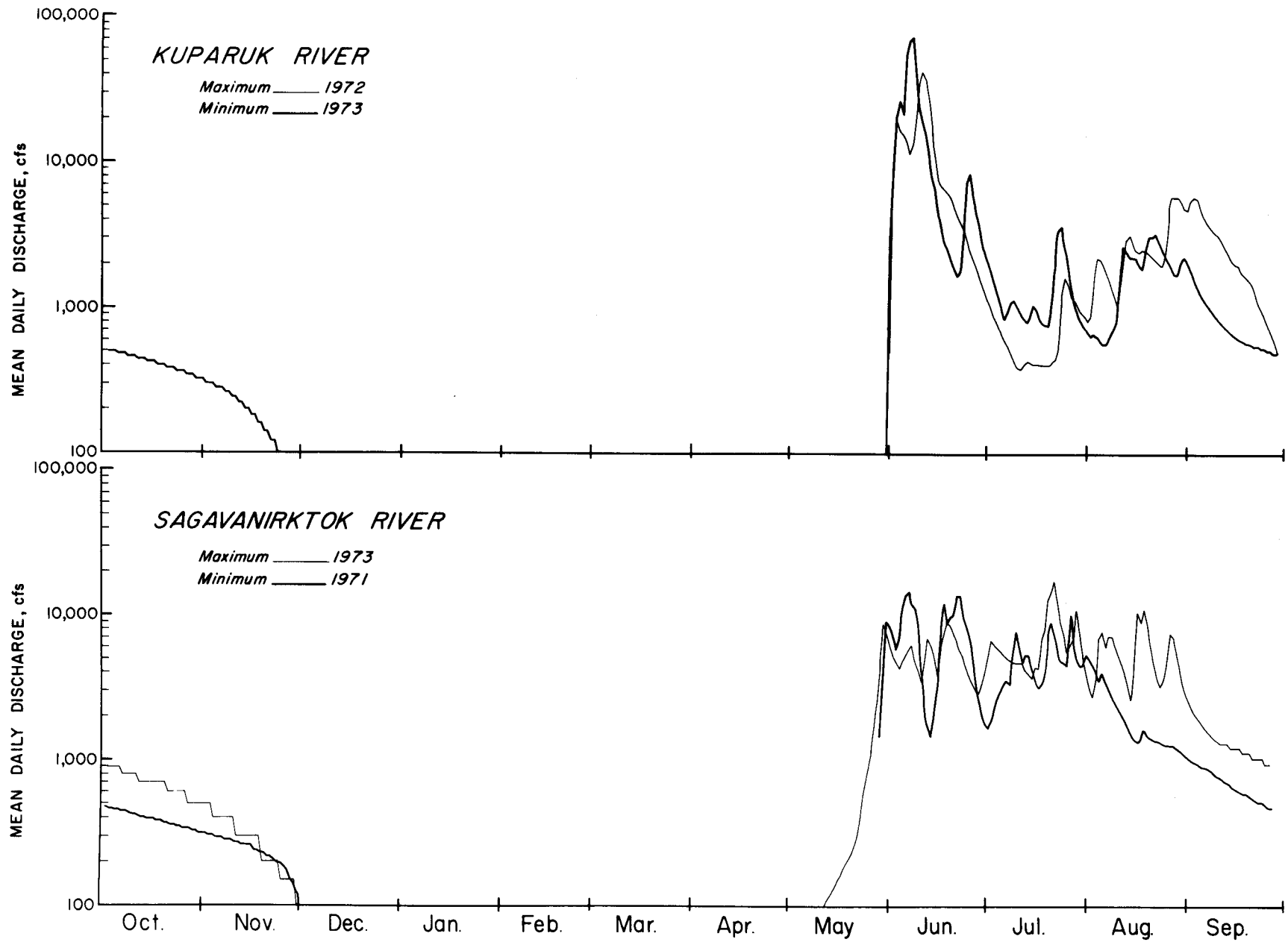
FIGURE 21-HYDROGRAPHS - Kuparuk River / Sagavanirktok

137

D. Flow Duration Curves:

Flow duration curves (Figures 22 through 27) are a rank ordering of the magnitudes of daily mean flow during the entire period of record. The plots are arranged so as to enable one to associate a given rate of flow with the percent of time flow exceeded this rate over the length of record, i.e., the axes are streamflow in cubic feet per second vs. percent of time. Since the range of flows measured over the length of record are the endpoints of the flow duration curves, the range is stated on each respective flow duration curve plot.

E. Flow-Mass Curves:

A flow-mass curve (Figure 28) is the cumulative sum of the flow of a stream over its length of record. Often flow-mass curves are valuable for reservoir studies, but they also are valuable as subtle indicators of streamflow variability and seasonability. Normally, flow drops off quickly in the late autumn and reaches its lowest point during March and early April. This is especially true of the Arctic rivers and those which are in the continental climatic zone. This is indicated by a cyclic flow-mass curve which is somewhat predictable and is essentially a seasonally controlled variable. Rivers confined to the coastal areas, especially the smaller streams such as Power Creek near Cordova, Lowell Creek and Spruce Creek near Seward; Myrtle Creek; and the Terror and Uganik Rivers on Kodiak Island, all have high variability of flow which usually continues throughout the year. These

138
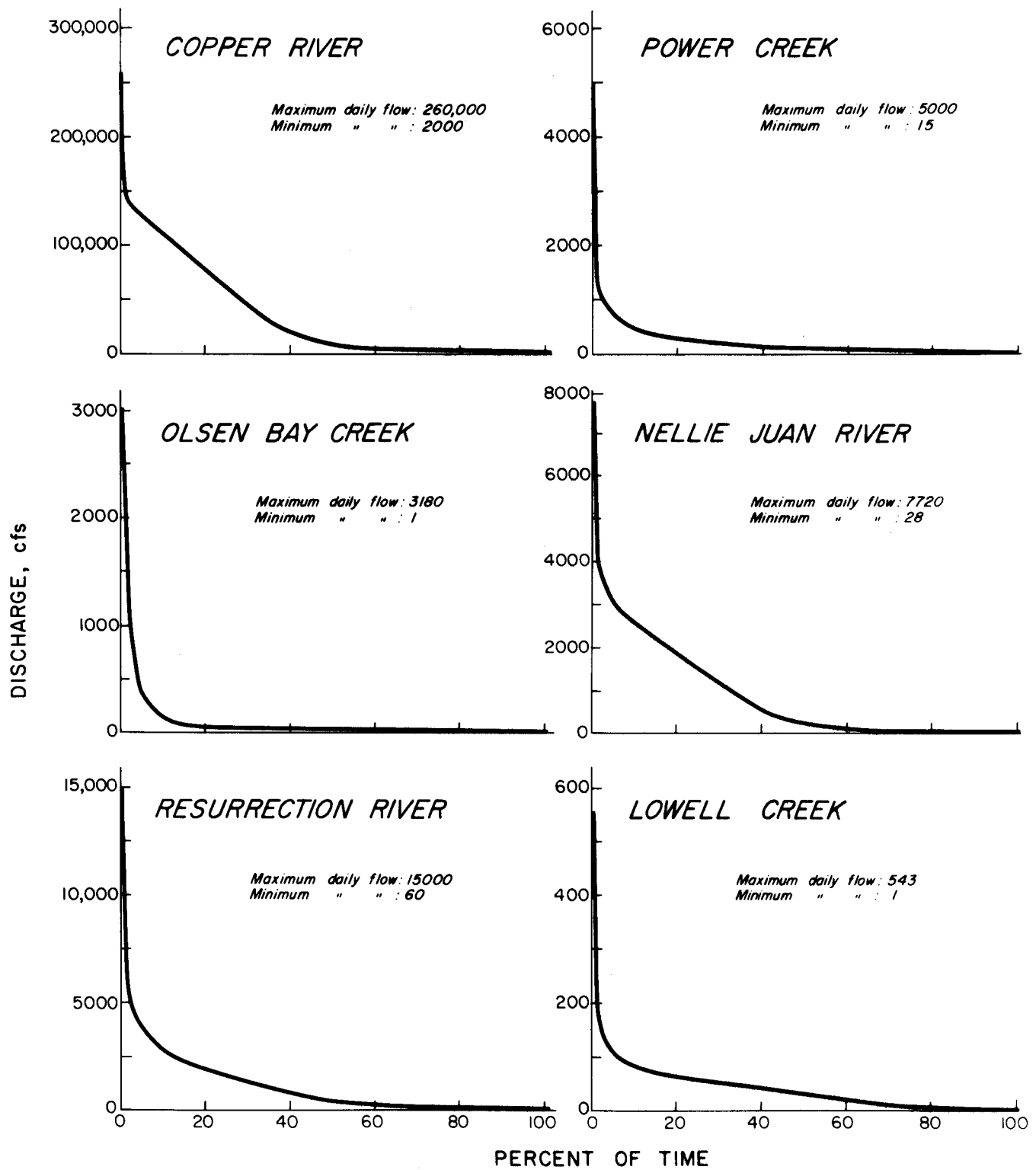
FIGURE 22 - FLOW DURATION CURVES

Copper River, Power and Olsen Bay Creeks, Nellie Juan and
Resurrection Rivers, and Lowell Creek

139
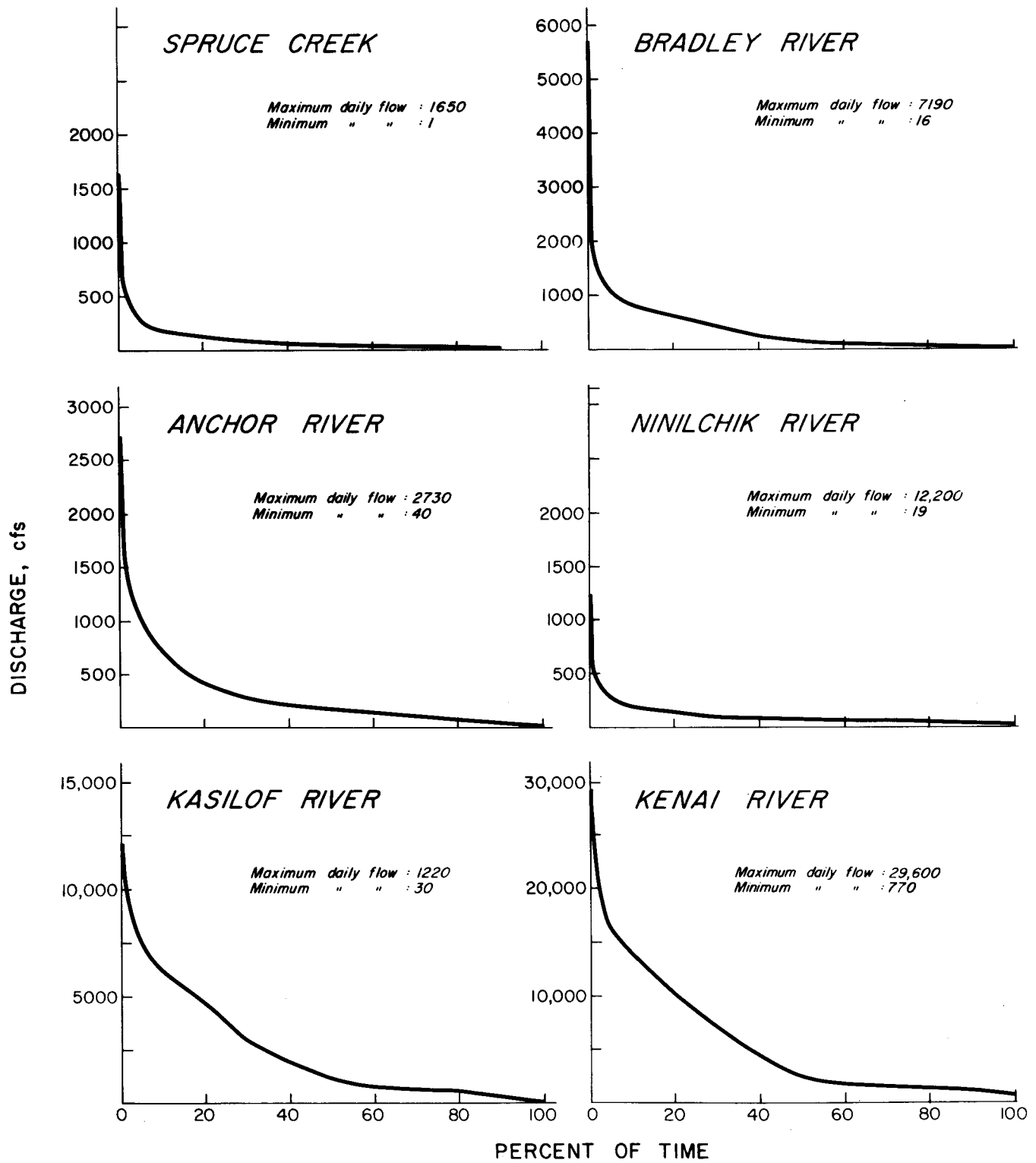
FIGURE 23 – FLOW DURATION CURVES

Spruce Creek, Bradley, Anchor, Ninilchik, Kasilof & Kenai Rivers

140
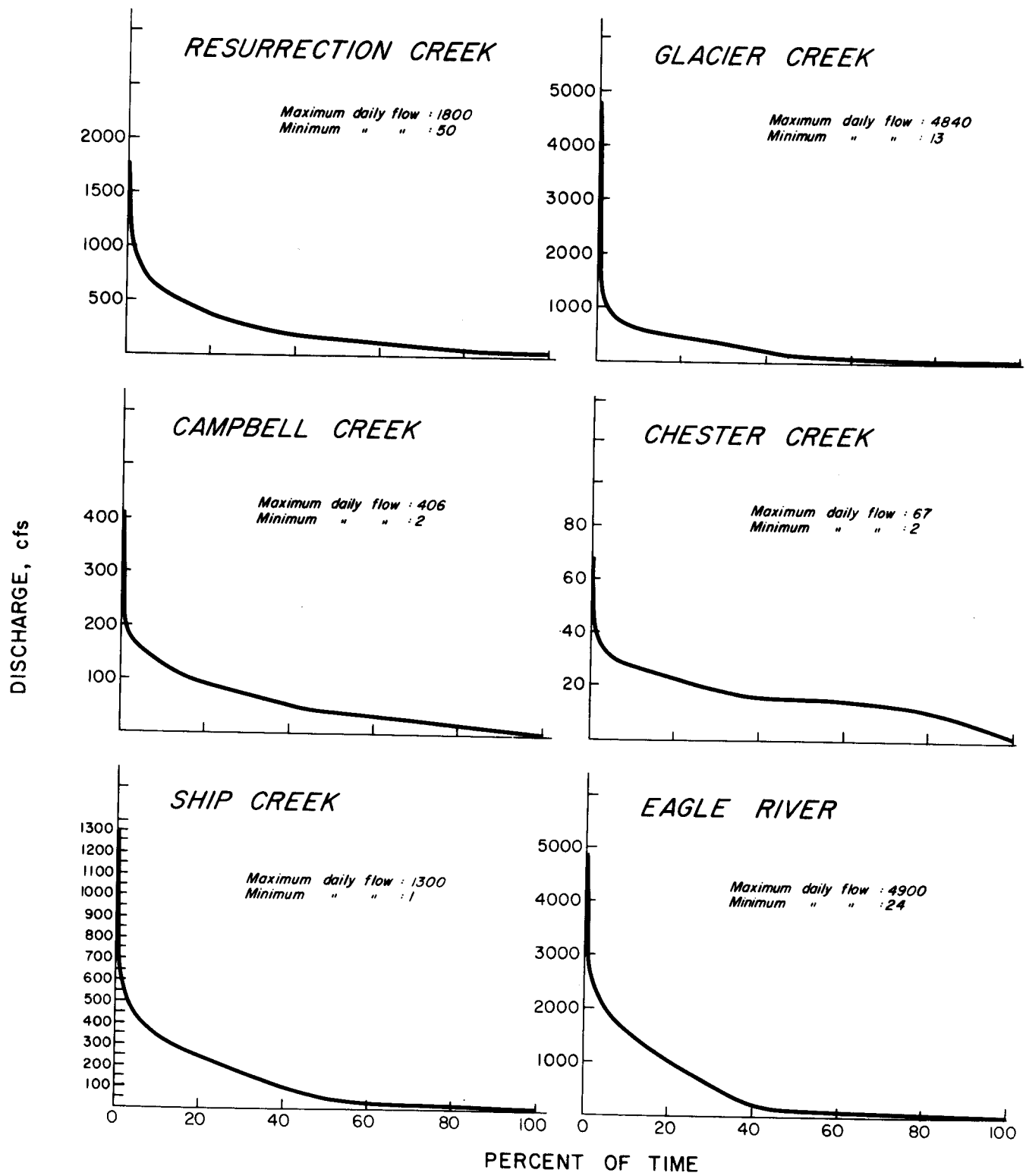
FIGURE 24 - FLOW DURATION CURVES

Resurrection, Glacier, Campbell, Chester, & Ship Creeks and Eagle River

141
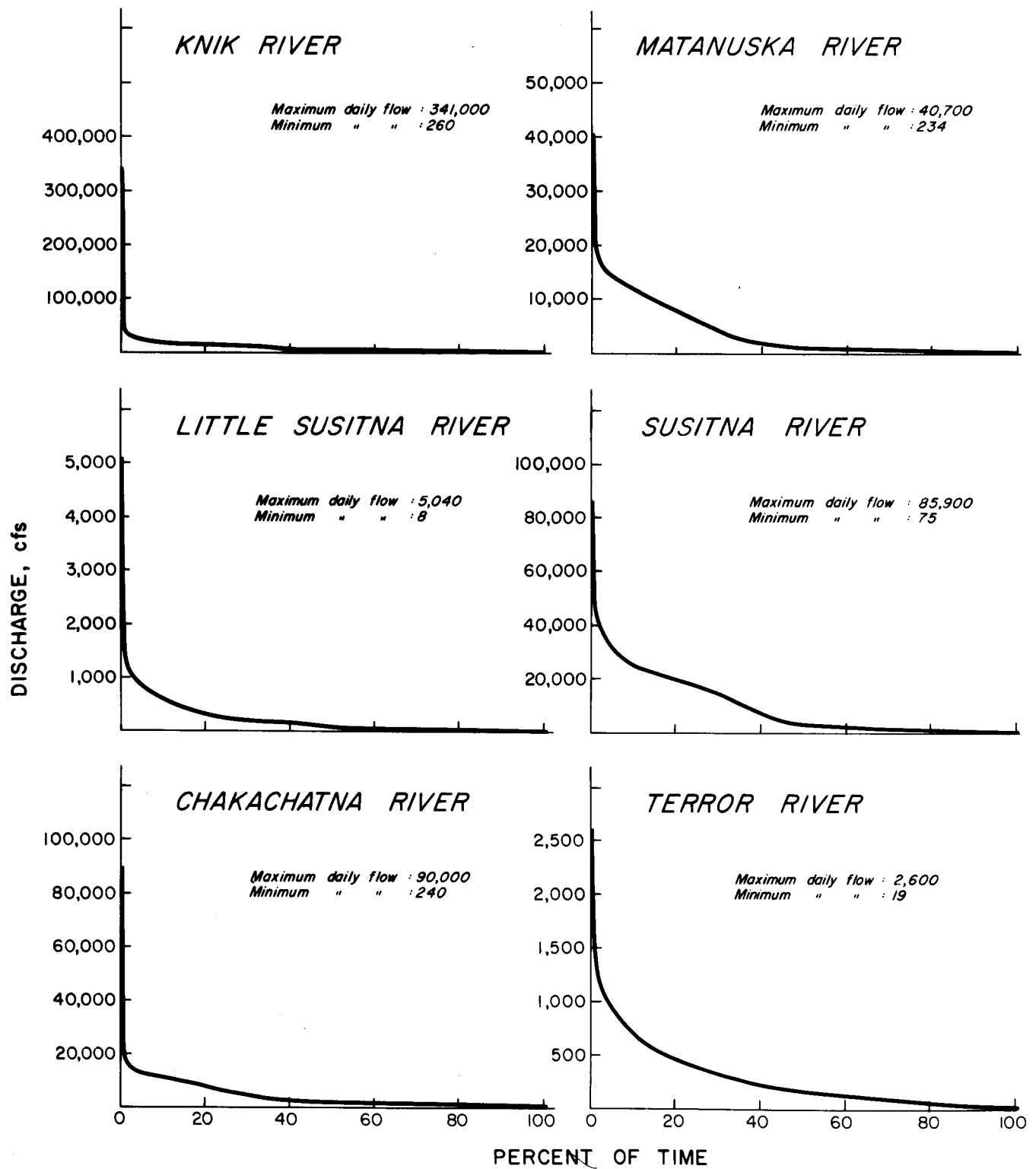
FIGURE 25 – FLOW DURATION CURVES

Knik, Matanuska, Little Susitna, Susitna, Chakachatna &
Terror Rivers

142
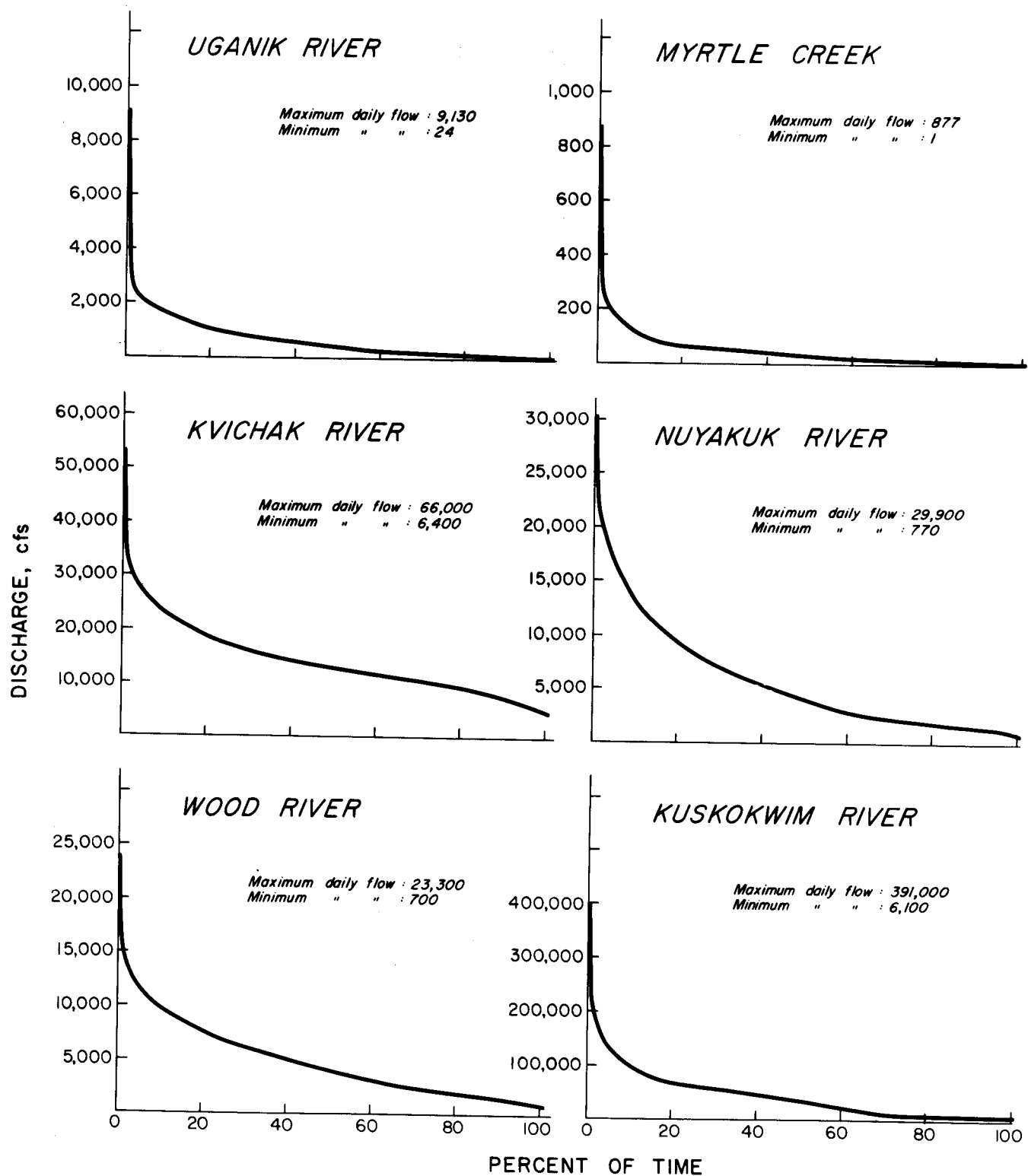
FIGURE 26 – FLOW DURATION CURVES

Uganik River, Myrtle Creek, Kvichak, Nuyakuk, Wood and Kuskokwim Rivers

143
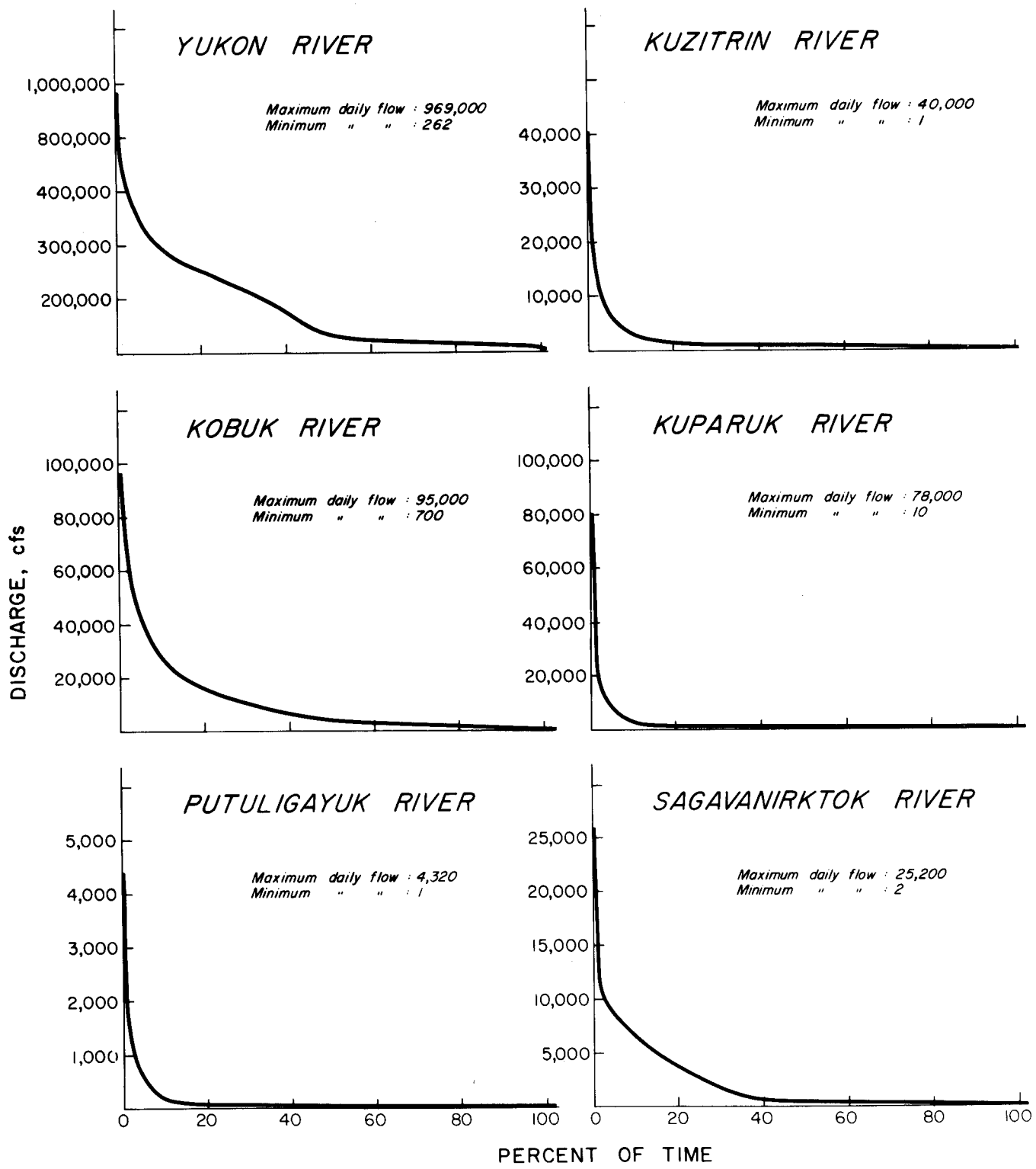
FIGURE 27 – FLOW DURATION CURVES

Yukon, Kuzitrin, Kobuk, Kuparuk, Putuligayuk and Sagavanirktok Rivers
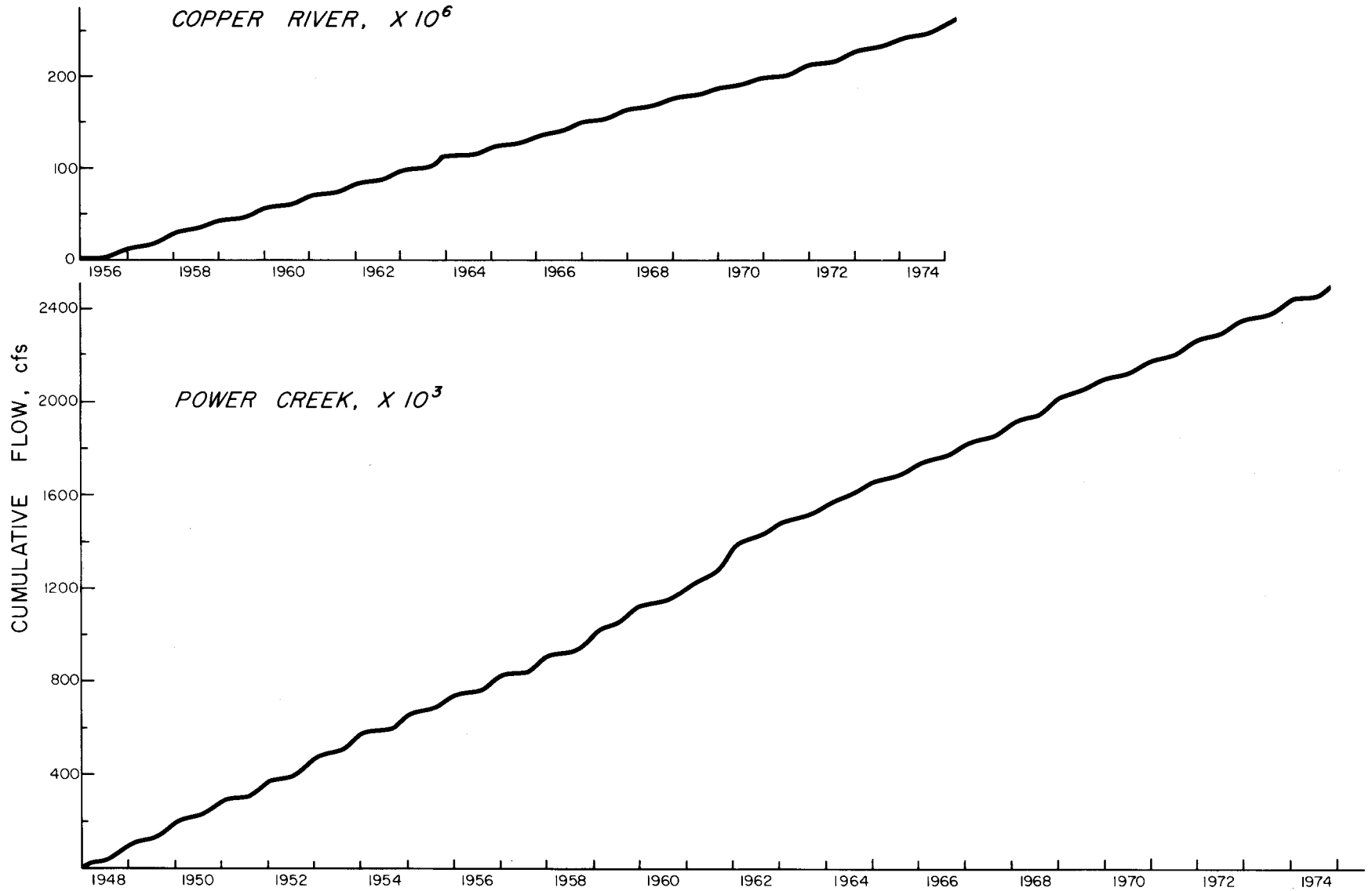
EXAMPLES OF FLOW MASS CURVES

FIGURE 28 – EXAMPLES OF FLOW MASS CURVES
Copper River and Power Creek

basins are probably more subject to thaw periods and rain-
storms in winter than are the larger coastal basins. Flow-
mass curves are illustrated by two examples, the Copper River
and Power Creek near Cordova. For the additional rivers, the
value of the average annual flow contribution is tabulated in
Table 5.

F.   Exceedance Series:

The following graphs (Figures 29 through 37) for each
river of OCS interest are plotted in order to show the his-
torical flow as a percentage of exceedance. This can best be
understood by discussing an example. For instance, the points
on the graph of the Copper River for July 1 (Figure 28) are
interpreted in the following way. Maximum flow on that date
was approximately 260,000 cubic feet per second (the uppermost
dark line). The second line (dashed) intercepts July 1 at
150,000 cubic feet per second. This is the 0.25 exceedance
curve, and indicates that on July 1, 25% of the years of
record had a flow which exceeded 150,000 cubic feet per second.
Likewise the third line (dotted) indicates that in one half of
the years of record (0.50 exceedance) flow exceeded 135,000
cubic feet per second on July 1. The bottom curve indicates
the minimum flow which has occurred on each date.

Period of record (P.O.R.) is indicated for each river on
the upper right edge of the exceedance graph. For some rivers,
the maximum and .25 exceedance curves will be the same because
only a few years of record exist for those rivers.

146

TABLE 5
AVERAGE ANNUAL FLOW-MASS VALUE

USGS Reference Number	River	Beginning Record CFS-Month	End of Record CFS	Period of Record (POR) Years	Avg. Annual Value CFS-Year
15212000	Copper	$ 440,200	242,396,420	19	8,343,310
15219000	W. F. Olsen Bay Cr.	799	359,122	6	59,720
15216000	Power Cr.	9,700	2,495,000	27	92,048
15237000	Nellie Juan R.	4,640	1,501,102	4.5	332,544
15237700	Resurrection R. Nr., Seward	36,518	1,551,409	3.33	403,944
15238500	Lowell Cr.	667	52,002	<1.0	15,415
15238600	Spruce Cr.	7,964	190,749	7.0	26,112
15239000	Bradly R.	20,656	2,516,850	17.0	1,468,835
15240000	Anchor R.	10,316	1,419,686	13.0	108,413
15241600	Ninilchik R.	6,597	395,959	10.4	37,390
15242000	Kasilof R.	128,660	18,290,219	21.0	864,836
15258000	Kenai R.	121,780	26,833,381	26.0	1,027,369
15267900	Resurrection Cr. (Hope)	11,320	633,374	7.0	88,865
15272550	Glacier Cr.	5,884	834,926	9.0	92,116
15274600	Campbell Cr.	2,577	166,715	8.0	20,517
15275100	Chester Cr.	399	44,224	9.75	4,495
15276000	Ship Cr.	6,200	382,945	12.5	30,139
15277100	Eagle R.	13,170	1,507,742	8.0	186,821
15281000	Knik R.	118,490	35,283,653	14.0	2,511,797
15284000	Matanuska R.	72,390	32,752,329	23.0	1,420,867
15290000	Little Susitna R.	4,237	2,764,635	27.0	102,393
15292000	Susitna R.	196,370	85,475,225	24.0	3,553,285
15294500	Chakachatna R.	62,670	17,308,733	13.0	1,326,620
15295700	Terror R.	1,017	463,929	4.0	115,728
15296000	Uganik R.	9,550	5,247,624	22.0	238,094
15297200	Myrtle Cr.	450	177,919	10.33	17,179
15300500	Kvichak R.	889,000	40,878,420	6.167	6,484,420
15302000	Nuyakuk R.	183,190	44,487,480	21.0	2,109,728

147

TABLE 5 CONTINUED

USGS Reference Number	River	Beginning Record CFS-Month	End of Record CFS	Period of Record (POR) Years	Avg. Annual Value CFS-Year
15303600	Wood R.	210,000	28,350,000	13.0	2,164,615
15304000	Kuskokwim R.	1,162,200	397,850,000	24.0	16,428,658
15564800	Yukon R. (Ruby)	785,000	1,122,000,000	18.0	62,289,722
15712000	Kuzitrin R.	48	48,970,000	11.0	4,451,813
15744000	Kobuk R. (Ambler)	270,000	28,100,000	8.0	3,478,750
15896000	Kuparuk R.	10	199,800	4.0	49,948
15896700	Putuligayuk R.	100	45,080	4.0	11,245
15910000	Sagavanirktok R.	35,000	2,715,000	4.0	670,000
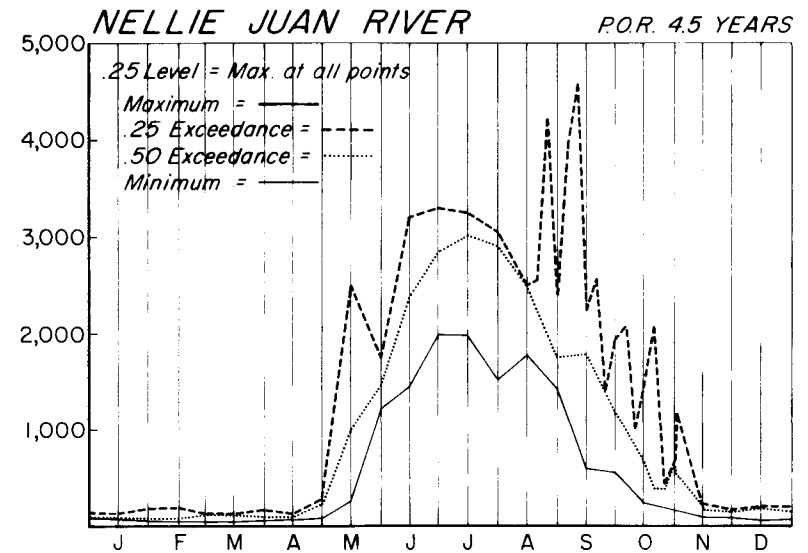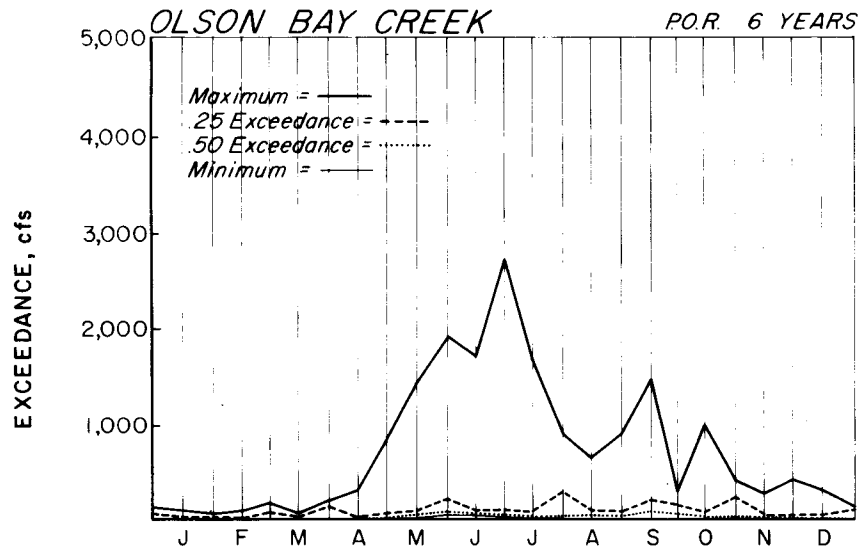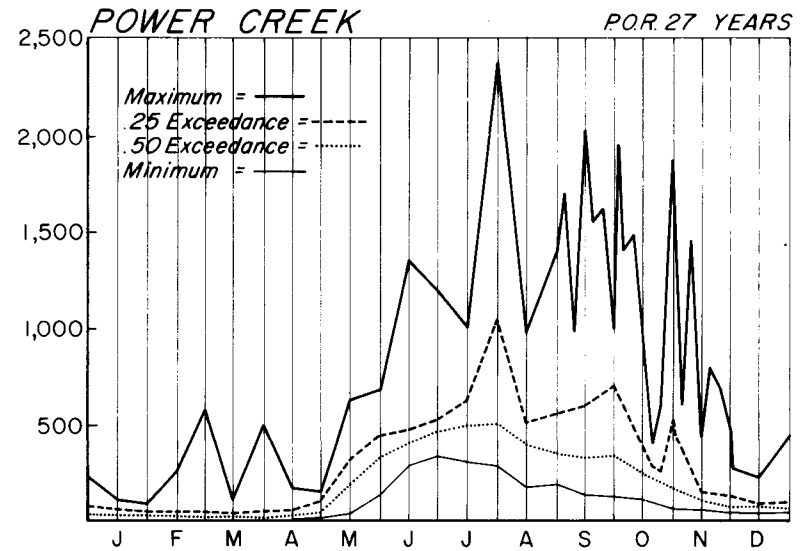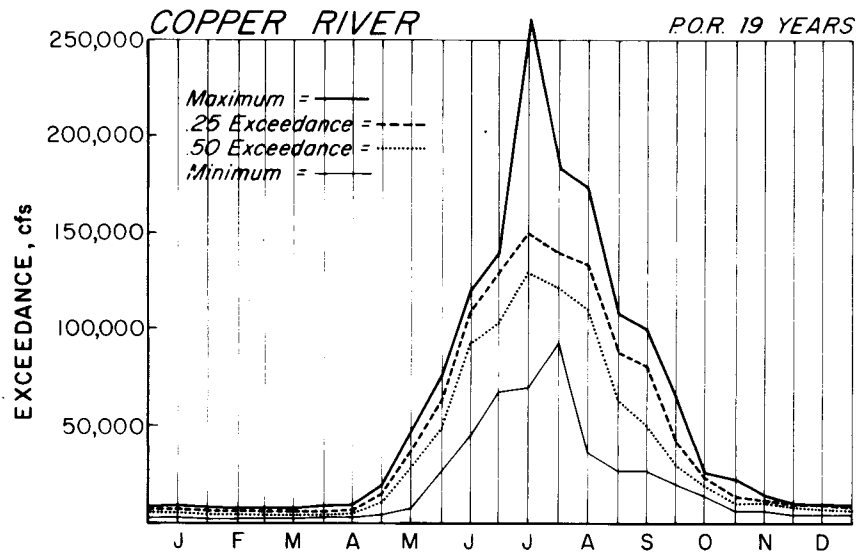
FIGURE 29 – EXCEEDANCE PROBABILITIES BASED ON PERIOD OF RECORD (POR)
Copper River, Power Creek, Olson Bay Creek, & Nellie Juan River

149
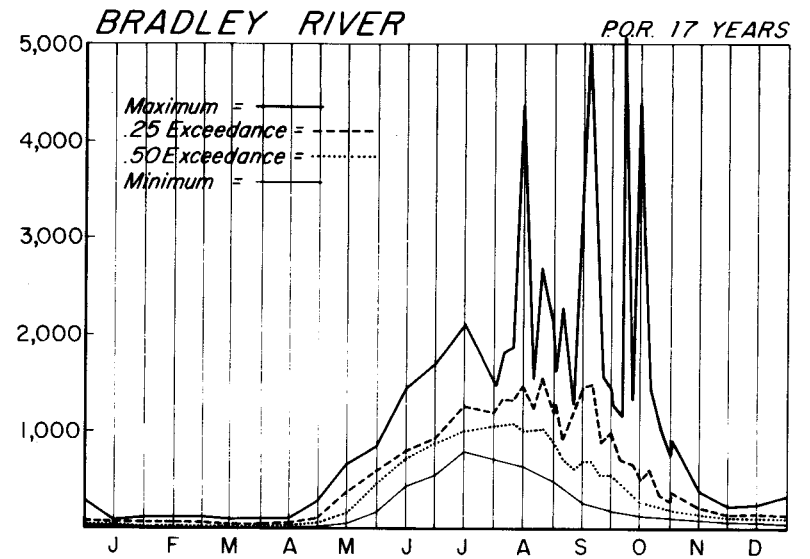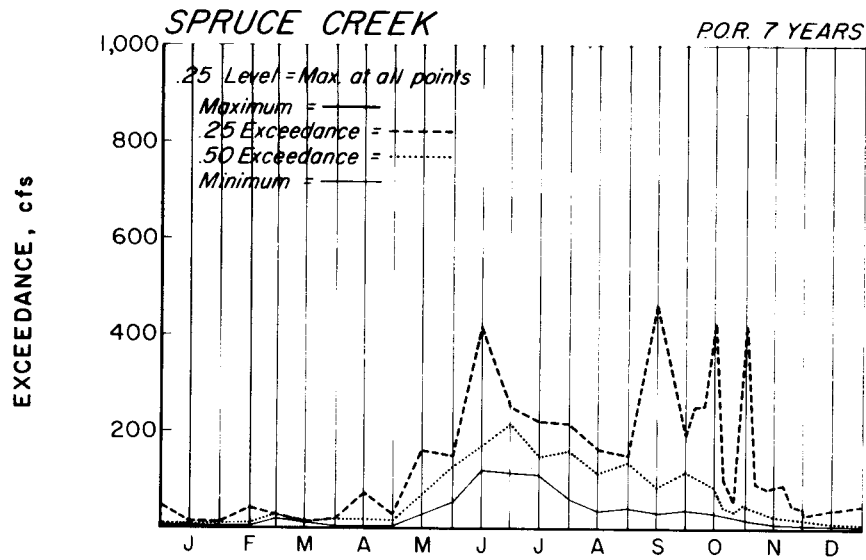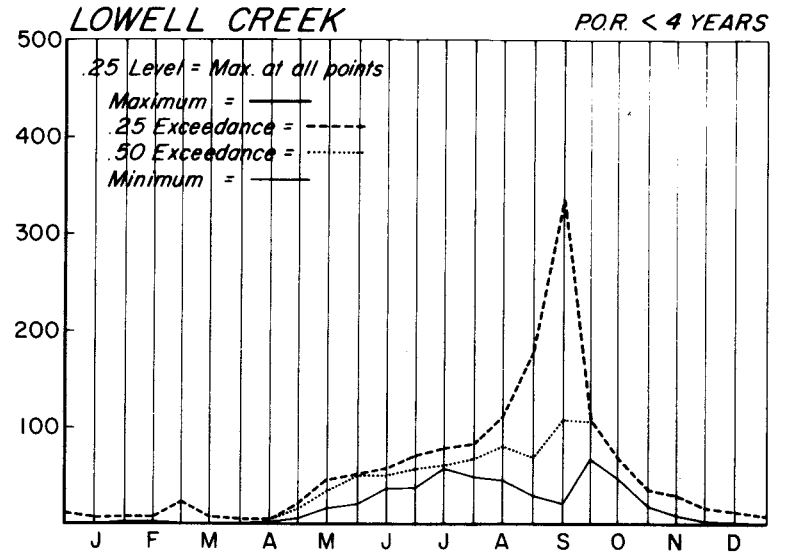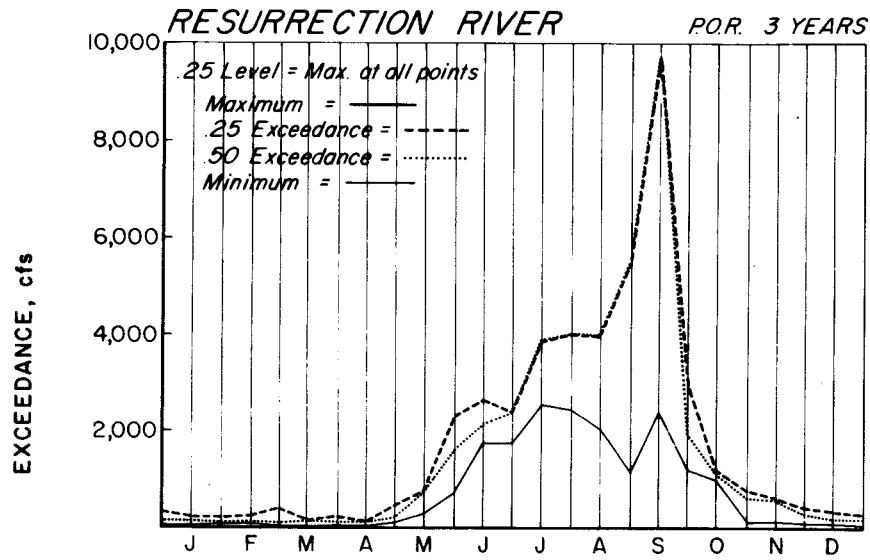
FIGURE 30 – EXCEEDANCE PROBABILITIES BASED ON PERIOD OF RECORD (POR)
Resurrection River, Lowell Creek, Spruce Creek & Bradley River
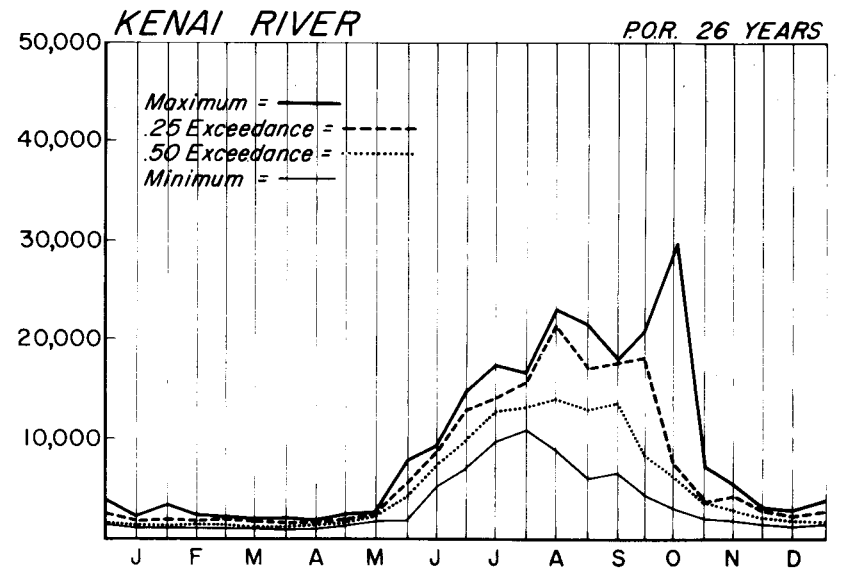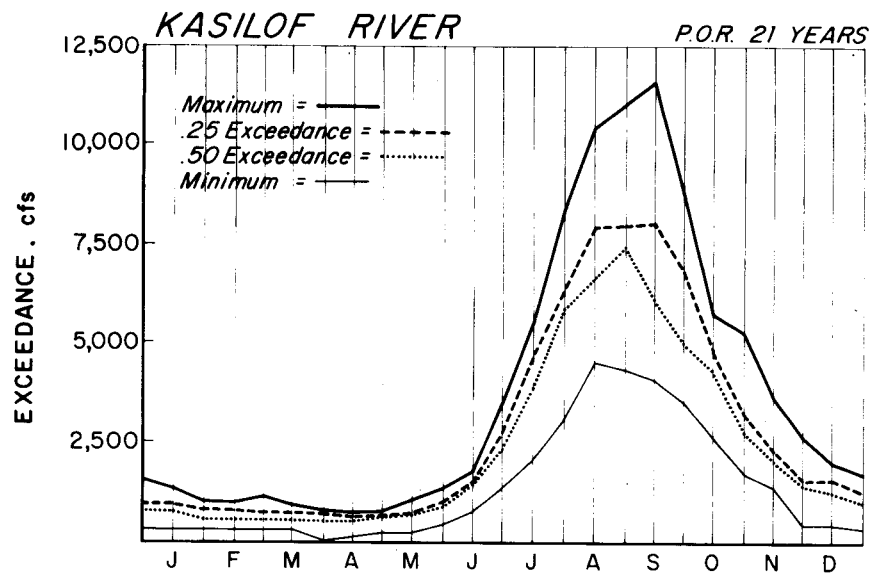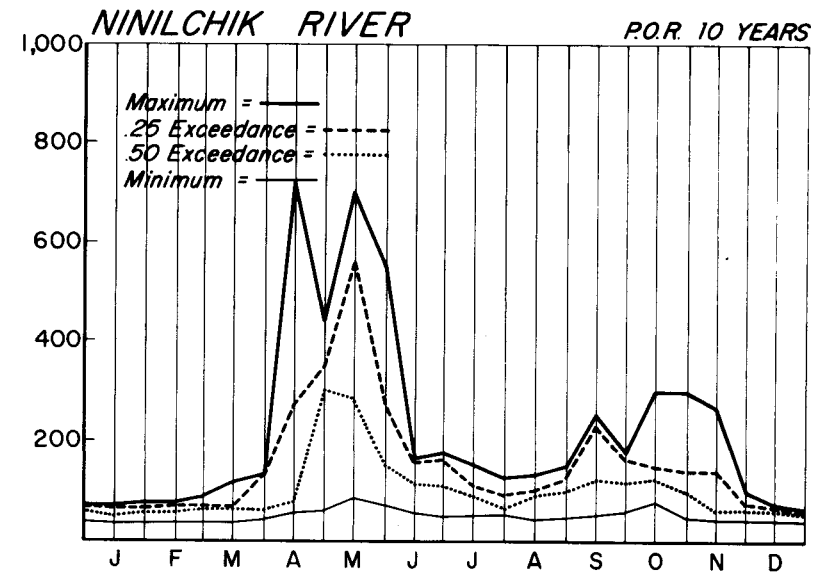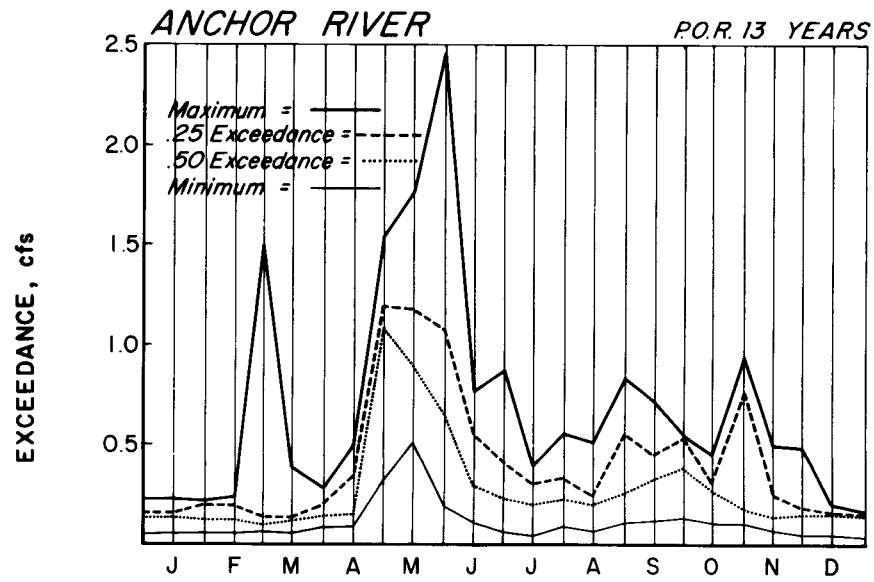
FIGURE 31—EXCEEDANCE PROBABILITIES BASED ON PERIOD OF RECORD (POR)
Anchor, Ninilchik, Kasilof & Kenai Rivers

151
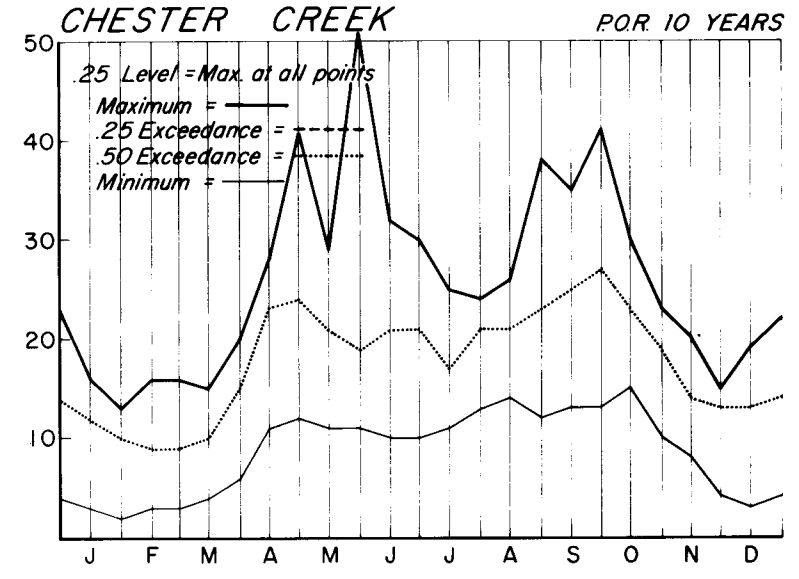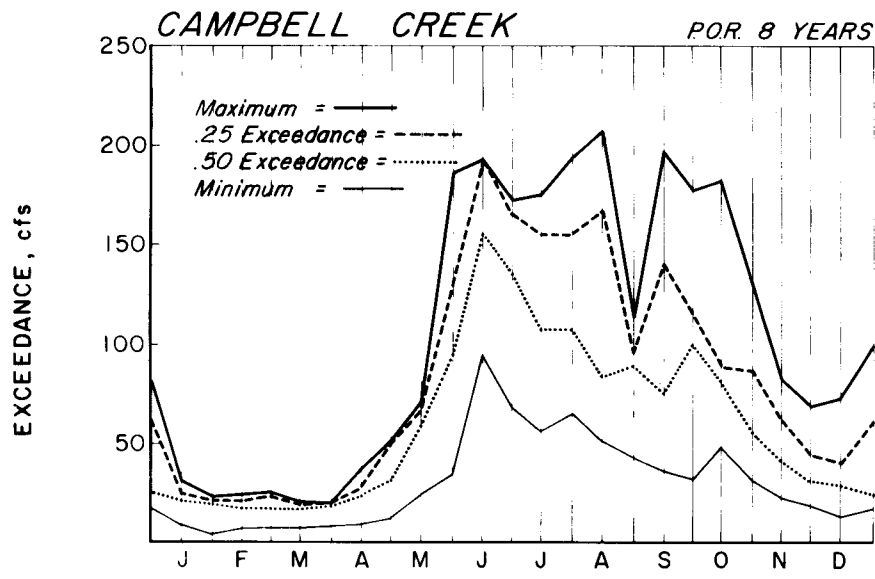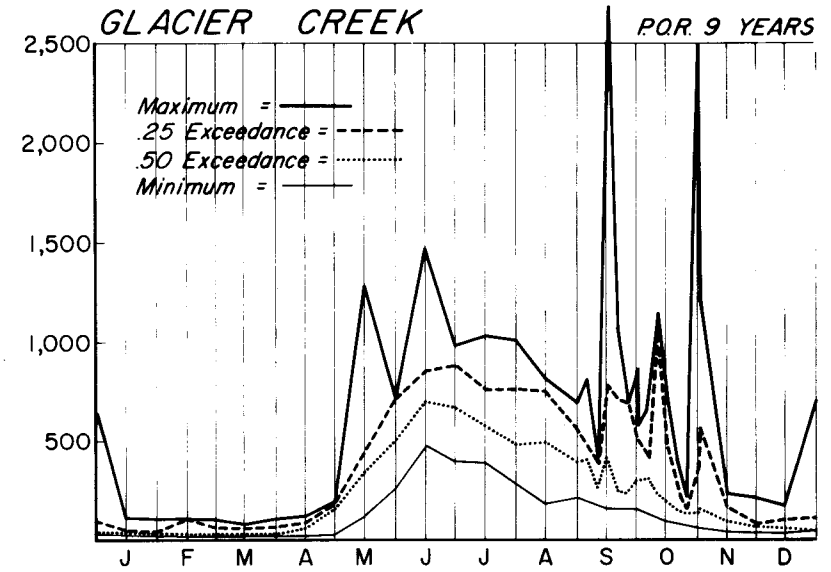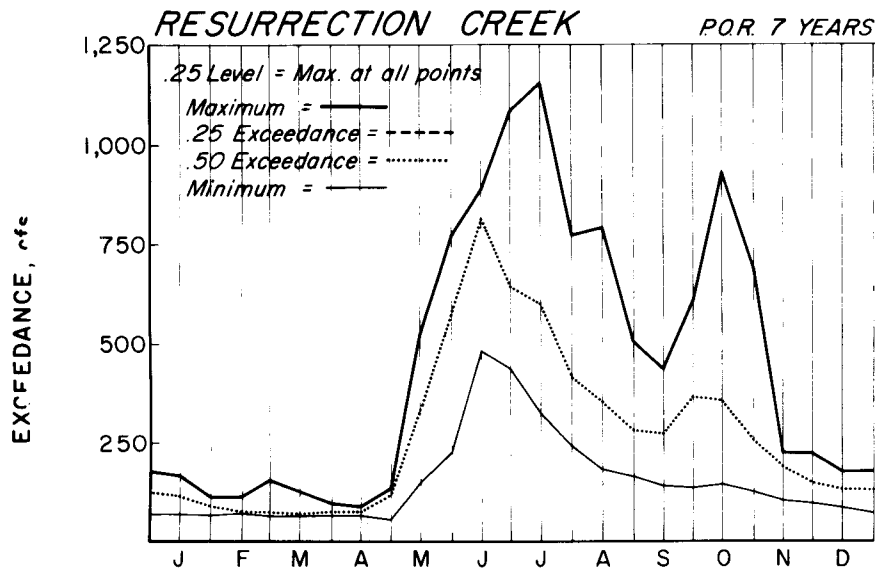
FIGURE 32 – EXCEEDANCE PROBABILITIES BASED ON PERIOD OF RECORD (POR)
Resurrection, Glacier, Campbell & Chester Creeks
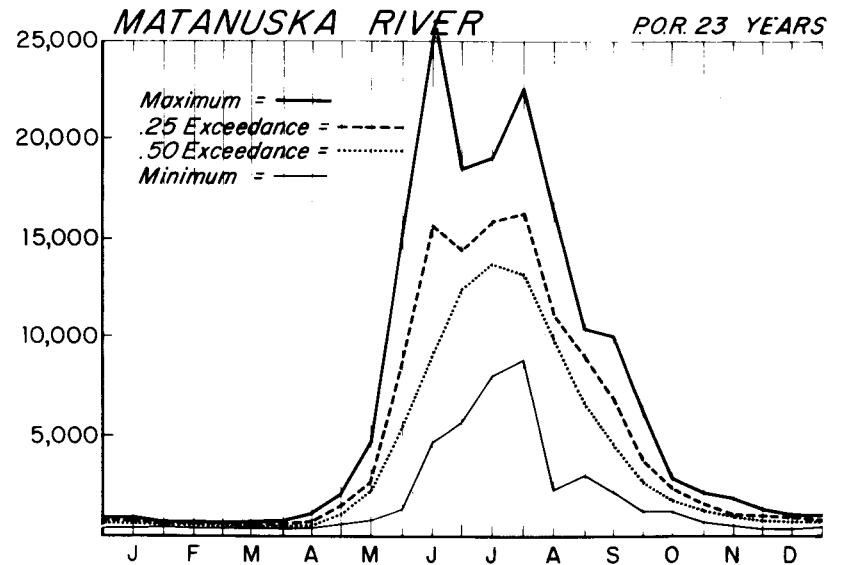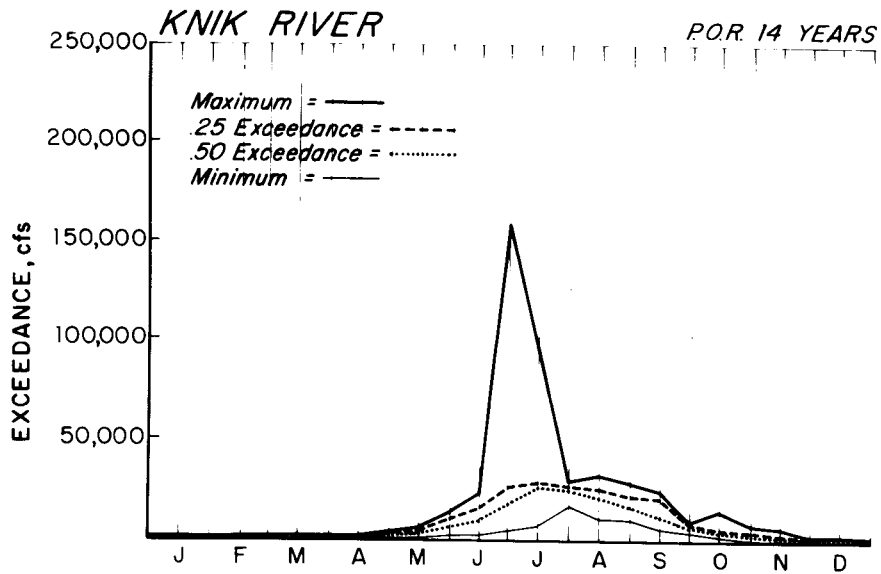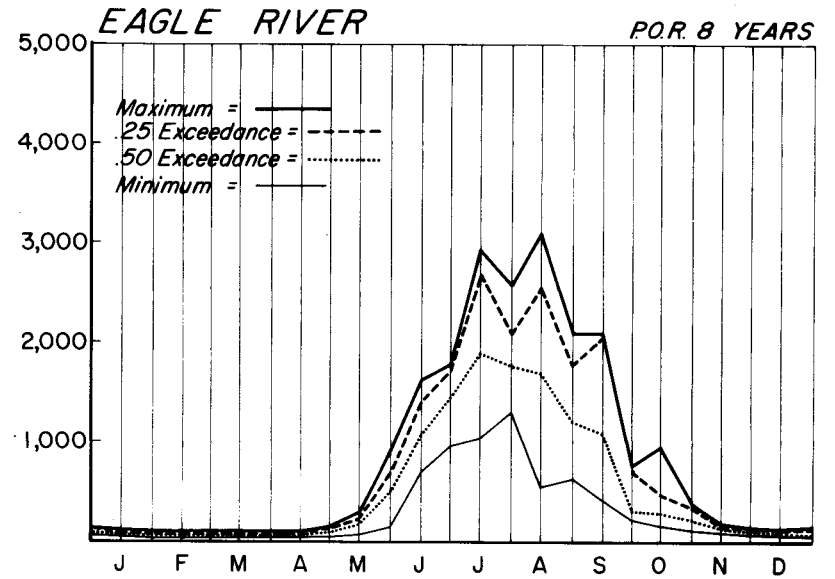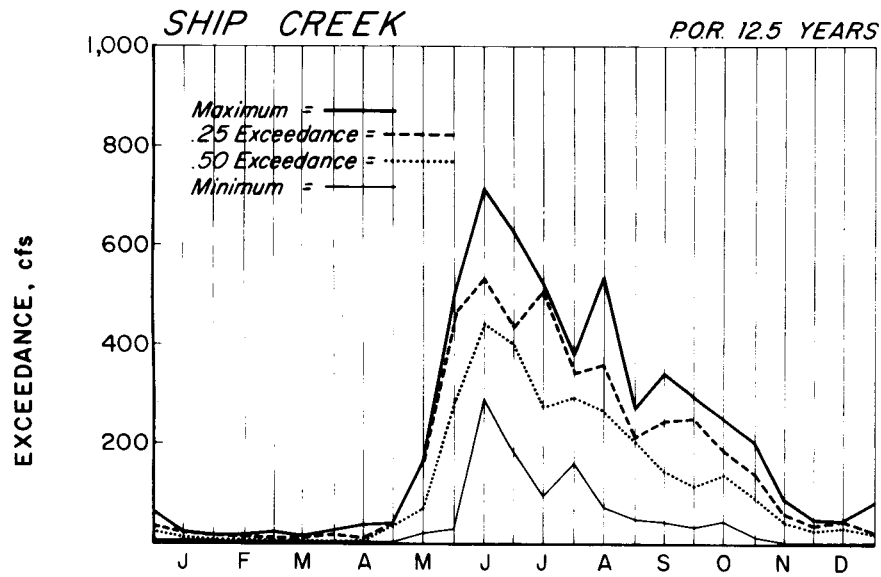
FIGURE 33 – EXCEEDANCE PROBABILITIES BASED ON PERIOD OF RECORD (POR)
Ship Creek, Eagle, Knik & Matanuska Rivers
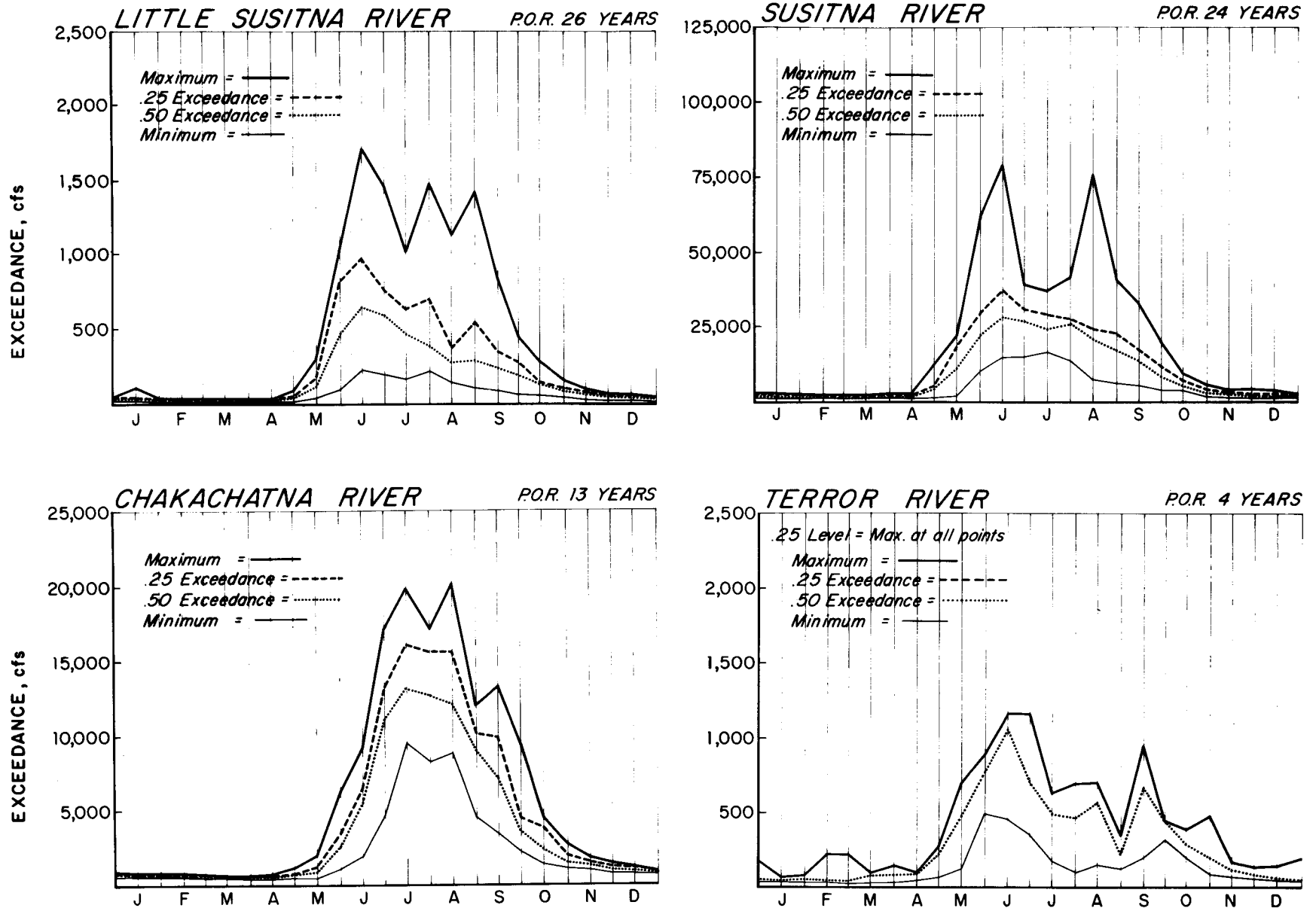
FIGURE 34 — EXCEEDANCE PROBABILITIES BASED ON PERIOD OF RECORD (POR)
Little Susitna, Susitna, Chakachatna & Terror Rivers

154
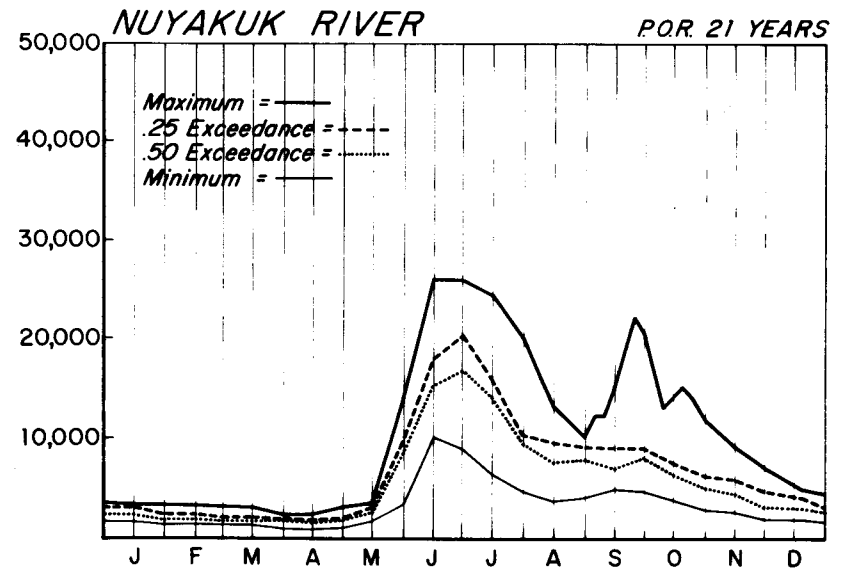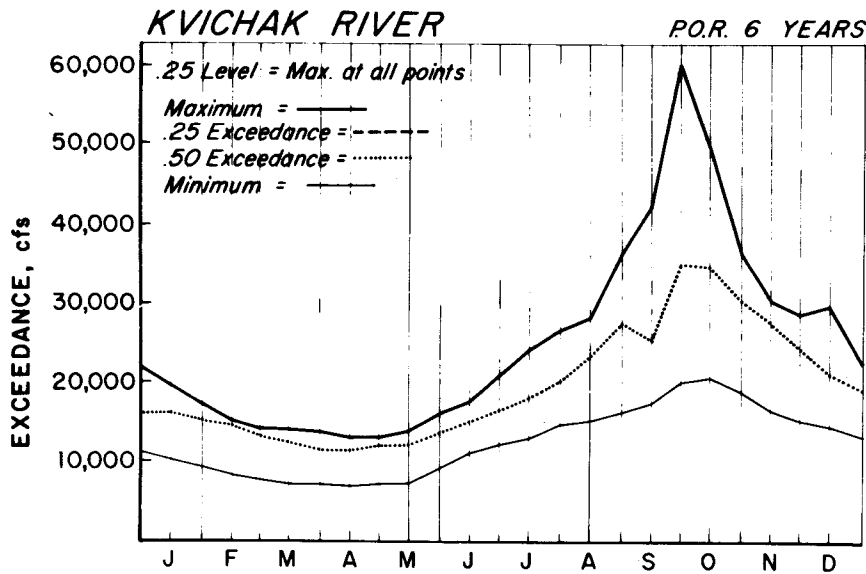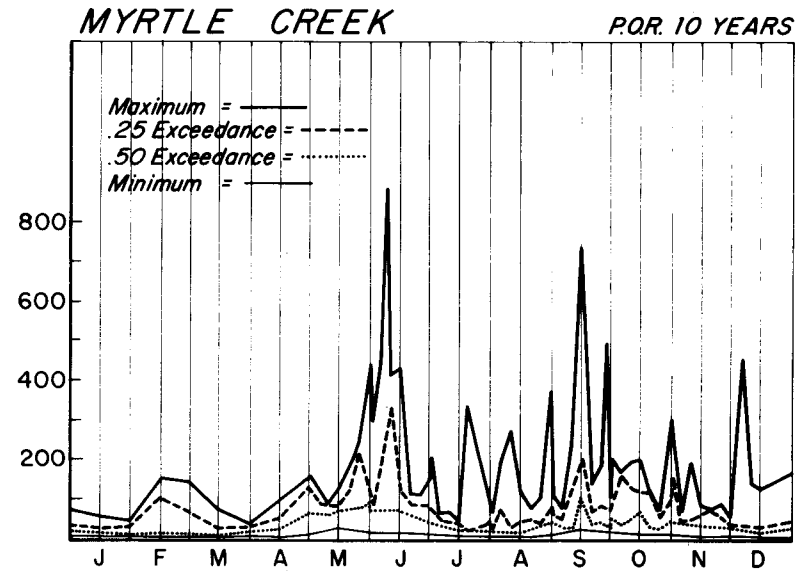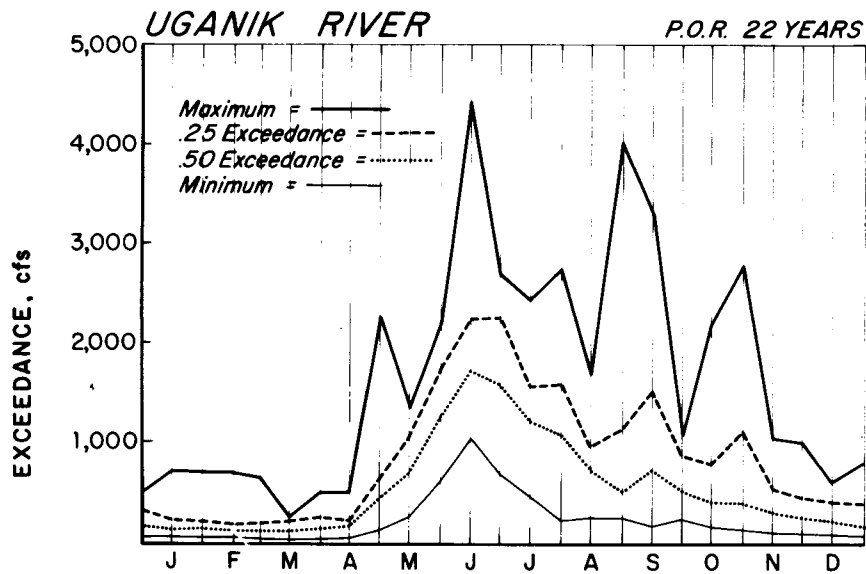
FIGURE 35 – EXCEEDANCE PROBABILITIES BASED ON PERIOD OF RECORD (POR)
Uganik River, Myrtle Creek, Kvichak & Nuyakuk Rivers

155
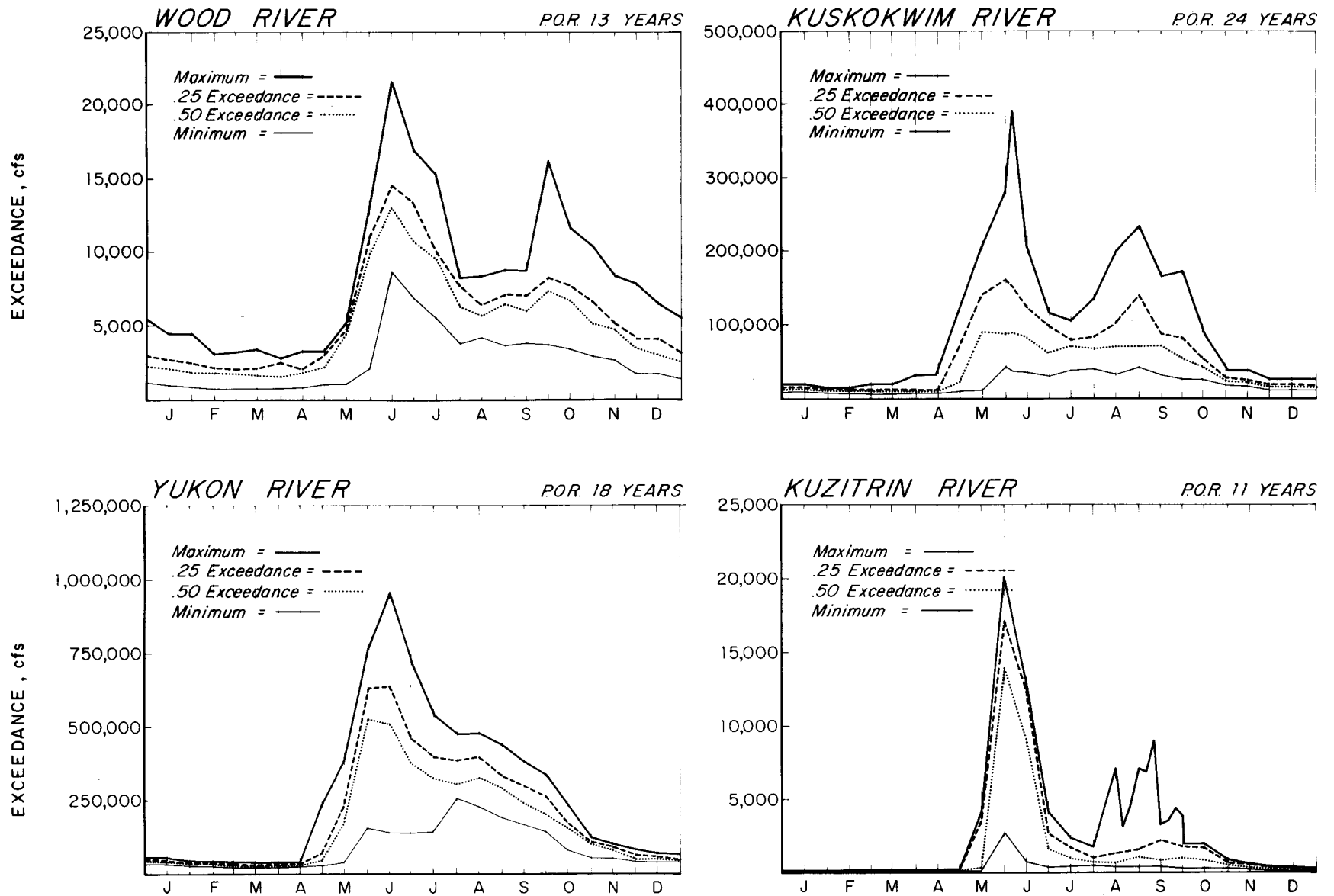
FIGURE 36 - EXCEEDANCE PROBABILITIES BASED ON PERIOD OF RECORD (POR)
Wood, Kuskokwim, Yukon, & Kuzitrin Rivers
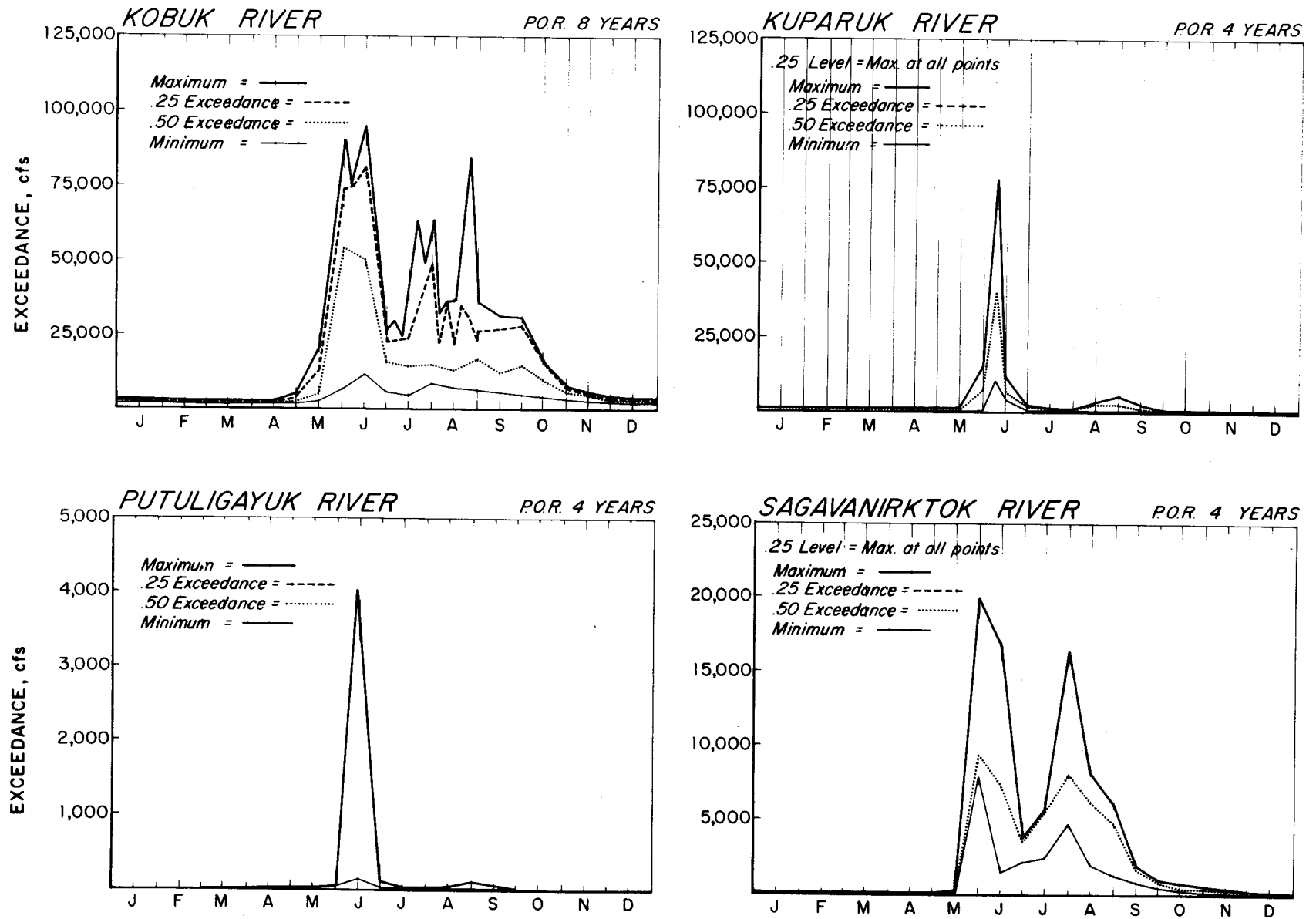
FIGURE 37 – EXCEEDANCE PROBABILITIES BASED ON PERIOD OF RECORD (POR)
Kobuk, Kuparuk, Putuligayuk & Sagavanirktok Rivers

157

G. Short-Term Variability Indices:

   Short-term variability (Figures 38 through 43) is an
important consideration in the hydrology of Alaskan coastal
streams, especially in the Arctic. Here seasonability is most
dramatic and large changes in flow can take place over a short
period of time. An extreme example is the Putuligayuk River,
a small river basin which is confined to the Arctic coastal
plain. Flow during June 1972 went from 0 cubic feet per second
on June 9, to 4000 cubic feet per second on June 13, then back
to 762 cubic feet per second on June 16.

   In order to evaluate the short term variability of a
stream, ratios were used. The maximum flows of 1, 3, 7, 10,
and 30 days duration for each year were ratioed to the mean
annual flow. These ratios were then plotted versus time to
yield a graphic description of short-term variability. The
plotted values are averages of the ratios for each water
year for the period of record of the stream.
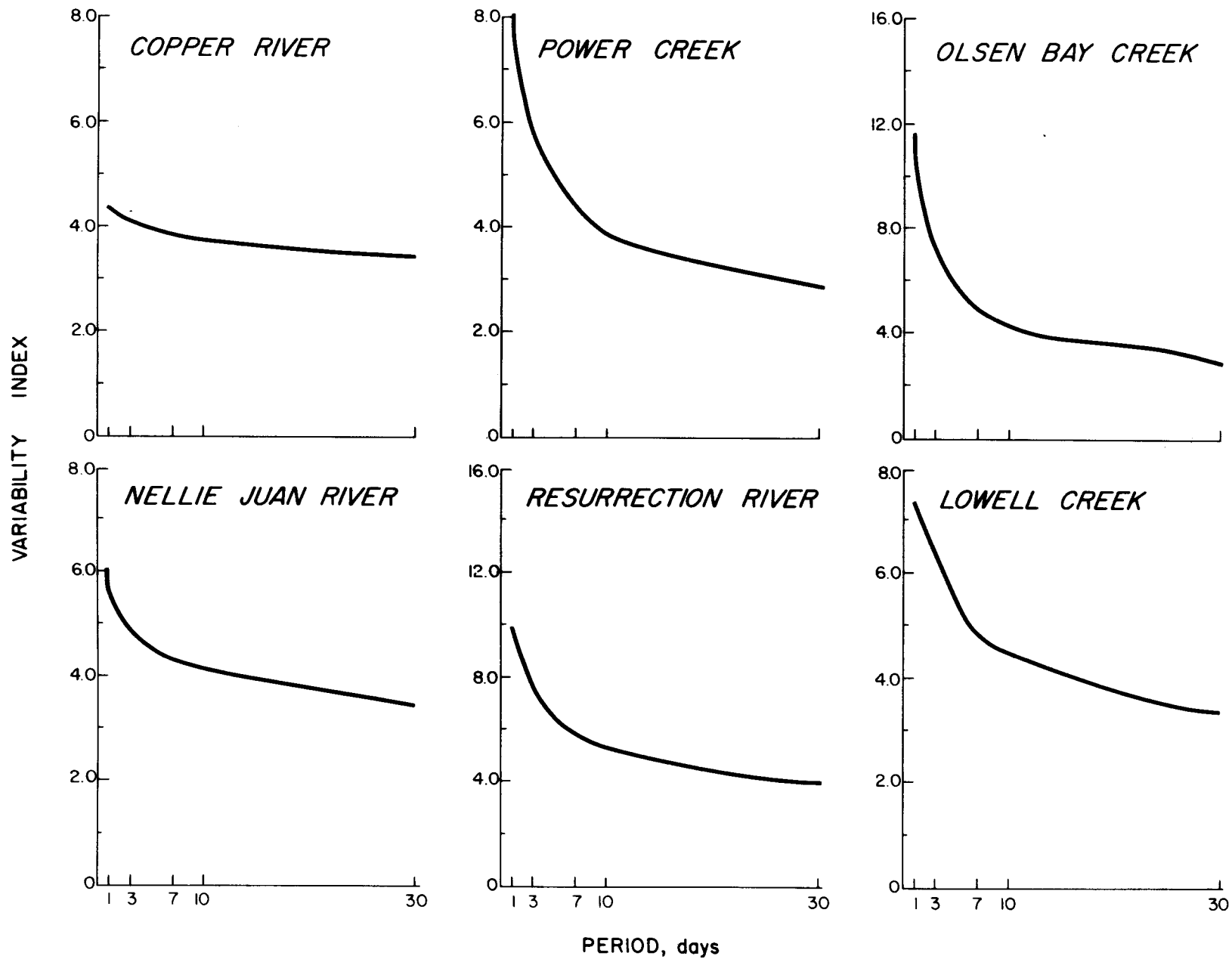
FIGURE 38 – SHORT-TERM VARIABILITY INDEX
Copper, Nellie Juan, Resurrection Rivers, Power, Olsen Bay & Lowell Creeks
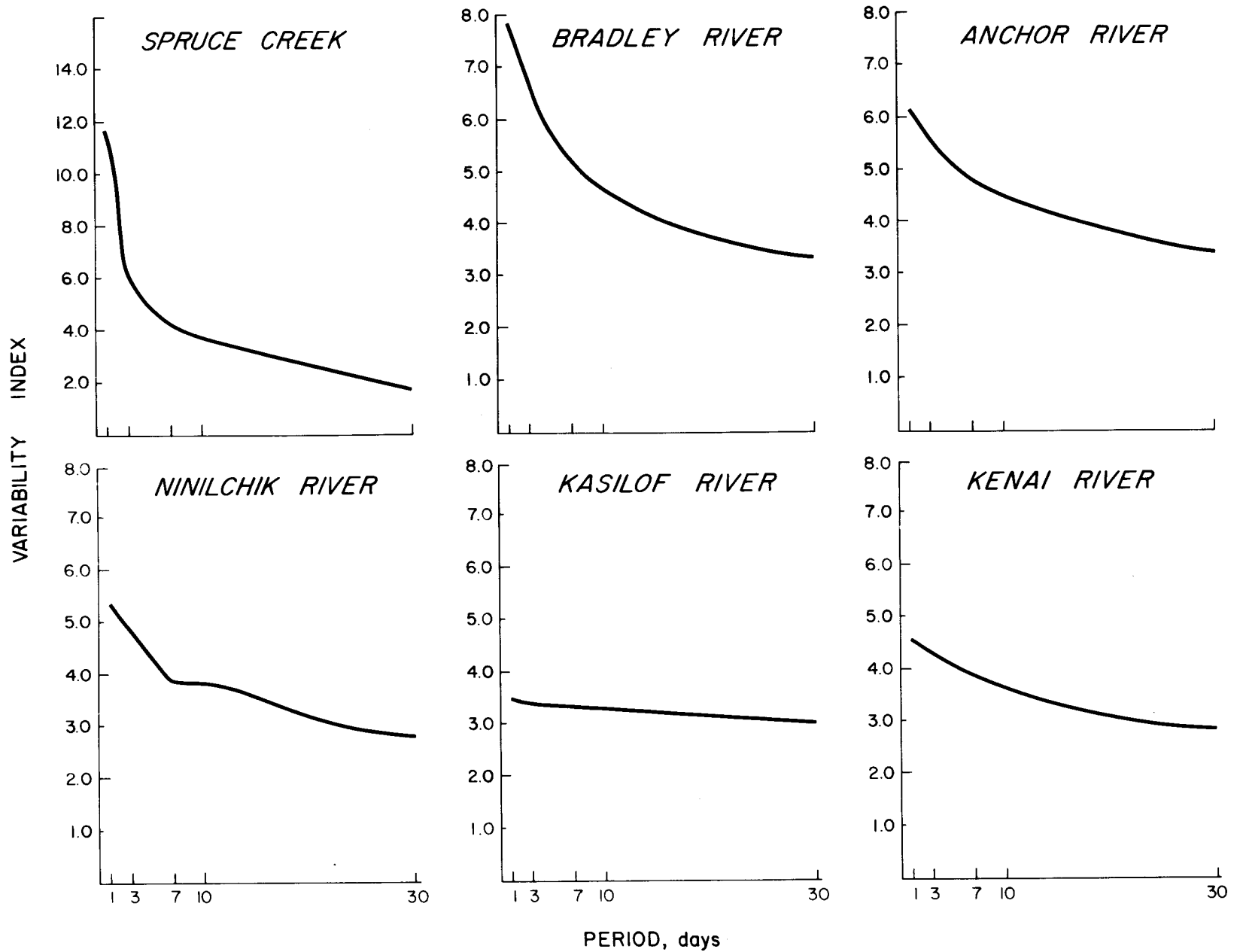
FIGURE 39 – SHORT-TERM VARIABILITY INDEX
Spruce Creek, Bradley, Anchor, Ninilchik, Kasilof & Kenai Rivers
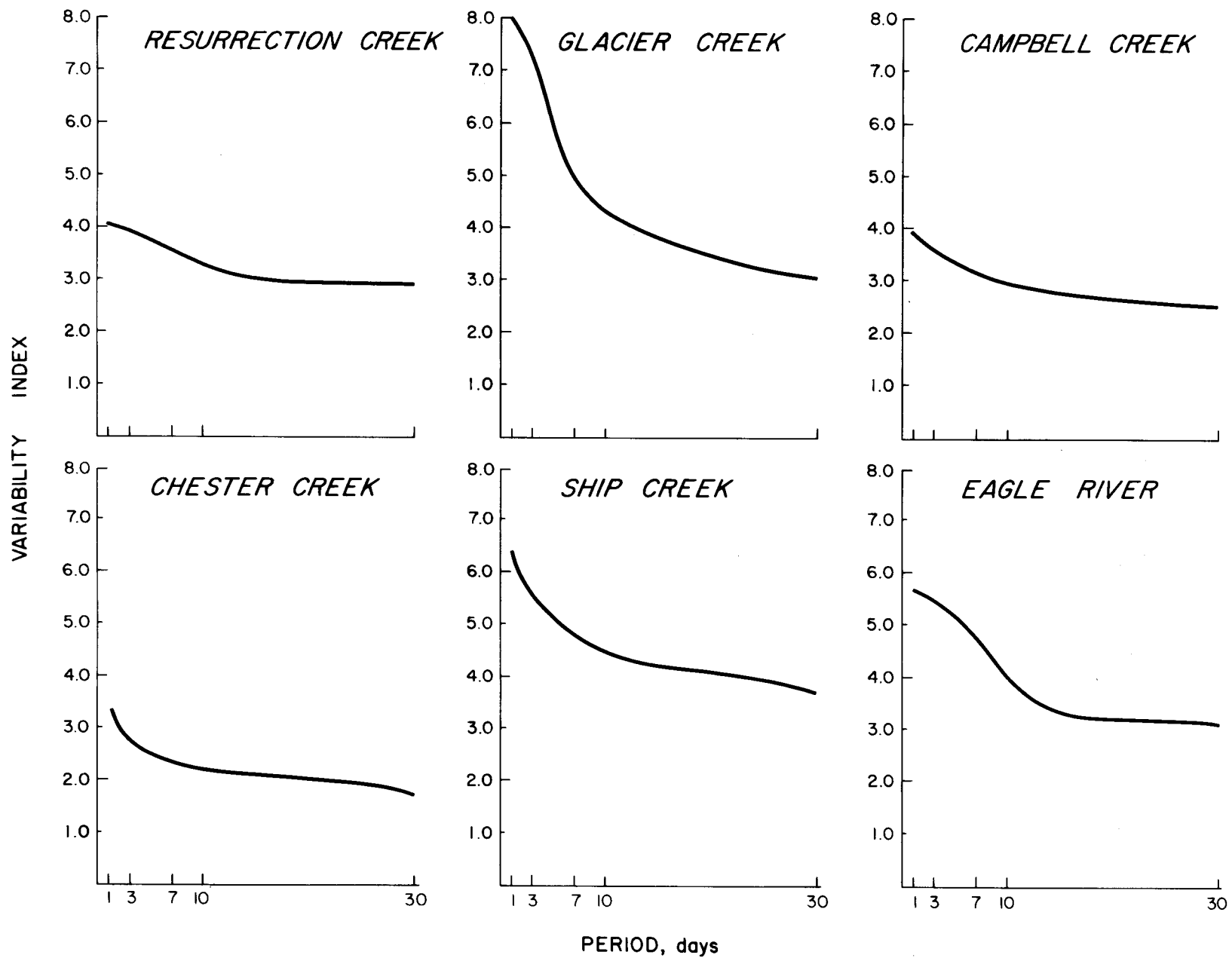
FIGURE 40 – SHORT- TERM VARIABILITY INDEX
Resurrection, Glacier, Campbell, Chester, Ship Creeks & Eagle River
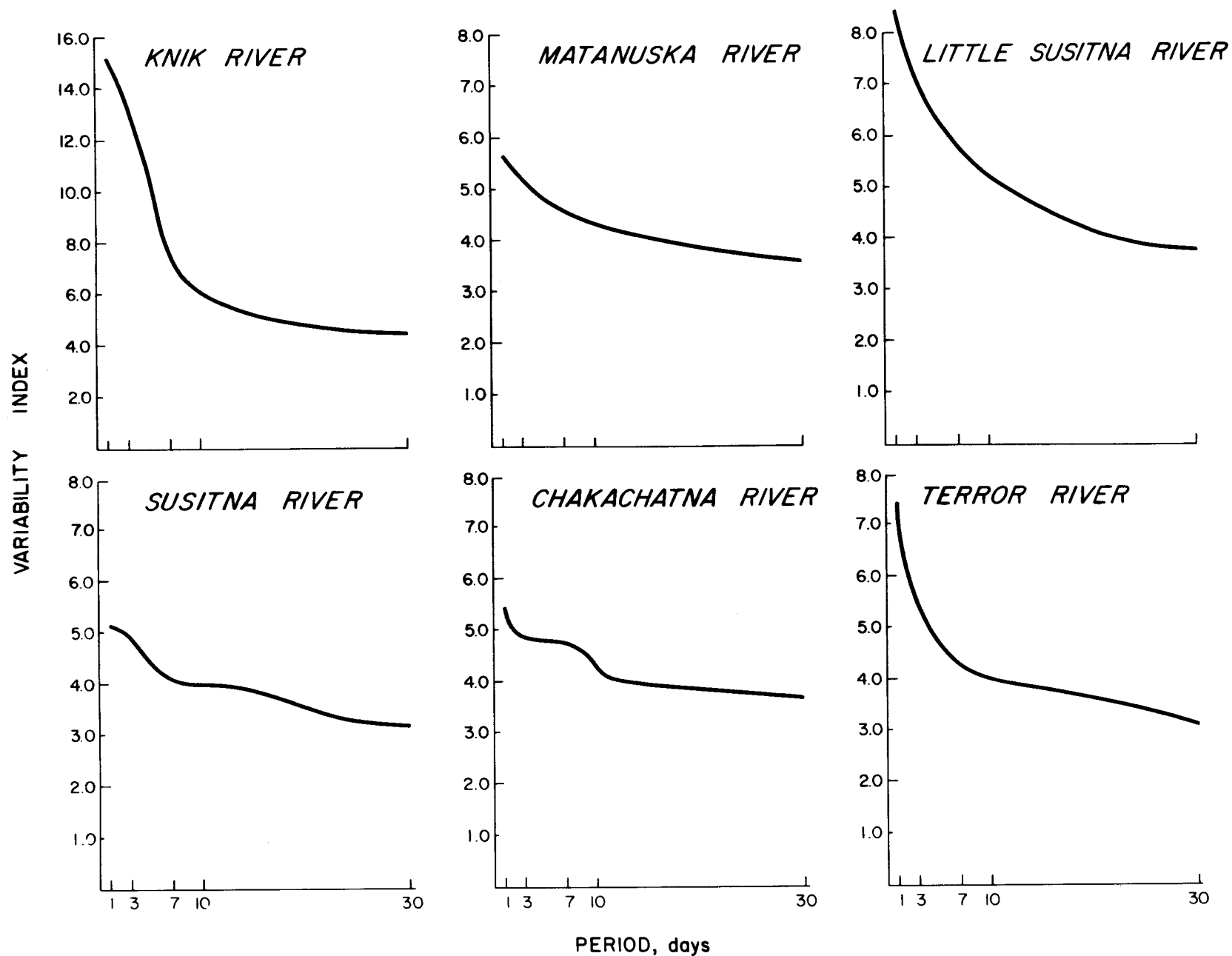
FIGURE 41 — SHORT-TERM VARIABILITY INDEX
Knik, Matanuska, Little Susitna, Susitna, Chakachatna & Terror Rivers

162
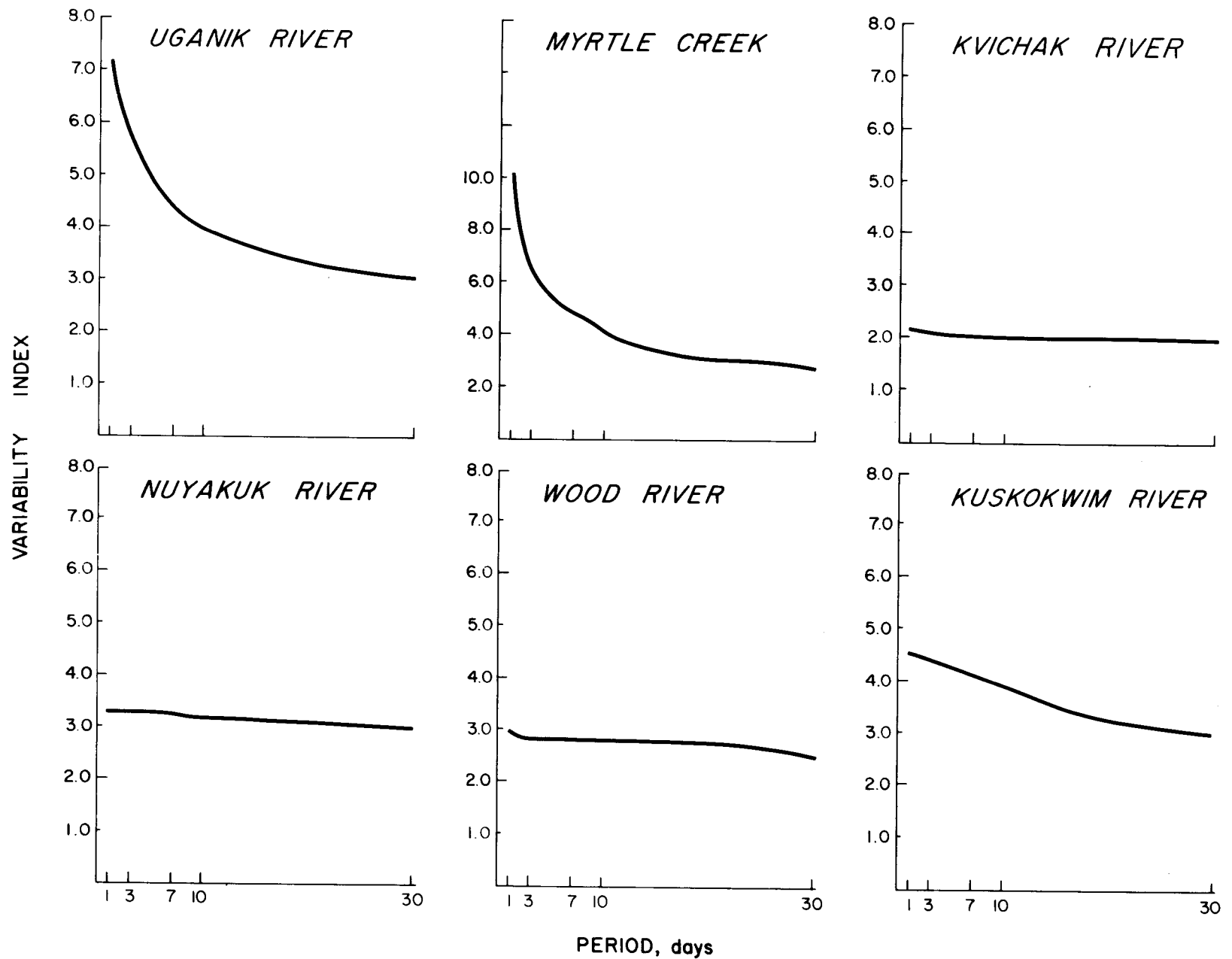
FIGURE 42 – SHORT-TERM VARIABILITY INDEX
Uganik, Kvichak, Nuyakuk, Wood, Kuskokwim Rivers & Myrtle Creek

163
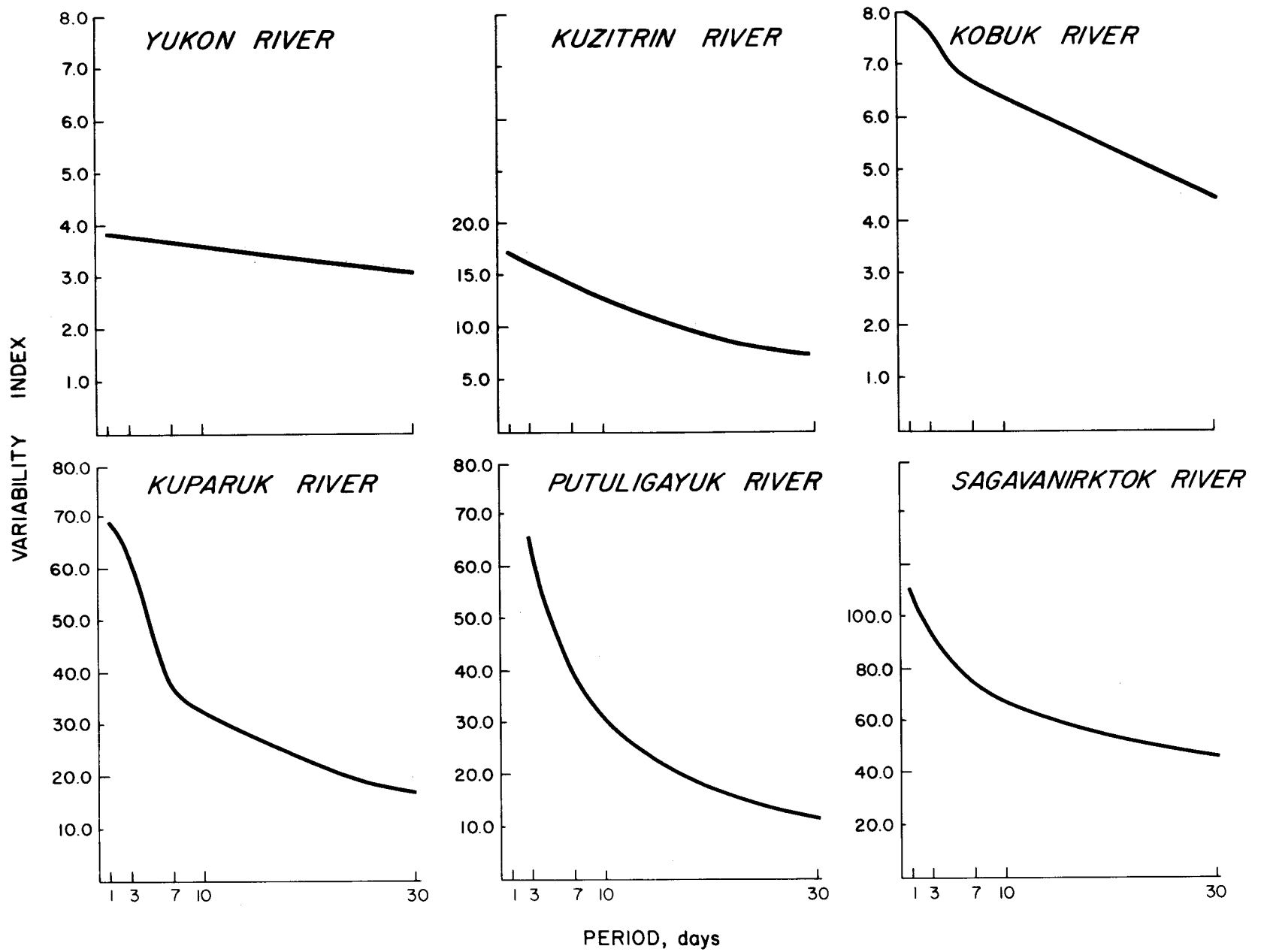
FIGURE 43 – SHORT–TERM VARIABILITY INDEX
Yukon, Kuzitrin, Kobuk, Kuparuk, Putuligayuk & Sagavanirktok Rivers

H.   Statistical Streamflow Parameters:

The statistical parameters given are based both on
monthly and annual variations. They are:

1. The mean daily flow by month, giving both the maximum
    and minimum daily flows for each month, and the year
    and day for each occurrence.

2. The maximum, minimum, and average daily flow data
    for the length of the streamflow record.

3. The mean monthly flow data, giving the maximum and
    minimum mean monthly flow and the respective years of
    occurrence.

4. The maximum and minimum mean annual flows for the
    length of record.

Rivers with less than 3 years of record are not included.
These parameters are listed by river in Appendix I.

I.   Sediment Relationships:

Although sediment load data for Alaskan streams is
available, most of it is not continuous and consequently
cannot be correlated with seasonal streamflow variations. For
a few rivers, however, continuous daily data is available for
one or more years which makes possible a correlation between
flows and sediment loads. This data for the Copper, Ninilchik,
Knik, and Matanuska Rivers has been plotted (Figures 44
through 53) along with the stream hydrograph for the corres-
ponding year of record. All the available continuous daily
records have been included here.
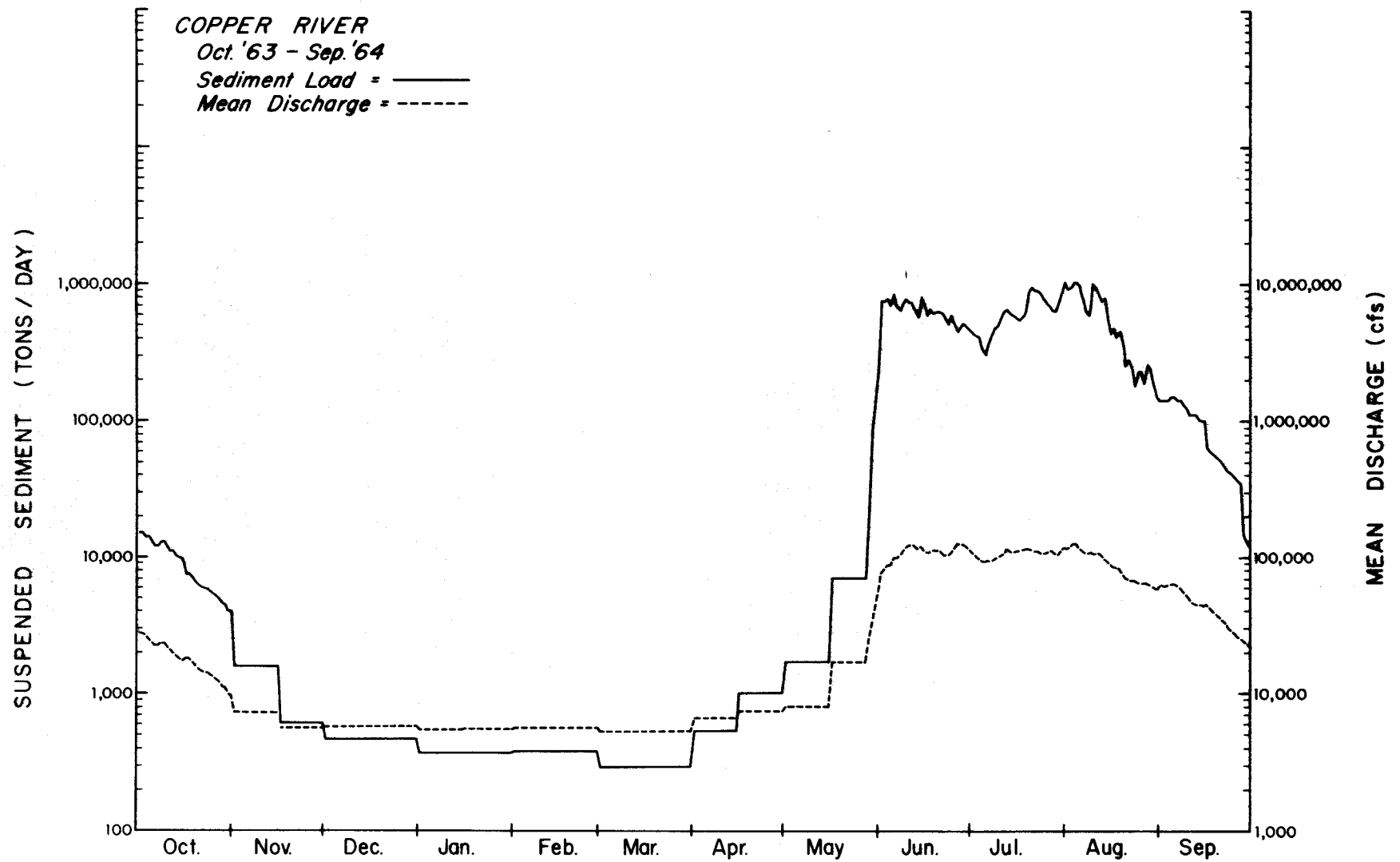
FIGURE 44 –SEDIMENT LOAD – HYDROGRAPH Copper River, 10/63 - 9/64
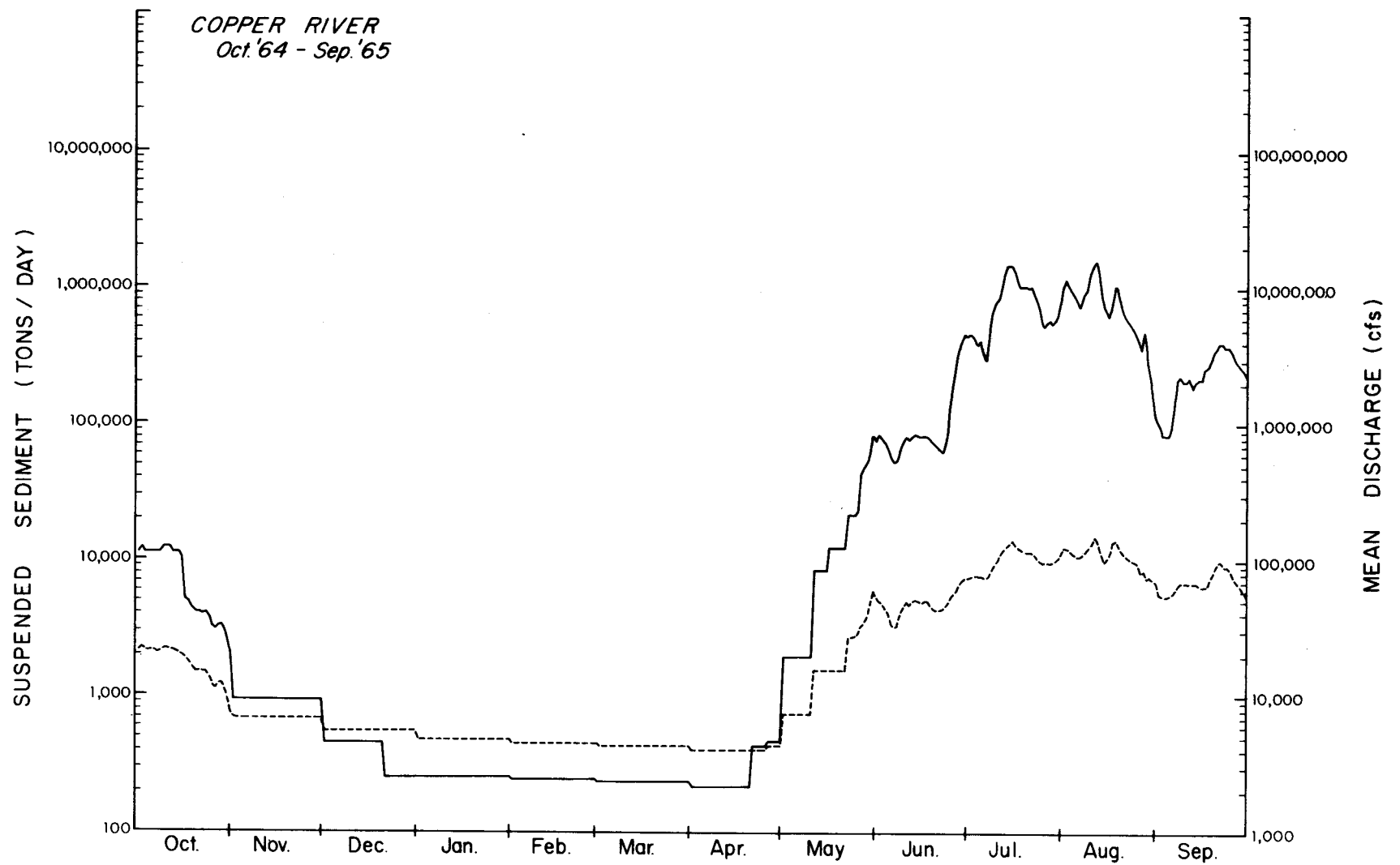
FIGURE 45-SEDIMENT LOAD – HYDROGRAPH Copper River 10/64 – 9/65
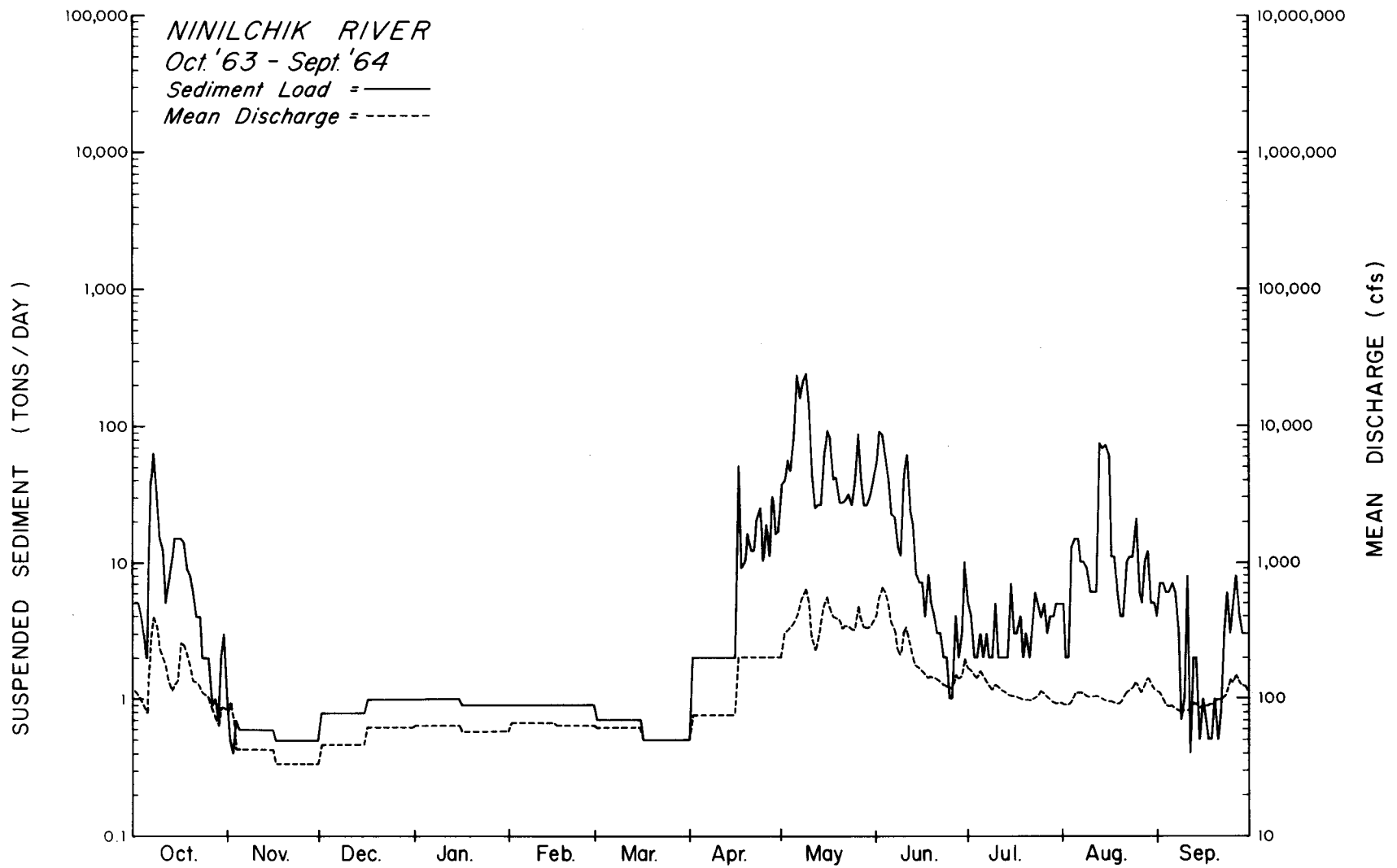
FIGURE 46-SEDIMENT LOAD-HYDROGRAPH Ninilchik River 10/63-9/64
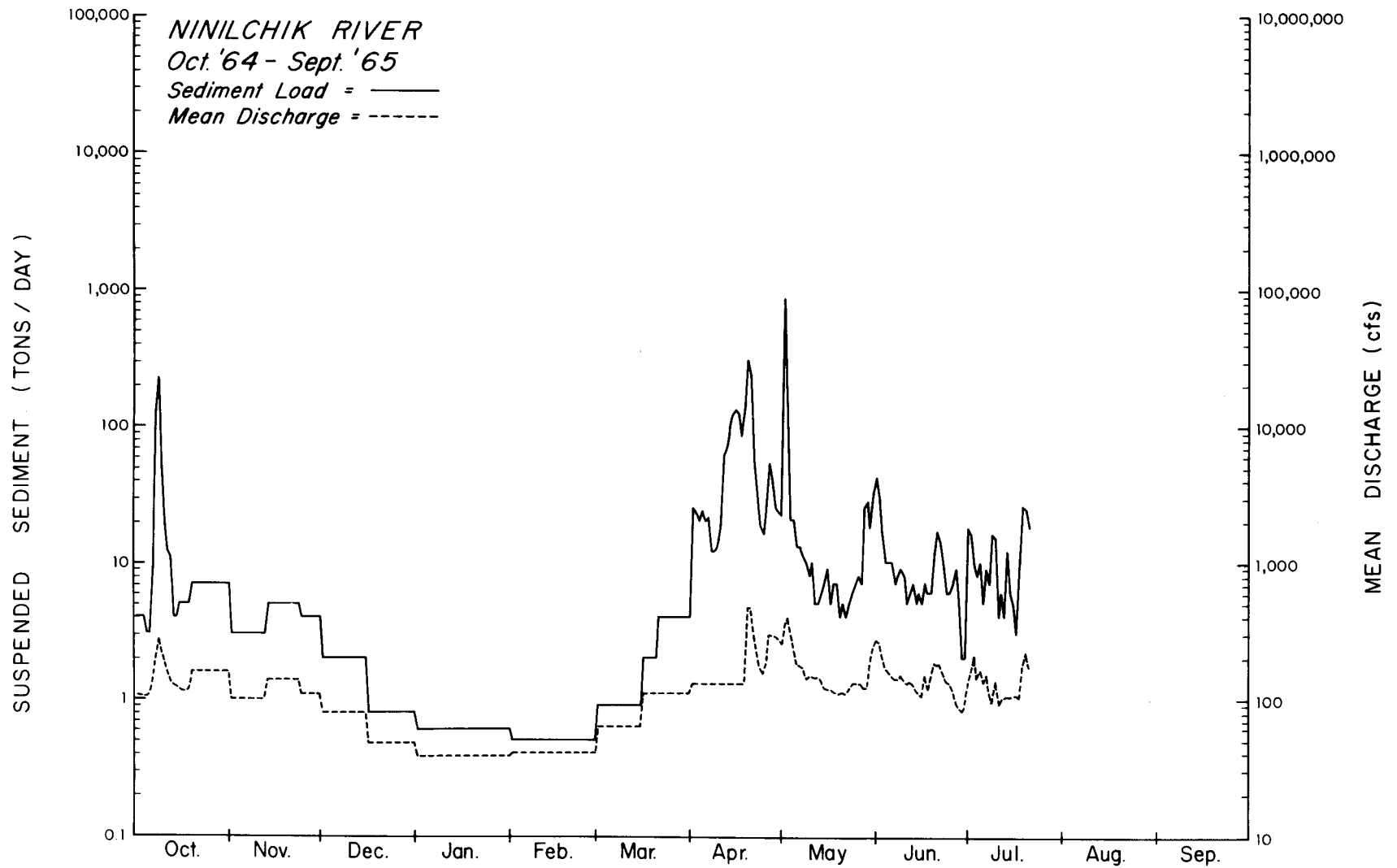
FIGURE 47-SEDIMENT LOAD-HYDROGRAPH Ninilchik River 10/64-9/65
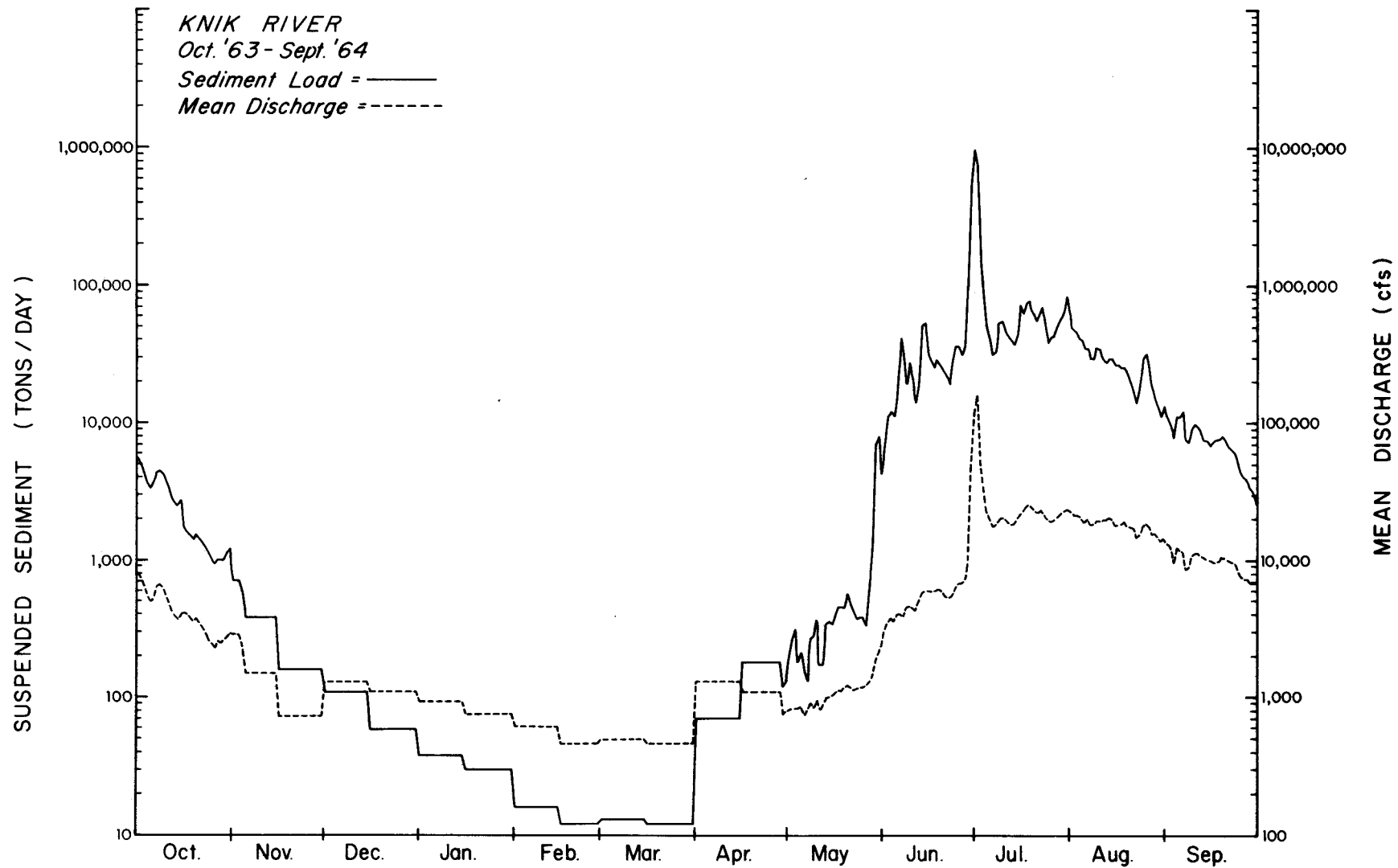
FIGURE 48 – SEDIMENT LOAD – HYDROGRAPH   Knik River 10/63 - 9/64
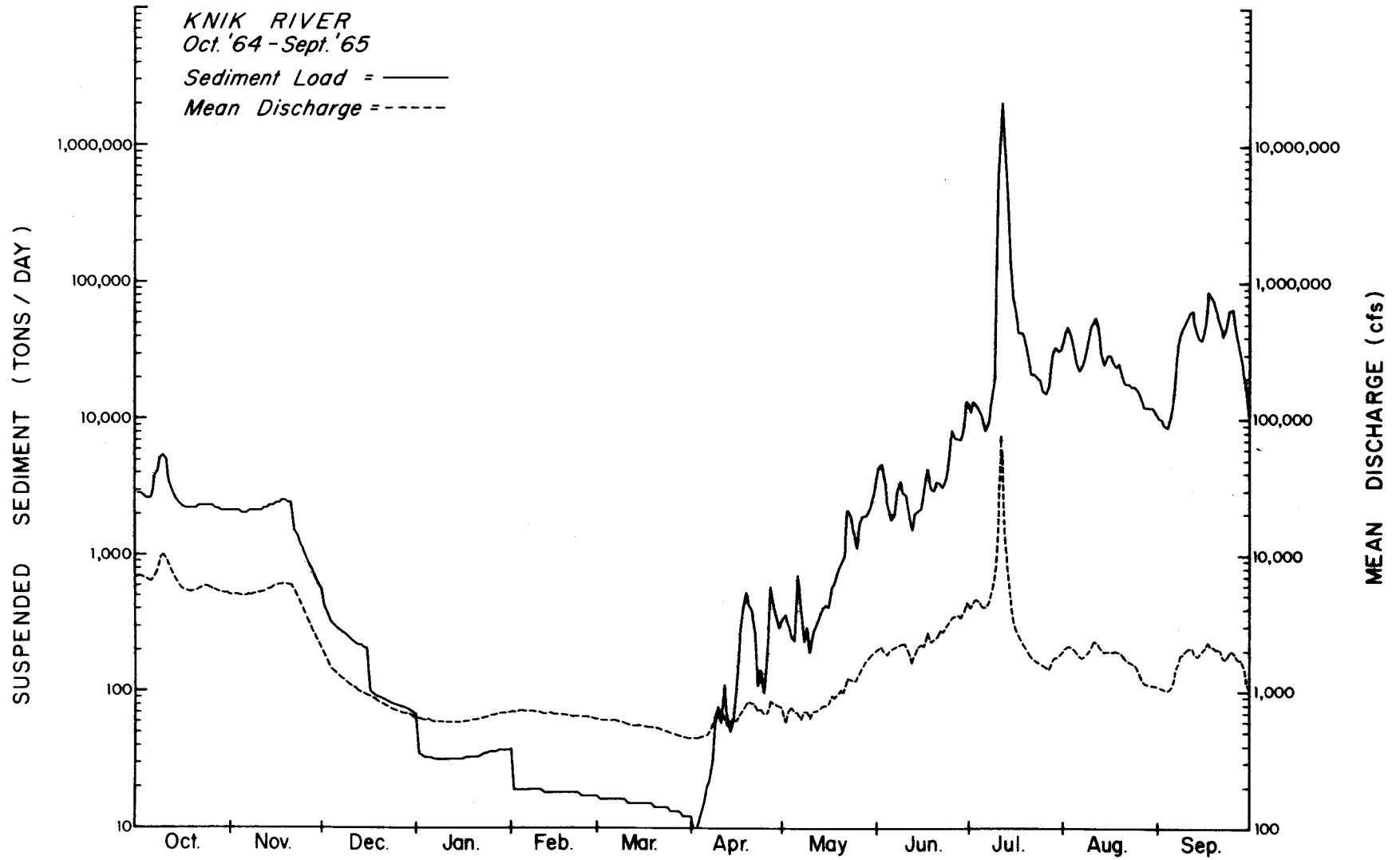
FIGURE 49 – SEDIMENT LOAD – HYDROGRAPH   Knik River   10/64 – 9/65
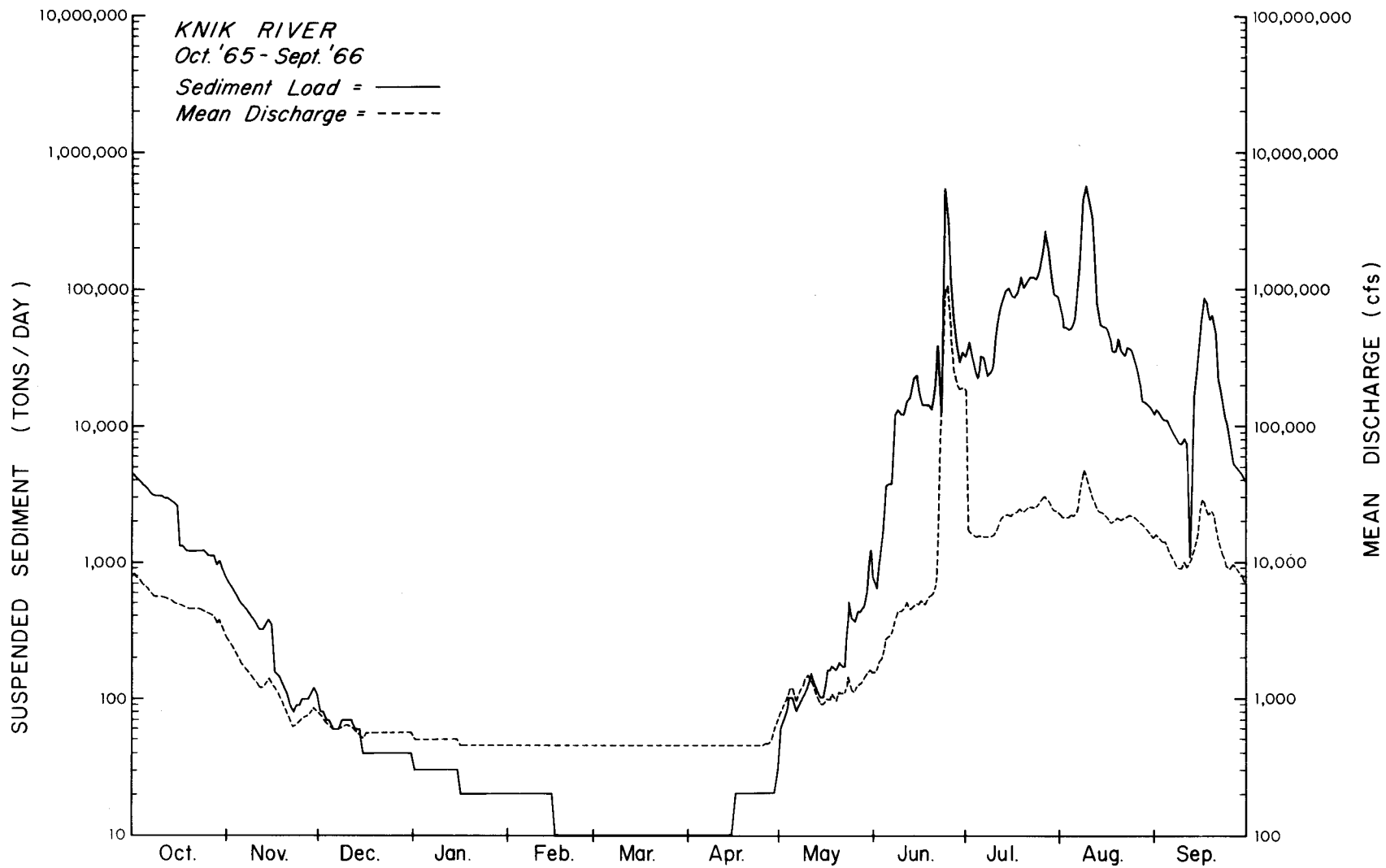
FIGURE 50 - SEDIMENT LOAD - HYDROGRAPH   Knik River   10/65 - 9/66
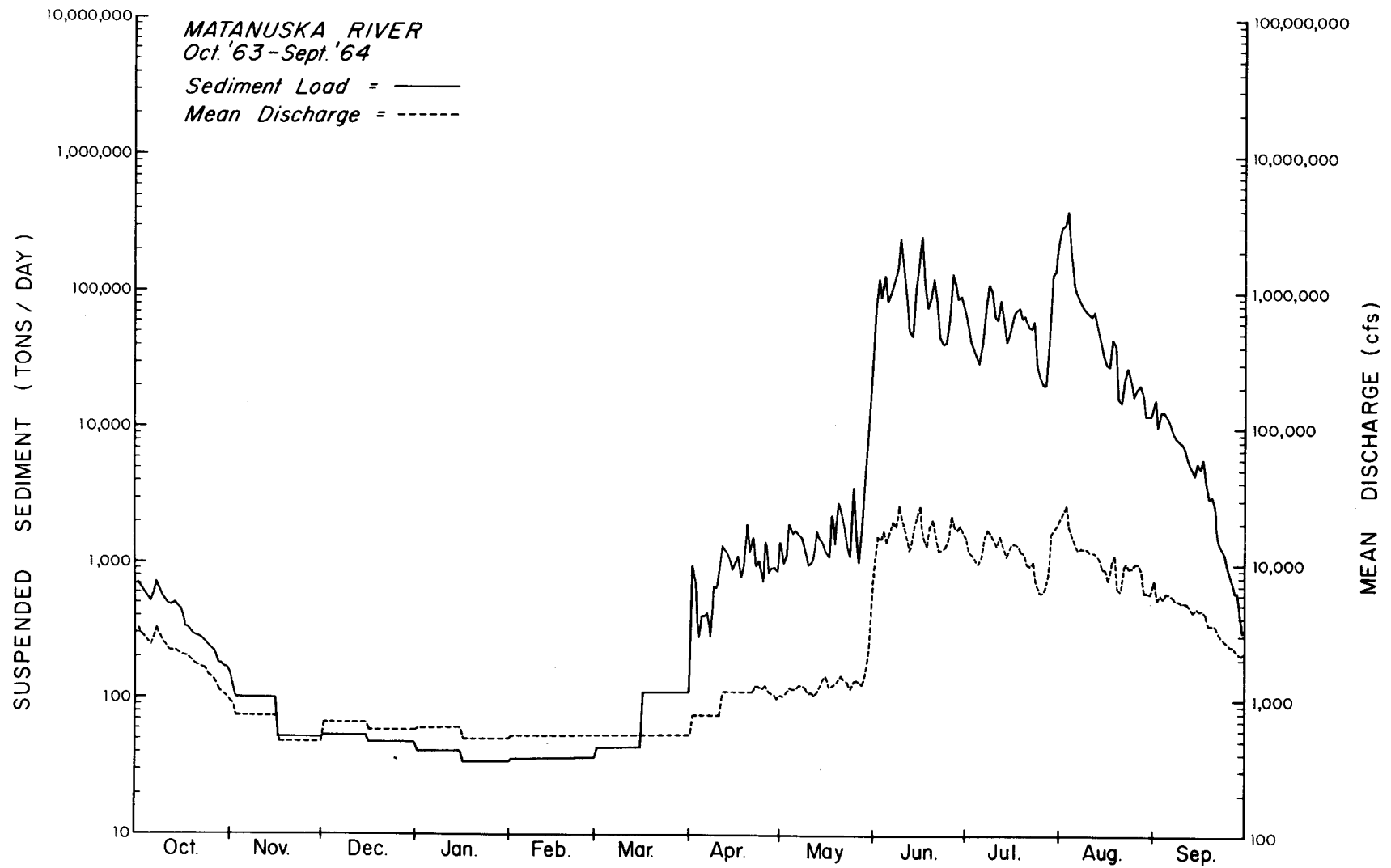
FIGURE 51 - SEDIMENT LOAD - HYDROGRAPH Matanuska River 10/63 - 9/64
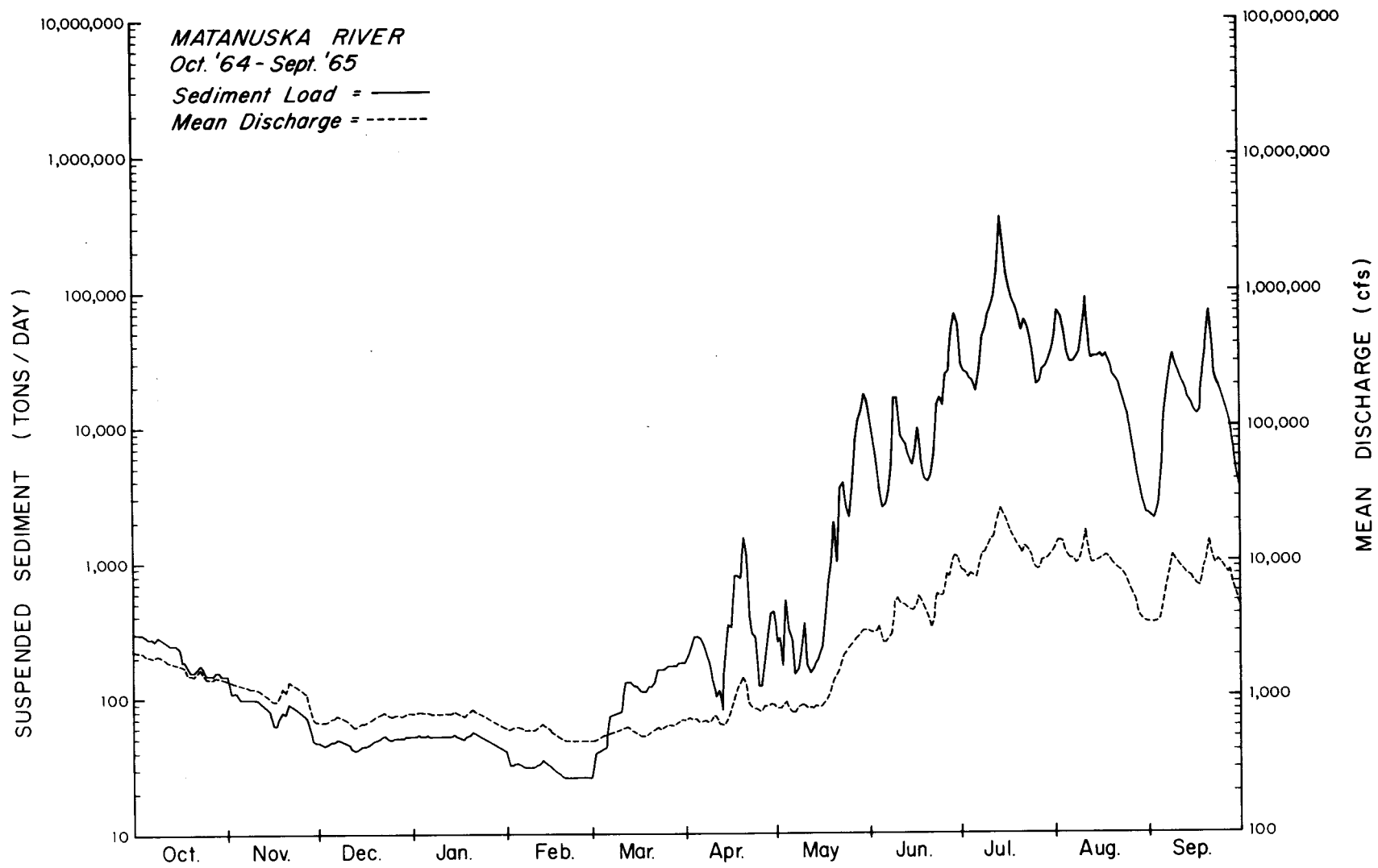
FIGURE 52-SEDIMENT LOAD -HYDROGRAPH Matanuska River 10/64-9/65
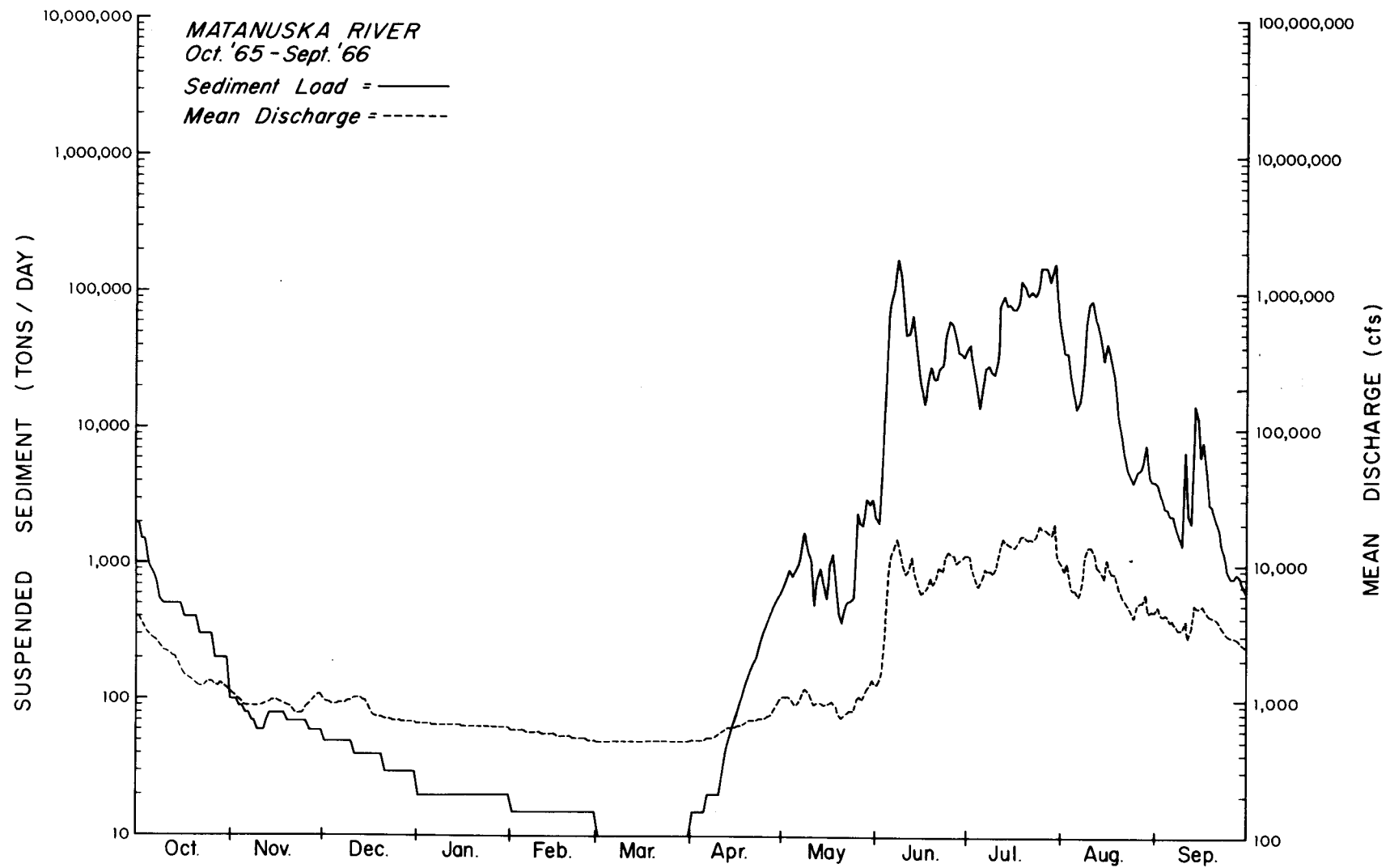
FIGURE 53—SEDIMENT LOAD—HYDROGRAPH Matanuska River 10/65-9/66

VII. DISCUSSION

A. Snowmelt Characterizations:

1. General observations - NOAA VHRR satellite imagery:

Snowmelt begins in the lowlands of the southern half of Alaska (south of the Yukon River) during the month of April and in the extreme southern part of the state in the month of March. Melt in interior Alaska often begins at about the same time as in the coastal areas and proceeds rapidly because of the drier conditions (lighter snow-packs) and the more continental climate.

First areas to become snowfree are the low-lying regions of the Tanana Valley, the Copper River valley north of Chitina, the Matanuska Valley, and low areas of the Yukon Valley above Rampart, and downstream from Tanana to Ruby. The valleys of the upper Sagavanirktok, Itkillik, Killik, and Anaktuvuk Rivers and some of their tributary valleys are also snowfree early in the season. However, these river valleys are more often subject to extensive wind erosion of the snowpack, particularly on steep slopes.

Snowmelt then spreads to the lower Koyukuk, and throughout the interior lowlands of the Tanana and Yukon Valleys. Slowly, the areal extent of snowmelt increases through the lowlands of the state, including the lower Kuskokwim River valley. As the days become warmer by mid-May, most of the elevations less than 900 meters are snowfree and coastal areas in the southern half of Alaska

are melting or snowfree. Enhanced thermal IR imagery from the NOAA-3 satellite indicates that on May 12, 1975, melting was occurring or complete at most elevations everywhere in Alaska except the coastal plain and lower foothills of the Arctic Slope region.

Generally, shorefast ice and snow near the western Alaskan coast lags other areas of melt. Probably this is a result of the "heat sink" effect of the shorefast ice, sea ice, ice-covered lakes, and the overall influence of the cooler marine climate. These combined effects also dominate the snowmelt on Alaska's Arctic Slope. The snowcover in this region is the last area of seasonal snow cover to disappear and often persists until early June. This results in an anomalous pattern of snowmelt in the North Slope region. The mid-elevations (600-900 meters) are the areas of snowmelt initiation on the Arctic Slope, and snowmelt proceeds in both directions from these elevations, with the lowest elevations often the last to become snowfree.

A chronology of the snowmelt in Alaska using NOAA imagery (of use in OCS characterization) follows for the years 1975 and 1976 (Table 6).

TABLE 6

NOAA IMAGERY OF USE IN OCS CHARACTERIZATION - 1975

NOAA IMAGERY ORBIT NO. & DATE	SNOWMELT OBSERVATION	PLUME OF SEDIMENT OR OVERFLOW	LOCATION OBSERVATION	FLOODING/ CAUSE	CIRCULATION FEATURE	NOTES
#2081 30 Apr. 75	Melting Temp. Present		Throughout Interior and Lower Yukon and Kuskokwim Valley			Some evidence of Snowfree area
#2093 01 May 75	Melting and Snowfree Areas Present		Interior (Tan. Valley) Yukon, Lower Kuskokwim		Coastal Weather Effects Domate	*
#2105 02 May 75	Matanuska Valley & Copper R. Valley Clear Observation Lowlands Snowfree		Cook Inlet, Copper River Valley & Interior			First Clear Weather Obs. of Cook Inlet & Copper R. Val.
#2143 05 May 75	Generally Snowfree in Cen. Yukon & Porcupine R. Valleys		Interior & Cook Inlet		Ice in Cook Inlet W. Side of Inlet	
#2156 06 May 75	Snowfree Area of North Slope Clearly Visible		N. Slope of Brooks Range		Clearing of Ice in Norton Sound	Sag R. Visible Effects of Flow or Haul Road
#2168 07 May 75	Further Melting Throughout Int. & Copper Valley		Entire State		Coastal Ice Degrading So. of Bering Str.	" "
#2193 09 May 75	Extensive Melt in Interior Alaska		S. Coast Cloudy - Rest of State Clear or P. Cldy.			Yukon R. Ice Still Intact
#2218 11 May 75	Extensive Further Melting Occurred		Entire State			Record High Temps Interior
#2231 12 May 75	75% Complete in Interior		North of Alaska Range			Brooks Range Melting
#2281 16 May 75	80% Complete So. of Brooks and No. of Alaska Range		Alaska N. of Alaska Range		Coastal Weather Variance Indicated	*Cloudy S. of Alaska Range
#2306 18 May 75	Melt Completed on Most Cook Inlet Lowlands		Entire State			Strong Wave Cloud/ Wind Effect

*Good Demonstrative Example

TABLE 6 (continued)

NOAA IMAGERY OF USE IN OCS CHARACTERIZATION - 1975

NOAA IMAGERY ORBIT NO. & DATE	SNOWMELT OBSERVATION	PLUME OF SEDIMENT OR OVERFLOW	LOCATION OBSERVATION	FLOODING/ CAUSE	CIRCULATION FEATURE	NOTES
19 thru 22 May Cloudy						
#2364 23 May 75	Melt Proceeding Coastal Lowlands Kusk-Yuk. Delta				Coastal Area Much Cloudier Again	
#2381 24 May 75	Ice Persists Along Coastal Areas (North of Togiak) Probably Shorefast		Yukon River Innoko R.	Aniak/Holycross Flood Ice Jam 1000 mi.		*Breakup of Rivers Dominate
#2444 29 May 75	Melt Complete Throughout Most of Brooks Range, Interior S. Central Seward Peninsula of Alaska	Ice Flooded Off Sag R. on N. Slope also off Canning R.	Entire State	Yukon Delta Flooded Ice Jam, Tidal Effects 1050 mi^2		Sag R. Not Visible for 4 previous Days Flow Initiation Indeterminate
#2494 02 June 75	Melt Complete Except for N. Slope					N. Slope Nearly Continuously Cloudy Since 29 May
#2506 03 Jun 75		Sea Ice Flooded Off: Sag, Colville, Canning, Sadlerochit, Hulahula, Jago, Oklilak	Kuparuk Nichilik Egaksrak Kukpowruk Kokolik Rivers		Sea Ice Still Intact Along Shore N. of Hazen Bay	
#25 1 05 Jun 75	Snow Definitely Melting on No. Slope	Major Overflow Water at Mouths of Most Rivers on No. Slope		Overflow Flooding No. Slope Rivers		
#2544 06 Jun 75			Northern Alaska	Kasegaluk Lagoon Completely Flooded by Overflow Water		

*Good Demonstrative Example

179

TABLE 6 (coninued)

NOAA IMAGERY OF USE IN OCS CHARACTERIZATION - 1975

NOAA IMAGERY ORBIT NO. & DATE	SNOWMELT OBSERVATION	PLUME OF SEDIMENT OR OVERFLOW	LOCATION OBSERVATION	FLOODING/ CAUSE	CIRCULATION FEATURE	NOTES
#2594 10 Jun 75	Coastal Shorefast Ice Generally Absent So. of Cape Rodney, Seward Peninsula No. Slope Snowmelt 50% Complete		Western Alaska & No. No. Slope			
#2607 11 Jun 75	Snowmelt on No. Slope 70% Complete		Entire State		Coastal Fog and Weather Again Evident	
#2619 12 Jun 75	No. Slope Snowmelt 80% Complete		Entire State		Coastal Weather * Again Evident-Fog- Stratus	
#2920 06 Jul 75	Teschekpuk L. Still Frozen Ice Still Intact No. of Icy Cape	Huge Sediment Plume off McKenzie R.	No. Slope			Ice Normally Still Present Along Beau- fort Sea Coast in Early July
#3132 23 Jul 75	Ice Lead Open to Barrow					Ice Close but Only Obstructs Passage Between Barrow & Smith Bay
#6538 20 Apr. 1976	Initiation of Melt in Interior Alaska		Tanana Valley			
#6563 22 Apr. 76	Increasing Melt in Interior Alaska and East Cook Inlet		Copper, Tanana Valleys and Cook Inlet			Sea Ice still at Maximum Extent but Discont.
#6576 23 Apr. 76	Interior Snowmelt also Cook Inlet Interior Areas		Interior Alaska and Cook Inlet			
#6601 25 Apr 76			Entire State		Wave Clouds-Strong Erosive Winds Indicated	Ice Free Wake S. of St. Law. Island
#6613 26 Apr 76	Extensive Melt in Tanana Valley Lowlands		Interior Third of State and Gulf Coast		Wave Clouds and High Cloudiness Windy Again- Esp. Aloft	Sea Ice intact

*Good Demonstrative Example

180

TABLE 6 (coninued)

NOAA IMAGERY OF USE IN OCS CHARACTERIZATION - 1976

NOAA IMAGERY ORBIT NO. & DATE	SNOWMELT OBSERVATION	PLUME OF SEDIMENT OR OVERFLOW	LOCATION OF OBJECTS	FLOODING CAUSE	CIRCULATION FEATURE	NOTES
#6638 28 Apr 76	Extensive Melt in Tanana, Yukon, Copper, Valleys	Sediment Plumes @ Copper, Bering Many other S. Coast Rivers, Cook Inlet	Interior, South Coast of Alaska		Sediment Plums Swept in Direction (Westward) of Alaska Current	
#6651 29 Apr. 76	West Side of Alaska Peninsula Melting Upper Kuskokwim R.	Plumes Permeate Water off S. Coast	W. Alaska Peninsula Upper Kuwkokwim Valley			
#6701 3 May 76	Melting Beginning in Brooks Range, Extensive in Interior Alaska				Wave Clouds in the Brooks Range, Leads in increasing off North Slope	
#6763 8 May 76	Moist Cloudy Air Spreading Slow Melt over Entire State S. of Brooks Range		Entire State		Coastal Weather Effects Evident	
#6776 9 May 76	N. Slope Melt Pattern Evident. 80% Snowfree S. of Brooks Range. Sag R. Flow Evident	Sag. R. Overflow Initiated	Entire State	Sag River Snowmelt Runoff	Norton Sound 50% Ice Free	
#6801 11 May 76		Canning R. Overflow in Addition to Sag. Also Jago and Sadlerochit Rivers	North Slope	N. Slope Snowmelt Runoff	Sea Ice very Degraded S. of Bering Straits	
12 May - 14 May			Clouded Everywhere			
#6876 17 May 76			Interior Alaska		Superb Example of Orographic Cloudiness in Yukon Tanana Uplands	
#6914 20 May 76 #6914 IR "	Melt 90% Complete S. of Brooks Range. New snow- fall N. of Brooks Range, Destroying Melt Pattern.		Entire State	Ice Jam on Middle Yukon (IR Image)	Ice covers Lake Iliamna S. Coast Clouded Nearly 10 Days Consecutively. IR Image Excellent Detail.	

*Good Demonstration Example

TABLE 6 (continued)

NOAA IMAGERY OF USE IN OCS CHARACTERIZATION - 1976

NOAA IMAGERY ORBIT NO. & DATE	SNOWMELT OBSERVATION	PLUME OF SEDIMENT OR OVERFLOW	LOCATION OF OBJECTS	FLOODING CAUSE	CIRCULATION FEATURE	NOTES
#6939 22 May 76	N. Slope still 95% Snowcovered Shorefast Ice Still Intact over Most of W. Coast		Entire State			
#6989 26 May 76	Colville River Channel Flow Evident		N. Slope	Snowmelt	Coastal Weather Evident	
#7026 29 May 76	Lake Iliamna Breaking up		S. of Alaska Range			
#7051 31 May 76 IR Image	Excellent Resolution of Snowfree areas south of Brooks Range to Coast		South of Brooks Range			
# 11665 (NOAA 3) 4 June 76	Snowmelt Progressing N. Slope Pattern very evident	Sea Ice Flooded Off: Sag Jago Kuparuk, Colville Sadlerochit Rivers. Also Kasegaluk Lagoon	N. Slope of Alaska	Snowmelt		
#11727 (NOAA 3) 9 June 76	Melt 40% Complete on N. Slope Pattern very evident		N. Slope of Alaska		Sea ice deteriorated 100 miles N. Bering Str. 90% ice free S. of Bring Strait.	
#7190 11 June 76	Snowmelt Continuing on N. Slope	Huge Flooded area off Colville River	N. Slope	Snowmelt and Ice Erosion		
#1176 (NOAA 3) 13 June 76	Snowmelt 80% Complete, still persistent snow around Sagavanirktak and Lower Kuparuk, on N. Slope		N. Slope		Ice deteriorating in Chukchi Sea	
#11814 (NOAA 3) 16 June 76	Snowmelt 95% complete, no more sea ice flooded		N. Slope			

*Good Demonstration Example

B. Regional Character of Streams - Climatic Influences

1. Gulf of Alaska Region: Climatic hazards.

The Gulf of Alaska is nearly surrounded on all its continental boundaries by high mountain ranges, including the Chugach, the Robinson, and the Kenai Mountains. Cook Inlet is also bounded by the ridges of the Aleutian Range on the west. This topography, combined with the moderating influence of the Alaska current, serves to give the Gulf coast region of Alaska its relatively mild and wet climate.

Rather than describe the snowmelt pattern of each basin individually, it was felt that discussion of specific anomalies and trends throughout the region would reveal more of the region's hydrologic character. Some of the individual basins are devoid of ground based snowmelt or snowcover measurements, whereas others contain USDA Soil Conservation Service snowcourses. In the past five years, an archive of satellite imagery from the LANDSAT (ERTS) and NOAA satellites has been accumulating. For remote areas and isolated river basins, these sources provide the best and most accurate snowmelt observations available. Snowmelt observations made from NOAA satellite imagery are tabulated in Table 6.

Many of the river basins in the Gulf Coast region of Alaska are subject to the hazard of glacier-dammed lake outburst floods. These floods are caused by the release, either sudden or gradual, of headwater areas of the streams. A detailed description of glacier-dammed lake

outburst floods and a list of streams subject to them has
been compiled by Post and Mayo (1971). Gulf Coast rivers
on which known glacier dammed lake outburst floods have
occurred are:

a. Knik River - this river is famous for the flood
    activity of Lake George, the largest glacier-dammed
    lake in Alaska; however, since 1966 Knik Glacier
    has failed to form an ice dam and the lake has not
    filled.

b. Snow and Kenai Rivers - floods on this river system
    originate from a glacier-dammed lake at the headwaters
    of the Snow River (Post and Mayo, 1971), a tributary
    to the Kenai River. Outburst floods have occurred
    since December 1911 and outburst peak discharge has
    varied regularly as a function of changes in the
    amount of water impounded due to glacier melt.
    Since 1961, the outburst flood peaks have exceeded
    the annual storm peaks.

c. Tazlina and Copper Rivers - the Tazlina basin,
    tributary to the Copper River contains four major
    lakes which are susceptible to outburst flooding.
    The flood history of the Tazlina River is much more
    complex than for the other examples mentioned here
    as more than one lake is involved, and changes in
    the basin have not been systematic.

d. Bering River - the Ungaged Bering River system
    includes Berg Lake, presently dammed by the Bering

glacier. This lake has a complex history and
presents one of the greatest potential floods of
any glacier-dammed lake in Alaska. Post and Mayo
(1971) state that catastrophic draining will occur
in the near future if the ice dam restraining Berg
Lake continues to thin, and the situation is be-
coming unstable. The ice dam now holding Berg Lake
could erode rapidly, thus releasing the entire lake
in a few hours. This could create a devastating
flood which would sweep the Bering River Valley
with a peak flow far exceeding 30000 cubic meters
per second ($\sim$ 1000000 CFS). As an additional
cautionary observation, it should be pointed out
that outburst floods are not seasonal in nature and
have occurred in winter as well as mid- to late
summer. It is also possible that outburst floods
could be caused by volcanic eruptions which rapidly
melt glacier ice on volcanic peaks thus resulting in
catastrophic floods which occur without warning.

2. South Bering Region: Climatic Hazards

Although glaciation is present in the Kvichak
River system and some glacier-dammed lakes have formed,
they are not considered to be a hazard to coastal
development because of the storage capacity of Lake
Iliamna, which would serve to moderate any rapid dis-
charges from glacier dammed lakes. The major climatic

hazards for this region are considered to be ice jams and severe storms.

A few small glacier-dammed lakes are also present in the headwaters of the Kuskokwim River; however, since they are small they also do not appear to represent any substantial hazard.

3. North Bering - Chukchi Region: Climatic Hazards

Again, as in the South Bering Region, the major hazards are spring ice jams and floods. Severe storms can be expected, but less often than in the South Bering Region.

4. Beaufort Sea Region: Climatic Hazards

The arctic rivers of Alaska have somewhat unique patterns of snowmelt in the respective basins which result in a mid-elevation snowmelt and a streamflow which begins before the river channel is free of ice. Water consequently will flow in the channel but on top of the ice. This results in large areas of flooded shorefast sea ice at the mouths of the rivers. A satellite image depicting this flooding hazard is shown in Figure 54. This flooding at the mouth is not pre-dictable as to its extent and is apparently quite variable from year to year. Walker (1972) observes that surface flooding of the Colville River extended 12 to 18 km from the Colville Delta. More data on this hazard is shown in Table 7. These measurements were made from NOAA satellite imagery.

FIGURE 54: NOAA SATELLITE IMAGE, ORBIT NO. 2519, June 4, 1975, VISIBLE band. This image clearly shows the North Slope snowmelt pattern. Runoff is flooding the shorefast sea ice off the mouths of the Colville, Kuparuk, Sagavanirktok and Canning Rivers.

TABLE 7

AREA (km^2) OF FLOODED SEA ICE

Date	Kuparuk River River	Sagavanirktok River	Colville River
21 May 74	--	61	15
26 May 74	10	151	50
4 June 74	30	185	61
6 June 74	30	40	120
4 June 75	101	208	219
9 June 75	69	179	276

C.   Snowmelt Characterizations-Regional:

1.   Gulf of Alaska Region:

Snowmelt along the south coast generally occurs from one to two weeks after it occurs in interior regions of Alaska. Johnson and Hartman (1969) indicate a seasonal lag of 3 to 14 days when comparing the coastal lag to the earlier summers of interior Alaska. The seasonal lag, heavier snows (especially at higher elevations), and marine climatic effects result in delayed runoff.

Snowfall, as well as rainfall, is generally greater in the Prince William Sound Coastal Area and the coast east of the Copper River Delta. U.S.D.A. Soil Conservation Service snowcourses are generally clustered around the Anchorage area and the Kenai Peninsula. They give a general, albeit incomplete in areal coverage, description of snowcover and water equivalents prior to the snowmelt period in the spring. The snowcourse locations are shown in Figure 55. Data for Gulf of Alaska snow-

188

courses for March, 1976, are given in Table 8 showing

average depths of snow given as an equivalent depth of

water, both for 1976 and for the period of record.

Snowfall is characterized as strongly influenced by

orographic effects and locally variable. Winter thaws

also can melt snow on the ground, and snow that falls at

low elevations along the coast seldom remains more than a

few weeks. As snowmelt becomes more extensive in late

spring (early to mid-May) the snowmelt pattern is determined

by slope aspect and elevation. The pattern is typical of

temperate areas, with melt proceeding from lowest to

higher elevations. Of the few relatively flat, low-lying

areas in the region such as the western Kenai Peninsula,

the Copper River Delta, and the Matanuska Valley; the

Kenai Peninsula and Matanuska Valley areas generally are the

first areas to become snowfree, usually in early May.

Chronological documentation of the snowmelt

patterns in the region are best documented by satellite

imagery. Table 6 gives chronological observations

using NOAA satellite imagery which is available for the

1975 and 1976 snowmelt periods. NOAA imagery is

available in both the visible band (.6 → .7 μ) and the

thermal infrared (10.5 → 12.5 μ) band. The resolution is

900 meters at nadir, which is about an order of magnitude

less than LANDSAT. However, NOAA imagery provides a much

better sequence of snowmelt since it is available

daily. At times, the infrared imagery is also a valuable

189

FIGURE 55: USDA snow courses in Alaska.

SNOW COURSES AND RELATED DATA MEASURING SITES

ALASKA

1977

LEGEND

State Boundary
State Capital
Town Less Than 5000 Population
Town 5000 to 25,000 Population
Town Over 25,000 Population

Towns of less than 5000 omitted from map unless
incorporated or required for orientation purposes

Lake or Reservoir
Large Stream
Small Stream
State Highway
Snow Data Measuring Site

INDEX OF ALASKA SNOW COURSES

MAP NO.	COURSE NAME	COURSE NO.	ELEV.	LAT.	LONG.	MEAS. DATES *	MEAS. BY
1	Arctic Valley #1	49MM1	500	61°13'N	149°40'W	2,3,4,5	c
2	Arctic Valley #2	49MM2	1000	61°13'N	149°37'W	2,3,4,5	c
3	Arctic Valley #3	49MM3	2030	61°14'N	149°35'W	2,3,4,5	c
4	Arctic Valley #4	49MM4	2330	61°14'N	149°33'W	2,3,4,5	c
5	Arctic Ski Bowl	49MM5	3000	61°15'N	149°31'W	2,3,4,5	c
6	Ship Creek	49MM7MPS	1750	61°08'N	149°28'W	2,3,4,5	a
7	Indian Pass	49MM8A	2350	61°05'N	149°29'W	2,3,4,5	a
8	Bird Creek	49MM6A	2350	61°06'N	149°20'W	2,3,4,5	a
9	South Campbell Creek	49MM11	1200	61°08'N	149°42'W	2,3,4,5,7	a
10	Mt. Alyeska	49LL15S	1200	60°57'N	149°05'W	2,3,4,5	a
11	Bertha Creek	49LL2	850	60°45'N	149°51'W	2,3,4,5	a,b
12	Kenai Summit	49LL3	1390	60°40'N	149°28'W	2,3,4,5	a
13	Moose Pass	49LL4	700	60°31'N	149°30'W	2,3,4,5	a
14	Jean Lake	50LL1	620	60°31'N	150°11'W	2,3,4,5	a
15	Bridge Creek (UP)	51KK1	1300	59°42'N	151°28'W	3,4,5	a
16	Bridge Creek (LO)	51KK2	1100	59°40'N	151°32'W	3,4,5	a
17	McArthur	52LL1A	120	61°00'N	152°00'W	2,3,4,5	a,c
18	Alexander Lake	50MM1A	200	61°45'N	150°54'W	2,3,4,5	a,c
19	Skwentna	51MM1A	160	61°58'N	151°12'W	2,3,4,5	a,c
20	Chelatna Lake	51NN1a	1650	62°31'N	151°29'W	2,3,4,5	a,c
21	Peters Hills	50NN1a	2010	62°31'N	150°57'W	2,3,4,5	a,c
22	Talkeetna	50NN2	350	62°18'N	150°05'W	2,3,4,5	a,c
23	Bald Mtn. Lake	49NN1A	2150	62°15'N	149°45'W	2,3,4,5	a,c
24	Fog Lakes	48NN2A	2250	62°47'N	148°29'W	2,3,4,5	a,c
25	Monahan Flat	4700lA	2710	63°18'N	147°39'W	2,3,4,5	a,c
26	Clearwater Lake	46NN1A	3100	62°59'N	146°58'W	2,3,4,5	a,c
27	Sanford River	45NN2A	2280	62°13'N	145°04'W	2,3,4,5	a,c
28	St. Anne's Lake	46MM1A	1990	61°53'N	146°03'W	2,3,4,5	a,c
29	Lake Louise	46NN2A	2400	62°17'N	146°30'W	2,3,4,5	a,c
30	Oshetna Lake	47NN1A	2950	62°23'N	147°29'W	2,3,4,5	a,c
31	Little Nelchina	47NN2A	4160	62°07'N	147°36'W	2,3,4,5	a,c
32	Willow Airstrip	50MM2	150	61°45'N	150°03'W	2,3,4,5	a,c
33	Independence Mine	49MM10	3300	61°45'N	149°25'W	3,4,5	a
34	Sheep Mountain	47MM2	2900	61°47'N	147°30'W	3,4,5	a
35	Tsaina River	45MM4	1500	61°12'N	145°30'W	3,4,5	a
36	Worthington Glacier	45MM2	2400	61°10'N	145°45'W	3,4,5	a
37	Lowe River	45MM3	550	61°06'N	145°50'W	3,4,5	a
38	Valdez	46MM2	50	61°08'N	146°20'W	2,3,4,5	a
39	Wolverine Glacier (A)	48LL1	2130	60°23'N	148°54'W	1,2,4,5,6,7	g
40	Wolverine Glacier (B)	48LL2	3610	60°25'N	148°55'W	2,3,4,5,6,7	g
41	Wolverine Galcier C	48LL3	4430	60°25'N	148°55'W	1,2,4,6,7	g
42	Gulkana Glacier A	45006	4590	63°15'N	145°29'W	2,3,4,5,6,7	g
43	Gulkana Glacier B	45007	5480	63°17'N	145°26'W	2,3,4,5,6,7	g
44	Gulkana Glacier C	45008	6360	63°19'N	145°29'W	5,6,7	g
45	Mankomen Lake	44NN1	3050	63°00'N	144°32'W	2,3,4,5	a
46	Tok Junction	43001	1650	63°18'N	143°00'W	2,3,4,5	a
47	Mentasta Pass	43NN1	2430	62°51'N	143°30'W	2,3,4,5	a
48	Haggard Creek	45NN1A	2540	62°42'N	145°28'W	2,3,4,5	a
49	Fielding Lake	45001A	3000	63°18'N	145°33'W	2,3,4,5	a
50	Ft. Greely	45005	1420	63°57'N	145°45'W	1,2,3,4,5,7	a
51	Granite Creek	45004	1240	63°57'N	145°24'W	1,2,3,4,5,7	a
52	Big Delta	45PP1	980	64°14'N	145°58'W	2,3,4,5	a
53	French Creek	46PP2MA	2010	64°43'N	146°40'W	2,3,4,5,7	a
54	Little Salcha	46PP3	1500	64°38'N	146°44'W	2,3,4,5,7	a
55	Caribou Mine	45PP2A	1115	64°40'N	145°40'W	2,3,4,5,7	a
56	Munson Ridge	46PP1AP	3100	64°52'N	146°13'W	2,3,4,5,7	a
57	Teuchet Creek	45PP3	1640	64°57'N	145°31'W	2,3,4,5	a
58	Upper Chena	44QQ1AP	3000	65°07'N	144°55'W	2,3,4,5,7	a
59	Lower Chena	44QQ6	2000	65°04'N	144°59'W	2,3,4,5,7	a
60	Monument Creek	45QQ2	1900	65°03'N	145°55'W	2,3,4,5	a
61	Mt. Ryan	46QQ1AP	2950	65°16'N	146°07'W	2,3,4,5,7	a
62	Little Chena	46QQ2AP	2200	65°08'N	146°32'W	2,3,4,5,7	a
63	Colorado Creek	46PP4S	750	64°52'N	146°39'W	1,2,3,4,5,7	a
64	Cleary Summit	47QQ1A	2230	65°03'N	147°24'W	1,2,3,4,5,7	a
65	Yak Pasture	47PP1	540	64°52'N	147°55'W	2,3,4,5	a
66	Bonanza Creek	48PP1	1150	64°45'N	148°20'W	2,3,4,5	b
67	Haystack Mtn.	47QQ2	1950	65°08'N	147°38'W	2,3,4,5	d
68	Caribou Creek	47QQ3	1440	65°09'N	147°35'W	2,3,4,5	d
69	Poker Creek	47QQ4S	1025	65°08'N	147°32'W	2,3,4,5,7	d
70	Farewell Lake	53NN1A	1090	62°34'N	153°35'C	3,4	a
71	Lake Minchumina	52001A	730	63°53'N	152°18'W	3,4	a
72	Wien Lake	51PP1A	1020	64°22'N	151°18'W	3,4	a
73	Lake Todatonten	52RR1a	980	66°10'N	152°55'W	3,4	a
74	Bettles Field	51RR1A	640	66°35'N	151°32'W	3,4	a
75	Anaktuvuk Pass	51TT1A	2100	68°09'N	151°41'W	3,4	a
76	Chandalar Lake	48SS1A	2040	67°30'N	148°30'W	3,4	a
77	Squaw Lake	48SS2a	2150	67°33'N	148°15'W	3,4	a
78	Arctic Village	45TT1A	2300	68°05'N	145°35'W	3,4	a
79	Koness Lake	44SS1A	1790	67°55'N	144°08'W	3,4	a
80	Coleen River	42SS1A	1100	67°44'N	142°28'W	3,4,7	a
81	Vundik Lake	43SS1a	950	67°23'N	143°45'W	3,4	a
82	Venetie	46SS1A	610	67°03'N	146°25'W	3,4,7	a
83	Fort Yukon	45RR1AM	430	66°35'N	145°15'W	3,4,7	a
84	Black River	42RR1A	650	66°36'N	142°45'W	3,4,7	a
85	Circle City	44QQ3A	600	65°50'N	144°05'W	3,4,7	a
86	Circle Hot Springs	44QQ5	860	65°29'N	144°39'W	3,4	a
87	Dempsey Creek	41RR2A	950	66°06'N	141°48'W	3,4	a
88	Nation River	41QQ1a	3050	65°25'N	141°40'W	3,4	a
89	Eagle Village	41PP1A	900	64°08'N	141°08'W	3,4,7	a
90	Boundary	41PP3A	3300	64°05'N	141°27'W	3,4	a
91	Chicken Airstrip	41PP2A	1650	64°05'N	141°45'W	3,4,7	a
92	Mt. Fairplay	42001a	3100	63°42'N	142°17'W	3,4,5	a
93	Douglas Ski Bowl	34JJ1	1640	58°16'N	134°27'W	3,4,5	b
94	Cropley Lake	34JJ2	1650	58°16'N	134°31'W	1,2,3,4	b
95	Eagle Crest	34JJ3	1000	58°17'N	134°32'W	1,2,3,4	b
96	Fish Creek	34JJ4	500	58°19'N	134°33'W	1,2,3,4	b
97	Upper Long Lake	33JJ2aS	1000	58°11'N	133°53'W	3,4,5,6,7	e
98	Speel River	33JJ3A	280	58°09'N	133°43'W	3,4,5,6,7	e
99	Petersburg Reservoir	32HH1	550	56°47'N	132°56'W	2,3,4,5	b
100	Mitkof Island	32HH2	1050	56°46'N	132°56'W	2,3,4,5	b
101	Crystal Lake	32HH3	1375	56°36'N	132°50'W	2,3,4,5	b
102	Harriet Top	31GG1	2000	55°29'N	131°37'W	3,4,5	b
103	Hunt Saddle	31GG2	1500	55°30'N	131°37'W	3,4,5	b
104	Lake Shore	31GG3	660	55°29'N	131°36'W	3,4,5	b
105	Log Cabin (B.C.)	34KK1	2880	59°45'N	134°58'W	3,4,5	e
106	Five Mile Camp	49RR1	400	65°55'N	149°48'W	2,3,4,5	i
107	Thirty Mile	50RR2a	1300	66°13'N	150°15'W	2,3,4,5	i
108	Prospect Creek	50RR1	980	66°47'N	150°45'W	2,3,4,5	i
109	Cold Foot Camp	50SS1	1000	67°16'N	150°10'W	1,2,3,4	i
110	Dietrich Camp	49SS1A	1550	67°42'N	149°45'W	2,3,4,5	i
111	Table Mountain	49SS3a	2200	67°58'N	149°45'W	2,3,4,5	i
112	Toolik River	49TT1	3100	68°37'N	149°26'W	7	d
113	Sagwon	48UU1	1000	69°26'N	148°34'W	7	d
114	Prudhoe Bay	48VV1	30	70°15'N	148°30'W	7	h
115	Barrow	56WW1	15	71°20'N	156°40'W	7	h
116	Meade River	57VV1	200	70°29'N	157°25'W	7	h
117	Barter Island	43VV1	15	70°08'N	143°37'W	7	h
118	Kavik River	47UU1	200	69°30'N	147°00'W	7	h
119	Candle	61QQ1	20	66°55'N	161°56'W	3,4	a,f
120	Kugruk River	62QQ1	225	65°40'N	162°27'W	3,4	a,f

<u>LEGEND</u>

* Numerals 1,2,3,4,5, and 6 refer to January 1, February 1, March 1, April 1, May 1, June 1, and 7 - for special dates.

* Letters refer to Agency that secures the snow survey, as follows:
   a. Soil Conservation Service
   b. Forest Service
   c. U.S. Army Corps of Engineers
   d. U.S. Army Cold Regions Research & Engineering Lab
   e. Alaska Power Administration
   f. Bureau of Land Management
   g. U.S. Geological Survey
   h. University of Alaska
   i. Alaska Pipeline Office

* Letters following the snow course no. refer to:
   A. Snow course and aerial stadia marker
   a. Aerial stadia marker only
   M. Soil Moisture Station
   P. Precipitation Storage Gage
   S. Snow Pillow

DRAINAGE BASIN and/or SNOW COURSE			Date of Survey	1976 Snow Depth (inches)	Water Content (inches)	PAST RECORD Water Content (inches)		Years of Previous Record
NAME	Number	Elevation				Last Year	Average +	
COPPER RIVER:								
Haggard Creek	34	2540	2/26	14	2.4	5.6	4.7	11
Little Nelchina	40	4160	2/29	19a	3.2e	6.0e	4.5	8
Mankomen Lake	32	3050	DELAYED REPORT			7.7	6.0	9
St. Anne's Lake	54	1985	2/29	17	3.4	6.1	4.4	11
Sanford River	37	2280	2/29	19a	3.4e	6.2e	4.7	9
Tsaina River	119	1550	2/26	43	11.5	16.7	12.3	3
Worthington Glacier	55	2500	2/26	56	18.5	25.9	15.1	9
MATANUSKA-SUSITNA:								
Alexander Lake	49	200	2/28	26	6.6	12.2e	9.6	12
Bald Mountain Lake	47	2150	2/28	14	3.6	7.2e	6.0	11
Chelatna Lake	44	1650	2/28	40a	8.0e	10.0e	8.6	12
Clearwater Lake	36	3100	2/28	16e	2.7e	6.3	4.9	10
Fog Lakes #2	96	2250	2/28	18	2.8	6.1	5.6	6
Independence Mine	51	3300	3/1	48	1.0	18.7	14.8	9
Lake Louise	41	2400	2/29	14	2.1	4.3	3.5	10
Monahan Flat	35	2710	2/28	25	4.4	9.0	6.3	11
Oshetna Lake	39	2950	2/29	13	2.2	4.5	3.3	12
Peters Hills	45	2010	2/28	49a	10.8e	14.3e	12.2	8
Sheep Mountain #2	120	2900	2/26	18	3.8	4.9	4.3	3
Skwentna	48	158	2/28	27	6.6	10.0	8.4	9
Talkeetna	46	350	2/28	25	5.8	10.4	7.0	9
Willow Airstrip	50	150	2/29	19	4.0	7.9	6.1	12
UPPER COOK INLET:								
Arctic Ski Bowl	65	3000	3/2	26	7.4	11.9	10.5	12
Arctic Valley #1	61	500	3/2	9	1.6	7.0	3.1	12
Arctic Valley #2	62	1000	3/2	12	1.8	6.3	3.2	12
Arctic Valley #3	63	2030	3/2	21	4.1	8.5	5.3	12
Arctic Valley #4	64	2330	3/2	23	4.8	8.5	5.8	12
Bird Creek	66	2350	2/27	39	12.2	20.4	13.8	9
Indian Pass	68	2350	2/27	50	15.3	17.4	16.5	9
McArthur	52	120	NO SURVEY			23.1e	17.4	11
Mt. Alyeska	128	1200	3/1	81	29.0	37.5	26.3	3
Ship Creek	67	1750	2/27	31	8.2	11.6	9.0	9
South Campbell Creek	129	1200	2/27	17	3.2	9.2	6.8	3
PRINCE WILLIAM SOUND:								
Lowe River	118	550	2/26	50	13.5	16.8	---	2
Valdez	117	50	2/26	50	15.7	16.5	---	2
KENAI PENINSULA:								
Bertha Creek	98	850	2/26	48	12.6	13.3	11.2	6
Bridge Creek, Lower	122	1100	2/25	33	9.0	14.6	10.6	4
Bridge Creek, Upper	121	1300	2/25	33	9.6	13.9	10.5	4
Jean Lake	101	620	2/26	14	3.0	4.8	3.1	6
Kenai Summit	99	1390	2/26	34	8.7	9.8	9.4	6
Moose Pass	100	700	2/26	22	5.9	7.0	4.8	6

a - aerial marker reading   e - estimated   N/S - No Survey

tool for use in determining the melting condition and extent of melting in a region. Further discussion of the use of NOAA satellite imagery for applications in snow hydrology are found in Seifert et al. (1975) and Kane et al. (1975).

2. Southern Bering Sea Region

Four rivers in this region are presently gauged by the U.S. Geological Survey. They are the Kvichak, Nuyakuk, Wood, and Kuskokwim. All these rivers excepting the Kuskokwim are strongly influenced by large lakes in their respective drainages. These lakes serve as storage mechanisms which moderate flow and consequently streamflow has a low index of seasonal variability. Snowmelt still contributes to most of the peak runoff events in these river systems, however, the seasonability is masked more so by the lake effects in this region than in any other subregion in Alaska. Snowmelt begins in this transitional region about May 1. and continues through early May, with no observed anomalies to the typical temperate elevational snowmelt pattern.

The Kuskokwim River more closely resembles an interior subarctic river system in most of its characteristics. Precipitation is generally lower and snowmelt runoff is the major contribution to streamflow. Consequently the Kuskokwim is also more seasonal and is subject to the additional hazard of ice-jam flooding. No chronology of ice jams is presently available. However, the U.S.

Weather Service River Forecast office in Anchorage does keep records of ice jams and they are often documented by on-site observation notes and photographs. Ice-jam flooding potential exists throughout the snowmelt period from roughly May 1 to the end of May. Ice-jam flooding can result in rapid, unpredictable increases in water levels and equally rapid releases of flood water. More discussion on ice jams is found in the section on the Yukon River in the North Bering-Chukchi Region.

There are observations which indicate subtle snow-melt anomalies in the South Bering region. Snowmelt initiates in the inland ($\sim$ 100 km inland) lowlands and slowly spreads coastward and upward in elevation. This slight anomaly is due to the seasonal lag caused by the shorefast and sea ice and cooler marine influence in the coastal areas. This influence becomes more apparent farther north as the climate becomes more arctic and the influences of sea ice become more pronounced. The anomaly attains its fullest development on Alaska's North Slope, and will be described further in the Beaufort Sea section. Except for the coastal areas, the snowmelt pattern is otherwise elevation-determined.

There are no snowcourses in this region.

3.   North Bering - Chukchi Sea Region:

Three rivers in this region are gauged by the U.S. Geological Survey: the Yukon at Ruby, the Kuzitrin River in Nome on the Seward Peninsula, and the Kobuk River at Ambler.

194

TABLE 9
National Weather Service AHOS/T Sites in Alaska
Installation completed in August 1976

Station	Sensor	
	Precip	River Gage
Healy	x	
Tanacross (Cathedral Bluffs)	x	
Sutton	x	
Little Susitna River	x	
Eagle River	x	
South Fork Eagle River	x	
Tuxedni Park	x	
Glen Alps	x	
Alyeska	x	
Lawing	x	
Auke Bay	x	
Little Rabbit Creek	x	

National Weather Service Proposed AHOS/S Sites
To be installed in the Summer of 1977

Station	Precip	River Gage
Stevens Village (Yukon River Bridge)	x	x
South Fork Campbell Creek (Anchorage)		x
North Pole (Chena River)		x
Little Chena River #2	x	x
Upper Chena River #3	x	x
Nenana (Tanana River)		x
Salchaket (Salcha River)		x
Harding Lake (Tanana River)	x	x
Ship Creek (Anchorage)		x
Eagle River		x

195

An attempt to characterize the snowmelt of the Yukon River basin is not a meaningful task. The Yukon drains such a huge area (259,000 sq. miles at Ruby) and encompasses nearly every climatic zone in the north. Rather than characterize the snowmelt, which is complex and best observed via satellite, this discussion will center on ice-jam observations and the hazards they produce, and some satellite observations of ice jams. (For a satellite chronology of the snowmelt, see Figs. 56-63, following Table 10).

Ice jams have been a seasonal event for Alaska natives since prehistory. Most native villages are associated with rivers and depend on them for food and transportation. Ice jams which flood villages are a fact of life on the Yukon and lower Kuskokwim rivers. At present it is nearly impossible to predict the location of ice jam formations. Present strategy involves monitoring of ice jams once the U.S.W.S. river forecast office is aware of their existence, and warning villagers up- and downstream of the situation. Recently (Bowers, 1976) installations have been made of real-time reporting networks which record precipitation and river stage. These new devices, called Automatic Hydrologic Observing Stations (AHOS/T) with a telephone coupler, have been installed (or will be installed) at the sites listed below (Table 9). AHOS/S sites are similar to AHOS/T except that the data are relayed via the GOES satellite. These real-time data systems will allow earlier detection

196

of rapid increases in river stage and, hopefully, more timely warnings.

The U.S.W.S. river forecast office for Alaska maintains records and photographs of ice jam floods. However, perhaps the most insightful examples of ice jam floods are those which have been observed via satellite. May, 1975, was a particularly fortunate observation period for users of satellite imagery, since the two major floods on the lower Yukon were both recorded by satellite imagery during that month. The first flood occurred near Holy Cross, Alaska, on May 24, 1975 and is best depicted on the thermal infrared imagery of the NOAA satellite. An enlargement of this image showing the flooded area is shown in Figure 62. The flooded area was measured with a polar compensating planimeter and was found to be 2590 $km^2 \pm 5\%$. NOAA imagery provided the only measurement of areal extent of this flood. A second flood, caused by ice jams and of even greater interest to offshore development interests, it occurred in the Yukon Delta on May 29, 1975. This flood was visible on both NOAA and LANDSAT imagery for that date. The LANDSAT image is shown in Figure 60 and a map of the area is shown as Figure 61.

The other river basins in the North Bering-Chukchi Region have no snowcourses, so the only means of characterizing them is via satellite observations. Both the Kuzitrin and Kobuk rivers begin the melt sequence about

197

May 8-10 each year. Both have elevationally related snowmelt patterns. Melt is 95% complete by June 10 and no significant glaciation is present in either basin.

Relating specifically to the Kobuk River, although Hotham Inlet remained frozen until at least June 10, 1975, there were never any signs of the sea ice being flooded by fresh water from the Kobuk River.

4. Beaufort Sea Region:

The north slope river basins have a unique and interesting snowmelt pattern which results mainly from a combination of severe climate variation and diverse physiography. The pattern is characterized by mid-elevation snowmelt initiation. The first areas to become snowfree in the North Slope are at those elevations between 300 and 600 meters. Runoff begins in late May and flows down channels which are still frozen and filled with ice. When this initial meltwater reaches the mouth of the rivers, it encounters still intact shorefast sea ice, and consequently the water flows out over the sea ice, flooding large areas of the ice until it finds a crack or other drainage route.

The snowmelt progresses from the mid-elevation range in both directions. The last areas to become snowfree are the highest peaks in the Brooks Range and the lowest nearshore coastal areas. This is the clearest example of seasonal lag and "thermal inertia" caused by the presence of a large area of sea ice offshore and surface lake ice

on the coastal plains, which delays snowmelt until mid-June. Melt occurs rapidly and snowcover is usually slight (< 20 cm), so that the region usually is 95% snowfree by June 25. Runoff is obviously very seasonal. As a further example of this seasonability of runoff, it is interesting to note that in the five years of record, 60 to 80% of all the volume of runoff in the Kuparuk River drainage occurred during the month of June.

A NOAA image (No. 2519), dated June 4, 1975, (Figure 54) shows most of the major seasonal features of interest to OCS development. Meltwater is flooding the shorefast ice at the mouths of the Colville, Kuparuk, Sagavanirktok, and Canning Rivers, and in Kasegaluk lagoon on the North-west coast of Alaska. The anomalous snowmelt pattern of the North Slope region is also very well documented on this image.

5.   Additional Snowmelt Information:

Table 10 classifies ungaged rivers by similarity to gauged streams. This is helpful and necessary since there are many streams which are ungaged, but which have climatic, basin-size, and topographic similarities to gaged basins. These are the characteristics that were used to develop the table.

C. NOAA Satellite Imagery:

A pictorial chronology of the 1975 snowmelt season follows. Figures 56 through 63. Figure captions stress the

Gaged River	Ungaged River	Region
Chakachatna River	Drift River MacArthur River Katnu River Grecian River Johnson River Beluga River	Gulf Coast - Cook Inlet
Nellie Juan River	Rude River Lowe River	
Little Susitna River	Chuit River Theodore River	
Eagle River	Peter's Creek Naknek River Egegik River Ugashik River	South Bering - Bristol Bay
Kuzitrin River	Utokok River Kokolik River Avalik River Kukpowruk River	North Bering - Chukchi
	Pitmegea River Kukpuk River Kivalina River Wulik River Hot Spring Creek Aglapuk River	Coastal Streams Draining N.W. Alaska
	Mudyutok River Buckland River Koyuk River	Seward Peninsula Drainages
	Tagagawik River	Selawik Basin
Kobuk River	Noatak River	Beaufort Sea-Arctic Alaska
Kuparuk River	Ikpikpuk River Shaviovik River	Low Elevation dist. and long stream length
Putuligayuk River	Meade River Ivisaruk River Kaoluk River Avalik River Okpiksak River Kadleroshilik River Fish Creek	Coastal Plain drainages

TABLE 10 Continued

Gaged River	Ungaged River	Region
Sagavanirktok River	Tamavariak River	Beaufort Sea
	Katakturuk River	
	Sadlerochit River	
	Hulahula River	Steep gradient,
	Jago River	Immature River
	Okpilak River	Some Braiding
	Aichilik River	
	Egaissrak River	
	Kongakut River	
	Marsh Creek	
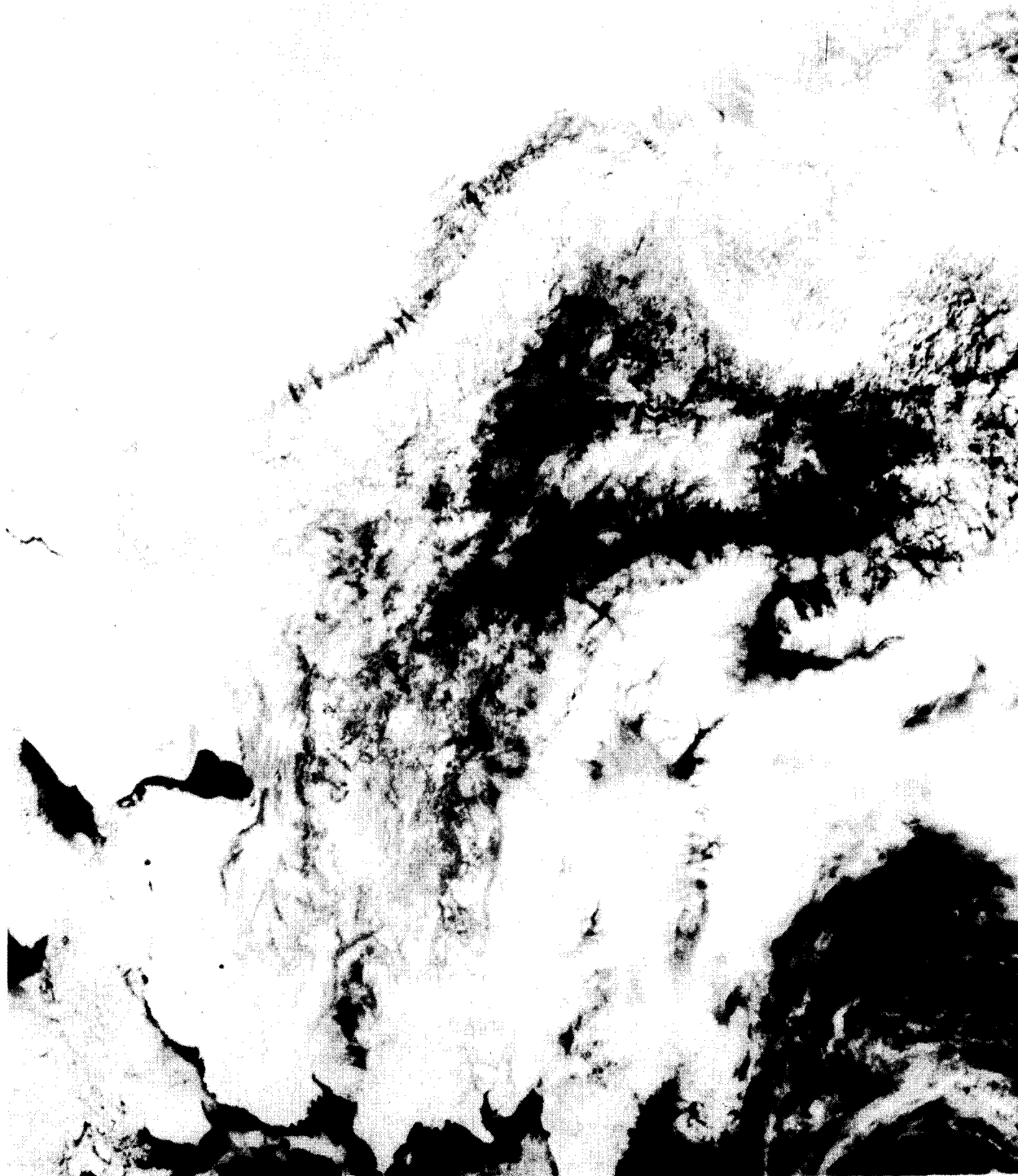
FIGURE 56: NOAA VISIBLE BAND IMAGE, ORBIT NO. 2093, May 1, 1975. This image depicts the earliest days of snowmelt. Unfortunately, the south coast is mostly clouded; however, the original darkening due to snowmelt is evident in the Tanana and Copper River Valleys.

FIGURE 57: NOAA IMAGE, ORBIT NO. 2206, May 10, 1975, VISIBLE BAND. About half the state has now had melting temperatures and conditions. Snowmelt is evident in the Yukon, Tanana, Copper basins and on the Alaska Peninsula. The lower Kuskokwim River area is also partly snowfree.

FIGURE 58: **This image is identical to that of Figure 57 except that it is in** the thermal infrared band (10.5 - 12.5 μ). This image is also specifically calibrated to depict both snowfree area (black) and areas at 0° C (stippled white and black). This imagery is quite valuable for monitoring rates and areal extent of snowmelt.
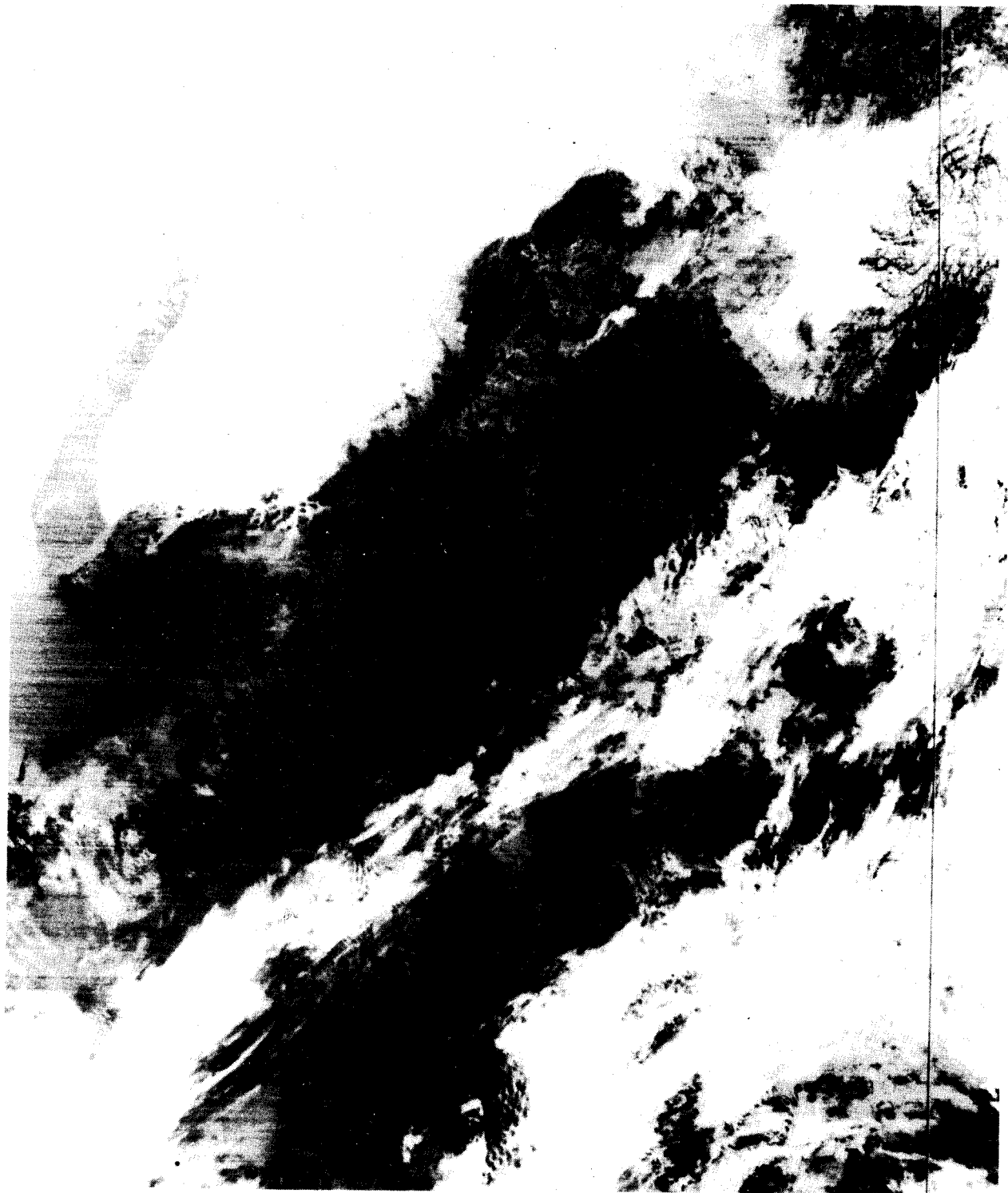
FIGURE 59: NOAA IMAGERY, ORBIT NO. 2256, May 14, 1975. Another infrared-enhanced image showing the areas of melting snow statewide in stippled white and the snowfree areas in black. The north slope snowmelt pattern is beginning to emerge at about this date. Note the Yukon River ice cover, indicated as a "melting" area.

FIGURE 60: LANDSAT IMAGE - ORBIT NO. 21363, SPECTRAL BAND 6, May 29, 1975. This image shows the large flooded area of the Yukon Delta, which was caused by a series of ice jams in the delta area. Much ice can still be seen in the main channels.

FIGURE 61

NORMAL CHANNEL SIZE OF YUKON RIVER, SAME SCALE AS
LANDSAT IMAGE FIGURE 60. (USGS)
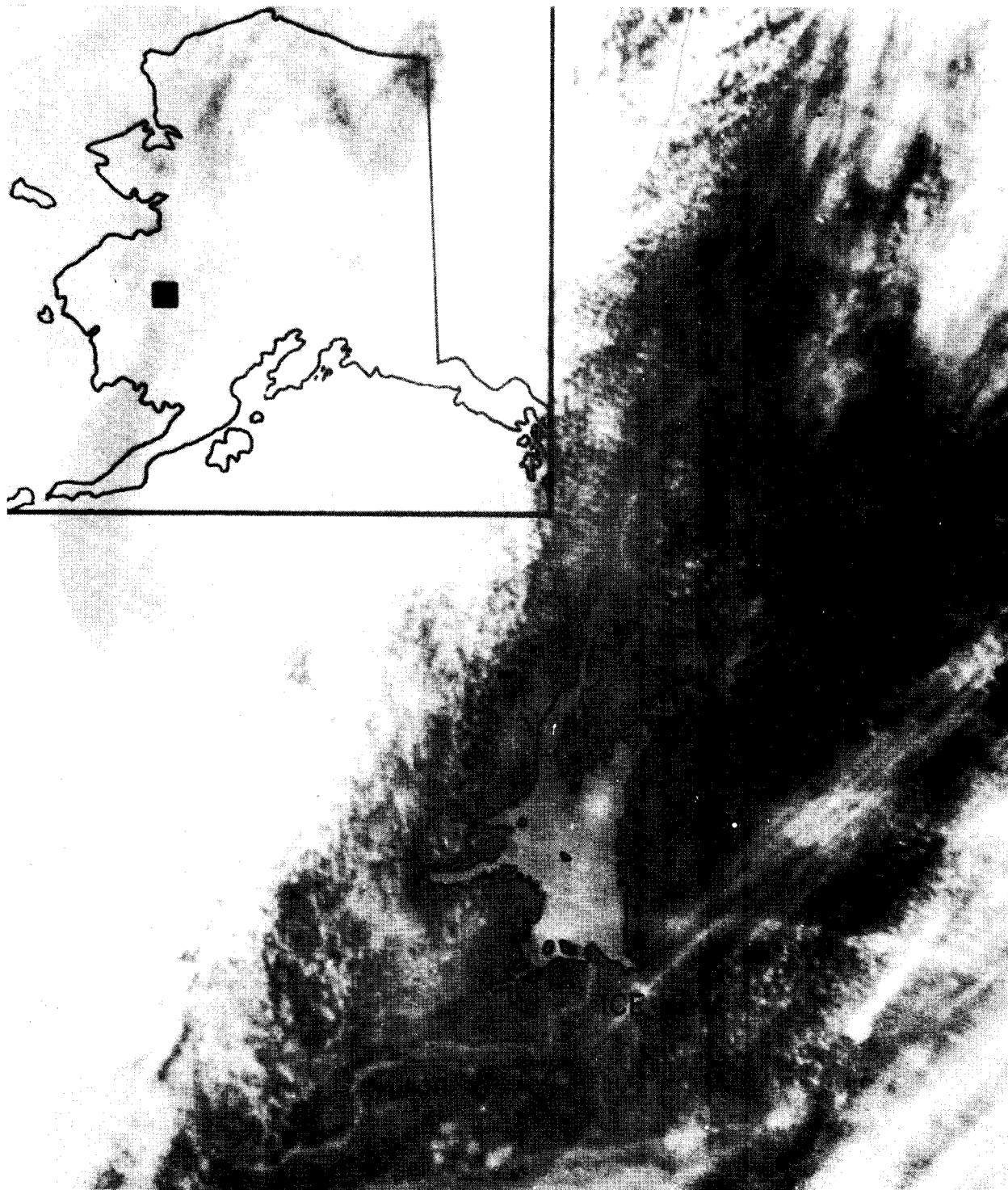
FIGURE 62: NOAA IR IMAGERY ENLARGEMENT, #2381, May 24, 1975. This is one of the most spectacular ice jam floods ever observed by satellite. The site is just upstream from the village of Holy Cross near the confluence of the Yukon and Innoko Rivers. The flooded surface area was measured using a polar compensating planimeter and found to be approximately 2590 km^2 · 5 .

FIGURE 63: NOAA IMAGE, ORBIT NO. 2619, June 12, 1975, VISIBLE BAND. Snow-
melt is 95% complete by this date throughout the state. This image is an
excellent example of the strong local influences of the oceans in coastal
Alaska.

salient features of the imagery as they relate to regional

and general snowmelt characterization.

VIII. CONCLUSIONS

Streams have been classified as encyclopedically as possible.
A conceptual understanding of the snowmelt and runoff process, conveyed
by description and especially through the use of satellite imagery has
also been attempted.

These characterizations should prove useful for engineering evalu-
ations of offshore sites as they might be affected by various hydrologic
hazards and seasonal variation.

IX. NEEDS FOR FURTHER STUDY

Characterization of the coastal streams of Alaska would be greatly
aided by additional gaging of streams. In particular, rivers which are
unique and should be gaged include the Colville, Utukok, Wulik, Koyuk,
and Canning Rivers. Such gaging would fill gaps in the understanding of
some of the more unique river systems in Alaska, as well as give perspective to the study of those rivers already gaged.

It was determined while doing background research for this study
that very little research, if any, has addressed the question of biological
responses to seasonal streamflow variations. This area deserves more
attention.

Local studies of orographic precipitation effects are necessary to
understand better this effect in Alaska. There is presently too little
available data for adequate assessment of snow depth increases with
elevation on either a local or regional basis.

The availability of fresh water in the Beaufort Sea/Chukchi regions is a critical factor in the orderly development of the areas. At present, too little is known about sources of winter and spring (April and May) flow to properly allocate water use by industry and yet still maintain adequate water levels in streams for fish populations. This is especially true in the Sagavanirktok River. Water use may well be one of the major onshore impacts of OCS development, and it is advisable to get more adequate and accurate information on the fresh water available, especially during the critically low late winter periods. For these reasons, it is strongly suggested that a detailed hydrologic reconnaissance be undertaken of all the major rivers in the Chukchi and Beaufort Sea drainages. Documentation of winter sources, flow regimes, springs, the possible availability of groundwater or subsurface flow in streambeds, and a study of minimum flows allowable are all required to ensure protection of the fish and hydrologic resources of the regions. Suggested rivers for hydrologic reconnaissance are the Canning, Sagavanirktok, Kuparuk, Colville, Ikpikpuk, Meade, Utukok, Kokolik, Kukpowruk, Kukpuk, and Wulik Rivers.

X.   ACKNOWLEDGEMENTS

XI. LITERATURE CITED

Anderson, D. M., L. W. Gatto, H. L. McKim, and A. Petrone. 1973.
Sediment distribution and coastal processes in Cook Inlet, Alaska.
In Symposium on Significant Results obtained from the Earth
Resources Satellite-1, Vol. 1, Tech. presentations, Section B,
GSFC, March 5-9, 1973, NASA SP-327. pp. 1323-1339.

Bilello, M. 1973. Measurements of snow and ice for correlation
with data collected by remote systems. *In* Advanced Concepts
and Techniques in the Study of Snow and Ice Resources, held
at Monterey, California, December 2-6, 1973, Nat. Acad. Sci.,
Wash., D.C. pp. 283-293.

Bowers, T. 1976. Personal Communication.

Campbell, W. J., and S. Martin. 1973. Oil and ice in the arctic
ocean: possible large scale interactions. July 6, 1973. Science
181(4094):56-58.

Carlson, R. F. 1972. The land hydrology of the south-central coastal
zone, *In* A Review of the oceanography and renewable resources of
the Northern Gulf of Alaska: Univ. of Alaska, Inst. of Marine
Science Report S72-23, Sea Grant Report 73-3, Sec. 7. pp. 149-
152.

Carlson, R. F. 1974. Permafrost hydrology: an Alaskan experience,
In Permafrost hydrology: Proceedings of a Workshop Seminar,
1974, Calgary, Alberta, February 26-28, 1974, Environment Canada,
Ottawa. pp. 45-49.

Environmental Protection Agency. 1975. Environmental Studies of an
Arctic Estuarine System - Final Report. Alexander *et al.*, Institute
of Marine Science, University of Alaska. EPA-660/3-75-026.

Guymon, G. L. 1974. Regional sediment yield analysis of Alaska streams. Journ. of the Hydraulics Div., ASCE, 100(HY1), paper 10255, Jan. pp. 41-41.

Johnson, P., and C. W. Hartman. 1969. Environmental Atlas of Alaska. Inst. of Water Resources, Univ. of Alaska, Fairbanks.

Kane, D. L., and R. F. Carlson. 1973. Hydrology of central arctic river basins of Alaska, Institute of Water Resources, Univ. of Alaska, Fairbanks. Report No. IWR-41. 51 pp.

Kane, D. L., R. F. Carlson, and R. D. Seifert. 1975. Alaskan arctic coast ice and snow dynamics as viewed by the NOAA satellites. Proceedings, Third Inter. Symp. on Ice Problems, Hanover, N.H. pp. 567-577.

McCloy, J. M. 1970. Hydrometeorological relationships and their effects on the levels of a small Arctic delta, Geografiska Annaler 52A(3-4). pp. 223-241.

Newbury, R. W. 1974. River hydrology in permafrost areas. *In* Permafrost Hydrology: Proceedings of a Workshop Seminar, 1974, Calgary, Alberta, February 26-28, 1974, Environment Canada. pp. 31-37.

Post, A., and L. Mayo. 1971. Glacier dammed lakes and outburst floods in Alaska, U.S. Geological Survey, Hydrol. Investigations HA-455.

Poulin, A. O. 1974. Hydrologic characteristics of snow-covered terrain from thermal infrared imagery. *In* Advanced Concepts and Techniques in the Study of Snow and Ice Resources, held at Monterey, California, December 2-6, 1973, Nat. Acad. Sci., Wash., D.C. pp. 494-503.

Reimnitz, E., and N. F. Marshall. 1965. Effects of the Alaska Earthquake and Tsunami on recent deltaic sediments. J. Geoph. Res. May 15. 70(10):2363-2576.

Reimnitz, E., and K. F. Bruder. 1972. River discharge into an ice covered ocean and related sediment dispersal. Geol. Soc. of Amer. Bull., 83(3):861-866.

Seifert, R. D., R. F. Carlson, and D. L. Kane. 1975. Operational applications of NOAA imagery in Alaska. *In* Operational Applications of Satellite Snowcover Observations, Washington, D.C., NASA SP-391. pp. 143-155.

Strahler, A. N. 1952. Hypsometric (Area-Altitude) Analysis of Erosional Topography, Bull. of the Geol. Soc. of America, 63. November. pp. 1117-1142.

Walker, H. J. 1973. Spring discharge of an Arctic river determined from salinity measurements beneath sea ice. Water Resources Research 9(2):474-480.

U.S. Coast and Geodetic Survey. 1964. United States Coast Pilot 9, Pacific and Arctic Coast. U.S. Government Printing Office, Washington.

APPENDIX

15212000 COPPER RIVER NEAR CHITINA, ALASKA
***** MEAN DAILY FLOW BY MONTH *****

MONTH	MAXIMUM	YEAR	DAY	MINIMUM	YEAR	DAY	AVERAGE
OCT	64500.	1957	1	7440.	1954	31	19582.
NOV	22000.	1957	1	5000.	1956	21	9311.
DEC	9900.	1956	1	4400.	1955	1	6766.
JAN	8500.	1961	1	2700.	1956	1	5528.
FEB	10000.	1958	28	2300.	1956	1	4757.
MAR	8000.	1974	1	2000.	1956	1	4532.
APR	16000.	1974	30	3000.	1959	1	5401.
MAY	80800.	1960	26	3800.	1959	1	29460.
JUN	170000.	1969	18	27300.	1970	1	82447.
JUL	260000.	1971	15	66400.	1970	21	118275.
AUG	226000.	1971	11	27000.	1969	29	102253.
SEP	130000.	1960	13	17700.	1958	30	51183.

***** YEARLY FLOW DATA *****

MAXIMUM	YEAR	MINIMUM	YEAR	AVERAGE
260000.	1971	2000.	1956	36855.

***** MEAN MONTHLY FLOW DATA *****

MONTH	MAXIMUM	YEAR	MINIMUM	YEAR
OCT	29035.	1957	13655.	1968
NOV	15060.	1957	6000.	1955
DEC	9000.	1960	4400.	1955
JAN	8500.	1961	2700.	1956
FEB	8000.	1974	2300.	1956
MAR	8000.	1974	2000.	1955
APR	10933.	1974	3000.	1959
MAY	49945.	1957	15403.	1964
JUN	114957.	1957	48050.	1970
JUL	143794.	1971	84423.	1970
AUG	135523.	1971	53361.	1969
SEP	83893.	1957	27933.	1969

***** MEAN ANNUAL FLOW DATA *****

MAXIMUM	YEAR	MINIMUM	YEAR
46411.	1957	26791.	1970

15210000 POWER CREEK NEAR CORDOVA, ALASKA
***** MEAN DAILY FLOW BY MONTH *****

MONTH	MAXIMUM	YEAR	DAY	MINIMUM	YEAR	DAY	AVERAGE
OCT	2150.	1954	31	70.	1950	31	293.
NOV	1880.	1957	4	40.	1973	30	170.
DEC	550.	1969	29	32.	1973	15	80.
JAN	580.	1958	7	20.	1972	28	57.
FEB	940.	1968	27	18.	1950	16	52.
MAR	1000.	1969	31	15.	1972	16	43.
APR	500.	1969	1	15.	1972	1	48.
MAY	909.	1961	16	20.	1972	1	185.
JUN	1540.	1958	16	138.	1950	1	434.
JUL	3340.	1958	27	281.	1959	27	548.
AUG	2470.	1954	2	176.	1969	14	490.
SEP	5000.	1949	25	94.	1959	21	476.

***** YEARLY FLOW DATA *****

MAXIMUM	YEAR	MINIMUM	YEAR	AVERAGE
5000.	1949	15.	1972	241.

***** MEAN MONTHLY FLOW DATA *****

MONTH	MAXIMUM	YEAR	MINIMUM	YEAR
OCT	594.	1952	123.	1950
NOV	334.	1957	53.	1950
DEC	190.	1969	37.	1950
JAN	129.	1961	25.	1951
FEB	175.	1968	19.	1972
MAR	134.	1968	15.	1972
APR	104.	1963	16.	1972
MAY	308.	1961	94.	1952
JUN	598.	1958	328.	1972
JUL	925.	1958	352.	1974
AUG	715.	1956	252.	1969
SEP	1024.	1951	218.	1969

***** MEAN ANNUAL FLOW DATA *****

MAXIMUM	YEAR	MINIMUM	YEAR
321.	1958	180.	1974

217

15219000 W F OLSEN BAY CREEK NEAR CORDOVA, ALASKA
***** MEAN DAILY FLOW BY MONTH *****

MONTH	MAXIMUM	YEAR	DAY	MINIMUM	YEAR	DAY	AVERAGE
SEP	2430.	1973	13	4.	1974	9	141.
OCT	1680.	1972	16	7.	1973	27	85.
NOV	830.	1972	19	3.	1973	24	63.
DEC	400.	1972	1	2.	1973	7	33.
JAN	150.	1973	9	1.	1966	3	15.
FEB	317.	1968	27	1.	1965	1	19.
MAR	355.	1969	31	1.	1966	1	18.
APR	500.	1973	30	2.	1972	1	36.
MAY	3000.	1973	28	10.	1972	1	193.
JUN	2400.	1973	30	25.	1974	30	231.
JUL	3180.	1973	13	11.	1974	31	221.
AUG	1550.	1973	6	5.	1974	23	118.

***** YEARLY FLOW DATA *****

MAXIMUM	YEAR	MINIMUM	YEAR	AVERAGE
3180.	1973	1.	1966	98.

***** MEAN MONTHLY FLOW DATA *****

MONTH	MAXIMUM	YEAR	MINIMUM	YEAR
SEP	889.	1973	18.	1969
OCT	501.	1972	20.	1957
NOV	424.	1972	5.	1973
DEC	218.	1972	4.	1966
JAN	95.	1973	2.	1965
FEB	85.	1973	2.	1966
MAR	87.	1973	2.	1972
APR	213.	1973	2.	1972
MAY	1503.	1973	36.	1971
JUN	1787.	1973	41.	1974
JUL	1841.	1973	19.	1974
AUG	831.	1973	14.	1958

***** MEAN ANNUAL FLOW DATA *****

MAXIMUM	YEAR	MINIMUM	YEAR
643.	1973	25.	1972

15237000 NELLIE JUAN RIVER NEAR HUNTER, ALASKA

***** MEAN DAILY FLOW BY MONTH *****

MONTH	MAXIMUM	YEAR	DAY	MINIMUM	YEAR	DAY	AVERAGE
DEC	220.	1952	11	55.	1951	16	128.
JAN	310.	1951	16	48.	1955	1	110.
FEB	430.	1963	18	40.	1952	1	95.
MAR	140.	1955	11	28.	1954	21	72.
APR	1760.	1955	18	43.	1963	3	157.
MAY	4340.	1951	16	53.	1954	1	738.
JUN	3890.	1952	21	1030.	1955	5	2110.
JUL	5690.	1961	10	1520.	1954	24	2790.
AUG	4990.	1951	9	1490.	1951	26	2343.
SEP	7720.	1951	11	480.	1952	18	1963.
OCT	3890.	1964	7	122.	1951	27	594.
NOV	1330.	1964	18	85.	1953	30	275.

***** YEARLY FLOW DATA *****

MAXIMUM	YEAR	MINIMUM	YEAR	AVERAGE
7720.	1951	28.	1954	897.

***** MEAN MONTHLY FLOW DATA *****

MONTH	MAXIMUM	YEAR	MINIMUM	YEAR
DEC	173.	1963	73.	1961
JAN	198.	1961	58.	1952
FEB	157.	1961	40.	1952
MAR	115.	1955	33.	1952
APR	433.	1955	50.	1954
MAY	1088.	1951	324.	1954
JUN	2552.	1964	1535.	1955
JUL	3445.	1952	2195.	1954
AUG	2600.	1963	1823.	1954
SEP	2779.	1963	1192.	1952
OCT	1025.	1963	451.	1951
NOV	517.	1952	138.	1961

***** MEAN ANNUAL FLOW DATA *****

MAXIMUM	YEAR	MINIMUM	YEAR
1098.	1963	861.	1954

15237700 RESURRECTION RIVER NEAR SEWARD, ALASKA
***** MEAN DAILY FLOW BY MONTH *****

MONTH	MAXIMUM	YEAR	DAY	MINIMUM	YEAR	DAY	AVERAGE
OCT	3260.	1954	21	200.	1955	31	957.
NOV	2000.	1967	3	150.	1955	26	479.
DEC	480.	1967	1	100.	1955	29	236.
JAN	392.	1958	1	90.	1955	7	175.
FEB	500.	1958	27	85.	1955	16	155.
MAR	430.	1958	1	60.	1955	11	152.
APR	543.	1955	19	70.	1956	4	135.
MAY	3050.	1955	31	150.	1955	1	558.
JUN	5340.	1955	7	750.	1956	1	2336.
JUL	4850.	1955	10	1800.	1956	1	2797.
AUG	15000.	1966	21	1230.	1955	29	3310.
SEP	14000.	1957	13	1160.	1955	2	4098.

***** YEARLY FLOW DATA *****

MAXIMUM	YEAR	MINIMUM	YEAR	AVERAGE
15000.	1966	60.	1966	1133.

***** MEAN MONTHLY FLOW DATA *****

MONTH	MAXIMUM	YEAR	MINIMUM	YEAR
OCT	1179.	1966	552.	1967
NOV	685.	1967	183.	1955
DEC	384.	1967	119.	1955
JAN	295.	1958	95.	1966
FEB	321.	1958	93.	1955
MAR	220.	1955	59.	1955
APR	338.	1955	98.	1966
MAY	885.	1958	351.	1955
JUN	2268.	1958	1830.	1966
JUL	3294.	1955	2529.	1967
AUG	4271.	1966	2439.	1955
SEP	5745.	1966	2409.	1955

***** MEAN ANNUAL FLOW DATA *****

MAXIMUM	YEAR	MINIMUM	YEAR
1350.	1966	1173.	1955

15238500 LOWELL CREEK AT SEWARD, ALASKA
***** MEAN DAILY FLOW BY MONTH *****

MONTH	MAXIMUM	YEAR	DAY	MINIMUM	YEAR	DAY	AVERAGE
MAY	63.	1958	23	8.	1958	1	29.
JUN	85.	1958	29	22.	1966	1	53.
JUL	101.	1966	12	37.	1967	3	66.
AUG	543.	1966	21	31.	1958	29	88.
SEP	400.	1966	18	19.	1958	24	105.
OCT	185.	1966	5	22.	1965	26	55.
NOV	95.	1957	3	7.	1965	30	23.
DEC	26.	1957	13	2.	1965	24	10.
JAN	12.	1958	1	1.	1966	1	6.
FEB	38.	1958	27	2.	1965	25	5.
MAR	24.	1958	1	2.	1966	1	5.
APR	16.	1957	26	3.	1965	1	7.

***** YEARLY FLOW DATA *****

MAXIMUM	YEAR	MINIMUM	YEAR	AVERAGE
543.	1966	1.	1966	42.

***** MEAN MONTHLY FLOW DATA *****

MONTH	MAXIMUM	YEAR	MINIMUM	YEAR
MAY	43.	1957	18.	1965
JUN	60.	1958	45.	1965
JUL	75.	1965	51.	1957
AUG	139.	1966	45.	1958
SEP	159.	1966	31.	1958
OCT	68.	1966	41.	1957
NOV	38.	1957	13.	1966
DEC	15.	1957	4.	1965
JAN	10.	1958	2.	1966
FEB	11.	1958	3.	1965
MAR	10.	1958	2.	1966
APR	9.	1957	6.	1958

***** MEAN ANNUAL FLOW DATA *****

MAXIMUM	YEAR	MINIMUM	YEAR
45.	1957	32.	1966

15238600 SPRUCE CREEK NEAR SEWARD, ALASKA

***** MEAN DAILY FLOW BY MONTH *****

MONTH	MAXIMUM	YEAR	DAY	MINIMUM	YEAR	DAY	AVERAGE
SEP	1160.	1972	3	14.	1968	24	117.
OCT	1650.	1969	11	16.	1957	30	97.
NOV	440.	1969	1	5.	1973	28	34.
DEC	153.	1969	19	2.	1973	13	14.
JAN	45.	1971	3	1.	1969	6	6.
FEB	80.	1970	11	1.	1969	1	12.
MAR	32.	1970	19	1.	1969	25	11.
APR	91.	1969	17	1.	1973	4	13.
MAY	220.	1969	22	1.	1972	1	53.
JUN	1000.	1969	17	51.	1973	2	174.
JUL	493.	1970	12	68.	1974	25	167.
AUG	704.	1970	20	31.	1974	25	118.

***** YEARLY FLOW DATA *****

MAXIMUM	YEAR	MINIMUM	YEAR	AVERAGE
1650.	1969	1.	1969	77.

***** MEAN MONTHLY FLOW DATA *****

MONTH	MAXIMUM	YEAR	MINIMUM	YEAR
SEP	220.	1974	56.	1968
OCT	333.	1969	38.	1973
NOV	63.	1969	10.	1973
DEC	51.	1969	4.	1973
JAN	15.	1970	1.	1969
FEB	31.	1970	1.	1969
MAR	15.	1970	1.	1969
APR	35.	1969	1.	1972
MAY	100.	1968	31.	1971
JUN	298.	1969	116.	1972
JUL	234.	1971	110.	1974
AUG	213.	1970	57.	1969

***** MEAN ANNUAL FLOW DATA *****

MAXIMUM	YEAR	MINIMUM	YEAR
105.	1970	57.	1968

15239000 BRADLEY RIVER NEAR HOMER, ALASKA
***** MEAN DAILY FLOW BY MONTH *****

MONTH	MAXIMUM	YEAR	DAY	MINIMUM	YEAR	DAY	AVERAGE
OCT	7190.	1969	14	90.	1958	30	436.
NOV	1380.	1957	3	50.	1963	29	131.
DEC	596.	1969	21	38.	1958	16	93.
JAN	300.	1961	16	24.	1972	27	66.
FEB	165.	1970	25	18.	1972	23	50.
MAR	150.	1968	3	16.	1972	26	41.
APR	115.	1970	1	16.	1972	1	44.
MAY	1190.	1961	17	24.	1972	1	254.
JUN	2890.	1958	22	170.	1973	1	722.
JUL	2230.	1971	14	549.	1972	1	1007.
AUG	5140.	1958	13	507.	1958	31	1034.
SEP	6000.	1961	12	184.	1968	24	861.

***** YEARLY FLOW DATA *****

MAXIMUM	YEAR	MINIMUM	YEAR	AVERAGE
7190.	1969	16.	1972	405.

***** MEAN MONTHLY FLOW DATA *****

MONTH	MAXIMUM	YEAR	MINIMUM	YEAR
OCT	1728.	1969	160.	1959
NOV	502.	1957	73.	1968
DEC	239.	1969	41.	1968
JAN	199.	1961	32.	1974
FEB	116.	1970	20.	1972
MAR	109.	1970	17.	1972
APR	103.	1970	17.	1972
MAY	593.	1960	87.	1964
JUN	1358.	1969	517.	1972
JUL	1394.	1971	788.	1959
AUG	1593.	1966	556.	1962
SEP	1557.	1966	306.	1959

***** MEAN ANNUAL FLOW DATA *****

MAXIMUM	YEAR	MINIMUM	YEAR
541.	1970	285.	1962

15240000 ANCHOR RIVER AT ANCHOR POINT, ALASKA
***** MEAN DAILY FLOW BY MONTH *****

MONTH	MAXIMUM	YEAR	DAY	MINIMUM	YEAR	DAY	AVERAGE
OCT	1530.	1957	22	80.	1956	26	351.
NOV	1550.	1957	3	70.	1955	21	232.
DEC	610.	1957	2	45.	1955	15	135.
JAN	400.	1961	16	45.	1956	1	128.
FEB	460.	1963	21	50.	1954	1	121.
MAR	1500.	1963	1	50.	1956	11	151.
APR	2230.	1959	29	80.	1956	1	323.
MAY	2730.	1964	31	188.	1963	27	914.
JUN	2500.	1964	1	52.	1957	26	392.
JUL	1080.	1964	28	47.	1957	15	228.
AUG	2000.	1963	23	40.	1955	21	252.
SEP	1960.	1961	12	103.	1962	2	347.

***** YEARLY FLOW DATA *****

MAXIMUM	YEAR	MINIMUM	YEAR	AVERAGE
2730.	1964	40.	1955	299.

***** MEAN MONTHLY FLOW DATA *****

MONTH	MAXIMUM	YEAR	MINIMUM	YEAR
OCT	611.	1957	197.	1962
NOV	832.	1957	89.	1955
DEC	259.	1957	50.	1955
JAN	284.	1961	50.	1954
FEB	285.	1963	50.	1954
MAR	681.	1963	57.	1956
APR	591.	1958	140.	1955
MAY	1312.	1964	473.	1963
JUN	808.	1955	131.	1957
JUL	355.	1964	133.	1957
AUG	382.	1955	106.	1962
SEP	599.	1961	129.	1962

***** MEAN ANNUAL FLOW DATA *****

MAXIMUM	YEAR	MINIMUM	YEAR
394.	1958	208.	1957

224

15241600 NINILCHIK RIVER AT NINILCHIK, ALASKA
***** MEAN DAILY FLOW BY MONTH *****

MONTH	MAXIMUM	YEAR	DAY	MINIMUM	YEAR	DAY	AVERAGE
MAY	1000.	1972	12	58.	1959	1	222.
JUN	650.	1964	2	44.	1959	29	123.
JUL	218.	1965	19	30.	1966	20	86.
AUG	350.	1971	7	39.	1959	10	88.
SEP	500.	1966	18	44.	1958	1	119.
OCT	394.	1963	7	36.	1969	23	121.
NOV	500.	1970	2	34.	1953	16	95.
DEC	100.	1967	1	40.	1973	18	57.
JAN	64.	1964	1	36.	1974	11	49.
FEB	80.	1970	26	36.	1974	1	53.
MAR	140.	1970	29	36.	1974	1	63.
APR	1220.	1974	24	40.	1968	1	159.

***** YEARLY FLOW DATA *****

MAXIMUM	YEAR	MINIMUM	YEAR	AVERAGE
1220.	1974	30.	1966	104.

***** MEAN MONTHLY FLOW DATA *****

MONTH	MAXIMUM	YEAR	MINIMUM	YEAR
MAY	381.	1964	82.	1959
JUN	238.	1964	62.	1959
JUL	124.	1965	60.	1959
AUG	144.	1966	48.	1959
SEP	199.	1966	55.	1959
OCT	203.	1966	78.	1968
NOV	248.	1967	41.	1953
DEC	70.	1967	42.	1965
JAN	52.	1972	37.	1974
FEB	67.	1970	36.	1974
MAR	108.	1970	37.	1974
APR	548.	1974	52.	1959

***** MEAN ANNUAL FLOW DATA *****

MAXIMUM	YEAR	MINIMUM	YEAR
139.	1965	76.	1970

15242000 KASILOF RIVER NEAR, KASILOF ALASKA
***** MEAN DAILY FLOW BY MONTH *****

MONTH	MAXIMUM	YEAR	DAY	MINIMUM	YEAR	DAY	AVERAGE
OCT	8720.	1957	1	1670.	1968	31	4001.
NOV	5230.	1969	1	580.	1955	30	2042.
DEC	2560.	1957	1	310.	1955	16	1142.
JAN	1510.	1970	1	290.	1956	1	716.
FEB	1100.	1970	21	280.	1956	1	569.
MAR	1100.	1970	1	23.	1964	31	515.
APR	792.	1961	5	19.	1964	2	517.
MAY	1200.	1967	25	205.	1964	1	664.
JUN	3380.	1958	30	409.	1964	1	1369.
JUL	8390.	1958	31	1310.	1965	1	3868.
AUG	11400.	1957	25	3050.	1955	1	6698.
SEP	12200.	1957	14	3250.	1970	30	6378.

***** YEARLY FLOW DATA *****

MAXIMUM	YEAR	MINIMUM	YEAR	AVERAGE
12200.	1957	19.	1964	2385.

***** MEAN MONTHLY FLOW DATA *****

MONTH	MAXIMUM	YEAR	MINIMUM	YEAR
OCT	5885.	1957	2584.	1968
NOV	3706.	1957	1161.	1955
DEC	1885.	1952	358.	1955
JAN	1156.	1968	290.	1956
FEB	955.	1961	280.	1956
MAR	919.	1970	270.	1956
APR	719.	1965	113.	1964
MAY	981.	1967	264.	1964
JUN	1821.	1953	824.	1952
JUL	5513.	1958	2093.	1965
AUG	10025.	1957	4168.	1965
SEP	10482.	1957	3982.	1969

***** MEAN ANNUAL FLOW DATA *****

MAXIMUM	YEAR	MINIMUM	YEAR
3196.	1958	1874.	1955

15266300 KENAI RIVER AT SOLDOTNA, ALASKA

***** MEAN DAILY FLOW BY MONTH *****

MONTH	MAXIMUM	YEAR	DAY	MINIMUM	YEAR	DAY	AVERAGE
MAY	7600.	1958	30	1100.	1955	1	2352.
JUN	14700.	1959	23	2520.	1971	2	7246.
JUL	17300.	1971	14	6820.	1972	1	11955.
AUG	23200.	1966	11	5800.	1959	30	13895.
SEP	26800.	1974	24	3700.	1958	29	12010.
OCT	29500.	1969	15	1830.	1958	31	6262.
NOV	7000.	1959	1	1300.	1973	28	2758.
DEC	3700.	1959	29	1100.	1973	13	1787.
JAN	8000.	1969	18	950.	1974	28	1516.
FEB	3200.	1959	1	900.	1974	8	1333.
MAR	2500.	1970	30	800.	1973	21	1200.
APR	2200.	1958	25	770.	1955	1	1218.

***** YEARLY FLOW DATA *****

MAXIMUM	YEAR	MINIMUM	YEAR	AVERAGE
29500.	1969	770.	1955	5513.

***** MEAN MONTHLY FLOW DATA *****

MONTH	MAXIMUM	YEAR	MINIMUM	YEAR
MAY	3351.	1958	1950.	1973
JUN	10219.	1959	4949.	1972
JUL	15239.	1971	9696.	1973
AUG	18968.	1955	8705.	1959
SEP	20843.	1967	5873.	1959
OCT	14375.	1969	2851.	1958
NOV	4507.	1969	1631.	1973
DEC	2828.	1959	1199.	1973
JAN	2342.	1969	1068.	1974
FEB	2417.	1969	913.	1974
MAR	1781.	1958	842.	1973
APR	1703.	1970	812.	1972

***** NEXT ANNUAL FLOW DATA *****

MAXIMUM	YEAR	MINIMUM	YEAR
6627.	1969	3832.	1974

15267900 RESURRECTION CREEK NEAR HOPE, ALASKA

***** MEAN DAILY FLOW BY MONTH *****

MONTH	MAXIMUM	YEAR	DAY	MINIMUM	YEAR	DAY	AVERAGE
OCT	1450.	1959	11	94.	1958	28	311.
NOV	577.	1970	1	90.	1958	25	175.
DEC	350.	1969	22	65.	1958	25	127.
JAN	170.	1970	1	52.	1974	25	95.
FEB	140.	1958	29	50.	1974	25	76.
MAR	170.	1958	4	50.	1959	1	73.
APR	120.	1971	30	50.	1972	29	74.
MAY	814.	1958	29	51.	1972	1	288.
JUN	1800.	1971	27	201.	1971	2	618.
JUL	1550.	1971	13	239.	1974	31	531.
AUG	1730.	1971	9	146.	1974	23	353.
SEP	555.	1971	5	122.	1959	27	243.

***** YEARLY FLOW DATA *****

MAXIMUM	YEAR	MINIMUM	YEAR	AVERAGE
1800.	1971	50.	1972	248.

***** MEAN MONTHLY FLOW DATA *****

MONTH	MAXIMUM	YEAR	MINIMUM	YEAR
OCT	656.	1959	131.	1958
NOV	235.	1957	98.	1958
DEC	192.	1969	77.	1958
JAN	133.	1970	55.	1959
FEB	110.	1958	44.	1974
MAR	123.	1958	50.	1974
APR	92.	1959	58.	1972
MAY	422.	1958	175.	1971
JUN	780.	1970	439.	1973
JUL	954.	1971	334.	1959
AUG	755.	1971	136.	1974
SEP	429.	1971	139.	1959

***** MEAN ANNUAL FLOW DATA *****

MAXIMUM	YEAR	MINIMUM	YEAR
335.	1970	175.	1974

15272550 GLACIER CREEK AT GIRDWOOD, ALASKA

***** MEAN DAILY FLOW BY MONTH *****

MONTH	MAXIMUM	YEAR	DAY	MINIMUM	YEAR	DAY	AVERAGE
OCT	2610.	1959	11	54.	1973	31	272.
NOV	1200.	1970	1	22.	1973	28	120.
DEC	1160.	1959	19	18.	1973	16	75.
JAN	632.	1970	1	16.	1974	21	42.
FEB	245.	1970	11	13.	1974	23	40.
MAR	207.	1970	18	13.	1974	15	32.
APR	197.	1959	26	13.	1972	1	55.
MAY	1450.	1959	22	21.	1972	1	301.
JUN	2260.	1959	16	225.	1972	5	609.
JUL	1470.	1971	13	277.	1972	2	593.
AUG	2700.	1966	8	101.	1974	25	490.
SEP	4840.	1957	17	83.	1958	25	475.

***** YEARLY FLOW DATA *****

MAXIMUM	YEAR	MINIMUM	YEAR	AVERAGE
4840.	1957	13.	1974	254.

***** MEAN MONTHLY FLOW DATA *****

MONTH	MAXIMUM	YEAR	MINIMUM	YEAR
OCT	817.	1959	99.	1973
NOV	255.	1970	31.	1973
DEC	309.	1959	34.	1973
JAN	140.	1970	21.	1974
FEB	145.	1970	16.	1974
MAR	97.	1970	14.	1974
APR	94.	1959	13.	1972
MAY	453.	1959	152.	1974
JUN	850.	1959	385.	1972
JUL	883.	1971	422.	1974
AUG	900.	1971	274.	1959
SEP	975.	1957	157.	1958

***** MEAN ANNUAL FLOW DATA *****

MAXIMUM	YEAR	MINIMUM	YEAR
355.	1970	162.	1974

15274600 CAMPBELL CREEK NEAR SPENARD, ALASKA
***** MEAN DAILY FLOW BY MONTH *****

MONTH	MAXIMUM	YEAR	DAY	MINIMUM	YEAR	DAY	AVERAGE
OCT	182.	1972	15	30.	1969	2	72.
NOV	130.	1970	1	18.	1973	30	44.
DEC	100.	1967	31	12.	1973	15	31.
JAN	80.	1968	1	4.	1974	28	21.
FEB	25.	1968	10	2.	1969	3	14.
MAR	24.	1970	1	6.	1971	1	14.
APR	85.	1968	24	7.	1971	1	22.
MAY	202.	1968	31	11.	1971	1	52.
JUN	222.	1972	16	28.	1971	3	120.
JUL	256.	1971	28	42.	1969	23	114.
AUG	405.	1971	9	40.	1974	23	98.
SEP	264.	1967	6	30.	1969	23	80.

***** YEARLY FLOW DATA *****

MAXIMUM	YEAR	MINIMUM	YEAR	AVERAGE
405.	1971	2.	1969	57.

***** MEAN MONTHLY FLOW DATA *****

MONTH	MAXIMUM	YEAR	MINIMUM	YEAR
OCT	128.	1972	41.	1968
NOV	81.	1972	23.	1973
DEC	68.	1972	17.	1973
JAN	35.	1973	8.	1974
FEB	21.	1968	7.	1974
MAR	19.	1970	6.	1971
APR	45.	1968	8.	1971
MAY	90.	1968	27.	1971
JUN	152.	1968	88.	1969
JUL	149.	1971	70.	1969
AUG	188.	1971	55.	1974
SEP	159.	1967	35.	1969

***** MEAN ANNUAL FLOW DATA *****

MAXIMUM	YEAR	MINIMUM	YEAR
71.	1967	38.	1969

15275100 CHESTER CREEK AT ARCTIC BLVD. IN ANCHORAGE, ALASKA
***** MEAN DAILY FLOW BY MONTH *****

MONTH	MAXIMUM	YEAR	DAY	MINIMUM	YEAR	DAY	AVERAGE
JUN	51.	1968	1	9.	1970	17	19.
JUL	47.	1969	25	9.	1970	8	19.
AUG	60.	1971	9	12.	1970	4	21.
SEP	57.	1967	5	11.	1969	9	23.
OCT	45.	1971	16	7.	1970	19	20.
NOV	33.	1967	21	5.	1970	30	14.
DEC	30.	1970	23	3.	1970	2	12.
JAN	24.	1968	3	2.	1971	25	11.
FEB	16.	1968	9	2.	1971	1	9.
MAR	23.	1974	31	2.	1971	4	11.
APR	36.	1968	17	5.	1971	10	18.
MAY	59.	1968	31	10.	1970	5	20.

***** YEARLY FLOW DATA *****

MAXIMUM	YEAR	MINIMUM	YEAR	AVERAGE
57.	1967	2.	1971	17.

***** MEAN MONTHLY FLOW DATA *****

MONTH	MAXIMUM	YEAR	MINIMUM	YEAR
JUN	33.	1968	10.	1970
JUL	24.	1968	12.	1970
AUG	33.	1971	15.	1974
SEP	36.	1967	13.	1970
OCT	29.	1971	11.	1970
NOV	21.	1967	9.	1970
DEC	18.	1967	5.	1970
JAN	17.	1968	3.	1971
FEB	15.	1968	3.	1971
MAR	15.	1968	4.	1971
APR	25.	1968	11.	1970
MAY	31.	1972	11.	1970

***** MEAN ANNUAL FLOW DATA *****

MAXIMUM	YEAR	MINIMUM	YEAR
22.	1968	10.	1971

231

15276500 SHIP CREEK AT ELMENDORF AFB, ALASKA
***** MEAN DAILY FLOW BY MONTH *****

MONTH	MAXIMUM	YEAR	DAY	MINIMUM	YEAR	DAY	AVERAGE
MAY	552.	1963	31	1.	1971	6	113.
JUN	827.	1971	26	31.	1971	3	383.
JUL	725.	1963	3	68.	1969	23	299.
AUG	1300.	1971	9	47.	1969	27	233.
SEP	789.	1967	18	28.	1969	26	171.
OCT	476.	1969	7	7.	1968	29	119.
NOV	203.	1970	1	2.	1968	14	44.
DEC	101.	1967	30	2.	1968	1	23.
JAN	51.	1968	1	1.	1970	4	10.
FEB	17.	1968	29	1.	1969	1	5.
MAR	34.	1965	26	1.	1969	1	5.
APR	48.	1965	26	1.	1969	1	11.

***** YEARLY FLOW DATA *****

MAXIMUM	YEAR	MINIMUM	YEAR	AVERAGE
1300.	1971	1.	1971	125.

***** MEAN MONTHLY FLOW DATA *****

MONTH	MAXIMUM	YEAR	MINIMUM	YEAR
MAY	227.	1968	20.	1971
JUN	594.	1964	245.	1969
JUL	508.	1963	118.	1969
AUG	450.	1971	82.	1969
SEP	380.	1967	40.	1969
OCT	185.	1965	36.	1968
NOV	75.	1970	10.	1968
DEC	34.	1965	2.	1968
JAN	18.	1966	2.	1969
FEB	12.	1964	1.	1969
MAR	15.	1965	1.	1969
APR	32.	1964	1.	1970

***** MEAN ANNUAL FLOW DATA *****

MAXIMUM	YEAR	MINIMUM	YEAR
150.	1964	70.	1970

15277100 EAGLE RIVER AT EAGLE RIVER, ALASKA
***** MEAN DAILY FLOW BY MONTH *****

MONTH	MAXIMUM	YEAR	DAY	MINIMUM	YEAR	DAY	AVERAGE
OCT	2740.	1969	7	80.	1970	20	320.
NOV	340.	1969	2	60.	1973	21	121.
DEC	170.	1967	30	50.	1973	10	81.
JAN	120.	1970	1	24.	1974	29	61.
FEB	90.	1970	1	24.	1974	1	50.
MAR	90.	1970	1	28.	1974	1	51.
APR	140.	1974	30	35.	1971	15	65.
MAY	1050.	1969	27	36.	1971	1	236.
JUN	2700.	1967	24	129.	1971	3	993.
JUL	3430.	1971	14	901.	1971	4	1701.
AUG	4500.	1971	9	465.	1969	25	1603.
SEP	4900.	1967	18	220.	1968	27	869.

***** YEARLY FLOW DATA *****

MAXIMUM	YEAR	MINIMUM	YEAR	AVERAGE
4900.	1967	24.	1974	516.

***** MEAN MONTHLY FLOW DATA *****

MONTH	MAXIMUM	YEAR	MINIMUM	YEAR
OCT	707.	1969	155.	1968
NOV	174.	1969	86.	1973
DEC	119.	1969	54.	1973
JAN	99.	1970	39.	1969
FEB	90.	1970	26.	1974
MAR	85.	1970	36.	1972
APR	79.	1969	36.	1971
MAY	355.	1968	82.	1971
JUN	1507.	1967	689.	1972
JUL	2115.	1967	1303.	1970
AUG	2221.	1967	874.	1969
SEP	1593.	1967	457.	1969

***** MEAN ANNUAL FLOW DATA *****

MAXIMUM	YEAR	MINIMUM	YEAR
709.	1967	418.	1969

233

15281000 KNIK RIVER NEAR PALMER, ALASKA
***** MEAN DAILY FLOW BY MONTH *****

MONTH	MAXIMUM	YEAR	DAY	MINIMUM	YEAR	DAY	AVERAGE
OCT	19100.	1969	13	850.	1958	30	4276.
NOV	7000.	1970	1	550.	1958	26	1784.
DEC	2700.	1960	10	500.	1973	1	897.
JAN	5000.	1961	22	450.	1960	16	657.
FEB	1800.	1961	1	290.	1962	15	570.
MAR	1500.	1970	30	260.	1962	1	478.
APR	2000.	1969	30	320.	1962	1	683.
MAY	14200.	1974	30	400.	1972	1	3089.
JUN	153000.	1964	30	1550.	1966	1	11717.
JUL	341000.	1961	26	4120.	1965	4	25098.
AUG	47600.	1966	8	9420.	1974	25	20845.
SEP	33800.	1967	19	4160.	1958	26	12102.

***** YEARLY FLOW DATA *****

MAXIMUM	YEAR	MINIMUM	YEAR	AVERAGE
341000.	1961	260.	1962	6899.

***** MEAN MONTHLY FLOW DATA *****

MONTH	MAXIMUM	YEAR	MINIMUM	YEAR
OCT	9419.	1969	2087.	1973
NOV	4844.	1964	637.	1958
DEC	1529.	1969	500.	1973
JAN	1401.	1961	474.	1966
FEB	1378.	1961	338.	1962
MAR	778.	1963	260.	1962
APR	1177.	1964	348.	1972
MAY	7223.	1969	1039.	1955
JUN	19957.	1969	2598.	1955
JUL	37454.	1960	17435.	1970
AUG	25103.	1971	15261.	1969
SEP	15962.	1974	8461.	1958

***** MEAN ANNUAL FLOW DATA *****

MAXIMUM	YEAR	MINIMUM	YEAR
7872.	1967	6317.	1970

15284000 MATANUSKA RIVER AT PALMER, ALASKA
***** MEAN DAILY FLOW BY MONTH *****

MONTH	MAXIMUM	YEAR	DAY	MINIMUM	YEAR	DAY	AVERAGE
OCT	6230.	1951	1	686.	1950	31	1920.
NOV	2100.	1971	1	380.	1958	30	971.
DEC	1300.	1971	1	350.	1958	1	716.
JAN	1000.	1961	16	310.	1959	16	615.
FEB	660.	1961	1	360.	1971	16	514.
MAR	580.	1965	30	340.	1957	20	466.
APR	2220.	1958	30	234.	1955	25	637.
MAY	18700.	1960	26	587.	1970	1	2715.
JUN	26600.	1964	8	1320.	1956	1	10081.
JUL	24800.	1965	13	5780.	1957	1	12848.
AUG	40700.	1971	10	2080.	1959	17	10147.
SEP	15600.	1951	5	1250.	1959	30	4885.

***** YEARLY FLOW DATA *****

MAXIMUM	YEAR	MINIMUM	YEAR	AVERAGE
40700.	1971	234.	1955	3898.

***** MEAN MONTHLY FLOW DATA *****

MONTH	MAXIMUM	YEAR	MINIMUM	YEAR
OCT	2923.	1951	1170.	1969
NOV	1793.	1971	568.	1958
DEC	1024.	1971	440.	1958
JAN	821.	1961	349.	1959
FEB	528.	1961	381.	1971
MAR	572.	1965	360.	1971
APR	985.	1964	465.	1972
MAY	6019.	1960	1007.	1966
JUN	17247.	1964	5415.	1955
JUL	15616.	1965	10340.	1969
AUG	15729.	1971	4992.	1959
SEP	8966.	1951	2123.	1969

***** MEAN ANNUAL FLOW DATA *****

MAXIMUM	YEAR	MINIMUM	YEAR
4815.	1957	2662.	1969

15290000 LITTLE SUSITNA RIVER NEAR PALMER, ALASKA
***** MEAN DAILY FLOW BY MONTH *****

MONTH	MAXIMUM	YEAR	DAY	MINIMUM	YEAR	DAY	AVERAGE
OCT	442.	1965	1	30.	1956	28	118.
NOV	140.	1970	1	18.	1968	27	57.
DEC	50.	1972	1	9.	1951	26	36.
JAN	100.	1961	13	16.	1959	16	28.
FEB	31.	1957	1	10.	1955	1	22.
MAR	30.	1965	27	8.	1957	11	18.
APR	72.	1953	30	8.	1956	1	21.
MAY	1510.	1974	30	12.	1955	1	199.
JUN	2810.	1949	21	90.	1971	1	675.
JUL	2080.	1957	20	167.	1958	15	516.
AUG	5040.	1971	10	102.	1974	25	444.
SEP	1880.	1957	19	57.	1969	30	284.

***** YEARLY FLOW DATA *****

MAXIMUM	YEAR	MINIMUM	YEAR	AVERAGE
5040.	1971	8.	1957	202.

***** MEAN MONTHLY FLOW DATA *****

MONTH	MAXIMUM	YEAR	MINIMUM	YEAR
OCT	210.	1972	51.	1958
NOV	81.	1957	24.	1968
DEC	47.	1965	17.	1954
JAN	54.	1961	17.	1959
FEB	29.	1958	14.	1952
MAR	28.	1968	10.	1956
APR	34.	1955	10.	1955
MAY	395.	1974	53.	1971
JUN	1176.	1949	289.	1959
JUL	1047.	1963	240.	1958
AUG	909.	1971	159.	1969
SEP	605.	1965	82.	1969

***** MEAN ANNUAL FLOW DATA *****

MAXIMUM	YEAR	MINIMUM	YEAR
313.	1949	96.	1959

15292000 SUSITNA RIVER AT GOLD CREEK, ALASKA
***** MEAN DAILY FLOW BY MONTH *****

MONTH	MAXIMUM	YEAR	DAY	MINIMUM	YEAR	DAY	AVERAGE
OCT	20100.	1949	1	1500.	1950	31	5688.
NOV	5300.	1957	1	950.	1959	26	2473.
DEC	4400.	1957	5	800.	1958	25	1765.
JAN	2600.	1958	6	700.	1959	14	1444.
FEB	2200.	1972	1	75.	1959	28	1204.
MAR	2100.	1961	16	660.	1950	11	1076.
APR	3700.	1953	26	700.	1974	1	1342.
MAY	55500.	1972	31	900.	1964	1	13533.
JUN	85900.	1964	7	10000.	1971	1	27986.
JUL	50000.	1967	21	11800.	1959	28	24079.
AUG	77700.	1971	10	5280.	1959	29	22987.
SEP	41000.	1959	1	3710.	1959	30	13786.

***** YEARLY FLOW DATA *****

MAXIMUM	YEAR	MINIMUM	YEAR	AVERAGE
85900.	1964	75.	1959	9751.

***** MEAN MONTHLY FLOW DATA *****

MONTH	MAXIMUM	YEAR	MINIMUM	YEAR
OCT	8212.	1957	3124.	1959
NOV	3954.	1957	1215.	1959
DEC	3264.	1957	866.	1959
JAN	2452.	1961	724.	1959
FEB	2028.	1972	699.	1959
MAR	1900.	1958	713.	1964
APR	2650.	1961	745.	1964
MAY	21887.	1972	3745.	1971
JUN	50577.	1964	15503.	1959
JUL	34400.	1953	16103.	1959
AUG	32623.	1957	8879.	1959
SEP	21243.	1951	5093.	1959

***** MEAN ANNUAL FLOW DATA *****

MAXIMUM	YEAR	MINIMUM	YEAR
11555.	1962	5595.	1959

152945-CHAKACHATNA RIVER NEAR TYONEK, ALASKA
***** MEAN DAILY FLOW BY MONTH *****

MONTH	MAXIMUM	YEAR	DAY	MINIMUM	YEAR	DAY	AVERAGE
OCT	9240.	1965	1	1000.	1971	27	2468.
NOV	2590.	1969	1	802.	1959	25	1206.
DEC	1300.	1959	1	590.	1959	16	813.
JAN	990.	1961	25	438.	1963	31	613.
FEB	890.	1961	6	360.	1960	16	505.
MAR	678.	1961	1	320.	1960	16	445.
APR	1000.	1971	29	240.	1960	16	441.
MAY	5980.	1960	31	310.	1964	1	1042.
JUN	19000.	1971	27	1000.	1965	1	5736.
JUL	19800.	1971	15	4430.	1965	1	12018.
AUG	90000.	1971	11	4390.	1959	31	12075.
SEP	14000.	1965	16	2010.	1960	29	6064.

***** YEARLY FLOW DATA *****

MAXIMUM	YEAR	MINIMUM	YEAR	AVERAGE
90000.	1971	240.	1960	3645.

***** MEAN MONTHLY FLOW DATA *****

MONTH	MAXIMUM	YEAR	MINIMUM	YEAR
OCT	4072.	1965	1351.	1971
NOV	1822.	1959	902.	1971
DEC	1007.	1963	650.	1965
JAN	817.	1961	480.	1965
FEB	780.	1961	381.	1960
MAR	550.	1970	325.	1960
APR	692.	1971	250.	1960
MAY	2381.	1971	471.	1964
JUN	10933.	1971	2114.	1965
JUL	14472.	1971	9960.	1970
AUG	16714.	1971	8415.	1969
SEP	10255.	1965	3347.	1959

***** MEAN ANNUAL FLOW DATA *****

MAXIMUM	YEAR	MINIMUM	YEAR
4558.	1971	3106.	1970

15295700 TERROR RIVER AT MOUTH NEAR KODIAK, ALASKA
***** MEAN DAILY FLOW BY MONTH *****

MONTH	MAXIMUM	YEAR	DAY	MINIMUM	YEAR	DAY	AVERAGE
MAR	394.	1965	23	19.	1957	1	69.
APR	237.	1965	19	24.	1956	1	94.
MAY	1430.	1965	30	60.	1958	1	351.
JUN	1820.	1964	16	290.	1957	30	774.
JUL	1850.	1958	23	96.	1957	30	490.
AUG	2010.	1964	13	85.	1957	3	357.
SEP	2500.	1956	26	111.	1958	2	435.
OCT	2600.	1965	2	77.	1965	31	277.
NOV	482.	1957	3	47.	1955	22	115.
DEC	500.	1957	25	34.	1954	30	75.
JAN	245.	1956	26	24.	1957	31	50.
FEB	320.	1958	12	19.	1957	23	62.

***** YEARLY FLOW DATA *****

MAXIMUM	YEAR	MINIMUM	YEAR	AVERAGE
2600.	1965	19.	1957	277.

***** MEAN MONTHLY FLOW DATA *****

MONTH	MAXIMUM	YEAR	MINIMUM	YEAR
MAR	164.	1965	27.	1956
APR	134.	1965	72.	1954
MAY	528.	1958	200.	1956
JUN	1055.	1956	553.	1957
JUL	625.	1955	194.	1957
AUG	533.	1964	243.	1957
SEP	708.	1957	249.	1954
OCT	327.	1955	251.	1957
NOV	210.	1957	57.	1965
DEC	154.	1957	48.	1955
JAN	75.	1966	39.	1957
FEB	142.	1958	27.	1957

***** MEAN ANNUAL FLOW DATA *****

MAXIMUM	YEAR	MINIMUM	YEAR
280.	1957	257.	1956

15296000 UGANIK RIVER NEAR KODIAK, ALASKA
***** MEAN DAILY FLOW BY MONTH *****

MONTH	MAXIMUM	YEAR	DAY	MINIMUM	YEAR	DAY	AVERAGE
OCT	8180.	1952	3	120.	1973	29	676.
NOV	9130.	1954	2	75.	1965	17	534.
DEC	2920.	1963	21	65.	1955	31	269.
JAN	4110.	1963	22	50.	1957	31	226.
FEB	1100.	1968	27	30.	1972	23	159.
MAR	2150.	1965	23	24.	1972	10	158.
APR	1440.	1953	30	30.	1972	1	231.
MAY	3420.	1951	31	130.	1952	1	844.
JUN	5540.	1969	8	493.	1955	6	1734.
JUL	5050.	1968	23	230.	1957	30	1361.
AUG	7480.	1963	30	193.	1957	3	827.
SEP	5530.	1966	27	164.	1952	20	797.

***** YEARLY FLOW DATA *****

MAXIMUM	YEAR	MINIMUM	YEAR	AVERAGE
9130.	1954	24.	1972	653.

***** MEAN MONTHLY FLOW DATA *****

MONTH	MAXIMUM	YEAR	MINIMUM	YEAR
OCT	2106.	1969	152.	1973
NOV	1378.	1959	100.	1973
DEC	520.	1969	82.	1973
JAN	1108.	1963	53.	1956
FEB	442.	1968	48.	1972
MAR	631.	1965	26.	1972
APR	383.	1953	69.	1972
MAY	1396.	1960	473.	1971
JUN	2885.	1969	1034.	1952
JUL	2426.	1971	457.	1967
AUG	1303.	1971	334.	1957
SEP	1523.	1957	254.	1964

***** MEAN ANNUAL FLOW DATA *****

MAXIMUM	YEAR	MINIMUM	YEAR
882.	1960	438.	1952

15297200 MYRTLE CREEK NEAR KODIAK, ALASKA
***** MEAN DAILY FLOW BY MONTH *****

MONTH	MAXIMUM	YEAR	DAY	MINIMUM	YEAR	DAY	AVERAGE
JUN	877.	1969	8	13.	1968	22	82.
JUL	333.	1971	19	2.	1963	24	35.
AUG	429.	1966	21	1.	1963	14	37.
SEP	722.	1969	14	8.	1968	1	62.
OCT	396.	1958	2	7.	1973	15	47.
NOV	254.	1967	1	4.	1955	21	38.
DEC	450.	1969	5	2.	1968	15	32.
JAN	250.	1955	20	2.	1969	1	20.
FEB	346.	1958	29	2.	1969	1	28.
MAR	330.	1965	8	1.	1972	3	25.
APR	257.	1966	26	2.	1972	1	32.
MAY	443.	1971	31	12.	1972	1	74.

***** YEARLY FLOW DATA *****

MAXIMUM	YEAR	MINIMUM	YEAR	AVERAGE
877.	1969	1.	1963	43.

***** MEAN MONTHLY FLOW DATA *****

MONTH	MAXIMUM	YEAR	MINIMUM	YEAR
JUN	175.	1969	15.	1963
JUL	87.	1971	8.	1967
AUG	72.	1967	7.	1969
SEP	107.	1969	30.	1968
OCT	120.	1969	20.	1973
NOV	63.	1972	11.	1973
DEC	112.	1969	3.	1968
JAN	48.	1955	2.	1969
FEB	79.	1958	2.	1969
MAR	108.	1955	1.	1972
APR	47.	1969	4.	1972
MAY	102.	1973	39.	1964

***** MEAN ANNUAL FLOW DATA *****

MAXIMUM	YEAR	MINIMUM	YEAR
57.	1970	34.	1964

15300500 KVICHAK RIVER AT IGUIGIG, ALASKA
***** MEAN DAILY FLOW BY MONTH *****

MONTH	MAXIMUM	YEAR	DAY	MINIMUM	YEAR	DAY	AVERAGE
AUG	35000.	1967	30	14600.	1974	1	22388.
SEP	43000.	1967	21	16000.	1974	1	25194.
OCT	56000.	1967	4	18400.	1973	30	31426.
NOV	35200.	1967	1	15000.	1973	27	24926.
DEC	32000.	1967	12	12500.	1973	30	20405.
JAN	21500.	1968	1	9000.	1959	23	14619.
FEB	17000.	1972	1	7500.	1959	23	12474.
MAR	14400.	1970	14	7000.	1959	5	11040.
APR	13800.	1970	1	6400.	1959	21	10259.
MAY	15000.	1972	26	7000.	1959	1	10810.
JUN	20400.	1972	30	9000.	1959	1	13742.
JUL	25800.	1972	31	12000.	1974	1	18153.

***** YEARLY FLOW DATA *****

MAXIMUM	YEAR	MINIMUM	YEAR	AVERAGE
56000.	1967	6400.	1959	18144.

***** MEAN MONTHLY FLOW DATA *****

MONTH	MAXIMUM	YEAR	MINIMUM	YEAR
AUG	28677.	1967	15248.	1974
SEP	40367.	1967	17237.	1974
OCT	47994.	1967	20432.	1973
NOV	30620.	1967	16523.	1973
DEC	25555.	1967	14103.	1973
JAN	18781.	1968	9726.	1959
FEB	15207.	1972	8143.	1959
MAR	14000.	1972	7065.	1959
APR	13080.	1970	6740.	1959
MAY	14032.	1972	7371.	1959
JUN	17873.	1972	10983.	1974
JUL	23594.	1972	13555.	1974

***** MEAN ANNUAL FLOW DATA *****

MAXIMUM	YEAR	MINIMUM	YEAR
23268.	1968	13420.	1974

1530200 NUYAKUK RIVER NEAR DILLINGHAM, ALASKA
***** MEAN DAILY FLOW BY MONTH *****

MONTH	MAXIMUM	YEAR	DAY	MINIMUM	YEAR	DAY	AVERAGE
OCT	19900.	1955	1	2900.	1953	31	5955.
NOV	12000.	1959	1	2100.	1953	21	4642.
DEC	7250.	1957	2	1700.	1957	25	2974.
JAN	3400.	1957	1	1300.	1954	16	2255.
FEB	3200.	1953	1	1200.	1954	16	1859.
MAR	3570.	1953	8	1000.	1954	16	1660.
APR	2300.	1955	1	770.	1950	16	1571.
MAY	13400.	1950	31	960.	1950	1	3555.
JUN	29900.	1959	20	3590.	1955	1	14638.
JUL	26100.	1958	1	4700.	1957	31	13259.
AUG	20300.	1971	1	3500.	1957	25	8112.
SEP	22900.	1955	26	4100.	1957	1	7827.

***** YEARLY FLOW DATA *****

MAXIMUM	YEAR	MINIMUM	YEAR	AVERAGE
29900.	1959	770.	1950	5800.

***** MEAN MONTHLY FLOW DATA *****

MONTH	MAXIMUM	YEAR	MINIMUM	YEAR
OCT	11523.	1955	3515.	1958
NOV	8886.	1957	2570.	1958
DEC	4887.	1957	1848.	1953
JAN	3176.	1951	1397.	1964
FEB	3200.	1953	1252.	1954
MAR	3041.	1953	1097.	1964
APR	2300.	1955	800.	1950
MAY	5890.	1951	1719.	1964
JUN	23293.	1959	10361.	1954
JUL	21852.	1958	5794.	1954
AUG	13834.	1971	3365.	1957
SEP	14373.	1955	5271.	1959

***** MEAN ANNUAL FLOW DATA *****

MAXIMUM	YEAR	MINIMUM	YEAR
7948.	1958	4235.	1954

15303000 WOOD RIVER NEAR ALEKNAGIK, ALASKA

***** MEAN DAILY FLOW BY MONTH *****

MONTH	MAXIMUM	YEAR	DAY	MINIMUM	YEAR	DAY	AVERAGE
OCT	16200.	1955	1	2800.	1957	25	5544.
NOV	10200.	1969	1	2200.	1957	26	4432.
DEC	7830.	1957	1	1300.	1956	30	3218.
JAN	5400.	1970	1	800.	1957	28	2231.
FEB	4400.	1963	1	700.	1957	13	1795.
MAR	3500.	1963	8	700.	1957	1	1527.
APR	3250.	1955	25	700.	1957	1	1554.
MAY	11900.	1955	31	990.	1956	1	4538.
JUN	23300.	1969	22	2800.	1956	1	11790.
JUL	16800.	1969	1	3680.	1963	28	8535.
AUG	8270.	1950	15	2720.	1959	29	5527.
SEP	17500.	1955	26	2940.	1959	5	5930.

***** YEARLY FLOW DATA *****

MAXIMUM	YEAR	MINIMUM	YEAR	AVERAGE
23300.	1969	700.	1957	4323.

***** MEAN MONTHLY FLOW DATA *****

MONTH	MAXIMUM	YEAR	MINIMUM	YEAR
OCT	9855.	1955	3395.	1958
NOV	8225.	1957	2500.	1957
DEC	5332.	1969	1500.	1955
JAN	4187.	1970	950.	1957
FEB	3451.	1963	727.	1957
MAR	3129.	1963	700.	1957
APR	2939.	1955	785.	1959
MAY	5595.	1950	990.	1956
JUN	18393.	1955	8003.	1958
JUL	13080.	1958	5046.	1958
AUG	7503.	1950	4245.	1959
SEP	9517.	1955	3912.	1957

***** MEAN ANNUAL FLOW DATA *****

MAXIMUM	YEAR	MINIMUM	YEAR
5054.	1955	3495.	1957

15304000 KUSKOKWIM RIVER AT CROOKED CREEK, ALASKA
***** MEAN DAILY FLOW BY MONTH *****

MONTH	MAXIMUM	YEAR	DAY	MINIMUM	YEAR	DAY	AVERAGE
OCT	172000.	1955	1	18000.	1958	31	44131.
NOV	37000.	1957	1	12000.	1956	16	23252.
DEC	25000.	1957	1	10000.	1955	1	14857.
JAN	19000.	1962	1	8400.	1955	1	12569.
FEB	14000.	1955	1	5900.	1955	1	11018.
MAR	19000.	1957	1	6100.	1956	1	10995.
APR	50000.	1957	13	7000.	1955	1	12755.
MAY	260000.	1957	7	10000.	1951	1	81751.
JUN	391000.	1954	5	28000.	1954	22	93575.
JUL	154000.	1957	28	30200.	1954	1	69596.
AUG	302000.	1953	28	33100.	1959	17	82243.
SEP	234000.	1953	1	25800.	1953	25	71313.

***** YEARLY FLOW DATA *****

MAXIMUM	YEAR	MINIMUM	YEAR	AVERAGE
391000.	1954	6100.	1956	43625.

***** MEAN MONTHLY FLOW DATA *****

MONTH	MAXIMUM	YEAR	MINIMUM	YEAR
OCT	74903.	1955	25525.	1958
NOV	34500.	1957	14000.	1956
DEC	25000.	1951	10000.	1955
JAN	19000.	1962	8400.	1955
FEB	14000.	1955	5900.	1955
MAR	19000.	1957	6100.	1956
APR	41000.	1957	8500.	1953
MAY	161558.	1957	22129.	1954
JUN	235057.	1954	33390.	1954
JUL	115577.	1953	44065.	1954
AUG	159761.	1953	41842.	1957
SEP	114770.	1951	31790.	1958

***** MEAN ANNUAL FLOW DATA *****

MAXIMUM	YEAR	MINIMUM	YEAR
62115.	1953	32173.	1959

15564800 YUKON RIVER AT RUBY, ALASKA
***** MEAN DAILY FLOW BY MONTH *****

MONTH	MAXIMUM	YEAR	DAY	MINIMUM	YEAR	DAY	AVERAGE
OCT	330000.	1955	1	57000.	1959	31	151279.
NOV	120000.	1957	1	41000.	1959	16	69494.
DEC	76000.	1957	1	31000.	1957	16	44443.
JAN	51000.	1968	1	29000.	1950	1	36323.
FEB	37000.	1952	1	23000.	1955	1	29915.
MAR	33000.	1955	1	17000.	1959	1	25915.
APR	40000.	1959	30	17000.	1959	1	27006.
MAY	800000.	1971	21	25000.	1972	1	229753.
JUN	959000.	1954	18	332.	1957	29	457437.
JUL	705000.	1954	1	262.	1959	31	292545.
AUG	524000.	1957	22	190000.	1955	31	317155.
SEP	498000.	1952	5	142000.	1953	30	244235.

***** YEARLY FLOW DATA *****

MAXIMUM	YEAR	MINIMUM	YEAR	AVERAGE
959000.	1954	262.	1959	161029.

***** MEAN MONTHLY FLOW DATA *****

MONTH	MAXIMUM	YEAR	MINIMUM	YEAR
OCT	199513.	1953	90323.	1958
NOV	98000.	1952	47000.	1953
DEC	64225.	1957	32935.	1959
JAN	50000.	1952	29000.	1955
FEB	37000.	1952	23000.	1955
MAR	33000.	1955	17000.	1959
APR	34000.	1955	18500.	1959
MAY	389710.	1971	104677.	1954
JUN	855099.	1954	517.	1957
JUL	548515.	1954	323.	1959
AUG	472355.	1957	225531.	1956
SEP	370033.	1952	153357.	1955

***** MEAN ANNUAL FLOW DATA *****

MAXIMUM	YEAR	MINIMUM	YEAR
227211.	1952	113755.	1959

15712000 KUZITRIN RIVER NEAR NOME, ALASKA
***** MEAN DAILY FLOW BY MONTH *****

MONTH	MAXIMUM	YEAR	DAY	MINIMUM	YEAR	DAY	AVERAGE
AUG	10000.	1965	8	305.	1971	15	1253.
SEP	8930.	1955	10	200.	1970	30	1434.
OCT	2310.	1954	8	130.	1970	30	713.
NOV	750.	1972	1	40.	1967	29	253.
DEC	300.	1972	1	10.	1957	25	107.
JAN	160.	1973	1	2.	1954	21	53.
FEB	120.	1973	1	1.	1971	28	35.
MAR	100.	1973	1	10.	1972	1	57.
APR	100.	1958	30	1.	1955	23	53.
MAY	30000.	1967	23	1.	1954	1	3159.
JUN	40000.	1971	3	310.	1970	30	5334.
JUL	4040.	1965	10	290.	1970	5	1120.

****** YEARLY FLOW DATA *****

MAXIMUM	YEAR	MINIMUM	YEAR	AVERAGE
40000.	1971	1.	1971	1454.

***** MEAN MONTHLY FLOW DATA *****

MONTH	MAXIMUM	YEAR	MINIMUM	YEAR
AUG	4125.	1955	350.	1971
SEP	4154.	1965	381.	1969
OCT	1355.	1955	187.	1970
NOV	448.	1972	83.	1967
DEC	212.	1972	23.	1957
JAN	142.	1973	10.	1958
FEB	108.	1973	2.	1955
MAR	85.	1973	10.	1972
APR	80.	1973	1.	1955
MAY	8252.	1967	212.	1954
JUN	11703.	1971	912.	1970
JUL	1871.	1967	345.	1970

***** MEAN ANNUAL FLOW DATA *****

MAXIMUM	YEAR	MINIMUM	YEAR
2258.	1955	675.	1959

15744000 KOBUK RIVER AT AMBLER, ALASKA

***** MEAN DAILY FLOW BY MONTH *****

MONTH	MAXIMUM	YEAR	DAY	MINIMUM	YEAR	DAY	AVERAGE
JUL	55500.	1957	21	3800.	1959	9	15435.
AUG	90400.	1973	22	5500.	1958	31	17852.
SEP	53500.	1955	10	4000.	1958	29	13331.
OCT	32100.	1955	1	2200.	1970	30	9271.
NOV	5500.	1973	1	1500.	1970	25	3523.
DEC	3400.	1972	1	1100.	1970	25	2041.
JAN	2600.	1973	1	900.	1959	21	1515.
FEB	2200.	1973	1	800.	1959	15	1256.
MAR	1800.	1973	1	800.	1957	1	1105.
APR	3400.	1950	30	700.	1957	1	1154.
MAY	95000.	1971	29	900.	1971	1	15824.
JUN	94000.	1958	13	4800.	1959	30	34775.

***** YEARLY FLOW DATA *****

MAXIMUM	YEAR	MINIMUM	YEAR	AVERAGE
95000.	1971	700.	1957	9971.

***** MEAN MONTHLY FLOW DATA *****

MONTH	MAXIMUM	YEAR	MINIMUM	YEAR
JUL	30977.	1957	5235.	1959
AUG	39752.	1973	8119.	1971
SEP	33253.	1955	4967.	1958
OCT	18584.	1955	2974.	1970
NOV	5000.	1955	1850.	1970
DEC	3052.	1972	1297.	1970
JAN	2426.	1973	951.	1959
FEB	2057.	1973	827.	1959
MAR	1753.	1973	800.	1957
APR	1550.	1973	900.	1971
MAY	30242.	1973	3945.	1966
JUN	61310.	1958	7810.	1959

***** MEAN ANNUAL FLOW DATA *****

MAXIMUM	YEAR	MINIMUM	YEAR
12615.	1958	5502.	1970

15896000 KUPARUK RIVER NEAR DEADHORSE, ALASKA

***** MEAN DAILY FLOW BY MONTH *****

MONTH	MAXIMUM	YEAR	DAY	MINIMUM	YEAR	DAY	AVERAGE
MAY	7200.	1971	31	10.	1972	1	213.
JUN	78000.	1973	8	380.	1971	30	12973.
JUL	3700.	1973	25	213.	1971	9	821.
AUG	6040.	1972	28	200.	1974	12	1343.
SEP	6040.	1972	4	20.	1974	30	1016.
OCT	500.	1972	1	20.	1973	21	185.
NOV	300.	1972	1	15.	1973	1	74.
DEC	50.	1972	1	10.	1973	1	17.
JAN	10.	1972	1	10.	1972	1	10.
FEB	10.	1972	1	10.	1972	1	10.
MAR	10.	1972	1	10.	1972	1	10.
APR	10.	1972	1	10.	1972	1	10.

***** YEARLY FLOW DATA *****

MAXIMUM	YEAR	MINIMUM	YEAR	AVERAGE
78000.	1973	10.	1972	1544.

***** MEAN MONTHLY FLOW DATA *****

MONTH	MAXIMUM	YEAR	MINIMUM	YEAR
MAY	7200.	1971	10.	1972
JUN	17884.	1973	5592.	1974
JUL	1392.	1973	300.	1971
AUG	2541.	1972	425.	1971
SEP	2733.	1972	192.	1974
OCT	406.	1972	62.	1973
NOV	174.	1972	15.	1973
DEC	24.	1972	10.	1973
JAN	10.	1972	10.	1972
FEB	10.	1972	10.	1972
MAR	10.	1972	10.	1972
APR	10.	1972	10.	1972

***** MEAN ANNUAL FLOW DATA *****

MAXIMUM	YEAR	MINIMUM	YEAR
1721.	1972	1542.	1973

***** MEAN DAILY FLOW BY MONTH *****

MONTH	MAXIMUM	YEAR	DAY	MINIMUM	YEAR	DAY	AVERAGE
AUG	25200.	1974	19	1300.	1971	31	5198.
SEP	6050.	1972	1	450.	1970	30	1525.
OCT	900.	1972	1	92.	1973	31	418.
NOV	500.	1972	1	14.	1973	30	148.
DEC	100.	1970	1	3.	1973	29	27.
JAN	20.	1973	1	2.	1974	5	5.
FEB	10.	1973	1	2.	1972	1	4.
MAR	10.	1973	1	2.	1971	1	4.
APR	10.	1973	1	2.	1971	1	4.
MAY	15000.	1972	31	2.	1971	1	1191.
JUN	20000.	1972	1	1500.	1971	15	7311.
JUL	18400.	1973	24	1750.	1971	3	5534.

***** YEARLY FLOW DATA *****

MAXIMUM	YEAR	MINIMUM	YEAR	AVERAGE
25200.	1974	2	1974	1873.

***** MEAN MONTHLY FLOW DATA *****

MONTH	MAXIMUM	YEAR	MINIMUM	YEAR
AUG	6731.	1974	2585.	1971
SEP	2271.	1972	792.	1971
OCT	690.	1972	245.	1971
NOV	273.	1972	40.	1973
DEC	59.	1972	7.	1973
JAN	15.	1973	2.	1974
FEB	10.	1973	2.	1972
MAR	10.	1973	2.	1971
APR	10.	1973	2.	1971
MAY	2954.	1974	185.	1971
JUN	9051.	1972	5583.	1973
JUL	7154.	1973	4005.	1974

***** MEAN ANNUAL FLOW DATA *****

MAXIMUM	YEAR	MINIMUM	YEAR
1845.	1972	1497.	1971

250

ANNUAL REPORT

GULF OF ALASKA STUDY OF MESOSCALE

OCEANOGRAPHIC PROCESSES

(GAS-MOP)

Dr. S. P. Hayes

Dr. J. D. Schumacher

Pacific Marine Environmental Laboratory
Environmental Research Laboratories
National Oceanic and Atmospheric Administration
3711 15th Avenue NE.
Seattle, Washington 98105

April 1, 1976

I. SUMMARY

The objective of this research is to describe the mesoscale oceanic circulation on the continental shelf in the Gulf of Alaska in order to characterize the intermediate scale advective and diffusive processes. These processes are inherently important to the assessment of potential pollution problems due to OCS petroleum development. The study discussed here, when combined with the meteorological research, additional physical oceanographic research, and the theoretical modeling research of other investigators, forms a coherent program to describe the physical milieu within the proposed OCS lease areas.

From the data collected and analyzed to date, several preliminary conclusions can be drawn: (1) the shelf break flow is dominated by the Alaskan current system; (2) this system varies in intensity and structure as it proceeds from Yakutat to Unimak Pass; (3) in the Northeast Gulf of Alaska over half of the nontidal variance of the current occurs with time scales of less than a week; (4) the oceanic response to the wind changes character from the midshelf region where it is consistent with Ekman setup to the inner shelf region where direct windstau setup becomes more important; (5) near the Copper River the mean flow is low and complex; (6) near Kodiak Island the shelf break flow is intense; however, on the shelf itself the flow is weak and tidally dominant; and (7) throughout the Gulf of Alaska a seasonal trend is clear with higher velocities occurring in winter.

The data from all regions are still being analyzed and intercompared. As this processing continues, we expect to refine our understanding of the flow on the continental shelf and the processes which drive it.

II. INTRODUCTION

A. General Nature and Scope of Study

The objective of this research is to describe the mesoscale oceanic circulation on the continental shelf in the Gulf of Alaska. Together with additional observational and theoretical programs, these studies will attempt to characterize the intermediate and large-scale advective and diffusive processes within proposed OCS lease areas.

The average circulation in the Gulf of Alaska has been attributed to the westward-flowing Alaskan Current. This large-scale phenomenon is produced by the response to the global wind forcing. On intermediate scales the circulation will be modified by bathymetry and, in addition, it will respond to a variety of local and nonlocal forcing functions. Locally, the wind-generated response will be important. These lead to near-surface Ekman flows, sea surface slopes (and hence barotropic velocity components), and modification of the density stratification (and hence baroclinic velocity fields). The nonlocal effects include tidal currents and shelf waves. These can significantly modulate the mean flow and hence the response to the local wind field.

In an ideal world, we could recreate the ocean in a computer model and generate the oceanic velocity fields from first principals. However, the real ocean is so rich in variability that a priori modeling is impractical. Rather, observational results must be accumulated and events documented in order that the models may be guided into the correct approximations. In this manner, the models may be used to extend the observational results, so that we may predict what will probably happen in a given situation.

The experimental program discussed here was designed with this philosophy in mind. The immenseness of the continental shelf in the Gulf of Alaska defies saturation of measurements. Instead, the program provided regional coverage

to establish the statistics of the velocity field at a few points. This was supplemented by process-oriented studies in areas which were selected so that either generic dynamics or specific problem sites could be studied. The dynamical studies relate the velocity field to the wind forcing, the bathymetry, the sea surface slope, and the density field. The process experiments are required in order to interpret the statistical observations.

B. Specific Objectives

The observational program is discussed in terms of the regional and process experiments defined above.

1. Regional Experiment

Four moorings, 62, WGC-1, WGC-2, and WGC-3, comprise the regional experiment. These were each separated by roughly 600 km, and they spanned the Gulf of Alaska Shelf from Yakutat to Unimak Pass. Their intent was to gather statistical data on the nature of the temporal and large-scale spatial velocity variability. Near mooring 62 (which was also part of the process experiment), bottom pressure measurements were made. In addition, there was a pressure gage on WGC-2. These provided the data for coupling the velocity field to the sea surface slope and hence the barotropic velocity component. Similarly, a large-scale CTD grid was occupied by a separate research group (Royer, University of Alaska). This provided the data for comparison of measured and inferred baroclinic velocities and a test for geostrophic and nongeostrophic components.

2. Process Experiments

These moderately intense studies of specific areas were carried out at three locations, with a preliminary historical analysis being done at a fourth

location. The time schedule for the field experiments had two of the studies (Icy Bay and Kodiak Island) ending in March 1977; thus, only very preliminary findings are available now.

a. Barotropic Response Studies (BARS) - Icy Bay

The specific objectives are to establish:

(1) Response of sea surface slope to wind.

(2) Correlation of velocity and sea surface slope changes.

(3) Dynamics of the wind-forced currents.

(4) Influence of topography on current.

(5) Cross-shelf and alongshelf coherence of the velocity field.

(6) Near-shore velocity field.

(7) Influence of nonlocal forcing.

b. Kodiak Island-Shelikof Strait (KISS)

The objectives are:

(1) Measure the velocity field in the Shelikof Straits and its temporal variations.

(2) Monitor the flow through the two other passages in Cook Inlet.

(3) Study the transition from estuarine to shelf circulation.

(4) Study the shelf circulation seaward of Kodiak Island and its relation to forcing.

c. Copper River Study

(1) Investigate the apparent gyral circulation behind Kayak Island in order to establish at least a minimum understanding of the current structure and probable driving mechanism.

(Note: This study was added to the original proposed studies at the request of Dr. Hess.)

d. <u>Lower Cook Inlet</u>

Historical analysis of data in order to define present state of knowledge and future observational requirements.

C. <u>Application to Petroleum Development Hazard Assessment</u>

Last year's annual report described the fate of oil in the marine environment and introduced the approach that physical oceanographic studies take to assess petroleum development impact. Once oil enters the marine environment it becomes a constituent. For the period it is found in a measurable amount in a volume of seawater, oil is a scalar quantity continuous in time and space. Further, assuming that oil is a conservative constituent, its concentration is altered locally, except at the boundaries, by processes of diffusion and advection only.

In the real world, diffusion or eddy coefficients are only vaguely understood with widely varying values; however, estimates of relative importance of advection and diffusion at a given location can be made. Such estimates can be based on relative magnitudes of kinetic energy in its two components: kinetic energy of mean flow (advective term) and kinetic energy of fluctuations (diffusion-type term). This latter quantity, called herein total variance, is distributed over a broad frequency range. The upper bound depends on sampling interval and lower bound on record length. Little net motion results from diurnal and higher frequencies, and thus these bands can be considered as contributing to dispersion. Remaining frequencies lead to fluctuations about the mean and will either reduce or augment mean flow.

Temporal impact of oil may be qualitatively assessed by examining partition of total kinetic energy. For example: flow consisting of a relatively high mean, weak low frequency, and moderate tidal components will result in high transport of a constituent in a constant direction. Flow consisting of

a weak mean and low frequency components but high tidal components will result in little net transport or a long residence time for the oil at that location with relatively high dispersion.

Current records from WGC-2C are characteristic of the first example. At this shelf break station there was a strong mean, 22 cm s^{-1}, low-frequency variance was 190 cm^2 s^{-2}, and the remaining high-frequency (6-25 hrs) variance was 414 cm^2 s^{-2}. At WGC-2D (on northern Albatross Bank, 92-m depth), there was a low mean, 3 cm s^{-1}, low-frequency variance was 142 cm^2 s^{-2} and high-frequency variance was 1,414 cm^2 s^{-2}. Using these measured and calculated values, it is clear that oil at WGC-2C will be transported, on the average of 25 km day^{-1}, or three times as far as oil at 2D. High-frequency energy at 2D is more than three times that at 2C, but quantification of diffusion is not possible from the data. It is clear that oil has a longer residence time on the bank, although reduction in concentration will occur more rapidly.

To apply this straightforward assessment is premature, since two critical factors are unknown. These are: (1) the spatial extent over which an Eulerian measurement can be extrapolated, and (2) a quantification of diffusion. The first unknown may be addressed indirectly by knowing the temporal and spatial character of the mass field; i.e., over what scale is the density field uniform. Additionally, direct determination of spatial coherence is one goal of process-oriented experiments, such as Icy Bay. Diffusion experiments can be designed, e.g., tracking a large number of drifters, but the representativeness of one experiment is questionable. Stochastic models, at this time, are the most common approach. Finally, this qualitative assessment is only one factor in a large matrix including direct effect of wind, impact on biota, effects of suspended particulate matter, economic considerations, etc., and is presented only as a first-order approximation to one subject of environmental assessment.

III. CURRENT STATE OF KNOWLEDGE

The historical data base and the recent results from the OCSEAP studies have been summarized in the past two annual reports (April 1975, April 1976) and in Hayes and Schumacher (1976). In addition, the final report of Ingraham et al. (1976) contains a description of the mean flow and seasonal variations. Briefly, the mean circulation in the Gulf of Alaska is dominated by the Alaskan gyre (Dodimead et al., 1963). The northern boundary of this gyre is the Alaskan Current. This westward flow generally parallels the coastline. There are indications that the flow intensifies as it proceeds westward along the Alaskan Peninsula (Favorite, 1967). This may be related to a change from an eastern boundary to a western boundary current (Thompson, 1972).

Seasonally, the Gulf of Alaska is dominated by the Aleutian Low in winter and the North Pacific High in summer. During winter this low-pressure system leads to winds from the southeast and severe storms. The onshore Ekman transport produces a downwelling situation on the continental shelf. In summer, lighter winds prevail and a relaxation of the wintertime setup ensues (Royer, 1975).

Prior to the OCSEAP studies, little information was available on the sea surface slope in the Gulf of Alaska. Some analyses of coastal sea level included Alaskan stations. Of note is the study of Pattullo et al. (1954), which concluded that the seasonal excursion of sea level (uncorrected for atmospheric pressure) was about 25 cm. Recently, Reid and Mantyla (1975) observed that the atmospheric pressure variations accounted for 50% of the sea level change. They tried to relate the seasonal variations to changes in the baroclinic structure of the Alaskan Current. However, their wintertime data set is sparse and the results are only suggestive.

Hayes and Schumacher (1976) showed a close correlation between the winds, the bottom-pressure variations, and the currents. The coherence was higher in winter than in spring. The latter period indicated the possible influence of forcing from the flow adjacent to the shelf break. Royer and Muench (1977) showed wavelike features in sea surface temperature which could influence coastal circulation.

IV. STUDY AREA

The study area is the Gulf of Alaska continental shelf (fig. R1). The regional experiment (moorings 62, WGC1, WGC-2, and WGC-3) extends from Icy Bay to Unimak Pass. Process experiments involved moorings in the Icy Bay, Copper River, and Kodiak Island regions.

V. PROGRAM RATIONALE AND METHODS OF DATA COLLECTION

The current meter and/or pressure gage moorings indicated in figure R1 have been maintained, and the data from these arrays have been processed. In addition, CTD data was collected in support of the mooring operations. Hydrographical data was collected using the following equipment:

Plessey 9040 CTD inputted to the PODAS system aboard the Discoverer;

Plessey 9040 CTD and Plessey 8400 data logger aboard the Miller Freeman.

Water samples were taken using a Rosette sampler equipped with Niskin bottles. Salinity samples were drawn and salinity determinations were made using the ship's inductive salinometer. Reversing thermometers (calibrated by NOIC) were employed to develop field correction factors for the CTD system.

Aanderaa RCM-4 current meters were used on the moored arrays. The tapes were processes by PMEL/UW's Aanderaa tape system (Charnell and Krancus, 1976).

The bottom pressure measurements are made with an internally recording pressure-temperature gage (PTG) designed by PMEL. The gage records on digital tape cassette the integral value of pressure and temperature once every 15 min. A technical report describing the gage is in preparation. Calibration of the gages is described in last year's annual report.

VI.   RESULTS

Seven cruises were conducted during this reporting period. Forty current meter and/or bottom-pressure gage arrays were deployed. A new series of arrays were moored in the Kodiak Island-Shelikof Strait region. These five arrays and seven from the Icy Bay region are to be recovered in March 1977. Additionally, 50 CTD stations were occupied in Icy Bay and off the Copper River, and two 25-hr time series were conducted.

The following list summarizes current meter and pressure gage moorings. Table 1 summarizes current meter records collected during this year.

Gulf of Alaska Current Meter and/or Pressure Gage Moorings

Mooring	Location	Dates
60A	60°05.4' N 145°70.7' W	2 July 74 - 3 Sept 74
B	60°07.3' N 145°46.1' W	2 Mar 76 - 18 May 76
C	60°07.8' N 145°48.7' W	18 May 76 - 19 Aug 76
61A	59°34.0' N 145°47.0' W	16 Aug 74 - 20 Nov 74
B	59°33.9' N 145°53.0' W	11 Mar 76 - 17 May 76
C	59°32.6' N 145°49.7' W	18 May 76 - 19 Aug 76
62A	59°34.0' N 142°10.5' W	17 Aug 74 - 1 Feb 75
B	59°34.0' N 142°13.5' W	2 Feb 75 - 27 Apr 75
C	59°33.6' N 142°11.7' W	28 Apr 75 - 4 June 75
D	59°33.0' N 142°05.3' W	5 June 75 - 18 Sept 75
E	59°33.0' N 142°05.3' W	19 Sept 75 - 20 Nov 75
F	59°34.7' N 142°11.4' W	21 Nov 75 - 5 Mar 76
G	59°35.6' N 142°06.0' W	6 Mar 76 - 16 May 76
H	59°37.6' N 142°06.2' W	16 May 76 - 21 Aug 76
I	59°38.1' N 142°05.0' W	22 Aug 76 - 21 Oct 76
J	59°38.1' N 142°06.1' W	21 Oct 76 - present

Mooring	Location	Dates
63	59°46.6' N 141°59.2' W	2 Feb 75 - 21 Feb 75
63½	59°46.7' N 141°59.1' W	3 Feb 75 - 10 May 75
69A	59°50.1' N 145°41.9' W	3 Mar 76 - 17 May 76
B	59°49.2' N 145°43.3' W	18 May 76 - 19 Aug 76
SLS 4	59°46.2' N 141°28.6' W	21 Nov 75 - 3 Mar 76
5	59°40.2' N 141°39.7' W	21 Nov 75 - 3 Mar 76
6	59°15.5' N 141°59.3' W	21 Nov 75 - 3 Mar 76
7	59°45.2' N 141°30.2' W	3 Mar 76 - 14 May 76
8	59°39.5' N 141°39.2' W	3 Mar 76 - 14 May 76
9	59°18.8' N 142°01.6' W	7 Mar 76 - 13 May 76
10	60°00.0' N 142°17.5' W	4 Mar 76 - 21 Aug 76
11	59°48.6' N 142°25.1' W	4 Mar 76 - 21 Aug 76
12	59°43.1' N 142°34.2' W	4 Mar 76 - 21 Aug 76
13	59°45.1' N 141°33.6' W	13 May 76 - 22 Oct 76
14	59°40.0' N 141°40.0' W	14 May 76 - 24 Oct 76
16	60°01.2' N 142°25.5' W	21 Aug 76 - present
17	59°49.5' N 142°31.3' W	21 Aug 76 - present
19	59°46.0' N 141°29.0' W	22 Oct 76 - present
20	59°40.0' N 141°40.0' W	21 Oct 76 - present
21	59°20.2' N 141°59.0' W	22 Oct 76 - present
KISS 1A	59°44.7' N 154°43.7' W	15 Oct 76 - present
2A	58°37.2' N 153°05.0' W	15 Oct 76 - present
3A	58°45.3' N 152°10.6' W	14 Oct 76 - present
4A	59°01.9' N 151°56.4' W	14 Oct 76 - present
5A	56°33.2' N 152°39.5' W	18 Oct 76 - present
WGC 1A	54°01.7' N 162°59.8' W	4 Sept 75 - 1 Nov 75

Mooring	Location	Dates
WGC 1B	54°01.4' N 163°01.8' W	2 Nov 75 - 12 Mar 76
1C	54°01.0' N 163°02.8' W	13 Mar 76 - 11 June 76
1D	54°01.0' N 163°05.0' W	11 June 76 - 30 Sept 76
1E	54°02.7' N 163°06.3' W	30 Sept 76 - present
WGC 2A	57°28.1' N 150°29.0' W	21 Sept 75 - 27 Nov 75
2B	57°26.7' N 150°29.0' W	28 Nov 75 - Lost
2C	57°26.9' N 150°29.6' W	10 Mar 76 - 8 June 76
2D	57°34.6' N 150°48.6' W	8 June 76 - 18 Oct 76
2E	57°33.8' N 150°49.3' W	20 Oct 76 - present
WGC 3A	55°05.1' N 157°09.5' W	11 Mar 75 - Lost
3B	55°11.5' N 156°58.0' W	10 June 76 - 17 Oct 76
3C	55°12.0' N 156°56.7' W	17 Oct 76 - present

The locations of the current meter moorings are summarized in figure R1. The mean current vectors for all current meter records are summarized in figures R2-R5.

B.   The following articles and technical reports have been published or submitted for publication during FY-77:

Charnell, R. L., and G. A. Krancus (1976): A processing system for Aanderaa current meter data. NOAA Tech. Memo. ERL PMEL-6.

Hayes, S. P., and J. D. Schumacher (1976): Description of wind, current, and bottom pressure variations on the continental shelf in the Northeast Gulf of Alaska from February to May 1975. Journal of Geophysical Research, 81:6411-6419.

Halpern, D., and J. R. Holbrook (1977): Moored near-surface current measurements during February 1975 on the Gulf of Alaska Outer Continental Shelf. Submitted to Journal of Geophysical Research.

Table 1. Statistics of currents from moored current meters deployed during the reporting period.

Mooring	Observation Period	Instrument Depth (m)	Instrument Serial No.	Record Length (days)	Mean Speed (cm/s)	Variance (cm²/s²) U	Variance (cm²/s²) V	Total Variance	Net Flow (cm/s)	Net Flow Direction
60B	3/2-5/18/76	20	1815	76.50	16.90	163.9	166.6	330.5	1.79	287°
	"	50	1451	"	16.04	152.8	141.4	294.2	2.26	210°
	"	100	600	"	10.62	53.9	78.8	132.7	3.51	162°
60C	5/18-8/19/76	20	1679	92.58	12.63	94.3	91.0	185.3	0.60	058°
	"	50	1675	"	10.62	59.5	69.2	128.7	1.92	108°
	"	90	1676	"	8.67	29.7	58.2	87.9	3.03	106°
61B	3/11-5/17/76	20	1454	67.50	25.72	240.6	274.3	514.9	17.61	250°
	"	50	1835	"						255°
	"	100	1667	"	26.08	268.5	328.7	597.2	15.48	250°
	3/11-3/23/76	162	1668	12.17	20.23	116.3	344.6	460.9	12.26	206°
61C	5/18-8/19/76	20	1687	93.79	18.00	133.8	199.8	333.6	7.35	245°
	5/18-8/2/76	50	1804	76.25						278°
	5/18-8/19/76	90	1805	93.79						265°
	"	163	1807	"	25.34	165.3	541.0	706.3	8.62	197°
62G	3/6-5/16/76	20	1683	71.38	28.04	318.3	254.7	573.0	18.87	321°
	"	50	1684	"	26.28	300.2	187.5	487.7	16.99	311°
	"	100	1669	"	21.70	174.6	146.9	321.5	14.13	314°
62H	5/16-8/21/76	20	1809	98.71	14.60	132.7	114.7	247.4	3.88	307°
	"	50	1810	"	15.43	137.8	108.9	246.7	5.29	312°
	"	100	1811	"	10.12	63.8	48.2	112.0	4.27	315°
	"	170	1814	"	8.29	40.5	34.2	74.7	3.39	349°
62I	8/22-10/21/76	20	1812	60.33	23.74	234.1	236.3	470.4	16.19	303°
	"	50	1977	"	22.78	236.7	175.5	412.2	13.88	299°
	"	100	2252	"	18.78	171.6	133.1	204.7	10.11	305°
	"	180	2258	"	10.00	67.6	56.4	124.0	2.62	343°
69A	3/3-5/17/76	20	604	75.58	21.70	216.2	291.6	507.8	6.47	319°
	"	50	1670	"	20.17	171.5	269.2	440.7	4.36	318°

Table 1 (Continued)

Mooring	Observation Period	Instrument Depth (m)	Instrument Serial No.	Record Length (days)	Mean Speed (cm/s)	Variance (cm²/s²) U	V	Total Variance	Net Flow (cm/s)	Net Flow Direction
69B	5/18-8/19/76	20	1824	93.33	21.46	218.7	311.9	530.6	5.57	328°
	"	50	1828	"	14.17	83.2	134.1	217.3	3.51	300°
	"	87	1829	"	10.41	37.8	92.2	130.0	2.04	273°
WGC 1C	3/13-6/11/76	20	1982	90.29	32.51	348.9	228.8	577.7	25.33	253°
	"	50	1978	"	30.81	275.6	182.7	458.3	24.36	254°
	"	100	1985	"	24.22	163.9	121.8	285.7	18.98	243°
	"	175	1832	"	11.41	69.5	56.6	126.1	7.55	225°
WCG 1D	6/11-9/30/76	20	1973	110.88	22.20	232.3	457.7	457.7	11.14	253°
	"	50	598	"	20.49	169.1	201.5	370.6	10.23	254°
WGC 2C	3/10-6/8/76	24	1977	90.21	30.17	322.0	281.5	603.5	21.62	226°
	"	54	1825	"	30.28	254.6	216.9	471.5	23.82	232°
	3/10-5/12/76	104	1818	63.29	30.26	233.1	194.6	427.7	25.54	235°
	3/10-6/8/76	179	1837	90.21	25.48	200.0	480.3	690.3	12.79	182°
WGC 2D	6/8-10/18/76	20	1678	124.67	34.67	631.1	780.4	1411.5	3.11	245°
	"	50	1808	"	31.95	466.2	721.7	1187.9	3.39	234°
	"	80	1455	"	20.26	177.1	337.3	514.4	1.10	178°
WCG 3B	6/10-10/17/76	20	1817	124.67	43.97	719.4	1166.9	1886.3	21.59	256°
	6/10-9/14/76	50	1831	96.04	41.03	597.2	1114.2	1711.4	16.42	261°
	6/10-10/17/76	98	1834	124.67						
SLS 8	3/3-5/14/76	49	1672	71.50	14.08	68.7	55.6	124.3	10.68	300°
	3/8-5/13/76	74	1673	66.46	12.96	63.6	48.0	111.6	9.78	299°
SLS 9	3/7-5/13/76	51	1677	66.67	21.96	241.0	284.7	525.7	6.85	329°
	"	100	1987	"	19.48	182.0	215.1	397.1	6.66	327°
	"	240	1988	"	15.69	131.0	129.0	260.0	7.66	317°
SLS 14	5/14-9/24/76	77	1830	124.67	12.48	91.0	77.3	168.3	5.17	300°
GASS 9	4/21-7/23/76	20	1768	93.75	49.60	1039.9	1163.9	2203.8	22.29	198°
	"	30	1769	"	43.55	811.9	885.7	1697.6	20.45	198°
	"	50	625	"	39.22	657.5	729.4	1386.9	19.60	202°
	"	100	1771	"						
	"	273	1773	"						
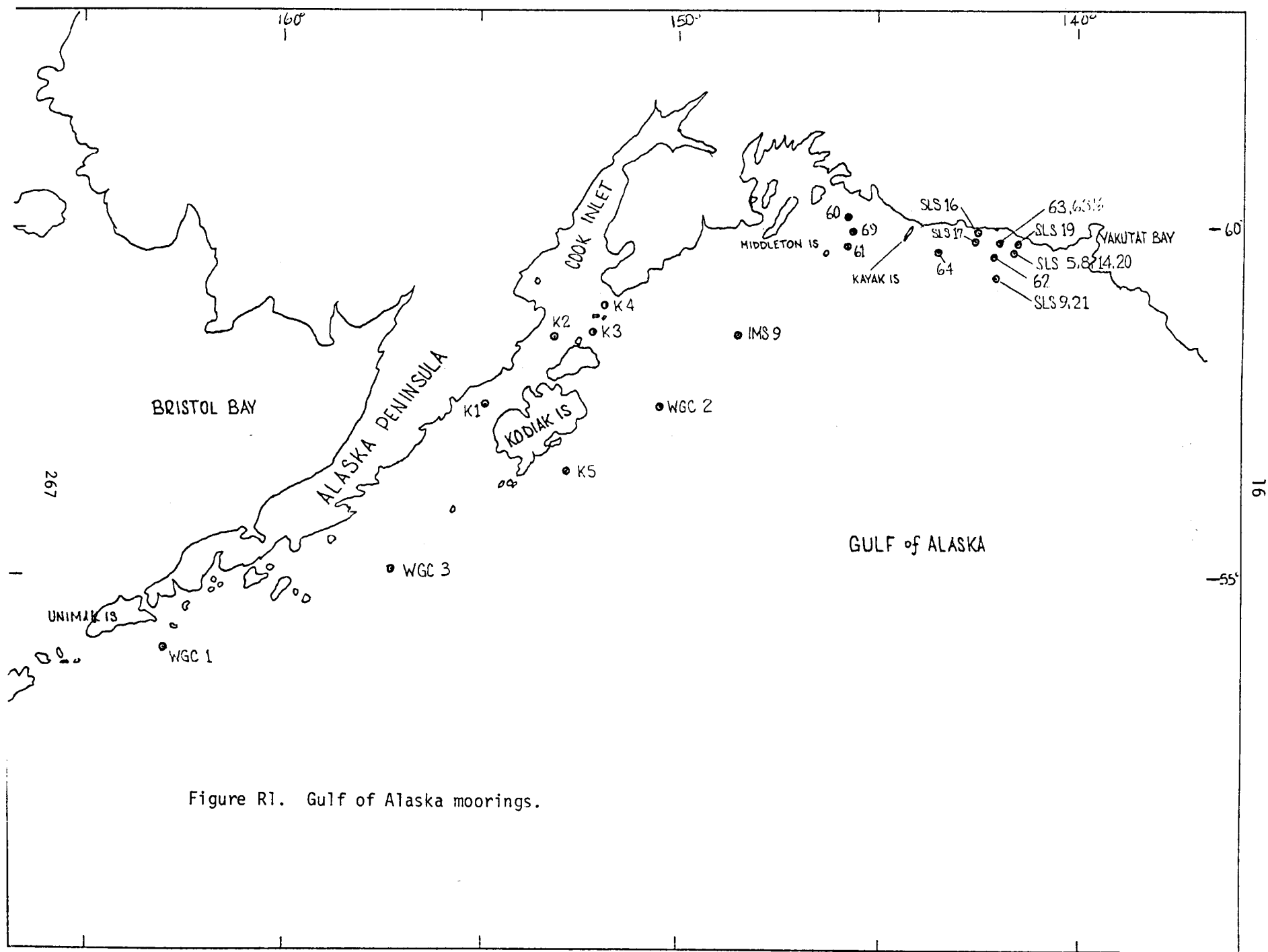
Figure R1.   Gulf of Alaska moorings.

FROM CHART 531

Figure R2a.

Depth Contours

100m — — — — —
187m ————————
500m —·····—·····

Speed Scale   cm/sec

| 60B | 61B | | SLS 8 |
| 62G | 69A | | SLS 9 |

20m 50m 100m 160m   50m 100m 240m
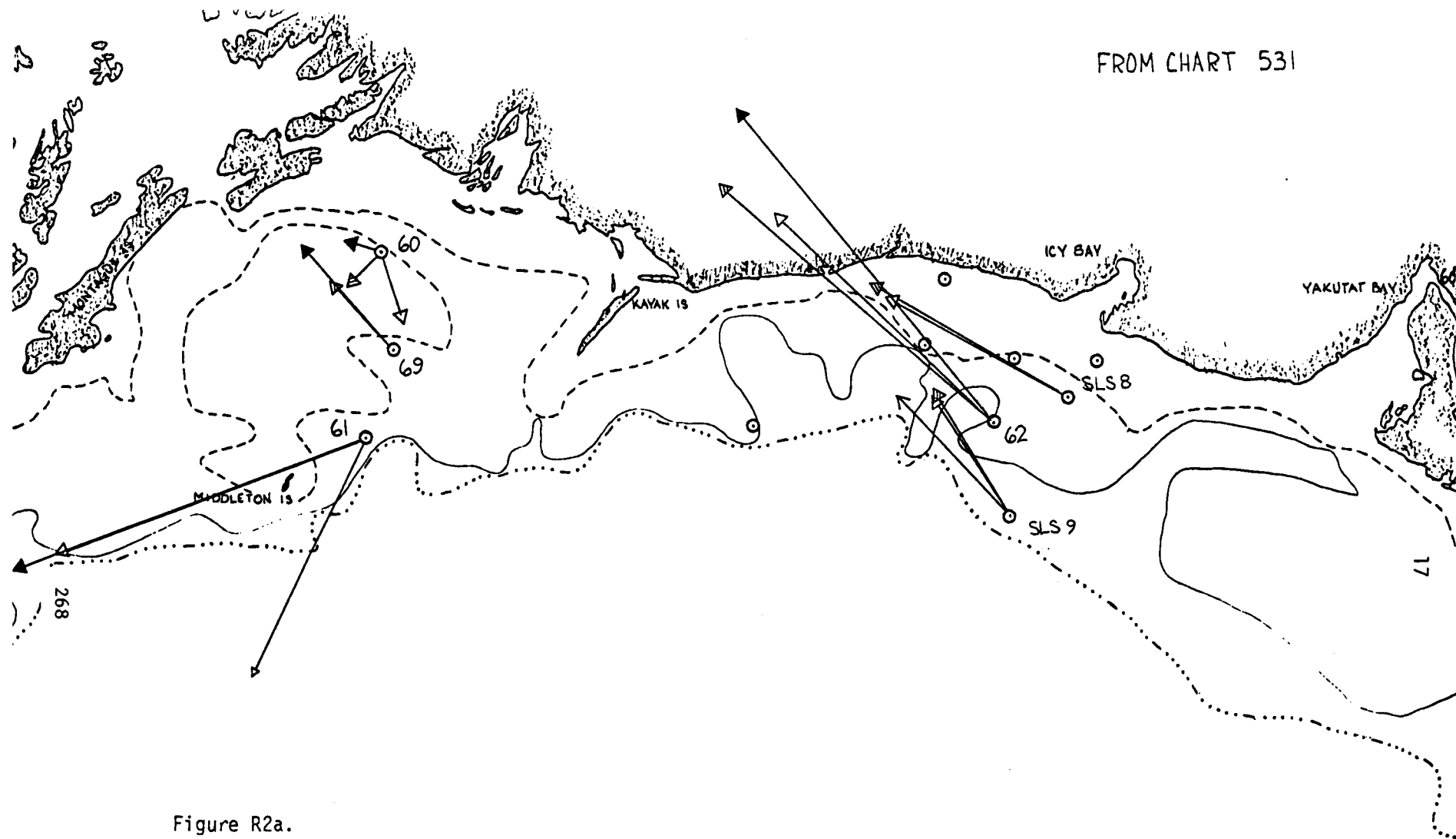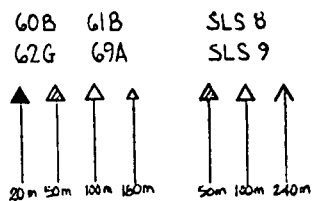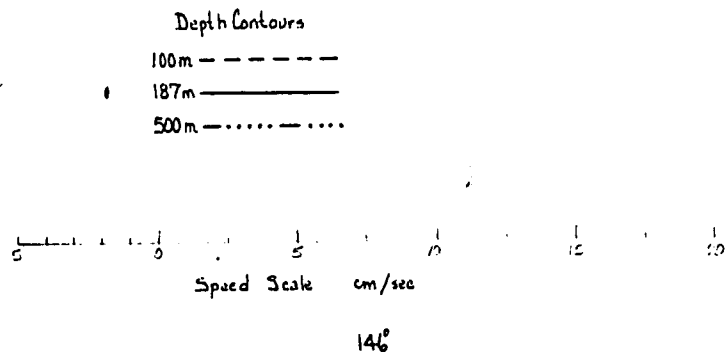
MARCH — MAY
1976
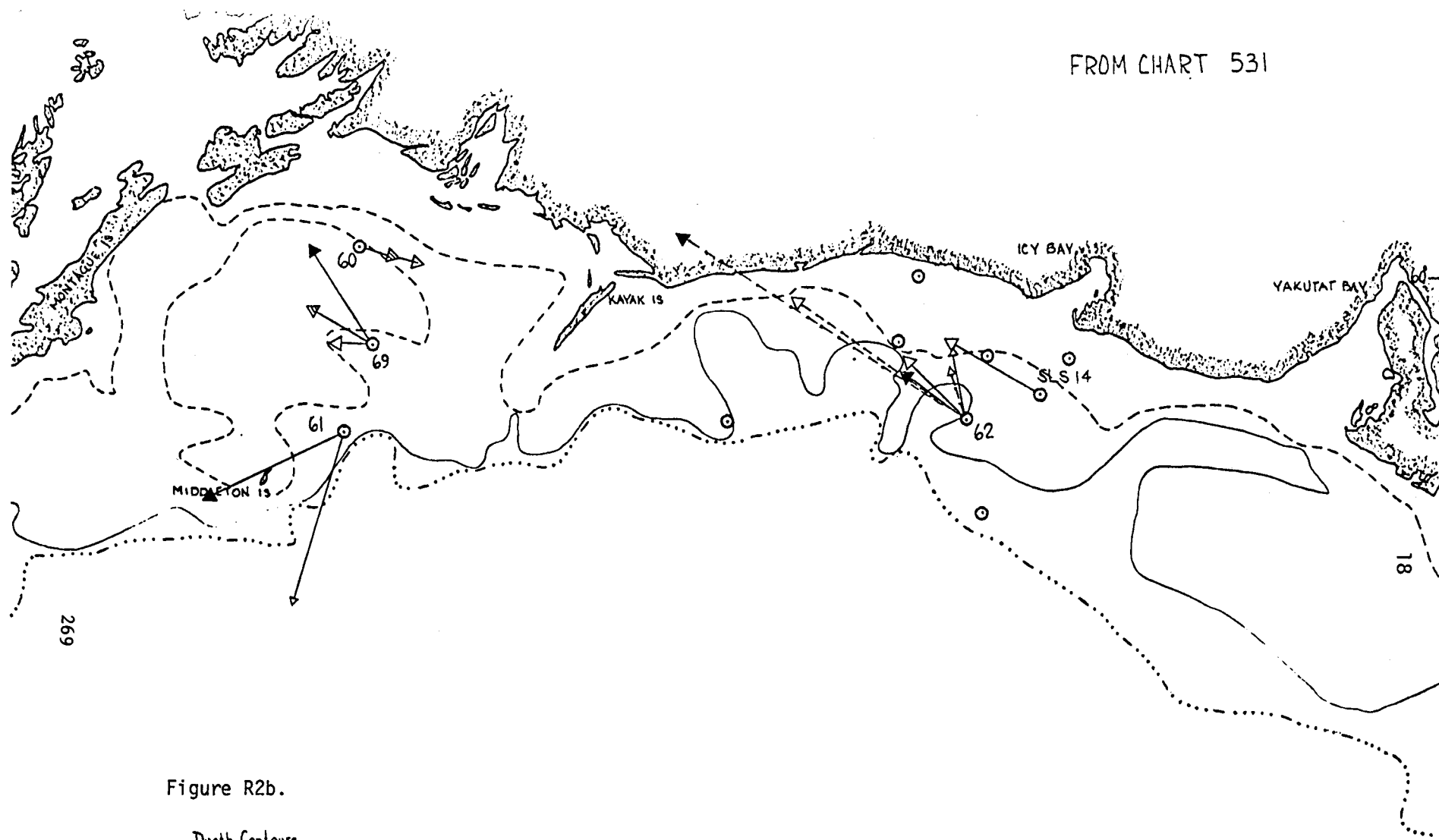
FROM CHART 531

Figure R2b.

Depth Contours

100 m — — — — —
187 m —————————
500 m — · · · · · — · · · · ·

Speed Scale   cm/sec

MAY — OCTOBER
1976

COOK INLET

SHELIKOF STRAIT

KENAI PENINSULA

KODIAK ISLAND

270

187m

WGC 2D

WGC 2C

GASS 9

Figure R-3.

FROM CHART 531

Depth Contours

100m — — — —
187m —————
500m — ·· — ·· —

Speed Scale   cm/sec

5   0   5   10   15   20

GASS 9B
WGC 2C

20m 50m 100m 175m

WGC 2D

20m 80m

FROM CHART 16006

ALASKA PENINSULA

WGC 3B

Figure R-4.

Speed Scale   cm/sec

Depth Contours

100 m — — — —
187 m ————
500 m — ···· — ····

54'—

FROM CHART 16006

ALASKA PENINSULA

UNIMAK ISLAND

WGC 1

Figure R-5.

Depth Contours

100m — — —
187m ————
500m ·······—·····

WGC 1D   WGC 1C

50m 20m   175m 100m 20m

Speed Scale   cm/sec

56°

272

21

54°

166°   164°   162°   160°

VII. DISCUSSION

The analysis and interpretation of the data is divided into a discussion of the results from the regional study and those from the process-oriented experiments. Since these two experiments are interactive, there is some overlap.

A. Regional Experiment

In this section a description of the mean flow is presented by geographical area: Icy Bay, Kodiak Island, and Western Gulf (see fig. R1). This description was primarily based upon the results from the regional arrays (stations 62, WGC-1, WGC-2, and WGC-3). All current meter records used were 35-hr low-pass filtered. The resultant time series was resampled at 6-hr intervals (unless noted otherwise). Station locations (fig. R1), current statistics, and observation period were given in Section VI (Results).

1. Icy Bay Region

Station 62 (see fig. 1) has been occupied continuously since August 1974, with the longest contiguous records at depths of 50 and 100 m. Several techniques were applied in order to define longshelf and cross-shelf flow axes. The 50-m depth mean flow for each mooring record was decomposed into u, v components and averaged. The resultant was 14.9 cm s^{-1} at 310° T. Rotary coherence analysis was also performed. The resulting ellipse axis orientations (confidence level and stability considered) support the result that the longshelf axis was 310° T, and the onshelf axis was 040° T. The local longshelf axis was close to the local topographic trend (305° T).

The schedule of mooring deployments permits some resolution of seasonal trends in mean flow. Moorings 62B, E, and F were considered representative of winter regime, while 62C, D, G, H, and I represent summer regime. For
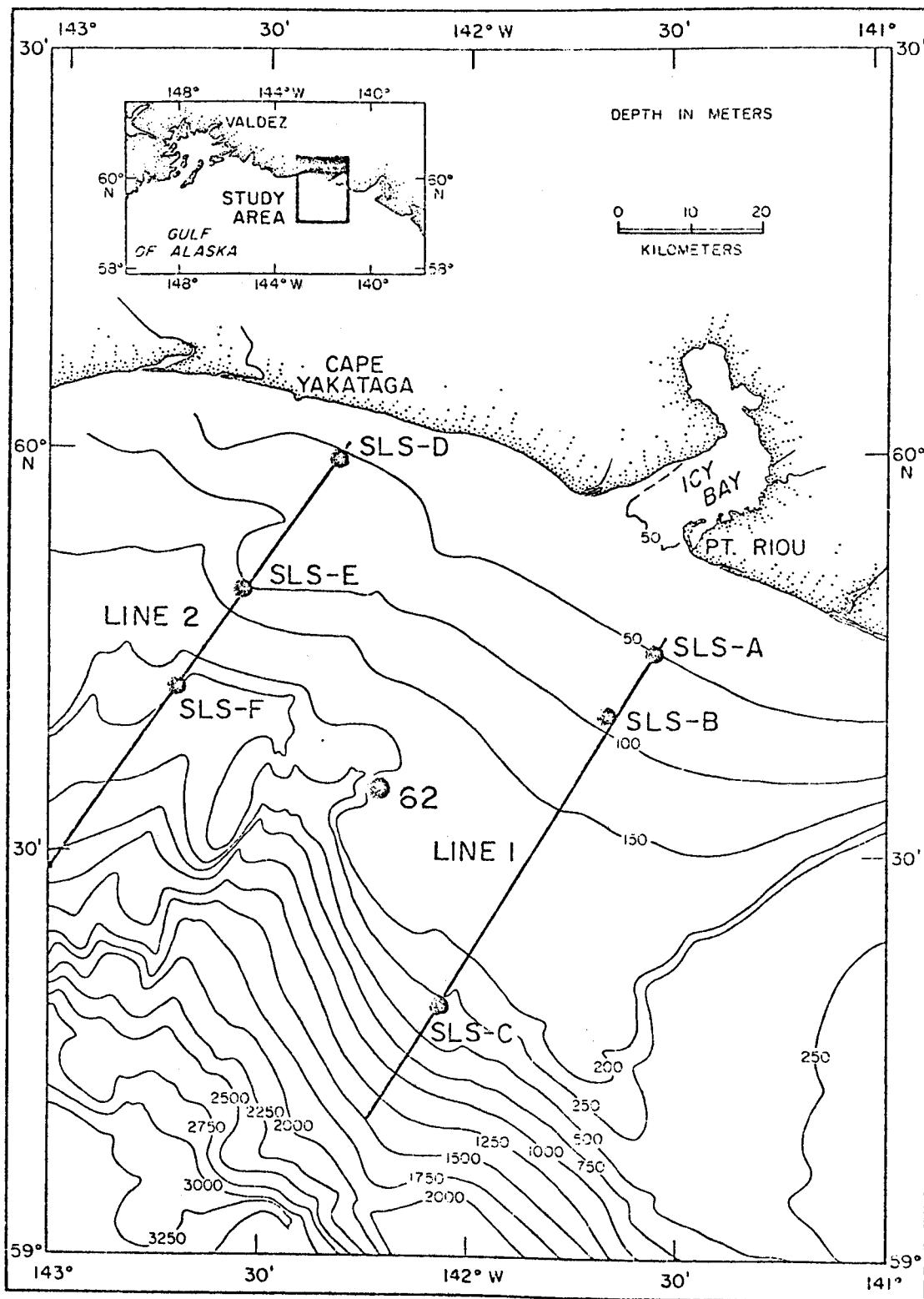
Figure 1. Icy Bay array. All moorings except 62 had pressure gages. All moorings except SLS-F had current meters at some time during the experiment.

the 20-month (February 75-October 76) record at 50 m, there were a total of 2,350 6-hourly observations. Overall, 89% had longshelf components. During the winter regime, the percent of longshore observations (90.5%) was greater than during the summer (88%). Greater longshelf speeds occurred during the winter regime; records from 62B and F, winter (fig. 2), indicated the highest values, with maximas of 56 and 74 cm s^{-1}. Maximum speeds along the negative longshelf axis occurred most often during the summer regime, with values of about 30 cm s^{-1}.

The cross-shelf flow was essentially negligible. During the winter regime, 43% of the observations had offshelf components, while 59% of the summer regime records had offshelf flow. Scatter diagrams from 62H and I are shown in figures 3 and 4. The record from mooring 62I was similar to records from the summer of 1975; however, 62H's record had a noticeably reduced mean flow and indicated that 57% of the observations had onshelf mean flow components.

To further examine seasonal trend and uniqueness of the record from 62H, mean velocities are presented as speed and direction by mooring duration (fig. 5). Records from 50- and 100-m depths were similar in magnitude, direction, and seasonal trend. There was a reduction in mean speed during 62H, except at 185-m depth, but this reduction did not continue through summer '76 (cf. 62I). Although records span only two summers, this reduction in mean speed appeared significant and warranted further investigation.

A progressive vector diagram (PVD), from 62H (50-m depth), constructed from 2.86-hr low-pass filtered data (resampled at 1-hr intervals), is shown in figure 6. This PVD started on 15 May 1976. Between 17-20 May there was an offshelf pulse, followed by 15 days of predominantly longshelf flow with a small onshelf component. From 4-7 June, flow was onshelf, followed by
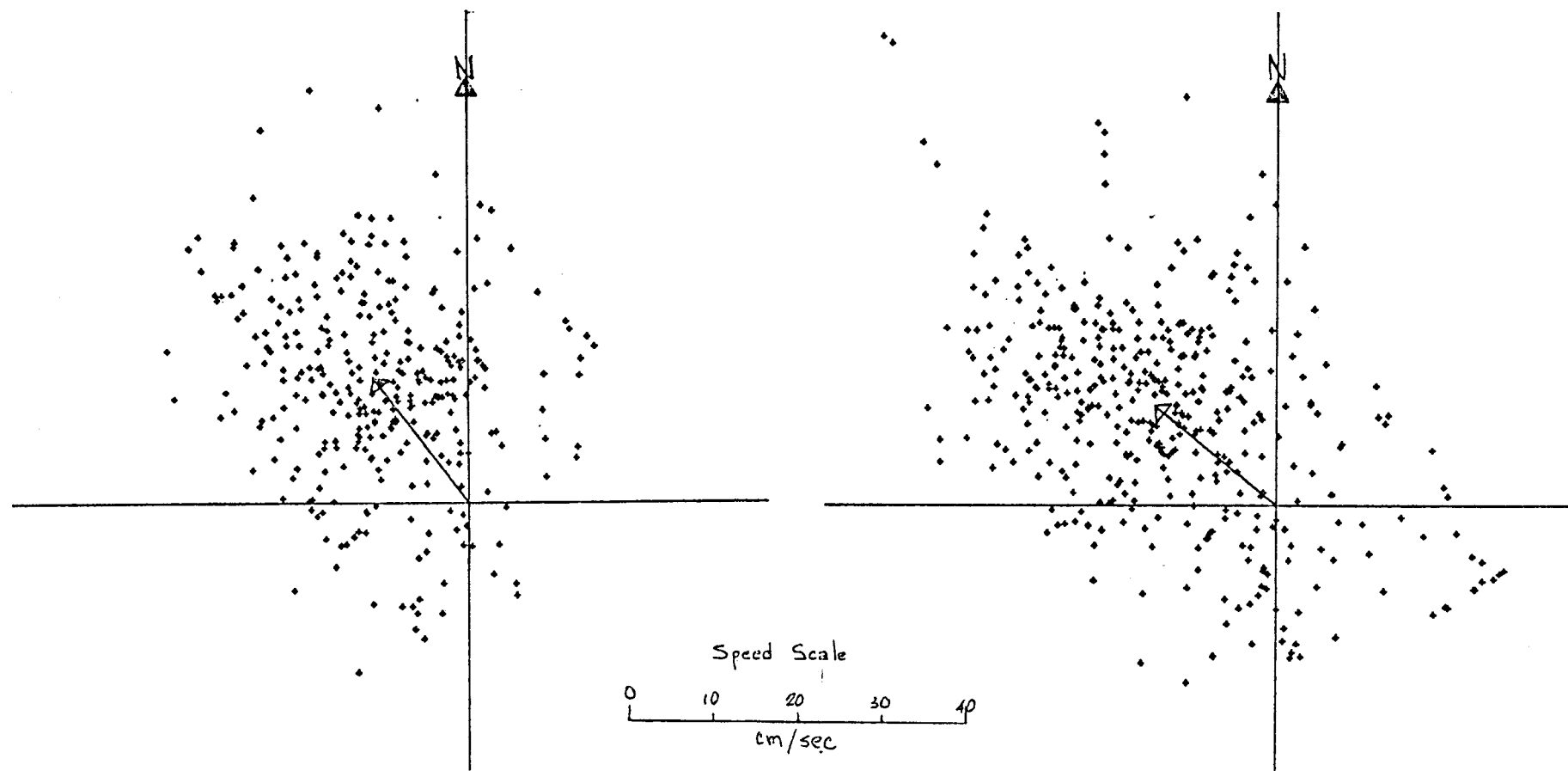
Mooring 62B   2 Feb 75 - 29 Apr 75
17.13 cm/sec
323⁰

Mooring 62F   20 Nov 75 - 5 Mar 76
17.16 cm/sec
309⁰

Figure 2. Current meter depths 50 m, moorings 62B and 62F.
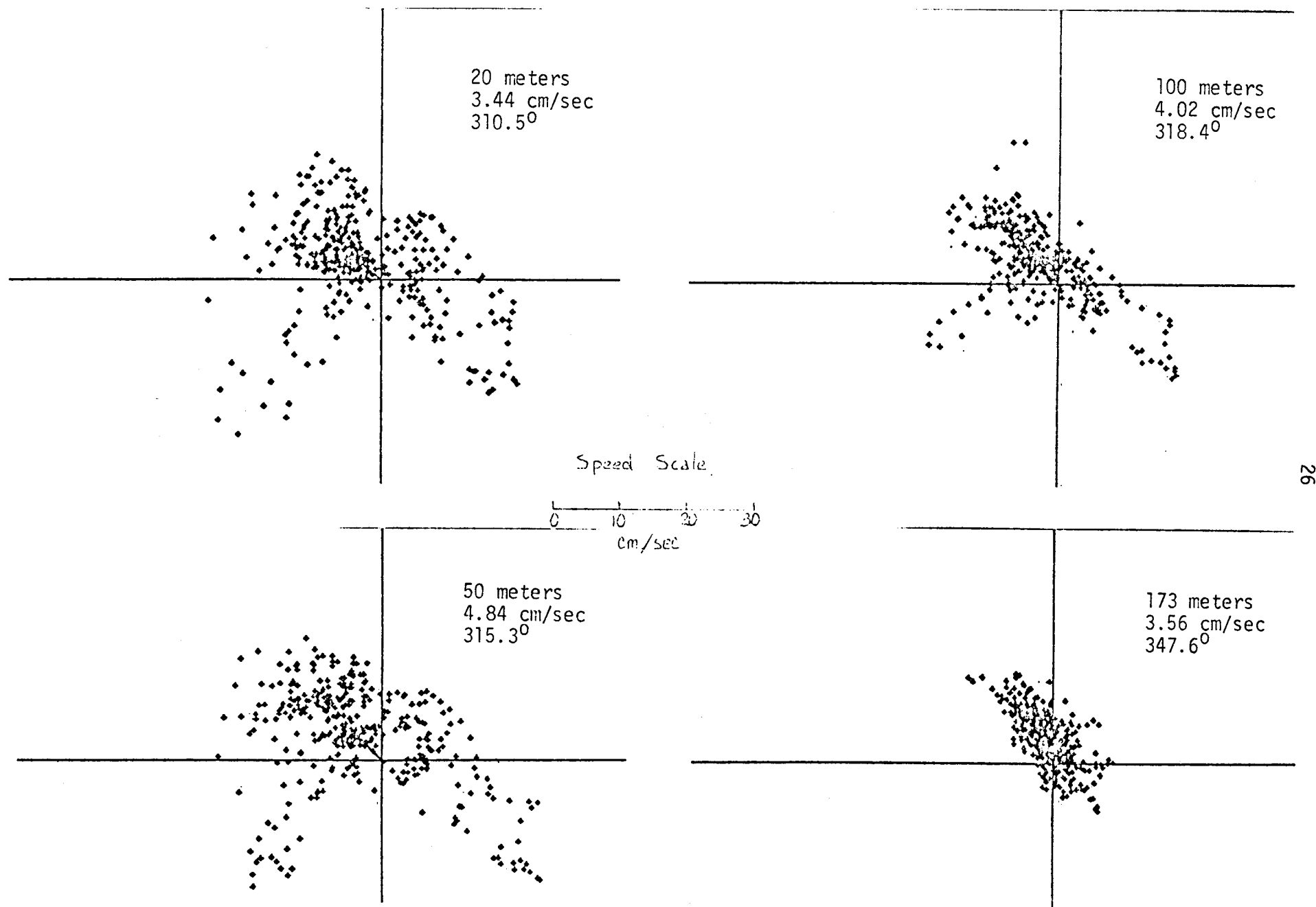
Figure 3. Scatter diagram from 62H, 14 May - 21 August 1976

20 meters
16.99 cm/sec
304.6°

100 meters
10.31 cm/sec
305.9°

Speed Scale

0   10   20   30   40   50
cm / sec

50 meters
14.40 cm/sec
300.5°

180 meters
2.65 cm/sec
344.5°
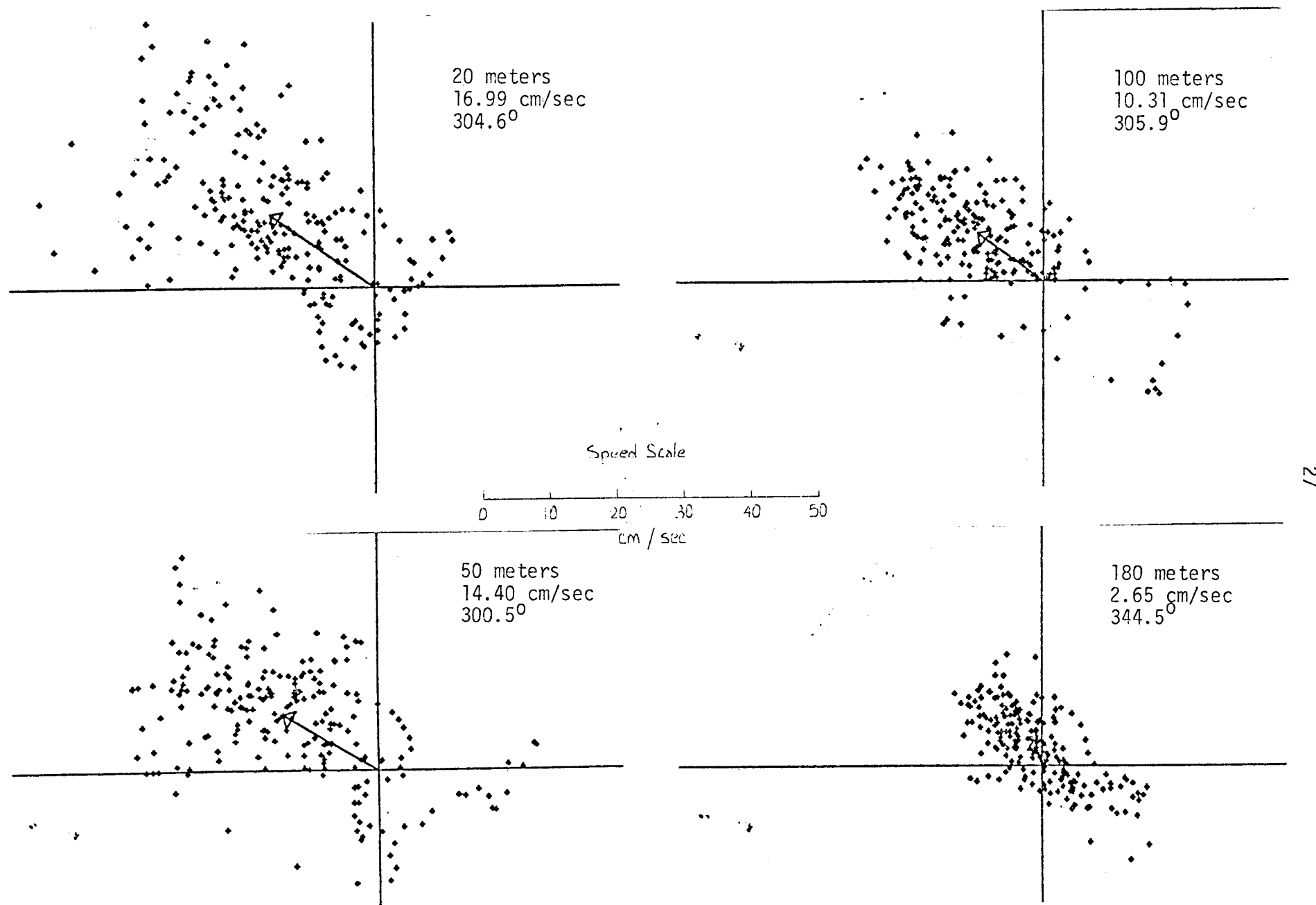
Figure 4.   Scatter diagram from 62I, 21 August - 21 October 1976.

a. Mean Speed

b. Mean Direction
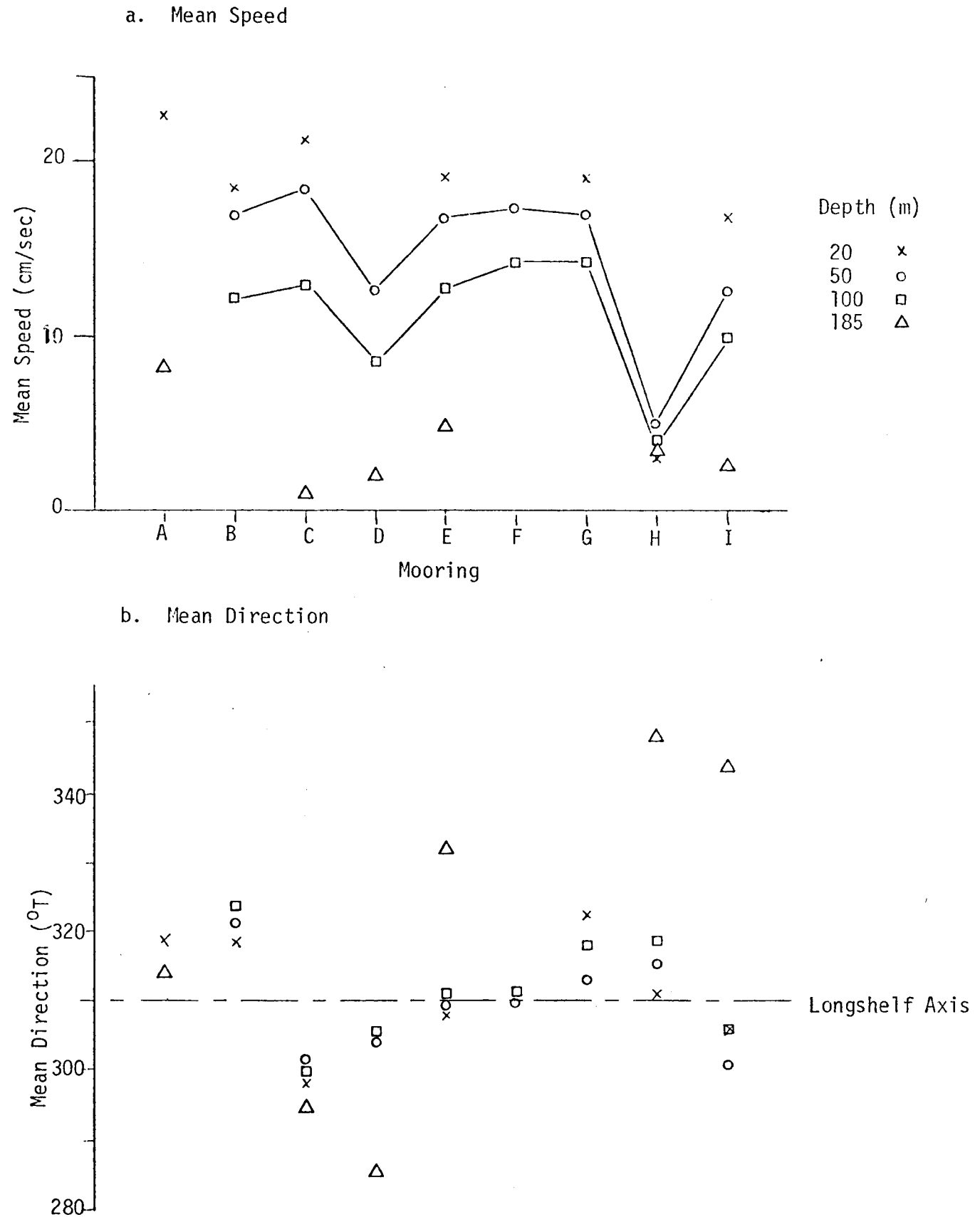
Figure 5. Mean Velocity at Station 62: August 1974 – October 1976.
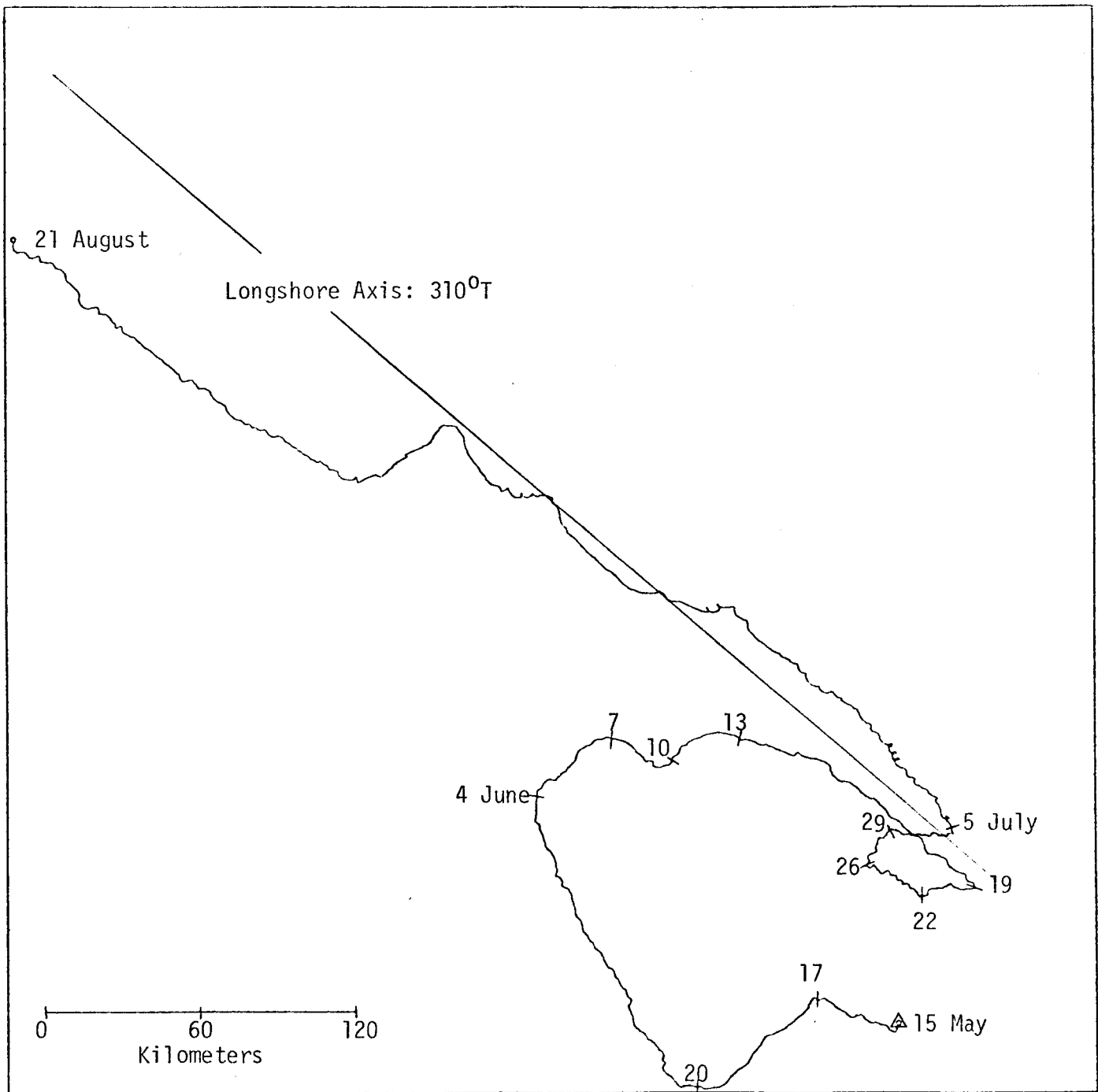
Figure 6. PVD from 50 m depth record at 62H, 15 May - 21 August 1976.

3 days of negative longshelf flow, and then onshelf flow for 2-1/2 days shifted to approximately negative longshelf flow for 6 days, ending on 19 June. The mean flow for the record described thus far was directed toward 030° T, which was substantially different than any record as shown in figure 5. The record from 62H indicated four more distinguishable direction changes between 19 June and 5 July. Each of these were low-speed (about 5 cm s^{-1}) and persisted for periods of approximately 3 days. The record for the remainder of mooring 62H appeared consistent with other summer regime data, with predominantly longshore flow (13.5 cm s^{-1}) and a smaller offshelf component (2.2 cm s^{-1}).

Some current records from nearby stations also indicated extended low-frequency fluctuations. Records from SLS-14 (occupied simultaneously with 62H) showed that low-frequency fluctuations occurred from 18 May to 13 June. After this period, mean flow was more consistent. The record from SLS9 (250-m depth contour) had a mean flow of about 7 cm s^{-1} at 329° T (50-m depth). Mean flow speed was consistent with depth, while direction veered 12° "contra sole" between 50 and 200 m. The PVD's (fig. 7) indicated flow containing low-frequency fluctuations. Additionally, these features tended to become aligned along the bathymetric axis, the effect increasing with depth. This also was shown in PVD's from 62H (fig. 8). However, records concomitant with SLS9 (fig. 9) did not indicate extended low-frequency fluctuations, but do show short-period (1-1/2 to 3 days) "eddylike" features. The passage of one such feature was indicated by noticeable changes in net speed, direction, and sigma-t (fig. 10). These features also have been noted in CTD sections across the Icy Bay shelf (fig. 11). During this event, the baroclinic flow indicated a speed of about 5 cm s^{-1} with clockwise rotation. Overall, these records indicated rather consistent longshelf flow (relative to local bathymetry). Similarly, winter-regime records from SLS-5 (moored at the same nominal site as SLS-8 and 14) indicated consistent longshelf flow.
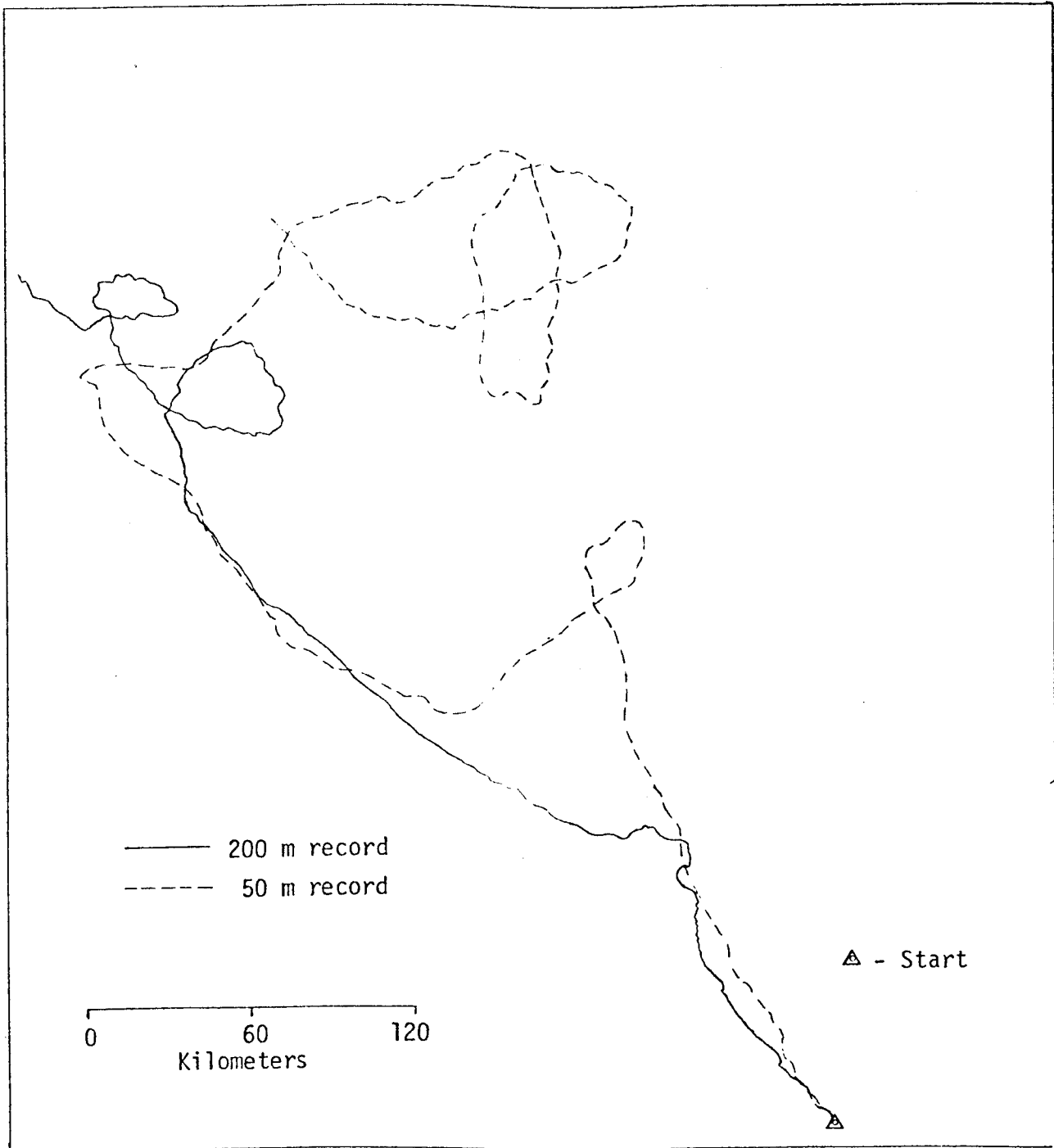
Figure 7. PVD's from 50 and 200 meter depths at SLS - C, 7 March -
12 May 1976.
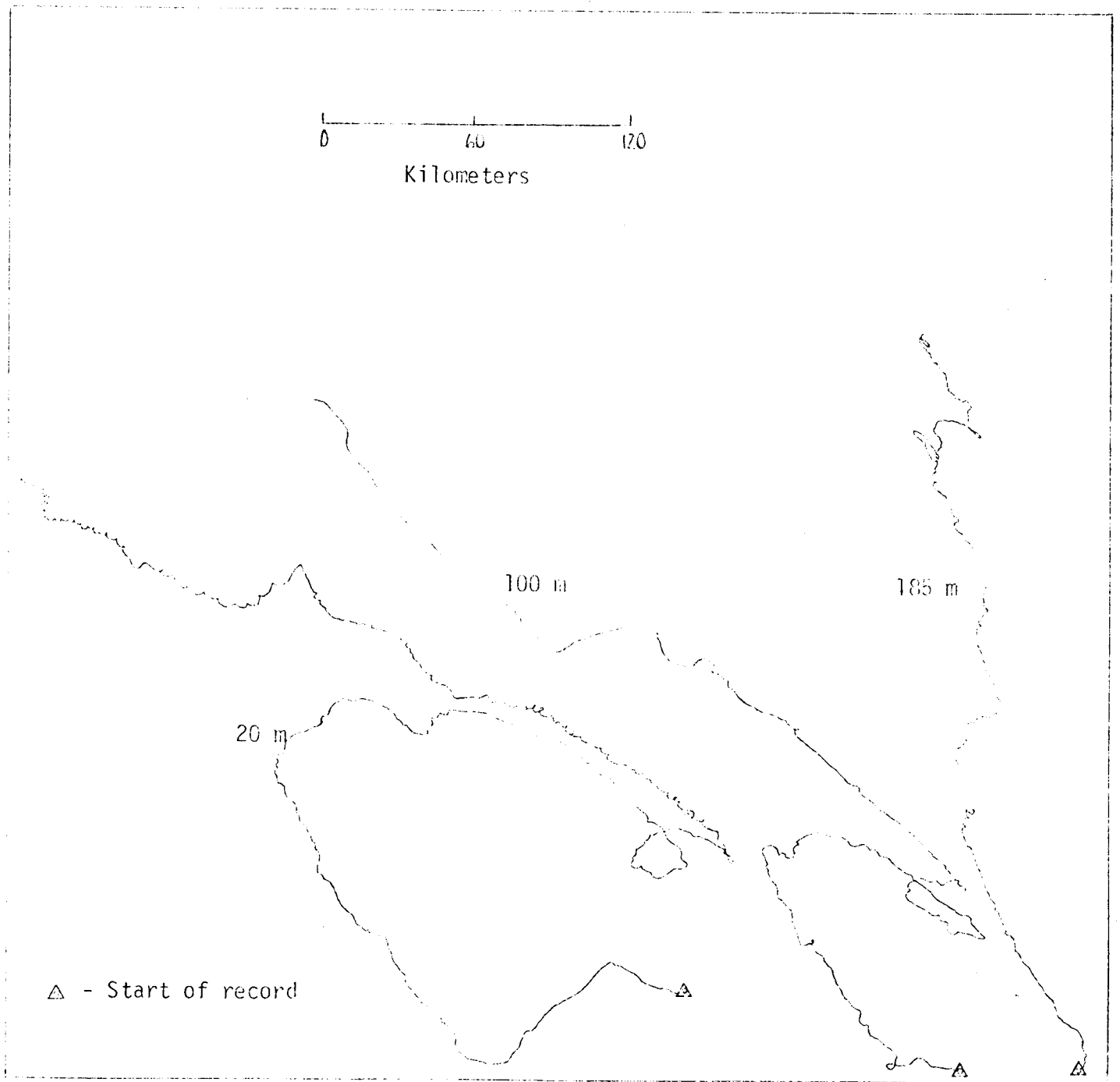
Figure 8. Composite of PVD's from mooring 62 H: 14 May - 21 August 1976.
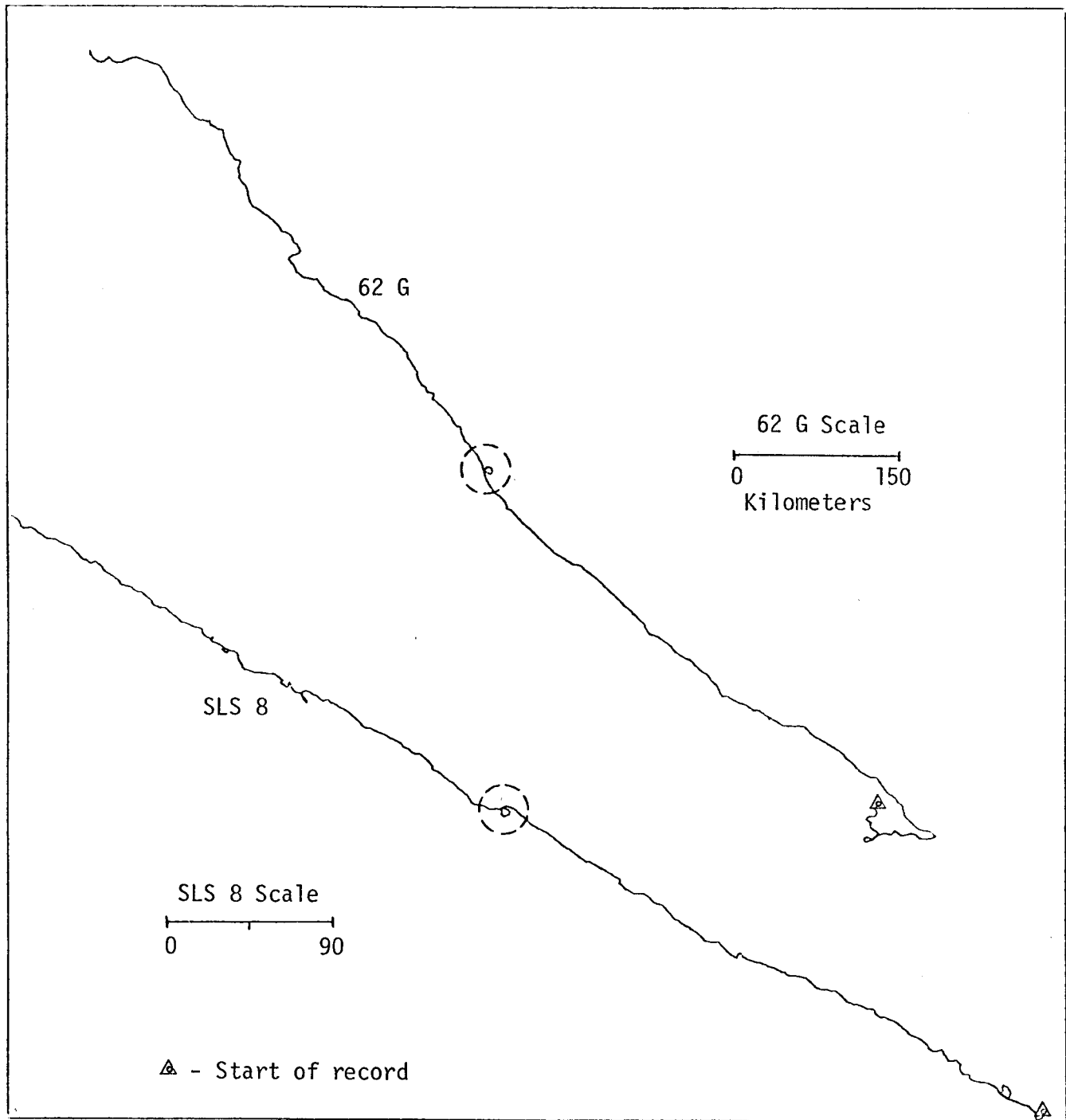
Figure 9.   PVD's at 50 m depth at SLS 8 (3 March - 17 May 1976) and 62 G
(5 March - 14 May 1976).   Note "eddy-like" feature encircled.
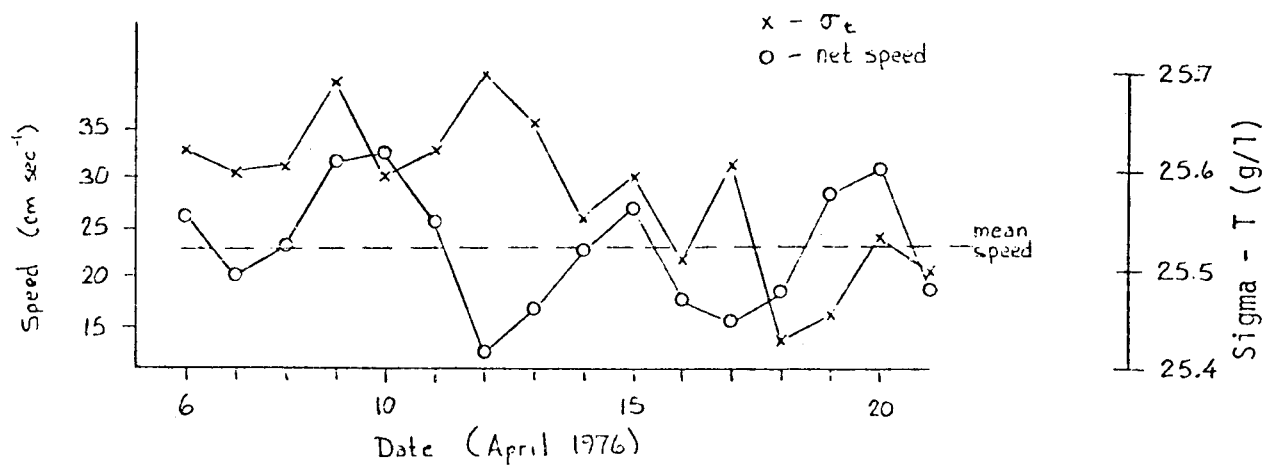
a. Net speed and Sigma - T values from 50 m depth record. Mean speed is for the 15 day segment.
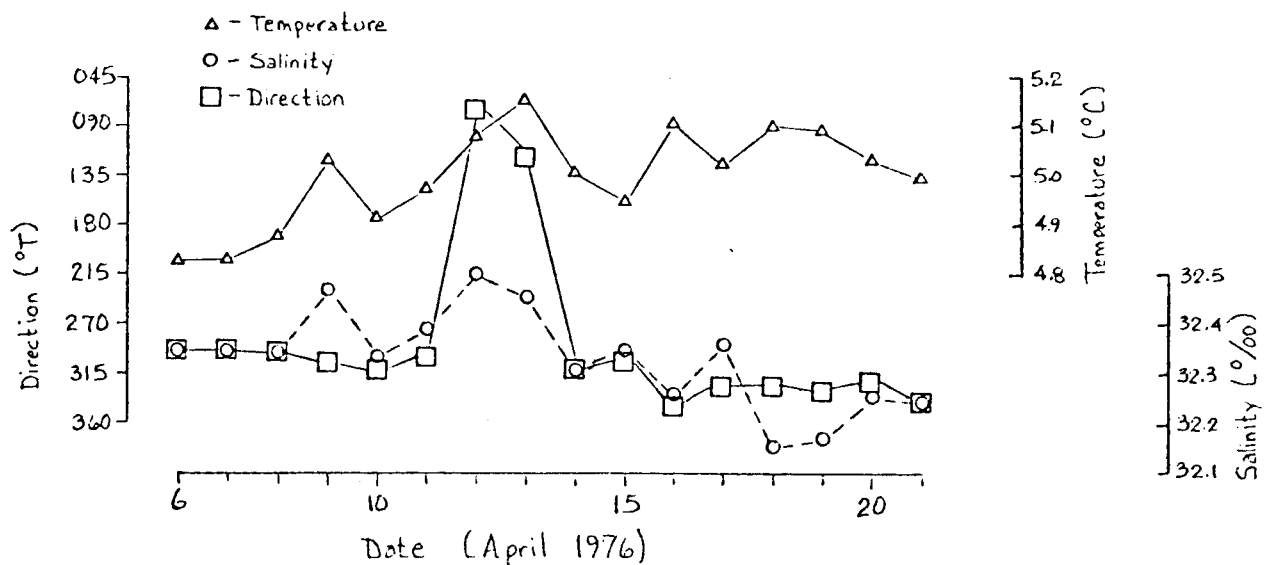
b. Direction, salinity, and temperature records during "eddy-like" feature. (Note period 11 - 14 April 1976.)

Figure 10. "Eddy-like" low frequency flow feature as indicated in 24-hour mean parameters.

Figure 11.   Sigma - T transect across Icy Bay shelf indicating "eddy-like" feature.   Station separation is approximately 10 km.   Line run 16 May 1976.
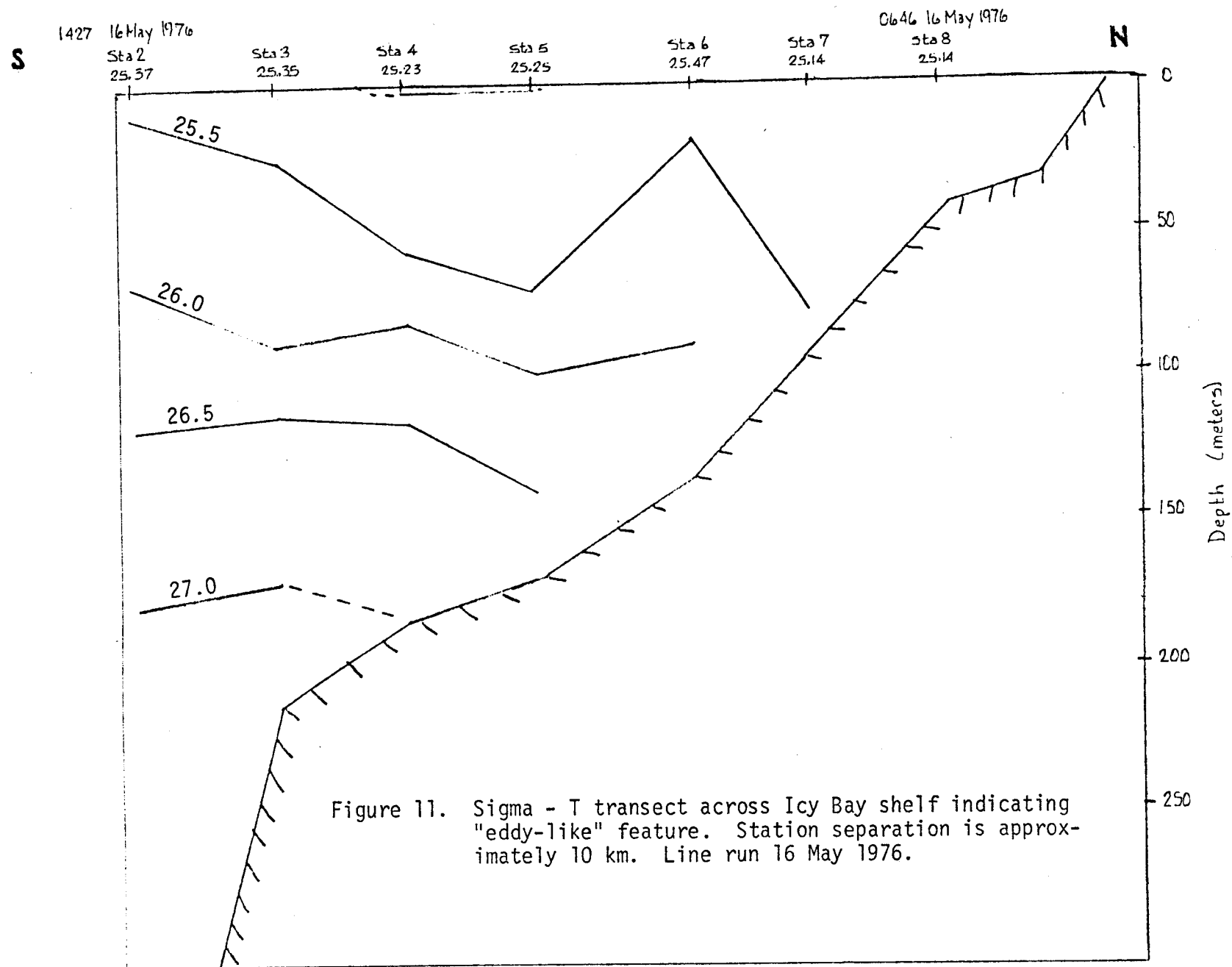
Summary. The dominant flow was along-shelf. Delineation of seasonal trends indicated two regimes: summer, or April through September; and winter, October through March. This conclusion was consistent with Ekman transport data for the periods 1950 to 1959 and December 1970 to October 1972 as presented in Royer (1975). The implication that meteorological conditions were related to mean flow seasonal trends was evident.

During winter, mesoscale meteorological conditions tended to augment local longshelf flow, reducing low-frequency fluctuations, while summer conditions required offshelf surface flow and a reduced longshelf component. Further, small-scale wind field investigations indicated strong offshore outbreaks during winter (Reynolds, Macklin, and Walter, 1977) along the Icy Bay shoreline. Such offshore winds may complicate the wintertime setup. Hayes and Schumacher (1976) described a barotropic model which accounted for about 50% of low-frequency flow during winter. This setup along the Icy Bay coast during winter increases the longshelf flow.

The extended low-frequency fluctuations in records from 62H are intriguing at this location for the following reasons: (1) previous current records collected at station 62 over a 20-month period do not contain such events; (2) after 5 July the record indicated consistent longshelf flow with an offshelf component; and (3) typical summer regime meteorological conditions indicated a tendency for upwelling or offshelf flow. Other current records from the Icy Bay shelf region usually indicated consistent mean flow parallel to depth contours, the exception being from SLS-14 which was occupied concurrently with 62H. There have been "eddylike" features in several current records; however, those features appeared as short-term (2-3 days) events. Current meter station SLS-9, located seaward of the shelf, indicated that low-frequency fluctuations are common at this shelf slope location.

Lagrangian drifter studies (Hansen, work unit 217) support the conclusion that mean flow was consistently longshelf and that,seaward of the shelf break, low-frequency fluctuations were typical (figs. 12 and 13). Wave- or eddy-like features have been documented by Royer and Muench (1977) west of the Icy Bay region, predominantly between Middleton Island and the southwestern end of Kodiak Island.

Analysis of current meter records from the shelf off the Oregon coast demonstrated the importance of "topographic steering" (Kundu and Allen, 1976). There, fluctuations roughly followed the direction of local bathymetry. It is likely that observed offshelf fluctuations in the Icy region were affected by bathymetry when propagated into the shelf. Due to bottom friction, "topographic steering" was a function of depth; low-frequency fluctuations became more linear with increasing depth. This was observed in offshelf records, and also in records from the shelf when extended fluctuations occurred during May-July 1976.

2. Kodiak Island

Station WGC-2 has been occupied since September 1975; however, mooring WGC-2B (winter 1975-76) was not recovered. The current measurement program around Kodiak Island was increased to six arrays (two current meters each) in October 1976 (see fig. R1 for locations of K1 to K5). Upon recovery in March '77, this pilot study will be completed.

The lack of records during winter conditions precludes a description of seasonal trends. Additionally, mooring WGC-2's location was moved from a shelf break environment to one on Northern Albatross Bank (100-m contour) for deployment of WGC-2D. The relocation was directed toward a better definition of circulation on the biologically highly productive Kodiak Shelf.
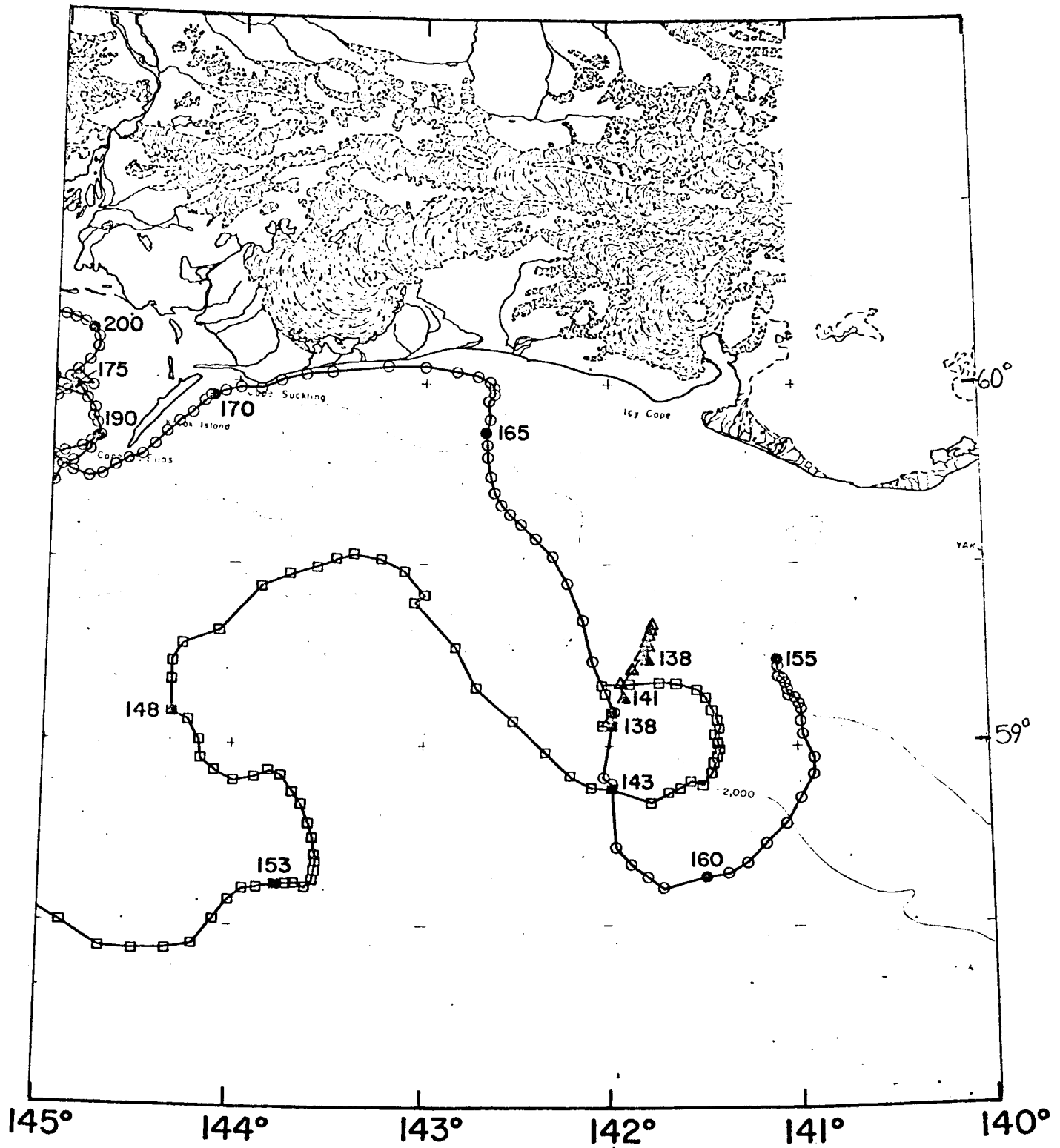
Figure 12. Lagrangian drifter trajectories, Gulf of Alaska, May - June, 1976.
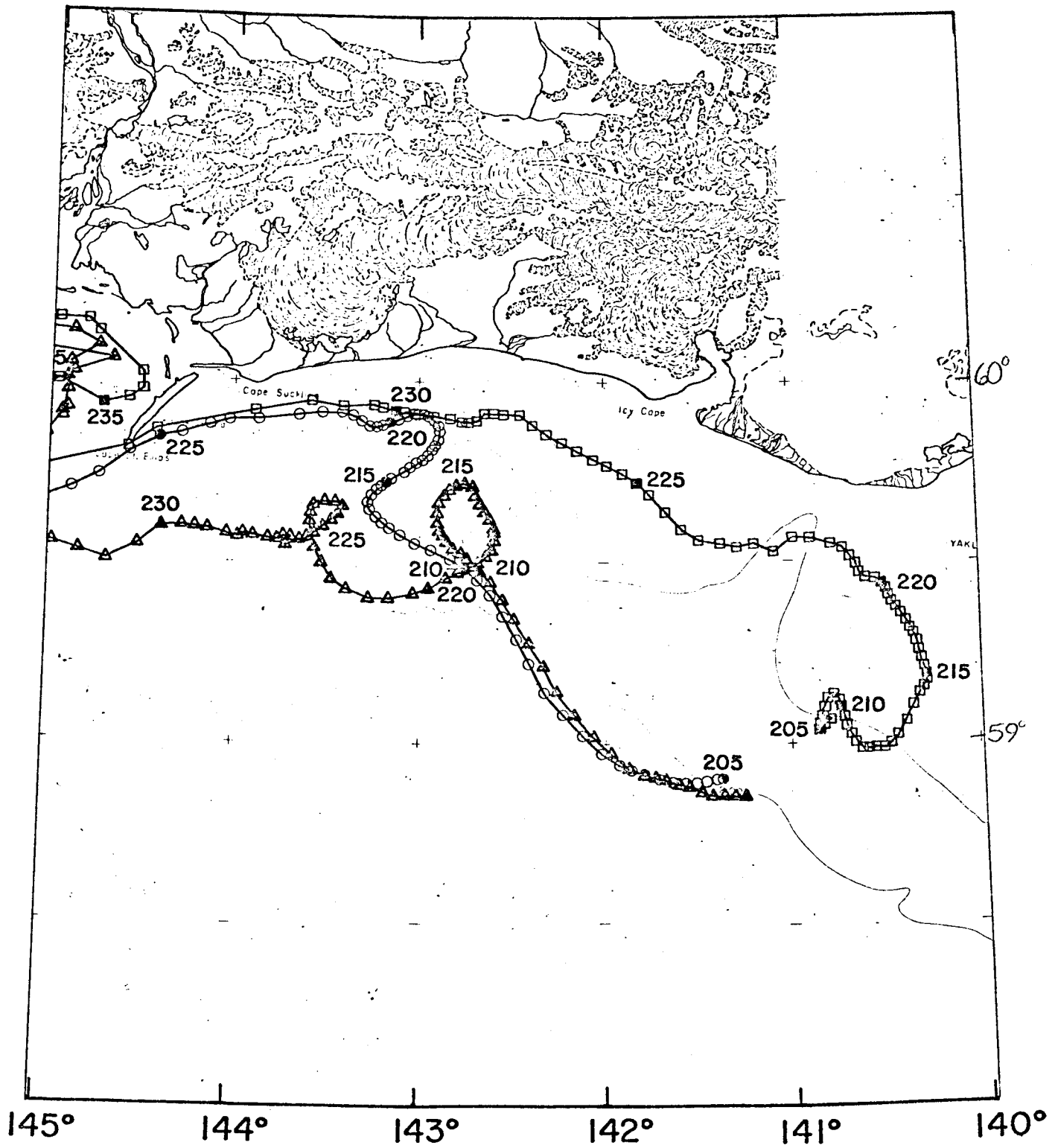
Figure 13.   Lagrangian drifter trajectories, Gulf of Alaska, July 1976.

Records from WGC-2A and C indicated that flow tended to be consistently longshelf towards the southwest. The mean flow at 100-m depth was about 25 cm s^{-1} for both records, while near-bottom flow (12 m off seafloor) had an offshelf component. There were no extended flow reversals as noted at station 62H in the Icy Bay region and little evidence for the shorter period "eddylike" features. The velocity field at this shelf break region was dominated by mean flow. In the record from WGC-2C, variance was 604 cm^2 s^{-2}, with 44% of this being contained in the major tidal frequency bands. The total kinetic energy is the sum of kinetic energy of the mean flow and of the variance. Records indicated that nontidal flow contained 81% of the total kinetic energy.

In contrast to WGC-2C, WGC-2D (moored at 92 m on the bank) indicated a significantly different circulation. A PVD (fig. 14) from the upper current record (20-m depth) clearly showed the dominance of tidal energy. The mean flow was reduced by a factor of 7, from 21.6 to 3.2 cm s^{-1}. This weak advection maintained a strong tendency to flow longshelf toward the southwest. Additionally, the record from near-bottom indicated flow with an offshelf component. As in shelf break records, there were no indications of either extended flow reversals nor "eddylike" features in the low-frequency flow.

An examination of energetics indicated that 90% of the variance was contained in tidal frequency bands. Nontidal flow accounted for approximately 11% of the total kinetic energy. Thus, in moving from the shelf break to the 92-m depth contour (approximately 15 km), two distinct circulation regimes were sampled.

Summary. The consistency both in direction and speed of records from the shelf break off Kodiak Island supports previous studies (Ingraham, Bakun, Favorite, 1976) which indicated that the Alaskan Current is intensified similar
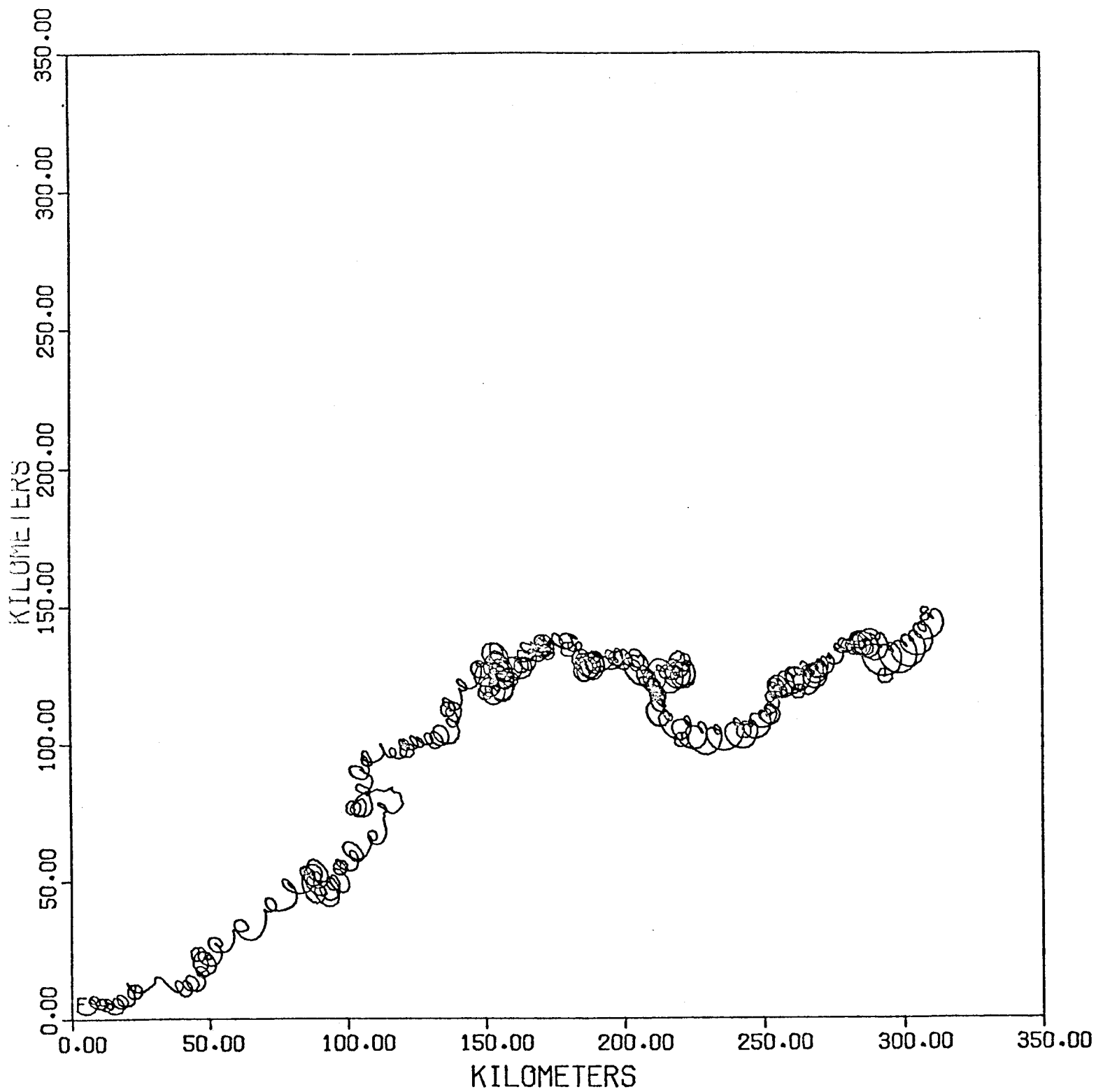
Figure 14. PVD from WGC 2D (20 m depth), 11 June - 20 October 1976.

to a western boundary current. This intensification was also shown in satellite imagery studies (Royer and Muench, 1977) and was indicated in CTD data (Royer, personal communication).

Baroclinic flow reversals (Royer, personal communication) and gyral circulation patterns as developed from a diagnostic model (Galt, personal communication) have been presented for the Kodiak Island shelf. Although these events are not evident in the record from WGC-2D, the low advective flow does imply that such events are possible, and further field experiments are necessary.

3. Northwestern Gulf of Alaska

Direct current measurements have been obtained from moored current meter arrays at two locations in the northwestern Gulf of Alaska. The first array from which data were obtained, WGC-1, was initially located approximately along the 200-m isobath about 130 km ESE of Unimak Pass at 54°01.7' N - 162°59.8' W. The array, WGC-1A, was at this position from September 4 - November 1, 1975, and obtained data from 50 m and 103 m. A second mooring at nearly the same location, WGC-1B, was emplaced from November 1, 1975 - March 12, 1976, but yielded no data due to malfunctioning of both current meters on the array. A third mooring, WGC-1C, was located about 1.3 km farther to the south than WGC-1A at 54°01.0' N - 163°02.8' W. Measurements at WGC-1C were obtained from depths of 20, 50, 100, and 175 m from March 12 - June 11, 1976. The most recent set of measurements, obtained from WGC-1D at the same location as WGC-1C and at depths of 20 and 50 m, covered the period June 11 - September 30, 1976. A fifth array, WGC-1E, is presently moored at the same approximate location as the previous WGC-1 arrays. We now have in hand a continuous record of currents, with the exception of the period from

November 1, 1975 - March 12, 1976, at WGC-1 from September 4, 1975 - September 30, 1976, or just over 1 year.

A second set of moored current arrays, WGC-3, has been located approximately along the 100-m isobath about 250 km southwest of Kodiak Island since March 11, 1975. The first of these arrays, WGC-3A, was not recovered. The second array, WGC-3B, yielded 20-m and 50-m records from June 10 - October 17, 1976, at 55°11.5' N - 156°58.0' W. A deeper meter (at 98 m) on the WGC-3B array malfunctioned and yielded no data, and the 50-m record was truncated by about 30 days due to malfunctioning of the meter. A third array, WGC-3C, is still deployed and has been in the water since October 17, 1976.

Mooring WGC-3 was located upstream from, although in shallower water than, WGC-1, as can be seen on figures R1, R4, and R5. The arrays were located to allow detection of possible coherence along the approximate axis of the Alaska Current-Alaska Stream system. WGC-1 is located such that it might be expected to show influence of transports through Unimak Pass between the North Pacific Ocean and the Bering Sea, while WGC-3 might be influenced by a cross-shelf flow originating in the Shelikov Strait. Both arrays are in a region suspected to contain complex flow because of a possible separation of the Alaska Current from the coastal region and concomitant change in character of the current from a western boundary to a drift-type current (see Thomson, 1972). Additional complications might be caused by the presence of Kodiak Island in the flow field. The following will not attempt to explain such complexities, but will address only the basic flow characteristics observed at each mooring.

The mean currents at WGC-1 were generally directed toward about 255°, or approximately parallel to the regional topography, throughout the mooring period (figs. R5 and 15-17). The deepest measurement obtained, from WGC-1C
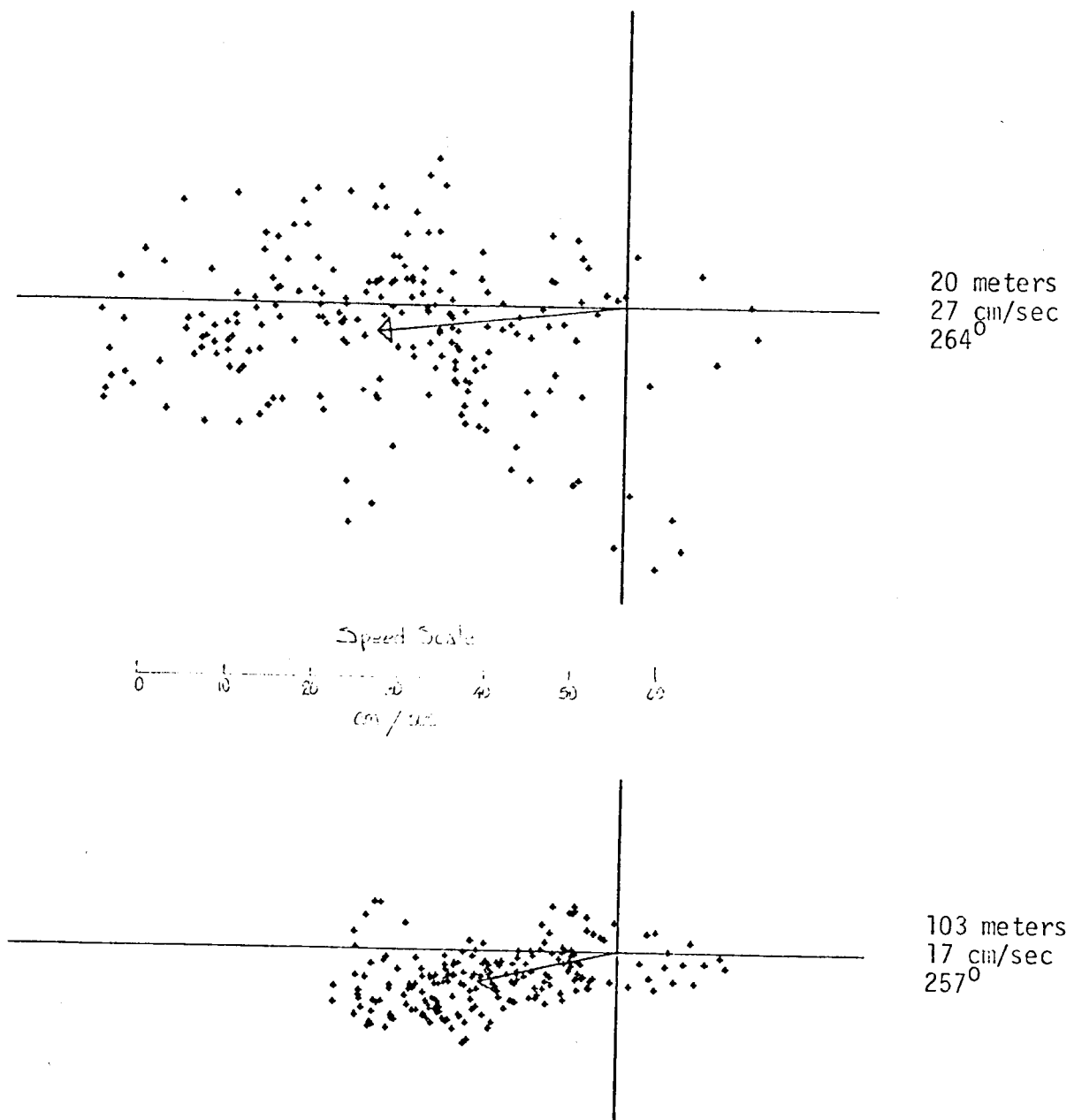
Figure 15. Scatter diagram from WGC 1A, 4 September - 1 November 1975.
Lat 54°01.7'N, Long 162°59.8'W.
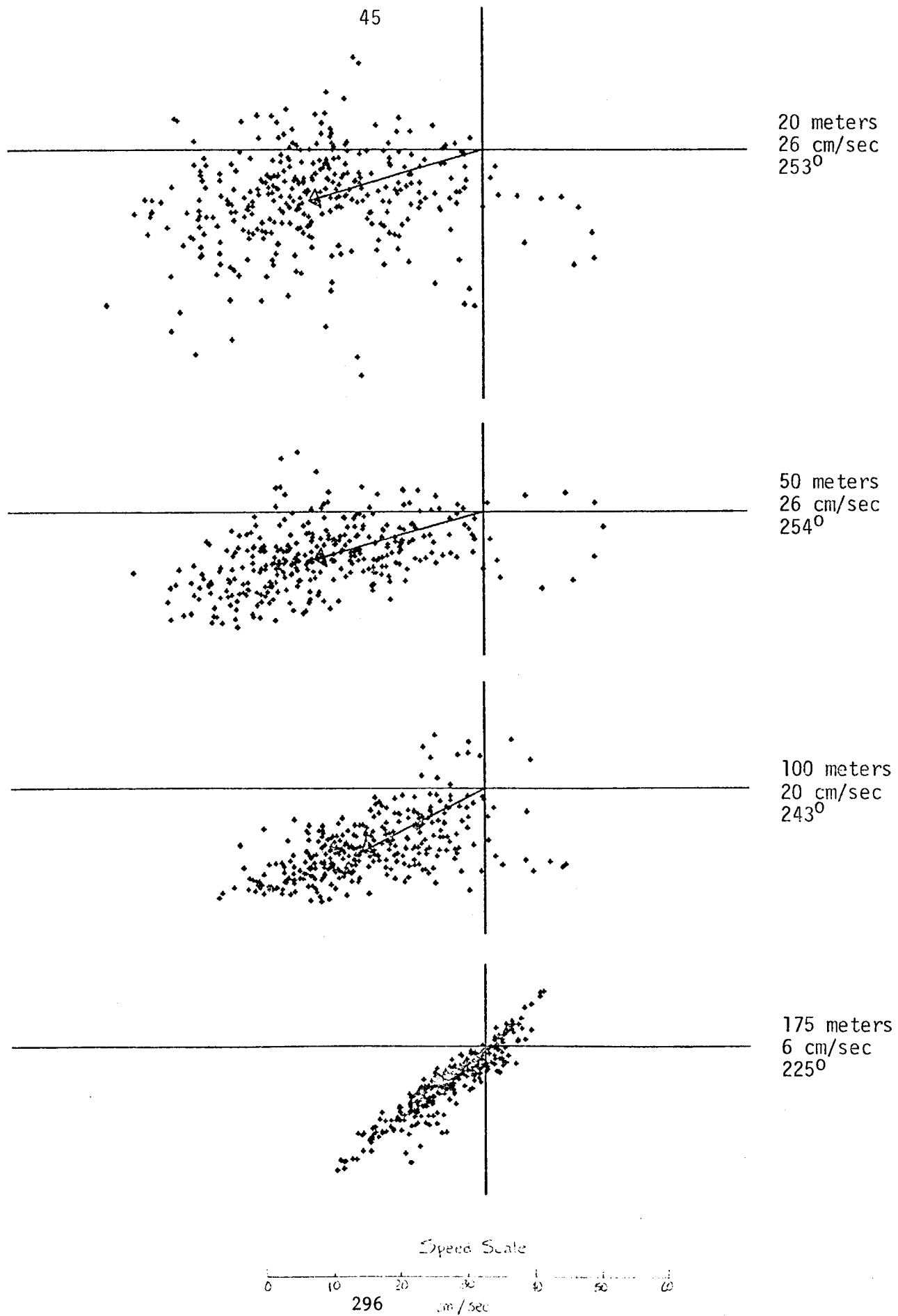
Figure 16. Scatter Diagram from WGC 1C, 13 March - 11 June 1976.
Lat 54°01.0'N, Long 163°02.8'W.
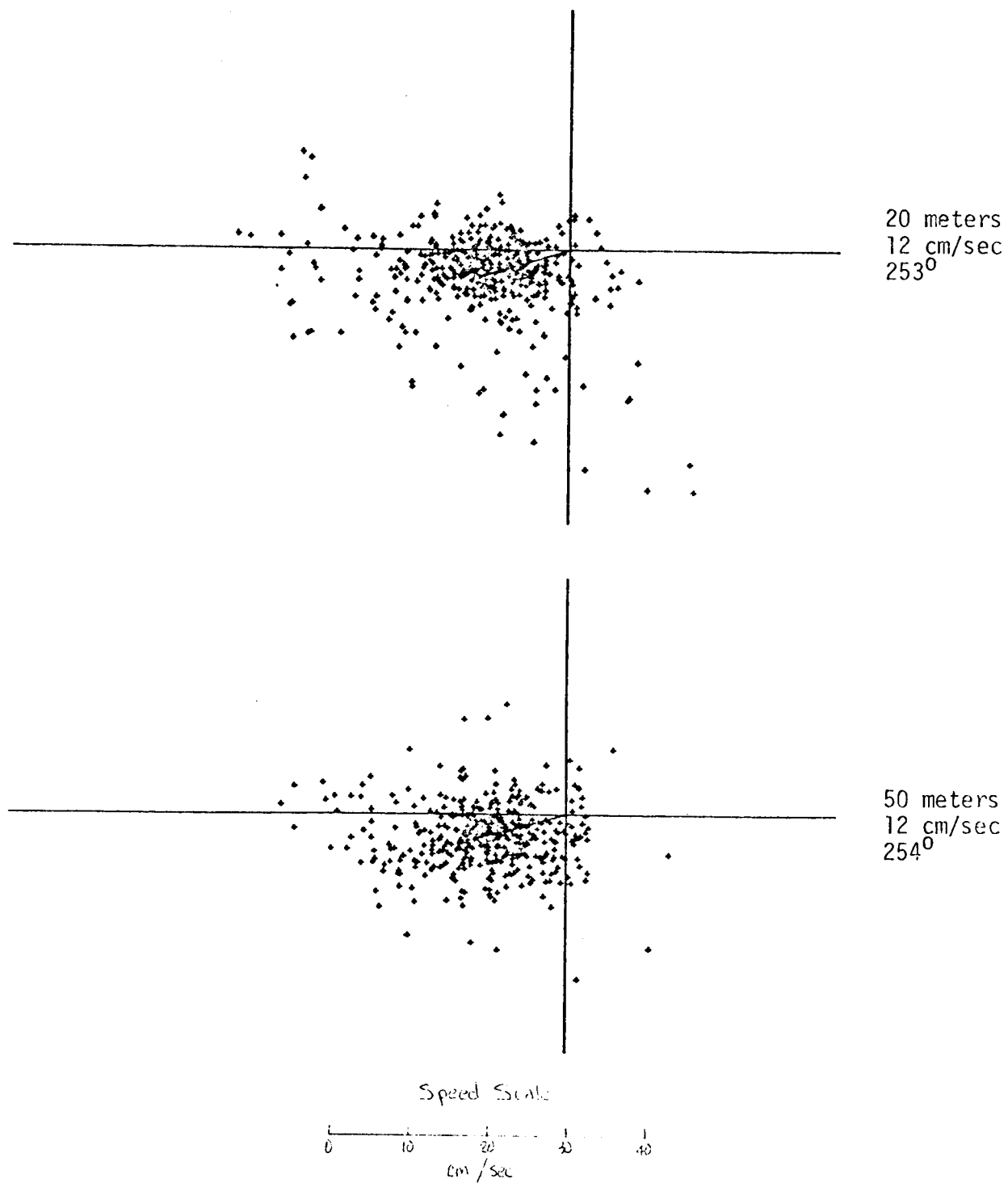
Figure 17. Scatter diagram from WGC 1D, 11 June - 20 October 1976. Lat 54°01.0'N, Long 163°05.0'W.

at 175 m, was the only exception and was directed toward about 225°. Since this measurement was obtained only about 10 m above the bottom, the directional deviation was likely a reflection of a bottom Ekman boundary layer causing the near-bottom current to veer to the left of the overlying currents. As seen from the scatter diagrams (figs. 15-17), the vector-averaged current speed did not decrease markedly between 20- and 50-m depths, although it had decreased markedly in time from WGC-1C (about 26 cm s^{-1}) to WGC-1D (about 12 cm s^{-1}). Both WGC-1A and WGC-1C indicated a roughly 35% decrease in speed between the upper 50-m and 100-m currents. At WGC-1C the current speed at 175 M had decreased still another 50% below that at 100 m. The decrease from the upper 50-m layer to 100 m suggests a degree of baroclinicity was present in the current--on the order of 35% if related to a 100-m reference level. The additional speed decrease at 175 m was likely related at least in part to presence of the bottom Ekman boundary layer, i.e., a frictional decrease.

It is difficult to say much at this time about the currents at WGC-3 because of the small amount of data available there. The mean surface current speed at WGC-3B was about 22 cm s^{-1} directed toward 257°, while the 50-m speed was about 16 cm s^{-1} directed toward 262° (fig. 18). Unlike currents at WGC-1, those at WGC-3 were therefore directed some 15-20° to the right of the local isobaths (fig. R4). The explanation for this is beyond the scope of the present treatment, but will likely be found in the presence of the complex bottom topography directly upstream from WGC-3 (fig. R4). The mean currents at both WGC-1 and WGC-3 can be seen to follow, in a general sense, the bottom topography and to substantiate the presence of the southwesterly extension of the Alaska Current. During the September-October 1975 and March-June 1976 periods, the current speeds in the upper 50 m were on the order of 25-30 cm s^{-1} at WGC-1, while during June-October 1976 the speeds
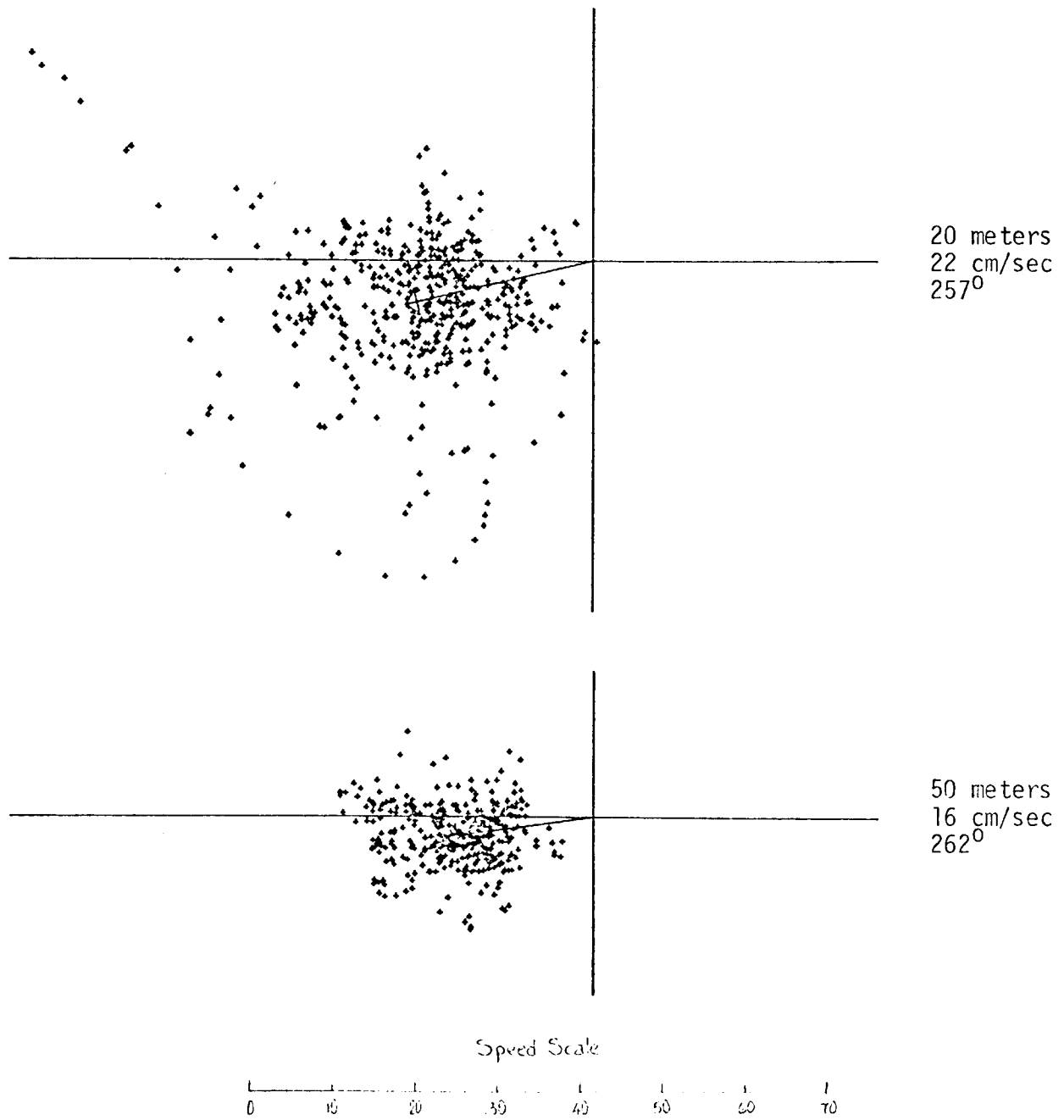
Figure 18. Scatter Diagram from WGC 3B, 10 June - 17 October 1976
(20 m depth) and 10 June - 16 September 1976 (50 m
depth). Lat 55°11.5'N, Long 156°58.0'W.

were lower, on the order of 12 cm s^{-1}. This variation likely reflects a seasonal change, the higher speeds being due to an overall spin-up of the system during winter 1975-76, and the lower speeds reflected the lower energy of the system following summer 1976.

The variance in flow at WGC-3 was considerably larger, up to a factor of 5 for the 2.9-hr filtered north-south variance, than at WGC-1. The variances computed from the 35-hr filtered data were, however, lower at WGC-3 than at WGC-1 (see table 1). The large high-frequency variance is due to a large tidal signal at WGC-3, at least a portion of which must reflect the presence of Shelikof Strait due to its north-south orientation. The lower frequency variance at WGC-1 is not well understood at this time, but is likely due to its location near Unimak Pass and possibly also to shelf waves. Variance was greater during the winter (WGC-1C) than during summer (WGC-1D), which suggests that winter storms were in part responsible for generating this variance.

The character of flow at both WGC-1 and WGC-3 can be illustrated by the 20-m progressive vector diagrams (figs. 19 and 20); deeper flow at each location exhibited the same character as the 20-m records. Flow at both locations showed no reversals and few perturbations other than tidal. Some wavelike features are manifestations of the low-frequency variance, and did not affect the net flow greatly (i.e., no reversals).

Summary. The flow along the shelf southwest of Kodiak Island and extending as far as about Unimak Pass was southwesterly, paralleled isobaths in general, and had speeds in the upper 50 m from 16-27 cm s^{-1}. Below that depth, speeds dropped off, and in the single available near-bottom measurement (WGC-1C at 175 m), an additional speed decrease and directional veering was probably due to presence of a bottom Ekman layer. Although data were inadequate for a
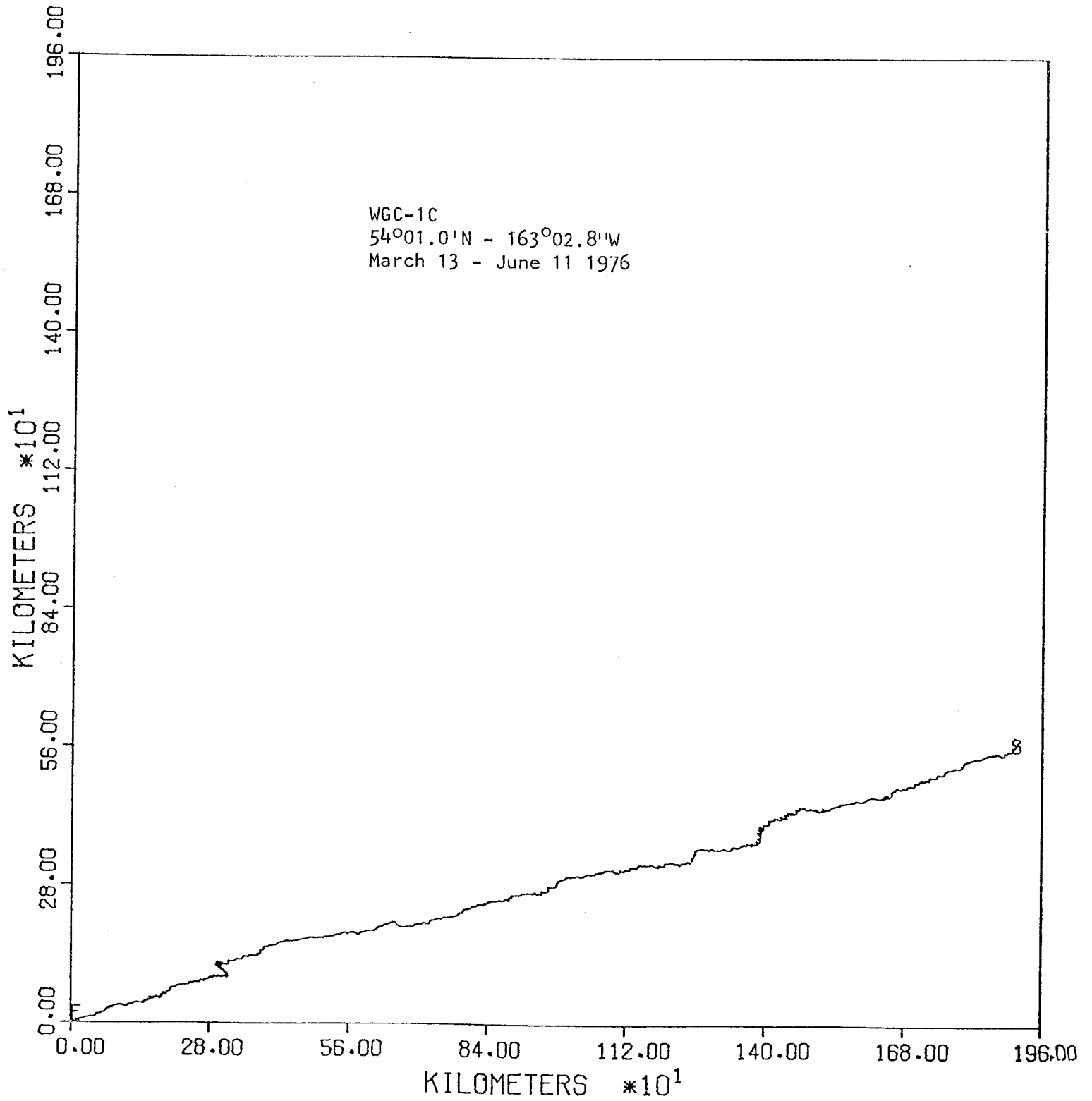
Figure 19 . Progressive vector diagram for WGC-1C, 20 m depth, from March 13 –
June 11 1966.
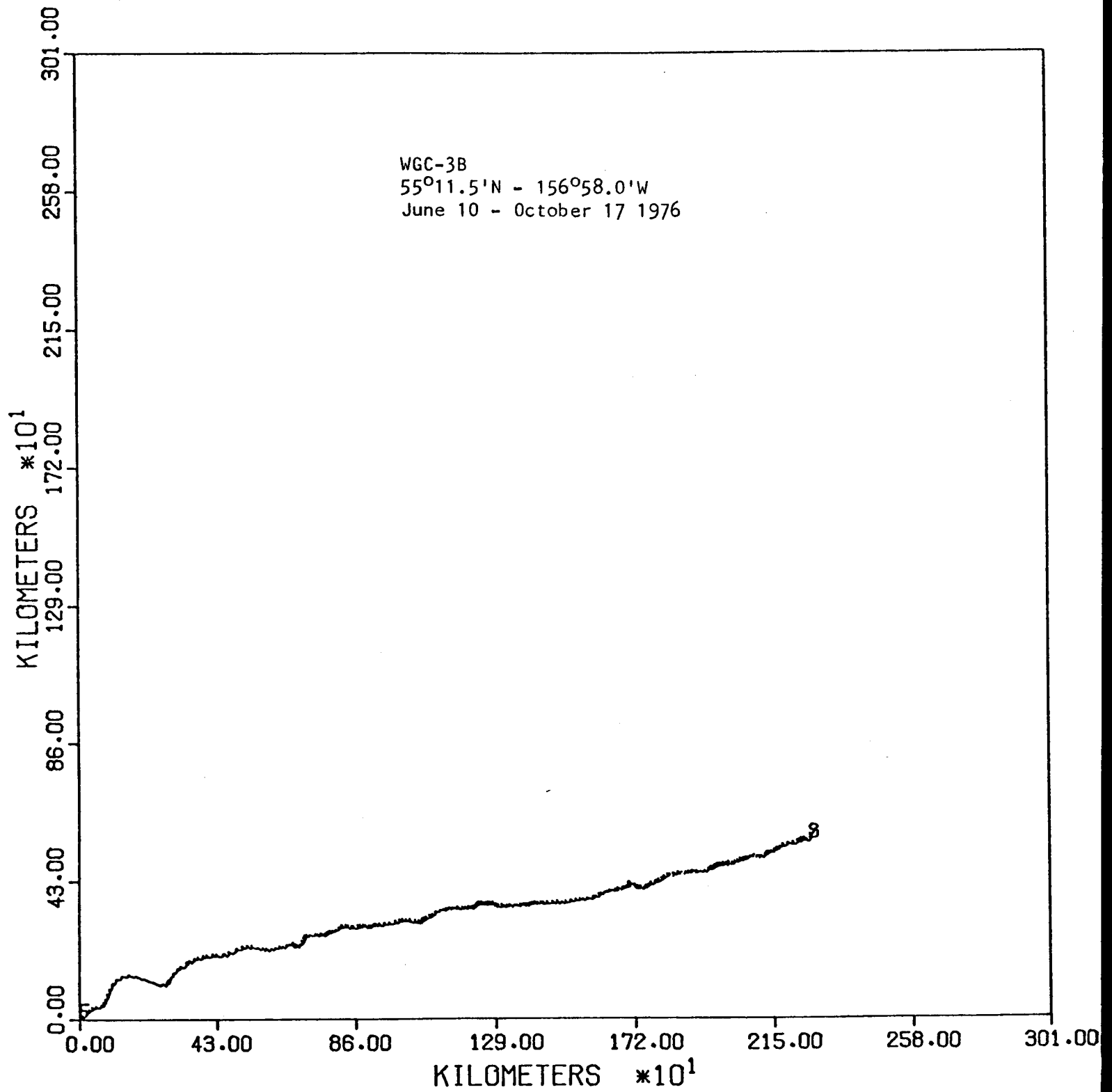
Figure 20. Progressive vector diagram for WGC-3B, 20 m depth, from June 10 – October 17 1976.

rigorous analysis, it appears that both mean speeds and low-frequency (nontidal) variance were larger during the winter months than during summer.

B. Process-Oriented Studies

The regional study and its preliminary results have provided a large-scale description of the flow around the Gulf of Alaska continental shelf. Given these statistical descriptions, several questions must be resolved before an attempt is made to incorporate the data into a model which describes the flow around the Gulf and across the shelf. The process experiments were designed to address two main questions: (1) What is the response of the current to forcing? and (2) How representative is a single current measurement? The forcing which drives the current is composed of direct, local wind forcing, density variations, and nonlocal fluctuations related to propagating perturbations (e.g., shelf waves) and offshelf effects. The current field on the shelf responds to these forcings in different ways which can be examined through the cross-shelf, alongshelf, and vertical coherences. It was clear from the outset that the saturation of measurements required in order to answer these questions could not be made throughout the Gulf. Rather, sites were chosen where either the problems could be studied in a generic manner or where there was a specific concern about the impact at the selected site. The preliminary discussion of three process studies are presented in this section.

1. Barotropic Response Study (BARS)

The location of this experiment is shown in figure 1. It consists of seven moorings, SLS-A, B, C, D, E, F, and 62. All SLS moorings had pressure gages and, at various times, current meters on all except F. Station 62 had current meters. This full array was deployed in March 1976 and was recovered in March 1977. The data discussed here are from the spring-summer period March-August 1976.

Current fluctuations associated with the wind are an important component
of the circulation on the shelf. Passage of storms will influence the cur-
rent on time scales of order a few days to a week. We observe that at SLS-B
about 75% of the nontidal variance is contained in oscillations with periods
of less than 8 days. Thus the focus of our analysis has been on wind-induced
oceanic currents.

The response of the ocean to variable winds can be discussed in terms
of a simple model. If the water depth, H, is much greater than the Ekman
layer thickness, d, then we expect, qualitatively, that the circulation will
follow Ekman (1905) dynamics. For winds to the west (+y), Ekman predicts
onshore transport in the surface layer, a sea-level setup at the coast, and
an alongshore flow which is driven by the sea surface slope. The cross-shelf
sea surface slope, $\frac{dn}{dx}$, is related to the northward wind stress, τy, by

$$\frac{dn}{dx} \sim \frac{\tau y}{d} \qquad\qquad\qquad (1)$$

If we assume the wind stress is proportional to the wind velocity squared
and the Ekman depth, d, is proportional to the wind speed, then the sea sur-
face slope is linearly related to the wind speed.

A second case occurs if the Ekman depth is of order H. This shallow
water problem was discussed by Welander (1957). The dominant wind forcing
is now the onshore wind stress component. The sea level slope is

$$\frac{dn}{dx} \sim \frac{\tau x}{H} \ . \qquad\qquad\qquad (2)$$

Note that the water depth rather than the Ekman depth now enters into the
relation. The slope is proportional to the wind velocity squared. Even in
deep water, onshore winds will cause a direct wind setup, but since d<<H,
the Ekman setup dominates.

We now consider the data. Figure 21 shows the low-pass filtered (40-hr cutoff) wind calculated by Fleet Numerical Weather Center, alongshore velocity at SLS-B, and four pressure gradients calculated from the records at SLS-B, D, E, and F. The wind and the current have been rotated into approximate alongshelf, cross-shelf axes. From the figure, it is clear that the velocity correlates better with the pressure gradient calculated across the entire shelf ($\Delta P_T = P_F - P_D$) than with the shallow gradient ($\Delta P_1 = P_E - P_D$). The cross-correlation function between the pressure differences and the alongshore currents were calculated, and the maximum correlation coefficients are shown in table 2. The lag associated with these is near zero. If only the records from March and April are considered, then the correlation coefficients all increase (e.g., $\Delta P_T - V$ correlation is 0.70). This is consistent with the results of Hayes and Schumacher (1976).

Table 2 also gives the correlation of the pressure gradients with the wind components. These results are quite interesting. In the deep water ($\Delta P_2 = P_F - P_E$) the pressure gradient is uncorrelated with the onshore wind, but highly correlated with the alongshore wind. This maximum correlation occurs with a lag of about 6 hours. In the shallower water, neither wind component yields large correlation; however, the onshore wind correlation is significant at the 95% level (about .20). These results qualitatively agree with the simple model above. The poor correlation in the shallow water is expected, since the calculated winds used cannot reflect the true local winds which drive the direct near-shore flow.

To further investigate the relation between the winds and the pressure gradient, the average pressure gradient associated with winds in 2 m/s bins was calculated. This is displayed in figure 22 for ΔP_1 and ΔP_2. The averaging removes some of the noise. The difference between the deep water and the
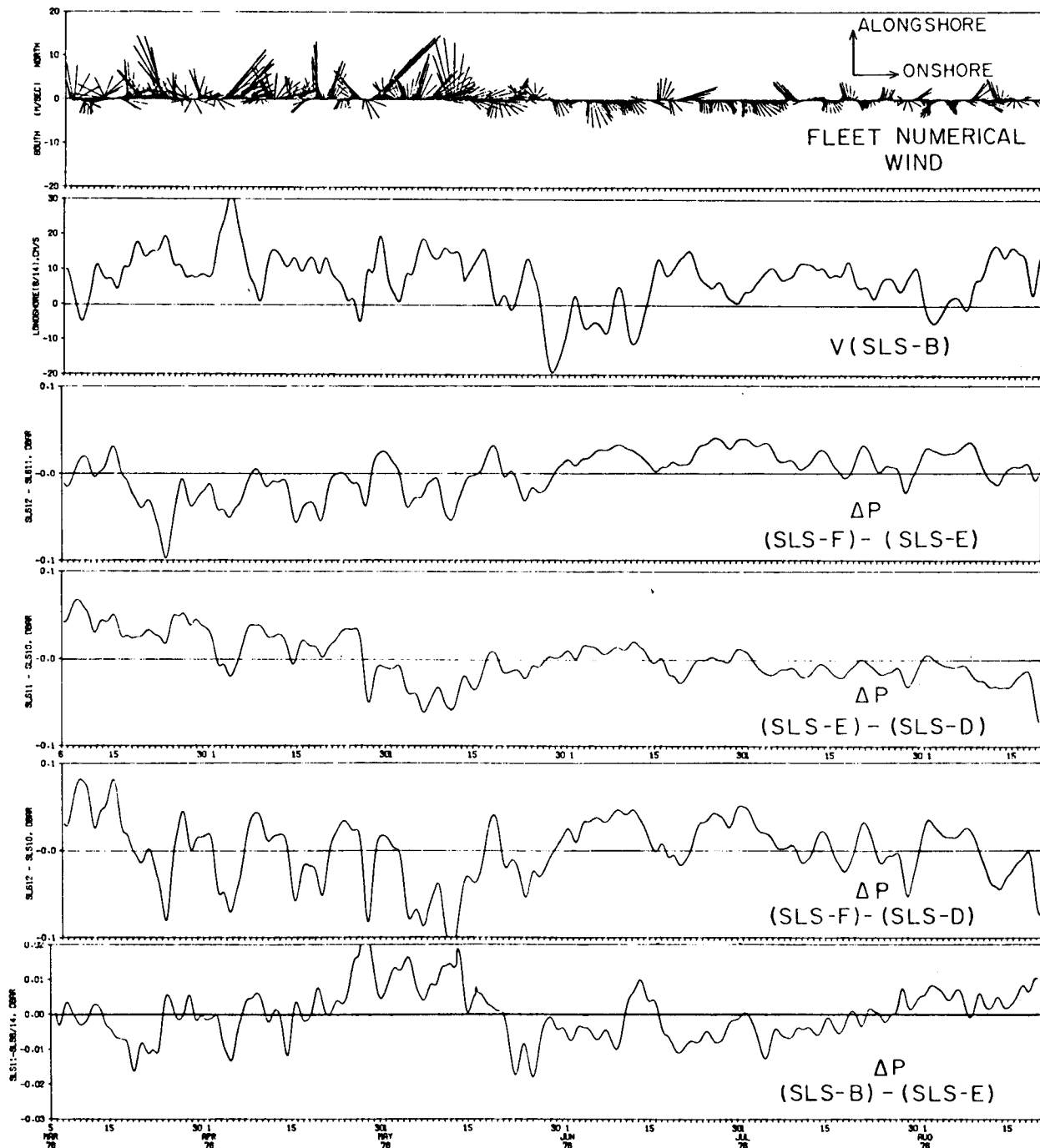
Figure 21. Low-pass filtered (40-hr cutoff) time series from the Icy Bay array from 5 March - 21 August 1976.

Table 2. Correlations between pressure gradients, currents (at SLS-B), and wind. Stations C, D, and E were in 50-, 100-, and 250-m depths, respectively. u and v are the cross-shelf and alongshelf components, respectively.

ΔP	Parameter	Correlation Coefficient
C-D	wind u	0.33
C-D	wind v	0.15
D-E	wind u	0.05
D-E	wind v	0.63
C-D	current v	0.28
D-E	current v	0.50
C-E	current v	0.55
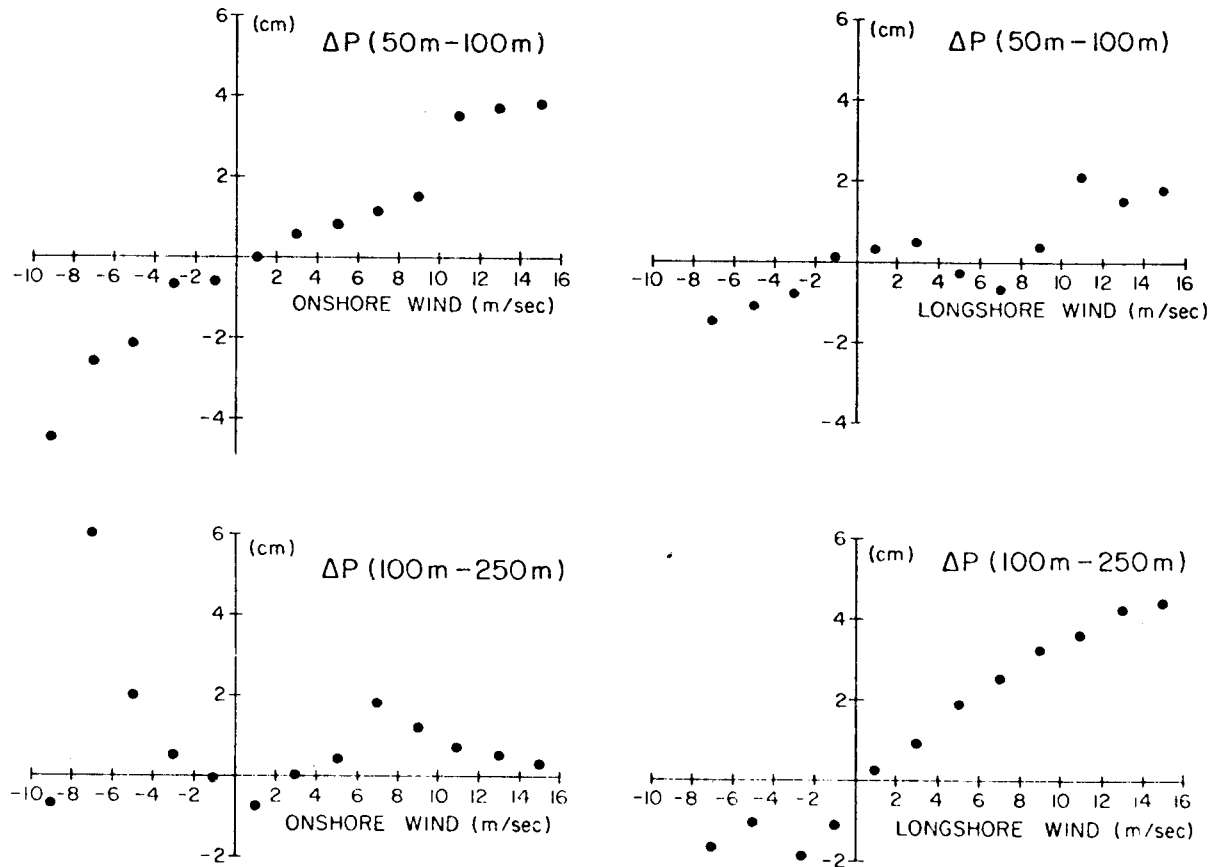
Figure 22. Cross-shelf pressure gradient between indicated depth contours versus onshore and alongshore wind.

shallow water response is clear. Although the onshore winds become dominant in the shallow water pressure gradient, it is not possible with these data to accurately define the functional relation between the pressure gradient and the wind.

The correlation between the winds and the alongshelf pressure gradient at the 100-m isobath was also calculated. This was small. It is expected that the alongshore slope may be more important in the initial setup of the flow. However, the high-frequency response has not yet been examined.

Turning now from the spring-summer pressure gradient studies, we consider some of the features of the combined current, pressure, and wind time series. Figure 23 shows the 9-month records from November 1975 through August 1976 of wind, current, and bottom pressure at SLS-B. The transition from winter to summer is seen in the wind field with the reduction in wind speed and a change in direction. The bottom pressure response is not as dramatic as was observed in spring 1975 (Hayes and Schumacher, 1976). Also, the current has a seasonal reduction, but the change is slow. The seasonality of the response of the ocean to the wind is seen in figure 24. The coherence between the wind and the bottom pressure shows a significant correlation for periods of 2-4 days in all cases. However, the lower frequency response is only observed in the spring and summer periods. This may be related to either a change in the forcing or a change in the response due to the increased stratification.

In addition to the current at SLS-B, long-term (20-month) current records are available at 62, and short-term (2-month) current records at SLS-C. In figure 25, scatterplots of the velocity components for three-time intervals at SLS-B and for SLS-C for the March-May period are shown. These present a contrast to those discussed in Section A for 62 (figs. 2 and 3). On the one
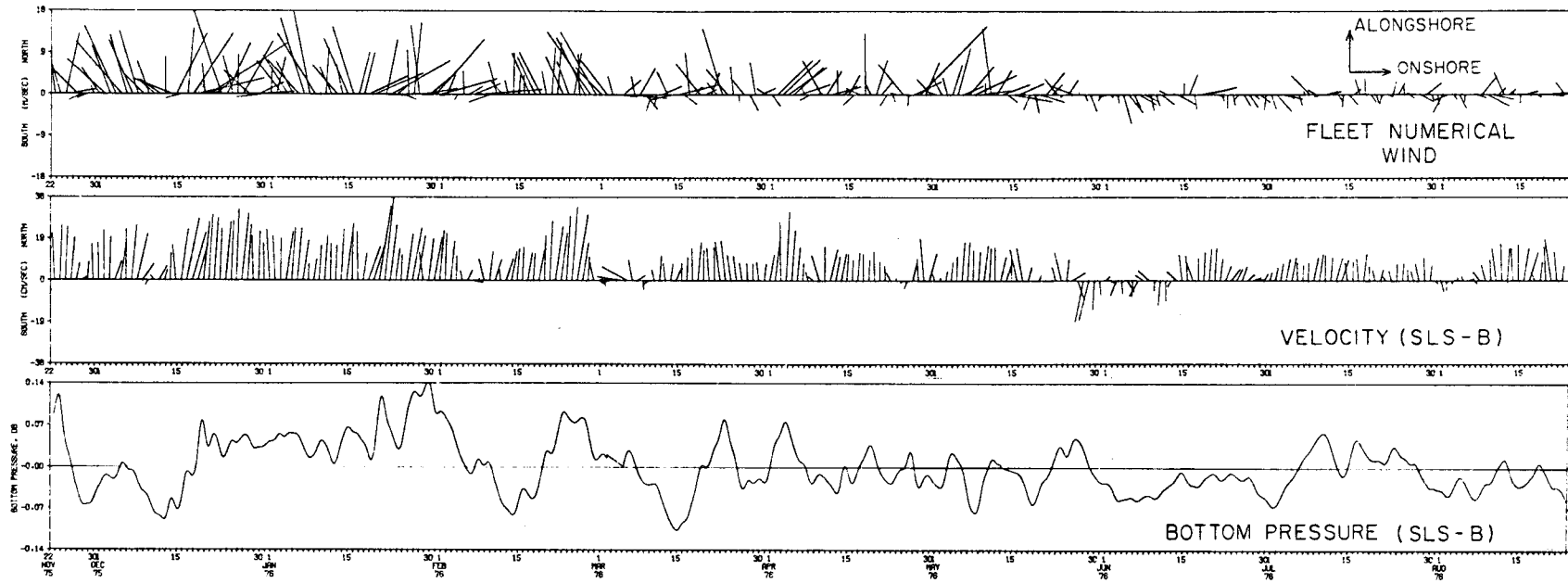
Figure 23.   Low-pass filtered time series at SLS-B from 22 November 1975 - 21 August 1976.
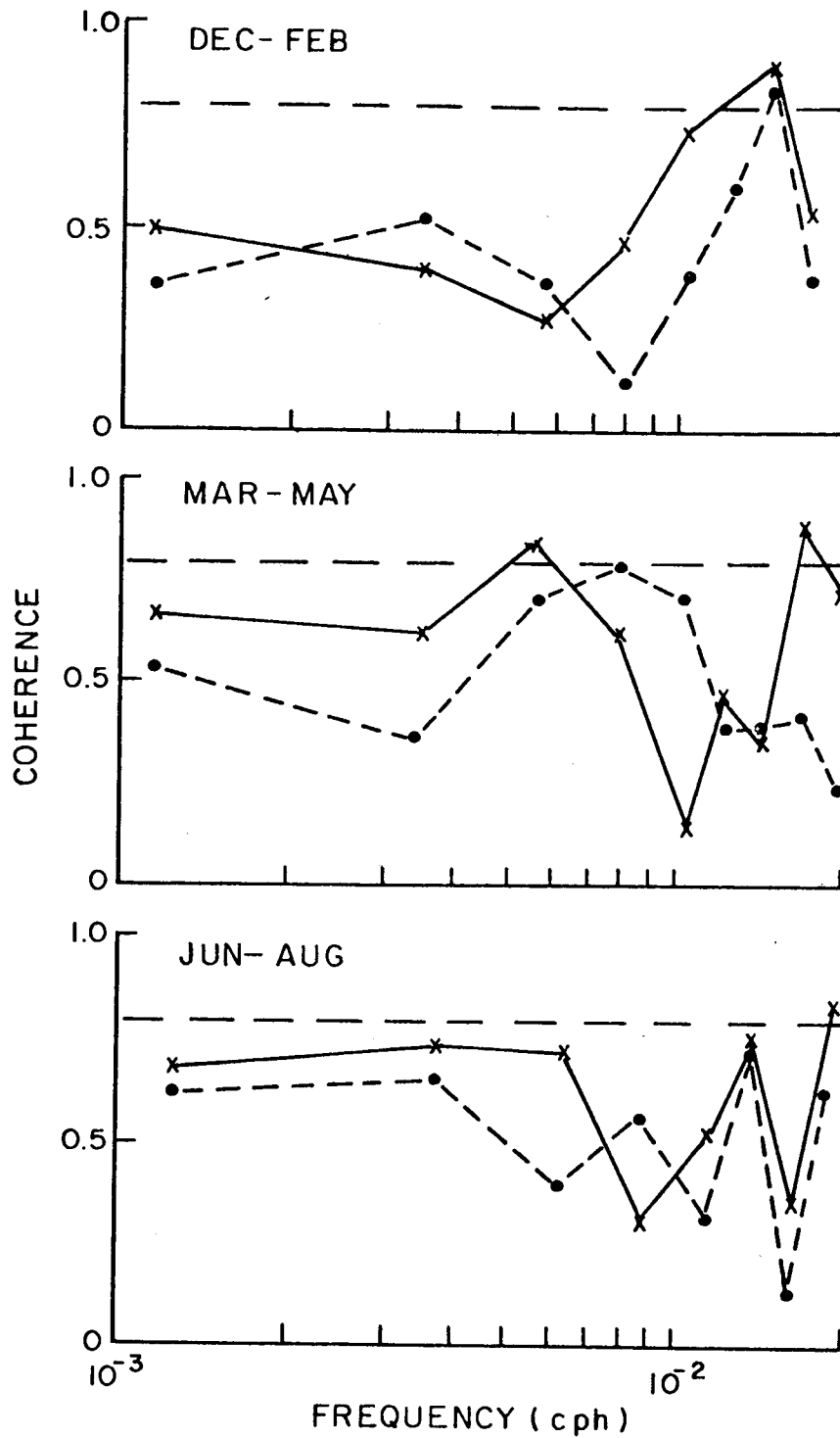
Figure 24. Coherence between alongshore (solid) and cross-shelf (dashed) wind and bottom pressure at SLS-B.

SLS - B (100 m contour)
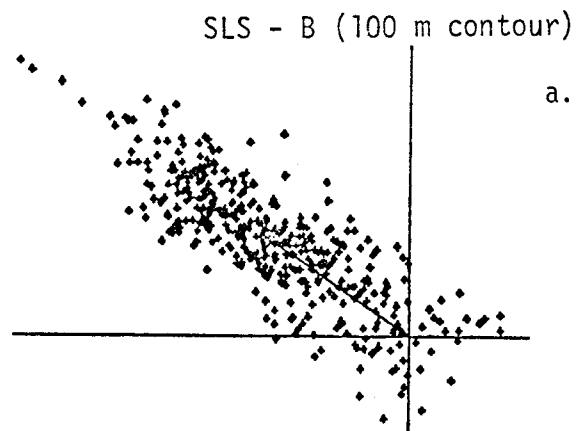
a. 20 November 1975–
    3 March 1976.

SLS - C (250 m contour)
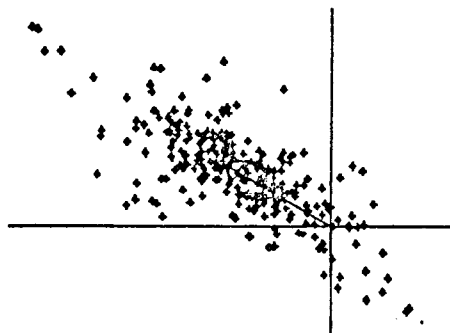
b. 3 March 1976–
    14 May 1976.
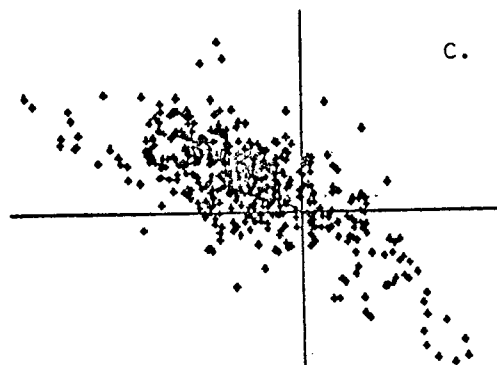
c. 14 May 1976–
    21 October 1976

7 March - 13 May 1976.

Speed   Scale

0   10   20   30   40   50

cm sec^{-1}
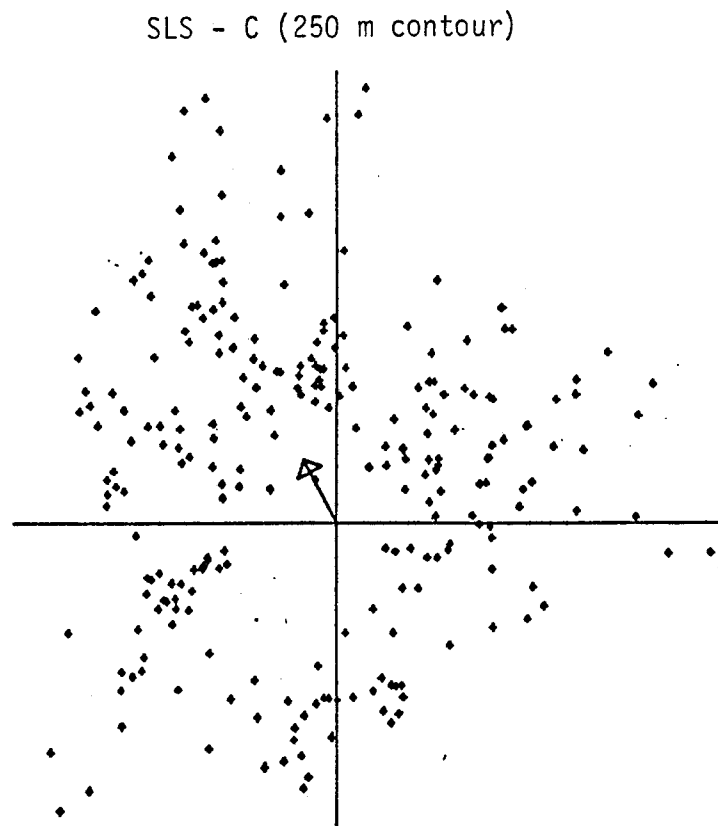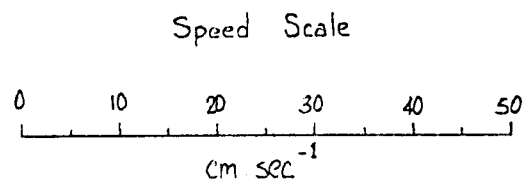
Figure 25.   Scatter diagrams for current records at SLS - B and SLS - C, 50 m depth.

hand, the currents at SLS-B are more colinear than those at 62. This is, presumably, caused by the bathymetric constraints as one proceeds farther onto the shelf. In agreement with this concept, the currents at SLS-C are quite variable. This produces a low mean velocity, although the speeds are relatively high.

The current records at 62 and SLS-B are compared for the winter and summer periods in figure 26. Flow is more unidirectional in winter than in summer. However, the wintertime alongshelf flow appears to have more high-frequency (periods, 2-4 days) energy than the summertime flow. The cross-shelf flow at SLS-B was always small. Station 62 shows a summertime increase in cross-shelf fluctuations. The relationship between the flow at 62 and at SLS-B is summarized by the cross-correlation function shown in figure 27. The longshore flow shows significant correlation in winter and essentially a decoupling of the flow in summer. Such correlations give an indication of the coherence of the flow across the shelf; however, rotation of velocity by the bottom contours are not fully accounted for.

Summary. The preliminary analysis of the data from the Icy Bay experiment indicates the following:

(1) Wind response in the deeper waters ($\geq$ 100 m) is consistent with Ekman dynamics (τ/d).

(2) Wind response in the shallower water (~50 m) shows increased importance of direct wind setup (τ/H).

(3) Coherence between wind and bottom pressure shows seasonal dependence with greater high-frequency (2-4 days) coherence in winter.

(4) Currents become increasingly colinear as one crosses onto the shelf. The mean velocity decreases seaward and shoreward of the shelf break. However, the offshelf speed is not much smaller. This is caused by the eddylike flow in the waters adjacent to the shelf break.
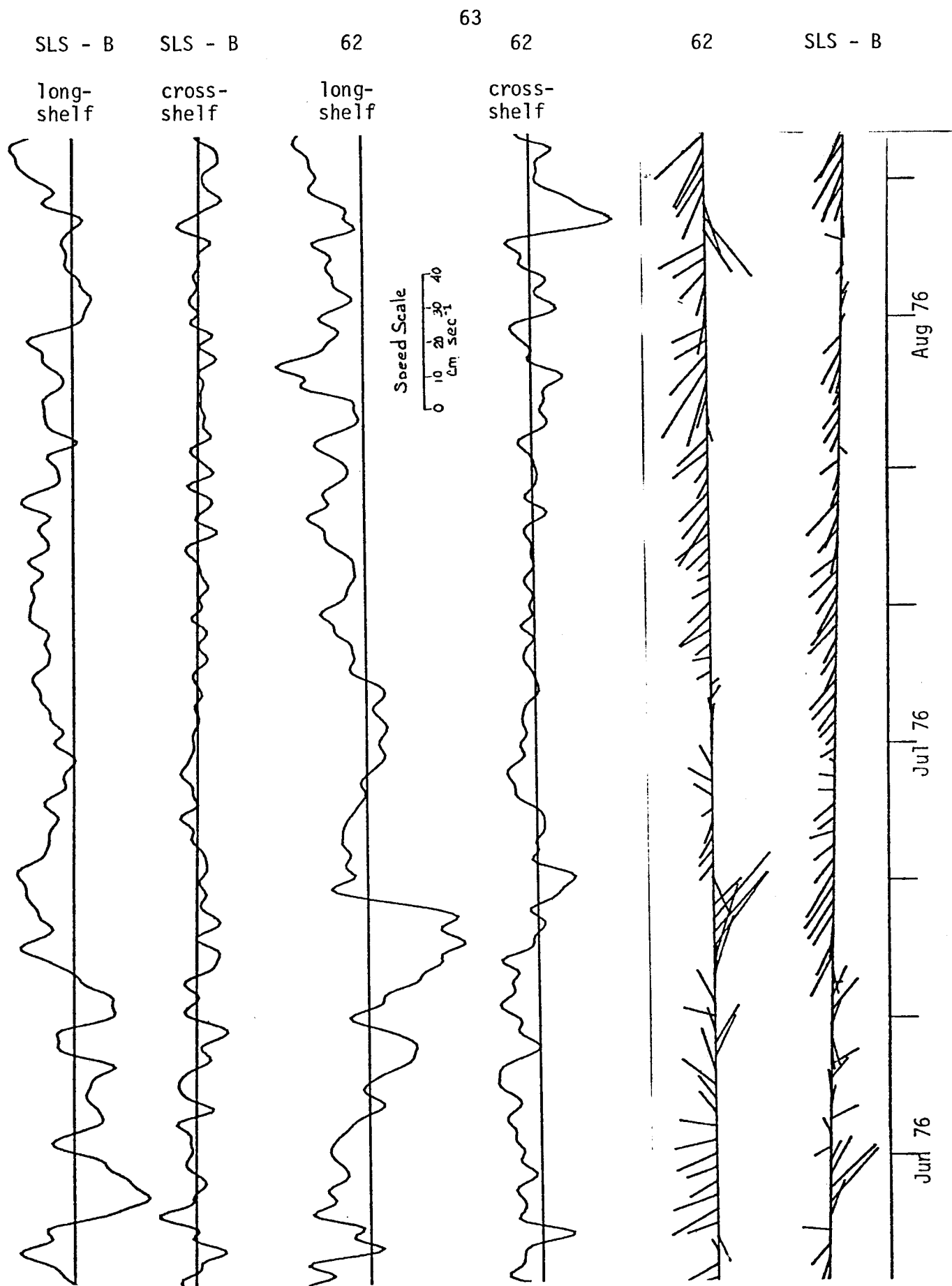
Figure 26 a.   Summer current records from 62 and SLS-B.   The longshelf
axis is 310°T.   Stick figures are daily low pass filtered
means on an East - West axis.
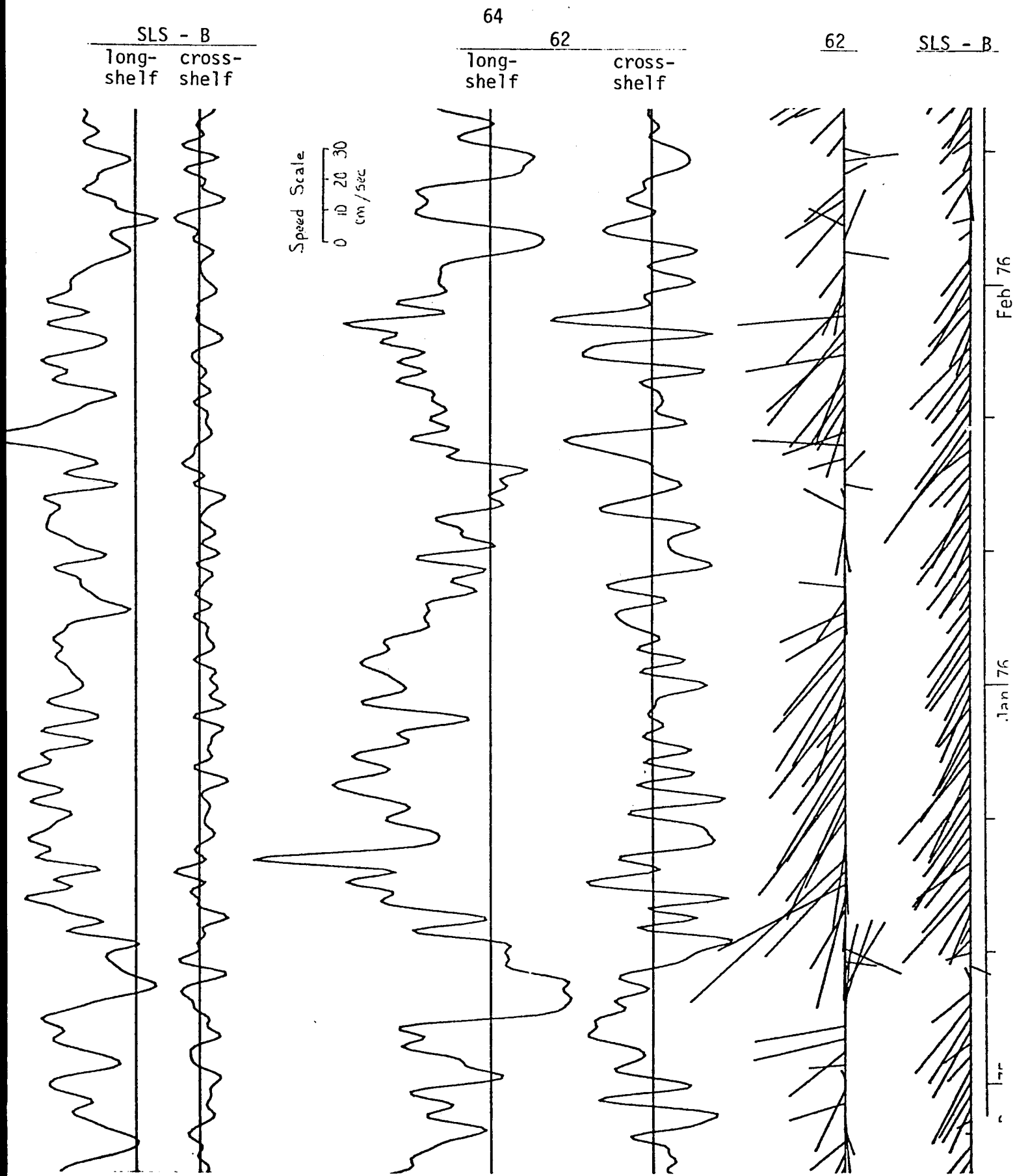
Figure 26 b.   Winter current records from 62 and SLS - B.
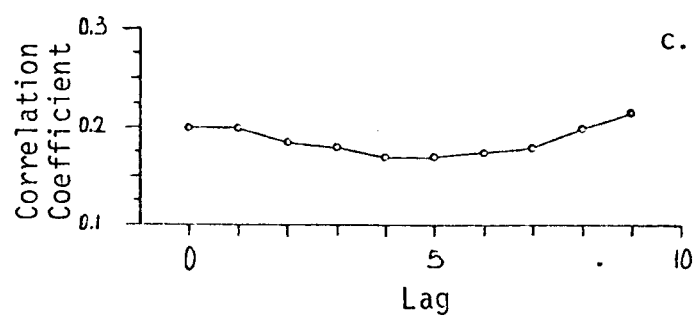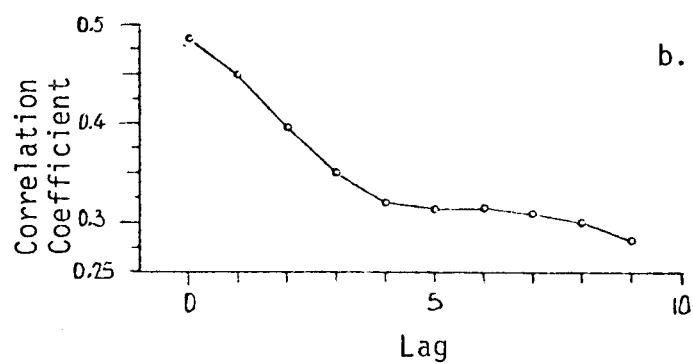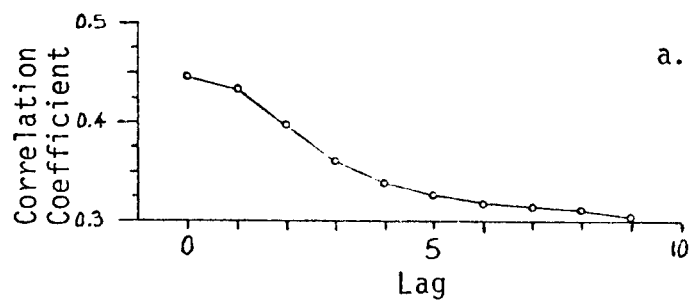
Figure 27.   Correlation coefficients at various lags (1 lag = 6 hours)
for longshore current components measured at station 62
and SLS-B.

As described in previous studies (Favorite, Dodimead, and Nasu, 1976; Ingraham, Bakun, and Favorite, 1976), the Alaskan current is variable and complex as it enters the Northeast Gulf of Alaska. Based on our observed velocities at 50 m, the wintertime transport on the shelf is about 0.5 SV, which is only about 10% of the total northward flow into the Gulf as estimated by Ingraham, Bakun, and Favorite (1976). The offshelf circulation has been described as variable. There was a definite tendency for these fluctuations to be linearized by shelf topography. The extent of the offshore influence on the shelf circulation has not been well established at this time.

The following sections describe experiments conducted during FY-77 but not defined in the work statement, i.e., these were reprogramed tasks to address specific petroleum development related questions. Section E, Copper River Study, discusses preliminary results from observations on the shelf west of Kayak Island. This experiment was generated in response to Dr. W. Hess' request for direct measurements in conjunction with numerical model studies by J. Galt. Section F, Lower Cook Inlet, addresses the question of circulation in Lower Cook Inlet as inferred from historical data sets (collected by NOS in 1973) in response to requirements established by OCSEAP.

2. Copper River Study

As noted in the FY-76 Annual Report and in Galt (1976), circulation on the shelf west of Kayak Island was complex. Nimbus buoy trajectories (Hansen, RU #217) tended to support the hypothesis that, during summer, gyral surface circulation existed as a quasi-permanent feature. The surface manifestation (as shown in satellite imagery) appeared as a clockwise gyre with the possibility of a more elongated counterclockwise flow shoreward. To investigate circulation as interpreted from direct measurements, three moored current

Meter arrays (stations 60, 61, and 69; see fig. R1) were deployed from March to October 1976. ·Forty CTD stations were also occupied to aid in interpretation.

Mean flow near the shelf break (figs. R2a and R2b) appeared to reflect the influence of longshelf flow due to the Alaska Current. As found in Icy Bay records, flow was stronger during late winter than in summer. At station 69, approximately 25 km shoreward of station 61 and on the same latitude as the western tip of Kayak Island, mean flow lacked seasonal speed trend and tended to flow consistently towards the northwest. Apparently some portion of the Alaskan Current flows onto the shelf across Tar Banks while the majority continues to flow westward along the shelf. Records from station 69 indicated very weak flow (<2 cm s^{-1}), which had a mean westward direction for the first 3 months and then a weaker eastward flow for the next 3 months.

These records support a picture of complex flow, particularly at station 60 as shown in a PVD (fig. 28; however, it appeared that either the moorings were located west of the feature or that the hypothesized gyral circulation was not incoherent on the spatial scale of moorings to permit observation. It was striking that the fluctuating portion of the total kinetic energy was 133 cm^2/s^2. This was only 9% of that observed on Albatross Bank, and 30% of that observed in Bristol Bay (station BC-2C) where mean flow was also weak. In this region both advective and dispersive effects were small.

3. Cook Inlet Historical Data Review

At the outset of the past year's activities in the Gulf of Alaska, no research was planned for Cook Inlet. New information obtained during 1973 from the region has, however, indicated potential environmental concern; this has established the Lower Cook Inlet region as a priority study area. In
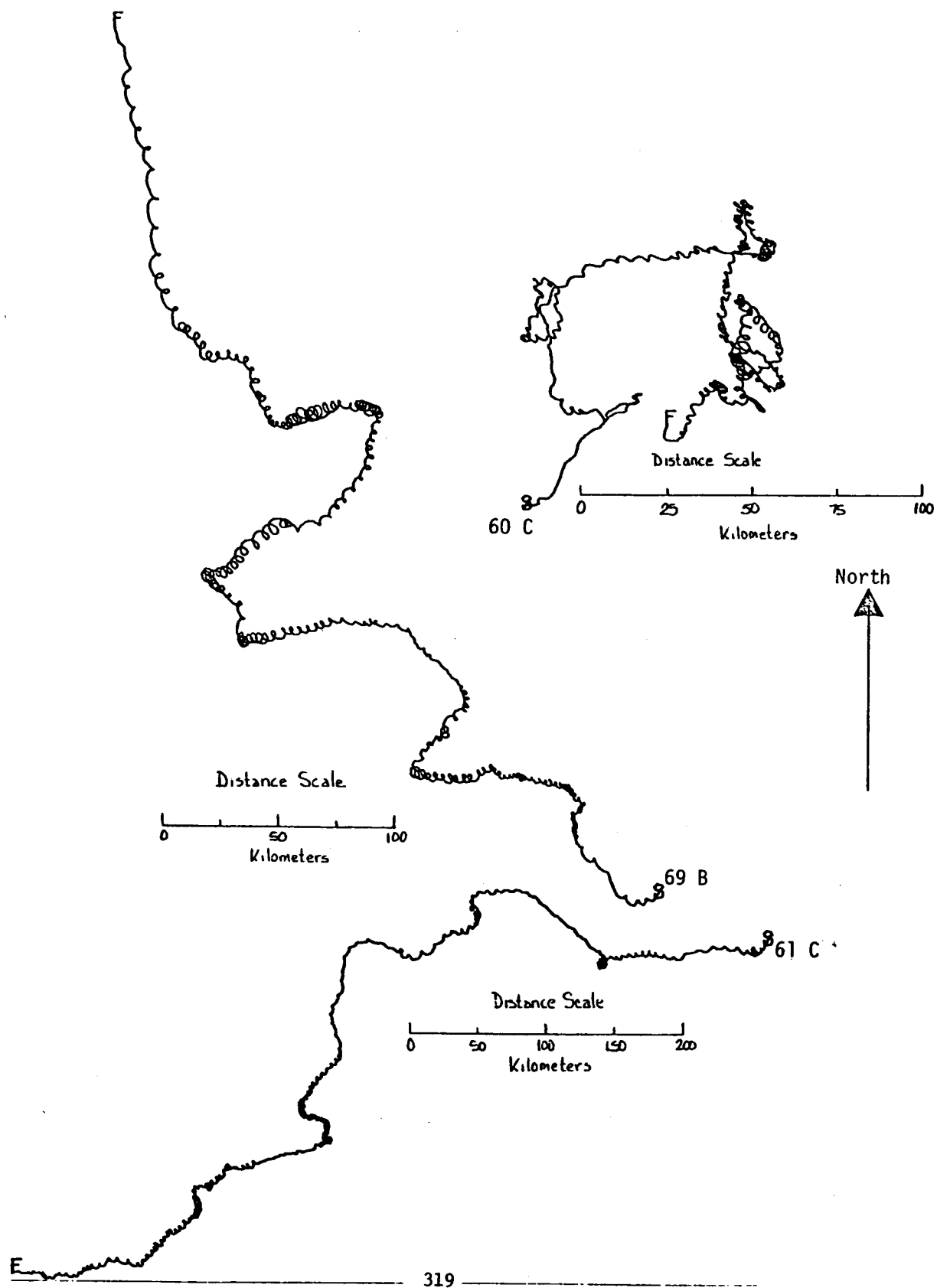
Figure 28.   PVD's from moorings 60 C, 69 B, and 61 C, 20 meter depth.

response to this need, a portion of the overall Gulf of Alaska research effort has been channeled into analysis of historical physical oceanographic data from Lower Cook Inlet. We define the area as that region lying south of the Forelands, extending southeast to the Barren Islands and to the southwest into Shelikov Strait (fig. 29).

Oceanographic temperature and salinity data have been obtained from Lower Cook Inlet during 1967, 1968, and 1973 (table 3). Information on circulation was obtained through use of moored current meters in 1973. The temperature and salinity data are presently being used to construct a picture of summer water characteristics, while the current records are being analyzed for mean and tidal flow structure. Preliminary data from these analyses were presented at a Cook Inlet synthesis meeting held in Anchorage during 15-18 November 1976. As a result of this meeting, a cooperative research effort in Lower Cook Inlet has been established with personnel from the Water Resources Division of the U.S. Geological Survey in Menlo Park, California.

Analyses carried out on available oceanographic and meteorological data have pointed out significant inadequacies in our environmental information base for Lower Cook Inlet, and have been instrumental in the initial steps toward correcting these inadequacies. These steps were: (1) participation in synthesis meetings to coordinate environmental information from Lower Cook Inlet; and (2) generation of a 1977-78 field program, when coupled with analysis and modeling, will enable us to address existing inadequacies.
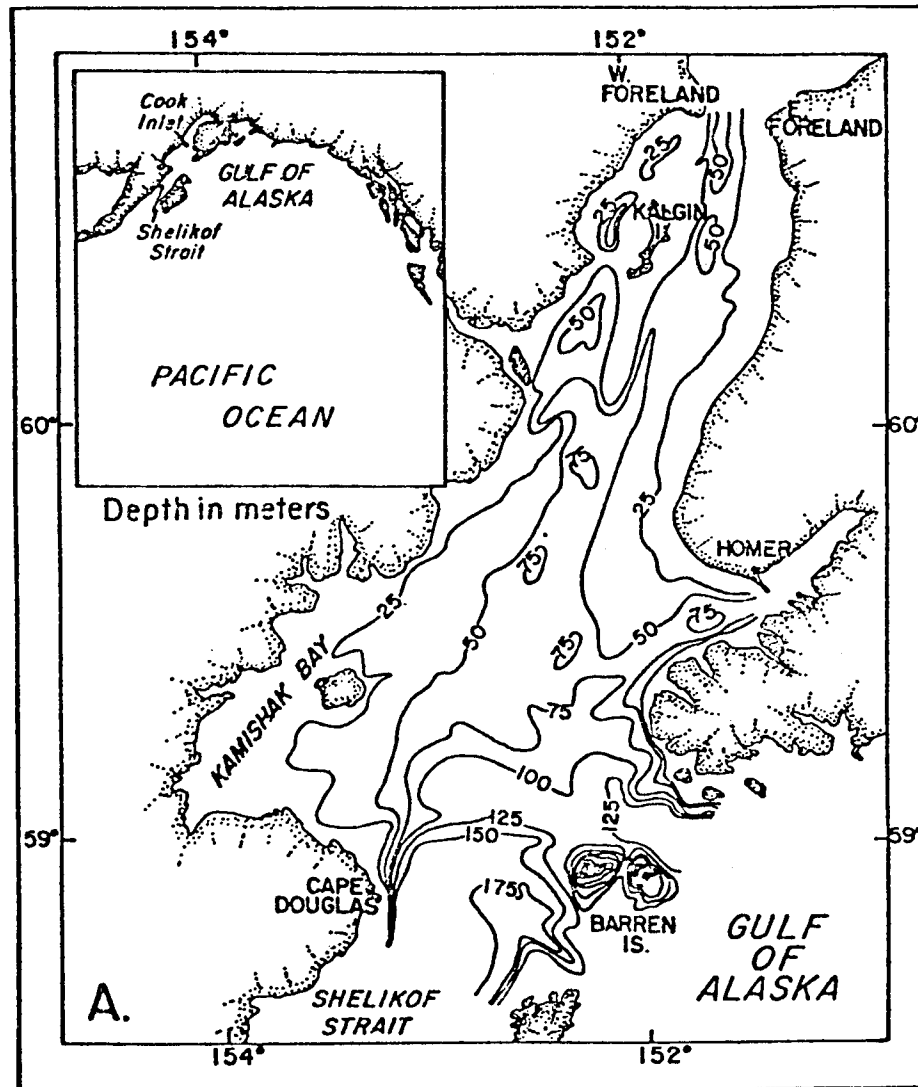
Figure 29. Lower Cook Inlet study area.

Table 3. Temperature, salinity, and current data available
from Lower Cook Inlet.

Date	Type of Data	No. of Stations	Source
June 1967	Temperature, salinity, oxygen, nutrients	24	NODC
May 1968	Temperature, salinity, oxygen, nutrients	40	NODC*
May 1973	Temperature, salinity	58	NOS
July 1973	Temperature, salinity	33	NOS
Aug-Sept 1973	Temperature, salinity	60	NOS
May-Sept 1973	Currents	26**	

 * Data have been plotted up in preliminary form by Kinney et al., 1970.
** Data were obtained at different times on the different stations during
   this interval.

VIII. CONCLUSIONS

The data analyzed to date have led to a preliminary description of the circulation on the continental shelf and its relation to offshelf flow, wind forcing, and seasonal baroclinic effects. From the regional array the statistics of the flow in the various base areas around the Gulf of Alaska can be contrasted. The process studies have produced more detailed understanding of the mechanisms influencing the circulation. The results can be summarized as follows:

1. The flow adjacent to the shelf is dominated by the Alaskan Current system. This current intensifies from the Northeast Gulf to the Kodiak region. It appears to be seasonally influenced by the large-scale meteorological forcing (Aleutian Low, winter; Pacific High, summer). Higher speeds and more uniform directions were characteristic of the winter regime.

2. In the Icy Bay region the Alaskan Current is complex; eddylike low-frequency fluctuations are common. The low-pass filtered (nontidal) speeds were high (about 30 cm s^{-1}); however, the mean velocity was small (7 cm s^{-1}) because of the direction variability. The largest mean velocity (15 cm s^{-1}) occurred at the shelf break. In the midshelf region (100-m depth), the flow velocity was again reduced (8 cm s^{-1}); however, the direction was fairly constant and aligned along the bathymetry.

3. At the shelf break (station 62) and at midshelf (SLS-B), a large fraction of the nontidal variance was contained in the frequency band from 0.133 to 1.0 cycles/day (50% and 75%, respectively). Thus, over half the low-frequency kinetic energy occurred between 1 and 7.5 days. Atmospheric forcing due to storm systems can be expected to contribute to the variance in this frequency band.

4. The response of the circulation to wind forcing in the Icy Bay region indicated that the dynamics change from the midshelf to the inner shelf region. In the deeper water the data are consistent with a sea level setup described by Ekman flow. In shallow water direct wind stress setup occurs. This latter process may contribute to a near-shore coastal jet.

5. On the shelf of the Copper River, it appeared that most of the Alaskan Current flowed along the shelf break; however, a small portion flowed north-westerly across Tar Banks towards the entrance to Prince William Sound. The complex flow behind Kayak Island was energetically weak at both tidal and low frequencies. This low velocity would increase the residence time of any drifting material.

6. Seaward of Kodiak Island, the Alaskan Current was a well-defined intense current. However, it apparently does not extend onto the shelf and has little influence on the current on the shelf where the flow was tidally dominated. Since there were no indications of large-scale upwelling, it appears that tidal mixing and low mean flow may be responsible for the high biological productivity in this region. The tidally dominated flow also implies a long residence time for pollutant material in this region.

7. In the western Gulf of Alaska, the shelf boundary velocities associated with the Alaskan Current were reduced from its high values near Kodiak. The flow southwest of Kodiak Island extending as far west as Unimak Pass was parallel to isobaths. It appears that the wintertime increase in velocity is common to this region also.

IX. NEEDS FOR FURTHER STUDY

The Gulf of Alaska physical oceanography program was initially planned to evolve from regional scale to process-oriented, site-specific studies. With completion of FY-77 operations and then extensive data analyses, a more complete description of regional scale circulation will be possible. The Icy Bay experiment, designed to examine processes on this shelf region, is at a similar stage of goal achievement. The physical oceanographic program must evolve to other key site-specific experiments

As identifiable both in present data gaps and at synthesis meetings held by the Project Office, there are four locations which require further field experiments: (1) Kodiak Island banks, (2) Lower Cook Inlet, (3) western Gulf of Alaska shelf, and (4) shelf region west of Kayak Island extending toward Kennedy/Stevenson Entrance. To address the goal of describing and understanding circulation on Kodiak Island banks and troughs will require at least 10 moored arrays, fine scale (5-km) CTD lines, and a meteorological buoy moored on the shelf. Bottom pressure gages moored across the shelf will not only enhance understanding of forcing mechanisms, but could also provide sea surface slope boundary conditions for modeling efforts. One result of the Lower Cook Inlet Synthesis Meeting was a well-defined experiment for this area. This would include seven moored current meter arrays, four separately moored bottom pressure gages, a meteorological buoy, surface drifters, fine-scale CTD lines, and surface velocity field measurements using Doppler Shift radar techniques. On the western Gulf shelf, an experiment similar to Icy Bay would best address physical oceanographic goals. This would require six arrays, three across shelf and four along the local bathymetry. Moorings would consist of two current meters each, and four bottom pressure gages would be included at selected sites. Again, a meteorological buoy is imperative.

Investigation of flow at Hurchinbrook Entrance and between Monteque Island and the mainland would help elucidate circulation in the final area identified above. It is recommended that this latter study be under Dr. Tom Royer's direction. Due to equipment and other funding limitations, it is recommended that the majority of arrays be moored for four winter (November-February) and summer (June-September) month periods, and at least one array be maintained continuously.

REFERENCES

Charnell, R. L., and G. A. Krancus (1976): A processing system for Aanderaa current meter data. NOAA Tech. Memo. ERL PMEL-6.

Ekman, V. W. (1905): On the influence of the earth's rotation on ocean currents. Arkiv for Matematik, Astronomi ock Fysik, 2:1-52.

Favorite, F., A. J. Dodimead, and K. Nasu (1976): Oceanography of the sub-arctic Pacific region, 1960-71. International North Pacific Fisheries Commission, Bull. 33, 187 pp.

Galt, J. A. (1976): Circulation studies on the Alaskan continental shelf off the Copper River Delta. U.S. Dept. of Commerce, NOAA, ERL, March.

Hayes, S. P., and J. D. Schumacher (1976): Description of wind, current, and bottom pressure variations on the continental shelf in the Northeast Gulf of Alaska from February to May 1975. Journal of Geophysical Research, 81:6411-6419.

Ingraham, W. J., A. Bakun, and F. Favorite (1976): Physical oceanography of the Gulf of Alaska. Final Report RU-357.

Kinney, P. J., J. Groves, and D. K. Button. Cook Inlet environmental data: R/V Acona cruise 065 - May 21-28, 1968. Rept. No. R-70-2, IMS, Univ. of Alaska, Fairbanks, 120 pp.

Kundu, P. K., and J. S. Allen (1976): Some three-dimensional characteristics of low-frequency current fluctuations near the Oregon coast. Journal of Physical Oceanography, 6:181-199.

Reynolds, R. M., S. A. Macklin, and B. Walter (1977): Arctic coastal air modification field studies in the Gulf of Alaska. Submitted to Journal of the Atmospheric Sciences.

Royer, T. C. (1975): Seasonal variations of waters in the northern Gulf of Alaska. Deep-Sea Research, 22:403-416.

Royer, T. C., and R. D. Muench (1977): On the ocean temperature distribution
in the Gulf of Alaska, 1974-1975. Journal of Physical Oceanography,
7:92-99.

Thomson, R. E. (1972): On the Alaskan Stream. Journal of Physical Oceanog-
raphy, 2:363-371.

Welander, P. (1957): Wind action on a shallow sea: Some generalizations on
Ekman's Theory. Tellus, 9:45-52.

ANNUAL   REPORT

RESEARCH UNIT: 140
REPORTING PERIOD: 4/1/76 - 3/31/77
PRINCIPAL INVESTIGATOR: JERRY GALT

Prepared by J. A. Galt, J. E. Overland, C. S. Smyth, Y. J. Han, C. H. Pease

SECTION I.   INTRODUCTION

The following report is a synopsis of modeling efforts in support of OCSEAP work around Alaska.   Included are program development for an advanced spill model for use anywhere along the Alaskan coast, diagnostic model studies of ocean surface currents around Kodiak, advection trajectory model studies in the Gulf of Alaska, a coastal marine meteorology model applied along the southeast Alaskan coast, a study of the circulation of the Bering Sea, and a report on the status of computer hardware and software in support of the modeling efforts.   The proponents of the various developmental pieces are as follows:

1. Advanced Model   - Galt, Karpen

2. Trajectory Model   - Galt, Pease

3. Diagnostic Model   - Galt, Watabayashi

4. Meteorological Model - Overland, Han, Galt

5. Bering Sea Model   - Han, Galt

6. Status of Computer   - Smyth, Galt

The basic framework of the advanced oil spill model has been completed. The program control modules are being tested interactively on the PDP11/34. Additional advanced model development is awaiting the implementation of an additional 32K words of memory and 2m byte disk capacity to the operating system.   Documentation in the form of a programmers and users manual is being written describing the special features of the overall model and the available algorithms.

The advanced model will incorporate each of the environmental models mentioned above and reference and mesh the output from each piece into a cohesive package. For example, the advanced spill model will take the results of the diagnostic model for a given region and the regional meteorological model over the same area and combine them through the techniques developed to predict advection and dispersion in the simple trajectory model.

The creation of the data base for these studies has been largely dependent on the help of other OCS investigators. Dr. Andy Bakun supplied wind data from FNWC for the simple trajectory model project. Dr. Tom Royer of the University of Alaska gave physical oceanographic data around Kodiak for use in the trajectory model. Mr. Bob Charnell supplied current meter data for the Gulf of Alaska. Dr. Stan Hayes offered sea surface elevation specifications for the diagnostic model. Dr. Jim Schumacher discussed current meter data in the Gulf of Alaska. Mr. Mike Reynolds supplied topographic information and initial verification winds for the regional meteorological model tests in exchange for a working copy of the model. And Dr. Felix Favorite of NMFS collected physical oceanographic station data used in the diagnostic model sutdies.

The following report includes preliminary results from several of the developmental models. These results represent only initial explorations into the current and wind conditions along the Alaskan continental shelf and are not final model predictions.

SECTION II. DIAGNOSTIC MODEL STUDY AROUND KODIAK

The diagnostic model developed at PMEL has been used to study the Kodiak Island region as part of the OCSEAP research. In this study a number of improvements have been incorporated into the model which make the model run more efficiently, clear up certain ambiguities related to the specification of boundary conditions and improve the graphics presentation. These recent developments are being documented in two technical reports in preparation (Watabayashi, 1977 and Watabayashi and Galt, 1977).

The diagnostic model was run using two separate sets of density data. The first set of stations were collected in April and May, 1972 (Favorite, et al, 1975) and were used as a preliminary check of the regional response to be expected from the model. Although not collected specifically for input to a model, these stations gave good coverage of the region of interest, made it possible to obtain a preliminary look at the currents, and experiment with various specifications of the open ocean boundary conditions. One difficulty with this data set, however, was that the station locations did not specifically resolve some of the complex bathymetry associated with the banks off shore from Kodiak. The second set of density data used for the study was collected in April, 1976 on the OCSEAP sponsored Moana Wave Cruise with Dr. T. Royer, Chief Scientist. In this case the data was specifically stationed to resolve the bathymetry. This second set of data was used for most of the investigations reported below.

The use of the diagnostic model on the Kodiak region was differ-
ent from previous studies in three specific ways that relate to the
formulation of the boundary conditions and forcing functions. As
before, the offshore sea surface elevation in deep water was deter-
mined by assuming a level of no motion at 1000 to 1200 meters and
along solid boundaries or coastlines, the sea surface elevation was
assumed to be constant. Along open boundaries across the shelf a new
procedure was carried out in two steps. First, the cross shelf sea
surface slope was assumed to be proportional to the on shore component
of the Ekman transport and inversely proportional to the depth, i.e.,

$$\frac{\partial \xi}{\partial \eta} \alpha \frac{\tau_s}{H}$$

where η is taken as a direction normal to an isobath and s is a direction
parallel to the isobath. With these values as a starting point, a re-
duced form of the model (ignoring the effects of bottom friction) solves
the resulting first order equations to indicate which boundary values
are strongly coupled. During this second stage, the coupled boundary
values are adjusted in a dynamically consistent manner that guarantees
a continuity balance and eliminates the extraneous lateral boundary
layers that were possible in some of the previous cases and which re-
quired numerical experimentation to correct. The third modification to
the program was to vary the strength of the wind stress and subsequent
surface Ekman mode for consistency with the sea surface slope condition.

Wind and current meter data for the Kodiak area was very limited.
At the time of the model experiments, one current meter mooring WGC-2C

333

(Charnell) was used along with wind data from FNWC (Bakun). The

current meter mooring was positioned on the 200 meter contour just

on the inner edge of the Alaskan Stream and showed consistently strong

flow to the SW along the isobath. The model was able to reproduce

this flow fairly well, but since the currents in this region were

dominated by the deep water baroclinic Alaska Stream, they were not

significantly affected by variations in the boundary condition settings.

Thus, this current meter was not particularly useful for exploring

variations in the flow. The wind data corresponding to the April-May,

76 period obtained from the FNWC pressure analysis showed a somewhat

different set of characteristics than we obtained from the Summer/Winter

analysis of the NEGOA area (ref. last year's annual report). The mean

winds were small relative to the variations associated with the storm

events. The record was clearly dominated by the passage of cyclones

where the wind direction reversed. Because of the reversals, no attempt

was made to run the model with mean wind values. Instead, a series of

test winds were created that could be used for the initial model studies.

Four   cases were considered, each with a uniform wind stress

blowing along the SW-NE axis (parallel to the coastline). This con-

figuration corresponded to various degrees of Ekman transport normal to

the coast (upwelling/downwelling) and was associated with the coastal

barotropic set-up through the boundary conditions. The cases run were

4, 2, 1 and -1 dynes/cm^2 towards the SW. Assuming a quadratic stress

law and typical values for the drag coefficient, this allows a maximum

wind case of approximately 30 kts. (mean wind). The model output for

334

these cases presents surface currents (figures 1 - 4) bottom currents (figures 5 - 8), and sea surface elevation (2, 1, -1 dynes/cm^2 cases included (figures 9 - 11).

From the preliminary results a number of tentative conclusions can be reached. These lead to the following qualified description of the regional flow.

Along the edge of the continental shelf the flow is dominated by the Alaskan Stream. Here the flow is relatively narrow with a maximum magnitude of approximately two knots. This is clearly an extension of the Stream that exists along the entire northern part of the Gulf of Alaska. It has been previously described by Favorite, et al, (1975) based on the April-May 1972 data from the RV Kelez cruise. By way of review, the Stream appears to intensify toward the west or, more accurately, toward the southwest as it flows down the Aleutian Chain. One of the features of the stream suggested by the '72 data and predicted by the model using both '72 and '76 data is a broadening of the Alaskan Stream just SW of the Trinity Islands. This appears to be associated with the bathymetry just downstream from Albatross Bank where a shoal is separated from the main section of the Bank by a deeper channel. The effects of variations in the wind stress have a minimal effect on the flow within the Alaskan Stream. This is built into the model through the boundary conditions and reflects our fundamental belief that this current is baroclinically controlled by processes with time scales that are long compared to local variations in the wind forcing.

335

The continental shelf SE of Kodiak can be characterized by a
series of banks separated by channels that provide deeper access to
the waters crossing the shelf.   Starting with Portlock Bank, this bank
and channel pattern repeats itself with Marmot Bank and then Albatross
Bank, which is itself cut in two by a channel off shore from Sitkalidak
Island.   Beyond Albatross Bank the 100 fa. contour again cuts in towards
shore south of the Trinity Islands.   Based on these preliminary model
studies, it appears that these deeper channels crossing the shelf have
a significant roll in the regional circulation.   Under the influence of
winds towards the SW (figures 1 - 3), these deeper channels tend to have
onshore _{surface} flow.   The effect is particularly pronounced south of Portlock
Bank and off Sitkalidak Island.   In both these cases, the cross shelf
channels lead into deeper regions oriented parallel to the coastline
and the flow can continue as a coastal current.   The channel SW of Marmot
Bank does not appear to develop the onshore flow using the '76 data.
With the '72 data this region developed weak onshore flow.   But with
limited access to deeper regions inshore, simple continuity arguments
suggest this channel will not develop as vigorous an onshore flow and
consequently, not contribute in a major way to the exchange of nearshore
waters with the waters of the outer continental shelf.   Under the influ-
ence of weak winds towards the NE (figure 4), the surface flow associated with these
channels is not obvious, although the channel off shore from Sitkalidak
Island appears to have flow inshore on the SW side and off shore on the
NE side.   Having studied only one case, these results must be considered
as little more than indicative of possible flow patterns.   A more realis-

Figure 1. Diagnostic Model Results Spring 76
Surface Currents
Wind Stress ← 4 dynes/cm^2

50 CM/SEC
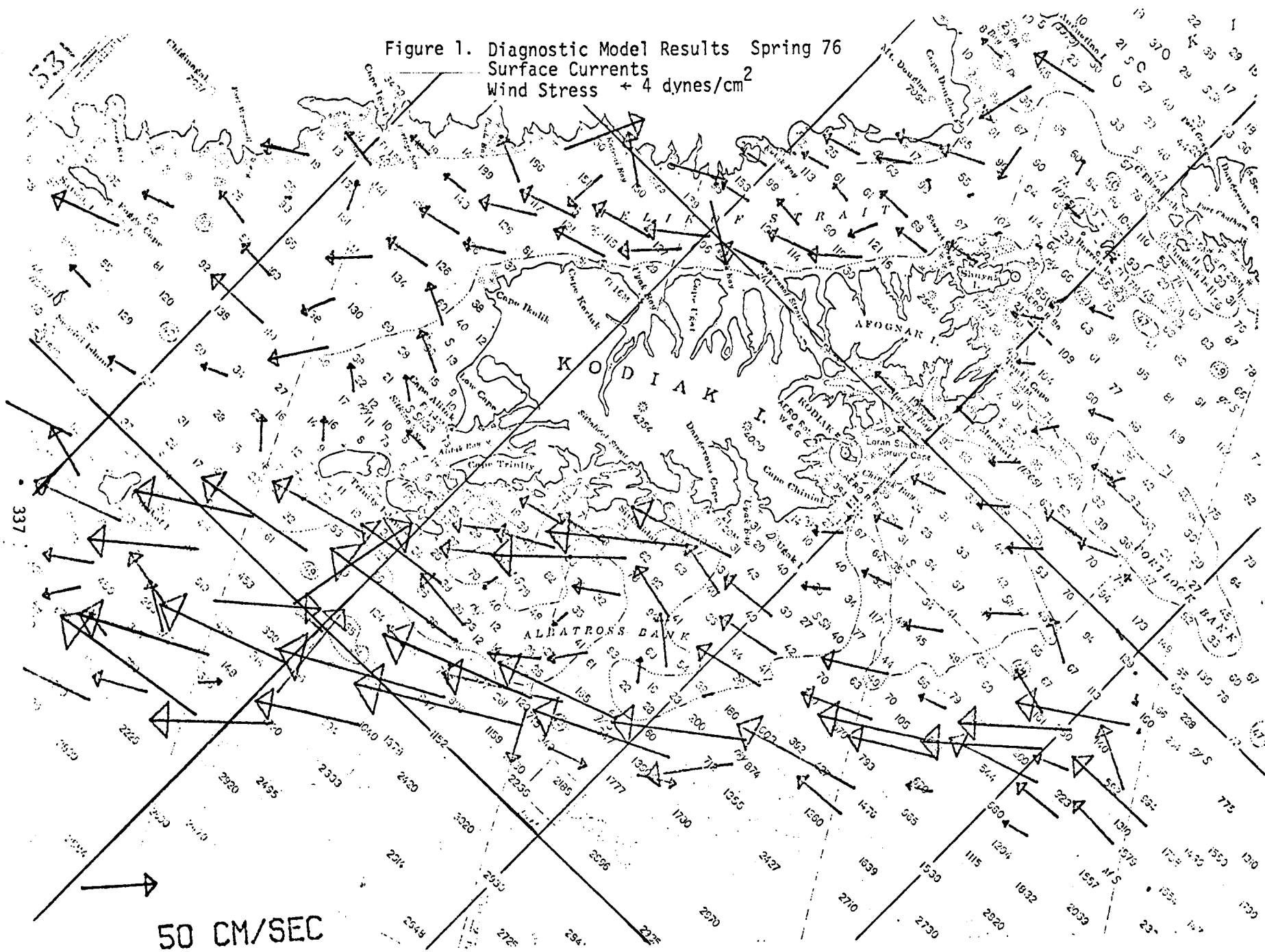
Figure 2. Diagnostic Model Results   Spring 76
Surface Currents
Wind Stress ←2 dynes/cm^2

50 CM/SEC
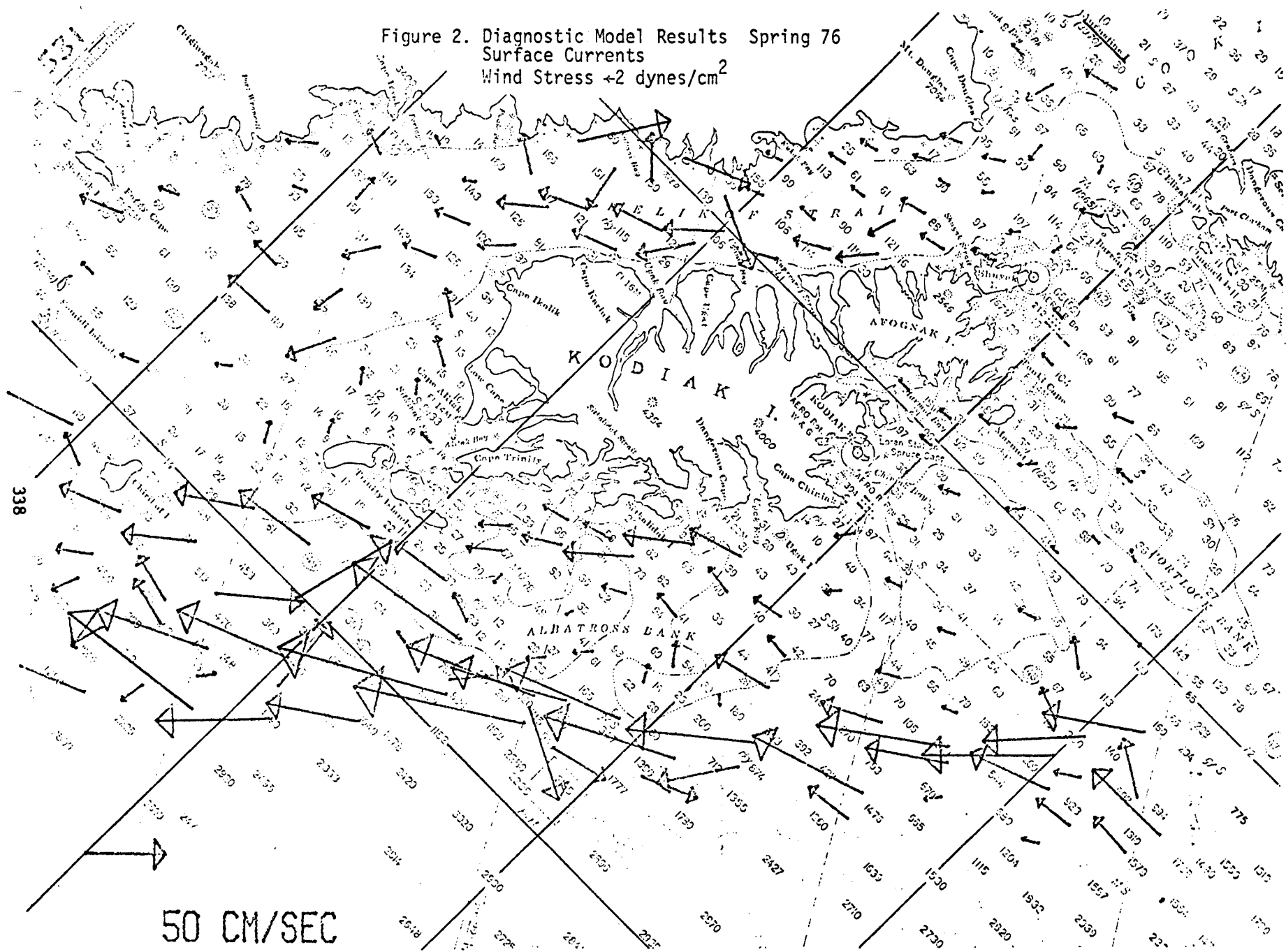
Figure 3. Diagnostic Model Results Spring 76
Surface Currents
Wind Stress ← 1 dyne/cm^2

50 CM/SEC
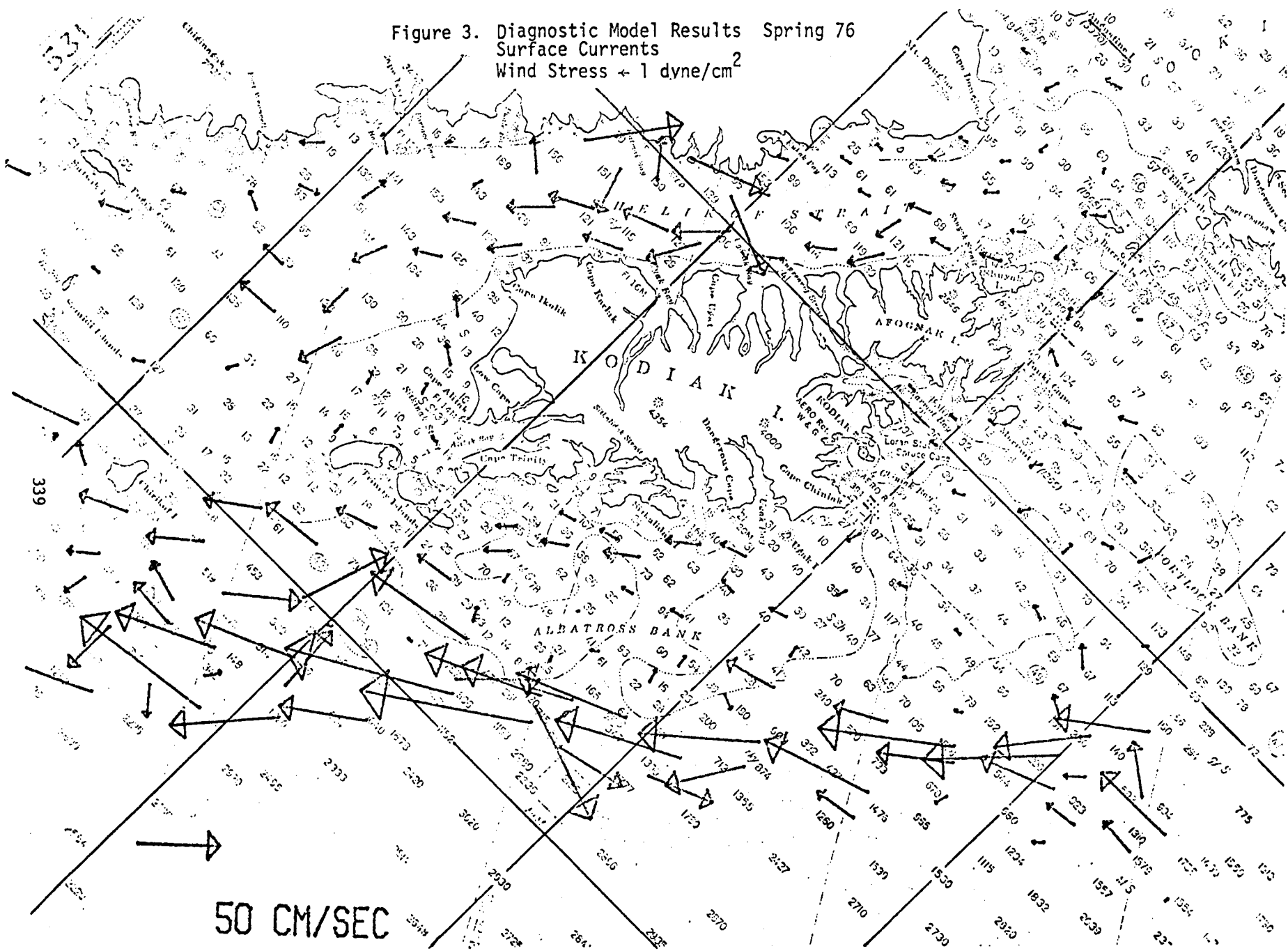
Figure 4. Diagnostic Model Results   Spring 76
         Surface Currents
         Wind Stress   1→ dyne/cm^2

50 CM/SEC
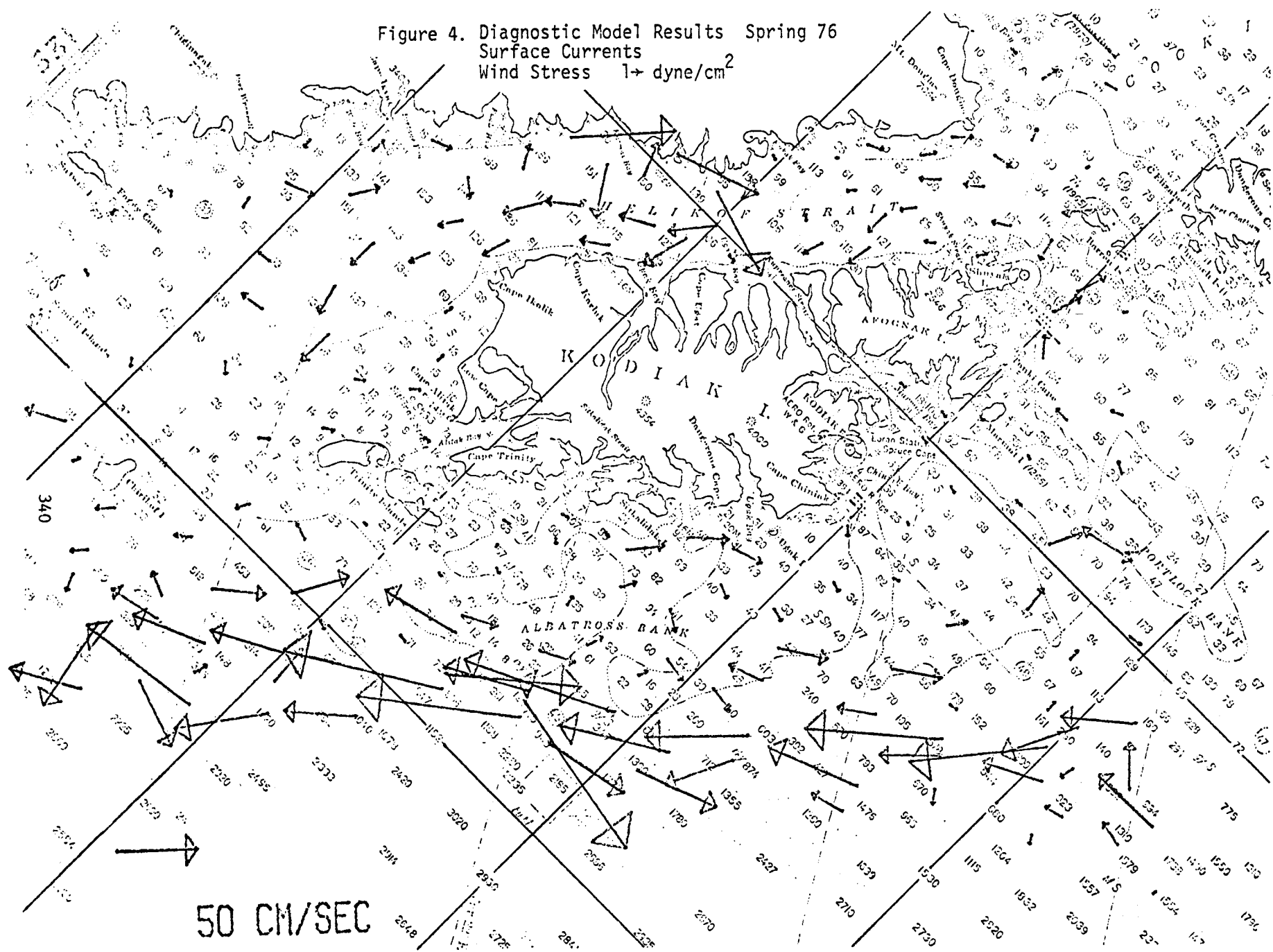
tic appraisal of the NE wind stress case will have to wait for better observational data and additional model tests.

One of the more interesting circulation features suggested by the present model studies is the coastal current. This is particularly well-developed along the south side of Kodiak between Dangerous Cape and Cape Trinity. For the case with strong wind to the SW, (figure 1), this flow obtains speeds of nearly two knots and is thus comparable in magnitude to the Alaskan Stream. As mentioned previously, this area has a relatively deep nearshore channel running inside the bank. In addition, this area has relatively free communication with the outer continental shelf via the channel through Albatross Bank. This current then appears to be caused by the barotropic set-up along the coast plus the extension of the onshore flow from this channel. With decreased winds toward the SW, the magnitude of this current drops off substantially, and the model shows speeds of a few tens of centimeters per second for a 1 dyne/cm^2 wind stress to the SW (figure 3). For the NE wind stress case, the direction of the coastal flow is seen to reverse with the region of strongest flow off Dangerous Cape, once again apparently associated with the channel across Albatross Bank. Without any observational data, it is difficult to evaluate how well the model is calibrated for this area. That we get current reversals for reasonable ranges of expected input parameters is interesting in itself and suggests that this area is worth more study, particularly since the actual direction of the flow may reverse and the region appears to have significant exchange of water across the shelf.

341

Figure 5. Diagnostic Model Results   Spring 76
            Bottom Currents
            Wind Stress   ÷ 4 dynes/cm^2

50 CM/SEC
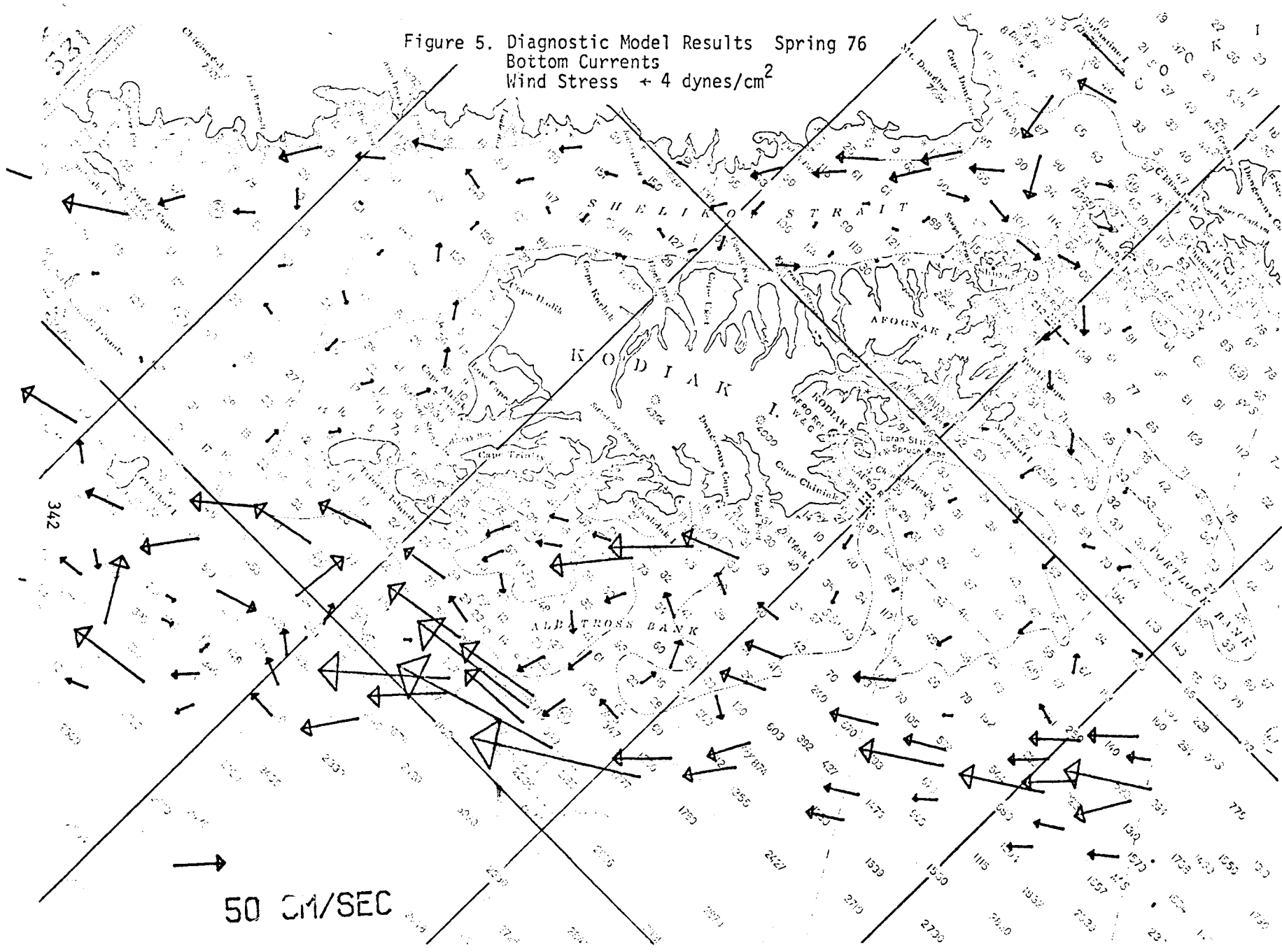
Figure 6. Diagnostic Model Results   Spring 76
Bottom Currents
Wind Stress ← 2 dynes/cm^2

50 CM/SEC
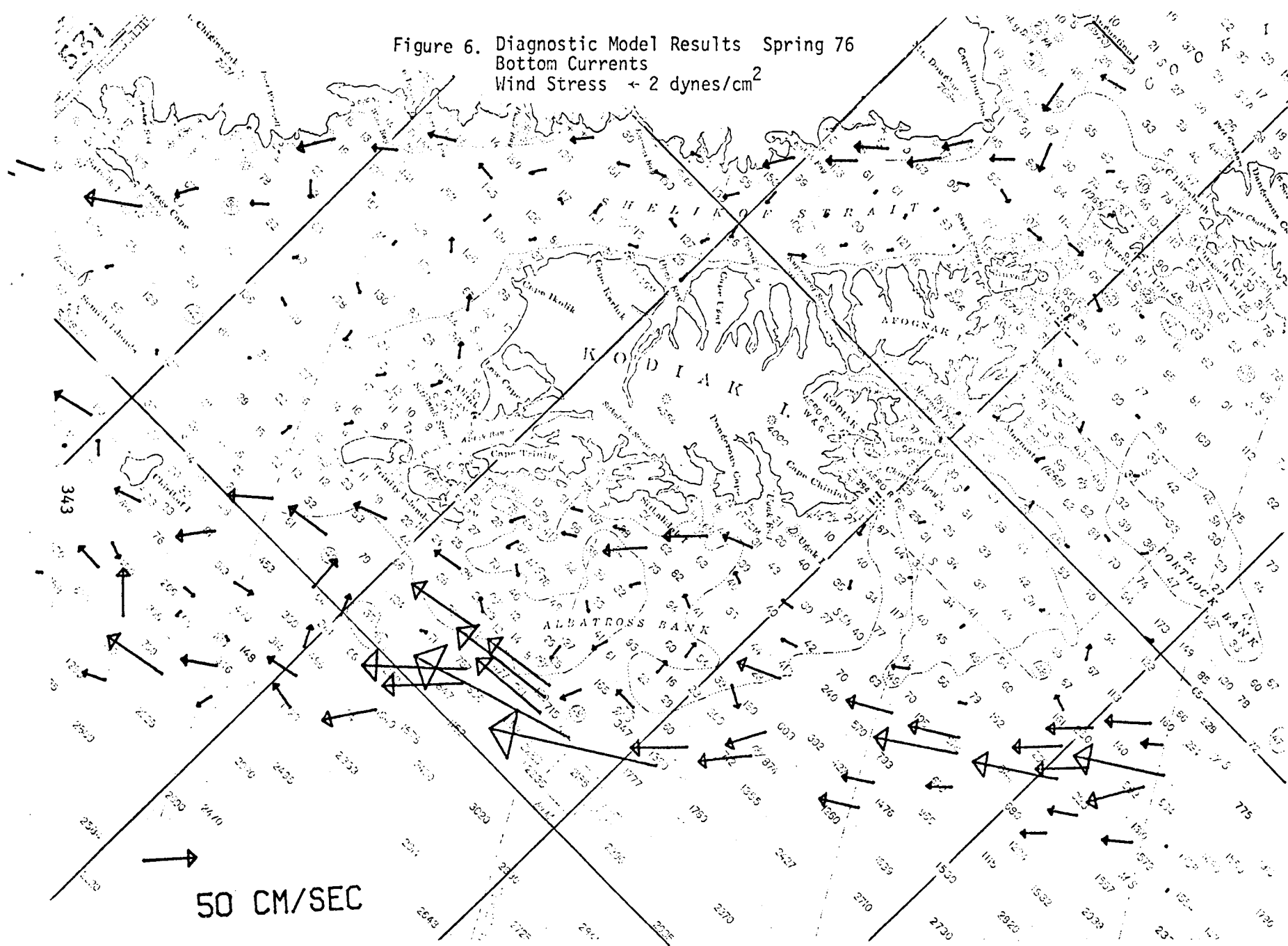
Figure 7. Diagnostic Model Results   Spring 76
Bottom Currents
Wind Stress   ← 1 dyne/cm^2

50 CM/SEC
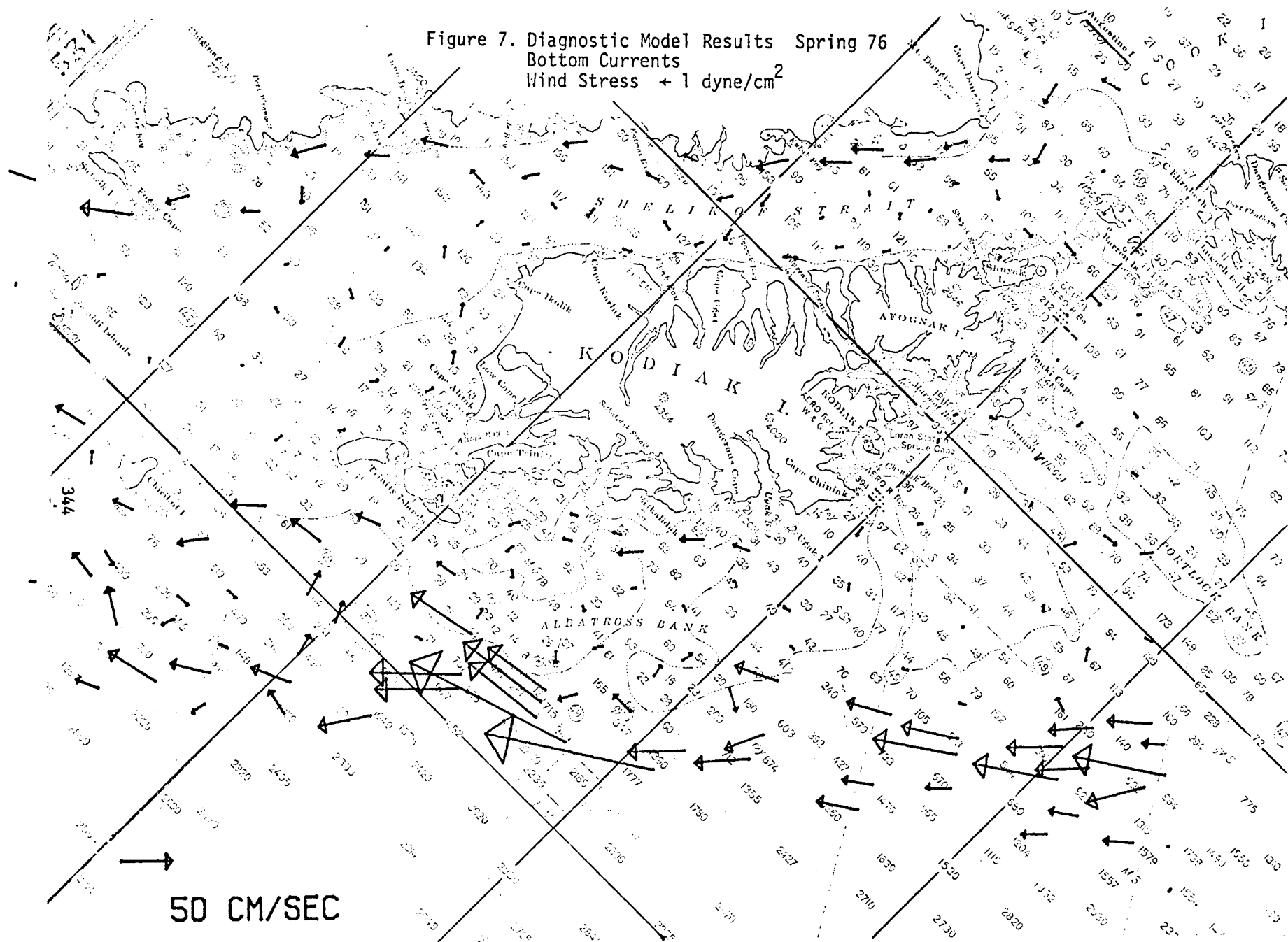
Figure 8. Diagnostic Model Results   Spring 76
          Bottom Currents
          Wind Stress $1 \rightarrow$ dyne/cm^2

50 CM/SEC
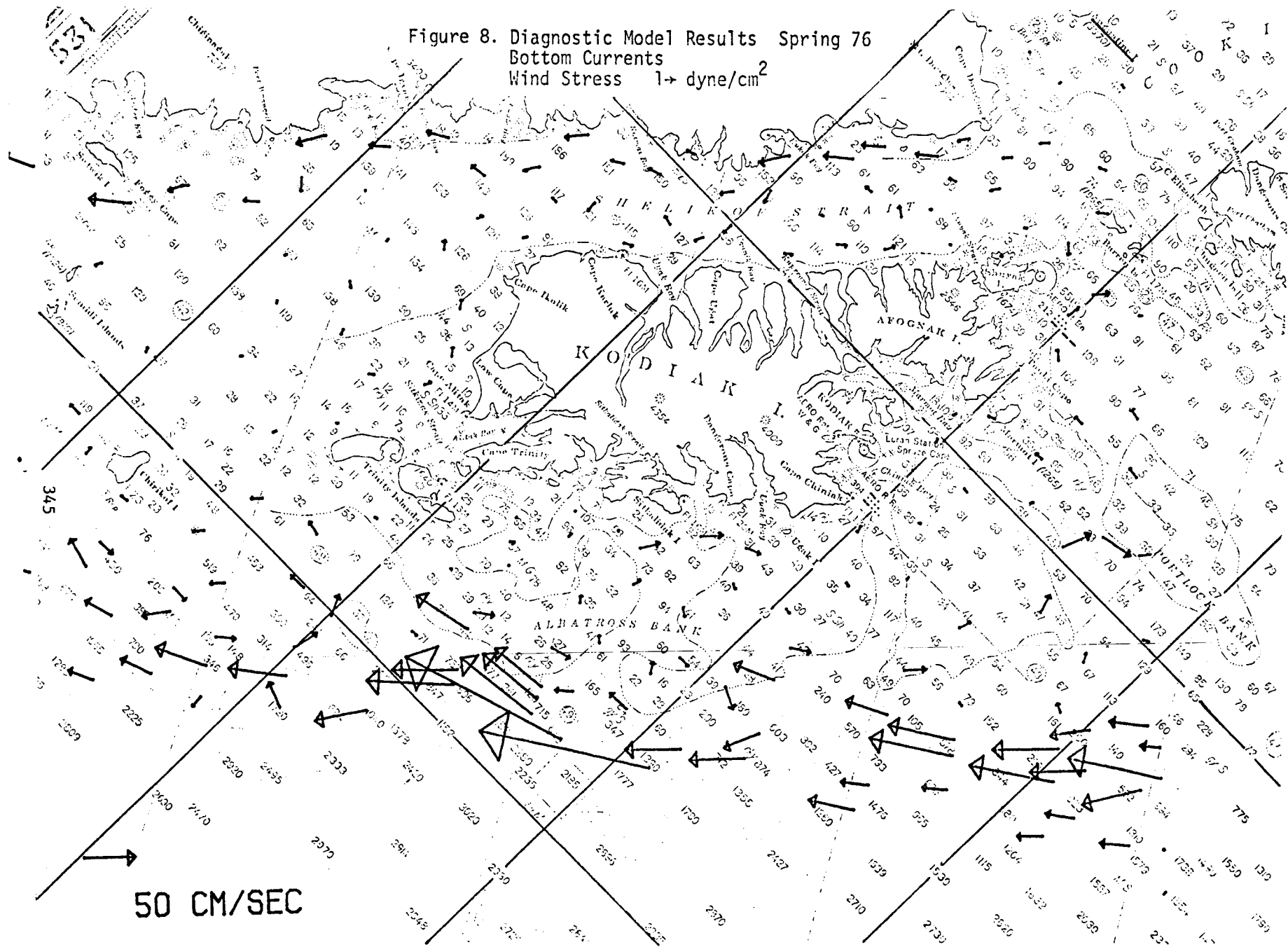
The model predicts bottom currents (geostrophic flow at the bottom) as well as surface currents. These are presented in figures 5 - 8 and can be described as generally similar to the surface flow patterns except that the bottom currents magnitudes tend to be smaller and their direction tends to be slightly different to compensate for the onshore or offshore transport of the surface Ekman flow. For example, comparing figures 1 and 5 for the area off Dangerous Cape indicates that the surface flow has a slight onshore component and consequently, the bottom flow shows a component offshore. Similarly, west of Kodiak off Low Cape, the surface currents show an offshore component and the deeper flow has an onshore component. In general, the bottom currents do not show a current reversal, but there are a few exceptional areas. A careful examination of figures 1 - 8 show that this may happen south of Portlock Bank and in some of the eastern regions of Shelikof Strait.

Figures 9 - 11 show the sea surface elevation predicted by the model. These correspond to streamlines for the flow just under the surface layer. There are two general features of these figures that are of interest. First, all the cases show a significant meander in the flow south of the Trinity Islands. This pattern is clearly related to the bathymetry and results in flow to the north (towards shore) in this region. The flow then appears to circulate in a counter clockwise loop continuing on to the southwest. Secondly, there is a major change in the surface contour closest to Kodiak Island between the SW stress and the NE stress cases (figures 10 - 11). This clearly indicates the poten-

346

Figure 9. Diagnostic Model Results Spring 76
Surface Elevation (Contour Interval
$\tau \leftarrow 2\ dyne/cm^2$ 6.4 cm.
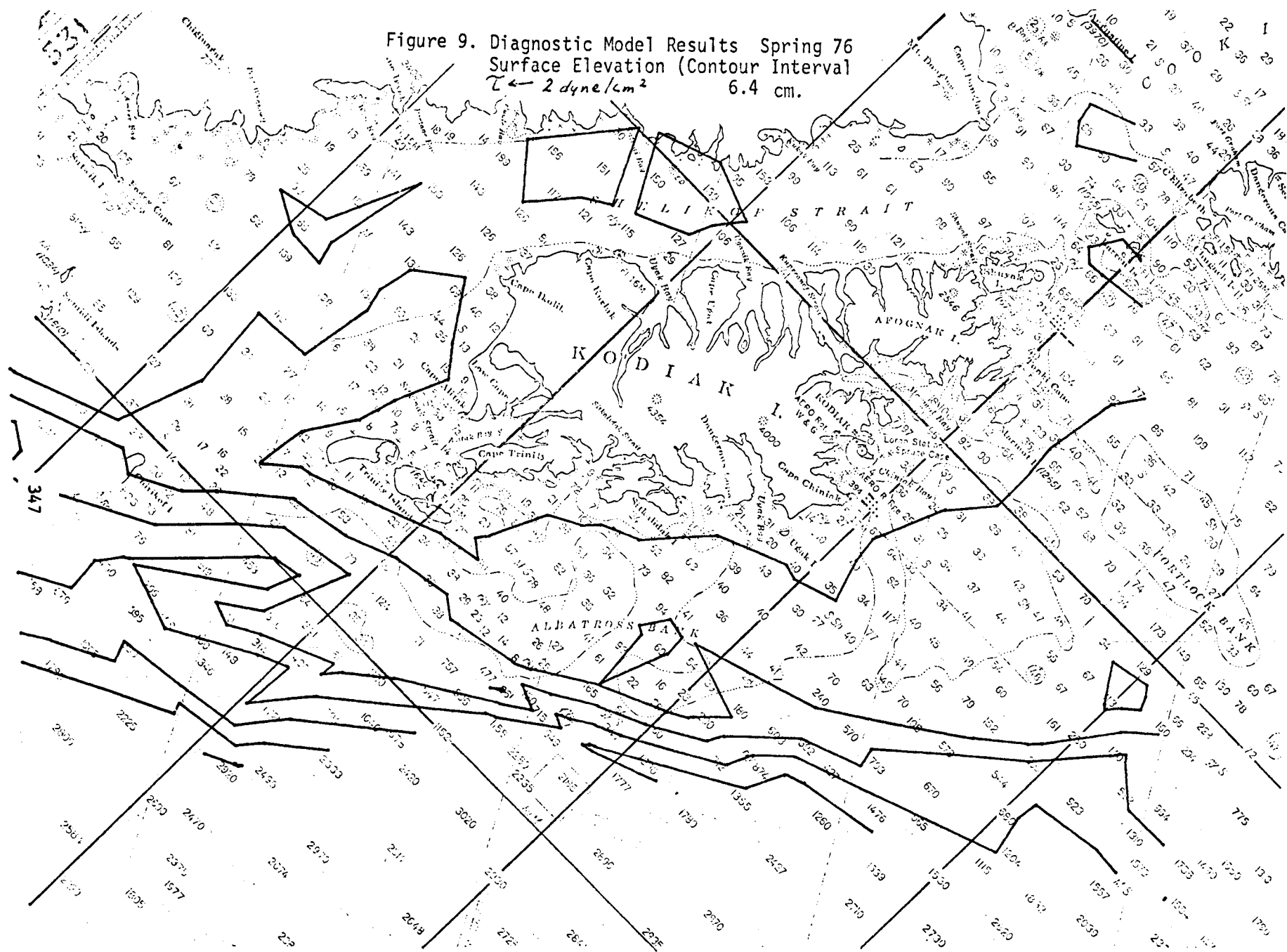
Figure 10. Diagnostic Model Results Spring 76
Surface Elevation (Contour Interval 6.6 cm.
$\tau \leftarrow 1\ dyne/cm^2$
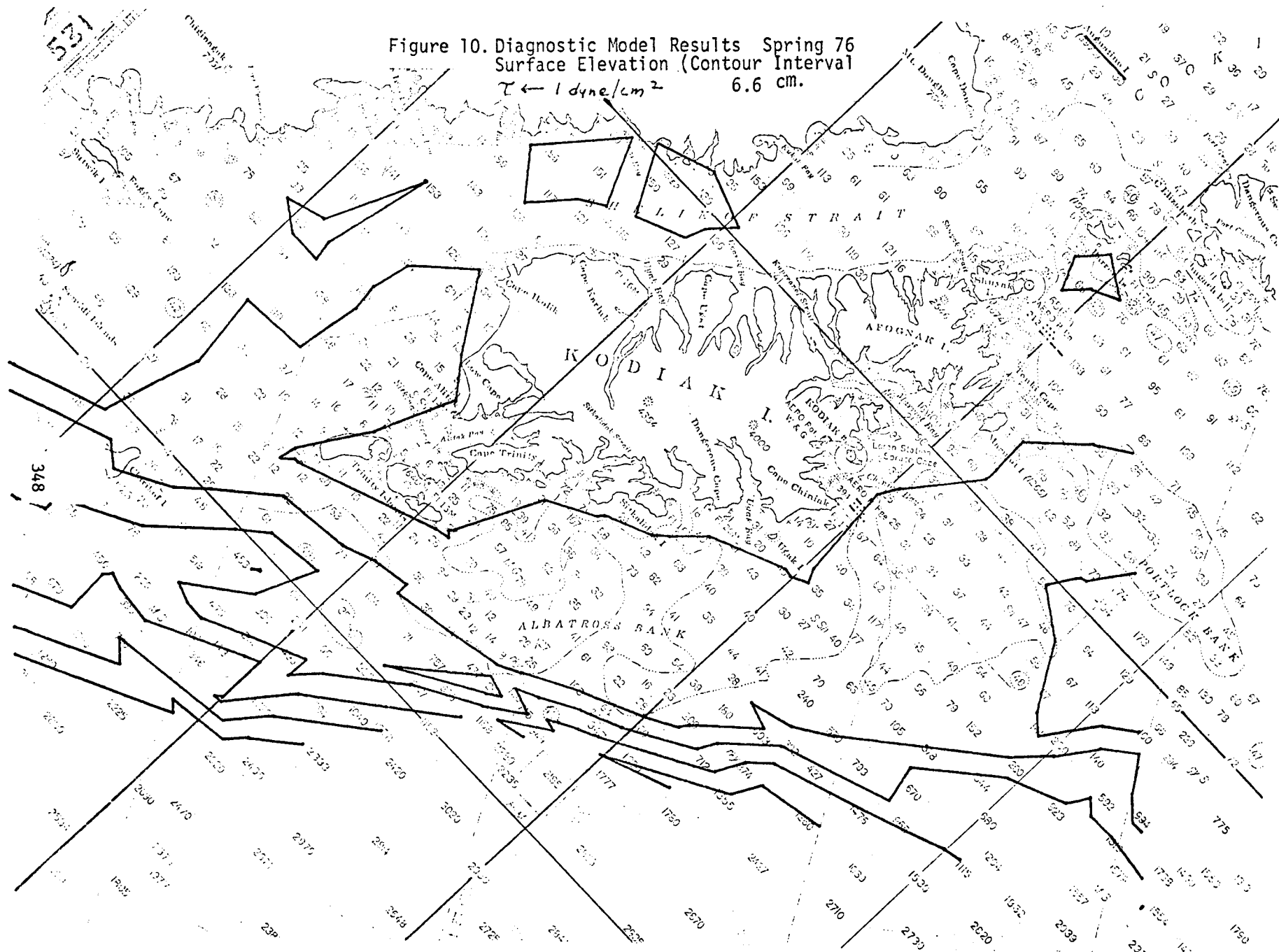
Figure 11. Diagnostic Model Results   Spring 76
Surface Elevation (Contour Interval 4.9 cm.
$\tau \rightarrow 1 \ dyne/cm^2$
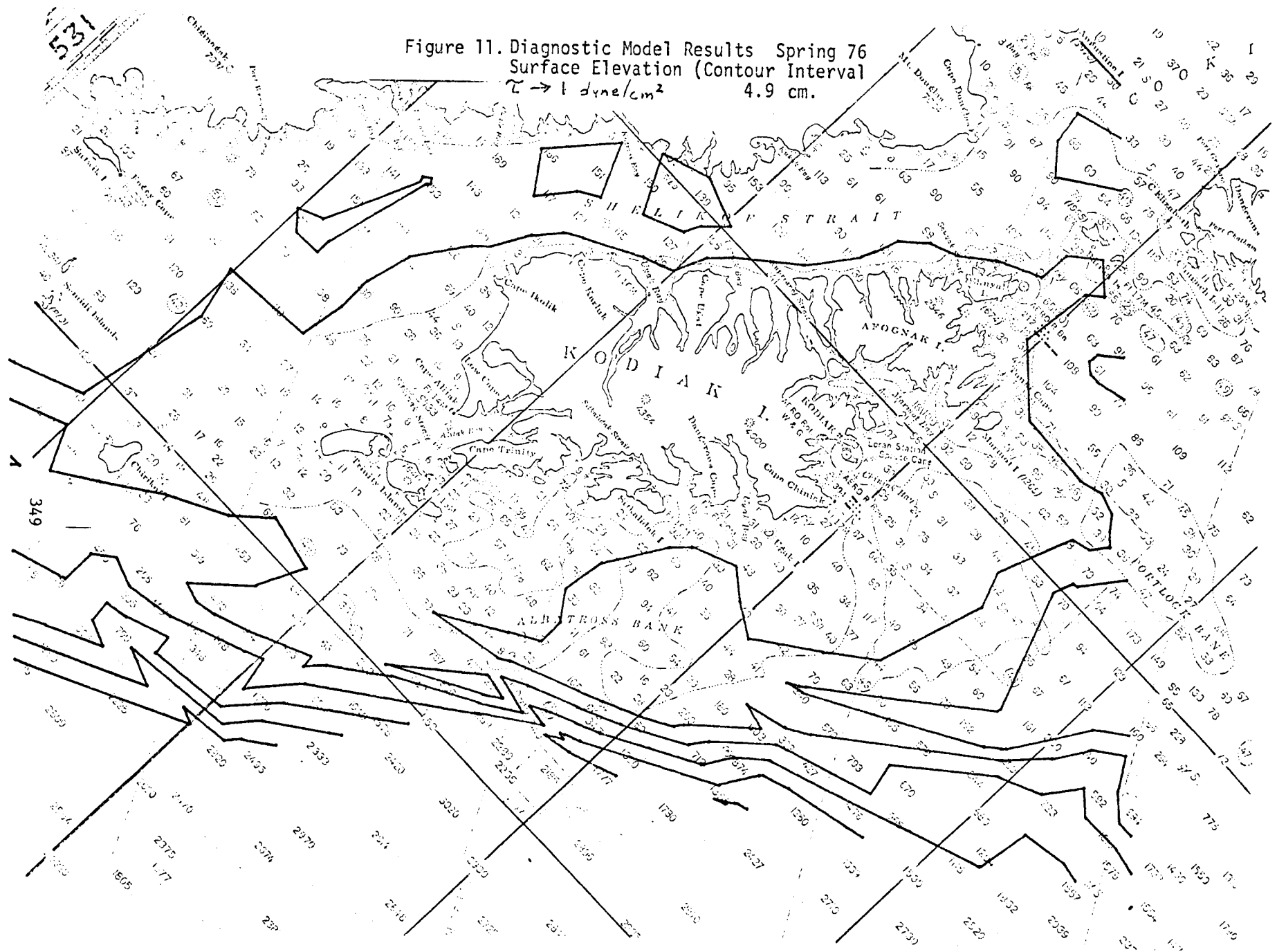
for reversing the direction of the coastal currents around Kodiak.

From these initial studies with the diagnostic model of the Kodiak area, a number of flow characteristics have been tentatively identified which allow speculation about the regional current dynamics. It should once again be emphasized that these studies have been made with essentially no current meter verification or wind field information. These represent only a first look with the model and subsequent studies should make it possible to strengthen or discard many of these conclusions. Future plans for applying the diagnostic model in the Kodiak region call for: 1) a recommendation for the inshore placement of current meter moorings to document flow conditions in the channels and over the banks, 2) running the model for additional stress fields, in particular investigating NW and SE stress cases, as well as more intense NE stress cases, 3) running the model with a mixed boundary value formulation to better resolve coastal currents and multiply connected domains, 4) keying the model to real time wind estimates and simulate time dependent trajectories for the region, and 5) analyzing observational data to establish the proportionality coefficient relating the sea surface slope to the wind stress.

Liaison with the Kodiak physical oceanographic components of the OCSEAP study will continue with primary communication carried out by personnel exchange with the appropriate PI's. Thus far the modeling results reported here have been presented, in part, at the OCSEAP Physical Oceanographers' Review Meeting (Lake Quinalt - Oct. '76) and the

350

Kodiak Lease Area Synthesis Meeting (Anchorage - March '77). In addition, USGS personnel (Smyth) working on OCS assessment modeling will be advised of the status of the Kodiak studies (April '77).

SECTION III.   TRAJECTORY MODEL STUDIES IN THE GULF OF ALASKA

The purpose of the preliminary trajectory model study is to investigate the possible formulations for an advective-diffusion model for the prediction of the movement of pollutant spills. We must legitimately ascertain if the various methods and options make any difference for prediction purposes. Such options should include trajectories based on real-time current meters and wind information with appropriate Ekman dynamics and those based on stochastic interpretations of ensemble data for the particular region of study.

The preliminary pollutant trajectory model has been written and tested with various input parameters for the Gulf of Alaska. The program allows the user to choose options of the type of physical processes to be studied. With these choices and the appropriate data inputs, the program is automatic for a given area of study. The program output is a data file or tape of trajectory positions and integer characters for the labelling of each new trajectory sequence. This data file or tape can then be read into an automatic machine-specific plot routine which will superimpose the trajectory information on a section of scaled coastline.

The component processes which can be used to run the trajectory model are: 1.) real-time currents using NEGOA current meter data for the region, to which the results of the diagnostic model ∧ 2.) mean
have also been keyed,
currents for the same current meter data, to which the results of
have also been keyed,
the diagnostic model   3.) mean plus stochastic currents based on

a Markov analysis of the same current meter record, 4.) real-time winds using six hour FNWC data for the region over the same time period as the current meter in the previous options, and 5.) mean plus stochastic winds based on a Markov analysis of the same wind record.

Figures 1 thru 6 show the results of the test cases of the model for the summer of 1974. Each trjectory on a plot runs for thirty days and they are initialized consecutively one day apart. The trajectory time step is every six hours, while the plots only give their location at the end of each week. The plotting routine also has the capability of tracing each individual trajectory with a line, but that was not implemented here since the runs were made with 50 differrent trajectories. The plotting package also has the capability of being used as a scatter diagram, showing a continuous cloud of points representing an overall view of the entire field of trajectory locations. This last feature would be most useful with a probability study.

Figure 1 shows the first case with a real-time ocean current and no wind. Simularly, The second case represented in figure 2 was run with a real-time current and a real-time wind. These two cases are very similar since the winds were light during the study period, except for the first few days. These results were reported earlier at NEGOA Synthesis Meeting in Anchorage.
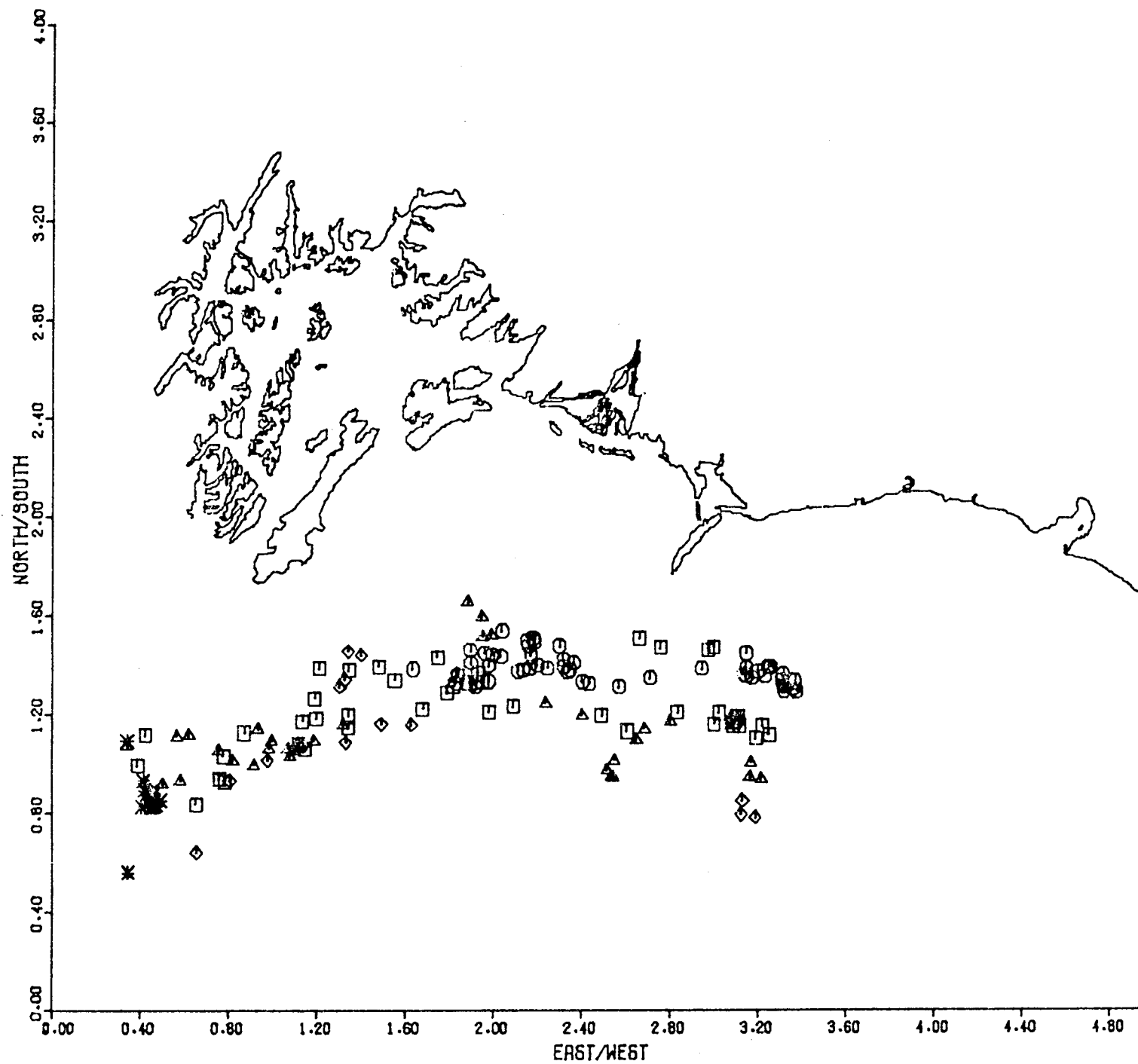
Figure 1. Trajectories based on real-time ocean currents only for summer 1974 in the Gulf of Alaska. Circles indicate end of first week, squares the second, triangles the third, and diamonds the fourth. Stars indicate the trajectory left the grid system before the end of the month.

Figure 2. Trajectories based on the real-time wind information for summer 1974 in the Gulf of Alaska. Symbols are the same as in Figure 1.

Figure 3 through 6 represent the results of cases using different stochastic formulations. The case shown in Figure 3 is based on a mean ocean velocity system plus a stochastic spreading component to the velocity. This case has no explicit wind formulation. Compared to the real-time results, the scatter is much greater while the bulk of the flow has a similar orientation toward the south or southwest. Figure 4 shows a case with a mean ocean system, but no ocean stochastic component. In addition, a downwind fraction of the mean wind and the stochastic wind are included. Compared to the three previous cases, the orientation of the predicted trajectories is markedly more towards the west and northwest for this fourth test. Figure 5 estimates the trajectories using the same set-up as that for Figure 4, except that an Ekman fraction of the stochastic wind is added in. This gives results more similar to those in the third case, with a large scatter, but a bulk orientation towards the south and southwest. Both case 3 and case 5 indicate several of the trajectories also beached east of Kayak Island and west along Montague Island. The last case is represented in Figure 6. This includes all the parts of the fifth case plus a stochastic ocean current component. The east/west scatter is similar to that for cases 3 and 5, but a much larger fraction of the trajectories beached to the north.

Preliminary initial results suggest that if you want to study specific events related to a pollutant spill that you will need information about the local conditions and time scale. It appears that the

V = VM + VS

GULF OF ALASKA TRAJECTORY PLOT
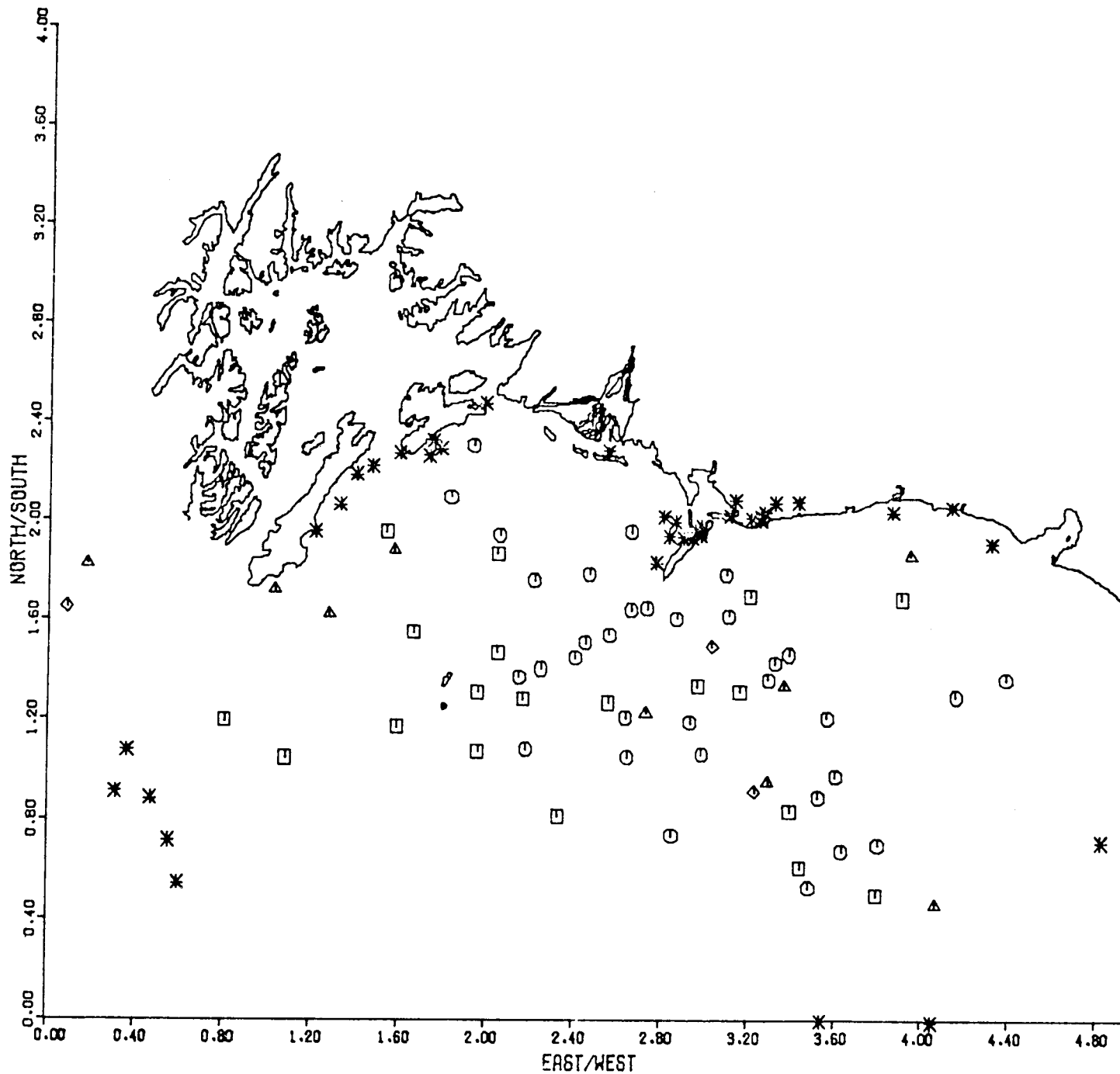
Figure 3. Trajectories based on a mean current system with stochastic spreading for summer 1974 in the Gulf of Alaska. Symbols are the same as in Figure 1.
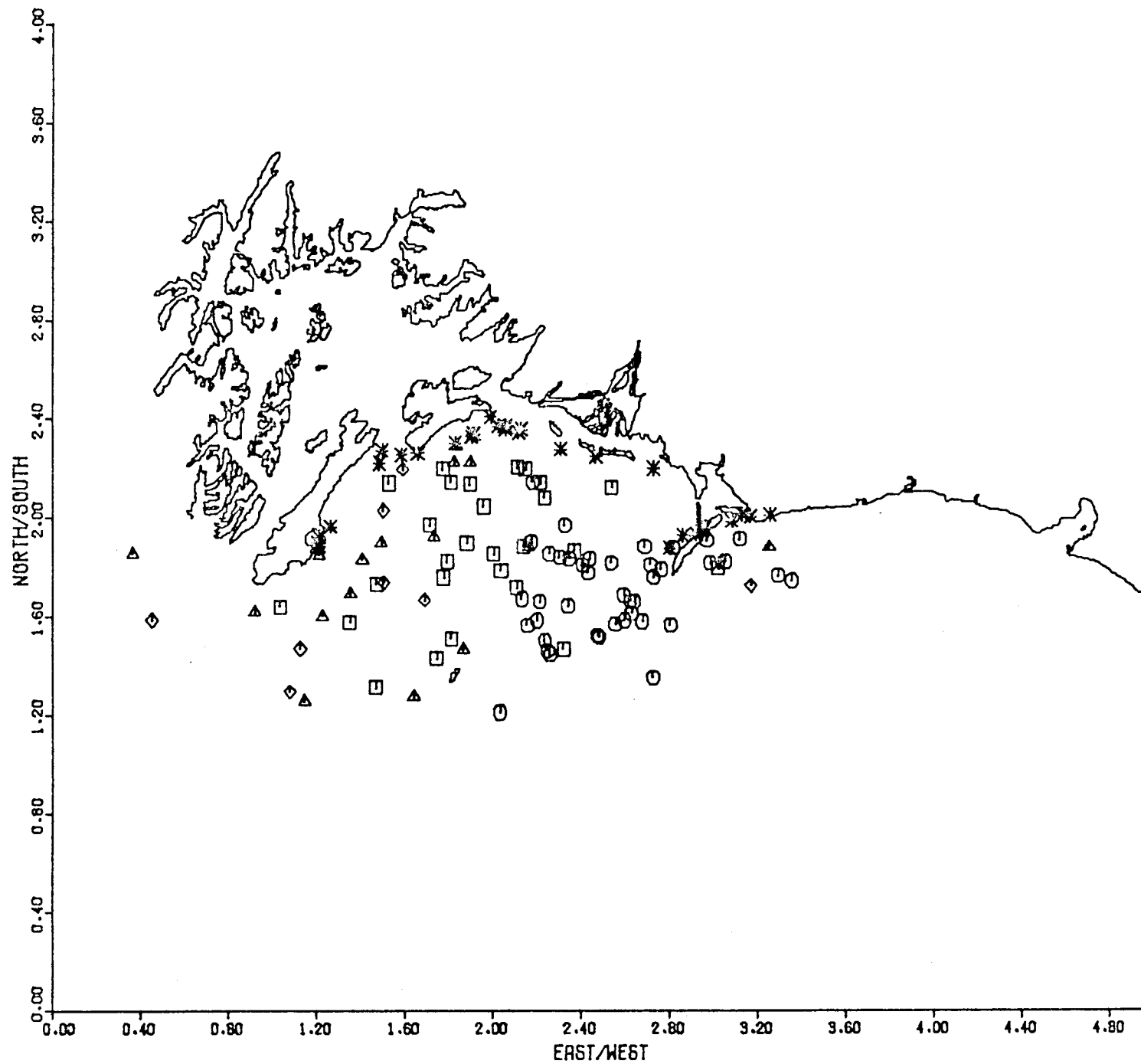
Figure 4. Trajectories based on a mean current system and mean plus stochastic downwind
information for summer 1974 in the Gulf of Alaska. Symbols are the same as Figure 1.
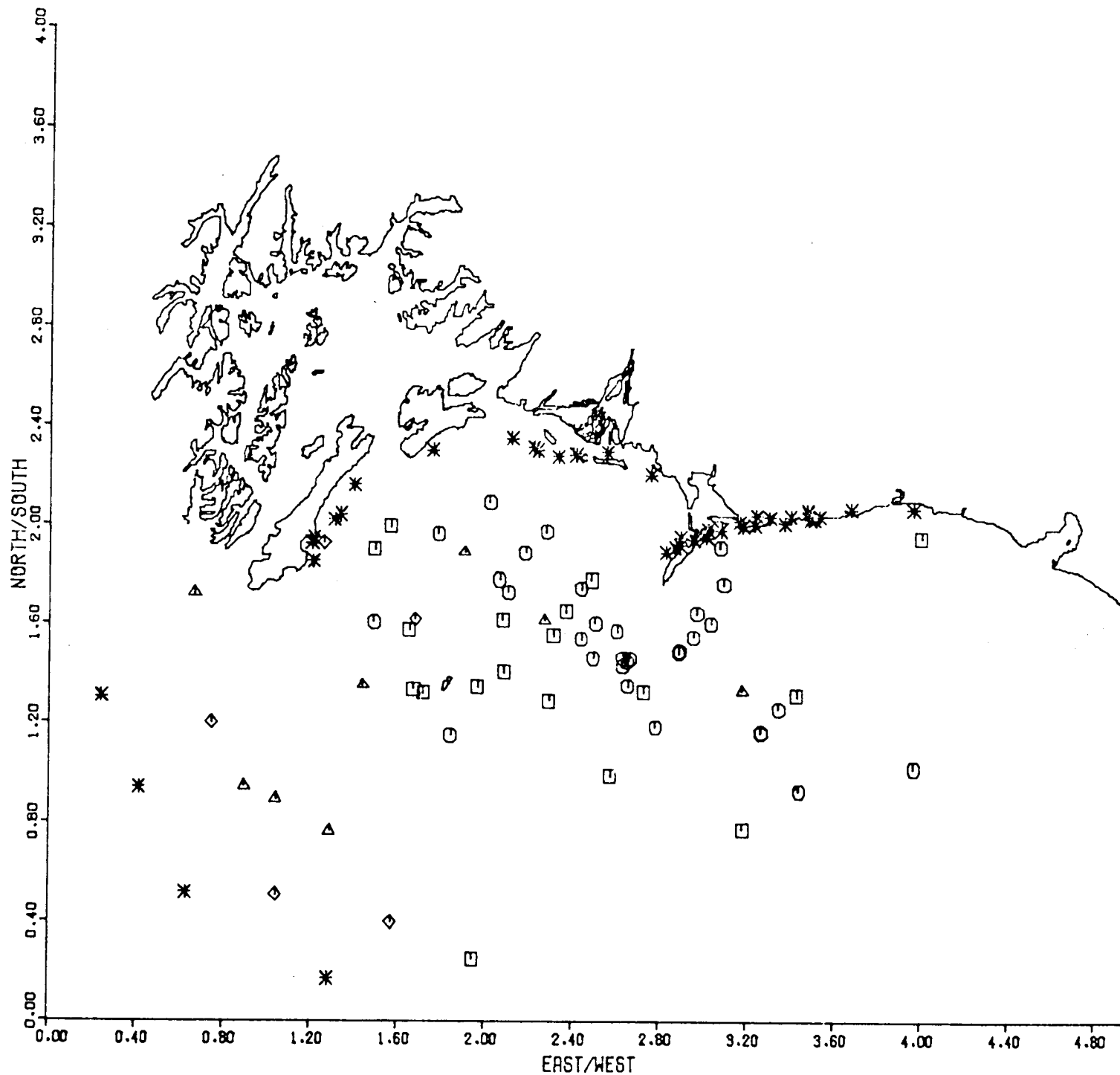
Figure 5. Trajectories based on a mean current system and mean plus stochastic downwind information and the Ekman effects of the stochastic part of the wind for summer 1974 in the Gulf of Alaska. Symbols are the same as Figure 1.

Figure 6. Trajectories based on a mean current system with stochastic spreading and mean plus stochastic downwind information and the Ekman effects of the stochastic part of the wind for summer 1974 in the Gulf of Alaska. Symbols are the same as Figure 1.

360

stochastic formulations give a good overview of an ensemble of possible occurrances of trajectories over a season, but do not give information related to specific events.

Another major point to be applied to an analysis of this study is that the winds and currents are not statistically independent. The major currents are Barotropic which are due to the set-up by the wind of a sea surface slope. So the correlation between the currents and the winds is not independent. This may introduce error into the cases with combined terms of wind and ocean currents. This problem makes a strong argument for the development of the independent regional meteorology model to be used in conjunction with the diagnostic model for trajectory inputs.

SECTION IV.   REGIONAL METEOROLOGICAL MODEL

IV-1.   Introduction

An important limitation of coastal marine meteorology is the inadequate specification of the local wind field at the desired spatial resolution. Typically, it is difficult to estimate near-shore wind fields directly from large scale synoptic patterns or scattered wind measurements because topography and discontinuities in surface roughness and heating give rise to significant mesoscale variations. For example, Fig. 1, reprinted from a NWS Technical Report to be published in early 1977, shows reported regions of ano-malous wind speed and direction along the Alaskan coast. The Alaska Region of the National Weather Service compiled Fig. 1 from a survey of the Coast Guard and other groups operating vessels in Alaskan waters. Strong ageostrophic winds exist in the passes of the south-east Alaskan coast and can be attributed to channelling around islands. The open coast is also subject to anomalous winds caused by high coastal mountains. Of particular importance are Katabatic winds, forced by the contrast of warm ocean temperatures and cold temperatures 50 - 100 km inland.

This section reports on one approach to ascertaining the magni-tude of mesoscale effects. A numerical model, which consists of fairly general conservation statements for mass, momentum, and heat, represents the behavior of the lower atmosphere. Within the context of its formulation, the model is used to document the implications of change in large scale flow, surface parameters, and assumed dynamics

362

363

Areas Coast Guard Encountered
Maximum Winds

Other Areas NWS Estimates Anomalous
Winds Occur
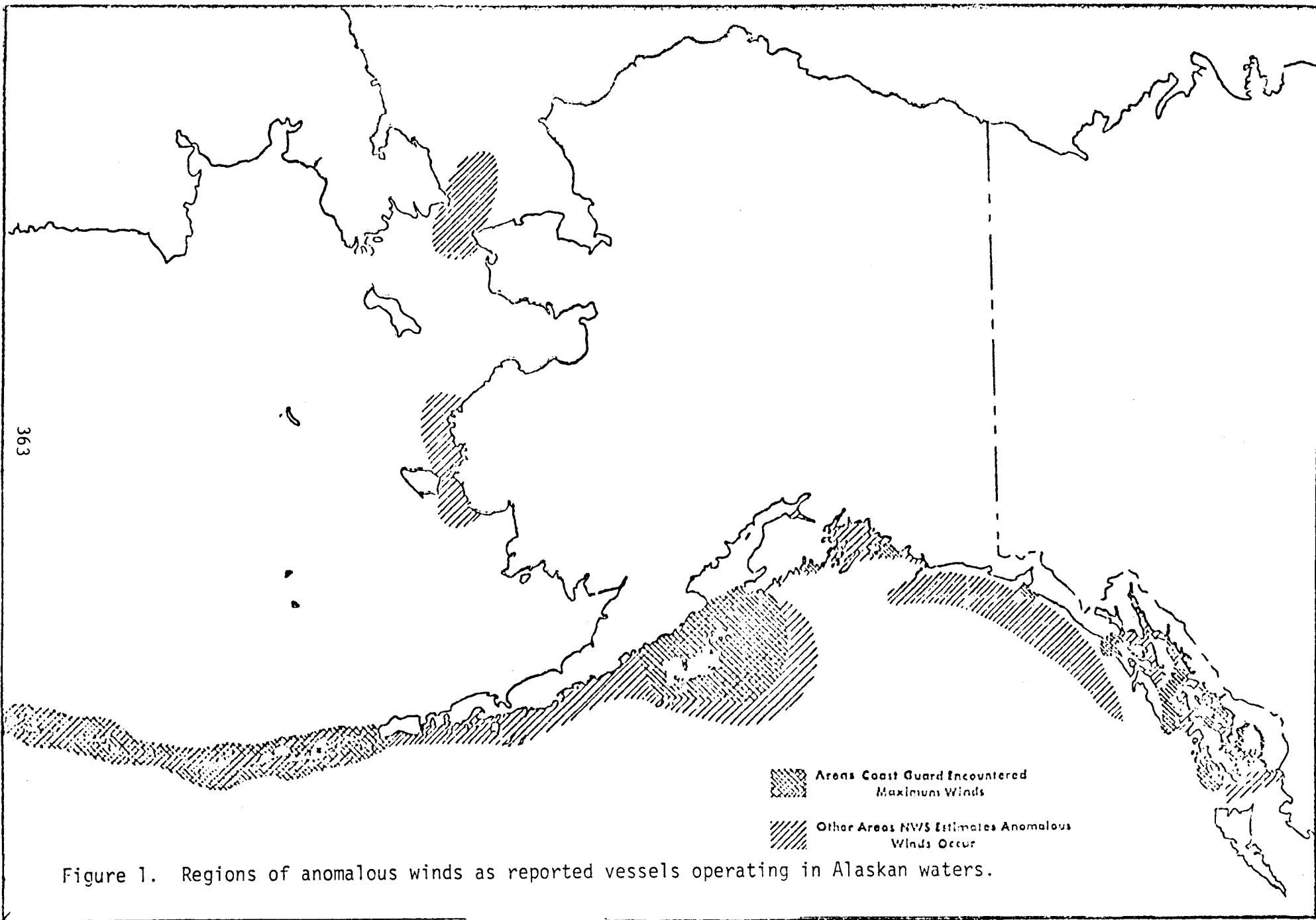
Figure 1. Regions of anomalous winds as reported vessels operating in Alaskan waters.

on the wind pattern in a limited region. A major goal is the ability to infer local winds at important maritime locations from the large scale flow pattern.

We have chosen to adapt a model proposed by Lavoie (1972, 1974). Lavoie treats the planetary boundary layer (PBL), typically 0.5 to 2 km deep, as a one layer, vertically integrated primitive equation model. The model solves for the two components of horizontal velocity, boundary layer height, and potential temperature throughout a limited region. Large scale geostrophic wind, surface elevation and temperature, and the stability of the air in the free layer above the PBL are specified as boundary conditions. Air temperature and PBL height are specified at the inflow boundaries. The local response is calculated by specifying smooth initial values of wind, temperature, and PBL height and then time stepping the equations of continuity, momentum, and heat conservation until an equilibrium state is obtained. The system is free to estimate land-water contrast, modification of the down wind environment by advection, and channelling by topography. The equilibrium state is considered to give the local winds which occur in conjunction with the given large scale pressure pattern. Since the model consists of only one layer, processes which depend upon vertical structure such as intensification of fronts cannot be directly resolved; however, the model should be well suited to estimating wind patterns in mountainous regions with strong orographic control.

A complete description of the model formulation and computer code is available as a forthcoming Technical Report. The remainder of this section discusses preliminary testing using Puget Sound as a base, and

364

initial application of the model along the Alaskan coastline.

IV-2.   Simulation for Puget Sound - Strait of Juan de Fuca

Puget Sound was selected as location to test the suitability of the model to simulate orographic control. The principal rationale was the accessibility of a large operational data base for verification as well as an existing digitized topographic grid.

We have initially selected to simulate two generalized meteorological flow conditions for the Puget Sound System, corresponding to summer and winter regimes. In the summer months, anticyclonic flow around a well-developed semi-permanent high pressure cell to the west of the region causes prevailing northwest winds offshore along the western coasts of Washington and Vancouver Island. By midwinter the prevailing flow is southwesterly, as the region comes more under the influence of the cyclonic circulation of the Aleutian low. An important winter case, however, that we have not chosen to investigate is high pressure to the east of the region which gives easterly winds, particularly along the Strait of Juan de Fuca.

A location map for western Washington is provided in Fig. 2. Topographic data for Puget Sound was obtained from a master tape at the National Center for Atmospheric Research (NCAR). The mesh is a 5 minute of latitude by 5 minute of longitude grid with an average elevation computed for each square. The NCAR tape also specified if the square was land, ocean, part land and ocean, or part lake. The NCAR elevation data was smoothed in both directions with a 1-2-1 type smoother (Shuman, 1957). Fig. 3 presents a view of the smoothed topo-
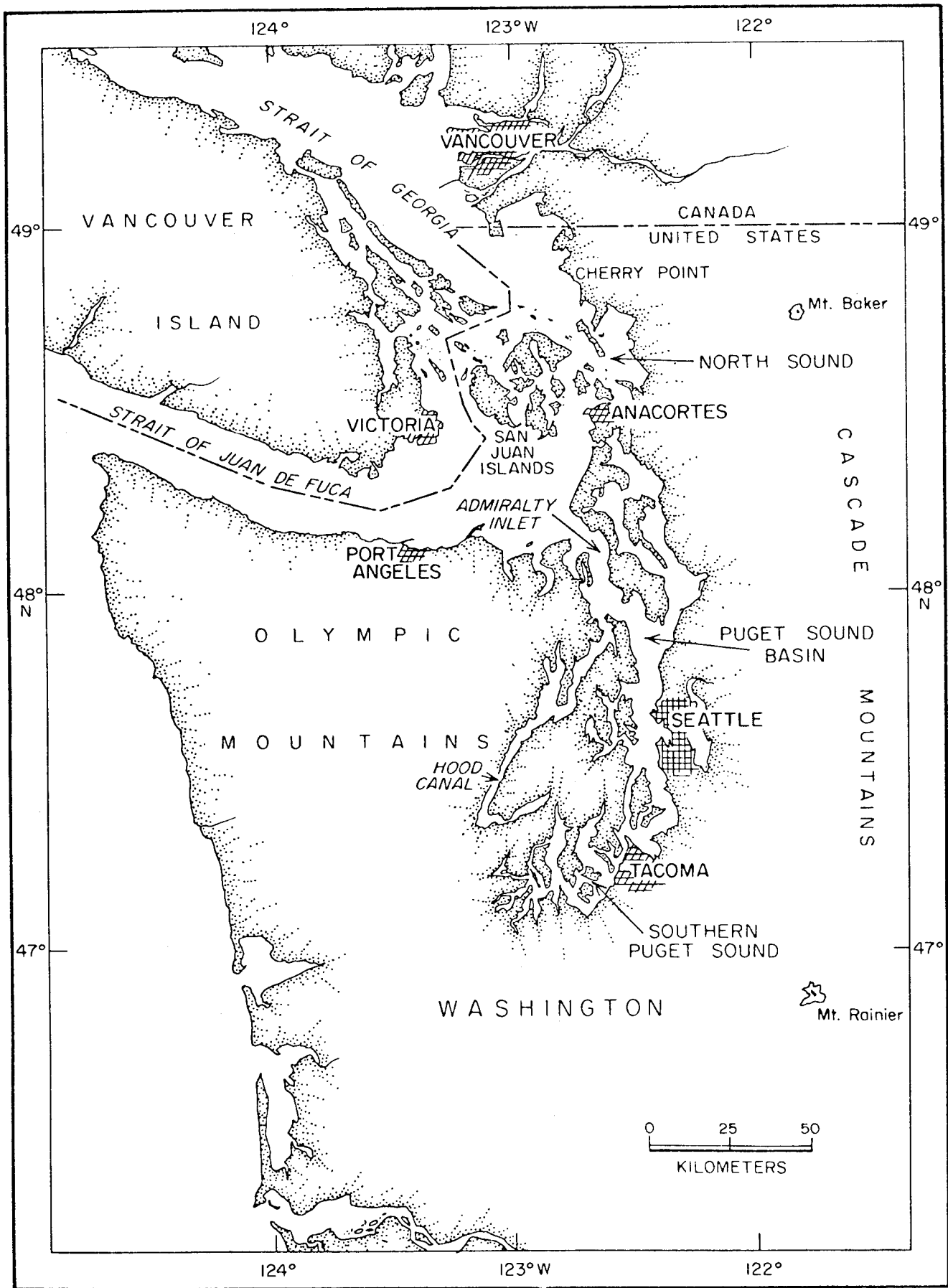
Figure 2.   Location map for the Puget Sound Basin.
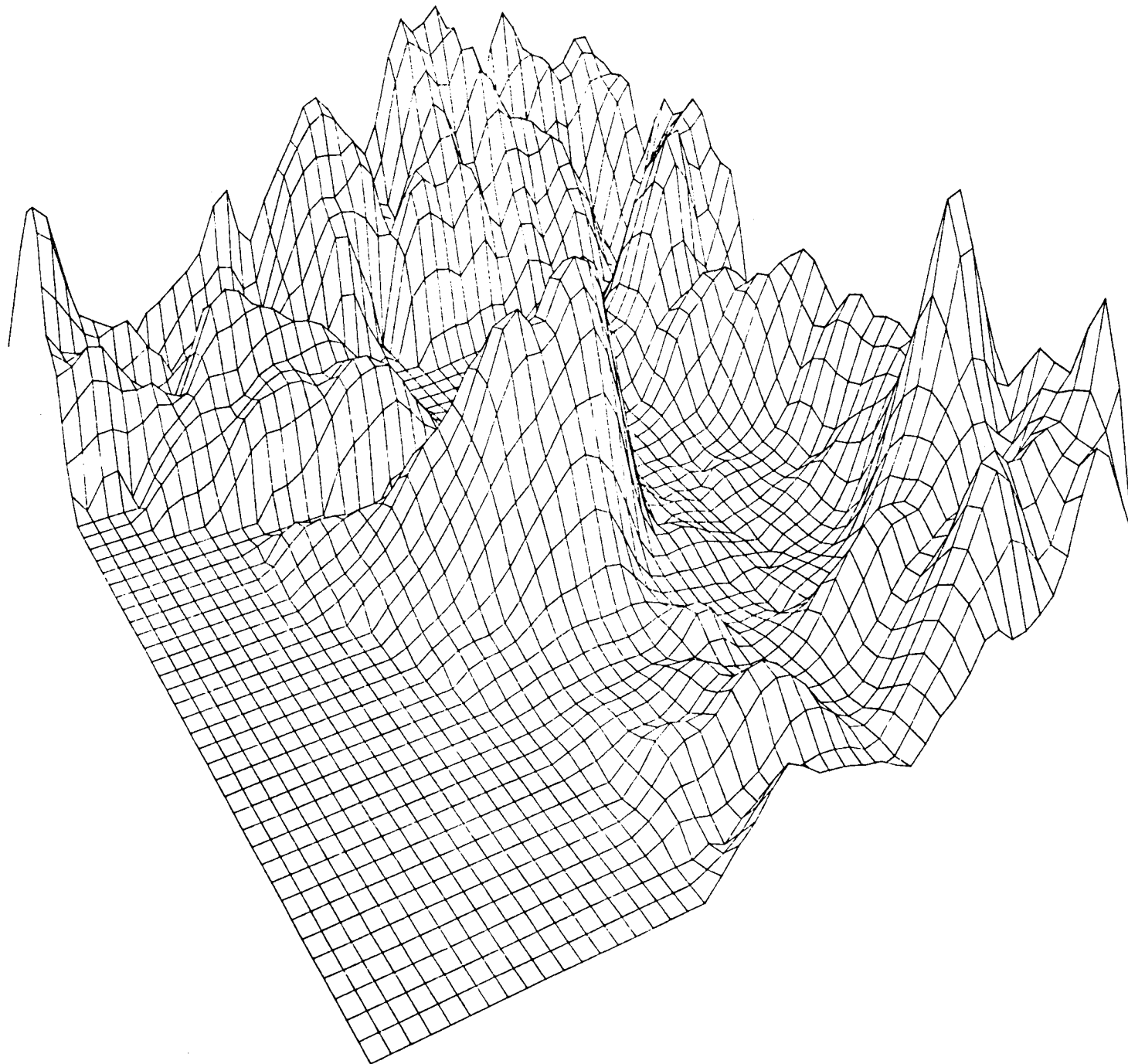
Figure 3. Topographic grid used in the computations as viewed from the southwest.

graphic grid as viewed from the southwest.

The following values of parameters and input conditions were used. They are generalized from measurements obtained during December, 1976.

$f = 1.08 \times 10^{-5}$ / sec $\quad$ = Coriolis parameter

$g = 980.6$ cm/sec^2 $\quad$ = gravity

$\Delta\theta = 3.0^\circ$K $\quad$ = inversion strength

$\theta_o = 282^\circ$K $\quad$ =reference atmospheric temperature

$C_D = 1.3 \times 10^{-3}$ (water) $\quad$ = surface momentum drag coefficient

$C_D = 9.0 \times 10^{-3}$ (land) $\quad\quad$ ditto

$C_H = 1.3 \times 10^{-3}$ (water) $\quad$ = surface heat exchange coefficient

$C_H = 7.0 \times 10^{-3}$ (land) $\quad\quad$ ditto

$h_i = 1.2$ Km $\quad$ = inversion height as specified on inflow boundaries

$v_g = 10$ m/s at 245° for SW flow = large scale geostrophic wind specified as constant over the model domain

$V_g = 10$ m/s at 335° for NW flow $\quad$ ditto

$E = 0.$ $\quad$ = entrainment rate of overlying stable air

The background large scale pressure gradient F_i is calculated to balance the specified geostrophic wind, V_g. The PBL height is initialized by h_i and velocities are initialized at 70% of the geostrophic wind.

Figures 4a and 4b show the calculated wind field and deviation of boundary layer height from h_i for the southwest wind case. Elevation contours are approximately 250m intervals. The deviation heights are dashed lines with a 200m contour interval. From the wind vectors one

368

VELOCITY VECTOR PLOT
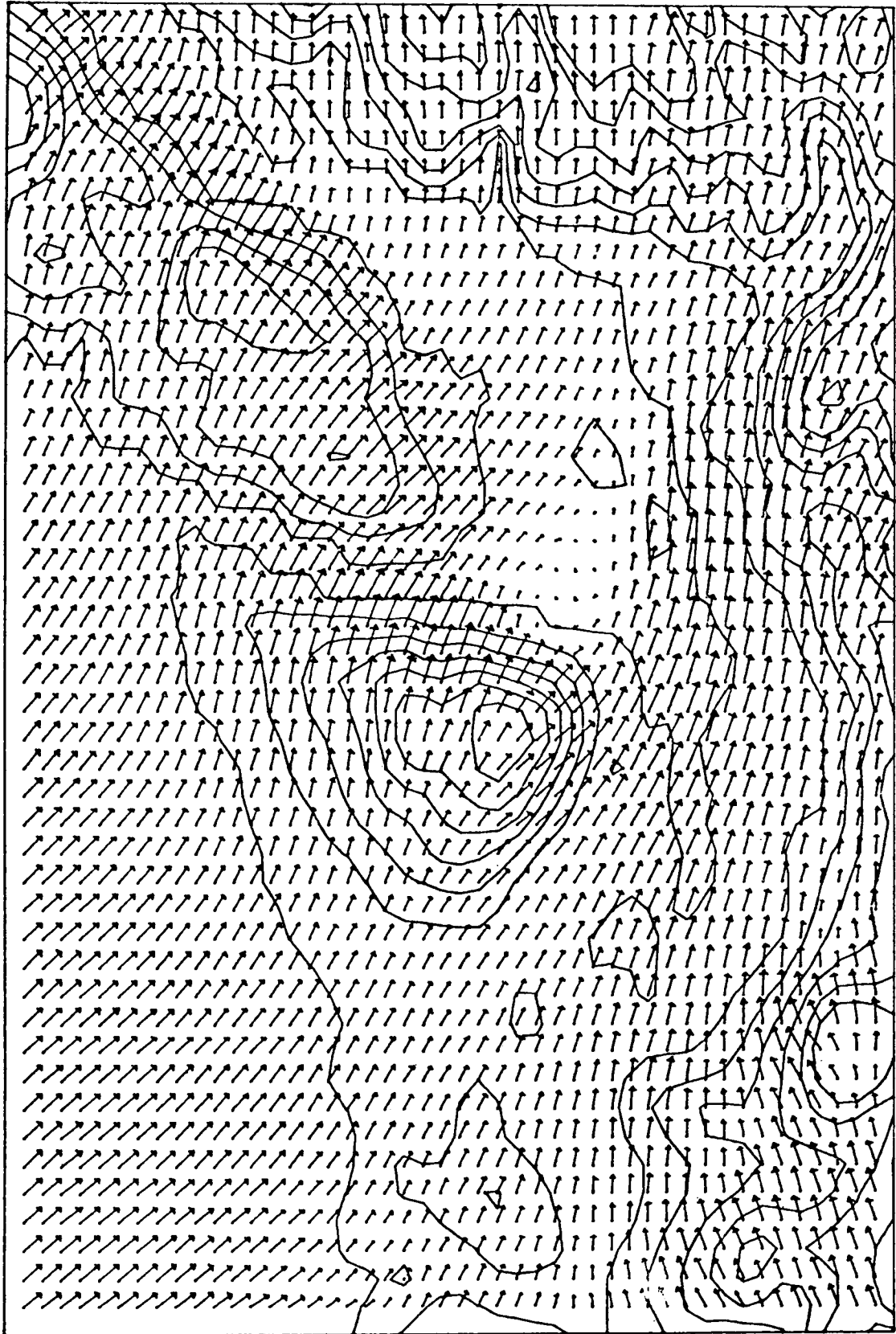
10 METERS PER SECOND

Figure 4a. Boundary layer winds for southwest geostrophic flow.

BOUNDARY LAYER HEIGHTS
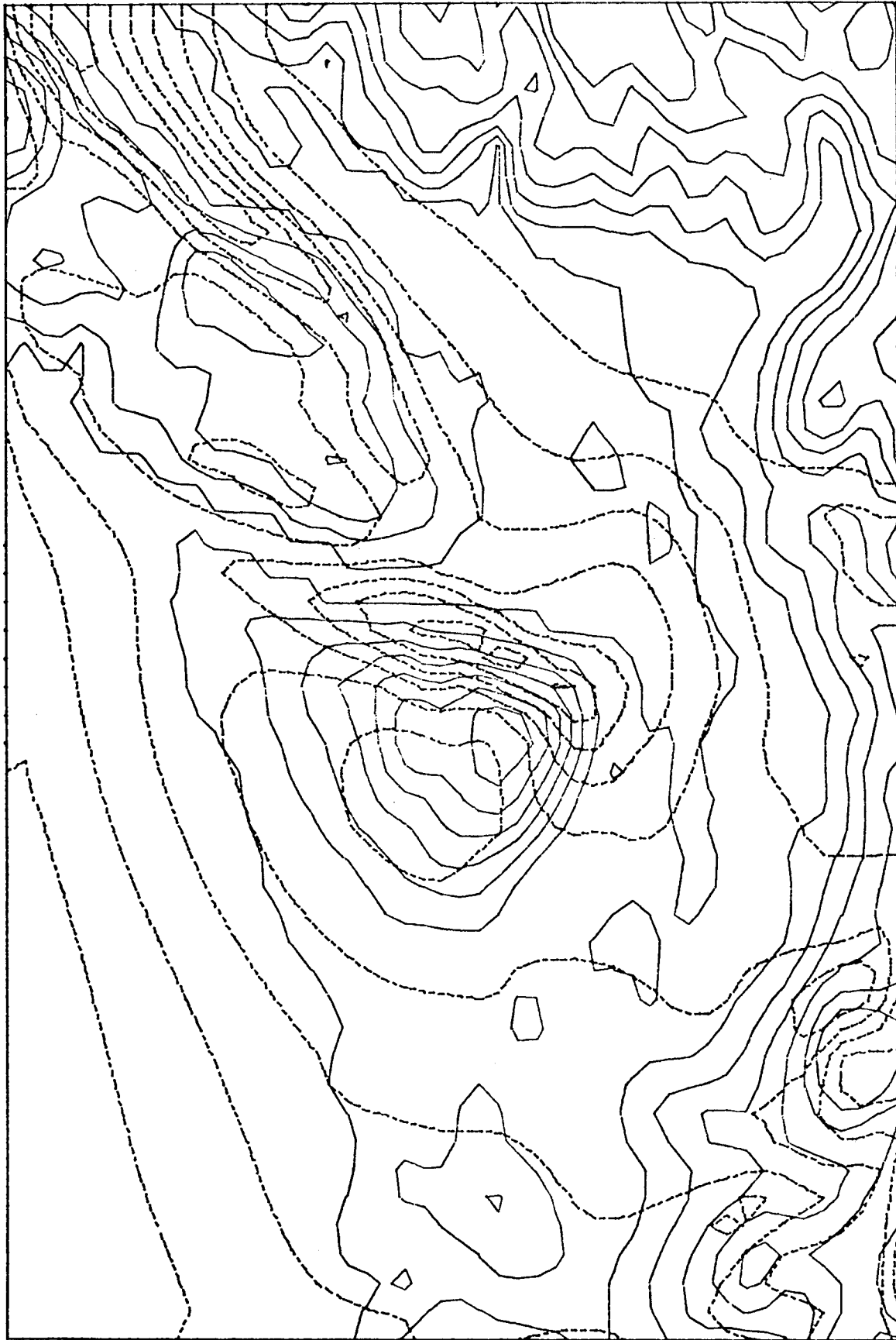
Figure 4b. Deviation of boundary layer height from the open ocean
reference height as shown by dashed lines. Broad local
maximums are on the windward side of Vancouver Island
and the Olympic Mountains. Sharp minimums are to the
N.E. of these same features.
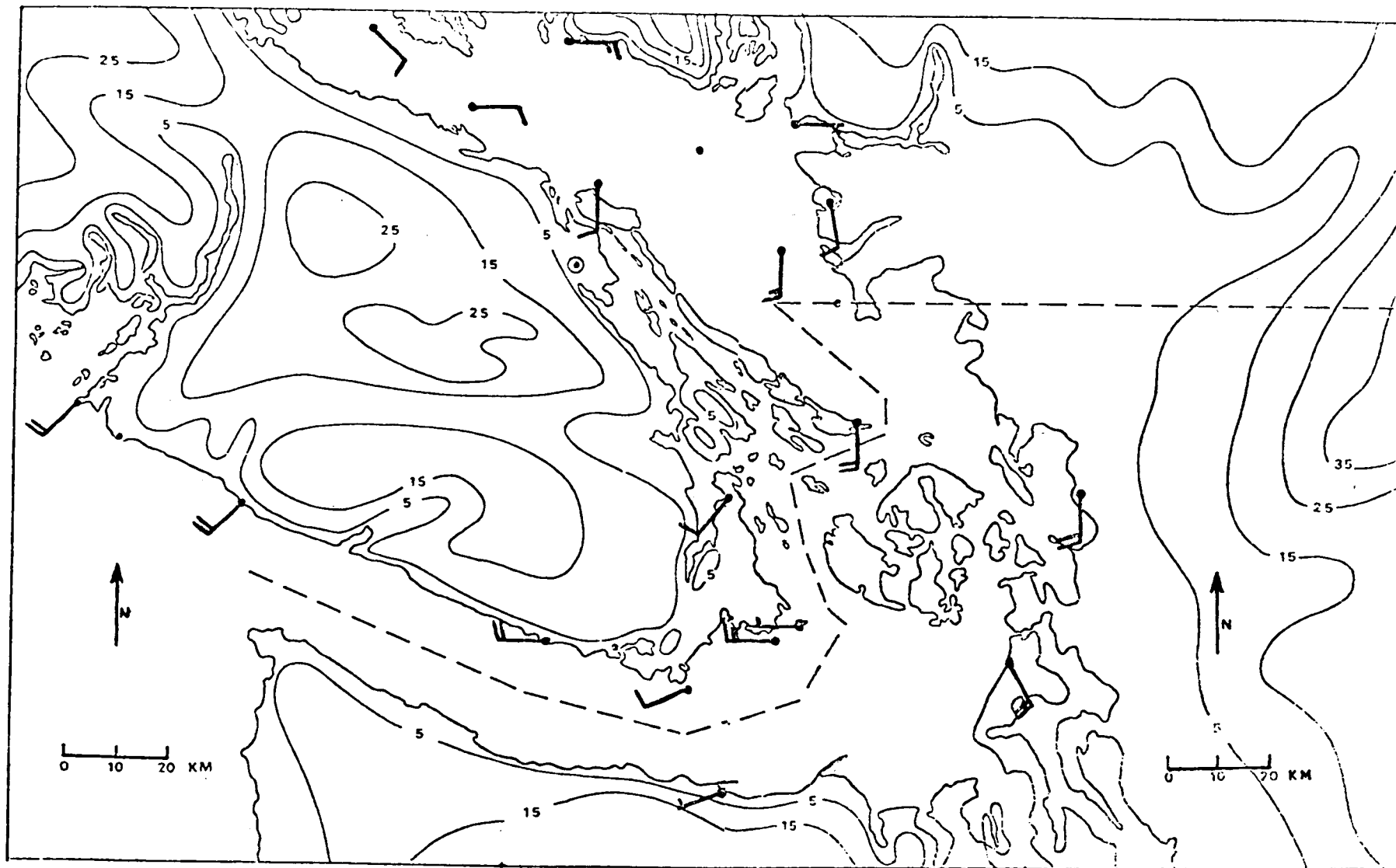
Figure 5. Reported winds for 0300-0400 GMT 25 October 1973. Sea level geostrophic wind is 13 m/s from 240°. Long wind barb is 10 kts and short barb is 5 kts (after Danard 1975.)

VELOCITY VECTOR PLOT

→
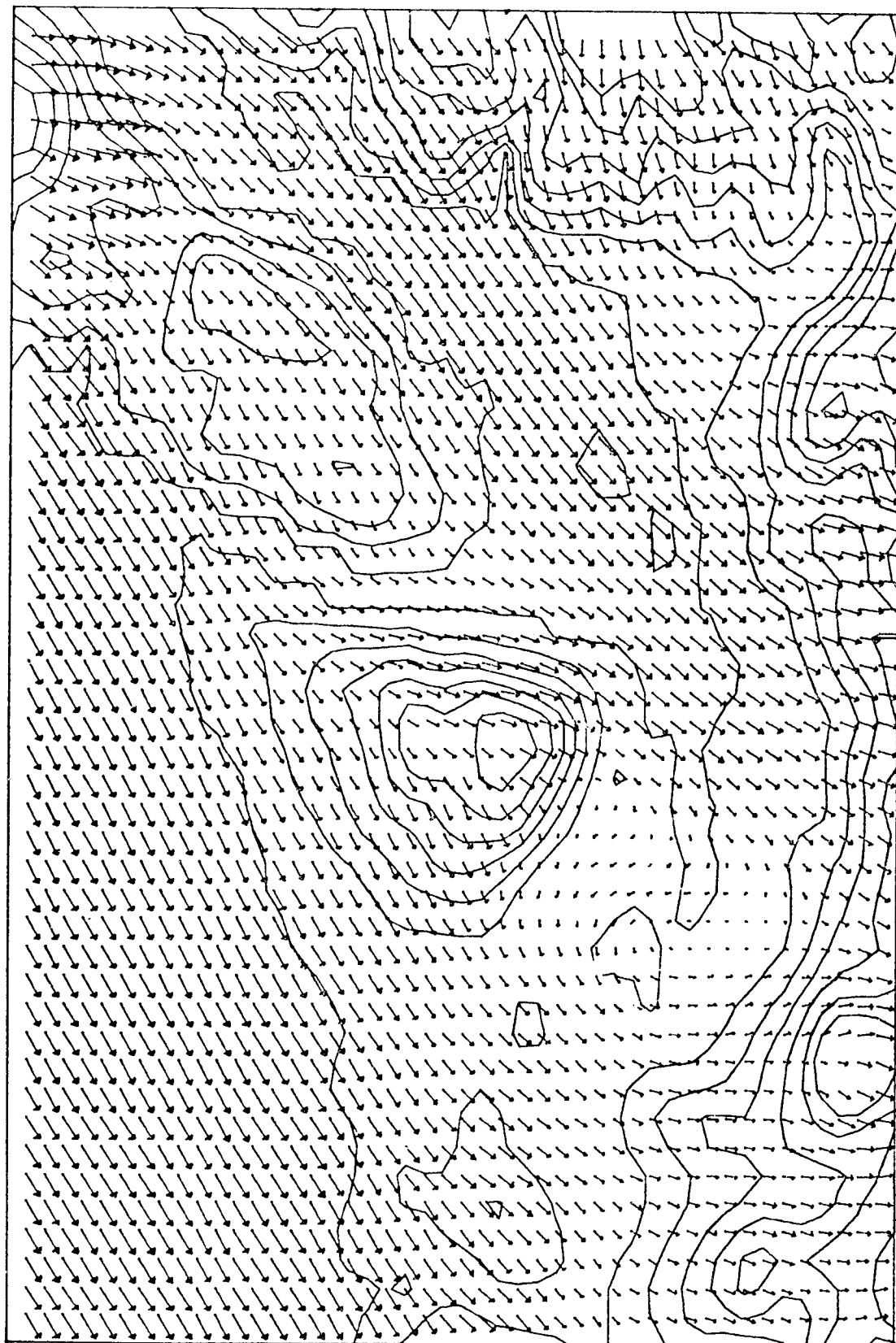
10 METERS PER SECOND

Figure 6a. Boundary layer winds for northwest flow.

BOUNDARY LAYER HEIGHTS
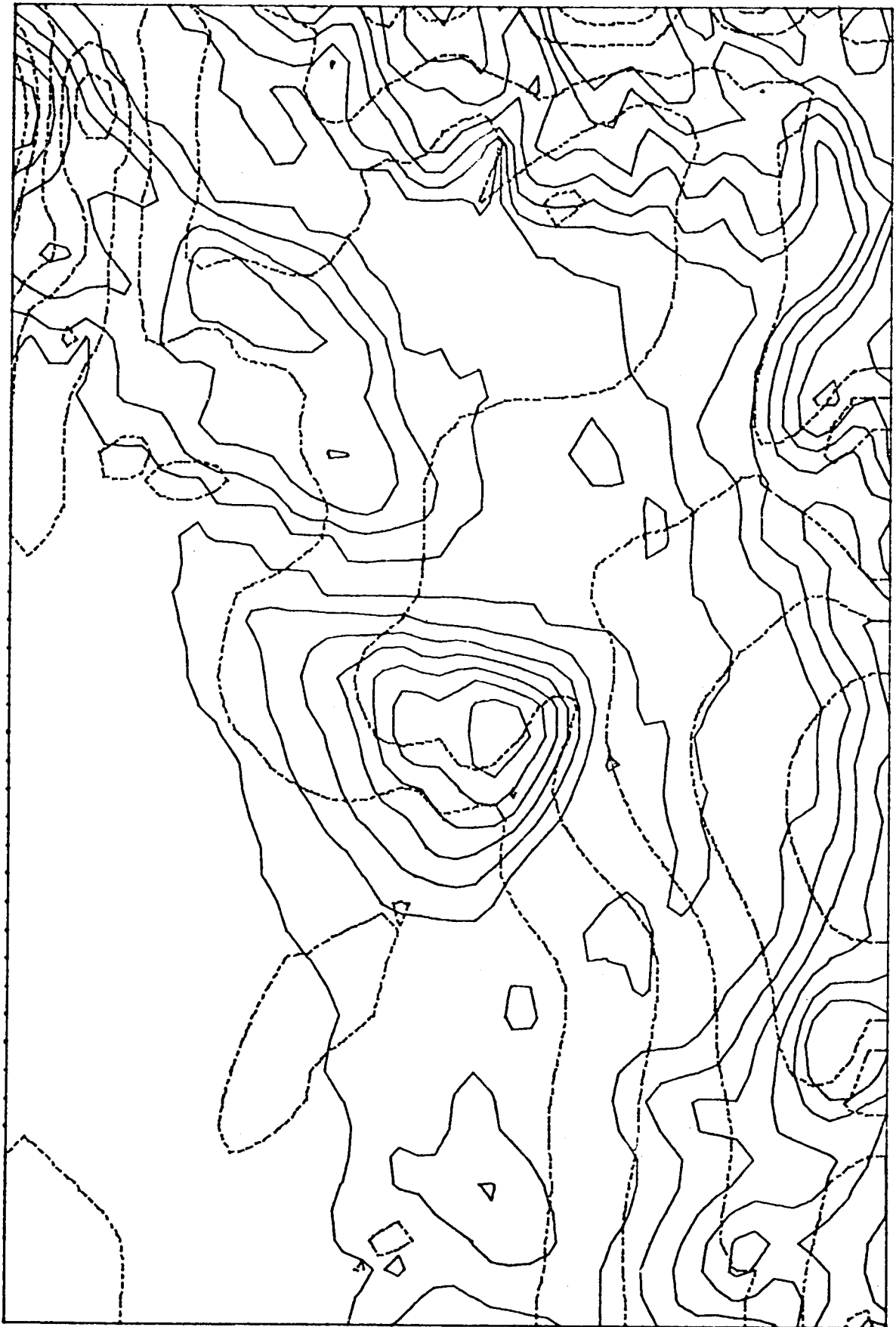
Figure 6b. Deviation of boundary layer height.

first notices that the flow is channelled by the Olympic Mountains. Winds over Puget Sound stronger and more southerly than off shore. Nearshore winds along the south coast of Vancouver Island and near the entrance to the Strait of Juan de Fuca are more southerly than farther off shore. The Strait of Georgia shows a large variation of local wind between the northern and southern end. Increased winds flow through the low point in the mountains of Vancouver Island and spill out over the inland waters. An eddy has formed at the east end of the Strait of Juan de Fuca near Port Angeles. The PBL deviations show a gentle rise over the windward side of the mountains with a pronounced lee wave trough on the downwind side of the Olympics and Vancouver Island.

For comparison, Fig. 5 gives observed anemometer winds at selected coastal stations which closely correspond to the synoptic situation depicted in Fig. 4a. As with the model, observed winter SW flow has strong winds along the east side of Puget Sound, with reduced flow in the region southeast of Vancouver Island. Winds at Victoria are less intense and more westerly than the model suggests. It may be that the position of the eddy and the magnitude of the pressure gradient that develops along the axis of the Strait of Juan de Fuca is very sensitive to the volume of air channelled through Puget Sound, which depends in turn on the orientation of the offshore flow.

Fig. 6a and 6b show velocity and height deviation for northwest winds. Channelling is indicated in the Strait of Juan de Fuca and especially by the Strait of Georgia. Height deviations are less intense than for the southwest wind case although the velocity field

374

indicates that the lee wave eddy is still a major feature.

In contrasting the wind and height fields for the two cases, northwest winds flow fairly closely to the orientation of the ridge line. Southwest winds funnel flow into Puget Sound but farther north inertia carries the major volume flux, velocity multiplied by PBL depth, cross contour through the low points in the ridge crest which induces a major local response in the height field.

The preliminary experiments indicate several persistent meso-scale features in the Puget Sound region. We can anticipate several important aspects. For offshore winds in the south to southwest quadrant one expects coastal winds and winds in Puget Sound to have a rather high coherency. Winds in the Strait of Juan de Fuca are very sensitive to adjacent terrain features. Direct over water measurements from the Straits will be very basic in understanding the induced flow patterns.

IV-3. Simulation of the Yukutat Region of Alaska

A location map for the Yukatat region, along the southeastern Alaska is shown in Fig. 7. Coastal modification along this coast is generally extensive enough to seriously affect estimates of surface winds for the region.

Little definitive exploration of the local meteorology of this region was accomplished before the study completed by Reynolds and Walter (1976). The data and cases shown in this section are based upon their recommendations.

The topographic grid is rectangular with a spacing of 5 km (Fig. 8). Other parameters are taken as:

$$f = 1.20 \times 10^{-4}/\text{sec}$$

$$g = 981.0 \text{ cm/sec}^2$$

$$\theta_n = 3°\text{K}$$

$$\theta_i = 274.°\text{K}$$

$$\theta_s = 282°\text{K (water)}$$

$$0_s = 274.°\text{K (land)}$$

$$C_D = 1.3 \times 10^{-3} \text{ (water)}$$

$$C_H = 5.0 \times 10^{-3} \text{ (land)}$$

$$h_i = 1.1 \text{ km}$$

$$V_g = 12 \text{ m/s at } 135° \text{ and } 355°$$

Note that a significant land water contrast in surface temperature is considered.

The results of the two cases of different prevailing winds are shown in Fig. 9 and 10. There are three major drainage regions easily
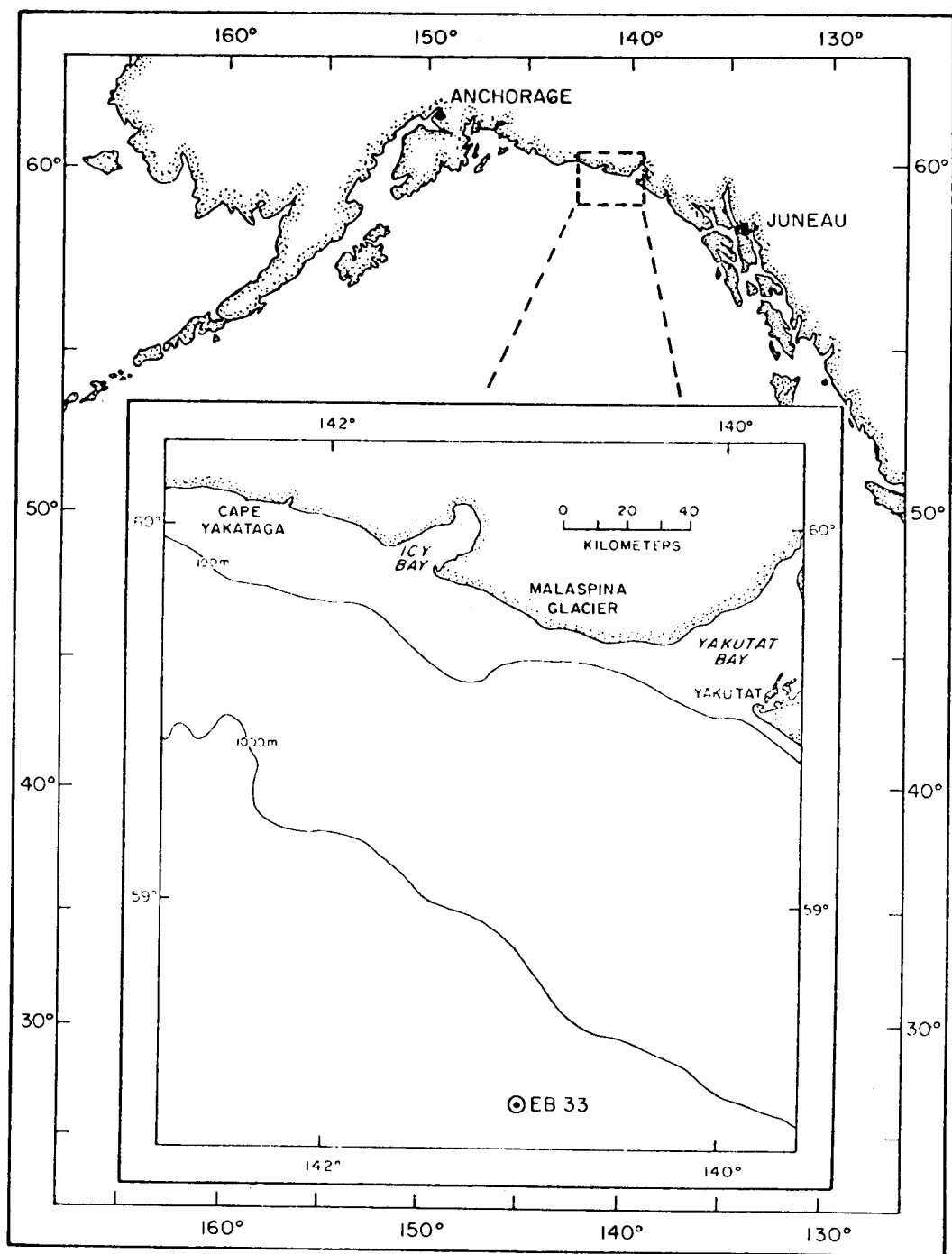
Figure 7.   Location map for southeast Alaska.
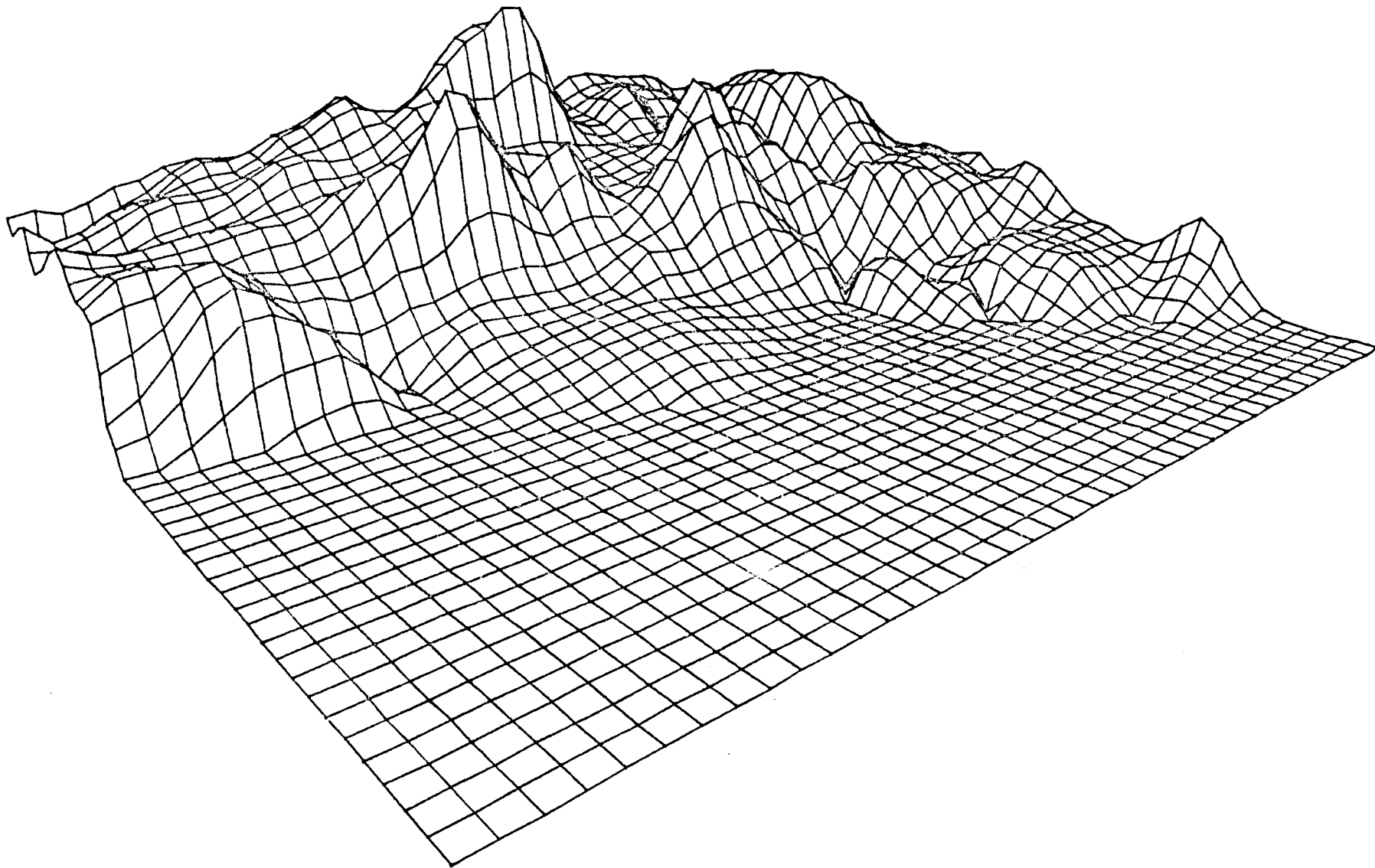
Figure 8. Topographic grid for Yukutat region as viewed from the west.

VELOCITY VECTOR PLOT
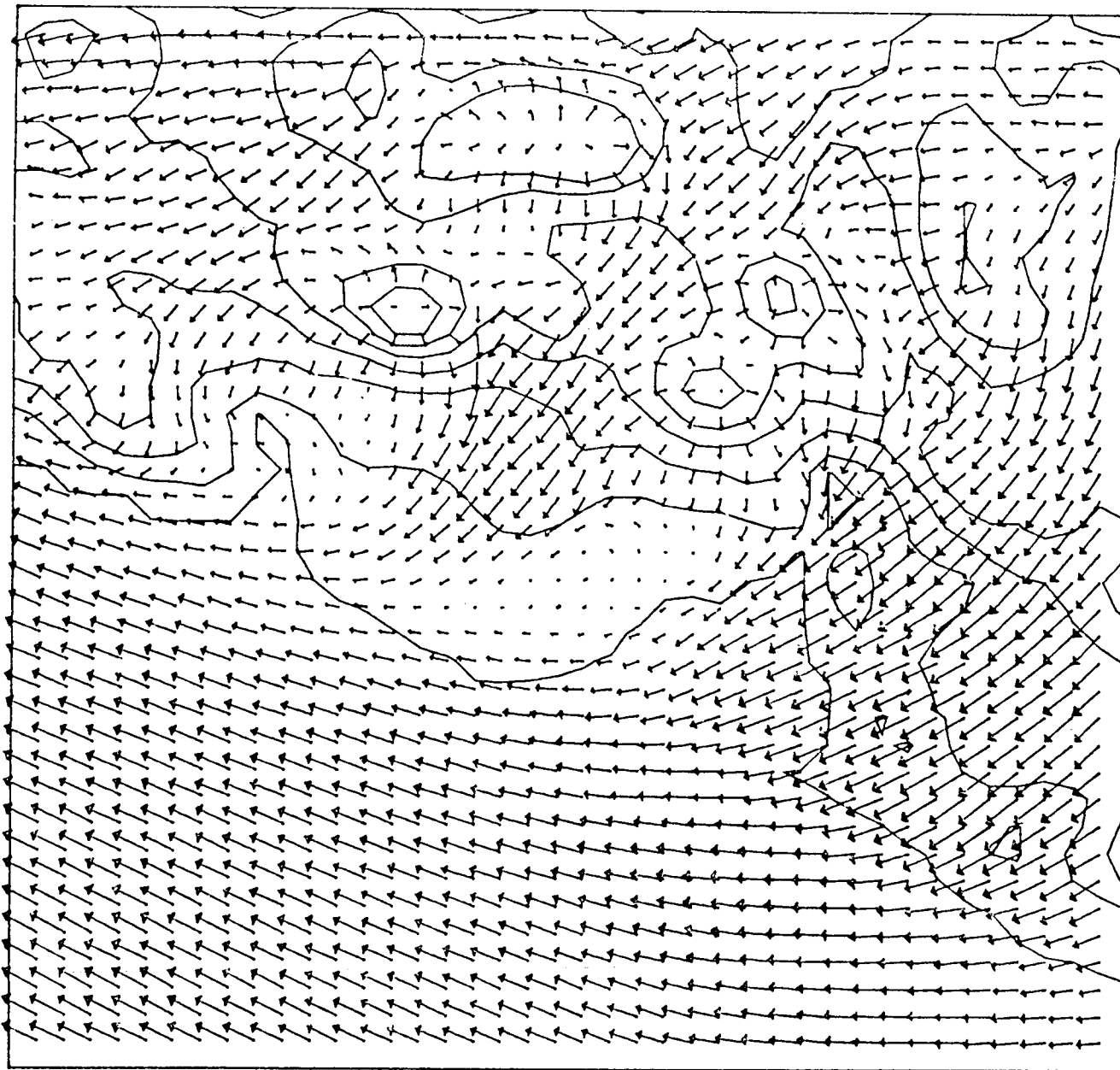
10 METERS PER SECOND

Figure 9. Geostrophic wind at 135° relative to top of figure at 13 m/s.

VELOCITY VECTOR PLOT
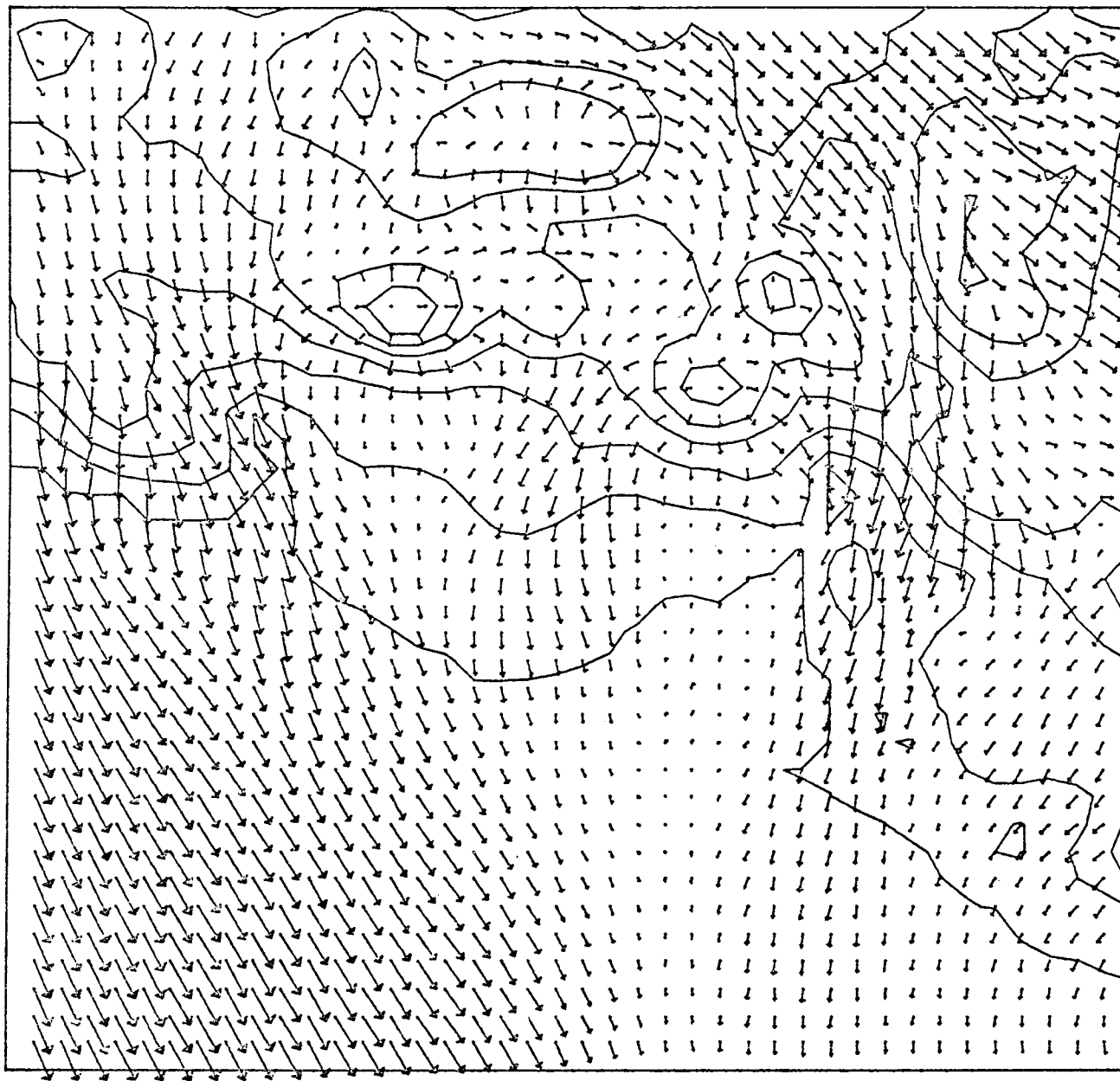
10 METERS PER SECOND

Figure 10. Geostrophic wind at 155° relative to top of figure at 13 m/s.

visualized in Fig. 8, separated by the major mountain peaks. In Fig. 9 for example, there are strong offland flow near Yukutat and across the Malaspina Glacier oriented nearly 90 to the unobstructed flow shown in the southwest corner. For northwest winds (Fig. 10) there are channelled winds in the Icy Bay area and suggestions of an eddy in the vicinity of Yukutat. Both cases show extensive channelling and horizontal wind shear south of Yukutat, one of the main regions of anomalous winds indicated by the Coast Guard in Fig. 1.

By way of comparison, we reproduce Fig. 11 from Reynolds and Walter (1976) showing a sequence of offshore wind measurements made in November 1975. This data is roughly consistent with the 135 case shown in FIg. 9. Fig. 11 does not show the extent of over water influence near the Glacier as indicated by the measurements.

It is now apparent that one must take a closer evaluation of the contrast between the land and ice as well as land and water.

IV-4. Conclusions

It is obvious from the lack of direct verification and smoothness of some of the fields that further analysis is needed in each region for model results to be directly applied. However, the model has fulfilled its original goal of dynamic exploration and suggesting important regional patterns. The model is at the stage where it can be used as an aid to field observations in making an assessment of regional flow patterns near Icy Bay.

Its easy adaptability to any area makes the model an important

381
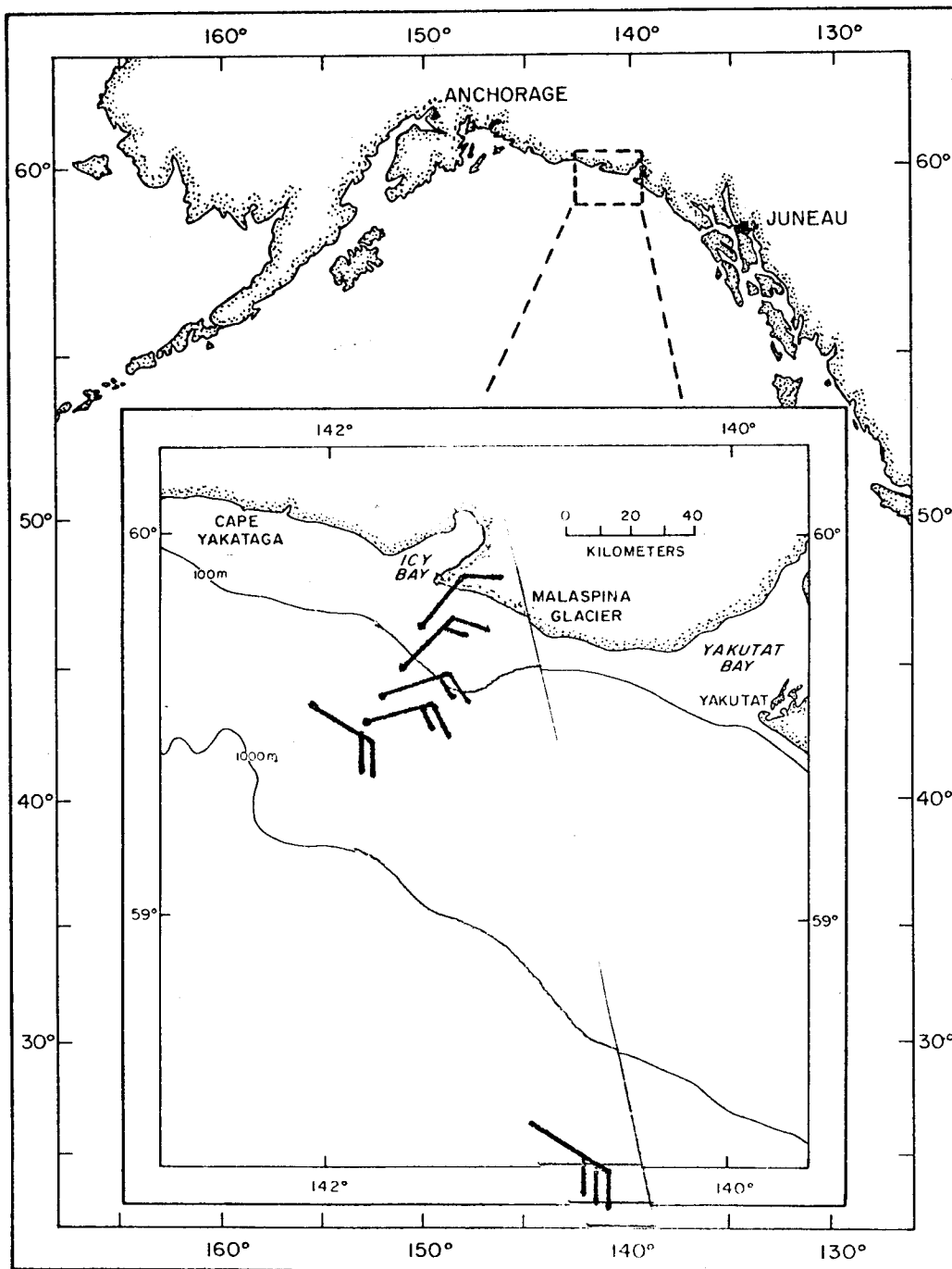
Figure 11. Icy Bay wind stations for geostrophic flow approximately 150° at 13 m/s (after Reynolds and Walter, 1976).

tool in recommending key locations for direct observations at other locations along the Alaskan coast.

SECTION V.   BERING SEA MODEL

V-1.   Introduction

The circulation of the Bering Sea is of particular interest because the region has great potential for the natural resources related industries such as fisheries, offshore mining industries, etc., and a thorough understanding of the current system in the sea is essential for the environmental assessment studies of the area.

Extensive studies of hydrographic data and a limited number of direct measurements indicate that the major currents in the sea are mainly driven by wind forcing, thermohaline forcing, interactions with the Pacific Ocean through numerous open passes along the Aleutian chain, and, to a limited extent, interactions with the Arctic Ocean through the Bering Strait. In addition, the bathymetry of the sea has been recognized as an important dynamical constraint. Our main effort has been to investigate the full, three dimensional structure of the currents using a numerical general circulation model which is sophisticated enough to include the above features. At the same time, we have constructed a simple diagnostic model to explore a certain aspect of the current system in the Bering Sea. We have

insert ⟶

made some preliminary calculations with this simple model. ∧ A brief review of the model and results is the subject of this report. A brief discussion of the mathematical model is presented in Section 2, together with the boundary conditions. Some preliminary results and their implications are discussed in Section 3.

Although this modeling effort is not being performed under BLM/OCSEAP sponsorship, it has potential relevance to the study of mass and momentum exchange near the shelf break, and is therefore included as a part of this report.

V-2. The Mathematical Model and Boundary Conditions

a. Model

The equations of motion for horizontal non-accelerated flow with a constant vertical eddy coefficient are:

$$-fv\rho_o = -\frac{1}{a\cos\phi}\frac{\partial p}{\partial\lambda} + \kappa\frac{\partial^2 u}{\partial z^2} \tag{1}$$

$$fu\rho_o = -\frac{1}{a}\frac{\partial p}{\partial\phi} + \kappa\frac{\partial^2 v}{\partial z^2} \tag{2}$$

The hydrostatic equation and the mass continuity equation are:

$$\frac{\partial p}{\partial z} = -g\rho_o \tag{3}$$

$$\frac{1}{a\cos\phi}\frac{\partial u}{\partial\lambda} + \frac{1}{a\cos\phi}\frac{\partial}{\partial\phi}(v\cos\phi) + \frac{\partial w}{\partial z} = 0 \tag{4}$$

In these equations spherical coordinates are used, with λ, ϕ, and z representing longitude, latitude, and height. The fluid is contained between the surface $z = \eta$ and the bottom $z = -H(\lambda, \phi)$. The model specifies two horizontal velocities and the pressure. The model assumes the fluid is homogeneous, thus the density ρ_o is a constant ($\rho_o = 1$.)

The boundary conditions are:

$$\kappa\,\rho_o\frac{\partial u}{\partial z} = \tau_c^\lambda, \quad \kappa\,\rho_o\frac{\partial v}{\partial z} = \tau_o^\phi \text{ and } W = \left(\frac{u}{a\cos\phi}\frac{\partial\eta}{\partial\lambda} + \frac{v}{a}\frac{\partial\eta}{\partial\phi}\right) \text{ at } z = \eta \tag{5}$$

$$\kappa\,\rho_o\frac{\partial u}{\partial z} = \tau_b^\lambda, \quad \kappa\,\rho_o\frac{\partial v}{\partial z} = \tau_b^\phi \text{ and } W = -\left(\frac{u}{a\cos\phi}\frac{\partial H}{\partial\lambda} + \frac{v}{a}\frac{\partial H}{\partial\phi}\right)$$

$$\text{at } z = -H(\lambda, \phi) \tag{6}$$

In (5) and (6) η is the free surface elevation; H is the depth of the sea; and τ_b^λ, τ_b^ϕ are the bottom stress components. Assuming that $\eta/H \ll 1$, we impose the boundary condition (5) at $z = 0$. Then the momentum equation (1) and (2) are vertically averaged to yield:

$$-f\bar{v} = -\frac{g}{a\,\cos\phi}\frac{\partial\eta}{\partial\lambda} + \frac{1}{H}(\tau_o{}^\lambda - R\bar{u}),\qquad(7)$$

$$f\bar{u} = -\frac{g}{a}\frac{\partial\eta}{\partial\phi} + \frac{1}{H}(\tau_o{}^\phi - R\bar{v})\qquad(8)$$

where

$$u = \frac{1}{H}\int_{-H}^{0}\rho_o u\,dz\qquad(9)$$

$$v = \frac{1}{H}\int_{-H}^{0}\rho_o v\,dz\qquad(10)$$

In (7) and (8) the component bottom stresses are taken as $R\bar{u}$ and $R\bar{v}$ where R is the coefficient of friction.

Integration of the continuity equation (4) with boundary conditions (5) and (6) yields:

$$\frac{1}{a\,\cos}\frac{\partial}{\partial\lambda}\left(\int_{-H}^{0}u\,dz\right) + \frac{1}{a\,\cos\phi}\frac{\partial}{\partial\phi}\left(\cos\phi\int_{-H}^{0}v\,dz\right) = 0\qquad(11)$$

Equation (11) simply states that the vertically integrated flow is horizontally nondivergent, which guarantees the existence of a stream function ψ such that

$$\bar{u} = \frac{1}{H}\int_{-H}^{0}u\,sz = -\frac{1}{a}\frac{1}{H}\frac{\partial\psi}{\partial\phi}\qquad(12)$$

$$\bar{v} = \frac{1}{H}\int^{0}v\,dz = \frac{1}{H}\frac{1}{a\,\cos\phi}\frac{\partial\psi}{\partial\lambda}\qquad(13)$$

Substituting (12) and (13) into (7) and (8), and applying the cur_z operator, defined by

$$cur_z(q_1, q_2) = \frac{1}{a\,\cos\phi}\frac{\partial q^2}{\partial\lambda} - \frac{\partial}{\partial\phi}(q_1\,\cos\phi)\qquad(14)$$

and simplifying by eliminating a factor of $1/(a^2\cos\phi)$, we get:

$$R \frac{\partial}{\partial \lambda}\left(\frac{1}{H^2 \cos\phi} \frac{\partial\psi}{\partial\lambda}\right) + \frac{\partial}{\partial\phi}\left(\frac{\cos\phi}{H^2} \frac{\partial\psi}{\partial\phi}\right) + \frac{\partial}{\partial\phi}\left(\frac{f}{H}\right)\frac{\partial\psi}{\partial\lambda} - \frac{\partial}{\partial\lambda}\left(\frac{f}{H}\right)\frac{\partial\psi}{\partial\phi}$$

$$= \frac{\partial}{\partial\lambda}\left(\frac{\tau_o^\phi}{H}\right) - \frac{\partial}{\partial\phi}\left(\frac{a\cos\phi}{H}\tau_o^\lambda\right) \qquad (15)$$

Eq. (15) is an inhomogeneous, linear, elliptic, second-order partial differential equation for the stream function ψ. For a given bathymetry $H(\lambda, \phi)$ and a prescribed surface stress distribution $\tau_o^\lambda(\lambda, \phi)$, $\tau_o^\phi(\lambda, \phi)$ it can be solved numerically by the relaxation method. It should be noted, however, that the highest order terms involve a small friction parameter R, and thus special care must be taken to maintain stability of the numerical method. This will be discussed in (c).

b. Surface Wind Stress and Open Boundary Conditions

Wind stress can be estimated by conventional drag law methods if the surface wind is known. Unfortunately, wind measurements over the Bering Sea are very sparse in space and time, since they generally come from a handful of ship stations. For the numerical model, therefore, wind stress is computed from surface pressure data. First, monthly mean pressure data provided by the National Climate Center, was interpolated quadratically from $5° \times 5°$ grid mesh into the model grid mesh $2°$ (long.) $\times 1°$ (lat.). The interpolated pressure data was then used to estimate geostrophic wind velocity, and the wind velocity at anemometer height was obtained by multiplying the geostrophic wind speed by a factor γ and changing the geostrophic wind direction by an angle α. The constant γ here is 0.7 while α is $19°$.

387

Strictly speaking, synoptic maps should be used in estimating wind stress as the variable part of the pressure could increase the wind stress estimate through the non-linearity of the drag law. In fact, the study by Aagaard (1970) strongly suggests that the stress computed from the monthly mean pressure could be easily underestimated by a factor of 2 or 3. On the basis of this study, we multiplied the monthly mean stress by 3.0 for the model calculation.

The annual mean wind stress was computed by averaging 12 months of wind stress data. This is shown in Figure (1). The computed monthly mean wind stress patterns for January and August are shown in Figures (2) and (3). The January map shows a typical winter pattern which is characterized by the northeasterly stress associated with a strong high pressure center over Siberia and a low pressure center over the North Pacific Ocean. On the other hand, the stress pattern in August (Figure (3)) shows a very weak stress over most of the sea, and somewhat stronger southwesterly stress over the southeast part of the basin. In general, the wind forcing in summer is weaker in order of magnitude than in winter.

At the open boundaries of the grid, estimates of vertically integrated transports are required. The model has four open boundaries along the Aleutian - Commander Island Arc: Kamtchatka Strait, Commander - Near Strait, Central Aleutian Pass and Western Aleutian Pass. Also the Bering Strait is modelled as an open boundary. The widths and depths of the open boundaries are adjusted to match the observed bathymetry within the limits imposed by grid resolutions.

WINDSTRESS VECTOR PLOT

1 DYNE/SQ CM
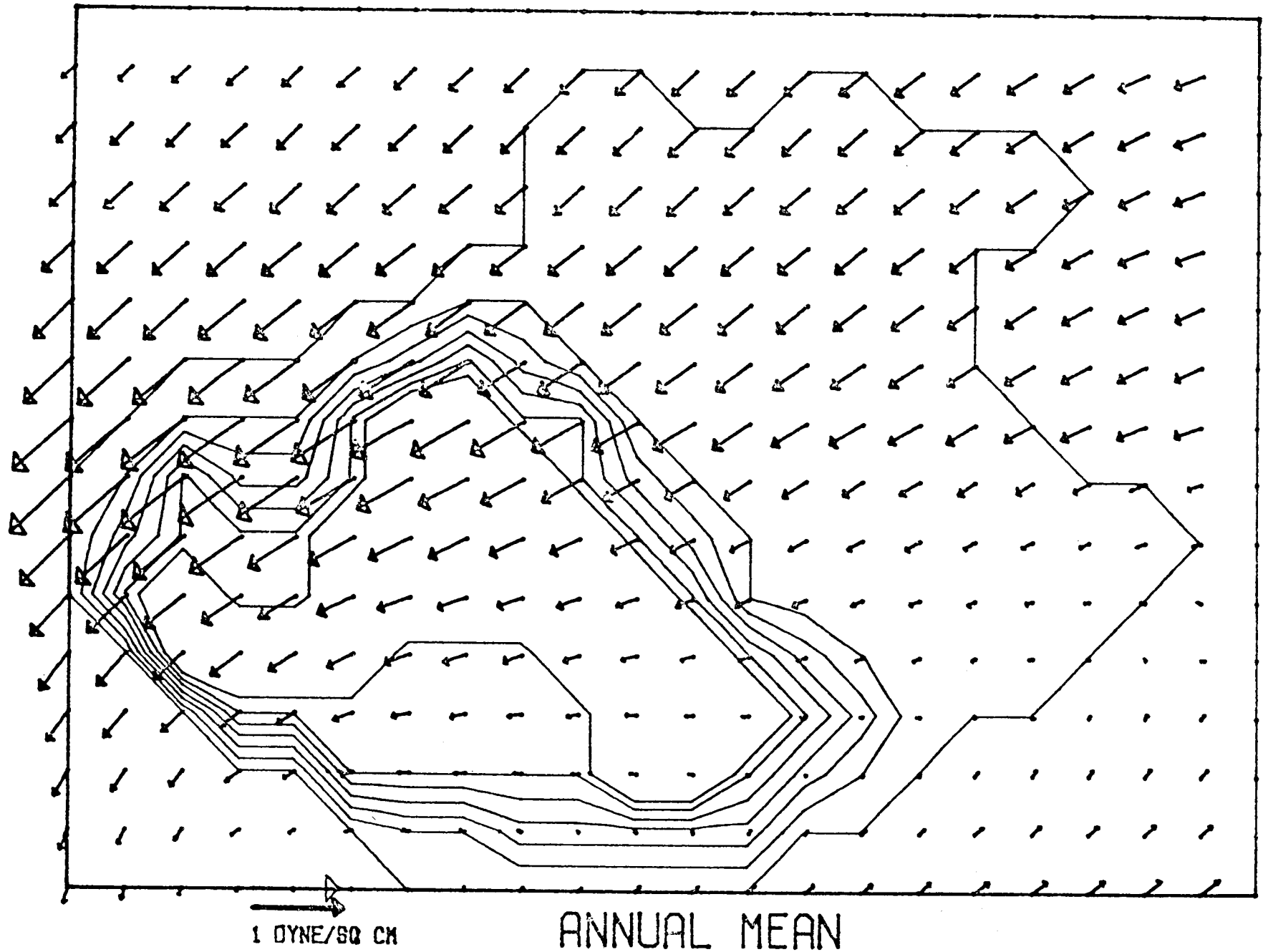
ANNUAL MEAN

Figure 1. Annual mean wind stress vector plot for the Bering Sea.

WINDSTRESS VECTOR PLOT

JANUARY MEAN

1 DYNE/SQ CM

390
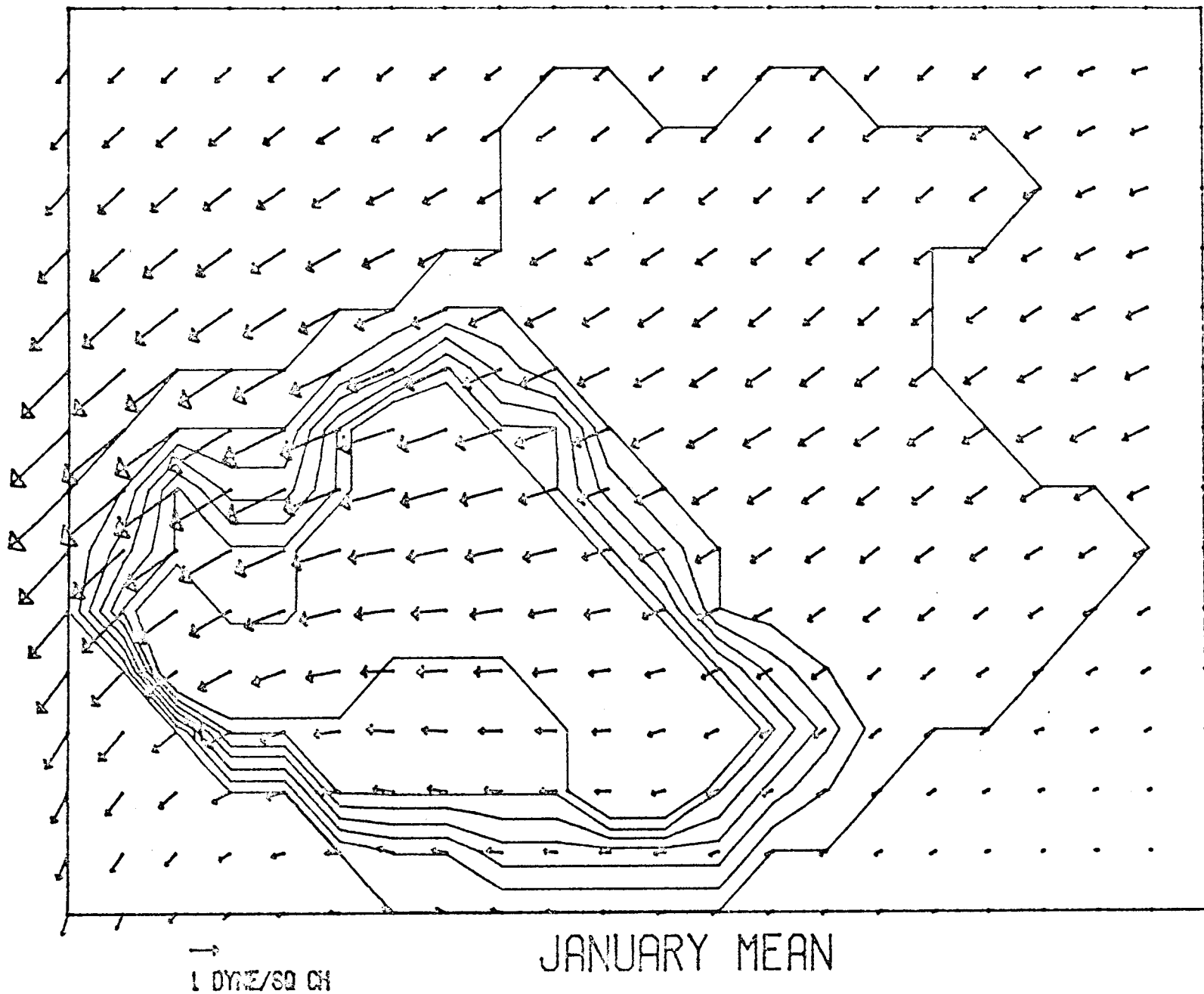
Figure 2.   January mean wind stress vectors for the Bering Sea.

WINDSTRESS VECTOR PLOT

1 DYNE/SQ CM
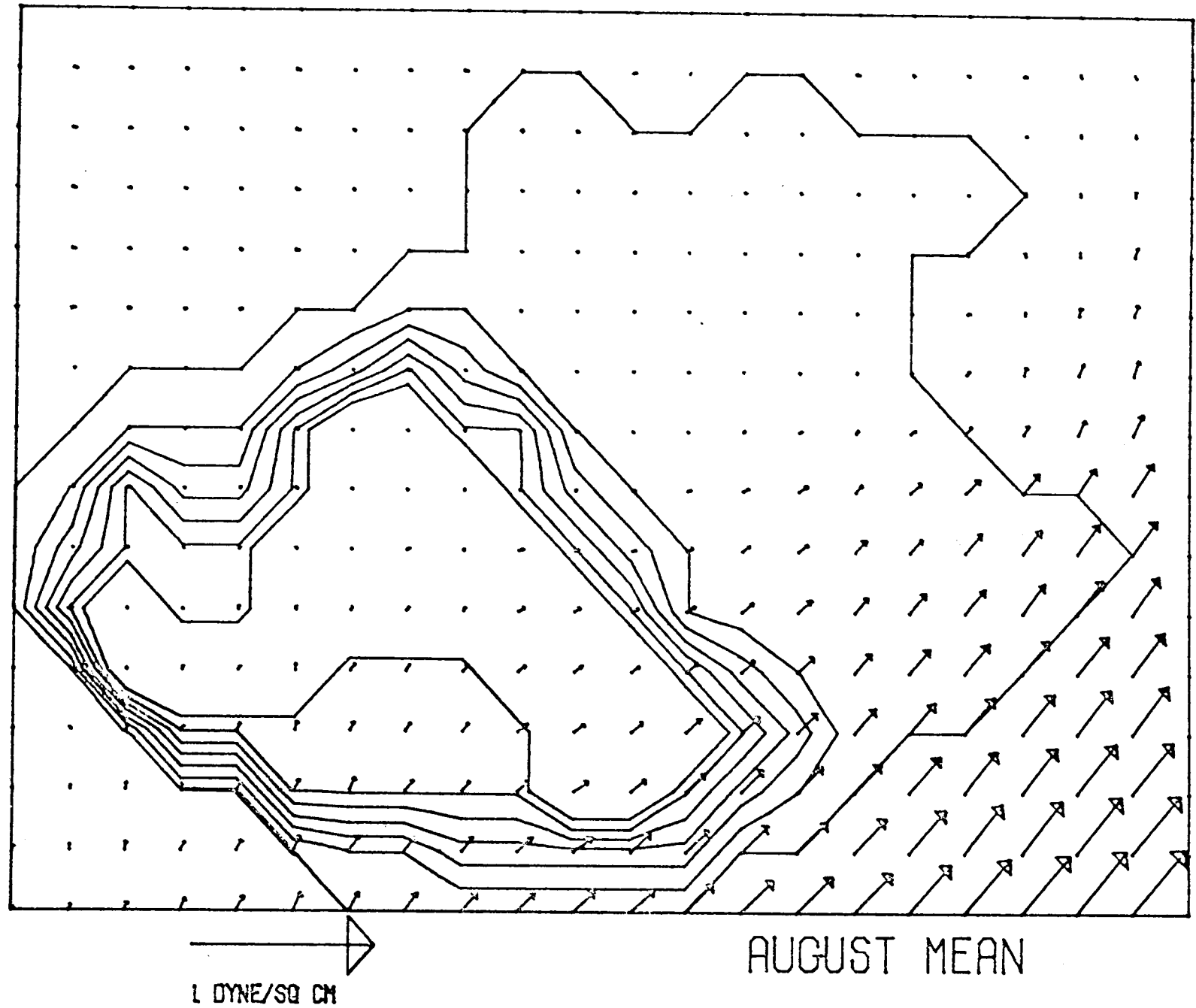
AUGUST MEAN

Figure 3. August mean wind stress vectors for the Bering Sea.

Integrated volume transport values on the open sections are chosen from various estimates presently available. It should be mentioned however, that at the present stage, there are many uncertainties in transport estimates at the various passes.

The chosen values of (annual mean) transports are given in Table (1). A net transport of 18sv outward through the Kamtchatka Strait is in close agreement with an estimate of 18.4sv by Arsenev (1967) and summer values (20sv) by Hughes et al, (1974). A net transport of 14sv inward across the commander - near Strait was taken from Arsenev (1967) which is greater than an estimate (10sv) by Favorite (1974) but less than Hughes et al (25sv). The total inflows through the Western and Central Aleutian are based on the estimates made by Arsenev (1967). For the Bering Strait, the total transport (1sv) outward was chosen from the estimate (1.1sv) by Arsenev (1967).

c. Numerical Procedures

We write the basic equation (15) in a compact form using Cartesian coordinate:

$$R \wedge^2 \psi + A \frac{\partial \psi}{\partial x} + B \frac{\partial \psi}{\partial y} = \phi \qquad (16)$$

where we denoted the right side of equation (15) ϕ. In (a) we have mentioned that Eq. (15) is the equation with small parameters at highest order terms. The shortcomings of the ordinary relaxation method for such an equation has been discussed by Sarkisian (1972) and Ilin (1969). For the present calculation, we adopted the method by

392

Table 1.

Mass transports at open boundaries

Kamchatka Strait	− 18sv.*
Commander − Near Strait	+ 14sv.*
Western Aleutian Pass	+ 4sv.
Central Aleutian Pass	+ 1sv.
Bering Strait	− 1sv.

* − Outward

+ Inward

Sarkisian (1972) "method of directional differences". The essence of the method is quite simple: derivatives of the first order terms are substituted for the difference forward and backward, depending on the sign of coefficients, in such a way that diagonal terms possess maximum weights. The diagonal dominance of the matrix then guarantees convergence of the iteration method.

The only drawback of the method of directional difference is a computational viscosity. According to Sarkisian, however, the accuracy of the solution for a particular example is within 10% when it is compared with the solution obtained by a more accurate method by Marchuk (1973).

V-3. Results and Suggestions

Solutions were obtained first for the case of annual mean wind stress together with specified mass inflow - outflow along the boundary. Solution for each twelve month period were also obtained, but since the results are still in the process of verification, we will very briefly discuss a few sample calculations and defer detailed analysis for another report.

With an annual mean wind stress from the general direction of northeast, contours of the streamfunction for the whole Bering Sea Fig. (4) show a strong cyclonic gyre in the western half of the deep basin. Transport in the eastern shelf region is less than 2sv. $(2 \times 10^6 m^3/sec)$. It is noted that the stream lines follow the bathy-
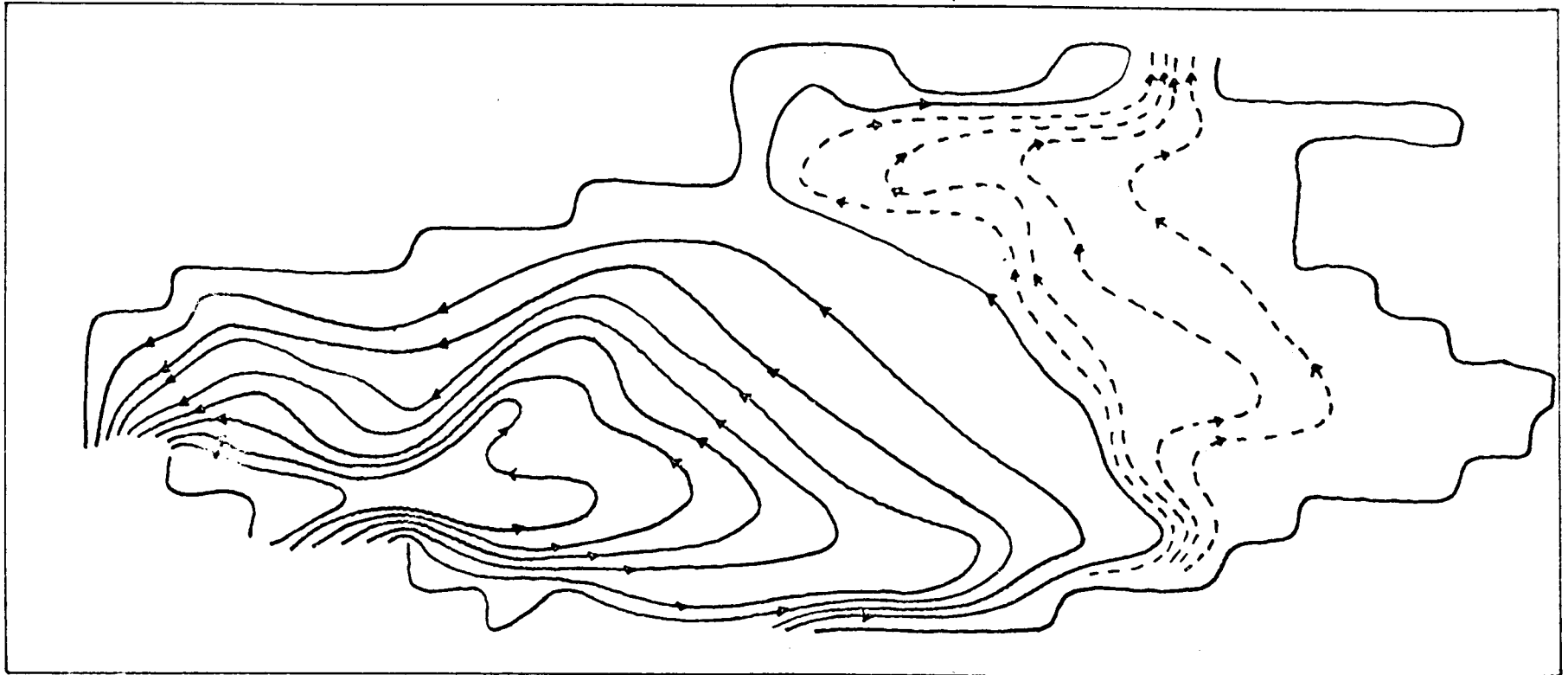
Figure 4. Circulation in the Bering Sea due to the annual mean wind with boundary source and sinks.

Transport Contours ——— 2.0 Sv (10^6 m^3/sec.)
--- 0.2 Sv

metry closely, indicating a topographic control of the flow by the dynamic constraint of potential vorticity. Fig. (5) shows vertically averaged velocity vectors for the annual mean case. The flow speed over the shelf is significantly stronger than in the deep basin due to shallowness of the shelf. To show a clearer picture of the circulation pattern in the deep basin, that portion was magnified and is shown in Fig. (6). Again, the velocity vectors clearly show a tendency to follow the bathymetry. To illustrate the flow characteristics in two different seasons, sample calculations for January and August are shown in Fig. (7) and (8). Although the general cyclonic gyres in the deep basin are maintained in both seasons, the intensity of the cross basin transport along the shelf break is significantly different depending on the season. Furthermore, the deep basin circulation in January shows three closed gyres which are conspicuously absent in August.

To investigate the direct influences of wind forcing and sources and sinks separately, two controlled experiments were made; one with wind forcing (annual mean) only (Fig. 9), and the other one with a source-sink only (Fig. 10). It is interesting to note that the August circulation is very similar to the one with the source-sink only. This might indicate that the circulation in summer is primarily driven by the mass source-sink specified along the boundary . It is also noted that the closed gyres in the deep basin in January are direct consequences of wind forcing, which showed up clearly in the experiment with wind forcing only.

396

VELOCITY VECTOR PLOT
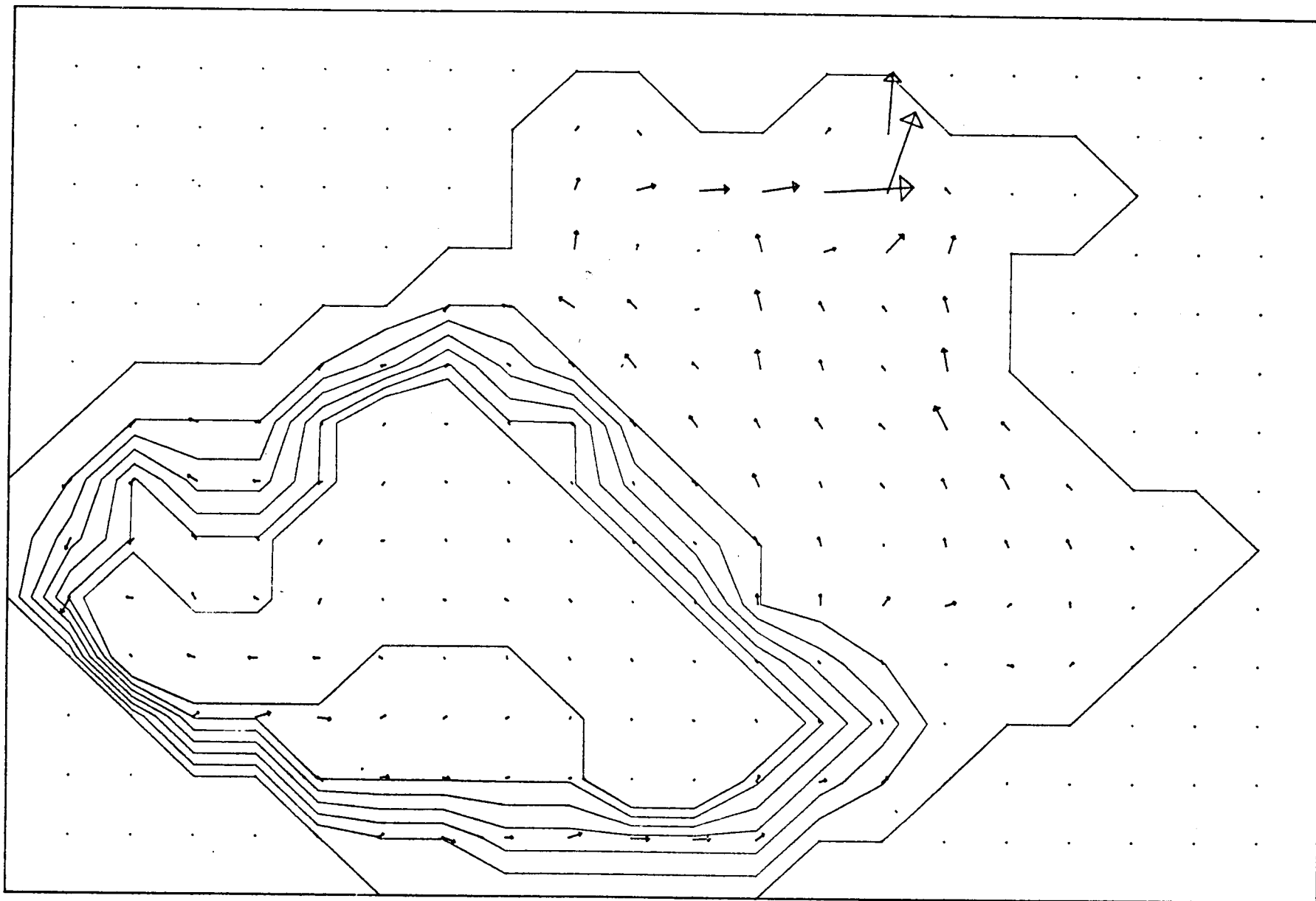
10CMETERS

Figure 5.   Vertically averaged velocity vectors for the annual mean case in the Bering Sea.

VELOCITY VECTOR PLOT

10 CM PER
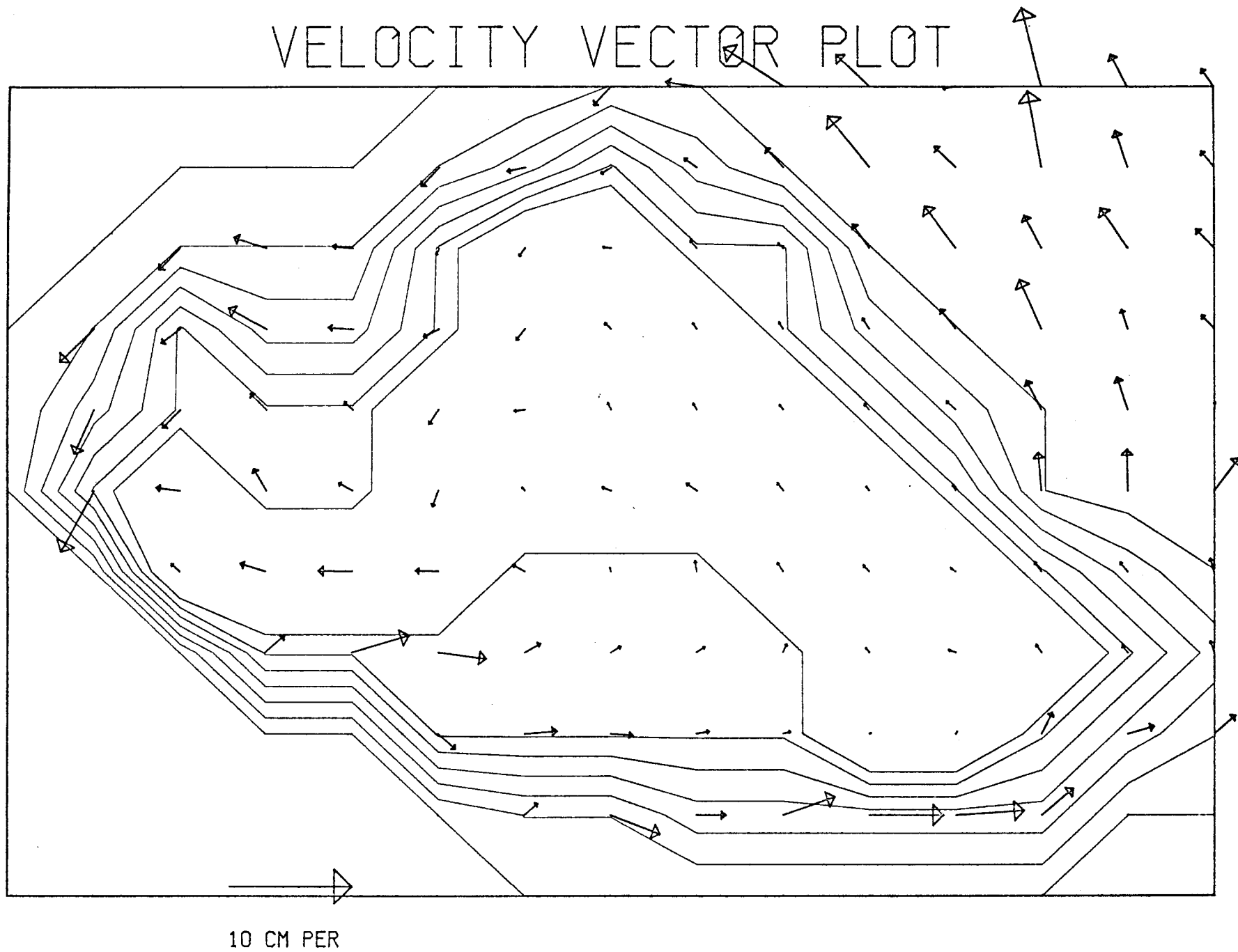
Figure 6.   Circulation pattern for the deep basin in the Bering Sea for the annual mean case.
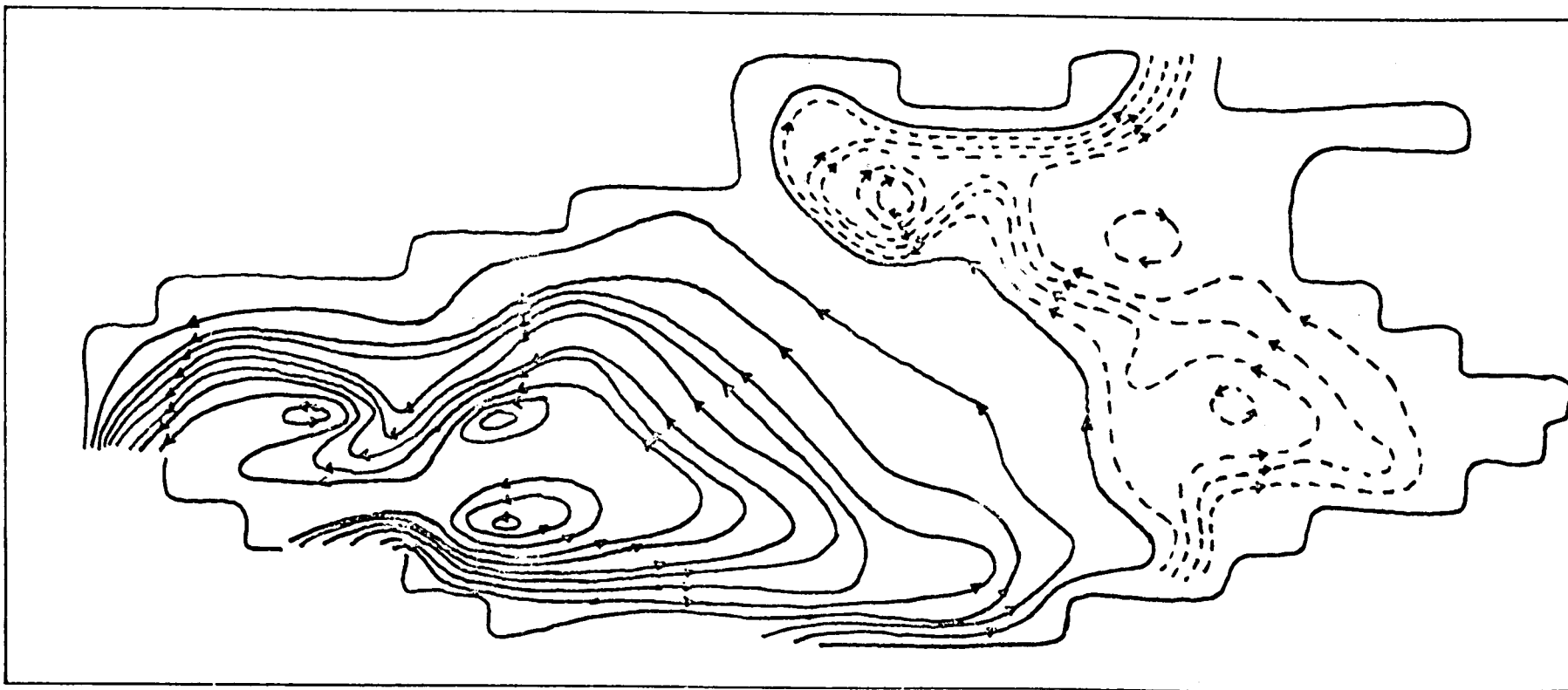
Figure 7. Circulation in the Bering Sea due to the January wind with boundary source and sinks. Transport Contours —— 2.0 Sv ($10^6 m^3$/sec.)
--- 0.2 Sv
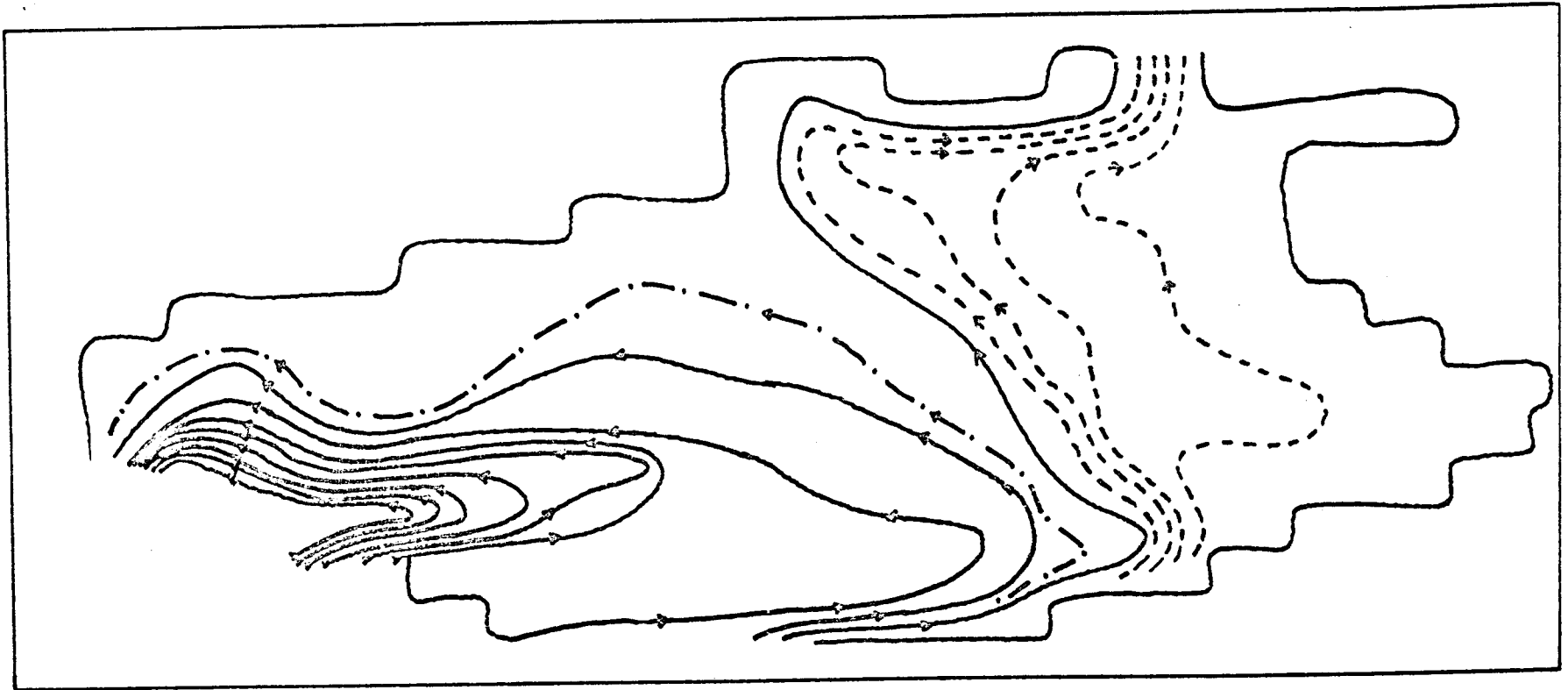
Figure 8. Circulation in the Bering Sea due to the August wind with boundary source and sinks.
Transport Contours —— 2.0 Sv ($10^6 m^3$/sec.)
—·— 1.0 Sv
——— 0.2 Sv
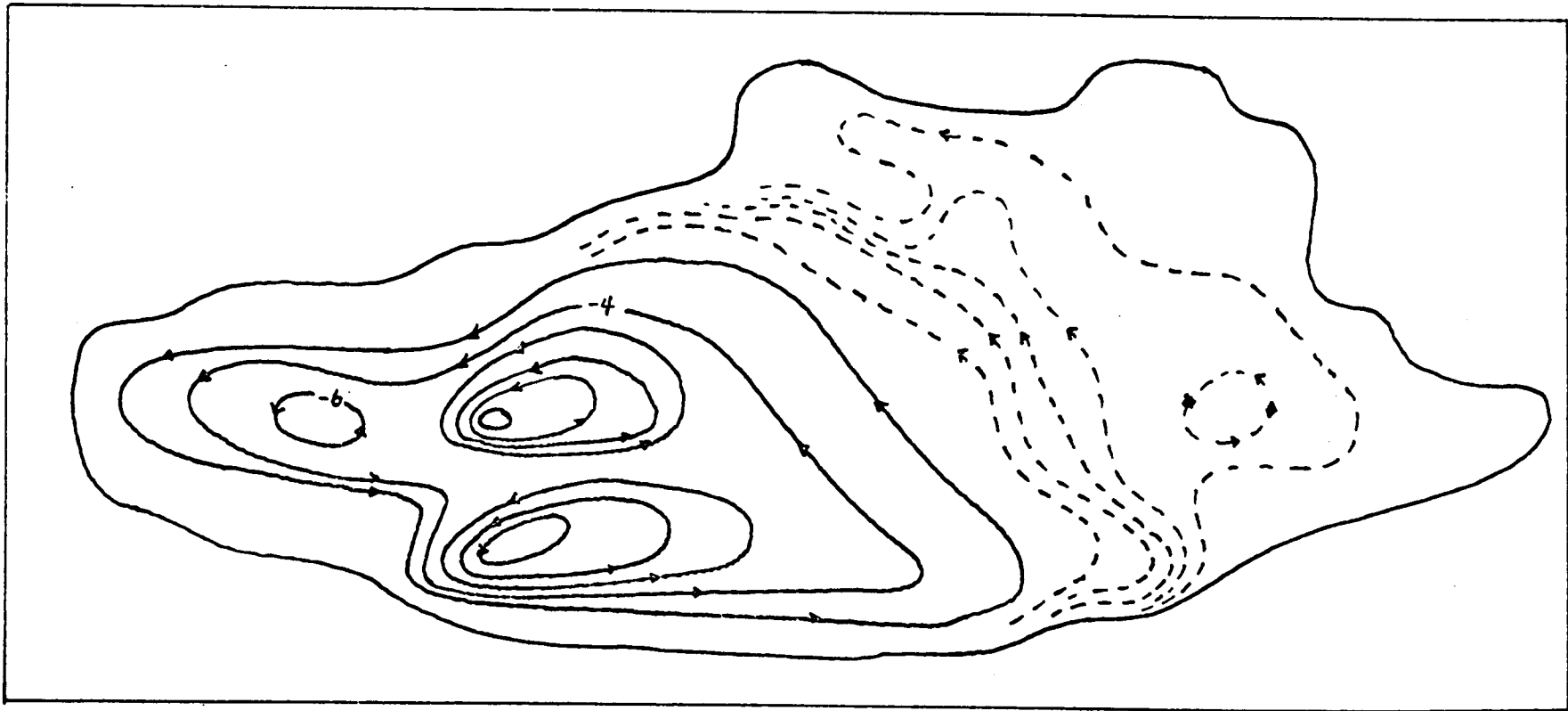
Figure 9.   Circulation in the Bering Sea due to the annual mean wind only.
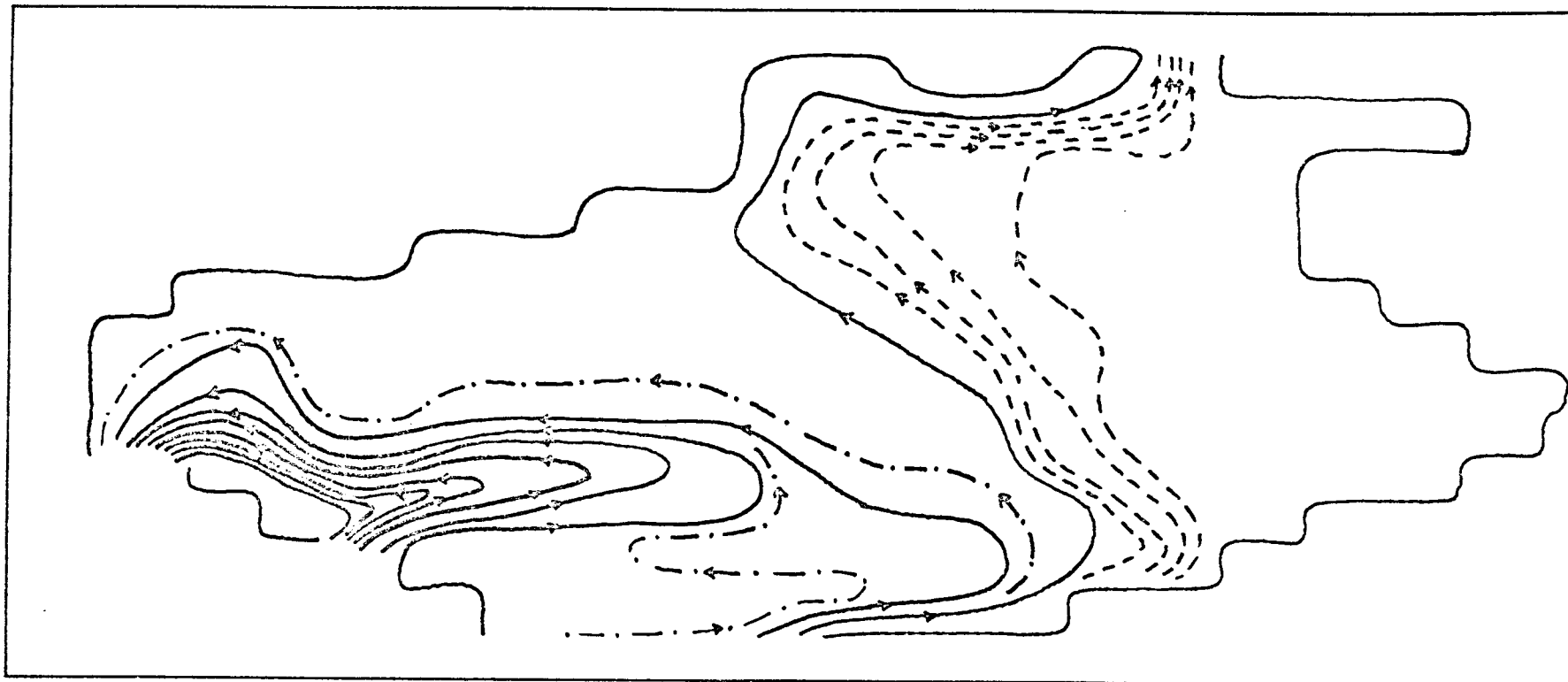
Figure 10. Circulation in the Bering Sea with sources and sinks only.
Transport Contours —— 2.0 Sv ($10^6 m^3$/sec.)
-.- 1.0 Sv
--- 0.2 Sv

It is suggested, based on the preliminary analysis above, that a simple model such as this can be valuable for exploring some fundamental physical processes in the Bering Sea. On the other hand, it must be recognized that the real ocean is baroclinic, and these results should be considered only a general guide in an effort to construct the full three-dimensional circulation pattern of the sea.

SECTION VI. STATUS OF COMPUTER

VI-1. Introduction

Graphics output is the most effective means of communicating the results of a numerical model run. The variables are embedded in a multidimensional space, and important features are geometrical or topological properties that must be "seen" to be understood. We have assembled a data processing system intended primarily for the storage and maintenance of graphic information; this system is integrated with other computer systems via telecommunications network links. Hardware development is nearly complete. System software development to fully utilize the equipment will require a minimum of an additional year. Applications software development, in particular an oil spill trajectory model, is underway.

VI-2. Hardware

The graphics system consists of

1. A 40 x 60 inch Talos graphic input tablet for map digitizing,

2. A Tektronix 4051 graphic calculator with tape cassette drive and a joystick.

3. A Tektronix 4662 plotter for hard copy plotting.

4. A DEC PDP-11/34 computer with 64k words of memory (32k currently installed), and 6m byte disk capacity (4m bytes installed).

5. A hard-wired serial communications link to the PMEL PDP-11/55 computer.

6. And a dial-up telephone port.

The peripheral devices all communicate via serial transmission lines. The dial-up telephone port will allow remote execution of a numerical model from any telephone (with suitable terminal equipment).

VI-3. Software

The manufacturer's RSX-11M operating system is used for all data processing functions. The computer is operated in a time-shared multi-programmed mode. This means that a number of programs run simultaneously, sharing resources. Program development, graphics input/output, data preparation, numerical model runs, and remote job operations can proceed at once.

A number of system modifications and extensions are being undertaken to support the particular set of peripheral devices in the system, and the special requirements of the modeling program. Because the applications programs are written under the DEC RSC11-M operating system, they are compatible with the DEC RSX11-D operating system on the PMEL PDP-11/55 with which the modeling computer can communicate via network software over a serial communications channel. The PDP-11/55 has a large disk capacity, magnetic tape drives, and other useful peripherals.

Because graphics is the heart of our man/machine inferface, a great deal of attention has been given to providing a rich set of graphics primitives. Improvement, integration, and simplification of these programs will continue to be a major objective.

SECTION VII. REFERENCES

Danard, 1975: A Numerical Model for Surface Winds in Juan de
        Fuca, Haro, and Georgia Straits. Report to Atmospheric
        Environment Services, Downsview, Ontario.

Lavoie, 1972: "A mesoscale numerical model of lake-affected storms."
        J. Atmos. Sci. 29, 1025-1040.

Lavoie, 1974: "A numerical model of tradewind weather on Oahu".
        Mon. Wea. Rev. 102, 630-637.

Reynolds and Walter, 1976: "Nearshore Atmospheric Modification"
        Annual Report to OCSEAP 1976.   Research Unit #347.

Shuman, 1957: "Numerical Methods in Weather Prediction: II Smoothing
        and Filtering" Mon. Wea. Rev. 85   357-361.

Second Annual Report

BRISTOL BAY OCEANOGRAPHIC PROCESSES (B-BOP)

J. D. Schumacher

R. L. Charnell

Pacific Marine Environmental Laboratory
Environmental Research Laboratories, NOAA

and

L. K. Coachman

Department of Oceanography
University of Washington

I. SUMMARY

Beginning in autumn 1975, investigations were begun in Bristol Bay to address environmental questions brought forward by the potential petroleum development of the Outer Continental Shelf. This work has been sponsored by the Outer Continental Shelf Environmental Assessment Program (OCSEAP). Hydrographic data have resolved a picture of the bay, characterizing the bay with three zones: Bering Shelf break water, Central Shelf water, and Coastal water. The Bering Shelf is oceanic in nature, and the Central Shelf water is highly stratified and bounded on the shoreward perimeter by a structure front separating it from a well-mixed coastal water. Current meter records can be characterized as dominantly tidal with low net flow. The net flows, however, confirm the counterclockwise flow around the shoreward perimeter of the Bay and the northwest flow along the slope. Winter circulation is poorly resolved; however, current reversals and phase differences in low-frequency periodicity are suggested. Heat budget analyses have been preliminarily examined and bottom-mounted pressure gage and atmospheric data have been collected.

II. INTRODUCTION

A. Objective

The objective of this work unit is to relate oceanic advective and diffusive processes to potential pollution problems due to OCS petroleum development. The two specific goals are:

1. To describe the general water circulation in the study area for both summer and winter regimes; and

2. To determine the spatial and temporal variability of the velocity field and obtain indications of spatial coherence.

B. Tasks

1. Hydrographic data acquisition. This task reflects the response to better define the density field in the light of previous efforts. Higher density sampling in the area of the structure front separating the regions of coastal water and Central Shelf water was undertaken to better delineate the magnitude and structure of the front. This task was undertaken to further delineate the now identifiable water mass distributions with associated differences in dynamics.

2. Current meter data. This task is required to describe the spatial and temporal variability at specific sites within the identified water masses of Bristol Bay. In particular, this task will attempt to obtain an estimate of spatial coherence in the velocity field on the scale of the bay.

3. Pressure gage data. This task is required to interpret sea-level perturbation time and length scales in relation to current dynamics. The effort is directed toward understanding meteorological effects on the circulation as a response to storm surge or as a potential driving mechanism for longer termed pulses observed.

4. _Meteorological data_. This task is required for correction of pressure gage information to determine the true oceanic response to storms. This requires the correlation of barometric pressures around the bay to determine the scale of meteorological events and their relation to the low-frequency currents.

Data from these activities will allow a description of the seasonal circulation throughout Bristol Bay in the light of its water mass structure. Also, in shorter time scales these activities will yield information on the variation in tidal current energies due to interference with locally generated internal tides. Such occurrences may lead to periods of locally low kinetic energy, thus reducing mixing. A better understanding of driving mechanisms for circulation will likewise follow from the combined density field, current meter, and pressure gage information.

C. Application to Petroleum Development Hazard Assessment

You are referred to the 1975 Annual Report for a description of the evolution of spilled oil in seawater. Present work relates to the location and duration of events discussed in that review. Each water mass as identified in last year's annual report will have its own effect on the history of petroleum contamination. The quiescent, highly stratified shelf region   might allow more time for volatiles to escape and cause a concentration of higher density particles to form at the interface between the two layers. This may allow a longer term effect on neritic and planktonic life forms with a long elapsed time before reaching the benthic zone at the bottom. If a source of contamination was located in the lower layer of the shelf area, a very long residence time could be expected, with the corresponding effect on benthic organisms. The stability of the area would also

restrict the surfacing of contaminants to the very low density components which would tend to volatilize upon reaching the surface. The well-mixed coastal region would allow a uniform contamination of the water column with a shorter elapsed time before reaching the bottom environment. Also, the residence time in the coastal water areas would be long, due to low mean flow. The Bering Sea Slope Current area along the shelf break is more oceanic in nature and the advection of contaminants there would be greater, though the advective flow pattern for the shelf break is still ill-defined.

III. STUDY AREA

This research unit addresses the physical oceanography of Bristol Bay (fig. 1). This area is defined as the area south of a line drawn between Nunivak Island and the Pribilof Islands and east of a line drawn between the Pribilof Islands and Unimak Pass. This region encompasses approximately 150,000 km^2. The average depth is approximately 55 m, with 50% of the area less than 50 m in depth. The area can be characterized as an equilateral diamond with the points oriented north-south and east-west. The 50-m contour bisects the area along a northwest-southeast line from the midpoint of the Pribilof-Nunivak line to Port Moller, with a departure from that line at the Alaskan Peninsula in the form of a shallow valley projecting three-quarters of the distance toward the easternmost point.

Freshwater input is primarily from the Kuskokwim River watershed which enters at the midpoint of the northeast line. The Kuskokwim accounts for about 50% of the freshwater runoff, and the balance enters from the watersheds of many smaller rivers in the eastern portion of the area. The total freshwater input amounts to approximately 1% of the volume of Bristol Bay.

For 5 months (November-March), about 60% of the area is ice-covered. The ice is 1-year winter ice, generally less than 1 m thick. Ice formation begins in sheltered areas in mid-October and builds to the most severe conditions in February and March. A general northward retreat of the ice begins in April. A representative contribution of freshened water due to sea-ice melt is about 0.6% of the volume of Bristol Bay.

The combined effect of ice melt and freshwater runoff is to charge the bay with fresher water, first in the early spring and again in midsummer, such that an equivalent of 1.5% of the volume is replaced in the space of 7 months. The character of the bay should show distinctly different regimes
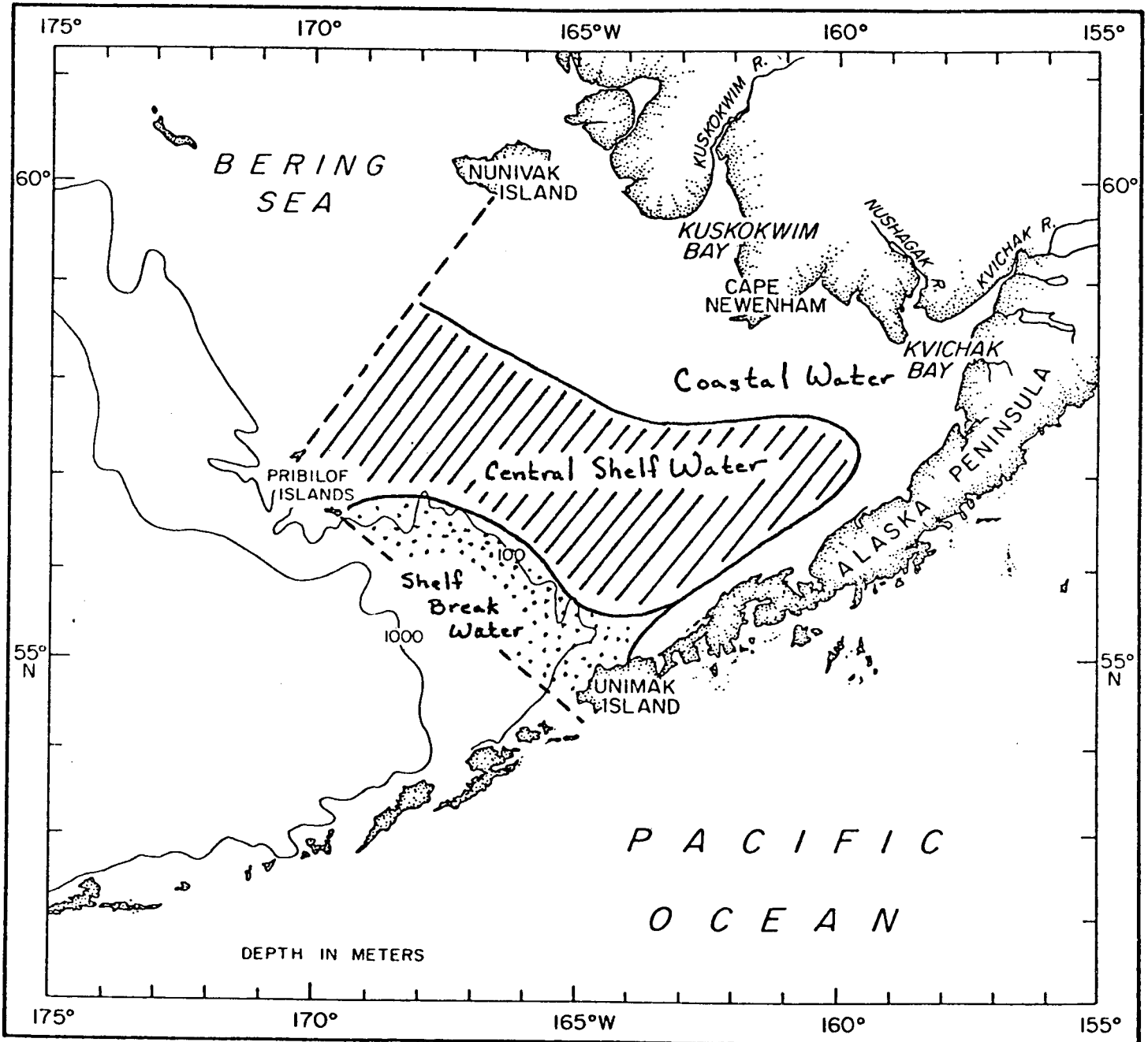
Figure 1

in summer and winter due to the very different conditions in those two seasons. It is reasonable to expect some marked differences between the information gathered in the two years of the program in that the 1975-76 season was very heavy in ice and the 1976-77 season is quite light in ice. The difference in the 1975-76 and 1976-77 seasons indicates that year-to-year differences could be substantial. At present there is insufficient information available to determine the range of year-to-year differences in a normal, or average, sense.

The connection with the western Gulf of Alaska waters is through Unimak Pass at the southern point of the area. Exchange with the Bering Sea waters can take place along the entire southwestern line of the area. Exchange along the northwestern line would be with the adjacent shelf of similar character. It would seem reasonable that the nature of all the exchanges will vary significantly with the varying environmental conditions on a year-to-year basis.

IV. PRESENT STATUS

A summary of oceanographic data collected prior to the initiation of the OCSEAP effort has been presented in the first annual report. The additions to the data base due to the OCSEAP effort have been considerable.

The hydrographic data summary (Appendix 1) reveals 12 cruises collecting CTD data under summertime conditions. It is evident from the cruise distribution that wintertime data is difficult to obtain, though it is sorely needed to complete the hydrographic picture. The figures in Appendix 1 describe the track lines during CTD cruises and show the broad scope of hydrographic data acquisition.

The summary of instrumented moorings (Appendix 2) outlines the density of current and bottom pressure data being collected. To date, 30 moorings have been deployed over 17 sites (fig. 2).

B-BOP

MOORING LOCATIONS
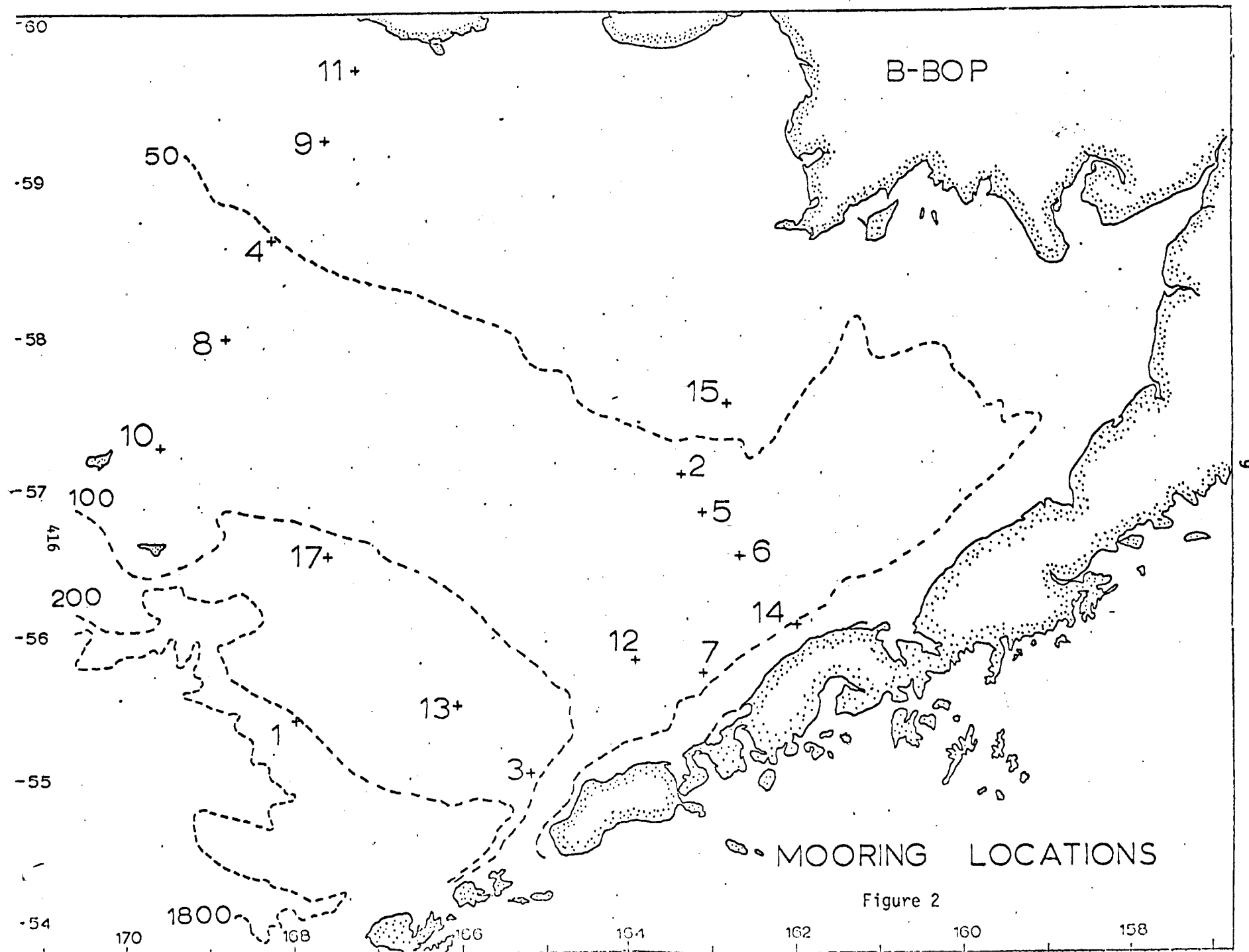
Figure 2

V. PROGRAM RATIONALE

To address the goals of this work unit, three long-term moored arrays, BC-2, -3, and -4, were maintained over the winter to assess flow under the ice and obtain information on the winter circulation.

Short-term arrays, BC-5, -6, -7, -8, -9, -10, -12, -13, -14, and -15, were deployed to better define the summer circulation by measuring currents flowing into and out of the bay. In addition, the arrays at BC-5, -6, and -4 were spaced to address cross-bay spatial coherence length scales.

VI. HYDROGRAPHY

Hydrographic data from June 1976 has been analyzed (Kinder, 1977, attached), and the major results are summarized.

1. The waters of the shelf are more clearly characterized by differences in vertical structure than by traditional temperature-salinity (water mass) categories. We propose three regions of stratification (during summer): coastal, shelf, and shelf break. The depth of water is the major factor influencing the distribution of vertical structure. The distribution of temperature and salinity is similar to those reported by Dodimead, et al. (1963), which was based on Redwing data from 1938-1941. Our data, however, reveal smaller scale features not shown by the earlier data.

2. Temperature fine structure was found throughout the shelf break region; this is probably related to the density instabilities reported by Coachman and Charnell (1977, attached).

3. The front, near the 50-m isobath, first noted by Muench (1976), has been confirmed. We believe that the balance between the rate of buoyancy input and the rate of tidally induced mixing determines the frontal location.

4. Salinity distributions and dynamic topographies show that the most intense flow is in the shelf break region and that the flow is to the northwest, paralleling the isobaths. Salinity distributions also suggest some flow into the bay along the Alaska Peninsula.

5. A high-salinity anomaly was found west of Cape Newenham.

We consider Kinder (1977) a preliminary report, and we continue to analyze this data and to investigate the seasonal changes over the shelf.

Coachman and Charnell (1977, attached) have reported on fine structure found in the shelf break region during March 1976. The widespread distribution of temperature fine structure suggests that the situation they found in March is not rare.

VII. CIRCULATION

As a first step in displaying the circulation within Bristol Bay, the vector mean flow for each mooring was calculated and plotted on figures 3 and 4. The records were loosely characterized as "winter" or "summer" (table 1). Caution must be exercised in interpreting this form of display because varying record lengths, overlapping seasons, and different depths are all displayed on the same figure. Nonetheless, displaying the net vectors yields a qualitative description of the general circulation.

Examining the summer net vectors, a number of general statements are indicated. The central shelf area is quiet when compared to the shelf break or coastal water shoal. The strongest flows are indicated at the shelf break, BC-3, with significant components along the shelf break and into the Bay. Flow has been postulated along the Aleutian Islands flowing to the northeast and joining with flow entering the Bering Sea through Unimak Pass. In the vicinity of station 3, the flow bifurcates and flows both along the shelf break and into Bristol Bay along the Alaskan Peninsula. The area of inflow to the bay is generally ice-free during winter, and the hydrographic data indicate tongue-like features projecting into the bay; these facts lend support to the existence of the inflow along the peninsula. The shelf break flow is well confirmed by the northwest flow at station 13. The highest percentage of transport must be along the shelf break due to the consistency of flow from the upper to the lower levels. The small fraction which enters Bristol Bay would seem to manifest itself as a narrow flow counterclockwise around the bay near the 50-m isobath, as indicated by the records at stations 14 and 15. The breadth of the current would be considerably less than 100 km, particularly along the peninsula where it would be constrained by the coast to a width of 50 km. The location of the current may be associated with the location of the structure front separating the coastal waters and the shelf area.

Table 1

Mooring	Observation Period	Instrument Depth (m)	Record Length (days)	Mean Speed (cm s^{-1})	Total Variance (cm^2 s^{-2})		Net Flow (cm s^{-1})
BC-2A Winter	8 Sept. 75– 5 Nov. 75	20	58		u 323.4 v 112.9	436.3	0.5 @ 305°T
		50	58				0.9 @ 306°T
BC-2B Winter	5 Nov. 75– 30 May 76	50	207	17.6	u 330.6 v 76.8	407.4	1.2 @ 089°T
BC-2C Summer	31 May 76– 26 Sept. 76	24	118	14.8	u 281.8 v 66.9	348.7	0.8 @ 324°T
BC-3A Winter	6 Nov. 75– 16 Mar. 76	20	130	29.1	u 435.3 v 595.1	1030.4	3.3 @ 010°T
BC-3B Summer	16 Mar. 76– 29 May 76	105	73	17.4	u 251.7 v 185.3	437.0	1.2 @ 342°T
BC-3C Summer	29 May 76– 28 Sept. 76	16	122	31.8	u 441.3 v 581.8	1022.1	17.2 @ 011°T
		100	122	20.5	u 265.6 v 270.4	536.0	6.7 @ 358°T
BC-4A Winter	7 Sept. 75– 4 Nov. 75	30	58	29.5	u 470.2 v 468.9	939.1	2.7 @ 297°T
		47	58	22.1	u 269.9 v 267.1	537.0	0.6 @ 315°T
BC-4B Winter	4 Nov. 75– 14 June 76	20					
BC-4C Summer	1 June 76– 25 Sept. 76	25	56	27.6	u 415.0 v 423.0	838.0	2.6 @ 312°T
		52	59	19.6	u 244.0 v 198.0	442.0	1.3 @ 301°T
BC-5A Summer	30 May 76– 27 Sept. 76	15	119	12.5	u 212.3 v 59.1	271.4	0.5 @ 192°T
		45	119	30.6	u 1182.1 v 202.6	1384.7	0.1 @ 345°T

Table 1 (Continued)

Mooring	Observation Period	Instrument Depth (m)	Record Length (days)	Mean Speed (cm s^{-1})	Total Variance (cm^2 s^{-2})		Net Flow (cm s^{-1})
BC-6A Summer	30 May 76 27 Sept. 76	20	120	11.3	u 219.3 v 43.3	262.6	0.6 @ 012°T
		50	120	16.6	u 392.7 v 59.0	451.7	1.0 @ 038°T
BC-8A Summer	1 June 76- 31 July 76	26	59	21.8	u 277.0 v 269.0	546.0	0.9 @ 088°T
		54	59	22.0	u 296.0 v 253.0	549.0	0.6 @ 342°T
BC-9A Summer	2 June 76- 31 July 76	17	59	27.8	u 424.0 v 417.0	841.0	0.1 @ 160°T
		27	59	24.7	u 352.0 v 355.0	707.0	0.3 @ 255°T
BC-12A Summer	19 Mar. 76- 12 June 76	39	84	9.1	u 155.0 v 44.0	199.0	0.6 @ 277°T
		87	14	14.3	u 262.0 v 87.0	349.0	1.3 @ 232°T
BC-13B Summer	6 June 76- 29 Sept. 76	100	35	17.3	u 231.8 v 143.7	375.5	1.6 @ 366°T
BC-14A Summer	30 May 76- 27 Sept. 76	21	124	21.4	u 721.0 v 123.7	844.7	3.5 @ 070°T
		40	124	11.9	u 299.9 v 57.4	357.3	0.8 @ 233°T
BC-15A Summer	31 May 76- 26 Sept. 76	20	118	28.8	u 695.5 v 259.0	954.5	2.4 @ 274°T

Summer
MOORING LOCATIONS

B-BOP

Figure 3

Figure 4

Winter MOORING LOCATIONS
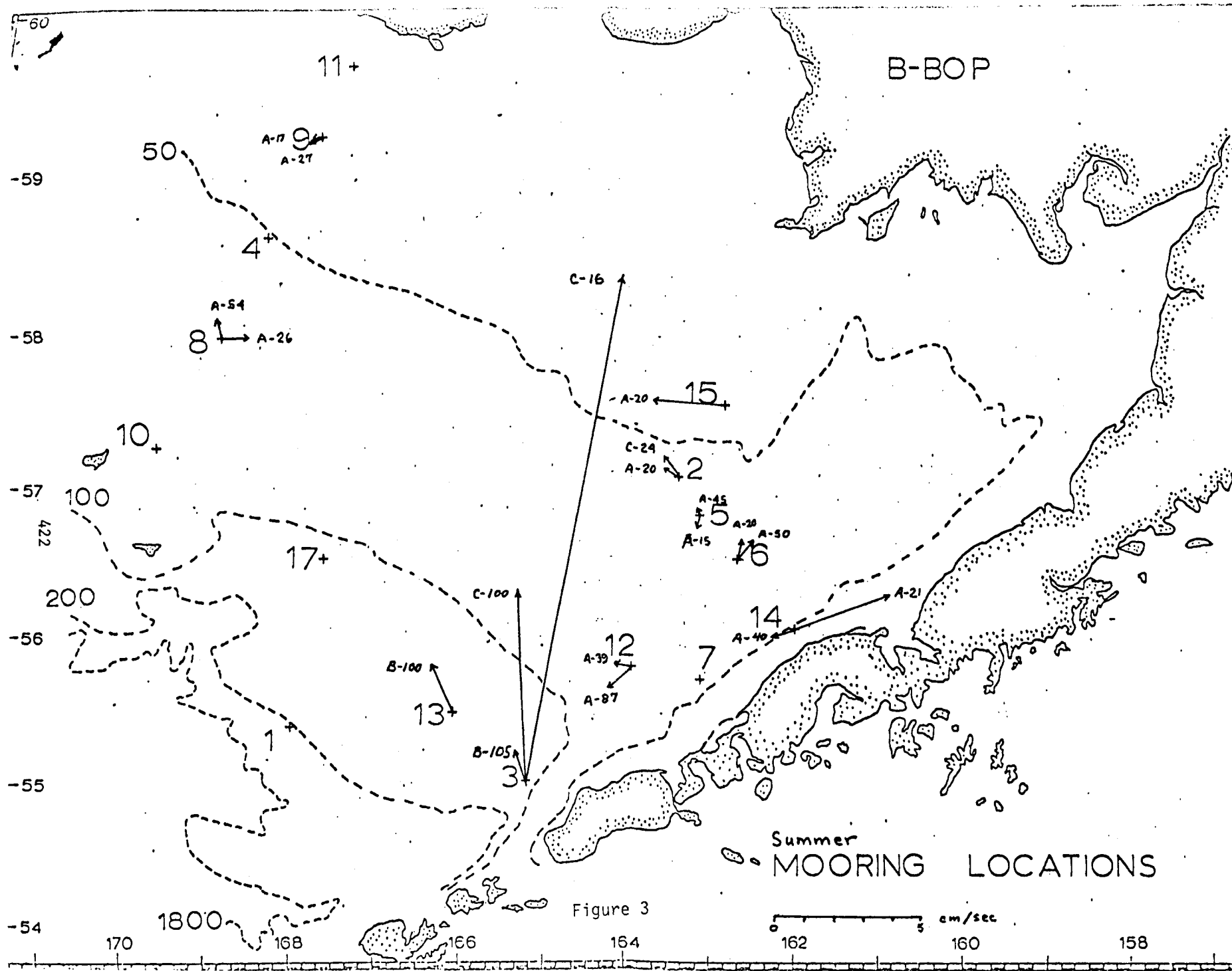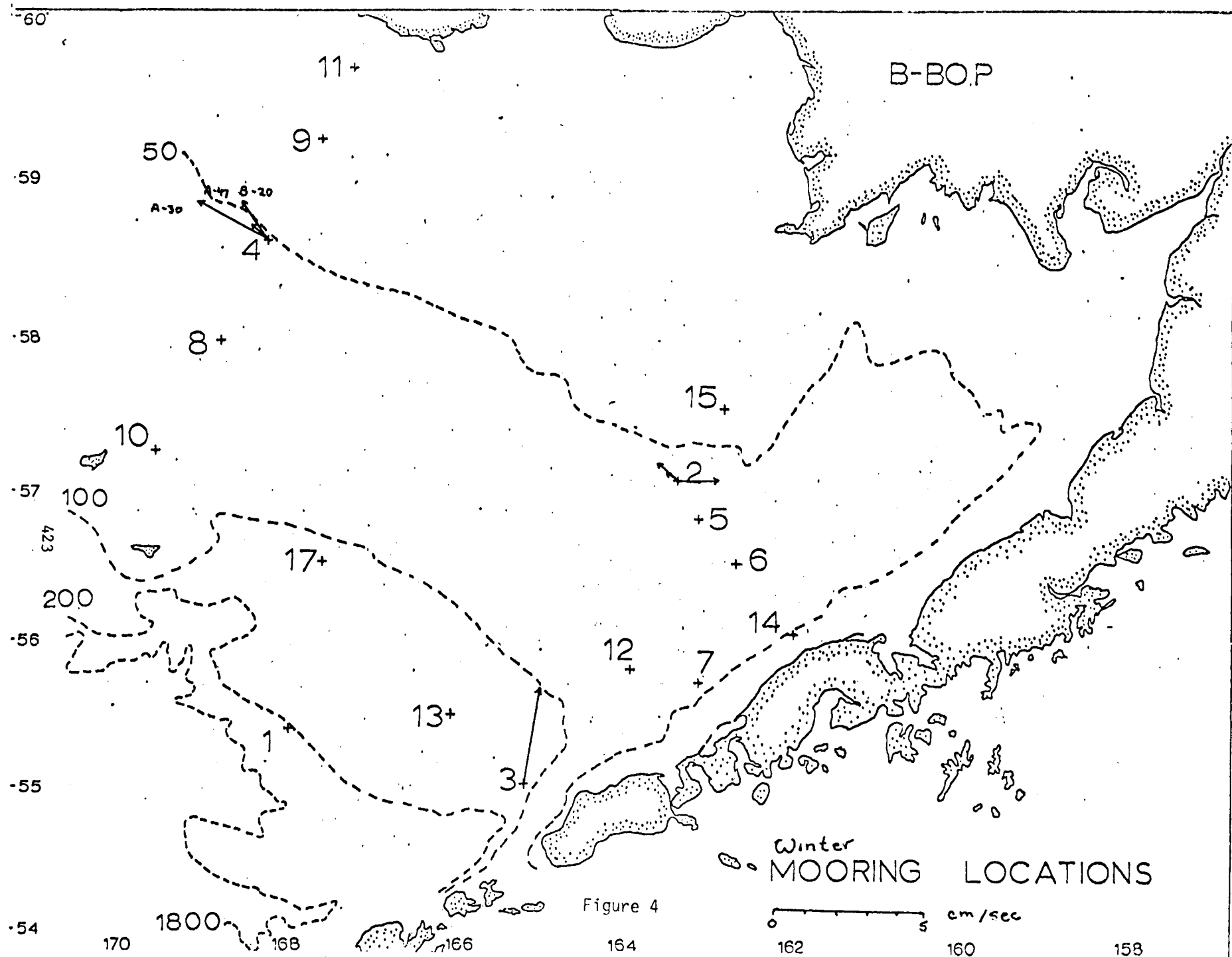
The front is generally found in the vicinity of the 50-m isobath. Current meter records from stations near the front show generally stronger flow than those distant from either side of the front. Currents away from the frontal area have net flows a third or less of the frontal stations. These low net velocities are a manifestation of generally high mean speeds with no consistent direction (figs. 5a and b). The net velocities do, however, represent the general drift, transport, of water in the area. This fact leads to the possibility that there exists a return flow, or displacement of bottom water out of the bay along the Alaskan Peninsula.

Winter records indicate inflow near Unimak Pass as in the summer records, lending support that this is the consistent picture. Outflow from the bay is indicated between Nunivak Island and the Pribilofs in the same vicinity and the front location in summertime. The interior records, however, do little to define the flow in the central reaches of the bay. Due to the lack of hydrographic data from under the ice, little speculation can be made concerning the details of the winter flow.

A. Low-Frequency Flow

The next logical step in understanding the flows within the bay is to examine the motions on a weekly time scale. This time scale allows the better resolution of seasonal changes and system responses. An attempt to interpret the low-frequency events will consist of examining the weekly averages to allow the history of each station to be characterized with regard to the hydrography.

Temperature provides the longest and most voluminous data set (fig. 6). A full year of records has been obtained from station 2. This station reveals a bit of the history of the shelf area. During the fall of 1975, the area was stratified with upper layer temperatures consistent with summer heating
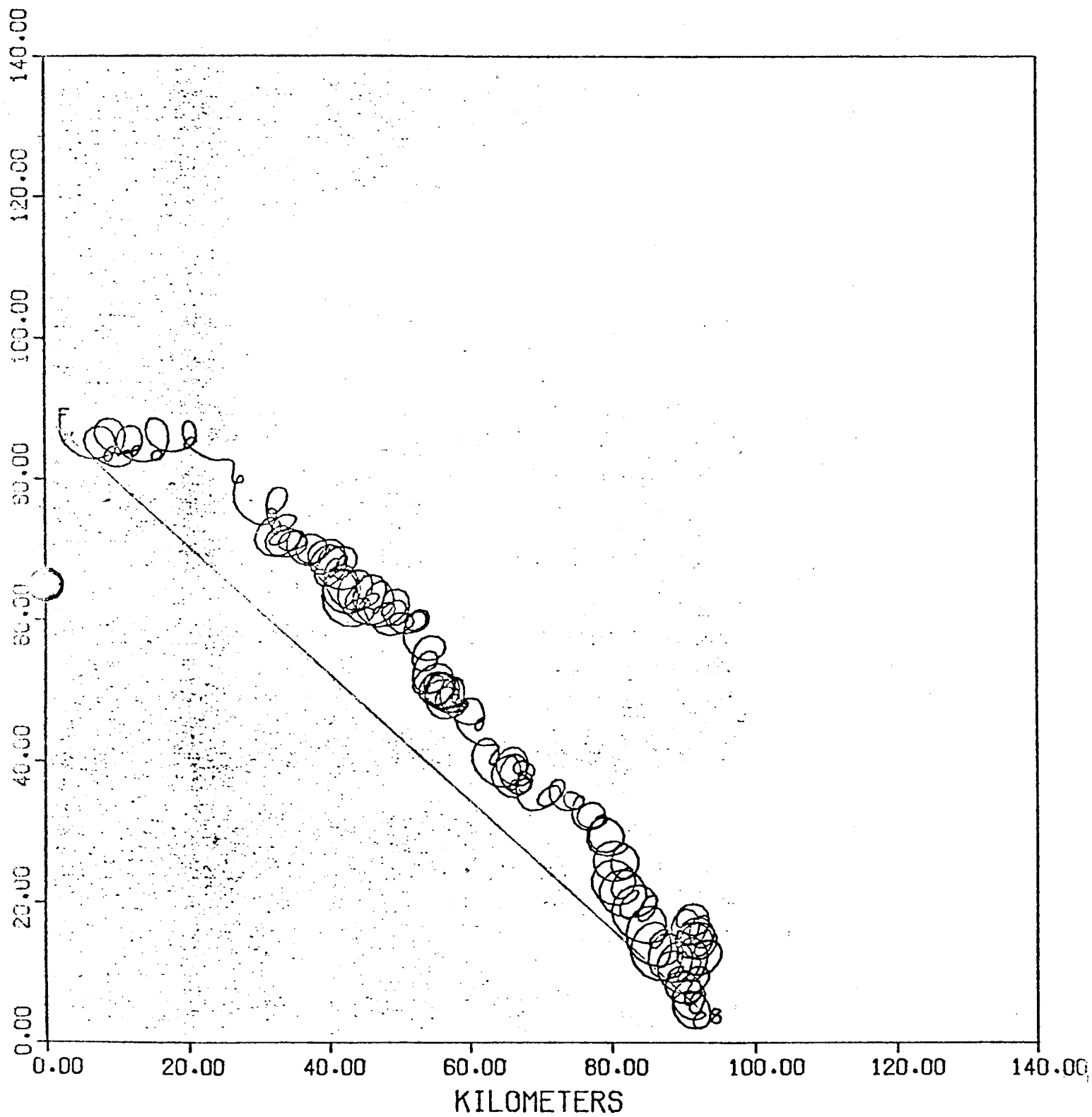
Figure 5b
PVD Station 4C depth 25 meters

425
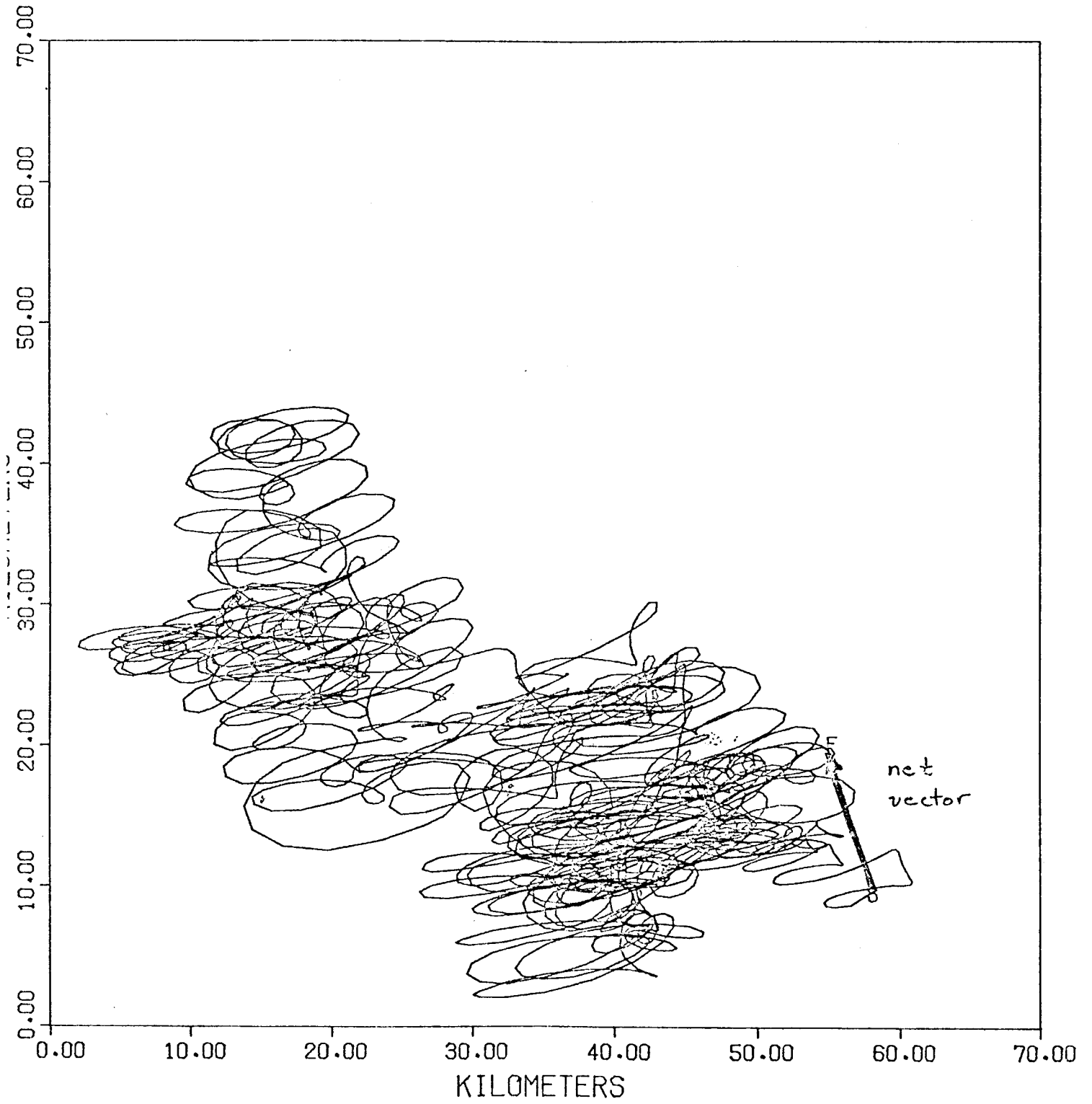
Figure 5a
PVD Station 5A depth 50 meters

TEMPERATURE-CURRENT METER STATIONS
BRISTOL BAY 1975-1976
7 DAY AVERAGES
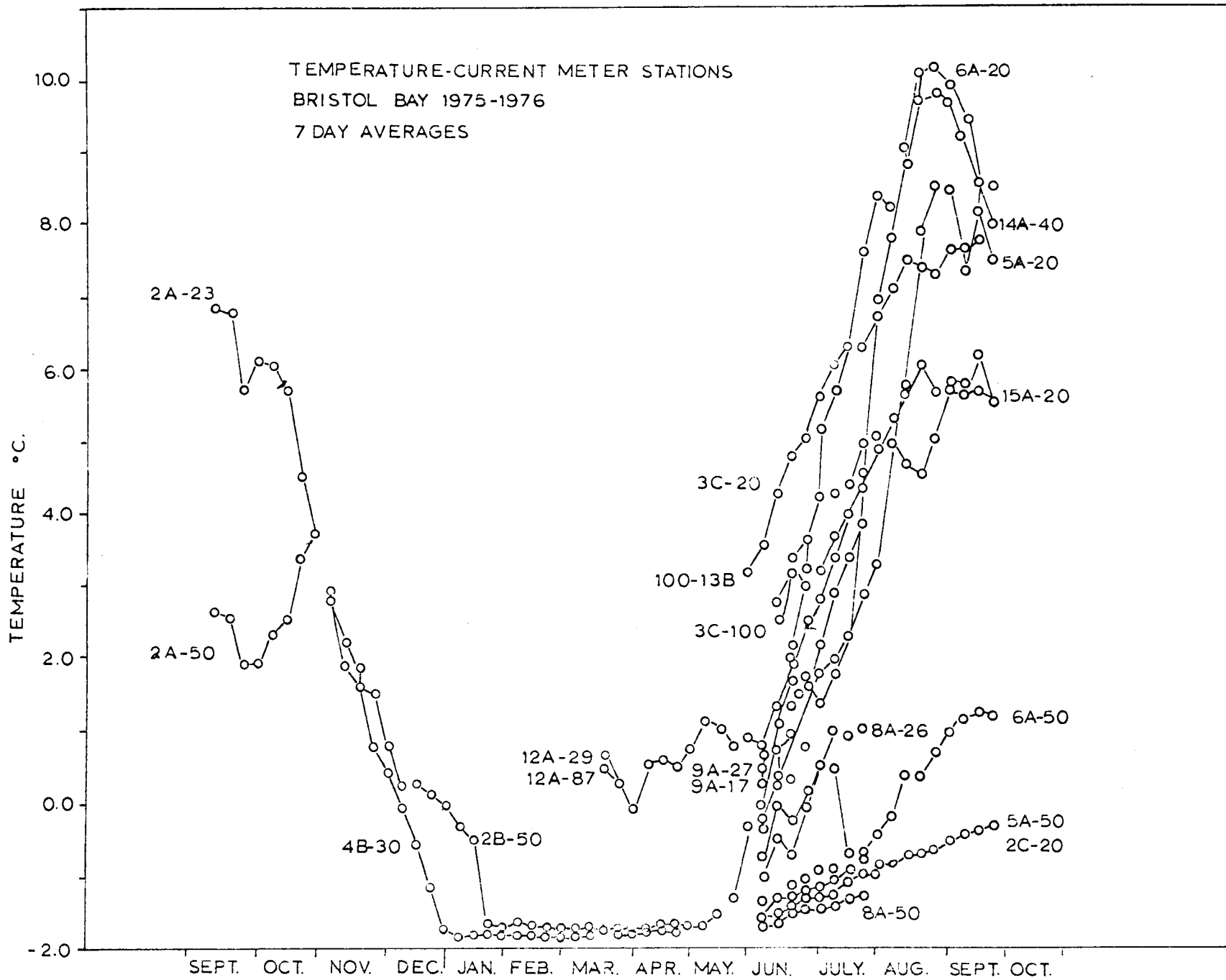
FIGURE 6

and lower layer temperatures slightly warmer than those of the summer of 1975, which would indicate a mild winter the season before, 1974. The surface waters cooled with the onset of winter and the lower waters warmed slightly, possibly due to the reduced stability, until early November when the water became isothermal. The point at which the water became isothermal has two possible explanations: either the stability was reduced to the point where the general region could be fully mixed by the winds and tide, or the front passed laterally across the station. Through the winter, stations 2 and 4 were in place and continued monitoring events. The waters over the majority of the bay continued cooling at nearly the same rate. A satellite photo from 10 December 1975 shows the formation of loose ice with many leads. The temperature record indicates the ice was fully formed and stabilized about the first of January. The ice remained over the central area until late May 1976, as characterized by water temperatures of -1.8, which is the freezing point of 32 $^o/_{oo}$ seawater. At the end of May, the seasonal heating began again over the entire bay. The summer heating at all stations along the shelf break and in the shallow mixed areas progressed at nearly the same rate regardless of depth.

In the shelf area the upper layers warmed as at the other stations, but the lower layers were effectively isolated from the seasonal heating. In the lower layer the increase in temperature over the summer was only 3°, while the upper layer warmed by 12°. The fact that waters offshore were considerably warmer and waters in the coastal region were likewise warmer substantiates the concept of very little lateral exchange with the shelf area lower layer. The hydrographic data from the summer of 1976 shows a very strong thermocline at 23 m, and this is reflected in the records of those current meter stations which had current meters just below the thermocline,

such as station 4 at 25 m and station 2 at 24 m, which had records similar
to those from stations with records from 50 m in the convective area.

Salinity (fig. 7) has a much smaller seasonal range in Bristol Bay than
might be expected considering the freshwater input from ice melt and runoff
in the summer. Salinities computed from the current meter's conductivity
sensors are not highly accurate, but the changes measured indicate events
passing the meter. Over the entire array of current meter measurements the
total salinity difference was two parts per thousand. Generally the varia-
tion at any one site was less than half a part per thousand. Further, the
largest changes occurred at those stations on the shelf break or vicinity,
such as stations 3 and 14. Within the shelf area, the upper layers showed
more variation than the lower layers, as expected. The largest change in
salinity at any one station occurred at station 15 toward the end of the
summer of 1976, indicating the transport of the low-salinity water from the
Kivichak River westward. Near the end of July there was a general decrease
in salinity at the shelf break stations and in the upper layers of the shelf
area of 0.1 to 0.3 parts per thousand, which could have been the response
to a major storm. The meters at station 3 and 14 indicated an increase of
0.2 parts per thousand in August, with the increase occurring at station 3
a few days before station 14. This again supports the view of inflow along
the Alaskan Peninsula. Thus salinity reveals no major seasonal effects, but
does give some insight into individual events.

The existence of periodic events in the current field are best illustrated
by the current records themselves. The weekly averaged "speeds," the averages
of the observed current magnitudes, are illustrated in figure 8. The pre-
dominant feature of the plot of mean speeds is the strong monthly periodicity
and the apparent separation into two levels of activity. The overall range
in mean speed is 40 cm/s with a dominant periodic variation of 10 cm/s.

SALINITY - CURRENT METER STATIONS

BRISTOL BAY   1975-1976
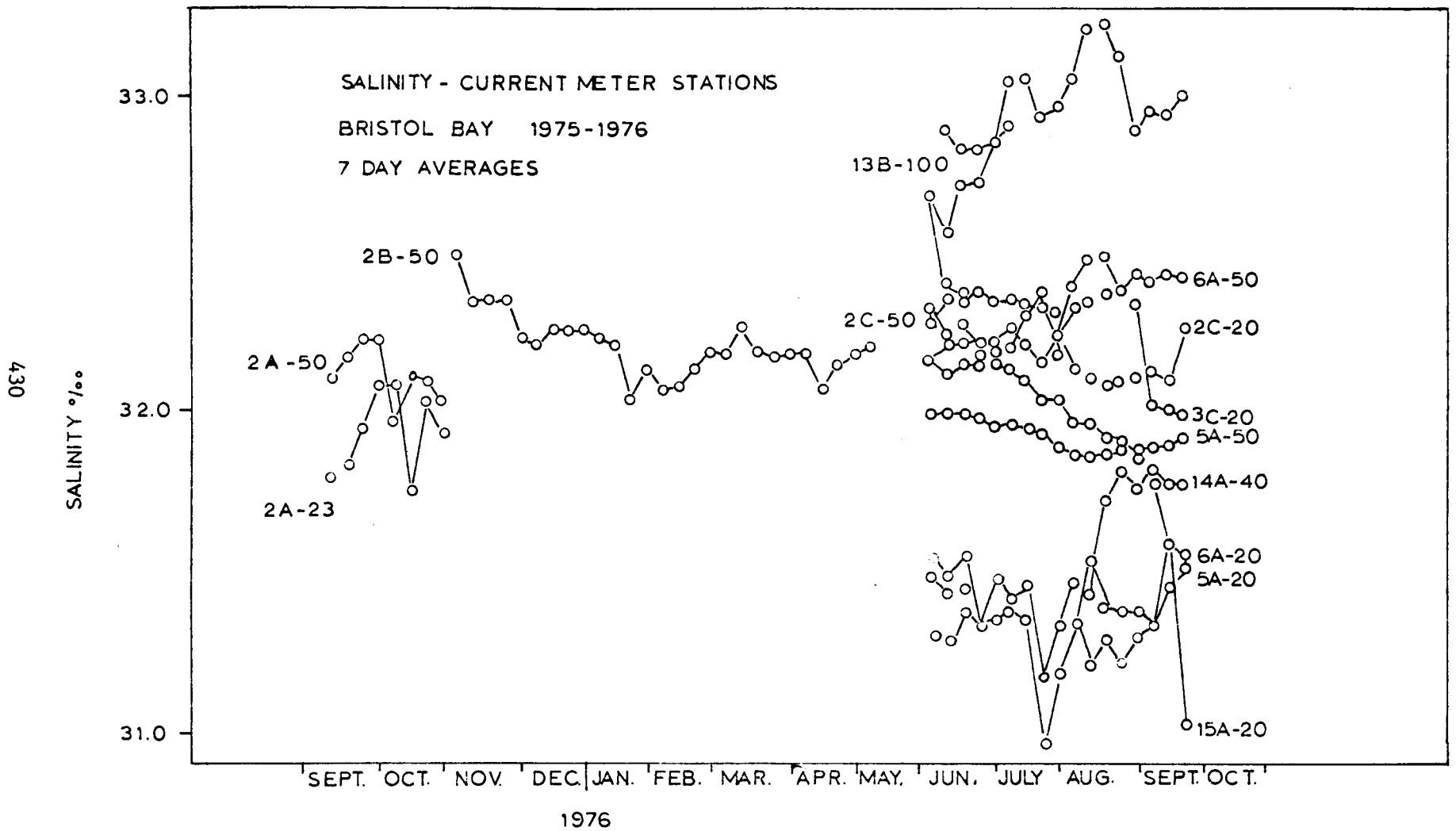
7 DAY AVERAGES

FIGURE 7

MEAN SPEEDS - CURRENT METER STATIONS
BRISTOL BAY
7 DAY AVERAGES
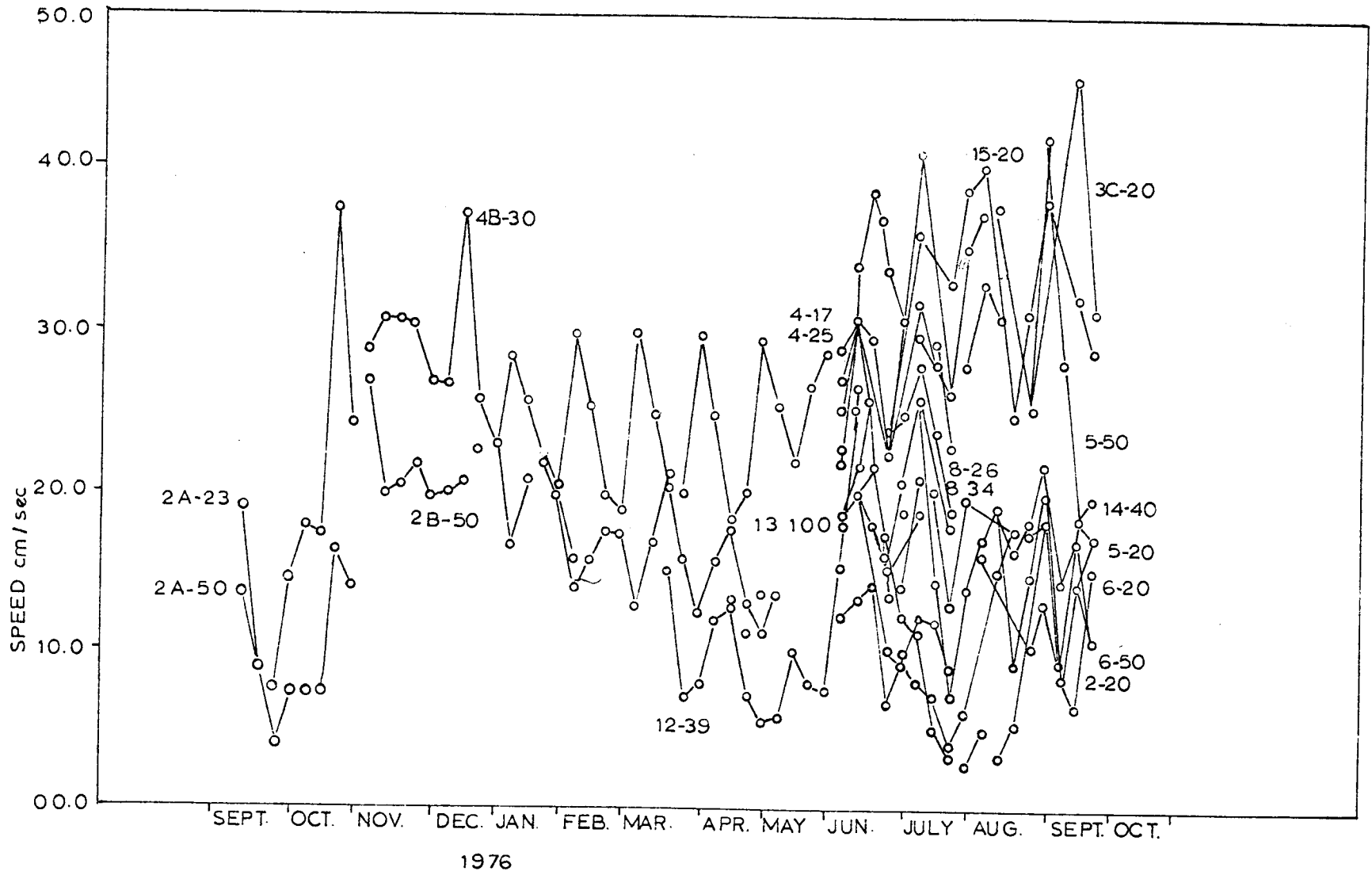
FIGURE 8

During the winter under the ice, the fluctuations in mean speed are very clean, with the striking feature that the phase of the fluctuation at northwestern end of the bay is 180 degrees out of phase with the fluctuations at the southeastern end of the bay. These fluctuations are particularly interesting, since they occur while the system is ice-covered and therefore not subject to wind stress directly. The winter record from station 4 is not out of phase with measurements in the rest of the bay during the summer months, this phase change relationship may be due to the ice lid on the system. The separation into two levels of energy is due to a tidal inference effect noted in the current meter records in the region of the shelf area. This effect is presently being investigated.

Interpretating 7-day averages of current vectors requires caution in that 7 days is not an integral number of semidiurnal periods. The effect can amount to approximately a 1-cm/s contribution to each weekly average, the component reversing sign every 2 weeks.

The north-south and east-west components for the longest station record, station 2, and example records for winter from station and summer records from station 6 are displayed in figure 9. These records show monthly periodicity and also allow a better examination of the seasonal differences. All the stations represented in the figure show little net flow in a north-south direction seasonally. The net transport over the year is then best examined in the east-west plot. At station 2, the highest activity occurs at the transition from winter to spring. The flow at station 2 is eastward through autumn and westward through the rest of the year, which could represent the formation and destruction of the shelf regime. Station 4 again shows periods where the sign of the fluctuation is 180 degrees out of phase with the fluctuations at station 2, but not as consistently as in the mean speed plot. Also,
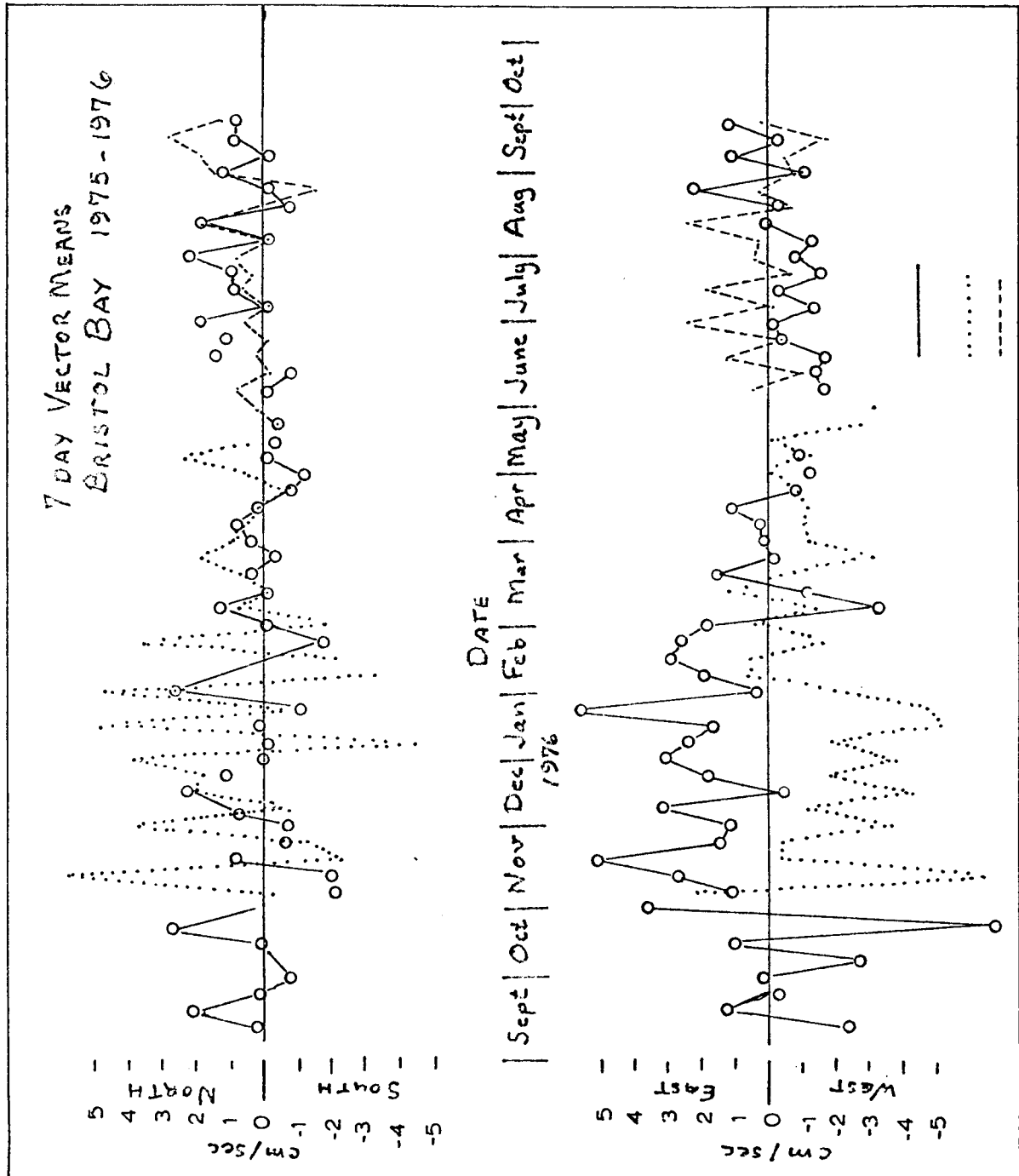
Figure 9

the seasonal trend during winter is opposite of that at station 2. Both station 2 and station 4 changed character in February in the sense that the variability has reduced, perhaps representing the spin down of the system after the wind stress has been removed by ice cover. Stations 2 and 6 were approximately 20 km apart during the summer and show rather good agreement in the current fluctuations. Neither station was particularly active; both had a net northward flow, but station 2 was predominantly westward and station 6 was eastward, indicating a more complicated flow regime than was resolved with the current meter spacing.

To provide some indication for driving forces, the weekly averaged vectors of current from station 2 during summer and weekly averaged wind vectors for the station 2 region were compared. The wind information was obtained from the Fleet Numerical Weather Facility projections, utilizing a numerical model with 3-degree grid spacing centered over station 2. The scale of the model grid results in wind projections which would cover most of Bristol Bay and thus affect records from all of the moorings. Figure 10 displays the vectors in a progressive vector diagram format. The striking feature is the similarity in long-term direction. This similarity is coincidental, and would not be so evident if compared with the other current meter stations. The similarity is probably due to absence of other forcing. Though the directions are quite similar, the variations do not seem to be strongly correlated. The reversal of wind between June 7 and June 28 had no apparent effect, with the exception of a slight reduction in current speed between June 20 and June 27. Likewise the high winds at the beginning and end of the record show no acceleration of the water mass.

Figure 11 is a visually smoothed trajectory of one Numbus-6 Lagrangian drifter deployed at the same time the summer moorings were placed in the bay.

Figure 10

BC-15

10 Aug

3 Aug

BC-2

BC-5

4 July

31 May

BC-6

14 July

Lagrangian Current
Nimbus-6 Drift Buoy
Visually Smoothed Track

BC-14
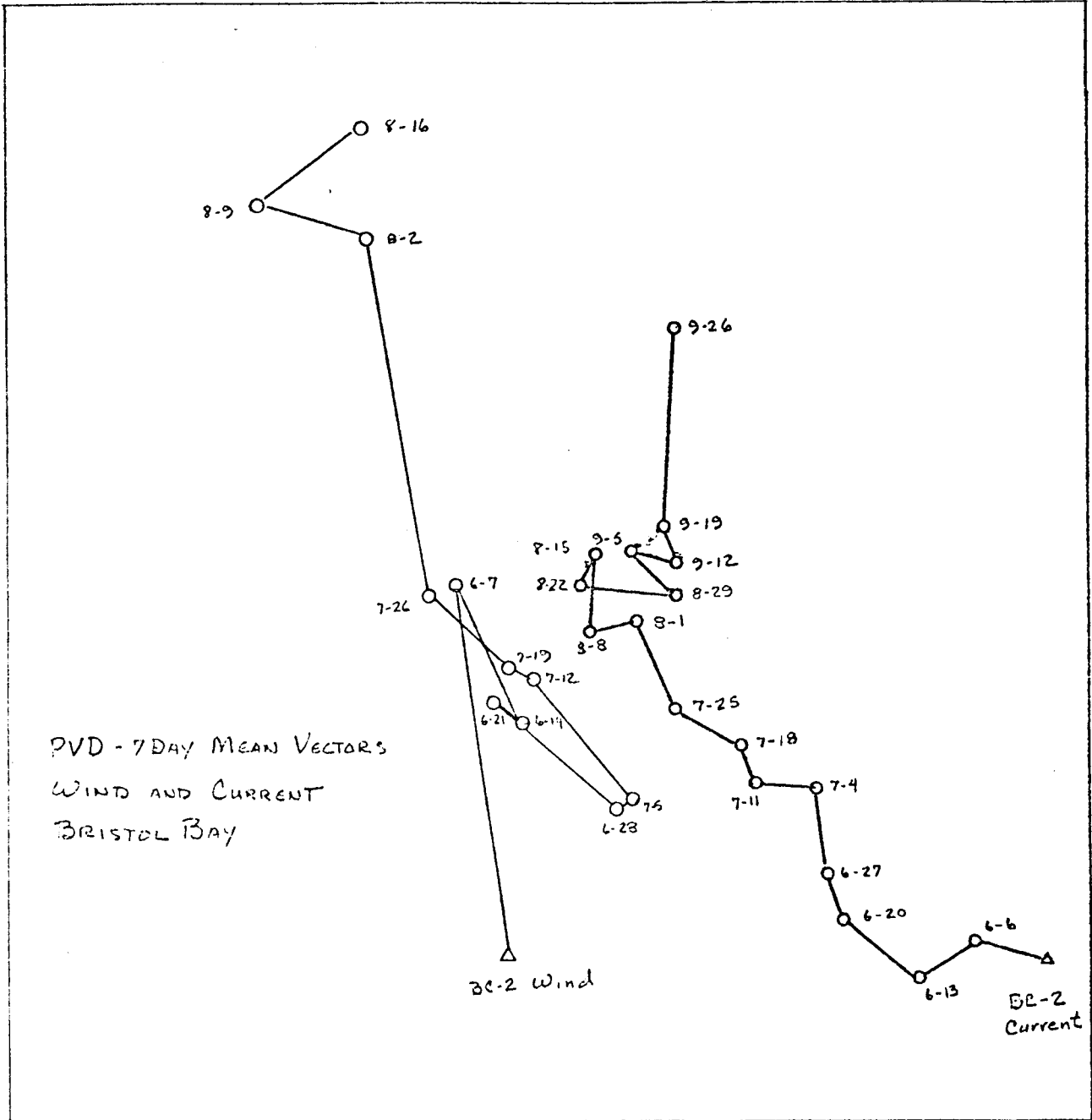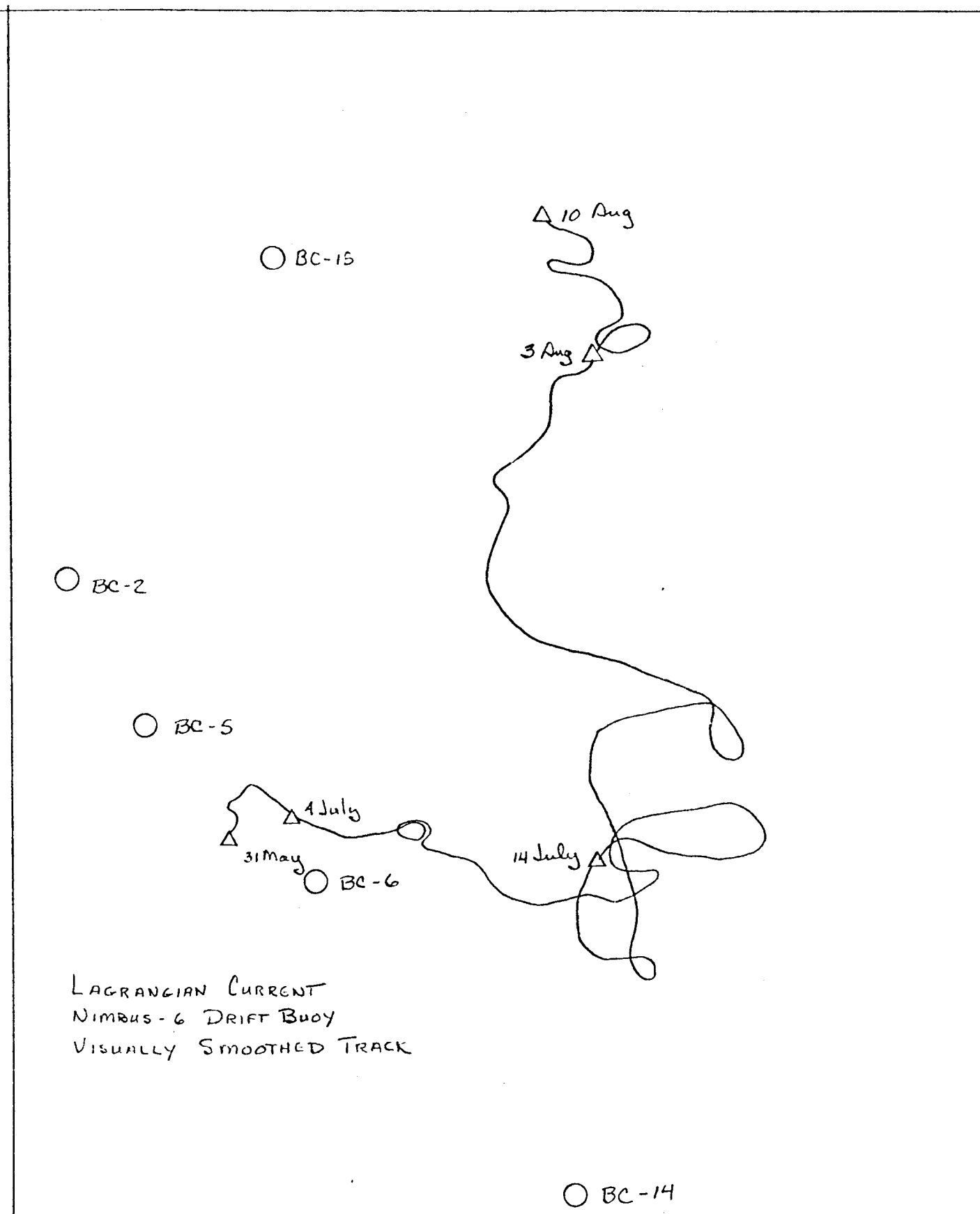
Figure 11

Throughout June there was very little motion in agreement with the current meter records from station 6. The first 2 weeks of July, however, the drifter made substantial excursions to the east and south with little corresponding motion in the record from station 6. Over the next month the drift was to the north with some small amount of east-west displacement. At this time there was a northward flow at station 6, though not large as the easterly flow. The similarity between the drifter trajectory and the wind PVD is quite striking after July 14. All of the drifters deployed at this time were recovered, but none were found with the drogue sheets attached. From the record presented, it can be estimated that the drogue was lost from this drifter around July 9.

Thus in the low-frequency flow there are periodicities of 1 month with some interesting phase variations over the space of the bay. The low-frequency data indicate seasonal changes in flow patterns and in particular will provide flow reversal from summer to winter at station 2. The lower frequency fluctuations in currents do not seem strongly coupled to low frequency in the wind field, though seasonal variations may show a stronger coupling. The drifter data show that while the drogues were attached the flow was very quiescent and in agreement to the current meter records.

B. High-Frequency Flow

For the purpose of the report, high-frequency flow will be considered only as flow fluctuations with periods of 24 hours and 12.5 hours, the dominant tidal bands. Table 2 lists the velocity components for each of these periods for the available data. The fact that stands out is that the motion is dominantly east-west. Nearly 75% of the diurnal flow is in the east-west direction and 63% of the semidiurnal flow is in the east-west direction averaged

over all the data. It is impossible at this stage of processing to determine
phase relations of the tidal currents across the bay to determine whether
or not the bay is sloshing back and forth as a solid body or as a wave propa-
gating in one or the other directions across the bay. Efforts are currently
underway to investigate this problem, however. There is a great deal of
variation in the magnitude of the tidal energy throughout the bay; the standard
deviations approximately equal the means. There are substantial variations
in tidal energy temporally, horizontally, and vertically. From the table
it is seen that the strongest tidal flows are in the lower layers of the
shelf area; the reason for this result is not yet understood. Periods have
been observed when the tidal current signal has virtually disappeared (fig. 12).
It is hypothesized that this is due to interfering internal waves in the
tidal frequencies. Perhaps this leads to amplification of the tidal motions
in the lower layers. The thorough investigation of tides within Bristol Bay
is underway.

Table 2. Tidal Component Energies $(cm/s)^2$

Station	Depth	24-hr - u	24-hr - v	12.5-hr - u	12.5-hr - v
BC-2C	20	73.0	0.5	147.2	46.1
BC-3B	50	93.5	3.5	171.3	53.1
BC-3C	20	46.4	30.0	181.0	268.6
BC-3C	100	34.4	30.0	148.9	161.8
BC-4C	25	46.2	57.0	312.8	302.6
BC-5A	20	51.1	3.0	101.6	30.1
BC-5A	50	322.7	22.1	659.8	122.3
BC-6A	20	50.0	4.6	101.3	18.0
BC-6A	50	106.6	15.5	213.3	24.8
BC-8A	26	37.4	35.7	205.0	201.4
BC-8A	54	52.4	37.4	211.6	188.9
BC-9A	17	69.5	92.4	306.6	296.3
BC-9A	27	74.8	81.4	233.9	208.0
BC-12A	39	27.3	5.4	52.1	16.5
BC-13B	100	39.1	10.7	132.2	92.1
BC-14A	37	72.2	18.3	152.0	19.6
BC-15A	20	148.4	3.8	449.7	213.2
Mean:		79.2	26.6	222.1	133.0
Standard deviation:		69.7	27.6	147.1	103.7

2.8 hour filter data
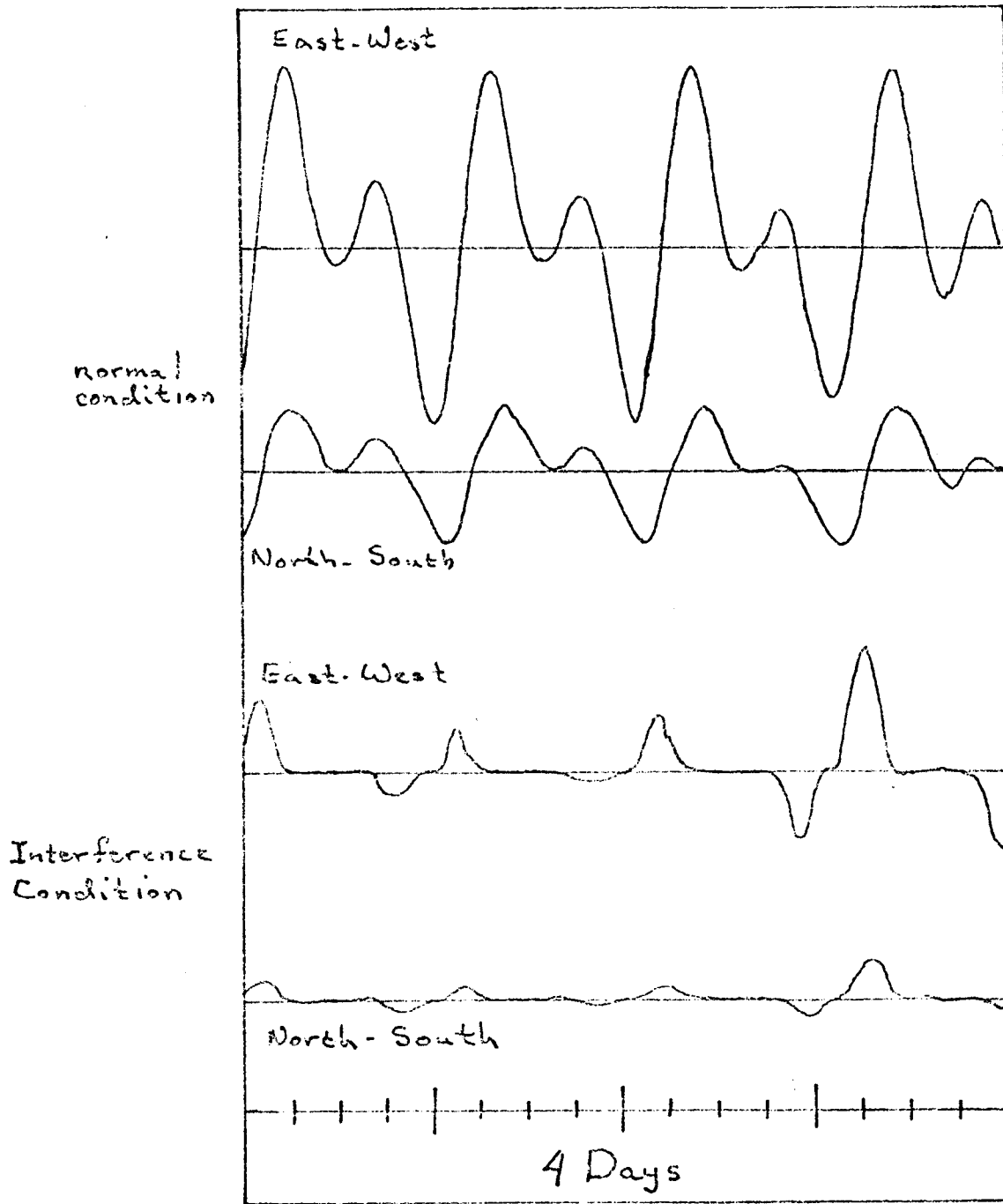
Figure 12

VIII. HEAT BUDGET OF THE EASTERN BERING SEA

This investigation it was felt, should be documented and the preliminary results made known because of their possible interest to OCSEAP investigators. The study is not complete, and some of the conclusions are tentative.

A. Results

Some very comprehensive oceanographic surveys of the eastern Bering Sea were completed as part of OCSEAP in summer 1976. The data are quite valuable for examining many oceanographic aspects of the region, but they are especially suitable for evaluating the heat content of this region and its changes during the seasonal heating.

The heat budget of a water column is altered by: (1) net surface exchange, which consists of net insolation, net long-wave radiation, evaporative heat flux, and conductive heat exchange between the ocean and atmosphere; (2) horizontal advection and diffusion of heat; and (3) vertical advection and diffusion of heat. Earlier heat budget studies were often hampered by little knowledge of horizontal temperature gradients or currents (horizontal heat advection), and the empirical formulas for estimating net insolation and net long-wave radiation varied so greatly that it was difficult to choose among them with confidence. A recent research effort in our laboratory has been to review and evaluate the formulas for estimating the radiative fluxes, and it is believed that these can now be specified to an accuracy of 5-10% over a period of about a month. In addition, the OCSEAP data provided direct current measurements, adequate spatial coverage to allow determination of the first and second derivative of heat content and oceanographic conditions such that a layer could be chosen deep enough to neglect vertical fluxes.

The following data sets were used: Moana Wave and Miller Freeman, 6-17 June 1976; Acona and Moana Wave, 7-10 August 1976; and Acona, 28-30 September 1976. The CTD data (1-m averages) were used to derive the heat content of the upper 50 m by vertical integration, and the individual station values were plotted. For each cruise, the heat content values were meaned by 1° x 1° areas; the values, however, were spatially weighted to the center of each 1° area after determination of the east-west and north-south gradients from the original plots. Values for the June and August cruises are shown in figures 13 and 14.

(At present the September data have not been treated in the detail accorded the June and August data. A number of the CTD casts have not been read off the tape due equipment problems; consequently the number of casts is quite small, and the weighting of the data results in rather uncertain values. If the remainder of the data can be retrieved, this data set can perhaps also be used.)

It should be noted that data exist outside of the area shown on the maps; in August, however, there were no data east of this area and very few to the north. It was decided not to use the data farther west because it is difficult to find a consistent level where the vertical advective and diffusive terms can be neglected. The data shown on the maps have been used in light of a model of heat conservation stated as follows:

$$\frac{\partial H}{\partial t} = Q - u \frac{\partial H}{\partial x} - v \frac{\partial H}{\partial y} + Ah\left(\frac{\partial^2 H}{\partial x^2} + \frac{\partial^2 H}{\partial y^2}\right)$$

where $\partial H/\partial t$ is the local change of heat content, Q is the net surface heat exchange, $u \frac{\partial H}{\partial x}$ and $v \frac{\partial H}{\partial y}$ are the horizontal advective terms where u is the east (x) component of velocity and v is the north (y) component of velocity, and remaining term is the horizontal diffusion of heat with A_h the eddy

thermal conductivity. Upon examination of the data base, it was decided to evaluate the various terms for the two 1° areas between 56°-57° N. and 164°-166° W.

The various terms in the equation, except Q, were determined by finite difference methods for space and time. The spatially dependent terms were computed from both June and August data, and a mean was used. The value of A_h used was 10^7 cm^2s^{-1}. Although this value cannot be stated with the confidence of a physical constant, numerous studies would suggest that it is unlikely to be in error by more than a factor of 2. The advective term is, of course, dependent on flow of the water. Current meters were not placed in either 1° area of interest, but there are data from two arrays to the southwest and three arrays to the northeast. The two arrays to the southwest were presumably in the Bering Slope Current; northwest flow of 2-19 cm/s was indicated. The three arrays between 56.5°-57.0° N., near 163° W., all showed net flow of 1cm s^{-1} or less with no consistent direction. In addition, maps of the geopotential anomaly (0/50 db) revealed the Bering Slope Current, but suggested very weak flow in the region of the two 1° areas of interest. Thus the advective terms are considered to be very small and have been neglected.

The net surface exchange consists of four components: Q_s, the net insolation; Q_b, the net long-wave radiation; Q_e, the evaporative flux; and Q_h, the conductive flux. Q_s and Q_b were determined by the empirical formulas and methods derived in our recent studies. The most critical factor for their determination is cloud cover, which was estimated from daily NOAA-4 satellite images (visual channel), corrected by +0.20 to agree with observer's estimates that were used to derive the cloud factors. Computations of Q_e and Q_h were made with bulk aerodynamic formulas using the transfer coefficients from a recent review paper with meteorological data from the National Climatic

Center. The computations are summarized in the following table, where single estimates of Q_s, Q_b, Q_e, and Q_h were made for the combined 1° areas rather than separately. Units are cal cm^{-2} min^{-1}.

Area (56°-57° N.)	$\partial H/\partial t$	Q_s	Q_b	Q_e	Q_h	$Ah\left(\dfrac{\partial^2 H}{\partial x^2} + \dfrac{\partial^2 H}{\partial y^2}\right)$	Residual
164°-165° W.	0.23	0.23	-0.02	-0.01	0	0.04	0.01
165°-166° W.	0.16	0.23	-0.02	-0.01	0	0.02	0.06

The residuals reveal the lack of an exact balance; if both areas are meaned, the value is 0.03 cal cm^{-2} min^{-1}, which is quite small considering the various approximations and uncertainties. The principal conclusion that emerges is that during this period the changes in heat content in this area were primarily controlled by surface exchange, with net radiation being by far the major factor.

Discussion. Do the results of this heat budget investigation, namely, that changes in summertime heat content are dominated by net radiation, generally apply to the shallow eastern Bering Sea as a whole? It seems likely that they do. First, there is considerable historical evidence that the flow is weak and variable, and all of the OCSEAP measurements on the continental shelf, except a few nearshore, have shown very weak net flow. Second, winds in summer are usually weak; hence the evaporative flux would be small. Finally, there is generally very little temperature gradient in the lower part of the water column. Vertical fluxes should usually be negligible, although in late summer or early fall (as suggested by the late September 1976 data) vertical diffusion of heat downward might assume some importance. It should be stressed that the above discussion applies only to summer. In winter, winds are strong, the air is cold, and latent and sensible heat fluxes are likely to be quite

large. In areas subject to ice formation, the surface heat exchanges may
be drastically altered.

The implication that net radiation almost wholly controls changes in
heat content during the summer is of interest for a number of reasons. First,
this simple (and rare) oceanic situation makes it quite straightforward to
apply a heat budget model. Thus the changes in heat content could have been
forecast using the formulas for estimating net insolation and net long-wave
radiation, with the only data input being cloud cover from satellite photo-
graphs. The fact that insolation acts on an almost motionless column of
water may have important implications to the primary productivity in this
area. Finally, this behavior of the environment is important to the eco-
system as a whole.

Heat content (Kcal/cm²)

7-10 August 1976
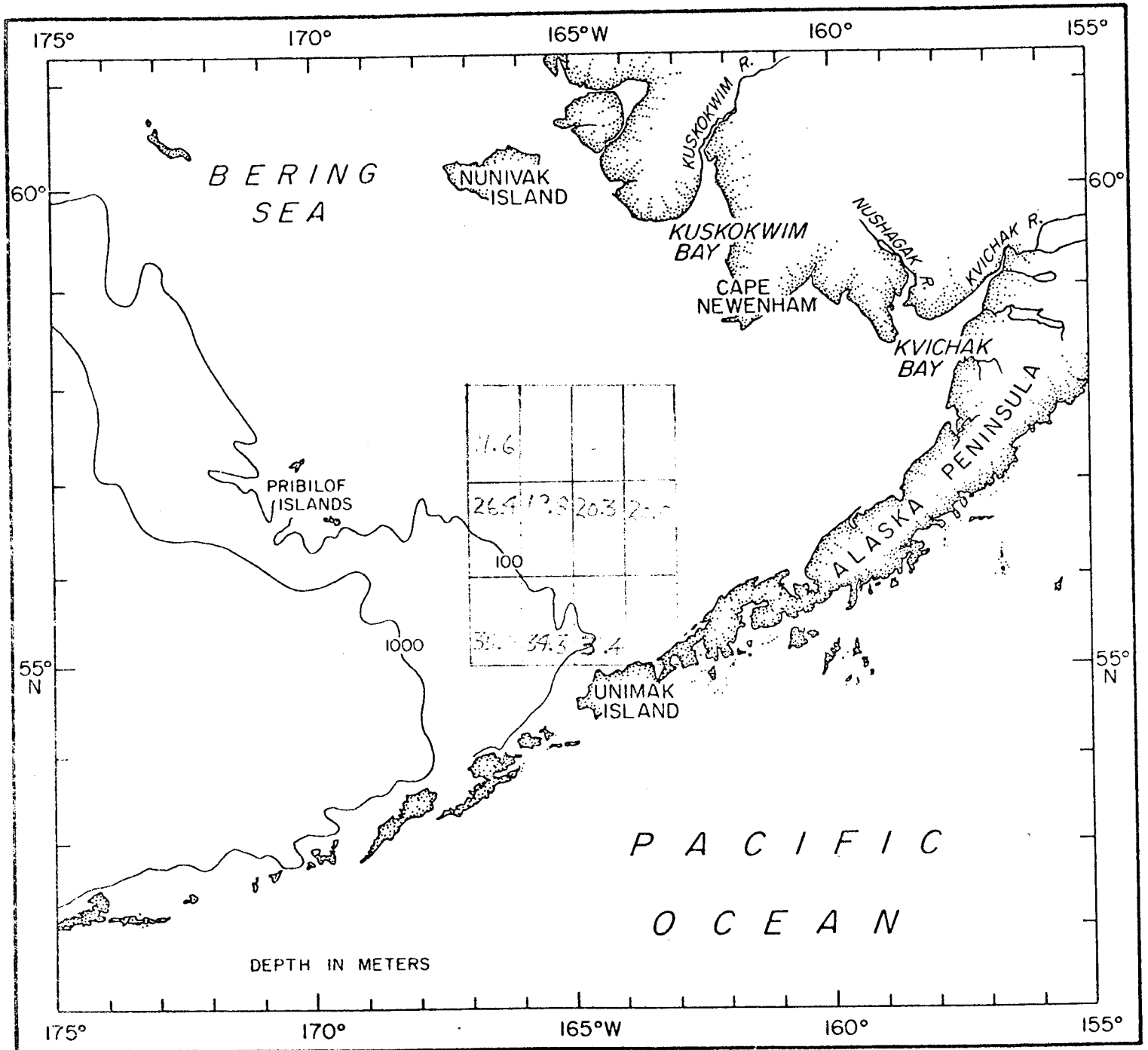
Figure 13

Heat Content (kcal cm⁻²,

6-17 June 1976
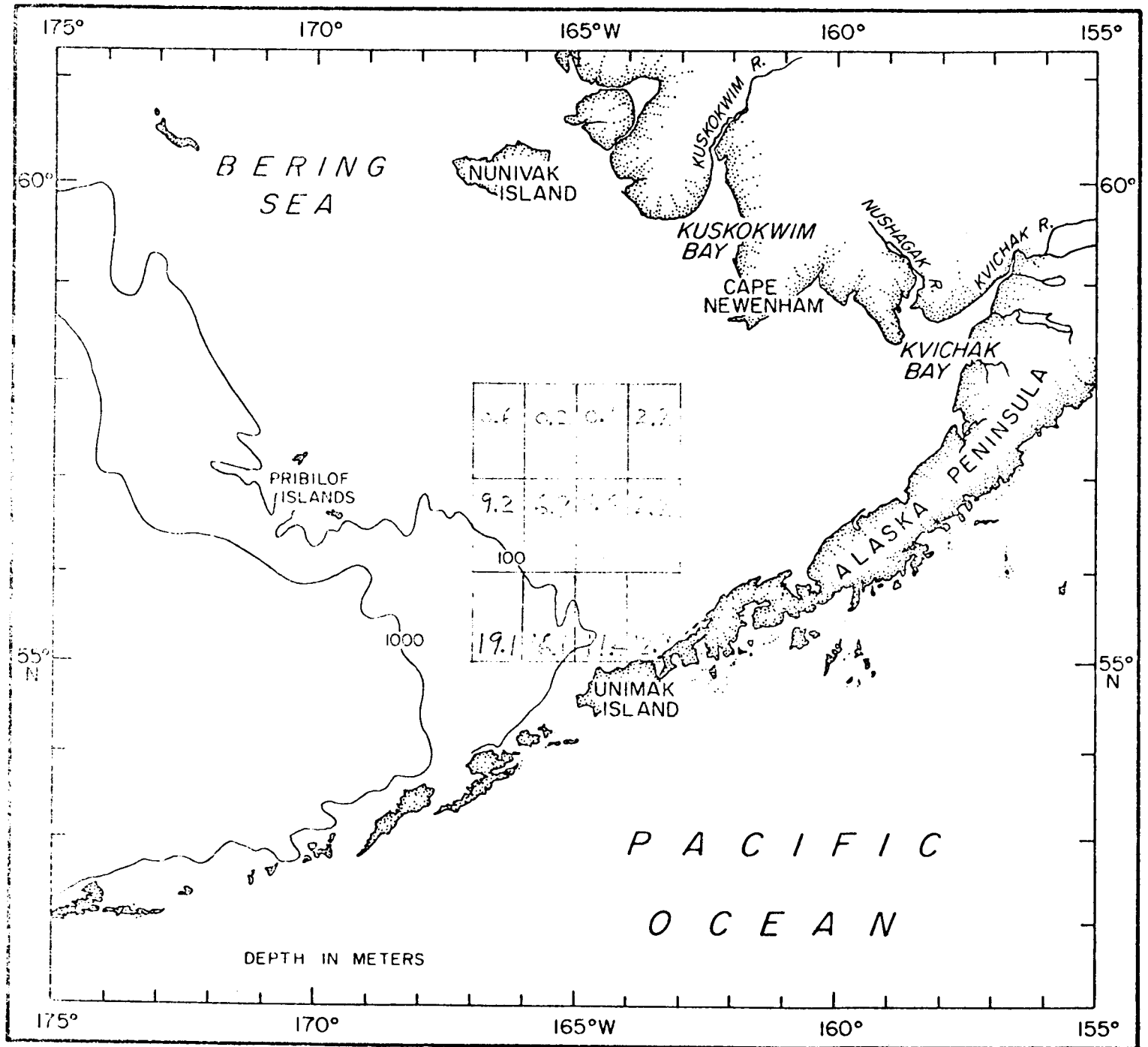
Figure 14

Bottom Mounted Pressure Gages and Meteorological Observations

The distribution of actual bottom pressure is central to the problem of circulation within Bristol Bay in that horizontal pressure gradient is one of the principle terms in the balance of forces. Combined with the atmospheric pressure field it is possible to separate baroclinic and barotropic components of the pressure field and thereby examine the contributions to the circulation of the various components of forcing such as geostrophy, slope current, and hydrostatic adjustment. The task of obtaining the required information is well underway.

Bottom mounted pressure gates have been deployed with a number of current meter arrays throughout Bristol Bay, Figure 15. These have been of the Aanderaa TG-2&3 type. Data from the pressure gages is now in processing and has yet to be fully examined. As noted in the last annual report events in the pressure record occurred concurrently with pulses in the current. As these records become available for analysis a complete picture of the pressure field can be formed.

The task of adjusting the records to account for atmospheric pressure requires (1) a study of the sea-level atmospheric pressure from around the bay, and (2) algorithm determined to allow for correction of the pressure gage records offshore. To date, atmospheric pressure records for the year 1975 are being analyzed for the purpose of program design and debugging and to provide information towards the design of the correct algorithm. If the correlation between shore station pressure records is linear the correction algorithm will be straight forward, however, if the spatial scale of atmospheric events is smaller than the horizontal scale of the bay, a more complex problem must be solved in order to provide the proper correction information. When the 1976 data are available from the National Climatic Center the results of the 1975 effort will be applied so that the effort of understanding the bottom pressure field can get underway.

Figure 15

MOORING LOCATIONS
● Bottom Mounted Pressure Gages
▲ Meteorologic Observation Station
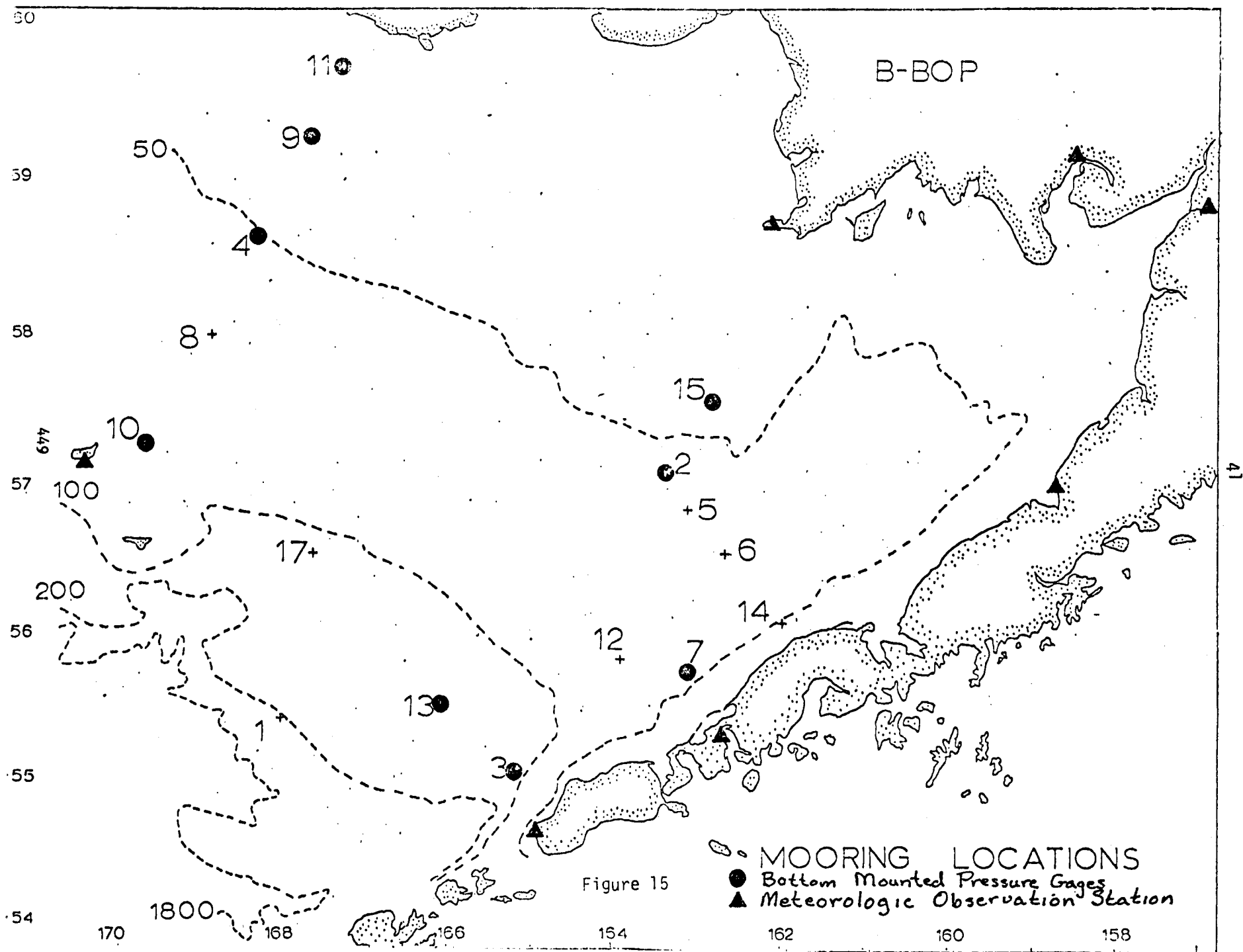
X.   Papers resulting from the Bristol Bay Investigations to date:

1.   FINESTRUCTURE IN OUTER BRISTOL BAY, L. K. Coachman and R. L.
       Charnell, Accepted in Deep sea Research for publication
       summer 1977.

2.   THE HYDROGRAPHIC STRUCTURE OVER THE CONTINENTAL SHELF NEAR
       BRISTOL BAY, ALASKA, JUNE 1976, T. H. Kinder, University of
       Washington Technical Report M77-3, January 1977.

3.   INTERNAL TIDES OF BRISTOL BAY, ALASKA, R. L. Charnell, H. O.
       Mofjeld, and J. D. Schumacher, in preparation.

4.   OBSERVATIONS OF MEDIUM SCALE FEATURES ALONG THE SEASONAL
       ICE EDGE IN THE BERING SEA, R. D. Muench and R. L. Charnell,
       Journal of Physical Oceanography, Vol. 7, #4, 1977.

XI. NEEDS FOR FURTHER STUDY

Hydrographic properties during winter conditions need examination. This would require running several CTD lines (off Cape Newenham, midway between this line and one run seaward from Nunivak Island) using helicopter ice techniques already developed. Additionally, it is recommended that three current meter arrays be deployed in the Kuskakwin Bay region; one at a site where historical data base exists and the other two separated by approximately 25 km on either side of the 50 m isobath. It should be noted that the three arrays recommended for the NCOP study (all south of the Bering Strait) will be located "downstream" of the B-BOP arrays and thus will provide a more coherent description and understanding of eastern Bering Sea shelf flow.

To further study flow on the St. George Basin area, Lagragian drifter studies are required since the high density of fishing operations inhibits its success of moored arrays. As is always required for understanding of forcing, meteorological data must be provided from a moored buoy.

In the context of these needs for further study the specific subjects for study can be classified into three categories:

A. Nearshore

1. A front is known to exist in certain areas of the bay; however, a detailed delineation of the front is lacking. A thorough survey of the front is required to delineate the zones of coastal water and shelf water.

2. The structure of the front is not presently known. A detailed examination of the currents and physical parameters of the front is required to define the generation mechanism of the front and current dynamics associated with the front.

3. To date, the investigations have not fully disclosed the disposition of freshwater inputs to the bay from river discharge and its relation to high-salinity anomalies located in the coastal waters.

4. Two high-salinity anomalies have been sampled within the coastal waters. The sourve anomalies and the distribution of the anomalies has to be addressed.

B. Central Shelf

The temporal and spatial distribution of the tidal current reductions noted in the summer season of 1976 is not known. Also, the cause of the current reduction is only speculated at the present time, and additional information is required before a firm mechanism can be developed.

C. Bering Sea Slope

1. Fine structure has been noted in the slope region. The extent of the fine structure and the lifetime of the structures are unknown. A better resolution of these questions will assist in understanding the source of the fine structure.

2. The success of current meter data acquisition on the slope has been marginal due to high equipment losses resulting from heavy fishing activity. Information on the circulation on the slope could be improved by the use of Lagrangian methods in the heavily fished region near Unimak Pass and current meter moorings farther "downstream" near St. George Basin.

D. General

1. The glaring need reflected in this report is the lack of winter data, either current or CTD. The spatial distribution of current meters wintering over has not been sufficient to resolve the winter current regime. Winter current meter stations are required to fill in the gaps in our knowledge. Also the collection of winter CTD data is critical to the understanding

of winter circulation. This problem may be best addressed by collection through the winter ice cover.

2. Present meteorological information is on a scale too large to resolve events which have a dimension less than that of the bay. To allow a better resolution of these smaller events, a meteorological buoy in the center of the bay is necessary. This would permit a distribution of small events to be drawn and the influence of small meteorological events on the water to be investigated.

XII. CONCLUSIONS

Investigations into the environment of Bristol Bay have been in operation for 2 years. A basic description of the physical oceanography of the bay has been drawn and questions concerning specific processes formulated.

Bristol Bay can be characterized as having three distinct zones: (1) the coastal waters where all the properties are uniform from the surface to the bottom; (2) the central shelf where the water column is highly stratified, forming a distinct two-layer system; and (3) the Bering Sea Slope where the characteristics are similar to that of the Bering Sea proper but reflect the effects of interaction with the shelf. The coastal water is well-mixed vertically and has modest horizontal gradients of salinity reflecting the influence of the freshwater discharge from rivers, though definite river effluent has yet to be identified. Currents measured in the coastal water thus far have been predominantly tidal with virtually no net flow when away from the zone of transition to central shelf waters. High salinity anomalies have been noted in the coastal waters, but their source and lifetime are not determined. The coastal waters are separated from the central shelf waters by a strong horizontal change in character from well-mixed to highly stratified. Thus structure front has yet to be well understood in terms of its effect on the circulation in the bay. Currents appear to be stronger near the front and in a direction which suggests a counterclockwise flow around the perimeter of the bay at the frontal zone, which needs further spatial delineation. Within the central shelf area, the currents are dominantly tidal with very low net flows. No consistent pattern of flow can be defined, and the tidal flow also contains periods of sustained reduced value. These two facts combine to make the central shelf area very sluggish in terms of advection through the area. At the shelf

break where the central shelf water and the Bering Sea meet, the currents are the strongest, though poorly sampled due to fishing pressure. Fine structure has been noted in the area, which is a rare phenomenon at best, the cause and extent of which is uncertain. The interaction at the shelf break is important in determining any exchange with the central shelf. Conclusions to this point are based primarily on summer data.

Winter influences on the circulation have yet to be fully determined. The general picture of circulation appears to be similar to the summer; however, details are poorly resolved. Current reversals have been noted, the extent and significance of which are yet to be ascertained. The winter hydrography is virtually unknown.

When the detailed processes have been addressed, a good description of Bristol Bay will have been formed.

APPENDIX 1

B-BOP HYDROGRAPHIC DATA SUMMARY

Dates	Stations[1]	Cruise	Region	Remarks
2-26 Aug. 75	48	Discoverer RP-4-DI-75B Leg I	Outer & inner Bristol Bay	Ship of oppor- tunity
2-11 Sept. 75	41	Discoverer RP-4-DI-75B Leg II	Outer Bristol Bay	
4-8 Nov. 75	14	Miller Freeman RP-4-MF-75B Leg I	Outer Bristol Ban	Analog data only
16-23 Mar. 76	27	Moana Wave RP-4-MW-76A	Unimak Pass	Stations near ice edge
16-18 June 76	19	Miller Freeman RP-4-MF-76A Leg IV	Nearly entire B-BOP grid less deep slope	3 lines of closely spaced (~ 5 nm) stations; 2 are across 50 m front
7-18 June 76	152	Moana Wave RP-4-MW-76A Leg VII		
30 June-8 July 76	59	Moana Wave RP-4-MW-76B Leg VIII	Outer Bristol Bay	Ship of oppor- tunity
3-10 Aug. 76	85	Acona 233	AS/CA inter- action zone	Moana Wave aborted after massive elec- tronic failure
5-9 Aug. 76	30	Moana Wave RP-4-MW-76C Leg II		
21-30 Sept. 76	66	Moana Wave RP-4-MW-76C Leg II	AS/CA inter- action zone	Digitizer failure on Moana Wave
29 Sept.-2 Oct. 76	42	Acona		
12-26 Nov. 75	32	Miller Freeman RP-4-MF-75B Leg II	Outer Bristol Bay	

[1]Does not include stations occupied at mooring sites or outside B-BOP grid.

B-BOP Stations
NOAA Ship DISCOVERER
12 AUGUST - 26 AUGUST 1975
RP-4-DI-75-1B

B-BOP Stations
NOAA Ship DISCOVERER
2 September - 11 September 1975
RP-4-DI-75B LEG II
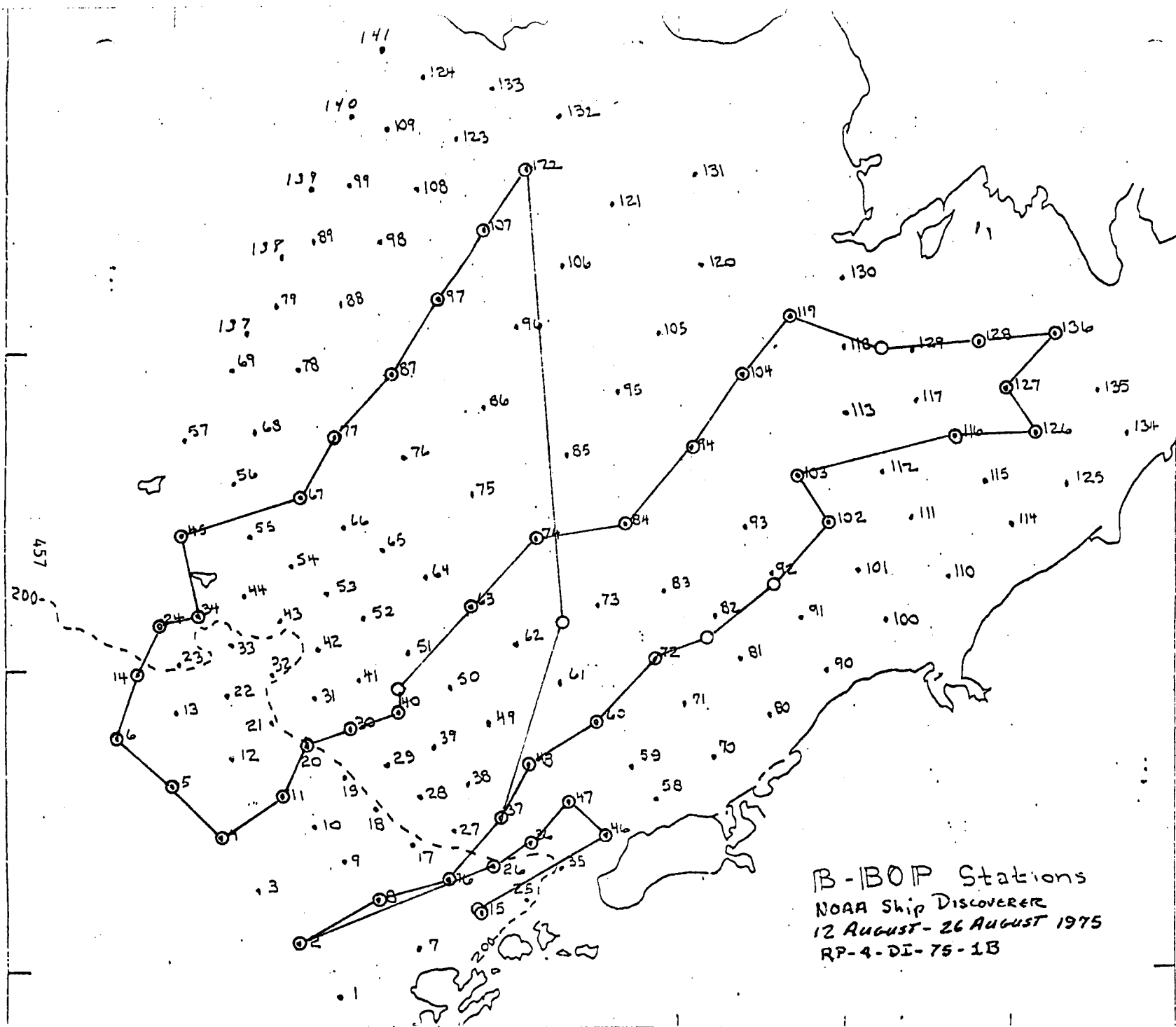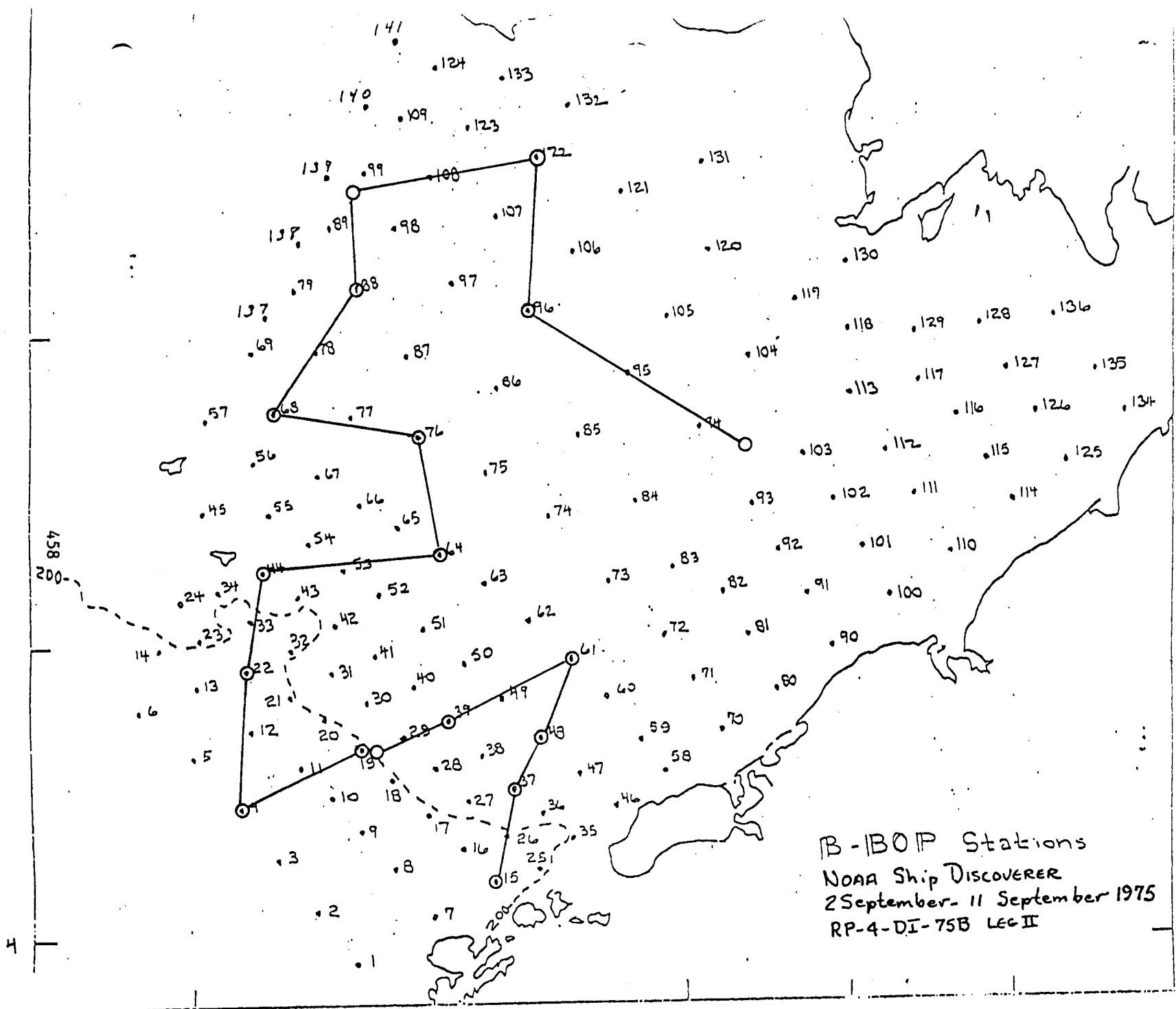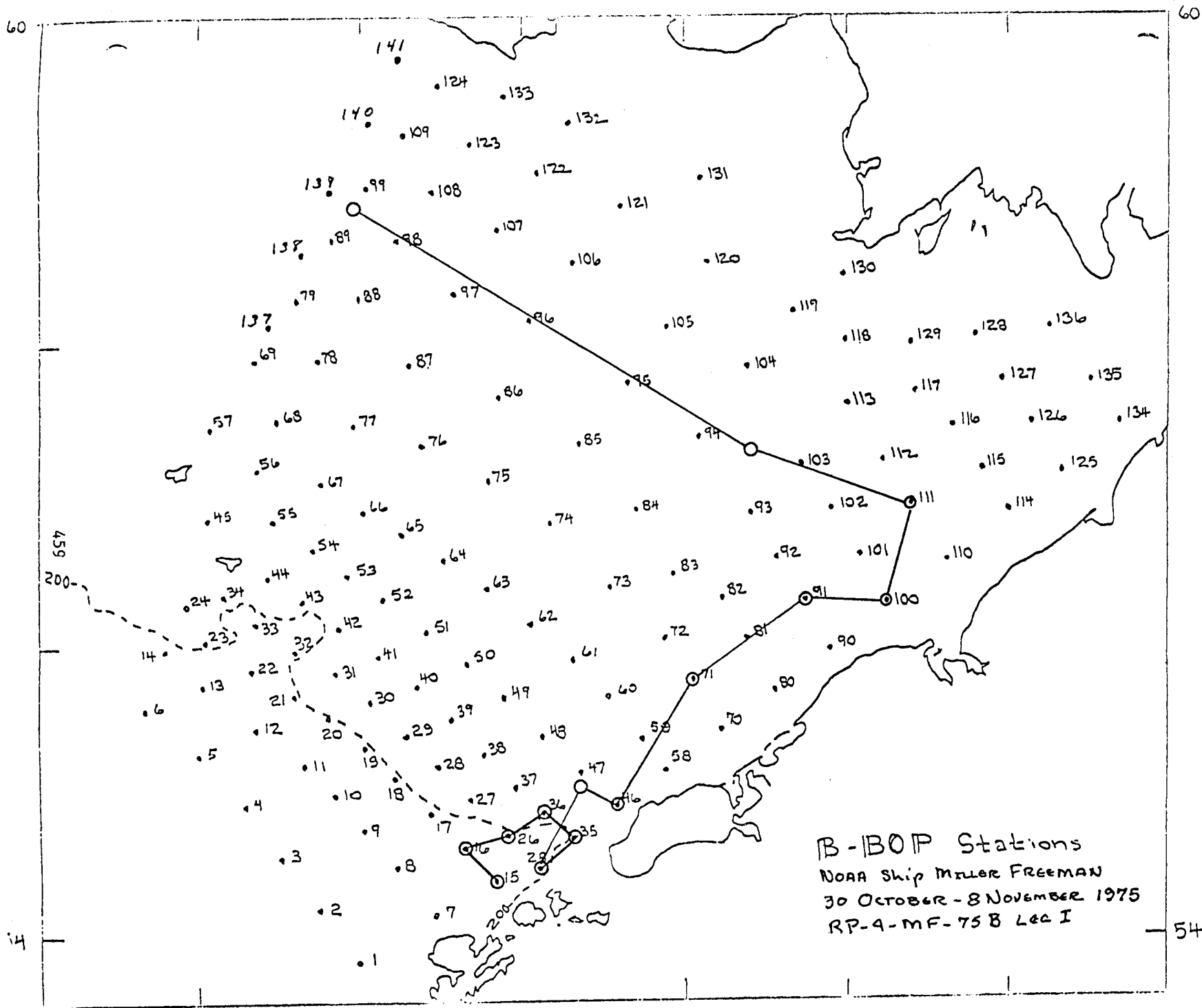
B-BOP Stations
NOAA Ship MILLER FREEMAN
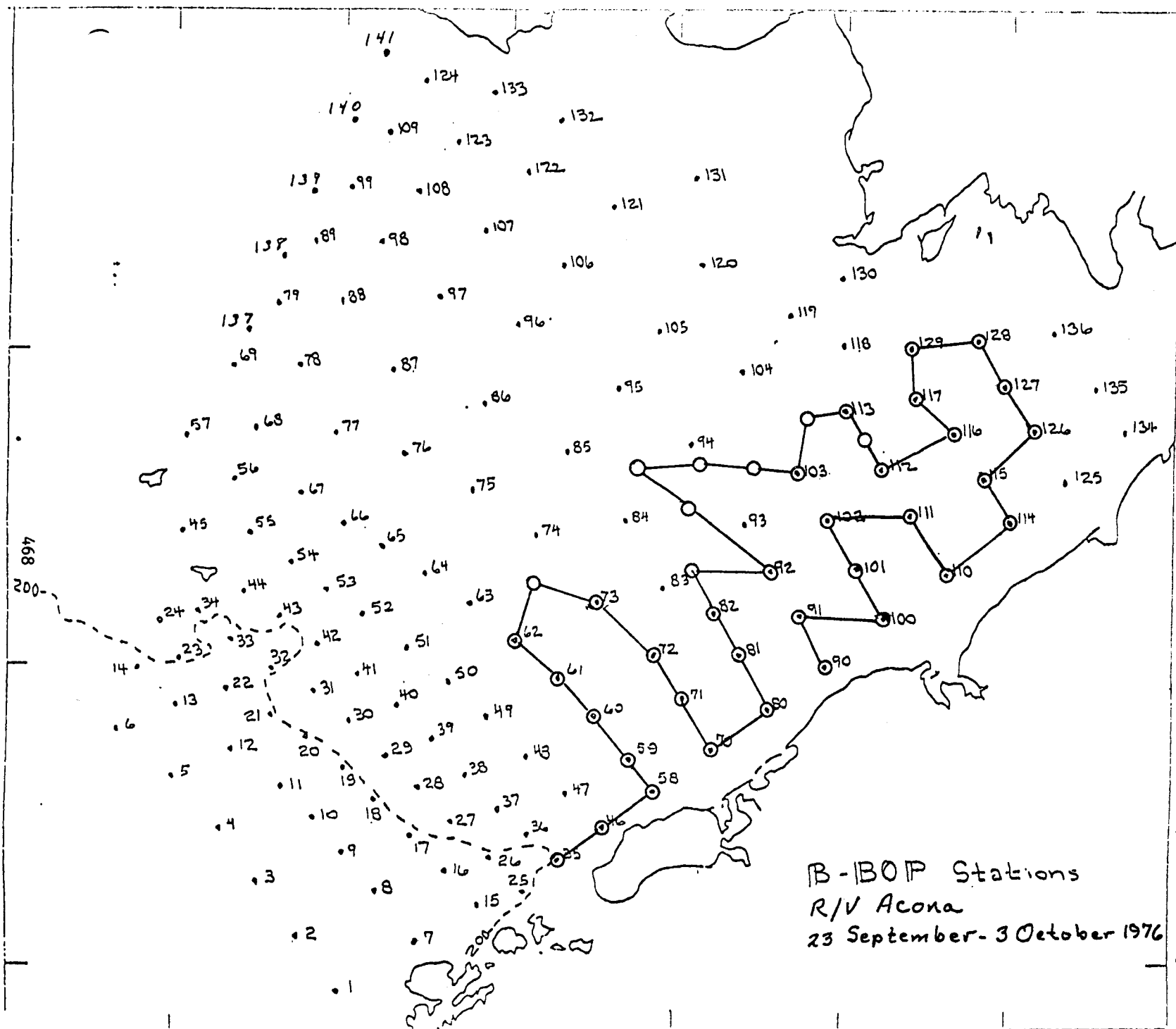30 October - 8 November 1975
RP-4-MF-75 B Leg I

B-BOP Stations

NOAA Ship MILLER FREEMAN

12 November - 26 November 1975

RP-4-MF-75 B LEG II

B-BOP Stations
R/V Moana Wave
8 March - 25 March 1976
RP-4-MW-76A Leg II

B-BOP Stations
NOAA Ship MILLER FREEMAN
7 June – 18 June 1976
RP-4-MF-76A LEG IV

B-IBOP Stations
R/V Moana Wave
26 May - 20 June 1976
RP-4-MW-76A LEG VI & VII

B-BOP Stations
M/V Moana Wave
30 June - 8 July 1976
RP-4-MW-76B-Leg VIII
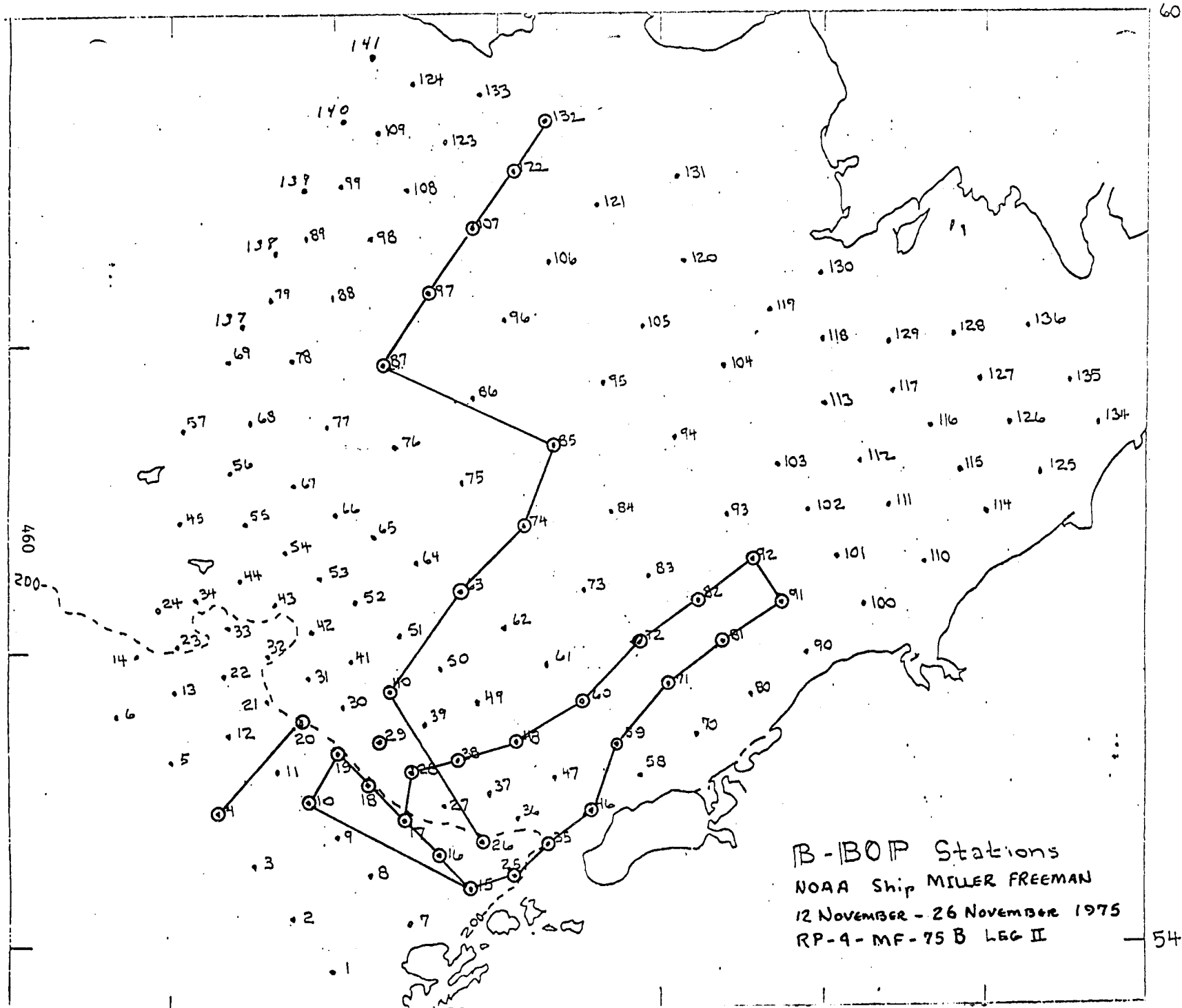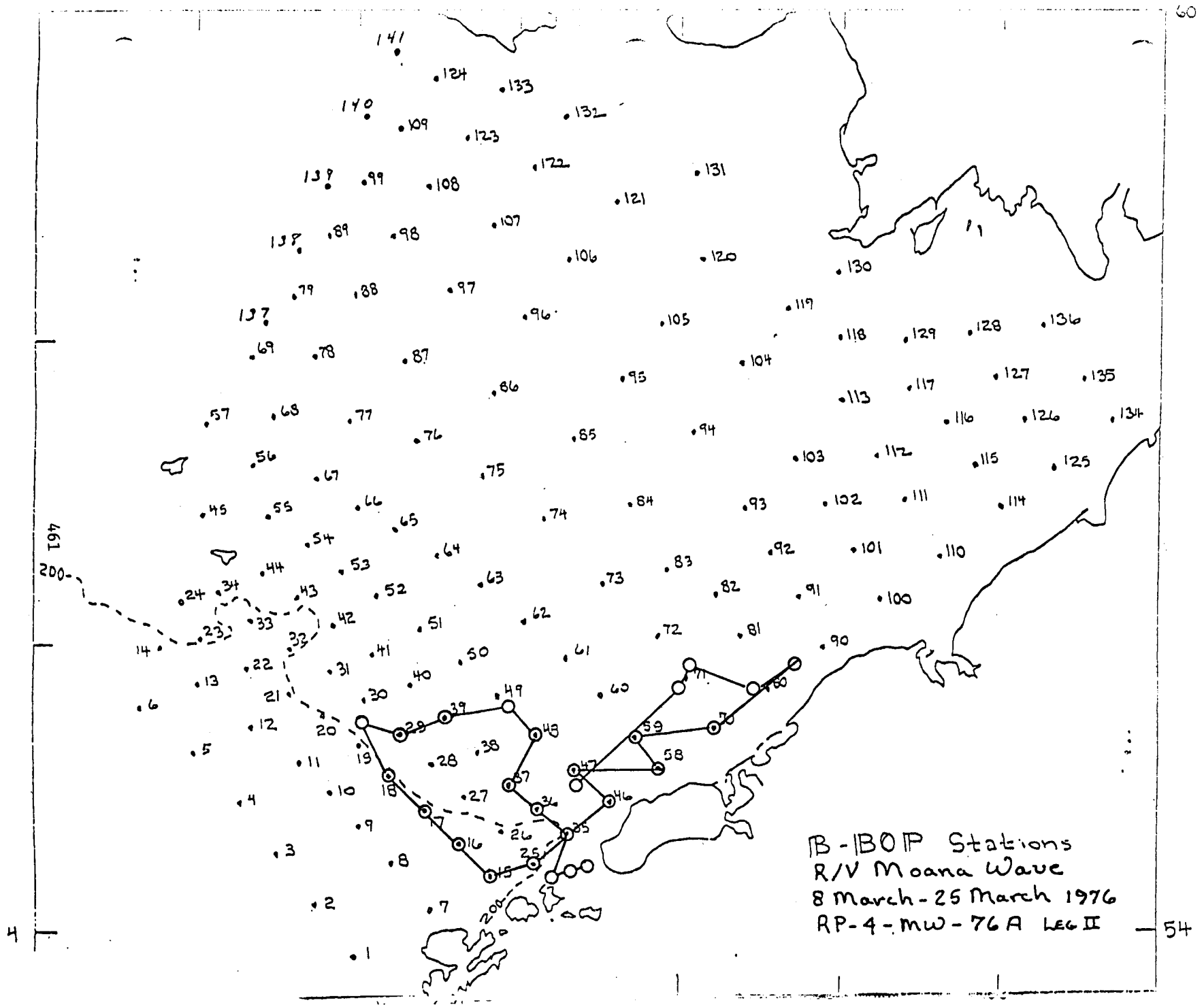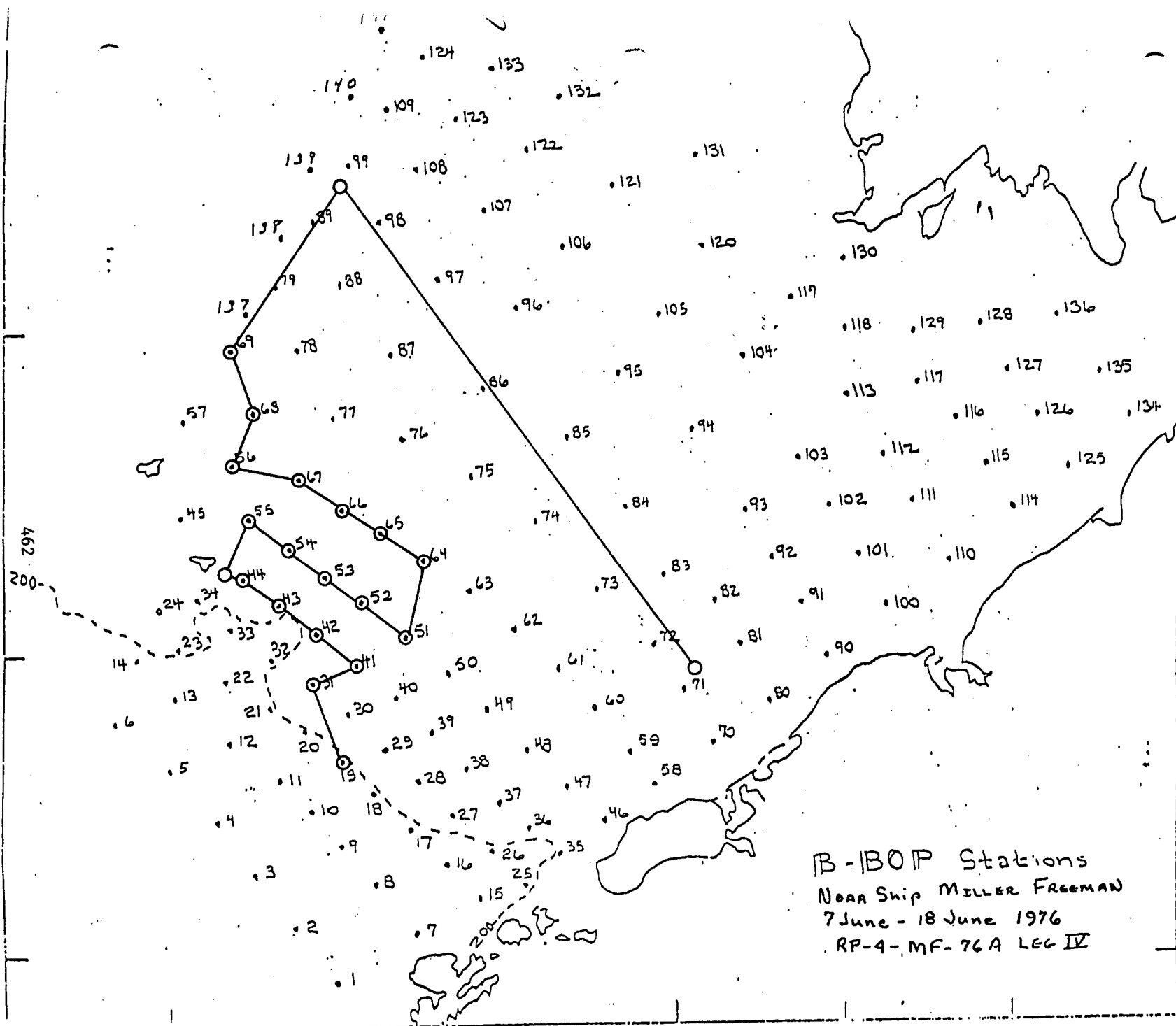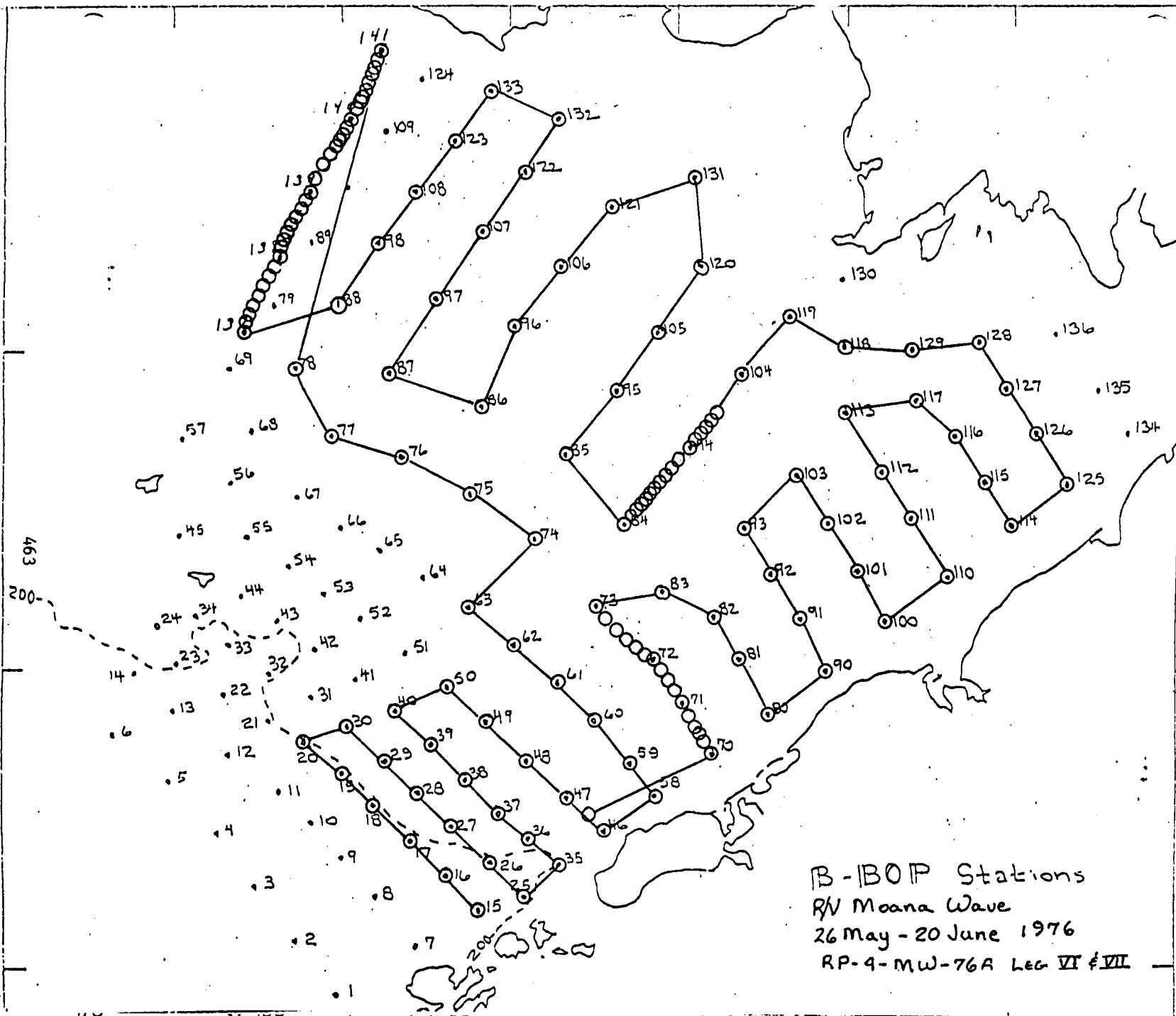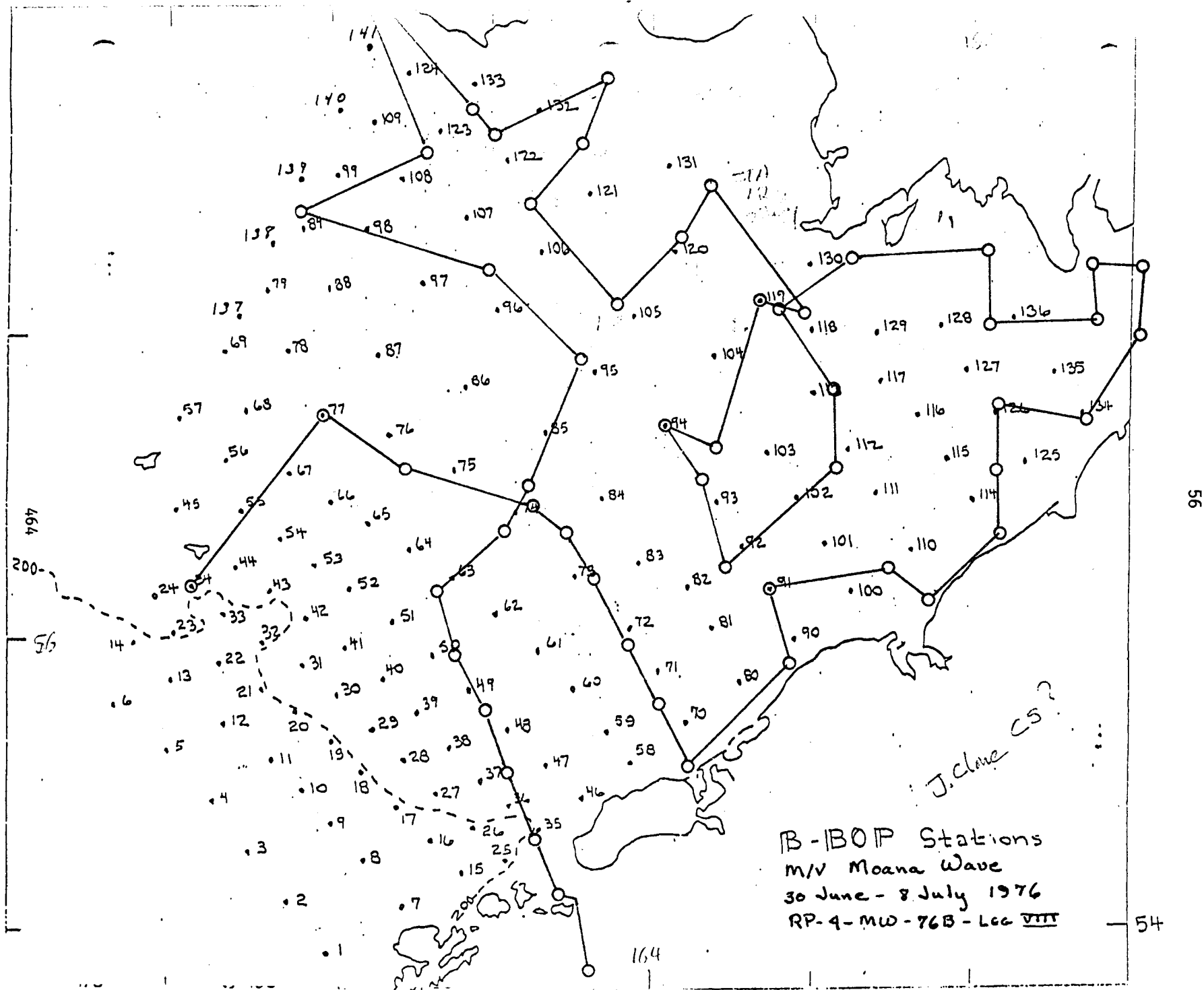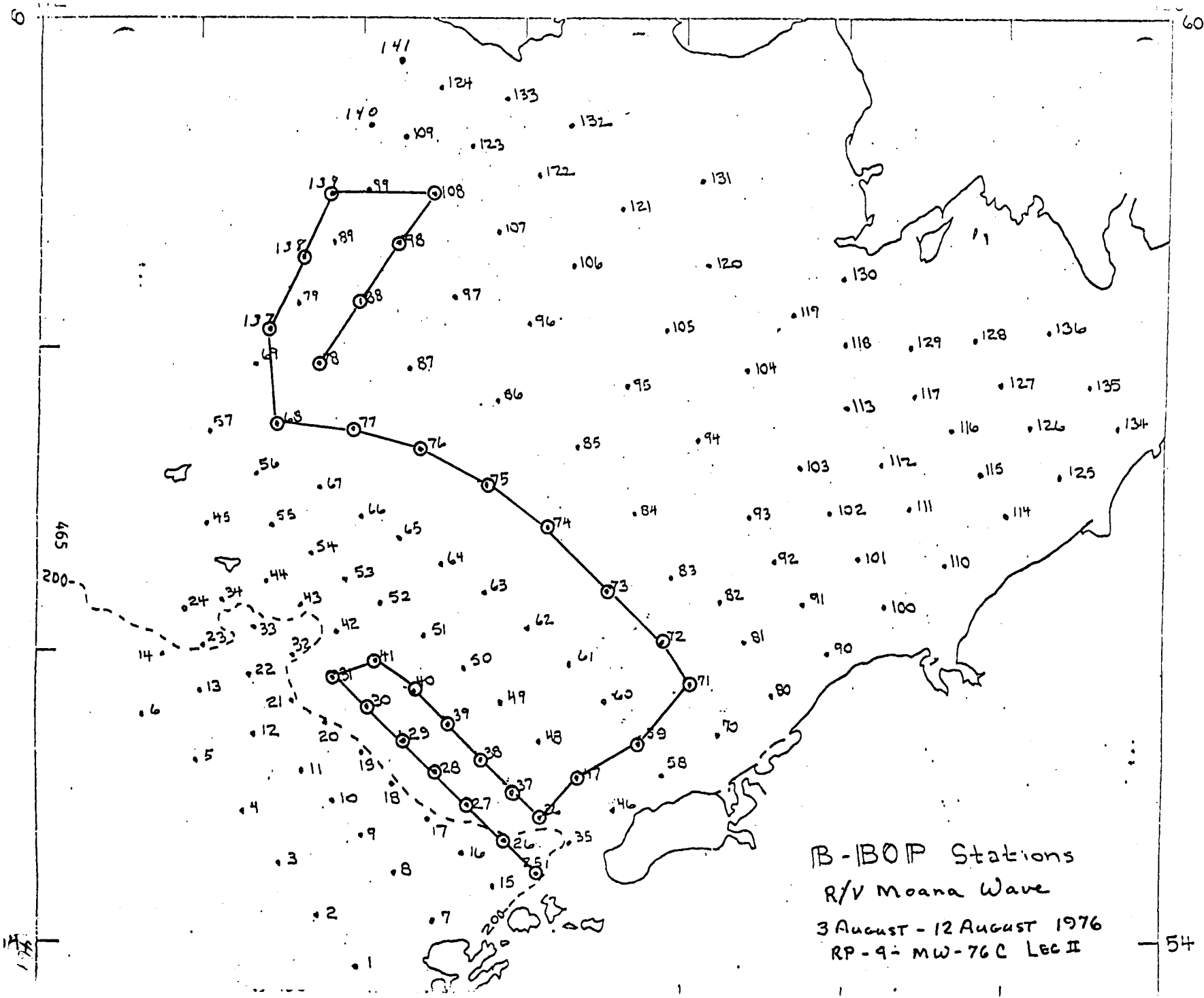
B-BOP Stations
R/V Moana Wave
3 August - 12 August 1976
RP-4-MW-76C Leg II

B-BOP Stations
R/V ACONA CRUISE #233
2 AUGUST - 13 AUGUST 1976

B-BOP Stations
R/V Moana Wave
17 September - 3 October 1976
RP-4-MW-76 C Leg V

B-BOP Stations
R/V Acona
23 September - 3 October 1976
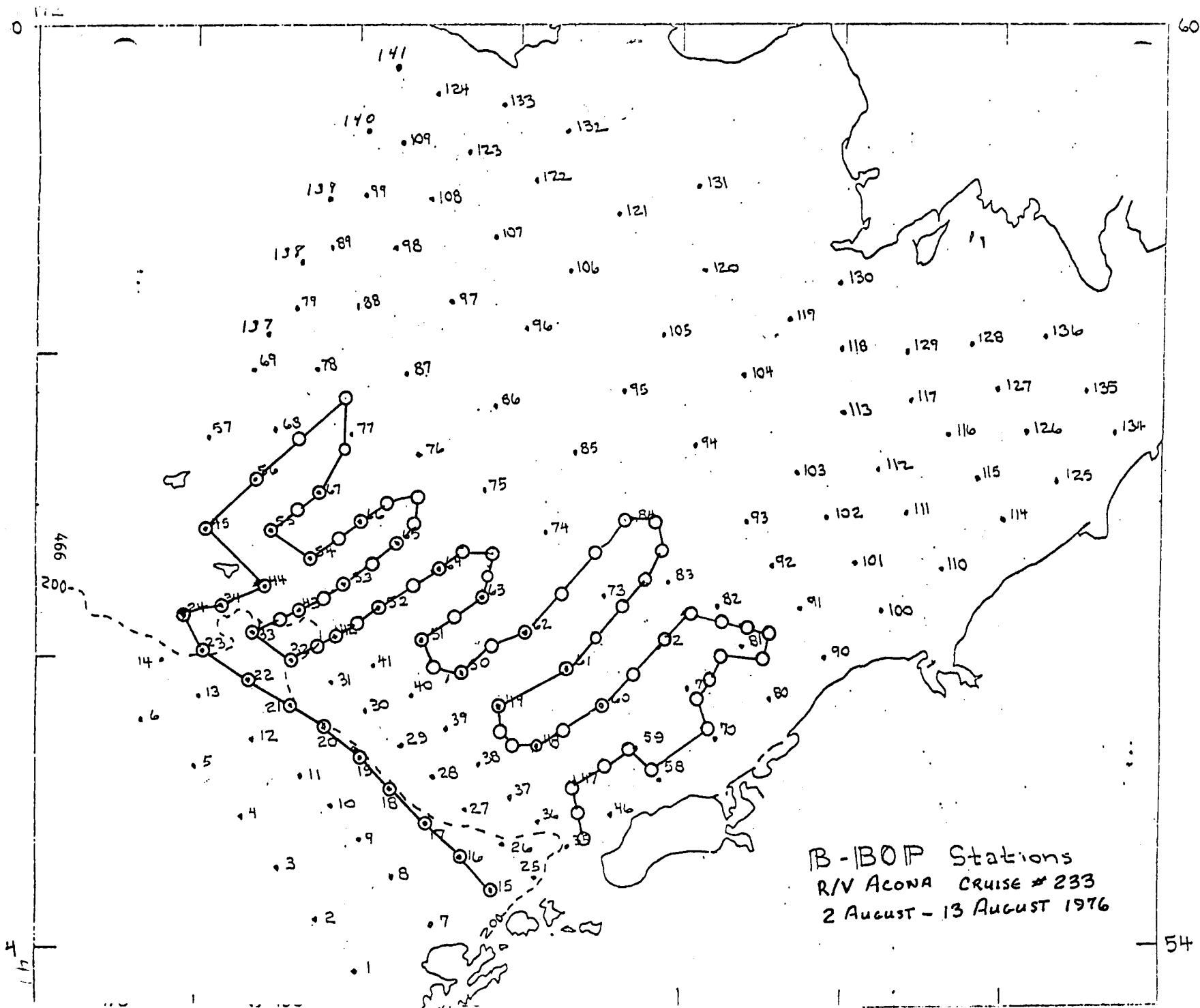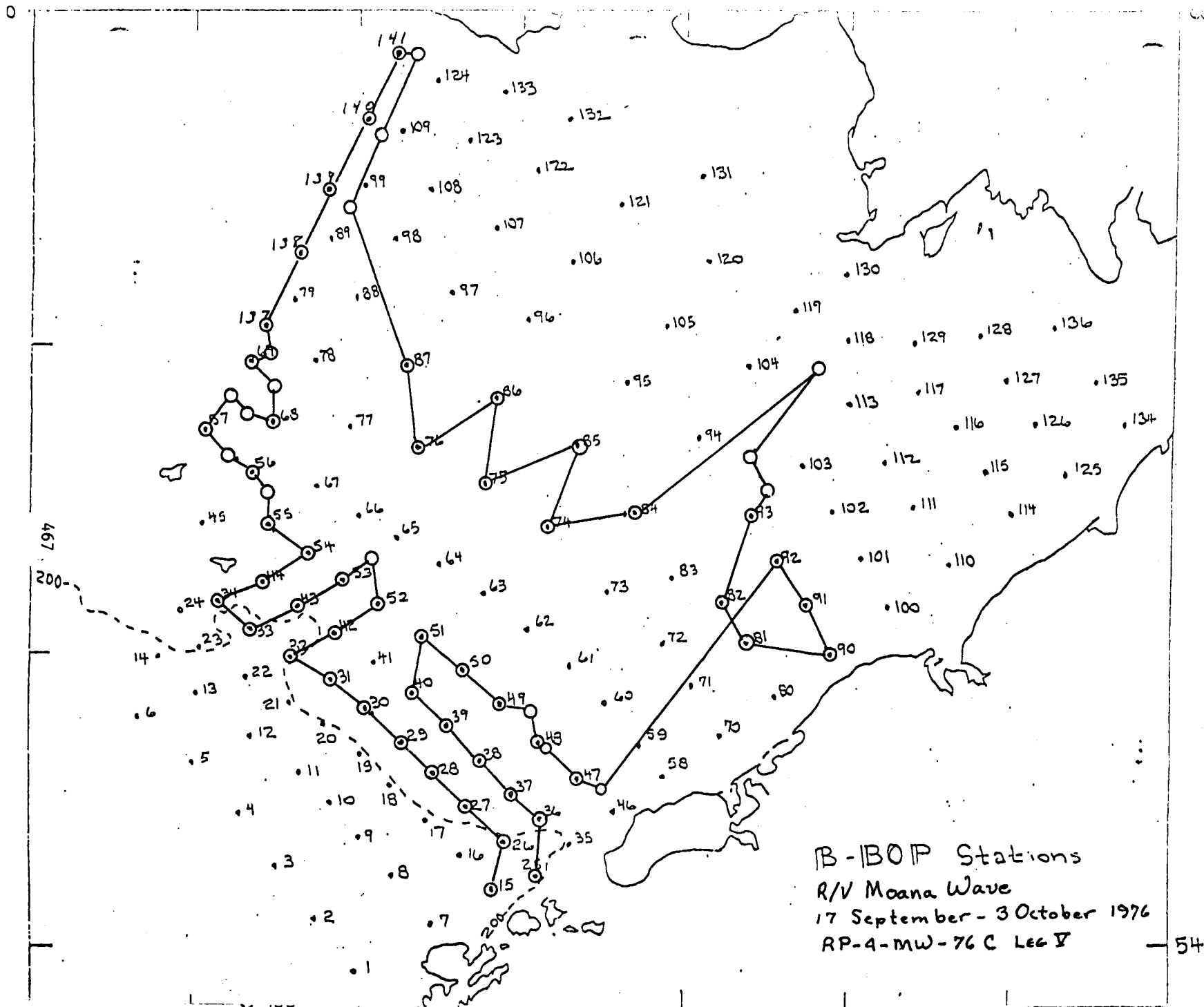
APPENDIX 2

B-BOP INSTRUMENT SUMMARY

Date	Location	Instruments[1]	Days[2]	Remarks
7 Sept.- 4 Nov. 75	BC-4A 58-37.0 168-14.0 55 m	2 RCM-4 1 TG-2	58	
6-21 Sept. 75	BC-1A 55-24.6 167-57.5 201 m	2 RCM-4 1 TG-2	3, 16	Trawled
8 Sept.- 5 Nov. 76	BC-2A 57-04.3 163-19.5 65 m	2 RCM-4 1 TG-2	58	
4 Nov. 75	BC-1B 55-24.0 167-58.0 205 m	2 RCM-4 1 TG-2	0	Trawled
4 Nov. 75- 14 June 76	BC-4B 58-37.0 168-14.1 55 m	2 RCM-4 1 TG-2	228	Partial recovery
5 Nov. 75- 30 May 76	BC-2B 57-03.7 168-21.8 65 m	2 RCM-4 1 TG-2	207	
6 Nov. 75- 16 Mar. 76	BC-3A 55-01.5 165-10.3 115 m	2 RCM-4	130	
16 Mar.- 29 May 76	BC-3B 55-01.3 165-04.8 116 m	2 RCM-4 1 TG-2	8, 73	
19 Mar.- 12 June 76	BC-12A 55-48.2 163-54.1 97 m	2 RCM-4	15, 85	

[1]RCM-4:   Aanderaa recording current meter, model 4.
 TG-2,3:   Aanderaa pressure gages, models 2 and 3.

[2]Number of days of usable data.

Date	Location	Instruments[1]	Days[2]	Remarks
20 Mar.- 30 May 76	BC-7A 55-42.3 163-01.3 67 m	2 RCM-4 TG-2	71 (TG-2)	
22 Mar.- 6 June 76	BC-13A 55-30.2 166-01.7 122 m	2 RCM-4 1 TG-2		
31 May- 26 Sept. 76	BC-2C 57-03.7 163-21.3 119 m	2 RCM-4 1 TG-2	23, 118	
29 May- 28 Sept. 76	BC-3C 55-01.8 165-09.8 114 m	2 RCM-4	122	
30 May- 27 Sept. 76	BC-6A 56-32.1 162-35.3 76 m	2 RCM-4	125	
6 June- 29 Sept. 76	BC-13B 55-30.1 165-49.4 122 m	2 RCM-4 1 TG-2	35	Trawled
30 May- 27 Sept. 76	BC-14A 56-02.3 161-50.0 51 m	2 RCM-4 1 TG-3	124	TG-3 not recovered
31 May- 26 Sept. 76	BC-15A 57-36.4 162-45.2 51 m	2 RCM-4 TG-2	118	one RCM-4 lost
1 June- 23 Sept. 76	BC-10A 57-16.6 169-32.8 66 m	1 RCM-4 1 TG-3	~ 60	
1 June- 24 Sept. 76	BC-8A 57-58.5 168-49.5 73 m	2 RCM-4	~ 60	

[1]RCM-4:   Aanderaa recording current meter, model 4.
 TG-2,3: Aanderaa pressure gages, models 2 and 3.
[2]Number of days of usable data.

Date	Location	Instruments[1]	Days[2]	Remarks
30 May- 27 Sept. 76	BC-5A 56-49.2 163-06.6 70 m	2 RCM-4	119	
1 June- 25 Sept. 76	BC-4C 58-35.8 168-20.7 58 m	2 RCM-4 1 TG-3	~ 60 Faded	
2 June- 24 Sept. 76	BC-9A 59-14.0 167-36.1 39 m	2 RCM-4	~ 60	
2 June- 24 Sept. 76	BC-11A 167-13.6 31 m	1 TG-3	~ 90	
27 Sept. 76	BC-2D 57-02.3 163-25.7 66 m	2 RCM-4 1 TG-2		
29 Sept. 76	BC-13C 55-47.2 165-13.8 108 m	2 RCM-4 1 TG-2		
26 Sept. 76	BC-15B 57-37.7 162-44.9 46 m	2 RCM-4 1 TG-2		
21 Sept. 76	BC-17A 56-34.0 167-33.0 108 m	2 RCM-4		
25 Sept. 76	BC-4D 58-36.6 168-21.7 55 m	2 RCM-4 1 TG-3		
24 Sept. 76	BC-9B 59-13.0 167-42.0 40 m	2 RCM-4 1 TG-3		

[1]RCM-4: Aanderaa recording current meter, model 4.
 TG-2,3: Aanderaa pressure gages, models 2 and 3.

[2]Number of days of usable data.

APPENDIX 3

Estimate of Funds Expended
by University of Washington
to 28 February 1977

Total Allocation (5/16/75-9/30/77): $330,400

A.   Salaries - faculty, staff & students   56,030

B.   Benefits   6,112

C.   Expendable Supplies & Equipment   18,210

D.   Permanent Equipment   67,020

E.   Travel   13,157

F.   Computer   107
         Consultation   4,000

G.   Other Direct Costs   26,633

H.   Indirect Costs   24,541

Total Expenditures   215,810

Remaining Balance $114,590

Annual Report

STD Measurements in Possible Dispersal Regions

of the Beaufort Sea

Knut Aagaard

Department of Oceanography

University of Washington

Seattle, Washington   98195

24 March 1977

I. Summary

Through a series of CTD sections across the Beaufort Sea shelf we have traced the seasonal hydrographic sequence from fall to spring in one year, and from fall to winter the next.

We have seen that not only are there large seasonal changes in the hydrography, but conditions are also different from one year to the next. The latter point is a caution to us, should we attempt to generalize from too short a time base. Nonetheless, the normal seasonal cycle has now probably been determined at least in outline.

One matter appears to stand out in importance: the Beaufort Sea shelf is certainly not neutral with respect to the Arctic Ocean to the north. Rather there are one or more forms of interaction, in which water and the substances it transports are exchanged between the shelf and the offshore regions. Certainly the salt budget calculations discussed in Section VII can be thus interpreted. It is likely that when the presence of widespread temperature maxima is better understood, it also will point to such an exchange. The most dramatic evidence of exchange is the series of four sections from fall 1976, in which an intense subsurface current core appears to be sweeping up the slope and onto the shelf, flooding at least one section to the innermost station with dense, saline water.

II. Introduction

The general objective of this research unit has been to provide seasonally distributed synoptic temperature-salinity mappings of the Beaufort Sea shelf and slope. In the first year of work the sections were distributed along the entire Alaskan shelf, one each going out from Pitt Point, Narwhal Island, and Humphrey Bay. They were run in the fall (October-November), winter (February), and spring (May). The intent was to provide broad areal coverage. The second year the sections were concentrated in two locations, *viz*. off Lonely and Oliktok. In each region two parallel lines of stations were run in order to more closely examine the east-west hydrographic structure. Because of the similarity in winter and spring conditions during the first year, we felt it sufficient the second year to sample only in the fall and winter.

The general thrust of this work is of course toward understanding the diffusive and advective processes which transport and disperse pollutants and substances of biological and geological importance.

III. Current state of knowledge

Except for the brief ice-free period during summer, hydrographic stations had never been taken in this area prior to the present work. Knowledge was therefore restricted to summer conditions, which briefly appear to be as follows. There are large temperature and salinity ranges (and gradients) on the shelf, with temperatures varying from near-freezing to more than 5°C, and salinities from brackish to greater than 33‰. In summer an eastward intrusion of relatively warm water originating in the Bering and Chukchi seas appears to be a regular feature of the circulation on the outer shelf, being typically located

seaward of the 40 m isobath. This water has been identified at least as far east as 143°W. Summer observations have also indicated the likelihood of an intermittent upwelling regime on the eastern part of the shelf. The upwelled water is relatively cold, low in oxygen, and high in nutrients. It has been postulated that the upwelling is a response to locally strong easterly winds and that the upwelled water on the shelf moves westward.

The work of the past year-and-a-half has added substantially to this picture, as will be discussed in Section VII of this report.

IV. Study area

The most general area of interest extends eastward from Point Barrow along the entire northern Alaskan coast, *i.e.*, from about 156°30'W to 141°W, a lateral distance of nearly 600 km. The shelf is narrow, with the shelf break typically 80-90 km offshore. The total runoff is relatively small, highly seasonal, and concentrated in a very few rivers of any consequence, the largest of which is the Colville. The area is covered by sea ice, both first- and multi-year, through all but 2-3 months. Even during the height of summer, ice is usually found well onto the shelf.

V. Data collection

The rationale of data collection has been discussed in the annual report of last year and in Section III of this report. In the second sequence of STD sections, run in the fall and winter of the present fiscal year (cruises W25 and W27), the station spacing was decreased somewhat from that of the first year, to about 5 nautical miles. The two parallel lines in each set were located about 15-20 miles apart. The idea was to get as much spatial resolution as possible.

During this second year we made certain changes in equipment and procedure. One was the installation of low-frequency navigation gear aboard the helicopter. This made possible a sizeable improvement in our ability to fix station locations. Another major improvement was to redesign the sensor package into a smaller format. It now fits down through an 8-inch auger hole, thus no longer requiring the laborious task of drilling and chiseling a hole four times the size. A third improvement was installation of a frequency counter along with the data logger, thus enabling constant monitoring of the sensor signals. This has improved the quality of the tapes considerably.

VI. Results

All data from cruises W21-W25 have been submitted to the project data office, properly formatted on magnetic tape. Pictorial representations of all the sections are included in Section VII of this report.

VII. Discussion

Figures 1-9 show the seasonal progression of the hydrography on the Beaufort shelf during 1975-1976. Cruise W21 was in the fall (October-November), W22 in
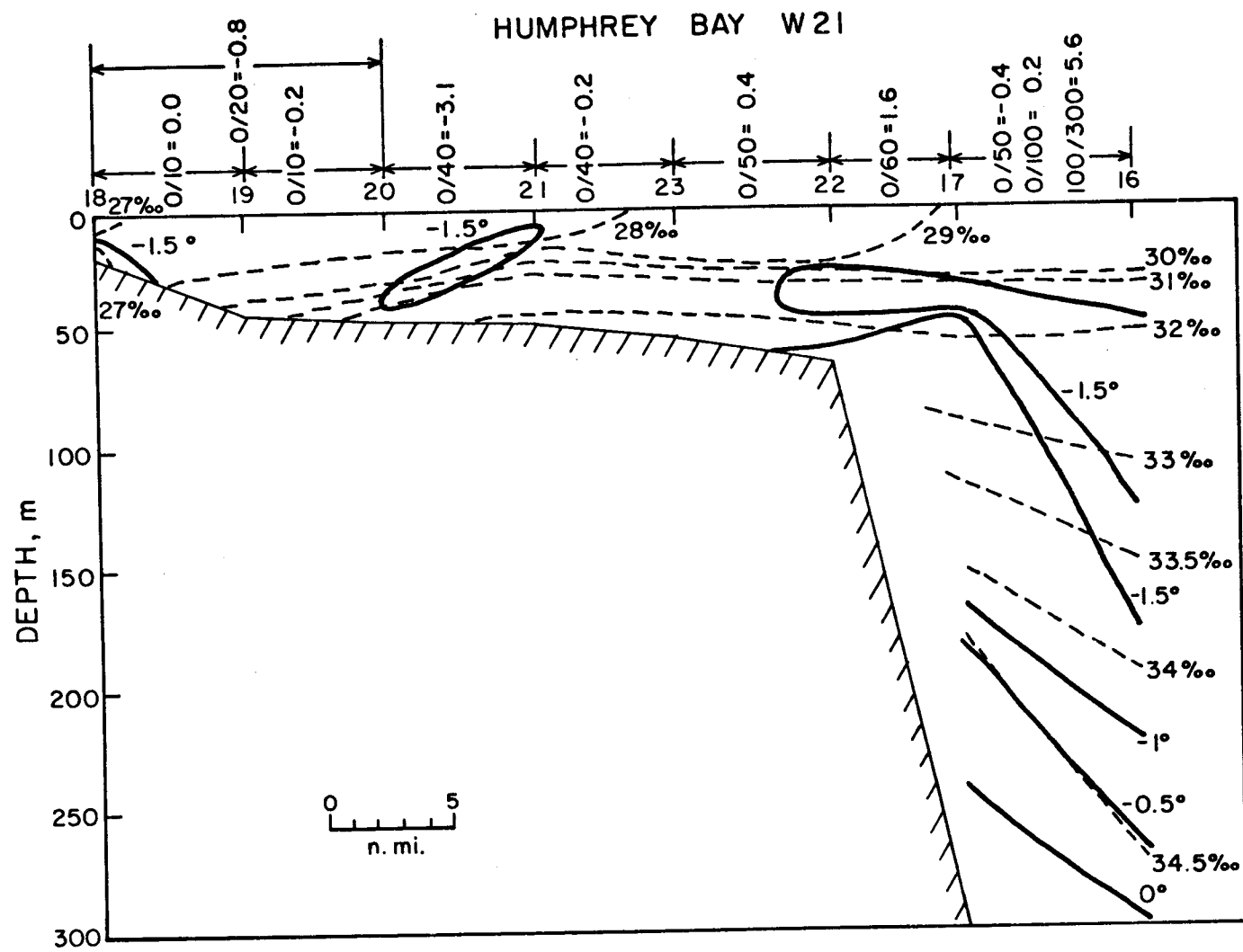
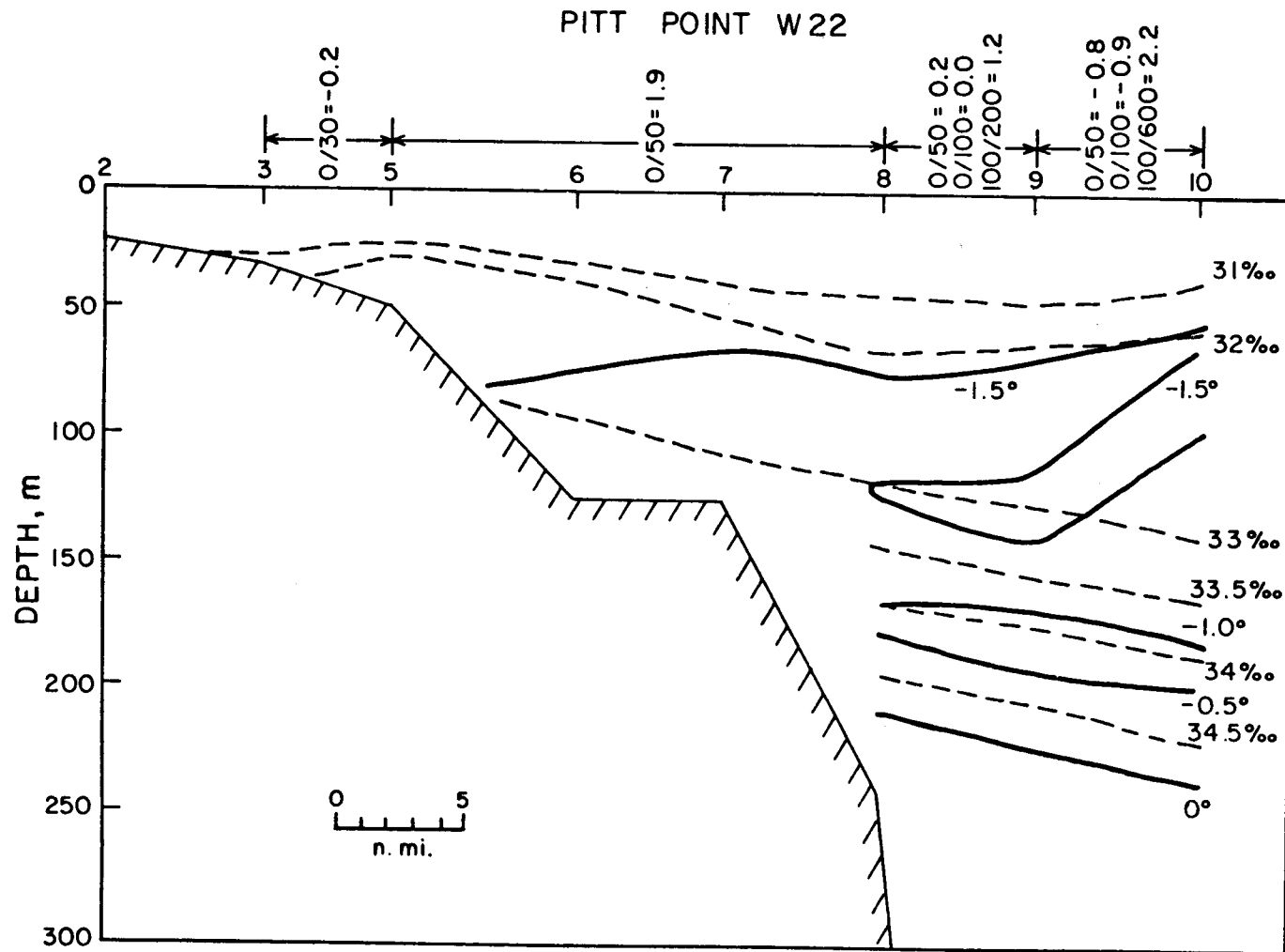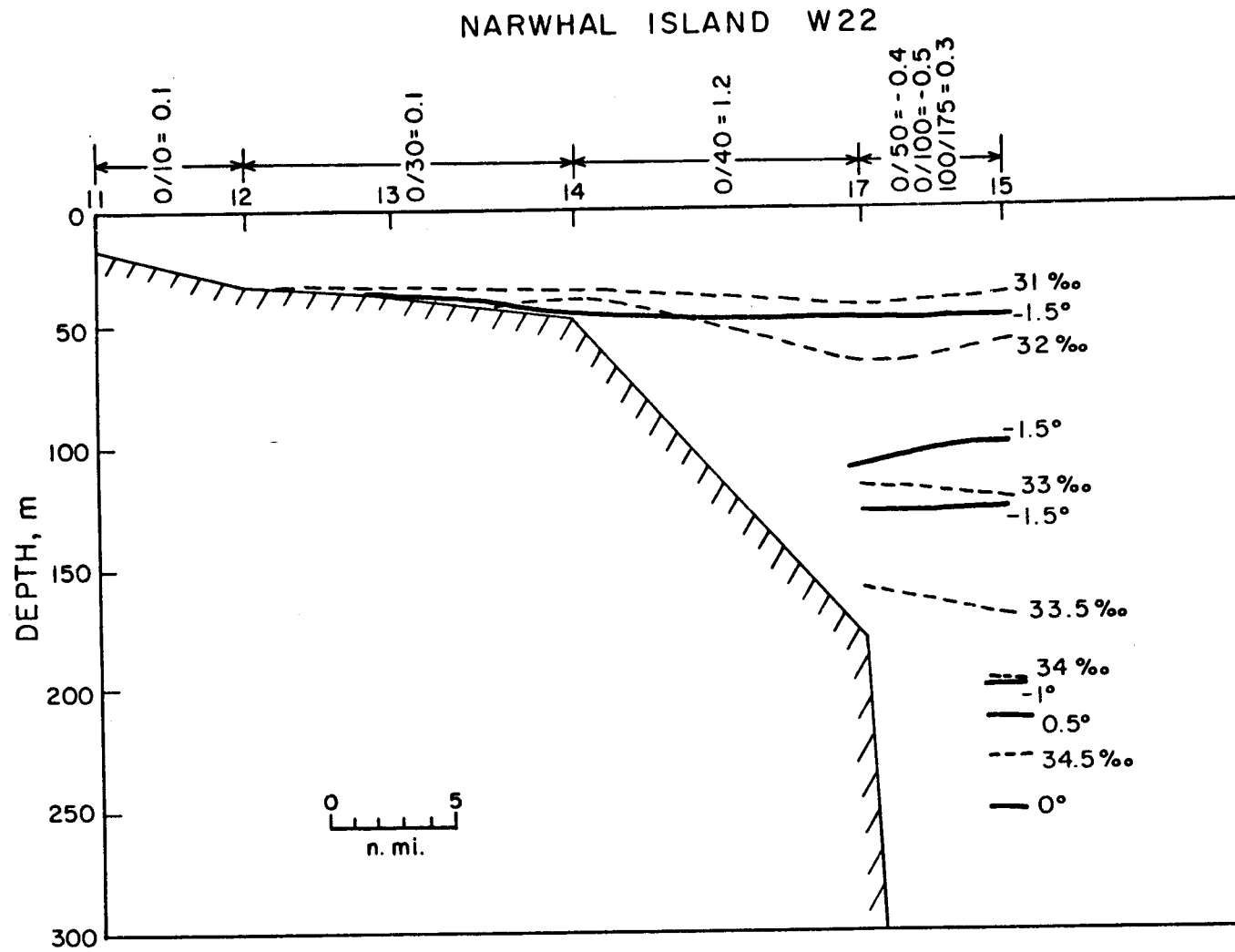PITT POINT W21
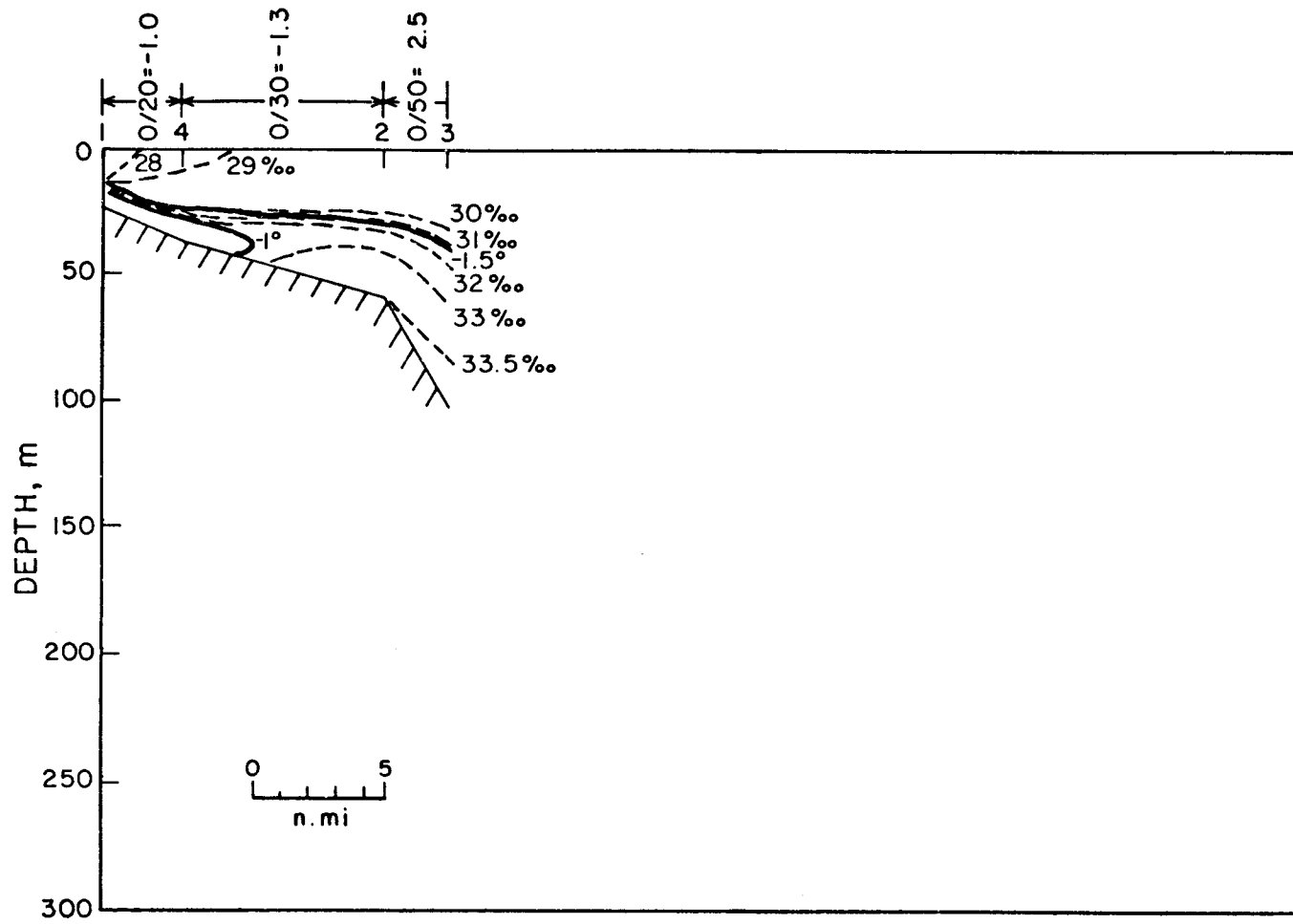
Figure 1

NARWHAL ISLAND W21
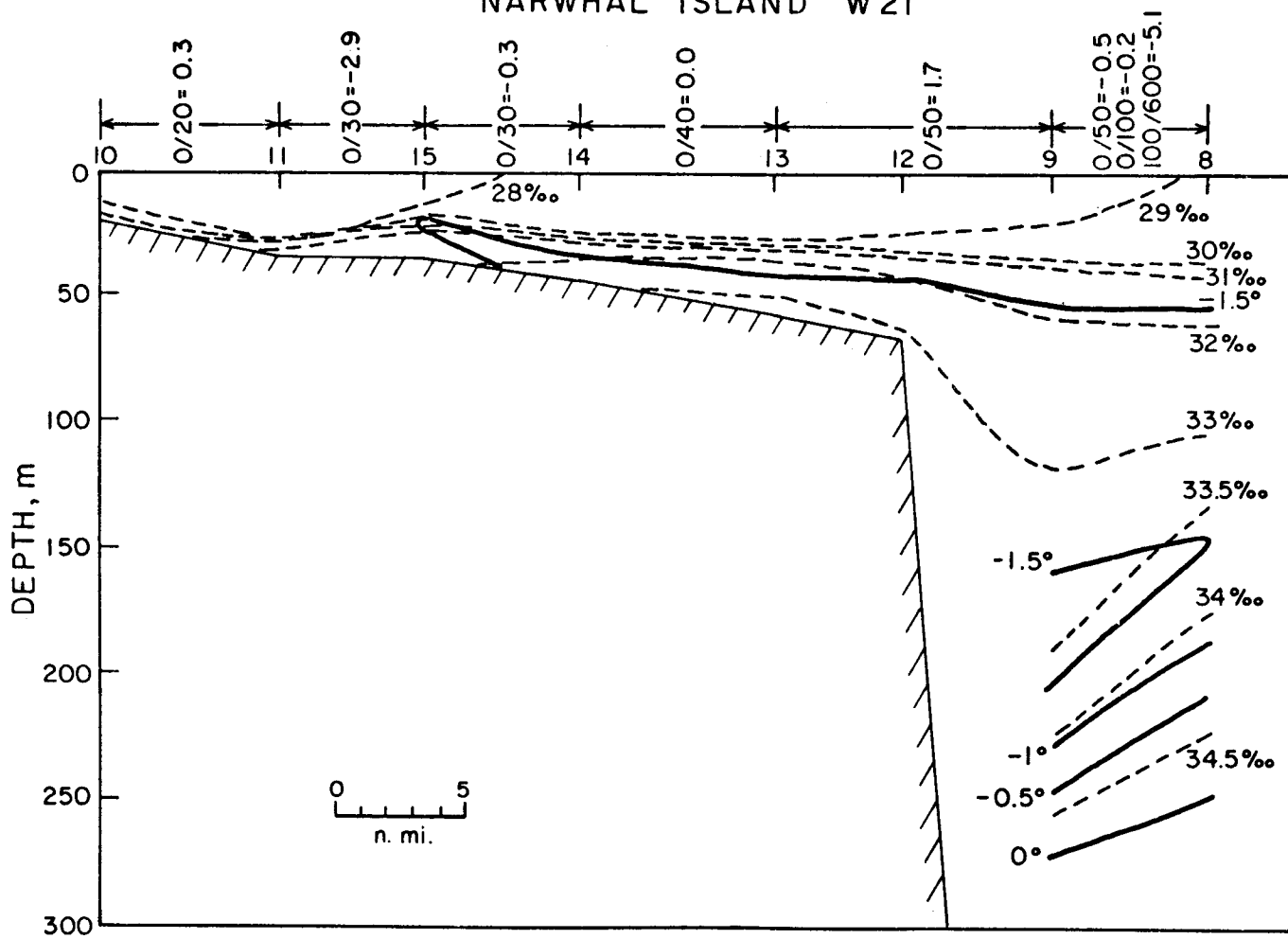
Figure 2
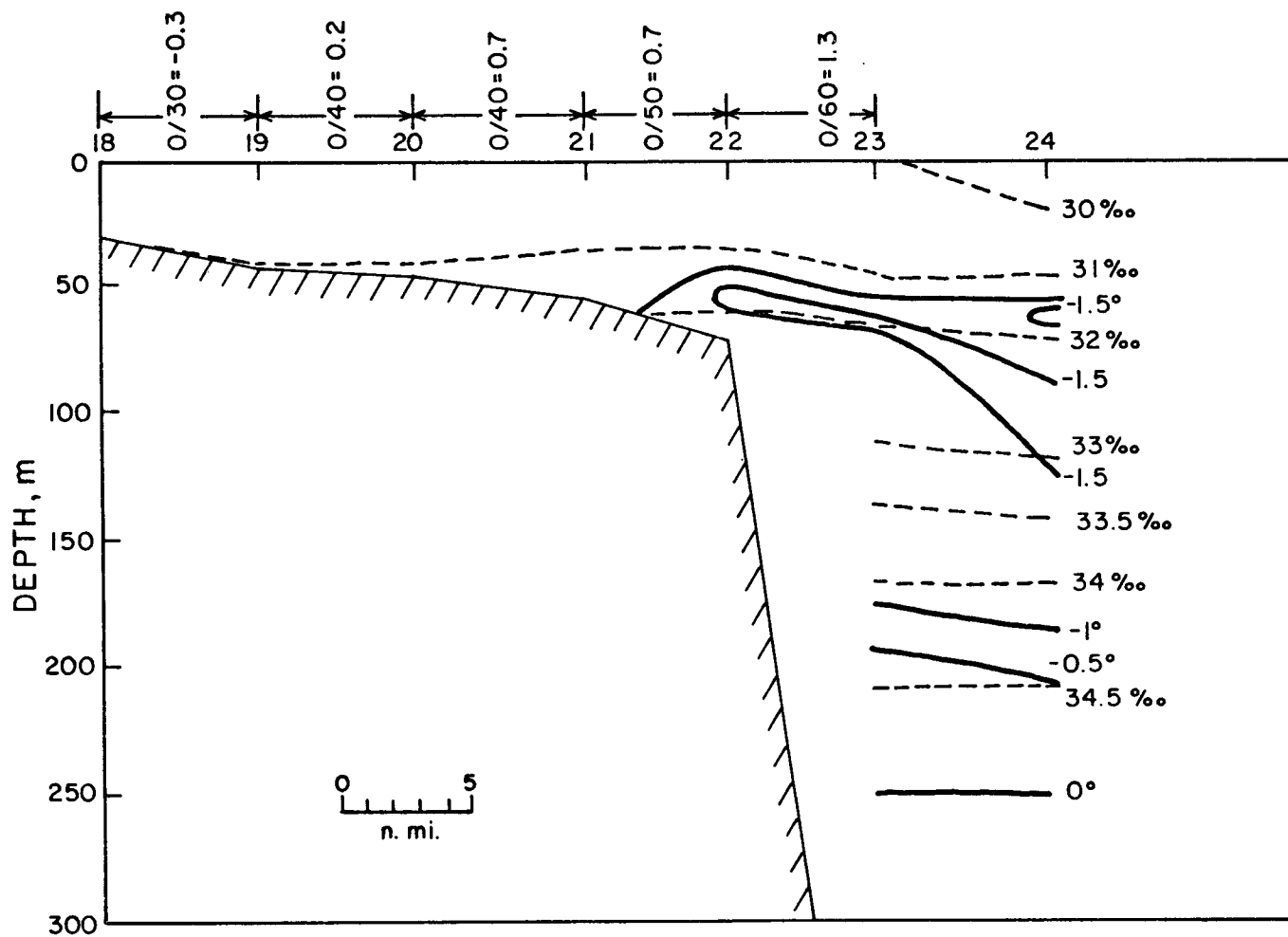
Figure 3

Figure 4

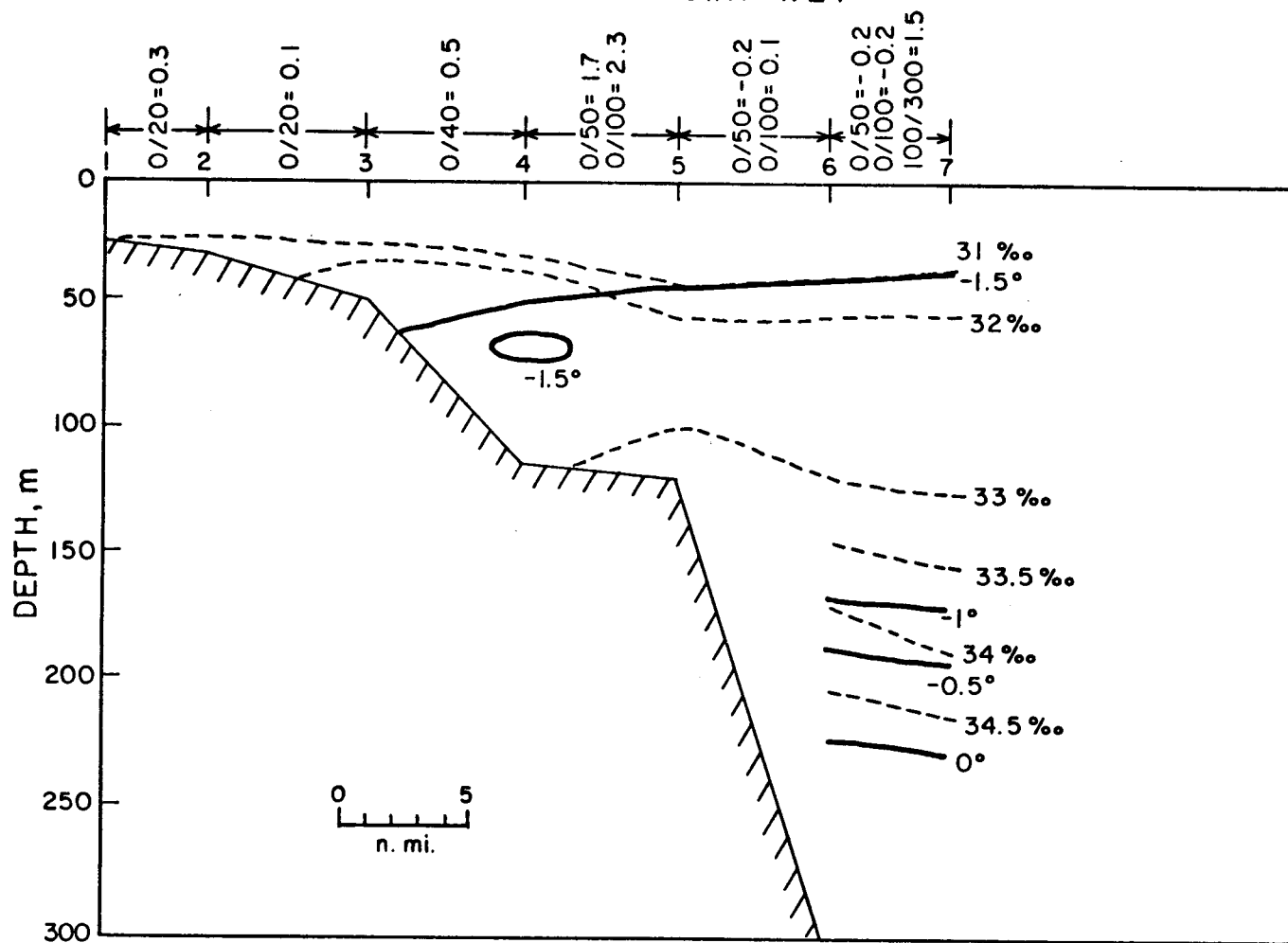NARWHAL ISLAND W22

Figure 5

Figure 6
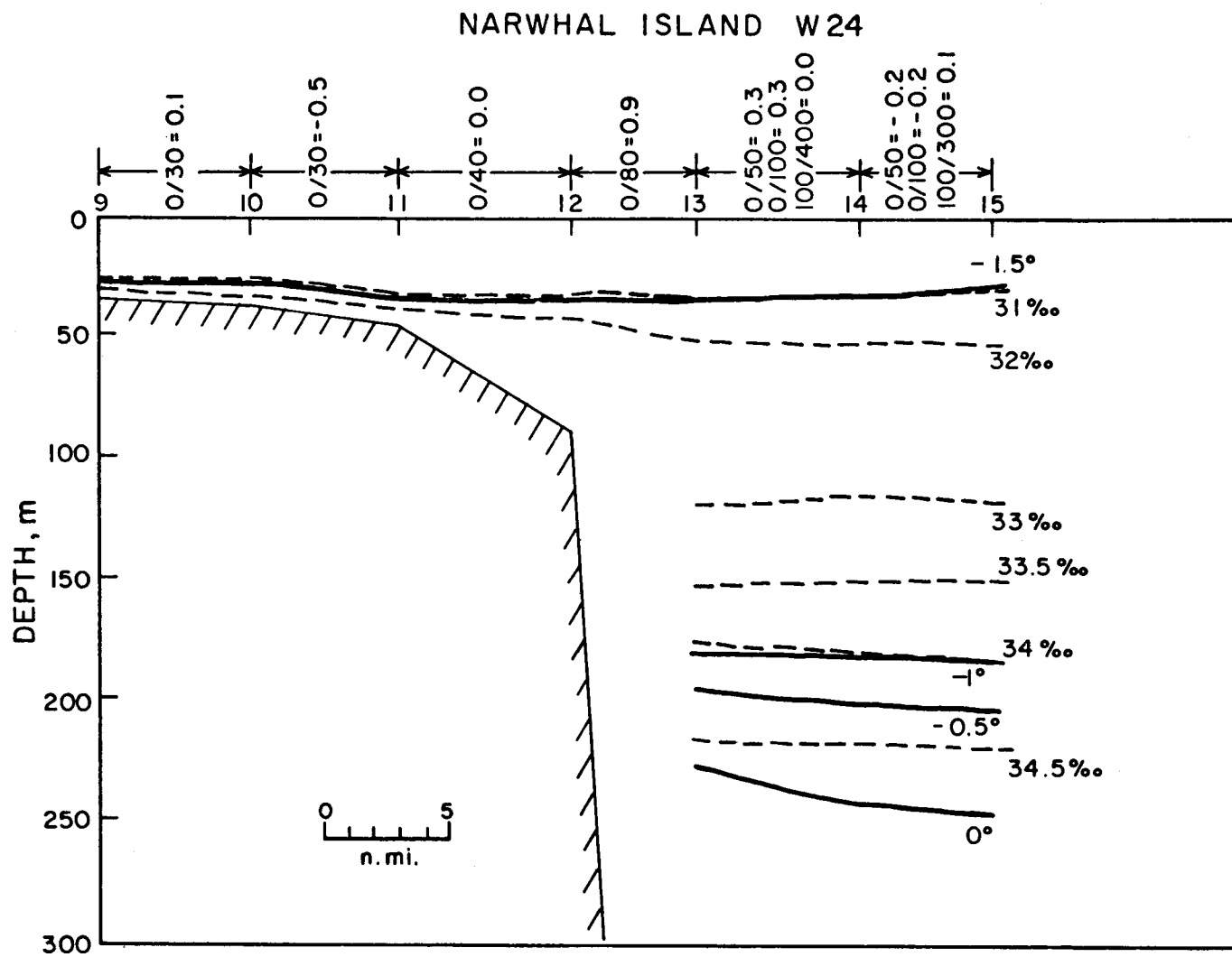
PITT POINT W24

Figure 7

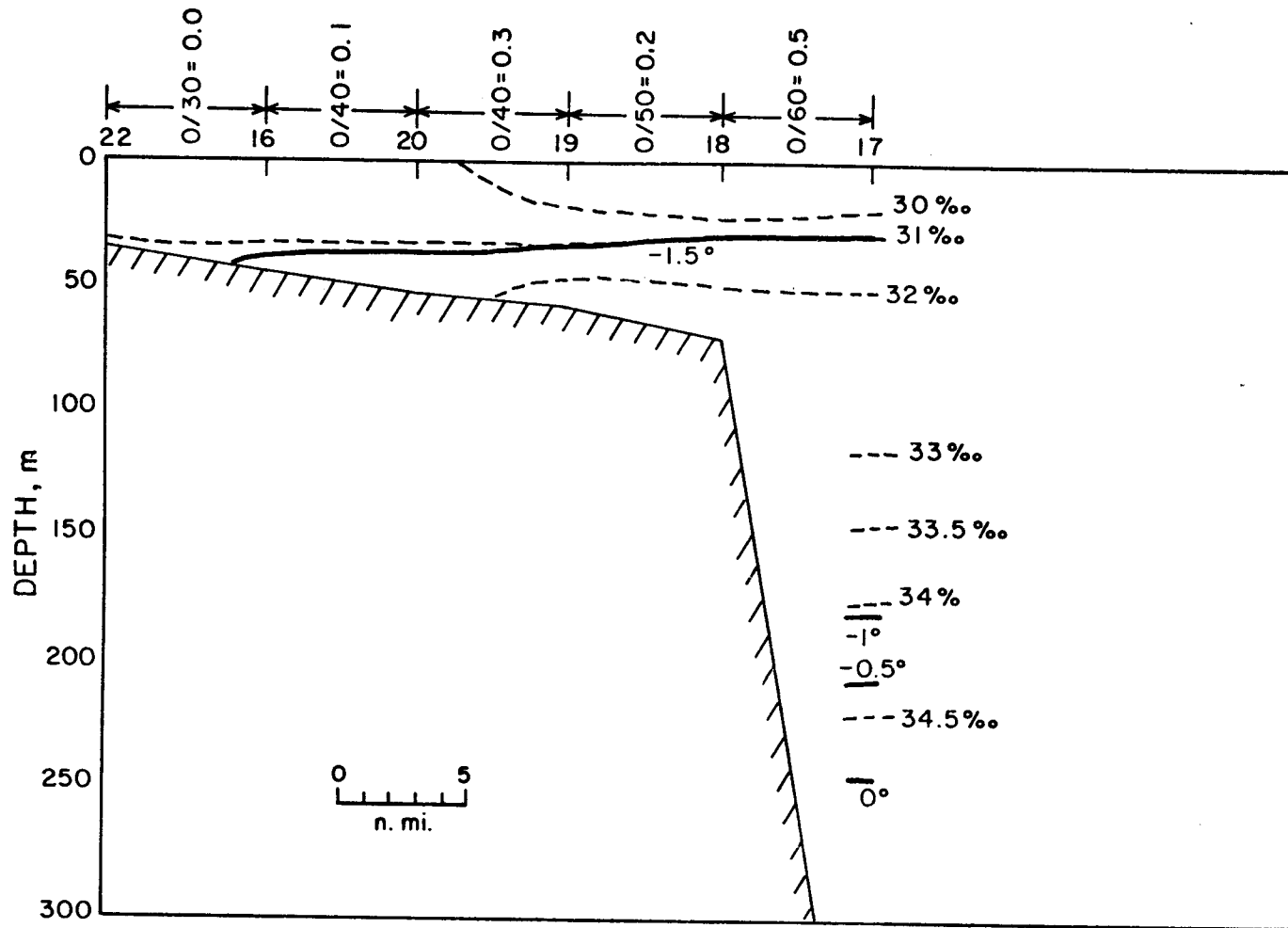Figure 8

HUMPHREY BAY   W24

Figure 9

the winter (February), and W24 in spring (May). The Pitt Point, Narwhal Island, and Humphrey Bay sections transect the western, central, and eastern shelf, respectively, and are assumed to have been representative of those regions.

In the fall (Figs. 1-3) the entire shelf was markedly stratified, with a strong salinity (and hence density) gradient below 20-30 m. Above the pycnocline the upper layer was of relatively low salinity (everywhere less than 30‰, and at station 18 less than 27‰) and nearly homogeneous in both temperature and salinity. An example is given in Figure 10, showing conditions at station 22 on the Humphrey Bay section. The temperatures in the upper isothermal layer were generally very close to the freezing point, with some tendency toward a slight supercooling (relative to the freezing point at one atmosphere). This upper homogeneous layer is the result of thermohalic convection driven by freezing. The process will continue throughout the winter, reducing the over-all shelf stratification. The fall sections also show a gradual seaward increase in upper-layer salinity, about 1-2‰ across the width of the shelf. Along with the salinity stratification, this represents a remnant of the previous summer hydrography, which is strongly influenced by runoff and ice melt. Finally, a number of the stations show a pronounced temperature maximum somewhere below the mixed layer. The presence of this maximum at the Pitt Point section is clearly seen in Figure 1, where it represents water of Bering Sea origin. We shall come back to this problem later in the discussion.

In the winter (Figs. 4-6) the overall stratification on the shelf was markedly less than in the fall, and the upper mixed layer extended deeper, typically below 30 m. At the same time the upper-layer salinity was also higher, being above 31‰ everywhere on the shelf. These features are apparent by contrasting Figure 10 with Figure 11, which shows conditions at station 22 on the Humphrey Bay winter section. [The two stations, W21-22 (Fig. 10) and W22-22 (Fig. 11), were taken at the same location.]

While both a reduced stratification and an increase in salinity are to be expected as winter progresses, due to the separation of salt by freezing, the salinity increase from station W21-22 to W22-22 is larger than reasonably can be explained by this process. Over 2 m ice would have to be formed from November to February for the salinity increase. That this result is not just a local one at this one station is shown by the total salt budget for both the Narwhal Island and Humphrey Bay sections. The mean salinity increase above 50 m over the shelf for the Narwhal Island section, between November and February, was 1.31‰, requiring the formation of about 270 cm ice. Similarly the increase for the Humphrey Bay section shoreward of station 22 was 1.51‰, which corresponds to forming about 370 cm ice. These calculated amounts of ice formation are almost certainly high by a factor of 2-3. On the other hand, changes in the salinity after February can readily be explained by freezing, or as being within the resolution of the methods. For example, from February (W22) to May (W24) the mean salinity in the Narwhal Island section increased by only 0.25‰, corresponding to 55 cm of ice formation; and the mean salinity in the Humphrey Bay section decreased -0.05‰, which is undoubtedly below the noise level. The conclusion must therefore be that during fall and early winter, there is a net advective flux of salt onto the Beaufort Sea shelf. Such a flux does not necessarily involve large volume transports. For example, if the new saltier water coming onto the shelf is 1‰ more saline than the water it replaces, then the flow rate of saline water onto the entire shelf region between the Narwhal Island and Humphrey Bay sections need not exceed 0.06 Sv in order to maintain the salt budget. The source of
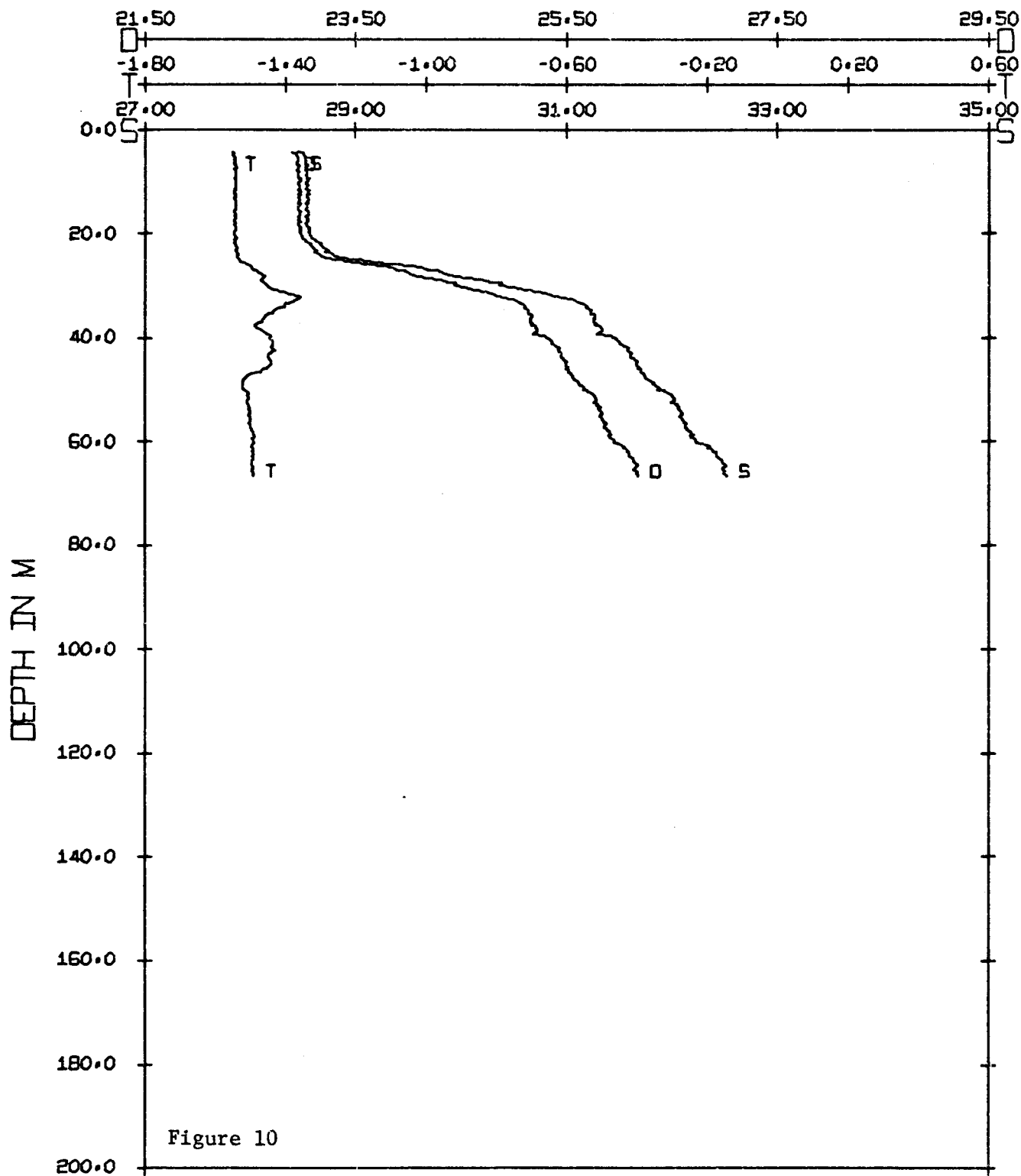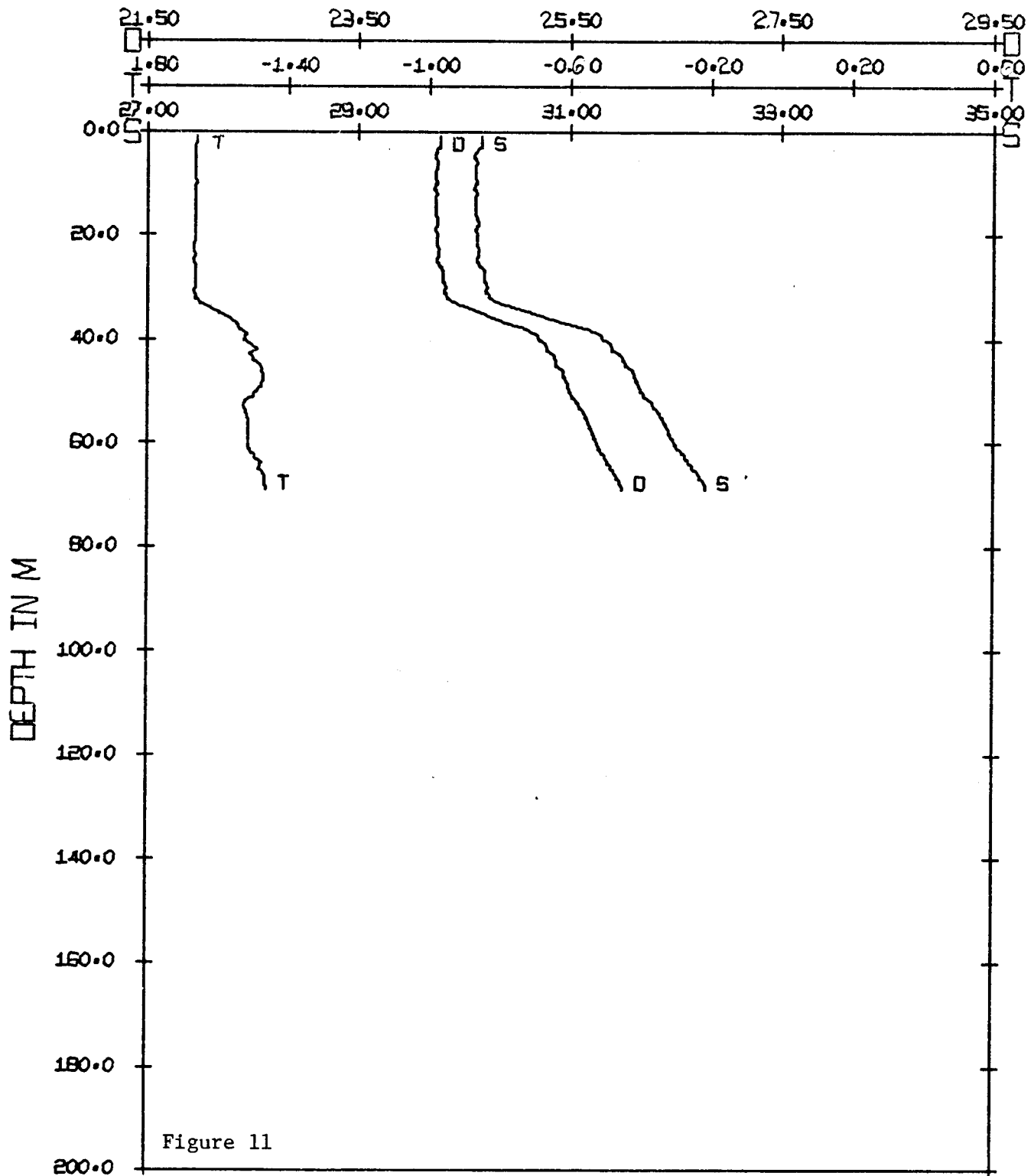
STD PLOT
TT 21   022

Figure 10

LATITUDE   70-29.7N
LONGITUDE   141-53.0W

T = TEMPERATURE - C
S = SALINITY - 0/00
D = SIGMA-T

DATE   10 NOV. 1975
BEGIN 2018

DEPTH IN M

STD PLOT
TT 22   022

Figure 11

T = TEMPERATURE - C

LATITUDE   70·29·5N   S = SALINITY   0/00   DATE   29 FEB· 1976
LONGITUDE 141-54·0W   D = SIGMA-T   BEGIN 1901

487

saline water must for the present be considered unknown. Conceivably it could lie in the Chukchi Sea, or alternatively it may be in the form of water upwelled from deeper levels in the Arctic Ocean.

Another feature of the winter salinity distributions is that except off Pitt Point the upper-layer salinity decreased seaward. At the Narwhal Island section the total decrease was 0.5‰ and at the Humphrey Bay section 0.8‰. In the spring sections (Figs. 7-9) there is a similar trend, this time at the Pitt Point section also. Several possible mechanisms suggest themselves. One is that relatively dense water sinking from the upper layer above the shelf moves into the Arctic Ocean at mid-depth and is replaced by less saline water moving inshore in the upper layer. Such a transverse circulation is in the cyclonic sense (looking westward along the shelf) and would be driven by a shallow salt source on the shelf. Freezing is of course an obvious example of such a salt source, its relatively greater intensity inshore conceivably being due either to the volume of water underlying a given surface area being less there, or to the amount of ice actually formed on the shelf being greater than offshore. Alternatively, relatively saline water being advected onto the shelf from the Chukchi Sea and later sinking from the shelf could also drive such a transverse circulation. Regardless of the details, a cyclonic circulation involves some form of free gravitational convection, being driven by a source of dense water at a relatively high elevation. The second possible mechanism responsible for the observed salinity distribution is upward movement of saline water onto the shelf from deeper levels in the Arctic Ocean. This water would have to flow in along the bottom of the shelf and then be subjected to a relatively effective vertical mixing on the inner or middle shelf. Such a transverse circulation is in the anticyclonic sense (looking westward) and would in effect be driven by a deep salt source seaward of the shelf. It thus represents a forced convection. A third possible mechanism is of course that the horizontal salinity gradient represents a baroclinic adjustment to a more-or-less steady geostrophic westward flow.

The temperatures in the winter sections were typically about 0.1° colder than in the fall, and in the upper layer the water showed a slight (on the average about 0.03°C) but definite supercooling. As in the fall, one or more subsurface temperature maxima were common.

The spring sections (Figs. 7-9) are very similar to those from winter. The salinity and density structure is about the same, but there are some slight differences in the temperature of the upper layer: it is not quite as cold, but is instead beginning to show a slight spring warming. Only four stations had near-surface temperatures below the freezing point. The temperature of the remaining stations varied from just above the freezing point to an extreme of about 0.16°C above at station 17. At the latter station, the upper 200 m of which are shown in Figure 12, the warming is restricted to a 5-m thick layer and is accompanied by a salinity that is slightly lower than that of the underlying water. As in the fall and winter, there generally were temperature maxima below the upper mixed layer.

The dynamic height differences between adjacent stations are also shown in Figures 1-9. For example, in Figure 1 the notation 0/20 = -1 between stations 1 and 4 means that the dynamic height at the surface relative to 20 db at station 1 was 1 dynamic centimeter higher than at station 4. Geostrophic motion at the surface relative to that at about 20 m would therefore be eastward. Had the sign been positive, it would have been westward. For a station separation of 5 nautical
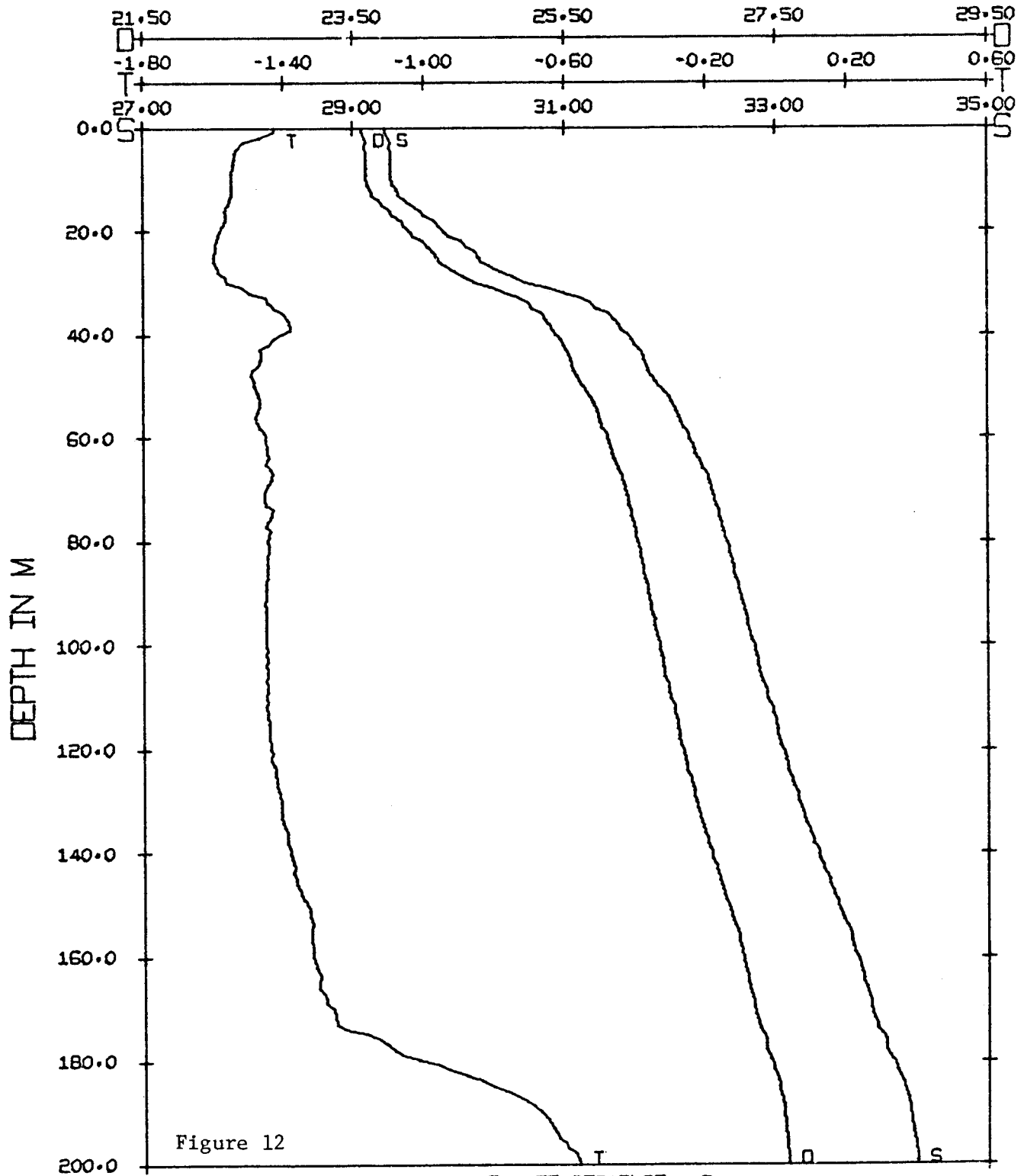
STD PLOT
W-24   17

Figure 12

LATITUDE   70-33·8N   T = TEMPERATURE - C   DATE   28 MAY 1976
LONGITUDE   141-44·0W   S = SALINITY - 0/00   BEGIN 2258
                              D = SIGMA-T

miles, a dynamic height difference of 1 dynamic centimeter corresponds to a relative geostrophic speed of just under 8 cm sec^{-1}. While there is of course no guarantee that dynamic height calculations for a shallow shelf regime have much significance in specifying the flow field, one might perhaps expect that any more-or-less persistent features in the dynamic topography at least indicate the mean flow directions. With this *caveat* the indicated flow in the fall was easterly on the inner and middle shelf and westerly on the outer shelf and slope. In the winter the only easterly flow was on the inner shelf, with westerly flow indicated on the middle and outer shelf. In the spring the flow was westerly over almost the entire shelf. The general westerly flow indicated along the slope in most of the sections is of course the intensified southern part of the Beaufort gyre. These speeds range from less than 1 cm sec^{-1} to 30 cm sec^{-1}.

There is an interesting dynamic topographic feature which appears on at least five of the sections, *viz.* a change in the sign of the calculated geostrophic shear at the outermost stations over the slope. The feature is, for example, clearly seen between stations 9 and 10 in Figure 4. The sign change occurs at about 100 m depth. Without knowing the absolute topography of some reference surface, the simplest interpretation is that there is a maximum in the westerly flow at the depth of the sign change, *i.e.*, a sub-surface current core. We shall return to this matter in discussing the observation from fall 1976.

Figures 13 and 14 show the sections taken during fall 1976 (31 October-4 November). The two Lonely sections are located about 15 miles apart, as are the two Oliktok sections. In certain respects the observed conditions are more like those encountered the previous winter, rather than like those of the fall. For example, very low salinities are missing in the W25 sections, water less saline than 29‰ being observed at only one station. In contrast, the upper water salinities in the W21 sections were less than 29‰ at all but four stations. Similarly, the over-all stratification in the W25 sections is closer to that in W22 and W24 than to that in W21. Another point of contrast is that in fall 1976 the salinity generally decreased seaward whereas in 1975 it had increased. The easterly flow over the inner and middle shelf indicated in the W21 sections is also missing in W25; instead westerly flow prevails. The winter temperature structure is not fully developed in the W25 sections, however. For example, one-fifth of the stations still show the surface layer to have been slightly above the freezing point, although admittedly within 0.01-0.02°C of freezing. About a third of the stations showed supercoooling in excess of 0.01°C.

By far the most remarkable feature of the W25 sections is the steeply inclined isopleths above the outer shelf and slope. In each case, Atlantic water which is normally found well below 200 m over the slope can be seen on the shelf. In the Oliktok East section (Fig. 14), water warmer than 0°C and more saline than 34.5‰ was observed at 91 m. To my knowledge, Atlantic water has previously been found this shallow only in the St. Anna Canyon, which indents the northern Kara Sea. In the Lonely West section (Figure 13) the effect of the onshore flow of relatively warm and saline water can be seen even at the innermost station, where the bottom 10 m were warmer than -1°C and above 34‰ in salinity. Whether such flushing of the shelf by dense water upwelling from off the slope is a rare phenomenon, is unknown. Six of the nine sections shown in Figures 1-9 do in fact portray the 33‰ isohaline climbing onto the shelf, three of them to above 50 m depth. Such a mechanism would of course provide the salt source needed to satisfy the salt budget calculations discussed earlier. It is appropriate to point out that neither during nor within at least 10 days prior to the section occupation
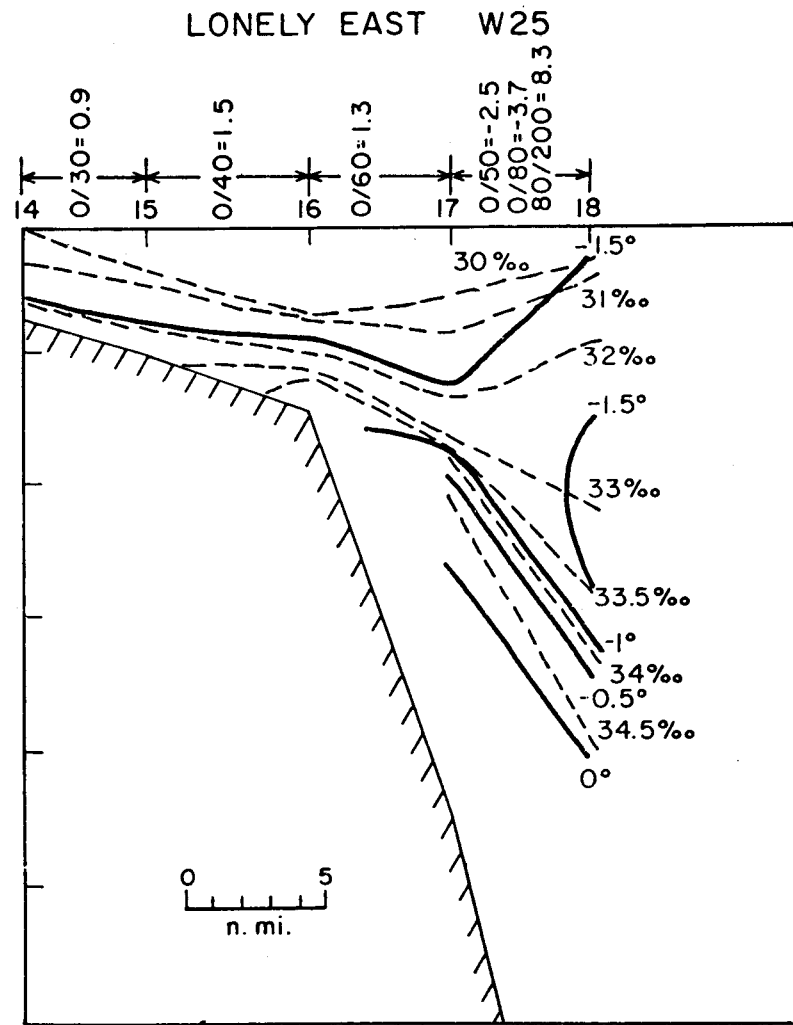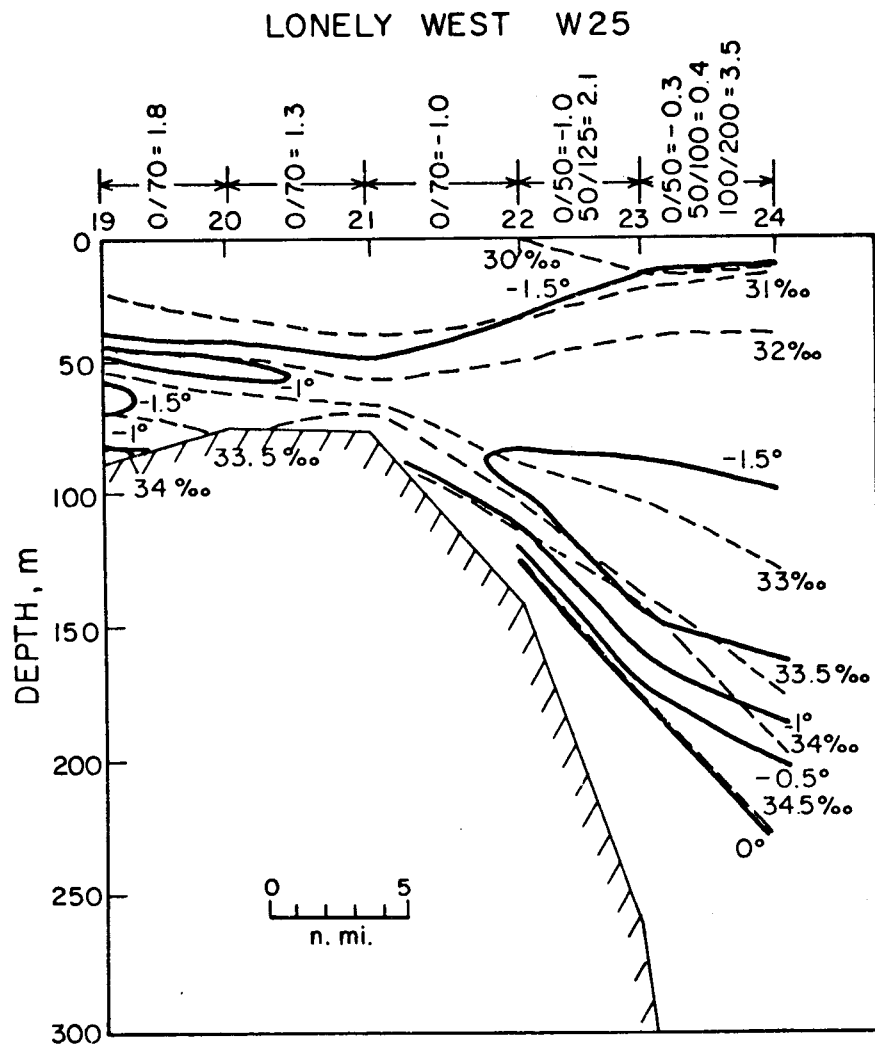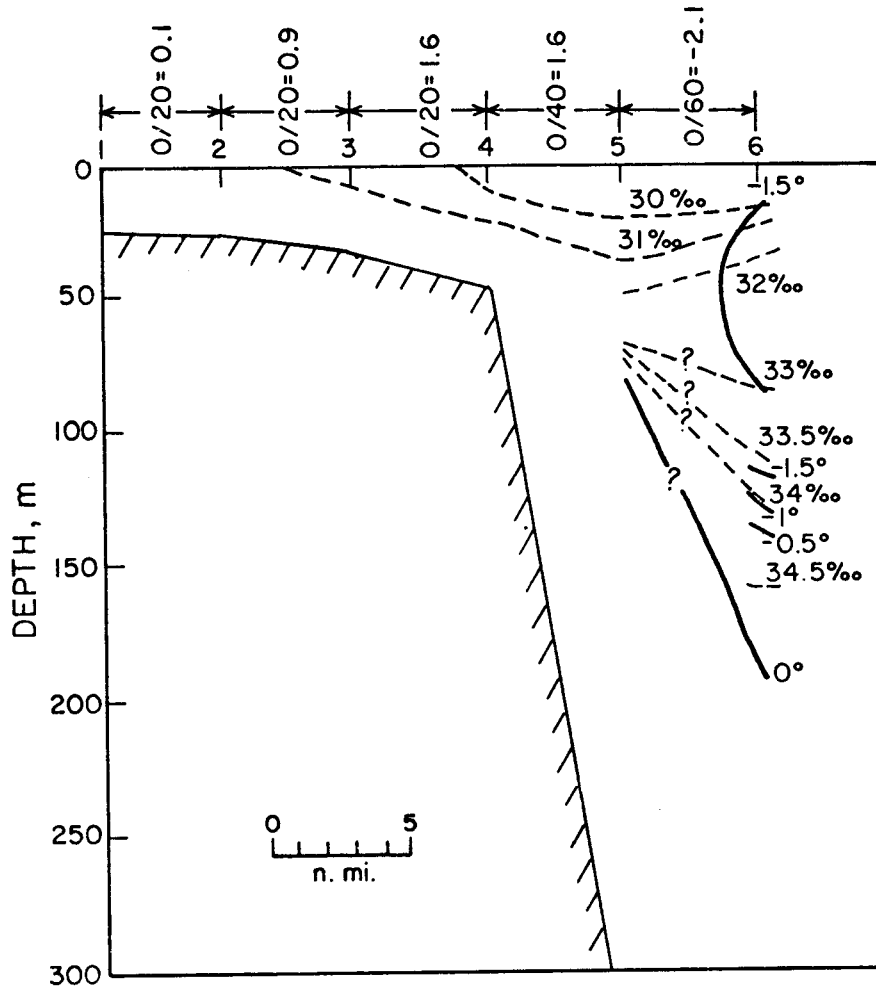
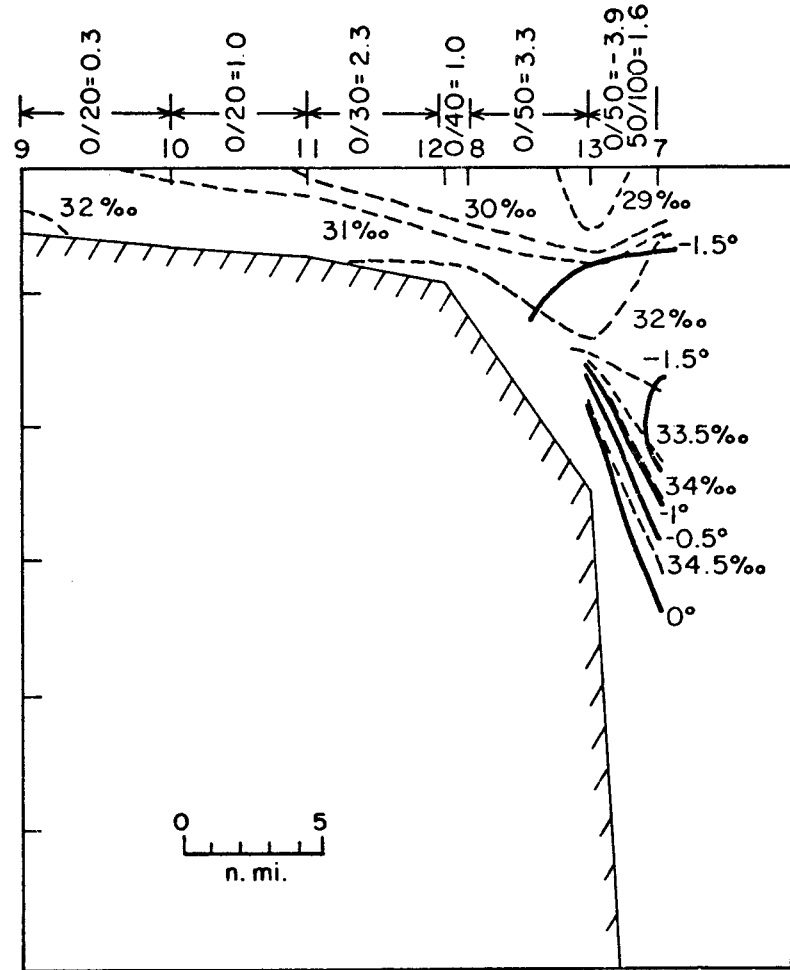Figure 13

OLIKTOK WEST W25

OLIKTOK EAST W25

Figure 14

were there strong easterly winds, such as have been proposed to drive summer upwelling.

Another notable feature of the W25 sections is the change in sign of the geostrophic shear at the outermost stations. This generally occurred between 50 and 80 m. A similar feature has been pointed out earlier for a number of the W21-W24 sections. Again the simplest interpretation is a high-speed core of westerly moving water at mid-depth. In the case of the Lonely East section, the geostrophic speed at 80 m relative to that 200 m is about 65 cm sec^{-1}, *i.e.*, well over 1 knot. Below 200 m the shear appears relatively small. It is important to note that the flow indicated by the dynamic topography is <u>not</u> aligned with the bottom topography, but has an onshore component. For example, between stations 23 and 17 this component at 80 m relative to 200 m was about 8 cm sec^{-1}.

The indications are thus of a rapid westerly flow of dense water along the slope and outer shelf, with the core of the current between 50 and 100 m. The flow is so inclined to the shelf edge as to flood portions of the shelf with saline water. In one observed instance (Fig. 13) the saline water extended at least 15-20 miles inshore from the shelf edge.

Finally, the general matter of subsurface temperature maxima merits a brief discussion. Apart from the Atlantic Water influence, such features can be seen at one or more stations on each of the W25 sections, as is also the case for each of the earlier cruises. For W25 the maxima are particularly prevalent at the two Lonely sections. Determining the source and mixing history of these features proves to be a very difficult problem, however. They vary greatly with respect to extent, temperature, density, and fine-scale structure. An example is given in Figure 15 and 16, showing conditions at station W25-6 from the Oliktok West section and at station W25-19 from the Lonely West section. At station 6 the two relatively small temperature maxima have associated salinities of 31.73 and 32.55%o and densities of 25.53 and 26.20 in σ_t. At station 19 there were also two maxima, but they were very large and had associated salinities of 32.09 and 33.34%o and densities of 25.82 and 26.85 in σ_t. In the case of station 19 it is probably safe to say that the upper maximum represents Bering Sea water that has flowed into the Beaufort past Point Barrow, while the lower maximum is the result of warm, saline water flowing up the slope as discussed earlier. However the origin and mixing history of the temperature structure at station 6 is certainly not clear. Even within a single closely spaced synoptic section, the T-S structure in the vicinity of the temperature maxima varies enormously. A case in point is the Lonely East section, stations W25-14 through W25-18, illustrated in Figures 17-21. Only at the two innermost stations is the hydrography strikingly similar.

VIII. Conclusions

We have seen that not only are there large seasonal changes in the hydrography, but conditions are also different from one year to the next. The latter point is a caution to us, should we attempt to generalize from too short a time base. Nonetheless, the normal seasonal cycle has now probably been determined at least in outline.
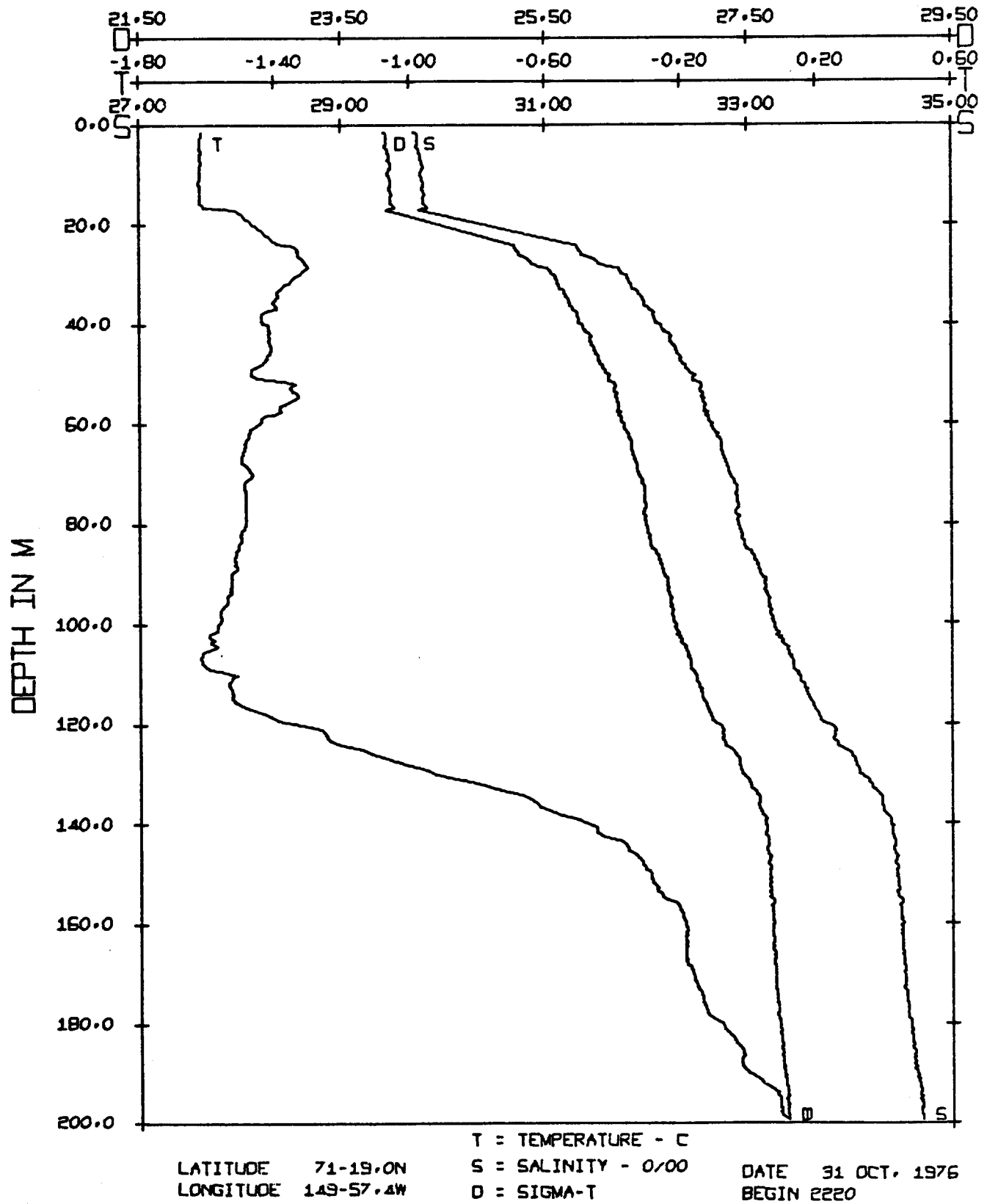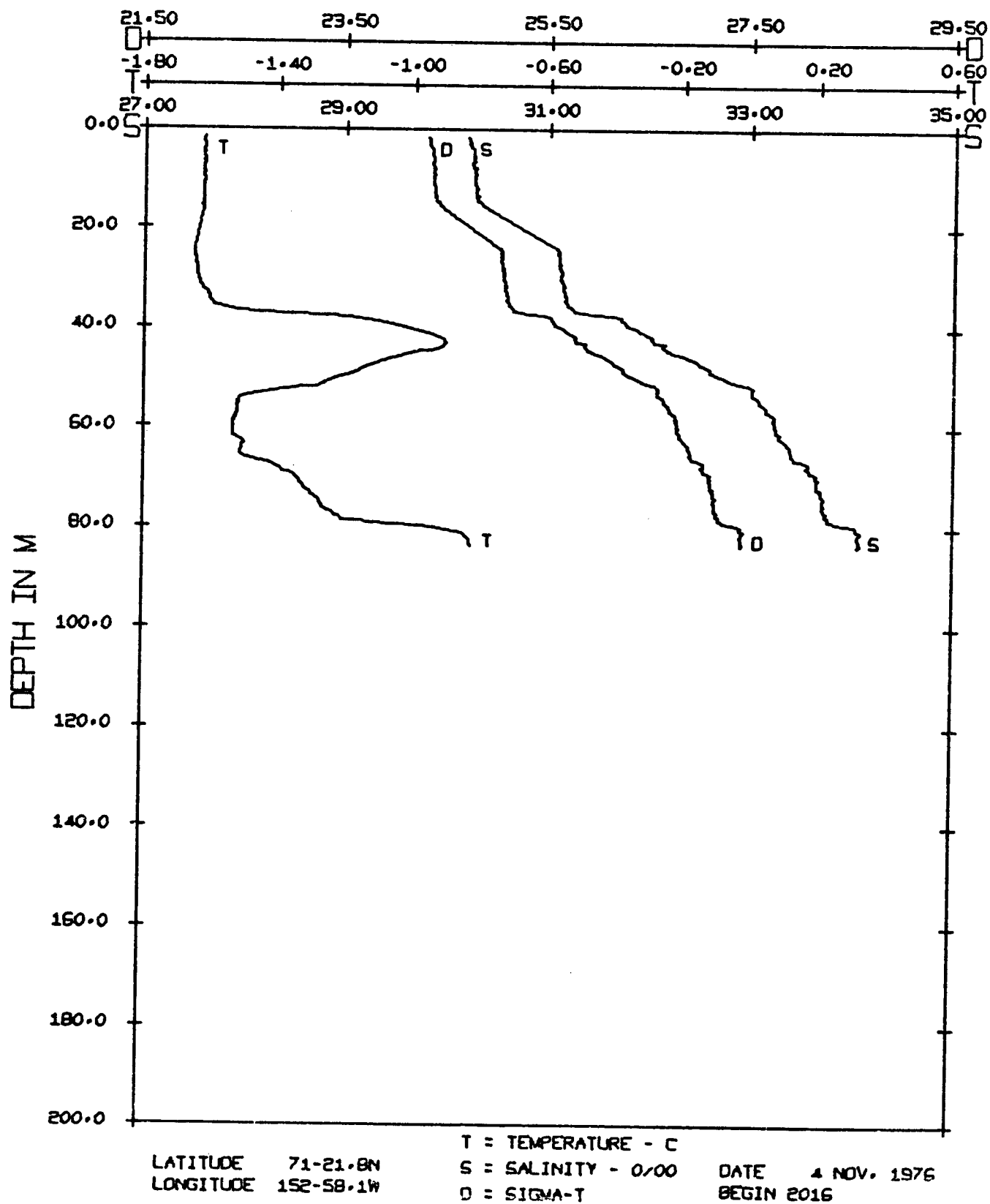
STD PLOT

W-25   6

LATITUDE   71-19.0N   T = TEMPERATURE - C   DATE   31 OCT. 1976
LONGITUDE   149-57.4W   S = SALINITY - 0/00   BEGIN 2220
                         D = SIGMA-T

Figure 15

STD PLOT

W-25   19

T = TEMPERATURE - C

S = SALINITY - 0/00

D = SIGMA-T

LATITUDE   71-21.8N
LONGITUDE   152-58.1W

DATE   4 NOV. 1976
BEGIN 2016

Figure 16

STD PLOT
W-25 014

LATITUDE 71-12.7N	T = TEMPERATURE - C
LONGITUDE 152-18.9W	S = SALINITY - 0/00 DATE 3 NOV. 1976
	D = SIGMA-T BEGIN 2123

Figure 17

STD PLOT
W-25   15
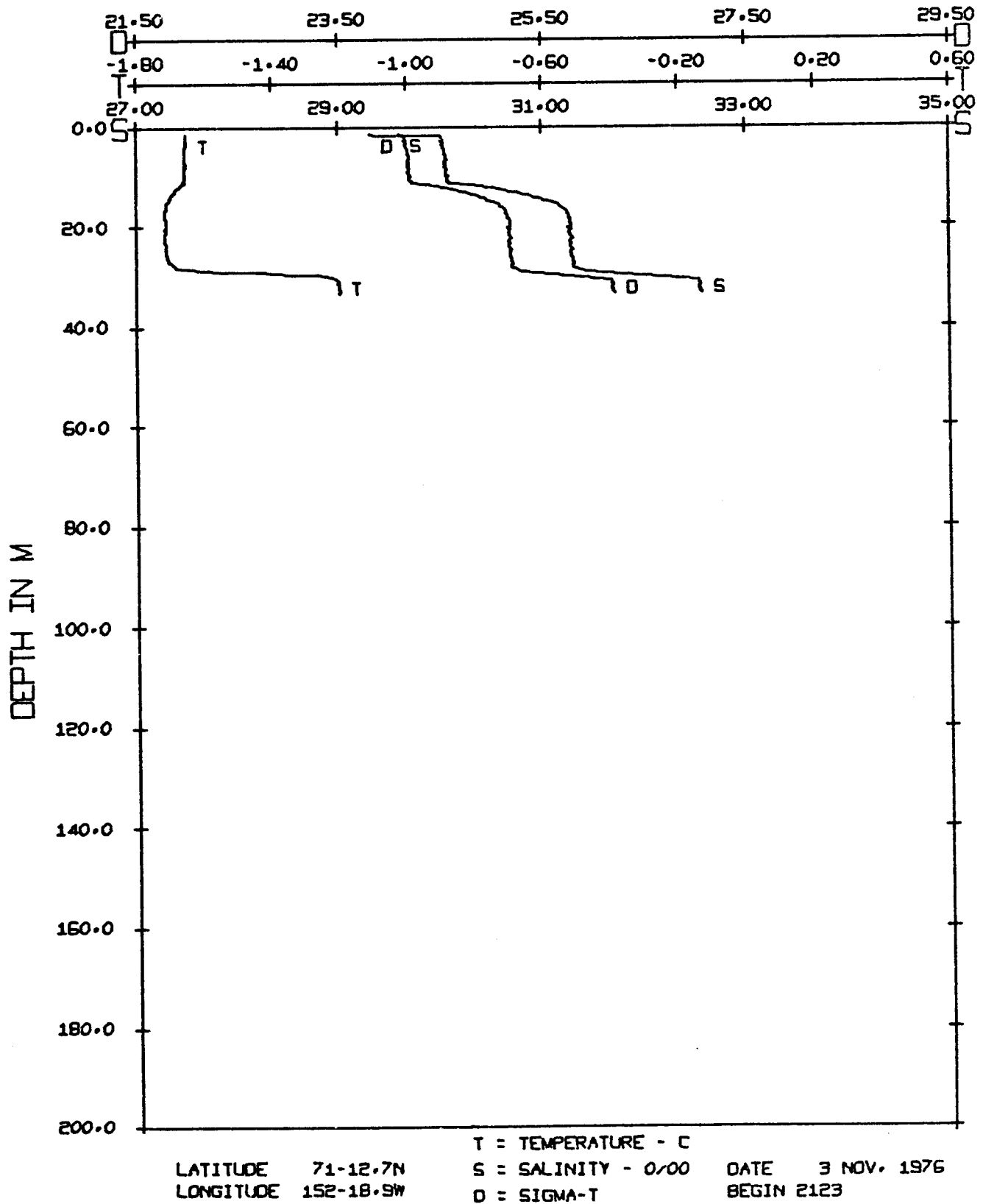
LATITUDE   71-17.3N   T = TEMPERATURE - C
LONGITUDE   152-10.4W   S = SALINITY - O/OO   DATE   3 NOV. 1976
                            D = SIGMA-T   BEGIN 2155

Figure 18

STD PLOT

W-25　　16

LATITUDE　　71-21.9N　　S = SALINITY - 0/00　　DATE　　3 NOV. 1975
LONGITUDE　152-04.5W　　D = SIGMA-T　　BEGIN 2225
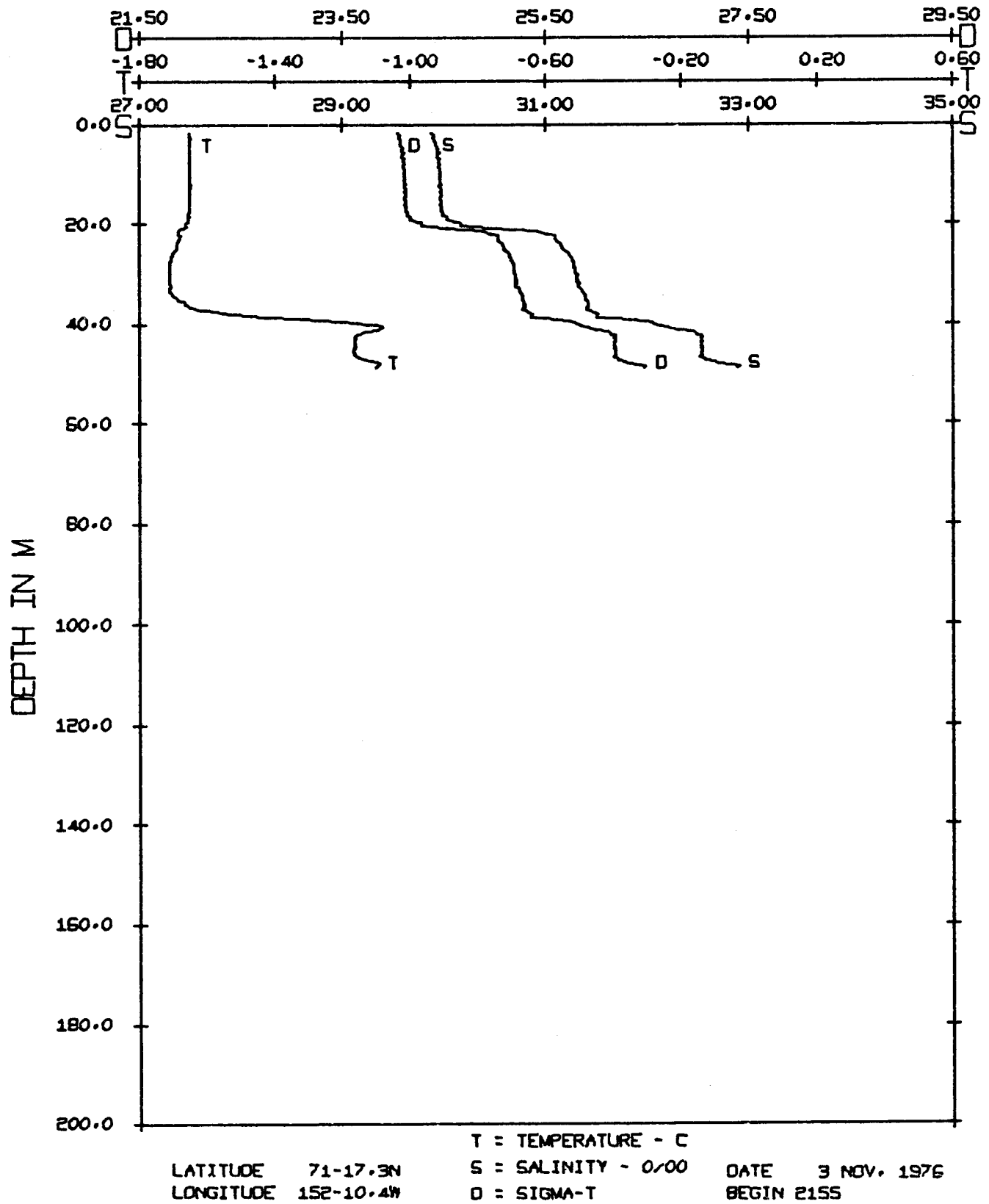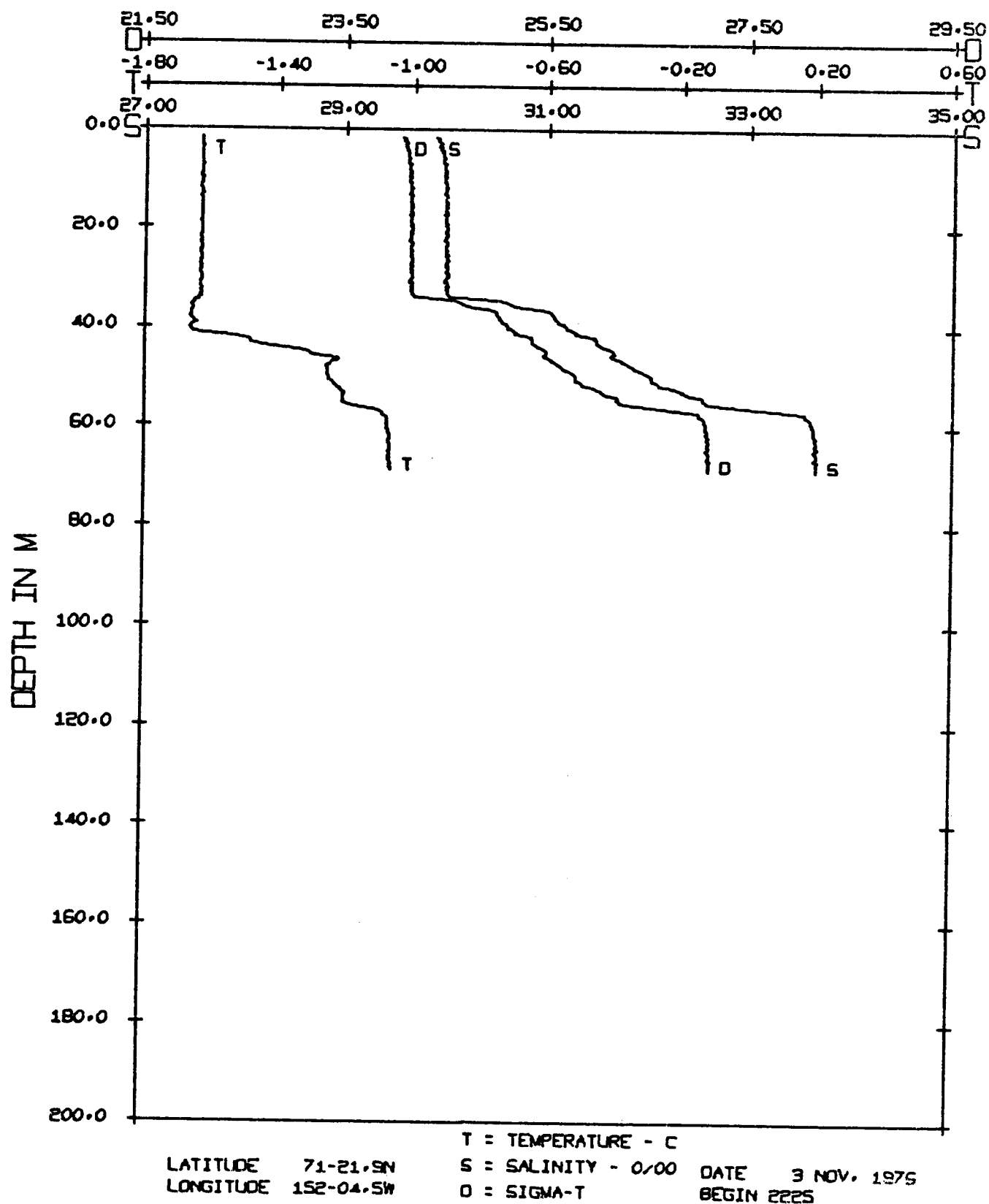
T = TEMPERATURE - C

Figure 19

STD PLOT

W-25　　17

LATITUDE　71-26.7N　　S = SALINITY - 0/00　　DATE　3 NOV. 1976
LONGITUDE　151-59.0W　　D = SIGMA-T　　BEGIN 2258

T = TEMPERATURE - C

Figure 20
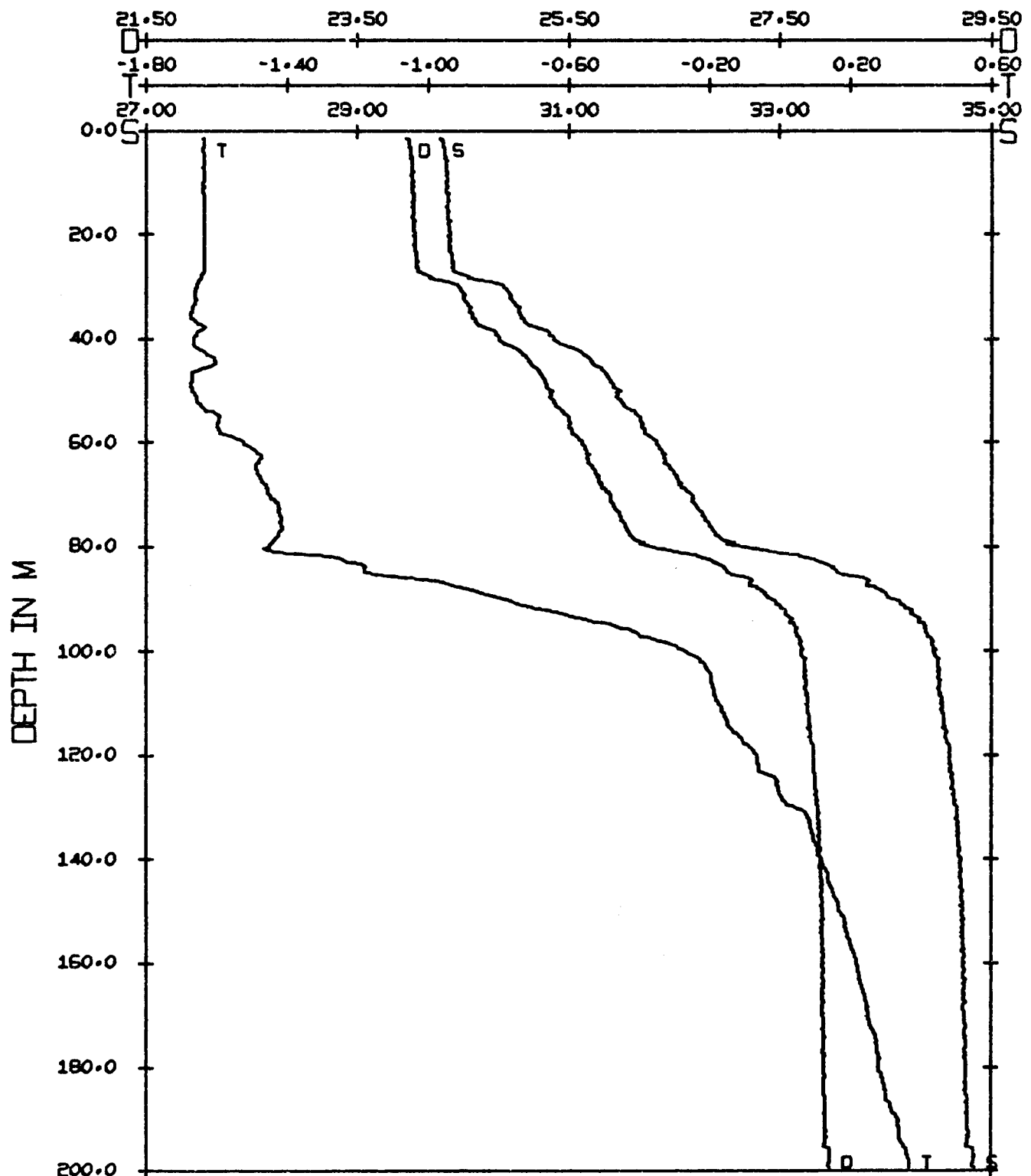
STD PLOT

W-25   18
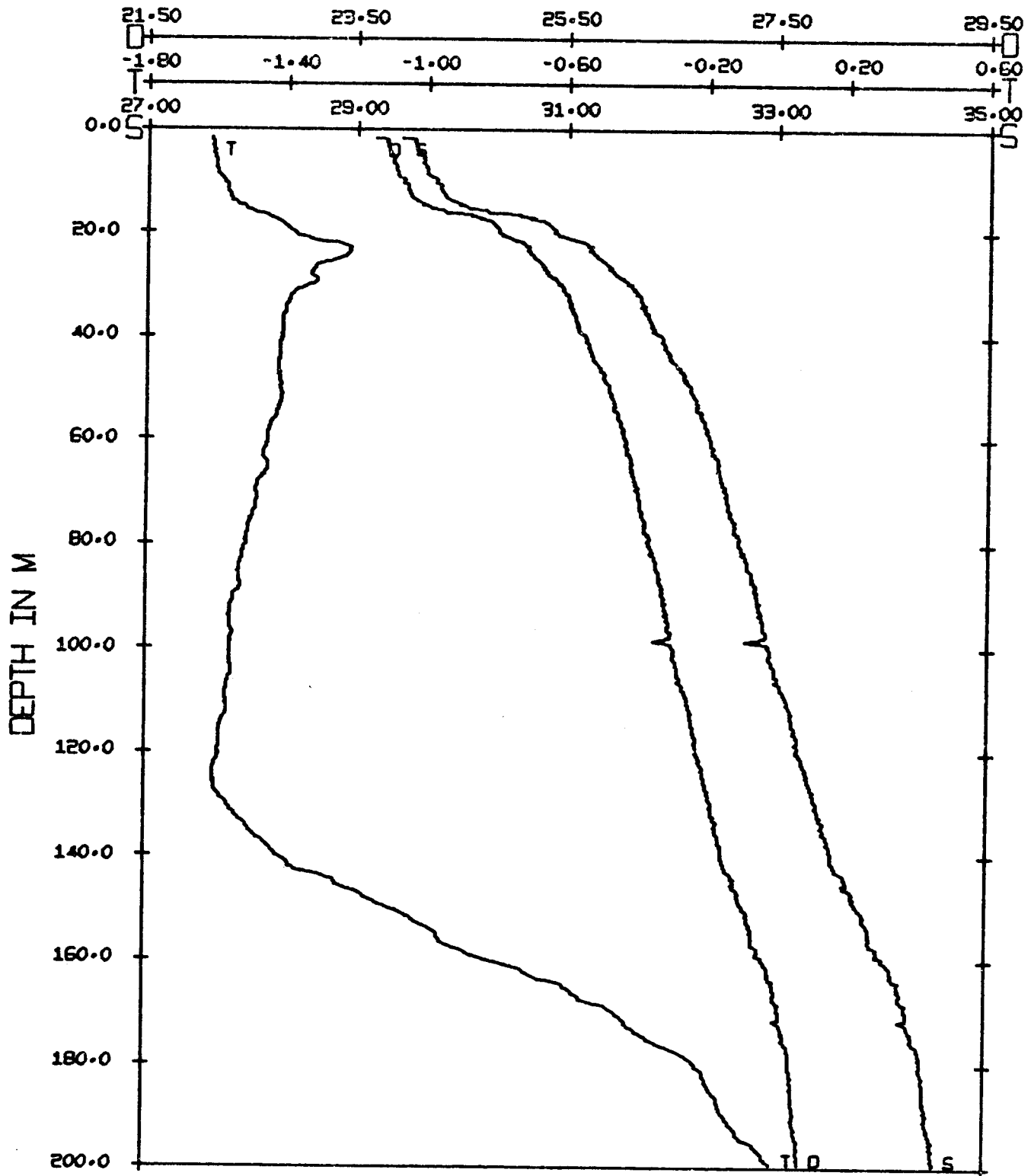
LATITUDE   71-31.2N
LONGITUDE   151-50.7W

T = TEMPERATURE - C
S = SALINITY - 0/00
D = SIGMA-T

DATE   3 NOV. 1976
BEGIN 2338

Figure 21

One matter appears to stand out in importance: the Beaufort Sea shelf is certainly not neutral with respect to the Arctic Ocean to the north. Rather there are one or more forms of interaction, in which water and the substances it transports are exchanged between the shelf and the offshore regions. Certainly the salt budget calculations discussed in Section VII can be thus interpreted. It is likely that when the presence of widespread temperature maxima is better understood, it also will point to such an exchange. The most dramatic evidence of exchange is the series of four sections from fall 1976, in which an intense subsurface current core appears to be sweeping up the slope and onto the shelf, flooding at least one section to the innermost station with dense, saline water.

IX. Needs for further study

The remainder of the contract year will be spent processing and analyzing the four sections from winter 1977. Additionally we will continue work on the earlier data. The question of exchange across the shelf, discussed briefly in Section VIII, will be the focus of much of this effort. Among the goals is achieving some understanding of the nature and significance of the temperature extrema.

X. Summary of 4th quarter operations

A. Field operations

The winter field work is described in the preliminary report on survey W27 (Ref.: M77-29), a copy of which is appended hereto.

B. Problems

The normal range of problems was encountered; there are no recommended changes.

C. Estimate of funds expended to 28 February 1977

Total allocation (5/16/75-9/30/77): $142,627

A.	Salaries - faculty and staff	$12,317	
B.	Benefits	1,446	
C.	Expendable supplies and equipment	3,811	
D.	Permanent equipment: Counter/timer $790 Calculator $750	23,281	
E.	Travel	4,640	
F.	Computer	2,924	
G.	Other direct costs	22,537	
H.	Indirect costs	5,986	

Total expenditures 77,395

Remaining balance 65,232

University of Washington

Department of Oceanography

Seattle, Washington 98195

Preliminary Report

University of Washington Participation in

NOAA UH-IH Helicopter CTD Survey W27

STD Measurements in Possible Dispersal Regions
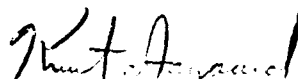
of the Beaufort Sea

4 - 11 March 1977

by

Richard B. Tripp

NOAA Contract 03-5-022-67, TA 1

Research Unit No. 151

Approved by:

Knut Aagaard, Research Associate Professor
Knut Aagaard, Research Associate Professor
Principal Investigator

Francis A. Richards, Professor
Francis A. Richards, Professor
Associate Chairman for Research

REF: M77-29

STD MEASUREMENTS IN BEAUFORT SEA

1. *Objectives*

To examine by means of STD measurements the possible sinking and spreading into the Canadian Basin of waters modified on the Beaufort Shelf. Cruise W27 is the second survey during this contract year in the examination of this possibly very important dispersal mechanism.

2. *Narrative*

Two sets of CTD stations, each consisting of two parallel lines normal to the coast, were occupied across the shelf. One set was off Lonely and the other off Oliktok. Station spacing was approximately five miles and parallel line spacing was fifteen miles. Pertinent CTD station information is listed in Appendix A.

The scenario of events is as follows:

__March 4, 1977__   Weather: cloudy, temperature -28°C, winds 015/10.
0903 AST - Tripp and Swift departed Barrow in helicopter N56RF (Barnhill and Winter) for the Lonely West section. There was some difficulty finding suitable ice. Most of the ice was rafted and > 6 ft.
1230 - After accomplishing two stations we departed for Lonely to refuel.
1450 - Departed Lonely for Station 3.
1850 - Landed at last site in this line. However, it was nearing total darkness and we had to abort the station.
2030 - Return to Barrow. A total of 5.6 hours of flight time were logged.

__March 5, 1977__   Weather: cloudy, light snow, temperature -28°C, winds 035/15.
0916 AST - Darnall and Swift departed Barrow in helicopter N56RF (Barnhill and Winter) for the Lonely East section.
1410 - Returned to Lonely to refuel after occupying Station 9. The fuel pump at the Husky camp was down and refueling was delayed for four hours.
2030 - Departed Lonely for Barrow. Severe icing conditions.
2110 - Returned to Lonely. A total of 3.7 hours of flight time were logged.

__March 6, 1977__   Bad weather: no flying was attempted.

__March 7, 1977__   Weather: clear; temperature -30°C, winds 090/16.
1145 AST - Darnall and Swift departed Lonely in helicopter N56RF (Barnhill and Winter) for Station 10 on the Lonely East section. After finishing the station, the heaters on the helicopter quit working. The radios became inoperative because of the cold.
1416 - Returned to Barrow. A total of 2.1 hours of flight time were logged.

__March 8, 1977__   No flying. Helicopter down for maintenance.

__March 9, 1977__   Weather: cloudy, temperature -27°C, winds calm.
0900 AST - Tripp and Darnall departed Barrow in helicopter N57RF (Feld and Winter) for Lonely.
1035 - Departed Lonely, after refueling, for the Oliktok West section.

503

March 9, 1977, cont'd.
1730 - Returned to Lonely for fuel after occupying Station 15.
1845 - Departed Lonely.
1935 - Returned to Barrow. A total of 5.7 hours of flight time were logged.

March 10, 1977   Weather: cloudy, temperature -28°C, winds 360/05.
0923 AST - Tripp and Darnall departed Barrow in helicopter N57RF (Feld and
       Winter) for Lonely.
1053 - Departed Lonely, after refueling, for the Oliktok East section.
1748 - Returned to Lonely for fuel after occupying Station 22.
1820 - Departed Lonely.
1920 - Returned to Barrow. A total of 6.1 hours of flight time were logged.

March 11, 1977   Weather: clear, temperature -32°C, wind 035/3.
0934 AST - Tripp, Darnall, and Lt. L. Ashim (U.S. Naval Postgraduate School)
       departed Barrow in helicopter N57RF (Feld and Winter) to complete the
       Lonely East section.
1350 - Returned to Lonely for fuel after occupying Station 25.

1450 - Departed Lonely.
1556 - Returned to Barrow. A total of 4.0 hours of flight time were logged.

During this time period, the ice was compact, quite broken and rafted.
The winds were light and prevailed from the northeast. A few narrow leads were
observed at the edge of the shelf. The refrozen leads were ∿ 3 ft thick and
the rest of the ice > 5 ft thick. There were some pieces of multi-year ice
throughout the area.

3. *Methods*

CTD casts were taken on each station utilizing a Plessy Model 9400 pro-
filing system with a redesigned sensor package capable of permitting its de-
ployment through an eight-inch auger hole. 110V power was supplied by a 2½ KW
Onan portable generator. This operation worked quite satisfactorily out of the
UH-IH helicopter. The data were stored on 7-track magnetic tape for reduction
ashore. In order to determine field correction factors for the conductivity
and temperature sensors, a water sample and temperature measurement were ob-
tained from a Nansen bottle one meter above the sensors.

Salinity samples were analyzed at Barrow utilizing a Hytech Model 6220
portable salinometer S/N 4917.

4. *Personnel*

R. B. Tripp	Principal Oceanographer	University of Washington
C. H. Darnall	Oceanographer	University of Washington
J. Swift	Graduate Student	University of Washington
Lt. Mike Barnhill	Pilot N56RF	NOAA
R. DeHart	Mechanic N56RF	NOAA
Lt. Don Winter	Pilot N57RF	NOAA
G. Feld	Mechanic N57RF	NOAA

5. *Acknowledgments*

The NOAA personnel participated in every aspect of the operation. Lt. Barnhill, Mr. Feld and Mr. DeHart's "can-do" approach was greatly appreciated, and certainly helped in accomplishing the mission.

APPENDIX A

| Consec. No.	Date/Time GMT March 1977	Latitude N	Longitude W	STD Depth M	Water Depth M
1	4-2158	71-22.0	152-57.6	83	84
2	2305	71-26.0	152-52.9	78	79
3	5-0154	71-30.1	152-43.3	6	74
4	0157	71-30.1	152-43.3	73	74
5	0247	71-34.4	152-38.0	126·	127
6	0358	71-39.9	152-30.3	366	367
7	2059	71-13.1	152-17.0	26	27
8	2251	71-17.5	152-11.6	48	49
9	2341	71-22.5	152-06.1	83	84
10	7-2234	71-25.8	151.54.2	220	221
11	9-2347	70-55.4	150-07.3	25	26
12	10-0023	70-59.9	150-05.4	27	28
13	0102	71-04.0	150-03.6	39	40
14	0141	71-08.6	150-01.7	56	57
15	0253	71-14.4	149-59.3	540	>541
16	2208	70-52.3	149-24.5	28	29
17	2244	70-58.0	149-21.9	31	32
18	2328	71-01.8	149-19.5	37	38
19	11-0021	71-06.9	149-20.7	42	43
20	0104	71-12.5	149-14.8	81	324
21	0127	71-12.5	149-14.8	323	324
22	0210	71-16.7	149-12.2	529	>530
23	2112	71-35.8	151-44.7	547	>548
24	2212	71-31.5	151-53.0	547	>548
25	2308	71-26.0	151-59.1	198	199
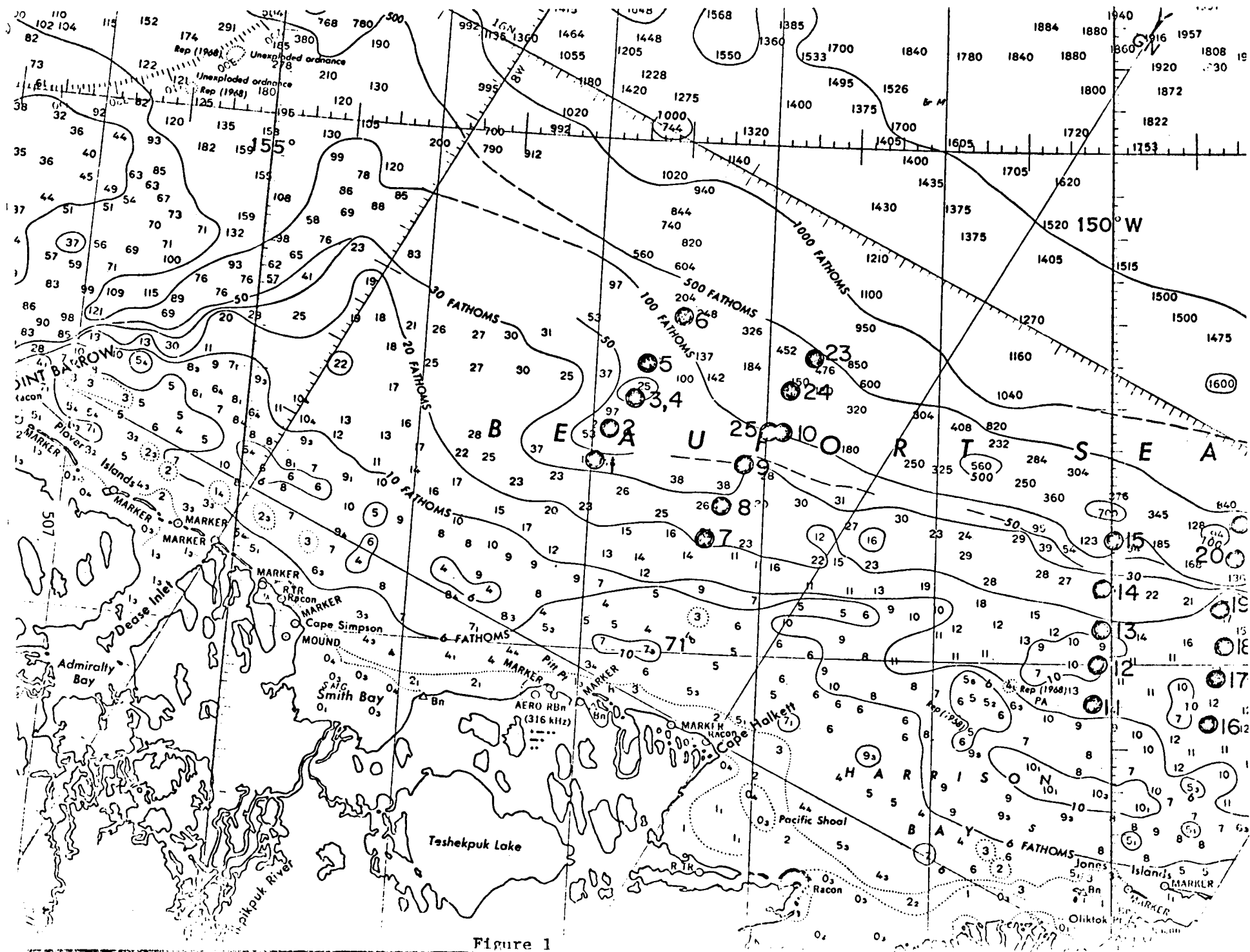
Figure 1

ANNUAL REPORT

YUKON DELTA COASTAL PROCESSES STUDY

William R. Dupré

Department of Geology
University of Houston
Houston, Texas

April 1, 1977

I SUMMARY

Objectives:

The overall objective of this project is to provide data on geologic processes in the Yukon-Kuskokwim delta region in order to better evaluate the potential environmental impacts of oil and gas exploration and production. The specific objectives of the study include the following:

1) Study the processes along the delta shoreline (e.g., tides, waves, sea-ice, river input) to develop a coastal classification including geomorphology, coastal stability, and dominant direction of sediment transport.

2) Study the processes active on the delta plain, including river breakup, river bank erosion and sedimentation, and the hydrology of the interconnected lakes and abandoned river channels.

3) Make a tectonic map of the delta region, delineating areas of Quaternary volcanism and faulting.

4) Make a geologic map of the delta area, emphasizing the delineation of depositional systems, in order to:

   a) establish a chronology of delta sublobes to serve as a datum by which the relative age of Quaternary faulting and volcanism can be measured.

   b) establish a chronology of storm-induced erosional events recorded in chenier-like sequences along the coast to estimate the recurrence interval of major storms in the region.

   c) determine the physical properties of the different geologic units, including the depth and stability of permafrost.

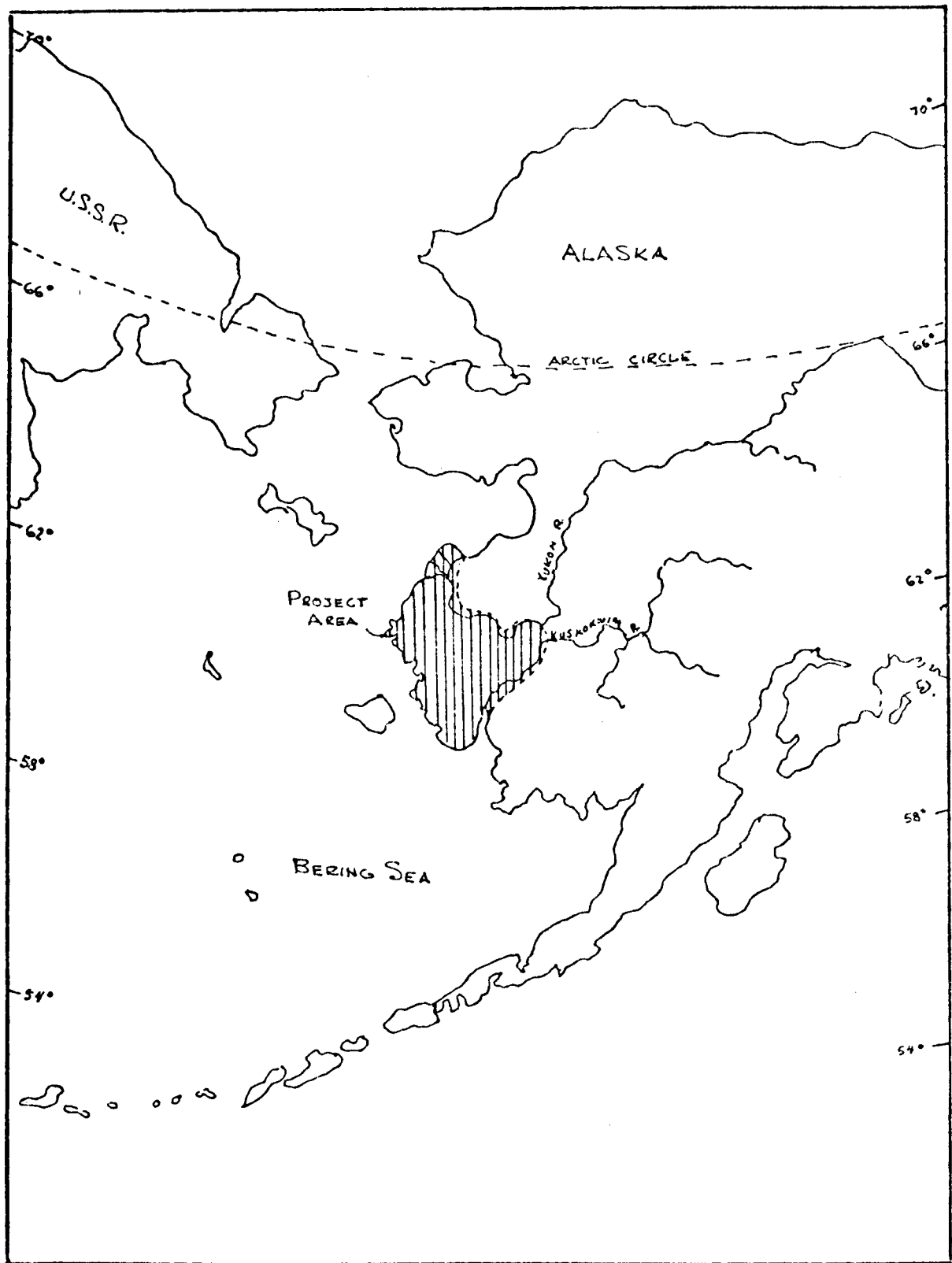   d) aid in the definition and extrapolation of biological habitats throughout the region.

Figure 1. Location of Project Area

Conclusions:

The Yukon-Kuskokwim delta region is characterized by widespread Quaternary tectonism. Northwest- and northeast-trending faults and structurally-controlled volcanic vents are mainly restricted to the onshore extension of the Nunivak Arch. Many of the northeast-trending faults may actually represent the slivering of the Kaltag fault, previously projected to the north of the delta. At least some of these faults appear to have had Holocene movement. The age of the volcanism is less certain, but most, if not all, of the activity appears to be pre-Holocene.

The presence of extensive permafrost is well evidenced by an abundance of geomorphic criteria as well as field investigations. It is locally absent beneath large lakes and rivers, as well as in areas of rapid deposition. Elsewhere it may be up to 600 feet thick, and may be present offshore of some areas of rapid erosion.

Flooding and river bank erosion along both the Yukon and Kuskokwim Rivers is strongly affected by the climatic extremes of this subpolar region. The largest floods are associated with ice breakup on the river, often accentuated by the effects of breached ice jams which form locally. Extreme floods may actually result in the complete diversion of the Yukon River, with disastrous consequences. Such events have occurred repeatedly during the Pleistocene; the most recent may have occurred only 1200 years ago.

Extensive floods may also occur both along the rivers and the coast due to late summer and early fall storms. These floods may actually result in larger amounts of erosion and sediment transport than occurs during breakup. Erosion rates are locally quite high along the river banks of the major rivers, and may be as high as 15 meters/year along some of the barrier islands along the coast.

The coastline is highly variable with respect to its morphology, processes, and overall coastal stability. Of particular importance in determining the relative coastal stability is the proximity of the Yukon River sediment input, the sheltering effects of barrier islands, laterally migrating tidal inlets, and local tectonic patterns. In spite of its heterogeneity, however, the dominant direction of longshore drift is toward the north, coincident with the oceanic and wave-generated currents.

Large areas of landfast ice fringe the delta region for almost half the year. The maximum extent of the shorefast ice varies little from year to year. Nevertheless, there is clear evidence of ice movement within this sheet of shorefast ice. Grounding of sea ice, combined with major storms, may be significant mechanisms for resuspending shelf sediments and allowing their transport across the shelf by oceanic currents.

Implications:

The siting of offshore facilities (e.g., drilling platforms, underwater pipelines) must take into account the extent and variability of shorefast ice, the probability of offshore permafrost, and the possible effects of altering offshore bathymetry in changing coastal stability. In addition, the effects

of possible oil spills must take into account not only the dominant
northward drift of water and sediments, but also the local and seasonal
variability of current patterns.

The selection of shoreline sites (e.g., docking and pipeline terminals) must take into account the present coastal stability, including the
possibility of erosion associated with major storm surges, even in an area
of long-term progradation. In addition, the effects of shorefast ice for
over half of the year must be considered.

Much of the delta is underlain by the on-land extension of the Nunivak Arch; this would seem to exclude most of the region for serious consideration for exploration. Nevertheless, the Quaternary faults and volcanoes
which characterize the zone constitute serious geologic constraints on the
selection of transportation corridors. The discontinuous permafrost and
the complex hydrology of the delta further complicate the location of such
corridors, as well as making it difficult to predict the effects of oil
spills.

Lastly, an understanding of the geologic processes and products
within the delta region will greatly aid in the definition and regionalization of biological habitats.

II. INTRODUCTION

The overall objective of this project is to provide data on geologic
processes in the Yukon-Kuskokwim delta region in order to better evaluate
the potential environmental impacts of oil and gas exploration and production. The specific objectives of the study include the following:

1) Study the processes along the delta shoreline (e.g., tides, waves, sea-ice, river input) to develop a coastal classification including geomorphology, coastal stability, and dominant direction of sediment transport.

2) Study the processes active on the delta plain, including river breakup, river bank erosion and sedimentation, and the hydrology of the interconnected lakes and abandoned river channels.

3) Make a tectonic map of the delta region, delineating areas of Quaternary volcanism and faulting.

4) Make a geologic map of the delta area, emphasizing the delineation of depositional systems, in order to:

   a) establish a chronology of delta sublobes to serve as a datum by which the relative age of Quaternary faulting and volcanism can be measured.

   b) establish a chronology of storm-induced erosional events recorded in chenier-like sequences along the coast to estimate the recurrence interval of major storms in the region.

   c) determine the physical properties of the different geologic units, including the depth and stability of permafrost.

   d) aid in the definition and extrapolation of biological habitats throughout the region.

This project was designed to provide as much information as possible to the problems of petroleum development in the region. A better understanding of the tectonic framework of the delta region should aid in the exploration of oil and gas. Those same tectonic features, to the extent to which they are active today, also provide serious constraints to the selection of transportation corridors, as does the existence of extensive permafrost and the actively shifting river courses.

A better understanding of coastal processes will aid in the siting of shoreline installations (e.g., docking and transfer facilities), as well as in evaluating the possible impacts of such facilities on coastal stability.

514

The siting of offshore facilities (e.g., drilling rigs, underwater pipelines) must take into account frequency and magnitude of a variety of nearshore processes, including those associated with sea-ice. An understanding of these processes, including their seasonal variability, will also aid in predicting the paths of possible oil spills. An inventory of coastal materials will also serve as baseline data should spills come onshore.

Lastly, a better understanding of the sub-arctic coastal processes by which the present coastal depositional systems formed, will aid in the interpreting older, potentially oil-bearing units which may have been formed under similar climatic conditions.

III. CURRENT STATE OF KNOWLEDGE

The Yukon River is the 17th largest river in the world providing over 90% of the sediment introduced into the Bering Sea (Lisitzin, 1972). Its freshwater discharge is sufficient to noticeably dilute the salinity of the waters in the Bering Sea. Yet for all its importance, relatively little is known of the Quaternary history of the region.

The ancestral Yukon River emptied into the Pacific in the vicinity of Cook Inlet during early Cenozoic time. Late Miocene uplift of the Alaska Range resulted in the diversion of the drainage system into the Bering Sea, where it has remained to the present (Nelson et al., 1974). Gradual submergence during late Miocene and Pliocene time was followed during the Pleistocene by repeated glacio-eustatic fluctuations of sea-level. Glacial intervals were characterized by emergence of the shallow Bering

Sea. During this time, the major rivers, including the Yukon and the Kuskokwim, emptied near the heads of major submarine canyons at the shelf edge (e.g., Scholl, Buffington et al., 1970; Hopkins, 1972). River valleys cut into the exposed continental shelf were filled during the most recent rise in sea-level with estuarine and marine sediments (e.g., Moore, 1964; Creager and McManus, 1967; Knebel and Creager, 1973). This was apparently accompanied by a general northward shift of the Yukon River to the north (Knebel and Creager, 1973; Shepard and Wanless, 1971).

Geologic mapping in the delta region (Hoare, 1961; Hoare and Coonrad, 1959a, 1959b; Hoare and Condon, 1966, 1968, 1971a, 1971b) has been largely concerned with defining the pre-Quaternary history of the region. Much work has been done on studying the Cenozoic sedimentary and tectonic history of the Bering Sea (e.g., Marlow and others, 1976), including studies of the Holocene sediments of the Yukon River at its mouth (Matthews, 1973) and on the Bering Sea shelf (McManus and others, 1974; Nelson and Creager, 1977). This study is the first, however, to deal in detail with the processes and events by which the present-day Yukon-Kuskokwim delta was formed.

IV. STUDY AREA

The combined Yukon-Kuskokwim delta complex (Figure 1) is an area of unique natural resources covering over 31,000 square miles. It has a large native population living in large part on a subsistence economy. It provides access to most of the spawning areas for salmon in the

516

region. It is, in addition, one of the most significant breeding grounds for migratory birds in North America. Probably no other area of similar size is as critical to so many species of water fowl as is the delta region (Joint Federal-State Land Use Planning Commisssion, 1975).

The delta region is largely a flat, featureless plain consisting of wet and dry tundra, interrupted by innumerable lakes, many of which are oriented. Many of these lakes have coalesced laterally to form very large bodies of water (e.g., Baird Inlet) connected to the sea by a series of ancient river channels. The flatness of the delta complex is interrupted by numerous small Quaternary shield volcanoes (generally less than 400 feet high), and the major uplifted massifs of the Askinuk Mts. (2340 feet of relative relief), the Kuzilvak Mts. (2190 feet of relative relief), and the Quaternary volcanic complex which forms Nelson Island (1485 feet relative relief).

The coastline is extremely varied, in part because of the heterogeneity of source material and in part because of the variability in tidal range. Extensive tidal flats and barrier islands flank the macro-tidal Kuskukwim delta, whereas prograding distributary mouth bars and mudflats flank the micro-tidal Yukon delta. Steep gravel beaches form along the cliffed shoreline at Cape Romanzof and Nelson Island, whereas sandy beaches form in the vicinity of Hooper Bay. Elsewhere eroding tundra cliffs form most of the shoreline.

V. SOURCES, METHODS, AND RATIONALE OF DATA COLLECTION

Hydrologic data on discharge are available in published form for the Kuskokwim RIver at Crooked Creek (1951-1965) and for the Yukon River at Kaltag (1957-1965). More recent data are presently unpublished, but are available from the Water Resources Division of the U.S. Geological Survey. A new gaging station was established on the Yukon River at Pilots Station in 1974, and will provide information on suspended and bedload sediment as well as discharge. Additional samples of both the bedload and suspended load of the Yukon and Kuskokwim Rivers are being collected as part of the field work.

River breakup in the delta region will also be monitored by aerial reconnaissance, supplemented by sampling of ice-borne sediments and measurements of ice thickness where possible. Special emphasis is being placed on the role of ice jams on flooding and river diversions. This monitoring program is designed to take advantage of the overflights flown by the River Forecast Service in Anchorage.

Much of the region has been mapped and published at a scale of 1:250,000 by Dr. Joe Hoare and associates at the U.S. Geological Survey. I have been using these maps in conuunction with 1950-1954 and 1973 aerial photography, as well as LANDSAT imagery, to prepare a geologic map of the delta region emphasizing the Quaternary depositional systems.

Field work is providing the ground truth for the mapping as well as samples for textural and mineralogic analyses and radiocarbon dating. Samples for dating are being selected to document the frequency of major shifts in the rivers course as well as major coastal storms. The distribution of

permafrost is also being studied, with special emphasis on defining the relationships between geomorphology, vegetation, and extent of ground ice. Hopefully the geologic mapping can be combined with data on morphology, vegetation, and physical properties to aid in the characterization of biological habitats and the definition of resource capability units.

Part of the field work consisted of coring a volcanic lake in the center of the delta region. The 5 1/2 meter core is presently being analysed by Dr. Tom Ager (U.S. Geological Survey) to determine frequency of volcanism in the region (via ash content), sources and rates of sedimentation, and evidence of climatic change (via pollen analysis).

Existing imagery is being used in combination with coastal overflights in a light plane to develop a coastal classification scheme. Baseline stations were established to characterize homogeneous intervals of the shoreline. Approximately twelve such stations were established in 1976 and will be reoccupied in 1977. Additional stations will be established at that time. Beach profiles are measured using a modified Emery method; offshore profiles are obtained with a Zodiac and fathometer. Sediment samples and process measurements (e.g. winds, waves) are also collected.

Bathymetric maps (dating back to 1898) are being used in conjunction with aerial photos (1954-1973) and baseline station profiles to determine rates and directions of shoreline change as well as dominant directions of nearshore sediment transport. LANDSAT imagery is also being used, and has proven invaluable in defining offshore sediment plumes and in studying the development of landfast ice in the region.

The results to date of this project can best be summarized in
a series of illustrations and tables, the significance of which are
described in section VII. These include:

1) A preliminary tectonic map (Figure 3)

2) A table of radiocarbon dates from the delta region (Table 1)

3) Generalized geologic map of the Yukon-Kuskokwim delta complex (Figure 4)

4) Selected portions of the geologic map of the delta region (Figure 5)

5) Map of sediment plumes off the Yukon delta as delineated on
   LANDSAT imagery (Figure 8)

6) Map showing the distribution of shorefast ice off the Yukon delta
   (Figure 9)

7) Map showing shoreline changes south of Cape Romanzof   (Figure 10)

Project No.	USGS No.	Lat.	Long.	Date
II-10	48	62°55'	164°06'	820±90
V-10	49	62°09'	164°59'	1350±80
V-9	50	62°02'	165°14'	34,400 (poss. reworked?)
V-4	51	61°32'	164°46'	1200±60
I-4	52	61°36'	166°10'	modern (contamined sample)
II-10	53	62°19'	165°12'	1890±85

Table 1

Radiocarbon dates - Yukon delta

VII. DISCUSSION

Tectonic Framework

Most of the major structural elements in the northern Bering Sea region apparently developed during late Cretaceous and early Cenozoic time (Hoare, 1961; Hopkins and Scholl, 1970), yet the location of the major zones of uplift and basins, as well as many of the transcurrent faults continue to be active to the present (Hoare, 1961; Grim and McManus, 1970). Of particular interest is the pattern of faulting and volcanism over much of the delta plain. The general trend and distribution of these features suggest that they reflect the on-land extension of the Nunivak Arch (Figure 2) previously recognized only
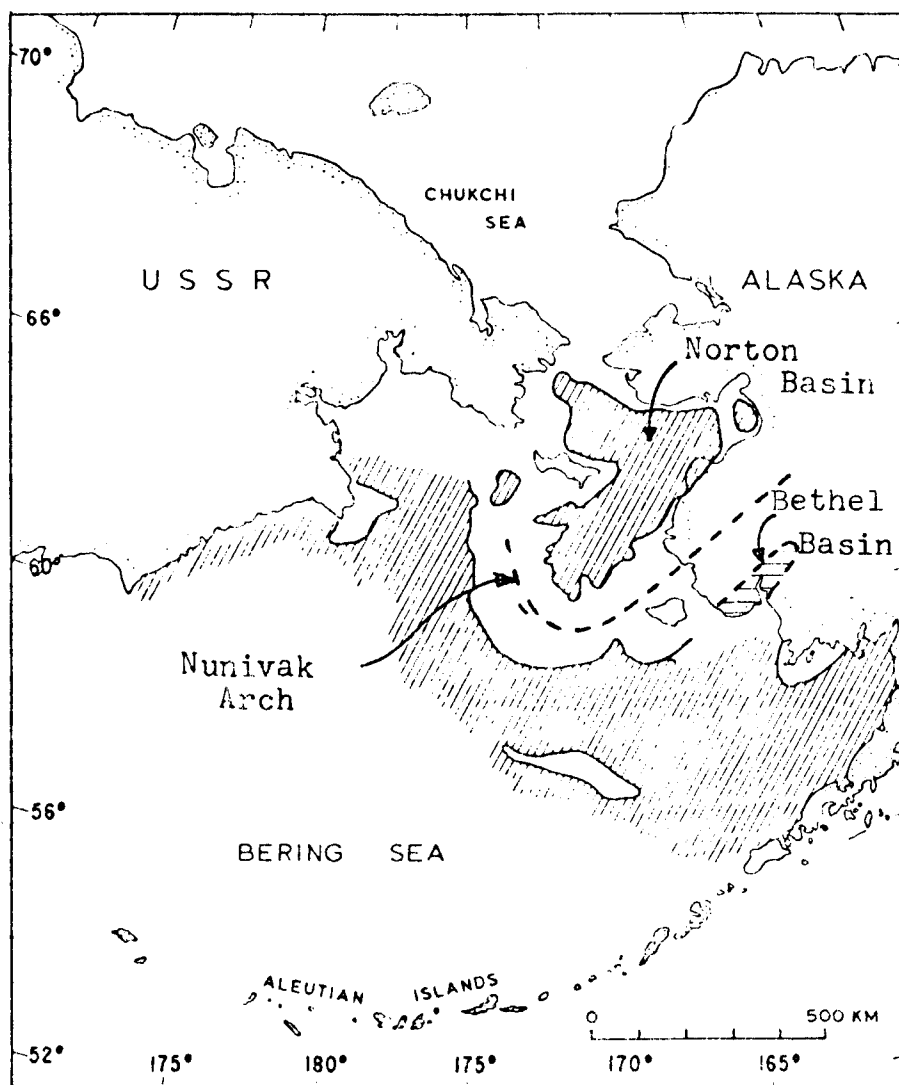
Figure 2- Major Cenozoic basins and areas of uplift, modified after Hoare, 1961; Nelson and others, 1974.

521

in the offshore (Scholl and Hopkins, 1969). Most of the newly
recognized faults, photo-linears, and measured joint sets within
the Quaternary deposits parallel previously mapped faults. Several
of these faults, (e.g., those parallel to the northwest face of
the Kuzilvak Mountains) appear to be a continuation of previously
mapped faults exposed in the Andreski Mountains. The Kuzilvak
Mountains are of particular interest because they appear to be a
fault-bound lozenge uplifted in response to transcurrent movement
along the fault zone. The Quaternary offsets along this zone had
been previously identified as a looped bar by Hoare and Condon (1966).

There is no evidence of the Kaltag fault passing through the
modern lobe of the Yukon delta, as previously suggested by Hoare and
Condon (1971). It is possible that it extends offshore, to the north
of the delta. It also seems possible, perhaps even likely, that it
splays into a series of southwest trending faults which transect the
Andreski Mountains and continue across the delta plain.

The age of the faulting remains uncertain, although the scarp
near the base of the Kuzilvak Mountains is remarkably well preserved.
The exact dating must await more extensive radiocarbon dating of the
various sublobes of the delta. Nonetheless, it seems likely that at
least some of the faults cut Holocene delta lobes.

The linear alignment of many of the volcanic vents, often on line
with the extension of mapped faults or major photo-linears, suggests that
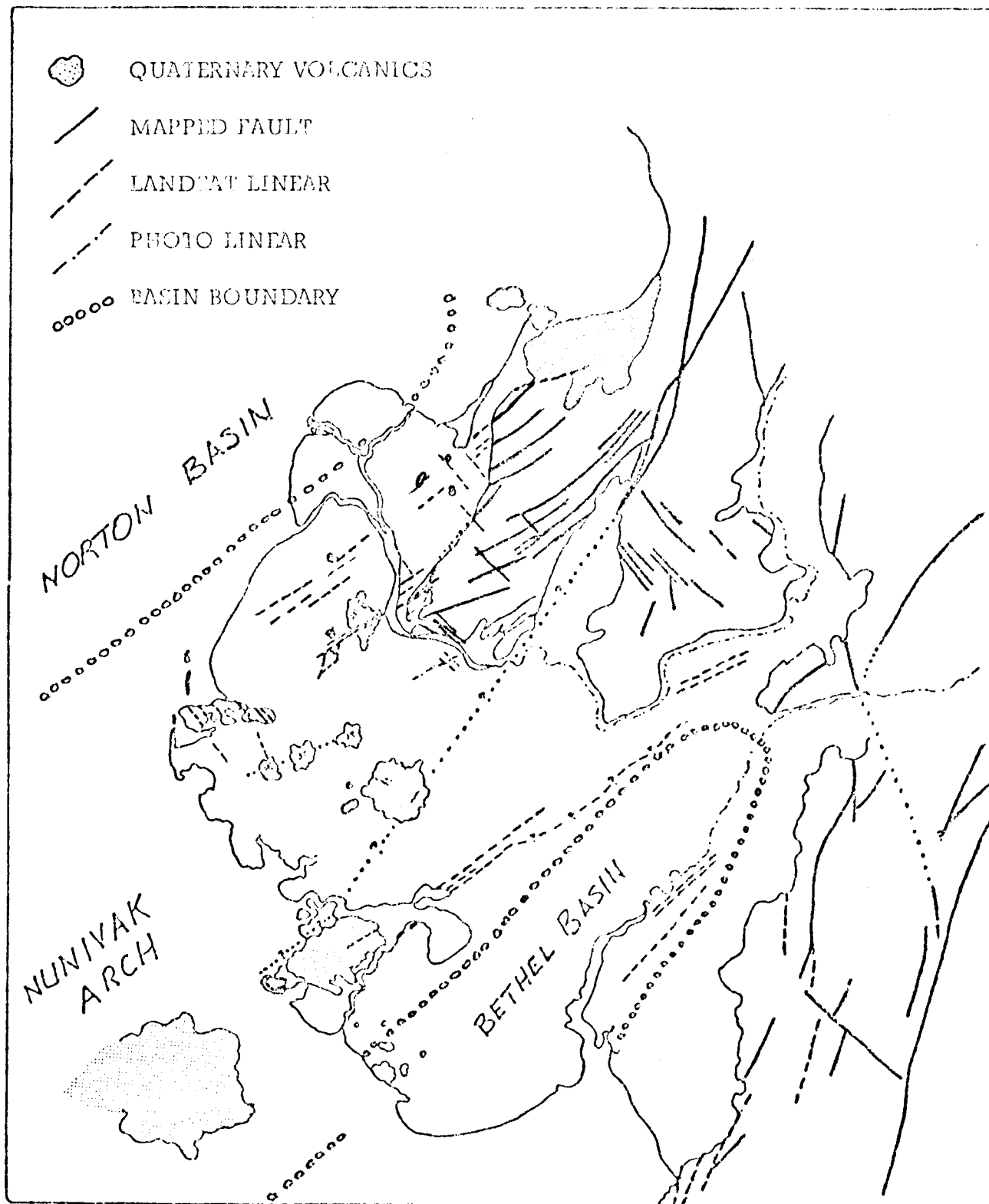the vents are structurally controlled. Whereas most of the volcanism

522

Figure 3– Tectonic map of the Yukon-Kuskokwim delta region (modified after Hoare, 1961; Beikman, 1974).

was apparently mild, forming low shield volcanoes, the presence of at least one caldera, cinder cones, and possible maars suggest that at least some of the volcanism was highly explosive, probably due to contact with ground water or permafrost.

Paleomagnetic data indicate that almost all of the volcanic rocks are normally polarized, hence are younger that 700,000 years B.P. (Hoare and Condon, 1971b). The volcanism probably occurred over a wide period of time, as indicated by the various degrees of weathering and slope modifications. A $5\frac{1}{2}$ meter core was obtained from a volcanic lake in the Ingaksiagwat Hills and is being analyzed for pollen and ash content by Dr. Tom Ager, U.S.G.S. There is a thick (10+cm) layer of ash approximately 40 cm below the base. This is probably correlative with an age of 3,000-4,000 year B.P., based on preliminary pollen chronology. The composition of the ash makes a local origin unlikely, however, and it seems more probable that its source is a major caldera eruption on the Alaskan pennisula (personal communication, B. Carter Hearn, U.S.G.S.).

There are not any other significant ash deposits within the core, which probably contains 60,000 to 90,000 years of record based on preliminary pollen analysis. This suggests either that volcanism in the delta was too far from the lake to have deposited ash, or that it predates the formation of the volcanic lake. The latter seems more likely, as some of the youngest volcanic vents (based on geomorphology) are within a few kilometers from the lake.

Delta Complex

The Yukon-Kuskokwim delta region consists of a complex assemblage of Quaternary depositional systems of various origins and ages (Figure 4). These include:

1) Abandoned meander-belt sequences marking past location of the Yukon River.

2) Extensive stabilized eolian deposits fringing many of the abandoned river courses.

3) Interfluvial and abandoned delta plain deposits, highly altered by thermokarst processes. These areas are largely covered with patterned ground and polycyclic thaw lakes.

4) Modern fluvial deposits, including active and abandoned meander belts deposits, natural levees and river bars.

5) Modern deltaic deposits, including active and abandoned distributaries, channel and distributary mouth bars, and prograding mudflats.

6) Modern bay and estuarine deposits, including large areas of prograding mudflats.

7) Sandy beaches and barrier islands locally bordered by low coastal dunes; formed by reworking of abandoned deltaic and eolian deposits.

Ancient River Courses: Major shifts in the location of the Yukon River have occurred several times during late Pleistocene time, and have resulted in extensive alteration of the meander-belt morphology. The mechanism by which such shifts (river avulsion) occur is unclear. They may be related to the Quaternary faulting in the area; alternatively, they may have occurred in response to flooding associated with major ice jams. Whatever their cause, they have resulted in the diversion of the Yukon River a hundred miles inland, causing a lateral shift of the Yukon delta of almost 150 miles to the north.
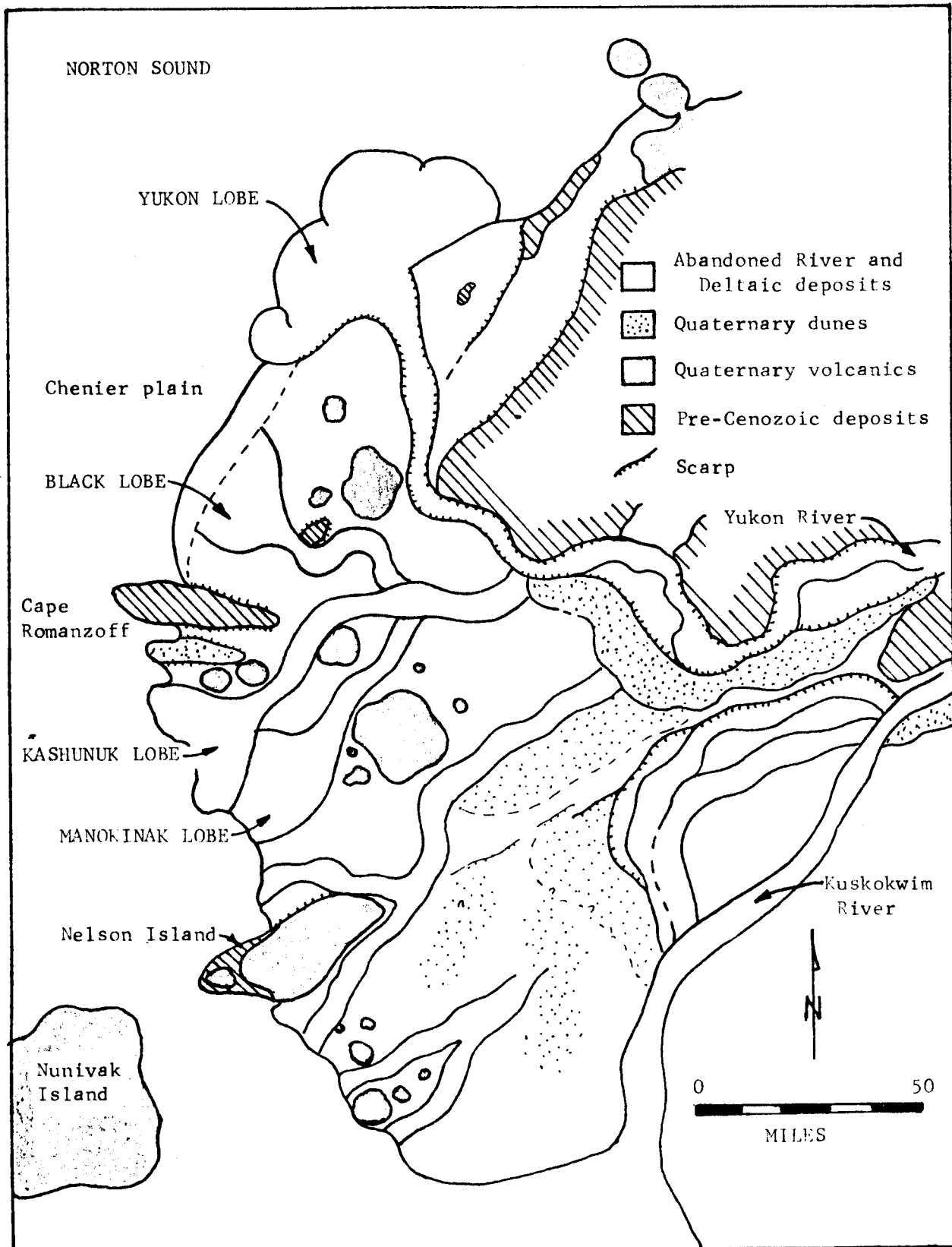
Figure 4 — Generalized geologic map of the Yukon-Kuskokwim
delta complex (modified after Beikman, 1974).

526

Radiocarbon samples were collected along the Black and Kashunuk Rivers to date the most recent sediments carried when they were the main course(s) of the Yukon (Table 1). Samples were also collected in the modern delta to date the oldest part of that delta. These dates should bracket the time of river avulsion, and provide an estimate as to the age of the modern delta. More dates are needed to clear up certain ambiguities in the area. Nonetheless, it seems likely that the Black River was abandoned approximately 1300 years ago, and the Kashunuk River about 1200 years ago. A sample from one of the oldest parts of the delta is approximately 830 years old. These dates suggest that the shift probably occurred about 1000-1200 years ago.

The question then arises as to the possibility of yet another shift, perhaps to reoccupy an older river course (e.g., the Kashunuk). Much water and sediment from the Yukon is diverted through the Kashunuk during Spring breakup. It certainly is possible for the Yukon to reoccupy the Kashunuk under natural conditions, much as the Mississippi would reoccupy the Atchafalaya Bayou and abandon its present course were it not for the intervention of the Corp of Engineers. The implications of such a shift of the Yukon are staggering, affecting the physiography, economy, and circulation patterns throughout the region. For that reason special caution is urged, particularly if construction is planned which might affect the hydrology of the river and increase the probability of river diversion.

Eolian deposits: Large areas of the delta are covered by eolian deposits. The wind-blown sand is deposited in several areas throughout the delta and is locally over 75 feet thick. The deposits appear to be of different ages.

These extensive dune fields are probably evidence of different climatic conditions in the area, as they are all presently stabilized. The dunes are re-activated, however, if vegetation is disturbed, as has happened in the vicinity of Hooper Bay. Therefore special care is needed during construction as these areas are highly vulnerable to erosion.

Lakes: Perhaps 50% of the delta plain is covered by lakes of different sizes and origins. The lake can be classified both as to origin and to degree of development. Some of the lakes are formed in abandoned river courses; others are formed as river levees act as a natural dam. Some are the result of volcanic eruption and collapse. Most, however, are the result of complex thermokaust processes associated with the melting and reformation of ground ice.

Once the lakes form, for whatever reason, they begin to expand laterally due to thermal erosion and wave action. Many of the larger lakes in the southern part of the region show a distinct orientation of long and short axes. The cause of the orientation is uncertain, but it is probably the result of the interaction between lake ice and strong, mutually perpendicular winds (c.f. Carson and Hussey, 1962). Many of these lakes have coalesed laterally to form larger bodies of water (e.g., Dall Lake, Baird Inlet).

Destructional phases of lake development can occur either slowly or rapidly. In some cases the lakes are drained rapidly due to the breaching of the lake either by coastal erosion or meandering rivers. In other cases the lake may fill slowly by sedimentation and vegetation. The patterns of emergent vegetation are important in determining patterns of ice development on the lake bottom (i.e. palsas).

Lakes of different origin and stages of development are characterized by different bathymetry, vegetation and perhaps water chemistry as well. As such, they may provide insight as to developing different schemes for classifying biological habitat.

Permafrost: The presence of discontinuous permafrost is well evidenced by an abundance of geomorphic criteria, including thermokarst lakes, palsas, patterned ground, solifluction lobes, and string bogs. Its existence was further substantiated by probing to frozen ground, examining rapidly eroding cut banks, and by the use of drillers reports of permafrost in the region.

Several types of ground ice were seen during the course of the field season. Pore ice and thin lenses of segregated (Taber) ice were seen, even in the Holocene deposits. The most impressive exposures were in older (late Wisconsian) deposits which cover much of the Yukon-Kuskokwim delta complex. In these areas, patterned ground was underlain by large ice wedges, up to a meter across at the top. These wedges appear to be truncated, and are probably inactive or only weakly active. Massive ice, similar to that described by MacKay (1971) in the northern part of Canada, is also present in these deposits. This massive ice is at least two meters thick (its base was not exposed), continuous over the length of large outcrops, and is generally non-foliated.

Preliminary field work has demonstrated a strong correlation between topography, soils type, vegetation, and depth of the active zone. However, the thickness of the permafrost could not be determined with present field methods. Nevertheless, interviews with engineers, and a report by Williams, 1970, give some evidence as to the distribution and thickness of permafrost in the region.

For example, almost all of the village of St. Marys is underlain by

permafrost (Chuck Kramer, Public Health Service, personal communication), although its distribution is highly variable. The active layer in blue clays is approximately 18-24", whereas patches of willows typically delineate areas of little or no permafrost. Depth to permafrost is relatively shallow along the Andreski River lowlands as well. The permafrost is usually at least 22 feet deep except where gravels are present, in which case the permafrost is absent. The presence of permafrost has caused innumerable construction problems in the region.

There is permafrost in much of the older parts of the modern Yukon delta, yet its thickness is probably on the order of 5-10 feet in most areas. Holocene fluvial deposits are underlain by over 35 feet of frozen ground near Bethel. The depth and distribution of the frozen ground appears to be controlled by the path of the meandering river. The major rivers and some of the larger lakes are underlain by unfrozen ground; even where the ground is frozen, unfrozen zones (taliks) may form in gravel layers.

The older (Wisconsinan) parts of the delta are underlain by great depths of permafrost, locally up to 600 feet (Williams, 1970). Depths up to 250 feet are present along the rapidly eroding coastal zone south of Cape Romanzof, thereby providing ideal conditions for the preservation of offshore permafrost, a possibility which needs closer attention in the future.

The distribution of the permafrost is also closely related to the thickness and distribution of the lake ice. Lakes are commonly thought to be underlain by unfrozen ground due to the presence of water beneath the ice. Most of the lakes are the result of thermokarst processes, hence tend to be

quite shallow (generally 3-5 feet). In these lakes, the thickness of the
ice is likely to be as great as the depth of the lake, thereby allowing
the lake to freeze to the bottom and permafrost to form beneath the lake.
Only a few of the lakes in the region appear not to freeze to the bottom;
these deeper lakes are probably underlain by unfrozen ground or rapidly
degrading permafrost.

In summary, permafrost is present throughout the region, in varying
contents and thickness, except in those few areas where rivers or deep lakes
provide sufficient insulation to prevent the underlying sediments from
freezing or where deposition has occurred so recently as to limit its
formation. In many ways, its distribution is similar to that of the Mac-
kenzie delta in Canada (as described by Smith, 1976), differing mainly in
the thickness of the frozen zone.

Coastal Environments:

Modern Yukon delta: The Yukon River has formed a high-constructional,
lobate delta, as would be expected by the relatively low wave regime,
shallow shelf, and relatively low clay content of the sediment load. There
are twelve active distributaries, but the two largest discharge most of the
water and sediment. The main distributaries appear to shift frequently,
probably due to ice jams in the delta area, thereby producing the arcuate
shape of the delta shoreline.

The delta is presently undergoing both constructional and destructional
phases of development. The constructional phase is characterized by pro-
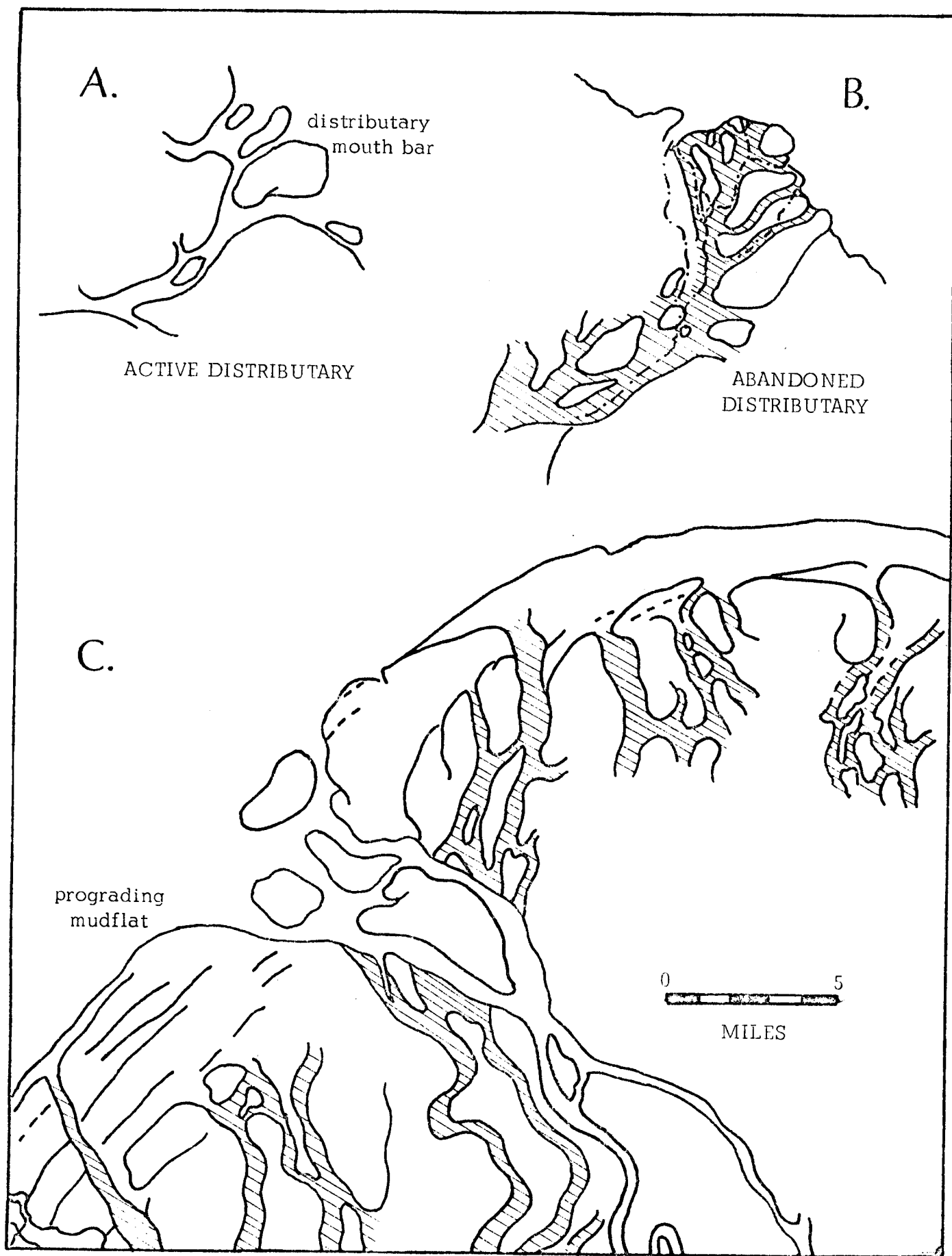gradation of distributary mouth bars and interdistributary mudflats.

531

Figure 5.   Depositional facies within the modern Yukon delta.

Erosion of the eastern-most part of the delta shoreline is presently occurring because of recent abandonment of a major distributary in the area. Subsidence does not occur during the destructional phase, in part because of the tectonic framework in the area and the relative lack of clays in the sediment load.

The modern delta is relatively young, having formed by river avulsion approximately 100 miles upstream. The timing of that event, hence the age of the delta, remains somewhat uncertain. A major decrease in the salinity of Norton Sound occurred approximately 5,000 years ago, and has been interpreted by Nelson and Creager (1977) as resulting from the shifting of the river to its present course. Radiocarbon dates from the delta plain, however, suggest the shift may have occurred as recently as 1200 years ago.

Chenier Plain and Tidal Mudflats: Some of the Yukon sediment is transported to the south via river-induced currents to be deposited within an extensive chenier plain in the vicinity of the Black River. It is presently an area of extensive, prograding tidal flats, but numerous erosional strandlines appear to record the effects of major storms in the region. Samples have been collected to date these shorelines, thereby giving an estimate as to the recurrence interval of these large storms.

Broad mudflats are also presently forming in partially protected bays in the region (e.g., Hooper Bay, Scammon Bay). These bays formed as river valleys were flooded during the post-Wisconsinan rise in sea level. The extent of the mudflats is in part a function of the tidal range which seems rather variable along much of the shoreline.

Extremely broad mudflats are present on the north side of Kuskokwim Bay. These mudflats, locally cut by meandering tidal channels, are up to 10 km. wide in some areas, making their study rather difficult. They will be studied in more detail next field season using a NOAA-provided helicopter.

Sandy Beaches and Barrier Islands: Sandy beaches are relatively uncommon along much of the delta region. They are extremely well developed in the vicinity of Hooper Bay, however, where coastal erosion of fluvial and eolian sediments provide a ready source of sand. They also form barrier islands in the vicinity of Cape Romanzof and south of Nelson Island. The barrier islands tend to form along the mesotidal areas of the coast. As tidal range increases the islands grade laterally into offshore sand shoals separated from the mainland by extensive tidal flats (Hayes, 1975). Tidal inlets separate both barrier islands and intervals of sand shoals.

A complex series of ridge and runnels as well as offshore sand bars extend up to a kilometer offshore just south of Hooper Bay. A small barrier island has formed in this area by the emergence and coalescence of these offshore bars, sometime between 1954 and 1973. These grade landward to sandy beaches which form along the base of cliffs, on spits, forelands, and barrier islands. These beaches typically consist of a series of welded ridge and runnels, a well developed berm, and a wind-modified back beach area, often littered with driftwood. These are locally fringed by vegetated sand dunes, many of which have been breached by strong, southwesterly storm-winds. Dunes are uncommon on the barrier islands, however, perhaps because of the extremely high rates of lateral migration (up to 15-20 meters/year - Figure 10).

534

<u>Gravel Beaches</u>: Small areas of gravel beaches are restricted to areas where outcrops of bedrock are exposed along the shore. This may include Quaternary volcanics as at St. Michaels, Jurassic (?) deposit at Pt. Romanoff, or cretaceous sediments at Cape Romanzof .

These locally derived gravels typically form small pocket beaches along the cliffed shoreline. The beaches are typically steep, with multiple berms and a cusped shoreline. Dunes may form where gravel beaches have prograded, such as at Tanumuk, on Nelson Island. The steep gravel beach grades rapidly offshore to a sandy bottom in most areas. The gravels overlie peat just to the northeast of Pt. Romanoff, where gravels have been transported via longshore drift during storms, having covered mudflats and blocked small streams.

Sediment Transport System

The Yukon River has a drainage area of over 855,000 km^2, and transports over 88 million metric tons of suspended sediment annually (Listzin, 1972, p. 37). Most of the sediment is silt and very fine sand; clay constitutes a relatively small proportion of the total load because of the dominance of mechanical weathering processes in subarctic environments (e.g., Hill and Tedrow, 1961).

An examination of selected hydrographs of the Yukon and Kuskokwim Rivers demonstrates the highly seasonal variation in discharge. The average discharge of the Yukon River is approximately 40,000 cfs during the winter months when the ice-covered river is fed mainly by base flow. Presumably, sediment transport is minimal during this interval. The major hydrologic event of the year is breakup when discharge may increase to over 1,000,000 cfs within a week or less. This is followed by a general decline

in discharge, interrupted by large floods associated with late summer-early fall storms. The effect of these storms is quite apparent on some of the Kuskokwim hydrographs (Figure 7). This decline in discharge continues until October or November, when the river freezed over and the winter cycle begins anew. This type of annual runoff pattern has been defined as a "nival" runoff regime by Church (1974).

River ice plays a major role in the shaping of sub-arctic and arctic deltas, particularly when it breaks up during the Spring. Breakup along the Yukon occurred relatively late in 1976. This appears to be the result of weather conditions, not only during breakup, but during freeze-up the previous year as well. Late fall of 1975 was characterized by prolonged intervals of sub-zero temperatures without significant snowfall. This resulted in unusually thick (up to 5 ft.) river ice. In addition, relatively mild conditions in the interior of Alaska, resulted in an early breakup inland at the same time the western part of the state (including the delta region) was having unseasonably cold weather. The late cold snap, accompanied by the thick ice retarded breakup and tended to increase the probability of ice jams and flooding.

Such complications make it extremely difficult to predict breakup conditions in the delta region, even as breakup occurs upstream. Some areas are, however, more likely to create ice jams than others, because of channel configurations. For example, the region around Holy Cross has been the site of ice jamming and flooding for 3 of the last 5 years, (River Forecast Service Personnel, personal communication). Ice jams result in the damming of the river and extensive upstream flooding.
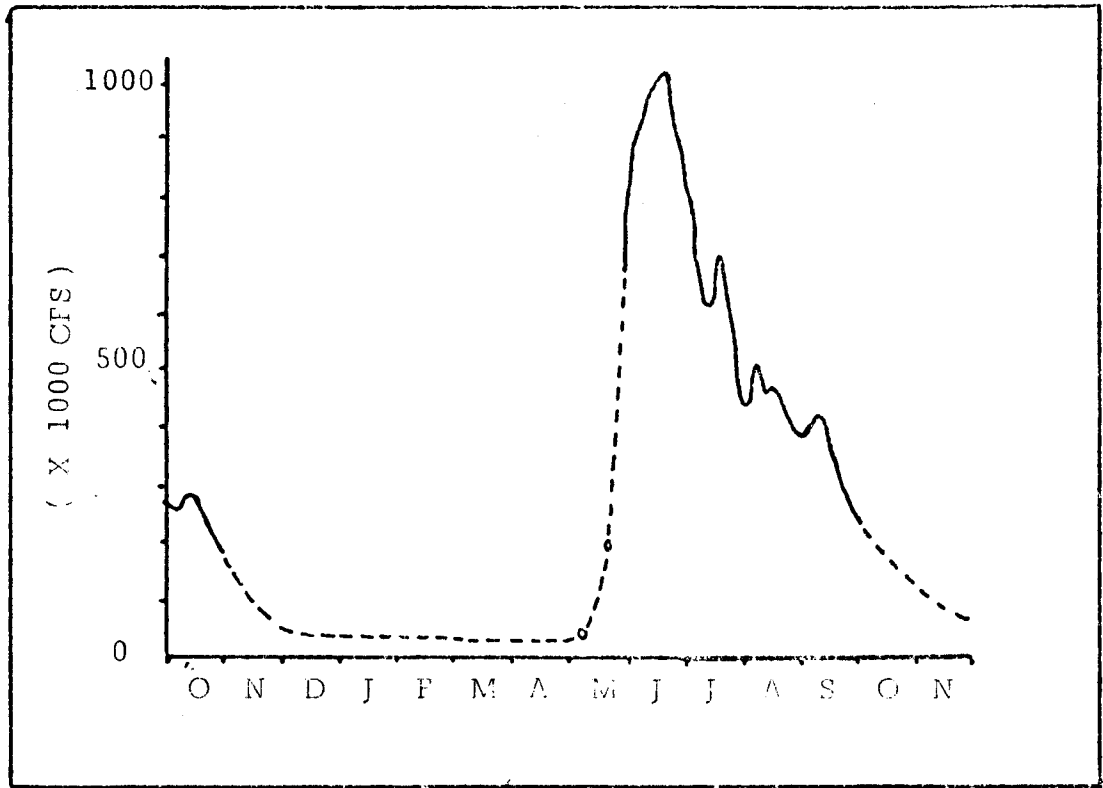
536

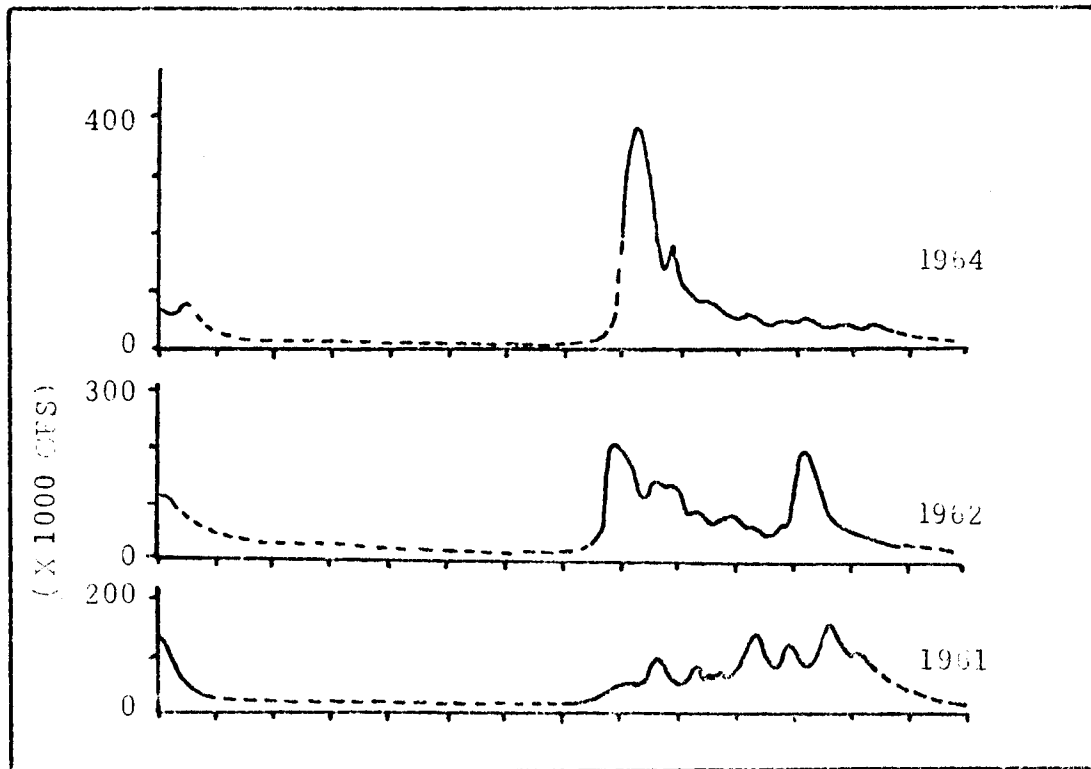Figure 6.   Hydrograph of Yukon River at Kaltag, 1963-1964.

Figure 7.   Selected hydrographs of Kuskokwim River at
Crooked Creek.

Rapid draining of these temporary lakes can result in extensive downstream

flooding as well. Serious river bank erosion is more likely to occur

associated with downstream flooding, although erosion is somewhat retarded

by the presence of frozen ground at this time of year.

Special note should be made of the role of sloughs in the draining

of ice jam lakes. These sloughs are partially abandoned river courses

which act as outlets by which upstream flooding is limited. Thus, any

construction which would tend to restrict flow in these sloughs would

seriously aggravate upstream flooding. This periodic re-occupation

prevents the complete abandonment of these channesl, creating a complex

channel pattern which differs from the classic meander-scroll belts in

more temperate climates. It seems likely that ice jams are the major

mechanism for channel diversion in the region.

The largest floods are associated with breakup, yet the total amount

of sediment transported during this event is probably less than that associated

with late summer-fall storms. This is because most of the water associated

with breakup is derived from snow melt, here is relatively sediment free.

In addition the ground is still frozen along much of the region, minimizing

the amount of sediment derived from riverbank erosion. This seems to be

corroborated by conversations with natives in the area who state that most

of the significant river erosion occurs associated with storms during the

late summer and fall. Most of the sediment in the Yukon River reaches

the Bering Sea via one of the major distributions in the delta. Large

amounts of sediment may bypass the delta, however, particularly during

major floods, and may reach the Bering Sea through a series of interconnected

lakes and partially abandoned river courses. In addition, at least some of the

sediment is permanently trapped in small deltas which form relatively large

538

lakes in the delta region. This complex pattern of sediment dispersion

makes it rather difficult to predict the path of waterborne pollutants,

particularly during floods.

Much of the sediment entering the coastal zone is deposited within

the modern delta, cheniers, and protected bays. There remains a significant

component of sediment transport both along the coast and across the

shelf as well (e.g., Nelson and Creager, 1977).

The general trend of nearshore sediment transport is to the north due

to the effect of local winds, southwesterly swell waves, major storms, and

the north-flowing Alaska Coastal Waters. When examined in detail, however,

the pattern becomes more complex. It is impossible to determine any dominant

direction of sediment transport in much of the southern part of the delta

region because of the effects of major tidal currents. Complex wave

refraction causes local reversals in the direction of sediment transport

(e.g., at Dall Point and along the southern end of some of the barrier

islands). River-induced currents off the mouth of the Yukon River have the

effect of locally reversing the direction of sediment transport. The

configuration of the Yukon delta shoreline and the offshore waves appear to

be mutually adjusted to minimize longshore currents. Northeasterly sediment

transport continues east of the active delta, toward St. Michaels.

Nelson and Creager (1977) have demonstrated that a significant amount

of Yukon-derived sediment enters the Alaska Coastal Waters, ultimately bypassing

Norton Sound to be deposited in the Chukchi Sea. A comparison of sediment

plumes off the Yukon delta (as delineated by LANDSAT imagery) with

shelf sediment distribution, oceanic currents and water masses also suggests

a strong correlation between the coastal waters and present-day sedimentation
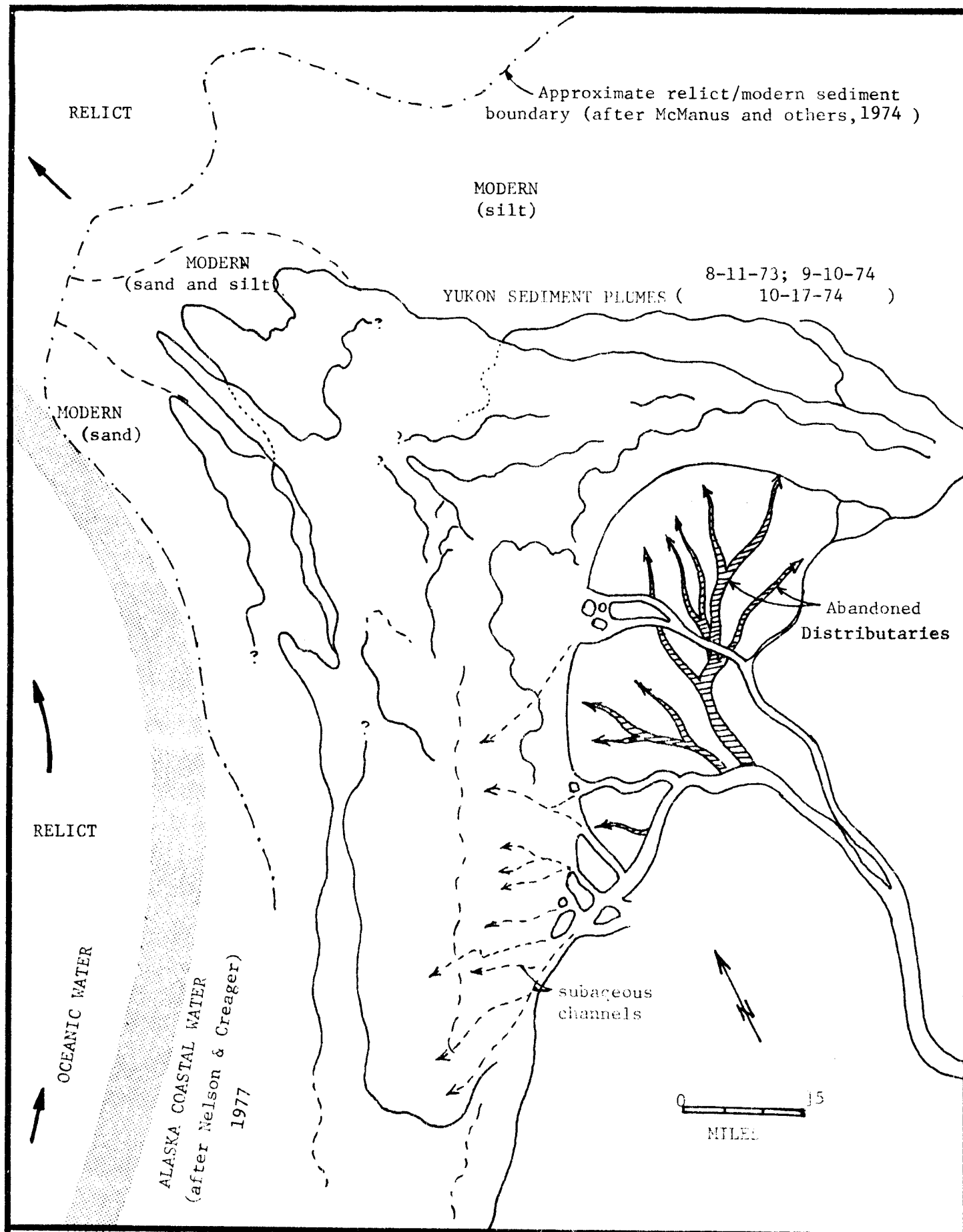
RELICT

Approximate relict/modern sediment
boundary (after McManus and others, 1974)

MODERN
(silt)

MODERN
(sand and silt)

YUKON SEDIMENT PLUMES (8-11-73; 9-10-74
                          10-17-74   )

MODERN
(sand)

Abandoned
Distributaries

RELICT

OCEANIC WATER

ALASKA COASTAL WATER
(after Nelson & Creager)
1977

subaqeous
channels

0   15

MILES

Figure 8- Comparison of offshore sediment plumes, modern and relict shelf sediments,
and oceanic currents and water masses off the Yukon delta.

patterns (Figure 8).

Once the Yukon sediment enters Norton Sound, it is diverted to the north and northwest with little or no mixing with oceanic water to the west. The modern shelf sediment as mapped by McManus and others (1974) is also confined to areas within the coastal water. This suggests that the contact between coastal and oceanic water is now and has been an effective barrier to diffusion of sediment to the west, thus supporting the idea that advective and shelf transport is a dominant process in the area. There is some evidence, however, that transport of bedload sediment is very sensitive to nearshore bathymetry, hence may not parallel suspended sediment transport.

It seems clear that LANDSAT imagery offers a valuable overview of suspended sediment transport across the shelf, thereby providing a first approximation as to the path of marine pollutants on the surface of Norton Sound. Pollutants on the surface are likely to be confined to the coastal waters where they will be transported to the north and northwest under most summer, fair-weather conditions. What is urgently lacking, however, is information on winds, waves, and currents under storm and winter conditions. This is particularly significant as much of the sediment on the shelf may be resuspended by storms (Matthews, 1973; Nelson and Creager, 1977). The grounding of sea ice is another mechanism which may be significant in resuspending shelf sediments (c.f. Reimnitz and Barnes, 1974).

Much information concerning the spatial and temperal distribution of sea ice can be obtained from existing LANDSAT imagery. This imagery demonstrates

that shorefast ice begins to form along the margins of the delta in October. It is most likely to form first over the shallow distributary mouth bars and mudflats along the delta front. The main river channels, including their extension offshore remain free of ice until November or December because of the greater depths and higher velocities.

The shoal areas off the major mouths of the delta continue to be delineated during the winter months by darker patterns on the ice. Aerial reconnaissance demonstrates these dark areas on the LANDSAT imagery are areas of aufeis formed where the shorefast ice has frozen to the bottom. No evidence could be found during overflights of major shoreline leads having been formed. Nevertheless, discussions with natives in the region suggest they do form in some areas and further field work is necessary before the dynamics of the nearshore ice is even approximately understood.

The seaward edge of the shorefast ice west of the Yukon is marked by a shear zone which remains remarkably constant throughout the winter (Figure 9); its location can be approximated by the 5-10 meter contour. In contrast, the shorefast ice north of the delta is more variable. Large areas of seasonal pack ice become relatively immobile during parts of the winter, and are welded to the pre-existing shorefast ice. The healed shear zone can be seen on the LANDSAT imagery, as can the newly formed shear zone, often 20 miles seaward of the old boundary. This suggests that, whereas the currents west of the Yukon delta are sufficient to prevent shorefast ice from extending beyond the 10 meter contour, the more sheltered portions of Norton Sound will often have seasonal pack ice temporarily attached to the shorefast ice, only to break off, typically at the old "healed" shear zone, later in the season.
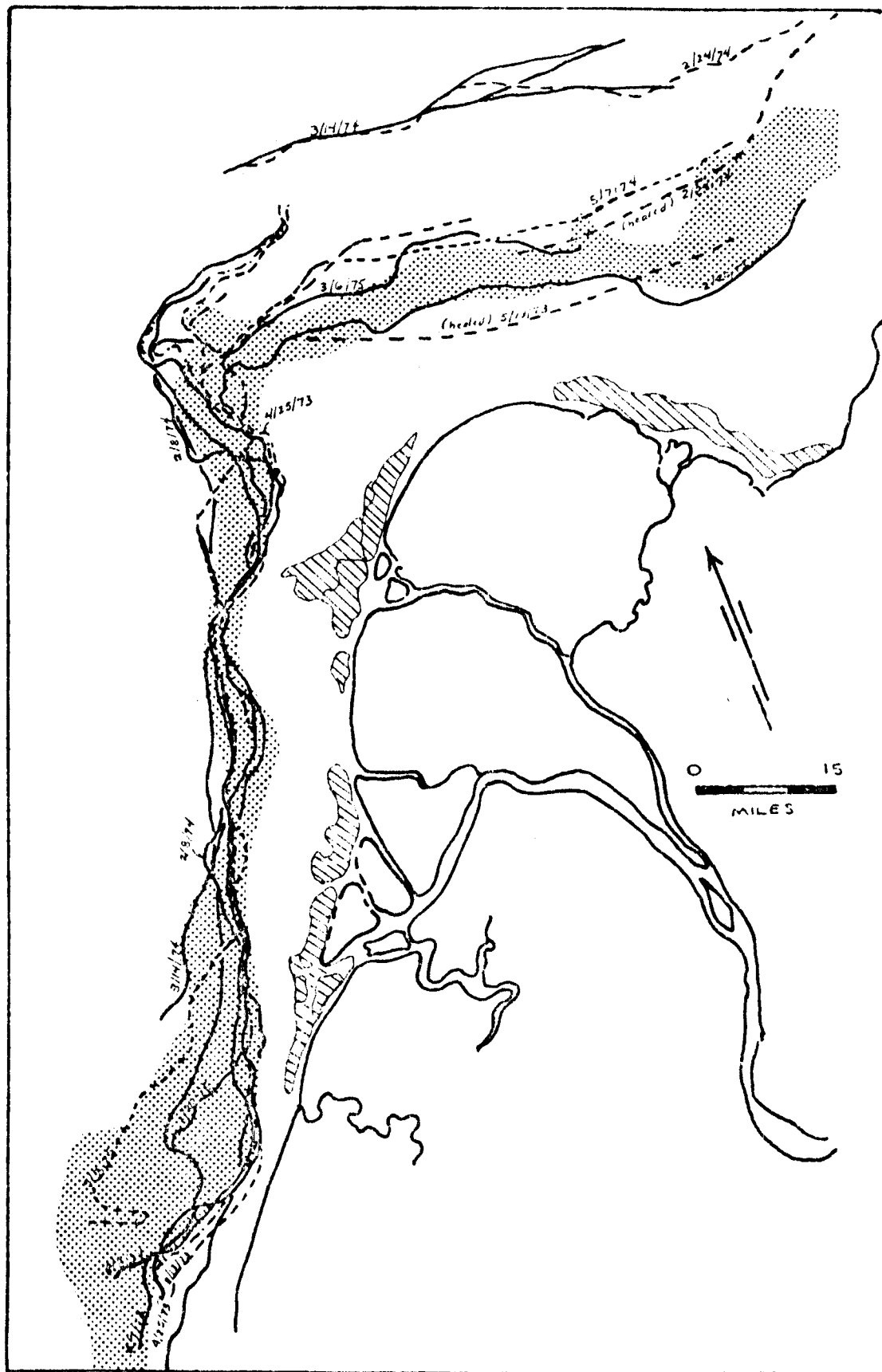
542

Figure 9 - Location of shear zones as determined from LANDSAT imagery, 3/13/73 to 3/6/75. Hatched areas delineate aufeis. Dotted area delineates the 5 to 10 meter bathymetric interval.

There is a relatively strong correlation between the distribution of shorefast ice and the 20 meter bathymetric contour off the Beaufort Sea (e.g., Stringer, 1974; Reimnitz and Barnes, 1974), although the explanation for this correlation remains uncertain (Reed and Sater, 1974, p. 300). In the northern Bering Sea the major circulation patterns, and in particular the Alaska current, appear a major factor in the distribution of the shorefast ice. The correlation with the 5-10 meter depths may be related the the thickness of the ice and to the pressure ridge keels, both of which may be less thick than their counterparts off the Beaufort Sea because of the thinner sea ice south of the Bering Straits. Pressure ridges and newly healed leads are common in the offshore part of the shorefast ice, however, suggesting it is a zone of significant ice movement. LANDSAT images obtained on successive days show a 5 x 10 mile sheet of floating ice detached from the main ice sheet and drift over 5 miles in 24 hours. Such ice mobility will make the siting of offshore drilling platforms extremely difficult.

Breakup was so delayed last spring that I was unable to observe the effects along the coast. Conversations with natives and non-natives in the area suggest that breakup along the delta is similar to that described by Walker (1973) along the Colville delta on the North Slope. In particular, they describe the riger flowing over the shorefast ice, causing the floating ice which delineates the offshore channels to sink and/or melt in place. LANDSAT images show that the sea ice doesn't stay long after breakup, either detaching and floating to the north or melting in place.

Coastal Stability:

Coastal stability is an especially important parameter as it provides some insights as to the suitability of an area for the establishment of shoreline facilities.

Comparison of 1954 and 1973 aerial photos indicates that several hundreds of feet of erosion has occurred along much of the coast in the last 30 years. Most of that erosion occurs during late summer/early fall storms, particularly in response to strong winds and elevated storm surges. How much erosion might occur in a single storm isn't known, although photography is available before and after the 1973 storm surge, and will be examined. Similarly, the recurrence interval of such storms isn't known. Some estimate of frequency of storms should be provided which some of the storm-generated chenier ridges are dated.

The variables which control the patterns of sedimentation and erosion are in many ways more important than the patterns themselves for, as these variables change, either naturally or as the result of man's activities in the region, so too will the coastal stability. The major factors which appear to determine coastal stability in this region include:

1) Proximity of fluvial sediment input: significant changes in the stability of the shoreline can be affected by changes in the location of major rivers or their distributaries.

2) General orientation of the coast: south-facing shorelines tend to be dominantly erosional, whereas the west-facing parts of the shoreline tend to be stable, or areas of deposition.

3) Presence of barrier island: provide partially sheltered intervals along which deposition on the mainland is likely to occur.
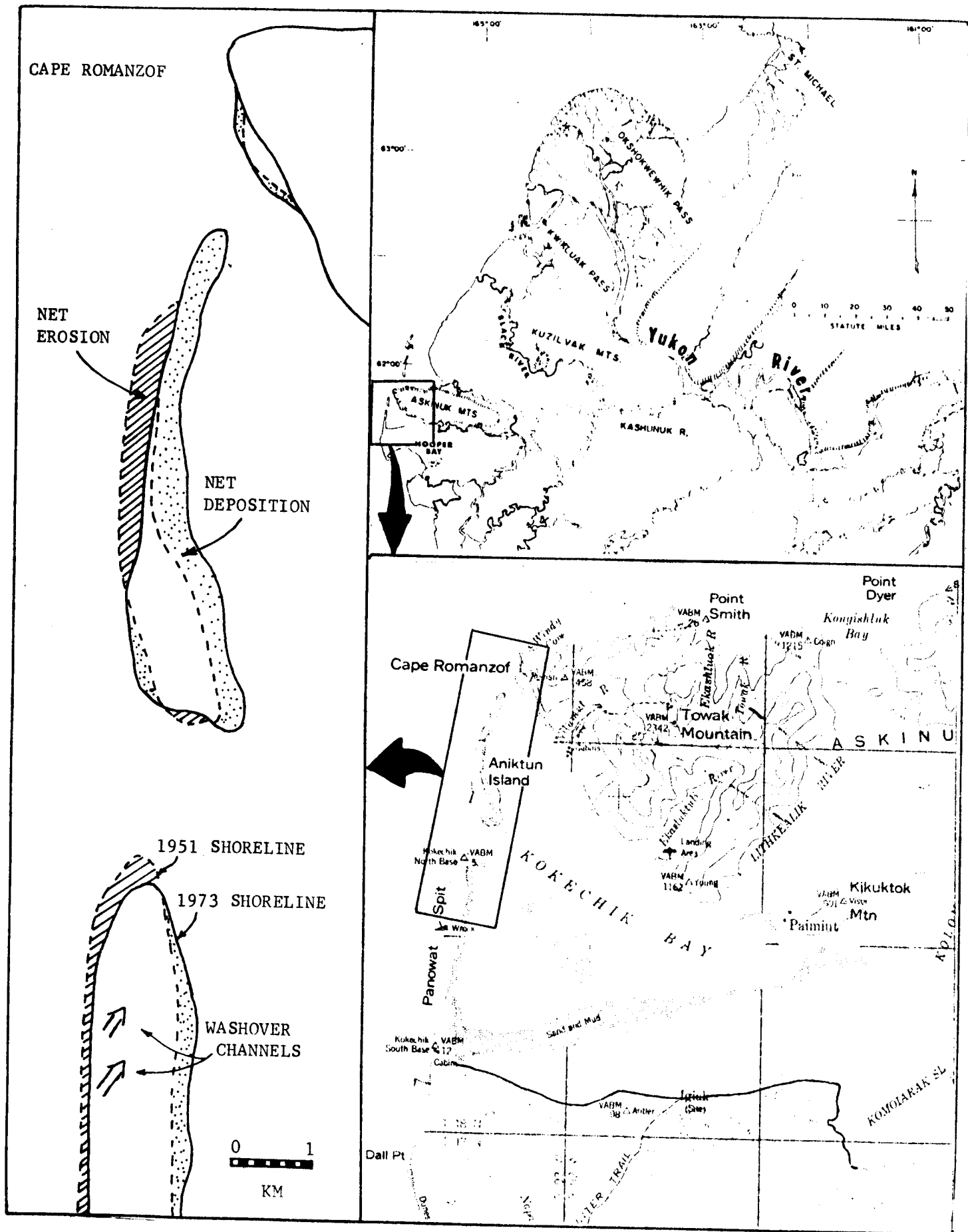
545

Figure 10 - Shoreline changes south of Cape Romanzof from 1951-1973. Maximum rate approaches 15-20 meters/year!

4) Prograding spits: protect large areas of inland bays, allowing the development of prograding mudflats.

5) Proximity of tidal and sub-tidal channels: lateral erosion of these channels can cause significant local erosion.

6) Major storms can cause significant erosion even in areas of long-term progradation.

7) Early forming shorefast ice can be an effective erosional agent when it has lifted and drifted offshore to return on a storm tide.

8) Tectonics: subsiding regions appear to be characterized by submergence and erosion of the shoreline.

Applications to Biological Habitat Studies:

An understanding of the geologic history of the delta region and the processes by which it continues to be shaped provide invaluable insights as to geologic hazards and engineering properties. Less obvious is the extent to which geologic processes and products combine to determine the topography, soils, and vegetation which are so important in defining biological habitats. Thus, it should be no surprise that the first report of pingo-like features (palsas) in the delta region was done to define their role as an important mink habitat (Burns, 1964). Similarly, the margins of abandoned distributary mouth bars mapped in the modern delta region have slopes and vegetation assemblages which, according to Bob Jones (U.S. Fish & Wildlife) are particularly important nesting areas.

Almost all of the delta is underlain by frozen ground. It is the selective melting of the permafrost which has resulted in the myriads of thermokarst lakes so important in making the area such a productive nesting area. This study is aimed at understanding the origins of these lakes,

including the processes by which they drain and/or fill, thereby defining a continuum of lake types which might aid in regionalization of nesting habitats.

VIII. CONCLUSION

The Yukon-Kuskokwim delta region is characterized by widespread Quaternary tectonism. Northwest- and northeast-trending faults and structurally-controlled volcanic vents are mainly restricted to the onshore extension of the Nunivak Arch. Many of the northeast-trending faults may actually represent the slivering of the Kaltag fault, previously projected to the north of the delta. At least some of these faults appear to have had Holocene movement. The age of the volcanism is less certain, but most, if not all, of the activity appears to be pre-Holocene.

The presence of extensive permafrost is well evidenced by an abundance of geomorphic criteria as well as field investigations. It is locally absent beneath large lakes and rivers, as well as in areas of rapid deposition. Elsewhere it may be up to 600 feet thick, and may be present offshore of some areas of rapid erosion.

Flooding and river bank erosion along both the Yukon and Kuskokwim Rivers is strongly affected by the climatic extremes of this subpolar region. The largest floods are associated with ice breakup on the river, often accentuated by the effects of breached ice jams which form locally. Extreme floods may actually result in the complete diversion of the Yukon River, with disastrous consequences. Such events have occurred repeatedly during the Pleistocene; the most recent may have occurred only 1200 years ago.

IX NEEDS FOR FUTURE STUDY

1) Obtain recent photography of the entire delta region, both as an aid to geologic mapping and to aid in establishing rates of erosion and deposition along river banks and lake margins.

2) Make more detailed studies of selected geologic units (emphasizing permafrost content, engineering properties, frequency of flooding, microtopography, vegetation, etc) to aid in the establishment of resource capability units and the characterization of biological habitats.

3) Coastal stations should be repeatedly re-occupied throughout the year, with special emphasis on assessing the effects of major storms on the coast. This should be coupled with a study of the effects of the 1974 storm surge in Norton Sound and existing weaterh data to generate a wave-climate model of the area. This would aid in predicting the effects of major storms on the coast, as well as providing insights as to the potential dispersion patterns of oil spills, etc.

4) In-situ monitoring of sediment transport during winter, breakup, and storm conditions, should be carried out in the Yukon River, in the nearshore coastal zone, and offshore on the shelf. This sampling program should also collect hydrologic and STD data, and be coincident with LANDSAT overflights when possible.

5) In-situ studies of ice dynamics deserve special attention. This could be coordinated with the study of LANDSAT imagery and sediment sampling programs. This should also be coordinated with studies of shelf sediments and the density of ice-gouging, as determined by side-scan sonar.

X SUMMARY OF FOURTH QUARTER OPERATIONS

Much of the laboratory work begun last quarter continues to the present. Onshore and offshore profiles of coastal stations are complete, but textural analysis of the coastal sediments and the formating of those data are in progress. Twelve samples of Yukon and Kuskokwim River sediments were sent to Tracy Vallier at Menlo Park, where they will be studied for both grain size and mineralogical analysis. In addition, samples submitted

to Steve Robinson at Menlo Park for radiocarbon dating are still in progress.

I spent four days in January visiting personnel in both the Marine Geology and Alaskan Geology branches of the U.S. Geological Survey at Menlo Park. The visit was extremely productive, both by providing new insights to the general geology in the area and in coordinating research efforts for this coming field season. I will be returning to California in early April to give a talk on the Yukon delta to the regional meeting of the G.S.A. (abstract attached).

LATE QUATERNARY HISTORY OF THE YUKON-KUSKOKWIM DELTA COMPLEX, ALASKA
   DUPRE, William R., Department of Geology, University of Houston,
      Houston, Texas 77004

The Yukon-Kuskokwim delta complex is in a tectonically-active region characterized by Quaternary faulting and structurally-controlled volcanism. Much of this deformation appears to represent an on-land extension of the Nunivak Arch.

Several abandoned courses of the Yukon River can be delineated, the older of which are fringed by extensive eolian sand deposits. There is little evidence, however, that the Yukon River once joined the Kuskokwim River, at least during the late Pleistocene. Most of the delta plain has been extensively altered by thermokarst processes, including the formation of polycyclic thaw lakes, many of which are strongly oriented. Dall Lake and Baird Inlet formed by expansion and lateral coalescence of thaw lakes initiated along former courses of the Yukon River.

The oldest courses of the Yukon appear to be in the southern part of the region. These were abandoned following a northward shift of the river to the vicinity of Cape Romanzoff where it continued to flow throughout most of the Holocene. At least three delta lobes formed in the area during the present highstand of sea-level.

The Yukon River subsequently shifted to its present course where it empties into Norton Sound approximately 1200 years ago. This was probably triggered by faulting or a massive ice jam approximately 100 miles inland. Thus the modern Yukon delta is a relatively young feature, as has been suggested by others on the basis of off-shore studies in the Bering Sea.

BIBLIOGRAPHY

Beikman, H. M., 1974.
  Preliminary geologic map of the southwest quadrant of Alaska; USGS open file map (2 sheets).

Brown, L. F. Jr., Fisher, W. L., Erxleben, A. W., and McGowen, J. H., 1971.
  Resource Capability Units: their utility in land-and water-use management with examples from the Texas coastal zone: Bureau of Economic Geology, the University of Texas at Austin, Geologic Circular 71-1, 22 p.

Carson, C. E., and Hussey, K. M., 1962.
  The oriented lakes of arctic Alaska; Jour. Geology, vol. 70, p. 417-439.

Church, M., 1974.
  Hydrology and permafrost with reference to northern North America in Permafrost Hydrology: Proceedings of Workshop Seminar, 1974: Canadian-National Committee, Int'l Hydrologic Decade, Envirnment Canada, Ottowa, p. 7-20.

Creager, T. S. and McManus, D. A., 1967.
  Geology of the floor of Bering and Chukchi Seas - American studies; in Hopkins, D. M. (ed.) The Bering Land Bridge, Stanford Univ. Press, Stanford, Calif., pp. 32-46.

Frazier, D. E., 1967.
  Recent deltaic deposits of the Mississippi River: their development and chronology; Trans. Gulf Coast Assoc, Geol. Soc., vol. 17, p. 287-315.

Grim, M. S. and McManus, D. A., 1970.
  A shallow-water seismic-profiling survey of the northern Bering Sea; Marine Geology, vol. 8, p. 293-320.

Hill, D. E., and Tedrow, J. C. F., 1961.
  Weathering and soil formation in the Arctic environment: Amer. Jour. Sci. vol. 259, p. 84-101.

Hoare, J. M., 1961.
  Geology and tectonic setting of lower Kuskokwin-Bristol Bay region, Alaska; Am. Assoc. Petroleum Geologists Bull., vol. 45, p. 594-611.

Hoare, J. M. and Condon, W. H ., 1966.
  Geologic map of the Kwiguk and Black Quadrangles, western Alaska; U.S.G.S. Misc. Geol. Invest. Map I-469.

Hoare, J. M. and Condon, W. H., 1968.
  Geologic map of the Hooper Bay Quadrangle, Alaska; U. S. G. S. Misc. Geol. Invest. Map I-523.

Hoare, J. M., and Condon, W. H., 1971(a)
    Geologic Map of the St. Michael Quadrangle, Alaska; U.S.G.S. Misc. Geol.
    Invest. Map I-682.

Hoare, J. M., and Condon, W. H., 1971(b)
    Geologic Map of the Marshall Quadrangle, western Alaska; U.S.G.S. Misc.
    Geol. Invest. Map I-668.

Hoare, J. M., and Coonrad, W. L., 1959.
    Geology of the Bethel Quadrangle, Alaska; U.S.G.S. Misc. Geol. Invest.
    Map I-285.

Hoare, J. M., and Coonrad, W. L., 1959.
    Geology of the Russian Mission Quadrangle, Alaska; U.S.G.S Misc. Geol.
    Invest. Map I-292.

Knebel, H. J., and Creager, J. S., 1973.
    Yukon River: evidence for extensive migration during the Holocene Trans-
    gression; Science, vol. 79, p. 1230-1231.

Lisitzin, A. P., 1972.
    Sedimentation in the world ocean; Soc. Economic Paleontologists and
    Mineralogists Spec. Pub. No. 17, 218 p.

Marlow, M S. and others, 1976.
    Structure and evolution of Bering Sea shelf south of St. Lawrence Island:
    Amer. Assoc. Pet. Geologist, vol. 60, p. 161-183.

Matthews, M. D., 1973.
    Flocculation as exemplified in the turbidity maximum of Acharon Channel,
    Yukon River delta, Alaska; Unpublished Ph.D. dissertation, Northwestern
    Univ., 88 p.

McManus, D. A., Venkatarathnam, K., Hopkins, D. M., and Nelson, C. H., 1974.
    Yukon River sediment on the northernmost Bering Sea shelf; Journal of
    Sed. Petrology, vol. 44, p. 1052-1060.

Moore, D. G., 1964.
    Acoustic reflection reconnaissance of coutinental shelves: eastern Bering
    and Chukchi Seas; in Moore, R. L. (ed.) Papers in marine geology, MacMillan
    Co., N. Y., pp. 319-362.

Nelson, C. H., and Creager, J. S., 1977.
    Displacement of Yukon-derived sediment from Bering Sea to Chukchi Sea
    during Holocene time: Geology, vol. 5, p. 141-146.

Nelson, C. H., Hopkins, D. M., and Scholl, D. W, 1974.
    Cenozoic sedimentary and tectonic history of the Bering Sea; in Hood,
    D. W., and Kelley, E. J. (ed.), Oceanography of the Bering Sea; Inst.
    Marine Sci., Univ. of Alaska, Fairbanks.

Reed, J. C., and Sater, (ed.), 1974.
    The coast and shelf of the Beaufort Sea; Arctic Institute of North
    America, 750 p.

Reimnitz, E., and Barnes, P., 1974.
in Reed and Sater (ed.), The coast and shelf of the Beaufort Sea; Arctic
Institute of North America.

Reimnitz, E., and Bruder, K. F., 1972.
River discharge into an ice-covered ocean and related sediment dispersal,
Beaufort Sea, coast of Alaska; Geol. Soc. Amer. Bull, vol. 83, p. 861-
866.

Scholl, D. W., Buffington, E. C , and Hopkins, D. M., 1968.
Geologic history of the continental margin of North America in the Bering
Sea; Marine Geology, vol. 6, p. 297-330.

Scholl, D. W., and Hopkins, D. M , 1969.
Newly discovered Cenozoic basins, Bering Sea shelf, Alaska; Amer. Assoc.
Pet. Geol. Bull., vol. 53, p. 2067-2078.

Shepard, F. P., and Wankss, H. R., 1971.
Our changing coastlines; McGraw Hill, New York, 579 p.

Smith, M. W., 1976.
Permafrost in the Mackenzie delta, Northwest Territories: Geological
Survey of Canada, Paper 75-28, 34 p.

Walker, H. J., 1973.
The nature of the seawater-freshwater interface during breakup in the
Colville River delta, Alaska; in Permafrost: the North American contribu-
tion to the Second International Conference; Nat'l Acad. Sci., p. 473-
476.

ANNUAL REPORT

Research Unit 217

LAGRANGIAN SURFACE CURRENT MEASUREMENTS
ON THE OUTER CONTINENTAL SHELF

Donald V. Hansen
NOAA/AOML
Miami, Florida

23 March 1977

ANNUAL REPORT - OCSEP

I.   Summary

The objectives of this work unit are to obtain Lagrangian current data for assessment of probable trajectories of oil spills in the Gulf of Alaska and the S.E. Bering Sea using drogued free drifting buoys located several times daily by a satellite positioning system. During the 1976 field season nine (9) buoys were deployed in the Gulf of Alaska, priamrily off Yakutat, and three (3) were deployed in the S.E. Bering Sea. These deployments were much more successful than those of 1975. Buoy lifetimes of up to eight (8) months have been achieved. Primary results from the Gulf of Alaska have been:

1.   Confirmation of the direction and speed of the westerly near surface current in the coastal area of the Northeast Gulf of Alaska.

2.   Definitive evidence for the existence of an anti-cyclonic eddy west of Kayak Island.

3.   Revelation of a strong tendency for materials introduced to the water surface over the continental shelf anywhere from Yakutat to Kayak Island to go ashore in the approaches to, or within, Prince William Sound.

4.   A suggestion from two short data series of an anti-cyclonic eddy east of Kodiak Island.

These evident inhomogeneities in the flow of the northern Gulf of Alaska make the original concept of using Lagrangian drifters to generate data for input to a statistical approach to oil spill trajectory modelling somewhat less attractive. Instead, it is the ability of the drifters to define specific spatial structure of the flow more efficiently than current meter moorings that has turned out to be of value in the Gulf of Alaska.

Primary results from the Bering Sea have been that in the quite shoal water where the deployments were made, the currents are much weaker than in the Gulf of Alaska, but confirm evidence from other kinds of data of a weak cyclonic flow in the S.E. Bering Sea. In this region the original concept of basing an oil spill trajectory model on Lagrangian statistics may be much more viable.

II. Introduction

The general objective of this work unit originally was to collect near surface Lagrangian current data for the N.E. Gulf of Alaska OCS region with particular emphasis on the lease tract area from Yakutat Bay to Prince William Sound. During the year the observational strategy was modified to obtain this type of data also from the Portlock Bank area east of Kodiak, and in the S.E. Bering Sea. The devices for acquiring this information are expendable free drifting (drogued) buoys located several times daily by the Random Access Measurement System aboard the NIMBUS-6 satellite. Two different buoy configurations have been used. A high endurance buoy using a drogue at 30 meters depth and carrying sea surface temperature, wind speed, and drogue loss sensors has been used for the challenging Gulf of Alaska environment, and a smaller, more economical buoy having a drogue at 10 meters was used in the more benign conditions of the Bering Sea in Summer.

The principal objective originally was to obtain Lagrangian statistical data on the relatively large scale coastwise current for input to advanced models. A secondary objective was to obtain sets of characteristic flow trajectories which have high visual impact and are easily understood by lay and professional people alike, and therefore are of substantial value for scenario discussion and other forms of debate on the subject of potential oil spill impacts. This philosophy seems still to be valid in the

Bering Sea, but the discovery of important inhomogeneities in the flow, such as semi-permanent eddies and persistent flow into coastal inlets, the relative importance of these has been reversed for the Gulf of Alaska. The drift buoys there have turned out to be most valuable for delineating specific spatial features of the flow more efficiently than can be done by current meter moorings or other methods. At the same time, the existence of such inhomogeneities makes the prospect of statistical modelling less attractive for the Gulf of Alaska OCS.

III.   Current State of Knowledge

The information available on circulation in the Gulf of Alaska OCS has increased dramatically during the last two years. Prior to the initiation of the project, however, no detailed Lagrangian data suitable for the needs of OCSEAP were available. Only a minor amount of new Lagrangian data were reported last year. The material presented in this report therefore comprise almost all of such information presently available.

IV.   Study Area

The area of study is the Gulf of Alaska OCS, primarily in the region of the westward flowing coastal currents. The area of interest is loosely bounded by Yakutat Bay to the east and Kodiak Island to the west in the coastal portion of the Gulf of Alaska gyre. During 1976 this work was extended to the S.E. Bering Sea, which will receive further attention during 1977.

V.   Sources, Methods, and Rationale of Data Collection

A buoy at 60°N is in view of the NIMBUS-6 satellite for about three orbits twice a day. This usually results in three to five valid positions per day. The parameter measurement is derived from count information betweeen successive orbits. The counters increment

at a rate proportional to the parameter sensed, therefore, the resultant information represents an integrated or averaged value of the parameter history between passes.

The buoy identification, time, doppler information, and count totals are relayed from the satellite receiving stations, to Goddard Spaceflight Center where the position and count data for the system user are determined. The user then converts the data into time series of position and parameters for further analysis.

As a general statement, the currents along the OCS Gulf of Alaska region are to the west, therefore, the buoy deployment area is at the eastern limits of the area. Deployments have been made in groups of three (3) buoys to provide a measure of statistical significance and cross shelf structure.

VI. Results

Design modifications effected following the disappointing experience of 1975 proved quite successful, at least for Summer conditions in the Gulf of Alaska. Of nine (9) buoys deployed in the Gulf of Alaska during 1976, five (5) were terminated by going ashore, in some cases continuing to transmit for up to six (6) months after stranding, and four (4) suffered electronic failure at sea. Three (3) of the buoys deployed in the Gulf of Alaska have been recovered and all three (3) of the buoys deployed in the S.E. Bering Sea were returned by fishermen. These returns and recoveries are quite valuable for interpretation of the trajectories and engineering analysis of the hardware.

Gulf of Alaska

Buoys 1105, 1133, and 1174 were deployed off Yakutat in May and June 1976. Buoys 1105 and 1133 initially moved south for 15-20 miles at which time 1105 stopped reporting, and 1133 reverted

to the westward movement indicated by the conventional wisdom for this region. Notable features of the trajectory of 1133 are (1) its movement crosses isobaths quite dramatically, suggesting that topographic control may not be a strong constraint for surface flows in this area and (2) the trajectory terminates on Middleton Island, extraordinarily bad luck from the point of view of the principal investigator, but probably indicative of expected behavior of surface pollutants. The eastward movement of buoy 1133 just prior to stranding on Middleton Island may be indicative of a quasi-permanent flow to the east in this area (Royer, personal communication). Buoy 1133 evidently fouled in a kelp bed or otherwise hung up offshore and continued transmitting for several days. This stationary position sequence suggests (our only assurance at present) that the drogue assembly remained attached to the buoy until the end. It also provided a special data base by which to evaluate accuracy of the locating system, and on the basis of which an objective data editing and filtering system has been designed. The location precision in this area turns out to be very close to NASA design specification (4 km r.m.s.).

The trajectory of buoy 1174 turned out to be especially interesting. Subsequent to a drift similar to those obtained in September 1975 as far as Cape Suckling, it closely skirted the east shore of Kayak Island, evidently to become trapped in an anticyclonic (clockwise) eddy just west of Kayak Island, and ultimately to beach on Montague Island. This particular occurrence provides some very strong evidence of the existence of an eddy west of Kayak, and has considerable relevance to lease activity in the area. It was thought remarkable that this buoy, deployed some 250 miles to the east, entered the eddy.

Boys 1142, 1203, and 1235, deployed off Yakutat in July exhibited quite surprising behavior. All of them initially followed the previously established general pattern of flow to the west and north. Buoys 1142 and 1235, deployed very close together, followed very similar paths for about 10 days before diverging into separate current structures. After having been dispersed from each other by distances exceeding 300 km at times, all three of these buoys subsequently became entrained in the anticyclonic eddy west of Kayak Island, as had buoy 1174 some two months earlier, and all three passed through the Hinchinbrook entrance to Prince William Sound. Ultimately all three were grounded in diverse interior waters of Prince William Sound, from which they continued transmission for several months. Buoys 1142 and 1235 were visually inspected by an aircraft commissioned by the Project Office in Juneau, and arrangements were made for Mr. Michael McCurdy of the Alaska Fish and Game Office in Cordova to attempt recovery of these buoys on his March cruise. On 21 March, Mr. McCurdy advised that he had successfully recovered buoys 1142 and 1235, and that he understood that buoy 1203 had been picked up by a fishing vessel and was being delivered to the USCG. Mr. McCurdy also reported that the buoys he recovered were still in generally good shape, and still had the drogue systems attached. One complete system was recovered, but the other drogue had to be cut off for consideration of safety in heavy weather. These recoveries and knowledge that the drogues were still attached are most valuable for interpretation of the data. It is now quite clear that movement of the buoys into Prince William Sound and subsequently was controlled by circulation rather than by high windage on an undrogued buoy. This result suggests the need for some special investigation of the water exchange between Prince William Sound and the adjacent continental shelf. Several possible explanations for the flow into

Prince William Sound come to mind, among which may be mentioned a barotropic flow into Hinchinbrook entrance and out of Montague Strait, a baroclinic exchange typical of estuaries, or "streaming" motion forced by Reynolds stresses associated with tidal currents. Each of these processes has different implications for transport of surface contaminants and each probably occurs to some extent. Further investigation of the vertical structure of the flow is required to evaluate the hazards.

Buoys 1473, 1540, and 1576, were deployed east of Kodiak Island, across the Portlock Bank out to the Alaska Stream in October. After a week, transmission from buoys 1473 and 1540 abruptly ceased, and three days later 1576 ceased as well. Some six and one-half weeks later 1540 transmitted for a few days intermittently from close off the southwest corner of Kodiak Island. It is believed that the transmission terminated due to a generic electronic failure. Results from an investigation of possible causes of this malfunction have been provided to the Project Office in Juneau. During their operational period, buoys 1540 and 1576 suggested the presence of a cyclonic eddy over Portlock Bank, and a meandering southwestward flow in the Alaska Stream. The path followed by buoy 1540 around Kodiak Island can only be speculated on. It is planned to repeat deployments in this region during 1977.

S.E. Bering Sea

The three buoys (503, 535, and 544) deployed in the S.E. Bering Sea during the Spring of 1976 were a lower cost design intended for less severe weather than must be expected in the Gulf of Alaska. These buoys reported their position only. They were drogued to the 10 meter depth in view of the relatively shoal water of the S.E. Bering Sea. This buoy design was so new that no drogue loss sensor was available in time to meet the deployment schedule (one of the

vicissitudes of using state of the art methods). As it turned out, all three of these buoys were recovered and returned by fishing vessels, and all had lost their drogues. There are therefore some remaining problems of interpretation of these data. The data collected over the first three months or so of the deployment indicate a weak but spatially coherent cyclonic circulation in S.E. Bering Sea, in agreement with other observations, but with a quite high level of temporal variability superimposed. The currents here are so weak as to make their detection quite difficult because of the position error of the satellite system. A Lagrangian statistical approach to oil spill impact modelling presently looks more attractive for this region than for the Gulf of Alaska. Present plans are for deployment of six (6) improved buoys in the S.E. Bering Sea during the Spring/Summer of 1977.

VII/VIII   Discussion/Conclusions

The results described above and illustrated in the accompanying illustrations and their implications for the NEGOA lease tracts require little discussion. At least during Summer conditions, materials released on the surface between Yakutat and Kayak Island will move generally westward at typical speeds of 10 miles/day or less. There is a pronounced tendency for movement inshore across the shelf, rather like the seasonal transport of pelagic organisms across the shelf in Spring, and for involvement of surface materials in an eddy west of Kayak Island, off the Copper River. The high percentage of buoys that have gone ashore on the approaches to or inside of Prince William Sound suggest these as likely impingement points for oil spilled on the surface over any part of the OCS as far away as Yakutat. Oil from the more distant points is likely to be well weathered before reaching the Prince William Sound area of course.

The systematic grounding of drifters east of or within Prince William Sound, while providing exactly the kind of information required by OCSEAP, has two negative aspects. First, it has limited the region of data coverage to less of the Gulf of Alaska OCS than was originally expected. Second, the original concept of a Lagrangian statistical model for oil spill impact evaluation is now less attractive. In effect, the contribution of Lagrangian data to OCSEAP needs in the Gulf of Alaska is more site specific than was envisaged.

The first of these negative aspects will be partially ameliorated by deployments in new areas (Portlock Bank) during the present funding period. Additional deployments in critical areas will satisfy the greater need. The second negative aspect should not really be seen as negative at all, but simply the natural result of obtaining a clearer understanding of the important processes and regions. It simply must be accepted that there are important inhomogeneities in the Gulf of Alaska OCS environment. It is believed that the most important of these east of Montague Island have been identified; future efforts should be directed to other areas of importance. One such area is Portlock Bank, for which further work is planned this year. Others will doubtless be identified.

The limited results obtained from the S.E. Bering Sea to date have served primarily to help define sampling strategy to be used there in 1977. Deployment of six (6) drifters is planned along the eastern margin of the St. George Basin. The flows are expected to be stronger in this region than farther east, and fishing activity has proved hazardous to current meter moorings. Data collected during 1976 will be related to current meter mooring data, and the Lagrangian dispersion concept will be investigated for applicability

in this region, but the weak currents in this area relative to
the accuracy of the locating systems, and the lack of precise
knowledge of time of drogue loss are impediments to a high quality
result.

Nearly all of the important results for the NEGOA region
were obtained prior to and were provided for use of the January
Synthesis Workshop.

IX.   Needs for Further Study

Three needs for further study, two specific and one general,
emerge from the results to date. First, the movement of drifters
into Prince William Sound raises a clear need for further investi-
gators of the nature of the water exchange between Prince William
Sound and the adjacent OCS. Such an investigation is probably
best done by means of moored current meters on other methodology
rather than by drifting buoys of the type used in this work unit.
A second specific need identified is for further investigation of
the existence of a quasi permanent eddy over Portlock Bank. Some
further information on this should be obtained this year, but it
must be expected that there will be some residual unanswered
questions or ambiguity. More generally, needs for further investi-
gation especially to the north and west of Kodiak Island must be
anticipated, for which drift buoys are appropriate and efficient.

X.   Summary of Fourth Quarter Operations

In spite of delay in receipt of project funds for procurement
of buoy hardware we expect to be able to meet achedules for deploy-
ment of six (6) drift buoys in the Bering Sea during the Spring of
1977. All purchase orders are out, and the timing is uncomfortably
close, but with luck we should be able to participate in the Bering
Sea cruise of Miller Freeman in May. Mr. David Pashinski has
extensive experience in this hardware and its deployment, and as

Chief Scientist for the cruise will be in charge of the deployments. The buoys to be used are of the same design (three (3) are the same refurbished hulls) as used in the Bering Sea last year, but modified for more secure drogue attachment and to include a drogue loss sensor. Present strategy is for concurrent deployment of six (6) buoys in the St. George Basin area. Buoy power is sufficient to maintain operations until the ice returns to the operating area.

Analysis will continue, primarily on data collected in the Bering Sea during 1976.

ILLUSTRATIONS

The following   figures show trajectories
of buoys deployed at the indicated times. Three
(3) digit numbers along the trajectories indicate
the Julian Day that the buoy was located at that
position.

DEPLOYED IN THE GULF OF ALASKA IN SEPT. 1975
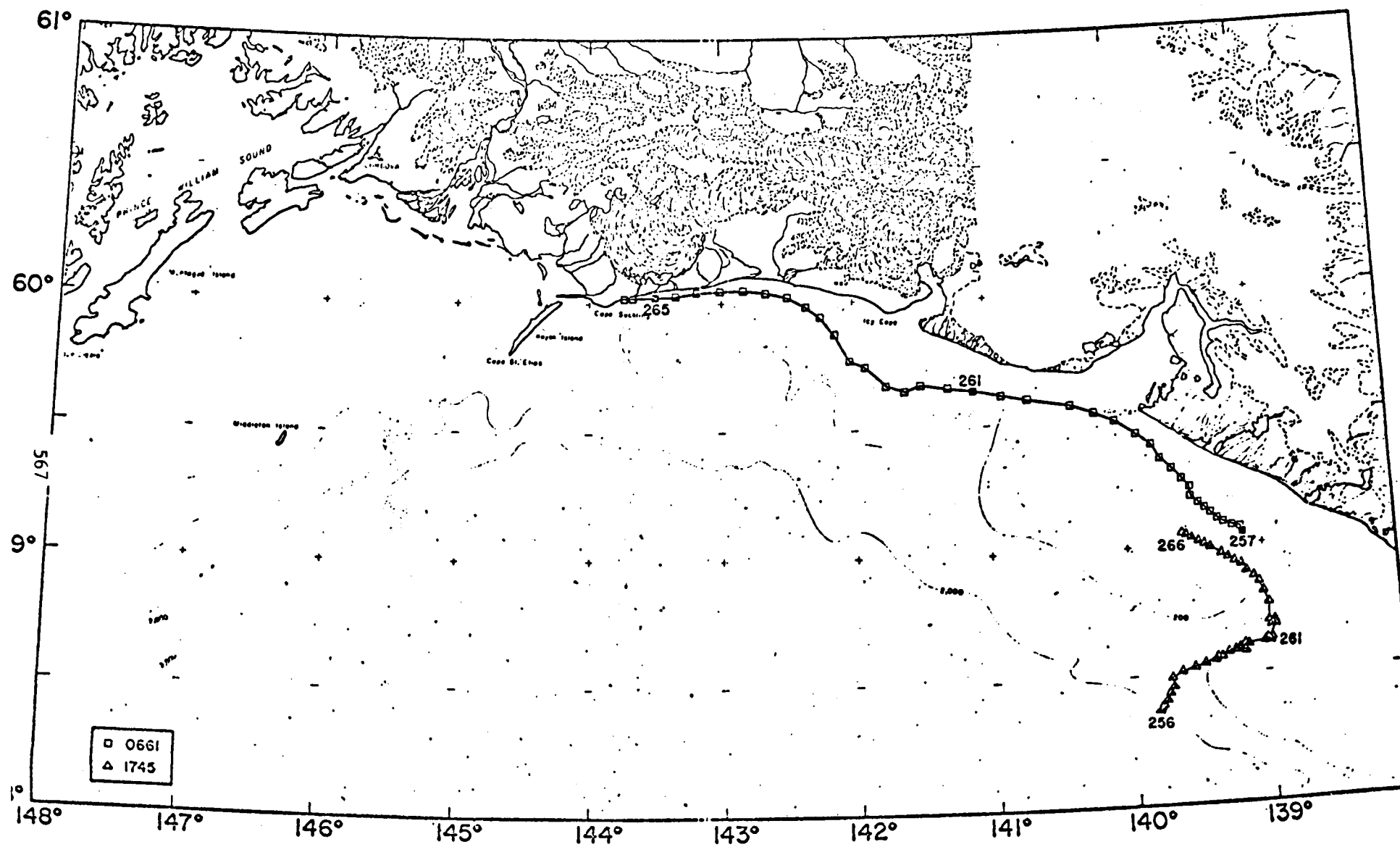
Figure 1.

DEPLOYED IN THE GULF OF ALASKA IN MAY-JUNE, 1976
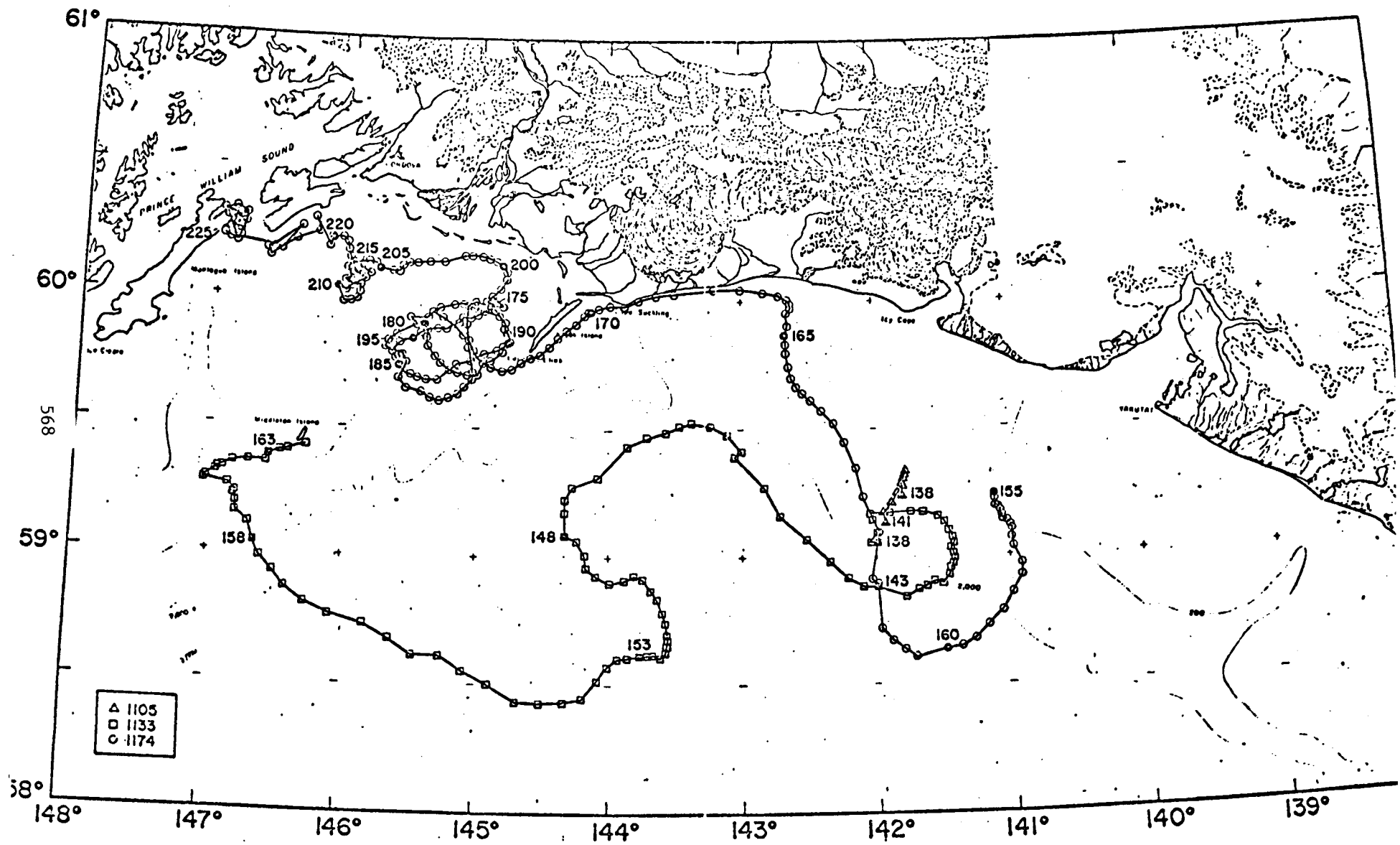
Figure 2.

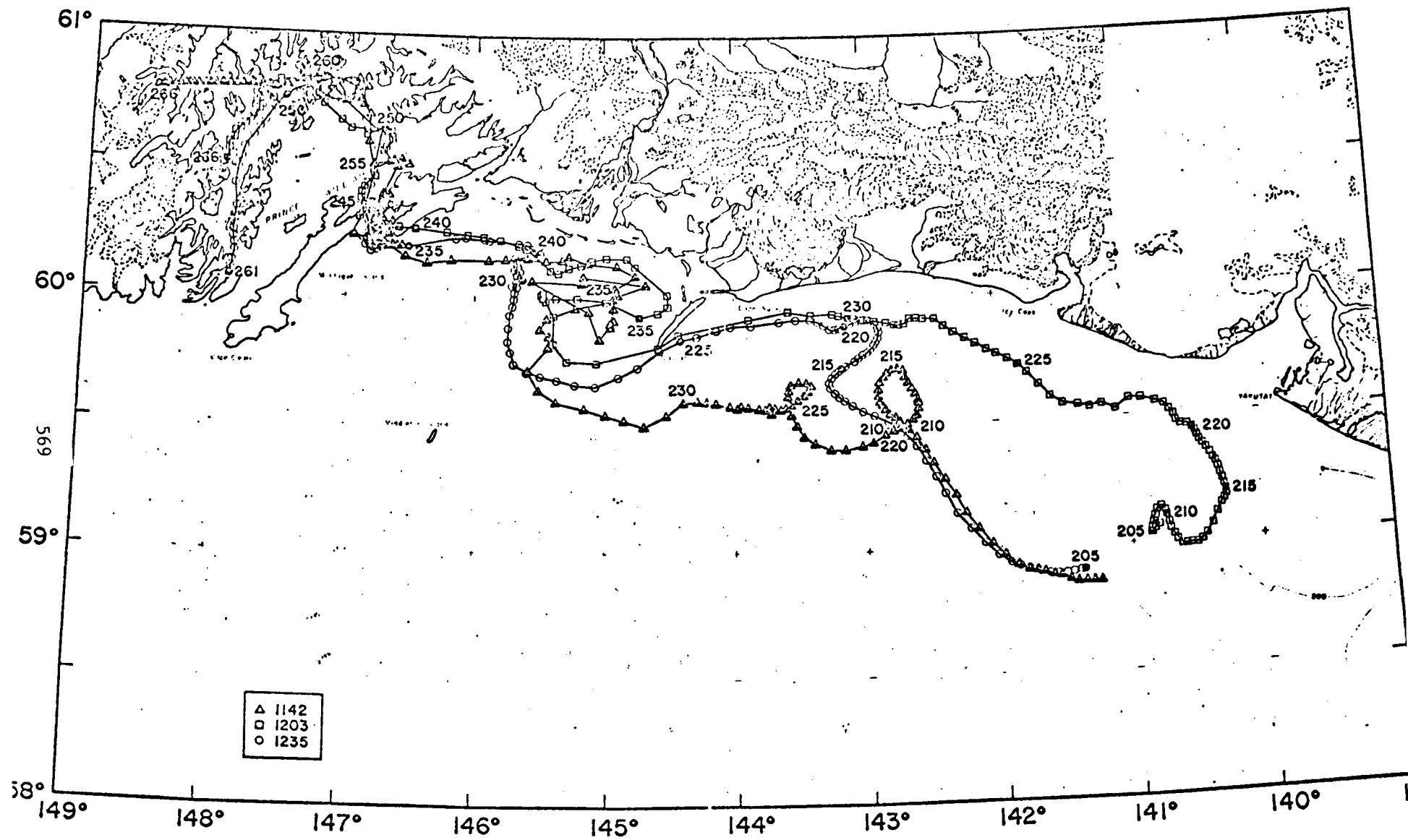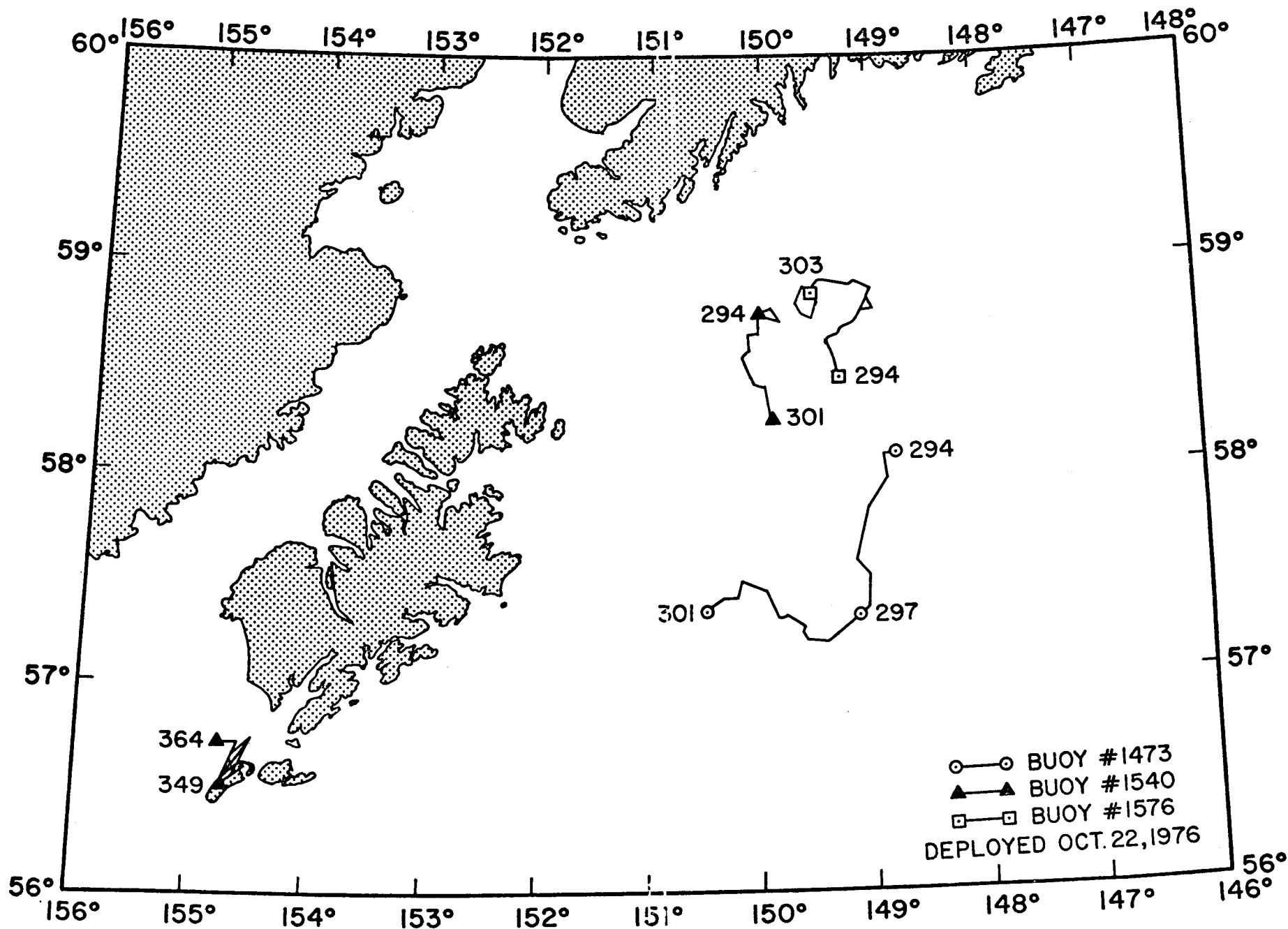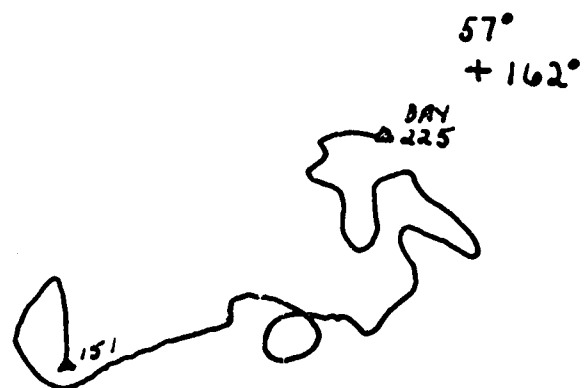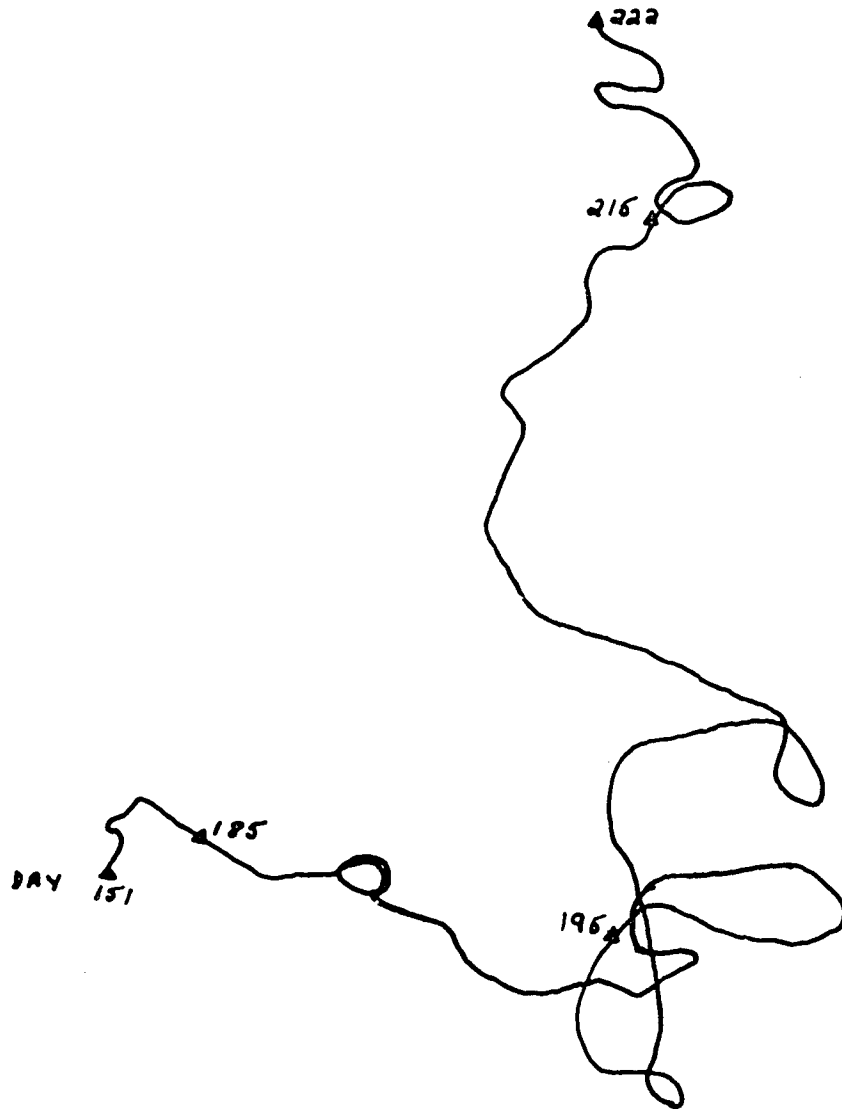DEPLOYED IN THE GULF OF ALASKA IN JULY 1976

Figure 3.

Figure 4.

57°
+ 162°

BAY
225

151

571

56°
+ 163°

Figure 5.

58°
+161°

222

216
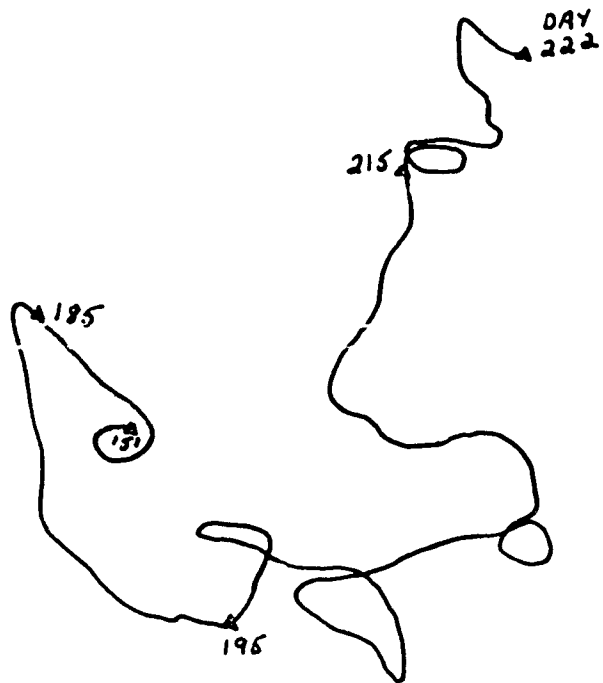
185

DAY 151

195

56°
+163°

Buoy I.D. 0535

Figure 6.

58°
+162°

DAY
222

215

185

151

196

56°
+164°

Figure 7.

Buoy I.D. O544

ANNUAL REPORT

Contract #03-5-022-91

Research Unit #244

Reporting period: 1 April 1976 –
31 March 1977

Number of Pages: 35 pages plus
Appendices

STUDY OF CLIMATIC EFFECTS ON FAST ICE EXTENT

AND ITS SEASONAL DECAY ALONG THE

BEAUFORT-CHUKCHI COASTS

Principal Investigator

R. G. Barry

Acting Director, Professor of Geography

Institute of Arctic and Alpine Research

University of Colorado

Boulder, Colorado 80309

31 March 1977

I. SUMMARY

The objectives of this project are (1) to delimit the extent of fast ice along the Beaufort and Chukchi coasts prior to and during the decay season; (2) to define and characterize the nature of the summer decay of fast-ice from remote sensing data; (3) to determine climatic processes and meteorological synoptic events contributing to the spatial and temporal characteristics of fast-ice breakup and to examine their amenability to predictive assessment.

The most significant hazard to petroleum development along the Beaufort Sea coast is posed by the occurrence of sea ice.

Major findings that can be identified as reasonably firm are as follows:

(1) Summer temperature conditions account for 65 percent of the variance in the distance off Pt. Barrow to the 4/8 concentration limit of pack ice on September 15. If wind speed and pressure data are included, 80 percent of the variance is accounted for.

(2) An accumulation of 250-400 thawing degree (F) days is required to remove the fast-ice and 400-550 TDDs for open water to extend up to 80 km off Pt. Barrow on September 15.

(3) Climatic data at Barrow show that the number of summers in which >400 TDDs were attained has declined from 88 percent for 1921-52 to 52 percent for 1953-75. In climatic terms, the 1975 summer was not a rare event.

(4) Synoptic types associated with southerly geostrophic winds and positive temperature departures predominate in mid-summer. The shift to these patterns appears to be a major determinant of ice breakup.

Preliminary results of direct significance to oil and gas developments include:

(1) A "calendar" of the fast-ice regime on the Beaufort Sea coast which provides a tentative framework for seasonal scheduling of operations in the nearshore zone.

(2) Hazards to petroleum development are identified within the fast-ice zone. These include: the occurrence of grounded ice masses within the 20m isobath, as a result of winter extension of the fast-ice edge; shear and pressure ridge features exerting significant forces on structures or bottom gouging will tend to occur further seaward in late winter; grounded ice ridges are discontinuous along the coast and therefore may not contain under-ice oil spills located within the fast-ice zone. The period of stable fast-ice inside about the 15m isobath extends approximately from February to early May.

II. INTRODUCTION

A. General Nature of the Study

Nearshore ice along Alaska's Beaufort Sea and Chukchi Sea coasts undergoes an annual cycle of formation, extension, modification, ablation and breakup. Many of the processes which contribute to this cycle are poorly understood or unknown, although it is generally recognized that meteorological and climatological factors are important influences for ice formation, motion, deformation, ablation and breakup. This study is attempting to interpret ice characteristics and their time variations from remote sensing data supplemented by aircraft and field observations. This derived information covering both the Beaufort and Chukchi coasts is then compared with concurrent coastal weather conditions and regional atmospheric pressure patterns. It is hoped that a systematic set of weather-ice relationships can be derived from the analysis.

B. Specific objectives

(1) Map ice characteristics and behaviour during the decay season from available remote sensing data for 1973-76.

(2) Generalize the results of (1) and individual case-studies in order to establish the recurrent and variable properties of the fast-ice prior to and during the decay season.

(3) Investigate surface weather data from the coastal stations and synoptic-scale atmospheric pressure patterns over the region to determine relationships between important ice-related weather "events" and the atmospheric circulation.

(4) Examine the possibilities for predictive assessments of climatic factors influencing fast-ice decay.

C. Relevance to Problems of Petroleum Development

Offshore petroleum development may involve temporary operations on the winter fast-ice surface or in the open waters during summer. Alternatively, large, ice-resistant structures may be used year-round (see: Clarke, 1976). An accurate assessment of the best operational modes and of the seasonal distribution of ice hazards requires that the normal patterns and variabilities of fast-ice characteristics and breakup processes be specified. Also, the pathways of pollutants deriving from oil spills or blow-outs are dependent to some degree on the season, and, in summer, on the relative progression of the breakup. It also seems significant that various faunal populations utilize the coastal environment, above and below the ice and in the open water areas. Seasonal and interannual variations in the weather and ice characteristics are important factors affecting the distribution and movements of these populations. These questions are elaborated in the report of the Beaufort Sea Synthesis Meeting (Feb. 1977).

III. CURRENT STATE OF KNOWLEDGE

The general characteristics of fast ice have been known for some time (e.g. Zubov, 1943), while more recent review of conditions in the Beaufort Sea fast-ice zone are given by Kovacs and Mellor (1974) and Reimnitz et al. (1976). The regional-scale dynamics of the fast-ice zone could not be effectively studied in detail until the launch of LANDSAT (formerly ERTS) in 1972. A good deal of literature has emerged since that time treating the information content of LANDSAT imagery of sea ice, but the OCSEAP Project represents the first systematic applied study of the regional scale surface morphology, composition and dynamics of fast-ice along the Beaufort and Chukchi Sea coasts.

Weather and climate have been studied by a number of authors (see, e.g., Watson, 1968; Selkregg, 1974; Holmgren and Weller, 1974) for the Alaska region, and the Arctic atmospheric circulation has likewise been treated (e.g. Keegan, 1958; Reed and Kunkel, 1960; Wilson, 1967; Hare, 1968; Weller and Bowling, 1974). However, the relationships between ice decay processes and weather variations has hitherto received little attention, especially on the detailed scale required for BLM planning.

IV. STUDY AREA

The fast ice zone along the Beaufort and Chukchi Sea coasts between Demarcation Point and the Bering Strait represents the study area for this project. The seaward extent is variable according to season and location.

V. DATA

A. Remote Sensing

Regional scale mapping of the ice characteristics and behaviour for 1973-76 has been carried out from LANDSAT imagery. Details of frames interpreted are given in the Quarterly Reports. Interpretation of categories of age, deformation, puddling of the ice, etc., is made with the aid of other remote sensing products (particularly aircraft SLAR and CIR) as well as reconnaissance observations and hand-held photography of the ice from aircraft. An analysis of digital radiance data for a particular melt-season LANDSAT scene was carried out under subcontract with the Laboratory for Applications of Remote Sensing, Purdue University (see Appendix 1), in order to determine the spectral information content of the LANDSAT data in summer.

B. Meteorological Data

The sources of data for the studies included here have been:

(1) National Weather Service station meteorological data for Barrow and Barter Island for 1953-75 and 1958-75 respectively. These data were published as local climatological data. Data used were temperature (sometimes converted into thawing degree days), wind speed and direction, barometric pressure, cloud cover. Synoptic weather data for Lonely, Oliktok, and Deadhorse were also used for case-study analyses.

(2) Geostrophic winds at sea level were calculated along the Beaufort and Chukchi coasts from the NMC grid-point pressure data.

(3) Regional patterns of atmospheric pressure and circulation have been classified for the Beaufort Sea area (Annual Rept., March 31, 1976, Appendix 4) and the Chukchi Sea area (Quarterly Rept. 03-6-022-35179, Sept. 30, 1976) on a daily basis for 1946-74 using NMC grid-point pressure data for 1200 GMT.

C. Climate-Ice Interaction Case Studies

These studies utilised the above data sources and also tabulations of the retreat of fast-ice and pack ice off Barrow on September 15 of each year since 1953 (Barnett, 1976). Each summer is ranked according to its ice severity.

The research strategy has focussed on identifying links between climatological parameters, synoptic patterns of atmospheric circulation and processes of ice decay in the near-shore zone. This has also necessitated the determination of the initial state of ice conditions in spring.

The analytical methods used in the case studies involved the characterization of particular ice events identified on LANDSAT imagery in terms of preceding and concurrent meteorological conditions. Indices employed in the analysis included cumulative thawing degree-days (sums of positive departures of daily average temperature above 32°F).

VI. RESULTS

A. Remote Sensing Interpretation and Mapping

Considerable progress has been made in the area of developing interpretive keys and methods for ice analysis using remote sensing data. The results of the LARSYS experiment show that the spectral information-content of melt-season LANDSAT data is limited mainly to the distribution and depth of surface melt pools on the ice (see Appendix 1). Correlative analysis of LANDSAT images, SLAR imagery, and CIR photography, supplemented by field observations, shows that the following ice features can be located and identified:

(1) Large fields of level, hummocked, and ridged ice.

(2) Differentiation of ice into 1st-year and older age categories, if the older ice inclusions are vast-floe (2-10km) size or greater.

(3) Ice puddling characteristics: the integrated effects of puddle depths and percent areal coverage.

(4) Large, well-grounded ice features in the fast-ice.

(5) Ice concentration vs. open water.

(6) Time changes in the ice (motions, puddling increases, drainage, breakup). It should be noted, however, that SLAR imagery and CIR photography are not available for all of the period (e.g. 1973) and that the LANDSAT coverage may be rendered useless by cloud cover.

The early summer limit of fast ice along the Beaufort Sea coast
for 1973-75 and the Chukchi Sea coast for 1973-76 (Stringer RU #257) is
mapped in Figs. 7 and 8 of the Sea Ice report prepared by R. G. Barry
for the Beaufort Sea Synthesis Meeting. These maps are being drafted
currently at the Arctic Project Office. The scale of LANDSAT imagery
does not allow differentiation of the narrow zone of bottom fast-ice
to about the 2m isobath.

The dates of significant ice decay events have been taken from
LANDSAT images for 1973-76 (Table 1). It should be stressed that these
phenomena are large-scale ($\geq$ 10 km^2) because of the satellite resolution.
Motions can occur on various scales in the "fast" ice during winter,
for example, but these motions are too small for LANDSAT to resolve.
These dates can be viewed as climatological averages, with a probable
variability (between years) of $\pm$ 10 days. The $\geq$ 14-day data gaps
caused by the LANDSAT orbit do not permit better time resolution.

Detailed ice-mapping analyses are still in progress, but relevant
preliminary conclusions can be stated at this point. The spring
flooding of estuarine ice areas is most prominent along a short section
of the coast including the Colville, Kuparuk and Sagavanirktok Rivers
(Fig. 1). Other rivers showing some evidence of this phenomenon on
LANDSAT imagery include the Canning, Sadlerochit, Hulahula, Jago and
Aichikik Rivers. Around mid-to-late June, the areas previously flooded
by these rivers begin to develop shore-polynyas which spread laterally
and seaward through mid-July. The largest of these (Colville) appears
to allow an avenue of motion for shoreward-moving ice when breakup
starts. Although the Meade, Chipp and Alaktok Rivers do not exhibit
large-scale flooding over the ice in May, they appear to enhance the
ice melt in Dease Inlet and Smith Bay through the creation of shore
polynyas in late June (Fig. 2).

Surface meltwater on the ice shows considerable variations, both
spatially in a given year and interannually at a given site. First-year
ice with relatively light deformation appears to pond the most melt-
water. These areas often drain in late June or early July. Nevertheless,
they are usually the first areas to melt through completely and break up.
When older ice floes are incorporated into the fast-ice, they tend to
persist late into the melt season. After the interstitial matrix of
first-year ice has melted, however, these floes become mobile.

Large, grounded ice masses can be found in the fast-ice in any
given year. Depending on the depth at which they became grounded, they
may or may not represent the seaward edge of fast ice. It is certain,
however, that well-grounded ice masses do not form a continuous,
shore-parallel strip along the coast (Fig. 3), but are separated by ice
which is either poorly-grounded or floating. The elevated ice deformation
features which comprise the groundings persist later into the melt
season than any other component of the fast-ice. In at least one year
(1975), several of these large, grounded masses survived the summer and
could be seen in the spring-summer fast-ice of 1976. When these

TABLE 1. AVERAGE DATES OF SIGNIFICANT STAGES IN SEASONAL FAST-ICE
REGIME ALONG THE BEAUFORT SEA COAST, 1973-76

Event	Average date
Rivers flooding onto nearshore ice	25 May
First appearance of ice-surface melt pools	10 June
First openings in previously-continous ice	29 June
End of stable ice period	7 July
Coastal zone largely ice-free within 10 m isobath limit	31 July
New ice formation	3 October
First continuous ice in fall	15 October

deformation features finally break up and begin to move, they often appear much brighter on the imagery than any surrounding summer pack ice, indicative of a raised surface. By implication, then, their keels, although not sufficiently deep to remain grounded, must still possess the potential for gouging and scouring if these pieces move onshore.

In 1972, 1973 and 1974 a coastwise parallel strip of open water and loose pack ice was present in August along most of the coast (Fig. 4). In 1975, the fast-ice melt was retarded by extremely low summer temperatures, and the polar pack ice was held close to shore. This was also the year, however, of several extensive, grounded ridge fields in the eastern part of outer Harrison Bay to Cross Island. LANDSAT imagery from August and September, 1975, indicates that these ice structures may have shielded the inner shelf from even more pack ice impingment than was observed. November, 1975, LANDSAT imagery indicates that the presence of these ice structures stabilized the incipient fast-ice sheet at a very early date. The systematic mapping of ice conditions from each summer's set of LANDSAT scenes is continuing. These maps form the documentation for the type of interpretations made above.

One particularly important case study in progress relates to the large grounded ridge fields off Oliktok in 1975-76. Initial analyses (see Quarterly Report, December 31, 1976) indicated that this feature was formed between March 25, 1975, and April 20, based on LANDSAT imagery. Subsequent analysis of NOAA satellite imagery shows that the feature was already in place by April 11 (see Figs. 5a). The severe winds accompanying the April 15 low pressure system in the Beaufort Sea were thus not responsible for the formation of this feature. The problem is further complicated because the AIDJEX detailed pressure and wind-stress fields are only available after April 10, so it seems quite likely that they "just missed" the formation of the ridges. At Barrow and Barter Island, seasonally-anomalous westerly winds were observed during two intervals between the formation dates, but the strongest winds in the period were from the (normal) easterly to northeasterly directions. This analysis is continuing, but the phenomenon appears to be more complex than was initially thought.

Analysis is presently underway of data gathered during field reconnaissance along the Beaufort and Chukchi coasts in 1976. A very good set of LANDSAT data have been received for the period, and the OCS SLAR appears to add much to the interpretive capability.

B. Synoptic Climatology

1. Beaufort Sea

A statistical clustering and classification algorithm has been applied to the NMC pressure grid data for a sector centered on the Beaufort Sea coast (58°-80°N, 125°-170°W). The results include a set of 21 characteristic pressure patterns which recur over the region through time. Each daily pressure grid for the 29-year period 1946-74

Table 2. Prevailing Wind Directions Associated with the Major Synoptic Types.

Type	Total Days	Determined Prevailing Direction (tens of degrees)	# of Days with Prevailing Direction	Prevailing Direction Alphabetic
Type 1	94	05 to 10	72	NE
Type 2	102	20 to 28	50	SW
Type 4	52	08 to 13	30	E-ESE
Type 5	47	23 to 31	36	W
Type 6	24	02 to 13	18	NE
Type 8	57	35 to 07	26	NNE
Type 9	5	08 to 13	4	ESE
Type 11	11	08 to 10	7	E
Type 14	23	08 to 10,26 to 28	6 & 5	Mixed
Type 16	13	08 to 10	9	E
Type 15	28	08 to 13,23 to 28	20	Mixed

Table 3. Wind Speeds Associated with Major Synoptic Types. (m.p.h.)

	June	July	August
TYPE 1	$\bar{v}$ = 14.75	15.34	12.69
	SD = 4.26	.5.09	5.09
	N = 47	22	25
TYPE 2	$\bar{v}$ = 9.07	11.90	10.70
	SD = 2.34	3.13	3.59
	N = 15	51	31
TYPE 4	$\bar{v}$ = 10.38	11.96	11.58
	SD = 4.00	5.61	3.01
	N = 13	10	25
TYPE 5	$\bar{v}$ = 11.32	10.79	9.63
	SD = 2.84	3.14	3.26
	N = 13	23	15
TYPE 6	$\bar{v}$ = 11.86	10.56	10.54
	SD = 2.98	3.13	3.25
	N = 5	10	12
TYPE 8	$\bar{v}$ = 9.57	10.75	11.05
	SD = 2.63	2.25	4.97
	N = 23	20	20

TABLE 4. PERSISTENCE OF CHUKCHI TYPES, FREQUENCY VS DURATION OF SPELLS

DAYS	TYPE 1	2	3	4	5	6	7	8	9	10	11	12	13	14	15	16	17	18	19	20	21	22	NT	MD
1	359	345	196	277	196	178	130	167	174	176	214	171	195	170	148	102	151	38	65	53	77	74	321	44
2	180	167	79	149	65	37	22	43	68	40	68	39	53	22	25	26	37	6	15	2	4	5	40	3
3	120	61	28	43	8	8	7	7	18	10	6	16	18	3	6	3	8	0	2	0	5	2	6	0
4	63	27	9	33	5	3	0	1	6	3	5	2	2	3	1	0	0	0	1	0	1	2	2	0
5	49	11	6	12	1	2	0	0	2	0	1	3	0	0	0	0	0	0	0	0	0	0	0	0
6	34	5	4	10	1	0	0	0	0	1	0	0	1	0	0	0	0	0	0	0	0	0	0	0
7	25	2	0	5	0	0	0	0	0	0	0	0	0	0	0	0	0	0	0	0	0	0	0	1
8	23	0	0	1	0	0	0	0	0	0	0	0	0	0	0	0	0	0	0	0	0	0	0	1
9	16	1	1	0	0	0	0	0	0	0	0	0	0	0	0	0	0	0	0	0	0	0	0	0
10	15	1	0	0	0	0	0	0	0	0	0	0	0	0	0	0	0	0	0	0	0	0	0	0
11	9	1	0	0	0	0	0	0	0	0	0	0	0	0	0	0	0	0	0	0	0	0	0	0
12	9	0	0	0	0	0	0	0	0	0	0	0	0	0	0	0	0	0	0	0	0	0	0	0
13	4	0	0	0	0	0	0	0	0	0	0	0	0	0	0	0	0	0	0	0	0	0	0	0
14	5	0	0	0	0	0	0	0	0	0	0	0	0	0	0	0	0	0	0	0	0	0	0	0
15	4	0	0	0	0	0	0	0	0	0	0	0	0	0	0	0	0	0	0	0	0	0	0	0
16	4	0	0	0	0	0	0	0	0	0	0	0	0	0	0	0	0	0	0	0	0	0	0	0
17	2	0	0	0	0	0	0	0	0	0	0	0	0	0	0	0	0	0	0	0	0	0	0	0
18	3	0	0	0	0	0	0	0	0	0	0	0	0	0	0	0	0	0	0	0	0	0	0	0
19	0	0	0	0	0	0	0	0	0	0	0	0	0	0	0	0	0	0	0	0	0	0	0	0
20	1	0	0	0	0	0	0	0	0	0	0	0	0	0	0	0	0	0	0	0	0	0	0	0
21	2	0	0	0	0	0	0	0	0	0	0	0	0	0	0	0	0	0	0	0	0	0	0	0
22	4	0	0	0	0	0	0	0	0	0	0	0	0	0	0	0	0	0	0	0	0	0	0	0
23	1	0	0	0	0	0	0	0	0	0	0	0	0	0	0	0	0	0	0	0	0	0	0	0
24	2	0	0	0	0	0	0	0	0	0	0	0	0	0	0	0	0	0	0	0	0	0	0	0
25	0	0	0	0	0	0	0	0	0	0	0	0	0	0	0	0	0	0	0	0	0	0	0	0
26	1	0	0	0	0	0	0	0	0	0	0	0	0	0	0	0	0	0	0	0	0	0	0	0
27	1	0	0	0	0	0	0	0	0	0	0	0	0	0	0	0	0	0	0	0	0	0	0	0
28	0	0	0	0	0	0	0	0	0	0	0	0	0	0	0	0	0	0	0	0	0	0	0	0
29	0	0	0	0	0	0	0	0	0	0	0	0	0	0	0	0	0	0	0	0	0	0	0	0
30	0	0	0	0	0	0	0	0	0	0	0	0	0	0	0	0	0	0	0	0	0	0	0	0
MEAN	3.5	1.8	1.7	1.9	1.4	1.3	1.2	1.3	1.5	1.3	1.3	1.4	1.4	1.2	1.2	1.2	1.3	1.1	1.3	1.0	1.2	1.2	1.2	1.3

584

10

has been classified with one or another of these characteristic
patterns based on a minimum sum of squared differences between
normalized grid-point pressures for the map pairs. Types 1-7 are
illustrated in Fig 6. The resulting synoptic catalog shows that
pressure patterns with lows to the SW, S and SE of Alaska and highs
or ridges over the Beaufort Sea are predominant from September to
May (Fig. 7). During the summer, patterns with high pressure to the
S and SE of Alaska are common, and low pressure systems are much more
frequent over central Alaska, in the Chukchi sea and along the
Beaufort Sea.

Analysis is continuing on the weather characteristics of these
patterns, but initial results show that many of the patterns possess
distinctive wind and temperature departures from average. Tables 2
and 3 summarize the average direction and wind speed characteristics
of the most frequent summer types at Barrow. These tables are based
on data for June 1964, 1965, 1966, 1971, 1973, 1974; July 1963, 1968,
1969, 1971, 1972, 1973, 1974; August 1962, 1968, 1969, 1971, 1973 and
1974. Detailed analysis of temperature departures associated with each
type are almost complete.

Case-study analyses show that some interannual variations in ice-
breakup conditions can be related to variations in the frequency of
these synoptic pressure patterns. The catalog of daily pressure patterns
and related statistics has been forwarded in magnetic tape format to
the OCS Data Manager's office in Juneau, and could be used by other
investigators interested in medium-range fluctuations of climate or
climate-related variables. The catalog affords a means of studying
fast-ice variations for earlier periods, for which no LANDSAT data
are available, when statistical ice-weather relationships has been
established and tested.

2. Chukchi Sea

A separate daily synoptic catalog for 1946-74 has been developed
for a rectangular sector centered on the Chukchi Sea coast (ca. 57°-
77°N, ca. 150°W-165°E) since the circulation patterns affecting the
two coasts appear to be sufficiently different so as to require
independent schemes. Maps of the key days of the 22 synoptic types
are included in Quarterly Report #03-5-022-91, December 31, 1976.
The four most frequent types are shown in Fig. 8 a-d. Types 1 and
4 have pronounced winter maxima of frequency whereas type 2 and
especially 3 occur more often in summer (Fig. 9).

These type frequencies and matrices of their transition frequencies
have been used to define synoptic circulation seasons. Indices, based
on between-month differences in type frequency and analogous differences
for the transition matrices, suggest that the most distinctive seasons
in terms of circulation patterns are summer (June-August), autumn
(September-October), and winter (November-May).

The frequency of spells of a given type is shown in Table 4. For example, there were 180 spells of type 1 lasting two days between 1946-74. The frequencies are not cumulative. The mean is calculated assuming that a type which only occurred singly would have a mean duration of 1.0 days (Table 7, Quarterly Report, December 31, 1976, was based on the assumption of a day's persistence such that this hypothetical case would yield a mean persistence of zero). Persistence of synoptic patterns is of importance with respect to influences on ice decay and these data will be incorporated in future climate-ice interaction studies.

C. Climate-Ice Interaction

The interpretation of climate-ice interaction is derived from the results of the following four sets of studies:

(1) A survey of "historical" data and LANDSAT-derived estimates of ice breakup along the Beaufort and Chukchi coasts.

(2) Wind velocities and synoptic types associated with the breakup and movement of pack ice and fast ice in the Beaufort Sea and case-studies of breakup patterns at Peard Bay, Barrow and eastward along the Beaufort coast.

(3) Analysis of meteorological factors associated with ice decay, breakup and retreat of the pact ice:

a) Analysis of breakup between Pt. Barrow and Cape Halkett for 1972-75 with associated temperature, surface wind, geostrophic wind and synoptic events.

b) Statistical analysis of the meteorological factors affecting the retreat of the pack ice off Barrow.

(4) Analysis of climatic trends in temperature and its relationship to the severity of ice conditions and navigability.

The available records of fast-ice breakup along the two coasts are summarized in Table 5. The "comments" point to the variable nature of these records and indicate the heterogeneity of data shown on the AEIDC map for the Chukchi Sea coast.

The complex character of interaction between wind velocity, synoptic pattern and motion of pack ice or fast ice is illustrated in Table 6. For this reason, a combination of statistical analyses supported by detailed case-studies has formed the basis of our study.

TABLE 5. DATES OF BREAK-UP ALONG THE BEAUFORT AND CHUKCHI SEA COASTS

Sources of information:

(1) Kniskern and Potocsky (1965), "Frost Degree Day, Related Ice Thickness curves, and Harbor Freeze-up and Breakup Dates for Selected Arctic Stations" Tech. Report TR-60, U.S. Naval Oceanographic Office, Washington, D. C.

(2) Source Map AEIDC

(3) National Weather Service, monthly climatological summaries for Alaska available since 1946 at NARL, Barrow, Alaska

Station	Earliest date ice broke in Spring	Latest date ice broke in Spring	Avg. date b.u.	Yrs. Data	Actual Years	Source of info. (See above)	Comments
Barter Isle	7/15	8/31	8/13	3	?,pre-1965	1	Avg. is too late, not enough data
Camden Bay/ Barter Isle	5/20*	7/25*	6/14*	9	1964-75 exc. 65, 69, 70	3	Dates & Avg. only apply to time when ice unsafe for man to walk on
Beaufort Sea/ Barter Isle	6/8*	7/10*	6/28*	8	1967-75 except 1969	3	
Camden Bay/ Barter Isle	6/25*	8/4*	7/18*	8	1964-75 exc. 65, 66, 69, 70	3	Dates & Aug. only apply to the time when boating or shipping was possible
Beaufort Sea/ Barter Isle	6/25*	8/4*	7/18*	8	1967-75 exc. 1969		
Barrow	6/27	8/7	7/15	8	1946-57 exc. 48, 51, 54, 55	3	
Barrow	6/30*	7/22*	7/14	4	1961, 1970 1972, 1975	3	*Dates apply to permit boating/ shipping. Few data.
Wainwright	6/7	7/26	6/29	7	?,poss. same as source 1	2	Probably Kuk River dates on the Chukchi, probably same data but error in source 2 avg.
Wainwright	6/7	7/26	7/5	7	?,pre-1965, poss. pre-1955	1	
Wainwright	6/27	7/26(1948)	7/10	13	1946-60 exc. 58, 59	3	Kuk River @ Wainwright
Pt. Lay	5/20	7/10	6/15	3	?	1	Dates possibly do not apply to Kokolik River. Too early for Chukchi
Pt. Lay	6/1	7/10	6/24	4	?,pre-1965	2	
Pt. Lay	5/7	7/10(1953)	6/5	6	1949-57 exc. 50, 52, 54	3	Kokolik River
Cape Lisburne	6/18	7/16	7/5	6	?	2	Chukchi. Only source.
Point Hope	5/30	7/8	6/20	8	?,pre-1965	1 & 2	Chuckchi Sea. Prob. all 3 Pt. Hope sources Same time period
Point Hope	6/2	7/8	6/16	7	1946-51 and 1954	3	
Kivalina	5/15	5/26	5/19	5	?	2	
Kotzebue	5/17	6/8	5/31	14	?,pre-1965	1 & 2	Kotz.breaks up much earlier than Kotz.Sound
Kotzebue	5/18	6/17	5/31	12	1946-59 exc. 47, 52	3	Ditto. Note similarities
Kotzebue	5/20*	7/27*	6/19*	10	1961-75 exc. 66,67,71,73,74	3	*applies to last ice only
Kotzebue	4/26	6/8	5/26	10	1961-75 exc. 62,66,67,73,74	3	*applies to date unsafe for man
Deering/ Kotzebue Sound	5/13	6/11	5/27	3	?	2	Few data; too early for the Sound.

Table 6 . Ice Movement and Associated Wind Directions, Speeds, and Synoptic Types.

LANDSAT Date	Direction Ice Movement	Wind Direction & Dates	Wind Speed (m.p.h.) & Dates	Synoptic Types & Dates	Ice Type Moving
B A R R O W A R E A					
3/18 to 3/23/73	ENE to WSW	06(all)	11.5,18.7,16.8, 11.7,17.4,14.8	3,1,1,1,1,1 (18th-23)	Pack
4/9 to 4/10/73		05(both)	12.2 & 6.9	1,1	
5/14/73	SW-NE	15,16,16,23 (11th-14th)	6.8,8.2,8.3, 11.5(11th-14)	12,12,10,4	Pack
10/21/73	S to N	16,16 (20th-21)	10.8,11.4 (20th-21)	3,3	Fast Ice
5/7 to 5/10/74	E – W	8,6,7,7 (7th-10)	10.1,13.7,15.5, 13.8	1,1,1,1	
7/20 to 7/21/74	to SW	34,01	6.9 & 6.8	14,14	Fast Ice
6/18/75	S to N	18,26,9 (16th-18)	8.8,12.4,11.4 16th-18th)	No Data	Attached Ice
4/25 to 4/27/75		5,3,5	12.7,10.8,7.9	No Data	Pack
B A R T E R I S L A N D A R E A					
3/8/73	W to E	15,27,27 (6th-8th)	5.3,19.7,17.7	13,1,1	Pack
4/13/73	SW – NE	34,26,25 32,9 (9th-13th)	11.2,7.2,4.8 6.8,7.3	17,4,1, 1,1	Pack
3/30/73	SE to NW	8,9 (29th-30)	21.4,21.6	1,1	
5/6/73		9,9,9 (4th-6)	21.4,22.4, 23.6	1,1,1	

Table 6 . Continued.

5/24/73		09	25.7	1	
6/21/74	SE – NW	9,9,9 (18th-20)	23.6,21.3, 16.1	21,21,1,16 (18th-31)	Pack
10/6/74		10,8,9	25.0,31.6,12.2 (4th-6th)	No Data	Shorefast
3/16/75	SW – NE	27,27,8	23.4,22.1,21.0 (14th-16th)	No Data	
before 4/3/75		10,10,10 9,11,1 (26th-31)	25.0,24.4,31.8 47.7,15.8 (26th-30)	No Data	Pack
4/4/75	to WSW	09	15.1	No Data	Pack

The major result of the statistical analysis of the meteorological factors affecting the retreat of the pack ice is shown in Table 7. The stepwise regression analysis shows that temperature in the form of thawing degree days (TDD's) is primarily accountable for the variance in the distance to the 4/8 concentration of pack ice on September 15. Also of some importance are the wind speed, pressure and number of days with southerly winds. The importance of summer TDDs is further demonstrated in Table 8 showing the relationship between ice severity and summertime TDDs. There is good correspondence between the rank of a summer at Barrow (in terms of TDDs) and the ice severity, although the relationship is less clear at Barter Island. The results are discussed in the next section.

VII. DISCUSSION

Interpretation of climate-ice interactions was initially based on a conceptual "word-model" of hypothetical links between climatic variables and ice response in summer, based on a literature survey, physical considerations, and preliminary inspection of remote sensing data. This scheme is summarized in Table 9. However, some of the complexities of the interrelationships will become apparent in the following discussion.

General associations between winds, synoptic type and movement of pack ice or fast ice were illustrated in Table 6, but the relationship of these events to summertime breakup requires elaboration. In summer, along the Beaufort Sea coast, southerly winds associated with higher temperatures would be expected to be most closely linked with breakup. Statistical analysis tends to confirm that southerly winds play at least a contributory role (Table 7), Table 3 shows that southerly to westerly flow occurs particularly with synoptic types 2 and 5, whereas other types give rise mainly to easterly airflow and should not produce a significant change from average ice conditions. On a time-scale of a few days there was a good correspondence between the timing of breakup between Pt. Barrow and Cape Halkett, as determined from LANDSAT imagery for 1972-75, and the occurrence of southerly geostrophic winds. Synoptic types 2 and 5 occurred on a majority of these days. The relationship was less clear, however, if examined in terms of observed southerly surface winds.

Preliminary analysis of breakup at Peard Bay on the Chukchi coast shows that, despite differences between this area and the coast eastward of Barrow in terms of fast-ice extent, the fast-ice breakup in Peard Bay is similar to that east of Barrow. This is probably due to the local occurrence of an east-west coast orientation and the presence of barrier islands which are common features of the Beaufort Sea coast, but not the Chukchi coast. There are also indications that southerly airflow may be of significance in Peard Bay. Geostrophic wind indices, computed for the Chukchi coast, shows evidence of long-term trends in summer airflow direction from southeasterly in the 1950's to easterly in the 1960's, returning to southeasterly since 1970 (Quarterly Report, 03-6-022-35179,

Table 7

RESULTS OF THE TWO STEPWISE REGRESSION ANALYSIS OF METEOROLOGICAL
DATA AND DISTANCE TO THE PACK ICE MARGIN OFF BARROW ON
SEPTEMBER 15, 1953-76

Variable Regression Analysis # 1		Regression Coeff.	% Variance Accounted For	F-ratio	Variable Regression Analysis # 2		Regression Coeff.	% Variance Accounted For	F-ratio
Summer TDD	X_1	0.262	65.4%	37.80	Summer TDD	X_1	0.219	65.4%	37.80
Windspeed	X_6	18.152	7.2%	4.97	S Wind	X_5	5.074	6.5%	4.43
Pressure	X_5	-164.676	7.5%	6.74	NE Wind	X_6	-4.821	2.4%	1.68
V Component	X_4	13.876	0.9%	0.83	NE*	X_4	2.800	3.4%	2.56
Winter FDD	X_2	-0.012	0.6%	0.53	E Wind	X_7	-1.826	0.9%	0.71
-U Component	X_3	1.952	0.4%	0.36	Types 2, 15	X_8	-0.984	0.4%	0.29
Cloud	X_7	7.631	0.3%	0.23	SE-SW*	X_2	-0.321	0.1%	0.04
			82.3%					79.1%	

(* geostrophic)

Table 8. Mildness/Severity of Summers Since 1953 in Terms of
Ice and Temperature at Barrow and Barter Island.

Summer	Ice severity Rank, Barrow to Prudhoe Bay (1 = mildest)	Summer TDD accumulation at Barrow (°F)	Rank Summer TDDs at Barrow (1 = mildest)	Summer TDD accumulation at Barter Is.	Rank Summer TDDs at Barter Is. (1 = mildest)
1953	15	366	17		
1954	9	925	1		
1955	22	303	22		
1956	20	321	20		
1957	11	636	8	844	2
1958	1	737	4	1118	1
1959	7	441	11	384	18
1960	17	351	18	439	13
1961	4	456	10	616	8
1962	3	721	5	669	5
1963	6	371	16	594	9
1964	18	311	21	406	16
1965	14	462	9	363	19
1966	13	389	13	571	10
1967	12	379	14	520	11
1968	2	760	3	737	3
1969	21	227	23	386	17
1970	19	375	15	430*	14
1971	16	426	12	618	7
1972	8	765	2	639	6
1973	5	645	7	717	4
1974	10	655	6	429	15
1975	23	346	19	461	12
Mean values		494		576	

* Estimate due to some missing data.

Table 9. **Postulated Climate - Ice Interactions in Summer**

Variable	State	Process	Ice Response	Links (a) Affected by	(b) Affect
1. Temperature anomaly	>o(<o)	Ice Melt	Rapid(slow) ablation	2,5,8	6,7,8
2. Cloud amount	High(low)	Net radiation	Slow(rapid) ablation	5	1,8
3. Wind speed	High(low)	Heat transfer	Enhances(retards) melt		1
4. Wind speed	High(low)	Ice dynamics	Enhances(retards) break-up		
5. Wind direction	Onshore(off—shore)	Ice dynamics	Retards(enhances) ice removal		1,2
6. Wind direction	Onshore(off-shore)	Temp. advection	Retards(enhances) ablation		1,2
7. Solid precipitation	High(low)	Albedo	Retards(enhances) ablation		8
8. Liquid precipitation	High(low)	Heat input	Advances(retards) ablation	1	
9. Net radiation	High(low)	Heat input	Advances(retards) ablation	1,2,6	1

September 30, 1976). Future case-studies should help to evaluate the possible significance of such shifts for ice breakup.

Regression analysis (detailed in the Quarterly Report for December 31, 1976) of summertime climatic parameters and pack ice retreat by mid-September tabulated by Barnett (1976) shows that geostrophic winds are not the best indicator of the distance off Barrow to the limit of 4/8 ice concentration (Table 7). Surface wind direction makes a small contribution to the variance, but thawing degree-day totals alone account for 65 percent of the variance of ice distance. This dominant temperature effect makes the role of other variable seem largely irrelevant at the present stage of our understanding.

This finding raises the question of the role of wind direction in determining the summer temperature. An analysis by Weaver (1970) shows that at Barrow, southerly winds bring significantly higher summer temperatures $(10.6^{o}C$ in July 1966) than onshore winds $(2.7^{o}C)$. It remains to be determined how much of the temperature-explained variance in Table 7 derives from this effect. Also, it is not clear whether the occurrence of open water off Pt. Barrow helps to determine the station temperature instead of the reverse, as we are assuming. Since water temperature remains close to freezing point the former effect should be limited.

Regardless of the possible interactions between air temperature, wind direction and the occurrence of open water, the correlation of +0.81 (Fig. 10) between summer thawing degree-days and pack ice retreat is high. Further investigation has been carried out using LANDSAT imagery for 1972-75. The following general relationships with thawing degree-days were found:

TDDs

(i)	<100	– initiation of ponding and rapid thawing of ice
(ii)	100-250	– fast ice breakup, some open water
(iii)	250-400	– fast ice largely gone, melting on pack ice
(iv)	400-550	– pack ice retreats, possibly to 80km north of Pt. Barrow
(v)	>550	– pack ice retreats more than 80 km

These categories show a significant change over time, based on climatic data at Barrow:

TDD categories	1921 to 1952	1953 to 1975
(i)	0	0
(ii)	1	1
(iii)	3	10
(iv)	12	4
(v)	16	8

The number of summers in which the pack ice did not retreat jumped from 4 in 32 years (12%) to 11 in 23 years (48%) in the last 55 years. There has been an average loss of 66 TDDs (a decrease from 559 for 1921-52 to 493 for 1953-75) or about $0.8^{o}F$ in the mean summer temperature over the same time

intervals. These findings will need to be assessed against the map evidence compiled by Hunt and Naske (RU #261) suggesting more open water conditions in August-September since about 1940 compared with ship records from 1860-1919.

VIII. CONCLUSIONS

The results of this project to date allow two broad sets of conclusions to be drawn. The first group are direct products of the climate-ice interaction studies and can be regarded as reasonably firm. The second set are more general and tentative inferences of significance for planning with regard to offshore petroleum development.

A. Ice Conditions and Climatic Effects (Reasonably firm)

(1) Summer temperature conditions, as indicated by accumulated thawing degree-days, account for 65 percent of the variance in the distance off Pt. Barrow of the southern limit of 4/8 concentration of pack ice on September 15. If windspeed and pressure data are incorporated in the regression, 80 percent of the variance is accounted for.

(2) An accumulation of 250-400 thawing degree (F) days is required to remove the fast ice and 400-550 TDDs for open water to extend up to 80km off Pt. Barrow on September 15.

(3) Climatic data at Barrow indicate a drop in summer temperature of nearly 1°F for 1953-75 compared with 1921-52. Correspondingly, the number of summers in which >400 thawing degree-days were attained has declined from 88 percent for 1921-52 to 52 percent for 1953-75. This implies that fewer summers with good shipping conditions have been experienced since the 1950's compared with the three preceding decades. Table 8 shows that in climatic terms, at least, the 1975 summer was not a rare event.

(4) The movement of pack ice, or broken fast-ice, along the Beaufort Sea coast is almost always in the same direction as the wind at Barrow and Barter Island, even though the moving ice may be hundreds of kilometers from these stations. However, the ice at Barrow moves with lighter winds than at Barter Island. Movement and breaking of ice observed on LANDSAT imagery in the vicinity of Barter Island has usually occurred with wind speeds averaging twice those during ice motion off Barrow. This may relate to the tendency for more open water in the Barrow area and the ice outlet via the Chukchi Sea.

(5) The synoptic pressure pattern types can be characterized seasonally in terms of broadly distinctive combinations of temperature and wind conditions. Thus, type 1 for the Beaufort Sea sector represents a pattern of polar easterly circulation, resembling the mean winter pattern, with strong NE winds and temperatures about or slightly below average. Types 2 and 5, which are frequent summer patterns, give rise to southerly geostrophic (southwesterly surface) winds and positive temperature departures.

The summertime shift to these types appears to be a major determinant of the ice breakup.

(6) Sections along the Chukchi Sea coast with an orientation towards east-west, particularly where there are sheltering barrier islands, will tend to have breakup characteristics similar to the Beaufort Sea coast between Pt. Barrow and Cape Halkett.

B.   Ice Conditions in relation to Petroleum Development (Tentative)

(1)   Hazards to Offshore Operations

(a)   Ice deformation features. Ridges and hummocks show more-or-less preferred locations from year to year (cf. maps prepared by W. Stringer RU #257 for the Beaufort Sea Synthesis Meeting: Sea Ice report, fig. 9). Examples are: offshore and west of Barter Island, in a line from Narwhal Island to a point approximately 80km due north of Atigaru Point in Harrison Bay, and approximately along the 20m isobath arcing around Pt. Barrow in the Chukchi Sea and Beaufort Sea. These areas are the scene of enormous shear and pressure forces, most of which (as interpreted from LANDSAT) seem to occur during the dark period November through February.

The edge of contiguous fast ice appears to be displaced progressively seaward through the winter months, based on interpretation of ice edges and puddling features on summer imagery. Each successive winter ice edge can be a site for ice deformation so that large grounded ice masses can occur well inside the 20m isobath. In general, however, the areal extent and intensity of ice deformation seems to be greatest near the late-winter fast ice edge in the so-called stamukhi zone (Reimnitz et al. 1976). This may be a consequence of the involvement of more massive polar floes and thicker first-year ice in ridge formation late in the season. Our case-study of ridging off Oliktok in late March - early April 1975 illustrates the anomalously large and well-grounded field of shear ridges that may form in this manner (see Section VI.A).

The implication is that permanent offshore structures may be subject to relatively large ice forces, even well inside the 20m isobath, but these forces would occur further seaward by late winter.

(b)   Grounded ice. As noted above, remote sensing data can be used to locate well-grounded ice only because it remains in situ late into the melt season. This type of ice is very discontinuous along the coast. During the decay season, therefore, under-ice oil spills occurring within the fast ice zone would not necessarily be contained within a band of grounded ice parallel to the coast. Nevertheless, the elongate ridges which parallel extensive segments of the Beaufort Sea coast in late winter have keels extending well below the level ice, even though they may be floating or only weakly grounded. These ridges might be

effective in temporarily containing most of an under-ice oil spill during February through May. Such trapping capability would rapidly diminish after late June as the fast ice begins to disintegrate leaving only well-grounded ridges in situ. This decay date also marks the end of the period when trapping could occur in the irregular bottom topography of the floating fast ice.

Our mapping has shown that well-grounded, deformed ice masses are occasionally found in waters < 10m deep. Structures and lines on the near-shore bottom must be able to withstand the forces generated by such features and associated bottom scour, even though the frequency and intensity of such events are much less than in the stamukhi zone.

(2) The Seasonal Fast-ice Regime

The results of our program, combined with other OCS studies, provide a preliminary scenario of the fast-ice regime that can serve as a tentative framework for seasonal scheduling of operations in the nearshore zone of the Beaufort Sea coast.

(i)   new ice formation - late September/early October
(ii) first continuous fast-ice sheet - mid/late October
      Unstable outside bays and the barrier islands
(iii) extension and modification of fast-ice - November to February
      No direct observations cover this period. The general
      sequence involves:

            - seaward progression of the ice edge
            - ridging of successive ice edges
            - incursions of older ice
            - grounded ice masses, formed in situ or driven
              shoreward (Kovacs)
(iv) stable fast-ice inside about the 15m isobath - February to
      April/May (Stringer)
(v)   estuarine flooding of ice - late May
(vi) puddling on ice - early June
(vii) melting and weakening of ice - June (Attached ice decays
      April/June)
(viii) breakup - late June to August
(ix) open water in favorable years - August/September
      Some deep-draft older ice and ridge fragments remain in
      the nearshore zone.

IX. NEEDS FOR FURTHER STUDY

A primary consideration in evaluating the results so far obtained is the limited number of seasons on which the detailed studies can be based. While the statistical analyses provide a useful overview it must be remembered that they assume linear relationships between the variables. It is likely, however, that ice/water-atmosphere feedbacks contribute to

non-linearity. For this reason, reasonable certainty can only be attached to our models when a range of different case-studies have been examined. LANDSAT data coverage for 1976 was much more complete than for the preceding years and can serve to test some of our findings to date.

Some specific topics for future work include:

1. Completion of imagery interpretation for the Beaufort and Chukchi coasts.
2. Assessment of the role of subsidiary factors involved in ice decay and retreat, particularly with respect to their coupling with air temperature and the occurrence of open water. The role of cloud cover needs to be examined.
3. Determination of the climatic characteristics of the synoptic types for the Chukchi sector.
4. Assessment of the effect of synoptic types on the breakup and consideration of possible feedbacks, due to the occurrence of open water, on the atmosphere. For example, does an early breakup in the Chukchi Sea influence the pattern of events further north by affecting air mass modification and storm tracks?
5. What changes in the large-scale atmospheric circulation are associated with the decrease in summer temperature at the Beaufort Sea coast? Are there indications of future long-term trends that would affect navigation, etc?
6. What climatic parameters that are primarily involved in determining the course of fast-ice breakup and pack ice retreat would be most important to forecast on short and long time scales?
7. More precise delimitation of the spatial and temporal occurrence of grounded ridges within the fast-ice zone.
8. An attempt to delineate ice hazards on a seasonal and geographical basis following the preliminary general outline presented in the Sea Ice report of the Beaufort Sea Synthesis Meeting (Barry, 1977).

X. SUMMARY OF FOURTH QUARTER ACTIVITIES

A. Office Activities

1. Schedule   The principal activities this quarter have been concerned with mapping and interpretation from remote sensing data and preparation of materials for the Beaufort Sea Synthesis Meeting (Barry, 1977) and for the Annual Report.

2. Personnel   R. G. Barry - Principal Investigator
R. Moritz - Graduate Research Assistant (1/2 time)
J. Rogers - Graduate Research Assistant (1/2 time)
G. Wohl - Graduate Research Assistant (1/2 time)
C. Wright - Professional Research Assistant (1/2 time)

3. <u>Methods</u>   Analysis of imagery and meteorological data follows previously described methods

4. Not applicable

5. <u>Data Analysed</u>

   (A) Remote Sensing Data

      (1) The LARSYS subcontract study was completed and is attached as a separate report in Appendix 1. Papers based on it are in preparation by Bartolucci and Moritz.

      (2) Maps of fast-ice limits have now been completed for the three Chukchi Sea coastal sectors for 1973-75. These are included as Appendix II, Maps 1-32, extending the series previously prepared for the Kotzebue sector for 1973 (Quarterly Report, December 31, 1976).

      (3) Interpreted maps of ice characteristics in the nearshore zone have now been prepared for the Barrow sector of the Beaufort coast for 1974 (Appendix III) and Prudhoe sector for 1973 (Appendix IV). Interpretation of the Barter Island maps for 1974 is in progress following preliminary delimitation of different ice zones.

   (B) Stages of Ice Decay on the Chukchi Sea Coast

Following the identification and dating of stages of ice decay on the Beaufort Sea coast (Quarterly Report, September 30, 1976, pp. 7-9), summarized and updated in Table 1 above, a similar analysis has been carried out for the Chukchi Sea coast. Dates are based on LANDSAT imagery which are available, at best, approximately every 18 days. This interval, combined with the problem of cloud obscuration, makes it improbable that the actual date of any defined ice event will coincide with a clear LANDSAT frame. For this reason, bracketing dates for non-occurrence and occurrence of each stage are tabulated.

The stages of ice decay recognized in this imagery analysis are defined as follows:

(i) Noticeable darkening in rivers due to thawing. Compared with the Beaufort Sea coast, there are few major rivers where this phenomenon may be observed.

(ii) Flooding of nearshore ice by rivers. Again, this is uncommon on the Chukchi Sea coast.

(iii) Surface darkening of the fast-ice due to <u>in situ</u> melting.

(iv)   First large-scale movements in the fast-ice.   These are
relatively obvious along this coast due to land-ice contrasts
on the imagery.   Also, the narrowness of the fast-ice along
the Chukchi Sea coast usually means that there are concurrent
major displacements in the pack ice.   These are favored by the
currents in the Chukchi Sea.

(v)   Fast-ice zone becomes ice free.   In contrast to the Beaufort
Sea coast, there is not always an ice-free strip between the land
and the pack ice; also, large but changing areas of open water
are usually obvious well into the pack-ice domain.

(vi)   First new ice in autumn.   New ice usually forms first in
embayments and lagoons making identification easy, although
the occurrence of pack ice in the nearshore zone may complicate
this task.

These six events have been catalogued from 1972-75 LANDSAT
imagery for the following 11 sectors:

Sector 1:   Pt. Franklin to Pt. Barrow (* indicates Peard Bay
            only in tables)
Sector 2:   Icy Cape to Pt. Franklin
Sector 3:   Pt. Lay area including Naokok to Icy Cape
Sector 4:   Water area of Sector 3 within the Barrier Islands
Sector 5:   Cape Beaufort
Sector 6:   Northern half of Cape Dyer including Cape Lisburne
            and eastward
Sector 7:   Southern half of Cape Dyer including Pt. Hope
Sector 8:   Cape Thompson southeastward
Sector 9:   Kivalina and northwestern Kotzebue Sound
Sector 10:   The immediate vicinity of Kotzebue
Sector 11:   Southern Kotzebue Sound

The results are summarized in Table 10.1 - 10.6
Supplementary information on breakup dates is given in Table 5.
This is summarized from various sources and may be based in some
cases on observations made during the 1940's.

(C)   Comparison of Summers 1972-76 with Long-term Climatic Data

Since LANDSAT data on ice conditions are only being examined
for the 1972-76 summers, it is important to compare the climatic
conditions during these years with long-term averages.   This is
done in Table 11, which shows mean thawing degree-days totals
for Kotzebue, Barrow and Barter Island and a ranking of the
1972 to 1976 summers in terms of standard deviation (S.D.)
departures.   At Barter Island, all four years lay within the
± 1 S.D. range about the mean.

TABLE 10.   DATES OF ICE EVENTS ON THE CHUKCHI SEA COAST

1.   Noticeable spring darkening in rivers due to thawing

Sector	1973		1974		1975	
	No Darkening	Darkening	No Darkening	Darkening	No Darkening	Darkening
1	4/11	5/19	4/4	No	2/23	5/16
2	4/11	NI	4/4	Infor-	2/23	5/16
3	4/11	NI	5/11	mation	5/1	5/16
4	4/11	NI	5/11		4/2	5/16
5	3/7	NI	3/20		5/1	5/16
6	3/7	NI	4/8		2/25	NI
7	3/7	NI	4/8		2/25	NI
8	3/7	5/19	4/8		2/25	NI
9	4/11	5/19	4/4		NI	NI
10	4/11	NI	4/4		NI	NI
11	4/11	NI	4/4		NI	NI

2. Flooding of near-shore ice by rivers

	1973		1974		1975	
Sector	No Flooding	Flooding	No Flooding	Flooding	No Flooding	Flooding
1	4/11	NI	4/4	5/28	2/23	NI
2	4/11	NI	4/4	5/28	2/23	NI
3	4/11	NI	5/11	NI	5/1	NI
4	4/11	NI	5/11	NI	4/2	NI
5	3/7	NI	3/20	NI	5/1	NI
6	3/7	NI	4/8	NI	5/1	NI
7	3/7	NI	4/8	NI	5/1	5/16
8	3/7	NI	4/8	NI	5/1	NI
9	4/11	5/19	4/4	NI	NI	5/16
10	4/11	5/31	4/4	NI	NI	6/1
11	4/11	NI	4/4	NI	NI	NI

3. Fast ice surface darkening due to in-situ melting

Sector	1973		1974		1975	
	No Melting	Melting	No Melting	Melting	No Melting	Melting
1	4/11	7/7	5/28	7/3	5/16	7/6
2	4/11	6/5	4/4	7/3	5/16	<7/28
3	4/11	6/5	5/11	<6/17	5/16	6/3
4	4/11	6/5	5/11	6/17	5/16	<7/28
5	4/11	6/4	3/20	5/31	5/1	5/16
6	3/7	4/11*	4/8	5/13*	4/2	5/16*
7	5/19	6/5	4/8	5/13	5/1	5/16
8	3/7	5/19	4/8	5/13	5/1	5/16
9	4/11	5/19	4/4	5/29	5/6	6/1
10	4/11	6/1	4/4	5/27	NI	6/1
11	4/11	6/1	4/4	5/28	NI	6/1

4. First large-scale movements in the fast ice

	1973		1974		1975	
Sector	No Movement	Movement	No Movement	Movement	No Movement	Movement
1	7/7	<8/14	5/28	>7/3	5/16	7/6
2	6/23	8/14	7/3	>7/6	5/16	7/28
3	6/5	6/23	5/11	6/17	6/3	<7/28
4		6/5	6/17	7/23	5/16	6/3
5	6/4	<6/23	6/17	7/7	6/3	<8/14
6	3/7	4/11	4/8	5/13*	4/2	5/16*
7	5/19	6/23	5/31	6/17	6/5	<8/14
8	5/19	6/23	6/17	<7/23	6/2	<8/14
9	6/1	6/2	5/29	7/3	6/1	6/18
10	6/1	<6/2	5/29	<7/3	6/1	6/18
11	6/1	6/18	5/28	7/3	6/1	6/18

* See category V, similar dates in both categories

< Event in this category occurred earlier than this date. Generally the category V event occurred on this date.

5. Fast ice zone becomes ice free

Chukchi Sector	1973 Not Ice Free	Ice Free	1974 Not Ice Free	Ice Free	1975 Not Ice Free	Ice Free	1972 Ice * Free
1	7/7	8/14	7/3	NI	7/28	9/1	7/31
2	6/5	8/14	7/6	NI	7/28	9/1	8/2
3	6/5	8/14	6/17	7/23	6/3	7/28	8/2
4	6/5	8/14	7/23	7/23	6/3	7/28	7/31
5	6/5	6/23	6/17	7/23	6/3	8/14	7/31
6	3/7	4/11	4/8	5/13	4/2	5/16	7/31
7	6/23	8/14	. 6/17	7/23	6/5	8/14	7/31
8	6/23	8/14	6/17	7/23	6/2	8/14	7/31
9	6/23	7/9	7/3	7/23	7/5	7/24	7/31
10	6/2	6/18	5/27	7/23	6/18	7/5	7/31
11	6/18	8/14	7/3	7/23	7/5	7/24	7/31

* No Information about the "Not Ice Free" Category

NI No Information; no appropriate satellite imagery

6. First new ice in Autumn

Sector	1973		1974		1975	
	No new Ice	New Ice	No new Ice	New Ice	No new Ice	New Ice
1	7/7	10/25*	7/3	NI	9/1	11/10
2	10/25	NI	7/6	10/4**	9/1	11/10
3	10/8	NI	7/23	NI	8/14	10/25***
4	NI	NI	7/23	10/4	8/14	10/25
5	6/23	NI	10/23	NI	9/1	10/25***
6	4/11	NI	10/22	NI	9/1	10/27***
7	NI	NI	10/22	NI	9/1	11/10
8	NI	NI	10/22	NI	9/1	10/27
9	10/6	NI	10/18	11/5***	10/27	11/10***
10	10/6	NI	9/10	10/18	10/27	11/10***
11	10/6	NI	10/18	11/5	10/27	11/10***

*   Peard Bay only

**   Icy Cape only

***   with floating, broken ice

TABLE 11.   AVERAGE THAWING DEGREE-DAYS AND 1972-76 SUMMER CONDITIONS

Parameter	Kotzebue	Barrow	Barter Island
Mean TDDs	1,944 (1943-76)	532 (1921-75)	583 (1948-75)
S.D.	204	182	176
Median	1,906	495	571
±1 S.D. range	1,740-2,148	350-714	407-759
1972	>1 S.D. warmer(2275)	>1 S.D. warmer(765)	above avg.(639)
1973	below avg.[1] (1748)	above avg. (645)	above avg.(717)
1974	above avg.[1] (2108)	above avg. (655)	below avg.(429)
1975	>2 S.D. colder(1521)	>1 S.D. colder(346)	below avg.(461)
1976	near avg. (1956)	near avg. (491)	near avg. (576)

---

[1] Denotes a total within 1 S.D. of the mean value.

6. <u>Milestone Chart and Data Submission Schedules</u>

    (A) Ice Mapping and Interpretation

        Actual or projected completion dates are tabulated below for each sector:

		Beaufort Sea			Chukchi Sea*	
	Barrow	Prudhoe	Barter Is.	Kotzebue		
1973	Jun 77	Mar 77	Jun 77	Dec 76	Mar 77	Mar 77
1974	Mar 77	Sep 76	Apr 77	Mar 77	Mar 77	Mar 77
1975	Sep 77	Jun 77	Sep 77	Mar 77	Mar 77	Mar 77
1976	Sep 77	Sep 77	Sep 77	Jun 77	Jun 77	Jun 77

---

*Preliminary maps of ice extent and major types.

        The analyses for the Beaufort Sea have been taking longer to complete since they have involved a more complete interpretation of ice melt features. The present maps of ice limits for the Chukchi coast will require additional interpretation during the next two quarters. Analysis of the 1976 imagery is expected to take at least six months since a much more complete set of data exists than for the earlier years. 1976 will also therefore provide more data for case studies.

    (B) Synoptic Climatology

        Analysis of weather characteristics associated with the Beaufort Sea synoptic types will be completed in a M.S. thesis to be completed during the next quarter by R. E. Mortiz. A tape of the synoptic catalog for the Chukchi sector will be forwarded during the next quarter also. These data will be used in the studies of climate-ice interaction.

    (C) Climate-Ice Interaction

        The case-studies of climate-ice interaction and assessment of the amenability of significant climatic and synoptic parameters to predictability are expected to be prepared as an interpretative report for September 30, 1977, along the lines of sections VII and VIII above.

B. <u>Problems/Recommended Changes</u>   None

C. <u>Estimate of Funds Expended</u> $18,000

REFERENCES

Barnett, D. G. 1976. A Practical Method of Long Range Ice Forecasting
    for the North Coast of Alaska, Pt. 1. FLEWEFAC Tech. Rept. #1,
    Suitland, Md. 16 pp.

Barry, R. G. (ed.) 1977. Sea Ice. Panel Report, Beaufort Sea Synthesis
    Meeting, (Barrow), OCSEAP Arctic Project Office, 14 pp. Mimeo +
    9 figures.

Clarke, E. S. 1976. Prototype Beaufort Sea Technology Scenario. Presented
    at Fourth International Conference on Port and Ocean Engineering
    under Arctic Conditions. Univ. of Alaska, Fairbanks. 31 pp. + figures.

Hare, F. K. 1968. The Arctic. Quart. J. Met. Soc, 94, 439-458.

Holmgren, B., Benson, C. and Weller, G. 1975. A Study of Breakup on
    the Arctic Slope of Alaska by Ground, Air and Satellite Observations.
    In: Climate of the Arctic, 24th Alaska Science Conf. (G. Weller
    and S. Bowling, eds.) Geophysical Inst., Fairbanks, 358-366.

Keegan, T. J. 1958. Arctic Synoptic Activity in Winter. J. Met., 15,
    513-521.

Kovacs, A. and Gow, A. J. 1976. Some Characteristics of Grounded Floebergs
    near Prudhoe Bay, Alaska. Appendix #1 to OCSEAP RU #88 report,
    March 31, 1976 (submitted to Arctic). 9 pp. + figs.

Kovacs, A. and Mellor, M. 1974. Sea Ice Morphology and Ice as a Geologic
    Agent in the Southern Beaufort Sea. In: The Coast and Shelf of the
    Beaufort Sea (J. C. Reed and J. Sater, eds.) Arctic Institute of North
    America, Washington, D. C. 113-161.

Reed, R. J. and Kunkel, B. 1960. The Arctic Circulation in summer.
    J. Met., 17, 489-506.

Selkregg, L. 1974. Alaska Regional Profiles: Arctic Region. University
    of Alaska AEIDC, Anchorage. 28 pp.

Watson, C. E. 1974. The Climate of Alaska. In: Climates of the States,
    NOAA Water Information Center, 481-501.

Weaver, D. F. 1970. Radiation regime over Arctic Tundra Lakes, 1966.
    Report, Dept. of Atmos. Sci., Univ. of Washington, Seattle, 112 pp.

Weller, G. and Bowling, S. (eds.) 1975. Climate of the Arctic, 24th
    Alaska Science Conference, Geophysical Inst., Fairbanks, 436 pp.

Wilson, C. 1967. Climatology. Introduction, Northern Hemisphere I.
    CRREL Report IA3, Cold Regions Research and Eng. Lab., Hanover, 141 pp.

Zubov, N. N. 1943. Arctic Ice. Translation by U. S. Navy Oceanographic
    Office and Amer. Met. Society. 491 pp.
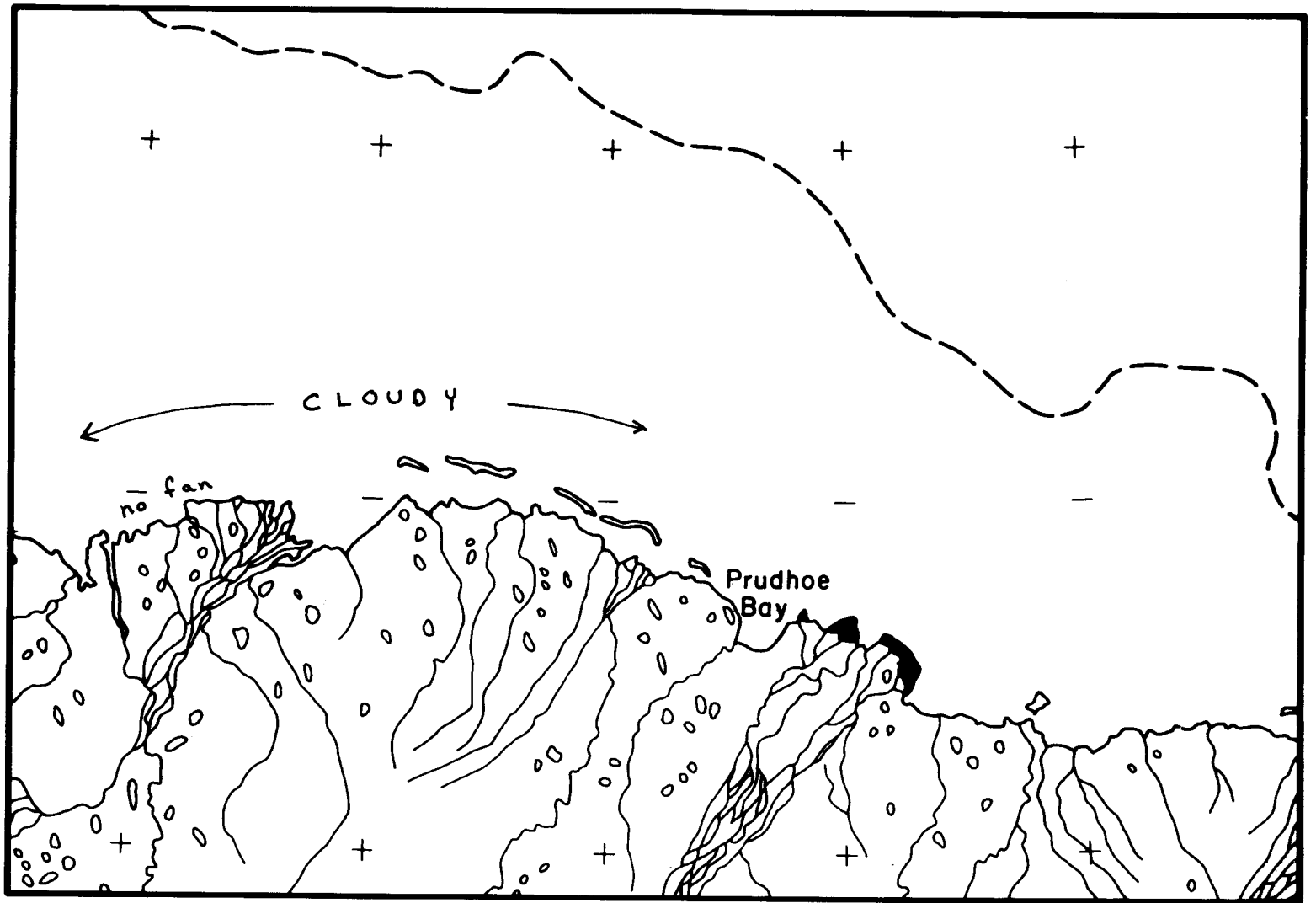
Near Shore Flooding, May 21, 1974, scene 1667-21162

FIGURE 1-a.
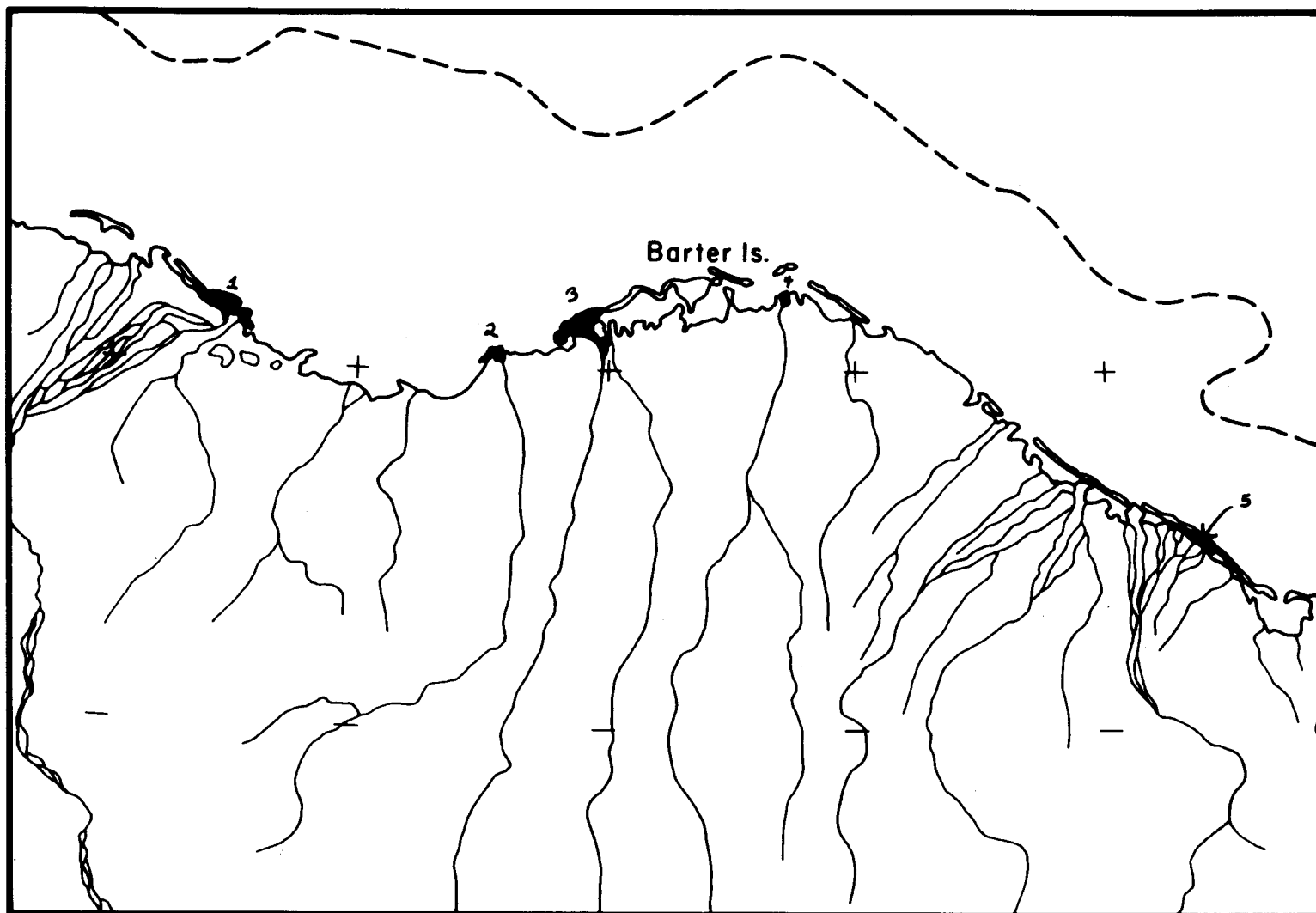
Near Shore Flooding, May 24, 1973 (1-3), scene
1305-21115; May 15, 1974 (4-5), scene 1661-20423

FIGURE 1-b.
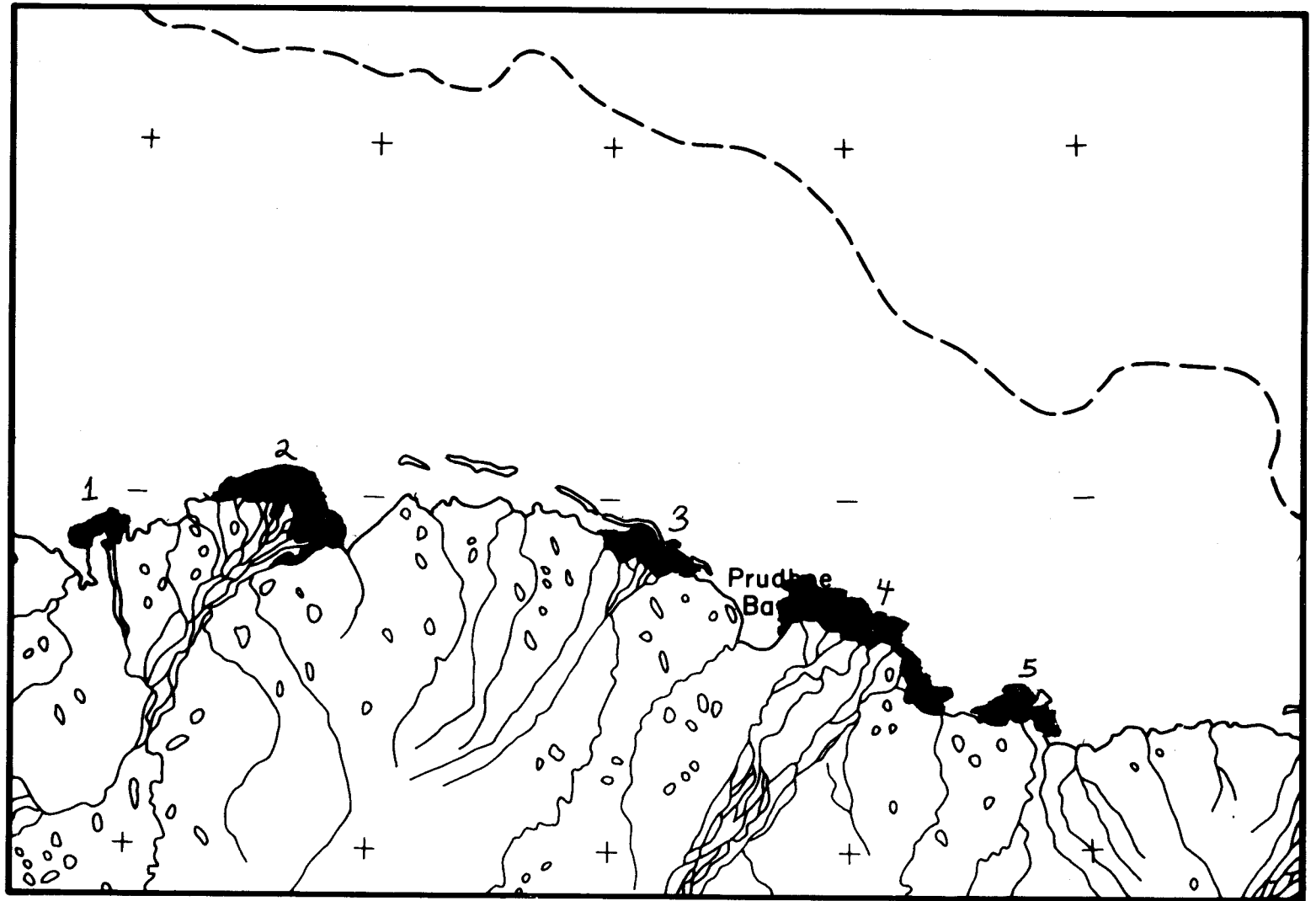
Near Shore Flooding, June 6, 1976 scene

2501-21051

FIGURE I-c.
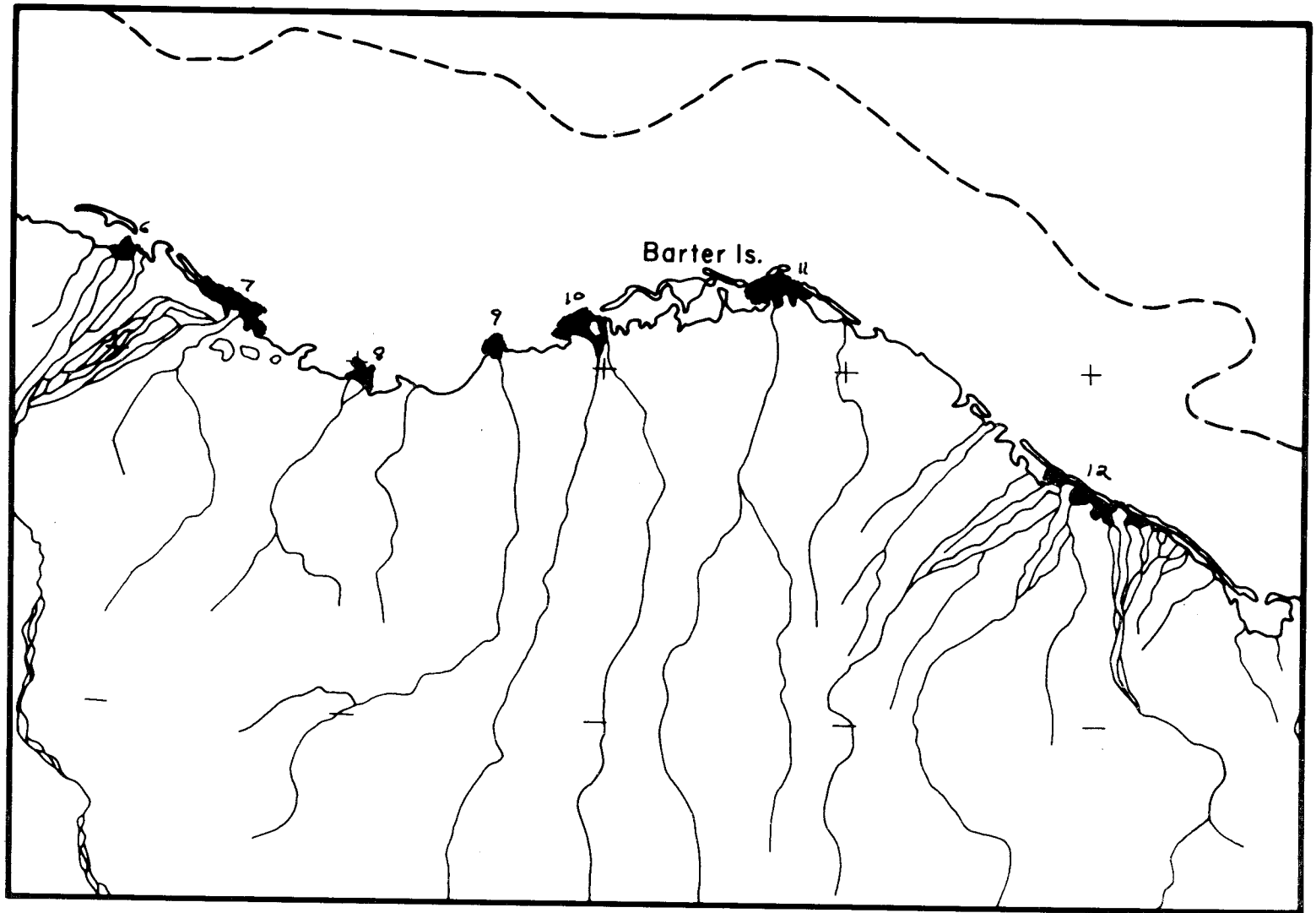
Near Shore Flooding, June 2, 1976 (10-12), scene
2497-20421; June 4, 1976 (6-9), scene 2497-20424

FIGURE 1-d.

FIGURE 2

26 JUNE, 1974: SCENE 1703-21151

THE CONTINUOUS ICE LIMIT (A) HAS BEEN EXTENDED WEST INTO OUTER HARRISON
BAY. NO MOTIONS COULD BE DETECTED WITHIN THE 25 JUNE CONTINUOUS ICE
LIMIT. PACK ICE (B) REMAINED COMPACTED AGAINST THE CONTINUOUS ICE EDGE.
PACK ICE DISPLACEMENTS IN THE TIME INTERVAL 25-26 JUNE ARE SHOWN ON THE
MAP AS SOLID ARROWS. THE "≢" SYMBOL DENOTES A "NO MOTION" CONDITION AT
A PARTICULAR POINT. THE SHEAR ZONE IS CLEARLY NOT LOCATED AT THE EDGE
OF CONTINUOUS ICE BUT RATHER SOME 15-20 KM SEAWARD OF IT. THE PREVAIL-
ING WIND DIRECTIONS FOR 25 JUNE AT BARTER ISLAND AND OLIKTOK ARE SHOWN
AS DOUBLE ARROWS (BTI AND OLI, RESPECTIVELY). THEIR RESPECTIVE MAG-
NITUDES WERE 5.7 and 6.2 M/SEC. THE ICE DRIFT BEYOND THE SHEAR ZONE
AGREED VERY WELL WITH EXPECTATIONS BASED ON ZUBOV'S RULE (ICE DRIFTS
AT 1/30TH TO 1/50TH THE WIND SPEED AND AT AN ANGLE OF ABOUT 30° TO THE
RIGHT OF THE WIND). THE PLOTTED VECTORS BEYOND THE SHEAR ZONE ARE
BETWEEN 1/35TH AND 1/50TH OF THE WIND SPEED AND 30 TO 40° TO THE RIGHT.
NEAR-SHORE ICE BETWEEN OLIKTOK AND THE EASTERN EDGE OF THE MAP REMAINED
SIMILAR TO THE PREVIOUS DAY EXCEPT THAT THE ICE BETWEEN PRUDHOE BAY AND
THE KUPARUK RIVER DELTA APPEARS TO HAVE DRAINED. THIS IS INDICATED ON
THE LANDSAT DATA BY THE DISAPPEARANCE OF THE DRAINAGE CRACKS AS WELL
AS BY A RELATIVE LIGHTENING IN TONE. THE NEWLY-IMAGED AREAS IN HARRISON
BAY EXHIBIT SEVERAL INTERESTING CHARACTERISTICS. FOREMOST IS THE PRES-
ENCE OF A LARGE GROUNDED ICE MASS AT N70°58', W150°42'. THE SEAWARD
"PUDDLING 3" BELT OF 25 JUNE TERMINATES IN EASTERN HARRISON BAY AT A
BOUNDARY WITH MUCH LIGHTER ICE, SSE OF THE LARGE GROUNDED MASS. THE
LIGHTER ICE HERE HAS A TEXTURE ON LANDSAT INDICATING A GREAT NUMBER OF
LIGHT-TONED FLOE-LIKE ICE PIECES EMBEDDED IN A SLIGHTLY DARKER MATRIX
OF ICE. ANALYSIS OF THE COLOR INFRARED PHOTOGRAPHY FROM 21 JUNE AND
APRIL SLAR IMAGERY IN THIS REGION LEADS US TO CONCLUDE THAT THE EASTERN
PORTION OF THIS ICE ("C") CONSISTS OF 2ND- AND/OR MULTI-YEAR ICE FLOES,
VARYING FROM SMALL TO VAST FLOE SIZE, AND EMBEDDED IN A 1ST-YEAR ICE
MATRIX. SHOREWARD OF THIS ICE, A CRESCENT-SHAPED BELT OF VERY DARK
TONE EXTENDS ACROSS THE BAY (DESIGNATED "PUDDLING 4" ON MAP). THE
SLAR IMAGERY SHOWS THIS TO BE RELATIVELY FLAT, UNDEFORMED ICE. SHORE-
WARD OF THIS BELT IS A SECOND ARCUATE ICE AREA OF LIGHTER TONE("D"),
WHICH HAS MODERATELY DEFORMED ICE WITH POORER PUDDLING DEVELOPMENT ON
26 JUNE. THE BOUNDARY AREA ("E") TO THE EAST OF THESE BELTS CONTAINS
SEVERAL PROMINENT RIDGES AND A NUMBER OF HEAVILY-HUMMOCKED AREAS.
MODERATE TO HEAVY PUDDLING CONDITIONS EXIST ON THE REMAINING HARRISON
BAY ICE, UP TO THE COLVILLE MOUTH AREA, WHERE OPEN WATER HAS EXTENDED
OUT FROM THE DELTA.

KEY:

SMOOTH ICE

Puddling 1
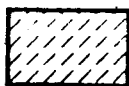
Puddling 2

Puddling 3

Puddling 4

ROUGH ICE

Ridging and
Hummocking

Grounding

Pack Ice

Open Water

40m Isobath — — —

Prudhoe
Bay

OLI

BTI
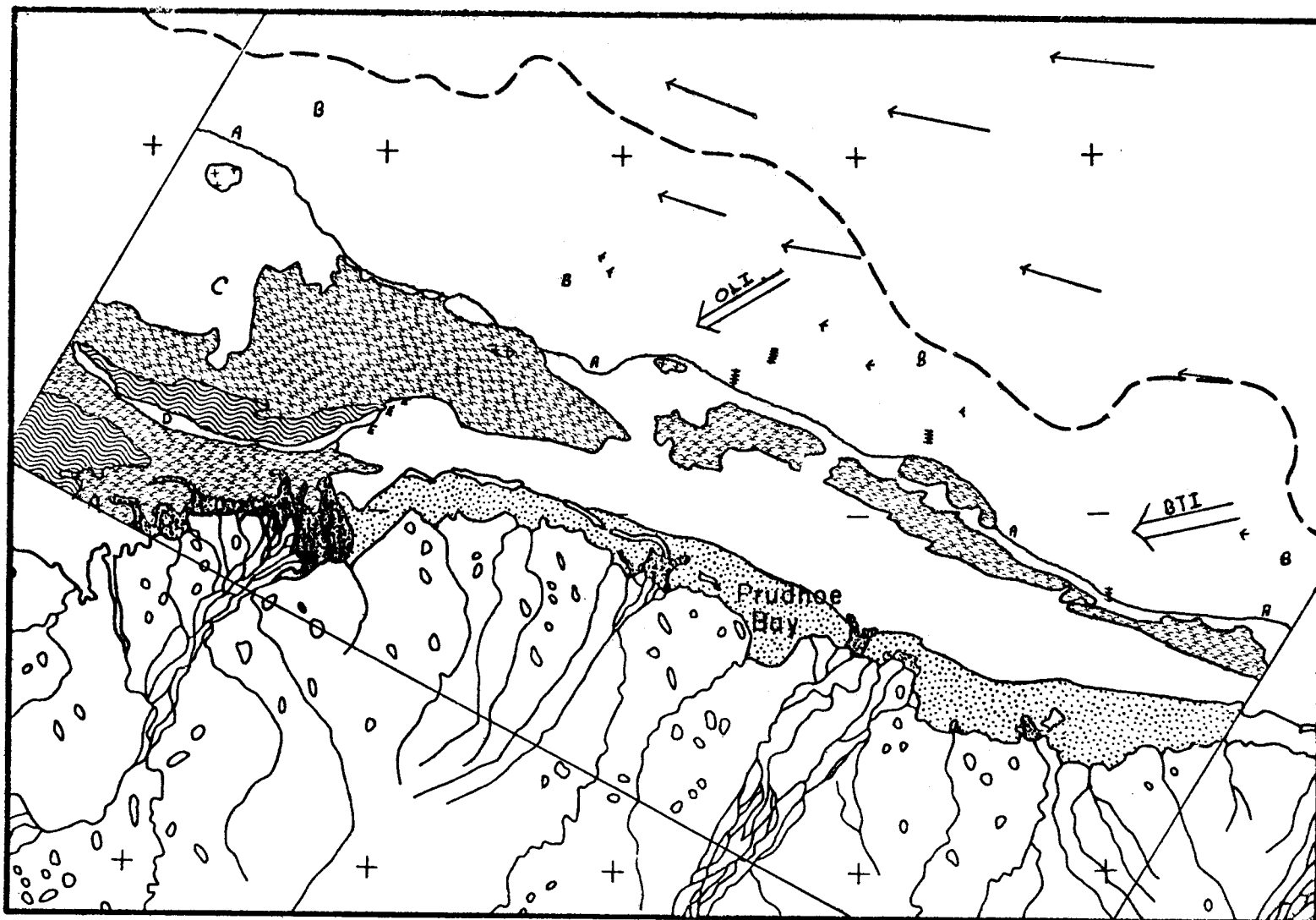
SHOREFAST SEA ICE

SURFACE MORPHOLOGICAL CHARACTERISTICS

BEAUFORT SEA COAST: PRUDHOE SECTOR

26 JUNE, 1974

FIGURE 2

FIGURE 3

THE CONTINUOUS ICE EDGE OF 26 JUNE HAS EXPERIENCED DISPLACEMENTS ALL
ALONG ITS EXTENT SHOWN ON THIS SCENE. 26 JUNE-14 JULY CONTINUOUS ICE
DISPLACEMENTS ARE SHOWN AS SOLID ARROWS. PACK ICE DISPLACEMENTS DURING
THE SAME INTERVAL ARE DEPICTED AS DOTTED ARROWS ON THE MAP. THE WELL-
GROUNDED NATURE OF THE THREE ICE MASSES SO DEPICTED ON THE MAP WAS
DETERMINED FROM THIS SCENE AND THE TWO FOLLOWING SCENES. IN THE MIDST
OF SHEARING AND/OR PRESSURED ICE FIELDS, ALL THREE MASSES REMAINED ES-
SENTIALLY STATIONARY. THE SHEARING ICE AROUND THE TWO WESTERNMOST
GROUNDED MASSES CREATED CRACKS (BLACK LINES) AND OPENINGS (SHOWN AS
OPEN WATER) IN THEIR VICINITY. THE DISPLACEMENTS OF PREVIOUSLY-CONTIN-
UOUS ICE APPEAR TO BE LARGER IN EASTERN HARRISON BAY THAN FURTHER EAST.
PACK ICE IS COMPACTED ALL ALONG THE PREVIOUSLY-CONTINUOUS ICE AND WAS
DISPLACED SOUTHWEST, THE SAME DIRECTION AS THE CONTINUOUS ICE. THE
MECHANISM OF BREAKUP, THEN, APPEARS TO BE THE SHOREWARD PRESSURING OF
CONTINUOUS ICE BY THE PACK. FAILURE HAS OCCURRED AT A GREAT MANY POINTS
IN THE ICE FIELD, LEAVING ONLY THE WELL-GROUNDED ICE IN PLACE. ALTHOUGH
LIMITED AREAS OF LIGHTER TONE REMAIN ON THIS SCENE, MOST OF THE NEAR SHORE
ICE IS NOW DEEPLY-PUDDLED (PUDDLING 4) OR MELTED COMPLETELY. THE OPEN
WATER AREAS OFF ALL THE MAJOR RIVERS HAVE INCREASED, MOST NOTABLY THOSE
OF THE COLVILLE, KUPARUK AND SAGAVANIRKTOK RIVERS. THE SHORE-POLYNYA
BREAKUP NW OF TIGVARIAK ISLAND (NOTED PREVIOUSLY) HAS DEVELOPED FURTHER
SINCE 12 JULY, WITH WIDER CRACKS AND OPEN WATER AREAS IN EVIDENCE.
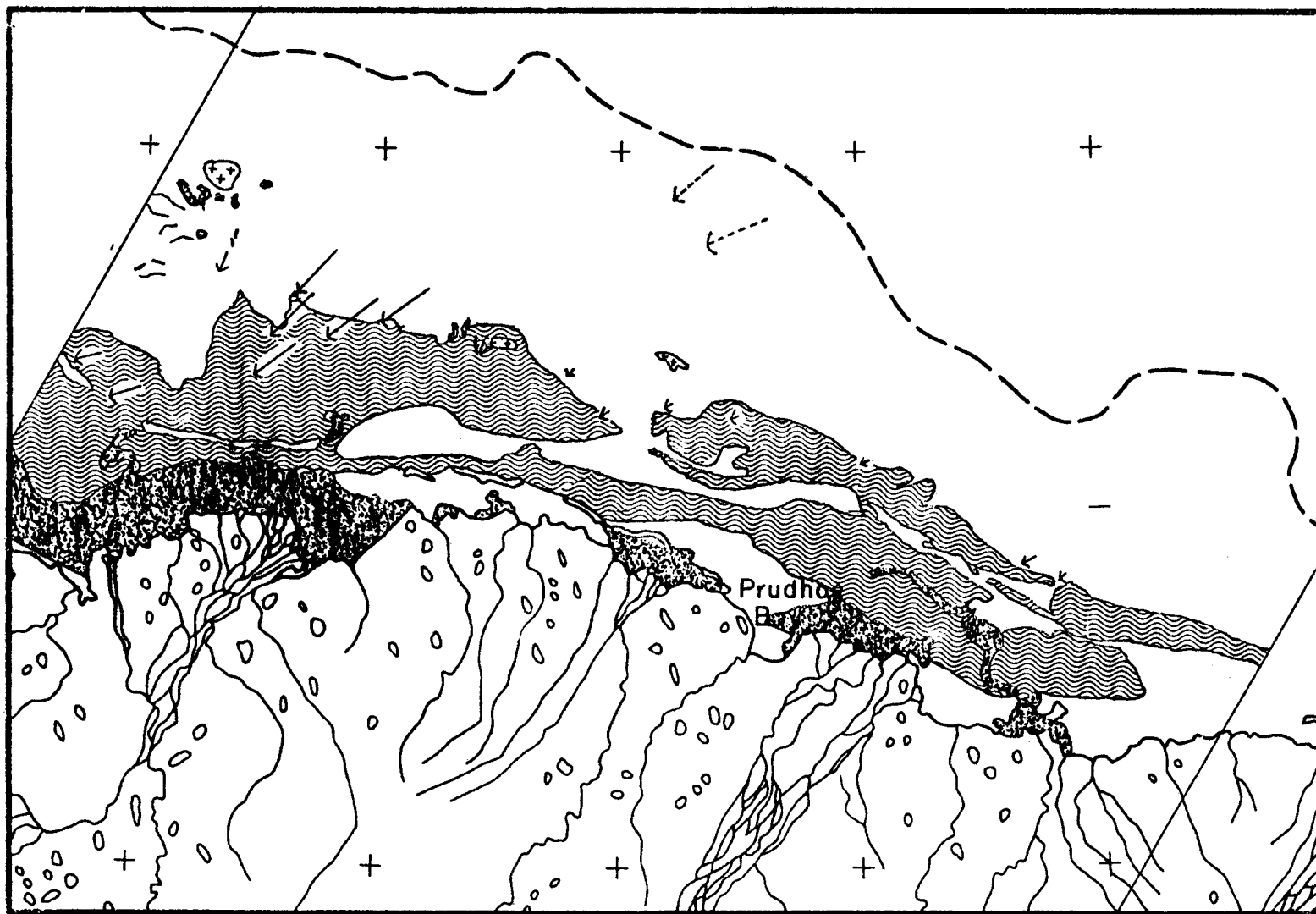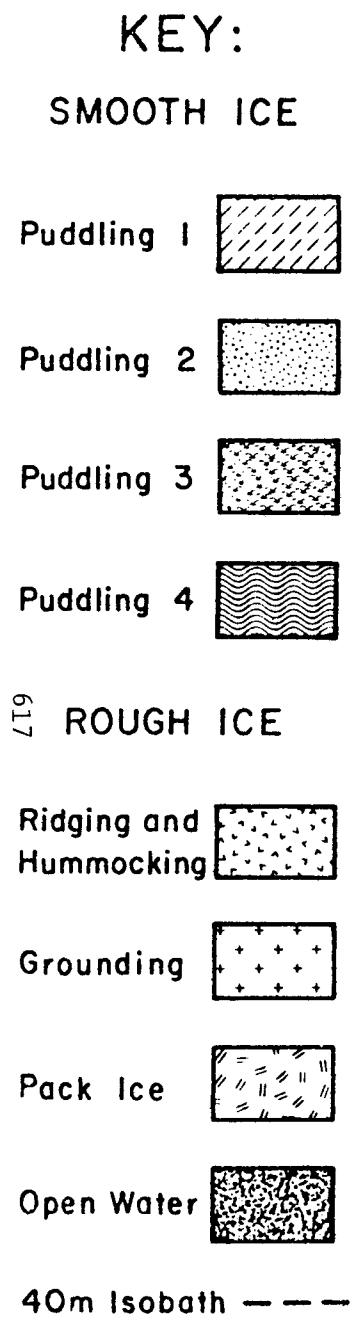
KEY:

SMOOTH ICE

Puddling 1

Puddling 2

Puddling 3

Puddling 4

ROUGH ICE

Ridging and
Hummocking

Grounding

Pack Ice

Open Water

40m Isobath — — —

617

Prudhoe
B

SHOREFAST SEA ICE
SURFACE MORPHOLOGICAL CHARACTERISTICS
BEAUFORT SEA COAST: PRUDHOE SECTOR
14 JULY, 1974

FIGURE 3

FIGURE 4

2 AUGUST, 1974: SCENE 1740-21194

ON THIS SCENE THE CONTINUOUS ICE SHEET OF 25-26 JUNE IS ESSENTIALLY GONE.
THE THREE LARGE GROUNDED MASSES NEAR THE FORMER CONTINUOUS ICE EDGE RE-
MAIN IDENTIFIABLE AND UNMOVED, ALTHOUGH THEY HAVE DECREASED IN AREA.   THE
FOURTH GROUNDED MASS NEAR BODFISH ISLAND IS DEPICTED AS "C".   TRULY
"SHOREFAST" ICE EXISTED BETWEEN THE SEAWARD GROUNDED MASSES AND THE COAST
EARLIER IN THE YEAR.   OPEN WATER NOW COVERS MOST OF THE FAST ICE ZONE,
WITH LOOSE PACK ICE (A) SEPARATING IT FROM COMPACT PACK ICE (B).   ALL
PACK ICE PRESENTS THE APPEARANCE OF ADVANCED SURFACE MELTING ON THIS SCENE.
SEVERAL LIGHT-TONED AREAS APPEARED ON THE LANDSAT DATA FOR THIS DATE IN
ZONE "B", WHICH, FROM THEIR SHAPE, APPEAR TO BE BROKEN UP FRAGMENTS OF
RIDGES WHICH FORMERLY COMPSED PART OF THE CONTINUOUS ICE.
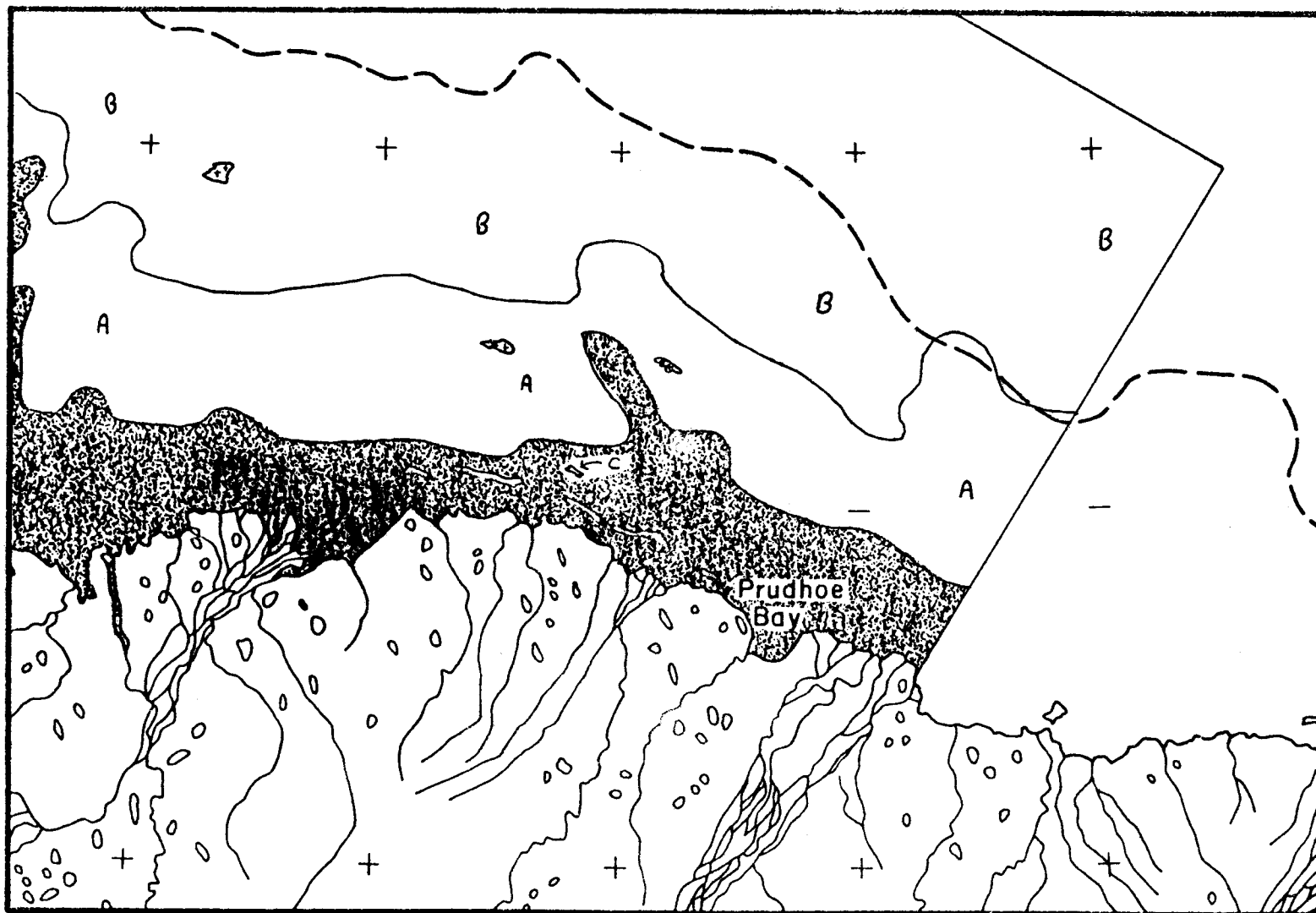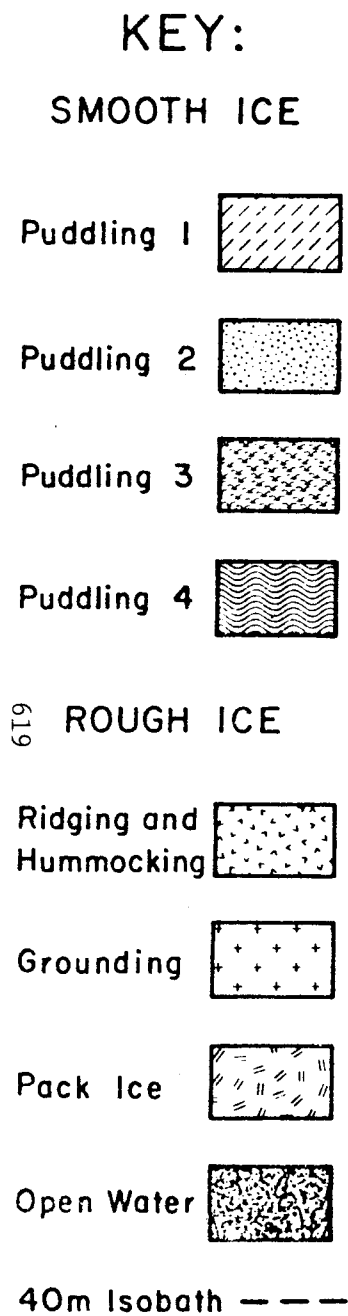
KEY:

SMOOTH ICE

Puddling 1

Puddling 2

Puddling 3

Puddling 4

619

ROUGH ICE

Ridging and
Hummocking

Grounding

Pack Ice

Open Water

40m Isobath — — —

SHOREFAST SEA ICE

SURFACE MORPHOLOGICAL CHARACTERISTICS

BEAUFORT SEA COAST: PRUDHOE SECTOR

2 AUGUST, 1974

FIGURE 4
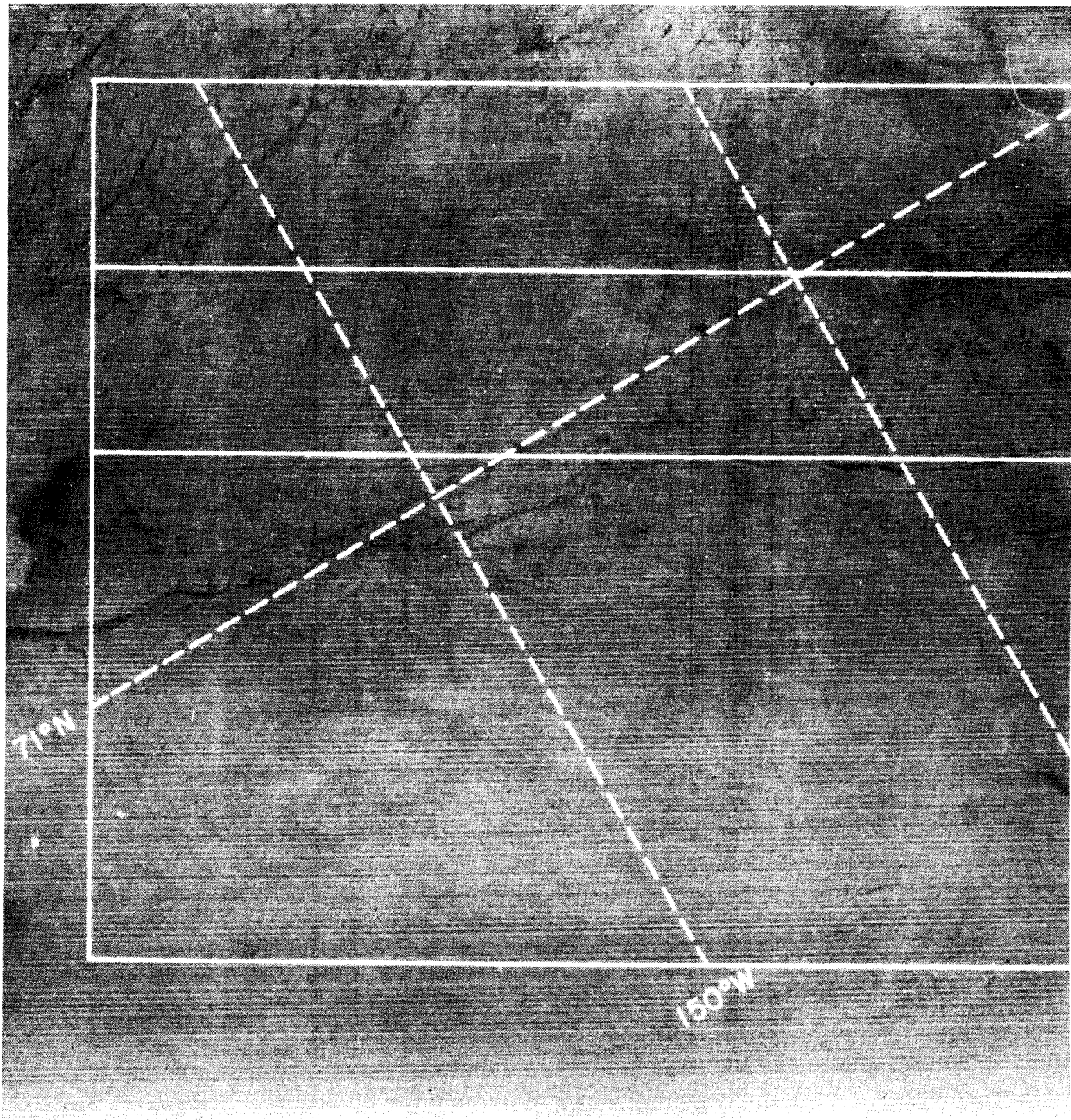
25 March, 1975. LANDSAT scene 1975-21163
LARGE RIDGE FIELD NOT ON SCENE

FIGURE 5-a.
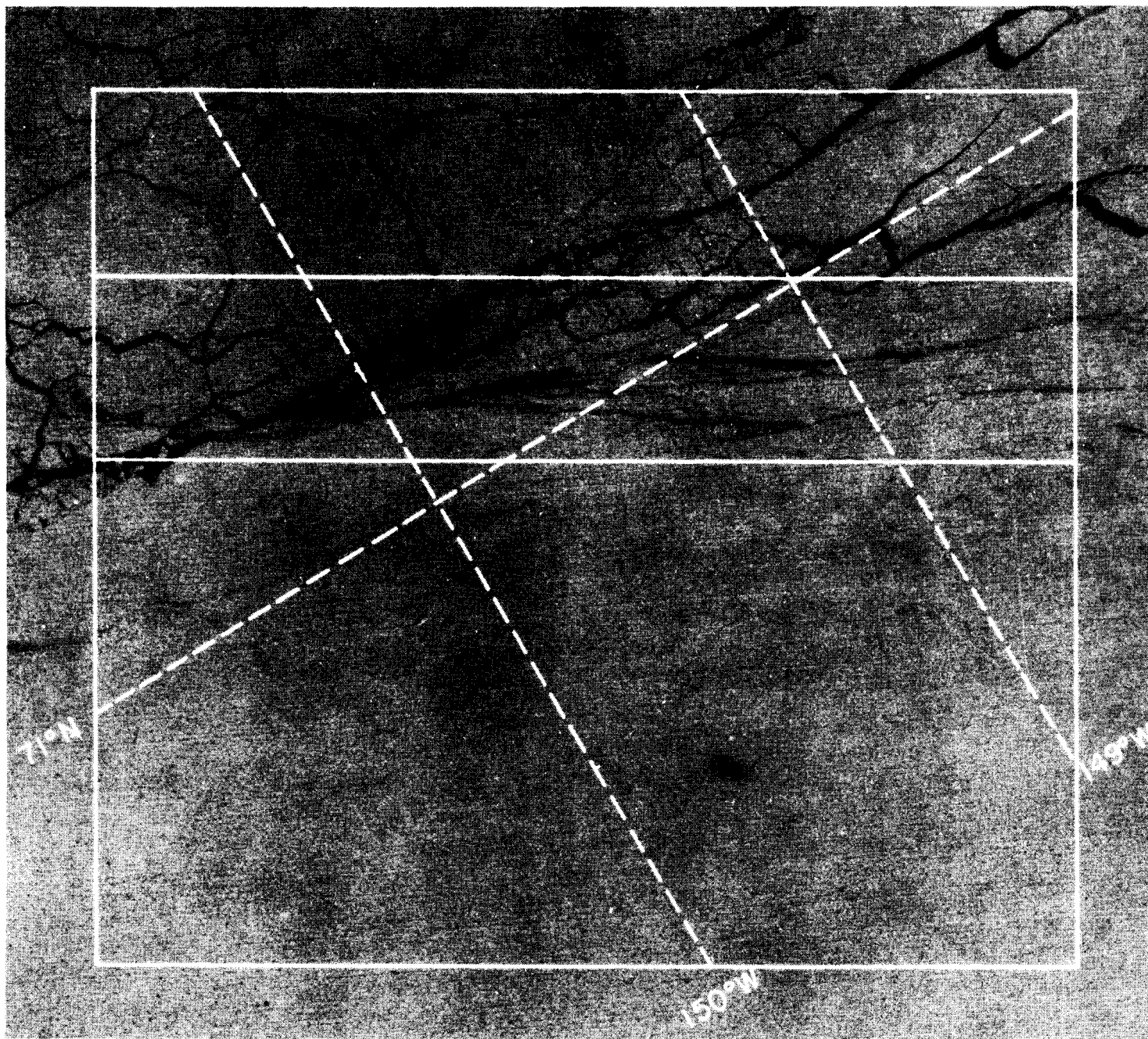
20 April, 1975. LANDSAT scene 2088-21170
LARGE RIDGE FIELD IN PLACE (center of white box)

FIGURE 5-b.

621
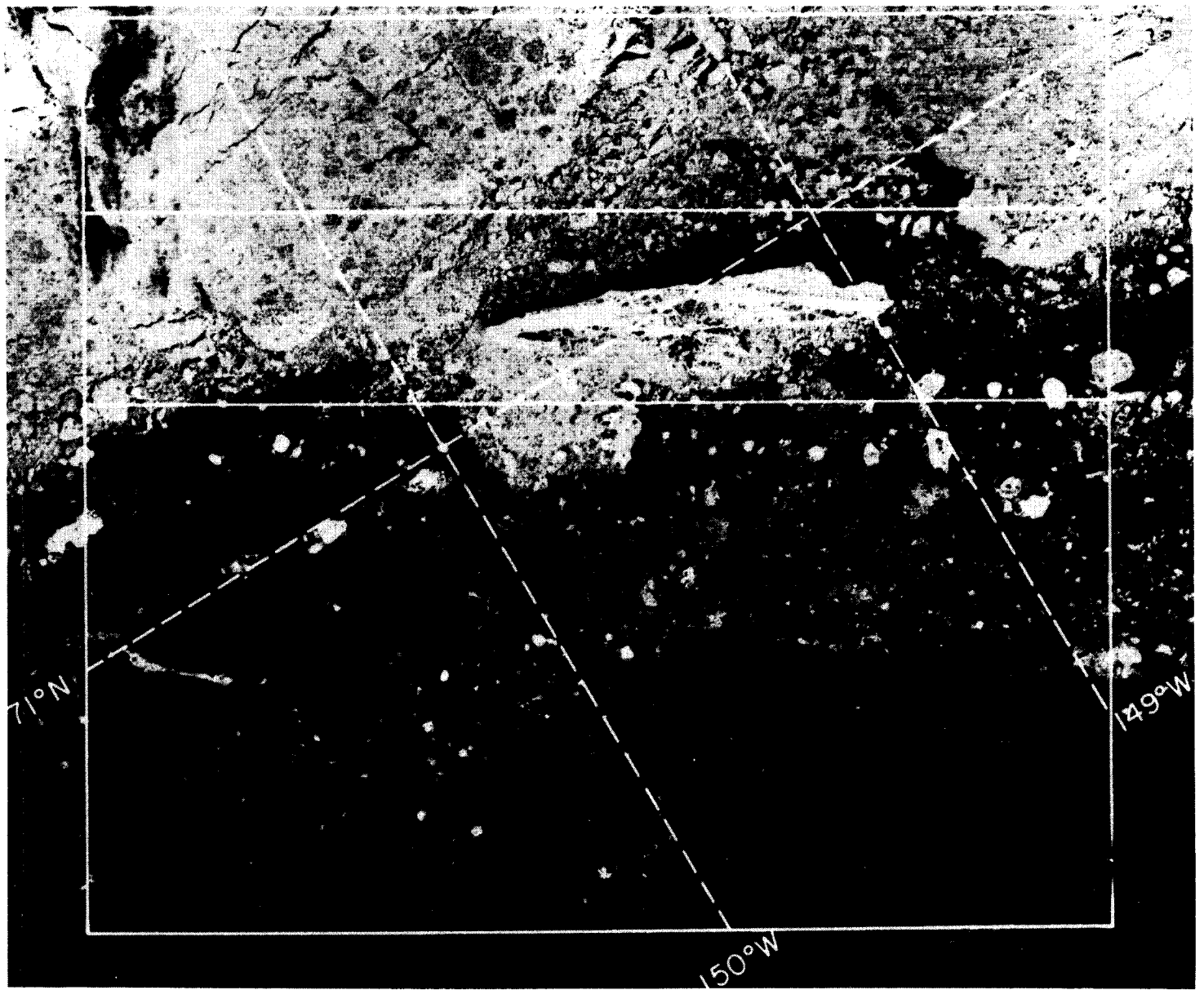
12 September, 1975. LANDSAT scene 2233-21213
LARGE RIDGE FIELD AT SUMMER'S END (pack ice to seaward)

FIGURE 5-c.

622
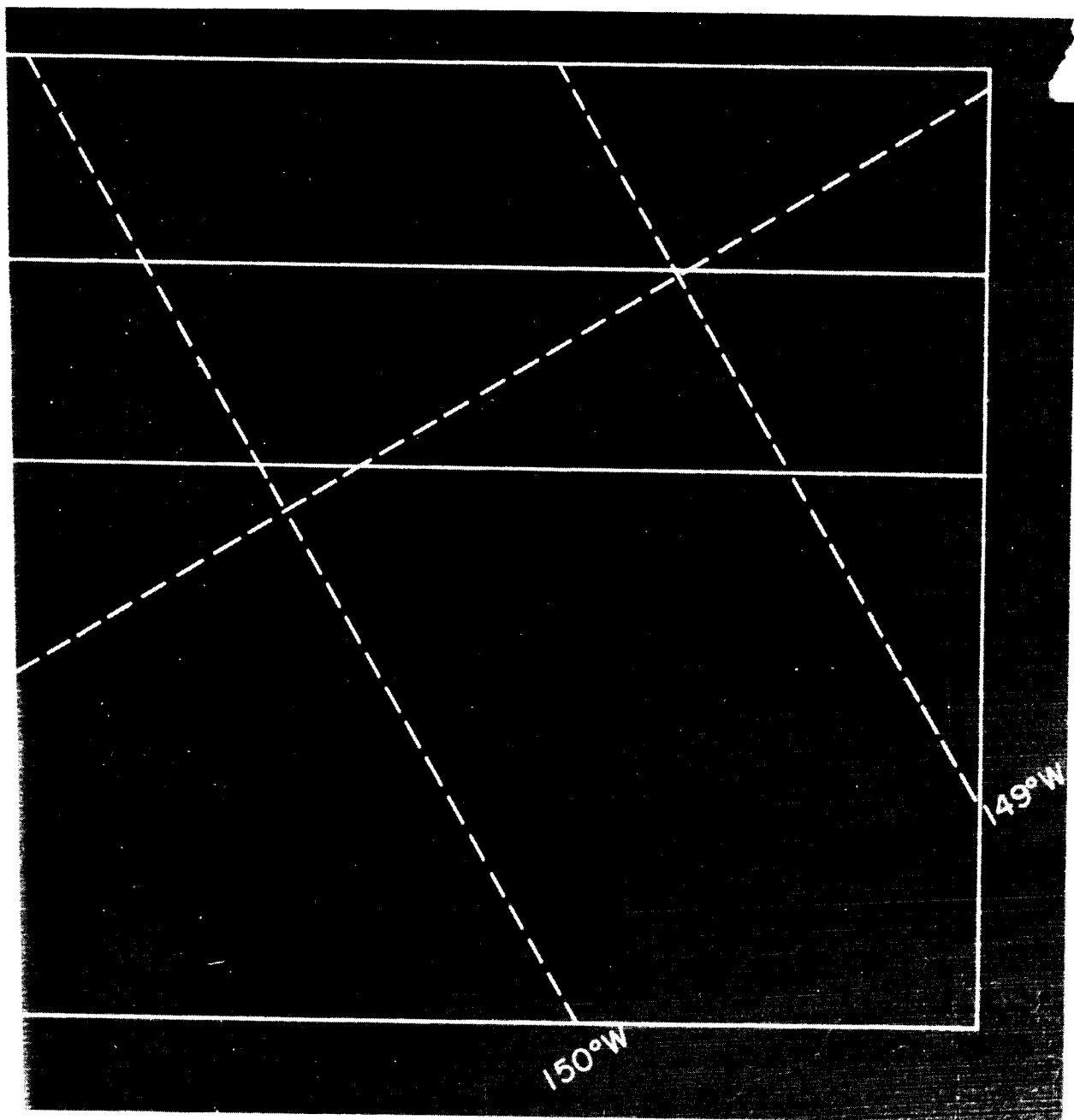
3 November, 1975. LANDSAT scene 2285-21094
POST-FREEZEUP CONDITIONS. FAST ICE BULDGES
SEAWARD AROUND LARGE RIDGE FIELD.

FIGURE 5-d.

623
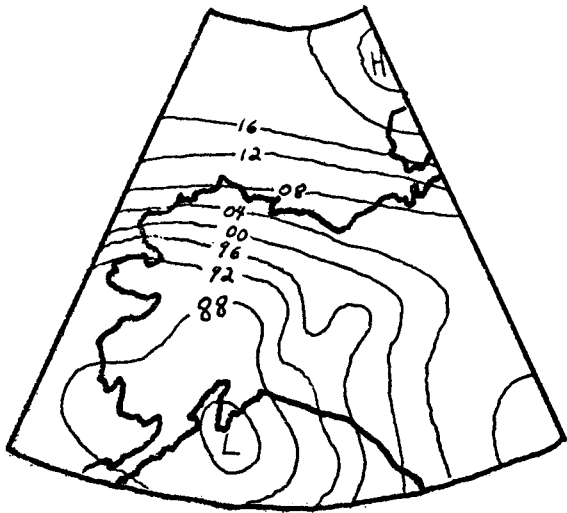
TYPE 1
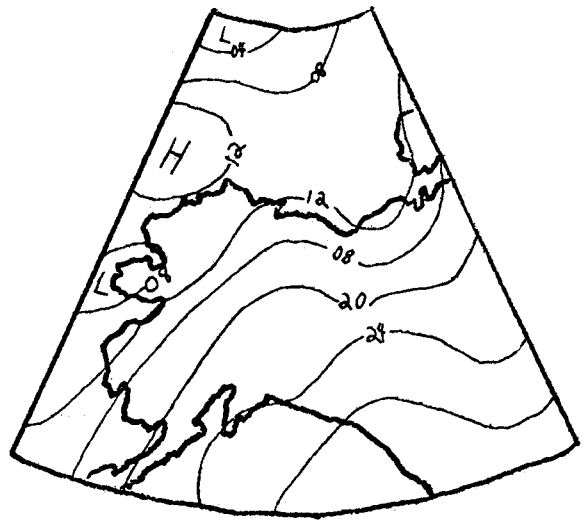
TYPE 2
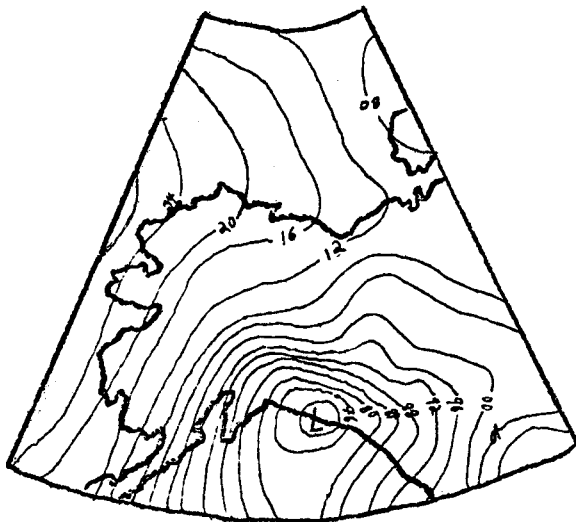
TYPE 3
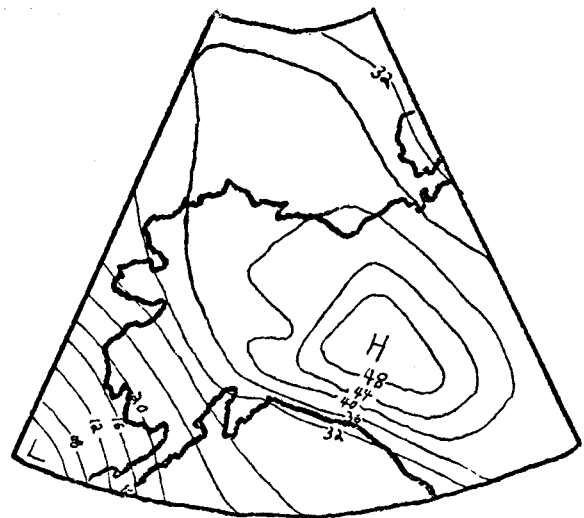
TYPE 4

BEAUFORT SYNOPTIC PRESSURE PATTERNS 1-4
FIGURE 6-a.
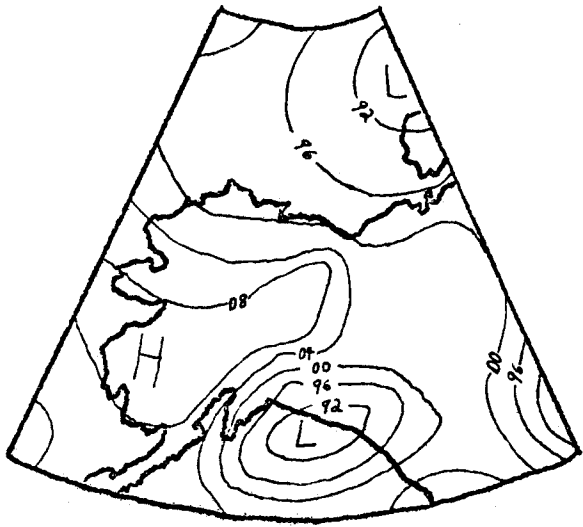
TYPE 5
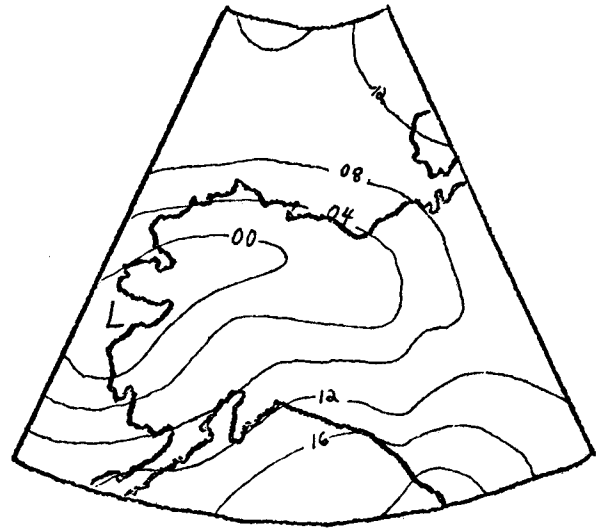
TYPE 6
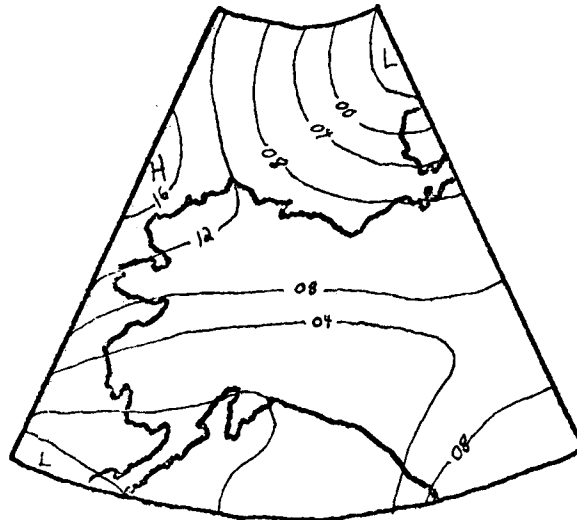
TYPE 7

BEAUFORT SYNOPTIC PRESSURE PATTERNS 5-7
FIGURE 6-b.
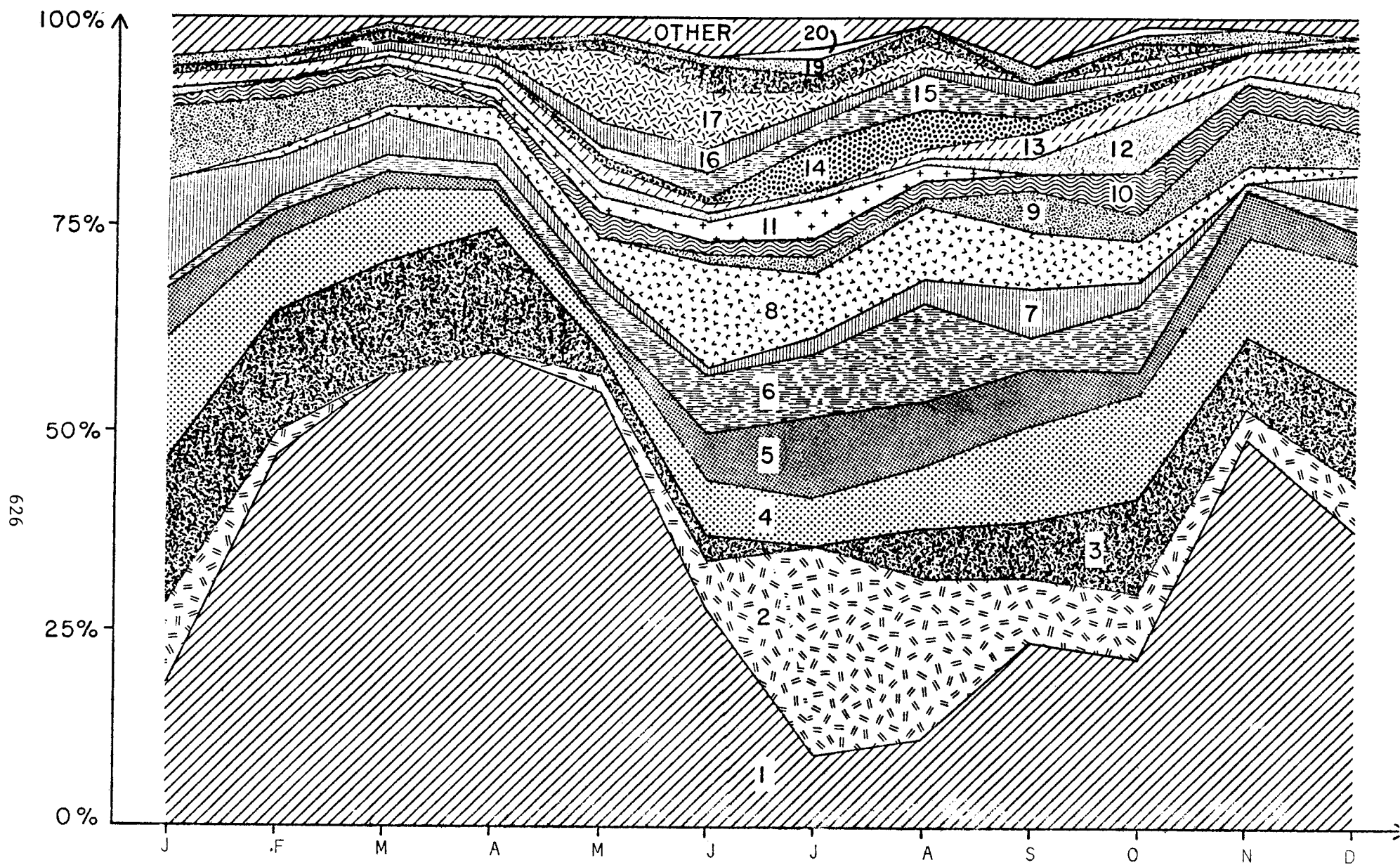
FREQUENCY OF BEAUFORT SYNOPTIC TYPES

September, 1968 to August, 1974

FIGURE 7
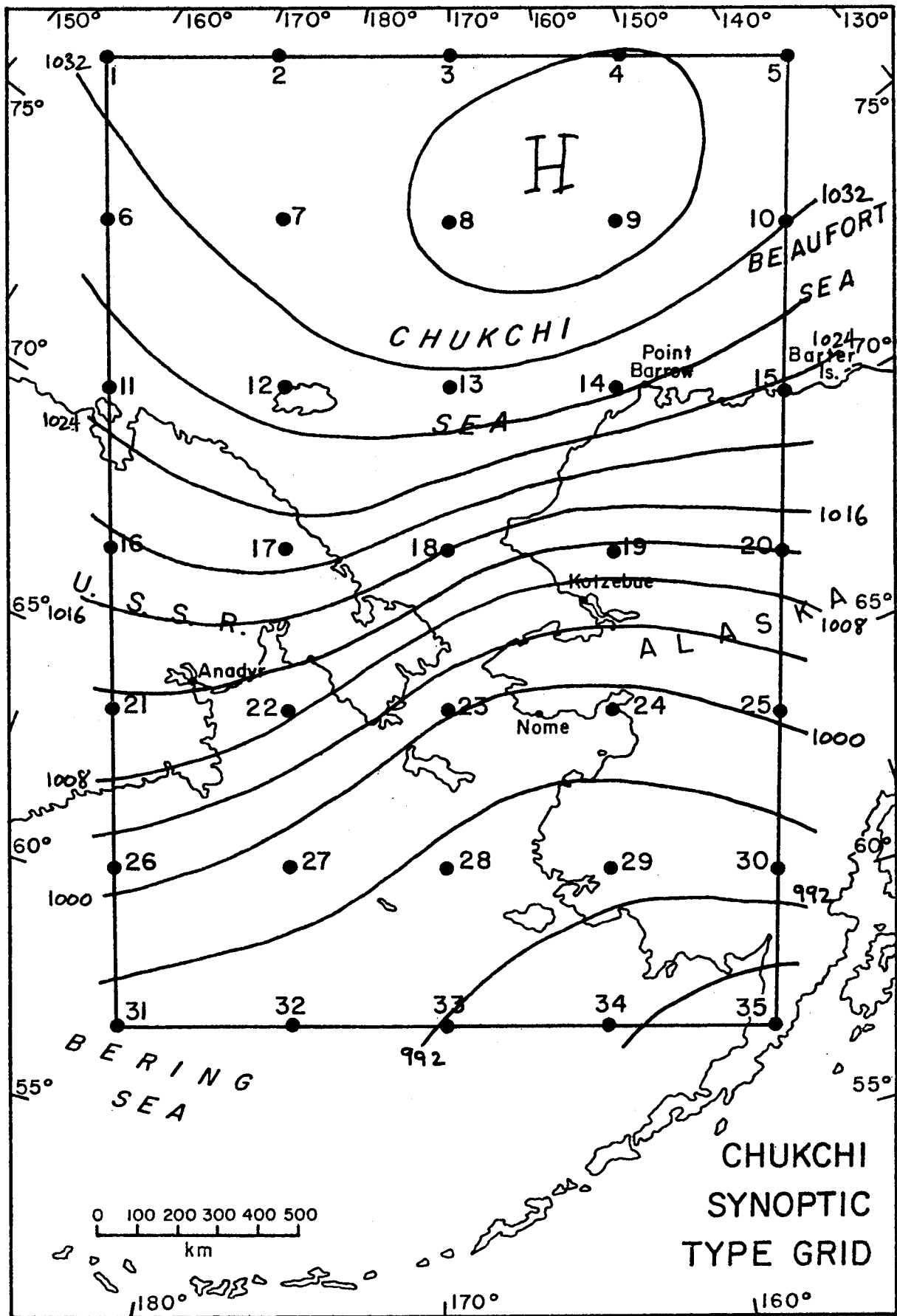
Characteristic isobar patterns for synoptic types 1-4 of the
Chukchi Sea catalog. (a) Type 1. Key Date 3/14/70.
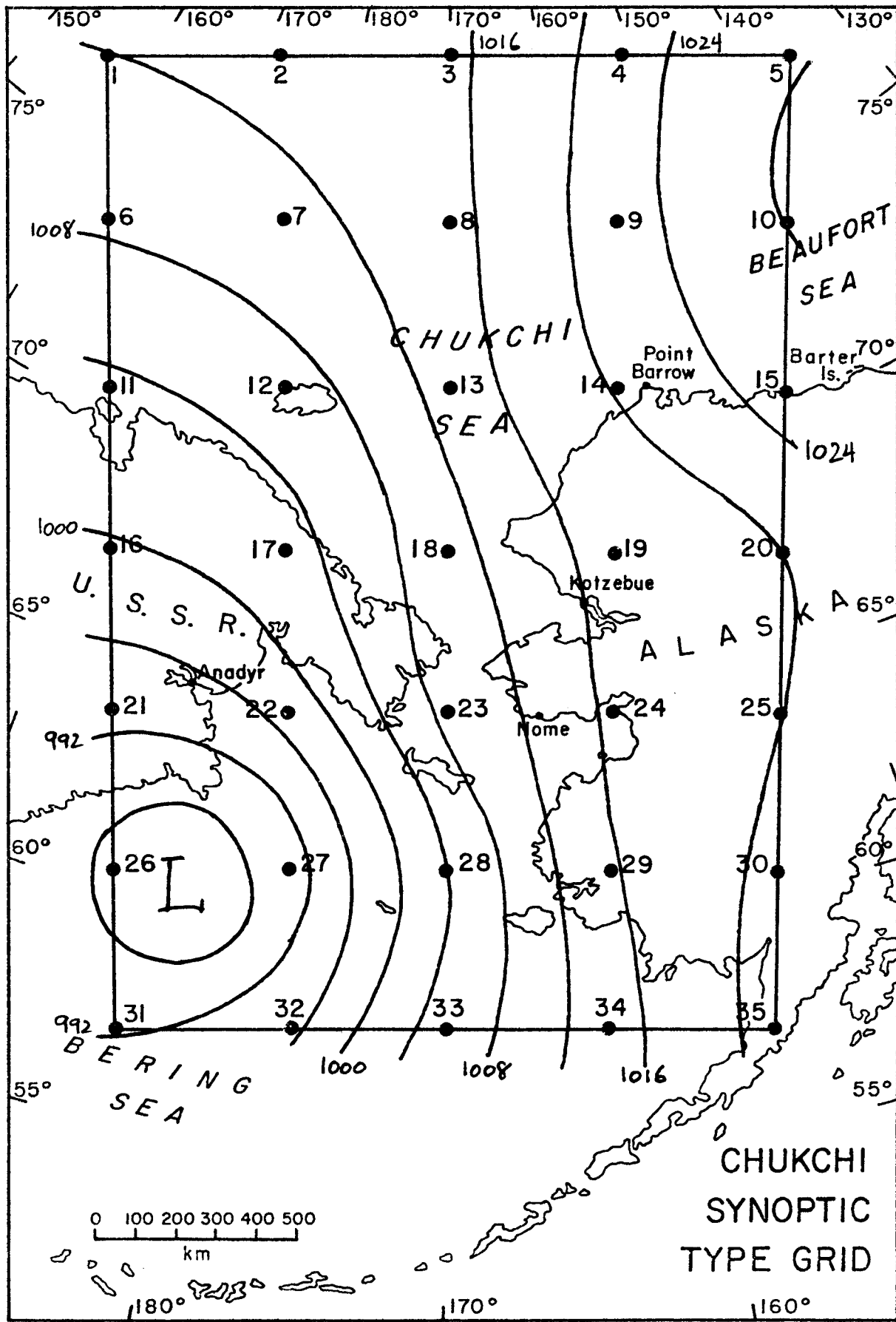
FIGURE 8-a

Characteristic isobar patterns for synoptic types 1-4 of the
Chukchi Sea catalog. (b) Type 2. Key Date 8/7/68.

FIGURE 8-b

628
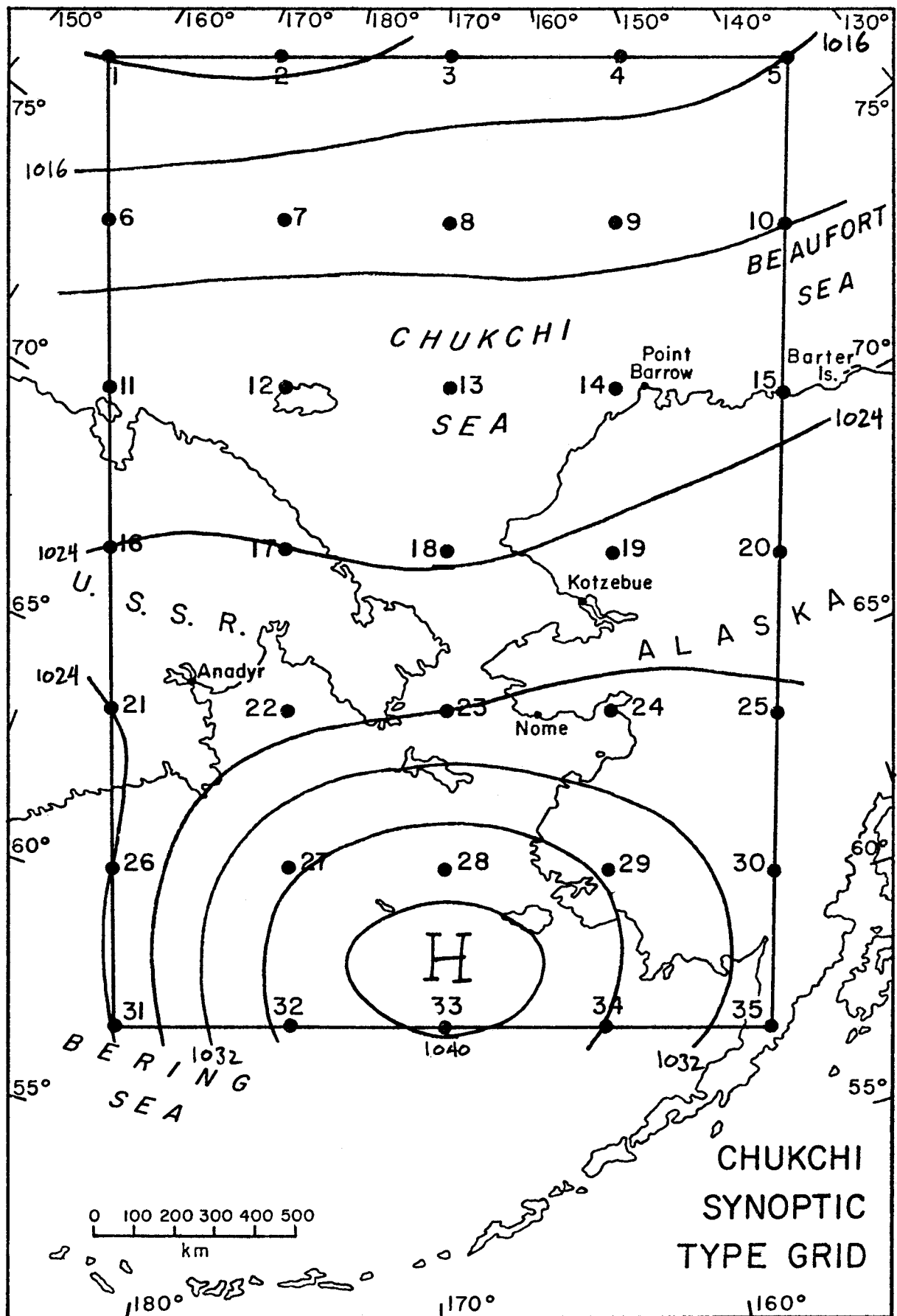
Characteristic isobar patterns for synoptic types 1-4 of the
Chukchi Sea catalog. (c) Type 3. Key Date 3/20/67.
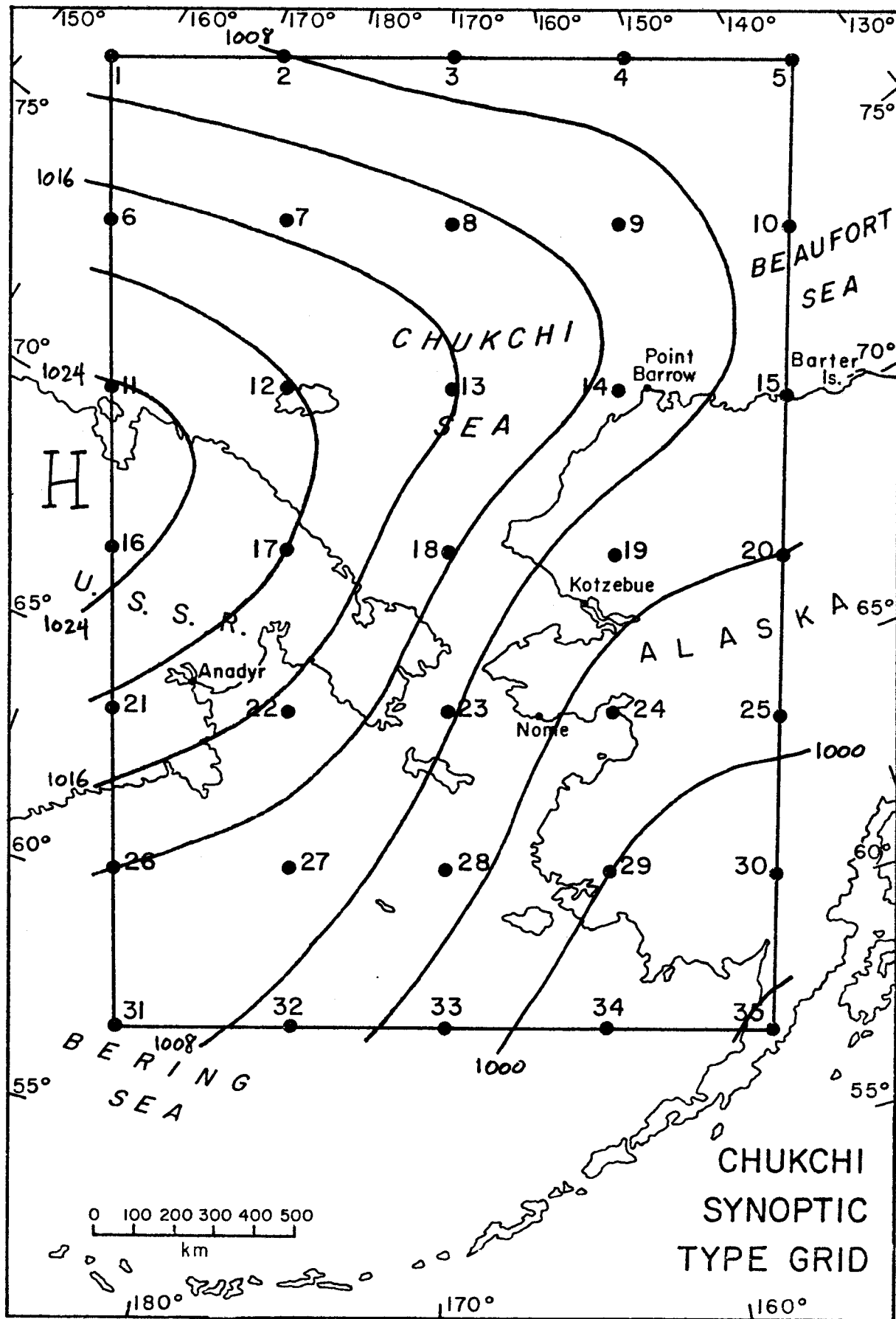
FIGURE 8-c

Characteristic isobar patterns for synoptic types 1-4 of the
Chukchi Sea catalog. (d) Type 4. Key Date 2/2/61.

FIGURE 8-d

% FREQUENCY OF CHUKCHI SYNOPTIC TYPES
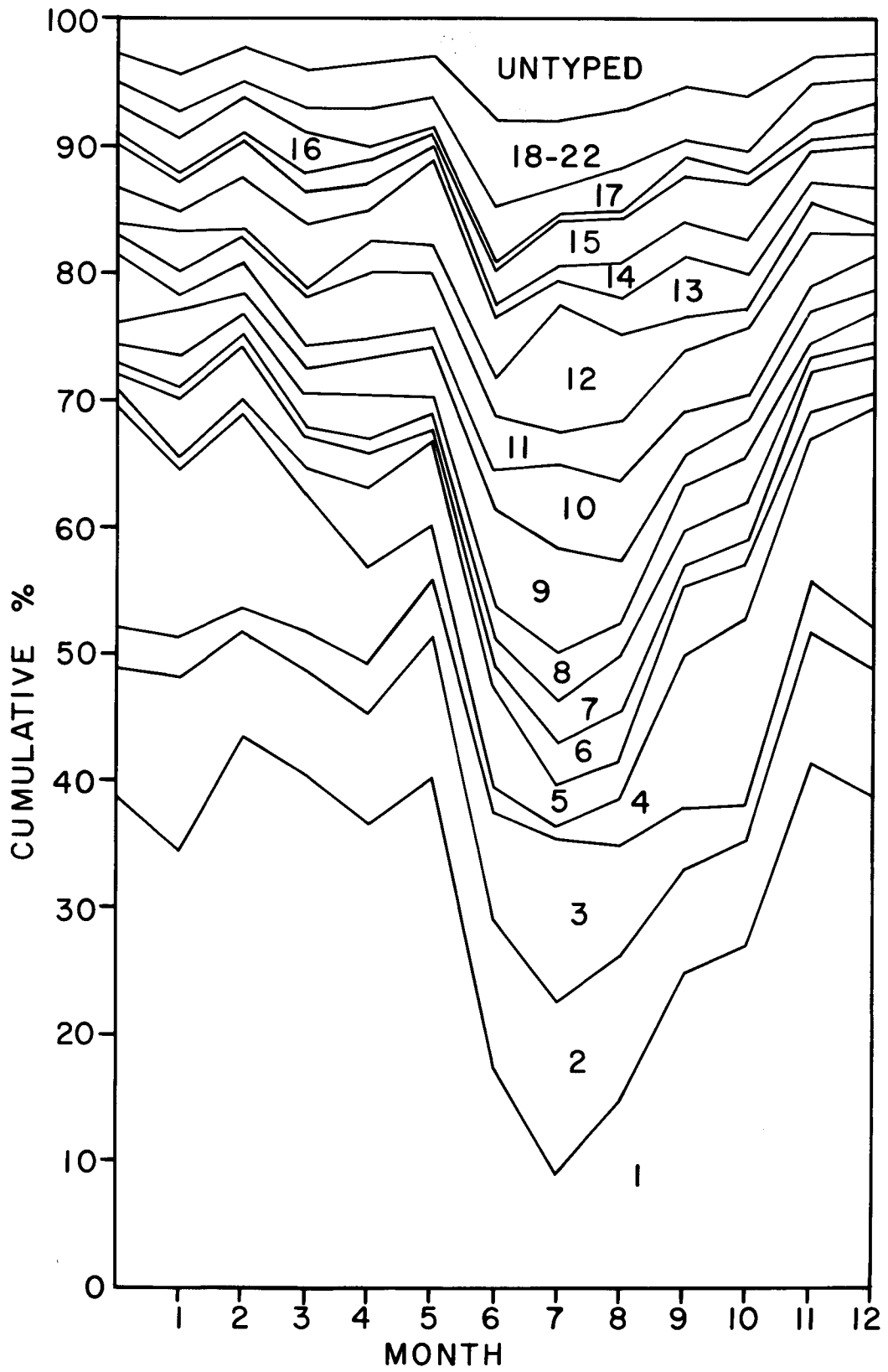
Relative frequency (percent) of synoptic types for the
Chukchi Sea sector, 1946-74.

FIGURE 9
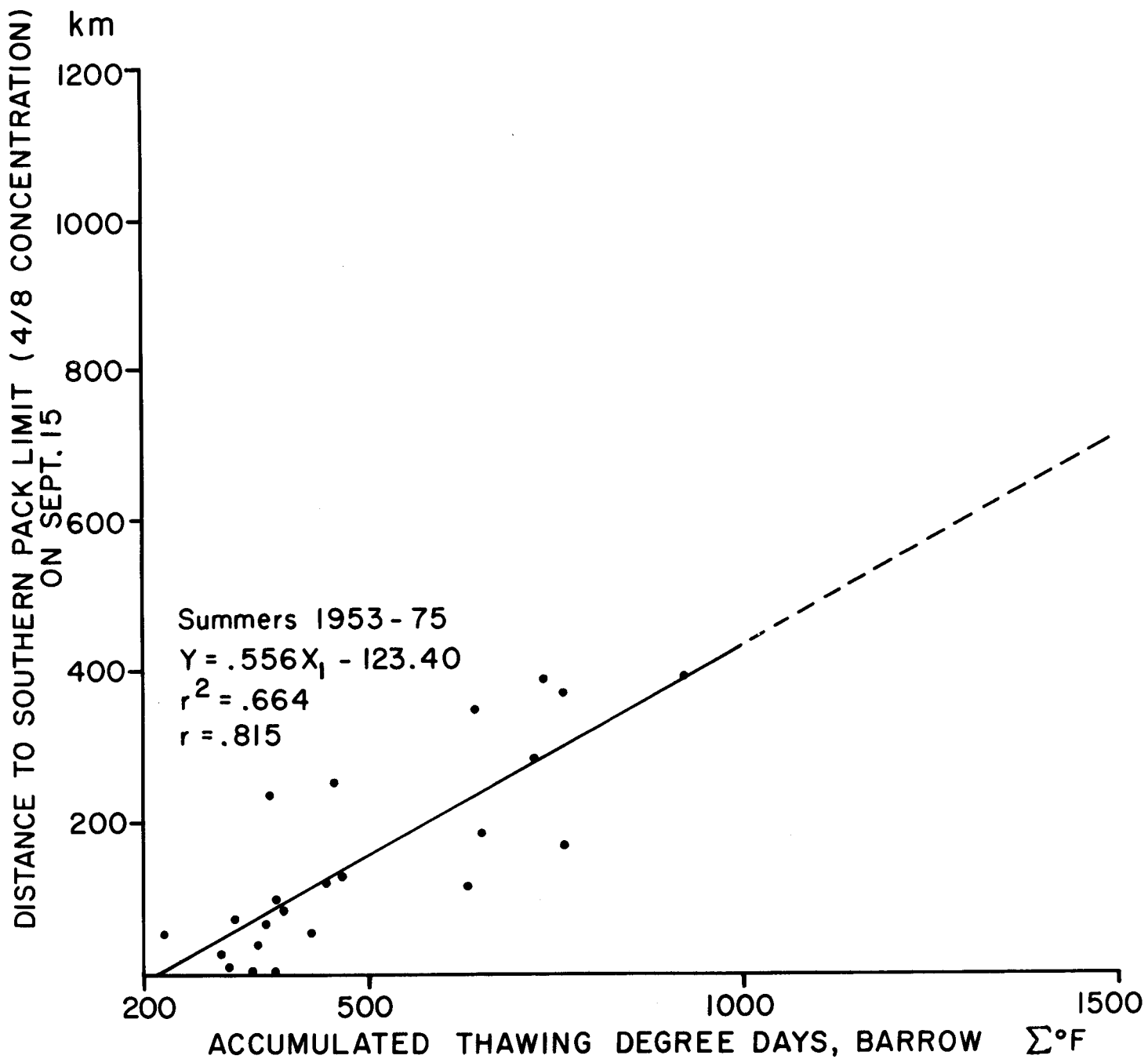
Distance to 4/8 ice concentration on September 15 off Point Barrow versus accumulated thawing degree days. Data for 1953-75. Projections illustrate the possible implications of higher summer temperatures, such as might occur in association with increasing CO_2 levels, assuming that a linear relationship obtains.

FIGURE 10

APPENDIX 1

REPORT OF THE LARSYS ANALYSIS

OF LANDSAT SPECTRAL INFORMATION

(Preliminary)

L. Bartolucci
Laboratory for the Application of Remote Sensing
Purdue University

and

R. E. Moritz
Institute of Arctic and Alpine Research
University of Colorado

INTRODUCTION

Near-shore waters along Alaska's Beaufort Sea Coast are covered by shore-fast sea ice for 9 to 10 months each year, and by April the fast ice extends 10 to 50 km seaward along the coast. Recent scientific interest in sea ice dynamics (Maykut, et al., 1972) and the prospects for offshore petroleum development in the region (Clarke, 1976) highlight the need for a better understanding of the behaviour and characteristics of shorefast sea ice. The LANDSAT satellite (formerly ERTS) has provided the first high-resolution, time-sequential data for monitoring the fast ice on a regional scale, since its launch in 1972. On the basis of available literature (McClain, 1972; Campbell, 1973; Barnes and Bowley, 1974; Hibler, et al., 1974; Reimnitz and Barnes, 1974; Stringer, 1974; Campbell, et al., 1975; Holmgren, et al., 1975) and inspection of melt season LANDSAT imagery of the Beaufort Shelf, it can be fairly stated that the amount of spectral and spatial ice information on these images exceeds our present interpretive capability. In this paper we present results of a multiband, computer-aided analysis of remote sensing data which was designed to improve this interpretive capability. The objectives of the study are:

   1) Evaluate computer-aided analysis techniques as applied to digital LANDSAT radiance data from melting shorefast sea ice.
   2) Determine the nature of the spectral and spatial ice information on the LANDSAT data, and the optimal techniques and tools for analysis of each information type.

ICE INFORMATION

The surface morphological characteristics of shorefast sea ice are most evident after the onset of melting (early June on the Beaufort Sea), but before ice breakup commences (about 10 July). Useful ice information which one might hope to resolve, interpret and map from remote sensing data include:

   1) Ice concentration: fraction of the sea surface covered by ice.
   2) Age categories: 1st-year, 2nd-year, and multi-year ice.
   3) Ice deformation: level ice, hummocked ice, pressure and shear ridge ice fields.
   4) State of ice surface: areal coverage and depth of melt pools vs. extent of bare ice or snow.
   5) Special ice features: dirty ice, grounded ice fields, ice islands. Interpretation and mapping of these phenomena are necessary for identification and understanding of ice hazards (e.g. surface albedos, initial ice thickness), and development of the fast ice canopy during the dark winter period (e.g. incursions of older ice, major grounded ice fields).

DATA AND METHODS

LANDSAT scene 1702-21093 (June 25, 1974, Figures 1 & 2) was chosen for analysis because of cloud-free skies, well developed puddling, and a relatively large amount of available correlative ice data, including SLAR imagery and color-IR photography of the study area. Hard copy images, including LANDSAT scenes over the study area before and after 25 June, SLAR images, and CIR photos were obtained for detailed "ice truthing" analyses of the study sector. The computer compatible tapes (CCT'S) for the southwest half of the selected scene were reformatted and geometrically corrected (Anuta, 1973) for use with the LARSYS computer processing system (Cardillo and Langrebe, 1960). Based on gray-scale printouts of the LANDSAT

radiance data, 7 representative fields, each with 10,201 picture elements (pixels), were chosen as input to the non-supervised classifier algorithms (Wacker, 1969). The digital processing sequence is illustrated in the flow chart (Figure 3). The saturated transformed divergence ("STD", see: Swain and Staff, 1972) between all pair-wise combinations of spectral classes was then used to merge spectrally non-separable classes from the 7 fields, resulting in nine spectral classes of LANDSAT pixels. All pixels on the ¼ scene were classified into these nine categories using the LARSYS Maximum Liklihood Classifier (Langrebe, et al., 1968). The results can be retreived as an alphanumeric map, color-coded slides, or as statistical information on the number of pixels classified into each category. Alphanumeric maps and test-field radiance statistics were used to compare ice characteristics (determined from SLAR, CIR, and LANDSAT hard copy) with the spectral classes at coincident locations.

RESULTS

Means and standard deviations of the spectral responses for each of the nine classes are shown in Table 1. Class #5 comprises pixels with a noise response in band 6, occurring every 6th scan line over certain parts of the scene (see: Portner, 1973), but is otherwise similar to #4. A coincident spectral plot of the mean responses ± 1 standard deviation is shown in Figure 4. It is note-worthy that all spectral responses decrease from band 4 through band 7, with the exception of #9. STD values for all 1, 2, 3, and 4 band combinations indicate that:

1) Band 6 is the single most effective band for correctly separating the spectral classes.

2) Spectral redundancy exists between the two visible bands (4 & 5) and also between the two photo-IR bands (6 & 7).

3) Three bands (4, 5, & 6) produce a classification with approximately the same % correct recognition of classes as a full 4-band classification.

4) The nine spectral classes are highly separable, yielding almost 100% correct recognition of classes.

Analysis of the surface types in relation to the LARSYS spectral classes produced the following results:

1) <u>Class 2</u> includes large fields of level, 1st-year ice with about 40% areal coverage of puddles and shallow-medium relative puddle depths. Also, several ridge systems, including at least one grounded system, were primarily composed of class 2 pixels.

2) <u>Class 3</u> is level, 1st-year ice with about 60% areal coverage of puddles having medium relative depths.

3) <u>Classes 4 & 5</u> are identical except for the 6th-line noise response in #5, band 6. Ice types include level to highly-deformed 1st-year ice, and, possibly, some older ice types. Puddling is generally poorly developed, with small areal coverage or very shallow depths or both. Some class 4 & 5 ice apparently drained between 6/21 and 6/25. Flat lake ice with little or no puddle development was also classified as 4 - 5. One large grounded ice mass, possibly a hummock field, was primarily classes 4 & 5.

4) <u>Class 6</u> is level to highly-deformed 1st-year ice. Puddling character-istics were intermediate between those of classes 2 and 3. Often class 6 appeared as "boundary pixels" between fields of class 2 and class 3, and thus represent a spatial average of these classes.

5) <u>Class 7</u> is open sea water.

6) <u>Class 8</u> is level, 1st-year ice with nearly 100% areal coverage of puddles

having relatively shallow depths. This class occurs predominantly on lake ice, but occasionally on the sea ice also.

7) <u>Class 9</u> includes relatively dry land surfaces, such as tundra, gravel, and the offshore barrier islands.

8) Class 10 occurred over 4 types of surface. These were: level, deeply-flooded 1st-year sea ice, wet-to-flooded tundra marshes, river channels in the vicinity of deltas, and sediment-laden water flowing out over the shorefast ice.

DISCUSSION AND CONCLUSIONS

Regarding the desired ice information, the following conclusions can be drawn:

1) Ice concentration can be accurately assessed from LANDSAT spectral information: class #7 was exclusively open sea water and all other classes over the sea were ice types.

2) Age categories could not be determined from the data sets, mostly because very little older ice was present on the scene. However, the one possible area of older ice was classified as predominantly #'s 4 & 5, which also include 1st-year ice types, causing us to be pessimistic about differentiation of ice ages from spectral information only. Areas of older ice on other LANDSAT scenes appear extremely bright in June, as do 1st-year fields with limited puddling development.

3) Ice deformation was partially distinguished: i.e. classes 3,8, and 10 (when 10 was ice) were always level ice. The remaining ice classes, however, contained ice ranging from level to highly-deformed.

4) Areal coverage and depth of melt pools on the ice surface are by far the most important factors in determining the spectral class of a given ice field. The separation of puddle depth from areal coverage within a pixel is difficult, however (see below).

5) Regarding special ice features: No ice islands could be identified on the ice truthing data sets, class #10 included ice covered by sediment-laden runoff, but was not distinct from several other surface types, and one large, grounded ice mass, possibly a hummock field, was primarily classified as #'s 4 & 5.

Calculations of direct-beam spectral reflectance, transmittance and absorptance effects in LANDSAT resolution elements (pixels) with variable proportional coverages of bare ice and puddles, and variable puddle depths have shown the strong dependence of the LANDSAT spectral responses on puddling. Figure 5 shows the schematic model for the calculations: each LANDSAT pixel encompasses a number of "bare ice" and "puddle" elements, so the spectral response is a weighted spatial average from the two surfaces. Figures 6-8 show the direct-beam spectral reflectances for various areal coverages and depths of puddles based on the model. Qualitative agreement with the LARSYS-generated classes is evident in that all curves drop from the visible to the photo-IR portion of the spectrum. High areal puddle coverage with shallow depths influences mainly the IR bands, while deep puddles cause significant decreases in the reflectance of visible bands also. These effects are a direct consequence of the strong wavelength-dependence of α_λ, the spectral attenuance coefficient for water. Thus most of the useful ice information characteristics are only distinguished if they happen to find surface expression in the puddling distribution.

A much better computer-aided classification of sea ice could be accomplished by including a X-band SLAR reflectance as a fourth or fifth spectral response at each point. The surface roughness of the ice fields can be assessed on this basis (Dunbar, 1975). It was also found that accurate location and interpretation of

ice features such as ridge systems, hummock fields, and, possibly, some ice age categories, can be made by manual interpretation of time-sequential, hard copy LANDSAT data, in conjunction with SLAR imagery and CIR photos. These analyses, however, require an interpretation of differential gray-tone areas with complex spatial configurations and the time changes in the ice fields. The infinite variety of spatial patterns which might, for example, be interpreted as a "ridged ice zone" by an image analyst cannot, at present, be quantified for use in automatic computer processing of LANDSAT data.

Finally, the redundancy of the two visible and two infrared bands indicates that considerable savings can be accomplished by using two or three bands for manual or machine processing of sea ice imagery during the melt season.
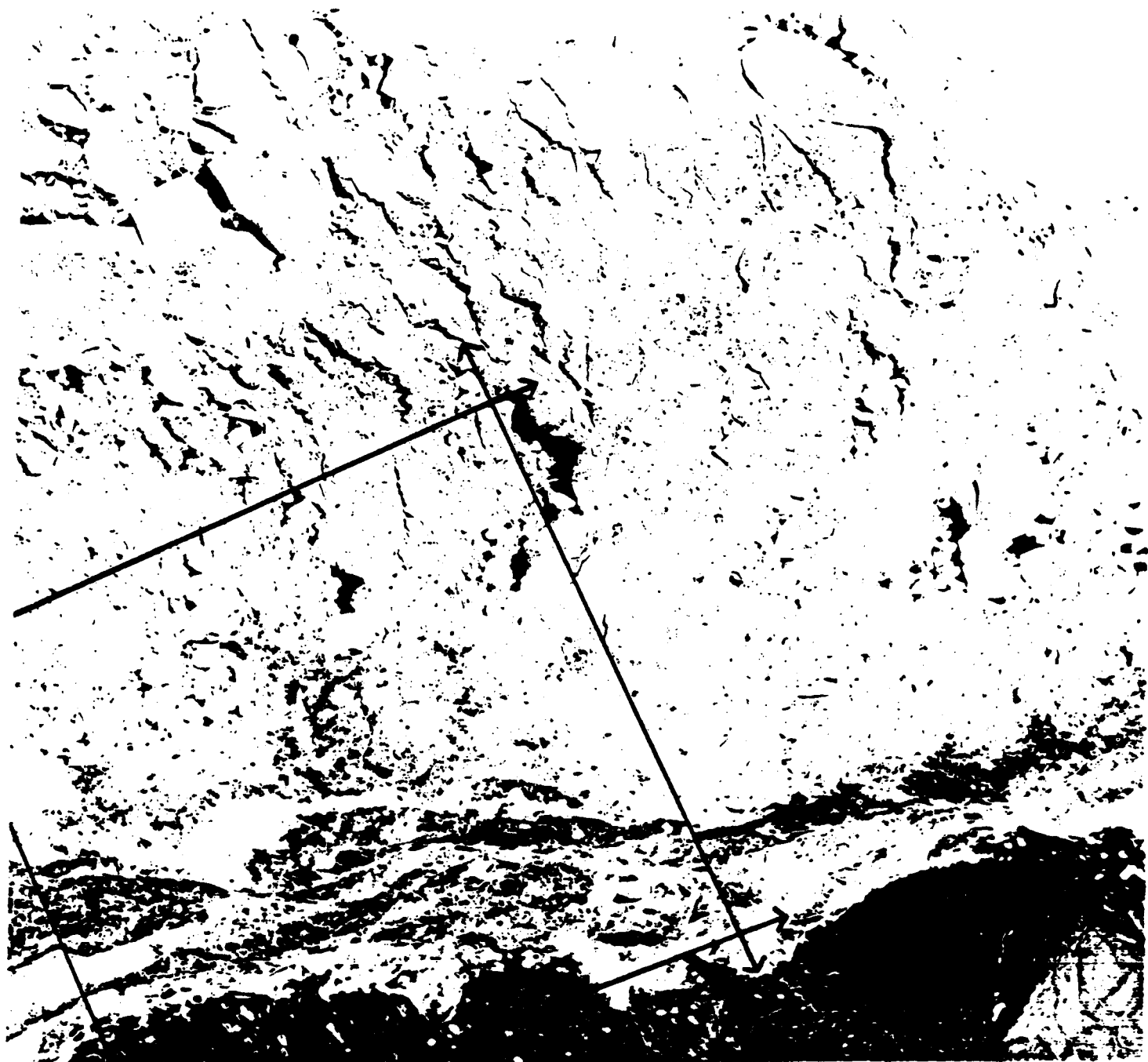
FIGURE I

LANDSAT Scene 1702-21093. LARSYS Classification Area

Outlined in Black.

Figure 2.

NORTHERN ALASKA

LANDSAT Frame ID: 1702-21093
June 25, 1974

```
          ┌─────────────────────────┐
          │     LANDSAT MSS Data     │
          │       (4 Bands)          │
          └─────────────────────────┘
                       │
                       ▼
          ┌─────────────────────────┐
          │   Gray-scale Printouts   │
          │       (4 Bands)          │
          └─────────────────────────┘
                       │
                       ▼
          ┌─────────────────────────┐
          │      Selection of 7      │
          │     Clustering Areas     │
          └─────────────────────────┘
                       │
                       ▼
          ┌─────────────────────────┐
          │    Clustering of Each    │
          │  Area into 10 Classes    │
          └─────────────────────────┘
                       │
                       ▼
          ┌─────────────────────────────┐
          │   Spectral Separability of  │
          │ All Pair-wise Combinations  │
          │        of Classes           │
          └─────────────────────────────┘
                       │
                       ▼
          ┌─────────────────────────┐
          │  Pool Together Spectrally│
          │    Similar Classes and   │
          │      Add Null Class      │
          └─────────────────────────┘
                       │
                       ▼
          ┌─────────────────────────┐
          │  Classification of Entire│
          │    Area into 9 Spectral  │
          │  Classes and 1 Null Class│
          └─────────────────────────┘
                       │
                       ▼
          ┌─────────────────────────┐
          │ Display Classification Map│
          └─────────────────────────┘
```

Figure 3. Sequence of processing and analysis steps for
            Fast-Ice mapping.

640

COINCIDENT SPECTRAL PLOT (MEAN PLUS AND MINUS ONE STD. DEV.) FOR CLASS(ES)

                                                                        LEGEND
                                                                          A = CLASS 1 NULL 0.2
                                                                          B = CLASS 2 2
                                                                          C = CLASS 3 3
                                                                          D = CLASS 4 4
                                                                          E = CLASS 5 5
                                                                          F = CLASS 6 6
                                                                          G = CLASS 7 7
                                                                          H = CLASS 8 8
                                                                          I = CLASS 9 9
                                                                          J = CLASS 10 10
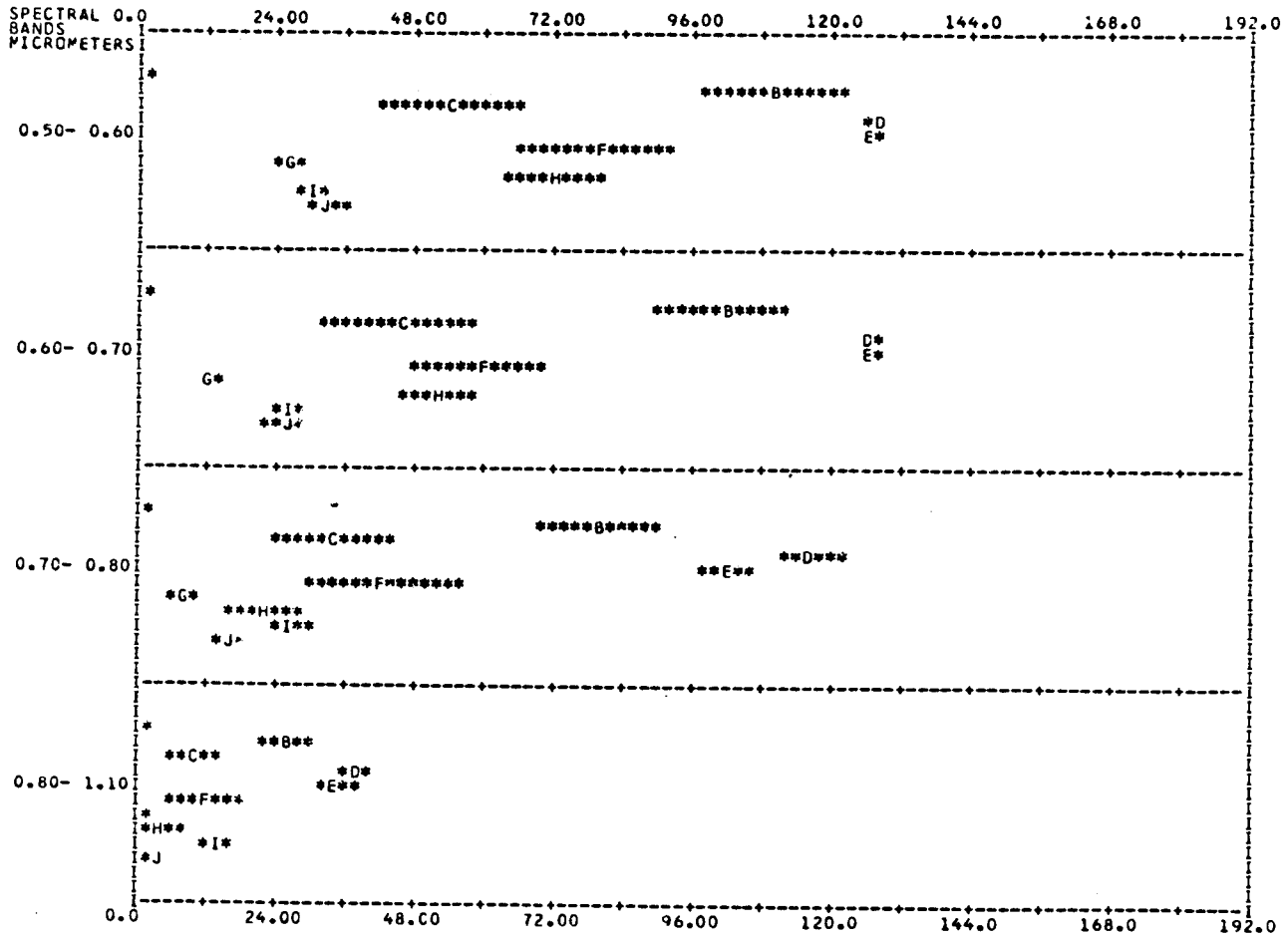
Figure 4.   Coincident spectral plot of all non-supervised
            classes used in the final Fast-Ice classification.

641
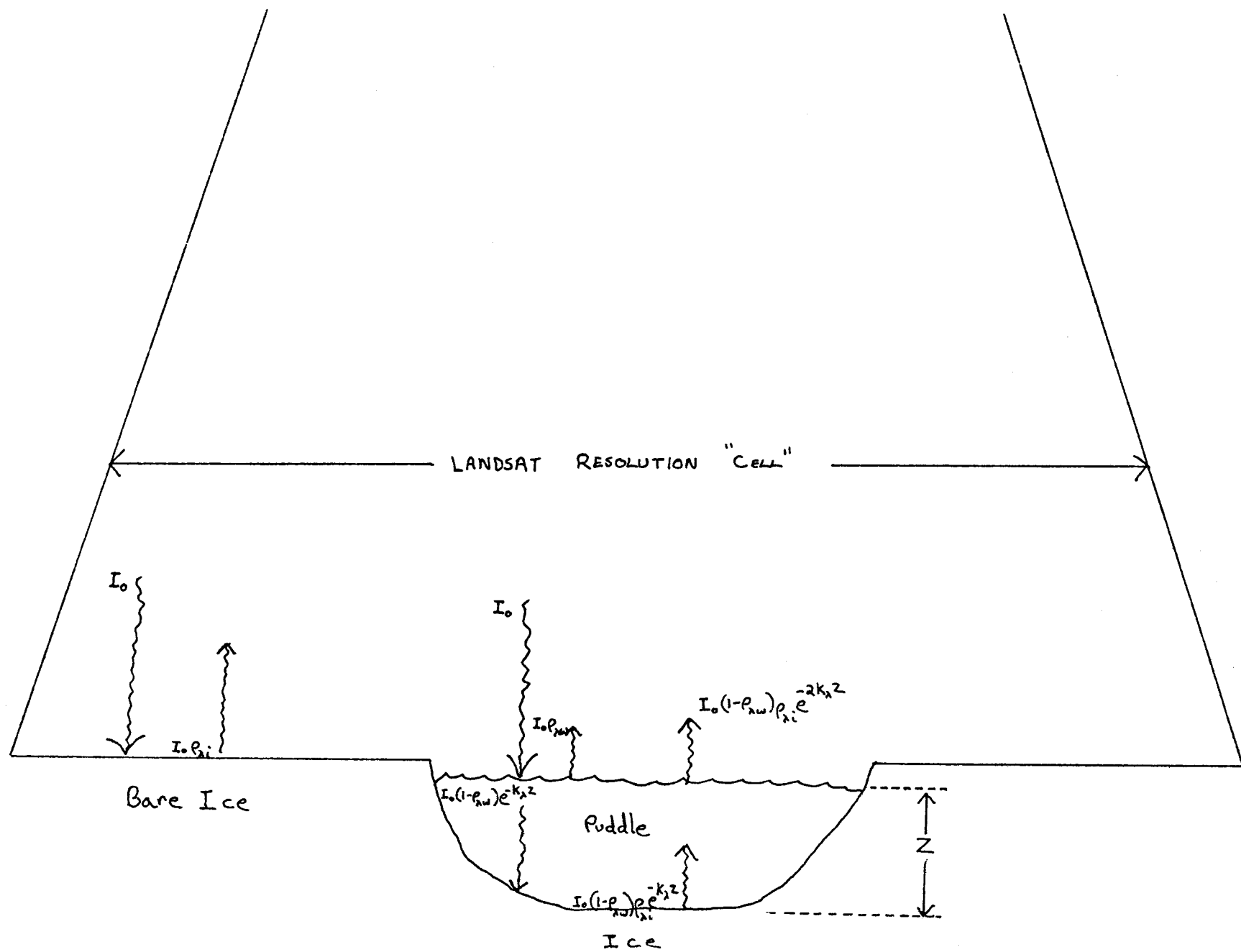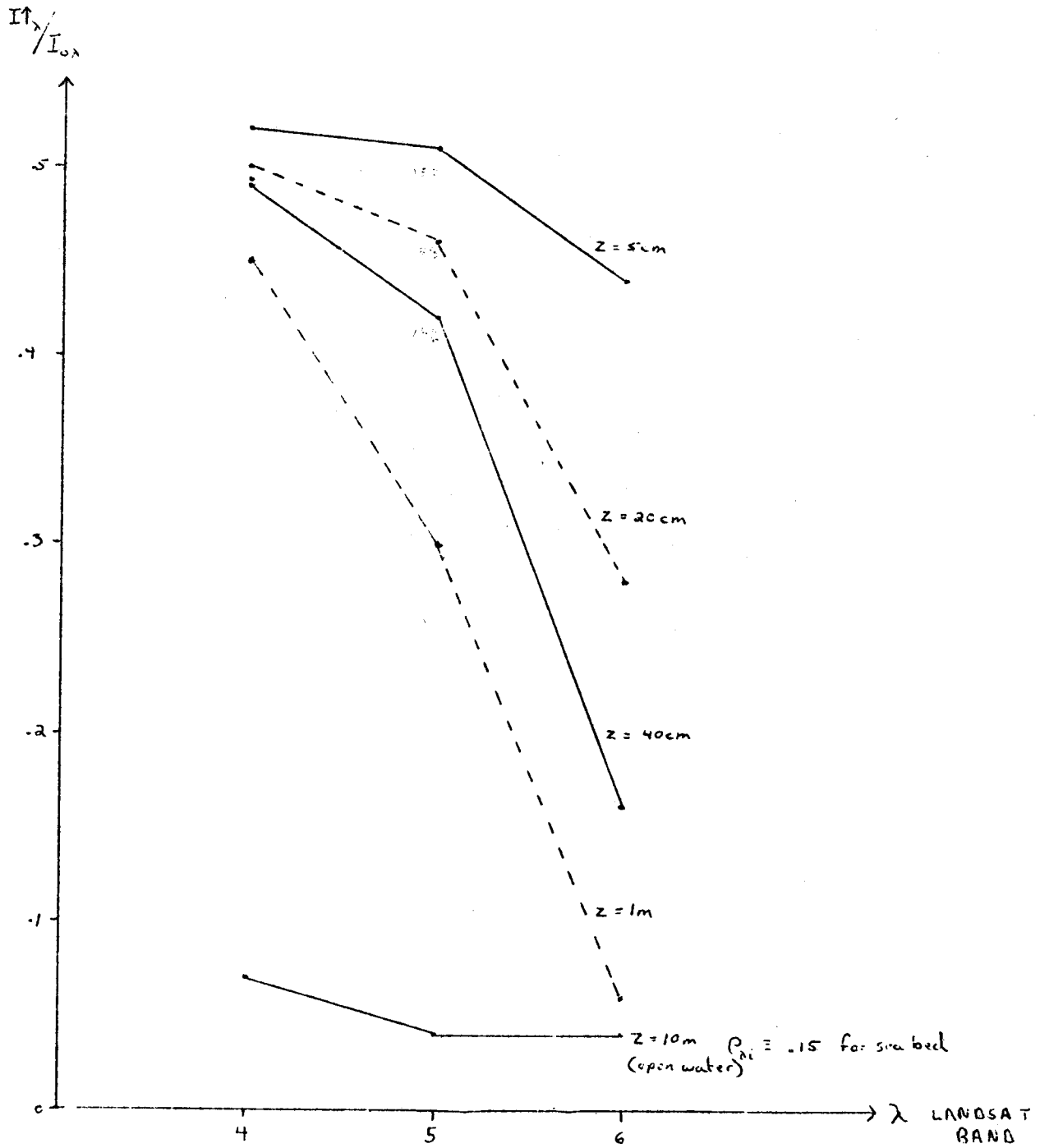
Figure 5

Figure 6

Spectral Reflectances for $A_i = 0$

$$\frac{I\uparrow_\lambda}{I_{o\lambda}} = A_i \rho_{\lambda i} + (1-A_i)\rho_{\lambda w} + (1-A_i)(1-\rho_{\lambda w})\rho_{\lambda c}\, e^{-2k_\lambda z}$$
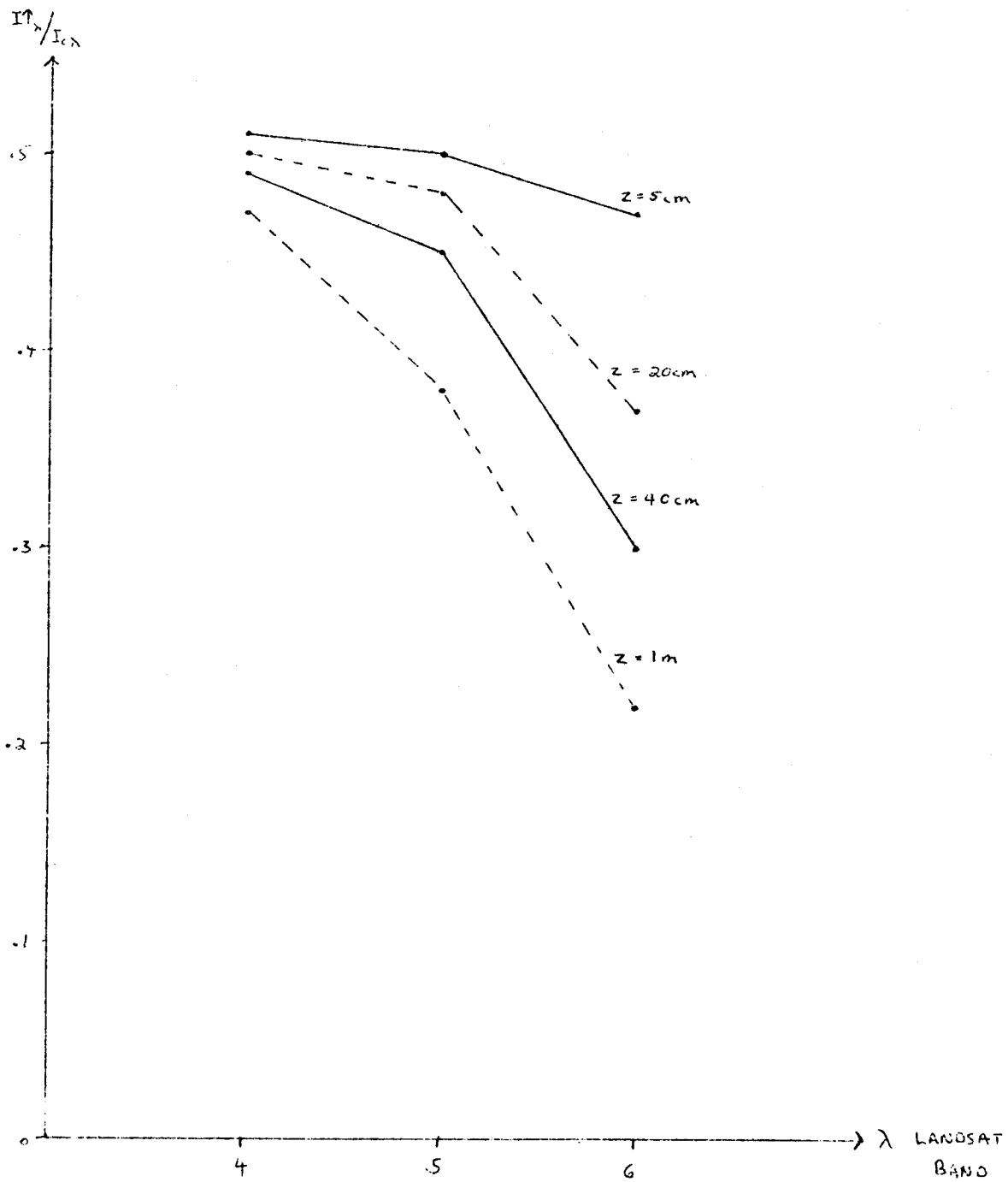
Figure 7

SPECTRAL REFLECTANCES FOR $A_c = 0.4$

Figure 8
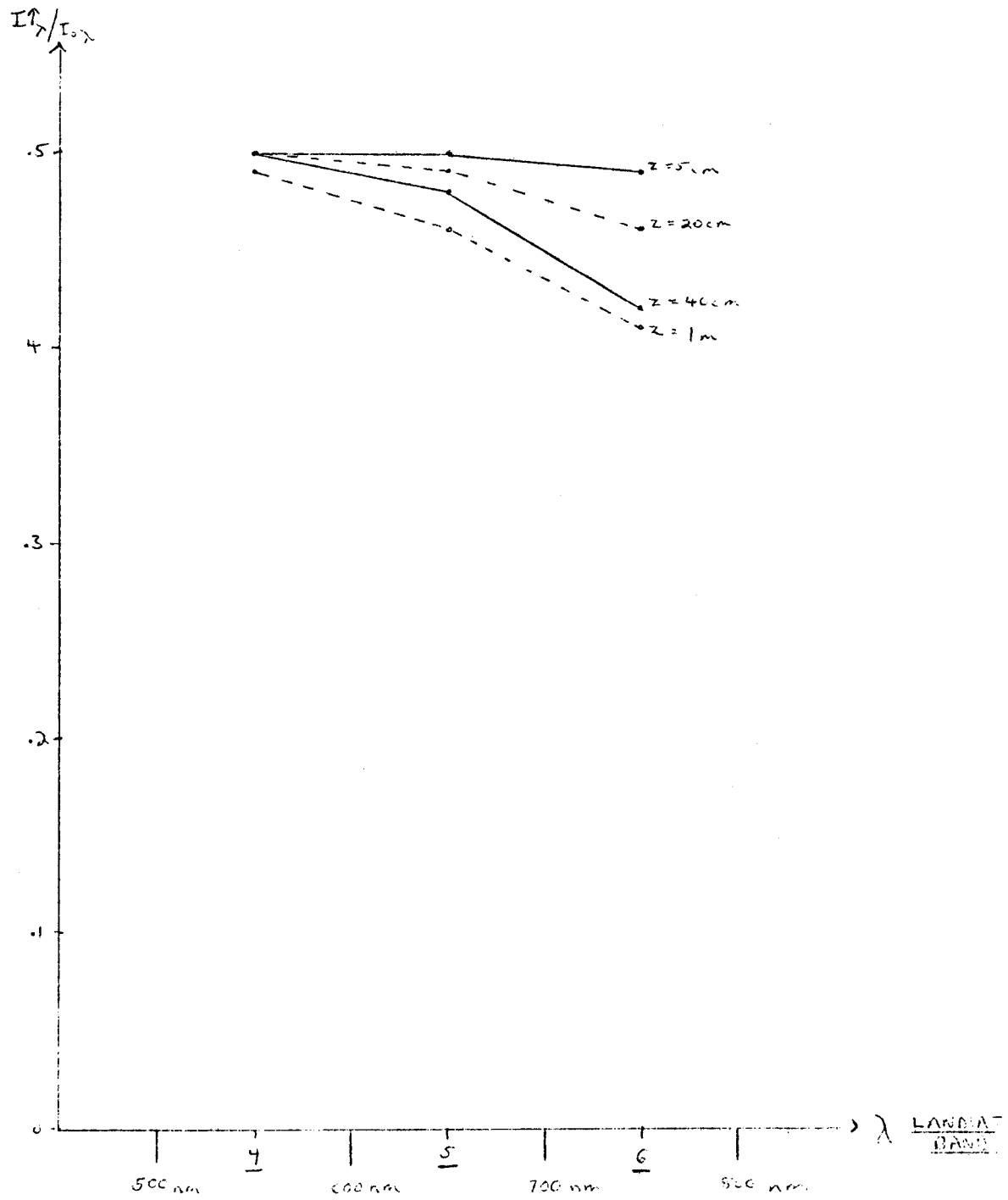
SPECTRAL REFLECTANCES FOR $A_i = 0.8$

Table 1. Mean Spectral Responses and Standard
Deviations for the Nine Non-Supervised
Classes of Fast Ice.

LANDSAT WAVELENGTH BANDS

Class #		4	5	6	7
2	Mean	110.2	101.4	79.7	25.6
	Std. Dev.	11.5	11.0	9.5	3.6
3	Mean	53.5	45.0	34.5	10.7
	Std. Dev.	12.3	12.5	10.5	3.9
4	Mean	127.0	127.0	116.8	38.0
	Std. Dev.	0.6	0.2	5.2	2.8
5 (noise)	Mean	126.9	126.6	101.7	34.3
	Std. Dev.	0.2	1.2	4.0	2.9
6	Mean	79.7	59.3	42.7	12.2
	Std. Dev.	12.9	10.7	13.1	5.4
7	Mean	25.7	12.9	7.7	0.9
	Std. Dev.	1.9	1.6	1.5	0.7
8	Mean	72.2	52.0	22.2	4.6
	Std. Dev.	7.3	6.4	6.0	2.5
9	Mean	29.3	25.7	26.9	13.6
	Std. Dev.	1.8	1.7	2.1	1.7
10	Mean	32.8	25.7	15.9	3.3
	Std. Dev.	3.5	3.1	2.1	1.4

APPENDIX II

MAPS OF NEAR-SHORE ICE CONDITIONS FOR THE

CHUKCHI SEA COAST, SUMMERS 1973-75

647

Map No. 1 : Barrow Sec., 23 MAR 73, 1243-22093

Legend A pack ice

1 shore fast ice

2 darker, newer (thinner) shore fast ice

The edge of the pack ice cannot be determined due to
cloud cover. The area between shore fast and pack
ice is covered with a very thin layer of new ice.
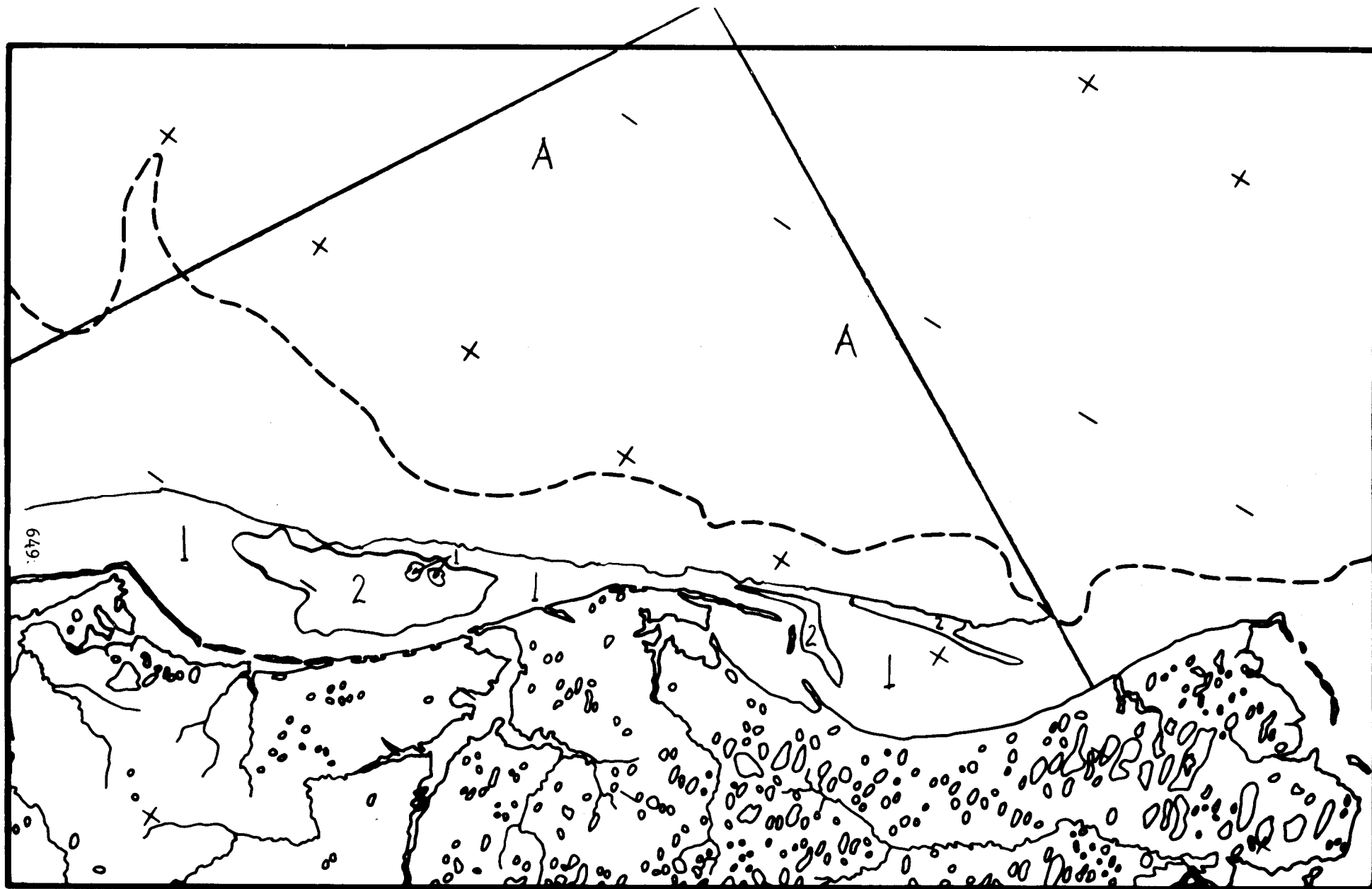
648

SHOREFAST SEA ICE
SURFACE MORPHOLOGICAL CHARACTERISTICS
CHUKCHI SEA COAST: BARROW SECTOR

23 March 1973

Map No. 2: Barrow Sec, 11 APR 73, 1262-22151

        Legend A pack ice - shows many leads and young ice

                  X open water with some new ice and floes

                  1 shore fast ice, nearly homogeneous but with indication of thinner ice seaward

                  2 new ice which formed in a large offshore lead

                  3 a combination of new, young and older floes in the lead area
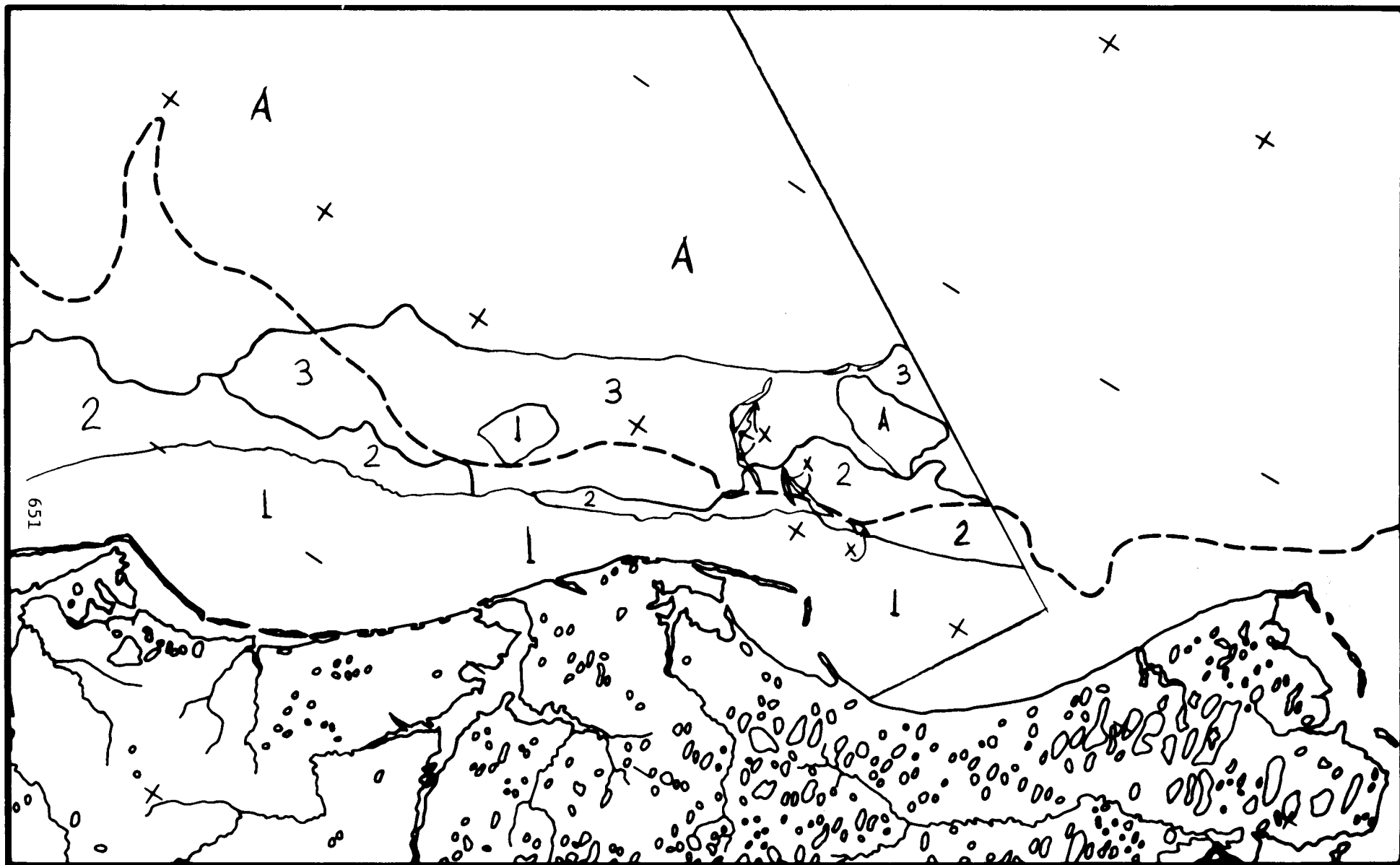
SHOREFAST SEA ICE
SURFACE MORPHOLOGICAL CHARACTERISTICS
CHUKCHI SEA COAST: BARROW SECTOR
11 April 1973

Map No. 3: Kotzebue Sec, 02 JUN 73, 1314-22043

Legend X open water

A pack ice

B primarily type 1 ice which has been broken,
75-90% ice coverage

1 generally flat, continuous, light tone, shore
fast ice

2 continuous shore fast ice that exhibits more
water on its surface than type 1

3 ice of types 1 and/or 2 which is disected
by many cracks

4 like types 1 and 2 except for increased amount
of surface melt water

5 no homogeneous ice made up of floes with varying
amounts of surface melt water

6 like type 5 but with more surface melt water

7 the lightest tone on this image, apparently flat
and thin

8 like type 7 but with melt water on the surface

9 flat ice with extensive and reletively deep
surface melt water

10 flooded or ice that is breaking up

11 partially obsured by clouds, but like type 5
with some young ice and more surface water
than type 6
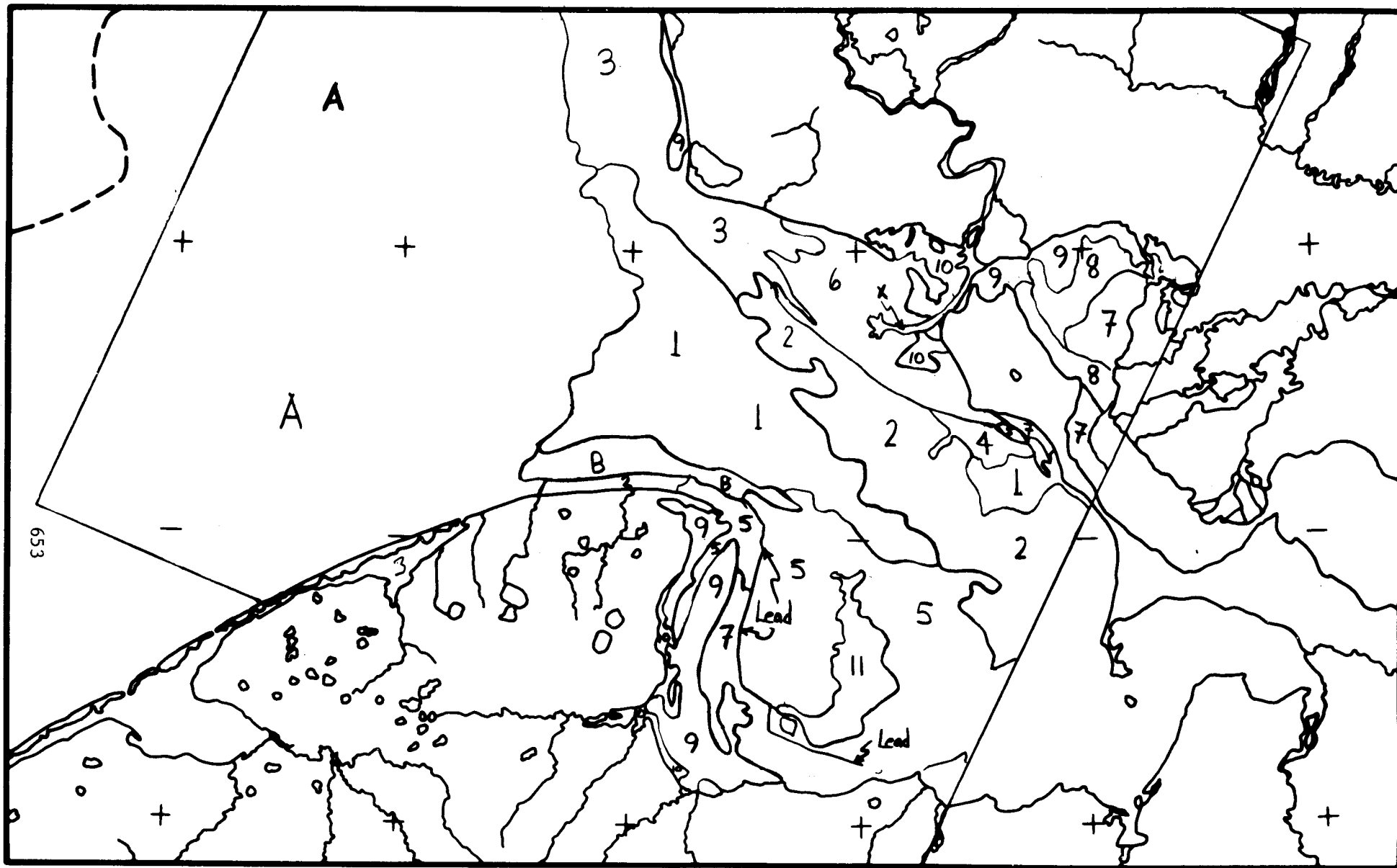
SHOREFAST SEA ICE
SURFACE MORPHOLOGICAL CHARACTERISTICS
CHUKCHI SEA COAST: KOTZEBUE SOUND SECTOR
2 June 1973

Map No. 4: Barrow Sec, 05 JUN 73, 1317-22203

Legend X open water

A pack ice

1-3 All three types are generally homogeneous
    shore fast ice types that exhibit an increasing
    amount of surface water from 1 to 3

4   slightly more surface water than type 3 but
    not as homogeneous

5   discontinuous ice (75-85% ice coverage) that
    would appear to be derived from ice type 3
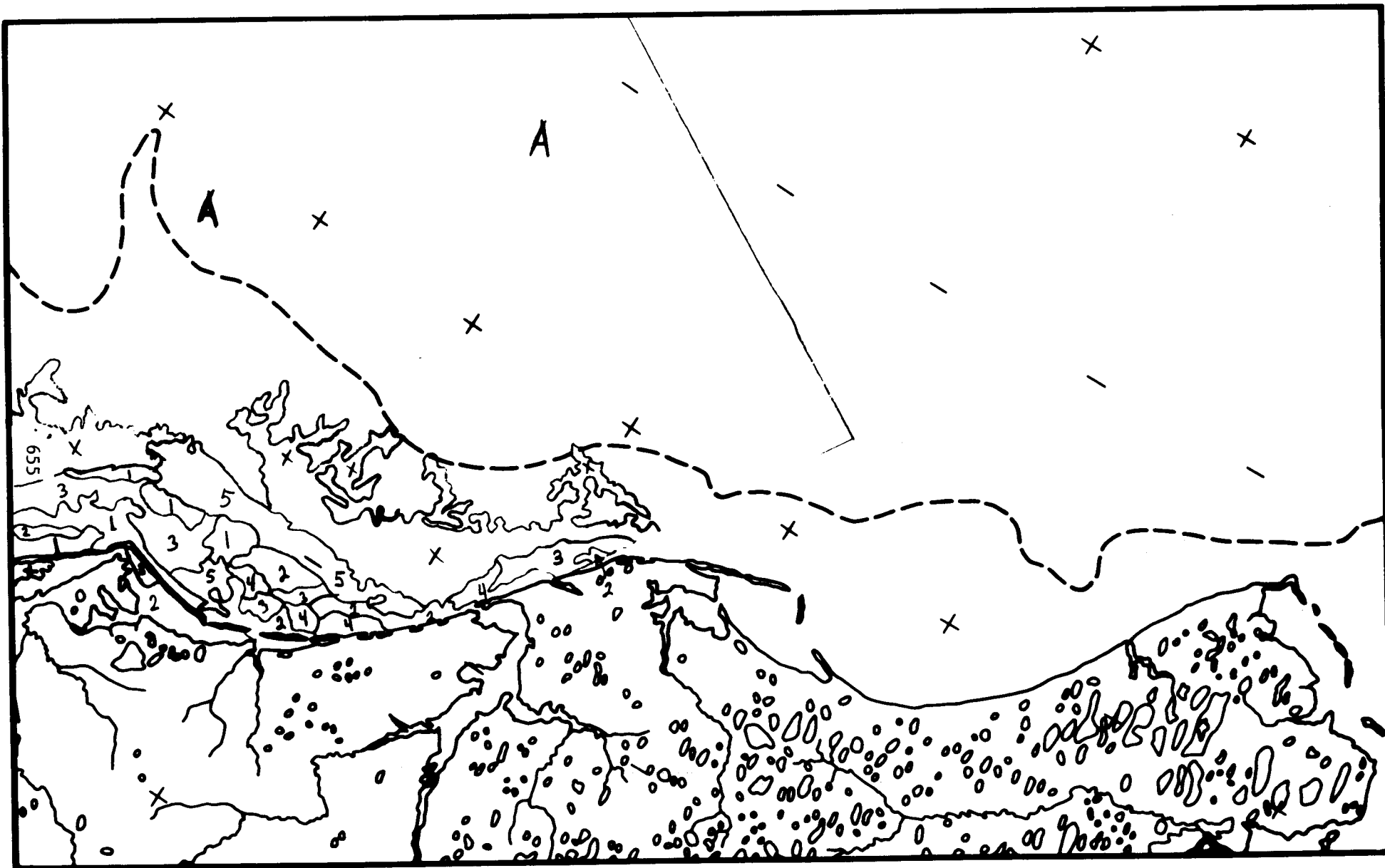
SHOREFAST SEA ICE
SURFACE MORPHOLOGICAL CHARACTERISTICS
CHUKCHI SEA COAST: BARROW SECTOR
5 June 1973

Map No. 5: Barrow Sec, 23 JUN 73, 1335-22201

Legend X open water

A pack ice

1-5 The shore fast ice in this frame is all con-
tinuous and very nearly homogeneous. Increasing
amounts of surface water is indicated from
the image from type 1 to type 5 which shows
an advanced stage of melting.

6   This type is not continuous at all points
and is breaking up. The ice is flooded at
most places and is probably very thin in
places too.
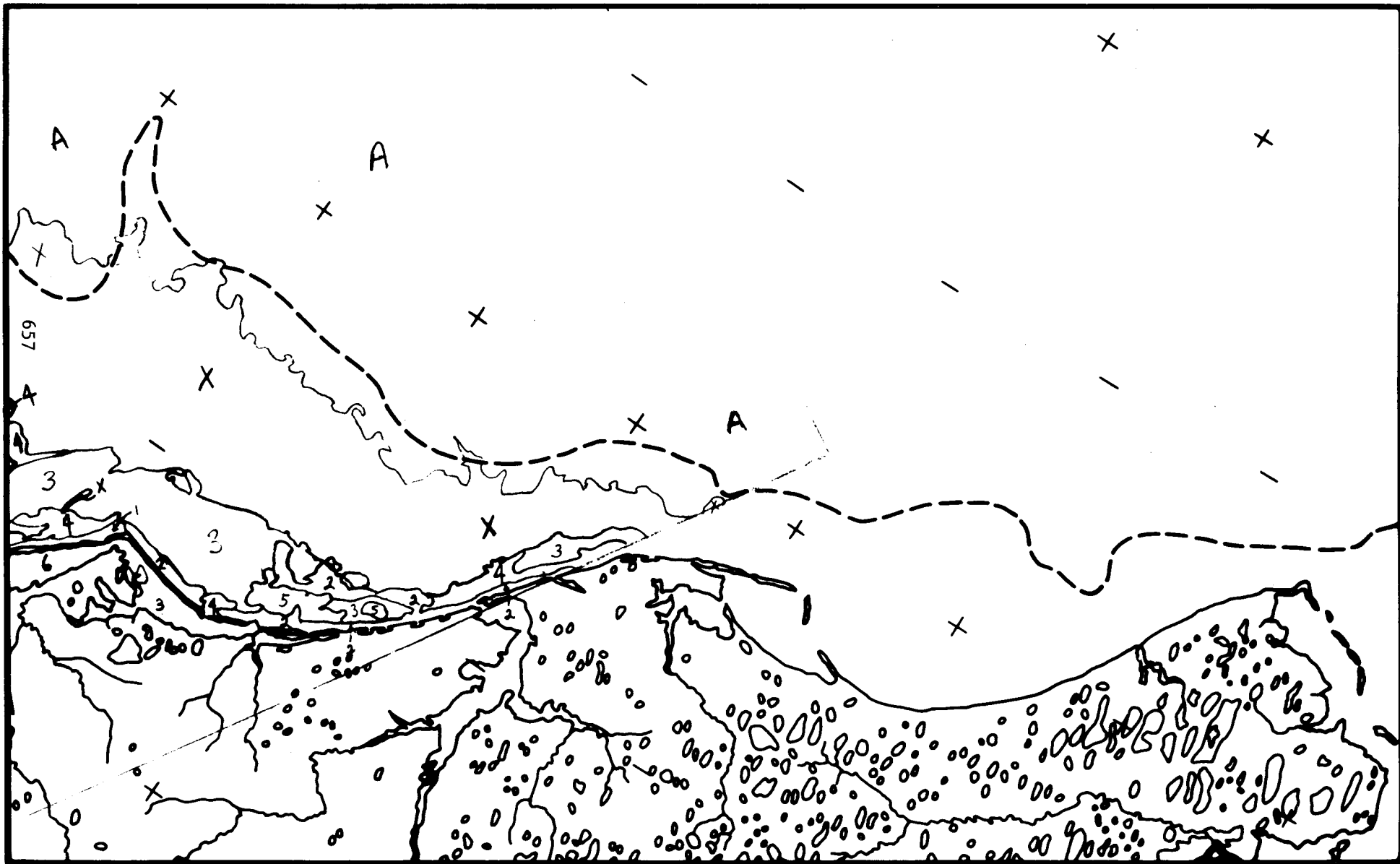
656

SHOREFAST SEA ICE
SURFACE MORPHOLOGICAL CHARACTERISTICS
CHUKCHI SEA COAST: BARROW SECTOR
23 June 1973

Map No.   6:   Point Hope Sec, 23 JUN 73, 1335-22210

Legend   X   open water

S   shore fast ice

1   floes which exhibit surface features of shore
fast ice

2-7 unconsolidated ice with increasing amounts of
surface melt water from 2 to 7

B   areas where ice concentration is less than
50%
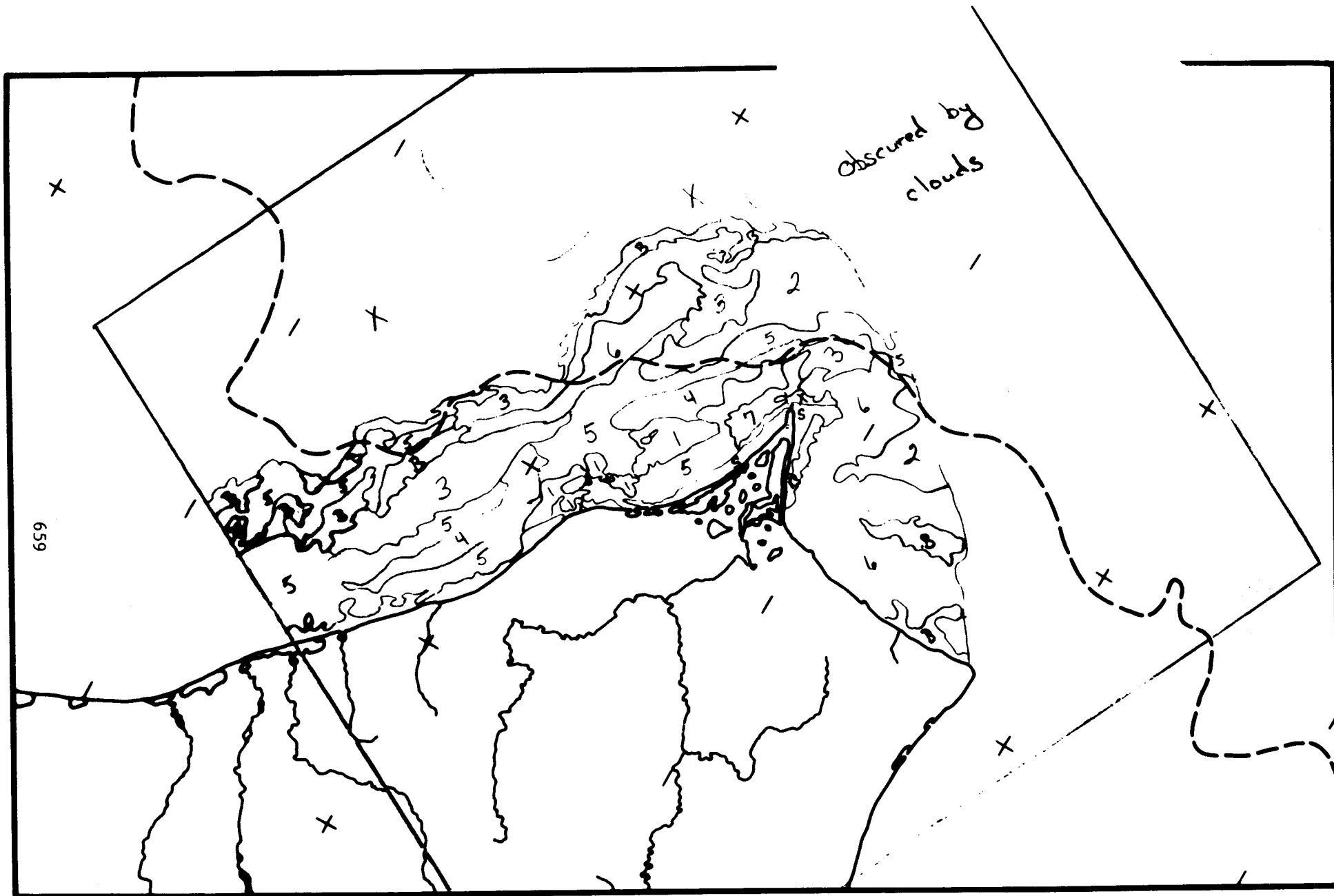
SHOREFAST SEA ICE
SURFACE MORPHOLOGICAL CHARACTERISTICS
CHUKCHI SEA COAST: POINT HOPE SECTOR

23 June 1973

Map No. 7: Barrow Sec, 07 JUL 73, 1349-21571

Legend X open water with or without floes (ice
           coverage <25%)

        A pack ice

        B flooded or partially flooded shore fast ice

        1 protected ice in bays and lagoons

        2 shore fast ice, known to be ridged from
           Point Barrow southwest for most if not all
           of its extent on this map

        3 apparently shore fast ice with much of its
           surface covered by shallow melt water

       4 & pack ice which has been pushed shoreward.
        5   Type 4 is generally continuous but type 5
            exhibits extensive melt and open water in
            small amounts.
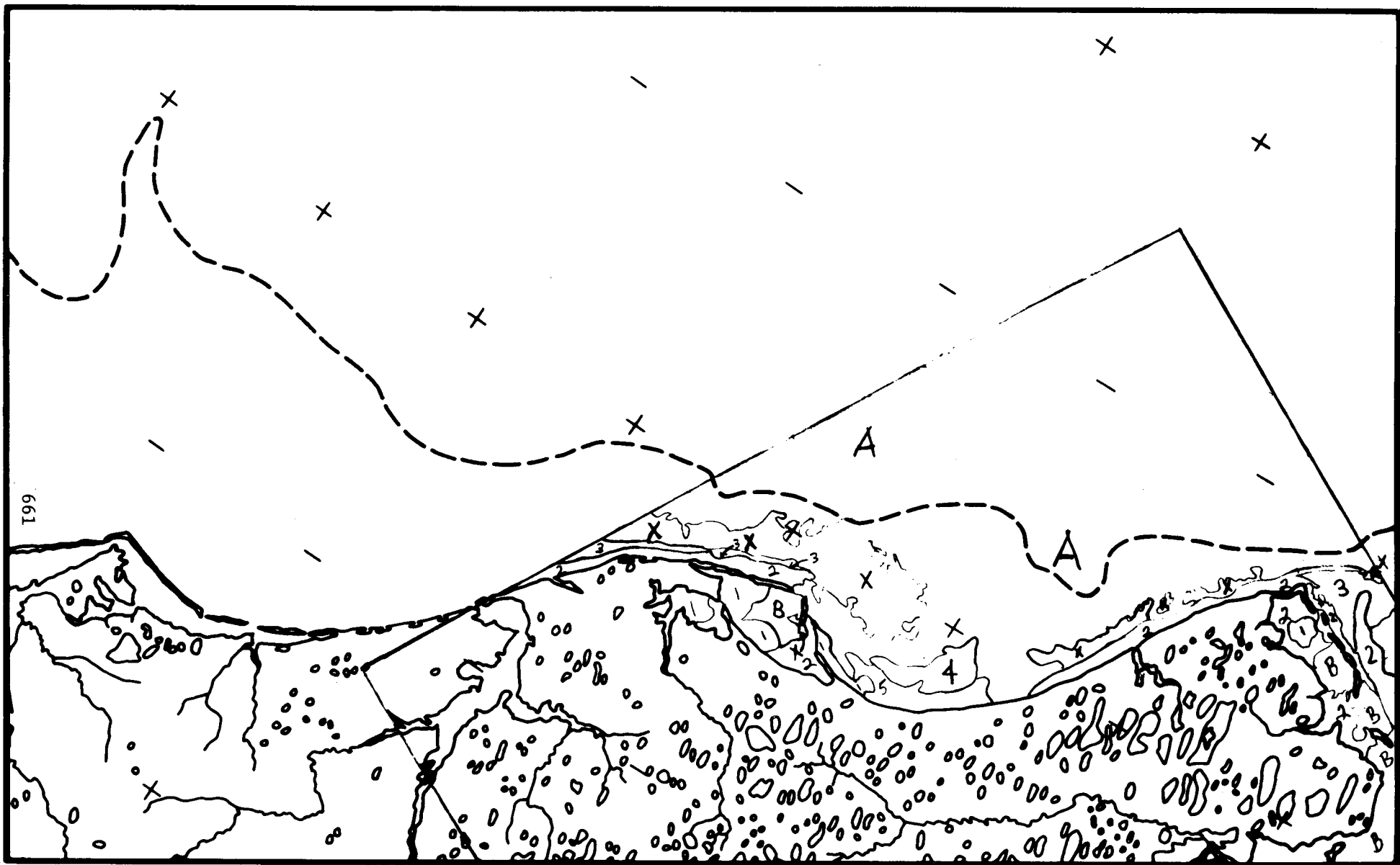
660

SHOREFAST SEA ICE
SURFACE MORPHOLOGICAL CHARACTERISTICS
CHUKCHI SEA COAST: BARROW SECTOR
7 July 1973

Map No.   8:   Point Hope Sec, 02 MAR 74, 1587-22162

          Legend   X   lead with refreezing ice

                 A   pack ice

                 1   shore fast ice

                 2   new and/or young ice near the lead

          Note: The pack ice Northeast to Southeast of Point

                 Hope has extensive new ice between older floes.
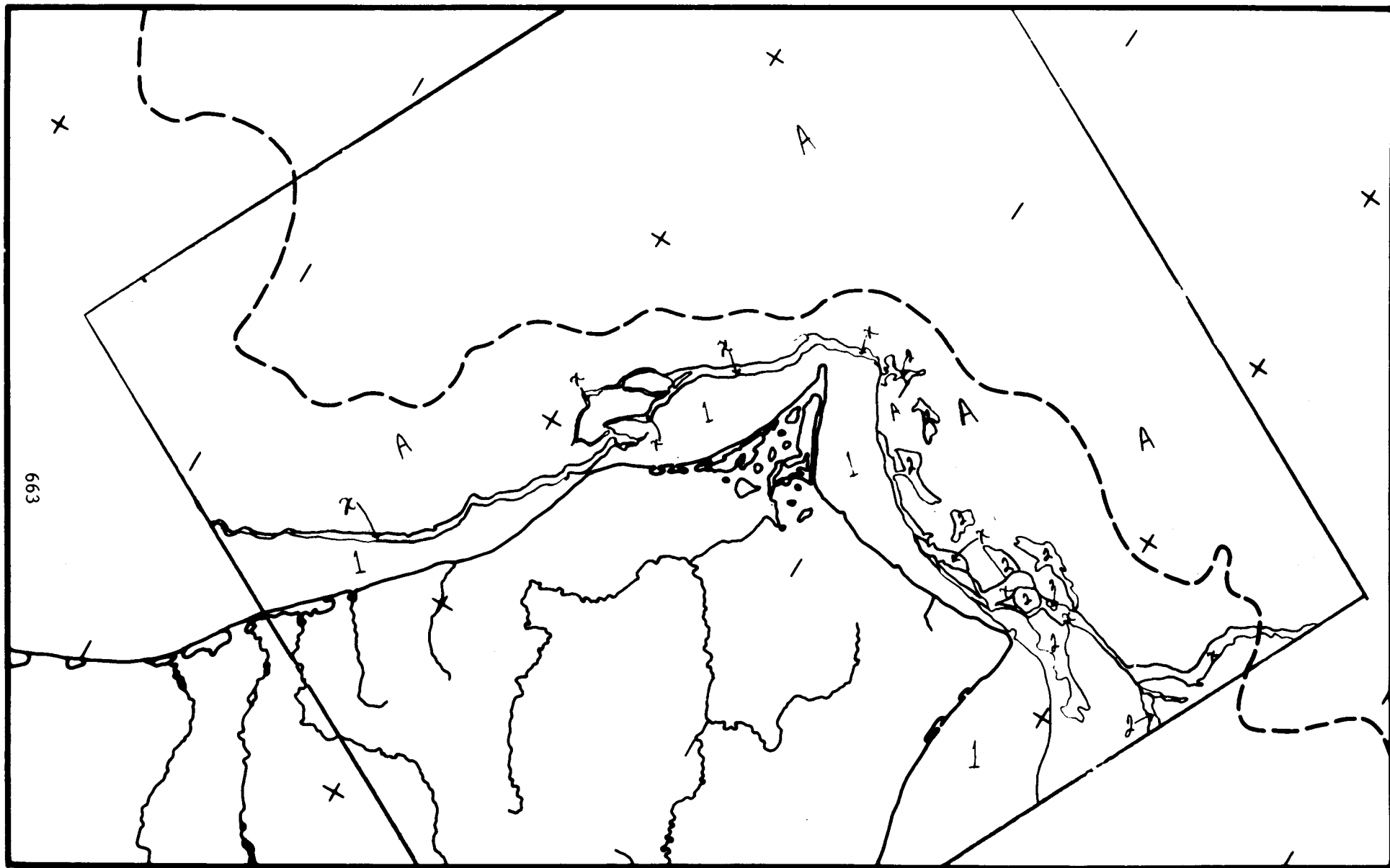
SHOREFAST SEA ICE
SURFACE MORPHOLOGICAL CHARACTERISTICS
CHUKCHI SEA COAST: POINT HOPE SECTOR

2 March 1974   1587 22162

Map No. 9: Point Hope Sec, 03 MAR 74, 1588-22220

Legend X area of young and/or new ice

A pack ice

1 shore fast ice

Note: Areas outlined in the pack ice but not

labeled are new ice forming in large leads.
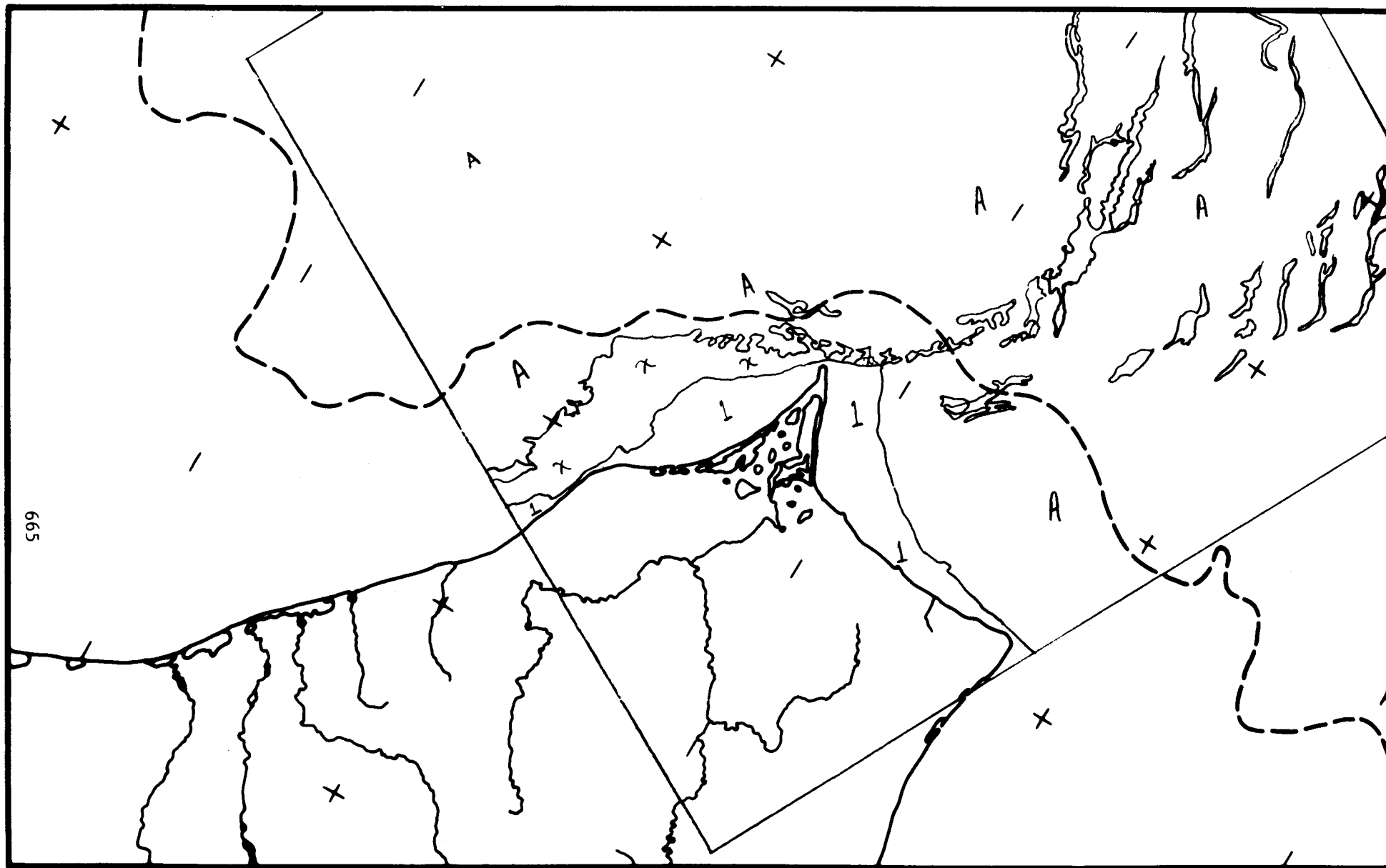
SHOREFAST SEA ICE
SURFACE MORPHOLOGICAL CHARACTERISTICS
CHUKCHI SEA COAST: POINT HOPE SECTOR

March 3, 1974   1588-22220

665

Map No. 10:   Barrow Sec, 18 MAR 74, 1603-22034

Legend   X   lead with new ice

A   pack ice with leads containing new ice

1   shore fast ice

2   older floes in the refreezing lead
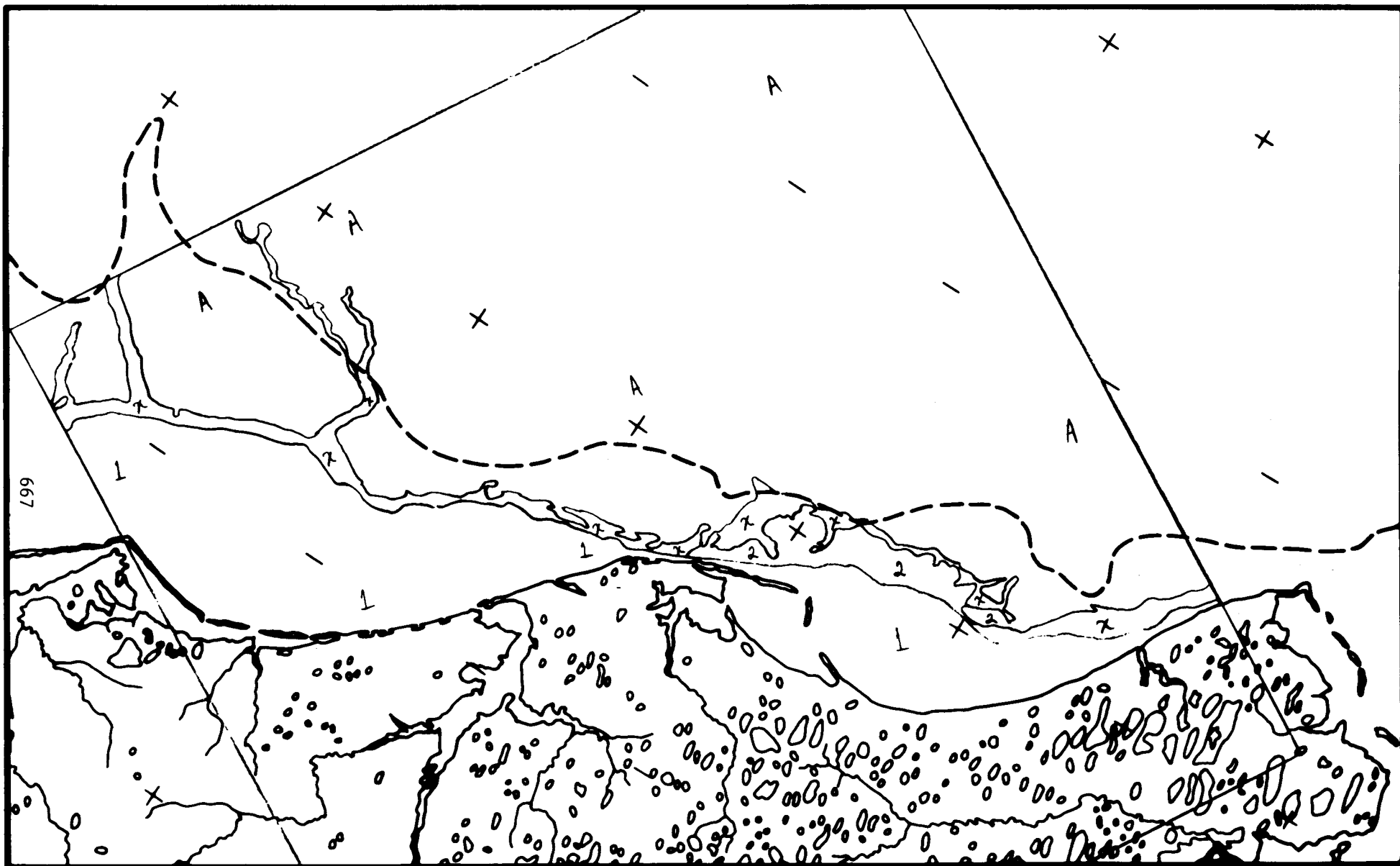
SHOREFAST SEA ICE
SURFACE MORPHOLOGICAL CHARACTERISTICS
CHUKCHI SEA COAST: BARROW SECTOR
March 18, 1974   1603-22034

Map No. 11: Point Hope Sec, 20 MAR 74, 1605-22160

        Legend X area of open water or new ice

             A pack ice with lead network

             1 shore fast ice

          _._. limit of extensive areas of new or

               young ice
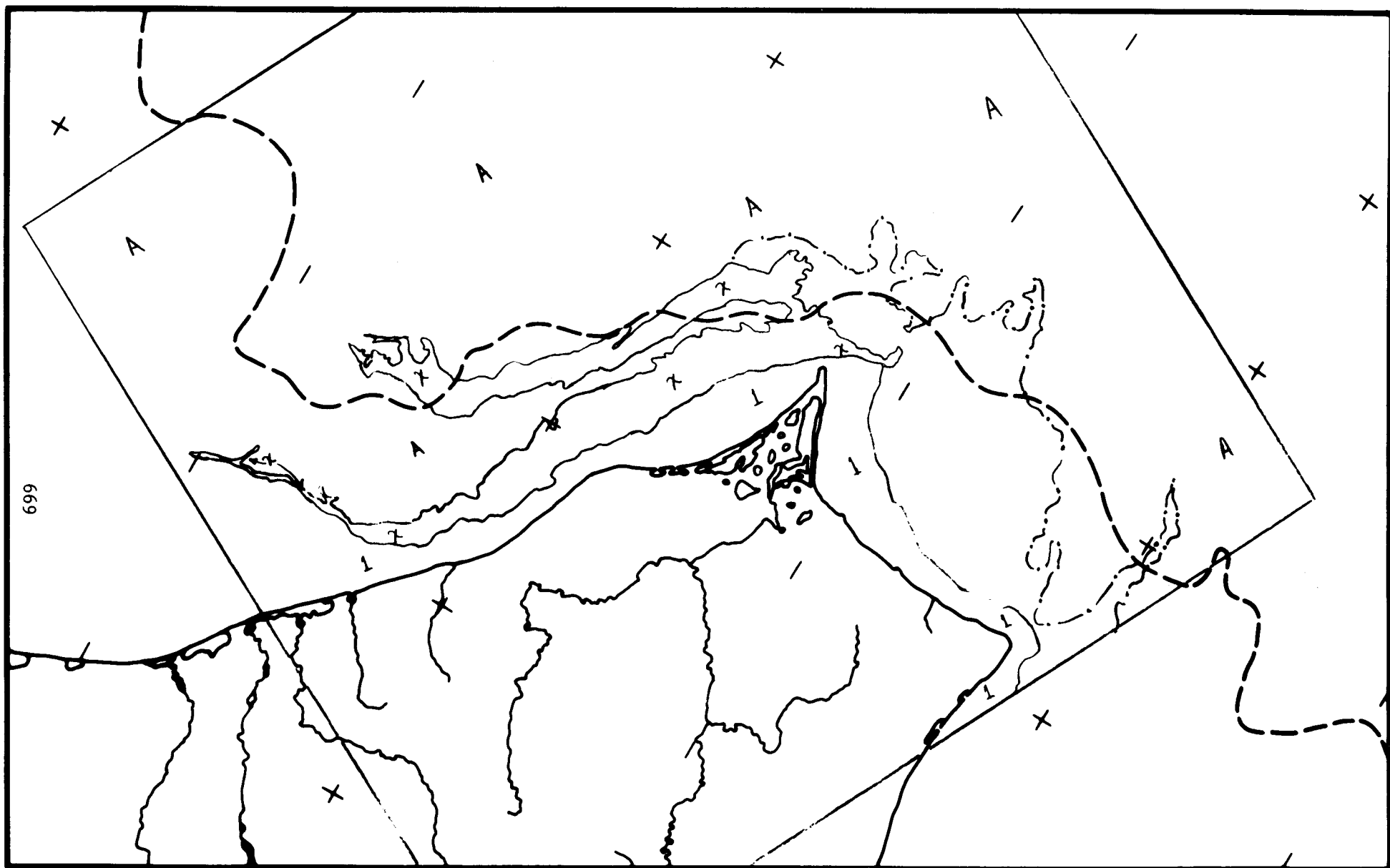
SHOREFAST SEA ICE
SURFACE MORPHOLOGICAL CHARACTERISTICS
CHUKCHI SEA COAST: POINT HOPE SECTOR

March 20, 1974   1605-22160

Map No. 12:   Point Hope Sec, 07 APR 74, 1623-22154

Legend   X   area of new ice

A   pack ice with lead network

1   shore fast ice

2   young ice within the new ice area

Note: There is also an area of young ice in the

pack due east of Point Hope.
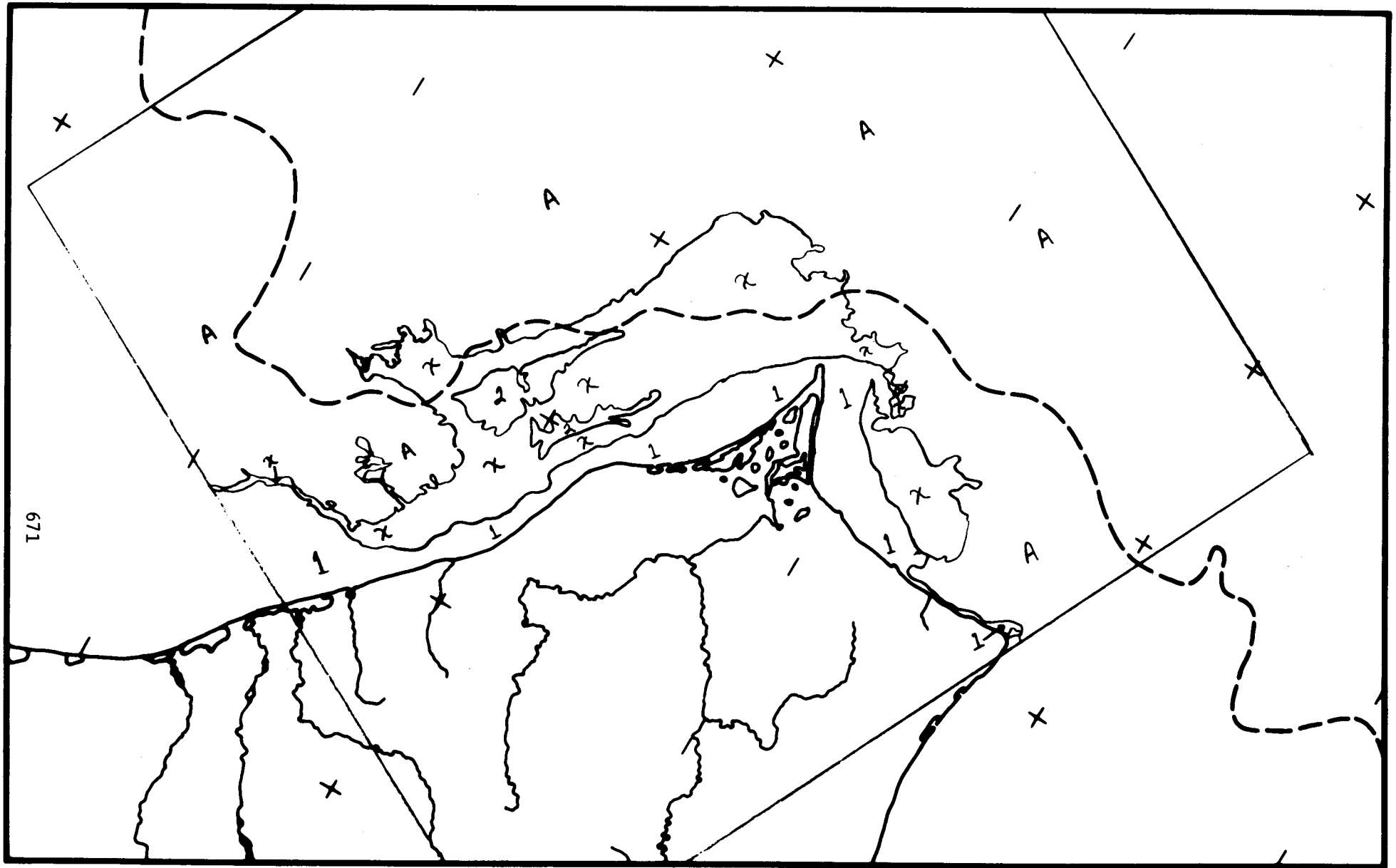
SHOREFAST SEA ICE
SURFACE MORPHOLOGICAL CHARACTERISTICS
CHUKCHI SEA COAST: POINT HOPE SECTOR
April 7, 1974   1623-22154

Map No. 13:   Point Hope Sec, 13 MAY 74, 1659-22144

        Legend X open water

                A pack ice

                1 shore fast ice, dry

                2 shore fast ice with evidence of surface
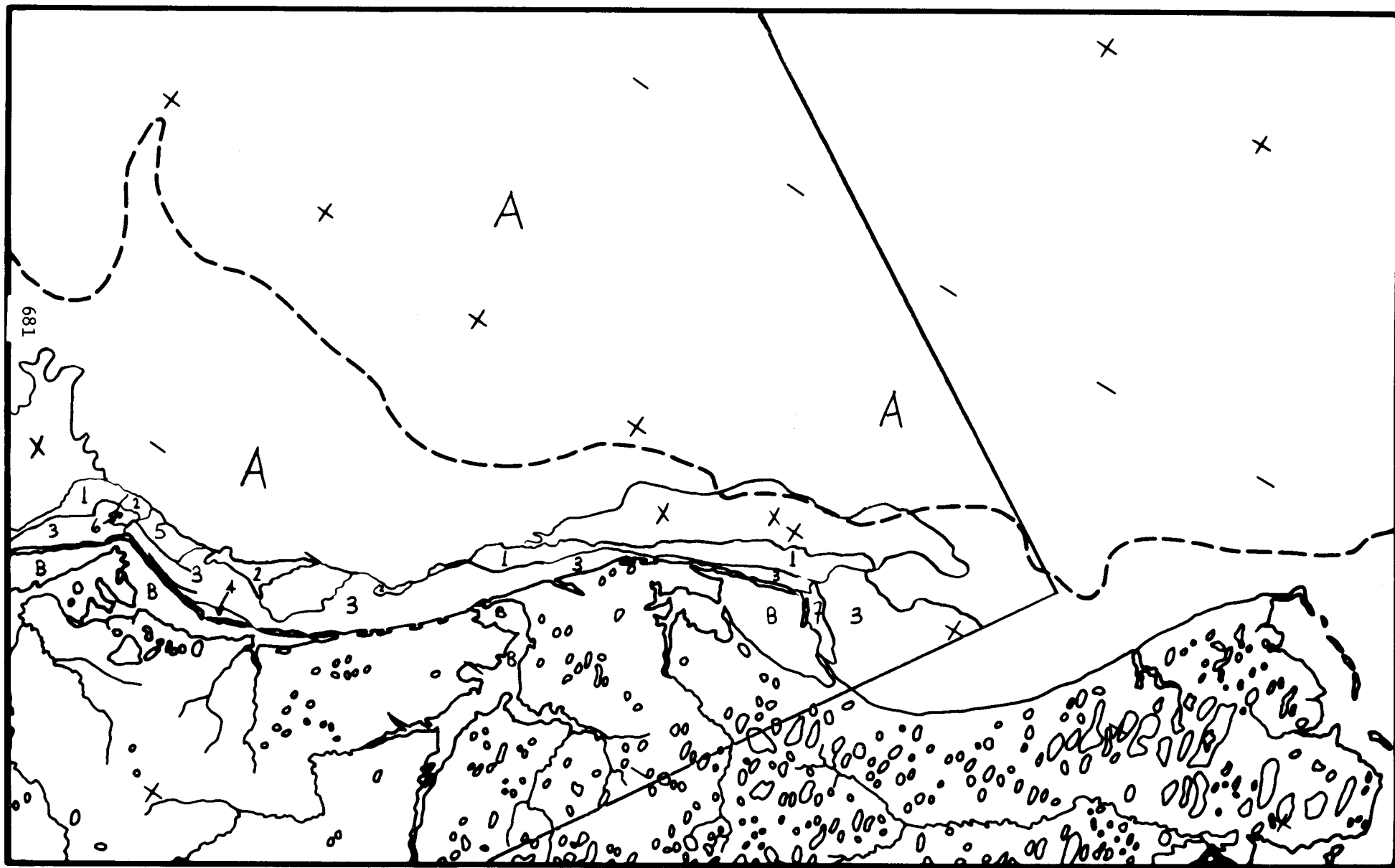
                    melt water
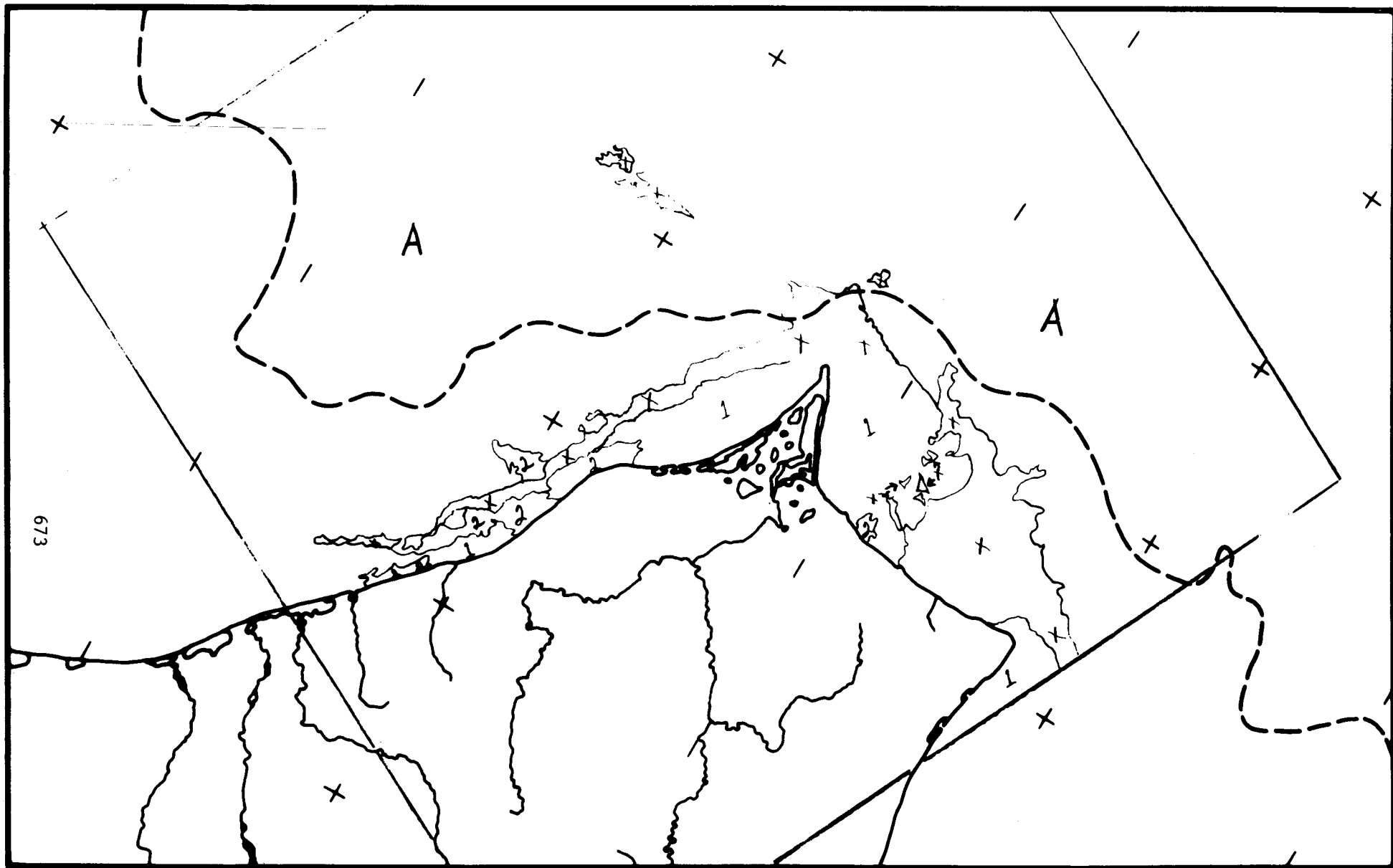
SHOREFAST SEA ICE
SURFACE MORPHOLOGICAL CHARACTERISTICS
CHUKCHI SEA COAST: POINT HOPE SECTOR
13 May 1974

Map No. 14:   Barrow Sec, 28 MAY 74, 1674-21561

        Legend X open water

                A pack ice

                1 shore fast ice exhibiting linear tonal
                   variations

                2 very uniform shore fast ice
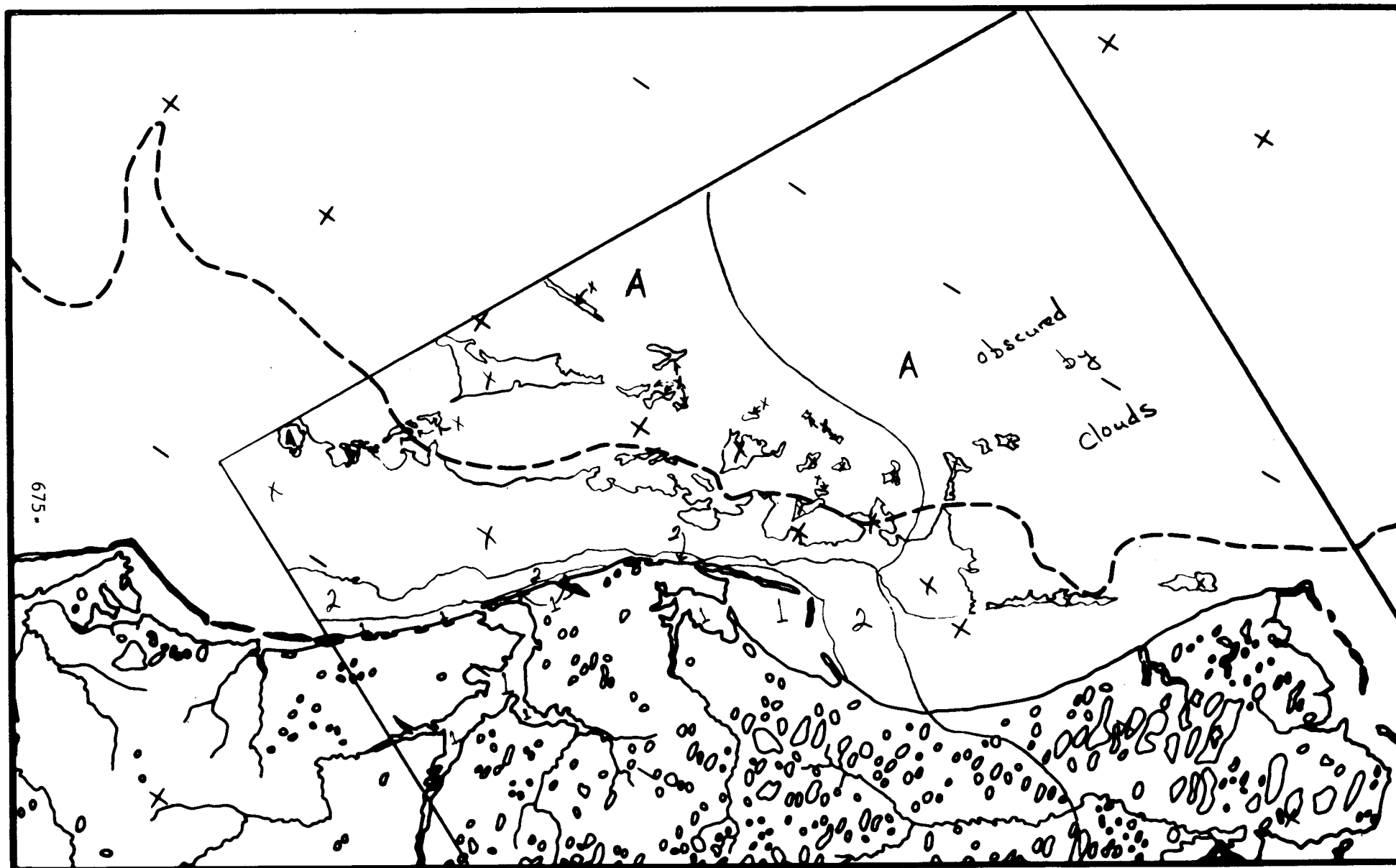
SHOREFAST SEA ICE
SURFACE MORPHOLOGICAL CHARACTERISTICS
CHUKCHI SEA COAST: BARROW SECTOR

28 May 1974

Map No. 15: Kotzebue Sec, 28 MAY 74, 1674-21573

Legend X open water

A pack ice

1 smooth protected ice

2 generally little surface water with few
   surface features

3 like type 2 but with more surface water and
   better defined surface features

4 this ice appears to be nonhomogeneous (mottled
   melt pattern) with different amounts of melt
   water in different areas

5 ice of this type has considerable amounts of
   melt water on the surface but is continuous

6 this ice type appears quite dark (much surface
   melt water) and cracks are clearly visible
   where the water has drained

7 a generalized ice type for rotten or nearly
   rotten ice found at the mouths of rivers
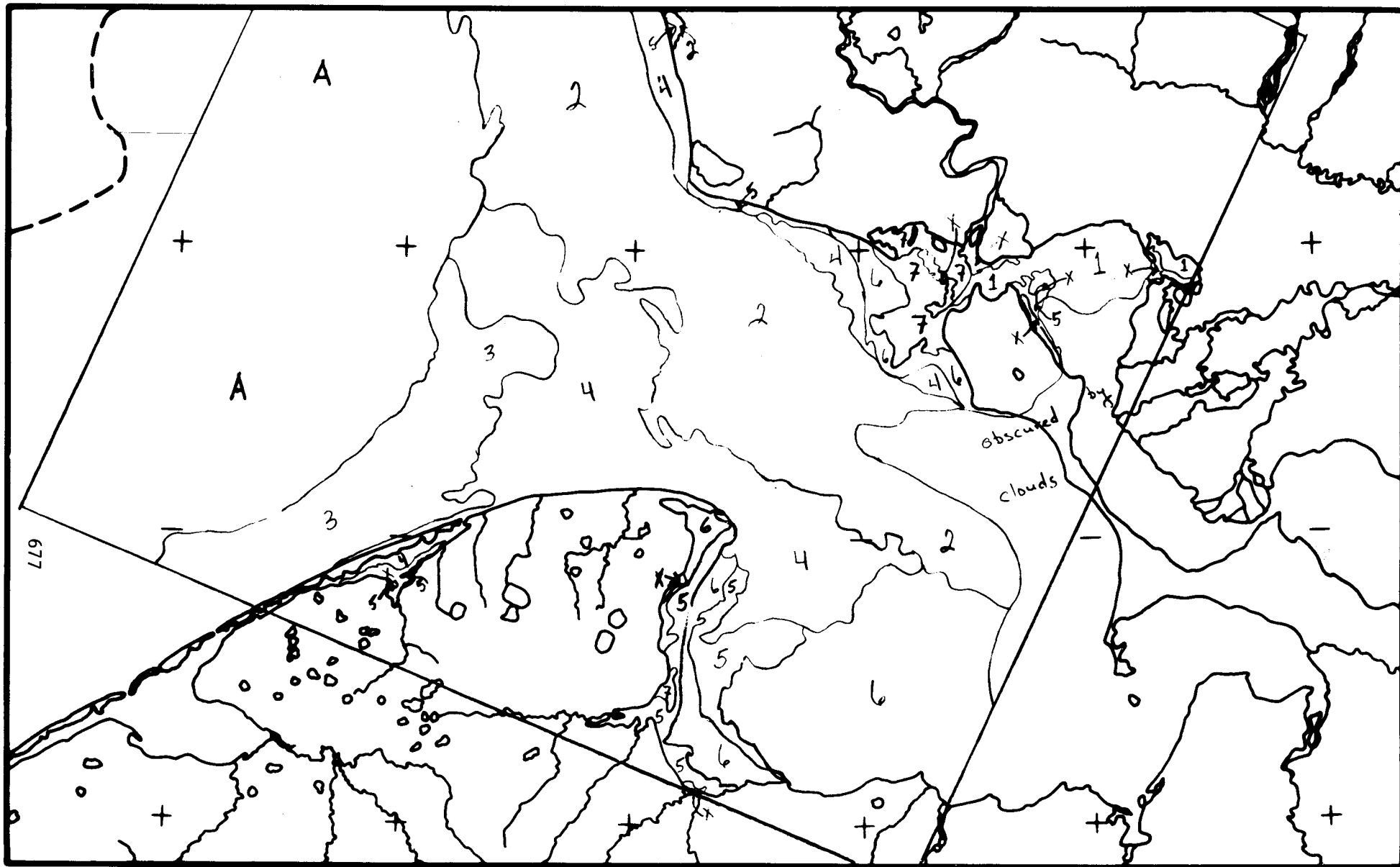
SHOREFAST SEA ICE
SURFACE MORPHOLOGICAL CHARACTERISTICS
CHUKCHI SEA COAST: KOTZEBUE SOUND SECTOR

28 May 1974

Map No. 16: Point Hope Sec, 31 MAY 74, 1677-22141

Legend   X   open water

A   pack ice

1   melt water and surface features are apparent
    on this ice. It is not entirely homogeneous.

2   a homogeneous ice type with an increased
    amount of surface water (as compared with
    type 1)

3   a nonhomogeneous ice type. All ice in this
    group has undergone considerable surface
    ablation (or flooding very close to the river
    mouth). Drain cracks are obvious as are areas
    of rotten ice. With these areas are individual
    floes that show much less surface water than
    the surrounding ice.

4   this shore fast ice has at least as much
    surface water as type 2 and in places shows
    more extensive melt due to runoff from the
    land. It is still continuous.
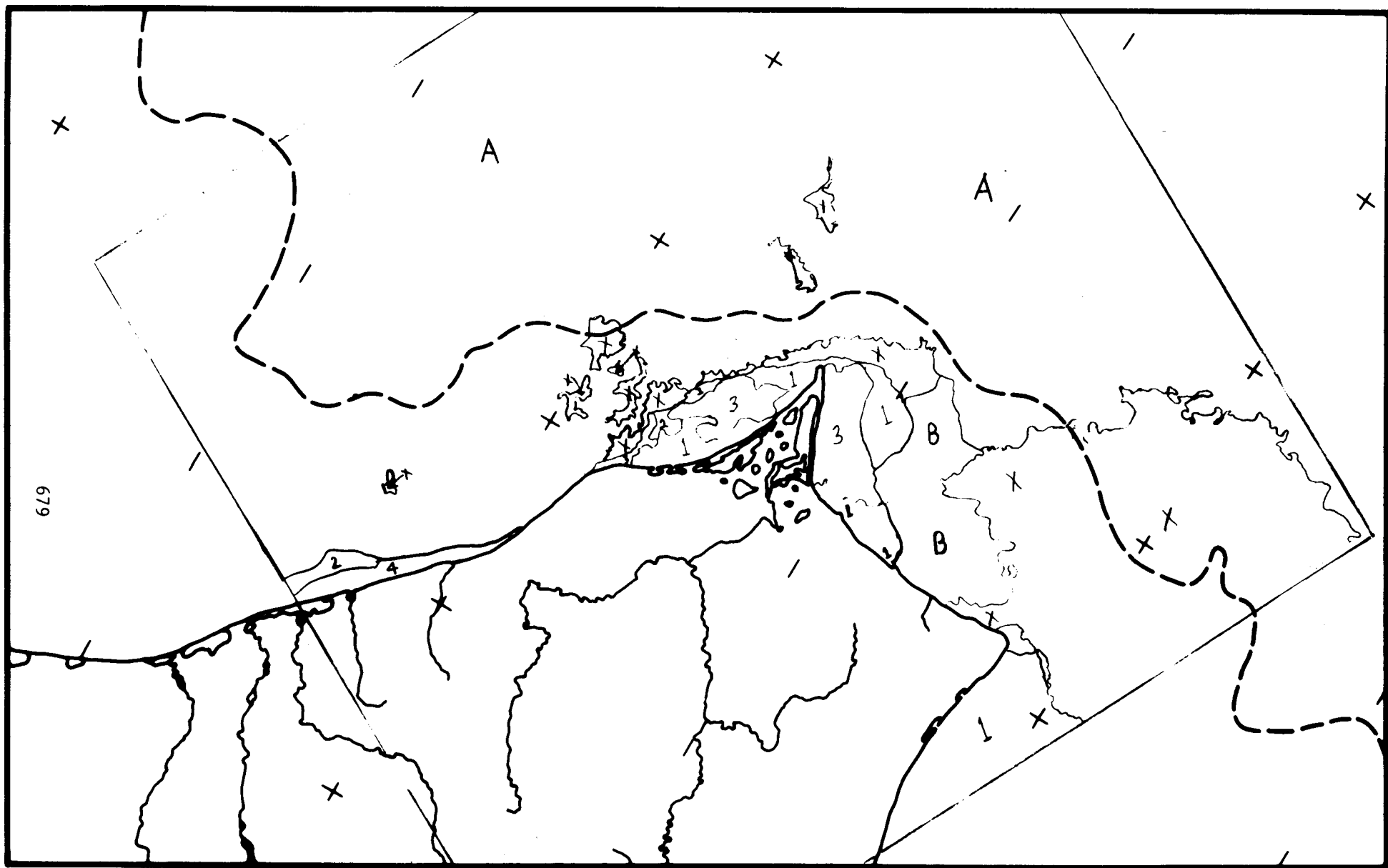
SHOREFAST SEA ICE
SURFACE MORPHOLOGICAL CHARACTERISTICS
CHUKCHI SEA COAST: POINT HOPE SECTOR

31 May 1974

Map No. 17:   Barrow Sec, 17 JUN 74, 1694-22071

Legend X open water with or without ice (ice coverage <25%)

A pack ice

B protected ice in bays, lagoons, etc. in advanced stages of decay. The area at the south west of the map has already developed large areas of open water within this area.

1 light tone area indicating small amounts of surface melt water. Not entirely homogeneous with some areas exhibiting increased amount of melt. The seaward edge does show some increased surface water too.

2 more homogeneous than type 1 but with more melt water on the surface

3 generally homogeneous ice (except in the northwest, near the edge of the map where 'dryer' floes appear with this ice type) exhibiting much surface melt water and clearly defined drain cracks. In the southeast map area the border line between types 3 and 5 and the line extending from it and the line just to the south indicate two narrow bands where the ice appears to be melting more rapidly or where forces have caused the ice to break up somewhat exposing some water.

4 very dark (wet) ice exhibiting some drain cracks

5 much like type 3 but with fewer drain cracks visible and not so homogeneous

6 a dark and featureless ice type except for a linear light band nearly traversing the area

7 this is the lightest and presumably dryest ice type on the map. There are some darker areas with this type and toward its eastern edge signs of advanced decay are detected.

SHOREFAST SEA ICE
SURFACE MORPHOLOGICAL CHARACTERISTICS
CHUKCHI SEA COAST: BARROW SECTOR

17 June 1974

Map No. 18:   Point Hope Sec, 17 JUN 74, 1694-22080

Legend   X   open water with or without ice (ice coverage
             <25%)

         A   pack ice, not continuous in most areas

         ---- this line indicates a lead, not continuous
               (or not distinguishable) along the entire
               line

         1   homogeneous ice with few distinguishable surface
             features

         2   contains more surface water than type 1 but also
             not as homogeneous with many areas of wetter ice

         3   mottled tone ice where either individual floes
             are well defined in terms of surface water or
             the ice is a conglomerate of different thickness
             of ice

         4   like type 3 but with less surface water in general

         5   in this type floes cannot be distinguished but
             there are changes in tone (surface water) showing
             no particular orientation except that increased
             melting is observed very near shore and in the
             southwest portion of this ice type

         6   clearly defined drain cracks and increased amounts
             of surface water characterize this ice type

         7   this near shore ice exhibits advanced melt and
             in isolated places rotten ice due to near shore
             effects (run off, air temperature, etc.)

         8   a small area of rotten ice
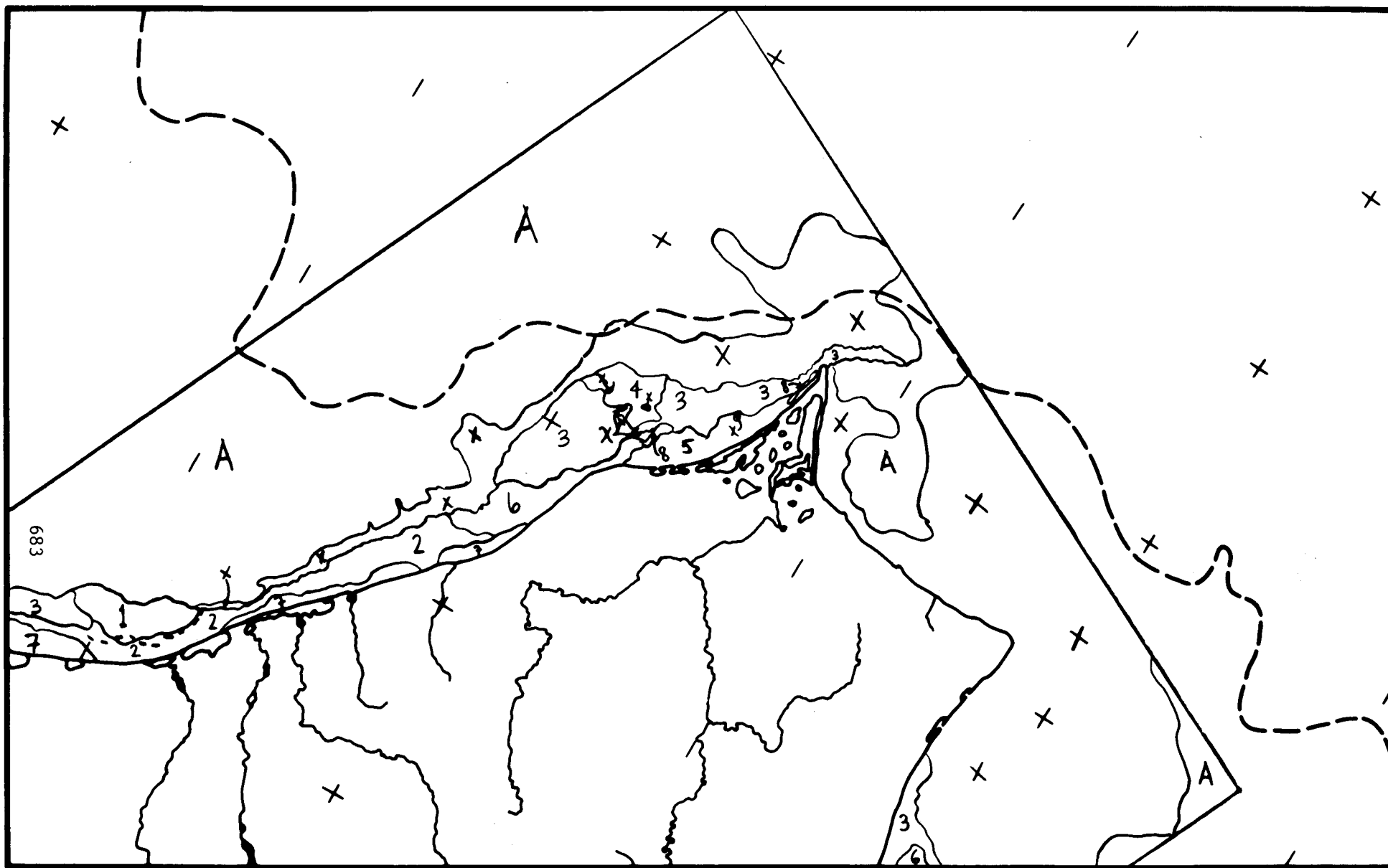
SHOREFAST SEA ICE
SURFACE MORPHOLOGICAL CHARACTERISTICS
CHUKCHI SEA COAST: POINT HOPE SECTOR
17 June 1974

Map No. 19: Barrow Sec, 03 JUL 74, 1710-21551

Legend X open water with <25% ice coverage

A pack ice

B ice in bays and lagoons which is rotten
in places

1 generally a uniform grey exhibiting linear
features roughly parallel to the shore

2 in this area individual floes may be dis-
tinguished due to their differing melt
water contents. The ice is continuous.

3 in overall tone much like type 2 but here
individual floes are not readily identified
although there are areas of differing melt
content

4 a very light toned area exhibiting few
surface features, probably well protected

5 a linear feature, possibly a grounded ridge

6 discontinuous ice, ice coverage 60% - 80%

7 continuous (probably) but at an advanced melt
stage

684

SHOREFAST SEA ICE
SURFACE MORPHOLOGICAL CHARACTERISTICS
CHUKCHI SEA COAST: BARROW SECTOR

3 July 1974

Map No. 20:   Kotzebue Sec, 03 JUL 74, 1710-21562

Legend   X   open water

1 discontinuous ice, coverage 20% - 50% except
  in the eastern Kotzebue sound where in a small
  area the coverage is up to 90 - 100%

2 a floe, broken in two, exhibiting an intricate
  surface melt pattern
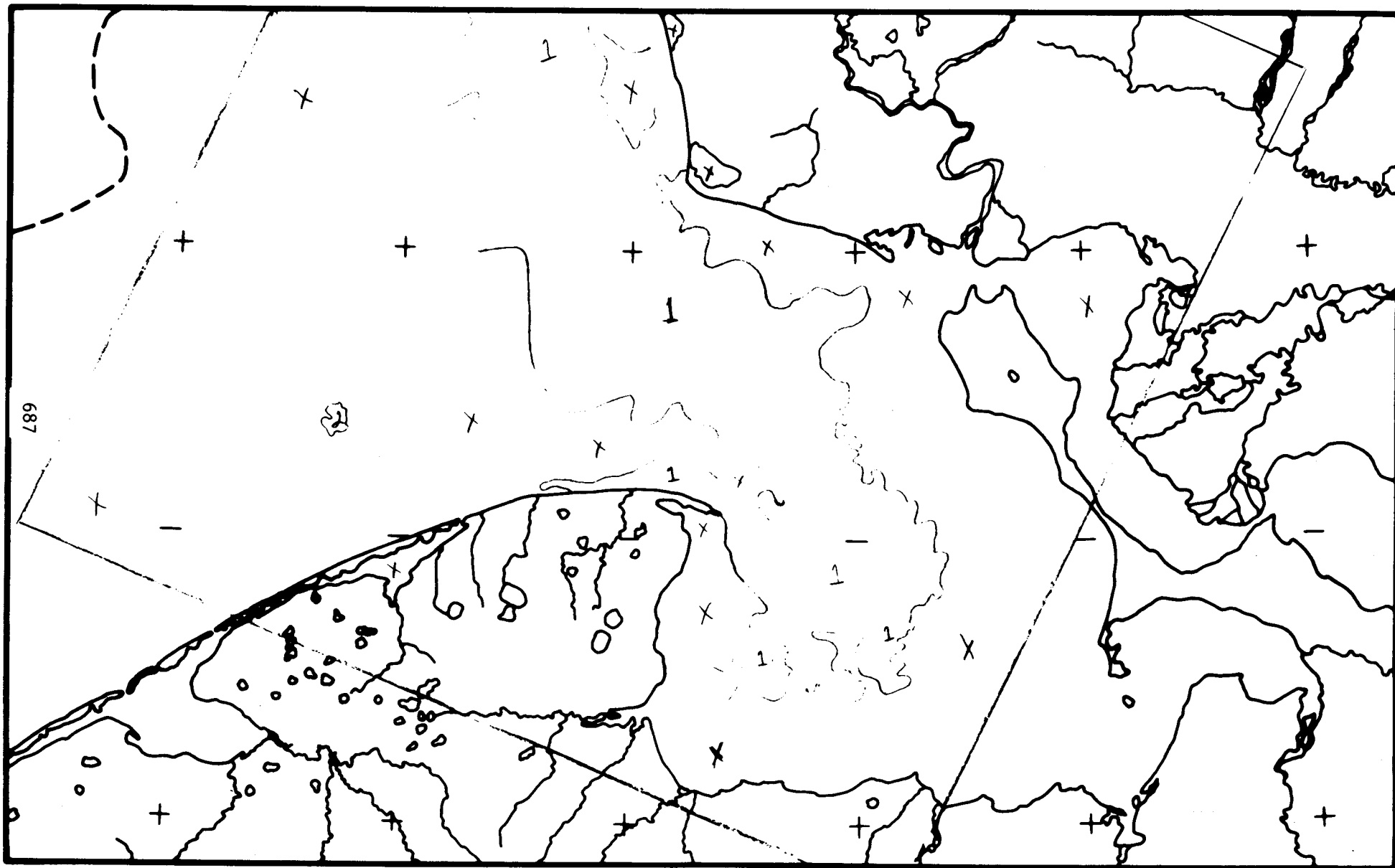
SHOREFAST SEA ICE
SURFACE MORPHOLOGICAL CHARACTERISTICS
CHUKCHI SEA COAST: KOTZEBUE SOUND SECTOR
3 July 1974

Map No. 21:   Point Hope Sec, 25 FEB 75, 1947-22043

                Legend: X   open water or new ice

                        A   pack ice disected by numerous leads

                        1   shore fast ice, the line thru the ice between
                            Point Hope and Cape Lisburne appears on the
                            imagery (possibly due to a shadow) but is
                            difficult to identify due to cloudiness.
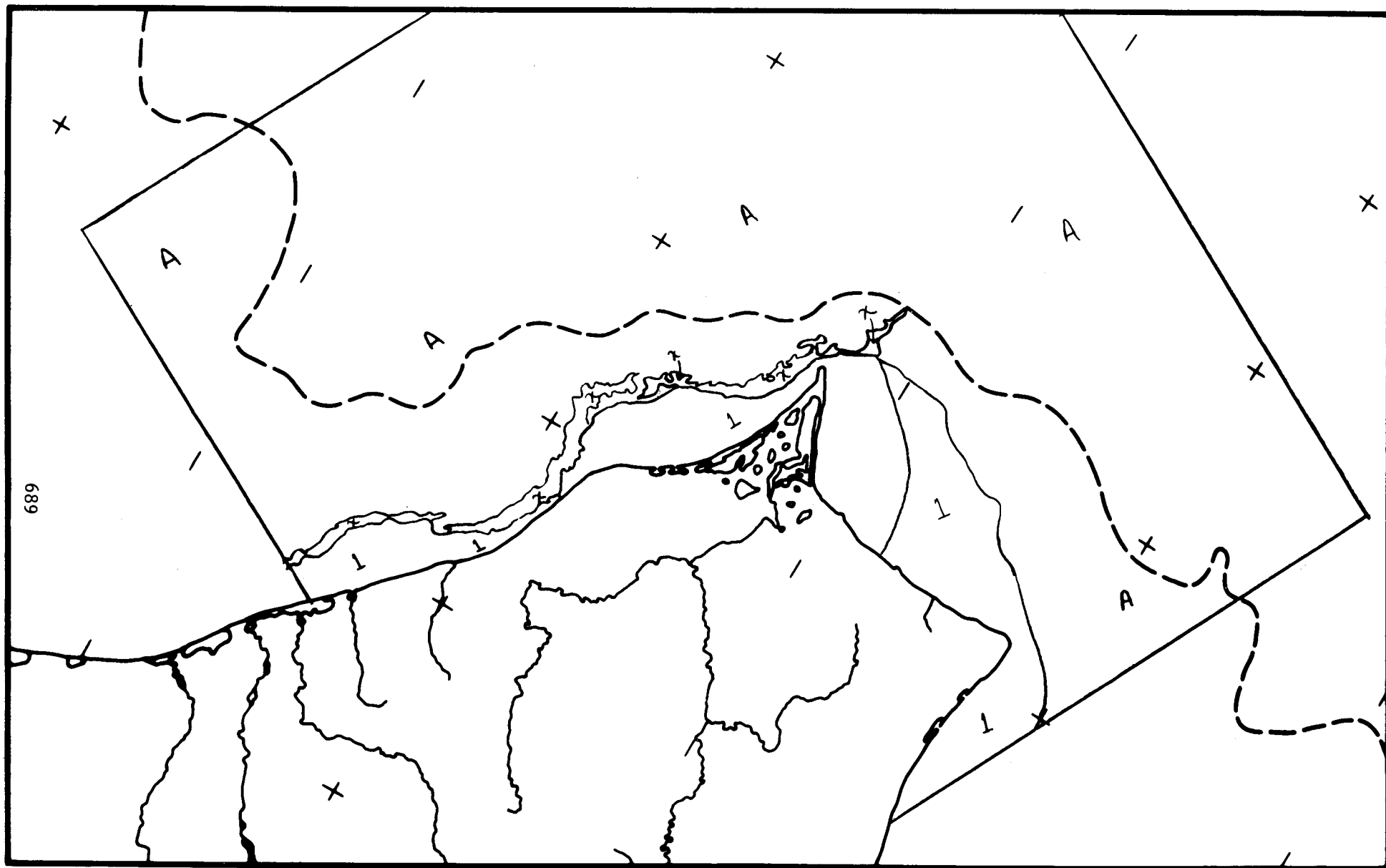
689

SHOREFAST SEA ICE
SURFACE MORPHOLOGICAL CHARACTERISTICS
CHUKCHI SEA COAST: POINT HOPE SECTOR

25 February 1975   1947-22043

Map No. 22: Barrow Sec, 01 APR 75, 1982-21562

Legend   X   new ice

A   pack ice

1   shore fast ice

_._.   shoreward of this line the pack ice has
been extensively broken. Seaward leads
are visible in the pack but no large
areas of new ice are seen.
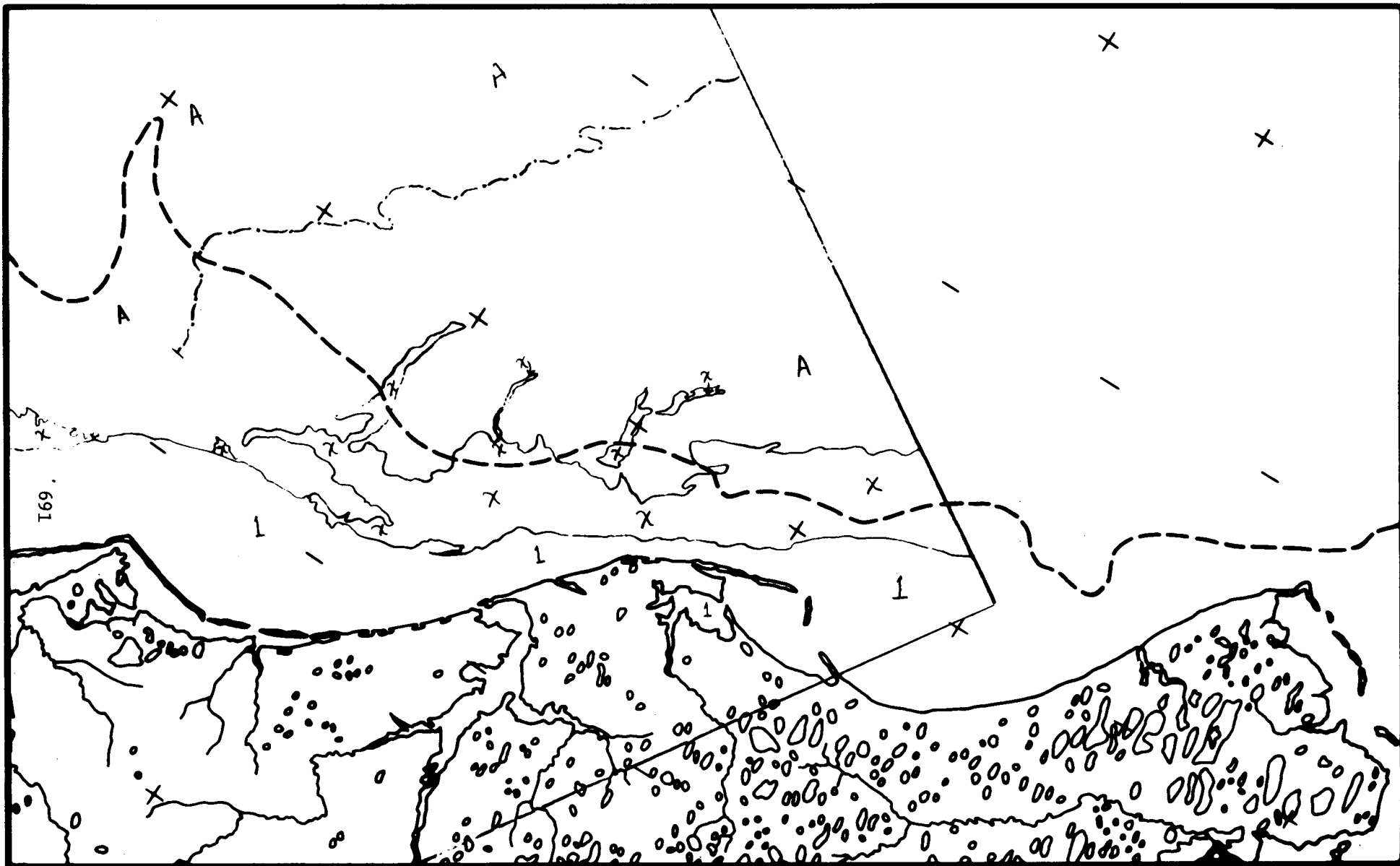
SHOREFAST SEA ICE
SURFACE MORPHOLOGICAL CHARACTERISTICS
CHUKCHI SEA COAST: BARROW SECTOR

1 April 1975   1982-21542

Map No. 23:   Point Hope Sec, 02 APR 75, 1983-22025

        Legend   X   new ice or open water

              A   pack ice

              1   shorefast   ice

              2   shorefast ice now broken away

            _._.   limit of severe fracturing in the pack
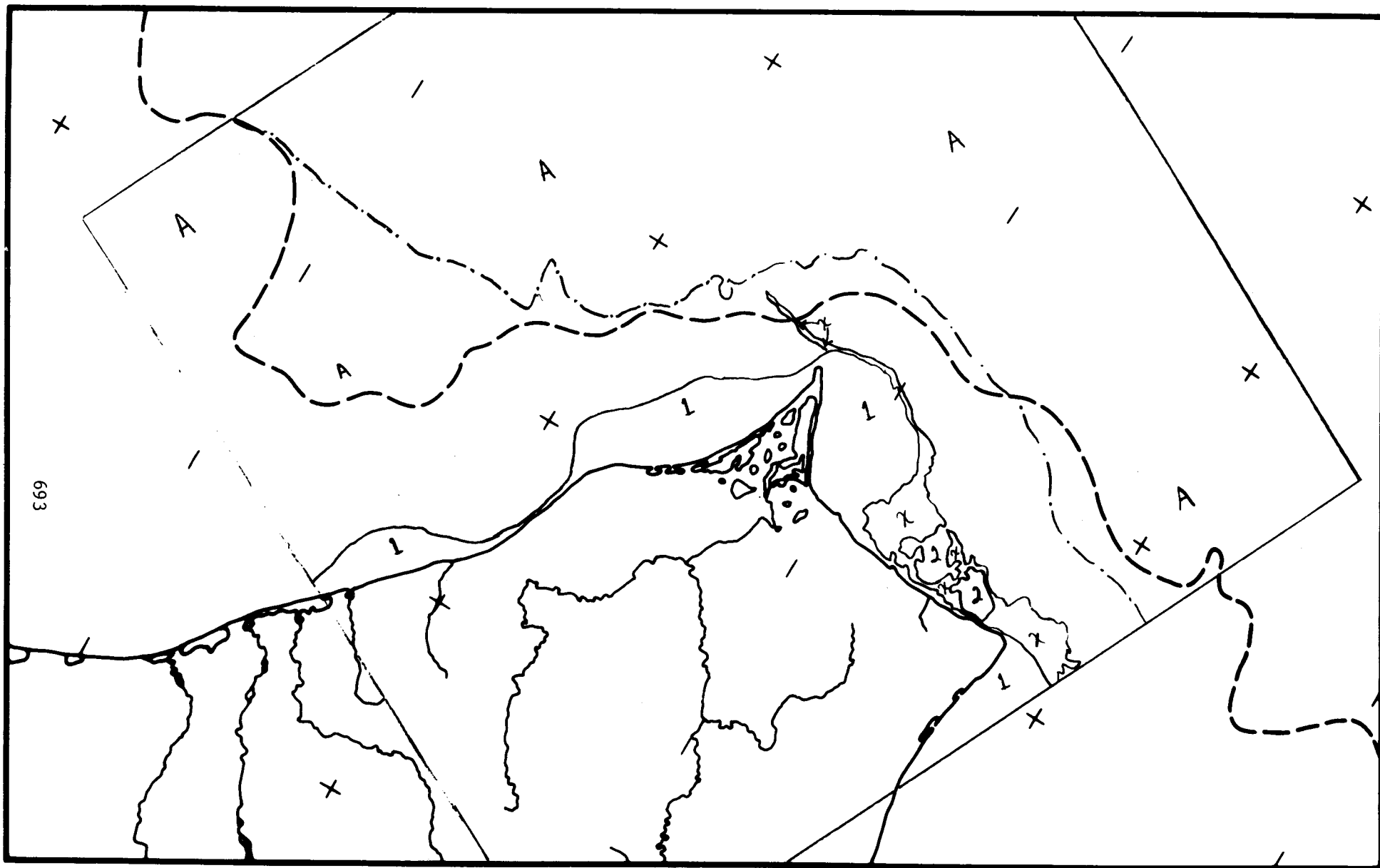
SHOREFAST SEA ICE
SURFACE MORPHOLOGICAL CHARACTERISTICS
CHUKCHI SEA COAST: POINT HOPE SECTOR

2 April 1975   1983-22025

Map No. 24 : Point Hope Sec, 12 APR 75, 2080-22151

        Legend X open water or new ice

                A pack ice

                1 shore fast ice

                2 young ice
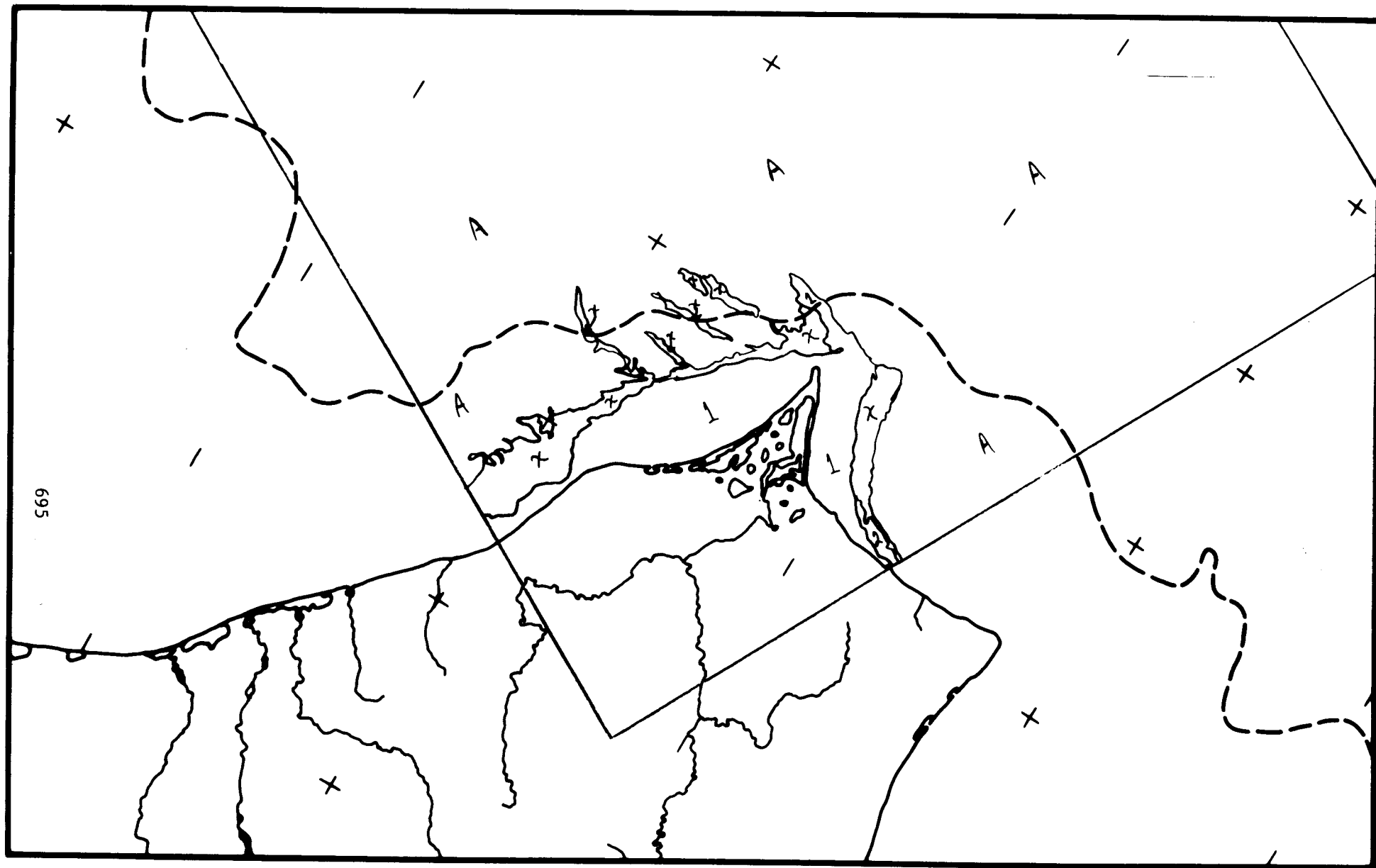
SHOREFAST SEA ICE
SURFACE MORPHOLOGICAL CHARACTERISTICS
CHUKCHI SEA COAST: POINT HOPE SECTOR

12 April 1975   2080-22151

Map No. 25:   Point Hope Sec, 29 APR 75, 2097-22090 & 2097-22093

     Legend   X   young and new ice

         A   pack ice

         1   shore fast ice - boundary indistinguishable

        _._. limit of severe fractures
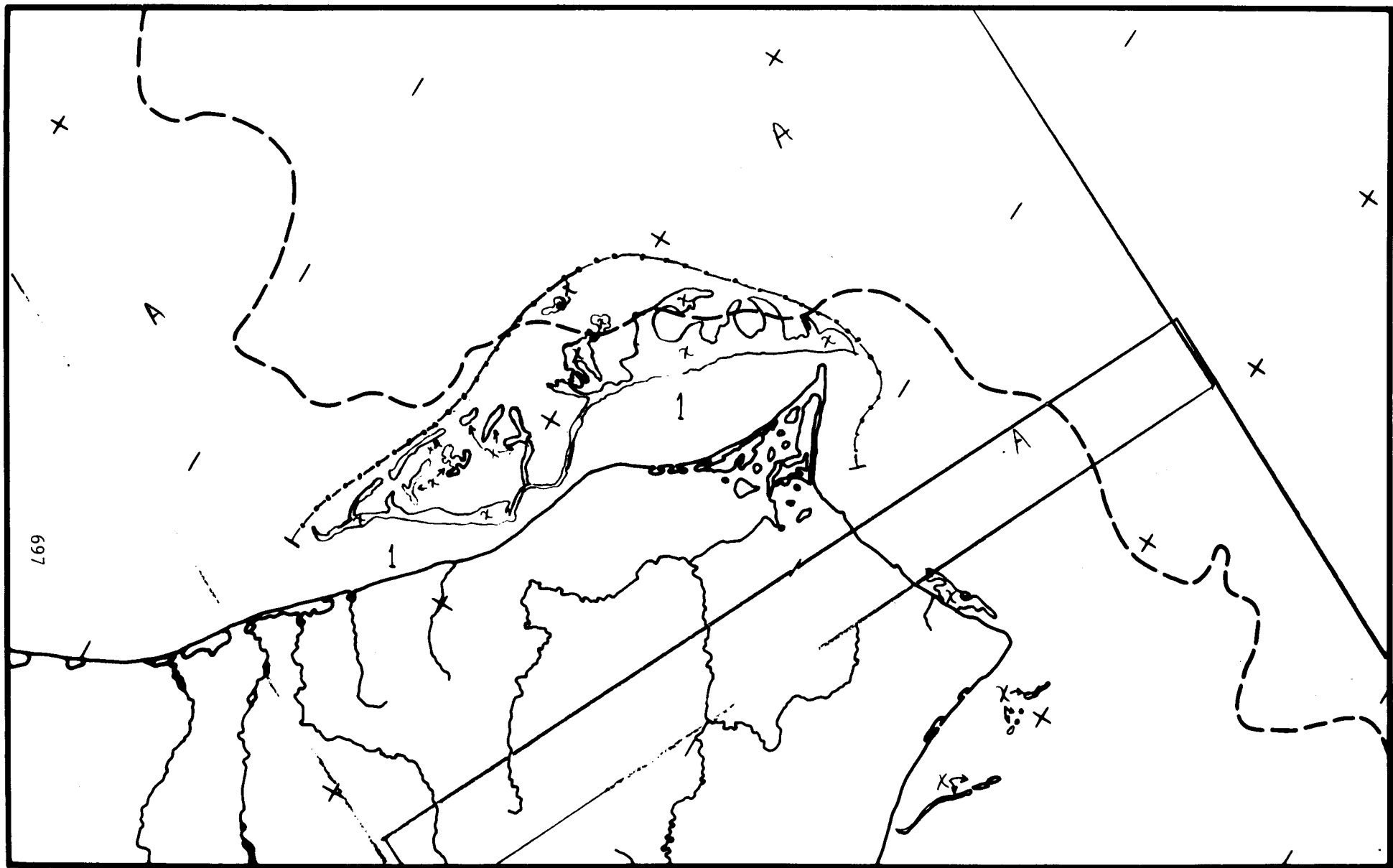
SHOREFAST SEA ICE
SURFACE MORPHOLOGICAL CHARACTERISTICS
CHUKCHI SEA COAST: POINT HOPE SECTOR

29 April 1975   2097-22093   2097-22090

Map No. 26: Point Hope Sec, 01 MAY 75, 2099-22203

        Legend X open water or new ice

                A pack ice, cannot distinguish shore fast ice
                   from pack ice on this image

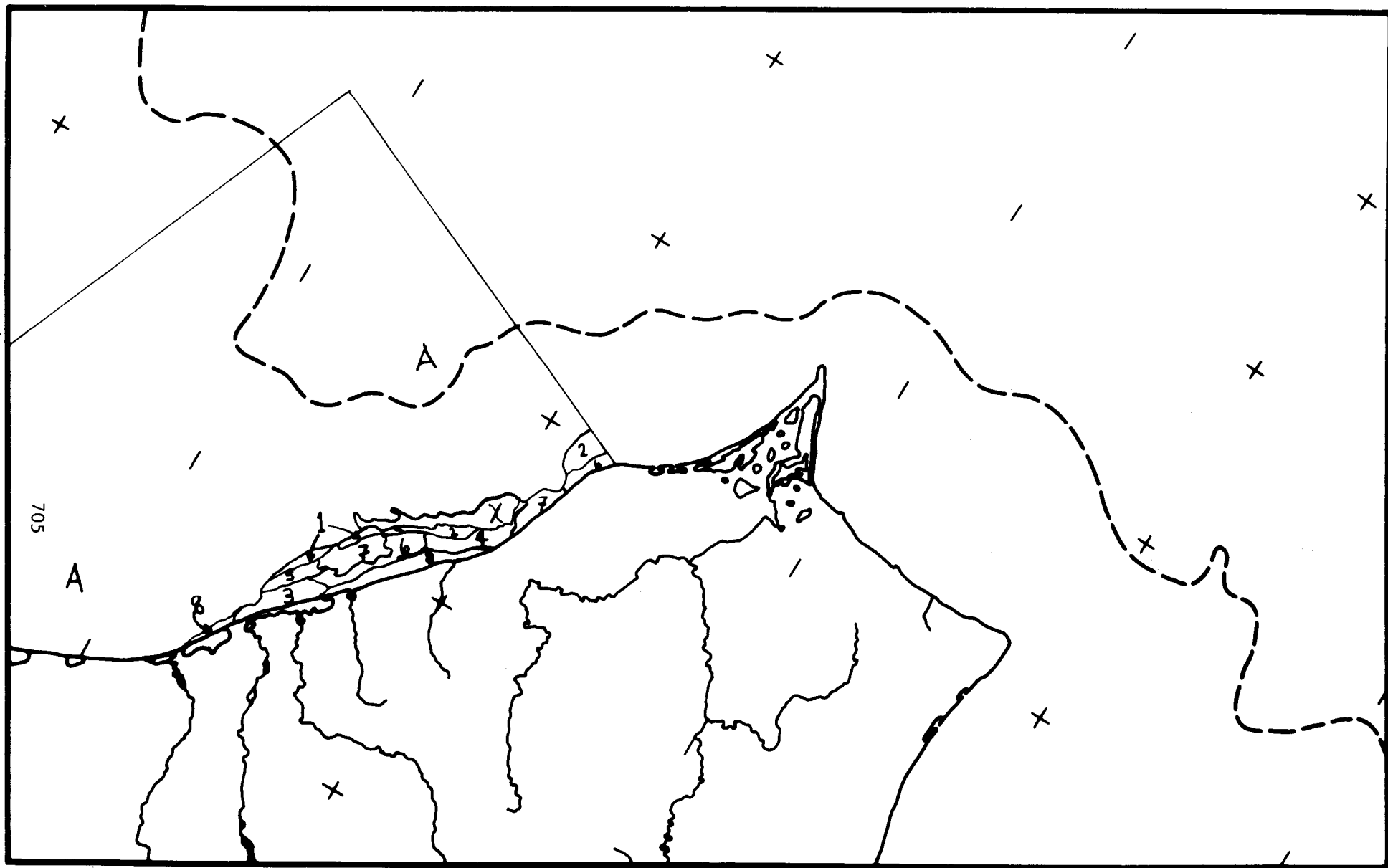   _._. limit of severe fracturing
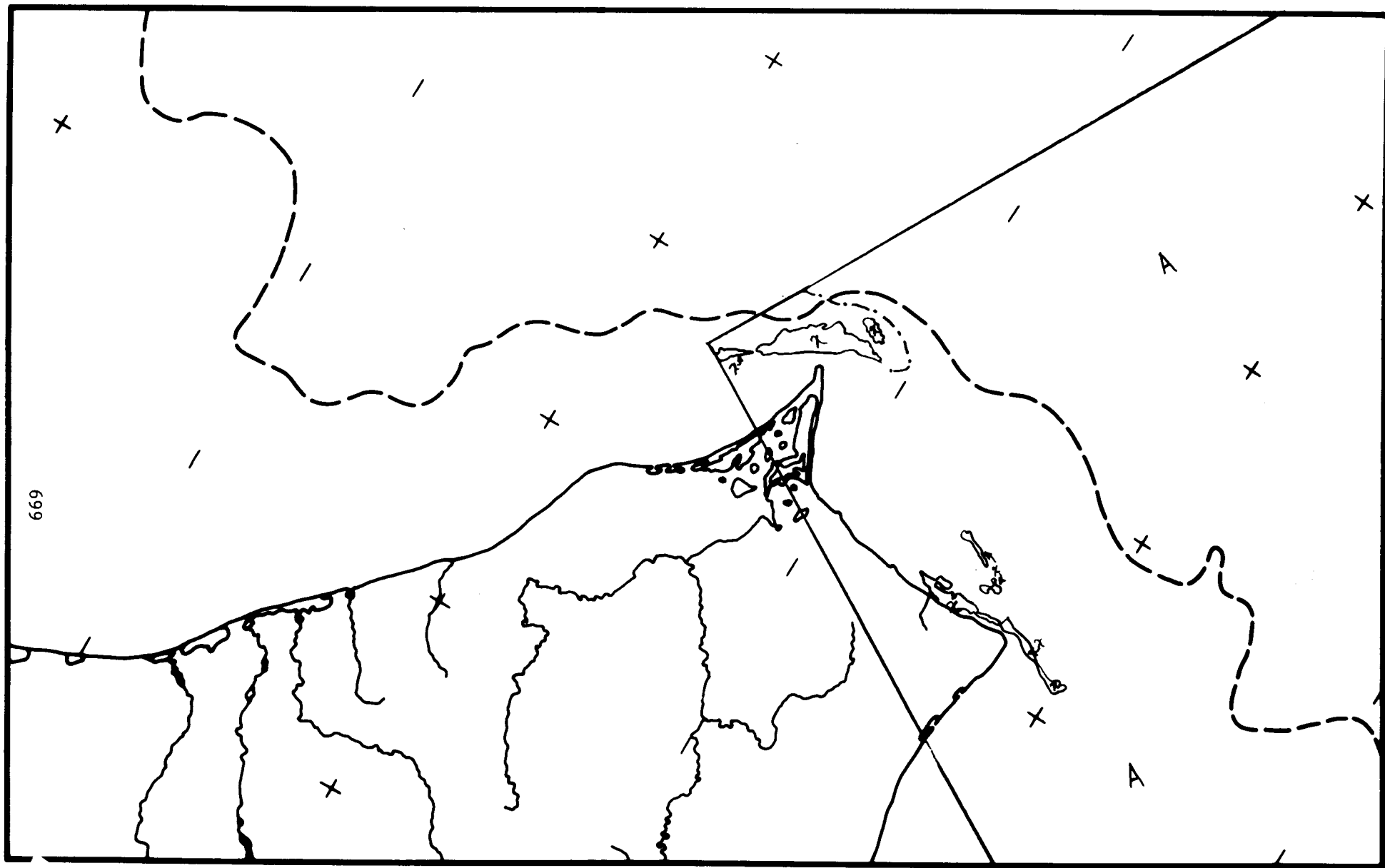
669

SHOREFAST SEA ICE
SURFACE MORPHOLOGICAL CHARACTERISTICS
CHUKCHI SEA COAST: POINT HOPE SECTOR

1 May 1975   2099-22203

Map No. 27: Barrow Sec, 14 MAY 75, 2112-21511

                Legend   X open water with nilas in bands

                         A pack ice, not continuous

                         1 shore fast ice, no evidence of melt

                         2 some darkening of the ice indicative of the

                              beginning of the melt
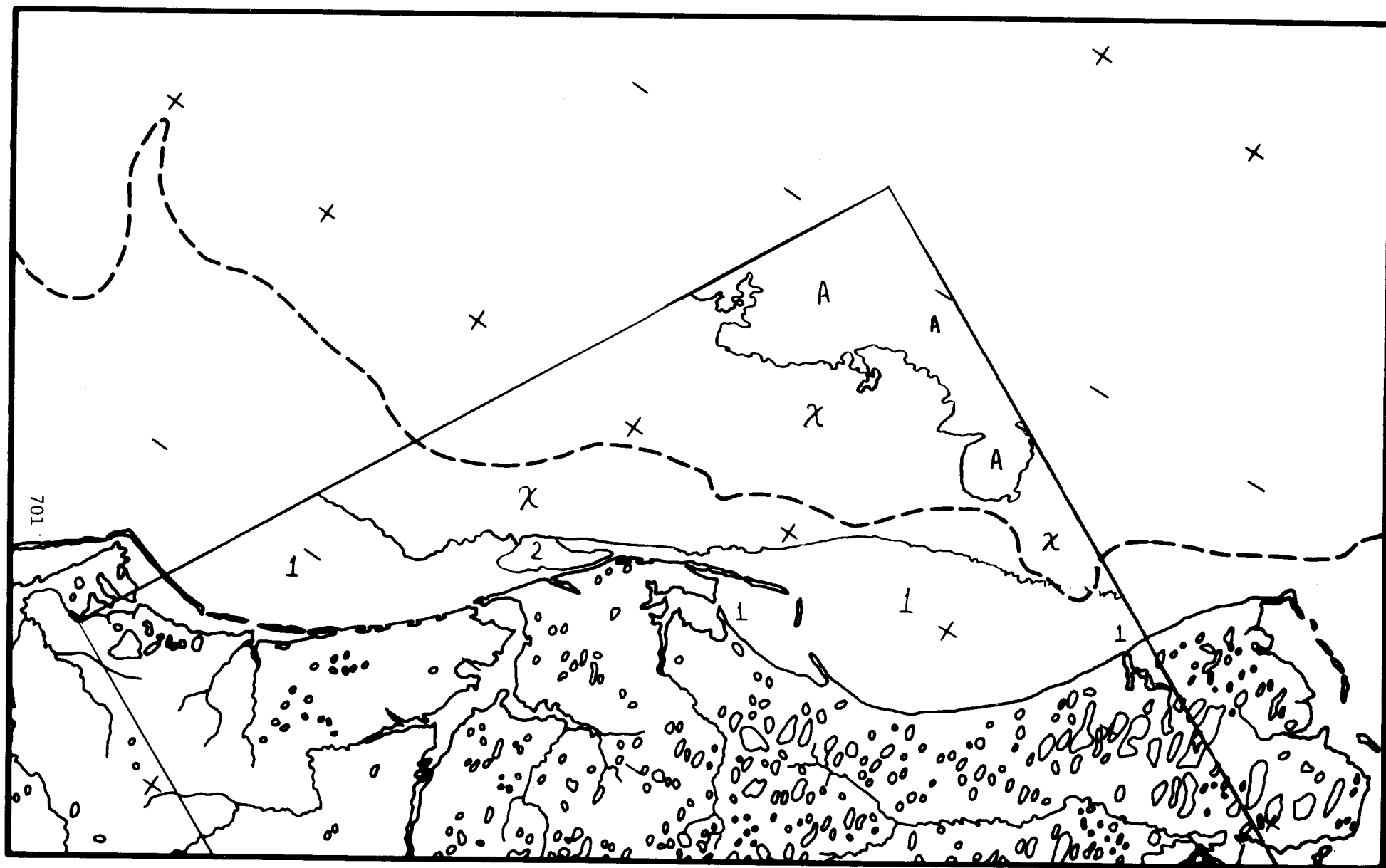
SHOREFAST SEA ICE
SURFACE MORPHOLOGICAL CHARACTERISTICS
CHUKCHI SEA COAST: BARROW SECTOR

14 May 1975   2112-21511

Map No. 28: Point Hope Sec, 16 MAY 75, 2114-22033

Legend X   open water

A   pack ice

1   homogeneous ice with some surface water

2   like type 1 but with an increased amount of
surface water. Some linear features are present.

3   an increasing amount of surface water and
numerous linear features without pattern
characterize this ice type

4   a near shore ice type with considerable
surface water and numerous drain cracks or
dry ridges visible

5   although not the darkest in appearance this
ice seems to be the furthest progresses in
melting there being a small opening to open
water in the middle of this type.
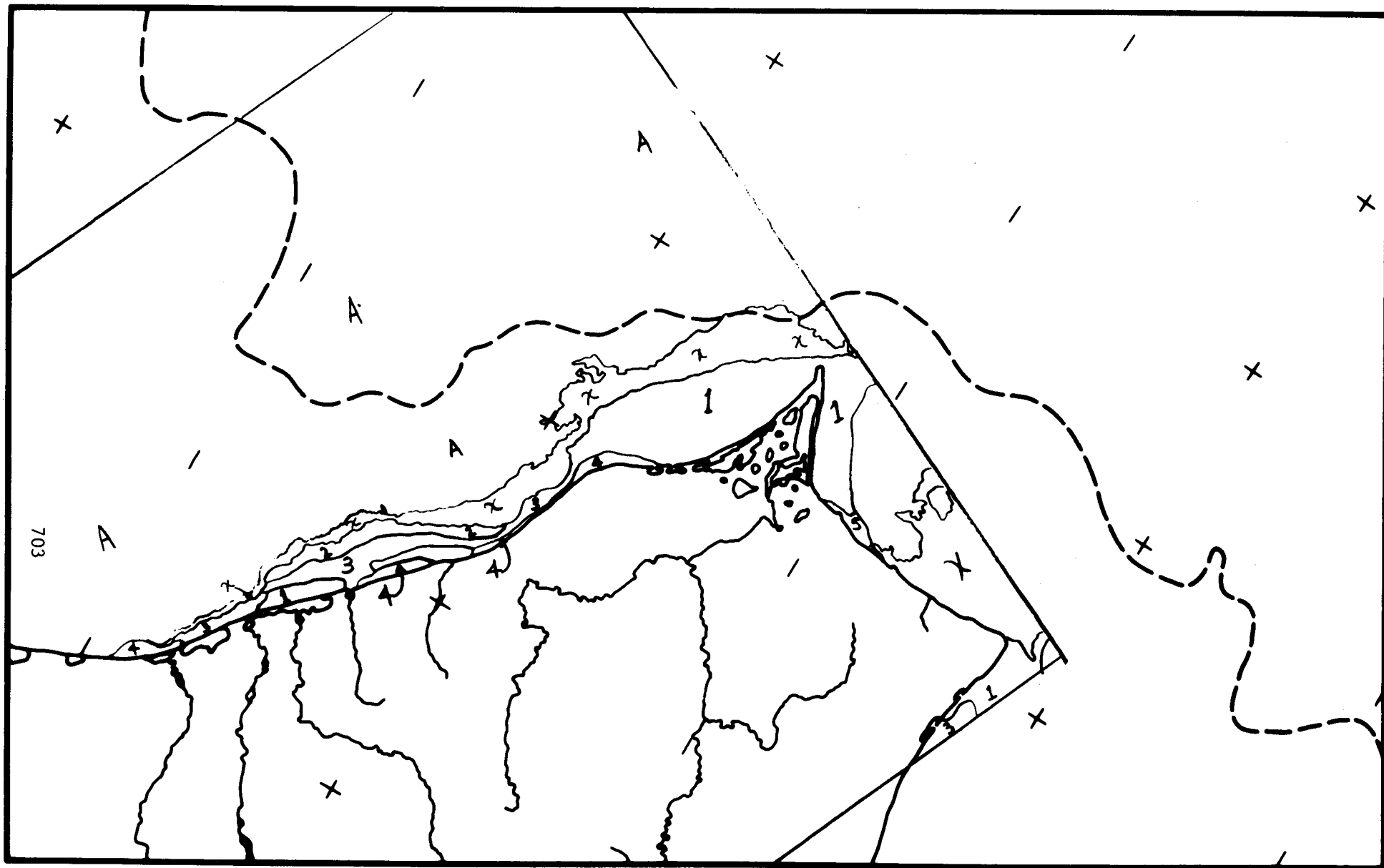
702

SHOREFAST SEA ICE
SURFACE MORPHOLOGICAL CHARACTERISTICS
CHUKCHI SEA COAST: POINT HOPE SECTOR
16 May 1975   E-2114-22033

Map No. 29:   Point Hope Sec, 02 JUN 75, 2131-21580

          Legend X open water

                 A pack ice

                 1 very light tone ice which, from its position, may be due to pressure ridging

                 2 generally homogeneous ice with surface melt water and some linear features

                 3 homogeneous ice with about the same surface water as type 2 but not exhibiting any linears

                 4 like type 3 but with an increased amount of surface water

                 5 this type has the same amount of surface water as does type 4 but does contain numerous linear features

                 6 an increasing amount of surface water with what appears to be individual floes discernable due to differing melt rates

                 7 considerable surface water and numerous linear featrues (here probably pressure ridges) are observed on this ice type

                 8 this near shore ice shows effects of surface run off and in places the ice appears rotten. This ice does appear well drained in places.

SHOREFAST SEA ICE
SURFACE MORPHOLOGICAL CHARACTERISTICS
CHUKCHI SEA COAST: POINT HOPE SECTOR
2 June 1975

Map No. 30: Point Hope Sec, 03 JUN 75, 2132-22034

           Legend X open water with or without floes

                   A pack ice

                   1 featureless ice with some surface water

                   2 slightly more surface water than type 1 and
                      with some lighter linear features visible,
                      otherwise like type 1

                   3 essentially featureless ice but with more
                      surface water than type 2

                   4 with more surface water than type 3 and with
                      distinct lighter linear features

                   5 this type has at least as much surface water
                      as type 4 and with bands containing more water

                   6 an area with numerous linear features and
                      considerable surface water

                   7 very light ice due either to extensive hummock
                      fields or drain cracks or both

                   8 very dark (wet) ice also containing linear
                      features

                   9 ice exhibiting evidence of shore influences,
                      run off etc.
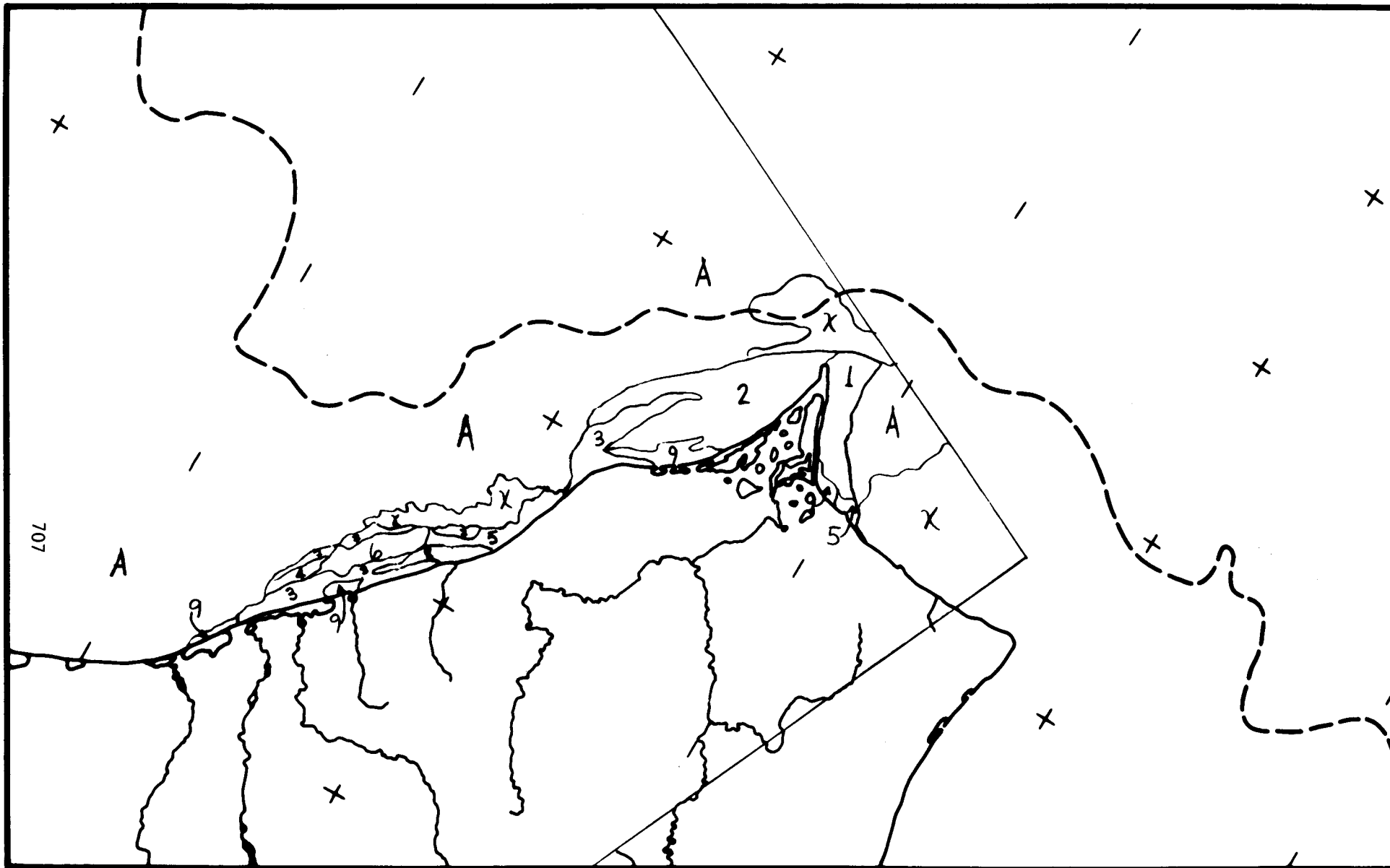
706

SHOREFAST SEA ICE
SURFACE MORPHOLOGICAL CHARACTERISTICS
CHUKCHI SEA COAST: POINT HOPE SECTOR

3 June 1975

Map No. 31:   Kotzebue Sound Sec, 19 JUN 75, 2148-21524

Legend   X   open water with or without some floes

A   pack ice

1   generally homogeneous ice with some bands
    exhibiting increased melt but overall fairly
    low amounts of surface melt water

2   also ice with little surface water but in
    this location water appear to be old refrozen
    leads transect the area

3   more surface melt water and a network of
    lighter linear features (old leads) characterizes
    this ice type

4   the same as type 3 but with more surface water
    and consequently more distinct linear features
    which show little or no signs of melting

5   this type has an intermediate amount of surface
    melt water and is divided into rounded elements
    but is continuous

6   like type 5 but with an increased amount of
    surface water

7   a noncontinuous ice type composed primarily of
    ice type 3 but in its northwestern reaches it
    is of ice type 1. Ice coverage varies from
    50% to 90%.

8   this ice exhibits large amounts of surface
    water and in places it is rotten and breaking up

9   this type is found near shore and is much like
    type 8 but would appear to be thinner and closer
    to dissolving or breaking up over its entire
    expanse

10 noncontinuous, unhomogeneous ice surrounding
    the small islands
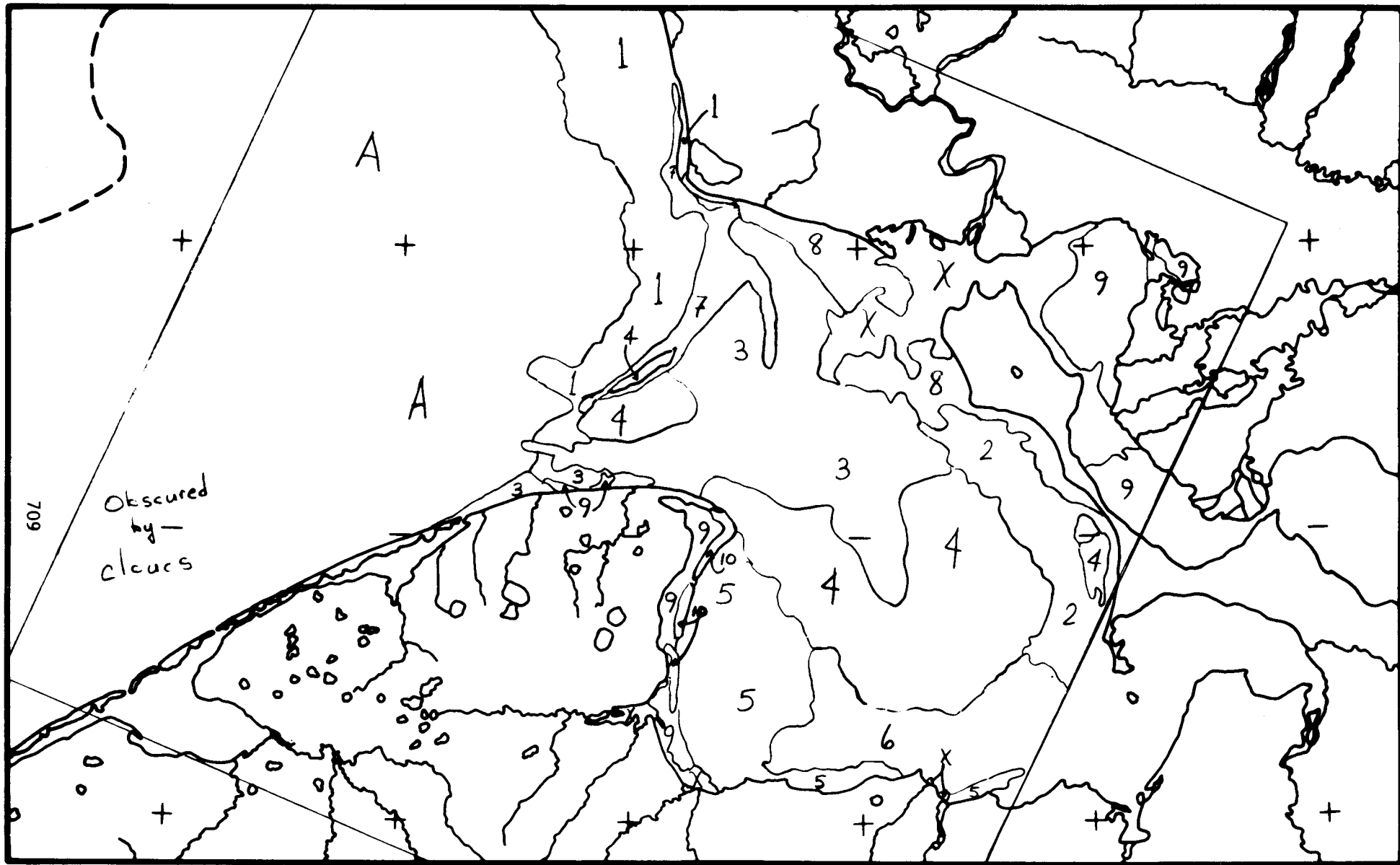
SHOREFAST SEA ICE
SURFACE MORPHOLOGICAL CHARACTERISTICS
CHUKCHI SEA COAST: KOTZEBUE SOUND SECTOR

19 June 1975

No map: Eastern Kotzebue Sound, 05 JUL 75, 2164-21411

No continuous ice is visible in this image, ice coverage

<20%.

Fig. 32. Summary of ice limits
along the Chukchi Sea coast
Summers 1973-75

15 MAY 73

26 MAY
74

16 MAY 75

14 MAY 75

11 MAY 74

05
JUNE
73

11 MAY 74   16 MAY
75

?-?-?-?

31 MAY 74

16 MAY 75

17 MAY 73   31 MAY 74

01 JUNE
75

28 MAY 74

02 JUNE 73

711
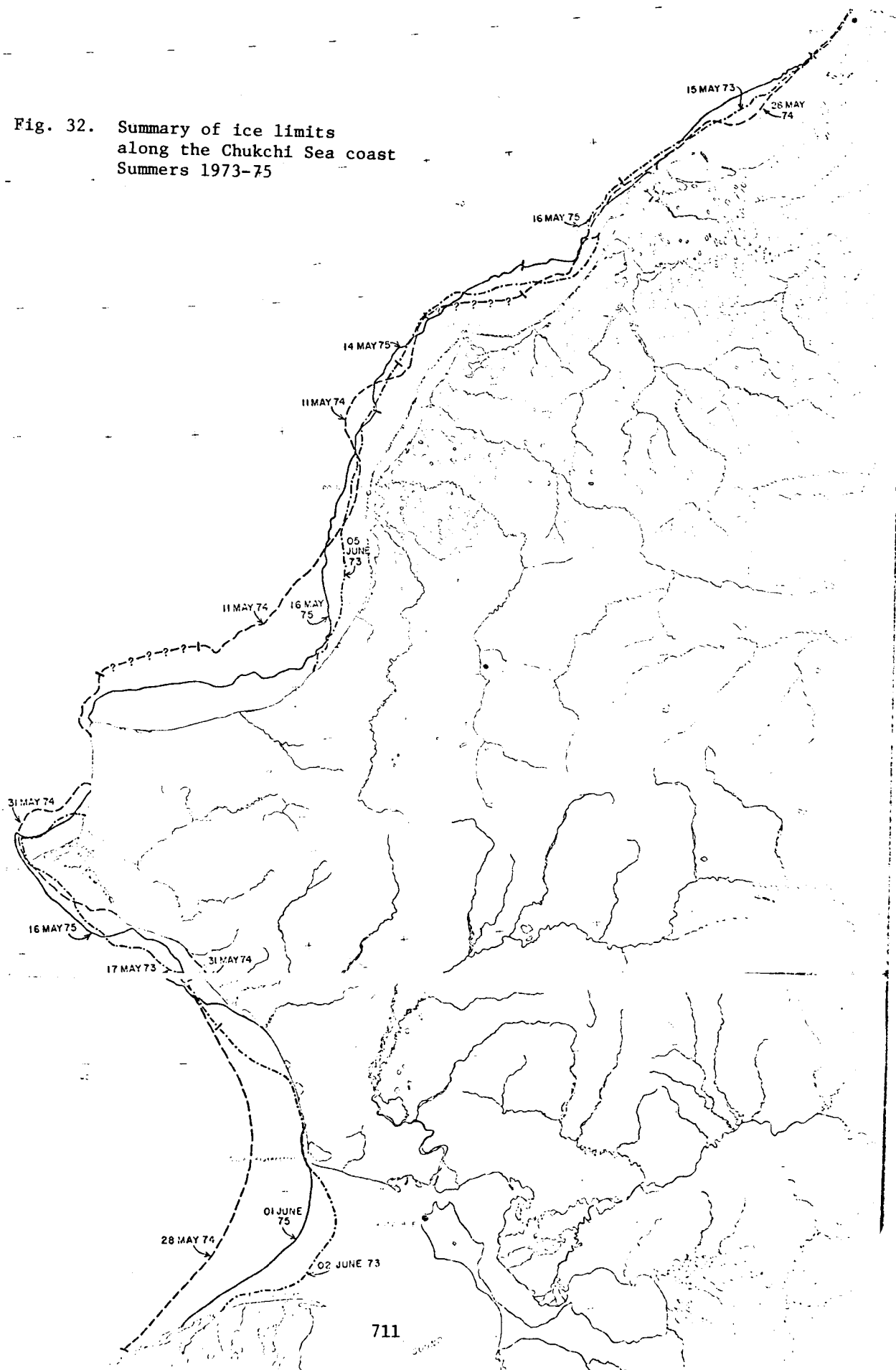
APPENDIX   III

MAPS OF NEAR-SHORE ICE CONDITIONS FOR THE BARROW SECTOR PREPARED

FROM 1974 DECAY SEASON LANDSAT IMAGERY

712

Introduction

The maps presented in the following section represent highly
nterpreted data products. In addition to the shape, tonal, textural,
and time-sequential information contained in the LANDSAT data, SLAR
imagery and color-infrared photography were consulted. Only those ice
features which appear important to the decay process and/or its
interpretation are mapped individually. Fields of fairly homogeneous
ice are designated with various symbols. On each map, a given symbol
represents only one type of ice (as interpreted) and the symbols are
numbered for cross-reference with the explanatory description for
each scene.

26 February 1974: Scene 1583-21524

This scene shows the near shore ice conditions between Barrow and
Lonely. A zone of ice with relatively light gray tone extends roughly
parallel to shore along the coast (1). This ice exhibits quite
uniform tone on the images, possibly indicating a nearly-level ice
surface. Zone 2, by contrast, is characterized by a generally darker
tone with more textural variation than zone 1. Some of this texture
must be due to ice surface roughness and the associated snowdrift
distribution. A number of large ridge systems (R) show up due to
shadow enhancement with the low sun elevation. These features were
also identified on the Appil SLAR imagery. A prominent "ice boundary"
(B) was identified, but could not be interpreted. Possibly it may
correspond to a zone of ridging or a refrozen crack or lead. Seaward
of this ice a system of cracks has developed in the previously-con-
tinuous ice (C). Zone 3 (west of Barrow) had a sightly-darker tone
than surrounding ice. Analysis of the April SLAR imagery showed this
to be highly-deformed ice along the fast ice edge in the Chukchi Sea.
Zone 4 contains pack ice and open water seaward of the continuous ice.
Several leads, including a prominent flaw lead along the ice edge,
appear in this zone. The pack ice floes were mainly greater than giant-
floe size, with some refrozen, new ice in the interstices between floes.
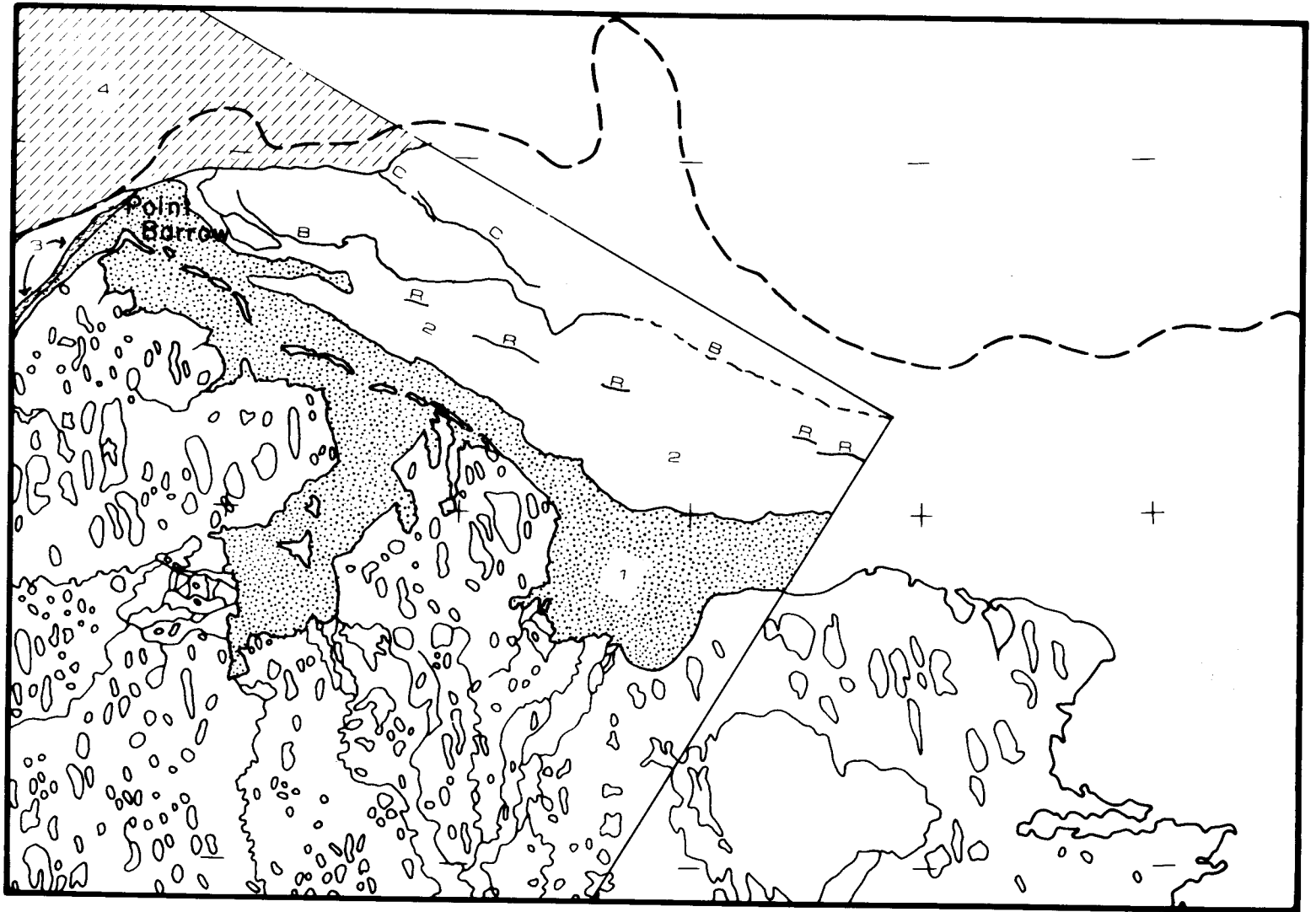
SHOREFAST SEA ICE
SURFACE MORPHOLOGICAL CHARACTERISTICS
BEAUFORT SEA COAST: BARROW SECTOR
26 FEB., 1974

16 March 1974: Scene 1601-21522

This scene shows much the same ice as the previous scene. Zone 1 is again distinguishable, based on its uniform, light gray tone. Two ice fields within this zone (5) are further differentiated because of a slightly-darker gray tone. In Smith Bay, the seaward edge of zone 5 may correspond to the fast ice edge during early winter. SLAR and CIR imagery show that the zone 5 ice seaward of Dease Inlet was somewhat rougher than the level, first-year ice inside the barrier Islands. Zone 2 again shows the darker gray tones and textural variations seen on 26 February, as well as the ridges (R). The lines designated as "G" correspond, again, to gray-tone contrasts that could not be positively interpreted. The most notable feature on this scene is zone 6, a refrozen lead, which opened up along the crack (C) which was mapped on 26 February. Analysis of April SLAR imagery showed that this same lead endured at least as late as 29 April, and was composed of extremely-smooth ice (first-year). Displacement vectors are shown for two segments of the ice edge that could be positively matched up. Zone 3, to the west and north of Barrow, consists of open water and thin ice in a partially-refrozen lead. Seaward of this lead the pack ice (4) consists primarily of giant-floe pieces. All of the important features of the ice fields to shoreward of the pack ice on this scene remained esentailly unchanged until sometime in May, when some of the ungrounded continuous ice began to crack and move.
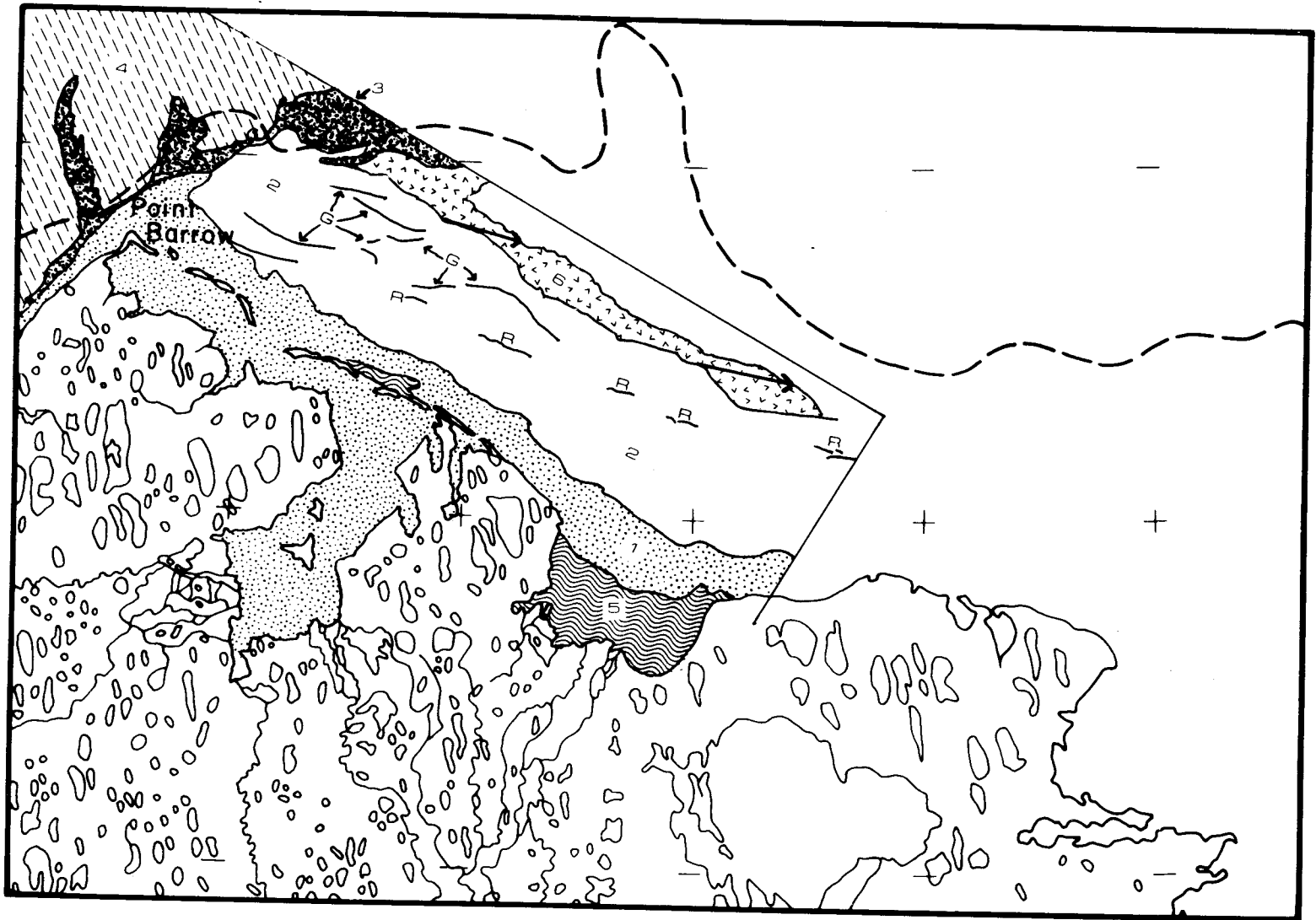
SHOREFAST SEA ICE
SURFACE MORPHOLOGICAL CHARACTERISTICS
BEAUFORT SEA COAST: BARROW SECTOR
16 MARCH, 1974

29 June 1974: Scene 1706-21322

This scene shows ice conditions between Admiralty Bay and Harrison
Bay, well after the onset of surface melting. The continuous ice lim-
it could be identified along the western 2/3 of this scene and is
designated as C. 8-9 tenths pack ice concentrations were present to
seaward along this edge. Several ice fields near shore are designated
as zone 1. These represent level, 1st-year ice with a light tone
on all LANDSAT bands, indicating a lack of puddle development. It
is possible that much of this ice has already undergone drainage of
surface meltwater through cracks and thawholes. Zone 2 is composed
of 1st-year, level ice which has the darkest tone of any ice on the
scene, indicating maximum puddle development at this time. Zone 3
contains ice with an intermediate gray tone, showing a considerable
amount of texture. Analysis of SLAR and CIR imagery shows this to
be lightly-deformed (small ridges and rafts) 1st-year ice, with def-
ormation increasing to seaward. Zone 4 showed a quite-distinct tone
on LANDSAT and CIR images, and was a rather uniformly rough ice type
on the SLAR. A detailed analysis of the CIR data lead us to conclude
that this ice was composed of up to 50% older floes (greater than 1st-
year age) which were frozen into the fast ice matrix of first-year
ice. Zone 5 presented a complexly-textured but light tone on the
LANDSAT images, and consists of mostly 1st-year ice, with deformation
ranging from level ice to large ridges. Well-developed surface pud-
dling was absent from most of this ice field, despite the presence
of numerous, locally flat ice pieces. In southern Harrison Bay, we
find a field of very dark ice, possibly puddled or covered with muddy
runoff from the Colville, and designated as "6". The Colville
shore polynya was just southeast of this ice.
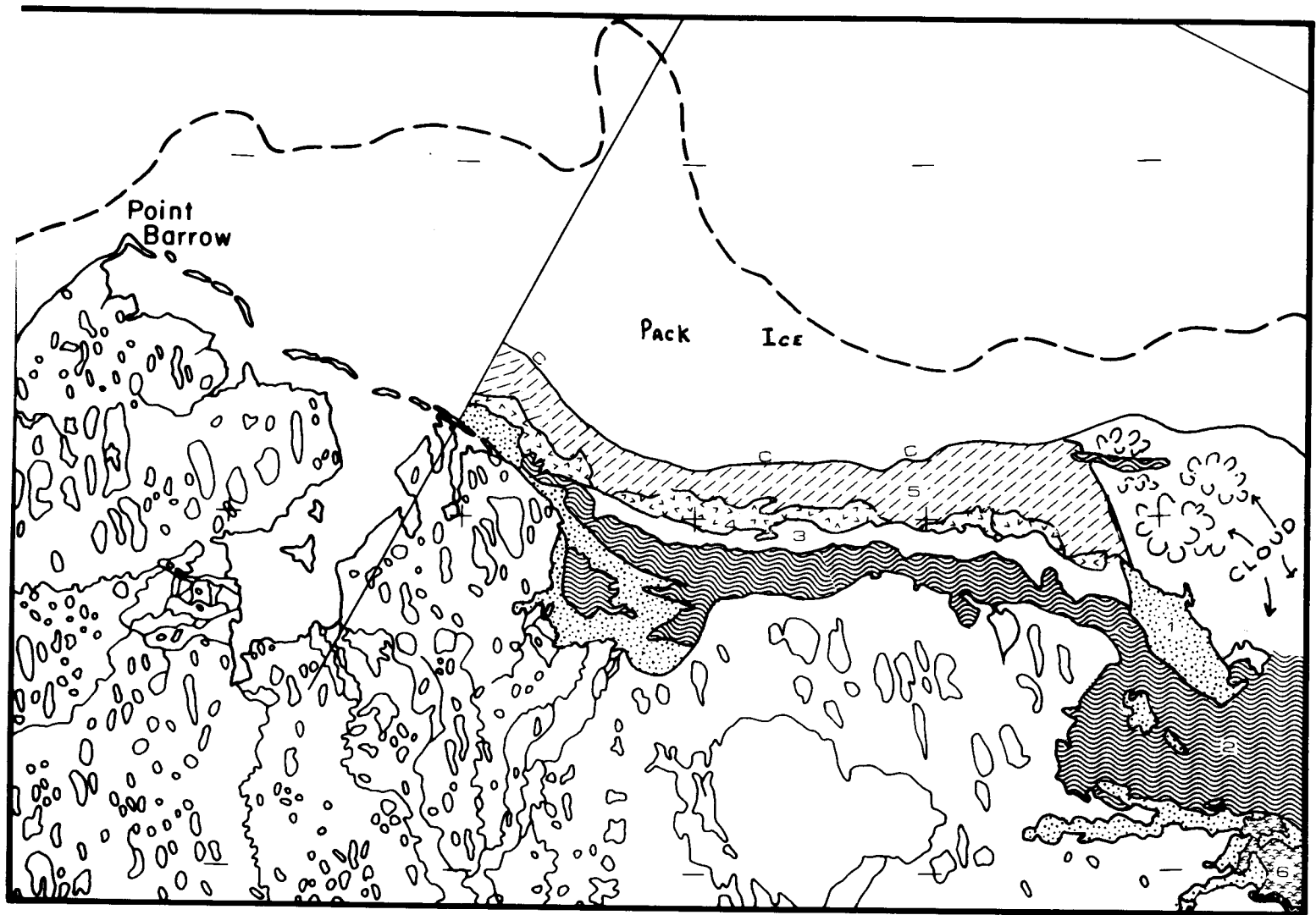
Point
Barrow

Pack   Ice

CLOUD

SHOREFAST SEA ICE
SURFACE MORPHOLOGICAL CHARACTERISTICS
BEAUFORT SEA COAST: BARROW SECTOR
29 JUNE, 1974

3 July 1974: Scene 1710-21551

This scene covered near shore ice conditions from Point Barrow to
Admiralty Bay. Zone 1 on this scene is level, 1st-year ice with
medium to heavy surface puddling development. Zone 2 is generally
the same type of ice as 1, but with a lighter tone on LANDSAT indic-
ating less surface meltwater. Some lineations appear in this ice,
possibly representing cracks through which surface water may have
drained. Zone 3 is the shoreward edge of a belt of fairly rough
ice (as interpreted from the SLAR). This ice appeared very distinct
on the 21 June CIR photographs, but could not be positively interp-
reted. It is possible that Zone 3 contains a high percentage of
older ice types. On LANDSAT, this ice gives some indication of light-
toned floes in a matrix of darker ice. Zone 4 is the lightest-toned
ice on the scene, and probably represents ice which has drained
completely. On the 21 June CIR photos this ice was not the lightest
ice in the area. Two elongate areas of dark-toned ice extend along
the seaward side of the barrier Islands (5). The SLAR imagery shows
that this ice is lightly deformed, with possible ridges along the
seaward edges of the zones. Apparently a good deal of surface melt-
water has been trapped between elevated ice features, causing the
dark tones on LANDSAT. To the west of Point Barrow a complex set
of linear features trends parallel to the coast. These features
appeared to be large ridge systems (on SLAR) and hummocky ice, and
are designated as "R" on the map. The lines on the map show the
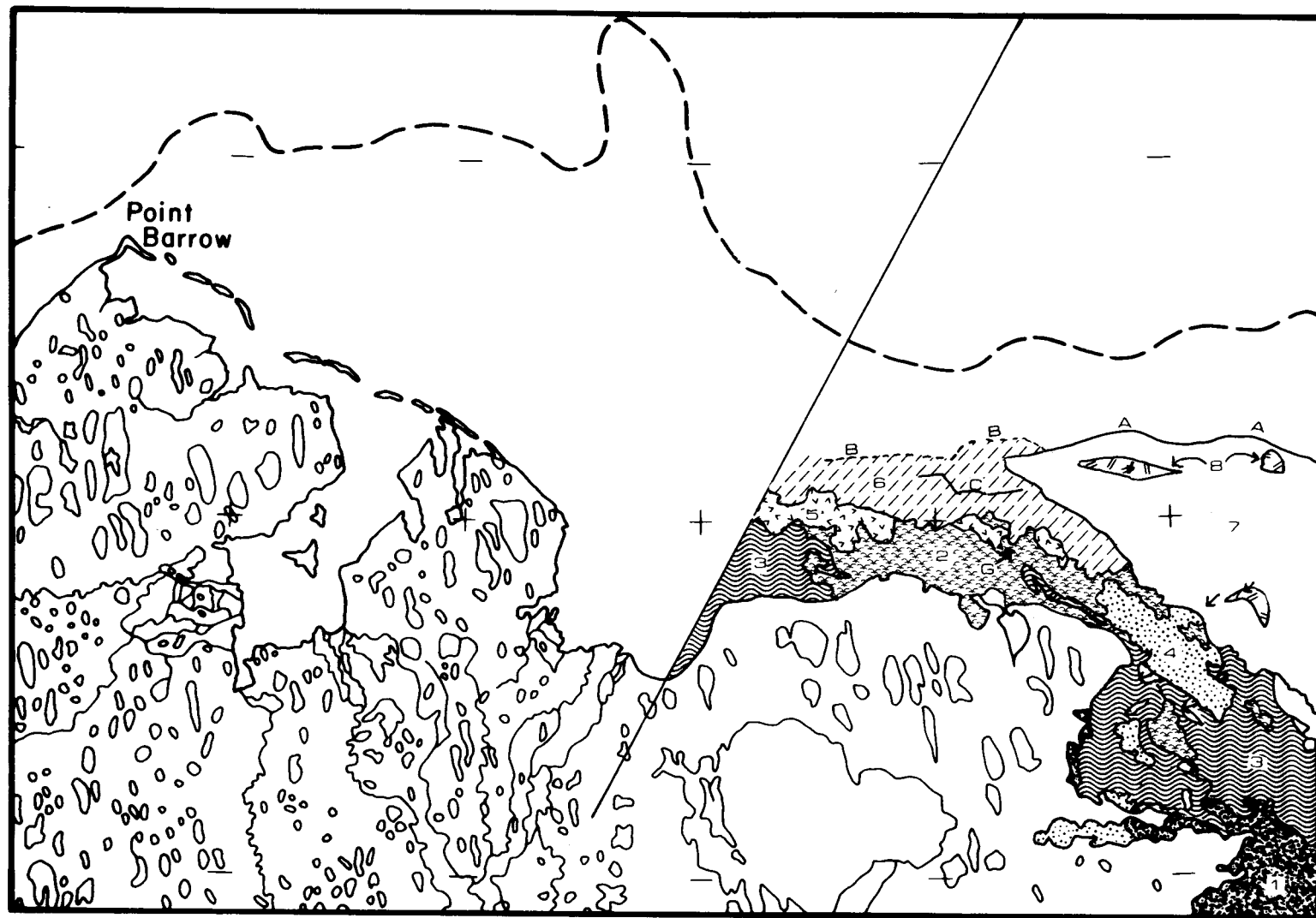general direction of these linears.
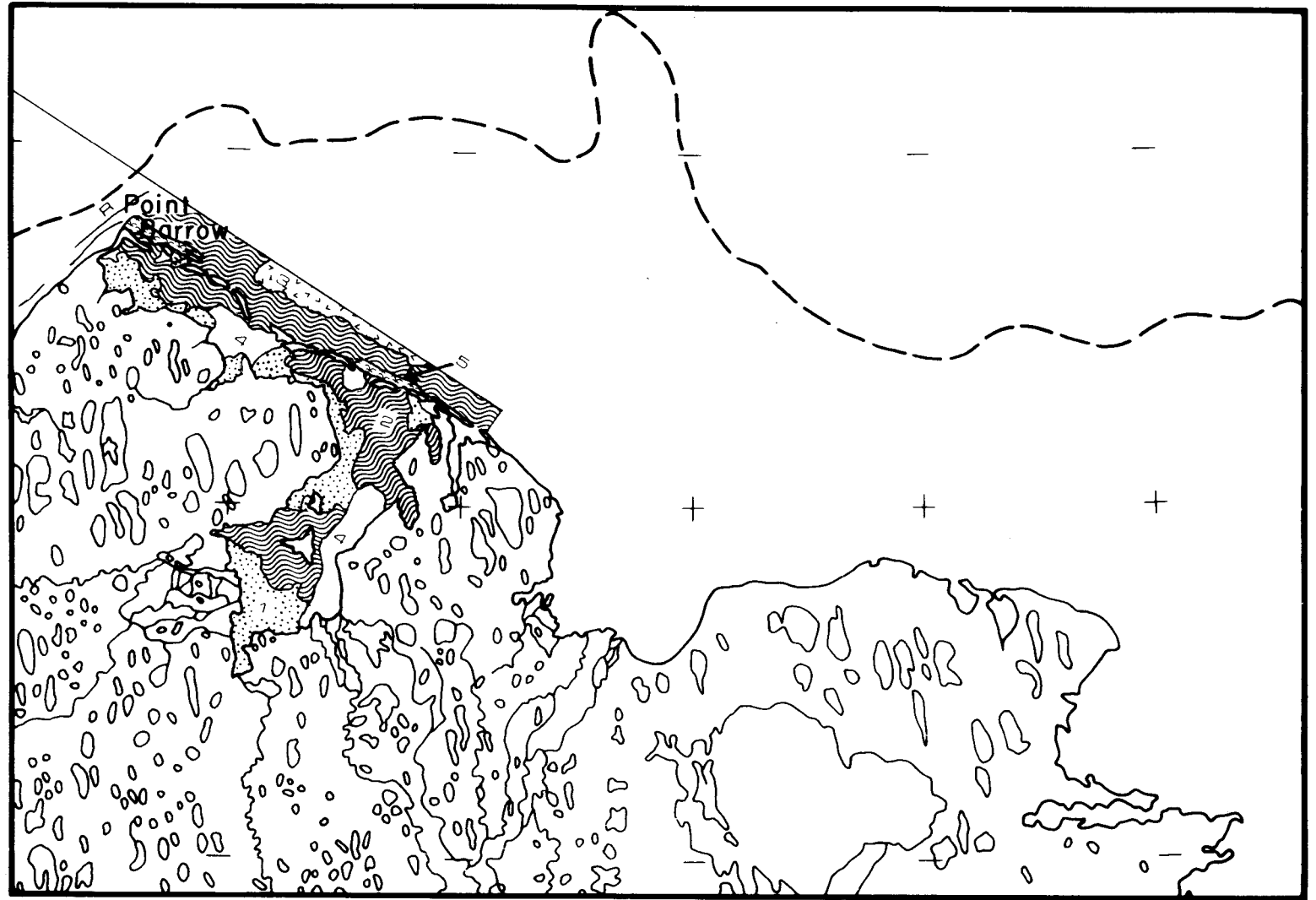
SHOREFAST SEA ICE

SURFACE MORPHOLOGICAL CHARACTERISTICS

BEAUFORT SEA COAST: BARROW SECTOR

3 JULY, 1974

16 July 1974: Scene 1723-21260

This scene shows ice conditions from Smith Bay to Harrison Bay. Zone
1 is open water in the Colville shore polynya. This zone has enlarged
considerably since 29 June. Some light-tone features within this zone
appear on the LANDSAT imagery, possibly indicating sediment in the
water or light fog over the water. Zone 2 is composed of open water
and fragmentary, decaying first-year ice pieces. This zone was form-
erly covered by level-to-lightly-deformed 1st-year ice with relatively
advanced puddle development. Within the shoreward portion of this
zone there are a number of light-tone ice features, possibly rep-
resenting drained ice or "bottom-fast" ice. The feature "G" is
a deformed ice mass with a considerable vertical relief (from SLAR).
This mass was later determined to be grounded. Zone 3 is also
composed of first-year ice in an advanced state of decay, with open
water spaces. However, the amount of open water is considerably
less than in zone 2. This ice was also in the most-heavily puddled
zone on June 29. Zone 4 is very light-toned ice which has apparently
cracked and broken since 29 June. Some open water spaces are evident
between pieces of this ice also, but it maintains a very light tone
with limited surface meltwater. This ice is 1st-year in age with
little or no surface deformation, and, off Cape Halkett, may rep-
resent ice which froze over later in winter than the ice to shoreward.
Seaward of zones 2 and 3 on the western 1/2 of the map is an area of
light-tone, floe-like elements in a matrix of open water and darker
ice (5). These floes are interpreted to be older ice floes. This
zone was covered by up to 50% older ice earlier in the melt season.
It is apparent that the breakup of this was not greatly delayed by
the greater thickness and albedo of the older ice floes, because the
1st-year interstices were able to melt out, mobilizing the older
floes. Zone 6 comprises mostly 1st-year ice with some areas of
heavy deformation. Occasional open water spaces appear in this zone
also. A prominent crack (C) formed in this zone between 29 June
and 16 July. The ice to shoreward of the crack was displaced 1 or
2 km west, while it was impossible to accurately determine displace-
ments to seaward. The indication is that the ice to seaward may
have been grounded. Two motion vectors were plotted in Harrison
Bay which show the WSW displacements occuring in the fast ice. Anal-
yses of the Prudhoe sector showed that during this season, pack ice
was pressuring the fast ice in towards shore. Perhaps the displacements
shoreward of C were results of this pressuring also. Zone 7 covered
most of outer Harrison Bay and consists mainly of 1st-year ice with
moderate to heavy deformation including some ridges. Very few openings
appeared in this ice on July 16, although some slight displacements
had taken place sinc 29 June. On LANDSAT imagery the tone was gen-
erally light, again indicating poorly-developed puddling. Zones 8
were flat, first-year ice fields which appeared much like zone 4
except that no open water was present. These fields may represent
areas which refreeze relatively late in the winter season. The con-
tinuous ice limit is fairly well-defined off Harrison Bay (A) but
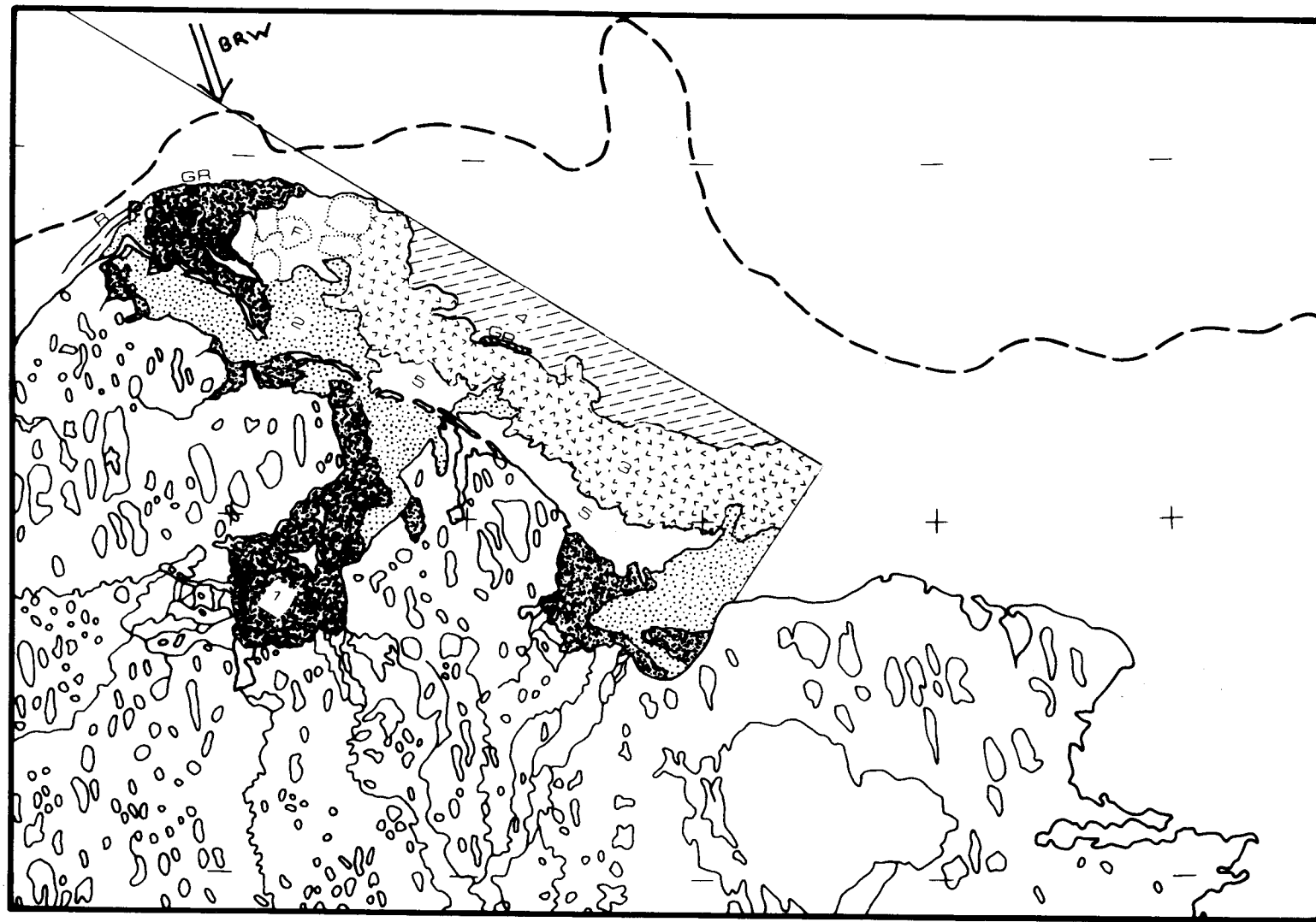is less definite to the west (B).

SHOREFAST SEA ICE
SURFACE MORPHOLOGICAL CHARACTERISTICS
BEAUFORT SEA COAST: BARROW SECTOR
16 JULY, 1974

Ice conditions between Point Barrow and Smith Bay are depicted on this scene. A definite continuous ice edge could not be drawn at this late stage in the decay season, due to numerous open water areas and the movements within formerly-shorefast ice. To the north and west of Point Barrow, however, a line of grounded ridges is designated as "GR". Pack ice was compact along this feature and the Barrow wind direction (double arrow) was such that the pack should have been forced shoreward. Because the ridges were firmly grounded, a polynya has formed in the "ice lagoon" to shoreward and is designated as zone 1 (open water) on the map. Other zone 1 areas have formed along the shoreline and in Admiralty and Smith Bays, which were formerly covered by 1st-year level ice. The features marked "F" are vast-floe size pieces of former fast ice, now floating in the ice lagoon formed by the grounded ridges. Zone 2 comprises 1st-year ice in a generally advanced state of decay. Some of this ice is heavily-puddled or rotten ice, although some light-toned ice (on LANDSAT) still persists in Elson Lagoon, zone 2. To the north and west of the spit leading to Pt. Barrow there is some older ice in zone 2. Zone 3 contains many relatively light-tone floes in a matrix of open water and rotten 1st-year ice. Some of these floes are older ice. This zone was partially composed of older floes earlier in the melt season. Zone 4 is somewhat more compact ice than zone 3, with less open water and less dark ice. The age of the ice in this zone is indeterminate on this scene. A large ridge system, located on February and March LANDSAT, April SLAR and June CIR photography remained stationary between zones 3 and 4 in the presence of shearing ice around it (GR). This ridge system is interpreted to be firmly grounded on the sea floor. Zone 5, just shoreward of zone 3, consists mainly of decayed 1st-year ice and open water. Some lighter-tone ice pieces in this area may represent the remnants of former ridge systems within the fast ice.
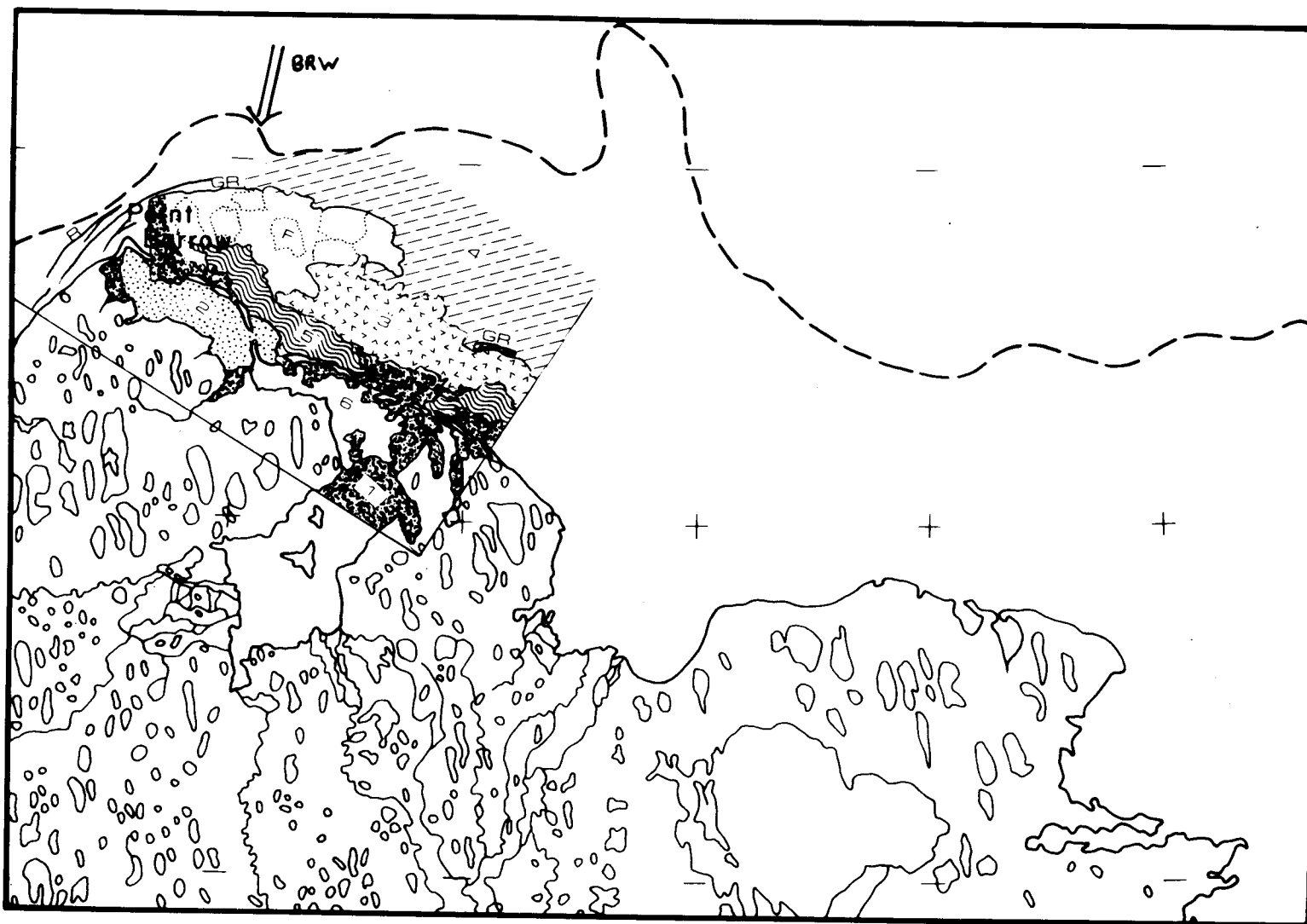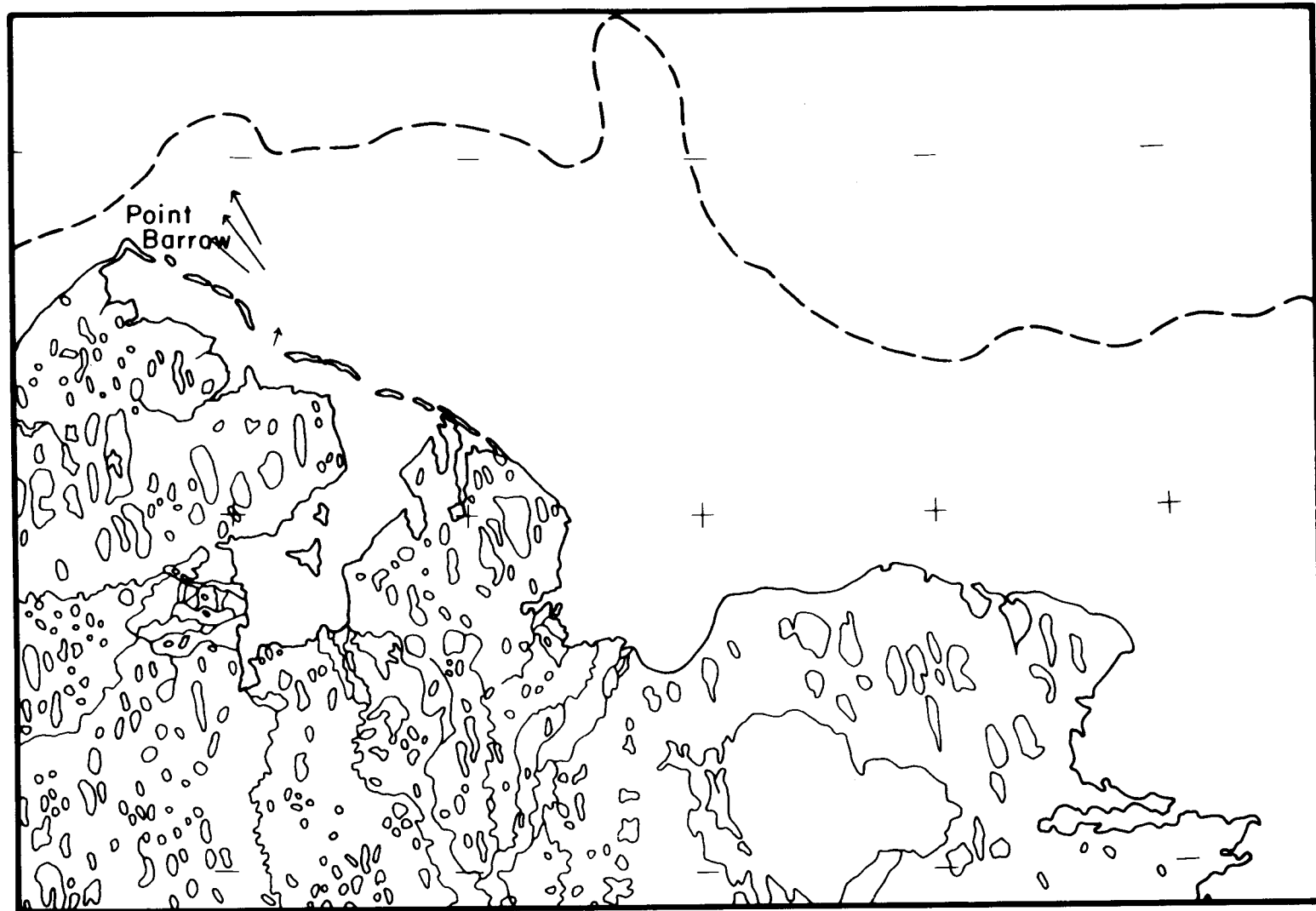
SHOREFAST SEA ICE
SURFACE MORPHOLOGICAL CHARACTERISTICS
BEAUFORT SEA COAST: BARROW SECTOR
20 JULY, 1974

21 July 1974: Scene 1728-21540

This scene shows ice conditions in the vicinity of Pt. Barrow. Some
notable changes occurred in the time interval 20-21 July. On this
scene, zone 2 represents partially-drained, 1st-year ice which has
broken up into floe-like ice pieces since 20 July. Zone 1 is open
water, and has undergone some areal enlargment near Dease Inlet. Zone
3 again represents light-toned floes in a matrix of open water and
rotten ice, some of which floes are older than 1st-year, especially
in the eastern part of Zone 3 on this map. Zone 4 is fairly-light
ice representing compact pack ice on this date. Zone 5 comprises
rotten, broken-up 1st-year ice which was formerly mainly level 1st-
year ice. Zone 6 contains 1st-year pans and floes of 5/10 concen-
tration in a matrix of open water. Both grounded ridge systems
(GR) have remained in place since 20 July. The floes in the ice
lagoon formed by the western grounded ridges have undergone displace-
ments since 20 July, but these are not in agreement with the Barrow
resultant wind vectors (double arrows). The displacement vectors
for the ice floes are shown on the supplementary map.

SHOREFAST SEA ICE
SURFACE MORPHOLOGICAL CHARACTERISTICS
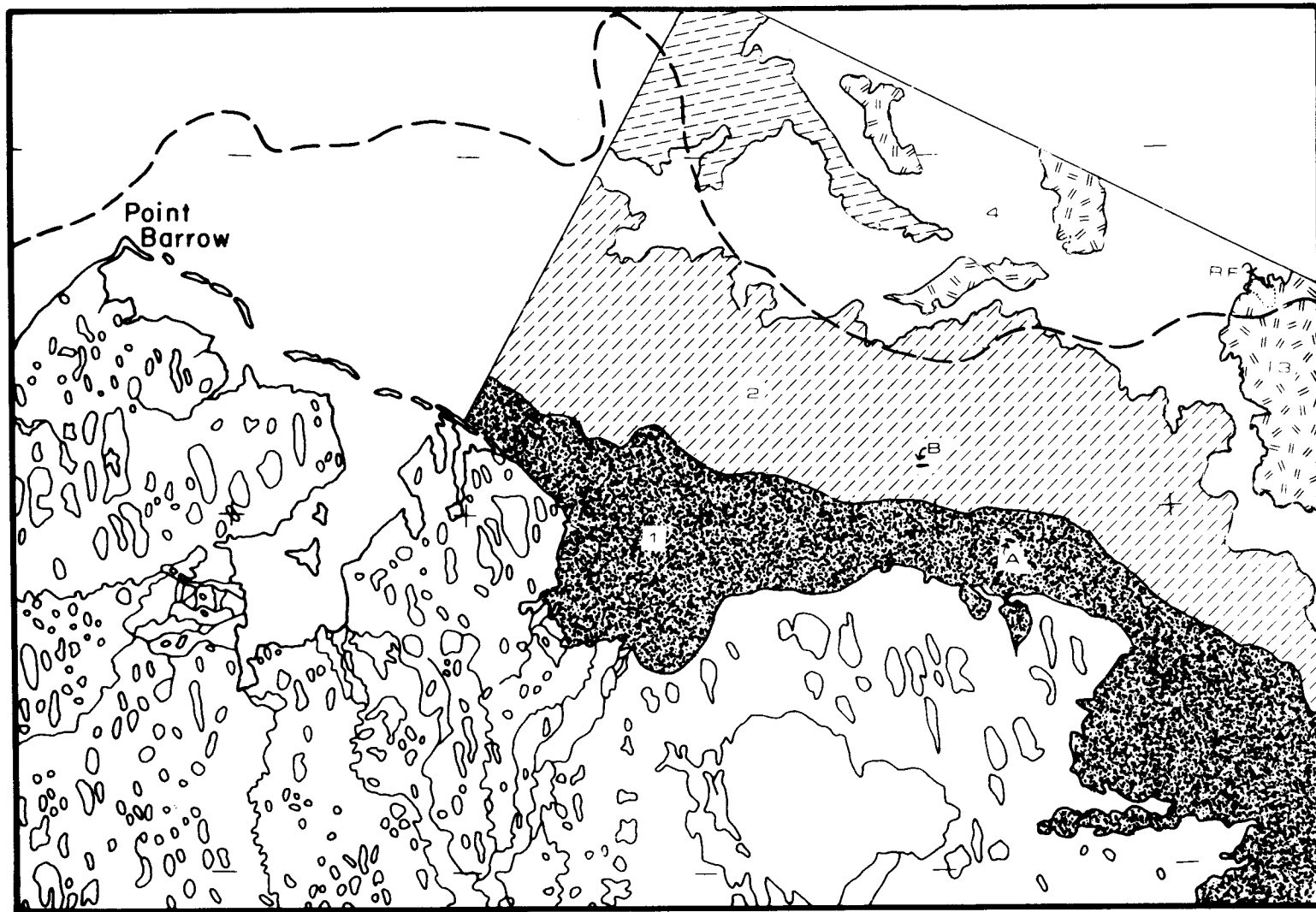BEAUFORT SEA COAST: BARROW SECTOR
21 JULY, 1974

SHOREFAST SEA ICE
SURFACE MORPHOLOGICAL CHARACTERISTICS
BEAUFORT SEA COAST: BARROW SECTOR
MOVEMENT 20→21 JULY

22 August 1974: Scene

On this scene we see the post-breakup conditions between Admiralty
Bay and Harrison Bay. Zone I is composed of open water and, at this
stage, represents a nearly-continuous shore lead along the entire scene.
One grounded ice mass in the shallows near shore remains in place
on this date (A). Zone 2 is very rarefied pack ice (less than 1/10
concentration) containing some large pieces of light-toned ice, some
of which pieces are probably ridge fragments from the formerly fast
ice. Zone 4 comprises pack ice in concentrations ranging from 2/10 to
about 7/10. The surfaces of these floes present the appearance of
advanced ablation. Zone 3 is covered by about 9/10 pack ice in
much the same conditions. The dotted enclosure designated "RF" be-
tween zones 3 and 4 in the northeastern map sector was identified as
a vast-floe size fragment from the ridges in Harrison Bay. These
ridges formed the late-June fast ice edge, just seaward of the large
grounded ice mass in outer Harrison Bay (see Prudhoe sector maps, 1974).
In zone 2, a second piece of ice was found to remain stationary through
the melt season and is designated as "B". This piece corrseponds in
position to a ridge system identified on the April SLAR and June CIR
data. Furthermore, it is located just seaward of the crack which
was mapped on the July 16 scene. It seems likely that B was grounded
firmly on the sea floor, and stabilized the fast ice around it during
early July. The ice to shoreward was weakened sufficiently so as to
fail under stress from winds and pressuring ice from the east.

SHOREFAST SEA ICE
SURFACE MORPHOLOGICAL CHARACTERISTICS
BEAUFORT SEA COAST: BARROW SECTOR
22 AUG., 1974

APPENDIX IV

MAPS OF NEAR-SHORE ICE CONDITIONS FOR THE PRUDHOE SECTOR PREPARED

FROM 1973 DECAY SEASON LANDSAT IMAGERY

.

Introduction

The maps presented in the following section represent highly
interpreted data products. In addition to the shape, tonal, textural,
and time-sequential information contained in the LANDSAT data,
Dr. Stringer's OCSEAP maps were consulted. SLAR and CIR images were
not available for 1973. Only those ice features which appear
important to the decay process and/or its interpretation are mapped
individually. Fields of fairly homogeneous ice are designated with
various symbols. On each map, a given symbol represents only one
type of ice (as interpreted) and the symbols are numbered for
cross-reference with the explanatory description for each scene.

14 March 1973:   Scene 1234-21175

This is a late winter scene showing several zones of differing grey
tones.   The continuous ice edge is quite distinct in the eastern
two/thirds of the frame, while in the western third it is rather
unclear.   The pack ice is very consolidated with little, if any,
open water, although there are many cracks (CR), refrozen leads
(RL), and ridges (R).   Light toned ice extends along the coast in
a band approximately 10 to 30 km wide (1).   The ice appears rela-
tively smooth, without major deformational features.   The seaward
edge of this zone may correspond to a former continuous ice edge.
There appears to be a zone (2) gradational between the continuous
ice (1) and the pack ice (3).   The ice appears rougher than zone
1, with possible ridging (R) along the seaward boundary and some
cracking and refrozen leads within the zone.   The eastern portion
of this zone appears more deformed than the western, having more
refrozen leads, smaller sized floe-like pieces of homogenous grey
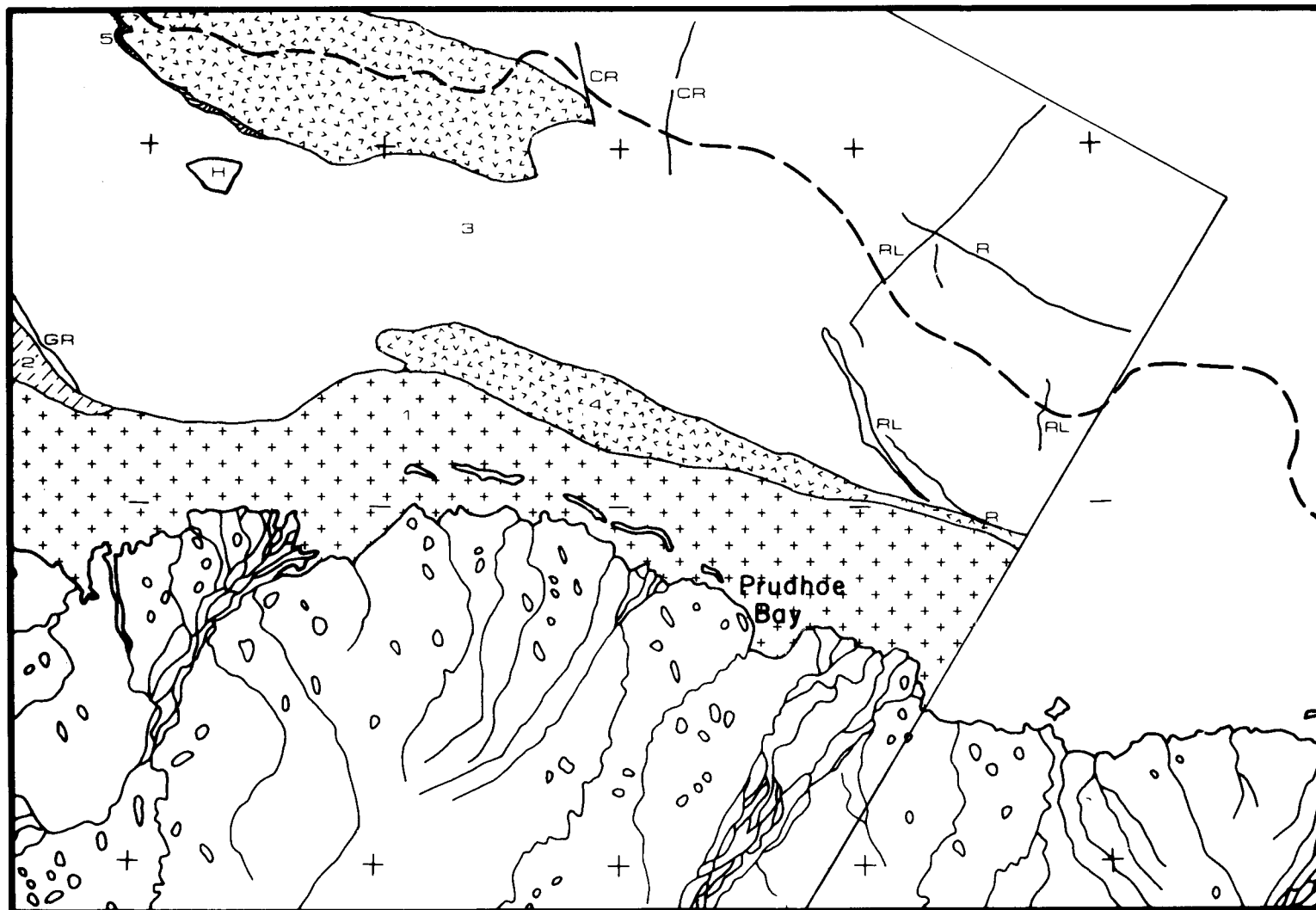ice, and more dark toned, possibly thinner ice.
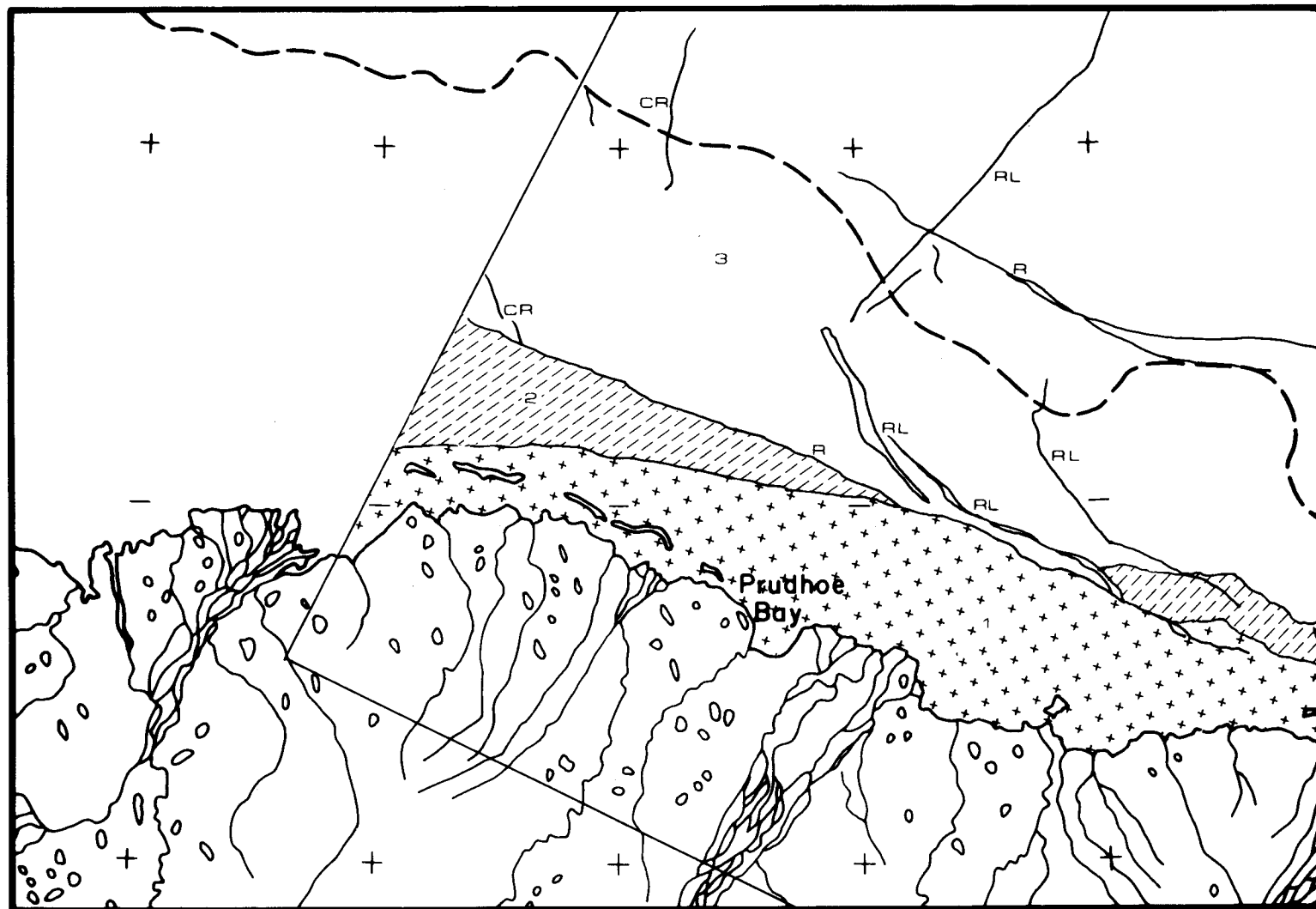
SHOREFAST SEA ICE

SURFACE MORPHOLOGICAL CHARACTERISTICS

BEAUFORT SEA COAST: PRUDHOE SECTOR

14 MARCH, 1973

16 March 1973:   Scene 1236-21292

This is another late winter scene with coverage into Harrison Bay.
The overall appearance of the ice is very similar to that of
14 March.   The continuous ice boundary is not well defined.   Light
toned, smooth-looking ice (1) continues along the coast in a band
approximately 10 to 25 km wide.   The seaward boundary of this zone
may be related to former continuous ice edges.   Seaward of zone 1
in western Harrison Bay is a zone of darker toned ice (2).   The
seaward edge of this zone is an extensively ridged or hummocked
zone (GR), possibly grounded.   The pack ice (3 and part of 4) is
well consolidated with little or no open water.   In outer Harrison
Bay the ice is composed of giant or larger sized floe elements
in a darker matrix of other ice.   There are many refrozen leads
(RL) and cracks (CR) in zone 3.   Two ridge systems (R) paralleling
the coast are noted in the eastern part of the zone, approximately
25 and 60 km from shore.   A hummock zone (H), possibly grounded,
is noted seaward of Harrison Bay.   Two areas of fairly light tone
(4) are present, one in the pack ice and one in the fast ice.
There is some cracking and possible ridging within the zones, but
they appear much more uniform than zone 3.   Shoreward of the larger
zone 4 is a narrow band of dark grey ice (5).   Possibly this re-
lates to movements of the pack ice or perhaps this is a ridge
system (the tone is similar to that of the large system on the
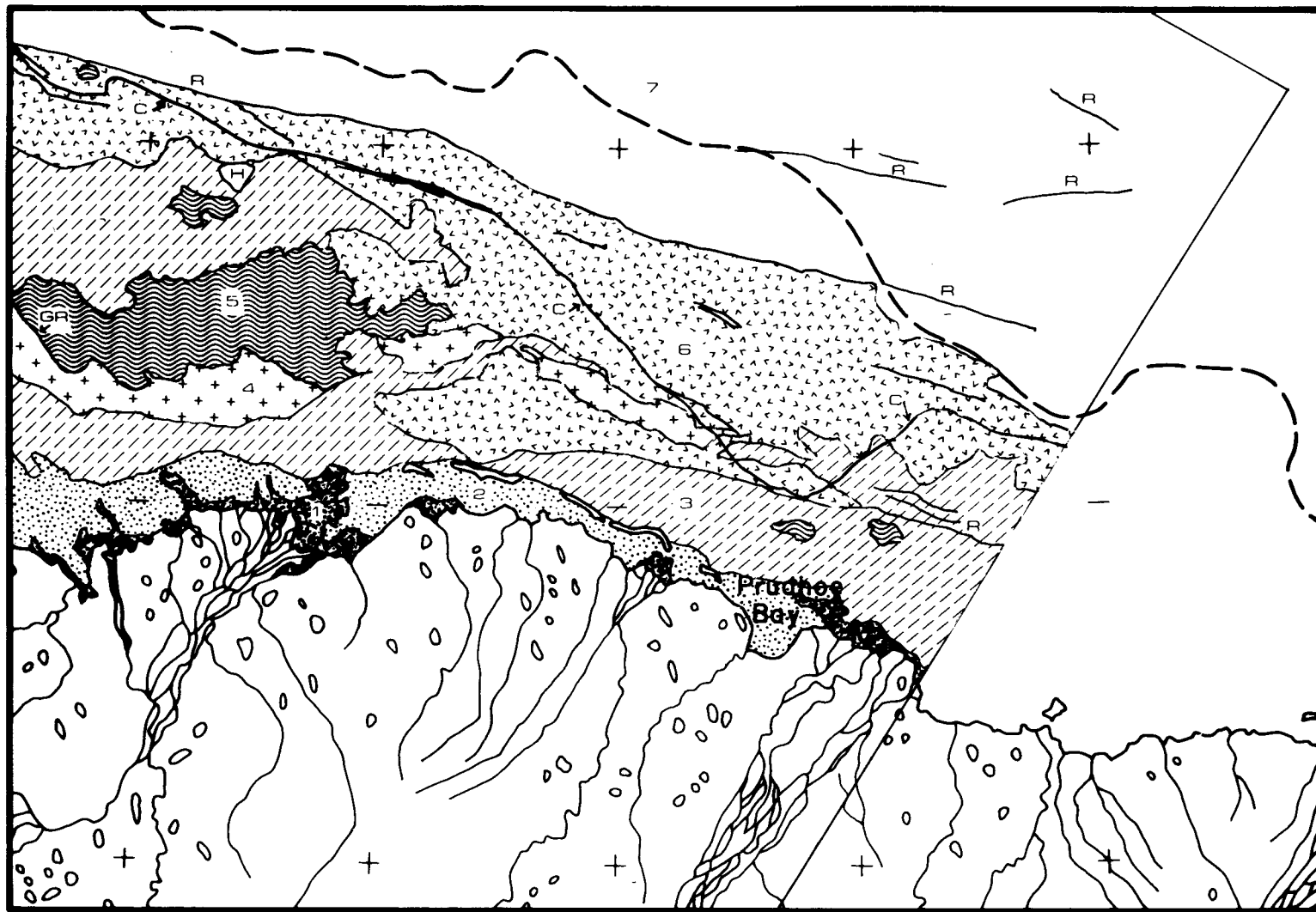seaward edge of zone 2).

SHOREFAST SEA ICE

SURFACE MORPHOLOGICAL CHARACTERISTICS

BEAUFORT SEA COAST: PRUDHOE SECTOR

16 MARCH, 1973

14 June 1973: Scene 1326-21284

In this late spring scene, the continuous ice edge is fairly
difficult to distinguish, but it has been roughly delimited (C).
There is much variation in the tone of the ice due to surface
meltwater and roughness differences. The pack ice (7 and part
of 6) is quite well consolidated. At river mouths and along the
coast (zone 1) the ice has either melted out or has been flooded
by meltwater. The nearshore ice (2) does not appear deformed.
There appears to be extensive puddling in this zone in varying
stages. Drainage has occurred in several areas, and drainage
cracks are present in interior Harrison Bay. The remainder of
the continuous ice zone appears to contain many deformational
features. Mapping in this zone was based on differential grey
tones. Zone 5 appears dark in all bands, so is probably most
heavily puddled. Zone 3 is composed of mottled light and dark
tones and is probably in various stages of puddling. The hummock
zone (H) noted on the 16 March frame is located in this zone.
Zone 6 is also composed of mottled light and dark tones, but
overall it appears lighter in all bands than zone 3. There are
many deformational features in this zone. Zone 4 appears to have
drained by this date. Without additional types of imagery (SLAR,
CIR) it is more difficult to interpret roughness and age charac-
teristics. There are two extensive ridge systems (R) paralleling
the shoreline. The system nearest the coast is also visible in
the 16 March frame. The outer system follows the 10 fm contour
and the continuous ice edge in the western part of the frame for
a short distance. In the eastern part of the frame this system
is approximately 20 km seaward of the 10 fm contour. The ridges
(GR) in outer Harrison Bay are especially prominent and have
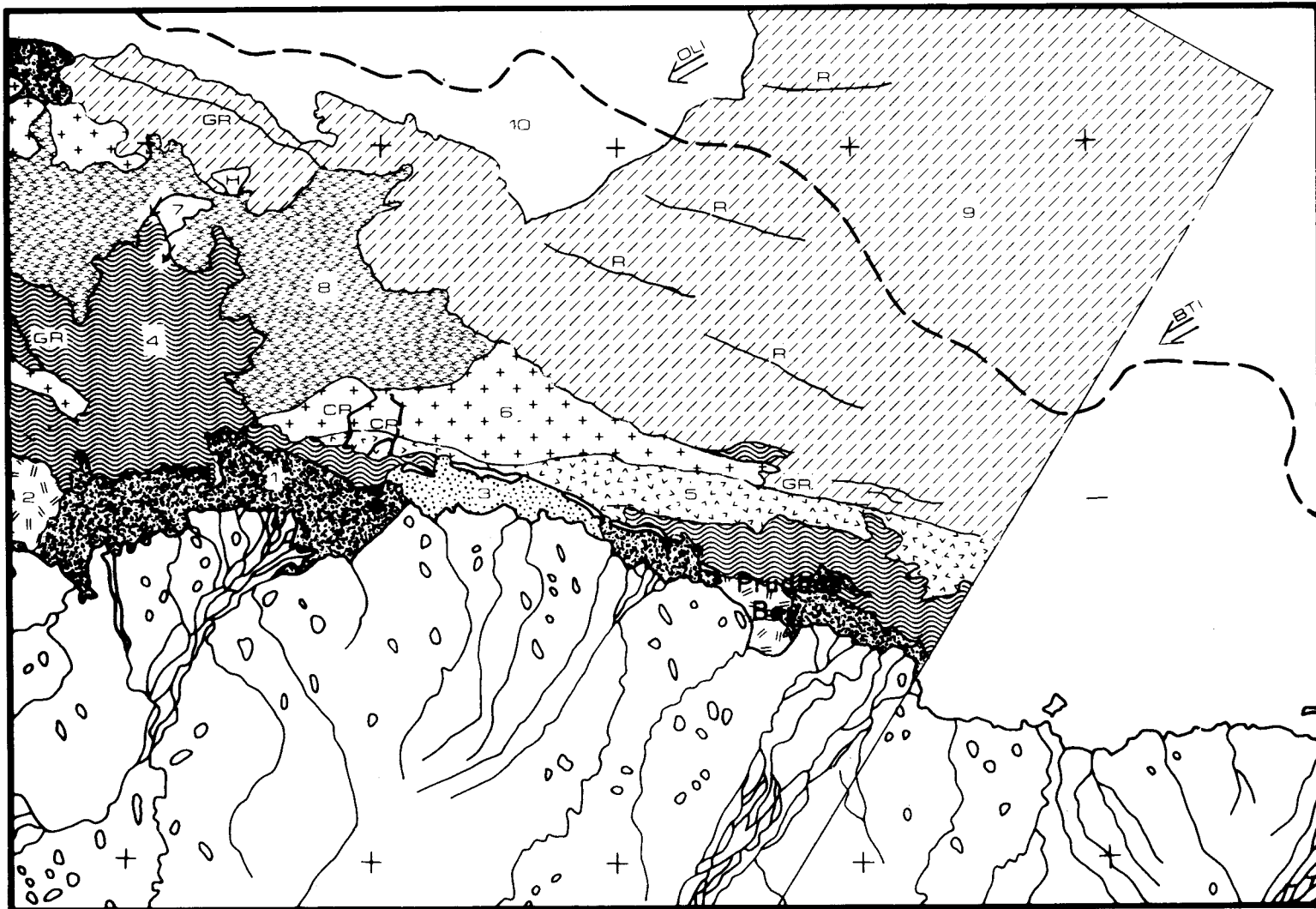remained stationary since 16 March.

SHOREFAST SEA ICE
SURFACE MORPHOLOGICAL CHARACTERISTICS
BEAUFORT SEA COAST: PRUDHOE SECTOR
14 JUNE, 1973

2 July 1973: Scene 1344-21283

In this early summer scene the character of the ice has changed
greatly. There is much more open water present, due to melting,
flooding of ice by river water, and movements in the fast and pack
ice. The western half of the frame has more open water than the
eastern half. In the western half the pack ice (zone 10) is frac-
turing and moving westward and the "continuous" ice appears to be
melting. Most movements in the continuous ice were too small to
be shown accurately on the map, however two displacements were of
sufficient magnitude (2 to 3 km) to be shown by arrows on the map.
Winds, shown by double arrows on the map, were from the ENE on
1 July for Oliktok (OLI) and Barter Island (BTI) at magnitudes of
5.4 m/sec and 4.9 m/sec respectively. In the eastern half, the
ice is quite continuous making it very difficult to locate the
shoreward edge of the pack ice (9). In the western half of the
frame the shoreward edge of the pack ice can be distinguished.
Large areas of open water (1) are present at the river mouths.
Much of the near shore smooth ice (2) has drained since 14 June.
Undrained smooth ice is designated 3. Much of this near shore
smooth ice has also disappeared since 14 June, especially in the
area of the Colville River shore polynya. There is a great deal
of variation in the amount of surface meltwater throughout the
"continuous" ice zone. Zones were mapped within this area based
on similar grey tones. Zone 4 appears to be the darkest, most
heavily puddled ice, although there are many light areas within
this zone. Zone 8 also appears quite dark overall, but has a
larger number of light areas than zone 4. Much of the ice in this
zone has broken up or melted since 14 June, and there is much open
water in this zone. Some of this ice may be older than first year,
but this distinction cannot be accurately made without SLAR and
CIR imagery. Zone 5 appears to be intermediate in puddling between
zones 4 and 6 in the eastern part of the frame. It is a fairly uni-
form medium grey tone with slight puddling variations. There are
large cracks (CR) in the western end, extending seaward through
zone 6. Two large areas (6) have drained since 14 June. The eastern
area appears quite deformed and gives some evidence of being grounded
(no movement since 16 March in certain places). There are large
cracks in the western part of this zone, possibly due to wind stress
and weakened ice. The ridge system along the shoreward edge of this
zone (GR) and extending to the east has been stationary since late
winter. A smaller area (7) that has drained since mid-June is
located just south of the hummock field (H) north of Harrison Bay.
A crack has developed along the shoreward edge of the hummock field.
It appears that the hummock field and the ridge system (GR) approx-
imately 5 km to the north of it are grounded. No movement seems to
have occurred between these two features. However, to the west of
the ridges open water is now present. Apparently an extension of
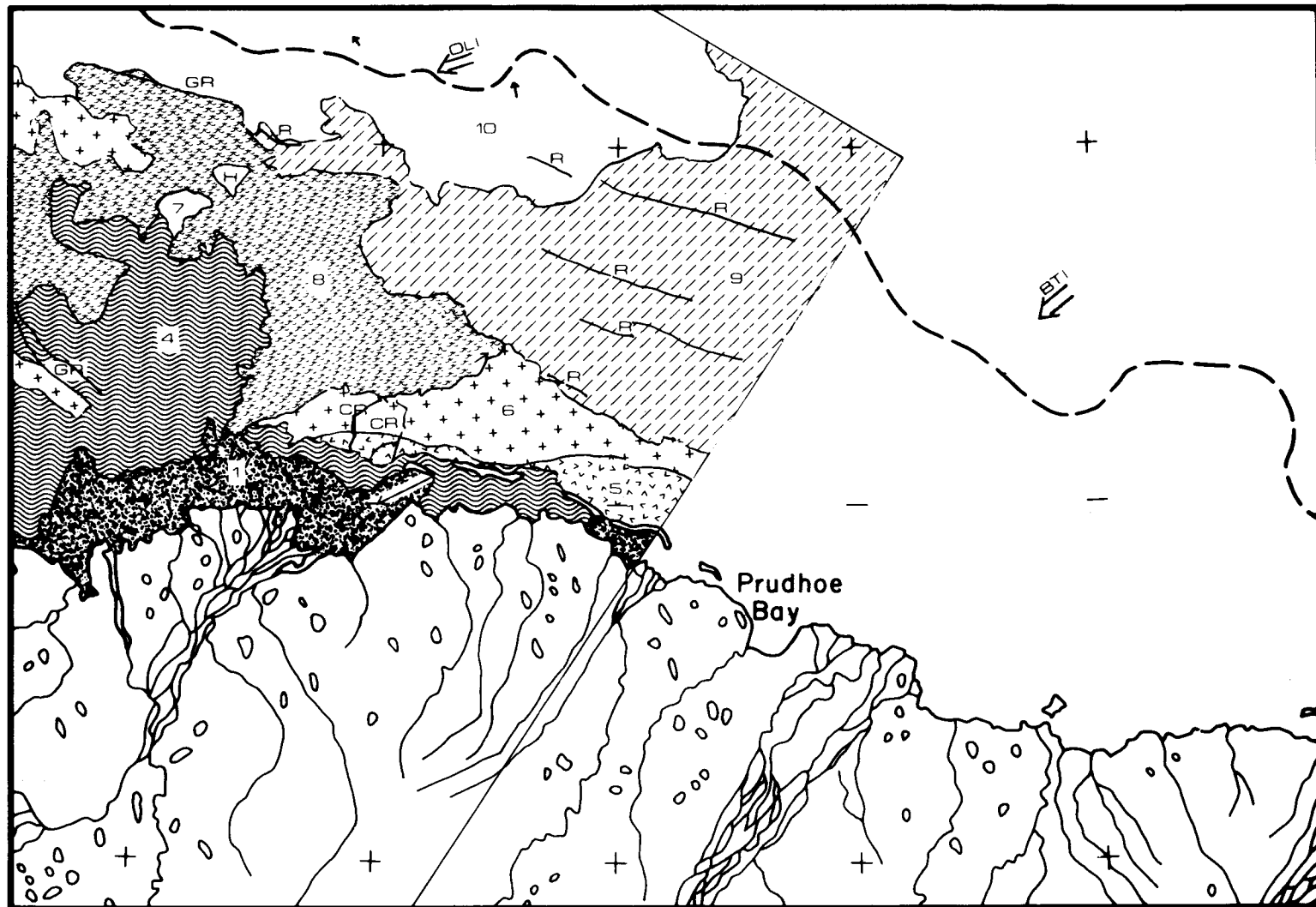these ridges has been rafted away.

SHOREFAST SEA ICE
SURFACE MORPHOLOGICAL CHARACTERISTICS
BEAUFORT SEA COAST: PRUDHOE SECTOR
2 JULY, 1973

3 July 1973:   Scene 1345-21342

This is an early summer scene which overlaps the previous frame suffi-
ciently to make detailed comparisons. The two scenes are quite
similar, although there have been many small movements and there is
slightly more open water at the mouth of the Colville River.   The
pack ice has moved northwestward several km. Displacements in the
ice are shown by arrows on the map. The major grounded features
(ridges in outer Harrison Bay, GR; hummock field, H; and ridges ap-
proximately 5 km seaward of the hummock field, GR) appear to have
remained stationary since the 2 July frame. Winds on 2 July, shown
by double arrows on the map, at Barter Island (BTI) and Oliktok (OLI)
were from the ENE and East at 2.9 m/sec and 4.5 m/sec respectively.
The amount of surface meltwater and the drainage characteristics of
the ice do not appear to have significantly changed since 2 July,
so the mapped grey zones are very similar for the two days.

SHOREFAST SEA ICE
SURFACE MORPHOLOGICAL CHARACTERISTICS
BEAUFORT SEA COAST: PRUDHOE SECTOR
3 JULY, 1973

23 August 1973:   Scene 1396-21162
24 August 1973:   Scene 1397-21220

In these two late summer frames, extending from the Colville River
to the Canning River, the ice is gone except for scattered frag-
ments.   It appears that none of the ice is grounded; most of it
being in very deep water.

743